ECN-C--04-079

TURBU OFFSHORE, COMPUTER PROGRAM FOR FREQUENCY DOMAIN ANALYSIS OF HORIZONTAL AXIS OFFSHORE WIND TURBINES

Implementation

T.G. van Engelen
H. Braam

SEPTEMBER 2004

Abstract

The design of offshore wind turbines requires to assess a huge amount of different sea-states and wind conditions. Therefor the calculational efficiency of a combined time/frequency domain approach is attractive. This was the reason for the development of the frequency domain tool TURBU Offshore. In addition, such a tool is very feasible for parameter studies; the dynamics of large offshore wind turbines use to be highly sensitive to the natural frequency values.
The implementation of TURBU Offshore is based on a modular linear model, with control loops included. The assumptions for structural and aerodynamic modelling are state of the art. A multi-blade transformation for three-bladed rotors eliminates the rotational coupling between the blades and the tower. Two-bladed rotors require a general handling of this coupling, which is however enabled by the model set-up. The program provides the mean loads, power spectra and periodic loads, which are merged to overall load histories for fatigue assessment. Besides, the power spectra make clear the relevance of poorly damped deformation modes.
Verification exercises point out that TURBU Offshore works well in stationary conditions and that it predicts damping rates and natural frequencies properly. It is expected that the use of TURBU Offshore in the design of wind turbines will yield substantial cost reduction for the nacelle, rotor and tower.
It is recommended to develop guidelines for the complementary use of TURBU Offshore with a time domain tool. The derivation of submodels for control design will be useful, just as the coupling of the linear structural dynamics model to an advanced aerodynamic code.

Acknowledgement

Danny Winkelaar is acknowledged for a substantial project contribution by way of fruitful discussions and reviewing the report.

Eric van der Hooft and Pieter Schaak are acknowledged for their outstanding support all over the project.

Luc Rademakers is acknowledged for creating the best possible conditions under the given constraints for carrying out the job.

Ben Hendriks is acknowledged for pleasant and effective project supervision.

Jaap ’t Hooft is acknowlegded for his understanding for the complications encountered during the course of this project.

Novem and the Dutch Ministry of Economic affairs are acknowledged for the financial grant of the project that has been executed under Novem project no. 2020-01-12-10-001 and ECN project no. 7.4152.

CONTENTS

SUMMARY

Problem statement
The design of offshore wind turbines significantly differs from that of onshore turbines by the huge amount of different sea-states to which they are subjected. Sea-states are combinations of mean wind speed and direction and significant wave height, period and direction. The large number of potential environmental conditions (sea states) makes it very time consuming to carry out a fatigue analysis with a time domain structural dynamics code like PHATAS [10] in the same straightforward way as for onshore wind turbines. For this reason, a combined time/frequency domain approach for fatigue analysis and sensitivity studies is very desirable: the high calculational speed of a frequency domain tool like TURBU Offshore allows for the evaluation of numerous sea-states that are close to a 'centre sea-state', which is assessed with a high-accuracy time domain tool like PHATAS.

Because large offshore wind turinbes tend to have low natural frequencies, the combined dynamic excitation by the wind and the waves may have a large impact on the structural integrity of the wind turbine. A frequency domain tool gives a quick insight in (undesired) dynamic interaction and thus allows for efficient parameter study of the choice of natural frequencies and damping.

Objective
The objective of the project TURBU Offshore [5] is to develop a computer program for frequency domain analysis of offshore wind turbines that enables the user

1. to evaluate the numerous load cases in a much faster way;
2. to determine the safety margins for the natural frequencies and the rotor speed;
3. to select the most important load cases for time domain analysis, for design purposes and for certification.

Because a frequency domain approach requires linearity of the equations of motion, the implemented wind turbine model in the program also enables the performance of stability analyses and control design.

Approach
A linear model of the whole wind turbine is the point of departure for frequency domain analysis. A modularised set-up has been obtained by idealising the wind turbine to an assemblage of distinct substructures or *components* – the tower/nacelle, the drive train, and the blades – which in turn consist of one or more discrete, rigid elements (see figure). This modularisation enables to include feedback control algorithms and to deal with special features like a (free) flapping hinge and dynamic yawing in a well organised and unconstrained way.

Other key features of the approach that has been adopted in the development of TURBU Offshore are the aerodynamic model and the modelling of the external forces. Also the rotational coupling between the blades and the tower is a key feature in linear wind turbine modelling.

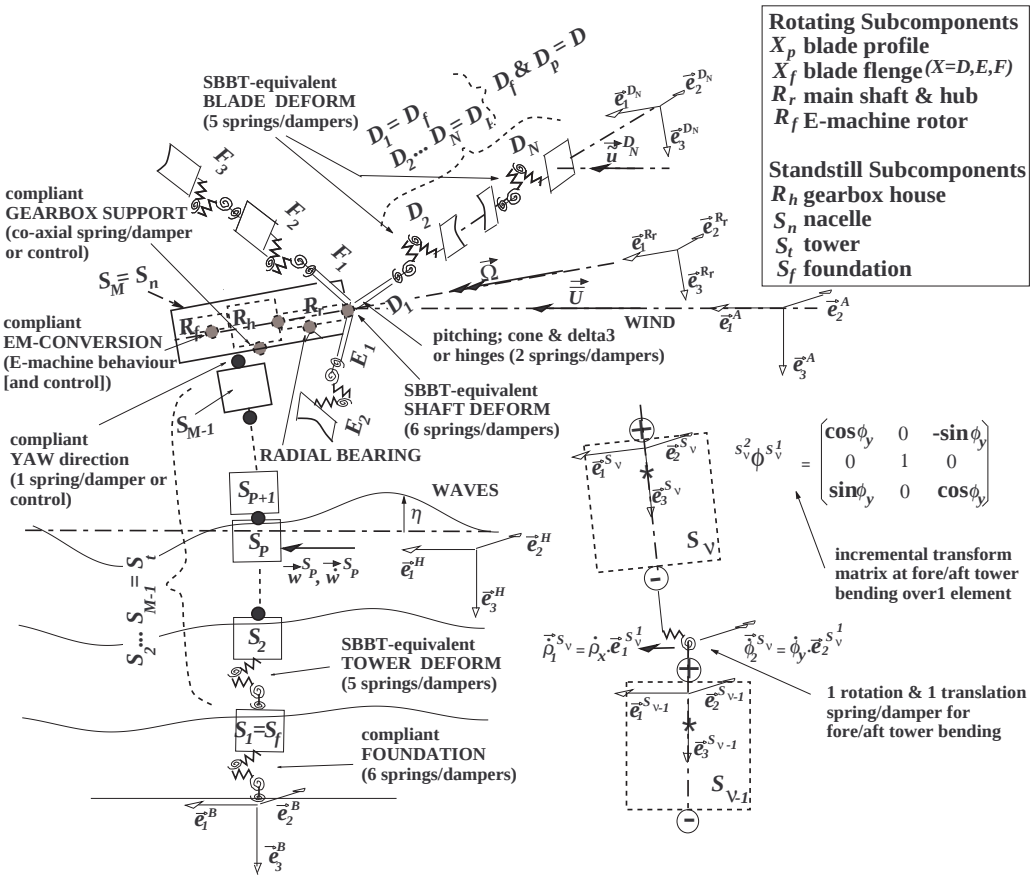

The wind turbine as an assembly of distinct substructures of elements

Substructures and subcomponents

All flexibility of a substructure is assumed to be concentrated at the attachments between the elements. The flexibility, or in broader sense the compliance, is represented by massless springs and dampers or any other mechanism for the generation of responsive loads for up to six degrees of freedom. The degrees of freedom allow for the modelling of structural deformation like tower and blade bending but also for the modelling of special degrees of freedom like foundation compliance, dynamic yawing, rotor shaft bending, pitch control and flapping hinges.

Each substructure is subdivided into different sets of elements, the subcomponents. The support structure is subdivided into subcomponents for the foundation, the tower, and the nacelle; the drive-train is modelled from submodels for the gearbox house, the generator rotor and the rotor shaft & hub; the rotor blades are subdivided into a so called 'flange' and 'profile' subcomponents.

Control algorithms are accommodated in the blade flange and generator rotor submodels. The set-up of the blade profile submodel allows for choosing the location of the aerodynamic axis, elastic axis and centre of gravity axis different from the pitch axis; it also allows for prebending and a cone and 'δ_3'-angle.

Aerodynamic model

To find the equilibrium position of the blades, the distribution of the axial and

tangential induction over the rotor plance is computed using Blade Element Momentum (BEM) theory with Prandtl's correction to account for the finite number of blades and corrections to the 2D lift polar to account for 3D-effects. Prandtl's correction is applied twice: at the blade tip and at the blade root.

Dynamic effects of the wake, also for yawed conditions, are taken into account by the engineering model as proposed by Schepers and Vermeer [12] or Glauert. The implemented wake model does not cater for instantaneous blade-specific changes. Therefor in each annulus only the transient behaviour of the annulus-average induction speed applies.

External forces
The environmental loads to be accounted for include those due to the wind, waves, soil movement, and gravity. Thus far only the longitudinal wind speed component is taken into account. Besides, periodic variations due to wind shear and tower passage are included; the former in accordance with IEC requirements and the latter via a semi-infinite dipole model.

The waves are assumed to have zero-average velocity, i.e. there is no current. The frequency domain approach enables by nature to account for the random character of the wind and the waves via power spectra and coherence functions.

Rotational coupling
The equations of motion for the integrated model, which results by connecting subcomponent models to component models and linking together the component models have coefficients that are periodic in the rotational frequency. This makes them not suitable for well-known solution procedures for systems of ordinary first order differential equations.

Because of the polar symmetry of rotors with three or more identical blades a simple transformation – the so-called multi-blade transformation, see Coleman & Feingold [3] – can eliminate the periodic coefficients in the full system equations. The only price to be payed for it consists in (i) multiplication of the wind speed variations with certain harmonic functions in the rotational speed before they enter the transformed model equations and (ii) multiplication of the output variables of the transformed model equations with similar harmonic functions.

The approach adopted for making the dynamic analysis of the complete structure more numerically efficient is a method proposed by Graig and Bampton [7]. The method allows for the significant reduction of the degrees of freedom in the blade and tower model without loss of accuracy in the dynamic behaviour of the lower bending modes; the number of modes to be included can be specified.

Results
The computer program TURBU Offshore has been developed for frequency domain analysis of offshore wind turbines with three blades or more. The set-up enables to include control algorithms and generalised degrees of freedom in a convenient way. The rotational coupling between the blades and the tower is eliminated via a multi-blade coordinate transform. The high rate of modularisation and the adopted model order reduction technique makes it possible to deal with the rotational coupling in a more general way (harmonic balancing, Floquet Transition Matrix method), which is required for the analysis of single- and

two-bladed rotors.

The implemented model set-up makes it also possible for aero-elastic stability analysis and control design. The incorporation of control loops makes it very valuable for realistic predictions of the stability. This becomes more important when the wind turbines become larger and larger.

The output of TURBU Offshore consists of the mean loads, power spectra for the stochastic loads and Fourier series for periodic loads. Overall load histories are assembled via a realisation algorithm and processed into load histograms for fatigue loading assessment.

Especially the power spectra provide a clear view on the relevance of poorly damped deformation modes for fatigue loading. This depends heavily on the rate of excitation, which depends on the power spectrum of wind and waves, the coherence of turbulence in the rotor plane and the rotational speed. The excitation by turbulence and waves is not taken into account in conventional aero-elastic stability analysis.

Conclusion
Calculations with the non-linear structural dynamics code PHATAS pointed out that TURBU Offshore works well in steady conditions.

Fast frequency domain load calculation with TURBU Offshore enables efficient assessment of the numerous load cases for offshore wind turbines (objective 1).

The validated calculation of damping rates and natural frequencies shows that TURBU Offshore can be used to determinte the safety margins with respect to the natural frequencies and the rotational speed (objective 2).

Since TURBU Offshore works properly both in load assessment and aero-elastic stability anlaysis, it will be suitable for the selection of the most important load cases for time domain analysis, design and certification (objective 3).

The use of TURBU Offshore will enable
- a higher level of design optimisation via fast frequency domain calculations,
- to get a better understanding in the dynamic deformation behaviour,
- to derive effective models for control optimisation and innovation.

Recommendations
It is recommended to develop guidelines for the complementary use of TURBU Offshore with a time domain tool like PHATAS. For the use of a frequency domain tool the linearised approximation must be valid in the conditions concerned. Mandatory load cases for certification should be the point of departure.

It is further recommended to derive submodels for control design and to use the integrated model in aero-elastic stability analysis. This would improve the dynamics in control design models and add control loops in stability analysis.

A third recommendation concerns the coupling of the integrated linear structural dynamics model of TURBU Offshore to an advanced aerodynamic code like AWSM. AWSM is expected to substantially reduce the number of uncertainties that accompany currently used BEM models.

SYMBOLS AND DEFINITIONS

The symbols and definitions are listed in three sections. The first section deals with the symbols. The descriptions may be superscripted by "^{DEF} ", which tells that a definition is given in a next section. The second section lists general definitions; the third one specific definitions of angles, coordinate systems, translations and points.

Symbols

A	:	state transition matrix in first order linear state space model
A	:	identifier for the wind field with coordinate system^{DEF} $\vec{e}^{\,A}$
$\underline{a}^{Q_k^{\mathrm{p}}}$	:	coordiantes of acceleration vector of point 'p' on structural element Q_k along axes of coordinate system $\vec{e}^{\,Q_k}$; point^{DEF} identifier $\mathrm{p} = \mathrm{a}, \mathrm{h}, *, \oplus, \ominus$ for aero- & hydrodynamic conversion, centre of gravity, element entry & exit; see also $\underline{q}^{Q_k^{\mathrm{p}}}$
B	:	input matrix in first order linear state space model
B	:	identifier for the turbine base with coordinate system^{DEF} $\vec{e}^{\,B}$
B	:	number of blades
C	:	output matrix in first order linear state space model
$C_{\mathrm{D}}^{X_k}$, $C_{\mathrm{L}}^{X_k}$, $C_{\mathrm{M}}^{X_k}$	:	drag, lift and moment coefficient for blade element X_k
$C_{\mathrm{M}}^{S_k}$	:	mass coefficient for under water tower element S_k
c^{X_k}	:	chord length of blade element X_k
D	:	feedthrough matrix in first order linear state space model
D, D_k	:	identifier for the first rotor blade and its k^{th} element; see X
D^{S_k}	:	diameter of tower element S_k
d^{W_m}	:	distance parameter in expression for Prandtl's correction factor in rotor annulus W_m
E, E_k	:	identifier for the second rotor blade and its k^{th} element; see X
E	:	elasticity modulus
F, F_k	:	identifier for the third rotor blade and its k^{th} element; see X
$F_{\mathrm{p}}^{W_m}$	:	Prandtl's correction factor for blade tip or blade root loss in rotor annulus W_m
${}^{\mathrm{a}}\underline{f}^{X_k^{\mathrm{a}}}$	:	coordinates of concentrated aerodynamic force in conversion point X_k^{a} along $\vec{e}^{\,X_k}$
${}^{\mathrm{h}}\underline{f}^{S_k^{\mathrm{h}}}$	:	coordinates of concentrated hydrodynamic force in conversion point S_k^{h} along $\vec{e}^{\,S_k}$
${}^{\mathrm{g}}\underline{f}^{Q_k^*}$	:	coordinates of concentrated gravity force in c.o.g. X_k^* along $\vec{e}^{\,Q_k}$
G	:	identifier for the earth surface with coordinate system^{DEF} $\vec{e}^{\,G}$
${}^{\mathrm{a}}G_{\mathrm{fq}_{k,j}}^{\mathrm{F}}$	:	matrix that maps the transformed distributed aerodynamic force loading ${}^{X_k}\Phi^{X_{k+j}^{\mathrm{cv}}} \cdot {}^{\mathrm{a}}\underline{q}_{\mathrm{f}}^{X_{k+j}^{\mathrm{cv}}}$ to the concentrated force ${}^{\mathrm{a}}\underline{f}^{X_k^{\mathrm{a}}}$; only depends on blade element width S; $_{j=[-1],0,[1]}$
${}^{\mathrm{a}}G_{\mathrm{tq}_{k,j}}^{\mathrm{F}}$	:	matrix that maps the transformed distributed aerodynamic force loading ${}^{X_k}\Phi^{X_{k+j}^{\mathrm{cv}}} \cdot {}^{\mathrm{a}}\underline{q}_{\mathrm{f}}^{X_{k+j}^{\mathrm{cv}}}$ to the concentrated torque ${}^{\mathrm{a}}\underline{t}^{X_k^{\mathrm{a}}}$; only depends on blade element width S; $_{j=[-1],0,[1]}$
${}^{\mathrm{a}}G_{\mathrm{tq}_k}^{\mathrm{M}}$	:	matrix that maps the distributed aerodynamic torque loading ${}^{\mathrm{a}}\underline{q}_{\mathrm{t}}^{X_k^{\mathrm{cv}}}$ to the concentrated torque ${}^{\mathrm{a}}\underline{t}^{X_k^{\mathrm{a}}}$; only depends on blade element width S
${}^{\mathrm{h}}G_{\mathrm{fq}_{k,j}}^{\mathrm{F}}$	:	matrix that maps the transformed distributed hydrodynamic force loading ${}^{S_k}\Phi^{H} \cdot {}^{\mathrm{h}}\underline{q}_{\mathrm{f}}^{S_{k+j}^{H}}$ to the concentrated force ${}^{\mathrm{h}}\underline{f}^{S_k^{\mathrm{h}}}$; only depends on tower element length L; $_{j=[-1],0,[1]}$
${}^{\mathrm{h}}G_{\mathrm{tq}_{k,j}}^{\mathrm{F}}$	:	matrix that maps the transformed distributed hydrodynamic force loading ${}^{S_k}\Phi^{H} \cdot {}^{\mathrm{h}}\underline{q}_{\mathrm{f}}^{S_{k+j}^{H}}$ to the concentrated torque ${}^{\mathrm{a}}\underline{t}^{S_k^{\mathrm{h}}}$; only depends on tower element length L; $_{j=[-1],0,[1]}$
G	:	shear modulus
g	:	gravitation
H	:	identifier for the wave field with coordinate system^{DEF} $\vec{e}^{\,H}$

${}^{(G)}\frac{\mathrm{d}}{\mathrm{d}t}\left({}^{Q_k^{\ominus}}\underline{h}^{Q_k}\right)$	:	time-derivative, relative to the earth, of the angular impulse coordinates of element Q_k along $\vec{e}^{\,Q_k}$ with respect to entry point $Q_k^{\ominus}$; contribution from motion of $Q_k^{\ominus}$ excluded ($\stackrel{\triangle}{=} {}^{Q_k^{\ominus}}\dot{\underline{h}}^{Q_k}$)
I^{Q_k}	:	matrix with inertia moments and products of element Q_k relative to the centre of gravity Q_k^* and valid in the final coordinate system^{DEF} $\vec{e}^{\,Q_k}$ of Q_k
i_{gb}	:	fast-to-slow transmission ratio of gearbox
$J_x^{Q_k}$, $J_y^{Q_k}$, $J_z^{Q_k}$	:	priniciples moments of inertia of Q_k (relative to c.o.g. Q_k^*, along main principle axes)
$\mathrm{J}_{i=m}^{k}(P_i)$	:	get (large) matrix by putting matrices $P_m \ldots P_k$ next to each other from left ro right ($k > m$)
$k_{\mathrm{FF}}(j)$, $k_{\mathrm{FF}}^{\oplus}(j)$	:	final element number of the foregoing subcomponent of the j^{th} subcompoment; first element number of j^{th} subcomponent; used without '(j)' if context allows
$k_{\mathrm{PP}}(j)$, $k_{\mathrm{PP}}^{\ominus}(j)$	:	first element number of the subsequent subcomponent of the j^{th} subcompoment; last element number of j^{th} subcomponent; used without '(j)' if context allows
L	:	length of tower elements $S_{2\ldots M-2}$; foundation and top elements S_1 and S_{M-1} have length $L/2$
M	:	number of elements in support structure S; $S_{\mathrm{f}} = \{S_1\},\ S_{\mathrm{t}} = \{S_{2\ldots M-1}\},\ S_{\mathrm{n}} = \{S_M\}$
M_{uw}	:	number of under water elements in support structure S
N	:	number of elements in a rotor blade X; $X_{\mathrm{f}} = \{X_1\},\ X_{\mathrm{p}} = \{X_{2\ldots N}\}$
P	:	number of rotor annuli in wake W
${}^{(G)}\frac{\mathrm{d}}{\mathrm{d}t}\left(\underline{p}^{Q_k}\right)$	:	time-derivative, relative to the earth, of the linear impulse coordinates of Q_k along $\vec{e}^{\,Q_k}$ ($\stackrel{\triangle}{=} \dot{\underline{p}}^{Q_k}$)
Q, Q_k	:	generic identifier for wind turbine 'component' and its k^{th} element ($Q = S, R, X, W$)
${}^{\mathrm{a}}\underline{q}_{\mathrm{f}}^{X_k^{\mathrm{cv}}}$, ${}^{\mathrm{a}}\underline{q}_{\mathrm{t}}^{X_k^{\mathrm{cv}}}$	:	coordinates of distributed aerodynamic force and torque loading on element X_k in its *conversion* coordinate system^{DEF} $\vec{e}^{\,X_k^{\mathrm{cv}}}$
${}^{\mathrm{a}}\underline{q}_{\mathrm{f}}^{X_{\mathrm{FF}}}$	:	distributed aerodynamic force loading on final element $X_{k_{\mathrm{FF}}}$ of foregoing subcomponent along coordinate system of $X_{k_{\mathrm{FF}}}$
${}^{\mathrm{a}}\underline{q}_{\mathrm{f}}^{X_{k_{\mathrm{FF}}}^{\mathrm{cv}}}$	:	distributed aerodynamic force loading on first element $X_{k_{\mathrm{PP}}}$ of subsequent subcomponent along coordinate system of $X_{k_{\mathrm{PP}}-1}$
${}^{\mathrm{h}}\underline{q}_{\mathrm{f}}^{S_k^H}$	:	coordinate vector of distributed hydrodynamic force loading on element S_k in the hydrodynamic coordinate system^{DEF} $\vec{e}^{\,H}$
$\underline{q}^{Q_k^{\mathrm{p}}}$	:	vector with coordinates of (geometric) vector $\vec{q}^{\,Q_k^{\mathrm{p}}}$ pertaining to point 'p' on structural element Q_k; the coordinates pertain to the axes of the coordinate system $\vec{e}^{\,Q_k}$ fixed to element Q_k; $\left(\underline{q}^{Q_k^{\mathrm{p}}}\right)^{Z_j}$ is the coordinate vector of $\vec{q}^{\,Q_k^{\mathrm{p}}}$ in $\vec{e}^{\,Z_j}$ of element Z_j; if 'p' is omitted, the vector q pertains to the whole element, such as for angular velocity etc.
${}^{\mathrm{a}}\underline{t}^{X_k^{\mathrm{a}}}$	:	coordinates of concentrated aerodynamic torque in conversion point X_k^{a} along $\vec{e}^{\,X_k}$
${}^{\mathrm{h}}\underline{t}^{S_k^{\mathrm{h}}}$	:	coordinates of concentrated hydrodynamic torque in conversion point S_k^{h} along $\vec{e}^{\,S_k}$
R	:	identifier for the drive-train
R_{h}, R_{f}, R_{s}, R_{h}	:	identifiers for subcomponents gearbox house, generator rotor, shaft system, rotor shaft & hub
r^{W_m/X_k}	:	radius of annulus W_m as concerns the intersection with the k^{th} element of the rotor blades
${}^{Q_k^{\mathrm{p1}}}\underline{r}^{Q_k^{\mathrm{p2}}}$	:	coordinates of place vector from point p1 to p2 on element Q_k; invariant in coord system $\vec{e}^{\,Q_k}$
$S_{\underline{x}_1\underline{x}_2}(f)$	:	spectrum matrix between (column) vectors $\underline{x}_1$ and $\underline{x}_2$; Fourier transform of $\mathrm{E}[\underline{x}_1(t+\tau)\cdot\underline{x}_2^{\dagger}]$
S, S_k	:	identifier for the support structure and its k^{th} element with coordinate system^{DEF} $\vec{e}^{\,S_{k=1\ldots M}}$
S_{f}, S_{t}, S_{t}	:	identifiers for subcomponents foundation, tower and nacelle
S	:	span width of blade elements $X_{2\ldots N-1}$; flange and tip elements X_1 and X_N have length $S/2$
$\mathrm{S}_{i=m}^{k}(P_i)$	:	get (large) matrix by putting matrices $P_m \ldots P_k$ above each other from top to bottom ($k > m$)
$\bar{U}$	:	average undisturbed longitudinal wind speed; along x-axis of wind field coord sys^{DEF} $\vec{e}^{\,A}$
$U_{\ell}^{X_k^{\mathrm{a}}}$, $U_{\mathrm{n}}^{X_k^{\mathrm{a}}}$	:	leadwise and normal relative wind speed for element X_k; equal -z and +x-coordinate of $\underline{u}^{X_k^{\mathrm{a}}}$
$U_{\mathrm{i}}^{W_m}$, $V_{\mathrm{i}}^{W_m}$	:	axial and tangential induction speed for annulus W_m; equal -x and -z-coordinate of $\underline{u}_{\mathrm{i}}^{W_m}$
$U_{\mathrm{i_o}}^{X_k}$, $\underline{U}_{\mathrm{i_o}}^{X}$	:	periodic axial induction speed for blade element X_k; column vector for blade X; along x-axis of rotor annulus coordinate system^{DEF} $\vec{e}^{\,W_m/X}$
${}^{\mathrm{t}}u^{W_m/X}$, ${}^{\mathrm{t}}\underline{u}^{W/X}$	:	undisturbed longitudinal turbulence in intersection rotor blade X / rotor annulus W_m and column vector for blade X; along x-axis of $\vec{e}^{\,A}$
${}^{\mathrm{t}}\hat{u}_p^{W_m}$, ${}^{\mathrm{t}}\underline{\hat{u}}_p$	:	p^{th} rotational mode of undisturbed longitudinal turbulence in rotor annulus W_m and column vector the for p^{th} mode for the rotor plane; along x-axis of $\vec{e}^{\,A}$

$u_{\mathrm{ro}}^{X_k}$, $\underline{u}_{\mathrm{ro}}^{X}$: undisturbed periodic wind velocity varation for element X_k by wind shear, tower stagnation and oblique infow; stacked in one column vector for blade X; along x-, y- and z-axis of blade base coordinate system^{DEF} $\vec{e}^{\,X_0}$

$u_{\mathrm{im}}^{W_m}$, $\underline{u}_{\mathrm{im}}^{W}$: induction velocity velocity vector rotor annulus W_m; stacked in one column vector for the wake; along axes of wake coordinate system^{DEF} $\vec{e}^{\,W_m/X}$ (blade-independent induction)

$\underline{u}^{X_k^{\mathrm{a}}}$, $\underline{u}^{X}$: coordinates of relative wind speed vector for blade element X_k along conversion coordinate system $\vec{e}^{\,X_k^{\mathrm{cv}}}$; stacked in one column vector for blade X

$\underline{v}^{Q_k^{\mathrm{p}}}$: coordinates of velocity vector of point 'p' on element Q_k along $\vec{e}^{\,Q_k}$; see $\underline{a}^{Q_k^{\mathrm{p}}}$

$\underline{v}$: input vector of linear first order state space model

W, W_m : identifier for the wake and its m^{th} annulus with coord sys^{DEF} $\vec{e}^{\,W_{m=1\ldots P}/X}$ ($X = D, E, \ldots$)

X, X_k : generic identifier for a rotor blade and its k^{th} element with coordinate system^{DEF} $\vec{e}^{\,X_{k=1\ldots N}}$

$X_{\mathrm{f}}, X_{\mathrm{p}}$: identifiers for subcomponents blade flange and blade structure

$\underline{y}$: output vector of linear first order state space model

$\underline{z}$: state vector of linear first order state space model

$\underline{\alpha}^{Q_k}$: coordinates of angular acceleration vector of structural element Q_k along $\vec{e}^{\,Q_k}$; see also $\underline{q}^{Q_k^{\mathrm{p}}}$

$\beta^{X_k^{\mathrm{d}}}$: flap angle^{DEF} for blade element X_k

$\gamma(f, d)$: coherence function of longitudinal turbulence

$\delta_{i\uparrow j}$, $\delta_{i\downarrow j}$: equals 1 if respectively $i \leq j$ and $i \geq j$, zero elsewise

γ^A, γ^{g}, γ^B : angles^{DEF} for the directional orientation of the longitudinal wind speed, waves and turbine base

${}^{G}\Phi^{A}$: matrix for coordinate transformation from wind field coordinate system^{DEF} $\vec{e}^{\,A}$ to geographic coordinate system^{DEF} $\vec{e}^{\,G}$

${}^{G}\Phi^{H}$: matrix for coordinate transformation from wave coordinate system^{DEF} $\vec{e}^{\,A}$ to geographic coordinate system^{DEF} $\vec{e}^{\,G}$

${}^{S_0}\Phi^{G}$: matrix for coordinate transformation from geographic coordinate system^{DEF} $\vec{e}^{\,G}$ to turbine base coordinate system^{DEF} $\vec{e}^{\,S_0} = \vec{e}^{\,B}$

${}^{R_{\mathrm{s}}}\Phi^{R_{\mathrm{h}}"}$: matrix for coordinate transformation from auxiliary gearbox house coordinate system^{DEF} $\vec{e}^{\,R_{\mathrm{h}}"}$ to shaft system c.s.^{DEF} $\vec{e}^{\,R_{\mathrm{s}}}$: transformation over main rotation $\int^t \Omega \mathrm{d}t$

${}^{S_k}\Phi^{S_0}$: matrix for coordinate transformation from turbine bse coordinate system^{DEF} $\vec{e}^{\,S_0} = \vec{e}^{\,B}$ to coordinate system^{DEF} $\vec{e}^{\,S_k}$ for support structure element S_k; involves forward transformation over rotations in entry points of elements $S_{1\ldots k}$

${}^{X_0}\Phi^{X_k^{\mathrm{cv}}}$: matrix for coordinate transformation from conversion coordinate system^{DEF} $\vec{e}^{\,X_k^{\mathrm{cv}}}$ to blade base coordinate system^{DEF} $\vec{e}^{\,X_0}$ of blade X; involves backward transformation over -(ζ^{X_k}) and -(-β^{X_k})

${}^{X_0}\Phi^{W_m/Xk}$: matrix for coordinate transformation from wake coordinate system^{DEF} $\vec{e}^{\,W_m/Xk}$ to blade base coordinate system^{DEF} $\vec{e}^{\,X_0}$ of blade X; involves backward transformation over -($\zeta_{\mathrm{i}}^{X_k}$)

${}^{X_k}\Phi^{X_0}$: matrix for coordinate transformation from blade base coordinate system^{DEF} $\vec{e}^{\,X_0}$ to coordinate system^{DEF} $\vec{e}^{\,X_k}$ for blade element X_k; involves forward transformation over (summed) rotations in the entry points of blade element $X_{1\ldots k}$

${}^{X_k}\Phi^{X_k^{\mathrm{cv}}}$: matrix for coordinate transformation from conversion coordinate system^{DEF} $\vec{e}^{\,X_k^{\mathrm{cv}}}$ to final coordinate system $\vec{e}^{\,X_k}$ of blade element X_k

$\phi_{i=1\ldots3}^{Q_k}$, $\underline{\phi}^{Q}$: potential rotation degrees of freedom^{DEF} in entry point of element Q_k and column vector with the dofs $\phi_{i=1\ldots3}^{Q_k}$ for $k = 1 \ldots K$ (K number of elements in Q)

$\phi_{\mathrm{inf}}^{X_k}$, $\phi_{\mathrm{set}}^{X_k}$, $\phi_{\mathrm{a}\frac{3}{4}c}^{X_k}$: inflow and setting angle^{DEF} and angle of attack on 3/4 chord position ($\equiv$ $\phi_{\mathrm{a}"}^{X_k}$) for element X_k

ϕ_{yw}, ϕ_{ti} : average yaw and invariant tilt angle^{DEF} of nacelle

ϕ_{cn}^{X}, ϕ_{pt}^{X}, $\phi_{\delta_3}^{X}$: cone, average pitch, and δ_3 angle^{DEF} of rotor blade X at the flange

φ_{yw}, φ_{gb}, $\varphi_{\mathrm{pt}}^{X}$: yaw, pitch and co-axial gearbox house deviation angle

$\phi_{\mathrm{pf}}^{X_k}$, $\phi_{\mathrm{pe}}^{X_k}$: orientation angles^{DEF} for flatwise and edgewise prebending of blade element X_k

$\phi_{\mathrm{tw}}^{X_k}$, $\phi_{\mathrm{ez}}^{X_k}$, $\phi_{\mathrm{pr}}^{X_k}$: orientation angles^{DEF} for chord line, neutral elastic z-axis and main principle z-axis of X_k

ψ,ψ_{f},ψ_{s},ψ_{r} : azimut angles^{DEF} for the main rotation, generator rotor, gearbox slow shaft and turbine rotor

θ^A, θ^B	:	angles^{DEF} for the tiltwise orientation of the longitudinal wind speed and the turbine base
$\rho_{i=1\ldots3}^{Q_k}$, $\underline{\rho}^Q$	:	potential translation degrees of freedom^{DEF} in entry point of element Q_k and column vector with the dofs $\rho_{i=1\ldots3}^{Q_k}$ for $k = 1 \ldots K$ (K number of elements in Q)
ζ^{X_k}, $\zeta_{\mathrm{i}}^{X_k}$	:	element lead angle^{DEF} and induction lead angle^{DEF} for blade element X_k
Ω	:	*the* wind turbine's rotational speed: $1/i_{\mathrm{gb}}$ times relative rotor speed of generator to nacelle
$\underline{\omega}^{Q_k}$	:	coordinates of angular velocity vector of structural element Q_k along $\vec{e}^{\,Q_k}$; see also $\underline{q}^{Q_k^{\mathrm{p}}}$

General definitions and abbreviations

azimuth
: pertains to an angle between two lines in rotor plane; see angle, azimuth, rotor

azimuthal ($\equiv$ 'azimuth like')
: pertains to an angle between two lines that set up a plane nearly parallel to the rotor plane; see angle, azimuthal, gearbox fast & slow shaft, AND angle, gearbox house deviation, azimuthal.

c.o.g. $\Leftrightarrow$ Q_k^* for structural element Q_k
: centre of gravity of a body

c.o.g.: short form centre of gravity of a body

compliant behaviour
: behaviour of (sub)component differs from fixed mounted rigid body motion

compliant behaviour, actuated
: 'non-rigid dynamic responsing' via controlled actuator

compliant behaviour, non-
: (sub)component behaves as fixed mounted rigid body motion

compliant behaviour, passive
: 'non-rigid dynamic responsing' via passive elements like springs and dampers

component $\Leftrightarrow$ Q; $Q = S,\ R,\ D,\ E\ F,\ W$ ($\equiv$ substructure)
: set of structural elements that is grouped together for modelling purposes; components are support structure S, drive-train R and rotor blades $D,\ E,\ F$; the wake W is also a 'component', although it is not built up from structural elements but from rotor annuli.

control data
: specification of control algorithm, actuator and sensor behaviour

coordinate system
: set of three perpendicular axes fixed to a body; unit vectors $\vec{e}_i$ along these axes defined in x-, y- and z-direction such that ('right-turning'):
  - $\rightarrow\ \vec{e}_3 = \vec{e}_1 \times \vec{e}_2 \ \Leftrightarrow\ \vec{e}_z = \vec{e}_x \times \vec{e}_y$
  - $\rightarrow\ \vec{e}_1 = \vec{e}_2 \times \vec{e}_3 \ \Leftrightarrow\ \vec{e}_x = \vec{e}_y \times \vec{e}_z$
  - $\rightarrow\ \vec{e}_2 = \vec{e}_3 \times \vec{e}_1 \ \Leftrightarrow\ \vec{e}_y = \vec{e}_z \times \vec{e}_x$

coordinate system, final $\Leftrightarrow$ $\vec{e}^{\,Q_k}$ for structural element $Q_k \equiv \vec{e}^{\,Q_k^3}$
: final coordinate system $\vec{e}^{\,Q_k}$ of a structurual element Q_k; it is *the* coordinate system of Q_k, which is fixed to the rigid body part of Q_k (see 'i.c.s.')

coordinate system, intermediate $\Leftrightarrow$ $\vec{e}^{\,Q_k^w}$ for element Q_k after w rotations
: intermediate coordinate system $\vec{e}^{\,Q_k^w}$ of a structural element Q_k; results from preceeding i.c.s. $\vec{e}^{\,Q_k^{w-1}}$ by rotation along its x-, y- or z-axis;
  - $\rightarrow\ \vec{e}^{\,Q_k^3}$ is identical to the final coordinate system of Q_k(see 'f.c.s');
  - $\rightarrow\ \vec{e}^{\,Q_k^0}$ is identical to the final coordinate system of Q_{k-1}; an i.c.s.

  also applies to coordinate systems $\vec{e}^{\,B}$ and $\vec{e}^{\,A}$ of turbine base and wind field

coordinate system, rotating
: coordinate system with y- and z-axis that rotate in average sense (with average rotor speed)

c.s. & coord sys : short form coordinate system

degree of freedom
: possibility for movement of a structural element Q_k relative to element Q_{k-1}, i.e. the element it is connected to 'in downward sense'; up to 6 of these relative movements occur in entry point $Q_k^{\ominus}$ (> 1 entry points only for rotor shaft); the relative movements are along a specific axis of an intermediate coordinate system (i.c.s) with signs corresponding to the arrow directions of the i.c.s.

degree of freedom, rotation
: capability to rotation for element Q_k relative to Q_{k-1}; the i^{th} rotation dof implies an angle of $\phi_i^{Q_k}$ rad along an axis of the $(i-1)^{\text{th}}$ intermediate coordinate system, i.e. along $\vec{e}_{\text{ra}}^{\,Q_k^{i-1}}$, with $\text{ra} = x,\ y,$ or z ; note that $\vec{e}^{\,Q_k^i}$ originates from $\vec{e}^{\,Q_k^{i-1}}$ by rotation over $\phi_i^{Q_k}$ along $\vec{e}_{\text{ra}}^{\,Q_k^{i-1}} \rightarrow \vec{e}_{\text{ra}}^{\,Q_k^i} \equiv \vec{e}_{\text{ra}}^{\,Q_k^{i-1}}$!

degree of freedom, translation
: capability to translation for element Q_k relative to Q_{k-1}; the j^{th} translation dof implies a translation of $\rho_j^{Q_k}$ m along an axis of an intermediate coordinate system $\vec{e}_{\text{ta}}^{\,Q_k^i}$, with $\text{ta} = x,\ y,$ or z;
note: all translation dof's are considered 'lumped' $\rightarrow$ invariant element size and 'forward-located points' like Q_k^* and $Q_{k+p}^{\oplus}$ are only affected in speed and acceleration by $\rho_j^{Q_k}$ via its time derivatives

dof : short form degree of freedom

drtr: drive train

element $\Leftrightarrow$ Q_k ($\equiv$ structural element)
: basic building block for component in wind turbine model; lumped mass & principle moments of inertia in c.o.g. Q_k^*, entry and exit point $Q_k^{\ominus}$ and $Q_k^{\oplus}$ for connection to foregoing Q_{k-1} and next Q_{k+1}; N elements in rotor blades $\{X\}$, M elements in support structure S and 4 elements in drive-train R; hydrodynamic conversion point S_k^{h} on S_k (if underwater); aerodynamic conversion point X_k^{a} on X_k; mass-less & rigid point connectons on Q_k; degrees of freedom and configuration angles in entry point $Q_k^{\ominus}$ 'at the side' of Q_{k-1};

f.c.s. : short form coordinate system, final

gb: gearbox

i.c.s. : short form coordinate system, intermediate

inertia, central scalar
: inertia scalar relative to c.o.g.

inertia, central principal moments $\Leftrightarrow$ J_x^{Xk}, J_y^{Xk}, and J_z^{Xk} for blade element X_k
: principal moments of inertia relative to centre of gravity in final coordinate system of X_k

inertia, cross product
: integral of ('distance to line' $\cdot$ 'coordinate along line')$\cdot$ 'particle mass'

inertia, moment
: integral over body of ('distance to line')$^2\cdot$ 'particle mass'

inertia, principal moments
: moments of inertia along coordinate system for which cross poducts of inertia equal 0, relative to any point

inertia, scalar
: moment of inertia or cross product of inertia for a body relative to a line and point

iTr : acronym transmission ratio gearbox

nelza : acronym neutral elastic z-axis angle

priza : acronym principal z-axis angle

rotor annulus
subtube W_k in the wake model W; widths of annuli $W_1 \ldots W_P$ such that each annulus exactly encapsulates the same number of structural elements ($N : P$ is integer)

SBBT-equivalent deformation $\Leftrightarrow$ slender beam bending theory equivalent deformation
deformation modelling of a structural element via three rotation and two or three translation springs characterised by SBBT-identical response of (SBBT = slender beam bending theory):
1 : distorsion angle [and axial strain] on torque [and axial force] at element-end
2 : bending angles & translations on bending torques and forces at element-end.

structurual element: see element

subcomponent
subset of structural elements within the element set of a component:
→ flange X_f and blade structure & profile X_p in rotor blade X ($X = D, E, F$ for $B = 3$);
→ gearbox house R_h, generator rotor R_f, gearbox slow shaft R_s, and rotor shaft&hub R_r in drive-train R;
→ foundation S_f, tower S_t and nacelle S_n in support structure S;
a subcomponent is the smallest entity for which a separate dynamic state space model is modelled

substructure: see component

supstr: support structure

transmission ratio gearbox $\Leftrightarrow$ i_gb
ratio between rotational speeds of gearbox fast shaft (= electric machine shaft) and gearbox slow shaft (= entry point of rotor shaft) at non-revolving gearbox house; at azimuthal gearbox house deviation speed $\frac{\mathrm{d}}{\mathrm{d}t}(\phi_3^{R_\mathrm{h}})$ relative to S_M, the gearbox slow shaft has azimuth speed $\frac{\mathrm{d}}{\mathrm{d}t}(\psi_\mathrm{s})$ relative to S_M that is equal to $\frac{\mathrm{d}}{\mathrm{d}t}(\psi_\mathrm{f}) + (i_\mathrm{gb} - 1)/i_\mathrm{gb} \cdot \frac{\mathrm{d}}{\mathrm{d}t}(\phi_3^{R_\mathrm{h}})$ (see 'angle, ...' in section on definitions for angles ψ_f, ψ_s, $\phi_1^{R_\mathrm{h}}$)

tilt0
identifies a rotation axis as 'tilt-wise' at t=0 (in rotating coord sys)

yaw0
identifies a rotation axis as 'yaw-wise' at t=0 (in rotating coord sys)

Angles, coordinate systems, translations, points

angle, blade, of attack $\Leftrightarrow$ $\phi_{\mathrm{a}_{\frac{3}{4}c}}^{X_k} \equiv \phi_{\mathrm{a}"}^{X_k}$
angle of attack on 3/4 chord position for blade element X_k; equals difference between inflow angle $\phi_\mathrm{inf}^{X_k}$ and setting angle $\phi_\mathrm{set}^{X_k}$ augmented with the cone-angle correction term $_{1/2}\, c^{X_k}/r^{W_m/X_k} \cdot \sin\beta^{X_k}$

angle, azimut, main $\Leftrightarrow$ ψ [deg] (>0 at clockwise orientation in fore-to-aft view)
rotation along the x-axis from the horizontal, as observed in the nacelle from the 'tilted coordinate system', over the time integral of the main rotational speed $\boldsymbol{\Omega}$

angle, blade, azimuth offset $\Leftrightarrow$ ${}^{R_\mathrm{r}}\psi^{X_0}$ [rad] (>0 at clockwise orientation in fore-to-aft view)
rotation along the x-axis of rotor plane coord system $\vec{e}^{\,R_\mathrm{r}}$ from $\vec{e}_y^{\,R_\mathrm{r}}$ to the neutral spanwise direction ($\equiv y$-axis) of blade X; for 3 bladed rotor ${}^{R_\mathrm{r}}\psi^{X_0}$ amounts to $2\pi \cdot (q-1)/B$, with $q = 1, 2, 3$, $B = 3$, for $X = D, E, F$

angle, blade, flap $\Leftrightarrow$ $\beta^{X_{k=1\ldots N}}$ [rad] (>0 at backward orientation)
rotation from the blade-neutral y-axis $\vec{e}_y^{\,X_0}$ to the projection of the elastic axis of X_k in the blade-neutral xy-plane (spanned by $\vec{e}_{x,y}^{\,X_0}$);

angle, blade, induction lead $\Leftrightarrow$ $\zeta_{\mathrm{i}}^{X_{k=1\ldots N}}$ [rad] (>0 at clockw orientation in fore-to-aft view)
rotation from the blade-neutral y-axis to the projection in the rotor plane of the line from rotor centre $R_{\mathrm{r}}^{\oplus}$ to X_k^{a}, the point on X_k for aerodynamic conversion

angle, blade, inflow $\Leftrightarrow$ $\phi_{\mathrm{inf}}^{X_{k=1\ldots N}}$ [rad] (>0 at counter clockwise orientation in root-to-tip view)
rotation from the leadwise axis of blade element X_k to the relative blade velocity vector on X_k (inflow angle);

angle, blade, initial in-wind-plane azimuthal $\Leftrightarrow$ $\xi_0^{X_{k=1\ldots N}}$ [rad] (>0 clockw or. in fore2aft view)
mean at $t = 0$ of the rotations from the horizonal line in the wind plane to the projections in the wind plane of the lines from the rotor centre $R_{\mathrm{r}}^{\oplus}$ to the points X_k^{a} for aerodynamic conversion

angle, blade, lead $\Leftrightarrow$ $\zeta^{X_{k=1\ldots N}}$ [rad] (>0 at clockwise orientation in fore-to-aft view)
rotation from the projection of elastic axis of X_k in the blade-neutral xy- plane to the actual elastic axis of X_k

angle, blade, nelza $\Leftrightarrow$ $\phi_{\mathrm{ez}}^{X_{k=1\ldots N}}$ [deg] (>0 at counter clockwise orientation in root-to-tip view)
rotation from blade-neutral z-axis to the neutral elastic z-axis of blade element X_k at zero pitch angle and no blade deformation (neutral elastic z-axis angle); $\equiv 0$ for blade flange element X_1

angle, blade, priza $\Leftrightarrow$ $\phi_{\mathrm{pz}}^{X_{k=1\ldots N}}$ [deg] (>0 at counter clockwise orientation in root-to-tip view)
rotation from blade-neutral z-axis to the principle z-axis of blade element X_k at zero pitch angle and no blade deformation (principal z-axis angle); $\equiv 0$ for blade flange element X_1

angle, blade, set $\Leftrightarrow$ $\phi_{\mathrm{set}}^{X_{k=1\ldots N}}$ [rad] (>0 at counter clockwise orientation in root-to-tip view)
rotation from the leadwise axis of blade element X_k to its chord line for the actual pitch angle and blade deformation state (setting angle);

angle, blade, twist $\Leftrightarrow$ $\phi_{\mathrm{tw}}^{X_{k=1\ldots N}}$ [deg] (>0 at counter clockwise orientation in root-to-tip view)
rotation from blade-neutral z-axis to the chord line of blade element X_k at zero pitch angle and no blade deformation (twist angle);

angle, blade flange, average pitch $\Leftrightarrow$ ϕ_{pt}^{X} [deg] (>0 at counter clockw. orient. in root2tip view)
average angle along $\vec{e}_y^{\,X_1^1} \equiv y$-axis in blade root after flapwise rotation (working point value of pitch angle)

angle, blade flange, pitch deviation $\Leftrightarrow$ $\varphi_{\mathrm{pt}}^{X} \equiv \varphi_2^{X_1}$ [deg] (>0 at counter clockw. orient. in root2tip view)
average angle along $\vec{e}_y^{\,X_1^1} \equiv y$-axis in blade root after flapwise rotation (working point value of pitch angle)

angle, blade flange, cone $\Leftrightarrow$ ϕ_{cn}^{X} [deg] (>0 at backward orientation)
fixed angle along blade neutral z-axis $\vec{e}_z^{\,X_1^0} = \vec{e}_z^{\,X_0}$ in blade flange via flapwise oriented offset of the blade's spanwise direction

angle, blade flange, δ_3 $\Leftrightarrow$ $\phi_{\delta_3}^{X}$ [deg] (>0 at clockwise orientation in fore-to-aft view)
fixed angle along $\vec{e}_x^{\,X_1^2}$ in blade flange, after flapwise rotation and pitching, via leadwise oriented offset of the blade's spanwise direction;

angle, blade structure, prebend edgewise $\Leftrightarrow$ $\phi_{\mathrm{pe}}^{X_{k=2\ldots N}}$ [deg] (>0 at clockw. or. in fore2aft view)
fixed angle along $\vec{e}_x^{\,X_k^2}$, after flapwise prebend and twist, via edgewise oriented offset, of the blade's spanwise direction

angle, blade structure, prebend flatwise $\Leftrightarrow$ $\phi_{\mathrm{pf}}^{X_{k=2\ldots N}}$ [deg] (>0 at backward orientation)
fixed angle along $\vec{e}_z^{\,X_k^1}$, after twist, via flapwise oriented offset of the blade's spanwise direction

angle, blade flange, deviation $\Leftrightarrow$ $\phi_i^{X_1}$ [rad] (>0 in accordance with c.s. $\vec{e}^{\,X_1}$, flap/pitch/lead)
set of 3 successive lumped rotations in entry point $X_1^{\ominus}$ of blade flange element X_1 (rotation dof's); bottum-up ordered as:

1: flap-hinge deviaton angle $\phi_1^{X_k}$ along $\vec{e}_z^{\,X_1^0} \equiv \vec{e}_z^{\,X_0}$
2: pitch deviation angle $\phi_2^{X_k}$ along $\vec{e}_y^{\,X_1^1}$
3: lead-hinge deviaton angle $\phi_3^{X_k}$ along $\vec{e}_x^{\,X_1^2}$

angle, blade structure, deformation $\Leftrightarrow$ $\phi_i^{X_{k=2\ldots N}}$ [rad] (>0 in acc. with c.s. $\vec{e}^{\,X_k}$, tors/flat/edge)
set of 3 successive lumped rotations in entry point $X_k^{\ominus}$ of blade structure element X_k (rotation dof's); bottum-up ordered as:

1: distorsion blade deformation angle $\phi_1^{X_k}$ along $\vec{e}_y^{\,X_k^0}$
2: flatwise blade deformation angle $\phi_2^{X_k}$ along $\vec{e}_z^{\,X_k^1}$
3: edgewise blade deformation angle $\phi_3^{X_k}$ along $\vec{e}_x^{\,X_k^2}$

set up, together with deformation translations, SBBT-equivalent blade element deformation

angle, foundation, deformation $\Leftrightarrow$ $\phi_i^{S_1}$ [rad] (>0 in acc. with c.s. $\vec{e}^{\,S_1}$, tors/fore-aft/sideward)
set of 3 successive lumped rotations in entry point $S_1^{\ominus}$ of tower element S_1 (rotation dof's); bottum-up ordered as:

1: distorsion foundation deformation angle $\phi_1^{S_1}$ along $\vec{e}_z^{\,S_1^0} \equiv \vec{e}_z^{\,B}$,
2: fore/aft foundation deformation angle $\phi_2^{S_1}$ along $\vec{e}_y^{\,S_1^1}$,
3: sideward foundation deformation angle $\phi_3^{S_1}$ along $\vec{e}_x^{\,S_1^2}$,

set up, together with deformation translations, overall foundation deformation (cross coupling between bending force and torque reactions on deformation angles and translations)

angle, gearbox, azimuthal, fast shaft (fast shaft equivalent) $\Leftrightarrow$ $\psi_{\rm f}$ [rad] (>0 at clockwise orientation in fore-to-aft view)
rotation of electric machine rotor along the x-axis of the final coordinate system $\vec{e}^{\,S_M}$ of the nacelle, i.e. relative to the nacelle; scaled as $\psi_{\rm f}' iTr$ it equals the *main* azimut angle ψ ($=\int^t \Omega_{\rm dt}$).

angle, gearbox, azimuthal slow shaft $\Leftrightarrow$ $\psi_{\rm s}$ [rad] (>0 at clockwise orientation in fore-to-aft view)
rotation of gearbox slow shaft along the x-axis of nacelle f.c.s. $\vec{e}^{\,S_M}$ ($\equiv \vec{e}_x^{\,R_{\rm h}}$); it amounts to $(i_{\rm gb}-1)/i_{\rm gb} \cdot \phi_3^{R_{\rm h}} + \psi$ and is the main azimut angle affected by azimuthal gearbox house deviation; see also 'gearbox fast shaft azimuthal angle' and 'transmission ratio gearbox'

angle, gearbox house, deviation (azimuthal) $\Leftrightarrow$ $\phi_{\rm gb} \equiv \varphi_3^{R_{\rm h}}$ [rad] (>0 in accordance with c.s. $\vec{e}^{\,R_{\rm h}}$)
rotation in entry point $R_{\rm h}^{\ominus}$ of gearbox house $R_{\rm h}$ along $\vec{e}_x^{\,R_{\rm h}^0} = \vec{e}_x^{\,S_M}$ (rotation d.o.f)

angle, nacelle, tilt, invariant $\Leftrightarrow$ $\phi_{\rm ti}^S$ [deg] (>0 at upward tilted turbine rotor)
rotation from the axis through the centre of the rotor shaft bearings to the 'in tower top plane' fore/aft axis of the nacelle

angle, nacelle, yaw, average $\Leftrightarrow$ $\phi_{\rm yw}^S$ [deg] (>0 at clockwise orientation in top-down view)
average rotation from the tower top x-axis to the 'in tower top plane' fore-aft axis of the nacelle

angle, nacelle, yaw, deviation $\Leftrightarrow$ $\varphi_{\rm yw} \equiv \varphi_1^{S_M}$ [deg] (>0 at clockwise orientation in top-down view)
lumped rotation in entry point $S_M^{\ominus}$ of nacelle element S_M along $\vec{e}_z^{\,S_M^0}$ (rotation dof)

angle, rotor, azimuth $\Leftrightarrow$ $\psi_{\rm r}$ [rad] (>0 at clockwise orientation in fore-to-aft view)
rotation from the horizontal in the rotor plane, as observed in the nacelle from its 'tilted coordinate system', towards the y-axis of the rotor hub's final coordinate system $\vec{e}^{\,R_{\rm r}}$; $\psi_{\rm r}$ is the *rotor* azimuth, i.e. *the* angular position of the turbine rotor; it aomunts to the sum of the gearbox slow shaft angle and main shaft distorsion angle amounts to $\psi + (i_{\rm gb}-1)/i_{\rm gb} \cdot \phi_3^{R_{\rm h}} + \phi_1^{R_{\rm r}}$.

angle, rotor shaft, deformation $\Leftrightarrow$ $\phi_i^{R_\mathrm{r}}$ [rad] (>0 in accordance with c.s. $\vec{e}^{\,R_\mathrm{r}}$, tors/yaw0/tilt0)
set of 3 successive lumped rotations in *exit* point $R_\mathrm{r}^{\oplus}$ of rotor shaft & hub element R_r (rotation dof's); bottum-up ordered as distorsion:

1: distorsion rotor shaft deformation angle $\phi_1^{R_\mathrm{r}}$ along $\vec{e}_x^{\,R_\mathrm{r}^0} \equiv \vec{e}_x^{\,R_\mathrm{s}} \equiv \vec{e}_x^{\,R_\mathrm{h}} \equiv \vec{e}_x^{\,S_\mathrm{n}}$

2: yaw0 rotor shaft deformation angle $\phi_2^{R_\mathrm{r}}$ along $\vec{e}_z^{\,R_\mathrm{r}^1}$

3: tilt0 rotor shaft deformation angle $\phi_3^{R_\mathrm{r}}$ along $\vec{e}_y^{\,R_\mathrm{r}^2}$

set up, together with deformmation translations, SBBT-equivalent rotor shaft deformation (cross coupling betweenbending force and torque reactions on deformation angles and translations)

angle, tower, deformation $\Leftrightarrow$ $\phi_i^{S_{k=2\ldots M-1}}$ [rad] (>0 in acc with c.s. $\vec{e}^{\,S_k}$, tors/fore-aft/sideward)
set of 3 successive lumped rotations in entry point $S_k^{\ominus}$ of tower element S_k (rotation dof's); bottum-up ordered as:

1: distorsion tower deformation angle $\phi_1^{S_k}$ along $\vec{e}_z^{\,S_k^0}$,

2: fore/aft tower deformation angle $\phi_2^{S_k}$ along $\vec{e}_y^{\,S_k^1}$,

3: sideward tower deformation angle $\phi_3^{S_k}$ along $\vec{e}_x^{\,S_k^2}$;

set up (with deform. translations) SBBT-equivalent tower element deformation;

angle, turbine base, direction $\Leftrightarrow$ γ^B [deg] (>0 at clockwise orientation in top-down view)
rotation from the south-to-north axis to the fore/aft direction of the tower at no deformation

angle , turbine base, tilt $\Leftrightarrow$ θ^B [deg] (>0 at upward tilt of nacelle front)
rotation from the actual fore/aft direction of the undeformed tower to the projection on earth of this fore/aft direction

angle, wave, direction $\Leftrightarrow$ γ^{g} [deg] (>0 at clockwise orientation in top-down view)
rotation from the south-to-north axis to the 10 minute average direction of horizontal wave propagation

angle, wind, direction $\Leftrightarrow$ γ^A [deg] (>0 at clockwise orientation in top-down view)
rotation from the south-to-north axis to the 10 minute average wind direction

angle, wind, slope $\Leftrightarrow$ θ^A [deg] (>0 if wind 'climbs')
rotation from projection on earth of 10 minute average wind direction to the actual wind direction

coordinate system, blade, base $\Leftrightarrow$ $\vec{e}^{\,X_0}$
base coordinate system for blade X with x-axis perpendicular to the rotor plane and y- and z-axis in radial and tangential direction of the blade at no pitch, no twist and no deformation, neither hinge angle nor cone and δ_3 angle; sets up the blade-neutral axial, radial and tangential directions; originates from rotor hub coordinate system $\vec{e}^{\,R_\mathrm{r}}$ by rotation along the x-axis over the blade azimuth offset angle ${}^X\psi^{R_\mathrm{r}}$.

coordinate system, blade, chord-wise $\Leftrightarrow$ $\vec{e}^{\,X^{\mathrm{set}}_{k=1\ldots N}}$
coordinate system with z-axis along chord line of blade element X_k; originates from blade element coordinate system $\vec{e}^{\,X_k}$ by rotation along along the y-axis over -(twist angle $\phi_{\mathrm{tw}}^{X_k}$ - nelza angle $\phi_{\mathrm{ez}}^{X_k}$)

coordinate system, blade, conversion *or* flap-&leadwise $\Leftrightarrow$ $\vec{e}^{\,X^{\mathrm{cv}}_{k=1\ldots N}}$
coordinate system with x- and z-axis pointing into the directions of the normal and (minus) lead wind speed component for blade element X_k; originates from blade-neutral coord sys $\vec{e}^{\,X_0}$ by successive rotation along the $z-axis$ over -(blade element flap angle β^{X_k}) and along the resulting intermediate $x-axis$ over +(blade element lead angle ζ^{X_k})

coordinate system, blade flange $\Leftrightarrow \vec{e}^{\,X_1}$
coordinate system along the neutral elastic axes of blade flange element X_1; originates from blade base coordinate system $\vec{e}^{\,X_0}$ by successive rotation along:
1: $\vec{e}_z^{\,X_0}$ over -(cone angle $\phi_{\rm cn}^{X}$) + (flapwise hinge deviation angle $\phi_1^{X_1}$)
2: $\vec{e}_y^{\,X_1^1}$ over -(average pitch angle $\phi_{\rm pt}^{X}$) + (pitch deviation angle $\phi_2^{X_1}$)
3: $\vec{e}_x^{\,X_1^2}$ over +(δ_3 angle $\phi_{\delta_3}^{X}$) + (lead hinge deviation angle $\phi_3^{X_1}$)
the neutral elastic x- and z-axis in the blade flange are assumed to coincide with the blade neutral x- and z-axis, so $\phi_{\rm ez}^{X_1} = 0$ and does not appear in the rotation along $\vec{e}_y^{\,X_1^1}$!

coordinate system, blade structure $\Leftrightarrow \vec{e}^{\,X_{k=2\ldots N}}$
coordinate system along the neutral elastic axes of blade element X_k; originates from preceeding coord system $\vec{e}^{\,X_{k-1}}$ by successive rotation along:
1: $\vec{e}_y^{\,X_k^0}$ over +(distors deform angle $\phi_1^{X_k}$ - neutral elastic z-axis angle incr ($\phi_{\rm ez}^{X_k} - \phi_{\rm ez}^{X_{k-1}}$))
2: $\vec{e}_z^{\,X_k^1}$ over +(flatwise angle $\phi_2^{X_k}$ - prebend flatwise angle $\phi_{\rm pf}^{X_k}$)
3: $\vec{e}_x^{\,X_k^2}$ over +(edgewise deformation angle $\phi_3^{X_k}$ + prebend edgewise angle $\phi_{\rm pe}^{X_k}$)

coordinate system, drive train, gearbox house $\Leftrightarrow \vec{e}^{\,R_{\rm h}}$, $\vec{e}^{\,R_{\rm h}"}$ coordinate system for gearbox house; $\vec{e}^{\,R_{\rm h}}$ originates from nacelle coordinate system $\vec{e}^{\,S_M}$ by rotation along the x-axis over azimuthal gearbox house deviation angle $\phi_3^{R_{\rm h}}$ (preceeded '0-rotations' along the y- and z-axis); auxiliary coordinate system $\vec{e}^{\,R_{\rm h}"}$ origing from $\vec{e}^{\,S_M}$ by rotation along the x-axis over $(i_{\rm gb}-1)/i_{\rm gb} \cdot \phi_3^{R_{\rm h}}$

coordinate system, drive train, generator rotor $\Leftrightarrow \vec{e}^{\,R_{\rm f}}$
rotating coordinate system with x-axis along length coordinate of gearbox fast shaft; originates from the nacelle coordinate system $\vec{e}^{\,S_M}$ by rotation along the x-axis over $\psi_{\rm f}$, being the time integral of *the* rotational speed $\boldsymbol{\Omega}$

coordinate system, drive train, gearbox shaft system $\Leftrightarrow \vec{e}^{\,R_{\rm s}}$
rotating coordinate system with x-axis along length coordinate of gearbox slow shaft; originates from aux. gearbox house coord system $\vec{e}^{\,R_{\rm h}"}$ by rotation along the x-axis over $\psi_{\rm f}/i_{\rm gb}$, being the co-axial rotation of the generator rotor with respect to the nacelle scaled with the gearbox transmision ratio

coordinate system, drive train, rotor shaft & hub $\Leftrightarrow \vec{e}^{\,R_{\rm r}}$ ($\equiv$ rotor coordinate system $\vec{e}^{\,R}$)
coordinate system on rotor shaft & hub with x-axis perpendicular to the rotor plane and y- and z-axis in neutral radial and tangential direction of the first blade; originates from $\vec{e}^{\,R_{\rm s}}$ viz. by by rotation along
1: $\vec{e}_x^{\,R_{\rm s}}$ over shaft distorsion angle $\phi_1^{R_{\rm r}}$
2: $\vec{e}_z^{\,R_{\rm r}^1}$ over yaw0-deformation angle $\phi_2^{R_{\rm r}}$
2: $\vec{e}_y^{\,R_{\rm r}^2}$ over tilt0-deformation angle $\phi_3^{R_{\rm r}}$

coordinate system, foundation $\Leftrightarrow \vec{e}^{\,S_1}$
coordinate system along the neutral elastic axes of support structure element S_1; originates from turbine base coordinate system $\vec{e}^{\,B}$ by foundation deformation rotations along
1: $\vec{e}_z^{\,S_0}$ over foundation distorsion angle $\phi_1^{S_1}$
2: $\vec{e}_y^{\,S_1^1}$ over foundation fore/aft deformation angle $\phi_2^{S_1}$
3: $\vec{e}_x^{\,S_1^2}$ over foundation sideward deformation angle $\phi_3^{S_1}$

coordinate system, geographic $\Leftrightarrow \vec{e}^{\,G}$
reference coordinate system fixed to the sea bottom; x-, y- and z-axis point from south to north, from west to east and vertically downward

coordinate system, hydrodynamic $\Leftrightarrow \vec{e}^{\,H}$
coordinate system with x-axis along horizontal wave movements and z-axis pointing vertically downward; originates from geographic coordinate system $\vec{e}^{\,G}$ by rotation along the z-axis over +(wave direction angle $\gamma^{\rm g}$)

coordinate system, nacelle $\Leftrightarrow \vec{e}^{\,S_M}$
coordinate system with x-axis pointing fore/aft in the average direction of the rotor shaft; originates from tower top coord sys $\vec{e}^{\,S_{M-1}}$ by rotation along
1: $\vec{e}_z^{\,S_{M-1}}$ over +(average yaw angle $\phi_{\rm yw}^S$) + (yaw deviation angle $\phi_1^{S_M}$)
2: $\vec{e}_y^{\,S_M^1}$ over -(tilt angle $\phi_{\rm ti}^S$)

coordinate system, rotor $\Leftrightarrow \vec{e}^{\,R}$: see rotor shaft & hub c.s. $\vec{e}^{\,R_{\rm r}}$ of drive train

coordinate system, rotor, average $\Leftrightarrow \vec{e}^{\,\bar{R}}$
coordinate system with x-axis perpendicular to the rotor plane in average position and with y- and z-axis rotating in average sense; originates from average nacelle coordinate system $\vec{e}^{\,\overline{S_M}}$ by rotation along the x-axis over $\bar{\boldsymbol{\Omega}} \cdot t$

coordinate system, rotor, fixed $\Leftrightarrow \vec{e}^{\,R_{\rm fx}}$
coordinate system with x-axis perpendicular to rotor plane and y- and z-axis pointing in the rotor plane's yaw- and tilt-direction; originates from rotor hub c.s. $\vec{e}^{\,R_{\rm r}}$ by rotation along the x-axis over -(rotor azimuth angle $\psi_{\rm r}$)

coordinate system, rotor annulus $\Leftrightarrow \vec{e}^{\,W_{m=1\ldots P}/Xz}$
coordinate system with x- and z-axis pointing into the axial and tangential direction of annulus W_m for blade X; originates from blade-neutral coordinate system $\vec{e}^{\,X_0}$ by rotation along along the x-axis over the 'ensemble-average' of the induction lead angles $\zeta_{\rm i}^{X_k}$ of the blade elements encapsulated by W_m.

coordinate system, tower $\Leftrightarrow \vec{e}^{\,S_{k=2\ldots M-1}}$
coordinate system along the neutral elastic axes of support structure element S_k; originates from coordinate system $\vec{e}^{\,S_{k-1}}$ by tower deformation rotations along
1: $\vec{e}_z^{\,S_k^0}$ over tower distorsion angle $\phi_1^{S_k}$
2: $\vec{e}_y^{\,S_k^1}$ over tower fore/aft deformation angle $\phi_2^{S_k}$
3: $\vec{e}_x^{\,S_k^2}$ over tower sideward deformation angle $\phi_3^{S_k}$

coordinate system, turbine base $\Leftrightarrow \vec{e}^{\,B}$
coordinate system with x-axis pointing purely fore/aft in the sense of the tower and z-axis pointing downward along the tower's length coordinate at no deformation; originates from geographic coord system $\vec{e}^{\,G}$ by rotation along along the z-axis over +(turbine base direction angle γ^B) and along the intermediate y-axis over -(turbine base tilt angle θ^B)

coordinate system, wind field $\Leftrightarrow \vec{e}^{\,A}$
coordinate system with x-axis along longitudinal wind speed and z- and y-axis respectively pointing downward and purely sideward; originates from geographic coordinate system $\vec{e}^{\,G}$ by rotation along the z-axis over +(wind direction angle γ^A) and along the intermediate y-axis over +(wind slope angle θ^A)

coordinate system, wind field, rotating $\Leftrightarrow \vec{e}^{\,A}$
coordinate system with x-axis in direction of longitudinal wind speed and with y- and z-axis rotating in average sense; originates from wind field coordinate system $\vec{e}^{\,A}$ by rotation along the $x - axis$ over the on-average evoluating azimuth angle $\bar{\boldsymbol{\Omega}} \cdot t$

translation, blade structure, deformation $\Leftrightarrow \rho_j^{X_{k=2\ldots N}}$ (>0 by c.s. $\vec{e}^{\,X_k}$, (axial/flat/edge)
set of 3 successive lumped translations in entry point $X_k^{\ominus}$ of blade element X_k (translation dof's); bottum-up ordered as:
1: axial blade deformation translation $\rho_1^{X_k}$ along $\vec{e}_y^{\,X_k^0}$,
2: flatwise blade deformation translation $\rho_2^{X_k}$ along $\vec{e}_x^{\,X_k^1}$,
3: edgewise blade deformation translation $\rho_3^{X_k}$ along $\vec{e}_z^{\,X_k^2}$,
set up, with deformation angles, SBBT-equivalent blade element deformation ($\rho_1^{X_k}$ unused)

translation, foundation, deformation $\Leftrightarrow$ $\rho_j^{S_1}$ (>0 by $\vec{e}^{\,S_1}$, axial/fore-aft/sideward)
set of 3 successive lumped translations in entry point $S_1^{\ominus}$ of foundation element S_1 (translation dof's); bottum-up ordered as:

1: co-axial foundation deformation translation $\rho_1^{S_1}$ along $\vec{e}_z^{\,S_1^0} \equiv \vec{e}_z^{\,B}$,

2: fore/aft foundation deformation translation $\rho_2^{S_1}$ along $\vec{e}_x^{\,S_1^1}$,

3: sideward foundation deformation translation $\rho_3^{S_1}$ along $\vec{e}_y^{\,S_1^2}$,

set up, with deformation angles, overall foundation deformation (cross copuling between bending force and torque reactions and rotation and translation deformation; $\rho_1^{S_1}$ unused)

translation, rotor shaft, deformation $\Leftrightarrow$ $\rho_j^{R_\mathrm{r}}$ (>0 by $\vec{e}^{\,R_\mathrm{r}}$, axial/yaw0/tilt0)
set of 3 successive lumped translations in entry point $R_\mathrm{r}^{\oplus}$ of rotor shaft & hub R_r (translation dof's); bottum-up ordered as:

1: axial rotor shaft deformation translation $\rho_1^{R_\mathrm{r}}$ along $\vec{e}_x^{\,R_\mathrm{r}^0} \equiv \vec{e}_x^{\,R_\mathrm{s}} \equiv \vec{e}_x^{\,R_\mathrm{h}} \equiv \vec{e}_x^{\,S_\mathrm{n}}$

2: yaw0 rotor shaft deformation translation $\rho_2^{R_\mathrm{r}}$ along $\vec{e}_y^{\,R_\mathrm{r}^1}$

3: tilt0 rotor shaft deformation translation $\rho_3^{R_\mathrm{r}}$ along $\vec{e}_z^{\,R_\mathrm{r}^2}$

set up, with deformation angles, SBBT-equivalent rotor shaft deformation ($\rho_1^{R_\mathrm{r}}$ relative to slow shaft R_s, $\rho_2^{R_\mathrm{r}}$ and $\rho_3^{R_\mathrm{r}}$ relative to nacelle S_n; cross coupling between bending force and torque reactions and translation and rotation deformations)

translation, tower, deformation $\Leftrightarrow$ $\rho_j^{S_{k=2\ldots M-1}}$ (>0 by $\vec{e}^{\,S_k}$, axial/fore-aft/sideward)
set of 3 successive lumped translations in entry point $S_k^{\ominus}$ of tower element S_k (translation dof's); bottum-up ordered as

2: axial tower deformation translation $\rho_1^{S_k}$ along $\vec{e}_z^{\,S_k^0}$,

2: fore/aft tower deformation translation $\rho_2^{S_k}$ along $\vec{e}_x^{\,S_k^1}$,

3: sideward tower deformation translation $\rho_3^{S_k}$ along $\vec{e}_y^{\,S_k^2}$,

set up, with deformation angles, SBBT-equivalent tower element deformation ($\rho_1^{S_1}$ unused)

point, blade, aerodynamic conversion $\Leftrightarrow$ $X^{\mathrm{a}}_{k=1\ldots N}$
location for concentrated aerodynamic loads on element X_k; lays on the aerodynamic axis in element X_k (X_1^{a} in interface X_1/X_0, $X^{\mathrm{a}}_{2\ldots N-1}$ 'mid-span', X_N^{a} at tip).

point, blade, centre of gravity $\Leftrightarrow$ $X^*_{k=1\ldots N}$

point blade base, entry from rotor shaft & hub $\Leftrightarrow$ $X_0^{\ominus}$ (coincides with $R_\mathrm{r}^{\oplus}$)
fictive location on blade X in the rotor centre

point blade base, exit to blade flange $\Leftrightarrow$ $X_0^{\oplus}$ (coincides with $X_1^{\ominus}$)
location on blade X in which the full span pitch actuator and flap- and leadwise blade hinges (or blade coning and δ_3 offset) are assumed; lays at interface X_0/X_1 on the pitch axis; the elastic neutral flatwise and edgwise bending line of element X_1 is *assumed* to intersect in this point

point, blade flange, entry $\Leftrightarrow$ $X_1^{\ominus}$: see $X_0^{\oplus}$

point, blade flange, exit to blade structure $\Leftrightarrow$ $X_1^{\oplus}$
intersection of the elastic neutral flatwise and edgwise bending line of blade element X_2 at interface X_1/X_2 (root to tip view); spanwise distance to entry $X_1^{\ominus}$ is 50% of spanwise length of elements $X_{2\ldots N-1}$

point, blade structrure, entry $\Leftrightarrow$ $X^{\ominus}_{k=2\ldots N}$
intersection of the elastic neutral flatwise and edgwise bending line of blade element X_k at interface X_k/X_{k-1} (root to tip view).

point, blade structure, exit $\Leftrightarrow$ $X^{\oplus}_{k=2\ldots N-1}$
intersection of the elastic neutral flatwise and edgwise bending line of blade element X_{k+1} at interface X_k/X_{k+1} (root to tip view); spanwise distance to entry $X^{\ominus}_{k=2\ldots N-1}$ all equall

point, blade structure, exit $\Leftrightarrow$ $X_N^{\oplus}$
intersection of the elastic neutral flatwise and edgwise bending line of blade element X_N at the outer side of X_N; spanwise distance to entry $X_N^{\ominus}$ is 50% of spanwise length of elements $X_{2\ldots N-1}$

point, foundation, entry $\Leftrightarrow S_1^{\ominus}$
location on the support structure S in which the visco/elastic foundation reaction are assumed (intersection of neutral elastic tower axis with 'mounting area' of tower)

point, foundation, exit to tower $\Leftrightarrow S_1^{\oplus}$
intersection of the elastic neutral bending lines of tower element S_2 at interface S_1/S_2; 'vertical' distance to entry $S_1^{\ominus}$ is 50% of length of elements $S_{2\ldots M-2}$

point, support structure, centre of gravity $\Leftrightarrow$ $S^*_{k=1\ldots M}$
The centre of gravity and inertia parameters for $S^*_{k=1\ldots M-1}$ follow from the tower dimensions; the inertia parameters for the nacelle elemenet S_M are enlarged with all inertia parameters of the generator rotor and gearbox house except their co-axial moment of inertia

point, support structure, hydrodynamic conversion $\Leftrightarrow S^{\mathrm{h}}_{k=1\ldots M_{\mathrm{uw}}}$
location for concentrated hydrodynamic loads on element S_k; assumed on the elastic neutral axis in element S_k (S_1^{h} in interface S_1/B, $S^{\mathrm{h}}_{2\ldots M_{\mathrm{uw}}}$ 'mid-height', with M_{uw} the number of underwater elements of S)

point, tower, entry $\Leftrightarrow S^{\ominus}_{k=2\ldots M-1}$
intersection of the elastic neutral bending lines of tower element S_k at interface S_k/S_{k-1}; 'vertical' distance to entry $S_1^{\ominus}$

point, tower, exit $\Leftrightarrow S^{\oplus}_{k=2\ldots M-2}$
intersection of the elastic neutral bending lines of tower element S_{k+1} at interface S_k/S_{k+1}; 'vertical' distance to entry $S_k^{\ominus}$ all equal

point, tower, exit to nacelle $\Leftrightarrow S^{\oplus}_{M-1}$
location on tower top in centre of yaw bearing; 'vertical' distance to entry $S^{\ominus}_{M-1}$ is 50% of length of elements $S_{2\ldots M-2}$

point, nacelle, entry $\Leftrightarrow$ $S_M^{\ominus}$: see tower exit to nacelle $S^{\oplus}_{M-1}$

point, nacelle, exit to gearbox house $\Leftrightarrow$ $S_M^{\oplus \mathrm{h}}$ (coincides with $R_{\mathrm{h}}^{\ominus}$)
location for co-axial support torque exchange with gearbox house R_{h} (not relevant because of *only* torque exchange; remaining dynamics added to nacelle)

point, nacelle, exit to generator rotor $\Leftrightarrow$ $S_M^{\oplus \mathrm{f}}$ (coincides with $R_{\mathrm{f}}^{\ominus}$)
location for co-axial generator torque exchange with the generator rotor on the fast shaft R_{f} (not relevant because of *only* torque exchange; remaining dynamics added to nacelle)

point, nacelle, exit to main shaft bearing $\Leftrightarrow$ $S_M^{\oplus \mathrm{b}}$ (coincides with $R_{\mathrm{r}}^{\ominus \mathrm{b}}$)
location for radial bearing force exchange with rotor shaft & hub R_{r} (not relevant because all load exchange between R_{r} and S_M is concentrated in the rotor centre $R_{\mathrm{r}}^{\oplus}$; see $S_M^{\oplus \mathrm{r}}$)

point, nacelle, exit to rotor shaft & hub entry $\Leftrightarrow$ $S_M^{\oplus \mathrm{r}}$ (coincides with $R_{\mathrm{r}}^{\ominus \mathrm{n}}$)
location for concentrated visco/elastic load exchange with the rotor shaft & hub R_{r}, chosen as the rotor centre $R_{\mathrm{r}}^{\mathrm{c}}$ (shaft bending model includes main bearing and 'fixed' gearbox house; shaft inertia moved to hub)

point, drive train, generator rotor entry $\Leftrightarrow$ $R_{\mathrm{f}}^{\ominus}$: see nacelle exit to generator rotor $S_M^{\oplus \mathrm{f}}$

point, drive train, generator rotor exit to shaft system $\Leftrightarrow$ $R_{\mathrm{f}}^{\oplus}$ (coincides with $R_{\mathrm{s}}^{\ominus \mathrm{f}}$)
location for co-axial torque exchange with gearbox shaft system R_{s} (not relevant because of torque exhange *only*).

point, drive train, gearbox house entry $\Leftrightarrow$ $R_{\mathrm{h}}^{\ominus}$: see nacelle exit to gearbox house $S_M^{\oplus \mathrm{h}}$

point, drive train, gearbox house exit to shaft system $\Leftrightarrow$ $R_{\mathrm{h}}^{\oplus}$ (coincides with $R_{\mathrm{s}}^{\ominus \mathrm{h}}$)
location for co-axial torque exchange with gearbox shaft system R_{s} (not relevant because of torque exchange *only*).

point, drive train, rotor, centre $\Leftrightarrow$ $R_{\mathrm{r}}^{\mathrm{c}}$ (coincides with $R_{\mathrm{r}}^{\ominus\mathrm{n}}$, $R_{\mathrm{r}}^{\oplus}$ and $X_0^{\ominus}$)
point on the axis of the rotor shaft such that coordinate vectors to the blade flange entry points $X_1^{\ominus}$ only have *spanwise* non-zero coordinates (y-direction)

point, drive train, rotor shaft & hub, centre of gravity $\Leftrightarrow$ R_{r}^{*}

point, drive train, rotor shaft & hub entry from shaft system $\Leftrightarrow$ $R_{\mathrm{r}}^{\ominus\mathrm{s}}$: see $R_{\mathrm{s}}^{\oplus\mathrm{r}}$

point, drive train, rotor shaft & hub entry from main bearing $\Leftrightarrow$ $R_{\mathrm{r}}^{\ominus\mathrm{b}}$: see $S_M^{\oplus\mathrm{b}}$

point, drive train, rotor shaft & hub entry from nacelle $\Leftrightarrow$ $R_{\mathrm{r}}^{\ominus\mathrm{n}}$: see $S_M^{\oplus\mathrm{r}}$ (coincides with $R_{\mathrm{r}}^{\oplus}$)

point, drive train, rotor shaft & hub exit to blade bases $\Leftrightarrow$ $R_{\mathrm{r}}^{\oplus}$ (coincides with $X_0^{\ominus}$)
location for load exchange between the rotor blades and the hub; as hub is rigid, concentrated loading may be assumed anywhere; chosen as the rotor centre $R_{\mathrm{r}}^{\mathrm{c}}$

point, drive train, shaft system entry from gearbox house $\Leftrightarrow$ $R_{\mathrm{s}}^{\ominus\mathrm{h}}$: see $R_{\mathrm{h}}^{\oplus}$

point, drive train, shaft system entry from generator rotor $\Leftrightarrow$ $R_{\mathrm{s}}^{\ominus\mathrm{f}}$: see $R_{\mathrm{f}}^{\oplus}$

point, drive train, shaft system exit to rotor shaft & hub $\Leftrightarrow$ $R_{\mathrm{s}}^{\oplus\mathrm{r}}$
location for co-axial torque change with rotor shaft&hub R_{r} (not relevant because of torque exchange *only*).

1. INTRODUCTION

The design of offshore wind turbines significantly differs from that of onshore turbines by the huge amount of different sea-states to which they are subjected. Sea-states are combinations of mean wind speed and direction and significant wave height, period and direction. The large number of potential environmental conditions (sea states) makes it very hard to accomplish a fatigue analysis in the same straightforward way as for onshore wind turbines with a time domain aerodynamic code like PHATAS or DUWECS.

Because large offshore wind turinbes tend to have low natural frequencies, the combined dynamic excitation by the wind and the waves may have a large impact on the structural integrity of the wind turbine. A frequency domain tool gives a quick insight in (undesired) dynamic interaction and thus allows for efficient parameter study of the choice of natural frequencies and damping.

For these reasons the frequency domain tool TURBU Offshore has been developed. Together with a time domain tool, TURBU Offshoe enables a combined time/frequency domain approach for fatigue analysis and sensitivity studies. A detailed underlying model description is given in [5]. This report describes the implementation of the computer program, subdivided in:

- outline of the computer program;
- description of the modelling approach;
- load calculation;
- input and output data;
- verification.

Chapter 2 gives an outline of the computer program. It consists of a short description of the subprograms for calculation of the working point conditions, the equations of motions, the dynamic analysis and postprocessing; the involved main functions are described including the data streams between the functions.

Chapter 3 describes the adopted modelling approach for the aerodynamic conversion, the rotor blades, the drive-train and the support structure. The parameters involved have a direct relation with the program input data.

Chapter 4 describes the implementation of the algorithms for load calculation. This concerns the mean, periodic and stochastic behaviour. Also postprocessing options are dealt with.

Chapter 5 describes the program input and output data. It deals with data to be supplied by the user and how these data are mapped to model parameters for use in the steady state and dynamic analysis. This chapter also describes the program output.

Chapter 6 describes the verification of the computer program TURBU Offshore. The verification pertains to the numerical validity of the software, the accuracy of steady state conditions, the validity of the implemented Craig Bamption model reduction method and the accuracy of the stochastic load calculation.

Appendix A describes the model implementations in accordance with the ap-

proach as adopted in [5]. This concerns the processing of the motion and load formulations into parameter matrices of so called state space models that represent the linearised dynamic properties of the equations of motion. Also the integration of the component models is dealt with.

Appendix B describes the implemented algorithms for the motions and loads. The developed program modules provide the mean values and partial derivatives to the 'determining variables' (sensitivity functions). These motion and load 'formulations' establish the required data for deriving the model implementations of the wind turbine components.

Appendix C describes how distributed aerodynamic loads are mapped to concentrated force and torque loads; the same mechanism is used for the hydrodynamic loading.

Appendix D gives a formal treatment of the mean, periodic and stochastic behaviour. This appendix is included in order to provide a calculation concept for the mean and periodic loads that is also valid for e.g. aerodynamically unbalanced rotors.

2. OUTLINE COMPUTER PROGRAM

This chapter gives an outline of the computer program TURBU Offshore. It consists of a short description of the subprograms for calculation of the working point conditions, the equations of motion, the dynamic analysis and postprocessing; the involved main functions are described including the data streams between the functions.

Section 2.1 gives an overview of the developed software, while in section 2.2 the main modules are discussed in respect of the implemented response and input model. The remaining software modules are referenced when dealing with the program layout in Appendix A and refchsnsys, and with the program input in chapter 5.

2.1 Software set-up

TURBU Offshore is a package of software modules in the MATLAB programming language [11]. A MATLAB module is an ASCII file with extension '.m', a so called *M-file*. An M-file accommodates a function or a script (M-function, M-script).

An M-function maps inputs to outputs through a function header and may have access to *global* variables and files. An M-script is just a block with M-code lines and has access to all variables within the scope of the *calling environment*, which can be another M-file or the interactive MATLAB shell:

- An M-script that is activated by typing the file name in the MATLAB shell runs as a computer program with the generated data available in the MATLAB workspace; we type such an M-script as an M-program.
- An M-script which name is stated in an M-function or other M-script can just be considered as a 'macro': stating the M-script's name implies straightforward execution of its code lines within the context of the calling M-file; we type such an M-script as an M-macro.

Note:

- An M-script on file <mfilename>.m is referred to as <mfilename>
- An M-function on file <mfilename>.m is referred to as <mfilename>()

TURBU Offshore involves four M-programs:

- TBUEOE: calculates average turbine state in working conditions;
- TBUEOM: parametrises integrated linear dynamic model in working point;
- TBUDYN: calculates power spectra and harmonics from dynamic excitation
- TBUHIS: composes load histories from average, stochastic and periodic loads.

The TURBU Offshore program package consists of six sets of M-files. Each of the first four sets contains the M-file for the individual program and the specific M-files called from this program. These sets are identified by the program names. The fifth set is identified by 'TBUGEN' and contains more generic M-files of TURBU Offshore, which are called on a deeper level. These five sets together are identified by 'MFILESTBU'. The sixth set contains the required M-files developed by ECN for general use, identified by 'MFILESECN'.

The M-file system 'MFILESTBU' is listed below:

1 TBUEOE
- TBUEOE: Calculate average deformation and loads for offshore wind turbine
- TBUAVR(): Calculate equilibrium conditions in analysis with TURBU Offshore
- TBUROTORPAR(): Defines rotor parameters in format TURBU Offshore
- TBUDRIVTRPAR(): Defines drive-train parameters in format TURBU Offshore
- TBUSUBSTRPAR(): Defines support structure parameters in format TURBU Offshore
- TBUEOMPAR(): Defines parametrising constants for equations of motion in fmt TURBU Offshore
- TBUPARNODES(): Defines entry point related parameters of structural elements Qk
-
- TBUAERCON(): Governs iteration procedure on axial and tangential aerodynamic impulse equations
- TBUSOLVEBEM(): Solves axial impulse equation in rotor annulus via iteration procedure
- TBUDEFRCON(): Calculates average deformation of blades, main shaft and tower

2 TBUEOM
- TBUEOM: Composes linear integrated dynamic model of offshore wind turbine
- TBUBLADEEOM(): Derives state space model for dynamic rotor blade behaviour
- TBUWAKEEOM(): Derives state space model for dynamic wake behaviour
- TBUDRIVTREOM(): Derives state space model for dynamic drive-train behaviour
- TBUSUPSTREOM(): Derives state space model for dynamic support structure behaviour
- TBUBLADEFSR(): Creates 'B' 1st order state space models with 2-subcomponent-blade-models
- TBUBLADEMODE(): linear place vectors from flange entry to blade elements' exit & cog
- TBUQRESPNOCP(): snsy matrix responsive loads on Qk to all dofs Q (no cross cpl)
- TBUR2SUBEOM(): Derives state space model for 2nd drive-train subcomp (generator rotor Rf)
- TBUR3SUBEOM(): Derives state space model for 3rd drive-train subcomponent (shaft&hub Rr)
- TBUS1SUBEOM(): State space model for 1st suppport structure subcomp (foundation Sf)
- TBUS2SUBEOM(): State space model for 2nd support structure subcomponent (tower St)
- TBUS3SUBEOM(): State space model for 3rd support structure subcomponent (nacelle Sn)
- TBUSENSENVLCOMP(): Composes fields in 'trg.sens' from corresponding fields in 'srcs'
- TBUSENSENVLINIT(): Inits fields in 'trg.sens' from envelope of fields in 'src.sens'
- TBUSENSVKSEQ(): Interchanges el.no. 'k' of snsy target with coord. no 'v' of snsy arg
- TBUSYSBKMX(): Sums columns for equal-name inputs in K- and B-mx of state space repres.
- TBUSYSFSR(): Creates 1st order state space model for overall wind turbine model
- TBUSYSFSRCONMAIN(): Connects 2 components via their 1st order state space representations
- TBUSYSFSRCONSUB(): Connects 2 subcomponents via their 1st order state space representations
- TBUSYSGHLKMX(): Assembles input, output and feedthrough mx's for mass/spring/damp system
- TBUSYSMDS2FSR: Converts mass/damper/spring model to 1st order state space representation
- TBUSYSMDSMX() : Derives mass, damper and stiffness matrix via Newton's approach
- TBUXCSUBEOM(): Derives state space model for pitch controlled rotational speed regulation
- TBUX1SUBEOM(): Derives state space model for 1st blade subomponent (flange Xf)
- TBUX2SUBEOM(): Derives state space model for 2nd blade subcmp (structure & profile Xp)

3 TBUDYN
- TBUDYN: Calculates dynamic loads on offshore wind turbine
- TBUBLADETURB(): Power spectra of rotational modes of long. turbulence in rotor annuli
- TBUBLADESHSH(): Amplitudes and phases of periodic wind speed by shear and stagnation
- TBUBLADEGRAV(): Amplitudes and phases of periodic gravity forces on blades
- TBUTOWERWAVE(): Power spectra of wave speeds and accelerations
- TBULOADSTO(): Power spectra setting up the stochastic wind turbine response
- TBULOADPER(): Amplitudes and phases setting up the harmonic wind turbine response
- TBUSYSMODE(): Analyses modal behaviour of overall wind turbine system
- TBUSYSMODECOMP(): Analyses isolated modal behaviour of rotor blade or support structure

4 TBUHIS
- TBUHIS: Composes load histories from average, stochastic and periodic loads
- TBUFFTSYN(): Gets stochastic time series from power spectra by inverse FFT
- TBUHARSYN(): Gets periodic time series from harmonics via amplitudes and phases
- TBUOUTPUT(): Sums average, stochastic and periodic load histories and store on files

5 TBUGEN

- TBUA2XMAP(): Defines subtubes of rotor annuli for interaction with blade elements
- TBUADDCAPX(): Adds 'token' (deflt 'X') to names of output signals
- TBUARR3DMUL(): Pre- and postmultiply the 2D-subarrays of 3D-array
- TBUARR3DSTAR(): Multiplies 2D-subarrays of in any number of 3D-arrays
- TBUAUXVEC(): Calculates auxiliary vectors for kinematics and angular impulse
- TBUSUPSTRCONS(): Calc. means and sensitivities of support struct conservative vectors
- TBUBLADEFLOW(): Linearised blade relative wind speed and angle of attack
- TBUBLADEIMP(): Calculate means and sensitivity matrices for impulse vectors rotor blade
- TBUBLADEKIN(): Linearises blade kinematics into mean vectors and senstivity matrices
- TBUBLADELOAD(): Linearised distributed and concentrated aerodynamic blade loads
- TBUBLADESET(): Linearised typical blade orientation angles and transformations
- TBUDAOAPERC(): Calc perturb on angle of attack based on axial wind speed variation
- TBUDRIVTRCONS(): Calc. means and sensitivities of drive-train conservative vectors
- TBUDRIVTRIMP(): Calc. means and sensitivity matrices of impulse vectors for hub Rr
- TBUDRIVTRKIN(): Linearises shaft& hub kinematics into means and senstivity matrices
- TBUELM2CROSEC(): Derives structural data for cross sections from element-data
- TBUFPRANDFA(): Calc Prandtl's tip corr fac & weight fac for wake dynamics in annulus
- TBUINERMX(): Composes inertia matrix for rigid body with distributed mass
- TBUMU4ELMS2ANN(): Calc. weights of blade element signals for use in rotor annuli
- TBUMX2ARRD(): Gets 3D-array from any number of 'equal-size 2D-arrays'
- TBUPHIMX(): Calculates (series of) 3*3 incremental transformation matrix
- TBUPHIMXDDROT(): Calc. (series of) sens. of 3*3 incr trafo matrix to ang. variation
- TBUQ2FTMAPMX(): Derives matrices for mapping distributed loading to concentrated force/torque
- TBUROTMX(): Gets matrix out left vector of out product for premultiplying right vec
- TBUSENSFPRAND(): Calc. partial derivatives of Prandtl's tip correction factor (Fpr)
- TBUSENSUTRANS(): Calc part drvs of transprt spd in intersection(annulus, blade elem)
- TBUSENSVKSEQ(): Interchanges el.no. 'k' of snsy target with coord. no 'v' of snsy arg
- TBUSHAFTPRISMATIC(): Calc. stiffness and damper matrices for prismatic approx. shaft
- TBUSSUBFTEX(): Assembles extern load vectors in supstr-subcomp element entry points
- TBUSUPSTRCONS(): Calc. means and sensitivities of support struct conservative vectors
- TBUSUPSTRIMP(): Calculates means and sensitivity matrices for impulse vectors supp str
- TBUSUPSTRKIN(): Linearises supp struct kinematics into means and sensitivity matrices
- TBUSUPSTRMODE(): Linear place vectors from foundation entry to sup str elements' exit & cog
- TBUSYSDOFPPFF(): DOF-vectors on subcomponents for export to neighbouring subcomps
- TBUSYSFTFT(): Assembles feedthrough load vectors in subcomponent element entry points
- TBUSYSFTPP(): Assembles feedthrough load vectors by actual on foregoing subcomponent
- TBUTRAFOMX(): Calculates transformation matrices in 3D multi-body structural model
- TBUTRANSP(): Transposes 2D-subarrays (matrices) in ND-arrays
- TBUWAKEFLOW(): Linearised transportation speed and Prandtl's correction factor
- TBUXSUBFTEX(): Assembles extern load vectors in blade-subcomponent element entry points

2.2 Software functionality

The key requirement for load calculation in the frequency domain is the availibity of models for the behaviour of the wind and waves and for the behaviour of the wind turbine when excited by the wind and waves. These models, classified respectively as the input and response model, are dealt with in the next two sections in reversed order.

2.2.1 Response model

The required response model is a linearised integrated dynamic model of the wind turbine, including control, aerodynamic conversion and wake dynamics. As a wind turbine rotates in average sense, the response model arises by linking a 'rotating model partition' to a 'stand still model partition'. Figure 2.1 gives a view

on the structural model, which sets up the major part of the response model.

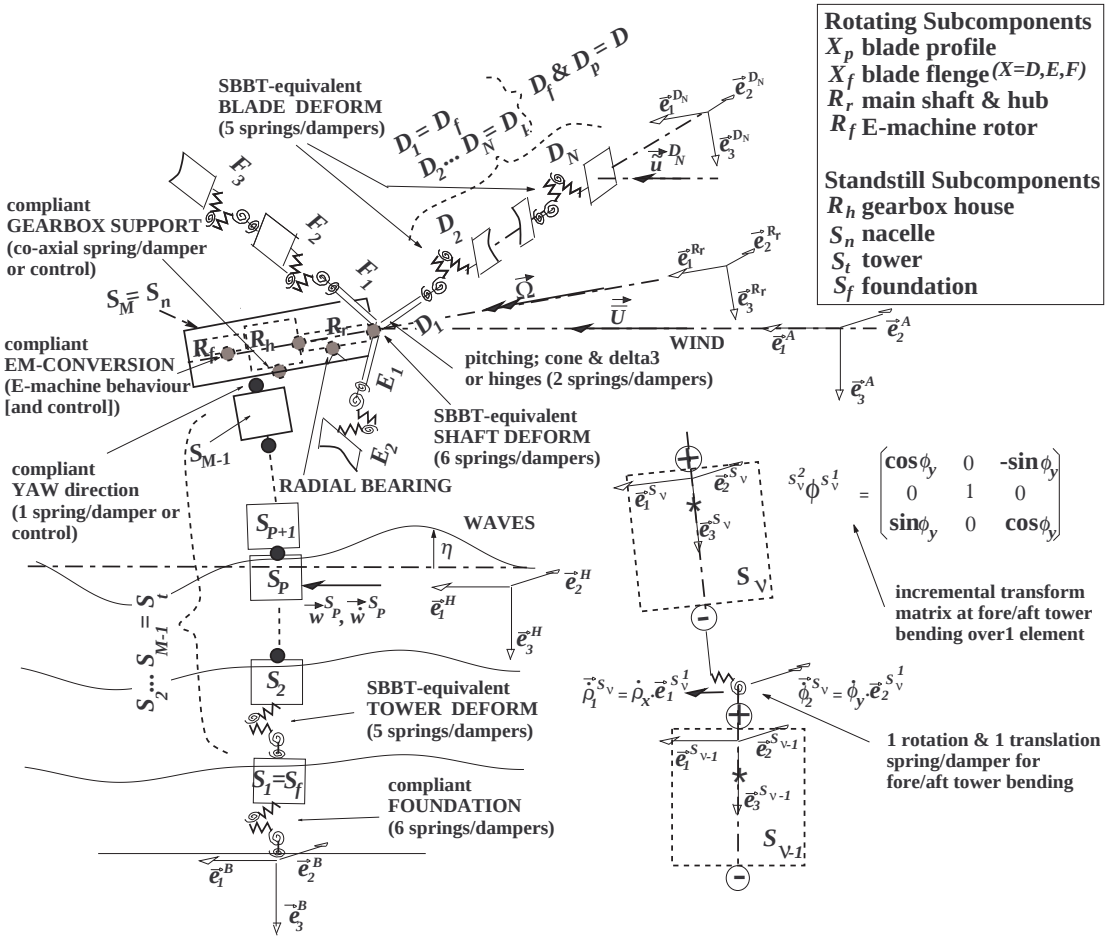

Figure 2.1 *The wind turbine as an assemblage of distinct substructures from elements*

The rotating partition comprises submodels for the air tube that encapsulates the rotor (A), the rotor blades (D, E, F), and the drive train as far as concerns the shaft system and hub (R_r) and the generator rotor (R_f). In accordance with the Blade Element Momentum theory, the response model of the air tube A is implemented as independent behaving rotor annuli A_1 ... A_P. A blade model X ($X = D, E, F$) consists of a blade flenge (X_f) and blade profile (X_p); it is implemented as a multi-body model with element X_1 for the blade flenge and elements X_2 ... X_N for the blade profile. In the associated M-code is implemented:

- axial and tangential aerodynamic impulse conservation in rotor annuli $\{A_m\}$ with 1st order dynamics for the 'ensemble average'[1] of the axial induction speed variation (TBUWAKEEOM(), TBUSOLVEBEM());
- 3D mechanic impulse conservation and slender-beam-bending-theory-equivalent (SBBT) elastic behaviour of blade elements $\{X_k,\ k = 2 \ldots N\}$ (TBUBLADEEOM());

[1] Average over B instantaneous values (B is number of blades)

- 3D mechanic impulse conservation, linear elastic flapwise and leadwise behaviour in case of hinges, and pitching torque control of blade root element X_1 (TBUBLADEEOM());
- 3D mechanic impulse conservation of rotor hub and SBBT main shaft bending via element R_{r}, and rigid body motion of generator rotor R_{f} (TBUDRIVTREOM()).

The standstill partition models the gearbox house of the drive train (R_{h}) and the complete support structure S. The support structure S consists of the foundation (S_{f}), tower (S_{t}) and nacelle (S_{n}), which also includes the main shaft bearing and the generator stator); it is implemented as a multi-body model with element S_1 for the foundation, elements S_2 .... S_{M-1} for the tower, and element S_M for the nacelle. In the associated M-code is implemented:

- 3D mechanic impulse conservation of the gearbox house via element $\mathrm{R_h}$, and, in case of compliant mounting, a co-axial angular spring-damper * * pair or linearly controlled support torque (TBUSUPSTREOM());
- 3D mechanic impulse conservation of the nacelle element S_{n} and, in case of yaw complicance, an angular spring-damper pair of linearly controlled torque (TBUSUPSTREOM());
- 3D mechanic impulse conservation and slender-beam-bending-theory-equivalent (SBBT) elastic behaviour of tower elements $\{S_j, j = 2 \ldots M-1\}$ and foundation element S_1 (TBUSUPSTREOM());

The implementation of the response model comprises the non-linear static behaviour and the parametrisation of the linearised dynamic behaviour. The former yields the average turbine state; the latter enables to assess the variations around the average turbine state.

Average turbine state & turbine data

The M-program TBUEOM solves the (non-linear) equations of equilibrium for the axial and tangential impulse in the rotor annuli and for the bending and torsion in the blades, drive-train and support structure. It calls functions TBUROTORPAR(), TBUDRIVTRPAR() and TBUSUPSTRPAR() for processing the supplied turbine data into the required format. Function TBUEOMPAR() is called for processing the site and environmental conditions into parametrising constants for the equations of motion; also the calculated average angular deformations are combined with the configuration rotations, like prebend and tilt, to the average relative rotations between blade elements and tower elements. On a lower level, the function TBUPARNODES() is called for defining the bottum-up ranked rotation and translation axes of degrees of freedom, or invariant rotations, between elements and for definition of flags that tell if a rotation or translation along an axis is a d.o.f. or not.

The average aerodynamic conditions are obtained with M-function TBUAERCON(); it executes an iteration procedure in which the more generic M-function TBUSOLVEBEM() is called every step for the actual solution of the aerodynamic impulse equation.

The average structural deformations are obtained with TBUDEFRCON().

Program TBUAVR governs the repetitive successive execution of TBUAERCON() and TBUDEFRCON() until the average turbine state is achieved.

Parametrisation of linear dynamic wind turbine model
The M-program TBUEOM composes the submodels for the variational behaviour of the wake, the blades, drive-train and support stucture, and connects these submodels to a linear integrated dynamic wind turbine model. The submodels are parameterised as linear first order state space models. The dynamic behaviour of such models is described by the following matrix/vector equations:

$$\begin{aligned} \frac{\mathrm{d}}{\mathrm{d}t}\left(\underline{z}\right) &= \boldsymbol{A}\cdot\underline{z}+\boldsymbol{B}\cdot\underline{v} \\ \underline{y} &= \boldsymbol{C}\cdot\underline{z}+\boldsymbol{K}\cdot\underline{v} \end{aligned}$$

Vectors $\underline{v}$, $\underline{z}$ and $\underline{y}$ respectively contain the inputs, state variables and outputs (all variations). The matrices $\boldsymbol{A}$, $\boldsymbol{B}$, $\boldsymbol{C}$ and $\boldsymbol{K}$ are respectively the transition, input, output and feedthrough matrix. Figure 2.2 shows the interdepency of the different submodels.

The names of the input, output and state variables are contiained in lists. These lists toghether with the matrix quadruple $\{\boldsymbol{A},\boldsymbol{B},\boldsymbol{C},\boldsymbol{K}\}$ form a data structure that completely describes the state space submodel.

M-program TBUEOM calls the following functions in order to obtain the integrated linear dynamic model:
- TBUBLADEEOM()
- TBUWAKEOM()
- TBUDRIVTREOM()
- TBUSUPSTREOM()
- TBUSYSFSRCONMAIN()
- TBUSYSFSR()

The component model generating M-functions TBUBLADEEOM() up to TBUSUPSTREOM() always first create the structure variables with fields for the mean values and for the partial derivatives of motions and loads. These motion and load 'formulations' are used for the parametrisation of the linearised equations of motion; they eventually map all motion and load variations to input variables from either an other component, which may also be the wake, or the environment (wind, gravitation). See Appendix B for the implemented motion and load formulations.

Rotor blade models
Function TBUBLADEEOM() governs the implemented dynamic blade behaviour. It returns state space models for the B blades D, E and F ($B = 3$), which exists, as mentioned above, as data structures with the parameter matrix quadruple and name lists for the input, state and output variables. The unique name of each input variable tells from which source it arises, which can be another component or the environment; the name of an output variable tells to which destination it is sent to. The state variable names tell in which component they exist. The parameter matrices and name lists are 'fields' in the sysD for blade D, etc. (compare 'structures' in the programming language 'C' or 'records' in the language 'PASCAL').

Function TBUBLADEEOM() loads the 'parametrising constants' that are output

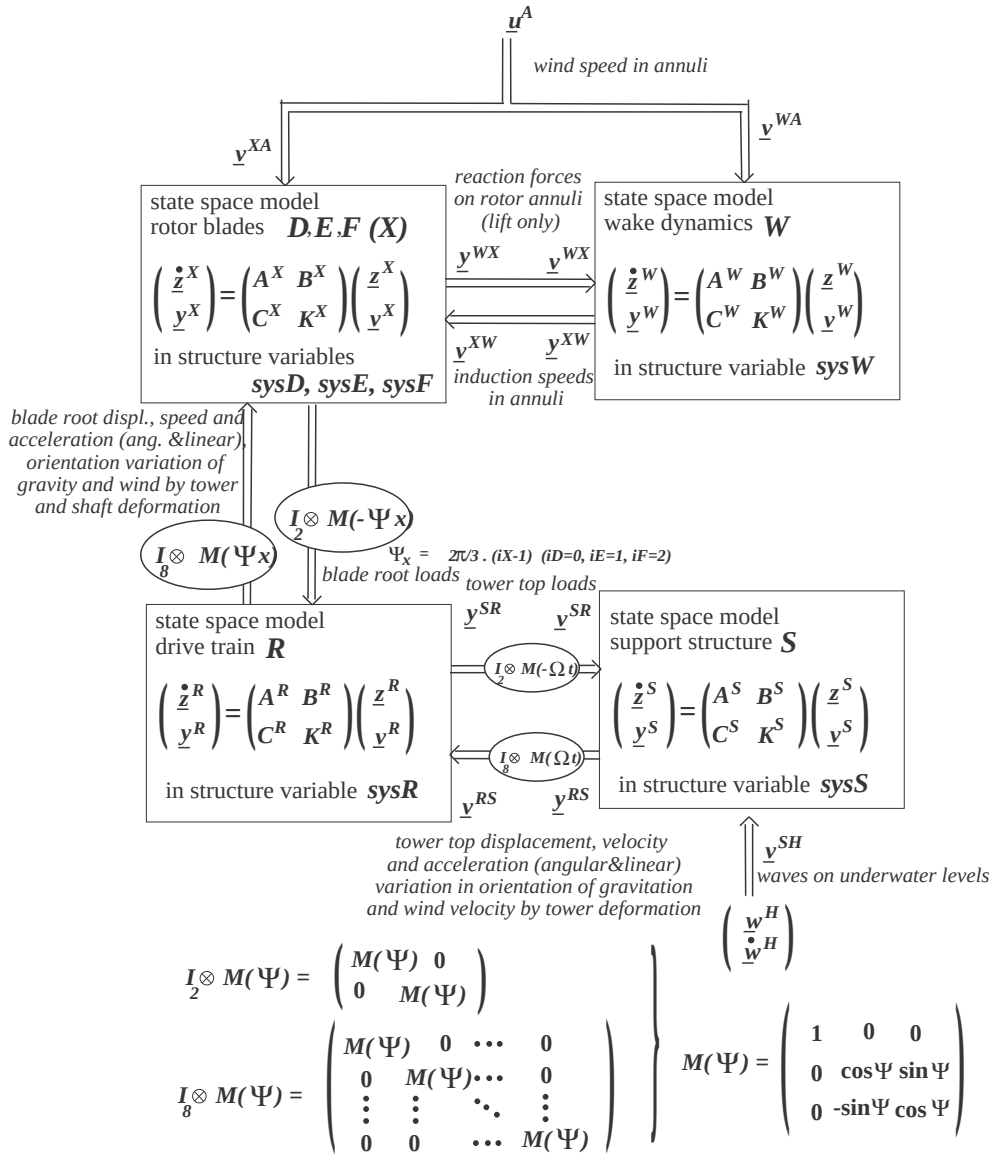

Figure 2.2 *Interdependency of state space models for the distinct substructures of the wind turbine*

of the equilibrium assessment by M-program TBUEOE. It then calls the general purpose functions TBUTRAFOMX() and TBUAUXVEC(). These functions provide transformation matrices and place vectors over the blade elements, with their sensitivities to the degree of freedoms. This is followed by calls to TBUBLADE-CONS(), TBUSYSDOFPPFF(), TBUBLADEMODE, TBUBLADEKIN(), TBUBLADEIMP(), TBUBLADEFLOW() and TBUBLADELOAD(), which provide the required motion and load formulations for setting up the state space models for the rotor blades.

Then, TBUBLADEEOM() governs the creation of the structure variables that accomodate the blade models in accordance with section A.2. It calls the functions TBUX1SUBEOM(), TBUXCSUBEOM(), TBUX2SUBEOM() that yield (blade-generic) subcomponent models for the flange X_{f}, the pitch actuator & control algorithm $X_{\mathrm{f_c}}$ and the profile & structure X_{p}. These submodels also exist as structure variables with fields for parameter matrices and signal lists: sysX1sub, sysXCsub, sysX2sub. These subcomponents are linked together to the blade-generic model sysX via two calls to TBUSYSFSRCOMPSUB(): first, the flange model is connected to the pitch control system; second, the profile & structure model is coupled to the flange & pitch control system. The connection mechanism is name-based: both subcomponent models are searched for matching pairs of input and output signal names. Their ranking numbers in the signal name lists coincide with column and row numbers in the input, output and feedthrough matrices.

Finally, a call to TBUBLADEFSR() provides the blade-specific models sysD, sysE and sysF for a three-bladed rotor. It creates 3 sets of signal name lists with, identifiers D, E and F instead of X. In addition, it slightly modifies and 'makes unique' the input and feedthrough matrix $(\boldsymbol{B}, \boldsymbol{K})$ per blade, namely for input variables from the drive-train the B and K-matrix now include:

- a transformation over the blade-specific azimut offset (0, 120 and 240 degrees for blade D, E and F);
- a rotation to translation mapping over the blade root length for the linear velocity and acceleration.

The latter enables to use drive-train kinematic variables *in the rotor centre* instead of *in the entry of the blade flange* as input signals. The input variables for the blade models are the angular and linear position, speed and acceleration vectors from the drive-train in the rotor centre, the induction speeds from the wake and the wind speed variations by turbulence, tower shadow and windshear, by yaw misalignment and by change in orientation via deformation of of the support structure and drive-train. This latter 'change in orientation' also yields gravity force variations. Output variables are the force and torque loads in the rotor centre and in the entry point of the blade flange, and the displacement variations of the c.o.g.'s of all blade elemenets.

Wake model

The function TBUWAKEEOM() is called for creation of the wake model W. It also starts with loading the 'parametrising constants' that are output of the equilibrium assessment by M-program TBUEOE. In addition, TBUWAKEEOM() 'gets input variables from TBUBLADEEOM()', namely the structure variables with load formulations with respect to the aerodynamic reaction forces by the blades on the wake. Then function TBUWAKEFLOW() is called, which provides the formulations of the transportation velocity and Prandtl's correction factor as required by wake model. Afterwards, the M-code in TBUWAKEEOM() provides the parameter matrices, the input and outupt signal name list and the state variable name list for the wake model in accordance with section A.3. This yields the structure variable sysW. Output variables are the induction speeds of the three rotor blades; input variables are the axial and tangential 'reaction forces by the rotor blades on the annuli' and the wind speed variations.

Via three subsequent calls to TBUSYSFSRCOMPMAIN() the three blade models and wake model are linked together. The linked model exists as structure variable sysDEFW.

Drive-train model
Function TBUDRIVTREOM() creates a component model for the drive-train in the structure variable sysR with fields for parameter matrices and name lists for input, output and state variables, based on loaded 'parametrising constants' that are output of TBUEOE. Function TBUDRIVTREOM() starts with calls to TBUTRAFOMX(), which provide transformation matrices with their sensitivities to the degree of freedoms. This is followed by calls to TBUDRIVTRCONS(), TBUDRIVTRKIN() and TBUDRIVTRIMP() for the required motion and load formulations.

Calls to TBUR2SUB(), TBURCSUB() and TBUR3SUB() yield subcomponent models for the generator rotor R_{f}, electrical system and generator torque control algorithm $R_{\mathrm{f_c}}$, and for the rotor shaft & hub R_{r} in accordance with section A.4. The obtained subcomponent models, sysR2sub, sysRCsub and sysR3sub, are linked together by twice calling TBUSYSFSRCOMPSUB(). Input variables are (i) the tower top motions and wind velocity and gravitation variations by orientation changes in the support structure, (ii) force and torque loads in the rotor centre, and (iii) gravity forces. Output variables are the motions in the rotor centre and fed-through wind speed and gravitation variations by orientation changes of the support structure and main shaft.

A call to TBUSYSFSRCOMPMAIN() in the governing M-program TBUEOM links the coupled blade and wake models to the drive-train model. The linked model exists as structure variable sysDEFWR.

Support structure model
Function TBUSUPSTREOM() creates a component model for the support structure as a structure variable sysS with fields for parameter matrices and name lists for input, output and state variables, based on loaded 'parametrising constants' that are output of TBUEOE. Function TBUSUPSTREOM() starts with calls to the general purpose functions TBUTRAFOMX() and TBUAUXVEC(). These functions provide transformation matrices and place vectors over the support structure elements, with their sensitivities to the degree of freedoms. This is followed by calls to TBUSUPSTRCONS(), TBUSYSDOFPPFF(), TBUSUPSTRMODE, TBUSUPSTRKIN(), TBUSUPSTRIMP() and TBUSUPSTRLOAD(), which provide the required motion and load formulations for setting up the state space models for the subcomponents of the support structure.

The subcomponent models are created by calls to TBUS1SUB(), TBUS2SUB(), TBUS3SUB() and TBUS3CSUB()[, TBUS4SUB() and TBUS4CSUB()]. This yields the models for the turbine foundation $sectionu\mathrm{f}$, the tower $sectionu\mathrm{t}$, the nacelle $sectionu\mathrm{n}$ and yawing acutator with control algorithm $sectionu\mathrm{n_c}$ [, and the gearbox house R_{h} and gearbox support torque actuator with control aogirhtm $R_{\mathrm{h_c}}$] in accordance with section A.5. The obtained subcomponent models are linked together by four times (six times) calling TBUSYSFSRCOMPSUB(). Input variables are (i) the tower top force and torque loads, (ii) wave speeds and force effective wave accelerations and (iii) gravity forces. Output variables are the motions in the tower top and the wind speed and gravitation variations by orientation

changes of the support structure.

Integrated linear model
A call to TBUSYSFSR() in the governing M-program TBUEOM links the coupled blade, wake and drive-train models to the support structure model for a *three* bladed wind turbine. The linked model exists as structure variable sysDEFWRS. This link is performed for a fixed azimuth angle while all parameter matrices of the resulting state space model are transformed in accordance with the algorithm of Coleman & Feingold [3]; in this 'Coleman tranformation' the same fixed azimuth angle is used. The resulting 'Coleman model' is used for load calculation, based on 'preprocessed' blade- and drive-train related inputs (wind speed variations, periodic gravity loading) and 'postprocessed' blade- and drive-train related outputs (blade loads and motion, main shaft deformation). This pre- and processing consists in modulation of inputs before they enter the Coleman model and in modulation of outputs after they have left the Coleman model. (see section 4.2).

2.2.2 Input model

Frequency domain load calculation requires the following inputs to the reponse model:
- power spectra of rotational modes of longitudinal turbulence in rotor annuli;
- power spectra of wave speeds and accelerations;
- amplitudes and phases of periodic wind speed by shear and tower stagnation;
- amplitudes and phases of periodic gravity forces on blades.

The power spectra are model formulations for the rotationally sampled wind turbulence by the rotor and the waves that hit the tower. The periodic wind speed variations model the effect of wind shear and tower stagnation on the rotating turbine blades; the periodic gravity forces the effect of gravitation on the blades.

As listed in section 2.1, these models are implemented in M-functions TBUBLADE-TURB(), TBUTOWERWAVE(), TBUBLADESHSH() and TBUBLADEGRAV() as used in M-program TBUDYN.

3. MODEL SET-UP

This chapter describes the model set-up for the implemented equations of motions. The modelling approach in [5] has been followed. Section section 3.1 deals with two basic concepts applied in the model; local coordinate systems and lumped degrees of freedom. The transformation matrices within and between elements are the means to express a vector in any coordinate system. The involved coordinate transformations are subject of section 3.2. The concept of multi-body modelling with a link to the blade and tower data is described in section 3.3. Section 3.4 describes the environmental influences and the relevant orientations. The set-up of the the *substructure*, or *component*, models is given in sections 3.6, 3.7 and 3.8 for the rotor blades, drive-train and support structure. Section 3.5 describes the wake model via the non-linear equations of equilibrium and linearised equations of motion.

3.1 Local coordinate systems and degrees of freedom

The final coordinate system is fixed to the rigid bar in an element (see e.g. fig 3.1 for element D_4) and originates form the final coordinate system of the foregoing element, e.g. D_3, by rotations along three axes in the connection point 'at the foot' of the element. The first axis for the rotations of Q_k is the x-, y-, z-axis of the foregoing final coordinate system $\vec{e}^{\,Q_{k-1}}$. The second axis belongs to the coordinate system that is obtained by rotating the final foregoing coordinate over that first rotation, that is to say the *first intermediate* coordinate system $\vec{e}^{\,Q_k^1}$ of element Q_k. The third rotation axis belongs to the coordinate system that is obtained by rotating along an axis of the *second intermediate* coordinate system $\vec{e}^{\,Q_k^2}$, which yields the *final* coordinate system $\vec{e}^{\,Q_k}$. See chapter 4 in [5] for a detailed treatment of the *incremental transformation matrices* between two intermediate coordinate systems.

So an element Q_k is equipped with three coordinate systems; the intermediate ones $\vec{e}^{\,Q_k^1}$ and $\vec{e}^{\,Q_k^2}$ and the final one $\vec{e}^{\,Q_k}$, which can also be considered as the third intermediate one. Each of these coordinate systems is always associated with a rotation ϕ_v ($v = 1, 2$ or 3) along an axis of the foregoing intermediate coordinate system, which may be a rotation degree of freedom. Such a rotation may also involve an invariant part in the context of the dynamic load calculations. This invariant part may concern a 'layout feature' such as the tilt angle $\phi^S_{\rm ti}$, or the average value of a rotation dof such as the average yaw angle $\phi^S_{\rm yw}$ or the average rotor shaft torsion $\bar{\phi}_1^{R_{\rm r}}$.

We also define the three translations ϕ_v ($v = 1, 2, 3$) on an element Q_k; they all have an invariant part equal to zero. If a rotation pertains to bending the accompanying translation is along the other bending axis of the same intermediate coordinate system; if a rotation pertains to torsion, the accompanying translation is along the same axis. The ranking order of rotations and translations in an element must be specified:

- rotations $\{\phi_v^{Q_k} | v = 1 \ldots 3\}$, are the bottom-up ranked rotations of element Q_k;

$\phi_v^{Q_k}$ is along an axis of $\vec{e}^{\,Q_k^v}$ for $v = 1 \ldots 3$; the rotation axes ordering depends on the substructure.
- translation $\{\rho_v^{Q_k} | v = 1 \ldots 3\}$, are the bottom-up ranked rotations of element Q_k; $\rho_v^{Q_k}$ is along an axis of $\vec{e}^{\,Q_k^v}$ for $v = 1 \ldots 3$; the translation axes ordering depends on the substructure.

The 'exit point' $Q_{k-1}^{\oplus}$ of element Q_{k-1} coincides with the 'entry point' $Q_k^{\ominus}$ of element Q_k. Springs and dampers, or other compliant devices like actuators, are assumed to be point structures (they have no size). Intermediate coordinate systems will coincide if not all three rotations are non-zero.

If a rotation is always zero, that is to say it has amean value equal to zero and it is not a dof, we yet let it exist in the rotation ranking order; this also holds for a translation with these properties.

A coordinate vector $\underline{q}^{Q_k}$ contains by convention the coordinates of a vector $\vec{q}$ on element Q_k along its (local) final coordinate system. We use:
- $q = \omega, \alpha, v, a$: angular and linear velocity and acceleration
- $q = t, f, q_{\mathrm{t}}, q_{\mathrm{f}}$: concentrated and distributed torque and force loading
- $q = \not{h}\,, p$: angular and linear impulse
- $q = r$: position vector

A position vector ${}^{Q_k^{\ominus}}\underline{r}^{Q_k^{\mathrm{p}}}$ runs along the *rigid* bar of element Q_k and does *not* include the dofs in the entry point $Q_k^{\ominus}$, so it has invariant coordinates along $\vec{e}^{\,Q_k}$. The effect of translations $\{\rho_v^{Q_k}\}$ on the position vector from $Q_k^{\ominus}$ to Q_k^{p} is *not* included. This is allowed because the translation dofs are very small with respect to the typical products 'element length times rotation dof value'. This even holds for the average values for the translation dofs! The translation dofs are only used for achieving slender beam theory equivalent tower and blade bending. The *average* translation values are *not* included in the expressions for the kinematic variables, however the *rate of change* of translations *is* included.

3.2 Coordinate transformations and variations

Transformation matrix ${}^{Q_k^w}\Phi^{Q_j}$ maps coordinates of a vector along the axes of coordinate system $\vec{e}^{\,Q_j}$ to those of the w^{th} intermediate coordinate system $\vec{e}^{\,Q_k^w}$. It holds:

$$ {}^{Q_k^w}\Phi^{Q_j} = {}^{Q_k^w}\Phi^{Q_k^{w-1}} \cdot \ldots \cdot {}^{Q_k^1}\Phi^{Q_{k-1}} \cdot {}^{Q_{k-1}}\Phi^{Q_{k-2}} \cdot \ldots \cdot {}^{Q_{j+1}}\Phi^{Q_j} \tag{3.1} $$

with ${}^{Q_m}\Phi^{Q_{m-1}}$ the transformation over one element, built up from incremental transformation matrices Φ_{x}, Φ_{y} and Φ_{z} in any order. The ordering of the incremental transformation matrices depend on the rotation axes of the bottom-up ranked rotation $\phi_1^{Q_m}$, $\phi_2^{Q_m}$ and $\phi_3^{Q_m}$. For example, these are the $z-$, $y-$ and $x-$axis for the blade flange element X_1 and the $y-$, $z-$ and $x-$axis for the blade structure elements $X_{2\ldots N}$:

$$ {}^{Q_m}\Phi^{Q_{m-1}} = \begin{cases} \Phi_{\mathrm{x}}(\phi_3^{Q_m}) \cdot \Phi_{\mathrm{y}}(\phi_2^{Q_m}) \cdot \Phi_{\mathrm{z}}(\phi_1^{Q_m}) & \text{for } Q = X \text{ and } m = 1 \\ \Phi_{\mathrm{x}}(\phi_3^{Q_m}) \cdot \Phi_{\mathrm{z}}(\phi_2^{Q_m}) \cdot \Phi_{\mathrm{y}}(\phi_1^{Q_m}) & \text{for } Q = X \text{ and } m = 2 \ldots N \end{cases} \tag{3.2} $$

For the mean and variation of the incremental transformation matrices then holds:

$$\bar{\Phi}_{\mathrm{x}} = \begin{pmatrix} 1 & 0 & 0 \\ 0 & \cos\bar{\phi} & \sin\bar{\phi} \\ 0 & -\sin\bar{\phi} & \cos\bar{\phi} \end{pmatrix} \quad \text{and} \quad \delta\Phi_{\mathrm{x}} = \frac{\mathrm{d}\Phi_{\mathrm{x}}}{\mathrm{d}\phi}\Big|_{\bar{\phi}} \cdot \delta\phi = \begin{pmatrix} 0 & 0 & 0 \\ 0 & -\sin\bar{\phi} & \cos\bar{\phi} \\ 0 & -\cos\bar{\phi} & -\sin\bar{\phi} \end{pmatrix} \cdot \delta\phi$$

$$\bar{\Phi}_{\mathrm{y}} = \begin{pmatrix} \cos\bar{\phi} & 0 & -\sin\bar{\phi} \\ 0 & 1 & 0 \\ \sin\bar{\phi} & 0 & \cos\bar{\phi} \end{pmatrix} \quad \text{and} \quad \delta\Phi_{\mathrm{y}} = \frac{\mathrm{d}\Phi_{\mathrm{y}}}{\mathrm{d}\phi}\Big|_{\bar{\phi}} \cdot \delta\phi = \begin{pmatrix} -\sin\bar{\phi} & 0 & -\cos\bar{\phi} \\ 0 & 0 & 0 \\ \cos\bar{\phi} & 0 & -\sin\bar{\phi} \end{pmatrix} \cdot \delta\phi$$

$$\bar{\Phi}_{\mathrm{z}} = \begin{pmatrix} \cos\bar{\phi} & \sin\bar{\phi} & 0 \\ -\sin\bar{\phi} & \cos\bar{\phi} & 0 \\ 0 & 0 & 1 \end{pmatrix} \quad \text{and} \quad \delta\Phi_{\mathrm{z}} = \frac{\mathrm{d}\Phi_{\mathrm{z}}}{\mathrm{d}\phi}\Big|_{\bar{\phi}} \cdot \delta\phi = \begin{pmatrix} -\sin\bar{\phi} & \cos\bar{\phi} & 0 \\ -\cos\bar{\phi} & -\sin\bar{\phi} & 0 \\ 0 & 0 & 0 \end{pmatrix} \cdot \delta\phi \tag{3.3}$$

For the variation of the transformation matrix ${}^{Q_k^w}\Phi^{Q_j}$ holds

$${}^{Q_k^w}\delta\Phi^{Q_j} = \begin{cases} \displaystyle\sum_{m=j+1}^{k} \sum_{v=1}^{3|w} {}^{Q_k^w}\bar{\Phi}^{Q_m} \cdot {}^{Q_m}\bar{\Phi}^{Q_m^{v+1}} \cdot \frac{\mathrm{d}^{Q_m^v}\Phi^{Q_m^{v-1}}}{\mathrm{d}\phi_v^{Q_m}}\Big|_{\bar{\phi}_v^{Q_m}} \cdot {}^{Q_m^{v-1}}\bar{\Phi}^{Q_{m-1}} \cdot {}^{Q_{m-1}}\bar{\Phi}^{Q_j} \cdot \delta\phi_v^{Q_m} & k > j \\ \displaystyle\sum_{v=w+1}^{3} {}^{Q_k^w}\bar{\Phi}^{Q_k^{v-1}} \cdot \frac{\mathrm{d}^{Q_k^{v-1}}\Phi^{Q_k^v}}{\mathrm{d}\phi_v^{Q_k}}\Big|_{\bar{\phi}_v^{Q_k}} \cdot {}^{Q_k^{v+1}}\bar{\Phi}^{Q_k} \cdot {}^{Q_k}\bar{\Phi}^{Q_j} \cdot \delta\phi_v^{Q_k} + & \\ \displaystyle\sum_{m=k+1}^{j} \sum_{v=1}^{3} {}^{Q_k^w}\bar{\Phi}^{Q_{m-1}} \cdot {}^{Q_{m-1}}\bar{\Phi}^{Q_m^{v-1}} \cdot \frac{\mathrm{d}^{Q_m^{v-1}}\Phi^{Q_m^v}}{\mathrm{d}\phi_v^{Q_m}}\Big|_{\bar{\phi}_v^{Q_m}} \cdot {}^{Q_m^{v+1}}\bar{\Phi}^{Q_m} \cdot {}^{Q_m}\bar{\Phi}^{Q_j} \cdot \delta\phi_v^{Q_m} & k <= j \end{cases} \tag{3.4}$$

Note that $\mathrm{d}^{Q_m^v}\Phi^{Q_m^{v-1}}/\mathrm{d}\phi_v^{Q_m}$ for example equals $\mathrm{d}\Phi_{\mathrm{x}}/\mathrm{d}\phi$ while $\mathrm{d}^{Q_m^{v-1}}\Phi^{Q_m^v}/\mathrm{d}\phi_v^{Q_m}$ then equals $\mathrm{d}\Phi_{\mathrm{x}}^{\mathrm{T}}/\mathrm{d}\phi$.

If we simply define the sensitivity of ${}^{Q_k^w}\Phi^{Q_j}$ to rotations that are outside the range between coordinate system $\vec{e}^{\,Q_k^w}$ and $\vec{e}^{\,Q_j}$ equal to zero, as well as the sensitivity to rotations in that range that are no dofs, then we can write with K elements in component Q:

$${}^{Q_k^w}\delta\Phi^{Q_j} = \sum_{m=1}^{K} \sum_{v=1}^{3} \frac{\partial^{Q_k^w}\Phi^{Q_j}}{\partial\phi_v^{Q_m}} \cdot \delta\phi_v^{Q_m} \tag{3.5}$$

Function tbutrafomx() calculates the sensitiviy matrices $\partial^{Q_k^w}\Phi^{Q_j}/\partial\phi_v^{Q_m}$ for all values of k, w, j, m and v. It also calculates the more limited matrix sets $\partial^{Q_k^w}\Phi^{Q_{k-1}}/\partial\phi_v^{Q_k}$ for $v = 1 \ldots w$ and $\partial^{Q_k^w}\Phi^{Q_k}/\partial\phi_v^{Q_k}$ for $v = w+1 \ldots 3$.

Next to these senstivity matrix sets, the function tbutrafomx() calculates the transformation matrix sets ${}^{Q_k^w}\bar{\Phi}^{Q_k^{w-1}}$, ${}^{Q_k^w}\bar{\Phi}^{Q_{k-1}}$ and ${}^{Q_k^w}\bar{\Phi}^{Q_j}$. It also calculates the 'internal' transformation matrices ${}^{Q_k}\bar{\Phi}^{Q_k^{\mathrm{tr}}}$ and ${}^{Q_k}\bar{\Phi}^{Q_k^{\mathrm{t_t}}}$ that map the time derivatives of

- rotational dofs $\dot{\varphi}_v^{Q_k}$ to the increment in the angular velocity vector along $\vec{e}^{\,Q_k}$
- translation dofs $\dot{\varrho}_v^{Q_k}$ to the increment in the linear velocity vector along $\vec{e}^{\,Q_k}$

It then holds:

$$
\begin{aligned}
{}^{Q_{k-1}}\underline{\omega}^{Q_k} &= {}^{Q_k}\bar{\Phi}^{Q_k^{\iota r}} \cdot \begin{bmatrix} \dot{\varphi}_1 \\ \dot{\varphi}_2 \\ \dot{\varphi}_3 \end{bmatrix}^{Q_k} \quad \text{with} \quad {}^{Q_k}\bar{\Phi}^{Q_k^{\iota r}} = \begin{bmatrix} {}^{Q_k}\underline{\bar{\Phi}}_{u_1}^{Q_k^1} & {}^{Q_k}\underline{\bar{\Phi}}_{u_2}^{Q_k^2} & {}^{Q_k}\underline{\bar{\Phi}}_{u_3}^{Q_k^3} \end{bmatrix} \\
{}^{Q_{k-1}^{\oplus}}\underline{v}^{Q_k^{\ominus}} &= {}^{Q_k}\bar{\Phi}^{Q_k^{\iota t}} \cdot \begin{bmatrix} \dot{\varrho}_1 \\ \dot{\varrho}_2 \\ \dot{\varrho}_3 \end{bmatrix}^{Q_k} \quad \text{with} \quad {}^{Q_k}\bar{\Phi}^{Q_k^{\iota t}} = \begin{bmatrix} {}^{Q_k}\underline{\bar{\Phi}}_{v_1}^{Q_k^1} & {}^{Q_k}\underline{\bar{\Phi}}_{v_2}^{Q_k^2} & {}^{Q_k}\underline{\bar{\Phi}}_{v_3}^{Q_k^3} \end{bmatrix}
\end{aligned}
\tag{3.6}
$$

The column vector ${}^{Q_k}\underline{\bar{\Phi}}_{u_1}^{Q_k^1}$ is the u_1^{th} column of the product ${}^{Q_k}\underline{\bar{\Phi}}^{Q_k^2} \cdot {}^{Q_k^2}\underline{\bar{\Phi}}^{Q_k^1}$ of average incremental matrices. The column number u_1 corresponds to the axis-number of the first *rotation* in entry Q_k ($1, 2, 3 \quad \Leftrightarrow \quad x, y, z$), etc.

The v_1^{th} column of that matrix product, notated as ${}^{Q_k}\underline{\bar{\Phi}}_{v_1}^{Q_k^1}$, corresponds to the axis-number of the first *translation* in entry Q_k, etc.

The linearised expression for the variation in the transformation matrix ${}^{Q_k^w}\Phi^{Q_j}$ is used for mapping coordinates from one to another coordinates system on component Q. The variation only applies at transformation of a vector $\underline{q}^{Q_j}$ if q has an average value non equal 0. We then use the tensor notation in order to denote the sensitivy to the rotation dofs $\phi_i^{Q_m}$ ($i = 1 \ldots 3,\ m = j+1 \ldots k$) of the coordinate variations between coordinate system $\vec{e}^{\,Q_j}$ and $\vec{e}^{\,Q_k}$ (say K elements in substructure Q):

$$
\left(\vec{q}^{\,Q_j}\right)^{Q_k} = {}^{Q_k}\bar{\Phi}^{Q_j} \cdot \underline{q}^{Q_j} + [\frac{\partial^{Q_k}\Phi^{Q_j}}{\partial \underline{\phi}^{Q}} \cdot \overline{\underline{q}}^{Q_j}] \cdot \delta\underline{\phi}^{Q} \tag{3.7}
$$

with:

$$
\begin{aligned}
[\frac{\partial^{Q_k}\Phi^{Q_j}}{\partial \underline{\phi}^{Q}} \cdot \overline{\underline{q}}^{Q_j}] \cdot \delta\underline{\phi}^{Q} = [\mathrm{O} \cdot \overline{\underline{q}}^{Q_j} \ldots \mathrm{O} \cdot \overline{\underline{q}}^{Q_j} \quad & \frac{\partial^{Q_k}\Phi^{Q_j}}{\partial \phi_1^{Q_{j+1}}} \cdot \overline{\underline{q}}^{Q_j} \ldots \\
\frac{\partial^{Q_k}\Phi^{Q_j}}{\partial \phi_3^{Q_k}} \cdot \overline{\underline{q}}^{Q_j} \quad & \mathrm{O} \cdot \overline{\underline{q}}^{Q_j} \ldots \mathrm{O} \cdot \overline{\underline{q}}^{Q_j}] \cdot \begin{bmatrix} \delta\phi_1^{Q_1} \\ \vdots \\ \delta\phi_3^{Q_j} \\ \delta\phi_1^{Q_{j+1}} \\ \vdots \\ \delta\phi_3^{Q_k} \\ \delta\phi_1^{Q_{k+1}} \\ \vdots \\ \delta\phi_3^{Q_K} \end{bmatrix}
\end{aligned}
\tag{3.8}
$$

3.3 Multi-body modelling approach

As already mentioned in the previous chapter, the rotor blades and tower are idealised to an assemblage of discrete, rigid elements, with all flexibility assumed

to be concentrated at the attachments between the elements (multi-body model). This section deals with the dimensioning of the rigid elements and the involved springs and dampers in order to establish a valid model for the rotor blades and (tubular) tower. Figure 3.1 shows for the rotor blade the physical structure and the subsequent steps towards the multi-body model on the base of which the governing equations for the blade are derived and implemented.

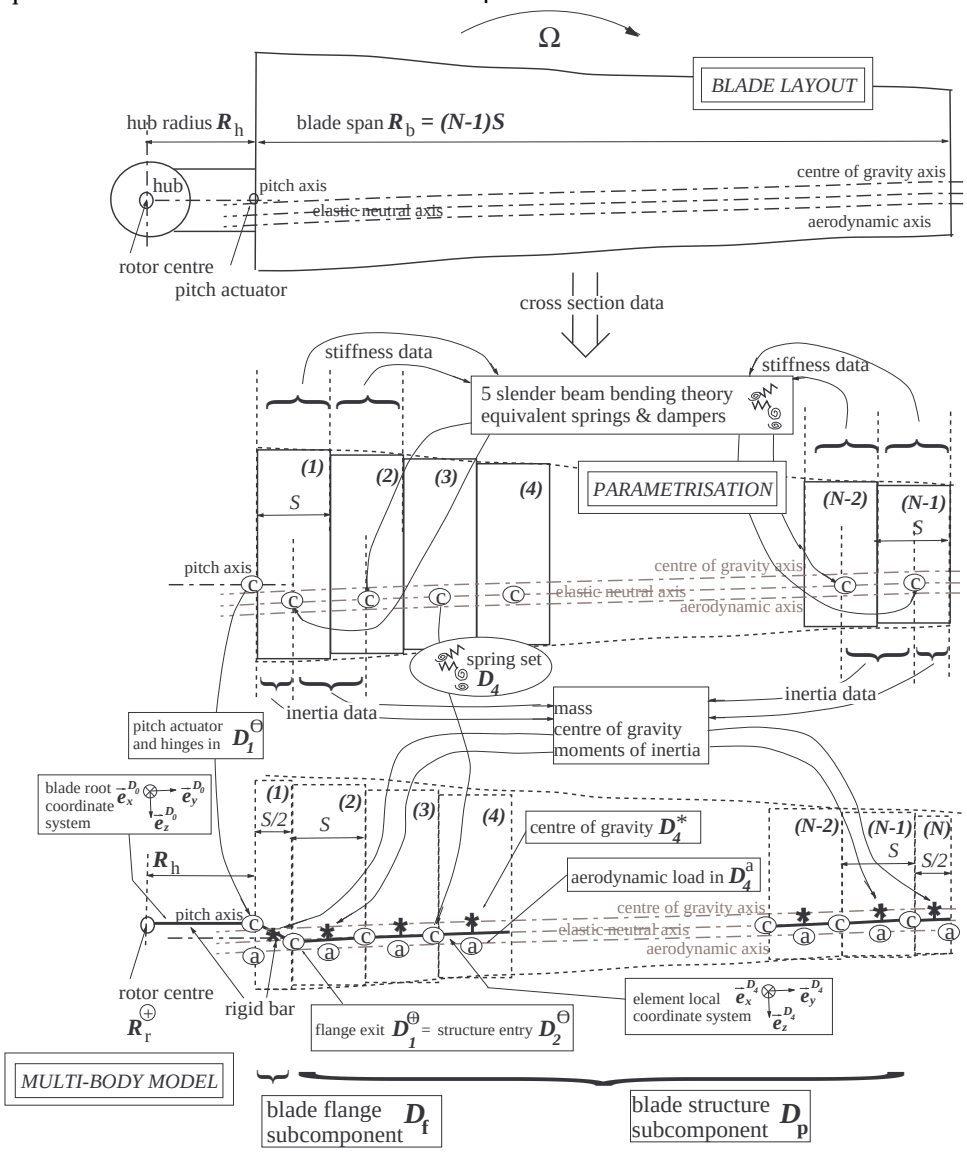

Figure 3.1 *From physical structure to multi-body blade model*

The elastic bending reactions in the elements of a multi-body model for a flexible structure (blade, tower) can be correctly parametrised by two angular and two linear springs. Our point of departure for such a parametrisation is equivalency with the slender beam bending theory as concerns the boundary conditions, see also e.g. [1]. In addition, we chose to avoid cross-couplings between angular and linear elastic reactions and chose the same location for all springs. Basic analysis of the slender beam bending theory points out that:

- Uncoupled bending directions are obtained by letting the orientations of the

springs coincide with the neutral (bending-)elastic axes;
- Cross-coupling in the '2×2' mapping from linear and angular spring deviations to elastic force and torque reactions *in the same bending direction* is avoided by choosing the location of the spring exactly 'mid-span' (at invariant elastic properties over the element);
- The well-known '2×2' mapping from torque and force loading (t,f) to angular and linear deviations (ψ,z) on the boundary of an element with bending stiffness EI and length L,

$$\begin{bmatrix} \psi \\ z \end{bmatrix} = \begin{pmatrix} L/\mathrm{E}I & L^2/2\mathrm{E}I \\ L^2/2\mathrm{E}I & L^3/3\mathrm{E}I \end{pmatrix} \cdot \begin{bmatrix} t \\ f \end{bmatrix} \tag{3.9}$$

is also obtained with a multi-body model if 'at mid-span' a linear spring is located with stiffness $12\mathrm{E}I/L^3$ [N/m] and angular spring with stiffness $\mathrm{E}I/L$ [Nm/rad].

Note that, next to *rotation* degrees of freedom, the implemented multi-body models for the blades and tower also include *translation* degrees of freedom. This is an extension on the model formulation in [5], which appeared inevitable for successful use of model reduction techniques. Besides, the extension guarantees accurate structural behaviour near the fixation.

For reasons of convenience in the formulation of the model equations, we chose to consider the conservation of angular momentum relative to the connection point with the foregoing element, e.g. the more inward blade or downward tower element (lower ranking number). Therefor, an SBBT-equivalent multi-body model with N-1 elements with 'mid-span' springs is mapped to a multibody model, characterised by:
- N elements with springs in the connection points of elements 2. . .N to foregoing elements;
- element 1 and N are half-size, while elements 2 . . . N-1 are full-size.

Define a connection point with a foregoing element as a *connector*, denoted in figure 3.1 by encircled 'c' markers. A connector may accommodate degrees of freedom. The orientation of coordinate systems on the elements of structural components as the rotor blade and tower are chosen such that their axes coincide with the 'directions of the degrees of freedom' in the connectors. Actually, they approximate as good as possible the neutral elastic axes. This choice also contributes to convenient derivation of the model equations.

The connector of the first element in the multi-body model may also acommodate degrees of freedom. In the blade model these dof's enable pitching and hinging in blade flange element X_1, which sets up the flange subomponent. In the support structure model, these are used for accomodating soil flexibility in element S_1, which sets up the foundation subcomponent S_f.

The mass properties of an element of the desired 'N element model' are derived from the mass distribution of *that* partition of the (flexible) structure to which the concerning (half- or full-size) element refers.

The damper values in the connectors are defined proportional to the stiffness values of the concerning springs in that point. The ratio can be freely chosen.

Figure 3.2 shows the physical layout of the support structure and the associated multi-body model; the intermediate model typed as ‘parametrisation’ in fig. 3.1 is omitted in this figure.

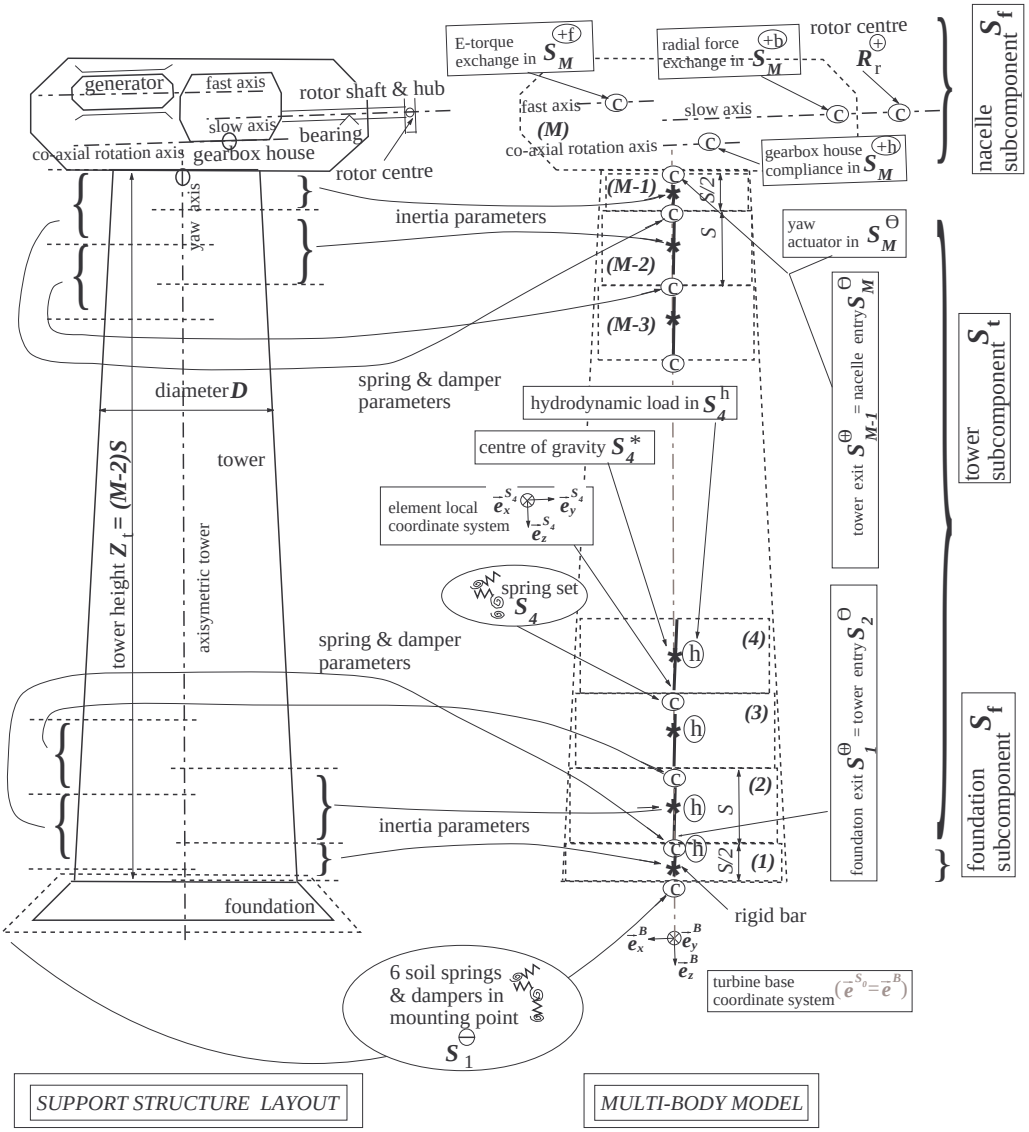

Figure 3.2 *From physical structure to multi-body support structure model*

3.4 Interacting components and the environment

A wind turbine can be considered to behave as a set of interacting components that are subjected to the environmental influences wind, waves and gravitation. Within the scope of TURBU Offshore these ‘components’ are dynamic models of the support structure (including the gearbox house), the drive-train, the rotor blades, the rotor annuli and the control. In order to compose an integrated model from these components, it is required to define the

- orientation of wind and waves relative to the earth and foundation;

- environmental influences as independent model inputs (exogeneous);
- model outputs for analysis of the integrated dynamic behaviour (exogeneous);
- inputs and outputs for the connection of components (interaction).

The first three topics are dealt with in the following subsections; the fourth one is dealt with in section A.1.

3.4.1 Orientation of wind, waves, turbine foundation

Figure 3.3 shows the 'environmental coordinate systems' of the wind turbine:
- geometric coordinate system $\vec{e}^{\,G}$
- aerodynamic coordinate system $\vec{e}^{\,A}$
- hydrodynamic coordinate system $\vec{e}^{\,H}$
- turbine base coordinate system $\vec{e}^{\,B}$

The aerodynamic coordinate system $\vec{e}^{\,A}$ originates from the geographic coordinate system $\vec{e}^{\,G}$ by rotation along $\vec{e}_z^{\,G}$ over the wind direction angle γ^A and along $\vec{e}_y^{\,A_1}$ over the wind slope angle θ^A; the *intermediate* coordinate system $\vec{e}_y^{\,A_1}$ is obtained from $\vec{e}^{\,G}$ by rotation over the direction angle γ^A along $\vec{e}_z^{\,G}$.

The hydrodynamic coordinate system $\vec{e}^{\,H}$ has a vertical downard pointing z-axis and originates from the geographic coordinate system $\vec{e}^{\,G}$ by rotation along the geographic z-axis $\vec{e}_z^{\,G}$ over the wave direction angle γ^{g}.

The turbine base coordinate system $\vec{e}^{\,B}$ originates from the geographic coordinate system $\vec{e}^{\,G}$ by rotation along $\vec{e}_z^{\,G}$ over the turbine base direction angle γ^B and along $\vec{e}_y^{\,B^1}$ over *minus* the turbine base slope angle θ^B; the *intermediate* coordinate system $\vec{e}_y^{\,B^1}$ is obtained from $\vec{e}^{\,G}$ by rotation over the direction angle θ^B along $\vec{e}_z^{\,G}$. The x-axis of $\vec{e}^{\,B}$ points purely fore/aft and the z-axis points co-axially downward in the sense of the foundation tower element S_1 at no soil deformation.

The transformation matrices ${}^A\Phi^G$, ${}^H\Phi^G$ and ${}^B\Phi^G$, which map coordinates along the geographic coordinate system $\vec{e}^{\,G}$ to coordinates along the aerodynamic, hydrodynamic, and turbine base coordinate system, are determined as follows (see also section 3.2, Eq. 3.3):

$$
\begin{aligned}
{}^A\Phi^G &= \Phi_{\mathrm{y}}(\theta^A)\cdot\Phi_{\mathrm{z}}(\gamma^A) = \begin{pmatrix} \cos\theta^A & 0 & -\sin\theta^A \\ 0 & 1 & 0 \\ \sin\theta^A & 0 & \cos\theta^A \end{pmatrix}\cdot\begin{pmatrix} \cos\gamma^A & \sin\gamma^A & 0 \\ -\sin\gamma^A & \cos\gamma^A & 0 \\ 0 & 0 & 1 \end{pmatrix} \\
{}^H\Phi^G &= \Phi_{\mathrm{z}}(\gamma^{\mathrm{g}}) = \begin{pmatrix} \cos\gamma^{\mathrm{g}} & \sin\gamma^{\mathrm{g}} & 0 \\ -\sin\gamma^{\mathrm{g}} & \cos\gamma^{\mathrm{g}} & 0 \\ 0 & 0 & 1 \end{pmatrix} \\
{}^B\Phi^G &= \Phi_{\mathrm{y}}(-\theta^B)\cdot\Phi_{\mathrm{z}}(\gamma^B) = \begin{pmatrix} \cos(-\theta^B) & 0 & -\sin(-\theta^B) \\ 0 & 1 & 0 \\ \sin(-\theta^B) & 0 & \cos(-\theta^B) \end{pmatrix}\cdot\begin{pmatrix} \cos\gamma^B & \sin\gamma^B & 0 \\ -\sin\gamma^B & \cos\gamma^B & 0 \\ 0 & 0 & 1 \end{pmatrix}
\end{aligned}
\tag{3.10}
$$

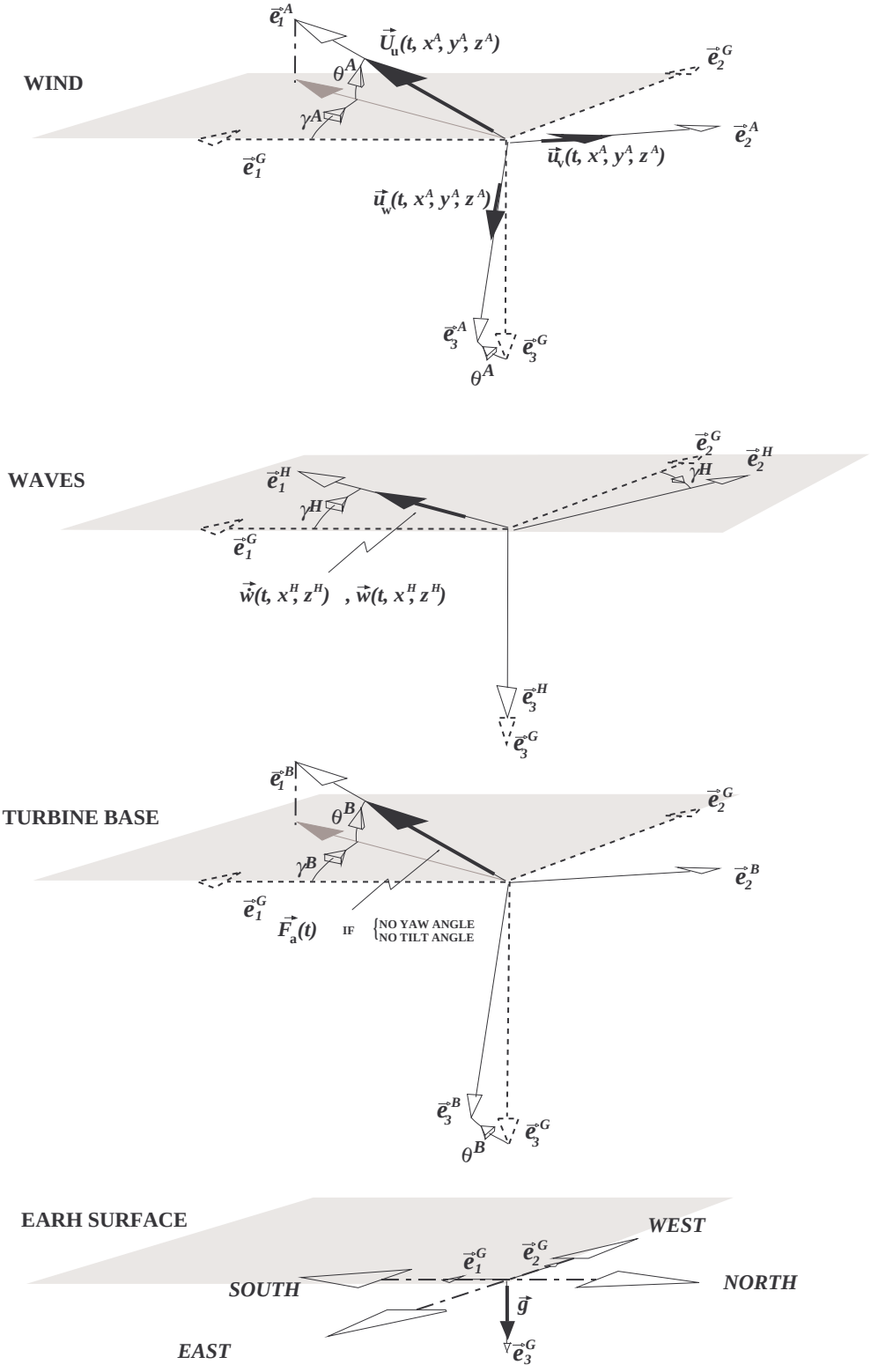

Figure 3.3 *Environmental coordinate systems of the wind turbine*

3.4.2 Exogeneous input variables

The environmental influences are modelled in the assessment of the dynamic wind turbine behaviour via the so called *exogeneous input variables*. These set up the 'independent input vector' $\underline{v}^G$, in which periodic and stochastic subvectors are distinghuised:

$$\underline{v}^G = \begin{bmatrix} \underline{v}^G_{\rm per} \\ \underline{v}^G_{\rm sto} \end{bmatrix}$$

$$\text{with: } \underline{v}^G_{\rm per} = \begin{bmatrix} \underline{u}^D_{\rm per} \\ \underline{u}^E_{\rm per} \\ \underline{u}^F_{\rm per} \\ \underline{g}^{D_0}_{\rm per} \\ \underline{g}^{E_0}_{\rm per} \\ \underline{g}^{F_0}_{\rm per} \\ \underline{g}^{R}_{\rm per} \\ \underline{u}^{D/R_{\rm fx}}_{\rm per} \\ \underline{u}^{E/R_{\rm fx}}_{\rm per} \\ \underline{u}^{F/R_{\rm fx}}_{\rm per} \end{bmatrix} \quad \text{and} \quad \underline{v}^G_{\rm sto} = \begin{bmatrix} \underline{u}^{W/D}_{\rm sto} \\ \underline{u}^{W/E}_{\rm sto} \\ \underline{u}^{W/F}_{\rm sto} \\ \underline{u}^{W/D/R_{\rm fx}}_{\rm sto} \\ \underline{u}^{W/E/R_{\rm fx}}_{\rm sto} \\ \underline{u}^{W/F/R_{\rm fx}}_{\rm sto} \\ \underline{w}^{S}_{\rm horz} \\ \dot{\underline{w}}^{S}_{\rm horz} \end{bmatrix} \tag{3.11}$$

Support structure model inputs

The exogeneous inputs to the support structure are the horizontal wave speeds and accelerations for the calculation of the hydrodynamic viscous and mass force variations on the $M_{\rm uw}$ under water elements. The subvectors $\underline{w}^S_{\rm horz}$ and $\dot{\underline{w}}^S_{\rm horz}$ respectively contain $M_{\rm uw}$ stochastic wave speed signals and force-effective wave acceleration signals (variations only). The orientation of all signals is along the x-axis of the hydrodynamic conversion system $\vec{e}^{\,H}$.

Drive-train model inputs

The periodic gravitation coordinates along the rotating coordinate system on the rotor hub $R_{\rm r}$ are accomodated by the 3-coordinate vector $\underline{g}^R_{\rm per}$ (x-coordinate identical to zero).

Rotor blade model inputs

The periodic wind speed variations on blade D are clustered in the periodic subvector $\underline{u}^D_{\rm per}$. This subvector contains for each of the N blade elements the periodic $x-$, $y-$ and $z-$coordinate along the *rotating* 'conversion coordinate system' $\vec{e}^{\,D^{\rm cv}_k}$ of the blade element. The $x-$ and $z-$axis of this coordinate system point in the normal and leadwise direction of the element, being the reference-directions for inflow angle; y-axis points spanwise). Subvectors $\underline{u}^E_{\rm per}$ and $\underline{u}^F_{\rm per}$ contain the periodic wind speed variations for blades E and F. The periodic variations are due to stagnation & windshear and also to oblique inflow. In the latter case the rotor blades experience periodic wind speed varations from the

average yaw and tilt component of the wind velocity vector as well as from the periodic axial induction variation that is associated with oblique inflow.

The stochastic wind speed variations on blade D by turbulence are clustered in the $N \cdot 3$-element subvector $\underline{u}_{\rm sto}^{W/D}$. The $k^{\rm th}$ set of 3-elements represent the $x-$, $y-$ and $z-$coordinate along $\vec{e}^{\,D_k^{\rm cv}}$. Idem for the subvectors $\underline{u}_{\rm sto}^{W/E}$ and $\underline{u}_{\rm sto}^{W/F}$ with respect to the blades E and F.

See also section B.5 up to Eq. B.182.

The periodic gravitation variations on blade D are accomodated by the three-element subvector $\underline{g}_{\rm per}^{D_0}$; it contains the x-, $y-$ and $z-$ coordinate along the rotating coordinate system $\vec{e}^{\,X_0}$ on the blade root. Subvectors $\underline{g}_{\rm per}^{E_0}$ and $\underline{g}_{\rm per}^{F_0}$ contain the correponding gravitation variations for the blades E and F. See also Eq. B.279 and B.282.

Wake model inputs

The exogeneous wake inputs are the periodic and stochastic wind speed variations for the calculation of the transporatioan speed and Prandtl's correction factor in the rotor annuli. They are accommodated by the respective subvectors sets $\{\underline{u}_{\rm per}^{D/R_{\rm fx}}, \underline{u}_{\rm per}^{E/R_{\rm fx}}, \underline{u}_{\rm per}^{F/R_{\rm fx}}\}$ and $\{\underline{u}_{\rm sto}^{W/D/R_{\rm fx}}, \underline{u}_{\rm sto}^{W/E/R_{\rm fx}}, \underline{u}_{\rm sto}^{W/F/R_{\rm fx}}\}$. Each subvector $\underline{u}_{\rm per}^{X/R_{\rm fx}}$ contains N sets of periodicly varying $x-$, $y-$ and $z-$coordinates for the N elements of blade X along the *non-rotating* coordinate system $\vec{e}^{\,R_{\rm fx}}$ that is fixed to the rotor plane. The periodic variations are due to stagnation & windshear and also oblique inflow. In the latter case the the transportion speed is affected by the associated periodic axial induction speed variations.

Each subvector $\underline{u}_{\rm sto}^{W/X/R_{\rm fx}}$ contains P sets of stochastic $x-$, $y-$ and $z-$coordinates along $\vec{e}^{\,R_{\rm fx}}$ for the intersections of the blade X with the P annuli.

Note on stochastic wind inputs for wake and blade model

Both the stochastic blade and wake model inputs are caused by the same turbulence, which is modelled annulus-wise. As only longitudinal turbulence is taken into account, the P-element vectors ${}^{\rm t}\underline{u}^{W/D}$, ${}^{\rm t}\underline{u}^{W/E}$ and ${}^{\rm t}\underline{u}^{W/F}$ accommodate the driving stochastic wind speed signals, which are located in the rotating intersection of each of the B blades ($B = 3$) with the rotor annuli. The orientation of the P signals for blade X is along the x-axis of the rotating aerodynamic conversion system $\vec{e}^{\,\tilde{A}/X}$. Assume that element X_k intersects with annulus W_m the following holds for the stochastic wake and blade model inputs in annulus m and on blade element k:

$$\begin{aligned}
\underline{u}_{\rm sto}^{W_m/D_k/R_{\rm fx}} &= \sum_{n=-1}^{1} {}^{X/R_{\rm fx}}\widehat{\underline{\Phi}}_{n_1}^{\tilde{A}/X} \cdot {\rm e}^{\jmath \cdot n\bar{\Omega}t} \cdot \Big[\, 0 \ldots 0_{(m-1)}\ 1\ 0_{(m+1)} \ldots 0_P \Big] \cdot {}^{\rm t}\underline{u}^{W/D} \\
\underline{u}_{\rm sto}^{W_m/D} &= \sum_{n=-2}^{2} {}^{X_k^{\rm cv}}\widehat{\underline{\Phi}}_{n_1}^{\tilde{A}/X} \cdot {\rm e}^{\jmath \cdot n\bar{\Omega}t} \cdot \Big[\, 0 \ldots 0_{(m-1)}\ 1\ 0_{(m+1)} \ldots 0_P \Big] \cdot {}^{\rm t}\underline{u}^{W/D}
\end{aligned} \tag{3.12}$$

The Fourier coefficient vectors ${}^{X/R_{\rm fx}}\widehat{\underline{\Phi}}_{1_n}^{\tilde{A}/X}$ and ${}^{X_k^{\rm cv}}\widehat{\underline{\Phi}}_{1_n}^{\tilde{A}/X}$ are the first column of the complex Fourier series matrices that correspond with the following periodic

transformation matrix formulations:

$$
\begin{aligned}
{}^{X/R_{\mathrm{fx}}}\widetilde{\bar{\Phi}}^{\tilde{A}/X} &= \Phi_{b1}\cdot\left[{}^{S_M}\bar{\Phi}^{A}\ \Phi_{\mathrm{d}}^{\mathrm{T}} + {}^{S_M}\bar{\Phi}^{A}\ \Phi_{\mathrm{c}}^{\mathrm{T}}\cdot\cos\bar{\Omega}t + {}^{S_M}\bar{\Phi}^{A}\ \Phi_{\mathrm{s}}^{\mathrm{T}}\cdot\sin\bar{\Omega}t\right]\cdot\Phi_{1b}\\
{}^{X_k^{\mathrm{cv}}}\widetilde{\bar{\Phi}}^{\tilde{A}/X} &= {}^{X_k^{\mathrm{cv}}}\bar{\Phi}^{X_0}\ \Phi_{b1}\cdot\left[\Phi_{\mathrm{d}}\ {}^{R_{\mathrm{h}^{\prime\prime}}}\bar{\Phi}^{A}\ \Phi_{\mathrm{d}}^{\mathrm{T}} + (\Phi_{\mathrm{d}}\ {}^{R_{\mathrm{h}^{\prime\prime}}}\bar{\Phi}^{A}\ \Phi_{\mathrm{c}}^{\mathrm{T}} + \Phi_{\mathrm{c}}\ {}^{R_{\mathrm{h}^{\prime\prime}}}\bar{\Phi}^{A}\ \Phi_{\mathrm{d}}^{\mathrm{T}})\cdot\cos\bar{\Omega}t + \right.\\
&\quad (\Phi_{\mathrm{d}}\ {}^{R_{\mathrm{h}^{\prime\prime}}}\bar{\Phi}^{A}\ \Phi_{\mathrm{s}}^{\mathrm{T}} + \Phi_{\mathrm{s}}\ {}^{R_{\mathrm{h}^{\prime\prime}}}\bar{\Phi}^{A}\ \Phi_{\mathrm{d}}^{\mathrm{T}})\cdot\sin\bar{\Omega}t + \Phi_{\mathrm{c}}\ {}^{R_{\mathrm{h}^{\prime\prime}}}\bar{\Phi}^{A}\ \Phi_{\mathrm{c}}^{\mathrm{T}}\cdot\cos^2\bar{\Omega}t +\\
&\quad \left.\Phi_{\mathrm{s}}\ {}^{R_{\mathrm{h}^{\prime\prime}}}\bar{\Phi}^{A}\ \Phi_{\mathrm{s}}^{\mathrm{T}}\cdot\sin^2\bar{\Omega}t + (\Phi_{\mathrm{c}}\ {}^{R_{\mathrm{h}^{\prime\prime}}}\bar{\Phi}^{A}\ \Phi_{\mathrm{s}}^{\mathrm{T}} + \Phi_{\mathrm{s}}\ {}^{R_{\mathrm{h}^{\prime\prime}}}\bar{\Phi}^{A}\ \Phi_{\mathrm{c}}^{\mathrm{T}})\cdot\sin\bar{\Omega}t\ \cos\bar{\Omega}t\right]\cdot\Phi_{1b}
\end{aligned}
\tag{3.13}
$$

Note that X is considered as the b^{th} blade for which holds:

$$
\Phi_{b1} = \begin{pmatrix} 1 & 0 & 0\\ 0 & \cos(.) & \sin(.)\\ 0 & -\sin(.) & \cos(.)\end{pmatrix}_{(\frac{\mathrm{b}-1}{\mathrm{B}}\cdot 2\pi)} \quad ; \quad \Phi_{1b} = \begin{pmatrix} 1 & 0 & 0\\ 0 & \cos(.) & \sin(.)\\ 0 & -\sin(.) & \cos(.)\end{pmatrix}_{(-\frac{\mathrm{b}-1}{\mathrm{B}}\cdot 2\pi)}
\tag{3.14}
$$

and that Φ_{d}, Φ_{c} and Φ_{s} are the coefficient matrices of the periodic transformation matrix over the on-average evoluating azimut angle $\bar{\Omega}t$ by Eq. 3.65.

The longitudinal wind speed variations in the rotor annuli ${}^{\mathrm{t}}\underline{u}^{W/X}$ are derived from the *homogeneous* variations ${}^{\mathrm{t}}\underline{u}^{\tilde{A}/X}$ via a filter with periodic coefficient that accounts for the azimut angle dependent distance between the wind and rotor/wake plane in corresponding circles (see pg 190 etc. in [4]).

These subvectors are used in the determination of the periodic transportation velocity in the intersection of a rotor blade and rotor annulus. See Eq. 3.28 through Eq. B.245.

The longitudinal wind speed variations by turbulence in the intersection of the blade D with each of the P rotor annuli are clustered in the stochastic subvector ${}^{\mathrm{t}}\underline{u}^{W/D}$. The same is done for the intersections of blades E and F with the rotor annuli, which results in subvectors ${}^{\mathrm{t}}\underline{u}^{W/E}$ and ${}^{\mathrm{t}}\underline{u}^{W/F}$.

The turbulence is oriented along the x-axis of the aerodynamic coordinate system $\vec{e}^{\,A}$. See section B.5 up to Eq. B.180.

3.4.3 Exogeneous output variables

The analysis of the integrated dynamic behaviour is facilitated via output signals that are defined on the models of the components. The 'exogeneous output vector' $\underline{y}^{G}$ is composed of subvectors with output variables from the rotor blades D, E, F, the wake model W, the drive train R, the support structure S:

$$
\underline{y}^{G} = \left[\ \underline{y}^{GD\,\mathrm{T}}\quad \underline{y}^{GE\,\mathrm{T}}\quad \underline{y}^{GF\,\mathrm{T}}\quad \underline{y}^{GW\,\mathrm{T}}\quad \underline{y}^{GR\,\mathrm{T}}\quad \underline{y}^{GS\,\mathrm{T}}\ \right]^{\mathrm{T}}
\tag{3.15}
$$

The composition of the exogeneous output subvectors are listed below and discussed afterwards (note that $X = D, E, F$ for blade no. 1,2,3).

$$\underline{y}^{GX} = \begin{bmatrix} {}^{\bar{X}_0^{\ominus}}\underline{r}^{X_1^{\oplus}/\bar{X}_0} \\ \vdots \\ {}^{\bar{X}_0^{\ominus}}\underline{r}^{X_N^{\oplus}/\bar{X}_0} \\ \underline{f}^{X_1^{\ominus}/X_0} \\ \underline{t}^{X_1^{\ominus}/X_0} \\ \varphi_{\mathrm{pt}}^{X} \end{bmatrix} \; ; \; \underline{y}^{GW} = \begin{bmatrix} \underline{u}_{\mathrm{i_m}}^{W} \end{bmatrix} \; ; \; \underline{y}^{GR} = \begin{bmatrix} {}^{\bar{R}_{\mathrm{r}}^{\mathrm{c}}}\underline{r}^{R_{\mathrm{r}}^{\mathrm{c}}/\bar{R}_{\mathrm{r}}} \\ \underline{\xi}^{R_{\mathrm{r}}^{\mathrm{c}}/\bar{R}_{\mathrm{r}}} \\ {}^{\mathrm{FT}}\underline{t}^{R_{\mathrm{r}}^{\mathrm{c}}} \\ \delta\Omega \\ t_{\mathrm{e}} \end{bmatrix} \tag{3.16}$$

and

$$\underline{y}^{GS} = \begin{bmatrix} {}^{\bar{S}_1^{\ominus}}\underline{r}^{S_1^{\oplus}/B} \\ \vdots \\ {}^{\bar{S}_1^{\ominus}}\underline{r}^{S_M^{\oplus}/B} \\ {}^{\mathrm{FT}}\underline{f}^{S_{M-1}^{\oplus}} \\ {}^{\mathrm{FT}}\underline{t}^{S_{M-1}^{\oplus}} \\ {}^{\mathrm{FT}}\underline{f}^{S_1^{\ominus}/B} \\ {}^{\mathrm{FT}}\underline{t}^{S_1^{\ominus}/B} \\ \varphi_{\mathrm{yw}} \\ \varphi_{\mathrm{gb}} \\ t_{\mathrm{gb}} \end{bmatrix} \tag{3.17}$$

Rotor blade outputs

Each rotor blade provides the following exogeneous output in the subvector $\underline{y}^{GX}$:

- exit point displacements relative to the average position of the rotor centre: ${}^{\bar{X}_0^{\ominus}}\underline{r}^{X_k^{\oplus}/\bar{X}_0}$ $(k = 1 \ldots N)$
- force and torque onto the blade flange$X_1^{\ominus}$: $\underline{f}^{X_1^{\ominus}/X_0}$, $\underline{t}^{X_1^{\ominus}/X_0}$
- pitch angle variation $\varphi_{\mathrm{pt}}^{X}$

The coordinate vector ${}^{\bar{X}_0^{\ominus}}\underline{r}^{X_k^{\oplus}/\bar{X}_0}$ describes the displacement variation of the exit points $X_k^{\oplus}$ relative to the average position of the rotor centre (== blade base $\bar{X}_0^{\ominus}$). Their coordinates are along the on-average rotating coordinate system $\vec{e}_{(.)}^{\,\bar{X}_0}$ on the blade base. Note that these outputs include the dynamic blade deformation as well as the dynamic rotor shaft deformation and modulated tower deformation.

The loads $\underline{f}^{X_1^{\ominus}/X_0}$, $\underline{t}^{X_0^{\ominus}/X_0}$ on the blade flange $X_1^{\ominus}$ are used for analysis of the blade root loads. Their coordinates are along the coordinate system of the blade blase X_0 in its actual position ($\vec{e}_{(.)}^{\,\bar{X}_0}$).

The pitch setpoint $\varphi_{\mathrm{pt}}^{X}$ is only output if pitch control applies.

Wake outputs

The wake model provides the following exogeneous output in subvector $\underline{y}^{GW}$:

- induction speed variation in rotor annuli: $\underline{u}_{\mathrm{i_m}}^{W}$

The wake induction vector $\underline{u}_{\mathrm{i_m}}^{W}$ consists of P subvectors, one in each rotor annulus. Such a subvector has 3 coordinates along the axes of the coordinate system in the cross section of a rotor annulus with a rotor blade. The x- and z-coordinates are equal to minus the axial and tangential induction speed components U_{i} and V_{i} in the cross section of rotor annulus W_m and blade X; the y-coordinate equals 0.

Drive-train outputs

The drive-train model (rotating part only) provides the following exogeneous output in subvector $\underline{y}^{GR}$:

- variation in the main rotational speed: $\delta\Omega$
- rotor centre displacements relative to its average position: $\delta^{\bar{R}_{\mathrm{r}}^{\mathrm{c}}}\underline{r}^{R_{\mathrm{r}}^{\mathrm{c}}/\bar{R}_{\mathrm{r}}}$
- rotor centre angular variations relative to its average orientation: $\delta\underline{\xi}^{R_{\mathrm{r}}^{\mathrm{c}}/\bar{R}_{\mathrm{r}}}$
- torsion and bending moments on the rotor shaft: ${}^{\mathrm{FT}}\underline{t}^{R_{\mathrm{r}}^{\mathrm{c}}}$
- generator counter torque to the drive train: t_{e}

The main rotational speed variation $\delta\Omega$ is the rotation of the slow gearbox shaft relative to the gearbox house. The 'measurable' slow shaft equivalent of the generator speed variation $\delta\Omega^{\mathrm{m}}$ is relative to the nacelle and also involves the coaxial gearbox house rotation $\varphi_3^{R_{\mathrm{h}}}$ (output of support structure). Only the fraction $(i_{\mathrm{gb}}-1)/i_{\mathrm{gb}}$ of the gearbox house rotation is fed-through into the gearbox slow shaft. For the measurable rotor speed variation $\delta\Omega^{\mathrm{m}}$ then holds:

$$\delta\Omega^{\mathrm{m}} = \delta\Omega + \tfrac{i_{\mathrm{gb}}-1}{i_{\mathrm{gb}}} \cdot \dot{\varphi}_1^{R_{\mathrm{h}}} \tag{3.18}$$

The coordinate vector $\delta^{\bar{R}_{\mathrm{r}}^{\mathrm{c}}}\underline{r}^{R_{\mathrm{r}}^{\mathrm{c}}/\bar{R}_{\mathrm{r}}}$ describes the displacement variation of the rotor centre $R_{\mathrm{r}}^{\mathrm{c}}$ relative to its average position $\bar{R}_{\mathrm{r}}^{\mathrm{c}}$. Their coordinates are along the on-average rotating coordinate system $\vec{e}_{(.)}^{\bar{R}_{\mathrm{r}}}$ in the rotor centre. The coordinate vector $\delta\underline{\xi}^{R_{\mathrm{r}}^{\mathrm{c}}/\bar{R}_{\mathrm{r}}}$ describes the angular variation of the rotor centre $R_{\mathrm{r}}^{\mathrm{c}}$ as three angular coordinates along the on-average rotating coordinate system $\vec{e}_{(.)}^{\bar{R}_{\mathrm{r}}}$ in the rotor centre. The decomposition of an angular position variation in x, y and z-coordinates is only valid for small rotations. Actually this linearisation introduces perturbations, which are by nature accepted in TURBU Offshore for the variations.

Note that both these drive-train outputs include the dynamic rotor shaft deformation as well as the modulated dynamic tower deformation.

The torsion and bending moments on the rotor shaft are clustered in the coordinate vector ${}^{\mathrm{FT}}\underline{t}^{R_{\mathrm{r}}^{\mathrm{c}}}$ along the coordinate system of the hub.

Support structure outputs

The support structure provides the following exogeneous output in subvector $\underline{y}^{GS}$:

- exit point displacements relative to the average position of the turbine base: $\delta^{\bar{S}_1^{\ominus}}\underline{r}^{S_k^{\oplus}/B}$ $(k = 1 \ldots M)$
- co-axial angular variation of the gearbox house: φ_{gb}
- force and torque loads on the tower top $S_M^{\ominus}$: ${}^{\mathrm{FT}}\underline{f}^{S_{M-1}^{\oplus}}$, ${}^{\mathrm{FT}}\underline{t}^{S_{M-1}^{\oplus}}$
- force and torque loads on the foundation entry $S_1^{\ominus}$: ${}^{\mathrm{FT}}\underline{f}^{S_1^{\ominus}/B}$, ${}^{\mathrm{FT}}\underline{t}^{S_1^{\ominus}/B}$
- yaw angle variation of the nacelle: φ_{yw}
- co-axial torque on the gearbox house: t_{gb}

The coordinate vector $\delta^{\bar{S}_0^{\ominus}} \underline{r}^{S_k^{\oplus}/B}$ describes the displacement variation of the exit points $S_k^{\oplus}$ relative to the average position $\bar{S}_0^{\ominus}$ of the foundation entry (= turbine base B). Their coordinates are along the invariant coordinate system $\vec{e}^{\,B}_{(.)}$ on the turbine base. For $k = M - 1$ it concerns the yaw bearing centre.

The force and torque loads ${}^{\mathrm{FT}}\underline{f}^{S_{M-1}^{\oplus}}$, ${}^{\mathrm{FT}}\underline{t}^{S_{M-1}^{\oplus}}$ are used for analysis of e.g. the yaw bearing loading. Their coordinates are along the coordinate system of the tower top element S_{M-1}.

The force and torque loads ${}^{\mathrm{FT}}\underline{f}^{S_1^{\ominus}/B}$, ${}^{\mathrm{FT}}\underline{t}^{S_1^{\ominus}/B}$ are used for analysis of the tower foot and the foundation. Their coordinates are along the coordinate system of the turbine base B ($\equiv S_0$).

The yaw angle variation φ_{yw} is only output if dynamic yaw control applies.

3.5 Aerodynamic modelling

The Blade Element Momentum theory, with extensions for transient wake behaviour and for yawed conditions, is the point of departure for the aerodynamic modelling. The governing equations for the equilibrium and for the linearised variations are listed in section 3.5.1. The involved transportation speed and Prandtl's correction factor, which accounts for the finite number of blades, are subject of section 3.5.2.

The implemented model equations are listed in section A.3 with the underlying implemented expressions for the transportation speed and Prandtl's correction factor by section B.8.

3.5.1 Blade Element Momentum theory, wake dynamics and oblique inflow

Point of departure for the Blade Element Moment theory is the assumption of aerodynamically independent behaving rotor annuli. The rotor annuli are chosen such that each annulus exactly encapsulates one or more blade elements and the the number of blade element N is an integer multilple of the number rotor annuli P. The blade layout by fig. 3.1 causes the inner and outer annulus to have a smaller width then the remaining annuli. For $N = P$, the inner and outer annuli have width $\frac{1}{2}S$, while this amounts to S for the remaning annuli. For $N = 2P$ the inner and out annulus width amount to $\frac{3}{2}S$, the remaning ones to $2S$.

As a reference, we use the non-rotating coordinate system $\vec{e}^{\,R_{\mathrm{r}}^{\mathrm{fx}}}$, which is fixed to the rotor plane; it is obtained from the hub coordinate system $\vec{e}^{\,R_{\mathrm{r}}}$ by rotation over *minus* the rotor azimuth angle. This coordinate system coincides with the one on the nacelle. The axial, transverse and vertical wind speed components are described along $\vec{e}^{\,R_{\mathrm{r}}^{\mathrm{fx}}}$. The x- and z-axis of the rotating coordinate systems $\vec{e}^{\,W_m/X_k}$ in annulus W_m coincides with the axial and tangential direction of blade element X_k.

The following two alineas deal with the equilibrium conditions and the linearised equations of motions for the dynamic wake behaviour.

Equations of equilibrium for the rotor annuli

To find the equilibrium position of the blades, the distribution of the axial and tangential induction over the rotor plance is computed using Blade Element Momentum (BEM) theory with Prandtl's correction factor in order to account for the finite number of blades:

$$\begin{aligned}
\tfrac{1}{2}\rho \cdot \sum_{k=k_1(m)}^{k_{\rm end}(m)} [C_{\rm L}(\bar{\phi}_{\rm a_{3/4c}}) \cdot c \cdot S \cdot \sqrt{\bar{U}_{\rm n}^2 + \bar{U}_\ell^2} \cdot \bar{U}_\ell \cdot \cos\bar{\beta}]^{X_k} &= \tfrac{2\pi}{B}\rho \cdot [\bar{r} \cdot \Delta\bar{r} \cdot \bar{F}_{\rm p} \cdot 2\bar{U}_{\rm i} \cdot \bar{U}_{\rm tr}]^{W_m} \\
\tfrac{1}{2}\rho \cdot \sum_{k=k_1(m)}^{k_{\rm end}(m)} [C_{\rm L}(\bar{\phi}_{\rm a_{3/4c}}) \cdot c \cdot S \cdot \sqrt{\bar{U}_{\rm n}^2 + \bar{U}_\ell^2} \cdot \bar{U}_{\rm n}]^{X_k} &= \tfrac{2\pi}{B}\rho \cdot [\bar{r} \cdot \Delta\bar{r} \cdot \bar{F}_{\rm p} \cdot 2\bar{V}_{\rm i} \cdot \bar{U}_{\rm tr}]^{W_m}
\end{aligned} \tag{3.19}$$

with:

$$\begin{aligned}
S^{X_k} &= \mu_k \cdot S \quad (\mu_k = \tfrac{1}{2} \text{ for } k = 1, N \text{; else } \mu_k = 1 \text{ (case } N = 2P)) \\
\bar{r}^{W_m} &= R_{\rm h} + \tfrac{1}{2}\sum_{k=1}^{k_1(m)-1} \mu_k \cdot S \cdot \cos\bar{\beta}^{X_k} + \tfrac{1}{2}\sum_{k=1}^{k_{\rm end}(m)} \mu_k \cdot S \cdot \cos\bar{\beta}^{X_k} \\
\Delta\bar{r}^{W_m} &= \sum_{k=k_1(m)}^{k_{\rm end}(m)} \mu_k \cdot S \cdot \cos\bar{\beta}^{X_k} \\
\bar{R} &= R_{\rm r} + \tfrac{1}{2}\sum_{k=1}^{N} \mu_k \cdot S \cdot \cos\bar{\beta}^{X_k}
\end{aligned} \tag{3.20}$$

Prandtl's correction is applied twice: at the blade tip and at the blade root. See section 3.5.2.

The 2D lift polars used in the rotor annuli are assumed to be corrected in order to account for 3D-effects.

The influence of the difference $\bar{\zeta}^{X_k} - \bar{\zeta}_{\rm i}^{X_k}$ between the element lead angle and induction lead angle is neglected (see fig. B.5 in section B.5.3). This pertains to the annulus width Δr in the right hand side as well as the mapping of the normal blade force to the axial force on the rotor annulus; only the cosinus of the flap angle $\bar{\beta}^{X_k}$ is involved.

The use of the full hub radius $R_{\rm r}$ in the expression for $\bar{r}^{W_m}$ instead of scaling by 'application of the cosinus rule on the induction lead angle $\bar{\zeta}_i$' introduces a relative error smaller than $\bar{\zeta}_i^2/(k_{\rm end}(m) + k_1(m) - 1) \cdot R_{\rm r}/S$.

An algorithm for simultaneous solving the aerodynamic equilibrium equations is implemented in M-function tbuaerconinit(). It works iteratively and calls M-function tbusolvebem() in each iteration.

Linearised equations of motion for the rotor annuli

The linearised model equations are used for the dynamic wake behaviour. They are obtained from the equations in section 12.2 of [5] by considering the linearised variation behaviour with the time dependent terms included. The state vector of the dynamic wake model consists of the 'ensemble average' axial induction speed

variations in the rotor annuli (average over B instantaneous values) and optionally also the 'ensemble average' tangential induction speed variations.

The following differential equation is the point of departure for obtianing the linearised model ($B = 3$):

$$\frac{\mathrm{d}}{\mathrm{d}t}\left(U_{\mathrm{i_m}}^{W_m}\right) = \sum_{k=k_1(m)}^{k_{\mathrm{end}}(m)} \left(\frac{-({}^{\mathrm{a_L}}f_1^{D_k} + {}^{\mathrm{a_L}}f_1^{E_k} + {}^{\mathrm{a_L}}f_1^{F_k})}{\rho \cdot 2\pi r^{W_m} \cdot \Delta r^{W_m} \cdot 2R^{W_m} \cdot \mathcal{F}_{\mathrm{a}}^{W_m} \cdot (\frac{F^{D_k}+F^{E_k}+F^{F_k}}{B}}) - \frac{U_{\mathrm{i_m}}^{D_k} \cdot U_{\mathrm{tr}}^{D_k} + U_{\mathrm{i_m}}^{E_k} \cdot U_{\mathrm{tr}}^{E_k} + U_{\mathrm{i_m}}^{F_k} \cdot U_{\mathrm{tr}}^{F_k}}{B \cdot R^{W_m} \cdot \mathcal{F}_{\mathrm{a}}^{W_m}} \right) \tag{3.21}$$

with:

$$\mathcal{F}_{\mathrm{a}}^{W_m} = \frac{2\pi}{\int_0^{2\pi} \left\{ \frac{1 \; - \; \left(r^{W_m}/R^{W_m}\right)\cos\psi}{\left[1 \; + \; \left(r^{W_m}/R^{W_m}\right)^2 \; - \; 2\left(r^{W_m}/R^{W_m}\right)\cos\psi\right]^{1.5}} \right\} \, \mathrm{d}\psi} \tag{3.22}$$

The lift force reactions ${}^{\mathrm{a_L}}f_1^{X_k}$ by the blades, along the x-axis of the annulus coordinate systems, correspond with the left hand term in the axial equilibirum equation 3.19 with a minus sign.

In this equation of motion, we assume the blade radius, annulus radii and widths to be equal to the average values $\bar{R}^{W_m}$, $\bar{r}^{W_m}$, and $\Delta\bar{r}^{W_m}$. We also assume frozen wake conditions for blade-local variations in inflow and structural conditons that *differ* from the *ensemble-average* variations in conditions. It then holds that $U_{\mathrm{i_m}}^{X_k} = U_{\mathrm{i}}^{W_m}$ for $X = D, E, F$; note that $U_{\mathrm{i_m}}^{D_k}$ is part of the expression for ${}^{\mathrm{a_L}}f_1^{D_k}$ etc. Equation 3.21 can then be dealt with without further algebraic manipulations:

If the blade-local variations were assumed 'equilibrium wake' then $U_{\mathrm{i_m}}^{X_k}$ would be composed from the annulus-average $U_{\mathrm{i}}^{W_m}$ and feedthrough contributions of the blade-local variations; this 'local equilibrium wake assumption' is effectively assumed in the model description [5], which is based on [10].

Define ϵ_k as the weighting factor for the relative contribution of blade element k to annulus m:

$$\epsilon_k = \mu_k \; / \sum_{\kappa=k_1(m)}^{k_{\mathrm{end}}(m)} \mu_\kappa \tag{3.23}$$

The variation expression for the equation of motion then is:

$$\frac{\mathrm{d}}{\mathrm{d}t}\left(U_{\mathrm{i_m}}^{W_m}\right) = \sum_{k=k_1(m)}^{k_{\mathrm{end}}(m)} \left(\frac{-(\delta^{\mathrm{a_L}}f_1^{D_k} + \delta^{\mathrm{a_L}}f_1^{E_k} + \delta^{\mathrm{a_L}}f_1^{F_k})}{\rho \cdot 2\pi \bar{r}^{W_m} \cdot \Delta\bar{r}^{W_m} \cdot 2\bar{R}^{W_m} \cdot \bar{\mathcal{F}}_{\mathrm{a}}^{W_m} \cdot \bar{F}_{\mathrm{p}}^{W_m}} \right) - \frac{\bar{U}_{\mathrm{tr}}^{W_m}}{\bar{R}^{W_m} \cdot \bar{\mathcal{F}}_{\mathrm{a}}^{W_m}} \cdot \delta U_{\mathrm{i_m}}^{W_m} +$$

$$\sum_{k=k_1(m)}^{k_{\mathrm{end}}(m)} \left(\frac{B \cdot {}^{\mathrm{a_L}}\bar{f}_1^{X_k}}{B \cdot \rho \cdot 2\pi \bar{r}^{W_m} \cdot \Delta\bar{r}^{W_m} \cdot 2\bar{R}^{W_m} \cdot \bar{\mathcal{F}}_{\mathrm{a}}^{W_m} \cdot (\bar{F}_{\mathrm{p}}^{W_m})^2} \right) \cdot (\delta F_{\mathrm{p}}^{D_k} + \delta F_{\mathrm{p}}^{E_k} + \delta F_{\mathrm{p}}^{F_k}) -$$

$$\sum_{k=k_1(m)}^{k_{\mathrm{end}}(m)} \epsilon_k \cdot \left(\frac{\bar{U}_{\mathrm{i}}^{W_m}}{B \cdot \bar{R}^{W_m} \cdot \bar{\mathcal{F}}_{\mathrm{a}}^{W_m}} \right) \cdot (\delta U_{\mathrm{tr}}^{D_k} + \delta U_{\mathrm{tr}}^{E_k} + \delta U_{\mathrm{tr}}^{F_k}) \tag{3.24}$$

The aerodynamic reaction force variations on the rotor annuli by the blades are dealt with in paragraph (iii) in section 3.6.3 with the required underlying relationships in paragraphs (i) and (ii). The variations in the transportation speed and Prandtl's correction factor are subject of section 3.5.2.

When we also assume no differences between tangential induction speed variations on the different blade in the same annulus ($\delta V_{\mathrm{i}}^{W_m/D_k} = \delta V_{\mathrm{i}}^{W_m/E_k} = \delta V_{\mathrm{i}}^{W_m/F_k}$), the equation for the annulus-wise accompanying tangential induction speed variation $\delta V_{\mathrm{i}}^{W_m}$ becomes:

$$\begin{aligned}\delta V_{\mathrm{i_m}}^{W_m} \;=& \sum_{k=k_1(m)}^{k_{\mathrm{end}}(m)} \left(\frac{-(\delta^{\mathrm{a_L}} f_3^{D_k} + \delta^{\mathrm{a_L}} f_3^{E_k} + \delta^{\mathrm{a_L}} f_3^{F_k})}{\rho \cdot 2\pi \bar{r}^{W_m} \cdot \Delta\bar{r}^{W_m} \cdot 2\bar{F}_{\mathrm{p}}^{W_m} \cdot \bar{U}_{\mathrm{tr}}^{W_m}} \right) + \\ & \sum_{k=k_1(m)}^{k_{\mathrm{end}}(m)} \left(\frac{B \cdot {}^{\mathrm{a_L}}\bar{f}_3^{X_k}}{B \cdot \rho \cdot 2\pi \bar{r}^{W_m} \cdot \Delta\bar{r}^{W_m} \cdot 2 \cdot (\bar{F}_{\mathrm{p}}^{W_m})^2 \cdot \bar{U}_{\mathrm{tr}}^{W_m}} \right) \cdot (\delta F_{\mathrm{p}}^{D_k} + \delta F_{\mathrm{p}}^{E_k} + \delta F_{\mathrm{p}}^{F_k}) - \\ & \sum_{k=k_1(m)}^{k_{\mathrm{end}}(m)} \epsilon_k \cdot \left(\frac{\bar{V}_{\mathrm{i}}^{W_m}}{B \cdot \bar{U}_{\mathrm{tr}}^{W_m}} \cdot (\delta U_{\mathrm{tr}}^{D_k} + \delta U_{\mathrm{tr}}^{E_k} + \delta U_{\mathrm{tr}}^{F_k}) \right)\end{aligned} \tag{3.25}$$

The tangential induction speed variations by Eq. 3.25 are calculated 'equilibrium wake'. This appears more realistic then assuming transition behaviour: the later version 4 of the aerodynamic code PHATAS [10] does not include anymore transient behaviour for the tangential induction $V_{\mathrm{i_m}}^{W_m}$ whereas the earlier version 3 did include. In TURBU Offshore, it is also allowed to include transient dynamics for the tangential induction speed. In that case the following equation of motion for $V_{\mathrm{i_m}}^{W_m}$ applies:

$$\begin{aligned}\tfrac{\mathrm{d}}{\mathrm{d}t}\big(V_{\mathrm{i_m}}^{W_m}\big) \;=& \sum_{k=k_1(m)}^{k_{\mathrm{end}}(m)} \left(\frac{-\gamma \cdot (\delta^{\mathrm{a_L}} f_3^{D_k} + \delta^{\mathrm{a_L}} f_3^{E_k} + \delta^{\mathrm{a_L}} f_3^{F_k})}{\rho \cdot 2\pi \bar{r}^{W_m} \cdot \Delta\bar{r}^{W_m} \cdot 2\bar{R}^{W_m} \cdot \bar{\mathcal{F}}_{\mathrm{a}}^{W_m} \cdot \bar{F}_{\mathrm{p}}^{W_m}} \right) - \frac{\gamma \cdot \bar{U}_{\mathrm{tr}}^{W_m}}{\bar{R}^{W_m} \cdot \bar{\mathcal{F}}_{\mathrm{a}}^{W_m}} \cdot \delta V_{\mathrm{i_m}}^{W_m} + \\ & \sum_{k=k_1(m)}^{k_{\mathrm{end}}(m)} \left(\frac{\gamma \cdot B \cdot {}^{\mathrm{a_L}}\bar{f}_3^{X_k}}{B \cdot \rho \cdot 2\pi \bar{r}^{W_m} \cdot \Delta\bar{r}^{W_m} \cdot 2\bar{R}^{W_m} \cdot \bar{\mathcal{F}}_{\mathrm{a}}^{W_m} \cdot (\bar{F}_{\mathrm{p}}^{W_m})^2} \right) \cdot (\delta F_{\mathrm{p}}^{D_k} + \delta F_{\mathrm{p}}^{E_k} + \delta F_{\mathrm{p}}^{F_k}) - \\ & \sum_{k=k_1(m)}^{k_{\mathrm{end}}(m)} \epsilon_k \cdot \left(\frac{\gamma \cdot \bar{V}_{\mathrm{i}}^{W_m}}{B \cdot \bar{R}^{W_m} \cdot \bar{\mathcal{F}}_{\mathrm{a}}^{W_m}} \right) \cdot (\delta U_{\mathrm{tr}}^{D_k} + \delta U_{\mathrm{tr}}^{E_k} + \delta U_{\mathrm{tr}}^{F_k})\end{aligned} \tag{3.26}$$

The factor γ is introduced for scaling the time scale of the transient dynamics relative to those of the axial induction speed. Choosing $\gamma = 1$ yields the same transient bevahiour; take $\gamma = 10$ for ten times as fast transients, etc.

3.5.2 Transportation speed and Prandtl's correction factor

The first part of this subsection gives the expressions as functions of the wind field velocity components and the induction speeds in the rotor annuli. The second paragraph describes the wind velocity components involved, which are relative to the rotor plane

(i) Expressions in wind velocity components

The transportation speed in the partition of rotor annulus W_m that intersects with blade X is identified as $U_{\rm tr}^{W_m/X}$ and is expressed as follows in the axial and yaw- and tiltwise wind speed components:

$$U_{\rm tr}^{W_m/X} = \sqrt{(U_{\rm ax}^{W_m/X} - F_{\rm p}^{W_m/X}\cdot U_{\rm i_m}^{W_m})^2 + (U_{\rm yaw}^{W_m/X})^2 + (U_{\rm tilt}^{W_m/X})^2} \tag{3.27}$$

The periodic axial induction variation by oblique inflow is catered for in the variation of $U_{\rm ax}^{W_m/X}$ (see Eq. B.240 and B.242 and B.248, $U_{\rm i_o}^{X_k}$).

The expression for Prandtl's correction factor $F_{\rm p}^{W_m/X}$ in the intersection of annulus W_m and element X_k and for the involved vortex distance parameter $d^{W_m/X}$ are:

$$\begin{aligned} F_{\rm p}^{W_m/X} &= \tfrac{2}{\pi}\cdot\arccos\left(\mathrm{e}^{-(\bar{R}-\bar{r}^{W_m})\pi/d^{W_m/X}}\right)\cdot\tfrac{2}{\pi}\cdot\arccos\left(\mathrm{e}^{-(\bar{r}^{W_m}-R_{\rm root})\pi/d^{W_m/X}}\right) \\ d^{W_m/X} &= \frac{2\pi\,\bar{r}^{W_m}}{B}\cdot\frac{U_{\rm tr"}^{W_m/X}}{\sqrt{\left(\bar{\Omega}\cdot\bar{r}^{W_m}\right)^2+\left(U_{\rm tr"}^{W_m/X}\right)^2}} \\ \text{with}\quad U_{\rm tr"}^{W_m/X} &= \sqrt{(U_{\rm ax}^{W_m/X} - U_{\rm i_m}^{W_m})^2 + (U_{\rm yaw}^{W_m/X})^2 + (U_{\rm tilt}^{W_m/X})^2} \end{aligned} \tag{3.28}$$

By use of overlined symbols (mean values) it is indicated that we neglect the influence of variation $\delta\Omega$ in the main rotation speed on $F_{\rm p}^{W_m/X}$ via $d^{W_m X_k}$ as well as the influence of variations in the rotor radius R and annulus radius r^{W_m}.

Just as in the expression for the blade relative wind speed we use the blade-independent identifier $U_{\rm i_m}^{W_m}$ for the non-oblique-inflow component of the axial induction speed instead of $U_{\rm i_m}^{W_m/X}$ because we assume azimuth-independency (see section A.3.1).

The axial, transverse and vertical undisturbed wind speed components are related to the x-, y- and z-axis of the non-rotating coordinate system fixed to the rotor plane. This coordinate system $\vec{e}^{\,R_{\rm fx}}$ originates from the rotor hub coordinate system $\vec{e}^{\,R_{\rm r}}$ by reverse rotation along the x-axis over the rotor azimuth angle $\psi_{\rm r}$ ($=\int^t\Omega{\rm d}t+(i_{\rm gb}-1)/i_{\rm gb}\cdot\phi_3^{R_{\rm h}}+\phi_1^{R_{\rm r}}$). We define the wind speed vector $\underline{u}^{W_m/X/R_{\rm fx}}$ to contain these wind speed components:

$$\underline{u}^{W_m/X/R_{\rm fx}} \triangleq \begin{bmatrix} U_{\rm ax}^{W_m/X} \\ U_{\rm yaw}^{W_m/X} \\ U_{\rm tilt}^{W_m/X} \end{bmatrix} \quad \text{(use Eq. B.240 and B.241 for mean } \bar{\underline{u}}^{R_{\rm fx}} \text{ and variation } \delta\underline{u}^{W_m/X/R_{\rm fx}}\text{)} \tag{3.29}$$

The mean $\bar{F}_{\rm p}^{W_m}$ of Prandtl's correction factor is equal all over the rotor annulus W_m and follows straightforward from Eq. 3.28 by use of the mean values for the axial induction speed and wind speed components ($\bar{U}_{\rm i_m}^{W_m}$, $\bar{\underline{u}}^{R_{\rm fx}}$). The variation of $F_{\rm p}^{W_m/X}$ depends on the actual values of the wind speed components in the intersection of annulus W_m and blade element X_k and of the axial induction in W_m (neglect tangential blade speed variations):

$$\delta F_{\rm p}^{W_m/X} = \frac{{\rm d}F_{\rm p}^{W_m/X}}{{\rm d}d^{W_m/X}}\cdot\frac{{\rm d}d^{W_m/X}}{{\rm d}U_{\rm tr"}^{W_m/X}}\cdot\left(\frac{\partial U_{\rm tr"}^{W_m/X}}{\partial\underline{u}^{W_m/X/R_{\rm fx}}}\cdot\delta\underline{u}^{W_m/X/R_{\rm fx}}+\frac{\partial U_{\rm tr"}^{W_m/X}}{\partial U_{\rm i_m}^{W_m}}\cdot\delta U_{\rm i_m}^{W_m}\right)$$

with $(\alpha_{\mathrm{t}_m} = -(\bar{R} - \bar{r}^{W_m})\pi/\bar{d}^{W_m},\ \alpha_{\mathrm{r}_m} = -(\bar{r}^{W_m} - R_{\mathrm{root}})\pi/\bar{d}^{W_m})$:

$$\frac{\mathrm{d}F_{\mathrm{p}}^{W_m/X}}{\mathrm{d}d^{W_m/X}} = \frac{4}{\pi^2 \bar{d}^{W_m}} \cdot \Big(\frac{\alpha_{\mathrm{t}_m} \cdot \mathrm{e}^{\alpha_{\mathrm{t}_m}} \cdot \arccos(\mathrm{e}^{\alpha_{\mathrm{r}_m}})}{\sqrt{1 - \mathrm{e}^{2\alpha_{\mathrm{t}_m}}}} + \frac{\alpha_{\mathrm{r}_m} \cdot \mathrm{e}^{\alpha_{\mathrm{r}_m}} \cdot \arccos(\mathrm{e}^{\alpha_{\mathrm{t}_m}})}{\sqrt{1 - \mathrm{e}^{2\alpha_{\mathrm{r}_m}}}} \Big)$$

$$\frac{\mathrm{d}d^{W_m/X}}{\mathrm{d}U_{\mathrm{tr}"}^{W_m/X}} = \frac{2\pi \bar{r}^{W_m}}{B} \cdot \frac{\big(\bar{\Omega} \cdot \bar{r}^{W_m}\big)^2}{\Big(\big(\bar{\Omega} \cdot \bar{r}^{W_m}\big)^2 + \big(\bar{U}_{\mathrm{tr}"}^{W_m}\big)^2 \Big)^{1.5}}$$

while:

$$\frac{\partial U_{\mathrm{tr}"}^{W_m/X}}{\partial \underline{u}^{W_m/X/R_{\mathrm{fx}}}} = \frac{(\bar{u}^{R_{\mathrm{fx}}})^{\mathrm{T}} + [\ -\bar{U}_{\mathrm{i_m}}^{W_m}\ \ 0\ \ 0\ ]}{\bar{U}_{\mathrm{tr}"}^{W_m}}$$

$$\frac{\partial U_{\mathrm{tr}"}^{W_m/X}}{\partial U_{\mathrm{i_m}}^{W_m}} = \frac{-\bar{U}_{\mathrm{ax}}^{R_{\mathrm{fx}}} + \bar{U}_{\mathrm{i_m}}^{W_m}}{\bar{U}_{\mathrm{tr}"}^{W_m}} \tag{3.30}$$

The mean $\bar{U}_{\mathrm{tr}}^{W_m}$ of the transportation speed follows straightforward from Eq. 3.27 by use of the mean values for the axial induction speed, wind speed components and Prandtl's correction factor ($\bar{U}_{\mathrm{i_m}}^{W_m}$, $\underline{\bar{u}}^{R_{\mathrm{fx}}}$, $\bar{F}_{\mathrm{p}}^{W_m}$) The variation of $U_{\mathrm{tr}}^{W_m/X}$ depends on the actual values of the wind speed components in the intersection of annulus W_m and blade element X_k and of the axial induction in W_m (neglect tangential blade speed variations):

$$\begin{aligned}\delta U_{\mathrm{tr}}^{W_m/X} = {} & \Big(\frac{\partial U_{\mathrm{tr}}^{W_m/X}}{\partial \underline{u}^{W_m/X/R_{\mathrm{fx}}}} + \frac{\partial U_{\mathrm{tr}}^{W_m/X}}{\partial F_{\mathrm{p}}^{W_m/X}} \cdot \frac{\partial F_{\mathrm{p}}^{W_m/X}}{\partial \underline{u}^{W_m/X/R_{\mathrm{fx}}}} \Big) \cdot \delta \underline{u}^{W_m/X/R_{\mathrm{fx}}} + \\ & \Big(\frac{\partial U_{\mathrm{tr}}^{W_m/X}}{\partial U_{\mathrm{i_m}}^{W_m}} + \frac{\partial U_{\mathrm{tr}}^{W_m/X}}{\partial F_{\mathrm{p}}^{W_m/X}} \cdot \frac{\partial F_{\mathrm{p}}^{W_m/X}}{\partial U_{\mathrm{i_m}}^{W_m}} \Big) \cdot \delta U_{\mathrm{i_m}}^{W_m}\end{aligned}$$

with:

$$\frac{\partial U_{\mathrm{tr}}^{W_m/X}}{\partial \underline{u}^{W_m/X/R_{\mathrm{fx}}}} = \frac{(\bar{u}^{R_{\mathrm{fx}}})^{\mathrm{T}} + [\ -\bar{F}_{\mathrm{p}}^{W_m} \cdot \bar{U}_{\mathrm{i_m}}^{W_m}\ \ 0\ \ 0\ ]}{\bar{U}_{\mathrm{tr}}^{W_m}}$$

$$\frac{\partial U_{\mathrm{tr}}^{W_m/X}}{\partial F_{\mathrm{p}}^{W_m/X}} = \frac{-\bar{U}_{\mathrm{i_m}}^{W_m} \cdot (\bar{U}_{\mathrm{ax}}^{R_{\mathrm{fx}}} - \bar{F}_{\mathrm{p}}^{W_m} \cdot \bar{U}_{\mathrm{i_m}}^{W_m})}{\bar{U}_{\mathrm{tr}"}^{W_m}}$$

$$\frac{\partial U_{\mathrm{tr}}^{W_m/X}}{\partial U_{\mathrm{i_m}}^{W_m}} = \frac{-\bar{F}_{\mathrm{p}}^{W_m} \cdot (\bar{U}_{\mathrm{ax}}^{R_{\mathrm{fx}}} - \bar{F}_{\mathrm{p}}^{W_m} \cdot \bar{U}_{\mathrm{i_m}}^{W_m})}{\bar{U}_{\mathrm{tr}"}^{W_m}}$$

while (use Eq. 3.30):

$$\frac{\partial F_{\mathrm{p}}^{W_m/X}}{\partial \underline{u}^{W_m/X/R_{\mathrm{fx}}}} = \frac{\mathrm{d}F_{\mathrm{p}}^{W_m/X}}{\mathrm{d}d^{W_m/X}} \cdot \frac{\mathrm{d}d^{W_m/X}}{\mathrm{d}U_{\mathrm{tr}"}^{W_m/X}} \cdot \frac{\partial U_{\mathrm{tr}"}^{W_m/X}}{\partial \underline{u}^{W_m/X/R_{\mathrm{fx}}}}$$

$$\frac{\partial F_{\mathrm{p}}^{W_m/X}}{\partial U_{\mathrm{i_m}}^{W_m}} = \frac{\mathrm{d}F_{\mathrm{p}}^{W_m/X}}{\mathrm{d}d^{W_m/X}} \cdot \frac{\mathrm{d}d^{W_m/X}}{\mathrm{d}U_{\mathrm{tr}"}^{W_m/X}} \cdot \frac{\partial U_{\mathrm{tr}"}^{W_m/X}}{\partial U_{\mathrm{i_m}}^{W_m}} \tag{3.31}$$

(ii) Wind velocity components relative to the rotor plane

The wind velocity components involved are the axial, yawwise and tiltwise wind speed components in the coordinate system $\vec{e}^{\,R_{\mathrm{fx}}}$ that is fixed to the rotor plane. These components, for the intersection of blade X with annulus W_m are the

coordinates of the wind speed vector $\underline{u}^{W_m/X/R_{\rm fx}}$, which is composed of a mean, periodic, stochastic and reactive part:

$$\underline{u}^{W_m/X/R_{\rm fx}} = \begin{bmatrix} \delta U_{\rm ax}^{W_m/X} \\ \delta U_{\rm yaw}^{W_m/X} \\ \delta U_{\rm tilt}^{W_m/X} \end{bmatrix} = \bar{\underline{u}}^{R_{\rm fx}} + \delta \underline{u}_{\rm sto}^{W_m/X/R_{\rm fx}} + \delta \underline{u}_{\rm per}^{W_m/X/R_{\rm fx}} + \delta \underline{u}_{\rm ori}^{W_m/X/R_{\rm fx}} \tag{3.32}$$

Figure 3.4 shows the interdependency of these wind speed subvectors and the 'driving variables and constants', that is to say:

- mean longitudinal wind speed;
- longitudinal turbulence;
- periodic variations by wind shear and tower stagnation;
- periodic axial induction speed variations by oblique inflow.
- orientation of the rotor plane relative to the longitudinal wind speed direction

See section 3.4.2, Eq. 3.12 for the relationship of the stochastic wind speed subvector with the longitudinal turbulence.

The longitudinal wind speed variatons ${}^{\rm r}u^{X_k^{\rm a}}$ by shear and stagnation are modelled in accordance with the IEC requirements with respect to wind shear and with a semi-infinite dipole model (see also pg 185, etc. in [4]). The periodic wind speed coordinates are calculated for the *blade elements*. Since an annulus may encapsulate a number of blade elements, the periodic windspeed vector for the 'wake model' is assembled in general as a weighted average over more blade elements:

$$\delta \underline{u}_{\rm per}^{W_m/X/R_{\rm fx}} = \sum_{k=k_1(m)}^{k_{\rm end}(m)} \epsilon_{k(m)} \cdot \left({}^{S_M}\bar{\Phi}^{A}_{(:,1)} \cdot {}^{\rm r}u^{X_k^{\rm a}} \right) - U_{\rm i_{obl}}^{W_m/X_d} \cdot \underline{e}_1 \tag{3.33}$$

The periodic coordinate values of the aerodynamic conversion point $X_k^{\rm a}$ relative to the tower top are approximated by

$$\begin{bmatrix} \tilde{x}^{X_k^{\rm a}} \\ \tilde{y}^{X_k^{\rm a}} \\ \tilde{z}^{X_k^{\rm a}} \end{bmatrix} = {}^{G}\bar{\Phi}^{S_M}.{}^{S_M^{\ominus}}\underline{r}^{S_M^{\oplus}} + {}^{G}\bar{\Phi}^{R_{\rm h"}}.{}^{R_{\rm h"}}\tilde{\Phi}^{R_{\rm s}}.{}^{R_{\rm s}}\bar{\Phi}^{X_0} \cdot \left(\begin{bmatrix} 0 \\ R_{\rm root} \\ 0 \end{bmatrix} + \sum_{i=1}^{k} {}^{X_0}\bar{\Phi}^{X_i}.{}^{X_i^{\ominus}}\underline{r}^{X_{i|k}^{\oplus|{\rm a}}} \right) \tag{3.34}$$

These coordinate values are used in the expressions below for the wind speed variations by wind shear and stagnation:

$$\begin{aligned} {}^{\rm r}u^{X_k^{\rm a}} &= {}^{\rm shr}u_{\rm u}(\tilde{z}^{X_k^{\rm a}}) + {}^{\rm tow}u_{\rm u}(\tilde{x}^{X_k^{\rm a}}, \tilde{y}^{X_k^{\rm a}}, \tilde{z}^{X_k^{\rm a}}) \quad \text{with} \quad (x, y, z = \tilde{x}^{X_k^{\rm a}}, \tilde{y}^{X_k^{\rm a}}, \tilde{z}^{X_k^{\rm a}}): \\ {}^{\rm shr}u_{\rm u}(z) &= \left(\left(\frac{Z_{\rm hub} - (z - z_{\bar{R}_P^{\oplus}})}{Z_{\rm hub}} \right)^{\alpha} - 1 \right) \cdot \bar{U}_{\rm u} \, . \\ {}^{\rm tow}u_{\rm u}(x, y, z) &= \frac{\cos\theta^A (\bar{U}_{\rm u} + {}^{\rm shr}u_{\rm u}(z)) \cdot D_{\rm tow}^2(z)}{8(x^2 + y^2)} \cdot \left(\left(\frac{x^2 - y^2}{x^2 + y^2} \right) \cdot \left(1 + \frac{z}{d} \right) + \frac{x^2 \cdot z}{d^3} \right) \end{aligned} \tag{3.35}$$

The involved parameters are the hub height $Z_{\rm hub}$, the exponential shear parameter α, the 'tilt angle' θ^A of the longitudinal wind speed relative to the earth surface G and the diameter parameter $D_{\rm tow}(z)$ equals the tower top diameter for $z < 0$

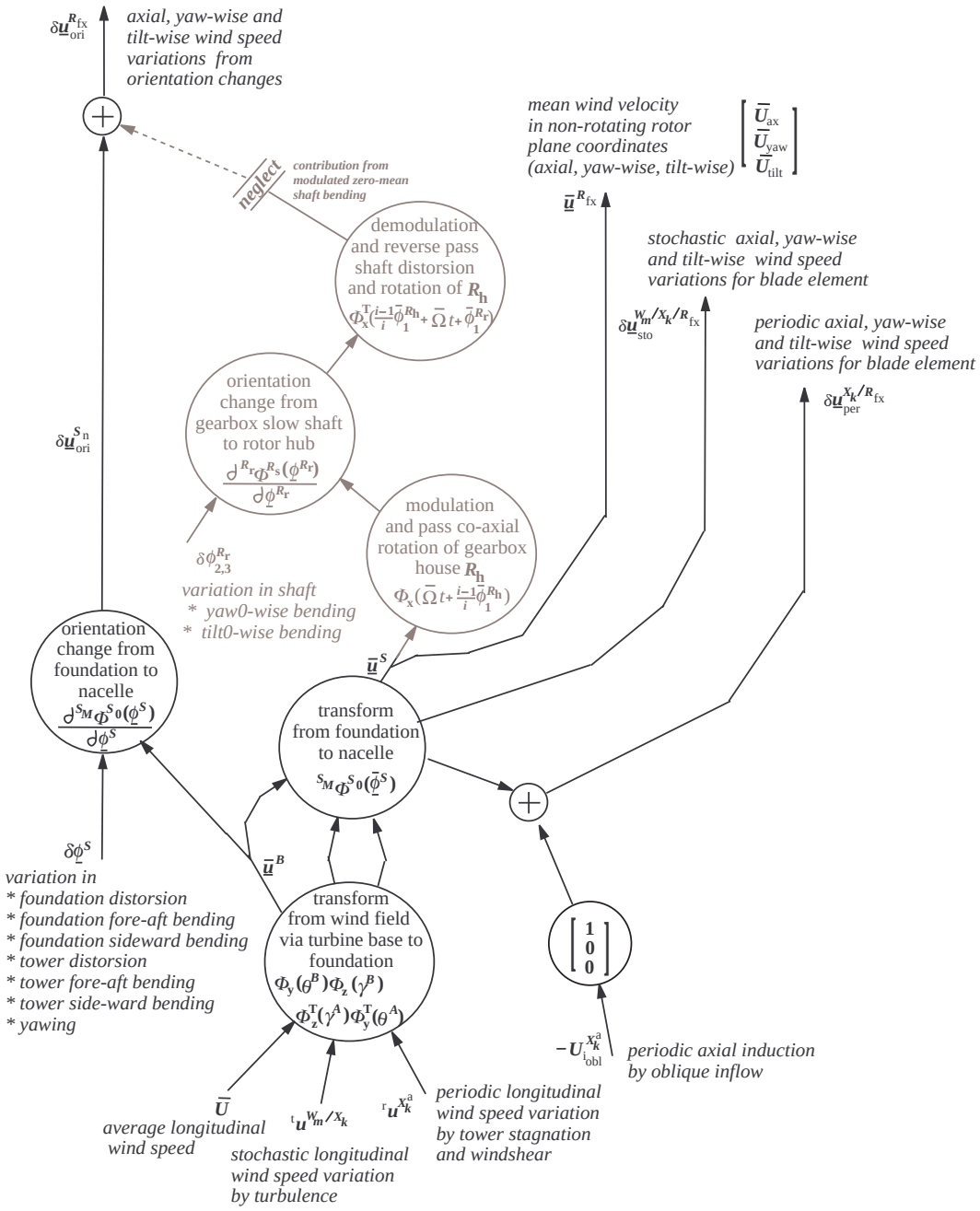

Figure 3.4 *Wind speed coordinates in rotor plane from mean longitudinal wind speed and from turbulence, tower stagnation & wind shear and inductive reaction on oblique-inflow*

('above tower top') and the actual tower diameter for $z > 0$ ('below tower top'). The distance parameter d is the vector sum of the instantaneous x, y and z-coordinate of X_k^{a}.

See Eq. 3.63 and 3.65 in section 3.7.1 for the transformation matrices ${}^{R_{\mathrm{h"}}}\tilde{\Phi}^{R_{\mathrm{s}}}$ and ${}^{R_{\mathrm{s}}}\bar{\Phi}^{X_0}$.

The *linearised* periodic axial induction speed variation $U_{\mathrm{i_o}}^{X_k}$ is a purely periodic and purely 'exogeneous' in the context of the linear model approach (see discussion near Eq. B.248 in section B.8.1). It is determined as follows:

$$U_{\mathrm{i_o}}^{W_m/X} = \bar{U}_{\mathrm{i}}^{W_m} \cdot \begin{cases} \frac{15\pi}{64} \cdot \frac{\bar{r}^{W_m}}{R} \cdot \tan(\bar{\chi}^{W_m}/2) \cdot \cos(\tilde{\Psi}^X + \bar{\Psi}_{\mathrm{off}}^{W_m}) & \text{(a)} \\ a_1 \cos(\tilde{\Psi}^X + \bar{\Psi}_{\mathrm{off}}^{W_k} - \Delta_1 \Psi) + & \\ \qquad a_2 \cos(2(\tilde{\Psi}^X + \bar{\Psi}_{\mathrm{off}}^{W_m}) - \Delta_2 \Psi) & \text{(b)} \end{cases}$$

with:

$$\begin{aligned} \bar{\chi}^{W_m} &= \arctan \frac{\sqrt{(\bar{U}_{\mathrm{yaw}})^2 + (\bar{U}_{\mathrm{tilt}})^2}}{\bar{U}_{\mathrm{ax}} - \bar{U}_{\mathrm{i}}^{W_m}} \\ \tilde{\psi}^X &= \bar{\Omega} \cdot t + \frac{(b-1)}{B} \cdot 2\pi + \bar{\phi}_3^{R_{\mathrm{h"}}} + \bar{\phi}_1^{R_{\mathrm{r}}} \\ \bar{\psi}_{\mathrm{off}}^{W_m} &= -\arctan \frac{\bar{U}_{\mathrm{tilt}}}{\bar{U}_{\mathrm{yaw}}} \end{aligned} \tag{3.36}$$

The parameters in the right hand side are the same as applied in PHATAS in function 'f_{skew}' [10]. Option (a) implies the parametrisation by Glauert while (b) implies a '2-harmonics engineering model' based on measured oblique inflow effects by Schepers and Vermeer [12].

See section B.8.1 for a detailed treatment of the mean and variation of the axial, transverse and vertical wind speed components.

3.6 Rotor blade modelling approach

The layout of the support structure model X is defined in section 3.6.1 by grouping the elements in subcomponents and via the orientation of rotations and translations between the elements. Two subcomponents are distinghuised: the blade flange X_{f} and the blade structure X_{p}. For the implemented 'motion formulations' of the kinematic and impulse variables see section B.3.1 and section B.3.2. The responsive loads on the flange elements differ from the slender beam theory equivalent spring and damper loads by Eq. 3.9 in section 3.3. These are subject of section 3.6.2. The aerodynamic loads on the tower are driven by the exogeneous 'wind' and 'gravity' input variables. The implemented 'load formulations' are in section B.7 and section B.10. The aerodynamic loads are also dealt with in section 3.6.3; the gravitation loads are not because they do not need any other user input than the gravitation constant g.

The implemented model equations are listed in section A.2.2 and A.2.3 for the blade profile and flange respectively.

3.6.1 Rotor blade layout

The blade X is modelled to be mounted to the hub at the location $X_1^{\ominus}$. At the hub side of $X_1^{\ominus}$ the blade base coordinate system $\vec{e}^{\,X_0}$ applies (see section B.2 and fig. 3.1). Figure 3.5 shows the blade layout while it also includes the main line of the derivation of the governing equations of motion.

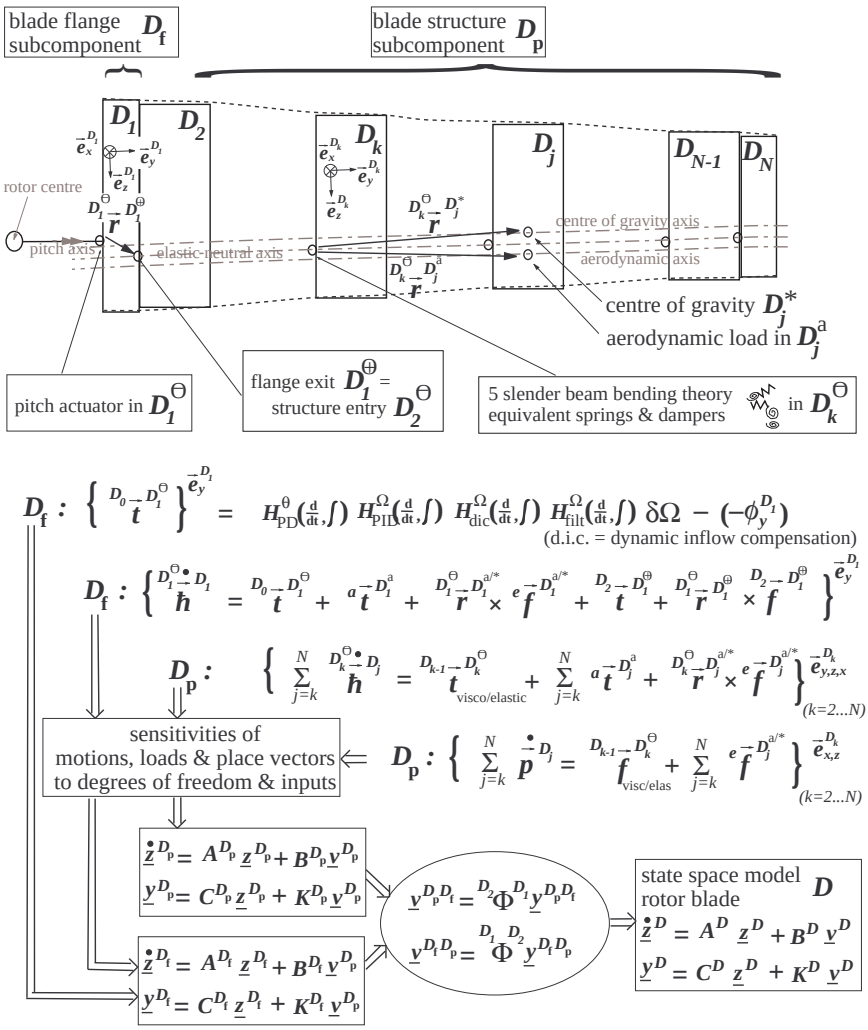

Figure 3.5 *Layout of the multi-body blade model with pitch control*

At the 'flange side' of $X_1^{\ominus}$, the coordinate system $\vec{e}^{\,X_1}$ is fixed to the rigid bar of the flange element X_1, with orientation defined by the pitch angle, and cone- and $\delta-3$-angle (either fixed or free). Coordinate system $\vec{e}^{\,X_1}$ originates from $\vec{e}^{\,X_0}$ by successive rotation along:

1. $\vec{e}_z^{\,X_0}$ (flap-hinge deviation angle $\phi_1^{X_1}$) - (cone angle ϕ_{cn}^{X})
2. $\vec{e}_y^{\,X_1^1}$ over (pitch deviation angle $\phi_2^{X_1}$) - (mean pitch angle ϕ_{pt}^{X} + neutral elastic z-axis angle $\phi_{\mathrm{ez}}^{X_1}$)
3. $\vec{e}_x^{\,X_1^2}$ over (lead-hinge deviation angle $\phi_3^{X_1}$) + (δ_3 angle $\phi_{\delta 3}^{X}$)

The (dummy) accompanying translations $\rho_{1,2,3}^{X_1}$ are along the x-, y- and z-axis.

The cone angle $\phi_{\rm cn}^{X}$ is the fixed angle along blade neutral z-axis in blade root via flapwise oriented offset of the blade's spanwise direction; >0 at backward orientation

The δ_3 angle is the fixed angle along the x-axis in the blade flange after flapwise rotation and pitching via leadwise oriented offset of the blade's spanwise direction; >0 at clockwise orientation in fore-to-aft view.

The average pitch angle $\phi_{\rm pt}^{X}$ is average angle along y-axis in blade root after flapwise rotation. It is the pitch angle that applies in the working point; >0 at counter clockwise orientaiton in root-to-tip view)

The 'neutral elastic z-axis angle' $\phi_{\rm ez}$ is the twist angle in structural sense. It is defined as the rotation from $\vec{e}_z^{\,X_0}$ to the neutral elastic z-axis of the blade element at zero pitch angle and no blade deformation and prebend, where $\phi_{\rm ez} > 0$ at counter clockwise orientation in root-to-tip view (nose-up); $\phi_{\rm ez} > 0$ is defined 0 for the blade flange element X_1.

The deviation angles $\{\vec{\phi}_i^{\,X_1}\}$ are rotation dofs that enable (bottum up ordered) devices for flap, pitch and lead motions in the blade flange.

The final coordinate systems of the blade structure elements $X_2 \ldots X_N$ are fixed to the rigid bars of these elements at the 'upward side' of the connector points $X_2^{\ominus} \ldots X_N^{\ominus}$. The orientation of the final coordinate system $\vec{e}^{\,X_k}$ is such that it approximates as good as possible the neutral elastic axes of the blade elements. It originates from foregoing final system $\vec{e}^{\,X_{k-1}}$ by blade deformation and blade structural rotations along:

1. $\vec{e}_y^{\,X_1}$ over (torsion deformation angle $\phi_1^{X_k}$ - neutral elastic z-axis angle increment $(\phi_{\rm ez}^{X_k} - \phi_{\rm ez}^{X_{k-1}})$)
2. $\vec{e}_z^{\,X_1^k}$ over +(flatwise deformation angle $\phi_2^{X_k}$ - prebend flatwise angle $\phi_{\rm pf}^{X_k}$)
3. $\vec{e}_x^{\,X_2^k}$ over +(edgewise deformation angle $\phi_3^{X_k}$ + prebend edgewise angle $\phi_{\rm pe}^{X_k}$)

The accompanying translations $\rho_{1,2,3}^{X_k}$ are along the y-, x- and z-axis.

The structural flatwise blade angle $\vec{\phi}_{\rm pf}^{\,X_1}$ is a fixed angle along the blade neutral z-axis via flatwise oriented offset of the blade's spanwise direction; >0 at backward orientation; the structural edgwise blade angle angle $\vec{\phi}_{\rm pe}^{\,X_1}$ is a fixed angle along blade neutral x-axis via edgewise orented offsset of the blade's spanwise direciton; >0 at clockwise orientation in fore-to-aft view.

The transformation matrix ${}^{X_k}\Phi^{X_{k-1}}$ is obtained by:

$$ {}^{X_k}\Phi^{X_{k-1}} = \begin{cases} \Phi_{\rm x}(\phi_3^{X_1} + \phi_{\delta 3}^{X}) \cdot \Phi_{\rm y}(\phi_2^{X_2} - \phi_{\rm pt}^{X}) \cdot \Phi_{\rm z}(\phi_1^{X_1} - \phi_{\rm cn}^{X}) & \text{(k=1)} \\ \Phi_{\rm x}(\phi_3^{X_k} + \phi_{\rm pe}^{X_k}) \cdot \Phi_{\rm z}(\phi_2^{X_k} - \phi_{\rm pf}^{X_k}) \cdot \Phi_{\rm y}(\phi_1^{X_k} - (\phi_{\rm ez}^{X_k} - \phi_{\rm ez}^{X_{k-1}})) & \text{(k>1)} \end{cases} \tag{3.37} $$

The deformation blade angles $\vec{\phi}_{1,2,3}^{\,X_{2\ldots N}}$ are rotation dofs that set up, with deformation translations $\vec{\rho}_{2,3}^{\,X_{2\ldots N}}$, the SBBT-equivalent blade deformation.

The rotation and translation dofs are collected in column vectors $\underline{\varphi}^X$ and $\underline{\varrho}^X$.

These vectors are composed of 3-element subvectors.

$$\underline{\varphi}^{X} = \begin{pmatrix} \varphi_1^{X_1} \\ \varphi_2^{X_1} \\ \varphi_3^{X_1} \\ \vdots \\ \varphi_1^{X_N} \\ \varphi_2^{X_N} \\ \varphi_3^{X_N} \end{pmatrix} \qquad \underline{\varrho}^{X} = \begin{pmatrix} \varrho_1^{X_1} \\ \varrho_2^{X_1} \\ \varrho_3^{X_1} \\ \vdots \\ \varrho_1^{X_N} \\ \varrho_2^{X_N} \\ \varrho_3^{X_N} \end{pmatrix} \tag{3.38}$$

These 'full dof vectors' are used in the motion and load formulations and eventually yield 'full size system matrices' for the equations of motion. After these full size matrices have been established, those rows and columns will be removed which pertain to rotation and translation 'directions' that do *not* accomodate dofs.

3.6.2 Responsive loads in flange

In case of active pitch control, the responsive torque load ${}^{\mathrm{RS}}t_2^{X_1^2}$ results from the inner loop of the pitch control, which is 'driven' by the pitch angle setpoint, which in turn results from the outer loop driven by the rotor speed 'measurement'. Actually, ${}^{\mathrm{RS}}t_2^{X_1^2}$ then amounts to minus the 'nose-up pitch angle adjustment torque' $t_{\mathrm{pt}}^{X_1}$.

The implemented pitch control system in TURBU Offshore regulates the rotational speed with the same pitch actuation torque t_{pt}^{X} on each rotor blade (collective pitch control). The pitch controller consists of an outer loop that generates a pitch angle variation setpoint $\varphi_{\mathrm{pt_r}}^{X}$ and an inner loop for realisation of this setpoint via the actuation torque t_{pt}^{X}. The outer loop is based on PID feedback of the rotational speed in conjunction with a lead-lag filter for dynamic inflow compensation and a low pass filter that prevents the feedthrough of rotational sampling effects, tower shadow, wind shear and tower vibration in $\varphi_{\mathrm{pt_r}}^{X}$. The x-coordinate of the angular velocity vector $\underline{\omega}^{X_{\mathrm{FF}(0)}}$ that is imported from the drive-train is used as the rotational speed. The 'equation of motion' for the outer loop is formulated in the time derivative operator $\frac{\mathrm{d}}{\mathrm{d}t}$ as follows

$$\varphi_{\mathrm{pt_r}}^{X} = K_\Omega \cdot \Big(\frac{\tau_{\mathrm{I}_\Omega}\cdot\frac{\mathrm{d}}{\mathrm{d}t}+1}{\tau_{\mathrm{I}_\Omega}\cdot\frac{\mathrm{d}}{\mathrm{d}t}} \Big) \cdot \Big(\frac{\tau_{\mathrm{D}_\Omega}\cdot\frac{\mathrm{d}}{\mathrm{d}t}+1}{\gamma_\Omega\cdot\tau_{\mathrm{D}_\Omega}\cdot\frac{\mathrm{d}}{\mathrm{d}t}+1} \Big) \cdot \Big(\frac{\tau_{\mathrm{D}_{\mathrm{dic}}}\cdot\frac{\mathrm{d}}{\mathrm{d}t}+1}{\tau_{\mathrm{I}_{\mathrm{dic}}}\cdot\frac{\mathrm{d}}{\mathrm{d}t}+1} \Big) \cdot \Big(\frac{b_n\cdot\frac{\mathrm{d}^n}{\mathrm{d}t^n}+\ldots+b_1\cdot\frac{\mathrm{d}}{\mathrm{d}t}+1}{a_n\cdot\frac{\mathrm{d}^n}{\mathrm{d}t^n}+\ldots+a_1\cdot\frac{\mathrm{d}}{\mathrm{d}t}+1} \Big) \cdot \omega_1^{X_{\mathrm{FF}(0)}} \tag{3.39}$$

The proportional (P) gain K_Ω and integral and differential (ID) time constants τ_{D_Ω}, τ_{I_Ω} as well as the time constants $\tau_{\mathrm{I}_{\mathrm{dic}}}$ and $\tau_{\mathrm{D}_{\mathrm{dic}}}$ of the lead-lag filter for dynamic inflow compensation depend on the working point conditions. The filter parameters $b_n \ldots b_1,\ a_n \ldots a_1$ mainly depend on the average rotational speed and the first natural frequency of the tower. All these parameters are to be derived with a control design tool. The multiplier γ_Ω amounts to ca. 0.1 and the involved denumerator factor does not influence the control behaviour. This factor mainly exists in order to be sure that the order of differentiation in the numerator $(n+3)$ does not exceed the one in the denumerator.

The inner loop is based on PD feedback of the pitch angle to the actuation torque. The angular dof variation along the y-axis that is imported from the flange element X_1, that is to say $\delta\phi_2^{X_1}$, represents *minus* the pitch angle variation. The 'equation of motion' is:

$$t_{\rm pt}^X \;=\; K_{\rm pt}\cdot\Big(\frac{\tau_{\rm D_{pt}}\cdot\frac{\rm d}{{\rm d}t}+1}{\gamma_{\rm pt}\cdot\tau_{\rm D_{pt}}\cdot\frac{\rm d}{{\rm d}t}+1}\Big)\cdot(\varphi_{\rm pt_r}^X-(-\delta\phi_2^{X_1})) \tag{3.40}$$

The proportional controller gain $K_{\rm pt}$ and differential time constant $\tau_{\rm D_{pt}}$ are chosen such that the pursued bandwidth for pitching $\omega_{0_{\rm pt}}$ [rad/s] is achieved under a sound damping rate $\beta_{0_{\rm pt}}$. The multiplier $\gamma_{\rm pt}$ amounts to ca. 0.1 and the involved denumerator factor does not influence the control behaviour; it just makes equal the the order of differentiation in the numerator and denumerator.

The parameters $K_{\rm pt}$ and $\tau_{\rm D_{pt}}$ are derived from the moment of inertia $J_{\rm pt}^X$ relative to the spanwise axis of the rotor blade for the desired bandwidth and damping rate:

$$\begin{aligned} K_{\rm pt} &= J_{\rm pt}^X\cdot\omega_{0_{\rm pt}}^2 \\ \tau_{\rm D_{pt}} &= 2\beta_{0_{\rm pt}}/\omega_{0_{\rm pt}} \end{aligned} \tag{3.41}$$

These expressions follow from a simplified but functional 2nd order approximation of the servo loop behaviour for pitch angle adjustment ($\varphi_{\rm pt}^X=-\phi_2^{X_1}$),

$$J_{\rm pt}^X\cdot s^2\varphi_{\rm pt}^X = K_{\rm pt}\big(\tau_{\rm D_{pt}}\cdot s+1\big)\cdot(\phi_{\rm pt_r}^{X_1}-\phi_{\rm pt}^X) \tag{3.42}$$

with the following characteristic equation:

$$J_{\rm pt}^X\cdot s^2 + K_{\rm pt}\cdot\tau_{\rm D_{pt}}\cdot s + K_{\rm pt} = 0 \tag{3.43}$$

3.6.3 Aerodynamic loads

The aerodynamic loads are modelled as concentrated loads in the 'aerodynamic conversion points' of the blade elements. These conversion points are in the (spanwise) middle of element X_2 up to X_{N-1}, at the rootside of X_1 and at the tipside of X_N. These locations result from the applied mapping mechanism for the by nature distributed aerodynamic loads on the elements and the layout of the multi-body model. The latter is characterised by:

- N elements with springs in the connection points of elements 2. . .N to foregoing elements;
- element 1 and N are half-size, while elements 2 . . . N-1 are full-size.

We choosed 'slender beam bending theory equivalency' as point of departure for the mapping of the distributed aero- loading to the concentrated forces and torques. The elastic behaviour is described by $N-1$ equal size elements with springs in the spanwise middle. The mapping mechanism implies the following:

- The distributed loading (force or torque per meter) of the $(N-1)$-element multi-body model is transformed into concentrated loads on the top and the bottom of each of the $N-1$ elements. The loads are such that the top loading of the foregoing element is correct and that the relative top deformation of the actual element relative to the top deformation of the foregoing element agrees with the results from the slender beam bending theory for uniform distributed loading.

The general expressions for the aerodynamic loads are given in the first paragraph, the mapping from the distributed to the concentrated loads in the second and the reaction loads on the rotor annuli are subject of the third paragraph. Expression for the involved blade relative wind speed and angle of attack are given in sections (iv) and (v) of this subsection.

For the implemented load formulations see section B.7.1, section B.7.2 and section B.7.3; the formulations for the blade relative wind speed and the angle of attack are in section B.5 and section B.6.

The reaction force loads on the rotor annuli are closely related to the blade force loads. The implemented formulations of these loads are given in section B.7.4.

(i) General expressions distributed aerodynamic loads

The spanwise aerodynamic load distribution results from the blade relative wind velocity by $\underline{u}^{X_k^{\mathrm{cv}}}$ and the blade setting angle $\phi_{\mathrm{set}}^{X_k}$ via the lift, drag and moment coefficient (C_{L}, C_{D}, C_{M}). The aerodynamic coefficient polars pertain to the angle of attack on the 1/4 chord position of the profile. In accordance with [10] a correction is made on this angle in case of flapwise blade deformation and/or coning; see Eq. 3.59. This modified angle of attack is typed as $\phi_{\mathrm{a}"}$.

The lift and drag effect can be expressed in forces per unit span length in the normal and leadwise direction of blade element, identified by x- and z-axis of the 'conversion' coordinate system $\vec{e}^{\,X_k^{\mathrm{cv}}}$. Fig. 3.6 shows the orientation of the coordinate systems with respect to blade element D_μ.

We define the coordinate vector ${}^{\mathrm{a}}\underline{q}_{\mathrm{f}}^{X_k^{\mathrm{cv}}}$ to contain these load components for blade element X_k in the first and third location. With the 'aerodynamic coefficient matrix' $\boldsymbol{C}_{\mathrm{LD}}$, the expression for ${}^{\mathrm{a}}\underline{q}_{\mathrm{f}}^{X_k^{\mathrm{cv}}}$ becomes:

$$
\begin{aligned}
{}^{\mathrm{a}}\underline{q}_{\mathrm{f}}^{X_k^{\mathrm{cv}}} \;\triangleq\; \begin{bmatrix} q_{\mathrm{n}}^{X_k} \\ 0 \\ q_{\ell}^{X_k} \end{bmatrix} \;&=\; \tfrac{1}{2}\rho c^{X_k} \cdot ||\underline{u}^{X_k}|| \cdot \boldsymbol{C}_{\mathrm{LD}}^{X_k}(\phi_{\mathrm{a}"}^{X_k}) \cdot \underline{u}^{X_k} \\
\text{with:}\quad \boldsymbol{C}_{\mathrm{LD}}^{X_k}(\phi_{\mathrm{a}"}^{X_k}) \;&=\; \begin{pmatrix} C_{\mathrm{D}}(\phi_{\mathrm{a}"} & 0 & -C_{\mathrm{L}}(\phi_{\mathrm{a}"}) \\ 0 & 0 & 0 \\ C_{\mathrm{L}}(\phi_{\mathrm{a}"}) & 0 & C_{\mathrm{D}}(\phi_{\mathrm{a}"}) \end{pmatrix}^{Xk}
\end{aligned}
\tag{3.44}
$$

with chord length c^{X_k} and the mass density of air ρ.

Next to this *force* loading, a blade section usually is subjected to aerodynamic *torque* loading per unit span via the aerodynamic moment coefficient C_{M}. This torque loading points along $\vec{e}_y^{\,X_k^{\mathrm{cv}}}$ in 'reverse sense', that is to say if $C_{\mathrm{M}} > 0$ an increase in wind speed intends to pitch the blade 'nose-up'[2]. We define the coordinate vector ${}^{\mathrm{a}}\underline{q}_{\mathrm{t}}^{X_k^{\mathrm{cv}}}$ to contain *minus* this load component for blade element X_k in the second location. With the 'aerodynamic coefficent vector' $\underline{\boldsymbol{C}}_{\mathrm{M}}$, the

[2] counter clockwise blade rotation along the spanwise-coordinate when looking from root to tip

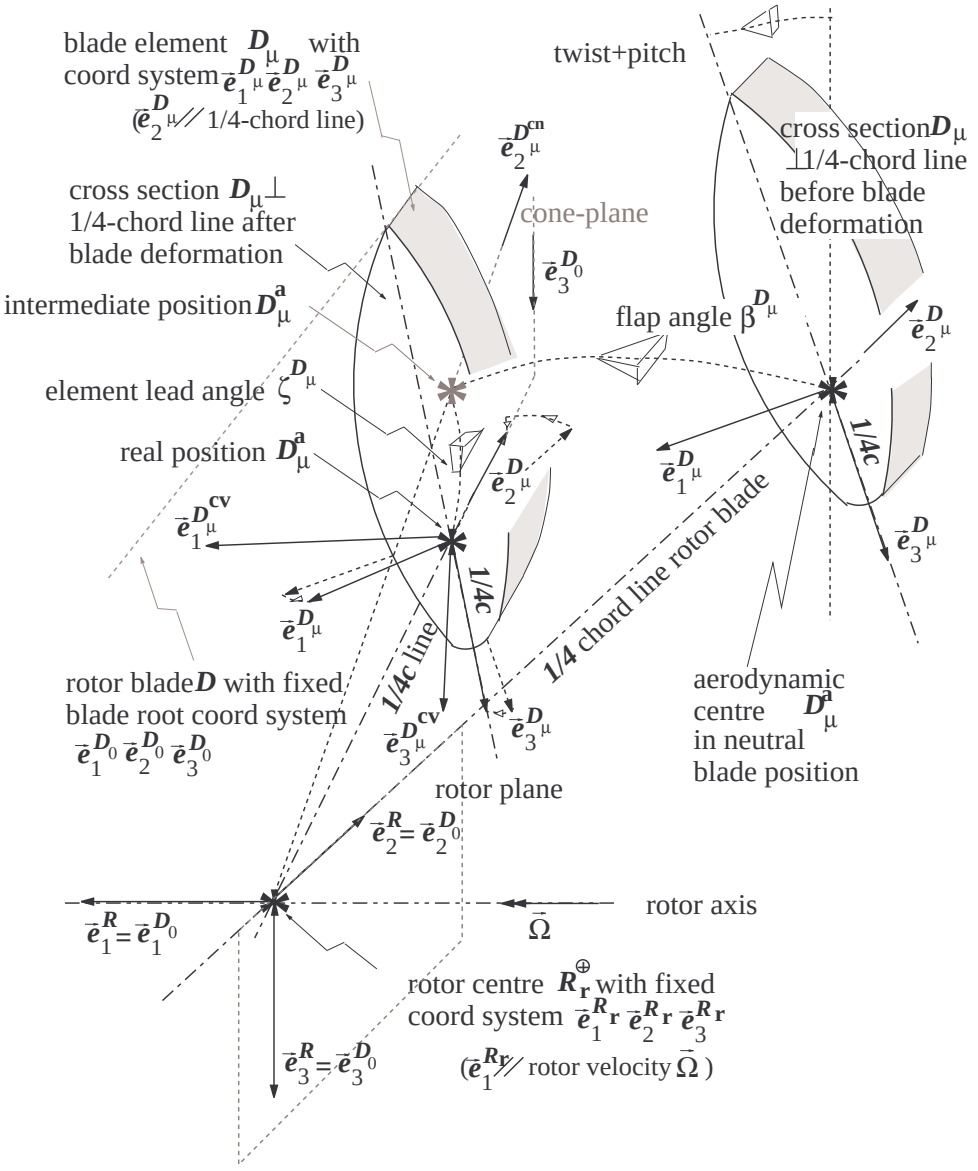

Figure 3.6 *Coordinate systems on 'neutral blade' and blade with prebending and deformation ($\vec{e}_{1,2,3}^{D_\mu} = \vec{e}_{x,y,z}^{D_\mu}$)*

expression for ${}^{\mathrm{a}}\underline{q}_{\mathrm{t}}^{X_k^{\mathrm{cv}}}$ becomes:

$$
{}^{\mathrm{a}}\underline{q}_{\mathrm{t}}^{X_k^{\mathrm{cv}}} \triangleq \begin{bmatrix} 0 \\ -q_{\mathrm{p}}^{X_k} \\ 0 \end{bmatrix} = \tfrac{1}{2}\rho (c^{X_k})^2 \cdot ||\underline{u}^{X_k}||^2 \cdot \underline{\boldsymbol{C}}_{\mathrm{M}}^{X_k}(\phi_{\mathrm{a}"}^{X_k})
$$

$$
\text{with:} \quad \underline{\boldsymbol{C}}_{\mathrm{M}}^{X_k}(\phi_{\mathrm{a}"}^{X_k}) = \begin{bmatrix} 0 \\ -C_{\mathrm{M}}(\phi_{\mathrm{a}"}) \\ 0 \end{bmatrix}^{Xk} \tag{3.45}
$$

The variation of ${}^{\mathrm{a}}\underline{q}_{\mathrm{f}}^{X_k^{\mathrm{cv}}}$ and ${}^{\mathrm{a}}\underline{q}_{\mathrm{t}}^{X_k^{\mathrm{cv}}}$ depends on the actual values of the components

and magnitude of the blade-relative wind velocity vector and on the (modified) angle of attack:

$$\begin{aligned}
\delta^{\mathrm{a}}\underline{q}_{\mathrm{f}}^{X_k^{\mathrm{cv}}} &= \tfrac{1}{2}\rho c^{X_k}\cdot\Big(\bar{\boldsymbol{C}}_{\mathrm{LD}}^{X_k}(\bar{\phi}_{\mathrm{a}"}^{X_k})\cdot\underline{\bar{u}}^{X_k}\cdot\delta||\underline{u}^{X_k}|| + \\
&\qquad ||\underline{\bar{u}}^{X_k}||\cdot\left.\frac{\mathrm{d}\boldsymbol{C}_{\mathrm{LD}}^{X_k}}{\mathrm{d}\phi_{\mathrm{a}"}^{X_k}}\right|_{\bar{\phi}_{\mathrm{a}"}^{X_k}}\cdot\underline{\bar{u}}^{X_k}\cdot\delta\phi_{\mathrm{a}"}^{X_k} + ||\underline{\bar{u}}^{X_k}||\cdot\bar{\boldsymbol{C}}_{\mathrm{LD}}^{X_k}(\bar{\phi}_{\mathrm{a}"}^{X_k})\cdot\delta\underline{u}^{X_k}\Big) \\
\delta^{\mathrm{a}}\underline{q}_{\mathrm{t}}^{X_k^{\mathrm{cv}}} &= \tfrac{1}{2}\rho(c^{X_k})^2\cdot\Big(2||\underline{\bar{u}}^{X_k}||\cdot\underline{\boldsymbol{C}}_{\mathrm{M}}^{X_k}(\phi_{\mathrm{a}"}^{X_k})\cdot\delta||\underline{u}^{X_k}|| + \\
&\qquad ||\underline{u}^{X_k}||^2\cdot\left.\frac{\mathrm{d}\underline{\boldsymbol{C}}_{\mathrm{M}}^{X_k}}{\mathrm{d}\phi_{\mathrm{a}"}^{X_k}}\right|_{\bar{\phi}_{\mathrm{a}"}^{X_k}}\cdot\delta\phi_{\mathrm{a}"}^{X_k}\Big)
\end{aligned} \tag{3.46}$$

Equation B.163 links the variation in magnitude of the relative wind velocity to variations in its coordinates. Make explicit definitions for the (intermediate) sensitivity functions to the blade relative wind speed and to the angle of attack:

$$\begin{aligned}
\frac{\partial^{\mathrm{a}}\underline{q}_{\mathrm{f}}^{X_k^{\mathrm{cv}}}}{\partial\underline{u}^{X_k}} &= \tfrac{1}{2}\rho c^{X_k}\cdot\Big(\bar{\boldsymbol{C}}_{\mathrm{LD}}^{X_k}\cdot\frac{\underline{\bar{u}}^{X_k}\cdot\underline{\bar{u}}^{X_k\,\mathrm{T}}}{||\underline{\bar{u}}^{X_k}||} + ||\underline{\bar{u}}^{X_k}||\cdot\bar{\boldsymbol{C}}_{\mathrm{LD}}^{X_k}\Big) \\
\frac{\partial^{\mathrm{a}}\underline{q}_{\mathrm{f}}^{X_k^{\mathrm{cv}}}}{\partial\phi_{\mathrm{a}"}^{X_k}} &= \tfrac{1}{2}\rho c^{X_k}\cdot||\underline{\bar{u}}^{X_k}||\cdot\left.\frac{\mathrm{d}\boldsymbol{C}_{\mathrm{LD}}^{X_k}}{\mathrm{d}\phi_{\mathrm{a}"}^{X_k}}\right|_{\bar{\phi}_{\mathrm{a}"}^{X_k}}\cdot\underline{\bar{u}}^{X_k} \\
\frac{\partial^{\mathrm{a}}\underline{q}_{\mathrm{t}}^{X_k^{\mathrm{cv}}}}{\partial\underline{u}^{X_k}} &= \tfrac{1}{2}\rho(c^{X_k})^2\cdot\Big(2\underline{\bar{\boldsymbol{C}}}_{\mathrm{M}}^{X_k}\cdot\underline{\bar{u}}^{X_k\,\mathrm{T}}\Big) \\
\frac{\partial^{\mathrm{a}}\underline{q}_{\mathrm{t}}^{X_k^{\mathrm{cv}}}}{\partial\phi_{\mathrm{a}"}^{X_k}} &= \tfrac{1}{2}\rho({}_cX_k)^2\cdot||\underline{u}^{X_k}||^2\cdot\left.\frac{\mathrm{d}\underline{\boldsymbol{C}}_{\mathrm{M}}^{X_k}}{\mathrm{d}\phi_{\mathrm{a}"}^{X_k}}\right|_{\bar{\phi}_{\mathrm{a}"}^{X_k}}
\end{aligned} \tag{3.47}$$

(ii) Mapping distributed to concentrated aerodynamic loads

Let ${}^{\mathrm{a}}\underline{f}^{X_k^{\mathrm{a}}}$ and ${}^{\mathrm{a}}\underline{t}^{X_k^{\mathrm{a}}}$ be the coordinates of the concentrated aerodynamic force and torque in the aerodynamic conversion point X_k^{a} along the axes of $\vec{e}^{\,X_k}$. The conversion point on the blade flange element, X_1^{a}, lays on the 25% chord point in the bottom cross section of X_1. The conversion points X_2^{a}... X_{N-1}^{a} lay on the 25% chord point 'mid span' while the point X_N^{a} lays in the cross section of the blade tip. The concentrated load vectors in X_k^{a} depend as follows on the distributed aerodynamic force and torque loads with normal, leadwise and pitchwise orientation ($1 \le k+j \le N$):

$$\begin{aligned}
{}^{\mathrm{a}}\underline{f}^{X_k^{\mathrm{a}}} &= \sum_{j=-1}^{1}{}^{X_k}\Phi^{X_{k+j}^{\mathrm{cv}}}\cdot{}^{\mathrm{a}}G_{\mathrm{fq}_{k,j}}^{\mathrm{F}}\cdot{}^{\mathrm{a}}\underline{q}_{\mathrm{f}}^{X_{k+j}^{\mathrm{cv}}} \\
{}^{\mathrm{a}}\underline{t}^{X_k^{\mathrm{a}}} &= {}^{X_k}\Phi^{X_k^{\mathrm{cv}}}\cdot{}^{\mathrm{a}}G_{\mathrm{tq}_k}^{\mathrm{M}}\cdot{}^{\mathrm{a}}\underline{q}_{\mathrm{t}}^{X_k^{\mathrm{cv}}} + \sum_{j=-1}^{1}{}^{X_k}\Phi^{X_{k+j}^{\mathrm{cv}}}\cdot{}^{\mathrm{a}}G_{\mathrm{tq}_{k,j}}^{\mathrm{F}}\cdot{}^{\mathrm{a}}\underline{q}_{\mathrm{f}}^{X_{k+j}^{\mathrm{cv}}}
\end{aligned} \tag{3.48}$$

The matrices ${}^{\mathrm{a}}G^{\mathrm{F}}_{\mathrm{fq}_{k,j}}$ and ${}^{\mathrm{a}}G^{\mathrm{M}}_{\mathrm{tq}_k}$ are determined as follows (replace 'fq' by 'tq' for ${}^{\mathrm{a}}G^{\mathrm{F}}_{\mathrm{tq}_{k,j}}$)

$$
{}^{\mathrm{a}}G^{\mathrm{F}}_{\mathrm{fq}_{k,j}} = \begin{cases} G^{\mathrm{L_{sh}}}_{\mathrm{fq}} \ , \quad G^{\mathrm{R_{sh}}}_{\mathrm{fq}} & (k{=}1;\, j{=}0{,}1) \\ G^{\mathrm{L}}_{\mathrm{fq}} \ , \quad G^{\mathrm{R}}_{\mathrm{fq}} + G^{\mathrm{L_{sh}}}_{\mathrm{fq}} \ , \quad G^{\mathrm{R_{sh}}}_{\mathrm{fq}} & (k{=}2...N{-}1;\, j{=}{-}1{,}0{,}1) \\ G^{\mathrm{L}}_{\mathrm{fq}} \ , \quad G^{\mathrm{R}}_{\mathrm{fq}} & (k{=}N;\, j{=}{-}1{,}0) \end{cases}
$$

$$
{}^{\mathrm{a}}G^{\mathrm{M}}_{\mathrm{tq}_k} = \begin{cases} \frac{1}{2}\,{}^{\mathrm{a}}G^{\mathrm{P}}_{\mathrm{tq}} & (k{=}1) \\ {}^{\mathrm{a}}G^{\mathrm{P}}_{\mathrm{tq}} & (k{=}2...N{-}1) \\ \frac{1}{2}\,{}^{\mathrm{a}}G^{\mathrm{P}}_{\mathrm{tq}} & (k{=}N) \end{cases}
\tag{3.49}
$$

The applied matrices only depend on S, the span width of elements X_2 ... X_{N-1} and twice the span width of elements X_1 and X_N:

$$
G^{\mathrm{L}}_{\mathrm{fq}} = \begin{pmatrix} 36S/384 & 0 & 0 \\ 0 & 0 & 0 \\ 0 & 0 & 36S/384 \end{pmatrix} \quad G^{\mathrm{R}}_{\mathrm{fq}} = \begin{pmatrix} 156S/384 & 0 & 0 \\ 0 & 0 & 0 \\ 0 & 0 & 156S/384 \end{pmatrix}
$$

$$
G^{\mathrm{L_{sh}}}_{\mathrm{fq}} = \begin{pmatrix} 156S/384 & 0 & 0 \\ 0 & 0 & 0 \\ 0 & 0 & 156S/384 \end{pmatrix} \quad G^{\mathrm{R_{sh}}}_{\mathrm{fq}} = \begin{pmatrix} 36S/384 & 0 & 0 \\ 0 & 0 & 0 \\ 0 & 0 & 36S/384 \end{pmatrix}
\tag{3.50}
$$

and:

$$
G^{\mathrm{L}}_{\mathrm{tq}} = \begin{pmatrix} 0 & 0 & -10S^2/384 \\ 0 & 0 & 0 \\ 10S^2/384 & 0 & 0 \end{pmatrix} \quad G^{\mathrm{R}}_{\mathrm{tq}} = \begin{pmatrix} 0 & 0 & -22S^2/384 \\ 0 & 0 & 0 \\ 22S^2/384 & 0 & 0 \end{pmatrix}
$$

$$
G^{\mathrm{L_{sh}}}_{\mathrm{tq}} = \begin{pmatrix} 0 & 0 & 22S^2/384 \\ 0 & 0 & 0 \\ -22S^2/384 & 0 & 0 \end{pmatrix} \quad G^{\mathrm{R_{sh}}}_{\mathrm{tq}} = \begin{pmatrix} 0 & 0 & 10S^2/384 \\ 0 & 0 & 0 \\ -10S^2/384 & 0 & 0 \end{pmatrix}
$$

$$
G^{\mathrm{p}}_{\mathrm{tq}} = \begin{pmatrix} 0 & 0 & 0 \\ 0 & S & 0 \\ 0 & 0 & 0 \end{pmatrix}
\tag{3.51}
$$

These mappings are derived in Appendix C.

Equation 3.48 shows that the concentrated load on X_k depend on the distributed force loads on elements X_{k-1}, X_k and X_{k+1}. Of course, the dependency on $\underline{q}^{X^{\mathrm{cv}}_{k-1}}$ does not apply for $k = 1$ and on $\underline{q}^{X^{\mathrm{cv}}_{k+1}}$ not for $k = N$. The variation of the concentrated loads is to be expressed in 'internal variables' of the subcomponent and input variables from the neighbouring subcomponents and related to the wind field and wake. This requires equation 3.48 to be rewritten. If X_k is the first element of a subcomponent then $\underline{q}^{X^{\mathrm{cv}}_{k-1}}$ is imported from the foregoing subcomponent. If X_k is the last element then $\underline{q}^{X^{\mathrm{cv}}_{k+1}}$ is imported from the subsequent subcomponent. Since the rotation dofs $\phi_v^{X_{k+1}}$ are neither 'internal variables' nor imported via input $\underline{\phi}^{X_{\mathrm{FF}}}$ from the *foregoing* subcomponent, these are fed in from the subsequent subcomponent via vector $\underline{\phi}^{X_{\mathrm{PP}}}$. Therefor, two 'neighbouring' distributed load coordinate vectors and one 'neighbour' angular dof vector are

defined as additional input variables to the subcomponent:

$$\begin{aligned} {}^{\mathrm{a}}\underline{q}_{\mathrm{f}}^{X_{\mathrm{FF}}} &\triangleq {}^{\mathrm{a}}\underline{q}_{\mathrm{f}}^{X^{\mathrm{cv}}_{k_{\mathrm{FF}}}} \\ {}^{\mathrm{a}}\underline{q}_{\mathrm{f}}^{X_{\mathrm{PP}}} &\triangleq {}^{\mathrm{a}}\underline{q}_{\mathrm{f}}^{X^{\mathrm{cv}}_{k_{\mathrm{PP}}}} \\ \underline{\phi}^{X_{\mathrm{PP}}} &\triangleq \underline{\phi}^{X_{k_{\mathrm{PP}}}} \end{aligned} \tag{3.52}$$

In these definitions k_{FF} is the number of the final element in the foregoing subcomponent and k_{PP} of the first element in the subsequent subcomponent (mnemonics '$_{\mathrm{FF}}$' and '$_{\mathrm{PP}}$' for heuristic expressions 'Final Foregoing' and 'Primary Post'). In the pursued expressions for the concentrated loads we will also use the symbols $k^{\oplus}_{\mathrm{FF}}$ and $k^{\ominus}_{\mathrm{PP}}$, which refer to the first and last element in the subcomponent, and a kind of generalised Kronecker-delta symbols:

$$\delta_{i\uparrow j} \triangleq \begin{cases} 1 & \text{if } i \le j \\ 0 & \text{if } i > j \end{cases} \quad ; \quad \delta_{i\downarrow j} \triangleq \begin{cases} 1 & \text{if } i \ge j \\ 0 & \text{if } i < j \end{cases} \tag{3.53}$$

With the defined symbols and additional subcomponent inputs the equations for the variation of the concentrated loads can be written as follows:

$$\begin{aligned} \delta^{\mathrm{a}}\underline{f}^{X^{\mathrm{a}}_k} = {} & \left({}^{X_k}\bar{\Phi}^{X^{\mathrm{cv}}_k} \cdot {}^{\mathrm{a}}G^{\mathrm{F}}_{\mathrm{fq}_{k,0}} \cdot \delta^{\mathrm{a}}\underline{q}_{\mathrm{f}}^{X^{\mathrm{cv}}_k} + \delta^{X_k}\Phi^{X^{\mathrm{cv}}_k} \cdot {}^{\mathrm{a}}G^{\mathrm{F}}_{\mathrm{fq}_{k,0}} \cdot {}^{\mathrm{a}}\overline{\underline{q}}_{\mathrm{f}}^{X^{\mathrm{cv}}_k} \right) + \\ & \Big(\delta_{(k,k_{\mathrm{FF}}\oplus)} \cdot \delta_{k_{\mathrm{FF}}\downarrow 1} \cdot \left({}^{X_k}\bar{\Phi}^{X^{\mathrm{cv}}_{k-1}} \cdot {}^{\mathrm{a}}G^{\mathrm{F}}_{\mathrm{fq}_{k,-1}} \cdot \delta^{\mathrm{a}}\underline{q}_{\mathrm{f}}^{X_{\mathrm{FF}}} + \delta^{X_k}\Phi^{X^{\mathrm{cv}}_{k-1}} \cdot {}^{\mathrm{a}}G^{\mathrm{F}}_{\mathrm{fq}_{k,-1}} \cdot {}^{\mathrm{a}}\overline{\underline{q}}_{\mathrm{f}}^{X^{\mathrm{cv}}_{k-1}} \right) + \\ & \qquad \delta_{k\downarrow k^{\oplus}_{\mathrm{FF}}+1} \cdot \left({}^{X_k}\bar{\Phi}^{X^{\mathrm{cv}}_{k-1}} \cdot {}^{\mathrm{a}}G^{\mathrm{F}}_{\mathrm{fq}_{k,-1}} \cdot \delta^{\mathrm{a}}\underline{q}_{\mathrm{f}}^{X^{\mathrm{cv}}_{k-1}} + \delta^{X_k}\Phi^{X^{\mathrm{cv}}_{k-1}} {}^{\mathrm{a}}G^{\mathrm{F}}_{\mathrm{fq}_{k,-1}} \cdot {}^{\mathrm{a}}\overline{\underline{q}}_{\mathrm{f}}^{X^{\mathrm{cv}}_{k-1}} \right) \Big) + \\ & \Big(\delta_{(k,k^{\ominus}_{\mathrm{PP}})} \cdot \delta_{k_{\mathrm{PP}}\uparrow N} \cdot \left({}^{X_k}\bar{\Phi}^{X^{\mathrm{cv}}_{k+1}} \cdot {}^{\mathrm{a}}G^{\mathrm{F}}_{\mathrm{fq}_{k,+1}} \cdot \delta^{\mathrm{a}}\underline{q}_{\mathrm{f}}^{X^{\ominus}_{\mathrm{PP}}} + \delta^{X_k}\Phi^{X^{\mathrm{cv}}_{k+1}} \cdot {}^{\mathrm{a}}G^{\mathrm{F}}_{\mathrm{fq}_{k,+1}} \cdot {}^{\mathrm{a}}\overline{\underline{q}}_{\mathrm{f}}^{X^{\mathrm{cv}}_{k+1}} \right) + \\ & \qquad \delta_{k\uparrow k^{\ominus}_{\mathrm{PP}}-1} \cdot \left({}^{X_k}\bar{\Phi}^{X^{\mathrm{cv}}_{k+1}} \cdot {}^{\mathrm{a}}G^{\mathrm{F}}_{\mathrm{fq}_{k,+1}} \cdot \delta^{\mathrm{a}}\underline{q}_{\mathrm{f}}^{X^{\mathrm{cv}}_{k+1}} + \delta^{X_k}\Phi^{X^{\mathrm{cv}}_{k+1}} \cdot {}^{\mathrm{a}}G^{\mathrm{F}}_{\mathrm{fq}_{k,+1}} \cdot {}^{\mathrm{a}}\overline{\underline{q}}_{\mathrm{f}}^{X^{\mathrm{cv}}_{k+1}} \right) \Big) \end{aligned} \tag{3.54}$$

and:

$$\begin{aligned} \delta^{\mathrm{a}}\underline{t}^{X^{\mathrm{a}}_k} = {} & \left({}^{X_k}\bar{\Phi}^{X^{\mathrm{cv}}_k} \cdot {}^{\mathrm{a}}G^{\mathrm{M}}_{\mathrm{tq}_k} \cdot \delta^{\mathrm{a}}\underline{q}_{\mathrm{t}}^{X^{\mathrm{cv}}_k} + \delta^{X_k}\Phi^{X^{\mathrm{cv}}_k} \cdot {}^{\mathrm{a}}G^{\mathrm{M}}_{\mathrm{tq}_k} \cdot {}^{\mathrm{a}}\overline{\underline{q}}_{\mathrm{t}}^{X^{\mathrm{cv}}_k} \right) + \\ & \left({}^{X_k}\bar{\Phi}^{X^{\mathrm{cv}}_k} \cdot {}^{\mathrm{a}}G^{\mathrm{F}}_{\mathrm{tq}_{k,0}} \cdot \delta^{\mathrm{a}}\underline{q}_{\mathrm{f}}^{X^{\mathrm{cv}}_k} + \delta^{X_k}\Phi^{X^{\mathrm{cv}}_k} \cdot {}^{\mathrm{a}}G^{\mathrm{F}}_{\mathrm{tq}_{k,0}} \cdot {}^{\mathrm{a}}\overline{\underline{q}}_{\mathrm{f}}^{X^{\mathrm{cv}}_k} \right) + \\ & \Big(\delta_{(k,k_{\mathrm{FF}}\oplus)} \cdot \delta_{k_{\mathrm{FF}}\downarrow 1} \cdot \left({}^{X_k}\bar{\Phi}^{X^{\mathrm{cv}}_{k-1}} \cdot {}^{\mathrm{a}}G^{\mathrm{F}}_{\mathrm{tq}_{k,-1}} \cdot \delta^{\mathrm{a}}\underline{q}_{\mathrm{f}}^{X_{\mathrm{FF}}} + \delta^{X_k}\Phi^{X^{\mathrm{cv}}_{k-1}} \cdot {}^{\mathrm{a}}G^{\mathrm{F}}_{\mathrm{tq}_{k,-1}} \cdot {}^{\mathrm{a}}\overline{\underline{q}}_{\mathrm{f}}^{X^{\mathrm{cv}}_{k-1}} \right) + \\ & \qquad \delta_{k\downarrow k^{\oplus}_{\mathrm{FF}}+1} \cdot \left({}^{X_k}\bar{\Phi}^{X^{\mathrm{cv}}_{k-1}} \cdot {}^{\mathrm{a}}G^{\mathrm{F}}_{\mathrm{tq}_{k,-1}} \cdot \delta^{\mathrm{a}}\underline{q}_{\mathrm{f}}^{X^{\mathrm{cv}}_{k-1}} + \delta^{X_k}\Phi^{X^{\mathrm{cv}}_{k-1}} \cdot {}^{\mathrm{a}}G^{\mathrm{F}}_{\mathrm{tq}_{k,-1}} \cdot {}^{\mathrm{a}}\overline{\underline{q}}_{\mathrm{f}}^{X^{\mathrm{cv}}_{k-1}} \right) \Big) + \\ & \Big(\delta_{(k,k^{\ominus}_{\mathrm{PP}})} \cdot \delta_{k_{\mathrm{PP}}\uparrow N} \cdot \left({}^{X_k}\bar{\Phi}^{X^{\mathrm{cv}}_{k+1}} \cdot {}^{\mathrm{a}}G^{\mathrm{F}}_{\mathrm{tq}_{k,+1}} \cdot \delta^{\mathrm{a}}\underline{q}_{\mathrm{f}}^{X^{\ominus}_{\mathrm{PP}}} + \delta^{X_k}\Phi^{X^{\mathrm{cv}}_{k+1}} \cdot {}^{\mathrm{a}}G^{\mathrm{F}}_{\mathrm{tq}_{k,+1}} \cdot {}^{\mathrm{a}}\overline{\underline{q}}_{\mathrm{f}}^{X^{\mathrm{cv}}_{k+1}} \right) + \\ & \qquad + \delta_{k\uparrow k^{\ominus}_{\mathrm{PP}}-1} \cdot \left({}^{X_k}\bar{\Phi}^{X^{\mathrm{cv}}_{k+1}} \cdot {}^{\mathrm{a}}G^{\mathrm{F}}_{\mathrm{tq}_{k,+1}} \cdot \delta^{\mathrm{a}}\underline{q}_{\mathrm{f}}^{X^{\mathrm{cv}}_{k+1}} + \delta^{X_k}\Phi^{X^{\mathrm{cv}}_{k+1}} \cdot {}^{\mathrm{a}}G^{\mathrm{F}}_{\mathrm{tq}_{k,+1}} \cdot {}^{\mathrm{a}}\overline{\underline{q}}_{\mathrm{f}}^{X^{\mathrm{cv}}_{k+1}} \right) \Big) \end{aligned} \tag{3.55}$$

The use of the (generalised) kronecker-delta functions and the feed-in loads from the neighbouring elements to the subcomponent guarantees the use of:

- distributed load variations that are *available* within the subcomponent;
- rotation dof position variations that are either internal in the subcomponent or fed in from the foregoing of following subcomponent.

(iii) Aerodynamic reaction loads on annuli

The reaction loads on the rotor annuli equal the concentrated force loads on the blade elements. In accordance with [10] it is assumed that this only pertains to the part of the aerodynamic forces due to *lift*. The reaction load from element X_k is to be supplied to the wake subsystem W as a coordinate vector along the annulus wise coordinate system $\vec{e}^{\,W_m/X_k}$ in the intersection of blade element X_k and rotor annulus W_m. We denote this coordinate vector as ${}^{\mathrm{aL}}\underline{f}^{W_m/X_k}$. The following applies:

$$ {}^{\mathrm{aL}}\underline{f}^{W_m/X_k} \;\triangleq\; \left(-{}^{\mathrm{aL}}\overline{f}^{X_k}\right)^{W_m/X_k} \;=\; -{}^{W/X_k}\Phi^{X_k} \,.\, {}^{\mathrm{aL}}\underline{f}^{X_k^{\mathrm{a}}} \qquad (3.56) $$

For the 'lift-only' element force ${}^{\mathrm{aL}}\underline{f}^{X_k^{\mathrm{a}}}$ applies the same expression as for the overall element force ${}^{\mathrm{a}}\underline{f}^{X_k^{\mathrm{a}}}$ (Eq. B.217). However, the mean and sensitivities and input variations of the involved distributed loads $\underline{q}^{X_{k+j}^{\mathrm{cv}}}$ in equations B.218 through B.230 are to be obtained with zero drag. This is accomplished by setting the drag-coefficient itself as well as its sensitivity to the angle of attack equal to zero in equations 3.47 and B.197. An other consequence is that also the 'lift-only' distributed force loads are to be imported from the neightbouring subcomponent. These are denoted as ${}^{\mathrm{aL}}\underline{q}_{\mathrm{f}}^{X_{\mathrm{FF}}}$, ${}^{\mathrm{aL}}\underline{q}_{\mathrm{f}}^{X_{\mathrm{PP}}}$ and are obtained via equations B.204 through B.210 for lift only; the coordinates are along the annulus-wise coordinate systems $\vec{e}^{\,W_m/X_{k_{\mathrm{L}}(n)}}$ and $\vec{e}^{\,W_m/X_{k_{1}(n)-1}}$ for subcomonent n (see also def. B.202).

(iv) Blade relative wind speed $\underline{u}$

The relative wind speed vector $\underline{u}^{X_k}$ for element X_k comprises the wind velocity component U_{n} in normal direction and U_ℓ in lead direction in the aerodynamic conversion point X_k^{a}; its coordinates are along the 'conversion coordinate system' $\vec{e}^{\,X_k^{\mathrm{cv}}}$ of the blade element. The linearised vector representation includes a mean, periodic, stochastic and reactive part; the latter is subdivided into parts caused by structural motion and by orientation change:

$$ \underline{u}^{X_k} = \begin{bmatrix} U_{\mathrm{n}} \\ U_{\mathrm{r}} \\ -U_\ell \end{bmatrix}^{X_k^{\mathrm{a}}} = \bar{\underline{u}}^{X_k} + \delta\underline{u}_{\mathrm{sto}}^{X_k} + \delta\underline{u}_{\mathrm{per}}^{X_k} + \delta\underline{u}_{\mathrm{mot}}^{X_k} + \delta\underline{u}_{\mathrm{ori}}^{X_k} \qquad (3.57) $$

Figure 3.7 shows the interdependency of these wind speed subvectors and the 'driving variables and constants' (structural motion excluded), that is to say:

- mean longitudinal wind speed;
- longitudinal turbulence;
- periodic variations by wind shear and tower stagnation;
- periodic axial induction speed variations by oblique inflow;
- periodic variations by oblique inflow;
- orientation of the rotor blade relative to the longitudinal wind speed direction.

See section 3.4.2, Eq. 3.12 for the relationship of the stochastic wind speed subvector with the longitudinal turbulence.

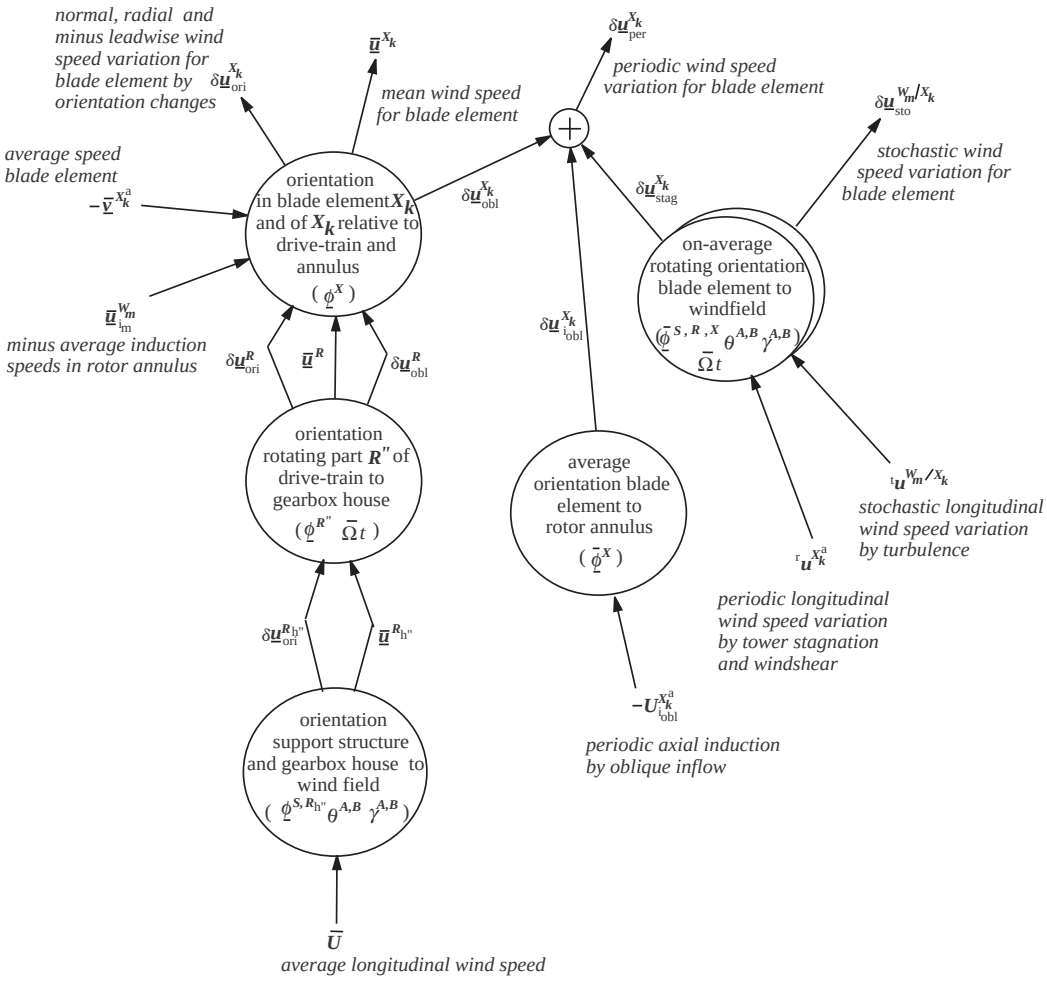

Figure 3.7 *Wind speed coordinates on blade element from mean longitudinal wind speed and from turbulence, tower stagnation & wind shear and inductive reaction on oblique-inflow*

For the periodic subvector holds:

$$\delta \underline{u}_{\mathrm{per}}^{X_k} \;=\; \delta \underline{u}_{\mathrm{obl}}^{X_k} + \delta \underline{u}_{\mathrm{stag}}^{X_k} + \delta \underline{u}_{\mathrm{i_{obl}}}^{X_k}$$

with:

$$\begin{aligned}
\delta \underline{u}_{\mathrm{obl}}^{X_k} &= {}^{X_k^{\mathrm{cv}}}\bar{\Phi}^{X_0} \cdot \Phi_{\mathrm{x}}\left({}^{R}\psi^{X_0}\right) \cdot \Phi_{\mathrm{x}}\left(\bar{\phi}_1^{R_{\mathrm{r}}}\right) \cdot \left(\Phi_{\mathrm{c}} \cdot \bar{\underline{u}}^{R_{\mathrm{h''}}} \cdot \cos\bar{\Omega}t + \Phi_{\mathrm{s}} \cdot \bar{\underline{u}}^{R_{\mathrm{h''}}} \cdot \sin\bar{\Omega}t\right) \\
\delta \underline{u}_{\mathrm{stag}}^{X_k} &= {}^{X_k^{\mathrm{cv}}}\bar{\Phi}^{X_0} \cdot \Phi_{\mathrm{x}}\left({}^{R}\psi^{X_0} + \bar{\phi}_1^{R_{\mathrm{r}}}\right) \cdot \left(\Phi_{\mathrm{d}} + \Phi_{\mathrm{c}}\cos\bar{\Omega}t + \Phi_{\mathrm{s}}\sin\bar{\Omega}t\right) \cdot {}^{R_{\mathrm{h''}}}\bar{\underline{\Phi}}_1^{A} \cdot {}^{\mathrm{r}}u^{X_k^{\mathrm{a}}} \\
\delta \underline{u}_{\mathrm{i_{obl}}}^{X_k} &= -{}^{X_k^{\mathrm{cv}}}\bar{\Phi}^{X_0} \cdot U_{\mathrm{i_{obl}}}^{X_k} \cdot \underline{e}_1
\end{aligned} \tag{3.58}$$

The periodic contribution $\delta \underline{u}_{\mathrm{obl}}^{X_k}$ from undisturbed oblique inflow is caused by 'modulation' of the mean yaw- and tiltwise wind speed components in the rotor.

See paragraph (ii) in section 3.5.2 for the contributions by tower stagnation and wind shear via ${}^{\mathrm{r}}u^{X_k^{\mathrm{a}}}$ and by axial induction speed varations via $U_{\mathrm{i_{obl}}}^{X_k}$.

See section B.5 for a detailed treatment of the mean and variation of the blade relative wind speed components. section B.5.3 lists the expressions of the mean value, reactive variation and stochastic and periodic variations for the blade relative wind speed. The mean value $\underline{\bar{u}}^{X_k}$ is given in Eq. B.179.

(v) Angle of attack $\phi_{\mathrm{a}_{3/4c}}$

In case of an (average) flap angle, it is assumed in accordance with [10] (pg 20) that the angle of attack on $_{3/4}$-chord governs the conversion through regularly obtained aerodynamic coefficient polars . Then the flap angle contributes to the effective angle of attack, which is then determined as:

$$\phi_{\mathrm{a}_{3/4\mathrm{c}}}^{X_k} = \phi_{\mathrm{inf}}^{X_k} - \phi_{\mathrm{set}}^{X_k} + \frac{1/2\, c^{X_k}}{r^{W_m/X_k}} \cdot \sin \beta^{X_k} \tag{3.59}$$

The angle $\phi_{\mathrm{a}_{3/4\mathrm{c}}}$, earlier referred to as $\phi_{\mathrm{a}^{\prime\prime}}$, mainly depends on the pitch angle and the twist angle *in aerodynamic sense*, which may differ from the twist angle *in structural sense*, usually referred to the structural pitch angle. The setting angle is also affected by (large) structural prebending and or deformation. Radius r^{W_m/X_k} is the radius of the rotor annulus that intersects with blade element X_k.

The twist angle in aerodynamic sense is defined as *the* twist angle ϕ_{tw}; it is defined as the rotation from the blade-neutral z-axis ($\vec{e}_z^{\,X_0}$) to the chord line of the blade element at zero pitch angle and no blade deformation of prebend, where $\phi_{\mathrm{tw}} > 0$ at counter clockwise orientation in root-to-tip view (nose-up).

The twist angle in structural sense is defined as the 'neutral elastic z-axis angle' ϕ_{ez}; it is defined as the rotation from $\vec{e}_z^{\,X_0}$ to the neutral elastic z-axis of the blade element at zero pitch angle and no blade deformation and prebend, where $\phi_{\mathrm{ez}} > 0$ at counter clockwise orientation in root-to-tip view (nose-up); $\phi_{\mathrm{ez}} > 0$ is defined 0 for the blade flange element X_1.

We introduce the chord-wise blade coordinate system $\vec{e}^{\,X_k^{\mathrm{set}}}$ with the z-axis along the chord line of X_k. By this definition, $\vec{e}^{\,X_k^{\mathrm{set}}}$ originates from *the* coordinate system $\vec{e}^{\,X_k}$ by rotation along the y-axis over $-(\phi_{\mathrm{tw}}^{X_k} - \phi_{\mathrm{ez}}^{X_k})$. The setting angle actually is the angle between the chord line and the lead direction of the blade element. It holds:

$$\begin{aligned}
{}^{X_k^{\mathrm{set}}}\Phi^{X_k} &= \begin{pmatrix} \cos\left(-(\phi_{\mathrm{tw}}^{X_k} - \phi_{\mathrm{ez}}^{X_k})\right) & 0 & -\sin\left(-(\phi_{\mathrm{tw}}^{X_k} - \phi_{\mathrm{ez}}^{X_k})\right) \\ 0 & 1 & 0 \\ \sin\left(-(\phi_{\mathrm{tw}}^{X_k} - \phi_{\mathrm{ez}}^{X_k})\right) & 0 & \cos\left(-(\phi_{\mathrm{tw}}^{X_k} - \phi_{\mathrm{ez}}^{X_k})\right) \end{pmatrix} \\
{}^{X_k^{\mathrm{set}}}\Phi^{X_k^{\mathrm{cv}}} &= {}^{X_k^{\mathrm{set}}}\Phi^{X_k} \,.\, {}^{X_k}\Phi^{X_k^{\mathrm{cv}}} \qquad (3.60) \\
\phi_{\mathrm{set}}^{X_k} &= -\arctan \frac{\vec{e}_z^{\,X_k^{\mathrm{set}}} \bullet \vec{e}_x^{\,X_k^{\mathrm{cv}}}}{\vec{e}_z^{\,X_k^{\mathrm{set}}} \bullet \vec{e}_z^{\,X_k^{\mathrm{cv}}}} = -\arctan \frac{{}^{X_k^{\mathrm{set}}}\Phi_{31}^{X_k^{\mathrm{cv}}}}{{}^{X_k^{\mathrm{set}}}\Phi_{33}^{X_k^{\mathrm{cv}}}}
\end{aligned}$$

The inflow angle $\phi_{\mathrm{inf}}^{X_k}$ equals the arctangent of the normal and leadwise relative speed on the blade element:

$$\phi_{\mathrm{inf}}^{X_k} = \arctan \frac{U_{\mathrm{n}}}{U_\ell} \tag{3.61}$$

Section B.6.2 lists the expressions of the mean value, sensitivity functions and stochastic and periodic variations for the angle of attack. Sensitivities to exactly the same variables apply as for the blade relative wind speed.

3.7 Drive-train modelling approach

The layout of the (rotating part of the) drive train model R is defined in section 3.7.1 by grouping the elements in subcomponents and via the orientation of rotations and translations between the elements. Two subcomponents are distinghuised: the (controlled) generator rotor $R_{\rm f}$ and the rotor shaft & hub $R_{\rm r}$. For the implemented 'motion formulations' of the kinematic and impulse variables see section B.2.1 and section B.2.2. The gearbox house subcomponent $R_{\rm h}$ has been moved from the drive-train model to the support structure because it stands still in average sense.

The responsive loads on both the generator rotor and the rotor shaft & hub differ from the slender beam theory equivalent spring and damper loads by Eq. 3.9 in section 3.3. These are subject of section 3.7.2.

The implemented model equations are listed in section A.4.1 and A.4.2 for the rotor shaft & hub and the generator rotor respectively.

3.7.1 Drive-train layout (rotating part)

The kinematic vectors for the gearbox slow shaft $R_{\rm s}$ are not explicitely avialable as structure variables; they are 'intermediate results' for the kinematic vectors of the rotor shaft & hub $R_{\rm r}$.

The drive-train model consists of the 'one-element-subcomponents' gearbox house $R_{\rm h}$, generator rotor & gearbox fast shaft $R_{\rm f}$, gearbox slow shaft $R_{\rm s}$ and main rotor shaft & hub $R_{\rm r}$. The subcomponents' $R_{\rm h}$, $R_{\rm f}$ and $R_{\rm s}$ only *rotate* relative to the nacelle in co-axial sense, that is to say along the (tilted) drive-train axis. These relative co-axial rotations are symbolised as $\varphi_{\rm gb} \equiv \phi_3^{R_{\rm h}}$, $\psi_{\rm f} \equiv 1/i_{\rm gb}\,\phi_3^{R_{\rm f}}$ and $\psi_{\rm s}$.

The gearbox house model is moved to the support structure while the gearbox slow shaft model $R_{\rm s}$ is only used for definition of intermediate kinematic variables (see section B.2.1).

The one-element subcomponent $R_{\rm r}$ has six degrees of freedom relative to $R_{\rm s}$. The involved six spring and damper pairs are located in the *exit* point $R_{\rm r}^{\oplus}$, being the rotor centre $R_{\rm r}^{\rm c}$; this is the only exception on the point of departure that all dofs are in the entry point of an element (see chapter on the integrated dynamic model 'for why'). The orientation of the final coordinate system $\vec{e}^{\,R_{\rm r}}$ is such that it approximates as good as possible the neutral elastic axes of the rotor shaft. It originates from $\vec{e}^{\,R_{\rm s}}$ by shaft deformation rotations along:

1. $\vec{e}_x^{\,R_{\rm s}}$ over +(shaft torsion angle $\phi_1^{R_{\rm r}}$)
2. $\vec{e}_z^{\,R_{\rm r}^1}$ over +(shaft 'yaw0-wise' shaft bending angle $\phi_2^{R_{\rm r}}$)
3. $\vec{e}_y^{\,R_{\rm r}^2}$ over +(shaft 'tilt0-wise' shaft bending angle $\phi_3^{R_{\rm r}}$)

The accompanying translations $\rho_{1,2,3}^{R_{\rm r}}$ are along the x-, y- and z-axis. The 'yaw0-wise' and 'tilt0-wise' identifiers pertain to yaw and tilt orientation in the initial

rotor shaft position; the bending dofs are all assumed zero-mean.

Next to the subcomponent related rotations $\phi_3^{R_{\rm h}}$, $\phi_3^{R_{\rm f}}$, $\psi_{\rm s}$ and $\phi_{1,2,3}^{R_{\rm r}}$, we define the following co-axial rotations:

$$\begin{array}{rcll} \phi_3^{R_{\rm h"}} & \stackrel{\triangle}{=} & \frac{i_{\rm gb}-1}{i_{\rm gb}} \cdot \phi_3^{R_{\rm h"}} & : \text{ feedthrough co-axial gearbox rotation into slow shaft} \\ \psi & \stackrel{\triangle}{=} & \frac{1}{i_{\rm gb}} \cdot \phi_3^{R_{\rm f}} & : \text{ main azimut angle } (\frac{\rm d}{{\rm d}t}(\psi) \stackrel{\triangle}{=} \text{main rotational speed } \Omega) \\ \psi_{\rm r} & \stackrel{\triangle}{=} & \psi_{\rm s} + \phi_1^{R_{\rm r}} & : \text{ rotor azimut angle, with } \psi_{\rm s} = \phi_3^{R_{\rm h"}} + \psi \end{array} \tag{3.62}$$

We assume that the fast and slow shaft rotate in the same direction[3] with transmission ratio $i_{\rm gb}$.

The following transformation matrices play a role in the derivation of the equations of motion for the drive train and in the exchange of motion and loading with the rotor blades:

$$\begin{array}{rcl} {}^{R_{\rm h"}}\Phi^{S_M} & = & \Phi_{\rm x}(\phi_3^{R_{\rm h"}}) \\ {}^{R_{\rm s}}\Phi^{R_{\rm h"}} & = & \Phi_{\rm x}(\psi) \\ {}^{R_{\rm r}}\Phi^{R_{\rm s}} & = & \Phi_{\rm y}(\phi_3^{R_{\rm r}}) \cdot \Phi_{\rm z}(\phi_2^{R_{\rm r}}) \cdot \Phi_{\rm x}(\phi_1^{R_{\rm r}}) \\ {}^{X_0}\Phi^{R_{\rm r}} & = & \Phi_{\rm x}({}^{R_{\rm r}}\psi^{X_0}), \quad \text{with } {}^{R_{\rm r}}\psi^{X_0} = {}_{0,2\pi/B,4\pi/B} \text{ for } X{=}D,E,F \end{array} \tag{3.63}$$

The main shaft deformation angles $\phi_{1,2,3}^{R_{\rm r}}$ are rotation dofs that set up, with deformation translations $\rho_{1,2,3}^{R_{\rm r}}$, the SBBT-equivalent shaft deformation. All main shaft inertia parameters are added to those of the (rigid) hub.

The transformation matrix ${}^{X_0}\Phi^{R_{\rm r}}$ caters for rotation of the base of rotor blade X relative to the hub over the 'azimut offset angle' ${}^{X_{\rm r}}\psi^{D_0}$.

In the transformation matrix ${}^{R_{\rm s}}\Phi^{R_{\rm h"}}$ over the main azimut angle ψ we can distinghuish the 'on-average rotating' transformation matrix ${}^{R_{\rm s}}\tilde{\Phi}^{R_{\rm h"}}$, the first order variation matrix $\delta^{R_{\rm s}}\Phi^{R_{\rm h"}}$ and the 'all over mean' transformation matrix ${}^{R_{\rm s}}\bar{\Phi}^{R_{\rm h"}}$. These are obtained by (note that ${}^{R_{\rm s}}\Phi^{R_{\rm h"}} \stackrel{\text{(orde 0,1)}}{=} {}^{R_{\rm s}}\tilde{\Phi}^{R_{\rm h"}} + \delta^{R_{\rm s}}\Phi^{R_{\rm h"}}$):

$$\begin{array}{rcll} {}^{R_{\rm s}}\tilde{\Phi}^{R_{\rm h"}} & = & \Phi_{\rm x}(\tilde{\psi}) & (\tilde{\psi} = \bar{\boldsymbol{\Omega}} \cdot t) \\ \delta^{R_{\rm s}}\Phi^{R_{\rm h"}} & \stackrel{\text{(orde 1)}}{=} & \Phi_{\rm x}(\tilde{\psi}) \cdot \begin{pmatrix} 0 & 0 & 0 \\ 0 & 0 & 1 \\ 0 & -1 & 0 \end{pmatrix} \cdot \delta\psi & (\delta\psi = \psi - \tilde{\psi}) \\ {}^{R_{\rm s}}\bar{\Phi}^{R_{\rm h"}} & = & \begin{pmatrix} 1 & 0 & 0 \\ 0 & 0 & 0 \\ 0 & 0 & 0 \end{pmatrix} & \end{array} \tag{3.64}$$

The transformation matrix ${}^{R_{\rm s}}\tilde{\Phi}^{R_{\rm h"}}$ associate with the average rotational speed is also expressed as a sum of harmonics of the invariant matrices $\Phi_{\rm d}$, $\Phi_{\rm c}$ and $\Phi_{\rm s}$:

$$\begin{array}{rcl} {}^{R_{\rm s}}\tilde{\Phi}^{R_{\rm h"}} & = & \Phi_{\rm d} + \Phi_{\rm c} \cdot \cos\bar{\Omega}t + \Phi_{\rm s} \cdot \sin\bar{\Omega}t \\ \multicolumn{3}{r}{\text{with } \Phi_{\rm d} = \begin{pmatrix} 1 & 0 & 0 \\ 0 & 0 & 0 \\ 0 & 0 & 0 \end{pmatrix} \quad \Phi_{\rm c} = \begin{pmatrix} 0 & 0 & 0 \\ 0 & 1 & 0 \\ 0 & 0 & 1 \end{pmatrix} \quad \Phi_{\rm s} = \begin{pmatrix} 0 & 0 & 0 \\ 0 & 0 & 1 \\ 0 & -1 & 0 \end{pmatrix}} \end{array} \tag{3.65}$$

[3] At opposite directions, the fedthrough rotation $\phi_3^{R_{\rm h"}}$ would amount to $(i_{\rm gb}+1)/i_{\rm gb} \cdot \phi_3^{R_{\rm h}}$

For dealing with the transportation velocity in the rotor annuli, we also define the in average sense fixed coordinate system $\vec{e}^{\,R_{\rm fx}}$ on the rotor hub. Its x-axis points perpendicular to the rotor plane and its y- and z-axis point in the rotor plane's yaw- and tilt-direction. This coordinate system originates from $\vec{e}^{\,R_{\rm r}}$ by rotation along the x-axis over minus the rotor azimuth angle $\psi_{\rm r}$:

$$ {}^{R_{\rm r}^{\rm fx}}\Phi^{R_{\rm r}} = \Phi_{\rm x}^{\rm T}(\psi_{\rm r}) = \Phi_{\rm x}^{\rm T}(\phi_3^{R_{\rm h"}}) \cdot \Phi_{\rm x}^{\rm T}(\psi) \cdot \Phi_{\rm x}^{\rm T}(\phi_1^{R_{\rm r}}) \tag{3.66} $$

3.7.2 Responsive loads by generator rotor and in rotor centre

Generator counter torque

In case of a variable speed system the generator torque control system yields a 'counter torque': if > 0 then it will slow down the rotational speed. The implemented generator torque control system in TURBU Offshore represents

- the servo behaviour of the E-system for the counter torque setpoint
- the steepness of the torque/speed curve for the actual working point in low frequencies;
- the feedback of generator speed variations for enhanced drive-train damping in a frequency range around the first collective leadwise blade bending natural frequency.

The transfer function formulation for the behaviour of the generator torque control system is:

$$ \begin{aligned} t_{\rm e} \;=\; & \Big(\tfrac{1}{s^2/\omega_{\rm te_0}^2 + 2\cdot\beta_{\rm te}s/\omega_{\rm te_0}+1}\Big)\cdot\tfrac{1}{i_{\rm gb}}\cdot\Big(\\ & K_{\rm pow}\cdot\Big(\tfrac{b_n\cdot\frac{{\rm d}^n}{{\rm d}t^n}+\ldots+b_1\cdot\frac{\rm d}{{\rm d}t}+1}{a_n\cdot\frac{{\rm d}^n}{{\rm d}t^n}+\ldots+a_1\cdot\frac{\rm d}{{\rm d}t}+1}\Big) + K_{\rm trs}\cdot\Big(\tfrac{h_m\cdot\frac{{\rm d}^m}{{\rm d}t^m}+\ldots+h_1\cdot\frac{\rm d}{{\rm d}t}+1}{g_m\cdot\frac{{\rm d}^m}{{\rm d}t^m}+\ldots+g_1\cdot\frac{\rm d}{{\rm d}t}+1}\Big)\Big)\cdot\dot{\varphi}_{\rm x}^{R_{\rm f}} \end{aligned} \tag{3.67} $$

The natural frequency $\omega_{\rm te_0}$ [rad/s] and exponential damping rate $\beta_{\rm te}$ characterise the servo behaviour of the electric system for the counter torque. These values depend on the electric system design.

The gain $K_{\rm pow}$ represents the steepness of the torque/speed curve (slow shaft equivalent) while the gain $K_{\rm trs}$ enhances the damping of the drive-train torsion (if < 0; slow shaft equivalent). The low-pass filter parameters $b_n \ldots b_1,\ a_n \ldots a_1$ mainly depend on the average rotational speed and the first natural frequency of the tower. The band- or high-pass filter parameters $h_m \ldots h_1,\ g_m \ldots g_1$ depend on the natural frequency of the first collective leadwise blade bending mode. All these parameters are to be derived with a control design tool.

Visco-elastic load reaction for rotor shaft with main bearing

The responsive loading for the rotor shaft involves visco-elastic loads for up to six degrees of freedom. Figure 3.8 shows the layout of the shaft model. The derivation below only deals with the elastic responsive loads. The same results are valid for the viscous responsive loads by just replacing stiffness by damper constants and dof position variations by dof speeds.

Via a slender beam theory approximation for the elastic deformation the model layout can be translated into four (sets of) equations between the degrees of

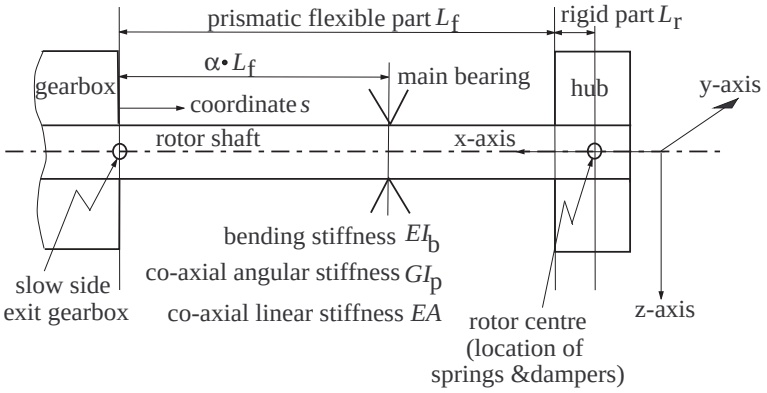

Figure 3.8 *Rotor shaft layout for visco-elastic responsive loading*

freedom in the rotor centre and the involved responsive loads by the rotor shaft in that same location. Consider angular and linear dofs along the x-, y- and z-axis, then the elastic reaction loads along the axes can be written as (similar expressions for viscous loads; replace 's' by 'd'):

$$\begin{aligned}
{}^{\mathrm{RS}}t_{\mathrm{x}}^{R_{\mathrm{r}}} &= -s_{\mathrm{t_x}\phi_{\mathrm{x}}}^{R_{\mathrm{r}}} \cdot \varphi_{\mathrm{x}}^{R_{\mathrm{r}}} \\
{}^{\mathrm{RS}}f_{\mathrm{x}}^{R_{\mathrm{r}}} &= -s_{\mathrm{f_x}\rho_{\mathrm{x}}}^{R_{\mathrm{r}}} \cdot \varrho_{\mathrm{x}}^{R_{\mathrm{r}}} \\
\begin{bmatrix} {}^{\mathrm{RS}}t_{\mathrm{y}}^{R_{\mathrm{r}}} \\ {}^{\mathrm{RS}}f_{\mathrm{z}}^{R_{\mathrm{r}}} \end{bmatrix} &= -\begin{pmatrix} s_{\mathrm{t_y}\phi_{\mathrm{y}}}^{R_{\mathrm{r}}} & s_{\mathrm{t_y}\rho_{\mathrm{z}}}^{R_{\mathrm{r}}} \\ s_{\mathrm{f_z}\phi_{\mathrm{y}}}^{R_{\mathrm{r}}} & s_{\mathrm{f_z}\rho_{\mathrm{z}}}^{R_{\mathrm{r}}} \end{pmatrix} \cdot \begin{bmatrix} \varphi_{\mathrm{y}}^{R_{\mathrm{r}}} \\ \varrho_{\mathrm{z}}^{R_{\mathrm{r}}} \end{bmatrix} \\
\begin{bmatrix} {}^{\mathrm{RS}}t_{\mathrm{z}}^{R_{\mathrm{r}}} \\ {}^{\mathrm{RS}}f_{\mathrm{y}}^{R_{\mathrm{r}}} \end{bmatrix} &= -\begin{pmatrix} s_{\mathrm{t_z}\phi_{\mathrm{z}}}^{R_{\mathrm{r}}} & s_{\mathrm{t_z}\rho_{\mathrm{y}}}^{R_{\mathrm{r}}} \\ s_{\mathrm{f_y}\phi_{\mathrm{z}}}^{R_{\mathrm{r}}} & s_{\mathrm{f_y}\rho_{\mathrm{y}}}^{R_{\mathrm{r}}} \end{pmatrix} \cdot \begin{bmatrix} \varphi_{\mathrm{z}}^{R_{\mathrm{r}}} \\ \varrho_{\mathrm{y}}^{R_{\mathrm{r}}} \end{bmatrix}
\end{aligned} \tag{3.68}$$

As we choosed the $x-$, $z-$ and y-axis as the bottom-up ranked rotation axes, the vectors of the dofs alongs the axes are expressed as follows in the angular dof vectors:

$$\begin{aligned}
\begin{bmatrix} \varphi_{\mathrm{x}}^{R_{\mathrm{r}}} \\ \varphi_{\mathrm{y}}^{R_{\mathrm{r}}} \\ \varphi_{\mathrm{x}}^{R_{\mathrm{r}}} \end{bmatrix} &= \begin{pmatrix} 1 & 0 & 0 \\ 0 & 0 & 1 \\ 0 & 1 & 0 \end{pmatrix} \cdot \begin{bmatrix} \varphi_1^{R_{\mathrm{r}}} \\ \varphi_2^{R_{\mathrm{r}}} \\ \varphi_3^{R_{\mathrm{r}}} \end{bmatrix} = \boldsymbol{P}_{\varphi}^{R_{\mathrm{r}}} \cdot \underline{\varphi}^{R_{\mathrm{r}}} \\
\begin{bmatrix} \varrho_{\mathrm{x}}^{R_{\mathrm{r}}} \\ \varrho_{\mathrm{y}}^{R_{\mathrm{r}}} \\ \varrho_{\mathrm{x}}^{R_{\mathrm{r}}} \end{bmatrix} &= \begin{pmatrix} 1 & 0 & 0 \\ 0 & 1 & 0 \\ 0 & 0 & 1 \end{pmatrix} \cdot \begin{bmatrix} \varrho_1^{R_{\mathrm{r}}} \\ \varrho_2^{R_{\mathrm{r}}} \\ \varrho_3^{R_{\mathrm{r}}} \end{bmatrix} = \boldsymbol{I} \cdot \underline{\varrho}^{R_{\mathrm{r}}}
\end{aligned} \tag{3.69}$$

The linear expressions searched for have to map the angular and linear dof vectors $\underline{\varphi}^{R_{\mathrm{r}}}$, $\underline{\varrho}^{R_{\mathrm{r}}}$ to the $x-$, $y-$ and $z-$ coordinates of the responsive torque and force

vectors:

$$ {}^{\mathrm{RS}}\underline{t}^{R_\mathrm{r}} = \begin{bmatrix} {}^{\mathrm{RS}}t_1^{R_\mathrm{r}} \\ {}^{\mathrm{RS}}t_2^{R_\mathrm{r}} \\ {}^{\mathrm{RS}}t_3^{R_\mathrm{r}} \end{bmatrix} \triangleq \begin{bmatrix} {}^{\mathrm{RS}}t_\mathrm{x}^{R_\mathrm{r}^1} \\ {}^{\mathrm{RS}}t_\mathrm{y}^{R_\mathrm{r}^3} \\ {}^{\mathrm{RS}}t_\mathrm{z}^{R_\mathrm{r}^2} \end{bmatrix} = {}^{\mathrm{RS}}\bar{\underline{t}}^{R_\mathrm{r}} + \frac{\partial^{\mathrm{RS}}\underline{t}^{R_\mathrm{r}}}{\partial \underline{\varphi}^{R_\mathrm{r}}} \cdot \underline{\varphi}^{R_\mathrm{r}} + \frac{\partial^{\mathrm{RS}}\underline{t}^{R_\mathrm{r}}}{\partial \underline{\varrho}^{R_\mathrm{r}}} \cdot \underline{\varrho}^{R_\mathrm{r}} \tag{3.70} $$

and

$$ {}^{\mathrm{RS}}\underline{f}^{R_\mathrm{r}} = \begin{bmatrix} {}^{\mathrm{RS}}f_1^{R_\mathrm{r}} \\ {}^{\mathrm{RS}}f_2^{R_\mathrm{r}} \\ {}^{\mathrm{RS}}f_3^{R_\mathrm{r}} \end{bmatrix} \triangleq \begin{bmatrix} {}^{\mathrm{RS}}f_\mathrm{x}^{R_\mathrm{r}^1} \\ {}^{\mathrm{RS}}f_\mathrm{y}^{R_\mathrm{r}^2} \\ {}^{\mathrm{RS}}f_\mathrm{z}^{R_\mathrm{r}^3} \end{bmatrix} = {}^{\mathrm{RS}}\bar{\underline{f}}^{R_\mathrm{r}} + \frac{\partial^{\mathrm{RS}}\underline{f}^{R_\mathrm{r}}}{\partial \underline{\varphi}^{R_\mathrm{r}}} \cdot \underline{\varphi}^{R_\mathrm{r}} + \frac{\partial^{\mathrm{RS}}\underline{f}^{R_\mathrm{r}}}{\partial \underline{\varrho}^{R_\mathrm{r}}} \cdot \underline{\varrho}^{R_\mathrm{r}} \tag{3.71} $$

For the sensitivities to the dof vectors then holds:

$$ \begin{aligned} \frac{\partial^{\mathrm{RS}}\underline{t}^{R_\mathrm{r}}}{\partial \underline{\varphi}^{R_\mathrm{r}}} &= -\begin{pmatrix} s_{\mathrm{t_x}\phi_\mathrm{x}}^{R_\mathrm{r}} & 0 & 0 \\ 0 & s_{\mathrm{t_y}\phi_\mathrm{y}}^{R_\mathrm{r}} & 0 \\ 0 & 0 & s_{\mathrm{t_z}\phi_\mathrm{z}}^{R_\mathrm{r}} \end{pmatrix} \cdot \boldsymbol{P}_\varphi^{R_\mathrm{r}} \quad ; \quad \frac{\partial^{\mathrm{RS}}\underline{t}^{R_\mathrm{r}}}{\partial \underline{\varrho}^{R_\mathrm{r}}} = -\begin{pmatrix} 0 & 0 & 0 \\ 0 & 0 & s_{\mathrm{t_y}\rho_\mathrm{z}}^{R_\mathrm{r}} \\ 0 & s_{\mathrm{t_z}\rho_\mathrm{y}}^{R_\mathrm{r}} & 0 \end{pmatrix} \\ \frac{\partial^{\mathrm{RS}}\underline{f}^{R_\mathrm{r}}}{\partial \underline{\varphi}^{R_\mathrm{r}}} &= -\begin{pmatrix} 0 & 0 & 0 \\ 0 & 0 & s_{\mathrm{f_y}\phi_\mathrm{z}}^{R_\mathrm{r}} \\ 0 & s_{\mathrm{f_z}\phi_\mathrm{y}}^{R_\mathrm{r}} & 0 \end{pmatrix} \cdot \boldsymbol{P}_\varphi^{R_\mathrm{r}} \quad ; \quad \frac{\partial^{\mathrm{RS}}\underline{f}^{R_\mathrm{r}}}{\partial \underline{\varrho}^{R_\mathrm{r}}} = -\begin{pmatrix} s_{\mathrm{f_x}\rho_\mathrm{x}}^{R_\mathrm{r}} & 0 & 0 \\ 0 & s_{\mathrm{f_y}\rho_\mathrm{y}}^{R_\mathrm{r}} & 0 \\ 0 & 0 & s_{\mathrm{f_z}\rho_\mathrm{z}}^{R_\mathrm{r}} \end{pmatrix} \end{aligned} \tag{3.72} $$

The stiffness parameters are derived from the shaft properties under the assumption of a prismatic beam, with flexible part of length L_f and rigid part of length L_p. The main bearing is located on distance αL_f from the begin of the flexible part of the main shaft (coincides with slow side gearbox exit in figure 3.8). If the shaft is non-prismatic, then the bending and coaxial stiffness values EI_b, GI_p and EA, are obtained by averaging over the flexible part L_f, which is exact for the coaxial stiffness values.

The stiffness parameters are obtained via the bending theory for slender beams. For the coaxial stiffness parameters holds:

$$ \begin{aligned} s_{\mathrm{f_x}\rho_\mathrm{x}}^{R_\mathrm{r}} &= \frac{EA}{L_\mathrm{f}} \\ s_{\mathrm{t_x}\phi_\mathrm{x}}^{R_\mathrm{r}} &= \frac{GI_\mathrm{p}}{L_\mathrm{f}} \end{aligned} \tag{3.73} $$

with E the elastic modulus, G the shear modulus, A the average surface of the shaft and I_p the average polar moment of inertia.

Although, the derivation of the bending stiffness and damper parameters is somewhat more complicated, it can still be manually done for the assumed non-conical shaft. The procedure is mentioned below for the stiffness parameters (similar for damping parameters). First the rigid shaft partition L_r is not taken into account, which yields an expression for the inverse stiffness matrix at the end of the flexible partition L_f. Afterwards, the stiffness parameters are shifted 'over the rigid partition', *after modifications related to the angular load and deformation*.

Assume the bending force F_z and bending torque M_y at the end of the flexible part ($s = L_\mathrm{f}$). Define the reaction force by the main shaft bearing F_s. Note that a force along the z-axis deforms the shaft in the same direction as torque along the y-axis (same orientation for 'linear and angular bending along the z-axis and y-axis'). The linear displacement $\varrho_\mathrm{z}(\alpha L_\mathrm{f})$ of the shaft in the main bearing relative to the slow side exit point of the gearbox must be zero. Slender beam bending theory then tells:

$$\varrho_\mathrm{z}(\alpha L_\mathrm{f}) \equiv 0 = \frac{F_\mathrm{s}\cdot(\alpha L_\mathrm{f})^3}{3EI_\mathrm{b}} + \frac{F_\mathrm{z}\cdot(\alpha L_\mathrm{f})^3}{3EI_\mathrm{b}} + \frac{(F_\mathrm{z}\cdot(1-\alpha)L_\mathrm{f} + M_\mathrm{y})\cdot(\alpha L_\mathrm{f})^2}{2EI_\mathrm{b}} \tag{3.74}$$

For the angular and linear displacement in $s = L_\mathrm{f}$ relative to the gearbox exit holds:

$$\begin{aligned}\varphi_\mathrm{y}(L_\mathrm{f}) &= \frac{F_\mathrm{s}\cdot(\alpha L_\mathrm{f})^2}{2EI_\mathrm{b}} + \frac{F_\mathrm{z}\cdot L_\mathrm{f}^2}{2EI_\mathrm{b}} + \frac{M_\mathrm{y}\cdot L_\mathrm{f}}{EI_\mathrm{b}} \\ \varrho_\mathrm{z}(L_\mathrm{f}) &= \frac{F_\mathrm{s}\cdot(\alpha L_\mathrm{f})^3}{3EI_\mathrm{b}} + \frac{F_\mathrm{s}\cdot(\alpha L_\mathrm{f})^2\cdot(1-\alpha)L_\mathrm{f}}{2EI_\mathrm{b}} + \frac{F_\mathrm{z}\cdot L_\mathrm{f}^3}{3EI_\mathrm{b}} + \frac{M_\mathrm{y}\cdot L_\mathrm{f}^2}{2EI_\mathrm{b}}\end{aligned} \tag{3.75}$$

Elimination of the support bearing force yields the 'inverse stiffness relationship' for the main shaft at the end of the flexible part:

$$\begin{bmatrix} \varphi_\mathrm{y}(L_\mathrm{f}) \\ \varrho_\mathrm{z}(L_\mathrm{f}) \end{bmatrix} = \begin{pmatrix} \frac{(1-\frac{3}{4}\alpha)L_\mathrm{f}}{EI_\mathrm{b}} & \frac{(1-\frac{3}{2}\alpha+\frac{1}{2}\alpha^2)L_\mathrm{f}^2}{2EI_\mathrm{b}} \\ \frac{(1-\frac{3}{2}\alpha+\frac{1}{2}\alpha^2)L_\mathrm{f}^2}{2EI_\mathrm{b}} & \frac{(1-\frac{9}{4}\alpha+\frac{6}{4}\alpha^2)-\frac{1}{4}\alpha^3)L_\mathrm{f}^3}{3EI_\mathrm{b}} \end{pmatrix} \cdot \begin{bmatrix} M_\mathrm{y} \\ F_\mathrm{z} \end{bmatrix} \tag{3.76}$$

Taking into account the rigid shaft partition L_r has two implications (assume force and torqe loading f_z and t_y in the rotor centre):

- the torque load in $s = L_\mathrm{f}$ is augmented with $f_\mathrm{c}\cdot L_\mathrm{r}$
- the linear displacement in $s = L_\mathrm{f} + L_\mathrm{r}$ is augmented with $\varphi_\mathrm{y}\cdot L_\mathrm{r}$

This yields the following 'inverse stiffness relationship' for the rotor centre:

$$\begin{bmatrix} \varphi_\mathrm{y}(L_\mathrm{f}+L_\mathrm{r}) \\ \varrho_\mathrm{z}(L_\mathrm{f}+L_\mathrm{r}) \end{bmatrix} = \begin{pmatrix} g_{11} & g_{12}+g_{11}\cdot L_\mathrm{r} \\ g_{21}+g_{11}\cdot L_\mathrm{r} & g_{22}+(g_{21}+g_{12})\cdot L_\mathrm{r}+g_{11}\cdot L_\mathrm{r}^2 \end{pmatrix} \cdot \begin{bmatrix} t_\mathrm{y} \\ f_\mathrm{z} \end{bmatrix} \tag{3.77}$$

with $g_{11}\ldots g_{22}$ the elements of the inverse stiffness matrix in Eq. 3.76.

For the associated 'target' stiffness matrix in Eq. 3.68 then holds:

$$\begin{pmatrix} s^{R_\mathrm{r}}_{\mathrm{t_y}\phi_\mathrm{y}} & s^{R_\mathrm{r}}_{\mathrm{t_y}\rho_\mathrm{z}} \\ s^{R_\mathrm{r}}_{\mathrm{f_z}\phi_\mathrm{y}} & s^{R_\mathrm{r}}_{\mathrm{f_z}\rho_\mathrm{z}} \end{pmatrix} = \begin{pmatrix} g_{11} & g_{12}+g_{11}\cdot L_\mathrm{r} \\ g_{21}+g_{11}\cdot L_\mathrm{r} & g_{22}+(g_{21}+g_{12})\cdot L_\mathrm{r}+g_{11}\cdot L_\mathrm{r}^2 \end{pmatrix}^{-1} \tag{3.78}$$

For the remaining bending stiffness parameters holds because of axi-symmetry and the reverse orientation of 'linear and angular bending along the y- and z-axis':

$$\begin{pmatrix} s^{R_\mathrm{r}}_{\mathrm{t_z}\phi_\mathrm{z}} & s^{R_\mathrm{r}}_{\mathrm{t_z}\rho_\mathrm{y}} \\ s^{R_\mathrm{r}}_{\mathrm{f_y}\phi_\mathrm{z}} & s^{R_\mathrm{r}}_{\mathrm{f_y}\rho_\mathrm{y}} \end{pmatrix} = \begin{pmatrix} s^{R_\mathrm{r}}_{\mathrm{t_y}\phi_\mathrm{y}} & -s^{R_\mathrm{r}}_{\mathrm{t_y}\rho_\mathrm{z}} \\ -s^{R_\mathrm{r}}_{\mathrm{f_z}\phi_\mathrm{y}} & s^{R_\mathrm{r}}_{\mathrm{f_z}\rho_\mathrm{z}} \end{pmatrix} \tag{3.79}$$

3.8 Support structure modelling approach

The layout of the support structure model S is defined in section 3.8.1 by grouping the elements in subcomponents and via the orientation of rotations and translations between the elements. Three subcomponents are distinguised: the foundation $S_{\rm f}$, the tower $S_{\rm t}$ and the nacelle $S_{\rm n}$. For the implemented 'motion formulations' of the kinematic and impulse variables see section B.1.1 and section B.1.2. The support structure model also includes the gearbox house subcomponent $R_{\rm h}$, which in average sense stands still. The gearbox house is included in the layout of the support structure in section 3.8.1; for its kinematic and impulse variables see the paragraph on $R_{\rm h}$ in section B.2.1 and section B.2.2.

The responsive loads on the foundation, nacelle and gearbox house elements differ from the slender beam theory equivalent spring and damper loads by Eq. 3.9 in section 3.3. These are subject of section 3.8.2. The hydrodynamic loads on the tower are driven by the exogeneous 'wave' input variables and are subject of section 3.8.3; for the implemented 'load formulations' see section B.9.

The implemented model equations are listed in section A.5.1, A.5.2, A.5.3 and A.5.4 for the gearbox house, nacelle, tower and foundation respectively.

3.8.1 Foundation, tower, nacelle, gearbox house

The support structure model is attached to the earth's surface in the point $S_1^{\ominus}$. At the 'earth side' of $S_1^{\ominus}$, the turbine base coordinate system $\vec{e}^{\,B}$ applies; see section 3.4.1 and fig. 3.3.

At the 'foundation side' of $S_1^{\ominus}$, the coordinate system $\vec{e}^{\,S_1}$ is fixed to the rigid bar of foundation element S_1, with orientation of the neutral elastic axes of the tower section that is mapped to element S_1. System $\vec{e}^{\,S_1}$ originates from $\vec{e}^{\,B}$ by foundation rotations along

1. $\vec{e}_z^{\,B}$ over +(foundation torsion angle $\phi_1^{S_1}$)
2. $\vec{e}_y^{\,S_1^1}$ over +(foundation fore/aft bending angle $\phi_2^{S_1}$)
3. $\vec{e}_x^{\,S_1^2}$ over +(foundation sideward bending angle $\phi_3^{S_1}$)

The accompanying translations $\rho_{1,2,3}^{S_k}$ are along the z-, x- and y-axis.

The final coordinate systems of the tower elements $S_2 \ldots S_{M-1}$ are fixed to the rigid bars of these elements at the 'upward side' of the connector points $S_2^{\ominus} \ldots S_{M-1}^{\ominus}$. The orientation of the final coordinate system $\vec{e}^{\,S_k}$ is such that it approximates as good as possible the neutral elastic axes of the blade elements. It originates from the foregoing final system $\vec{e}^{\,S_{k-1}}$ by tower deformation rotations along

1. $\vec{e}_z^{\,S_{k-1}}$ over +(tower torsion angle $\phi_1^{S_k}$)
2. $\vec{e}_y^{\,S_k^1}$ over +(tower fore/aft bending angle $\phi_2^{S_k}$)
3. $\vec{e}_x^{\,S_k^2}$ over +(tower sideward bending angle $\phi_3^{S_k}$)

The accompanying translations $\rho_{1,2,3}^{S_k}$ are along the z-, x- and y-axis.

The final coordinate system of the nacelle element S_M is fixed to the rigidly assumed nacelle body at the 'upward side' of $S_M^{\ominus}$. Coordinate system $\vec{e}^{\,S_M}$

originates from the tower top system $\vec{e}^{\,M-1}$ by rotation along

1. $\vec{e}_z^{\,S_{M-1}}$ over +(yaw deviation angle $\phi_1^{S_M}$) + (mean yaw angle $\phi_{\rm yw}^S$)
2. $\vec{e}_y^{\,S_M^1}$ over -(tilt angle $\phi_{\rm ti}^S$);

The (dummy) accompanying translations $\rho_{1,2,3}^{S_k}$ are along the z-, x- and y-axis.

The mean yaw angle $\phi_{\rm yw}^S$ is defined as the average rotation from the tower top x-axis to the 'in tower top plane' fore-aft axis of the nacelle; >0 at clockwise orientation in top-to-bottom view. The nacelle deviation angle $\phi_1^{S_M}$ is a rotation dof that enables to include yaw compliance in the dynamic calculations.

The tilt angle $\phi_{\rm ti}^S$ is defined as the rotation from the axis through the centre of the rotor shaft bearings to the 'in tower top plane' fore/aft axis of the nacelle; >0 at upward tilted turbine rotor.

The transformation matrices ${}^{S_k}\Phi^{S_{k-1}}$ between the elements of the support structure elements are obtained by:

$$ {}^{S_k}\Phi^{S_{k-1}} = \begin{cases} \Phi_{\rm x}(\phi_3^{S_k}) \cdot \Phi_{\rm y}(\phi_2^{S_k}) \cdot \Phi_{\rm z}(\phi_1^{S_k}) & \text{for } k = 1 \text{ and } k = 2 \ldots M-1 \\ \Phi_{\rm x}(\phi_3^{S_{\rm k}} \equiv 0) \cdot \Phi_{\rm y}(-\phi_{\rm ti}^S) \cdot \Phi_{\rm z}(\phi_1^{S_k} + \phi_{\rm yw}^S) & \text{for } k = M \end{cases} \tag{3.80} $$

The deformation tower angles $\phi_{1,2,3}^{S_{2\ldots M-1}}$ are rotation dofs that set up, with deformation translations $\rho_{1,2,3}^{S_{2\ldots M-1}}$, the SBBT-equivalent tower deformation.

All theoretically possible rotation and translation dofs are collected in column vectors $\underline{\varphi}^S$ and $\underline{\varrho}^S$. These vectors are composed of 3-element subvectors.

$$ \underline{\varphi}^S = \begin{pmatrix} \varphi_1^{S_1} \\ \varphi_2^{S_1} \\ \varphi_3^{S_1} \\ \vdots \\ \varphi_1^{S_M} \\ \varphi_2^{S_M} \\ \varphi_3^{S_M} \\ \varphi_1^{R_{\rm h}} \\ \varphi_2^{R_{\rm h}} \\ \varphi_3^{R} \end{pmatrix} \qquad \underline{\varrho}^S = \begin{pmatrix} \varrho_1^{S_1} \\ \varrho_2^{S_1} \\ \varrho_3^{S_1} \\ \vdots \\ \varrho_1^{S_M} \\ \varrho_2^{S_M} \\ \varrho_3^{S_M} \\ \varrho_1^{R_{\rm h}} \\ \varrho_2^{R_{\rm h}} \\ \varrho_3^{R_{\rm h}} \end{pmatrix} \tag{3.81} $$

These 'full dof vectors' are used in the motion and load formulations and eventually yield 'full size system matrices' for the equations of motion. After these full size matrices have been established, those rows and columns will be removed which pertain to rotation and translation 'directions' that do *not* accomodate dofs.

Note that the one-element subcomponent nacelle $S_{\rm n}$ may *rotate* relative to the tower top in up to three directions (yaw, roll, tilt)).

Note that the one-element subcomponent gearbox house $R_{\rm h}$ only *rotates* relative to the nacelle in *co-axial* sense (along the tilted drive-train axis).

3.8.2 Responsive loads in foundation & nacelle

Non-SBBT-equivalent responsive loads in the sense of section 3.3 occur in the foundation, the nacelle and the gearbox house.

(i) soil flexibility

Figure 3.9 shows the layout of the foundation model. The derivation below only deals with the elastic responsive loads. The same results are valid for the viscous responsive loads by just replacing stiffness by damper constants and dof position variations by dof speeds.

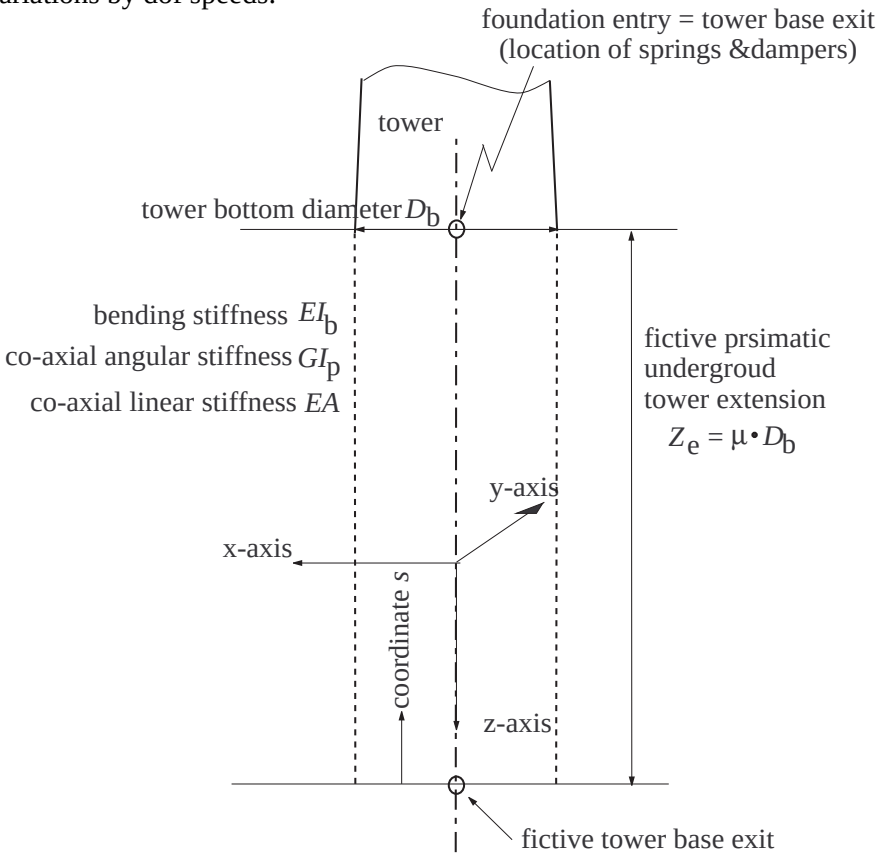

Figure 3.9 *Fictive tower extension for visco-elastic responsive loading on foundation*

The elastic foundation behaviour can be captured in four linear equations between degrees of freedom in the real foundation entry $S_1^{\ominus} \equiv B$ (turbine base) *on* the earth surface and responsive loads at that same location. This allows to let element S_1 model the foundation S_f as a one-element subcomponent. With angular and linear dofs along the x-, y- and z-axis, the elastic reaction loads along the axes can be written as (note the cross coupling parameters like $s^{S_1}_{t_x \rho_y}$); similar expressions

for viscous loads → replace 's' by 'd'):

$$
\begin{aligned}
{}^{\mathrm{RS}}t_{\mathrm{z}}^{S_1} &= -s_{\mathrm{t_z}\phi_{\mathrm{z}}}^{S_1} \cdot \varphi_{\mathrm{z}}^{S_1} \\
{}^{\mathrm{RS}}f_{\mathrm{z}}^{S_1} &= -s_{\mathrm{f_z}\rho_{\mathrm{z}}}^{S_1} \cdot \varrho_{\mathrm{z}}^{S_1} \\
\begin{bmatrix} {}^{\mathrm{RS}}t_{\mathrm{x}}^{S_1} \\ {}^{\mathrm{RS}}f_{\mathrm{y}}^{S_1} \end{bmatrix} &= -\begin{pmatrix} s_{\mathrm{t_x}\phi_{\mathrm{x}}}^{S_1} & s_{\mathrm{t_x}\rho_{\mathrm{y}}}^{S_1} \\ s_{\mathrm{f_y}\phi_{\mathrm{x}}}^{S_1} & s_{\mathrm{f_y}\rho_{\mathrm{y}}}^{S_1} \end{pmatrix} \cdot \begin{bmatrix} \varphi_{\mathrm{x}}^{S_1} \\ \varrho_{\mathrm{y}}^{S_1} \end{bmatrix} \\
\begin{bmatrix} {}^{\mathrm{RS}}t_{\mathrm{y}}^{S_1} \\ {}^{\mathrm{RS}}f_{\mathrm{x}}^{S_1} \end{bmatrix} &= -\begin{pmatrix} s_{\mathrm{t_y}\phi_{\mathrm{y}}}^{S_1} & s_{\mathrm{t_y}\rho_{\mathrm{x}}}^{S_1} \\ s_{\mathrm{f_x}\phi_{\mathrm{y}}}^{S_1} & s_{\mathrm{f_x}\rho_{\mathrm{x}}}^{S_1} \end{pmatrix} \cdot \begin{bmatrix} \varphi_{\mathrm{y}}^{S_1} \\ \varrho_{\mathrm{x}}^{S_1} \end{bmatrix}
\end{aligned}
\tag{3.82}
$$

With bottom-up ranked rotation axes in z-, y- and x-direction and corresponding z-, x- and y-axes for translatoin, the vectors of the dofs alongs the axes are expressed as follows in the angular dof vectors for S_1:

$$
\begin{aligned}
\begin{bmatrix} \varphi_{\mathrm{x}}^{S_1} \\ \varphi_{\mathrm{y}}^{S_1} \\ \varphi_{\mathrm{z}}^{S_1} \end{bmatrix} &= \begin{pmatrix} 0 & 0 & 1 \\ 0 & 1 & 0 \\ 1 & 0 & 0 \end{pmatrix} \cdot \begin{bmatrix} \varphi_1^{S_1} \\ \varphi_2^{S_1} \\ \varphi_3^{S_1} \end{bmatrix} = \boldsymbol{P}_{\varphi}^{S_1} \cdot \underline{\varphi}^{S_1} \\
\begin{bmatrix} \varrho_{\mathrm{x}}^{S_1} \\ \varrho_{\mathrm{y}}^{S_1} \\ \varrho_{\mathrm{z}}^{S_1} \end{bmatrix} &= \begin{pmatrix} 0 & 1 & 0 \\ 0 & 0 & 1 \\ 1 & 0 & 0 \end{pmatrix} \cdot \begin{bmatrix} \varrho_1^{S_1} \\ \varrho_2^{S_1} \\ \varrho_3^{S_1} \end{bmatrix} = \boldsymbol{P}_{\varrho}^{S_1} \cdot \underline{\varrho}^{S_1}
\end{aligned}
\tag{3.83}
$$

The linear expressions searched for have to map the angular and linear dof vectors $\underline{\varphi}^{S_1}$, $\underline{\varrho}^{S_1}$ to the $x-$, $y-$ and $z-$ coordinates of the responsive torque and force vectors:

$$
{}^{\mathrm{RS}}\underline{t}^{S_1} = \begin{bmatrix} {}^{\mathrm{RS}}t_1^{S_1} \\ {}^{\mathrm{RS}}t_2^{S_1} \\ {}^{\mathrm{RS}}t_3^{S_1} \end{bmatrix} \triangleq \begin{bmatrix} {}^{\mathrm{RS}}t_{\mathrm{x}}^{S_1^1} \\ {}^{\mathrm{RS}}t_{\mathrm{y}}^{S_1^3} \\ {}^{\mathrm{RS}}t_{\mathrm{z}}^{S_1^2} \end{bmatrix} = {}^{\mathrm{RS}}\bar{\underline{t}}^{R_{\mathrm{r}}} + \frac{\partial^{\mathrm{RS}}\underline{t}^{S_1}}{\partial \underline{\varphi}^{S_1}} \cdot \underline{\varphi}^{S_1} + \frac{\partial^{\mathrm{RS}}\underline{t}^{S_1}}{\partial \underline{\varrho}^{S_1}} \cdot \underline{\varrho}^{S_1}
\tag{3.84}
$$

and

$$
{}^{\mathrm{RS}}\underline{f}^{S_1} = \begin{bmatrix} {}^{\mathrm{RS}}f_1^{S_1} \\ {}^{\mathrm{RS}}f_2^{S_1} \\ {}^{\mathrm{RS}}f_3^{S_1} \end{bmatrix} \triangleq \begin{bmatrix} {}^{\mathrm{RS}}f_{\mathrm{x}}^{S_1^1} \\ {}^{\mathrm{RS}}f_{\mathrm{y}}^{S_1^2} \\ {}^{\mathrm{RS}}f_{\mathrm{z}}^{S_1^3} \end{bmatrix} = {}^{\mathrm{RS}}\bar{\underline{f}}^{R_{\mathrm{r}}} + \frac{\partial^{\mathrm{RS}}\underline{f}^{S_1}}{\partial \underline{\varphi}^{S_1}} \cdot \underline{\varphi}^{S_1} + \frac{\partial^{\mathrm{RS}}\underline{f}^{S_1}}{\partial \underline{\varrho}^{S_1}} \cdot \underline{\varrho}^{S_1}
\tag{3.85}
$$

For the sensitivities to the dof subvectors in S_1 then holds:

$$\frac{\partial^{\mathrm{RS}}\underline{t}^{S_1}}{\partial\underline{\varphi}^{S_1}} = -\begin{pmatrix} s^{S_1}_{\mathrm{t_x}\phi_\mathrm{x}} & 0 & 0 \\ 0 & s^{S_1}_{\mathrm{t_y}\phi_\mathrm{y}} & 0 \\ 0 & 0 & s^{S_1}_{\mathrm{t_z}\phi_\mathrm{z}} \end{pmatrix} \cdot \boldsymbol{P}^{S_1}_{\varphi} \; ; \quad \frac{\partial^{\mathrm{RS}}\underline{t}^{S_1}}{\partial\underline{\varrho}^{S_1}} = -\begin{pmatrix} 0 & s^{S_1}_{\mathrm{t_x}\rho_\mathrm{y}} & 0 \\ s^{S_1}_{\mathrm{t_y}\rho_\mathrm{x}} & 0 & 0 \\ 0 & 0 & 0 \end{pmatrix} \cdot \boldsymbol{P}^{S_1}_{\varrho}$$

$$\frac{\partial^{\mathrm{RS}}\underline{f}^{S_1}}{\partial\underline{\varphi}^{S_1}} = -\begin{pmatrix} 0 & s^{S_1}_{\mathrm{f_x}\phi_\mathrm{y}} & 0 \\ s^{S_1}_{\mathrm{f_y}\phi_\mathrm{x}} & 0 & 0 \\ 0 & 0 & 0 \end{pmatrix} \cdot \boldsymbol{P}^{S_1}_{\varphi} \; ; \qquad \frac{\partial^{\mathrm{RS}}\underline{f}^{S_1}}{\partial\underline{\varrho}^{S_1}} = -\begin{pmatrix} s^{S_1}_{\mathrm{f_x}\rho_\mathrm{x}} & 0 & 0 \\ 0 & s^{S_1}_{\mathrm{f_y}\rho_\mathrm{y}} & 0 \\ 0 & 0 & s^{S_1}_{\mathrm{f_z}\rho_\mathrm{z}} \end{pmatrix} \cdot \boldsymbol{P}^{S_1}_{\varrho} \tag{3.86}$$

The stiffness parameters are derived via the bending theory for slender beams under the assumption of a prismatic flexible beam with diameter equal to the tower bottom diameter D_b and length Z_e equal to $\mu \cdot D_\mathrm{b}$. The bending and coaxial stiffness values are EI_b, GI_p and EA, which pertain to the elastic behaviour of the tower bottom. For the coaxial stiffness parameters holds:

$$\begin{aligned} s^{S_1}_{\mathrm{f_x}\rho_\mathrm{x}} &= \frac{EA}{Z_\mathrm{e}} \\ s^{S_1}_{\mathrm{t_x}\phi_\mathrm{x}} &= \frac{GI_\mathrm{p}}{Z_\mathrm{e}} \end{aligned} \tag{3.87}$$

with E the elastic modulus, G the shear modulus, A the tower bottom surface $\frac{1}{4}\pi(D_\mathrm{b}^2 - (D_\mathrm{b} - \delta_\mathrm{b})^2$ and I_p the polar moment of inertia.

For the derivation of the bending stiffness paramaters, assume the bending force f_y and bending torque t_x in the tower base, that is to say Z_e m from the *fictitious* tower base. Note that a force along the y-axis deforms the shaft in the same direction as a torque along the x-axis (same orientation for 'linear and angular bending along the y-axis and x-axis'). The angular and linear displacement in $s = Z_\mathrm{e}$ relative to the fictitious turbine base yields the 'inverse stiffness relationship':

$$\begin{bmatrix} \varphi_\mathrm{x}(Z_\mathrm{e}) \\ \varrho_\mathrm{y}(Z_\mathrm{e} \end{bmatrix} = \begin{pmatrix} \frac{Z_\mathrm{e}}{EI_\mathrm{b}} & \frac{Z_\mathrm{e}^2}{2EI_\mathrm{b}} \\ \frac{Z_\mathrm{e}^2}{2EI_\mathrm{b}} & \frac{Z_\mathrm{e}^3}{3EI_\mathrm{b}} \end{pmatrix} \cdot \begin{bmatrix} f_\mathrm{y} \\ t_\mathrm{x} \end{bmatrix} \tag{3.88}$$

The inverse yields the pursued bending stiffness parameters for 'linear and angular bending along the y- and x-axis':

$$\begin{pmatrix} s^{S_1}_{\mathrm{t_x}\phi_\mathrm{x}} & s^{S_1}_{\mathrm{t_x}\rho_\mathrm{y}} \\ s^{S_1}_{\mathrm{f_y}\phi_\mathrm{x}} & s^{S_1}_{\mathrm{f_y}\rho_\mathrm{y}} \end{pmatrix} = \begin{pmatrix} \frac{4EI_\mathrm{b}}{Z_\mathrm{e}} & -\frac{6EI_\mathrm{b}}{Z_\mathrm{e}^2} \\ -\frac{6EI_\mathrm{b}}{Z_\mathrm{e}^2} & \frac{12EI_\mathrm{b}}{Z_\mathrm{e}^3} \end{pmatrix} \tag{3.89}$$

For the remaining bending stiffness parameters holds because of axi-symmetry and the reverse orientation of 'linear and angular bending along the x- and y-axis':

$$\begin{pmatrix} s^{S_1}_{\mathrm{t_y}\phi_\mathrm{y}} & s^{S_1}_{\mathrm{t_y}\rho_\mathrm{x}} \\ s^{S_1}_{\mathrm{f_x}\phi_\mathrm{y}} & s^{S_1}_{\mathrm{f_x}\rho_\mathrm{x}} \end{pmatrix} = \begin{pmatrix} s^{S_1}_{\mathrm{t_x}\phi_\mathrm{x}} & -s^{S_1}_{\mathrm{t_x}\rho_\mathrm{y}} \\ -s^{S_1}_{\mathrm{f_y}\phi_\mathrm{x}} & s^{S_1}_{\mathrm{f_y}\rho_\mathrm{y}} \end{pmatrix} \tag{3.90}$$

The co-axial and bending stiffness parameters are used in Eq. 3.86 for the sensitivities of the responsive loads to the dof subvectors in S_1.

(ii) free, flexible or controlled yawing and roll and tilt flexibility
The responsive force and torque loads can be visco-elastic in three directions each while the responsive torque along the (co-axial) z-axis is the yaw actuation torque t_{yw} if active yaw control is applied. No cross couplings are assumed between a pair of an angular and linear dof on the one side and a pair of a visco-elastic responsive force and torque on the other side.

In case of active yaw control, the control system yields a co-axial 'counter torque' t_{yw} on the nacelle: if > 0 it will turn the nacelle back towards its initial position when the actual deviation $\varphi_{\mathrm{yw}} > 0$ (clockwise deviation at top-down view on tower). The responsive torque load ${}^{\mathrm{RS}}t_3^{S_M}$ then amounts to minus the 'counter clockwise oriented yaw actuation torque' t_{yw}

The implemented yawing torque control system in TURBU Offshore represents
- the servo behaviour for yawing torque setpoint;
- the feedback of yaw angle deviations.

The transfer function formulation for the behaviour of the yawing torque control system is:

$$t_{\mathrm{yw}} = \left(\frac{1}{s^2/\omega_{\mathrm{yw}_0}^2+2\cdot\beta_{\mathrm{yw}}s/\omega_{\mathrm{yw}_0}+1}\right)\cdot K_{\mathrm{yw}}\cdot\left(\frac{\tau_{\mathrm{iyw}}\cdot\frac{\mathrm{d}}{\mathrm{d}t}+1}{\tau_{\mathrm{iyw}}\cdot\frac{\mathrm{d}}{\mathrm{d}t}}\right)\cdot\left(\frac{b_n\cdot\frac{\mathrm{d}^n}{\mathrm{d}t^n}+\ldots+b_1\cdot\frac{\mathrm{d}}{\mathrm{d}t}+1}{a_n\cdot\frac{\mathrm{d}^n}{\mathrm{d}t^n}+\ldots+a_1\cdot\frac{\mathrm{d}}{\mathrm{d}t}+1}\right)\cdot\varphi_{\mathrm{yw}} \tag{3.91}$$

The natural frequency ω_{yw_0} and exponential damping rate β_{yw} characterise the servo behaviour of the actuator for the yawing torque. These values depend on the applied actuator.

The gain K_{yw} represents the proportional feedback gain while τ_{iyw} represent the integral time-constant for the zero-offset regulation of the yaw angle deviation φ_{yw}. The (generalised) filter parameters $b_n \ldots b_1,\ a_n \ldots a_1$ allow the control system to be active only in a certain frequency range and may add some additional feedback dynamics. These control parameters are to be derived with a control design tool.

(iii) co-axial support torque control on gearbox
A gearbox torque control system generates a co-axial 'counter torque' t_{gb} on the gearbox house: if > 0 it will turn the gearbox house back towards its initial position when the actual displacement $\varphi_{\mathrm{gb}} > 0$.

The implemented gearbox torque control system in TURBU Offshore represents
- the servo behaviour for gearbox support torque setpoint;
- the feedback of angular gearbox displacements.

The transfer function formulation for the behaviour of the gearbox torque control system is:

$$t_{\mathrm{gb}} = \left(\frac{1}{s^2/\omega_{\mathrm{gb}_0}^2+2\cdot\beta_{\mathrm{gb}}s/\omega_{\mathrm{gb}_0}+1}\right)\cdot K_{\mathrm{gb}}\cdot\left(\frac{\tau_{\mathrm{igb}}\cdot\frac{\mathrm{d}}{\mathrm{d}t}+1}{\tau_{\mathrm{igb}}\cdot\frac{\mathrm{d}}{\mathrm{d}t}}\right)\cdot\left(\frac{b_n\cdot\frac{\mathrm{d}^n}{\mathrm{d}t^n}+\ldots+b_1\cdot\frac{\mathrm{d}}{\mathrm{d}t}+1}{a_n\cdot\frac{\mathrm{d}^n}{\mathrm{d}t^n}+\ldots+a_1\cdot\frac{\mathrm{d}}{\mathrm{d}t}+1}\right)\cdot\varphi_{\mathrm{gb}} \tag{3.92}$$

The radiated natural frequency ω_{gb_0} and exponential damping rate β_{gb} characterise the servo behaviour of the actuator for the gearbox torque. These values depend

on the applied actuator.

The gain K_{gb} represents the proportional feedback gain while $\tau_{\mathrm{i_{gb}}}$ represent the integral time-constant for the zero-offset regulation of the gearbox house deviation φ_{gb}. The (generalised) filter parameters $b_n \ldots b_1,\ a_n \ldots a_1$ enable to have the control system only active in a certain frequency range and may add some additional feedback dynamics. These control parameters are to be derived with a control design tool.

3.8.3 Hydrodynamic loads

The hydrodynamic loads are modelled as concentrated loads in the 'hydrodynamic conversion points' of the tower elements. These conversion points are in the (spanwise) middle of element S_2 up to $S_{M_{\mathrm{uw}}}$ and at the bottomside of S_1. These locations result from the applied mapping mechanism for the by nature distributed hydrodynamics loads on the elements and the layout of the multi-body model. See intro in section B.7 for the multi-body model layout and the mapping mechanism that is based on slender beam bending theory equivalency.

(i) General expressions distributed hydrodynamic loads
The hydrodynamic load distribution over the under water section of the tower is expressed in the speed and acceleration of the waves and the tower elements via the drag and mass coefficient. The load is a (horizontal) force per unit tower length that points along the x-axis of the hydrodynamic coordinate system $\vec{e}^{\,H}$. We define the coordinate vector $\underline{q}_{\mathrm{f}}^{S_k^{\mathrm{h}}}$ to contain the horizontal load component in the first location. With $\boldsymbol{C}_{\mathrm{V}}^{S_k}$ and $\boldsymbol{C}_{\mathrm{M}}^{S_k}$ the 'hydrodynamic viscous and mass coefficient matrices', the expression for $\underline{q}_{\mathrm{f}}^{S_k^{\mathrm{h}}}$ becomes:

$$\underline{q}_{\mathrm{f}}^{S_k^{\mathrm{h}}} \triangleq \begin{bmatrix} q_{\mathrm{horz}}^{S_k^{\mathrm{h}}} \\ 0 \\ 0 \end{bmatrix} = \tfrac{1}{2}\rho_{\mathrm{H}} \cdot D^{S_k^{\mathrm{h}}} \cdot \boldsymbol{C}_{\mathrm{V}}^{S_k} \cdot (|\underline{w}^{S_k^{\mathrm{h}}}|. \times \underline{w}^{S_k^{\mathrm{h}}}) + \tfrac{1}{4}\rho_{\mathrm{H}} \cdot \pi (D^{S_k^{\mathrm{h}}})^2 \cdot \boldsymbol{C}_{\mathrm{M}}^{S_k} \cdot \dot{\underline{w}}^{S_k^{\mathrm{h}}}$$

$$\text{with } \boldsymbol{C}_{\mathrm{V}}^{S_k} = \begin{pmatrix} C_{\mathrm{V}}^{S_k^{\mathrm{h}}} & 0 & 0 \\ 0 & 0 & 0 \\ 0 & 0 & 0 \end{pmatrix} \text{ and } \boldsymbol{C}_{\mathrm{M}}^{S_k} = \begin{pmatrix} C_{\mathrm{M}}^{S_k^{\mathrm{h}}} & 0 & 0 \\ 0 & 0 & 0 \\ 0 & 0 & 0 \end{pmatrix} \tag{3.93}$$

The '. $\times$ ' operation means 'element by element' multiplication.
Parameters $C_{\mathrm{V}}^{S_k^{\mathrm{h}}}$ and $C_{\mathrm{M}}^{S_k^{\mathrm{h}}}$ are the hydrodynamic viscous and mass coeffient for element S_k in under water level of the hydrodynamic conversion point S_k^{h}. Parameter $D^{S_k^{\mathrm{e}}}$ is the tower diameter in that under water level; ρ_{H} is the specific mass of the water.

For the relative wave speed and wave acceleration vector hold:

$$\begin{aligned} \underline{w}^{S_k} &= \begin{bmatrix} w_{\mathrm{horz}}^{S_k^{\mathrm{h}}} \\ 0 \\ 0 \end{bmatrix} - {}^{H}\Phi^{S_k} \cdot \underline{v}^{S_k^{\mathrm{h}}} \\ \underline{\dot{w}}^{S_k} &= \begin{bmatrix} \dot{w}_{\mathrm{horz}}^{S_k^{\mathrm{h}}} \\ 0 \\ 0 \end{bmatrix} - \frac{C_{\mathrm{M}}^{S_k^{\mathrm{h}}} - 1}{C_{\mathrm{M}}^{S_k^{\mathrm{h}}}} \cdot {}^{H}\Phi^{S_k} \cdot \underline{a}^{S_k^{\mathrm{h}}} \end{aligned} \tag{3.94}$$

The horizontal wave speed w_{horz} and acceleration $\dot{w}_{\mathrm{horz}}$ pertain to the underwater level for hydrodynamic conversion point S_k^{h} and follow from the wave spectrum and the dispersion relation; see section 10.3 in [5]. The hydrodynamic load is also affected by the tower speed $\underline{v}$ and tower acceleration $\underline{a}$ in the point S_k^{h}.

The orientation of the waves with respect to the turbine foundation element S_{f} *in the undeformed state* (coordinate system $\vec{e}^{\,S_0}$ follows from the direction angle of the horizontal wave speed and the slope and direction of the turbine base (see §3.4.1). This is implemented via the (time-invariant) transformation matrix ${}^{S_0}\Phi^{H}$. Matrix ${}^{S_k}\Phi^{H}$ transforms coordinates along $\vec{e}^{\,H}$ to coordinates along the 'structural tower element coordinate system' $\vec{e}^{\,S_k}$ with co-axial z-axis; the x- and y-axis of $\vec{e}^{\,S_k}$ coincide with the neutral (bending-)elastic axes for sideward and foreaft oriented tower deformation. The matrix depends on soil compliance and tower deformation, and on the orientation difference between the waves and the tower base. It then holds:

$$\begin{aligned} {}^{H}\Phi^{S_0} &= {}^{H}\Phi^{G} \,.\, {}^{G}\Phi^{B} = {}^{G}\Phi^{B} \cdot \left({}^{B}\Phi^{G}\right)^{\mathrm{T}} \\ {}^{H}\Phi^{S_k} &= {}^{H}\Phi^{S_0} \,.\, {}^{S_0}\Phi^{S_k} \end{aligned} \tag{3.95}$$

(ii) Mapping distributed to concentrated hydrodynamic loads

Let ${}^{\mathrm{h}}\underline{f}^{S_k^{\mathrm{h}}}$ and ${}^{\mathrm{h}}\underline{t}^{S_k^{\mathrm{h}}}$ be the coordinates of the concentrated hydrodynamic force and torque in the hydrodynamic conversion point S_k^{h} along the axes of $\vec{e}^{\,S_k}$. The conversion point on the foundation element, S_1, lays in the centre point of the bottom cross section of S_1. The conversion points S_2^{h}... $S_{N_{\mathrm{uw}}}^{\mathrm{h}}$ lay in the centre point 'mid span' of the under water support structure elements S_2 up to $S_{N_{\mathrm{uw}}}$. The expressions for the hydrodynamic *concentrated* load vectors in the *distributed* load vectors are similar to those for the aerodynamic ones. However there is no co-axial hydrodynanmic torque loading and tower bending includes linear displacements along the x- and y-axes instead of the x- and z-axes.

Taking into account that:

- For the blades, positive distributed forces along the x-axis yield negative concentrated torques along the z-axis and positive distributed forces along the z-axis yield positive concentrated torques along the x-axis.
- For the tower, positive distributed forces along the x-axis yield negative concentrated torques along the y-axis and positive distributed forces along the y-axis yield positive concentrated torques along the x-axis.

The expressions for the concentrated hydrodynamic forces are the same as for the concentrated aerodynamic forces, except that distributed torque loading is omitted

and that matrix elements 'on z-axis locations' are shifted to 'y-axis locations': ($1 \leq k+j \leq M_{\mathrm{uw}}$):

$$\begin{aligned} {}^{\mathrm{h}}\underline{f}^{S^{\mathrm{h}}_k} &= \sum_{j=-1}^{1} {}^{\mathrm{h}}G^{\mathrm{F}}_{\mathrm{fq}_{k,j}} \cdot {}^{S_k}\Phi^{H} \cdot \underline{q}_{\mathrm{f}}^{S^{\mathrm{h}}_{k+j}} \\ {}^{\mathrm{h}}\underline{t}^{S^{\mathrm{h}}_k} &= \sum_{j=-1}^{1} {}^{\mathrm{h}}G^{\mathrm{F}}_{\mathrm{tq}_{k,j}} \cdot {}^{S_k}\Phi^{H} \cdot \underline{q}_{\mathrm{f}}^{S^{\mathrm{h}}_{k+j}} \end{aligned} \tag{3.96}$$

The matrices ${}^{\mathrm{h}}G^{\mathrm{F}}_{\mathrm{fq}_{k,j}}$ are determined as follows (replace 'fq' by 'tq' for ${}^{\mathrm{h}}G^{\mathrm{F}}_{\mathrm{tq}_{k,j}}$)

$${}^{\mathrm{h}}G^{\mathrm{F}}_{\mathrm{fq}_{k,j}} = \begin{cases} G^{\mathrm{L_{sh}}}_{\mathrm{fq}} \ , & G^{\mathrm{R_{sh}}}_{\mathrm{fq}} & (k{=}1;\, j{=}0{,}1) \\ G^{\mathrm{L}}_{\mathrm{fq}} \ , & G^{\mathrm{R}}_{\mathrm{fq}} + G^{\mathrm{L_{sh}}}_{\mathrm{fq}} \ , \quad G^{\mathrm{R_{sh}}}_{\mathrm{fq}} & (k{=}2 \ldots M_{\mathrm{uw}}{-}1;\, j{=}{-}1{,}0{,}1) \\ \mu_{M_{\mathrm{uw}}} \cdot G^{\mathrm{L}}_{\mathrm{fq}} \ , & \mu_{M_{\mathrm{uw}}} \cdot G^{\mathrm{R}}_{\mathrm{fq}} & (k{=}M_{\mathrm{uw}};\, j{=}{-}1{,}0) \end{cases} \tag{3.97}$$

The applied matrices only depend on L, being the height of elements S_2 ... $S_{M_{\mathrm{uw}}}$ and twice the height of element S_1:

$$G^{\mathrm{L}}_{\mathrm{fq}} = \begin{pmatrix} 36L/384 & 0 & 0 \\ 0 & 36L/384 & 0 \\ 0 & 0 & 0 \end{pmatrix} \quad G^{\mathrm{R}}_{\mathrm{fq}} = \begin{pmatrix} 156L/384 & 0 & 0 \\ 0 & 156L/384 & 0 \\ 0 & 0 & 0 \end{pmatrix}$$

$$G^{\mathrm{L_{sh}}}_{\mathrm{fq}} = \begin{pmatrix} 156L/384 & 0 & 0 \\ 0 & 156L/384 & 0 \\ 0 & 0 & 0 \end{pmatrix} \quad G^{\mathrm{R_{sh}}}_{\mathrm{fq}} = \begin{pmatrix} 36L/384 & 0 & 0 \\ 0 & 36L/384 & 0 \\ 0 & 0 & 0 \end{pmatrix} \tag{3.98}$$

and:

$$G^{\mathrm{L}}_{\mathrm{tq}} = \begin{pmatrix} 0 & -10L^2/384 & 0 \\ 10L^2/384 & 0 & 0 \\ 0 & 0 & 0 \end{pmatrix} \quad G^{\mathrm{R}}_{\mathrm{tq}} = \begin{pmatrix} 0 & -22L^2/384 & 0 \\ 22L^2/384 & 0 & 0 \\ 0 & 0 & 0 \end{pmatrix}$$

$$G^{\mathrm{L_{sh}}}_{\mathrm{tq}} = \begin{pmatrix} 0 & 22L^2/384 & 0 \\ -22L^2/384 & 0 & 0 \\ 0 & 0 & 0 \end{pmatrix} \quad G^{\mathrm{R_{sh}}}_{\mathrm{tq}} = \begin{pmatrix} 0 & 10L^2/384 & 0 \\ -10L^2/384 & 0 & 0 \\ 0 & 0 & 0 \end{pmatrix} \tag{3.99}$$

The multiplier $\mu_{M_{\mathrm{uw}}}$ for the most upward under water element $S_{M_{\mathrm{uw}}}$ is the ratio between the length of the underwater partition of element $S_{M_{\mathrm{uw}}}$ and half the element length ($L/2$).

Equation 3.96 tells that the concentrated load on S_k depend on the distributed force loads on elements S_{k-1}, S_k and S_{k+1}. Of course, the dependency on $\underline{q}^{S^{\mathrm{h}}_{k-1}}$ does not apply for $k = 1$ and on $\underline{q}^{S^{\mathrm{h}}_{k+1}}$ not for $k = M_{\mathrm{uw}}$. The variation of the concentrated loads is to be expressed in 'internal variables' of the subcomponent and input variables from the neighbouring subcomponents and related to the wind field and wake. This needs to rewrite the equation 3.96. If S_k is the first element of a subcomponent then $\underline{q}^{S^{\mathrm{h}}_{k-1}}$ is fed in from the foregoing subcomponent. If X_k is the last element then $\underline{q}^{S^{\mathrm{h}}_{k+1}}$ is fed in from the subsequent subcomponent. Since the hydrodynamic loads are assumed 'zero-mean', there is no need to feed in the rotation dofs $\phi_v^{S_{k+1}}$ from the subsequent subcomponent via a vector $\underline{\phi}^{S_{\mathrm{PP}}}$. Thus,

(only) the two 'neighbouring' distributed load coordinate vectors are defined as additional input variables to the subcomponent:

$$\begin{aligned} {}^{\mathrm{h}}\underline{q}_{\mathrm{f}}^{S_{\mathrm{FF}}} &\triangleq {}^{\mathrm{h}}\underline{q}_{\mathrm{f}}^{S^{\mathrm{h}}_{k_{\mathrm{FF}}}} \\ {}^{\mathrm{h}}\underline{q}_{\mathrm{f}}^{S^{\ominus}_{\mathrm{PP}}} &\triangleq {}^{\mathrm{h}}\underline{q}_{\mathrm{f}}^{S^{\mathrm{h}}_{k_{\mathrm{PP}}}} \end{aligned} \tag{3.100}$$

In these definitions k_{FF} is the number of the final element in the foregoing subcomponent and k_{PP} of the first element in the subsequent subcomponent (mnemonics '$_{\mathrm{FF}}$' and '$_{\mathrm{PP}}$' for heuristic expressions 'Final Foregoing' and 'Primary Post'). In the pursued expressions for the concentrated loads we will also use the symbols $k^{\oplus}_{\mathrm{FF}}$ and $k^{\ominus}_{\mathrm{PP}}$, which refer to the first and last element in the subcomponent, and the 'generalised Kronecker-delta symbols' $\delta_{i\uparrow j}$ and $\delta_{i\downarrow j}$ (see Eq. 3.53. The equations for the variation of the concentrated loads can now be written as follows (see Eq. 3.54 and 3.55 for the aerodynamic concentrated loads, but note that the hydronamic loads are zero-mean):

$$\begin{aligned} \delta^{\mathrm{h}}\underline{f}^{S^{\mathrm{h}}_k} &= {}^{X}{}_{k}\bar{\Phi}^{X^{\mathrm{cv}}_k} \cdot {}^{\mathrm{h}}G^{\mathrm{F}}_{\mathrm{fq}_{k,0}} \cdot \delta\underline{q}_{\mathrm{f}}^{X^{\mathrm{h}}_k} + \\ &\left(\delta_{(k,k_{\mathrm{FF}}\oplus)} \cdot \delta_{k_{\mathrm{FF}}\downarrow 1} \cdot {}^{S}{}_{k}\bar{\Phi}^{H} \cdot {}^{\mathrm{h}}G^{\mathrm{F}}_{\mathrm{fq}_{k,-1}} \cdot \delta^{\mathrm{h}}\underline{q}_{\mathrm{f}}^{S_{\mathrm{FF}}} + \delta_{k\downarrow k^{\oplus}_{\mathrm{FF}}+1} \cdot {}^{S}{}_{k}\bar{\Phi}^{H} \cdot {}^{\mathrm{h}}G^{\mathrm{F}}_{\mathrm{fq}_{k,-1}} \cdot \delta\underline{q}_{\mathrm{f}}^{S^{\mathrm{h}}_{k-1}}\right) + \\ &\left(\delta_{(k,k^{\ominus}_{\mathrm{PP}})} \cdot \delta_{k_{\mathrm{PP}}\uparrow N} \cdot {}^{S}{}_{k}\Phi^{H} \cdot {}^{\mathrm{h}}G^{\mathrm{F}}_{\mathrm{fq}_{k,+1}} \cdot \delta^{\mathrm{h}}\underline{q}_{\mathrm{f}}^{S^{\ominus}_{\mathrm{PP}}} + \delta_{k\uparrow k^{\ominus}_{\mathrm{PP}}-1} \cdot {}^{S}{}_{k}\bar{\Phi}^{H} \cdot {}^{\mathrm{h}}G^{\mathrm{F}}_{\mathrm{fq}_{k,+1}} \cdot \delta\underline{q}_{\mathrm{f}}^{S^{\mathrm{h}}_{k+1}}\right) \end{aligned} \tag{3.101}$$

and:

$$\begin{aligned} \delta^{\mathrm{h}}\underline{t}^{S^{\mathrm{h}}_k} &= {}^{S}{}_{k}\bar{\Phi}^{H} \cdot {}^{\mathrm{a}}G^{\mathrm{F}}_{\mathrm{tq}_{k,0}} \cdot \delta\underline{q}_{\mathrm{f}}^{X^{\mathrm{h}}_k} + \\ &\left(\delta_{(k,k_{\mathrm{FF}}\oplus)} \cdot \delta_{k_{\mathrm{FF}}\downarrow 1} \cdot {}^{S}{}_{k}\bar{\Phi}^{H} \cdot {}^{\mathrm{h}}G^{\mathrm{F}}_{\mathrm{tq}_{k,-1}} \cdot \delta^{\mathrm{h}}\underline{q}_{\mathrm{f}}^{S_{\mathrm{FF}}} + \delta_{k\downarrow k^{\oplus}_{\mathrm{FF}}+1} \cdot {}^{S}{}_{k}\bar{\Phi}^{H} \cdot {}^{\mathrm{h}}G^{\mathrm{F}}_{\mathrm{tq}_{k,-1}} \cdot \delta\underline{q}_{\mathrm{f}}^{S^{\mathrm{h}}_{k-1}}\right) + \\ &\left(\delta_{(k,k^{\ominus}_{\mathrm{PP}})} \cdot \delta_{k_{\mathrm{PP}}\uparrow N} {}^{S}{}_{k}\Phi^{H} \cdot {}^{\mathrm{h}}G^{\mathrm{F}}_{\mathrm{tq}_{k,+1}} \cdot \cdot \delta^{\mathrm{h}}\underline{q}_{\mathrm{f}}^{S^{\ominus}_{\mathrm{PP}}} + \delta_{k\uparrow k^{\ominus}_{\mathrm{PP}}-1} \cdot {}^{S}{}_{k}\bar{\Phi}^{H} \cdot {}^{\mathrm{h}}G^{\mathrm{F}}_{\mathrm{tq}_{k,+1}} \cdot \delta\underline{q}_{\mathrm{f}}^{S^{\mathrm{h}}_{k+1}}\right) \end{aligned} \tag{3.102}$$

The use of the (generalised) kronecker-delta functions and the feed-in loads from the neighbouring elements to the subcomponent guarantees the use of distributed load variations that are *available* within the subcomponent.

4. LOAD CALCULATION

This chapter describes the calculation of the steady state and the dynamic loading. The dynamic loading is subdivided into periodic and stochastic loading.

The calculation of loads in the frequency domain involves the transformation of the power spectrum and coherence function of the wind turbulence and waves to the power spectra of forces and torques. In addition the (almost) periodic loads are to be determined from the azimut dependent gravity loading and wind speed variations caused by wind shear, oblique inflow and tower shadow. These loads, together with the mean loads, are to be linked together in order to assess the fatigue loading, usually via rainflow counting.

The first section deals with the mean loads, which are derived from the time-average turbine state. This average turbine state also provides the required working point dependent parameters of the component models for the linearised dynamic behaviour. The component models are created in accordance with the implementation descriptions in Appendix A.

Before the dynamic load calculations can be performed, the component models must be linked together and are to be made feasible for frequency domain analysis. The latter is catered for by the elimination of the periodic model coefficients via a multi-blade coordinate transformation as proposed by Coleman & Feingold [3]; this is subject of section 4.2. In order to speed up the computations, it is possible to reduce the orders of the component models for the rotor blades and the tower; a feasible method is the one proposed by Craig & Bamption [7], which is subject of section 4.3.

The last three sections of this chapter pertain to the calcalation of the stochastic and periodic loads and to the fatigue assessment on the obtained results.

4.1 Mean loads

The average turbine state involves the mean values for the loads, deformations and induction speeds. The induction speeds are obtained by solving the non-linear equations of equilibrium for the axial and tangential impulse in the rotor annuli in accordance with the BEM theory. This is done in conjuntion with solving the static bending and distorsion equations for the blades, rotor shaft and support structure. See also section 2.2.1 and section 3.5. However, mean loads also arise from loads that periodic in a rotating coordinate system but are invariant in a stand still coordinate system. These are all lumped together in the feedthrough loads by the drive-train on the support structure.

Point of departure for the mean feedthrough loads by the drive-train on the support structure is the time-average of the transformation from the coordinate system on the gearbox slow shaft to that of the gearbox house by Eq. A.22 (time-average

demodulated loads from drive-train):

$$\begin{bmatrix} {}^{\mathrm{FT}}\underline{\bar{f}}^{S^{\oplus}_{\tilde{\mathrm{n}}}R_{\mathrm{r}}} \\ {}^{\mathrm{FT}}\underline{\bar{t}}^{S^{\oplus}_{\tilde{\mathrm{n}}}R_{\mathrm{r}}} \\ {}^{\mathrm{FT}}\underline{\bar{t}}^{S^{\oplus}_{\tilde{\mathrm{n}}}R_{\mathrm{f}}} \end{bmatrix} = \overline{\begin{pmatrix} \Phi^{\mathrm{T}}_{\mathrm{x}}(\bar{\Omega}t) & \mathrm{O} & \mathrm{O} \\ \mathrm{O} & \Phi^{\mathrm{T}}_{\mathrm{x}}(\bar{\Omega}t) & \mathrm{O} \\ \mathrm{O} & \mathrm{O} & \Phi^{\mathrm{T}}_{\mathrm{x}}(\bar{\Omega}t) \end{pmatrix} \cdot \begin{bmatrix} {}^{\mathrm{FT}}\underline{f}^{S^{\oplus}_{\tilde{\mathrm{n}}}R_{\mathrm{r}}} \\ {}^{\mathrm{FT}}\underline{t}^{S^{\oplus}_{\tilde{\mathrm{n}}}R_{\mathrm{r}}} \\ {}^{\mathrm{FT}}\underline{t}^{S^{\oplus}_{\tilde{\mathrm{n}}}R_{\mathrm{f}}} \end{bmatrix}} \tag{4.1}$$

Combination of Eq. A.188 and A.196 on the one side and Eq. A.197 and A.216 on the other side yields the required expression for the non-demodulated loads from the drive-train:

$$\begin{bmatrix} {}^{\mathrm{FT}}\underline{f}^{S^{\oplus}_{\tilde{\mathrm{n}}}R_{\mathrm{r}}} \\ {}^{\mathrm{FT}}\underline{t}^{S^{\oplus}_{\tilde{\mathrm{n}}}R_{\mathrm{r}}} \\ {}^{\mathrm{FT}}\underline{t}^{S^{\oplus}_{\tilde{\mathrm{n}}}R_{\mathrm{f}}} \end{bmatrix} = \begin{pmatrix} \boldsymbol{I} & \mathrm{O} \\ \mathrm{O} & \boldsymbol{T}_{\mathrm{gb_s}} \\ \mathrm{O} & \boldsymbol{T}_{\mathrm{gb_f}} \end{pmatrix} \cdot \begin{bmatrix} {}^{R_{\mathrm{s}}}\Phi^{R_{\mathrm{r}}} \cdot \left(-\underline{\dot{p}}^{R_{\mathrm{r}}} + {}^{\mathrm{g}}\underline{f}^{R^{*}_{\mathrm{r}}} + \sum_{b=1}^{3} \Phi_{1b} \cdot {}^{\mathrm{FT}}\underline{f}^{X_{b_{\mathrm{PP}(1)}}}\right) \\ {}^{R_{\mathrm{s}}}\Phi^{R_{\mathrm{r}}} \cdot \left(-{}^{R^{\mathrm{c}}_{\mathrm{r}}}\underline{\dot{h}}^{R_{\mathrm{r}}} + {}^{R^{\mathrm{c}}_{\mathrm{r}}}\underline{r}^{R^{*}_{\mathrm{r}}} \times {}^{\mathrm{g}}\underline{f}^{R^{*}_{\mathrm{r}}} + \sum_{b=1}^{3} \Phi_{1b} \cdot {}^{\mathrm{FT}}\underline{t}^{X_{b_{\mathrm{PP}(1)}}}\right) \end{bmatrix} \tag{4.2}$$

The demodulation matrix $\Phi^{\mathrm{T}}_{\mathrm{x}}(\bar{\Omega}t)$ can be decomposed into an invariant part and two harmonic parts as in Eq. 3.65. This enables to split up the feedthrough loads from the drive train into a mean and periodic part when the mean loads on the support structure are considered. For the mean feedthrough torque from the rotor shaft then holds:

$$\begin{aligned} {}^{\mathrm{FT}}\underline{\bar{t}}^{S^{\oplus}_{\tilde{\mathrm{n}}}R_{\mathrm{r}}} &= \Phi^{\mathrm{T}}_{\mathrm{d}} \cdot {}^{\mathrm{FT}}\underline{\bar{t}}^{S^{\oplus}_{\tilde{\mathrm{n}}}R_{\mathrm{r}}} + \Phi^{\mathrm{T}}_{\mathrm{c}} \cdot \overline{\cos\bar{\Omega}t \cdot \delta^{\mathrm{FT}}\underline{t}^{S^{\oplus}_{\tilde{\mathrm{n}}}R_{\mathrm{r}}}_{\mathrm{per}}} + \Phi^{\mathrm{T}}_{\mathrm{s}} \cdot \overline{\sin\bar{\Omega}t \cdot \delta^{\mathrm{FT}}\underline{t}^{S^{\oplus}_{\tilde{\mathrm{n}}}R_{\mathrm{r}}}_{\mathrm{per}}} \\ \text{with } \delta^{\mathrm{FT}}\underline{t}^{S^{\oplus}_{\tilde{\mathrm{n}}}R_{\mathrm{r}}}_{\mathrm{per}} &= \boldsymbol{T}_{\mathrm{gb_s}} \cdot {}^{R_{\mathrm{s}}}\Phi^{R_{\mathrm{r}}} \cdot \left({}^{R^{\mathrm{c}}_{\mathrm{r}}}\underline{r}^{R^{*}_{\mathrm{r}}} \times \delta^{\mathrm{g}}\underline{f}^{R^{*}_{\mathrm{r}}}_{\mathrm{per}} + \sum_{b=1}^{B} \Phi_{1b} \cdot \delta^{\mathrm{FT}}\underline{t}^{X_{b_{\mathrm{PP}(1)}}}_{\mathrm{per}}\right) \end{aligned} \tag{4.3}$$

See Eq. A.197 ahd A.199 for the first term in the right hand side of the expression for ${}^{\mathrm{FT}}\underline{\bar{t}}^{S^{\oplus}_{\tilde{\mathrm{n}}}R_{\mathrm{r}}}$ (also for ${}^{\mathrm{FT}}\underline{\bar{f}}^{S^{\oplus}_{\tilde{\mathrm{n}}}R_{\mathrm{r}}}$).

The mean rate of change of impulse coordinates along a *stand still* coordinate system in average sense like $\vec{e}^{\,R_{\mathrm{h}}}$ of course always equal zero.

The periodic feedthrough torque $\delta^{\mathrm{FT}}\underline{t}^{X_{b_{\mathrm{PP}(1)}}}_{\mathrm{per}}$ from rotor blade X_b in the rotor centre has aerodynamic and gravition contributions. See Eq. A.117, A.104 and A.73, A.56, A.56 for the composition of feedthrough loads in the rotor blades.

The periodic terms in the aerodynamic forces concern variations in the normal and leadwise directed forces on the blade elements. For a rotation symmetric turbine rotor (three or more blades) these periodic force variations do *not* result in mean load coordinates along the stand still coordinate system $\vec{e}^{\,R_{\mathrm{h}}}$.

The periodic gravity force variations on the rotor blade elements *do* result in mean coordinates along $\vec{e}^{\,R_{\mathrm{h}}}$. For the periodic feedthrough forces from the rotor blades

by gravitation into the rotor centre holds (coordinates along blade base c.s. ${}^{X_{b_0}}\vec{e}$):

$$\begin{aligned}
\delta^{\mathrm{FT_g}}\underline{f}_{\mathrm{per}}^{X_{b_{\mathrm{PP}(1)}}} &= \sum_{k=1}^{N} m^{X_k}\cdot\Phi_{b1}\cdot{}^{R_\mathrm{r}}\bar{\Phi}^{R_\mathrm{s}}\cdot(\Phi_\mathrm{c}\cdot\cos\bar{\Omega}t+\Phi_\mathrm{s}\cdot\sin\bar{\Omega}t)\cdot\underline{\bar{g}}^{R_{\mathrm{h''}}}\\
\delta^{\mathrm{FT_g}}\underline{t}_{\mathrm{per}}^{X_{b_{\mathrm{PP}(1)}}} &= \sum_{k=1}^{N}(R_{\mathrm{root}}\cdot\underline{e}_2+\sum_{j=1}^{k}{}^{X_0}\bar{\Phi}^{X_j}\cdot{}^{X_j^{\ominus}}\underline{r}^{X_{j|k}^{\oplus|*}})\times\\
&\qquad (m^{X_k}\cdot\Phi_{b1}\cdot{}^{R_\mathrm{r}}\bar{\Phi}^{R_\mathrm{s}}\cdot(\Phi_\mathrm{c}\cdot\cos\bar{\Omega}t+\Phi_\mathrm{s}\cdot\sin\bar{\Omega}t)\cdot\underline{\bar{g}}^{R_{\mathrm{h''}}})
\end{aligned}\tag{4.4}$$

Place vector ${}^{X_j^{\ominus}}\underline{r}^{X_{j|k}^{\oplus|*}}$ points to exit point $X_j^{\oplus}$ if $j<k$ and to c.o.g. X_j^* if $j=k$.

See Eq. B.277 for the mean gravitation vector $\underline{\bar{g}}^{R_{\mathrm{h''}}}$ along $\vec{e}^{\,R_{\mathrm{h''}}}$.

If we now consider the expression above for $\delta^{\mathrm{FT_g}}\underline{t}_{\mathrm{per}}^{X_{b_{\mathrm{PP}(1)}}}$ in the second and third term in the right hand side of Eq. 4.3 then time-averaging implies the following

- harmonic product $\cos\bar{\Omega}t\cdot\sin\bar{\Omega}t$ yields multiplier 0;
- harmonic products $\cos\bar{\Omega}t\cdot\cos\bar{\Omega}t$ and $\sin\bar{\Omega}t\cdot\sin\bar{\Omega}t$ yield multiplier $\frac{1}{2}$

Together with the expression for the periodic rotor shaft gravity torque loading,

$${}^{R_\mathrm{r}^\mathrm{c}}\underline{r}^{R_\mathrm{r}^*}\times\delta^{\mathrm{g}}\underline{f}_{\mathrm{per}}^{R_\mathrm{r}^*}={}^{R_\mathrm{r}^\mathrm{c}}\underline{r}^{R_\mathrm{r}^*}\times m^{R_\mathrm{r}}\cdot{}^{R_\mathrm{r}}\bar{\Phi}^{R_\mathrm{s}}\cdot(\Phi_\mathrm{c}\cdot\cos\bar{\Omega}t+\Phi_\mathrm{s}\cdot\sin\bar{\Omega}t)\cdot\underline{\bar{g}}^{R_{\mathrm{h''}}}\tag{4.5}$$

it holds for the contribution of the periodic gravity loads on the rotor blades to the mean torque along $\vec{e}^{\,R_\mathrm{h}}$ in the rotor centre:

$$\begin{aligned}
&\Phi_\mathrm{c}^{\mathrm{T}}\cdot\overline{\cos\bar{\Omega}t\cdot\delta^{\mathrm{FT}}\underline{t}_{\mathrm{per}}^{S_{\tilde{\mathrm{n}}}^{\oplus}R_\mathrm{r}}}+\Phi_\mathrm{s}^{\mathrm{T}}\cdot\overline{\sin\bar{\Omega}t\cdot\delta^{\mathrm{FT}}\underline{t}_{\mathrm{per}}^{S_{\tilde{\mathrm{n}}}^{\oplus}R_\mathrm{r}}}=\\
&\quad\tfrac{1}{2}\Phi_\mathrm{c}^{\mathrm{T}}\cdot\boldsymbol{T}_{\mathrm{gb_s}}\cdot{}^{R_\mathrm{s}}\bar{\Phi}^{R_\mathrm{r}}\cdot({}^{R_\mathrm{r}^\mathrm{c}}\underline{r}^{R_\mathrm{r}^*}\times m^{R_\mathrm{r}}\cdot{}^{R_\mathrm{r}}\bar{\Phi}^{R_\mathrm{s}}\cdot\Phi_\mathrm{c}\cdot\underline{\bar{g}}^{R_{\mathrm{h''}}})+\\
&\quad\tfrac{1}{2}\Phi_\mathrm{s}^{\mathrm{T}}\cdot\boldsymbol{T}_{\mathrm{gb_s}}\cdot{}^{R_\mathrm{s}}\bar{\Phi}^{R_\mathrm{r}}\cdot({}^{R_\mathrm{r}^\mathrm{c}}\underline{r}^{R_\mathrm{r}^*}\times m^{R_\mathrm{r}}\cdot{}^{R_\mathrm{r}}\bar{\Phi}^{R_\mathrm{s}}\cdot\Phi_\mathrm{s}\cdot\underline{\bar{g}}^{R_{\mathrm{h''}}})+\\
&\quad\tfrac{1}{2}\Phi_\mathrm{c}^{\mathrm{T}}\cdot\boldsymbol{T}_{\mathrm{gb_s}}\cdot{}^{R_\mathrm{s}}\bar{\Phi}^{R_\mathrm{r}}\cdot(\sum_{b=1}^{B}\Phi_{1b}\cdot\sum_{k=1}^{N}(R_{\mathrm{root}}\cdot\underline{e}_2+\sum_{j=1}^{k}{}^{X_{b_0}}\bar{\Phi}^{X_{b_j}}\cdot{}^{X_{b_j}^{\ominus}}\underline{r}^{X_{b_{j|k}}^{\oplus|*}})\times\\
&\qquad\qquad m^{X_{b_k}}\cdot\Phi_{b1}\cdot{}^{R_\mathrm{r}}\bar{\Phi}^{R_\mathrm{s}}\cdot\Phi_\mathrm{c}\cdot\underline{\bar{g}}^{R_{\mathrm{h''}}})+\\
&\quad\tfrac{1}{2}\Phi_\mathrm{s}^{\mathrm{T}}\cdot\boldsymbol{T}_{\mathrm{gb_s}}\cdot{}^{R_\mathrm{s}}\bar{\Phi}^{R_\mathrm{r}}\cdot(\sum_{b=1}^{B}\Phi_{1b}\cdot\sum_{k=1}^{N}(R_{\mathrm{root}}\cdot\underline{e}_2+\sum_{j=1}^{k}{}^{X_{b_0}}\bar{\Phi}^{X_{b_j}}\cdot{}^{X_{b_j}^{\ominus}}\underline{r}^{X_{b_{j|k}}^{\oplus|*}})\times\\
&\qquad\qquad m^{X_{b_k}}\cdot\Phi_{b1}\cdot{}^{R_\mathrm{r}}\bar{\Phi}^{R_\mathrm{s}}\cdot\Phi_\mathrm{s}\cdot\underline{\bar{g}}^{R_{\mathrm{h''}}})
\end{aligned}\tag{4.6}$$

For the mean feedthrough force on the support strcuture by the rotor shaft R_r a much simpler expression holds. Note that

$$\Phi_\mathrm{c}^{\mathrm{T}}\cdot\Phi_\mathrm{c}=\Phi_\mathrm{s}^{\mathrm{T}}\cdot\Phi_\mathrm{s}=\begin{pmatrix}0&0&0\\0&1&0\\0&0&1\end{pmatrix}\tag{4.7}$$

so that:

$$\begin{aligned}
&\Phi_\mathrm{c}^{\mathrm{T}}\cdot\overline{\cos\bar{\Omega}t\cdot\delta^{\mathrm{FT}}\underline{f}_{\mathrm{per}}^{S_{\tilde{\mathrm{n}}}^{\oplus}R_\mathrm{r}}}+\Phi_\mathrm{s}^{\mathrm{T}}\cdot\overline{\sin\bar{\Omega}t\cdot\delta^{\mathrm{FT}}\underline{f}_{\mathrm{per}}^{S_{\tilde{\mathrm{n}}}^{\oplus}R_\mathrm{r}}}=\\
&\qquad\begin{pmatrix}0&0&0\\0&1&0\\0&0&1\end{pmatrix}\cdot(m^{R_\mathrm{r}}+\sum_{b=1}^{B}\sum_{k=1}^{N}m^{X_{b_k}})\cdot\underline{\bar{g}}^{R_{\mathrm{h''}}}
\end{aligned}\tag{4.8}$$

For the mean feedthrough torque by the generator rotor $R_{\rm f}$, there are no contributions from periodic rotor blade loading as only the co-axial torque is non-zero.

4.2 Multi-blade coordinate transformation

In general, the equations of motion in the fixed frame of reference will have periodic coefficients which make them not suitable for well-known solution procedures for systems of ordinary first order differential equations. Because of the polar symmetry of rotors with three or more identical blades a simple transformation – the so-called multi-blade transformation – can eliminate the periodic coefficients in the homogeneous equations, see Coleman & Feingold [3]. Here, we also subject the input and output variables to this multi-blade transformation, which eliminates the periodic coefficients from the 'particular equations' as well.

In our model structure, the homogeneous equations correspond to the first order state transition model, which is completely defined in the state transition matrix $\boldsymbol{A}$ of the state space representation. The 'particular equations' correspond to the dynamic input/output behaviour in which all parameter matrices of the state space representation play a role.

The time-invariancy of the 'particular equations' allows straightforwad mapping of the power spectra of the wind and wave variations towards the power spectra of the blade and tower loads via linear constant transfer functions. The only price to be payed for the elminated periodic coefficients consists in the consideration of modulated inputs and outputs.

Linking together the submodels of the rotating and standstill model partition of the wind turbine yields a linear model with a time-dependent coupling in the rotor azimut angle $\psi_{\rm r}$.

$$\begin{array}{rcl} \underline{\dot{z}} & = & \boldsymbol{A}(\psi_{\rm r}) \cdot \underline{z} + \boldsymbol{B}(\psi_{\rm r}) \cdot \underline{v} \\ \underline{y} & = & \boldsymbol{C}(\psi_{\rm r}) \cdot \underline{z} + \boldsymbol{K}(\psi_{\rm r}) \cdot \underline{v} \end{array} \tag{4.9}$$

The link of the rotating to the standstill model partition is performed for a chosen, fixed, value of the azimut angle, say $\bar{\psi}$ in M-function TBUSYSFSR(). The resulting parameter matrices $\boldsymbol{A}$, $\boldsymbol{B}$, $\boldsymbol{C}$ and $\boldsymbol{K}$ all will depend on the value of $\bar{\psi}$. These parameter matrices are to be pre- and postmultiplied with matrices that also depend on $\bar{\psi}$, vizually in accordance with the Coleman & Feingold transformation [3]. For 3 blades or more, the inverse of the Coleman transformation matrices $T_{z_{\rm cm}}$, $T_{v_{\rm cm}}$ and $T_{y_{\rm cm}}$ maps variables with coordinates in a rotating coordinate system, that is to say the rotor and drive-train variables, to variabales in a non-rotating coordinate system; variables with 'non-rotating' coordinates are left unchanged. Then, the parameter matrices $\boldsymbol{A}_{\rm cm}$, $\boldsymbol{B}_{\rm cm}$, $\boldsymbol{C}_{\rm cm}$ and $\boldsymbol{K}_{\rm cm}$ that are obtained from the scheme below do *not* depend on $\bar{\psi}$:

$$\begin{array}{rcl} \boldsymbol{A}_{\rm cm} & = & T_{z_{\rm cm}}^{-1}(\bar{\psi}) \cdot \Big(\boldsymbol{A}(\bar{\psi}) \cdot T_{z_{\rm cm}}(\bar{\psi}) - \dot{T}_{z_{\rm cm}} \Big) \\ \boldsymbol{B}_{\rm cm} & = & T_{z_{\rm cm}}^{-1}(\bar{\psi}) \cdot \boldsymbol{B}(\bar{\psi}) \cdot T_{v_{\rm cm}}(\bar{\psi}) \\ \boldsymbol{C}_{\rm cm} & = & T_{y_{\rm cm}}^{-1}(\bar{\psi}) \cdot \boldsymbol{C}(\bar{\psi}) \cdot T_{z_{\rm cm}}(\bar{\psi}) \\ \boldsymbol{K}_{\rm cm} & = & T_{y_{\rm cm}}^{-1}(\bar{\psi}) \cdot \boldsymbol{K}(\bar{\psi}) \cdot T_{v_{\rm cm}}(\bar{\psi}) \end{array} \tag{4.10}$$

These matrices parametrise the following linear time invariant system with modulated pre- and postprocessing:

$$\begin{aligned} \underline{\epsilon} &= T_{v_{\rm cm}}^{-1}(\psi_{\rm r}) \cdot \underline{v} \quad ; \quad \underline{\dot{q}} = \boldsymbol{A}_{\rm cm} \cdot \underline{q} + \boldsymbol{B}_{\rm cm} \cdot \underline{\epsilon} \\ & \qquad\qquad \underline{\eta} = \boldsymbol{C}_{\rm cm} \cdot \underline{q} + \boldsymbol{K}_{\rm cm} \cdot \underline{\epsilon} \quad ; \quad \underline{y} = T_{y_{\rm cm}}(\psi_{\rm r}) \cdot \underline{\eta} \end{aligned} \tag{4.11}$$

For a 3-bladed rotor the blade-related state variables are to be processed 'in sets of 3' with the *inverse* of the Coleman transformation matrix-kernels. This means that each subvector of corresponding state variables on the 3 blades, such as the flatwise angular deformation in the entry point of a blade element, is mapped to a state subvector of the pursued linear time-invariant model ('Coleman-model') by premultiplication with a 3×3 matrix. The 'real-life' corresponding blade states z^D, z^E, z^F are mapped as follows to the Coleman-model blade states q_1, q_2, q_3:

$$\begin{bmatrix} q_1 \\ q_2 \\ q_3 \end{bmatrix} = \begin{pmatrix} \frac{1}{3} & \frac{1}{3} & \frac{1}{3} \\ \frac{2}{3}\sin(\psi_{\rm r}) & \frac{2}{3}\sin(\psi_{\rm r}+\frac{2}{3}\pi) & \frac{2}{3}\sin(\psi_{\rm r}+\frac{4}{3}\pi) \\ \frac{2}{3}\cos(\psi_{\rm r}) & \frac{2}{3}\cos(\psi_{\rm r}+\frac{2}{3}\pi) & \frac{2}{3}\cos(\psi_{\rm r}+\frac{4}{3}\pi) \end{pmatrix} \cdot \begin{bmatrix} z^D \\ z^E \\ z^F \end{bmatrix} \tag{4.12}$$

For the drive-train related state variables, it matters if they represent coordinates of quantities along the x-, y- or z-coordinate of the rotating coordinate system on the rotor shaft. The x-, y- and z-coordinates are to be processed with the 1st, 2nd and 3rd row of the *inverse* of the transformation matrix over the rotor shaft azimut angle along the x-axis. So the Coleman-model drive-train states q_1, q_2, q_3 are obtained from the real-life states $z_{\rm x}^{R_{\rm r}}$, $z_{\rm y}^{R_{\rm r}}$, $z_{\rm z}^{R_{\rm r}}$, vizually the angular and linear shaft deformation degrees of freedom, by:

$$\begin{bmatrix} q_1 \\ q_2 \\ q_3 \end{bmatrix} = \begin{pmatrix} 1 & 0 & 0 \\ 0 & \cos(\psi_{\rm r}) & -\sin(\psi_{\rm r}) \\ 0 & \sin(\psi_{\rm r}) & \cos(\psi_{\rm r}) \end{pmatrix} \cdot \begin{bmatrix} z_{\rm x}^{R_{\rm r}} \\ z_{\rm y}^{R_{\rm r}} \\ z_{\rm z}^{R_{\rm r}} \end{bmatrix} \tag{4.13}$$

The Coleman-model can be used for load calculation if the blade- and drive-train related inputs are *azimut-dependent preprocessed* (wind speed variations, periodic gravity loading), and if the blade- and drive-train related outputs *azimut-dependent postprocessed* (blade loads and motion, main shaft deformation); see Eq. 4.11.

For a 3-bladed rotor, the blade-related inputs are to be 'preprocessed' 'in sets of 3' with the *inverse* of the Coleman transformation matrix-kernels. This means that each subvector of corresponding input quantities on the 3 blades, such as a wind velocity coordinate in the 'conversion coordinate system' of a blade element, is to be premultiplied with 3×3 matrix before it is used as input to the obtained linear time-invariant model. The 'real-life' corresponding blade inputs v^D, v^E, v^F are mapped as follows to the 'Coleman-model' blade inputs ϵ_1, ϵ_2, ϵ_3:

$$\begin{bmatrix} \epsilon_1 \\ \epsilon_2 \\ \epsilon_3 \end{bmatrix} = \begin{pmatrix} \frac{1}{3} & \frac{1}{3} & \frac{1}{3} \\ \frac{2}{3}\sin(\psi_{\rm r}) & \frac{2}{3}\sin(\psi_{\rm r}+\frac{2}{3}\pi) & \frac{2}{3}\sin(\psi_{\rm r}+\frac{4}{3}\pi) \\ \frac{2}{3}\cos(\psi_{\rm r}) & \frac{2}{3}\cos(\psi_{\rm r}+\frac{2}{3}\pi) & \frac{2}{3}\cos(\psi_{\rm r}+\frac{4}{3}\pi) \end{pmatrix} \cdot \begin{bmatrix} v^D \\ v^E \\ v^F \end{bmatrix} \tag{4.14}$$

Inversely, each subvector of real-life blade outputs on the corresponding blades, say y^D, y^E, y^F, is obtained from the Coleman-model blade output subvector η_1,

η_2, η_3 via the 3×3 Coleman transformation matrix-kernel itself:

$$\begin{bmatrix} y^D \\ y^E \\ y^F \end{bmatrix} = \begin{pmatrix} 1 & \sin(\psi_{\mathrm{r}}) & \cos(\psi_{\mathrm{r}}) \\ 1 & \sin(\psi_{\mathrm{r}} + \frac{2}{3}\pi) & \cos(\psi_{\mathrm{r}} + \frac{2}{3}\pi) \\ 1 & \sin(\psi_{\mathrm{r}} + \frac{4}{3}\pi) & \cos(\psi_{\mathrm{r}} + \frac{4}{3}\pi) \end{pmatrix} \cdot \begin{bmatrix} \eta_1 \\ \eta_2 \\ \eta_3 \end{bmatrix} \tag{4.15}$$

Drive-train inputs and outputs, which exist as coordinates along the rotating coordinate system on the rotor shaft, are also pre- and postprocessed. However, for these variables, the x-, y- and z-coordinates are to be processed with the 1st, 2nd and 3rd row of (the inverse, in case of inputs, of) the transformation matrix over the rotor shaft azimut angle along the x-axis. So the Coleman-model drive-train inputs ϵ_1, ϵ_2, ϵ_3 are obtained from the real-life inputs $v_{\mathrm{x}}^{R_{\mathrm{r}}}$, $v_{\mathrm{y}}^{R_{\mathrm{r}}}$, $v_{\mathrm{z}}^{R_{\mathrm{r}}}$ by:

$$\begin{bmatrix} \epsilon_1 \\ \epsilon_2 \\ \epsilon_3 \end{bmatrix} = \begin{pmatrix} 1 & 0 & 0 \\ 0 & \cos(\psi_{\mathrm{r}}) & -\sin(\psi_{\mathrm{r}}) \\ 0 & \sin(\psi_{\mathrm{r}}) & \cos(\psi_{\mathrm{r}}) \end{pmatrix} \cdot \begin{bmatrix} v_{\mathrm{x}}^{R_{\mathrm{r}}} \\ v_{\mathrm{y}}^{R_{\mathrm{r}}} \\ v_{\mathrm{z}}^{R_{\mathrm{r}}} \end{bmatrix} \tag{4.16}$$

and the Coleman-model drive-train outputs η_1, η_2, η_3 are mapped to real-life outputs $y_{\mathrm{x}}^{R_{\mathrm{r}}}$, $y_{\mathrm{y}}^{R_{\mathrm{r}}}$, $y_{\mathrm{z}}^{R_{\mathrm{r}}}$ by:

$$\begin{bmatrix} y_{\mathrm{x}}^{R_{\mathrm{r}}} \\ y_{\mathrm{y}}^{R_{\mathrm{r}}} \\ y_{\mathrm{z}}^{R_{\mathrm{r}}} \end{bmatrix} = \begin{pmatrix} 1 & 0 & 0 \\ 0 & \cos(\psi_{\mathrm{r}}) & \sin(\psi_{\mathrm{r}}) \\ 0 & -\sin(\psi_{\mathrm{r}}) & \cos(\psi_{\mathrm{r}}) \end{pmatrix} \cdot \begin{bmatrix} \eta_1 \\ \eta_2 \\ \eta_3 \end{bmatrix} \tag{4.17}$$

The proof that the azimuth dependency in the left hand side of Eq. 4.11 is eliminated by the transformation matrices in accordance with the submatrices in Eq. 4.12 ... 4.17 is not stated here. A generic proof is based on manually tracing a number of interactions between the rotating and standstill part and linking each interacting variable to a specific input, state or output variable.

4.3 Order reduction in substructure models

The approach adopted to the dynamic analysis of the complete structure is a method proposed by Graig and Bampton [7]. The method is closely related to a method proposed by Hurty [8, 9], known as *component-mode synthesis*, and a similar method developed by Gladwell [6], generally referred to as *branch-mode analysis*. The method allows to significantly reduce the degrees of freedom in the blade and tower model without loss of accuracy in the dynamic behaviour of the first two to four bending modes.

All methods have in common that the structure is regarded as a collection of substructures and, in the spirit of Rayleigh-Ritz, the motion of each substructure is represented by a linear combination of 'component modes'. The methods differ to some extent in the definition of the modes, but in general one assumes that they are generated by solving some form of substructure eigenvalue problem.

In the component mode synthesis method (Hurty [8]) the system equations of motion are derived by first deriving the equations of motion of each individual substructure separately and then coupling the equations by subjecting them

to given constraints, where the latter reflect the interacting forces between the various substructures. The motion of each substructure is described in terms of 'component modes', which are divided into three classes, namely, rigid-body modes, constraint modes and normal modes. The motion is represented by a linear combination of the component modes multiplied by time-dependent generalised coordinates. Integration over each substructure permits the derivation of the substructure Lagrange's equations. Then, the equations of motion for the entire structure are obtained in terms of the system generalised coordinates by assembling. The method is essentially a Rayleigh-Ritz type discretisation procedure, combined with truncation at the substructure level. It is a way of simulating complex structures by only a limited number of degrees of freedom.

The above procedure makes a sharp distinction between determinate and indeterminate constraints. In reality no such distinction exists and all boundary constraints should really receive equal treatment. This is the essence of an idea advanced by Graig and Bampton [7], who suggest that all constraints can be regarded as boundary constraints and there is no need to identify rigid-body modes specifically. It is only necessary to distinguish between external and internal degrees of freedom. The constraint modes are defined as the mode shapes due to successive unit displacements at the boundary points. The interior modes are simply the normal modes of the substructure with totally constrained boundary nodal points. The method is generally referred to as 'fixed constraint mode' method, because the modes used to describe the motion corresponds to fixed constraints. For more details the reader is referred to the paper by Graig and Bampton [7].

4.4 Stochastic loads from turbulence and waves

The required input spectrum matrix $\boldsymbol{S}$ pertains to the longitudinal wind turbulence ${}^{\mathrm{t}}u^{W_m/X}$ as experienced on the rotating blades $\{X\}$ and the wave speed w and acceleration $\dot{w}$. As a logical consequence of the Blade Elementum Momentum theory, the turbulence is considered in the intersections of the blades with a discrete number of rotor annuli (P). The hydrodynamic conversion is also discretised; each of the N_{uw} underwater elements of the support structure is linked to a water segment in which identical wave behaviour is assumed.

The stochastic consideration of the longitudinal turbulence for the average rotor speed $\bar{\Omega}$ then yields a $B\cdot P\times B\cdot P$ spectrum matrix that accounts for the rotational sampling effect. For the waves a $2\cdot N_{\mathrm{uw}}\times 2\cdot N_{\mathrm{uw}}$ spectrum matrix results, which includes the correlation between the horizontal wave speed and acceleration. The overall input spectrum matrix for a 3-bladed rotor then looks like:

$$\boldsymbol{S}_{\underline{v}\underline{v}}(\omega)=\begin{pmatrix} \boldsymbol{S}_{{}^{\mathrm{t}}\underline{u}^{W/D}{}^{\mathrm{t}}\underline{u}^{W/D}}(\omega) & \boldsymbol{S}_{{}^{\mathrm{t}}\underline{u}^{W/D}{}^{\mathrm{t}}\underline{u}^{W/E}}(\omega) & \boldsymbol{S}_{{}^{\mathrm{t}}\underline{u}^{W/D}{}^{\mathrm{t}}\underline{u}^{W/F}}(\omega) & \mathrm{O} & \mathrm{O} \\ \boldsymbol{S}_{{}^{\mathrm{t}}\underline{u}^{W/E}{}^{\mathrm{t}}\underline{u}^{W/D}}(\omega) & \boldsymbol{S}_{{}^{\mathrm{t}}\underline{u}^{W/E}{}^{\mathrm{t}}\underline{u}^{W/E}}(\omega) & \boldsymbol{S}_{{}^{\mathrm{t}}\underline{u}^{W/E}{}^{\mathrm{t}}\underline{u}^{W/F}}(\omega) & \mathrm{O} & \mathrm{O} \\ \boldsymbol{S}_{{}^{\mathrm{t}}\underline{u}^{W/F}{}^{\mathrm{t}}\underline{u}^{W/D}}(\omega) & \boldsymbol{S}_{{}^{\mathrm{t}}\underline{u}^{W/F}{}^{\mathrm{t}}\underline{u}^{W/E}}(\omega) & \boldsymbol{S}_{{}^{\mathrm{t}}\underline{u}^{W/F}{}^{\mathrm{t}}\underline{u}^{W/F}}(\omega) & \mathrm{O} & \mathrm{O} \\ \mathrm{O} & \mathrm{O} & \mathrm{O} & \boldsymbol{S}_{\underline{w}^S\underline{w}^S}(\omega) & \boldsymbol{S}_{\underline{w}^S\underline{\dot{w}}^S}(\omega) \\ \mathrm{O} & \mathrm{O} & \mathrm{O} & \boldsymbol{S}_{\underline{\dot{w}}^S\underline{w}^S}(\omega) & \boldsymbol{S}_{\underline{\dot{w}}^S\underline{\dot{w}}^S}(\omega) \end{pmatrix} \tag{4.18}$$

The modulation of inputs and outputs that is involved with the Coleman transformed model representation makes the output vector a so called cyclo stationary process. This implies that its covariance function matrix is periodic in the rotational frequency ($T = 2\pi/\bar{\Omega}$). In that case, the spectrum searched for is the Fourier transform of the *period-average* covariance function $\tilde{\boldsymbol{C}}$ (superscript † stands for complex conjugate transpose):

$$\boldsymbol{S}_{\underline{y}\underline{y}}(\omega) = \int_{-\infty}^{\infty} \mathrm{e}^{-\jmath\cdot\omega\tau}\cdot\tilde{\boldsymbol{C}}_{\underline{y}\underline{y}}(\tau)\mathrm{d}\tau \quad \text{with} \quad \tilde{\boldsymbol{C}}_{\underline{y}\underline{y}}(\tau) = \frac{1}{T}\int_0^T \mathrm{E}\left[\underline{y}(t+\tau)\cdot\underline{y}^{\dagger}(t)\right]\mathrm{d}t \tag{4.19}$$

The transfer function matrix $\boldsymbol{H}$ in the frequency domain representation of the Coleman transformed model

$$\underline{\eta}(\omega) = \boldsymbol{H}(\omega)\cdot\underline{\epsilon}(\omega) \quad \text{with} \quad \boldsymbol{H}(\omega) = \boldsymbol{C}_{\mathrm{cm}}\left(\jmath\omega\cdot\boldsymbol{I} - \boldsymbol{A}_{\mathrm{cm}}\right)^{-1}\cdot\boldsymbol{K}_{\mathrm{cm}}\ , \tag{4.20}$$

together with the coefficient matrices $\hat{\boldsymbol{U}}_m$ and $\hat{\boldsymbol{\Gamma}}_n$ in the Fourier series formulation of the input and output modulation

$$\underline{\epsilon}(t) = \sum_{m=-1}^{1}\hat{\boldsymbol{U}}_m\cdot\mathrm{e}^{\jmath\cdot m\bar{\Omega}t}\cdot\underline{v}(t) \quad ; \quad \underline{y}(t) = \sum_{n=-1}^{1}\hat{\boldsymbol{\Gamma}}_n\cdot\mathrm{e}^{\jmath\cdot n\bar{\Omega}t}\cdot\underline{\eta}(t)\ , \tag{4.21}$$

are the building blocks for mapping the input spectrum to the output spectrum:

$$\begin{aligned}\boldsymbol{S}_{\underline{y}\underline{y}}(\omega) = \sum_{n=-1}^{1}\sum_{m=-1}^{1}\sum_{\nu=-1}^{1}\sum_{\mu=-1}^{1}\hat{\boldsymbol{\Gamma}}_n\cdot\boldsymbol{H}(\omega-n\bar{\Omega})\cdot\hat{\boldsymbol{U}}_m\cdot \\ \boldsymbol{S}_{\underline{v}\underline{v}}(\omega-(n+m)\bar{\Omega})\cdot\hat{\boldsymbol{U}}_{\mu}^{\dagger}\cdot\boldsymbol{H}^{\dagger}(\omega-n\bar{\Omega})\cdot\hat{\boldsymbol{\Gamma}}_{\nu}^{\dagger}\end{aligned} \tag{4.22}$$

with all combinations of n, m, ν and μ excluded for which $n+m-\nu-\mu \neq 0$.

4.5 Periodic loads from gravitation, wind shear, tower shadow and oblique inflow

The periodic gravitation influence on the rotor blades can be modelled via a 3-coordinate vector per blade with non-zero periodic coordinate values in the span- and leaadwise direction of the blade root ($\underline{g}_{\mathrm{per}}^{D_0}$ for blade D). The periodic wind speed variations will differ over the blade elements and thus require a specific vector per blade element. Thus the periodic wind speed variations are modelled in a large vector per blade with $3\cdot N$ coordinates ($\underline{u}_{\mathrm{per}}^{D}$ for blade D). The overall periodic input vector is the 'stack' of the blade indivual periodic gravitation and wind speed vectors and can be written as Fourier series with coefficent vectors $\underline{\hat{v}}_\ell$ of dimension $B\cdot 3\cdot(N+1)$. For a 3-bladed rotor the periodic input vector looks like:

$$\underline{v}_{\mathrm{per}}(t) = \begin{bmatrix}\underline{g}_{\mathrm{per}}^{D_0}(t)\\ \underline{u}_{\mathrm{per}}^{D}(t)\\ \underline{g}_{\mathrm{per}}^{E_0}(t)\\ \underline{u}_{\mathrm{per}}^{E}(t)\\ \underline{g}_{\mathrm{per}}^{F_0}(t)\\ \underline{u}_{\mathrm{per}}^{FD}(t)\end{bmatrix} = \sum_{\ell=-L}^{L}\underline{\hat{v}}_\ell\cdot\mathrm{e}^{\jmath\cdot\ell\bar{\Omega}t} \tag{4.23}$$

The required modulation for the input vector of the Coleman transformed model yields a Fourier series with coefficients $\underline{\hat{\epsilon}}_k$ ranging from $-L-1$ to $L+1$:

$$\underline{\epsilon}_{\rm per}(t) \;=\; \sum_{k=-L-1}^{L+1} \underline{\hat{\epsilon}}_k \cdot {\rm e}^{\jmath \cdot k\bar{\Omega}t} \quad \text{with} \;\; \underline{\hat{\epsilon}}_k \;=\; \sum_{m=\max(-1,k-L)}^{\min(1,k-L)} \hat{\boldsymbol{U}}_m \cdot \underline{\hat{v}}_{k-m} \tag{4.24}$$

The desired periodic output variables are obtained as a Fourier series with coefficient vectors $\underline{\hat{y}}_p$ that range from $-L-2$ to $L+2$. The determination of $\underline{\hat{y}}_p$ requires the availability of the Fourier coefficient vectors $\underline{\hat{\eta}}_k$ of the Coleman model output variables. The latter follow straightforward from the input Fourier coefficients $\underline{\hat{\epsilon}}_k$ via the transfer function matrix $\boldsymbol{H}$ in the very frequency $k\bar{\Omega}$ for $k = p - n$:

$$\underline{y}_{\rm per}(t) \;=\; \sum_{p=-L-2}^{L+2} \underline{\hat{y}}_p \cdot {\rm e}^{\jmath \cdot p\bar{\Omega}t} \quad \text{with} \;\; \underline{\hat{y}}_p = \sum_{n=\max(-1,p-L-1)}^{\min(1,p-L-1)} \hat{\boldsymbol{\Gamma}}_n \cdot \boldsymbol{H}((p-n)\bar{\Omega}) \cdot \underline{\hat{\epsilon}}_{p-n} \tag{4.25}$$

4.6 Assessment of the fatigue loading

The usual way to assess the fatigue loading occurs via rainflow counting on load histories, which resuls in load histograms. The load histories can be obtained from the mean values, power spectra and Fourier series for the periodic loads. Stochastic time series can be generated from the power spectra via a so called realisation algorithm.

The generation of contemparary load histories on different spots or in different directions in a cross section requires a realisation algorithm that also accounts for the cross power spectra between the loads. These cross power spectra are available via the off-diagonal elements of the output spectrum matrix. Such a multivariable realisation algorithm is also used for the generation of stochastic wind fields, e.g. as implemented in the computer program SWIFT [13].

Next to this approach, direct translation of power spectra into load histograms is possible. This is common practice in conventional offshore engineering, in which the fatigue governing loads are purely stochastic. Algorithms are e.g. provided by Dirlik and examined for application on wind turbines [2]. If however the mean and periodic loads have considerable influence on the fatigue damage, it is recommended to apply this approach carefully.

5. INPUT AND OUTPUT DATA

This chapter describes the program input and output data. Section 5.1 deals with the data to be supplied by the user and how these data are mapped to model parameters for use in the steady state and dynamic analysis. Section 5.2 describes the program output.

5.1 User input

The input to be supplied by the user pertains to:
- turbine rotor [with pitch control]
- drive-train [with generator control [and gearbox support control]]
- support structure [with yaw control]
- site and average environmental conditions

5.1.1 Turbine rotor parameters

The required program input for the turbine rotor consists of a 'master data file', the M-script `<TurbineIdf>_xdata.m`. This M-script contains
- direct specifications of lumped parameters via 'assignment statements';
- indirect specifications of cross sectional or tabular data via 'lists with filenames'.

This program input is processed into intermediate ASCII-format data files with parameters that pertain to the elements of the implemented multi-body blade model. The following intermediate files apply (dimensions only listed if non-SI):
- `<TurbineIdf>_xgeomaero.dat`: chord length, twist and cone angle
- `<TurbineIdf>_xgeommech.dat`: distance to the profile nose and to the chord of the elastic axis and the centre of gravity axis as well as the co-axial deviation relative to the chord of the neutral elastic z-axis (nelze) and the principle inertia z-axis; the nelza-angle allows for letting differ the 'aerodynamic pitch' (twist) from the 'structural pitch' angle;
- `<TurbineIdf>_xdeform.dat`: moments of inertia for flatwise, edgewise and co-axial deformation and the elasticity and shear modulus;
- `<TurbineIdf>_xmotion.dat`: mass 'per unit span' and moments of inertia per unit span for flatwise, edgewise and co-axial angular motion;
- `<TurbineIdf>_rprofile.dat`: ranking number per spanwise location in the lists of provided files with lift, drag and pitch moment coefficient data.

Contents description of master file `<TurbineIdf>_xdata.m`:

`Nelm, B`
: Number of elements in the multi-body blade models; number of rotor blades.

`NbyNann`
: Specifies rotor annuli; each rotor annulus exactly encapsulates `NbyNann` blade elements.

`Spanb [m]; Rroot [m]; muRroot4Fp [-]`
: Netto blade length (does not include blade root); length of blade root; fraction of blade root length that is used in Prandtl's correction factor for the blade root (usually 0.5).

`mbb [kg]; yXcog [m]`
Netto mass rotor blade; spanwise distance from blade flange to centre of gravity of blade.

`phiCone, phiDelta3 [dg]`
Cone angle and 'delta$_3$' angle of the rotor blades.

`FlagStrucPitch [0/1]`
Flag for taking into account structural pitch of the rotor blades.

`FlagFlatBlade, FlagEdgeBlade, FlagTorsBlade [0/1]`
Flags for taking into account flatwise, edgewise and co-axial blade deformation.

`shingeflap, shingelead, shingepitch [Nm/rad]`
stiffness values for the flapping, lagging and pitching hinge in the blade flange; if specified `Inf` then no degree of freedom (rigid); `shingepitch` can also be specified `NaN`, which implies pitch control.

`s2dBlade, s2dHinge [(Nm/rad)/(Nm/(rad/s))]`
ratio between stiffness and damper constants in attachments of blade elements; `s2dBlade` pertains to the blade profile & structure X_{p}; `s2dHinge` to the flange X_{f}; if specified `Inf` then zero damping applies; they have no meaning at rigid blades or no hinges; `s2dHinge` has no meaning in pitching direction if pitch control applies.

`AlfaMin, AlfaMax [dg]; Naoa`
Minimum and maximum value for the angle of attack in the profile coefficient tables to be created for the blade elements; number of angle of attakc values in these tables.

`ae_file`
Name of file with aerodynamic blade data. The file referred to must contain ASCII-format columns with repectively radial locations [m], chord lengths [m], relative thickness values [%], aerodynamic pitch angle values [dg], offset values [m] of the aerodynamic centre relative to the elastic centre in chordwise direction and perpendicular to the chordwise direction.

`xst_file`
Name of file with structural blade data. The file referred to must contain ASCII-format columns with repectively radial locations [m], mass per unit values [m/kg], offset values [m] of the centre of gravity relative to the elastic centre, inertia radii [m] for flat- and edgwise blade motion, offset values [m] of the shearing centre relative to the elastic centre (not used), elasticity and shear modulus [N/m^2], inertia moments [m^4] for flatwise, edgewise and co-axial deformation, shear factors [-] for forces in z and x-direction (not used), cross section surface [m^2] and structural pitch angle [dg].

`files4clalfa, files4cdalfa, files4cmalfa`
Lists with names of files with lift, drag and pich moment coefficient data; such a list is a cell string array, e.g.:

```
files4clalfa={'cl_d15.dat','cl_d21.dat','cl_d32.dat','cl_cyl.dat'};
```

The ordering of file names in the list must be such that the profile thickness increases with increasing ranking number in the list. Each file that is referred to must contain to ASCII-format columns with respectively the angle of attack value and profile coefficient values; the data must cover the range {`AlfaMin, AlfaMax`}.

`profthickness [%]`
List with the relative thickness values [%] of the profiles to which the coefficient files in the name lists `files4clalfa, files4cdalfa, files4cmalfa` pertain, e.g.:

```
profthickness = [15, 21, 32, 100];
```

`Komega [rad/(rad/s), TIomega, TDomega, TDdic, TIdic [s]`
proportional control gain of rotor speed feedback and belonging integral and differential time constant; differential and integral time constant in lead-lag filter for dynamic inflow compensation.

`aFiltomega, bFiltomega`
arrays with denemurator and numerator coefficients in descending order for low pass filter in rotor speed control loop

`Kpitch [Nm/rad), TDpitch [s], gamTDpitch [-]`
proportional control gain of servo system for pitch angle control and belonging differential time constant and multiplier for elimination of very high frequent differential action.

5.1.2 Drive-train parameters

The required program input for the drive-train consists of a 'master data file', the M-script `<TurbineIdf>_rdata.m`. This M-script contains

- direct specifications of lumped parameters via 'assignment statements';
- indirect specifications of cross sectional data via a 'filename'.

This program input is processed into lumped parameters for the one-element subcomponents of the drive-train without intermediate data files.

Contents description of master file `<TurbineIdf>_rdata.m`:

`mHub [kg], xyzHubc [m], xyzRre [m], JHubxyz [kgm`^{2}`]`
overall mass of hub, x,y,z-coordinates of centre of gravity of hub relative to yaw axis in acc. with `FlagXNacDownwind, etc.` (see section 5.1.3); dito x,y,z-coordinates of rotor centre relative to yaw-axis; moments of inertia relative to x,y,z-coordinates in acc.with `FlagXNacDownwind, etc.`.

`rng4tors, rng4bend`
range of the length-coordinate along the rotor shaft (starting from the gearbox slow side exit) for determination of the distorsion stiffness; dito range, but now for determination of the bending stiffness.

`dRse2Brc, dShe2Rre [m]`
distance from slow gearbox exit to centre of the main bearing; distance of the end of (the flexible part of) the rotor shaft to the rotor centre

`s2dSh [(Nm/rad) /(Nm/(rad/s))]`
ratio between stiffness and damper constants in the rotor centre that model the rotor shaft flexibility.

`mRh [kg], xyzRh [m], JRhxyz [kgm`^{2}`]`
overall mass of gearbox house, x,y,z-coordinates of centre of gravity of gearbox house relative to yaw axis in acc. with `FlagXNacDownwind, etc.` (see section 5.1.3); moments of inertia relative to x,y,z-coordinates in acc.with `FlagXNacDownwind, etc.`.

`mRf [kg], xyzRf [m], JRfxyz [kgm`^{2}`]; iTr [-]`
overall mass of generator rotor, x,y,z-coordinates of centre of gravity of generator rotor relative to yaw axis in acc. with `FlagXNacDownwind, etc.` (see section 5.1.3); moments of inertia relative to x,y,z-coordinates in acc.with `FlagXNacDownwind, etc.`; gearbox transmission ratio; note that the co-axial moment of inertia represents the **fast shaft equivalent**, so the **real** value.

`sdCtorqRh, sdEtorqRf [Nm/rad, Nm/(rad/s)]`
gearbox house co-axial angular stiffness and damper constant; generator rotor co-axial angular stiffness and damper constant; if specified `Inf` then no degree of freedom; both sdCtorqRh(1) and sdCtorqRf(1) may be specified `Nan`, which implies respectively gearbox support torque control and generator counter torque control.

`rst_file`
Name of file with structural rotor shaft data. The file referred to must contain ASCII-format columns with repectively shaft locations relative to the slow gearbox exit [m], mass per unit values [m/kg], offset values [m] of the centre of gravity relative to the elastic centre, inertia radii [m] for motion in bending directions, offset values [m] of the shearing centre relative to the elastic centre (not used), elasticity and shear modulus [N/m^2], inertia moments [m^4] for bending in two directions (must be equal) and co-axial deformation, shear factors [-] for forces in z and x-direction (not used) and cross section surface [m^2].

`Omega0te [rad/s], Beta0te [-])`
Cut-off frequency and damping rate of generator counter torque servo system.

`Kpow, Ktrs [Nm/(rad/s)`
proportional control gains of rotor speed feedback for electric power control and distorsion reduction.

`aFiltpow, bFiltpow, aFilttrs, bFilttrs`
arrays with denemurator and numerator coefficients in descending order for low-pass filter in electric power control loop and band- or high-bass filter in distorsion rejection control loop

5.1.3 Support structure parameters

The required program input for the support structure consists of a 'master data file', the M-script `<TurbineIdf>_sdata.m`. This M-script contains

- direct specifications of lumped parameters via 'assignment statements';
- indirect specifications of cross sectional data via a 'filename'.

This program input is processed into intermediate ASCII-format data files with parameters that pertain to the elements of the implemented multi-body support structure model. The following intermediate files apply (dimensions only listed if non-SI):

- `<TurbineIdf>_tgeomhydro.dat`: tower diameter and wall thickness
- `<TurbineIdf>_tdeform.dat`: moments of inertia for fore-aft, sidward and co-axial deformation and the elasticity and shear modulus;
- `<TurbineIdf>_tmotion.dat`: mass 'per unit span', additional (water) mass per unit span, and moments of inertia per unit span for fore-aft, sideward and co-axial angular motion;

Contents description of master file `<TurbineIdf>_sdata.m`:

`Melm`
Number of elements in multi-body support structure model

`Ztow, Dbtow, Dttow, Lground [m]; rhoTower [kg/m`^{3}`]`
height up to tower top centre; tower bottom and tower top diameter; length of the (lower) rigid part of the tower; specific tower mass.

`CM, CV [-]; FlagFill [0/1]`
mass constant for water inertia in Morison's equation, drag constant for viscous behaviour water in Morison's equation; flag if tower no/yes (0/1) is filled with water

`FlagFrafTower, FlagSideTower, FlagTorsTower[0/1]`
Flags for taking into account fore-aft, sideward and co-axial tower deformation.

`FlagxNacDownwind, FlagzNacUpward, FlagxNacHoriz [0/1]`
Flags for interpretation of the provided nacelle data:
`FlagxNacDownwind`: x-coord. nacelle points **1/0** $\Leftrightarrow$ **yes/no** down-wind
`FlagzNacUpward`: z-coord. nacelle points **1/0** $\Leftrightarrow$ **yes/no** upward
`FlagxNacHoriz`: x-coord. nacelle is **1/0** $\Leftrightarrow$ **yes/no** horizontal (untilted)

`mNac [kg], xyzcNac [m], JNacxyz [kgm`^{2}`], phiTiltNac [dg]`
overall mass nacelle, x,y,z-coordinates in acc. with `FlagXNacDownwind, etc.` of centre of gravity relative to yaw axis; moments of inertia relative to x,y,z-coordinates in acc.with `FlagXNacDownwind, etc.`; tilt angle of nacelle

`sSnroll, sSntilt, sSnyaw [Nm/rad]`
stiffness values for the rolling, tilting and yawing motion of the nacelle;
if specified `Inf` then no degree of freedom (rigid); `sSnyaw` can also be specified `NaN`, which implies yaw control.

`LbyDbot [m/m]`
ratio of 'underground tower extension' L to tower bottom diameter D for for valuation of (cross-coupled) soil springs (typically ca. 3.5 in offshore conditions); if specified `[]` (empty) then the specified values for `sSfphiD, sSfrhoD [N/m]` are used.

`sSftors [Nm/rad], sSfaxial [N/m]; sSfphiD [Nm/rad], sSfrhoD [N/m]`
stiffness values for the co-axial foundation motion; stiffness values for the fore-aft and sideward foundation motion; if specified `Inf` then no degree of freedom (rigid); if `LbyDbot` specified non-empty then `sSfphiD, sSfrhoD` are overruled by the tower extension modelling approach.

`s2dNac, s2dTow, s2dSf [(Nm/rad)/(Nm/(rad/s))]`
ratio between stiffness and damper constants in attachments of support structure elements; `s2dNAc` pertains to the nacelle S_{n}; `s2dTow` to the tower S_{t}; `s2dSf` to the foundation S_{f}; they have no meaning at rigidly modelled attachments; if specified `Inf` then zero damping applies; `s2dyaw` has no meaning in pitching direction if pitch control applies.

`tst_file`
Name of file with structural tower data. The file referred to must contain ASCII-format columns with repectively height locations [m], mass per unit values [m/kg], offset values [m] of the centre of gravity relative to the elastic centre, inertia radii [m] for fore-aft and sideward tower motion, offset values [m] of the shearing centre relative to the elastic centre (not used), elasticity and shear modulus [N/m^2], inertia moments [m^4] for fore-aft, sideward and co-axial deformation, shear factors [-] for forces in x and y-direction (not used) and cross section surface [m^2].

`Omega0tgb [rad/s], Beta0tgb [-])`
Cut-off frequency and damping rate of gearbox support torque servo system.

`Kgb, TIgb [Nm/(rad/s)`
proportional control gain for gearbox house deviation feedback and belonging integral timeconstant.

`aFiltgb, bFiltgb`
arrays with denemurator and numerator coefficients in descending order for low-pass filter in gearbox house support torque control loop.

`Omega0tyw [rad/s], Beta0tyw [-])`
Cut-off frequency and damping rate of yawing torque servo system.

`Kyw, TIyw [Nm/(rad/s)`
proportional control gain for yaw angle feedback and belonging integral timeconstant.

`aFiltyw, bFiltyw`
arrays with denemurator and numerator coefficients in descending order for low-pass filter in yaw angle control loop.

5.1.4 Site data and average conditions

The required program input for the site and average conditions consists of a 'master data file', the M-script `<TurbineIdf>_odata.m`. This M-script contains

- direct specifications of lumped parameters via 'assignment statements';
- indirect specifications of turbulence and wave data via a 'filename'.

This program input is processed without intermediate data files.

`Prat [W], rho, rhoWater [kgm`^{3}`], depth [m]; grav [m/s`^{2}`]`
rated electric power; specific air mass; specific water mass; average water depth; gravitation

`Vw [m/s], Om [rad/s], Th [dg], eta [-]`
working point values of wind speed, rotor speed and pitch angle; if the pitch angle is specified `Inf` then the aerodynamic equilibrium will be searched for either the maximum power (partial load) or the rated power (full load); overall conversion efficiency (off course not including aerodynamic conversion).

`phiYawNac, phiDirBase, phiTiltBase [dg]`
mean yaw angle nacelle w.r.t. tower top (>0 at clockwise in top-down view); rotation from south-to-north axis to fore/aft direction of undeformed tower (>0 at clockwise orientation in top-down view); rotation from actual fore/aft direction of undeformed tower to the projection on earth of this direction (>0 at upward tilting).

`phiYawNac, phiDirBase, phiTiltBase [dg], alphashear [-]`
wave direction (>0 at clockwise oriented in top-down view); wind slope (>0 at climbing wind velocity); wind direction (>0 at clockwise oriented in top-down view); exponential factor wind shear.

`oturba_file`
Name of file with turbulence data 'a'; it must contain ASCII-format columns with frequency values [Hz] and with auto power spectral densitity values [(m/s)^2/Hz].

`oturbb_file`
Name of file with turbulence data 'b'; it must contain ASCII-format columns frequency values [Hz] and coherence values for first distance value [(m/s)^2/Hz] in column 2, coherence value for second distance value [(m/s)^2/Hz] in column 3, etc.; note that the first row contains in the first location a dummy datapoint, and in the second and further locations the distance values [m] to which the coherence values pertain.

`owave_file`
Name of file with wave data; it must contain ASCII-format columns frequency values [Hz] and auto power spectral densitity values of the water surface elevation [(m/s)^2/Hz]

5.2 Program output

The program output consists of

- power spectra of load signals;
- frequencies, damping rates and mode shapes of modal modes;
- linear parametrisation of the wind turbine model.

5.2.1 power spectra of load signals

The core results of the computer program consist in power spectra of load signals. These are the bending moments and shearing forces in the blade roots, on the tower top and in the turbine base. Auxiliary software modules are provided for reconstruction of time series from the spectra; the rate of correlation between flap- and leadwise blade loading and fore-aft and sideward tower loading is catered for.

5.2.2 Modal modes

The computer program also enables to perform modal mode analysis on the integrated model from which the periodic coefficients have been eliminated (see section 4.2). The model output section provides the displacements of the tower element and nacelle relative to the fixed, geographic, coordinate system and provides the displacements of the rotor blade elements relative to the rotating coordinate system on the rotor hub.

5.2.3 Linear wind turbine parametrisation

As an intermediate result during program execution, a linear model of the wind turbine becoms available. This model can be used for stability analysis in control design and for fast time-domain simulation when the performance of a designed controller is assessed during the iterative controller development process.

6. VERIFICATION

This chapter describes the verification of the computer program TURBU Offshore. The verification pertains to the numerical validity of the software, the accuracy of steady state conditions, the validity of the implemented Craig Bamption model reduction method and the accuracy of the stochastic load calculation.

6.1 Numerical validity software modules

All developed M-functions contain a test section in it. This means that a 'calling protocol' is included in the comments of the function that tells how to test the function. Many tests are based on implementation the same functionality in two ways. One way is the straightforward, easy way; the other way is the more complicated but much more efficient way. In the test call the results are numerically compared. The relative error must amount to approximately 10^{-14} or smaller, as MATLAB works in double precision. Next to these 'all-over tests', each function has always been verified 'by hand' for a very simple, but yet representative, case.

6.2 Steady state conditions

The aerodynamic model that is implemented in TURBU Offshore is the same as that in PHATAS, as far as concerns the behaviour in *unstalled conditions*. The error terms in the axial and tangential impulse balance, which are simultaneously solved, point out if the convergence is sound. These convergence results are stored on file during the determination of the stead state.

6.3 Craig Bampton model reduction

As mentioned in section 3.4, the Craig Bampton model reduction method exloits the so called 'internal modes' of a flexible structure. Figure 6.1 shows for the in-plane tower bending behaviour the two constrained 'static' modes in the left and middel graph and the first three internal modes in the right graph.

The plots in figure 6.2 show the transfer function behaviour from the shearing force 'Dtop' on the tower top to the linear and angular acceleration of the tower top. The dotted lines pertain to the reduced order model; the solid lines to the full order model. The plots in figure 6.3 show the frequency responses on the the bending moment 'Mtop' on the tower top. For a sound coupling of substructure model, these transfer functions of the reduced order model must be correct.

The plots in figure 6.4show the transfer function behaviour from the horizontal wave acceleration in the 'middle-depth' under water level to the linear and angular acceleration of the tower top. The dotted lines pertain to the reduced order model; the solid lines to the full order model. The plots in figure 6.5 show these responses on wave acceleration near the surface level. For a sound propagation of wave influence into the drive-train and rotor, these transfer functions of the reduced order model must be correct.

It is also important that the transfer functions from these excitation signals to the horizontal speed of the under water tower segments is correct for the reduced order model.

The plots in figure 6.6 show the response of the 'middle-depth' and 'surface level' horizontal tower speed to the tower top force 'Dtop', while figure 6.7 show the reponse of these speed signals to the tower top bending moment 'Mtop'.

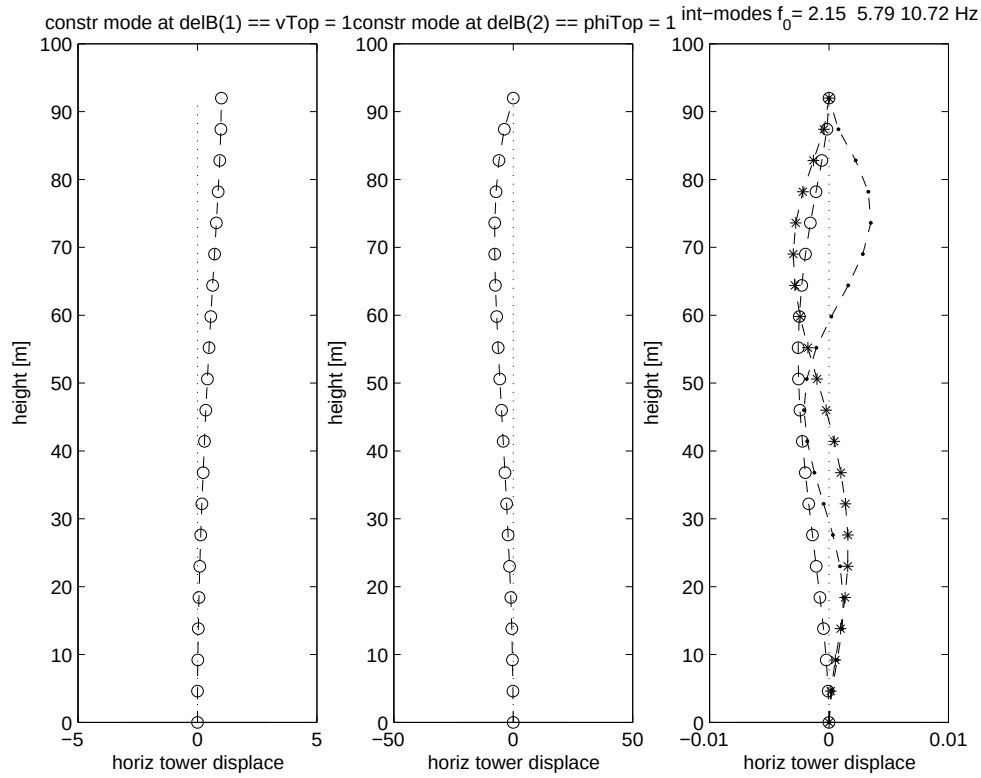

Figure 6.1 *The two constrained and first three internal bending modes*

The plots in figure 6.8 and figure 6.9, show the horizontal tower speed responses for the wave acceleration on 'middle-depth' and 'surface level'.

It can be concluded that all transfer functions to the tower top motions are exact for the considered number of bending modes. Also the approximated dynamic behaviour of the 'surface level' horizontal tower speed is very accurate. Close to the sea-bottom, the approximation is a bit less accurate, but near the eigenfrequencies, the behaviour still agrees very well with the unreduced model.

6.4 Accuracy of stochastic load calculation

The verification of stochastic load calculation has been preliminarily performed. The in-plane overall dynamic wind turbine behaviour had been implemented via the multi-body model method. The transfer function from the generator torque to the main shaft distorsion of the multi-body model was verified against the frequency response that was obtained from a PHATAS run under stochastic conditions. A noise test signal was superponed on the generator torque during the PHATAS simulation. The transfer function from the generator torque to the shaft distorsion in PHATAS was obtained via a Fourier Transform based system identification technique. Figure 6.10 shows the gain and phase shift of both transfer functions.

The dots represent the estimated transfer function from PHATAS; the solid line is the transfer function obtained from straightforward analysis of the available state space model of the multi-body implementation. The two peaks in the reponse represent (i, at 1.7 Hz) the second in-plane tower bending mode that interacts with shaft distorsion and collective

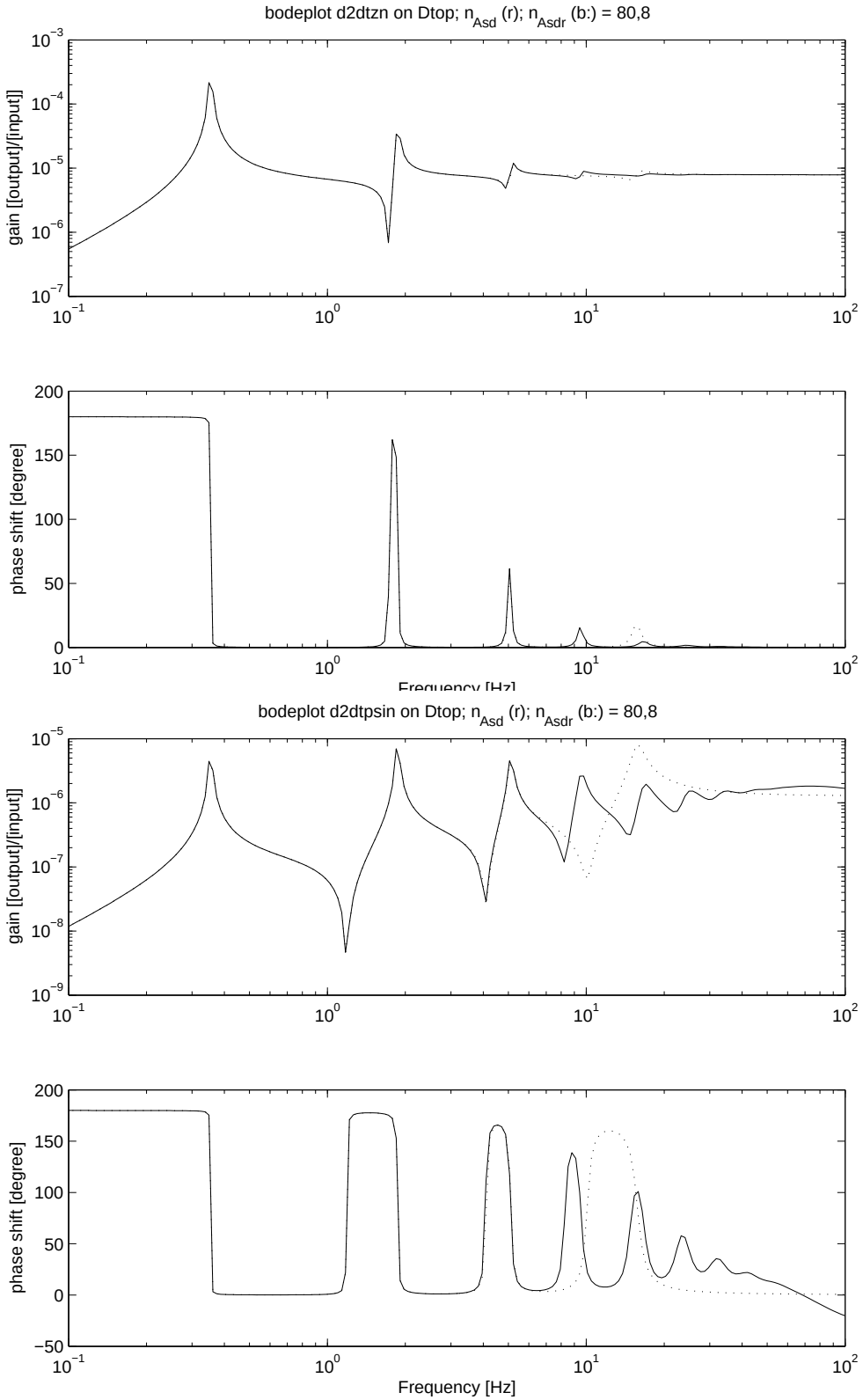

Figure 6.2 *Tower top motion response on shearing force on tower top*

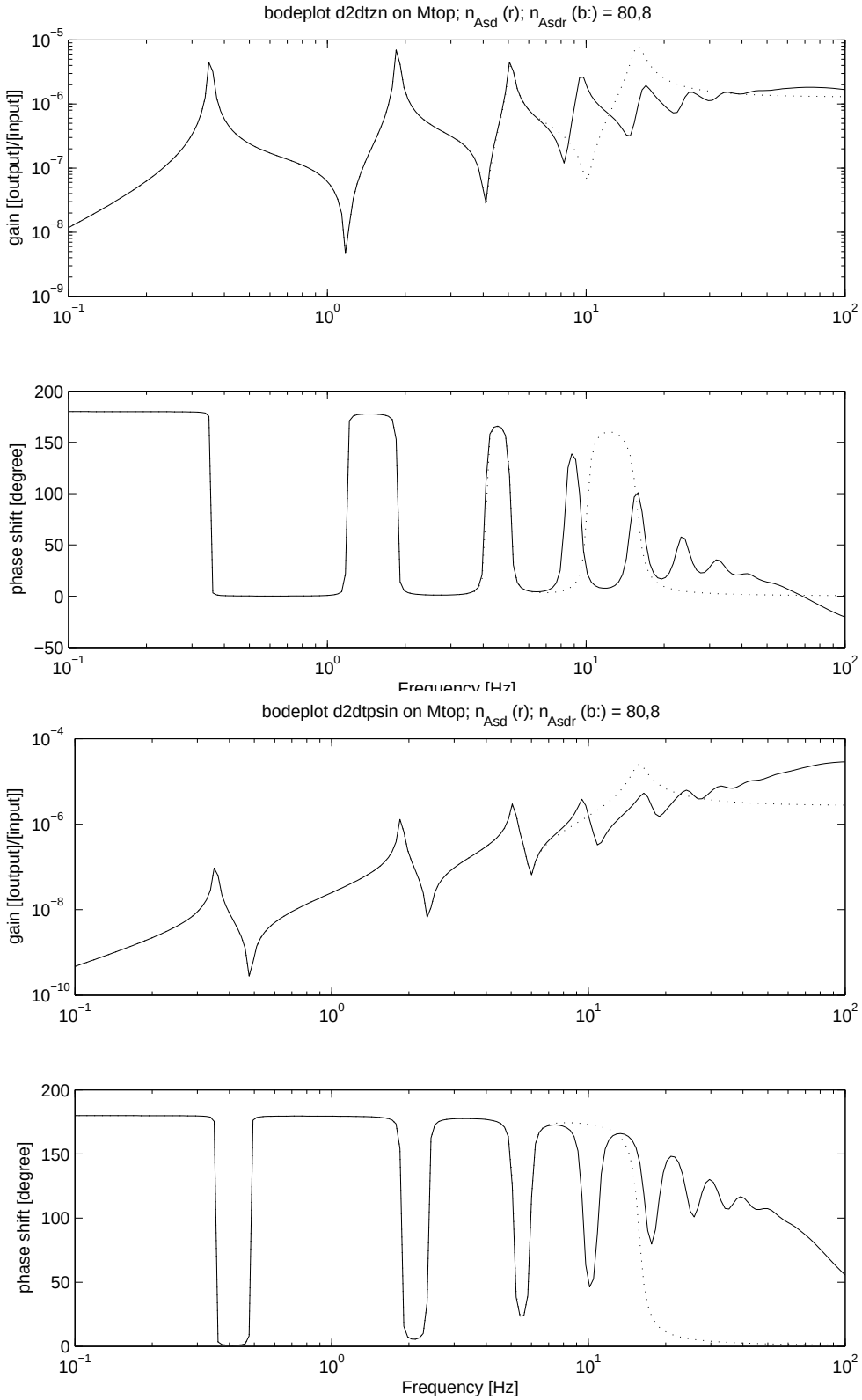

Figure 6.3 *Tower top motion response on bending moment on tower top*

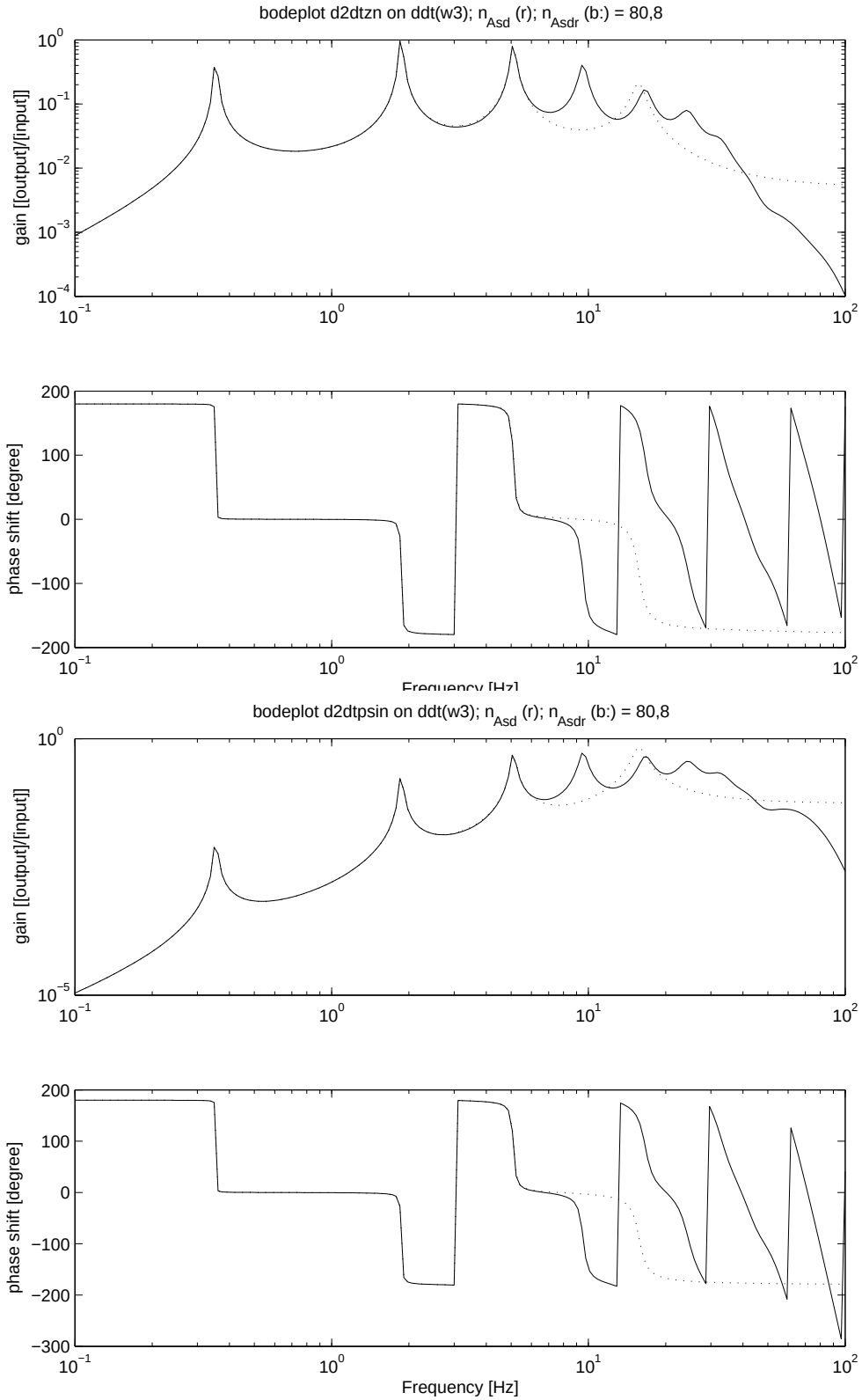

Figure 6.4 *Tower top motion response on 'middle-depth' horizontal wave acceleration*

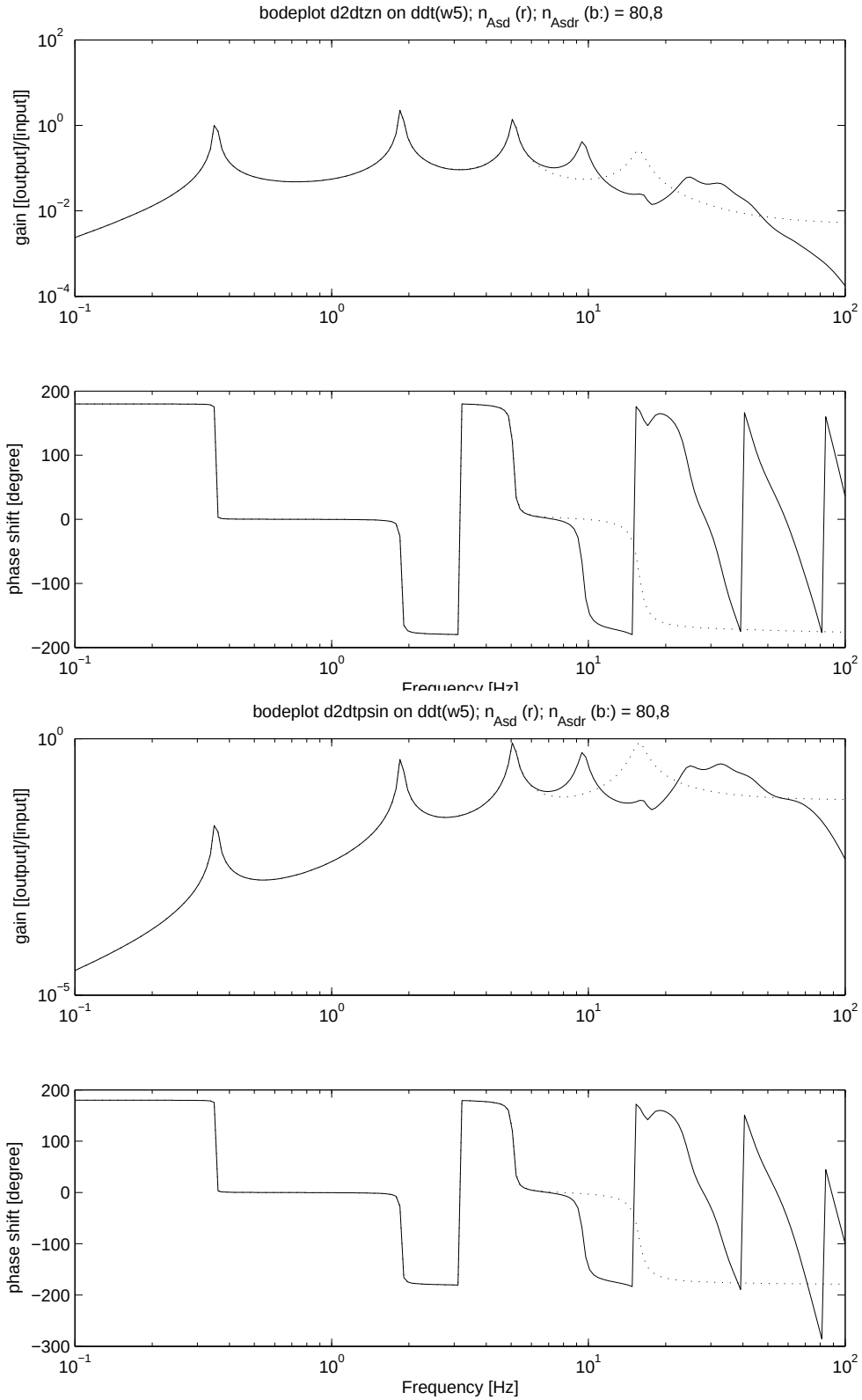

Figure 6.5 *Tower top motion response on 'surface level' horizontal wave acceleration*

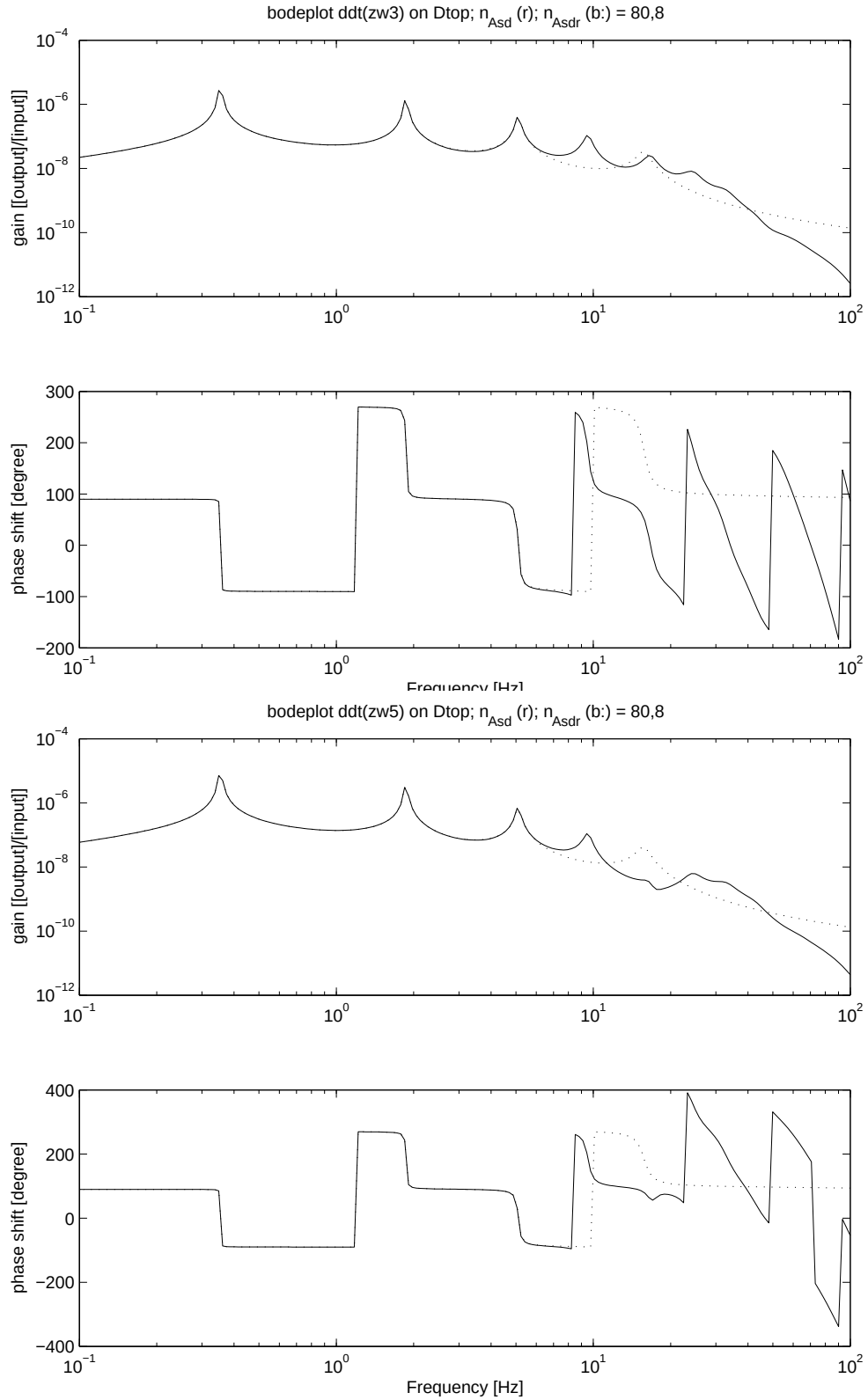

Figure 6.6 *'middle-depth' (upper graph) and 'surface level' (lower graph)s horizontal tower speed response on shearing force on tower top*

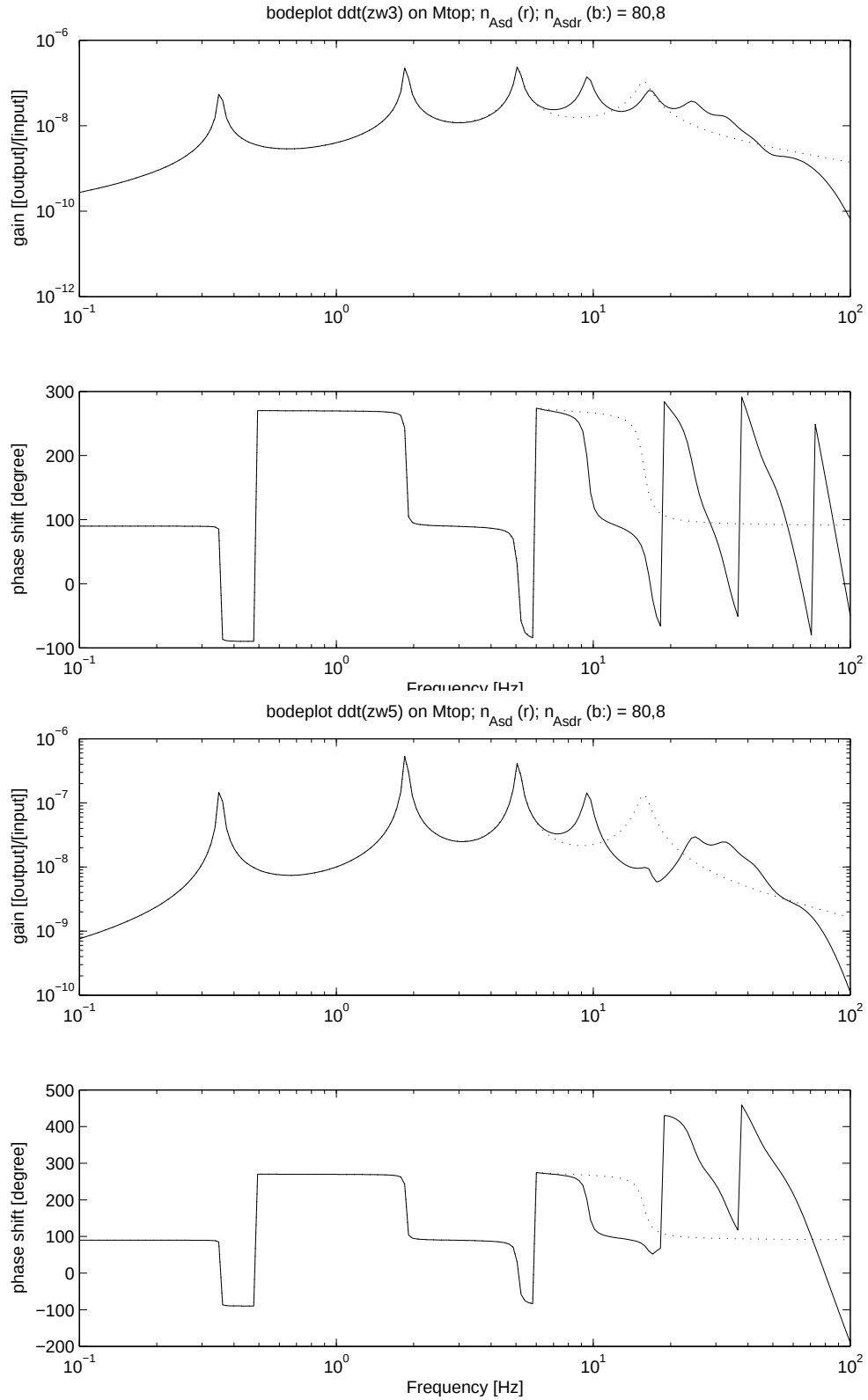

Figure 6.7 *'middle-depth' (upper graph) and 'surface level' (lower graph) horizontal tower speed response on bending moment on tower top*

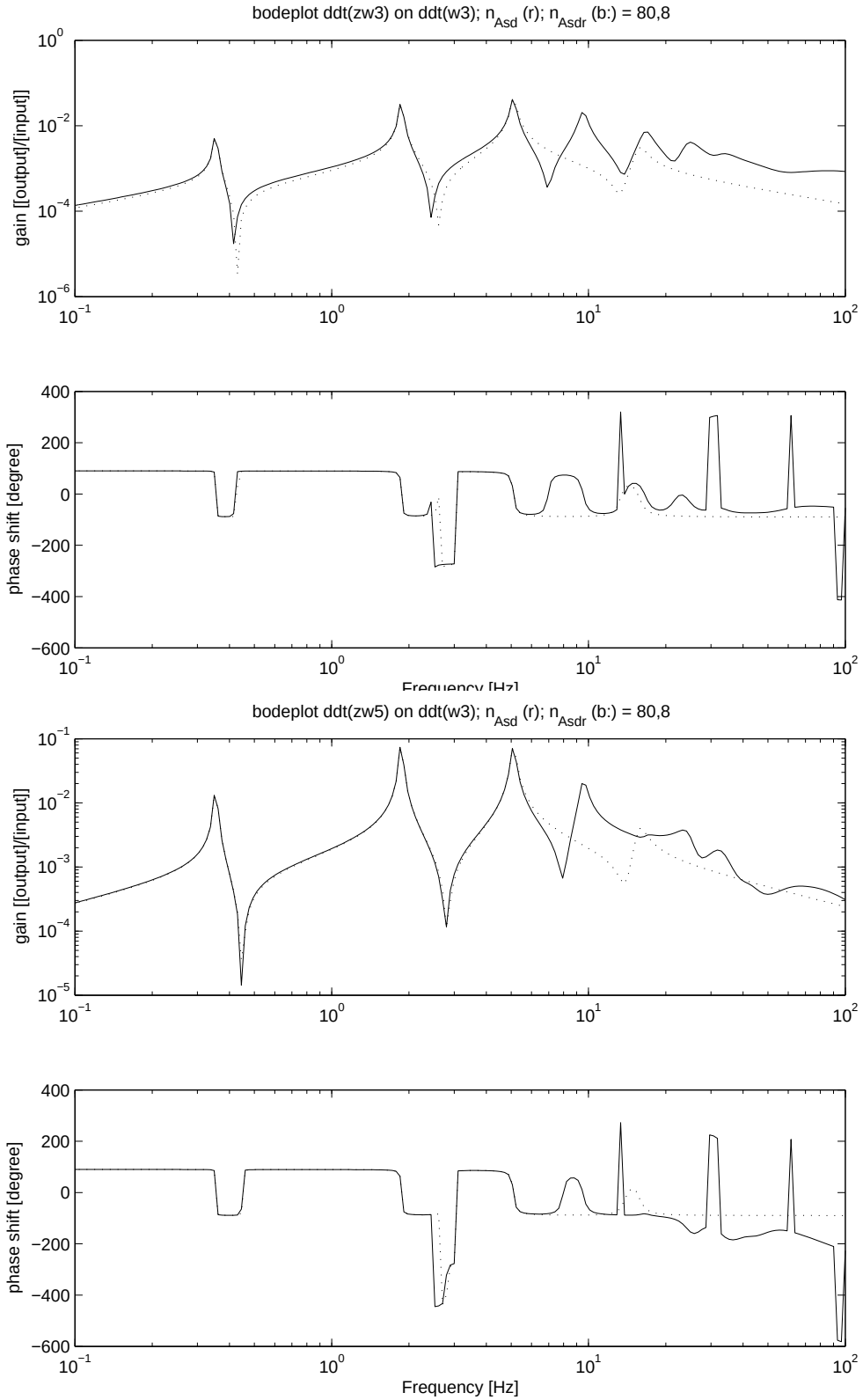

Figure 6.8 *'middle-depth' (upper graph) and 'surface level' (lower graph) horizontal tower speed response on 'middle-depth' horizontal wave acceleration*

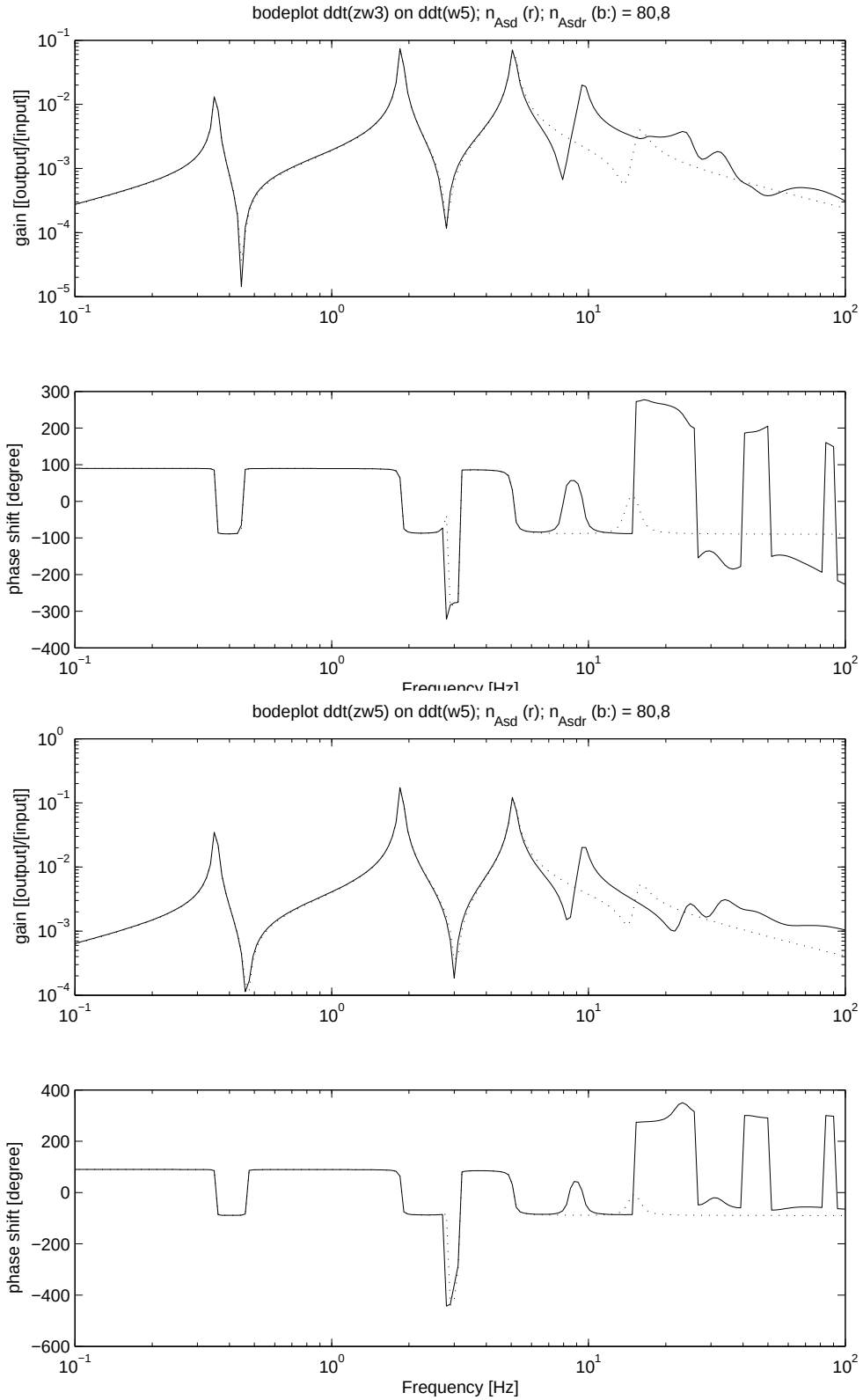

Figure 6.9 *'middle-depth' (upper graph) and 'surface level' (lower graph) horizontal tower speed response on 'surface level' horizontal wave acceleration*

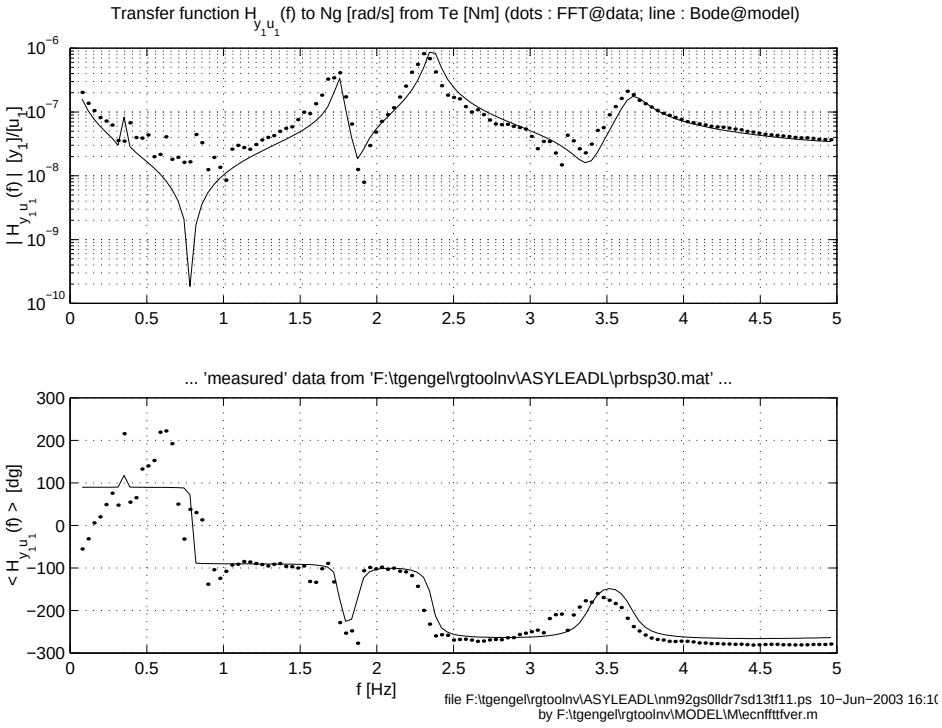

Figure 6.10 *Transfer function from generator torque to shaft distorsion*

lead-lag blade bending and (ii, at 2.3Hz) the first collective lead lag bending mode that interacts with shaft distorsion.

It can be concluded that the resemblance is very good.

7. CONCLUSIONS AND RECOMMENDATONS

Summary of results

The computer program TURBU Offshore has been developed for frequency domain analysis of offshore wind turbines with three blades or more. The modularised set-up of the model enables to include control algorithms and generarlised degrees of freedom in a convenient way. The rotational coupling between the blades and the tower is eliminated via a multi-blade coordinate transformation, which moves the periodicity of model parameters to harmonic operations on the input and output variables. The high rate of modularisation, together with the model order reduction technique for the blades and tower, also allows for the application of more general methods for handling the periodic coefficients, like the harmonic balance method and the Floquet Transition Matrix method. This is required for the analysis of single- and two-bladed rotors, which do not possess polar symmetry since the inertia of the rotor disc changes with the angular position.

The implemented model set-up makes it possible to carry out aero-elastic stability analysis and control design. The incorporation of control loops in the program modules of the rotor blades and drive-train makes it very valuable for realistic predictions on the stability. Since the size of the wind turbine is ever increasing, the natural frequencies decrease and thus interfere more and more with the bandwidth of power and speed control.

The output of TURBU Offshore consists of the power spectra of the loads on the blades, drive-train and support structure. These can be transformed into time series for the stochastic loads with a spectral representation method. In addition, the mean values of the loads and Fourier series for the periodic loading are provided. Thus the overall load histories can be assembled and subject to rainflow counting. The resulting load histograms are used for fatigue assessment in load cases.

Especially the power spectra provide a clear view on the relevance of poorly damped modes of the blades, support structure or whole system. This relevance, or ‘danger’ of such modes, depends heavily on the level of excitation. This very excitation, which is sized by the power spectrum of wind and waves, the coherence of turbulence in the rotor plane and the rotational speed, is catered for by the power spectra. Current aero-elastic stability analysis does not take into account the excitation by turbulence and waves.

Conclusions

Calculations with the non-linear aerodynamic code PHATAS pointed out that, in steady conditions, the mean and variational loads are appropriately assessed with TURBU Offshore.

The availability of TURBU Offshore, in which a numerically efficient method for load calculation in the frequency domain has been implemented, enables to take account of the numerous load cases for offshore sited wind turbines in a much faster way than nowadays possible with time domain tools (objective 1).

Reliable aero-elastic stability results have been obtained with TURBU Offshore in a benchmark exercise in the EU-project STABCON. The valid representation of damping rates and natural frequencies proves the feasibility of TURBU Offshore for the determination of ‘safety margins’ concerned with the natural frequencies and the rotational speed (objective 2).

The use of TURBU Offshore, which appears also to produce reliable aero-elastic stability results, will be effective for the selection of the most important load cases for time domain analysis, for design purposes and for certification (objective 3).

The cost of the turbine construction can be reduced significantly via TURBU Offshore, because

- the integrated linear model will provide a better understanding of deformation modes that involve both the blades and the drive train and the support structure;
- the frequency domain approach allows ample load case analyses, which enable to achieve a much higher level of design optimisation;
- the modularised set-up allows for the derivation of very effective control design models, which enable more accurate process control and the applicaton of innovative concepts like individual pitch control and free yawing.

Recommendations

It is recommended to develop guidelines for the complementary use of frequency domain tools like TURBU Offshore and time domain tools like PHATAS for load case analysis. Frequency domain analyses may severly under- or overestimate the dynamic loading if the linearised approximation is not valid for the conditions concerned. The linearised approximation is the point of departure for every frequency domain tool, which tells that only relatively small variations around the (ten-minute) average conditions are accounted for correctly. Mandatory load cases for certification should be the point of departure.

In order to take full advantage of the development of TURBU Offshore it is recommended to derive submodels of the structural dynamics and wind and wave loads for the design of control algorithms. This also holds for the use of the integrated model in aero-elastic stability analysis. Until now the models used for control design do not account sufficiently well for the dynamic interactions while the models for aero-elastic stability analysis do not include control loops.

Another fruitful option is expected to be the coupling of the integrated linear structural dynamics model of TURBU Offshore to an advanced aerodynamic code like AWSM. AWSM is expected to substantially reduce the number of uncertainties that accompany currently used BEM models.

REFERENCES

[1] R.L. Bielaw. *Rotary Wing Structural Dynamics and Aeroelasticity*. American Institute of Aeronautics and Astronautics, Inc., 370 L'Enfant Promenade, SW, Washington, DC 20024-2518, USA, 1995.

[2] N.W.M. Bishop and F. Sheratt. Fatigue life prediciton from power spectral density data. *Environmental Engineering*, Vol. 2, Nos 1 and 2, March and June 1989.

[3] Coleman, R.P. and A.M. Feingold. "Theory of Self-Excited Mechanical Oscillations of Helicopter Rotors with Hinged Blades". NASA TN 3844, NASA, Februari 1957.

[4] T.G. van Engelen, L.D. Hofland, and J.H. Vugts. Turbu offshore, computerprogramma voor frequentiedomein analyse van horizontale as offshore windturbines; fase I: Modelbeschrijving. Technical Report ECN-C–02-73, 2002.

[5] Engelen, T.G. van, L.D. Hofland, and J.H. Vugts. "TURBU Offshore Computer Programme for Frequency Domain Analysis of Horizontal Axis Offshore Wind Turbines Fase I: Mode Description". Technical Report ECN-C--02-073, Energy research Centre of the Netherlands ECN, Petten, The Netherlands, November 2002.

[6] Gladwell, G.M.L. "Branch Mode Analyses of Vibrating Systems". *Journal of Sound and Vibration*, Vol. 1:41–59, 1964.

[7] Graig Jr, R.R. and M.C.C. Bampton. "Coupling of Substructures for Dynamic Analyses". *AIAA Journal*, Vol. 6(7):1313–1319, 1968.

[8] Hurty, W.C. "Dynamic Analysis of Structural Systems by Component Mode Synthesis". Rept. 32-530, Jet Propulsion Lab., Pasadena, California, December 1964.

[9] Hurty, W.C. "Dynamic Analysis of Structural Systems Using Component Modes". *AIAA Journal*, Vol. 3(4):678–685, 1965.

[10] C. Lindenburg and J.G. Schepers. PHATAS-IV aeroelastic modelling. Technical Report ECN-CX--00-27, ECN Petten, the Netherlands, 2000.

[11] The Mathworks, Inc., 24 Prime Park Way, Natck, MA 01760-1500, USA; www.matlab.com. *MATLAB The Language of Technical Computing*, 6th edition.

[12] Schepers, J.G. "An Engineering Model for Yawed Conditions, Developed on the Basis of Wind Tunnel Measurements". Technical Report ECN-RX--98-057, Netherlands Energy Research Foundation ECN, Petten, The Netherlands, 1999.

[13] D. Winkelaar. *SWIFT, Program for Three-Dimensional Wind Simulation, Part 1: Model Description and Program Verification*. ECN Wind Energy, Petten, the Netherlands, December 1992.

APPENDIX A. IMPLEMENTED EQUATIONS OF MOTION

This appendix describes the implemented equations motion in accordance with the model set-up as described in chapter 3. Section A.1 describes the interaction signals between the components and what the 'connection conditions' are. The equations of motions and the associated program modules for the rotor blades, wake, drive-train and support structure are described in A.2, section A.3, A.4 and A.5.

A.1 Interaction signals for connection of components

The first four subsections describe the input and output variables for the rotor blades, rotor annuli, drive-train, support structure and control. The inputs and outputs are clustered in subvectors; each subvector has a superscript that consists of a 'source identifier' and 'destination identifier'. For exammple the input vector $\underline{v}^{RD}$ contains the feedthrough loads from rotor blade D into the rotor centre of the drive train R in the coordinate system of the hub; the output vector $\underline{y}^{RS}$ contains the kinematic vectors of the support structure including the gearbox house in the exit point to the rotating part of the drive-train in the (stand still) coordinate system of the gearbox house. These subsection also describes the exogenous input variables per component and the contribution of each component to the 'exogeneous' output vector. The control has the disposal of all exogeneous output variables as 'measurement signals'.

The last subsection describes how to convert outputs from one component into inputs for another component. Straightforward 'one to one' conversion is not valid for the interactions with the drive-train: rotor blade I/O requires transformation over the blade's azimut offset angle; support structure I/O over the 'on-average evaluating' main azimut angle $\bar{\Omega}t$.

A.1.1 Rotor blades I/O-variables

The input that is required by each rotor blade X is given by:

- periodic wind speed variation on blade: $\underline{u}_{\mathrm{per}}^{X}$
- periodic gravitation variation on blade base: $\underline{g}_{\mathrm{per}}^{X_0}$
- stochastic wind speed variation in intersection annuli/blade: ${}^{\mathrm{t}}\underline{u}^{W/X}$
- induction speed variation in rotor annuli: $\underline{u}_{\mathrm{i_m}}^{W}$
- kinematic vectors on blade blase exit: $\underline{\omega}^{X_{\mathrm{FF}(0)}}$, $\underline{\alpha}^{X_{\mathrm{FF}(0)}}$, $\underline{v}^{X^{\oplus}_{\mathrm{FF}(0)}}$, $\underline{a}^{X^{\oplus}_{\mathrm{FF}(0)}}$
- wind speed variation by orientation change up till hub: $\underline{u}_{\mathrm{ori}}^{X_{\mathrm{FF}(0)}}$.
- gravitation variation by orientation change up till hub: $\underline{g}_{\mathrm{ori}}^{X_{\mathrm{FF}(0)}}$
- angular and linear displacement vectors on blade blase exit: $\underline{\xi}^{X_{\mathrm{FF}(0)}}$, $\underline{x}^{X_{\mathrm{FF}(0)}}$

Note that the angular and linear displacements vectors are expressed along the blade base coordinate system in its *average* position $\vec{e}^{\,\bar{X}_0}$, while the kinematic vectors and orientation change related variables are to be expressed along the blade base coordinate system in its *actual* position $\vec{e}^{\,X_0}$.

The exogeneous input subvectors $\underline{u}^{X}_{\rm per}$, $\underline{g}^{X_0}_{\rm per}$ and ${}^{\rm t}\underline{u}^{W/X}$ have been dealt with in the previous section.

The wake induction vector $\underline{u}^{W}_{\rm i_m}$ contains for each rotor annulus *minus* the 'annulus-average' axial and tangential induction speed in the x- and z-location.

The blade base exit $X_0^{\oplus}$ coincides with the entry point $X_1^{\ominus}$ of the first blade element. The coordinate system along the blade base is rotated over the azimut offset angle relative to the coordinate system on the hub. The I/O between the rotor blades and hub is dealt with in detail in paragraph (vi).

The input vector $\underline{v}^{X}$ of each rotor blade has the following composition:

$$\underline{v}^{X} = \begin{bmatrix} \underline{v}^{XG} \\ \underline{v}^{XW} \\ \underline{v}^{XR} \end{bmatrix} \quad \text{with} \quad \underline{v}^{XG} = \begin{bmatrix} \underline{u}^{X}_{\rm per} \\ \underline{g}^{X_0}_{\rm per} \\ {}^{\rm t}\underline{u}^{W/X} \end{bmatrix}$$

$$\text{and} \quad \underline{v}^{XW} = \begin{bmatrix} \underline{u}^{W}_{\rm i_m} \end{bmatrix} \;;\; \underline{v}^{XR} = \begin{bmatrix} \underline{\omega}^{X_{\rm FF(0)}} \\ \underline{\alpha}^{X_{\rm FF(0)}} \\ \underline{v}^{X^{\oplus}_{\rm FF(0)}} \\ \underline{a}^{X^{\oplus}_{\rm FF(0)}} \\ \underline{u}^{X_{\rm FF(0)}}_{\rm ori} \\ \underline{g}^{X_{\rm FF(0)}}_{\rm ori} \\ \underline{\xi}^{X_{\rm FF(0)}} \\ \underline{x}^{X_{\rm FF(0)}} \end{bmatrix} \tag{A.1}$$

Each rotor blade needs to provide the following interaction output:

- aerodynamic force load reactions to the wake W: ${}^{\rm aL}\underline{f}^{W_m/X_k}$ for $(k = 1 \ldots N)$
- feedthrough force and torque on the rotor centre $X_0^{\ominus}$: ${}^{\rm FT}\underline{f}^{X^{\ominus}_{\rm PP(1)}}$, ${}^{\rm FT}\underline{t}^{X^{\ominus}_{\rm PP(1)}}$ (=${}^{\rm FT}\underline{f}^{X_0^{\ominus}}$, ${}^{\rm FT}\underline{t}^{X_0^{\ominus}}$)

The coordinate vector ${}^{\rm aL}\underline{f}^{W_m/X_k}$ is the reaction load from blade element X_k on the wake. It is supplied as a coordinate vector along the annulus wise coordinate system in the intersection of blade element X_k and rotor annulus W_m. It equals minus the concentrated force load on X_k, *but only as concerns the force component caused by lift.*

The feedthrough loads ${}^{\rm FT}\underline{f}^{X^{\ominus}_{\rm PP(1)}}$, ${}^{\rm FT}\underline{t}^{X^{\ominus}_{\rm PP(1)}}$ in the rotor centre $X_0^{\ominus}$ have coordinates along the coordinate system of the blade blase X_0.

The output vector $\underline{y}^{X}$ of a rotor blade has the following composition:

$$\underline{y}^{X} = \begin{bmatrix} \underline{y}^{GX} \\ \underline{y}^{WX} \\ \underline{y}^{RX} \end{bmatrix} \quad \text{with} \quad \underline{y}^{WX} = \begin{bmatrix} {}^{\rm aL}\underline{f}^{W_m/X_1} \\ \vdots \\ {}^{\rm aL}\underline{f}^{W_m/X_N} \end{bmatrix} \;;\; \underline{y}^{RX} = \begin{bmatrix} {}^{\rm FT}\underline{f}^{X^{\ominus}_{\rm PP(1)}} \\ {}^{\rm FT}\underline{t}^{X^{\ominus}_{\rm PP(1)}} \end{bmatrix} \tag{A.2}$$

The exogeneous output subvector $\underline{y}^{GX}$ provides the element displacements and blade flange loads and pitch angle variation (see Eq. 3.16).

A.1.2 Rotor annuli I/O-variables

The input that is required by the rotor annuli in the wake model W is given by:

- periodic wind speed variation on intersection blade/annuli: $\underline{u}_{\mathrm{per}}^{X/R_{\mathrm{fx}}}$
- stochastic wind speed variation in intersection annuli/blade: ${}^{\mathrm{t}}\underline{u}^{W/X}$
- aerodynamic force load reactions from the blades: ${}^{\mathrm{a_L}}\underline{f}^{W_m/D_k}$ for $(k = 1 \ldots N)$
- wind speed variation by orientation change up till nacelle: $\underline{u}_{\mathrm{ori}}^{S_{\mathrm{n}}}$

The input vector $\underline{v}^W$ to the wake has the following composition:

$$\underline{v}^W = \begin{bmatrix} \underline{v}^{WG} \\ \underline{v}^{WD} \\ \underline{v}^{WE} \\ \underline{v}^{WF} \\ \underline{v}^{WS} \end{bmatrix} \quad \text{with} \quad \underline{v}^{WG} = \begin{bmatrix} \underline{u}_{\mathrm{per}}^{D/R_{\mathrm{fx}}} \\ \underline{u}_{\mathrm{per}}^{E/R_{\mathrm{fx}}} \\ \underline{u}_{\mathrm{per}}^{F/R_{\mathrm{fx}}} \\ {}^{\mathrm{t}}\underline{u}^{W/D} \\ {}^{\mathrm{t}}\underline{u}^{W/E} \\ {}^{\mathrm{t}}\underline{u}^{W/F} \end{bmatrix} ; \; \underline{v}^{WS} = \begin{bmatrix} \underline{u}_{\mathrm{ori}}^{S_{\mathrm{n}}} \end{bmatrix} \quad \text{and}$$

$$\underline{v}^{WD} = \begin{bmatrix} {}^{\mathrm{a_L}}\underline{f}^{W_m/D_1} \\ \vdots \\ {}^{\mathrm{a_L}}\underline{f}^{W_m/D_N} \end{bmatrix} ; \; \underline{v}^{WE} = \begin{bmatrix} {}^{\mathrm{a_L}}\underline{f}^{W_m/E_1} \\ \vdots \\ {}^{\mathrm{a_L}}\underline{f}^{W_m/E_N} \end{bmatrix} ; \; \underline{v}^{WF} = \begin{bmatrix} {}^{\mathrm{a_L}}\underline{f}^{W_m/F_1} \\ \vdots \\ {}^{\mathrm{a_L}}\underline{f}^{W_m/F_N} \end{bmatrix} \tag{A.3}$$

The wake model needs to provide the following interaction output:

- induction speed variation in rotor annuli: $\underline{u}_{\mathrm{i_m}}^{W}$

The wake induction vector $\underline{u}_{\mathrm{i_m}}^{W}$ contains for each rotor annulus *minus* the 'annulus-average' axial and tangential induction speed in the x- and z-location. Since blade-local affection of the induction speed is not taken into account, only *one* induction vector $\underline{u}_{\mathrm{i_m}}^{W}$ applies, which contains the annulus-average axial and tangential induction speed values. This vector is input to all rotor blades.

The output vector $\underline{y}^W$ of the wake has the following composition:

$$\underline{y}^W = \begin{bmatrix} \underline{y}^{GW} \\ \underline{y}^{XW} \end{bmatrix} \quad \text{with} \quad \underline{y}^{XW} = \begin{bmatrix} \underline{u}_{\mathrm{i_m}}^{W} \end{bmatrix} \tag{A.4}$$

The exogeneous output subvector $\underline{y}^{GW}$ also provides the wake induction vector for analysis [and control] (see Eq. 3.16).

A.1.3 Drive-train I/O-variables (rotating part only)

The input that is required by the rotating part of the gearbox consists of:

- periodic gravitation variation on hub: $\underline{g}_{\mathrm{per}}^{R}$
- processed feedthrough force and torque from the rotor blades:
  ${}^{\mathrm{FT}}\underline{f}^{D_0^{\ominus}/R_{\mathrm{r}}}$, ${}^{\mathrm{FT}}\underline{t}^{D_0^{\ominus}/R_{\mathrm{r}}}$, ${}^{\mathrm{FT}}\underline{f}^{E_0^{\ominus}/R_{\mathrm{r}}}$, ${}^{\mathrm{FT}}\underline{t}^{E_0^{\ominus}/R_{\mathrm{r}}}$, ${}^{\mathrm{FT}}\underline{f}^{F_0^{\ominus}/R_{\mathrm{r}}}$, ${}^{\mathrm{FT}}\underline{t}^{F_0^{\ominus}/R_{\mathrm{r}}}$
- processed angular displacment & kinematic vectors from the gearbox house:
  $\underline{\xi}^{R_{\tilde{\mathrm{h}}}}$, $\underline{\omega}^{R_{\tilde{\mathrm{h}}}}$, $\underline{\alpha}^{R_{\tilde{\mathrm{h}}}}$
- processed linear displacement & kinematic vectors from nacelle:
  $\underline{x}^{S_{\tilde{\mathrm{n}}}^{\oplus \mathrm{r}}}$, $\underline{v}^{S_{\tilde{\mathrm{n}}}^{\oplus \mathrm{r}}}$, $\underline{a}^{S_{\tilde{\mathrm{n}}}^{\oplus \mathrm{r}}}$

- processed wind speed and gravitation variation by orientation change up to the gearbox house: $\underline{u}_{\mathrm{ori}}^{R_{\tilde{\mathrm{h}}"}}$, $\underline{g}_{\mathrm{ori}}^{R_{\tilde{\mathrm{h}}"}}$

Note that the displacement vectors $\underline{\xi}^{R_{\tilde{\mathrm{h}}"}}$, $\underline{x}^{S_{\tilde{\mathrm{n}}}^{\oplus \mathrm{r}}}$ are obtained by transformation over the average main rotation $\bar{\Omega}t$ along the x-axis from the displacement vectors on the exit point of the support structure; the involved coordinates of the latter displacement vectors respectively are along the 'feedthrough coordinate system' of the gearbox house in its *average* position and the final coordinate system of the nacelle in its *average* position.

The kinematic and orientation change related vectors are also obtained by transformation over $\bar{\Omega}t$ from the belonging vectors on the exit point of the support structure; the involved coordinates of the latter vectors are now along the 'feedthrough coordinate system' of the gearbox house in its *actual* position $\vec{e}^{\,R_{\tilde{\mathrm{h}}"}}$.

The input vector $\underline{v}^R$ of the drive-train has the following composition:

$$\underline{v}^R = \begin{bmatrix} \underline{v}^{RG} \\ \underline{v}^{RD} \\ \underline{v}^{RE} \\ \underline{v}^{RF} \\ \underline{v}^{RS} \end{bmatrix} \quad \text{with} \quad \underline{v}^{RG} = \begin{bmatrix} \underline{g}_{\mathrm{per}}^{R} \end{bmatrix} \; ; \; \underline{v}^{RS} = \begin{bmatrix} \underline{\omega}^{R_{\tilde{\mathrm{h}}"}} \\ \underline{\alpha}^{R_{\tilde{\mathrm{h}}"}} \\ \underline{v}^{S_{\tilde{\mathrm{n}}}^{\oplus}} \\ \underline{a}^{S_{\tilde{\mathrm{n}}}^{\oplus}} \\ \underline{u}_{\mathrm{ori}}^{R_{\tilde{\mathrm{h}}"}} \\ \underline{g}_{\mathrm{ori}}^{R_{\tilde{\mathrm{h}}"}} \\ \underline{\xi}^{R_{\tilde{\mathrm{h}}"}} \\ \underline{x}^{S_{\tilde{\mathrm{n}}}^{\oplus}} \end{bmatrix}$$

$$\text{and} \quad \underline{v}^{RD} = \begin{bmatrix} {}^{\mathrm{FT}}\underline{f}^{D_0^{\ominus}/R_{\mathrm{r}}} \\ {}^{\mathrm{FT}}\underline{t}^{D_0^{\ominus}/R_{\mathrm{r}}} \end{bmatrix} \; ; \; \underline{v}^{RE} = \begin{bmatrix} {}^{\mathrm{FT}}\underline{f}^{E_0^{\ominus}/R_{\mathrm{r}}} \\ {}^{\mathrm{FT}}\underline{t}^{E_0^{\ominus}/R_{\mathrm{r}}} \end{bmatrix} \; ; \; \underline{v}^{RE} = \begin{bmatrix} {}^{\mathrm{FT}}\underline{f}^{F_0^{\ominus}/R_{\mathrm{r}}} \\ {}^{\mathrm{FT}}\underline{t}^{F_0^{\ominus}/R_{\mathrm{r}}} \end{bmatrix} \tag{A.5}$$

The drive-train needs to provide the following interaction output:

- kinematic vectors in the rotor centre: $\underline{\omega}^{R_{\mathrm{r}}^{\mathrm{c}}}$, $\underline{\alpha}^{R_{\mathrm{r}}^{\mathrm{c}}}$, $\underline{v}^{R_{\mathrm{r}}^{\mathrm{c}}}$, $\underline{a}^{R_{\mathrm{r}}^{\mathrm{c}}}$
- wind speed variation by orientation change up till hub: $\underline{u}_{\mathrm{ori}}^{R}$.
- gravitation variation by orientation change up till hub: $\underline{g}_{\mathrm{ori}}^{R}$
- angular and linear displacement vectors in the rotor centre: $\underline{\xi}^{R_{\mathrm{r}}^{\mathrm{c}}}$, $\underline{x}^{R_{\mathrm{r}}^{\mathrm{c}}}$
- feedthrough loads from rotor shaft on nacelle in rotor centre: ${}^{\mathrm{FT}}\underline{f}^{S_{\tilde{\mathrm{n}}}^{\oplus} R_{\mathrm{r}}}$, ${}^{\mathrm{FT}}\underline{t}^{S_{\tilde{\mathrm{n}}}^{\oplus} R_{\mathrm{r}}}$
- feedthrough torque from generator rotor on nacelle in rotor centre: ${}^{\mathrm{FT}}\underline{t}^{S_{\tilde{\mathrm{n}}}^{\oplus} R_{\mathrm{f}}}$

The kinematic vectors and variations by orientation change up till the hub, which are input to the rotor blades, are coordinate vectors along the actual coordinate system $\vec{e}^{\,R_{\mathrm{r}}}$ of the rotor hub.

The angular and linear displacments vectors, wich are input to the rotor blades, are coordinate vectors along the rotor hub coordinate system in its *average* position $\vec{e}^{\,\bar{R}_{\mathrm{r}}}$.

The feedthrough loads to the support structure are coordinate vectors along the coordinate system $\vec{e}^{\,R_{\mathrm{s}}}$ of the gearbox slow shaft. The transformation from R_{s} to R_{r} involves the main shaft distorsion and bending (section 3.7.1, Eq. 3.63).

The output vector $\underline{y}^R$ of the drive-train has the following composition:

$$\underline{y}^R = \begin{bmatrix} \underline{y}^G \\ \underline{y}^{XR} \\ \underline{y}^{SR} \end{bmatrix} \quad \text{with} \quad \underline{y}^{XR} = \begin{bmatrix} \underline{\omega}^{R_\mathrm{r}} \\ \underline{\alpha}^{R_\mathrm{r}} \\ \underline{v}^{R_\mathrm{r}^\mathrm{c}} \\ \underline{a}^{R_\mathrm{r}^\mathrm{c}} \\ \underline{u}_\mathrm{ori}^{R_\mathrm{r}} \\ \underline{g}_\mathrm{ori}^{R_\mathrm{r}} \\ \underline{\xi}^{R_\mathrm{r}^\mathrm{c}} \\ \underline{x}^{R_\mathrm{r}^\mathrm{c}} \end{bmatrix} \; ; \; \underline{y}^{SR} = \begin{bmatrix} {}^{\mathrm{FT}}\underline{f}^{S_\mathrm{n}^\oplus R_\mathrm{r}} \\ {}^{\mathrm{FT}}\underline{t}^{S_\mathrm{n}^\oplus R_\mathrm{r}} \\ {}^{\mathrm{FT}}\underline{t}^{S_\mathrm{n}^\oplus R_\mathrm{f}} \end{bmatrix} \tag{A.6}$$

The exogeneous output subvector $\underline{y}^{GR}$ provides the linear and angular displacements and the torque load in the centre of the hub (see Eq. 3.16).

A.1.4 Support structure & gearbox house I/O-variables

The required input by the support structure and the gearbox house consists of:

- horizontal wave speeds and wave accelerations: $\underline{w}_\mathrm{horz}^S$, $\underline{\dot{w}}_\mathrm{horz}^S$
- feedthrough force and torque on the nacelle exit in the rotor centre : ${}^{\mathrm{FT}}\underline{f}^{S_\mathrm{n}^{\oplus\mathrm{r}}}$, ${}^{\mathrm{FT}}\underline{t}^{S_\mathrm{n}^{\oplus\mathrm{r}}}$

The exogeneous input subvectors $\underline{w}_\mathrm{horz}^S$ and $\underline{\dot{w}}_\mathrm{horz}^S$ have been dealt with in the previous section.

The input vector $\underline{v}^S$ of the support structure with gearbox house has the following composition:

$$\underline{v}^S = \begin{bmatrix} \underline{v}^{SG} \\ \underline{v}^{SR} \end{bmatrix} \quad \text{with} \quad \underline{v}^{SG} = \begin{bmatrix} \underline{w}_\mathrm{horz}^S \\ \underline{\dot{w}}_\mathrm{horz}^S \end{bmatrix}$$
$$\text{and} \quad \underline{v}^{SR} = \begin{bmatrix} {}^{\mathrm{FT}}\underline{f}^{S_\mathrm{n}^\oplus R_\mathrm{r}} \\ {}^{\mathrm{FT}}\underline{t}^{S_\mathrm{n}^\oplus R_\mathrm{r}} \\ {}^{\mathrm{FT}}\underline{t}^{S_\mathrm{n}^\oplus R_\mathrm{f}} \end{bmatrix} \tag{A.7}$$

The support structure has to provide the following interaction output:

- angular kinematic vectors from the gearbox house: $\underline{\omega}^{R_\mathrm{h"}}$, $\underline{\alpha}^{R_\mathrm{h"}}$
- linear kinematic vectors from nacelle: $\underline{v}^{S_\mathrm{n}^\oplus}$, $\underline{a}^{S_\mathrm{n}^\oplus}$
- wind speed and gravitation variation by orientation change up to the gearbox house: $\underline{u}_\mathrm{ori}^{R_\mathrm{h"}}$, $\underline{g}_\mathrm{ori}^{R_\mathrm{h"}}$
- angular displacement vector from the gearbox house: $\underline{\xi}^{R_\mathrm{h}^"}$
- linear displacement vector from nacelle: $\underline{x}^{S_\mathrm{n}^\oplus}$
- wind speed variation by orientation change up to the nacelle: $\underline{u}_\mathrm{ori}^{S_\mathrm{n}}$

All interaction outputs but the last three are coordinate vectors along the coordinate system $\vec{e}^{\,R_\mathrm{h}^"}$ on the gearbox house. The orientation of this coordinate system results from (i) the orientation of the turbine foundation relative to the earth and (ii) all rotations in the support structure and (iii) the fed-through coaxial gearbox house rotation into the gearbox slow shaft, which amounts to $(i_\mathrm{gb}-1)/i_\mathrm{gb}$ times the true gearbox house rotation $\phi_1^{R_\mathrm{h}}$.

The coordinates of the displacement outputs are along the 'feedthrough' gearbox house coordinate system in its average position $\vec{e}^{\,\bar{R}_{\mathrm{h}}"}$.

The last output $\underline{u}_{\mathrm{ori}}^{S_{\mathrm{n}}}$ has coordinates along the the nacelle's coordinate system $\vec{e}^{\,S_{\mathrm{n}}}$.

The composition of the output vector of the support structure is (in the implementation the interaction outputs to the wake and the drive-train are output variables of the fourth subcomponent in the support structure (R_{h})):

$$\begin{aligned}
\underline{y}^{S} &= \begin{bmatrix} \underline{y}^{GS} \\ \underline{y}^{WS} \\ \underline{y}^{RS} \end{bmatrix} \quad \text{with} \quad \underline{y}^{WS} = \begin{bmatrix} \underline{u}_{\mathrm{ori}}^{S_{\mathrm{n}}} \end{bmatrix} = \begin{bmatrix} \underline{u}_{\mathrm{ori}}^{S_{\mathrm{FF}(4)}} \end{bmatrix} \\
\underline{y}^{RS} &= \begin{bmatrix} \underline{\omega}^{R_{\mathrm{h}}"} \\ \underline{\alpha}^{R_{\mathrm{h}}"} \\ \underline{v}^{S_{\mathrm{n}}^{\oplus}} \\ \underline{a}^{S_{\mathrm{n}}^{\oplus}} \\ \underline{u}_{\mathrm{ori}}^{R_{\mathrm{h}}"} \\ \underline{g}_{\mathrm{ori}}^{R_{\mathrm{h}}"} \\ \underline{\xi}^{R_{\mathrm{h}}"} \\ \underline{x}^{S_{\mathrm{n}}^{\oplus}} \end{bmatrix} \equiv \begin{bmatrix} \underline{\omega}^{S_{\mathrm{FF}(4)}} \\ \underline{\alpha}^{S_{\mathrm{FF}(4)}} \\ \underline{v}^{S_{\mathrm{FF}(4)}^{\oplus}} \\ \underline{a}^{S_{\mathrm{FF}(4)}^{\oplus}} \\ \underline{u}_{\mathrm{ori}}^{S_{\mathrm{FF}(4)}} \\ \underline{g}_{\mathrm{ori}}^{S_{\mathrm{FF}(4)}} \\ \underline{\xi}^{S_{\mathrm{FF}(4)}} \\ \underline{x}^{S_{\mathrm{FF}(4)}} \end{bmatrix}
\end{aligned} \tag{A.8}$$

The exogeneous output subvector $\underline{y}^{GS}$ provides the linear displacement vectors for the elements, the coaxial gearbox speed, and the force and torque load vectors on the tower top and the foundation (see Eq. 3.17).

A.1.5 I/O-mappings between components

All interactions but those in which the drive train is involved consist of 'one to one' conversion of output subvectors to input subvectors:

$$\begin{array}{lcl}
\underline{v}^{WD} = \underline{y}^{WD} & ; & \underline{v}^{WE} = \underline{y}^{WE} \quad ; \quad \underline{v}^{WF} = \underline{y}^{WF} \quad ; \quad \underline{v}^{WS} = \underline{y}^{WS} \\
\underline{v}^{DW} = \underline{y}^{XW} & & \\
\underline{v}^{EW} = \underline{y}^{XW} & & \\
\underline{v}^{FW} = \underline{y}^{XW} & &
\end{array} \tag{A.9}$$

Use X_b as specific blade identifier instead of D, E etc. It holds

$$\{X_b | b = 1, 2, 3\} \equiv \{D, E, F\} \tag{A.10}$$

The mapping from the blade output subvector $\underline{y}^{RX_b}$ to the drive train input subvector $\underline{v}^{RX_b}$ includes transformation over the blade's azimut offset angle relative to the hub; the reverse mapping also includes this transformation but has also to deal with the spanwise offset over the hub radius to the blade flange. The mappings are given by:

$$\begin{aligned}
\underline{v}^{X_b R} &= {}^{X_0^{\oplus}}T^{X_0^{\ominus}} \cdot \phi_{b1}^{(8)} \cdot \underline{y}^{XR} \\
\underline{v}^{RX_b} &= \Phi_{1b}^{(2)} \cdot \underline{y}^{RX_b}
\end{aligned} \tag{A.11}$$

The matrix ${}^{X_0^{\oplus}}T^{X_0^{\ominus}}$ accounts for the blade hub radius. The 'eight-block-diagonal' matrix $\phi_{b1}^{(8)}$ transforms over *plus* the azimut offset angle $2\pi(b-1)/B$ along the rotor axis; the 'two-block-diagonal' matrix $\phi_{1b}^{(2)}$ over *minus* this azimut offset angle.

The mappings from output to input subvectors between the support structure and the drive-train includes transformation over the 'on-average evaluating' main azimut angle

$\bar{\Omega}t$:

$$\begin{aligned} \underline{v}^{SR} &= \tilde{\Phi}^{\mathrm{T}(3)} \cdot \underline{y}^{SR} \\ \underline{v}^{RS} &= \tilde{\Phi}^{(8)} \cdot \underline{y}^{RS} \end{aligned} \tag{A.12}$$

The 'three-block diagonal' matrix $\tilde{\Phi}^{\mathrm{T}(3)}$ transforms over *minus* the average main azimut angle $\bar{\Omega}t$; the 'eight-block diagonal' matrix $\tilde{\Phi}^{(8)}$ over *plus* the average main azimut angle.

The I/O-mapping with the drive-train involved are cleared up below.

Drive-train outputs into the rotor blades

The processed output vectors from R apply in the entry point of the blade flange, that is to say the exit point $X_0^{\oplus}$ of the blade base. However, the actual output vectors of R are related to the rotor centre $R_{\mathrm{r}}^{\mathrm{c}}$. So, the mapping involves the coordinate transformation over the azimut offset as well as the spanwise offset over the root radius R_{root}. For the mapping of the *actual* output vector of R to the *processed* output vector for blade X_b then holds:

$$\left(\underline{v}^{X_b R} \equiv \begin{bmatrix} \underline{\omega}^{X_{b_{\mathrm{FF}(0)}}} \\ \underline{\alpha}^{X_{b_{\mathrm{FF}(0)}}} \\ \underline{v}^{X_{b_{\mathrm{FF}(0)}}^{\oplus}} \\ \underline{a}^{X_{b_{\mathrm{FF}(0)}}^{\oplus}} \\ \underline{u}_{\mathrm{ori}}^{X_{b_{\mathrm{FF}(0)}}} \\ \underline{g}_{\mathrm{ori}}^{X_{b_{\mathrm{FF}(0)}}} \\ \underline{\xi}^{X_{b_{\mathrm{FF}(0)}}} \\ \underline{x}^{X_{b_{\mathrm{FF}(0)}}} \end{bmatrix} \right) = {}^{X_0^{\oplus}}T^{X_0^{\ominus}} \cdot \phi_{b1}^{(8)} \cdot \left(\begin{bmatrix} \underline{\omega}^{R_{\mathrm{r}}} \\ \underline{\alpha}^{R_{\mathrm{r}}} \\ \underline{v}^{R_{\mathrm{r}}^{\mathrm{c}}} \\ \underline{a}^{R_{\mathrm{r}}^{\mathrm{c}}} \\ \underline{u}_{\mathrm{ori}}^{R_{\mathrm{r}}} \\ \underline{g}_{\mathrm{ori}}^{R_{\mathrm{r}}} \\ \underline{\xi}^{R_{\mathrm{r}}} \\ \underline{x}^{R_{\mathrm{r}}^{\mathrm{c}}} \end{bmatrix} \equiv \underline{y}^{X R} \right) \tag{A.13}$$

The block diagonal matrix $\phi_{b1}^{(8)}$ contains eight transformation matrices Φ_{b1} over the azimut offset angle $2\pi(b-1)/B$. We implicitely introduce the 'diagonalisation operator' diag:

$$\Phi_{b1}^{(8)} \triangleq \mathrm{diag}\big(\Phi_{b1} \ \ldots \ \Phi_{b1}\big) \triangleq \begin{bmatrix} \Phi_{b1} & \cdots & \mathrm{O}_{(1,8)} \\ \vdots & \ddots & \vdots \\ \mathrm{O}_{(8,1)} & \cdots & \Phi_{b1} \end{bmatrix} \quad \text{with} \quad \Phi_{b1} = \Phi_{\mathrm{x}}(\tfrac{2\pi(b-1)}{B}) \tag{A.14}$$

The mapping matrix ${}^{X_0^{\oplus}}T^{X_0^{\ominus}}$ from the blade base entry to the blade base exit caters in the first four block rows and columns for the offset over the blade root radius via the 'kinematic mapping matrix' ${}^{X_0^{\oplus}}T_{\mathrm{kin}}^{X_0^{\ominus}}$ and thus looks like:

$${}^{X_0^{\oplus}}T^{X_0^{\ominus}} = \begin{bmatrix} {}^{X_0^{\oplus}}T_{\mathrm{kin}}^{X_0^{\ominus}} & \mathrm{O}_{(12\times3)} & \mathrm{O}_{(12\times3)} & \mathrm{O}_{(12\times6)} \\ \mathrm{O}_{(3\times12)} & \boldsymbol{I}_{(3\times3)} & \mathrm{O}_{(3\times3)} & \mathrm{O}_{(3\times6)} \\ \mathrm{O}_{(3\times12)} & \mathrm{O}_{(3\times3)} & \boldsymbol{I}_{(3\times3)} & \mathrm{O}_{(3\times6)} \\ \mathrm{O}_{(6\times12)} & \mathrm{O}_{(6\times3)} & \boldsymbol{I}_{(6\times3)} & {}^{X_0^{\oplus}}T_{\mathrm{dsp}}^{X_0^{\ominus}} \end{bmatrix} \tag{A.15}$$

with the kinematics related submatrix ${}^{X_0^{\oplus}}T_{\rm kin}^{X_0^{\ominus}}$ given by ($R_{\rm rt}$ short form of $R_{\rm root}$):

$$
{}^{X_0^{\oplus}}T_{\rm kin}^{X_0^{\ominus}} = \begin{bmatrix}
\boldsymbol{I}_{(3\times3)} & & & \mathrm{O}_{(3\times3)} & & & \mathrm{O}_{(3\times3)} & \mathrm{O}_{(3\times3)} \\
\mathrm{O}_{(3\times3)} & & & \boldsymbol{I}_{(3\times3)} & & & \mathrm{O}_{(3\times3)} & \mathrm{O}_{(3\times3)} \\
\begin{bmatrix} 0 & 0 & -R_{\rm rt} \\ 0 & 0 & 0 \\ R_{\rm rt} & 0 & 0 \end{bmatrix} & & & \mathrm{O}_{(3\times3)} & & & \boldsymbol{I}_{(3\times3)} & \mathrm{O}_{(3\times3)} \\
\begin{bmatrix} 0 & \bar{\Omega}R_{\rm rt} & 0 \\ -2\bar{\Omega}R_{\rm rt} & 0 & 0 \\ 0 & 0 & 0 \end{bmatrix} & & & \begin{bmatrix} 0 & 0 & -R_{\rm rt} \\ 0 & 0 & 0 \\ R_{\rm rt} & 0 & 0 \end{bmatrix} & & & \mathrm{O}_{(3\times3)} & \boldsymbol{I}_{(3\times3)}
\end{bmatrix}
\tag{A.16}
$$

and the displacment related submatrix ${}^{X_0^{\oplus}}T_{\rm dsp}^{X_0^{\ominus}}$ given by ($R_{\rm rt}$ short form of $R_{\rm root}$):

$$
{}^{X_0^{\oplus}}T_{\rm dsp}^{X_0^{\ominus}} = \begin{bmatrix}
\boldsymbol{I}_{(3\times3)} & & & \mathrm{O}_{(3\times3)} \\
\begin{bmatrix} 0 & 0 & -R_{\rm rt} \\ 0 & 0 & 0 \\ R_{\rm rt} & 0 & 0 \end{bmatrix} & & & \boldsymbol{I}_{(3\times3)}
\end{bmatrix}
\tag{A.17}
$$

The submatrix $\{4,1\}$ in ${}^{X_0^{\oplus}}T_{\rm kin}^{X_0^{\ominus}}$ is obtained by writing Eq. B.124 in the appropriate format for the spanwise offset over the root radius:

$$
\begin{aligned}
\frac{\partial \underline{a}^{X_0^{\oplus}}}{\partial \underline{\omega}^{X_{\rm FF(0)}}} &= \mathrm{J}^3_{w=1}\Big({}^{R_{\rm r}^{\rm c}}r_w^{X_0^{\oplus}} \cdot \underline{\bar{\omega}}^{X_0} - 2\bar{\omega}_w^{X_0} \cdot {}^{R_{\rm r}^{\rm c}}\underline{r}^{X_0^{\oplus}} + (\underline{\bar{\omega}}^{X_0} \bullet {}^{R_{\rm r}^{\rm c}}\underline{r}^{X_0^{\oplus}}) \cdot \underline{e}_w\Big) \\
\text{with} \quad {}^{R_{\rm r}^{\rm c}}r_w^{X_0^{\oplus}} &= \delta_{w2} \cdot R_{\rm rt} \quad ; \quad \underline{\bar{\omega}}^{X_0} = \begin{bmatrix} \bar{\Omega} \\ 0 \\ 0 \end{bmatrix} \quad ; \quad {}^{R_{\rm r}^{\rm c}}\underline{r}^{X_0^{\oplus}} = \begin{bmatrix} 0 \\ R_{\rm rt} \\ 0 \end{bmatrix}
\end{aligned}
\tag{A.18}
$$

The submatrices $\{3,1\}$ and $\{4,2\}$ in ${}^{X_0^{\oplus}}T_{\rm kin}^{X_0^{\ominus}}$ and $\{2,1\}$ in in ${}^{X_0^{\oplus}}T_{\rm dsp}^{X_0^{\ominus}}$ are clear by considering the vector products $\delta\underline{\omega}^{X_{\rm FF(0)}} \times {}^{R_{\rm r}^{\rm c}}\underline{r}^{X_0^{\oplus}}$ and $\delta\underline{\alpha}^{X_{\rm FF(0)}} \times {}^{R_{\rm r}^{\rm c}}\underline{r}^{X_0^{\oplus}}$.

For the mean angular and linear speed and the linear acceleration that are fed into the blade entry point $X_1^{\ominus}$ holds:

$$
\begin{aligned}
\underline{\bar{\omega}}^{X_{\rm FF(0)}} &= \underline{\bar{\omega}}^{X_0} &&= \begin{bmatrix} \bar{\Omega} & 0 & 0 \end{bmatrix}^{\rm T} \\
\underline{\bar{v}}^{X_{\rm FF(0)}^{\oplus}} &= \underline{\bar{\omega}}^{X_0} \times {}^{R_{\rm r}^{\rm c}}\underline{r}^{X_0^{\oplus}} &&= \begin{bmatrix} 0 & 0 & \bar{\Omega}R_{\rm rt} \end{bmatrix}^{\rm T} \\
\underline{\bar{a}}^{X_{\rm FF(0)}^{\oplus}} &= \underline{\bar{\omega}}^{X_0} \times (\underline{\bar{\omega}}^{X_0} \times {}^{R_{\rm r}^{\rm c}}\underline{r}^{X_0^{\oplus}}) &&= \begin{bmatrix} 0 & -\bar{\Omega}R_{\rm rt}^2 & 0 \end{bmatrix}^{\rm T}
\end{aligned}
\tag{A.19}
$$

Rotor blade outputs into the drive-train

The processed output subvectors from R apply in the exit point $R_{\rm r}^{\oplus}$ of the rotor hub, which coincides with the rotor centre $R_{\rm r}^{\rm c}$. The 'processing' consists in the backward tansformation of the output subvector from each rotor blade X_b over the azimuth offset angle towards the coordinate system on the rotor hub. For the mapping of the actual outputs from X_b to the processed outputs for R then holds:

$$
\Big(\ \underline{v}^{RX_b} \equiv \begin{bmatrix} {}^{\rm FT}\underline{f}^{X_{b_0}^{\ominus}/R_{\rm r}} \\ {}^{\rm FT}\underline{t}^{X_{b_0}^{\ominus}/R_{\rm r}} \end{bmatrix}\ \Big) = \Phi_{1b}^{(2)} \cdot \Big(\ \begin{bmatrix} {}^{\rm FT}\underline{f}^{X_{b_{\rm PP(1)}}^{\ominus}} \\ {}^{\rm FT}\underline{t}^{X_{b_{\rm PP(1)}}^{\ominus}} \end{bmatrix} \equiv \underline{y}^{RX_b}\ \Big)
\tag{A.20}
$$

The block diagonal matrix $\Phi_{1b}^{(2)}$ is composed out of two transformation matrices over *minus* the azimut offset angle $2\pi\cdot(b-1)/B$ ($b = 1, 2, 3$):

$$
\Phi_{1b}^{(2)} \triangleq \mathrm{diag}\Big(\Phi_{1b} \ \ \Phi_{1b}\Big) \quad \text{with} \quad \Phi_{1b} = \Big(\ \Phi_{\rm x}(\tfrac{-2\pi(b-1)}{B}) \equiv \Phi_{\rm x}^{\rm T}(\tfrac{2\pi(b-1)}{B}) \equiv \Phi_{b1}^{\rm T}\ \Big)
\tag{A.21}
$$

Drive train outputs into the support structure
The processed output subvectors from R apply in the exit point $S_{\mathrm{n}}^{\oplus \mathrm{r}}$ of the nacelle. The 'processing' consists in the backward tansformation of the output subvectors from R over the main rotation towards the *stand still* coordinate system on the gearbox house. This transformation only includes the 'on-average evaluating' main azimuth angle $\tilde{\psi}(\equiv \bar{\Omega} t)$ (see section 3.7.1). For the mapping of the actual outputs from R to the processed outputs for S then holds:

$$\left(\underline{v}^{SR} \equiv \begin{bmatrix} {}^{\mathrm{FT}}\underline{f}^{S_{\mathrm{n}}^{\oplus} R_{\mathrm{r}}} \\ {}^{\mathrm{FT}}\underline{t}^{S_{\mathrm{n}}^{\oplus} R_{\mathrm{r}}} \\ {}^{\mathrm{FT}}\underline{t}^{S_{\mathrm{n}}^{\oplus} R_{\mathrm{f}}} \end{bmatrix} \right) = \tilde{\Phi}^{\mathrm{T}(3)} \cdot \left(\begin{bmatrix} {}^{\mathrm{FT}}\underline{f}^{S_{\tilde{\mathrm{n}}}^{\oplus} R_{\mathrm{r}}} \\ {}^{\mathrm{FT}}\underline{t}^{S_{\tilde{\mathrm{n}}}^{\oplus} R_{\mathrm{r}}} \\ {}^{\mathrm{FT}}\underline{t}^{S_{\tilde{\mathrm{n}}}^{\oplus} R_{\mathrm{f}}} \end{bmatrix} \equiv \underline{y}^{SR} \right) \tag{A.22}$$

The block diagonal matrix $\tilde{\Phi}^{\mathrm{T}(3)}$ is composed out of three transformation matrices over *minus* the on-average evaluating main azimut angle:

$$\tilde{\Phi}^{\mathrm{T}(3)} \triangleq \mathrm{diag}\left(\tilde{\Phi}^{\mathrm{T}} \;\; \tilde{\Phi}^{\mathrm{T}} \;\; \tilde{\Phi}^{\mathrm{T}}\right) \quad \text{with} \quad \tilde{\Phi}^{\mathrm{T}} = \left(\Phi_{\mathrm{x}}(-\bar{\Omega} t) \equiv \Phi_{\mathrm{x}}^{\mathrm{T}}(\bar{\Omega} t) \right) \tag{A.23}$$

Support structure outputs into the drive-train
The processed output subvectors from S apply in the exit point $S_{\mathrm{n}}^{\oplus \mathrm{r}}$ of the nacelle, that coincides with the rotor centre $R_{\mathrm{r}}^{\mathrm{c}}$, which in turn coincides with the hub exit point $R_{\mathrm{r}}^{\oplus}$. The 'processing' consists in the tansformation of the output subvectors from S over the main rotation towards the *rotating* coordinate system on the slow gearbox shaft. This transformation only includes the 'on-average evaluating' main azimuth angle $\tilde{\psi}(\equiv \bar{\Omega} t)$ (see section 3.7.1). The variation around $\tilde{\psi}$ is taken into within the rotating part of the drive-train itself and has the same effect on orientation changes as the main shaft distorsion. For the mapping of the actual outputs from S to the processed outputs for R then holds (see Eq. B.35, B.165, B.278):

$$\left(\underline{v}^{RS} = \begin{bmatrix} \underline{\omega}^{R_{\tilde{\mathrm{h}}"}} \\ \underline{\alpha}^{R_{\tilde{\mathrm{h}}"}} \\ \underline{v}^{S_{\tilde{\mathrm{n}}}^{\oplus \mathrm{r}}} \\ \underline{a}^{S_{\tilde{\mathrm{n}}}^{\oplus \mathrm{r}}} \\ \underline{u}_{\mathrm{ori}}^{R_{\tilde{\mathrm{h}}"}} \\ \underline{g}_{\mathrm{ori}}^{R_{\tilde{\mathrm{h}}"}} \\ \underline{\xi}^{R_{\tilde{\mathrm{h}}"}} \\ \underline{x}^{R_{\tilde{\mathrm{h}}"}} \end{bmatrix} \right) = \tilde{\Phi}^{(8)} \cdot \left(\begin{bmatrix} \underline{\omega}^{R_{\mathrm{h}"}} \\ \underline{\alpha}^{R_{\mathrm{h}"}} \\ \underline{v}^{S_{\mathrm{n}}^{\oplus}} \\ \underline{a}^{S_{\mathrm{n}}^{\oplus}} \\ \underline{u}_{\mathrm{ori}}^{R_{\mathrm{h}"}} \\ \underline{g}_{\mathrm{ori}}^{R_{\mathrm{h}"}} \\ \underline{\xi}^{R_{\mathrm{h}"}} \\ \underline{x}^{S_{\mathrm{n}}^{\oplus}} \end{bmatrix} \equiv \begin{bmatrix} \underline{\omega}^{S_{\mathrm{FF}(4)}} \\ \underline{\alpha}^{S_{\mathrm{FF}(4)}} \\ \underline{v}^{S_{\mathrm{FF}(4)}^{\oplus}} \\ \underline{a}^{S_{\mathrm{FF}(4)}^{\oplus}} \\ \underline{u}_{\mathrm{ori}}^{S_{\mathrm{FF}(4)}} \\ \underline{g}_{\mathrm{ori}}^{S_{\mathrm{FF}(4)}} \\ \underline{\xi}^{S_{\mathrm{FF}(4)}} \\ \underline{x}^{S_{\mathrm{FF}(4)}} \end{bmatrix} = \underline{y}^{RS} \right) \tag{A.24}$$

The block diagonal matrix $\tilde{\Phi}^{(8)}$ is composed out of six transformation matrices over the on-average evaluating main azimut angle:

$$\tilde{\Phi}^{(8)} \triangleq \mathrm{diag}\left(\tilde{\Phi} \;\; \tilde{\Phi} \;\; \tilde{\Phi} \;\; \tilde{\Phi} \;\; \tilde{\Phi} \;\; \tilde{\Phi} \;\; \tilde{\Phi} \;\; \tilde{\Phi}\right) \quad \text{with} \quad \tilde{\Phi} = \Phi_{\mathrm{x}}(\bar{\Omega} t) \tag{A.25}$$

A.2 Rotor blade model

The submodel for the dynamic blade behaviour is obtained with M-function tbubladeeom(). Straightforward application of the mechanic impulse law for the blade elements $X_2 \ldots X_N$ yields 5 second order differential equations per element ($X = D, E, F$ for $B = 3$). The average conditions are obtained by considering the average coordinate vectors of loads and motions in the rotating coordinate systems on the blade elements.

The model equations are obtained in two steps. First, two seperate state space models are derived; one for the blade flange element and one for the $N-1$ blade structure elements. Afterwards, these two models are connected and set up *the* state state space model for the rotor blade. These two submodels are respectively derived in section A.2.2 and A.2.3. The connection of the submodels is dealt with in section A.2.4. The sections on the acutal model derivation are preceeded by section A.2.1 on the general equations of motions for the blade elements.

A.2.1 General equations of motion for rotor blades

Application of the angular and linear impulse laws for the N blade elements yield N sets of two vector equations that involve the aerodynamic and gravitation loading as well as the *response loading* by the foregoing element. Response load coordinates along axes relative to which a degree of freedom is defined are modelled visco/elastic or are modelled to arise from a control loop. The degrees of freedom for a rotot blade element are located in the entry point $X_k^{\ominus}$. The general expression for the k^{th} equation set is

$$\begin{aligned}
\sum_{j=k}^{N}\Big({}^{(G)}\frac{\mathrm{d}}{\mathrm{d}t}\Big({}^{X_k^{\ominus}}\vec{h}^{\,X_j}\Big)\Big)_{i_v}^{X_k^v} &= \Big({}^{X_{k-1}}\vec{t}^{\,X_k^{\ominus}}\Big)_{i_v}^{X_k^v} + \\
&\sum_{j=k}^{N}\Big({}^{\mathrm{a}}\vec{t}^{\,X_j^{\mathrm{a}}} + {}^{X_k^{\ominus}}\vec{r}^{\,X_j^{\mathrm{a}}} \times {}^{\mathrm{a}}\vec{f}^{\,X_j^{\mathrm{a}}} + {}^{X_k^{\ominus}}\vec{r}^{\,X_j^*} \times {}^{\mathrm{g}}\vec{f}^{\,X_j^*}\Big)_{i_v}^{X_k^v} \qquad \text{(A.26)}\\
\sum_{j=k}^{N}\Big({}^{(G)}\frac{\mathrm{d}}{\mathrm{d}t}\Big(\vec{p}^{\,X_j}\Big)\Big)_{\ell_v}^{X_k^v} &= \Big({}^{X_{k-1}}\vec{f}^{\,X_k^{\ominus}}\Big)_{\ell_v}^{X_k^v} + \sum_{j=k}^{N}\Big(\Big({}^{\mathrm{a}}\vec{f}^{\,X_j^{\mathrm{a}}} + {}^{\mathrm{g}}\vec{f}^{\,X_j^*}\Big)_{\ell_v}^{X_k^v}
\end{aligned}$$

The notation $\big(\vec{q}\big)_{i_v}^{X_k^v}$ implies the i_v^{th} coordinate of vector $\vec{q}$ along the v^{th} intermediate coordinate system ${}^{X_k^v}\vec{e}$ of element X_k (see section 3.1). The first, second and third intermediate (= final) coordinate system for $k = 2 \ldots N$ are obtained by rotations relative to element X_{k-1} along the y-, z- and x-axis (in $X_k^{\ominus}$).

The respective orientations of these rotations are 'pitchwise', 'flatwise' and 'edgewise'. The relative translations in $X_k^{\ominus}$ are along the y-, x- and z-axis. The rotation and translation ordering makes i_v to be equal to 2,3 and 1 for $v = 1, 2, 3$ and ℓ_v to be equal to 2,1 and 3.

The orientations of the rotations for $k = 1$ are 'flapwise', 'pitchwise' and 'leadwise', so along the z-, y- and x-axis). The belonging translations are along the x-, y- and z-axis. Then i_v equals 3,2, 1 and ℓ_v equals 1,2,3.

See also section 3.6.1.

A relative rotation of translation may be a degree of freedom (dof), but this is not required. If relative rotation i_v or translation ℓ_v is a dof, then the belonging coordinate of the impulse equation in the v^{th} intermediate coordinate system adds an scalar equation of motion to the required set for a rotor blade.

Moving the terms for $j = k+1 \ldots N$ in the left hand sides of Eq. A.26 to the right hand side and separating the k^{th} term in the right hand side 'sum-terms' from the remaining ones yields the first step for the pursued recursive expressions (omit the coordinate system

specification 'X_k^v' and use $\dot{\vec{\hbar}}$ and $\dot{\vec{p}}$ for the time derivatives relative to earth G):

$$\begin{aligned}
{}^{X_k^\ominus}\dot{\vec{\hbar}}^{X_k} &= {}^{X_{k-1}}\vec{t}^{\,X_k^\ominus} + {}^{\mathrm{a}}\vec{t}^{\,X_k^{\mathrm{a}}} + {}^{X_k^\ominus}\vec{r}^{\,X_k^{\mathrm{a}}} \times {}^{\mathrm{a}}\vec{f}^{\,X_k^{\mathrm{a}}} + {}^{X_k^\ominus}\vec{r}^{\,X_k^*} \times {}^{\mathrm{g}}\vec{f}^{\,X_k^*} + \\
&\quad \sum_{j=k+1}^{N} \left(-{}^{X_k^\ominus}\dot{\vec{\hbar}}^{X_j} + {}^{\mathrm{a}}\vec{t}^{\,X_j^{\mathrm{a}}} + {}^{X_k^\ominus}\vec{r}^{\,X_j^{\mathrm{a}}} \times {}^{\mathrm{a}}\vec{f}^{\,X_j^{\mathrm{a}}} + {}^{X_k^\ominus}\vec{r}^{\,X_j^*} \times {}^{\mathrm{g}}\vec{f}^{\,X_j^*} \right) \\
\dot{\vec{p}}^{X_k} &= {}^{X_{k-1}}\vec{f}^{\,X_k^\ominus} + {}^{\mathrm{a}}\vec{f}^{\,X_k^{\mathrm{a}}} + {}^{\mathrm{g}}\vec{f}^{\,X_k^*} + \\
&\quad \sum_{j=k+1}^{N} \left(-\dot{\vec{p}}^{X_j} + {}^{\mathrm{a}}\vec{f}^{\,X_j^{\mathrm{a}}} + {}^{\mathrm{g}}\vec{f}^{\,X_j^*} \right)
\end{aligned} \tag{A.27}$$

The rate of change of angular impulse in Eq. A.26 and A.27 actually is the *biased* angular impulse ($\hbar$ is used instead of h), which excludes the term that is set up by the linear acceleration of the reference point $X_j^\ominus$. The summed biased angular impulse change relative to $X_k^\ominus$ equals the torque load in $X_k^\ominus$ (see discussion in §5.1.3 of [5]). For the angular and linear impulse of the element X_j holds (no coordinate system reference):

$$\begin{aligned}
{}^{X_k^\ominus}\dot{\vec{\hbar}}^{X_j} &= {}^{X_k^\ominus}\vec{r}^{\,X_j^*} \times m^{X_j} \cdot \vec{a}^{\,X_j^*} + \boldsymbol{I}^{X_j} \bullet \vec{\alpha}^{\,X_j} + \vec{\omega}^{\,X_j} \times \boldsymbol{I}^{X_j} \bullet \underline{\omega}^{X_j} \\
\dot{\vec{p}}^{X_j} &= m^{X_j} \cdot \vec{a}^{\,X_j^*}
\end{aligned} \tag{A.28}$$

so that:

$${}^{X_k^\ominus}\dot{\vec{\hbar}}^{X_j} = {}^{X_{k+1}^\ominus}\dot{\vec{\hbar}}^{X_j} + {}^{X_k^\ominus}\vec{r}^{\,X_{k+1}^\ominus} \times \dot{\vec{p}}^{X_j} \tag{A.29}$$

We introduce the feedthrough torque and force load ${}^{\mathrm{FT}}\vec{t}^{\,X_k^\ominus}$ and ${}^{\mathrm{FT}}\vec{f}^{\,X_k^\ominus}$ from element X_{k+1} onto element X_k in its entry point:

$$\begin{aligned}
{}^{\mathrm{FT}}\vec{t}^{\,X_k^\ominus} &= {}^{X_k^\ominus}\vec{r}^{\,X_{k+1}^\ominus} \times \sum_{j=k+1}^{N} \left(-\dot{\vec{p}}^{X_j} + {}^{\mathrm{a}}\vec{f}^{\,X_j^{\mathrm{a}}} + {}^{\mathrm{g}}\vec{f}^{\,X_j^*} \right) + \\
&\quad \sum_{j=k+1}^{N} \left(-{}^{X_{k+1}^\ominus}\dot{\vec{\hbar}}^{X_j} + {}^{\mathrm{a}}\vec{t}^{\,X_j^{\mathrm{a}}} + {}^{X_{k+1}^\ominus}\vec{r}^{\,X_j^{\mathrm{a}}} \times {}^{\mathrm{a}}\vec{f}^{\,X_j^{\mathrm{a}}} + {}^{X_{k+1}^\ominus}\vec{r}^{\,X_j^*} \times {}^{\mathrm{g}}\vec{f}^{\,X_j^*} \right) \\
{}^{\mathrm{FT}}\vec{f}^{\,X_k^\ominus} &= \sum_{j=k+1}^{N} \left(-\dot{\vec{p}}^{X_j} + {}^{\mathrm{a}}\vec{f}^{\,X_j^{\mathrm{a}}} + {}^{\mathrm{g}}\vec{f}^{\,X_j^*} \right)
\end{aligned} \tag{A.30}$$

The angular and linear impulse equation can then be formulated as follows:

$$\begin{aligned}
{}^{X_k^\ominus}\dot{\vec{\hbar}}^{X_k} &= {}^{X_{k-1}}\vec{t}^{\,X_k^\ominus} + {}^{\mathrm{FT}}\vec{t}^{\,X_k^\ominus} + {}^{\mathrm{a}}\vec{t}^{\,X_k^{\mathrm{a}}} + {}^{X_k^\ominus}\vec{r}^{\,X_k^{\mathrm{a}}} \times {}^{\mathrm{a}}\vec{f}^{\,X_k^{\mathrm{a}}} + {}^{X_k^\ominus}\vec{r}^{\,X_k^*} \times {}^{\mathrm{g}}\vec{f}^{\,X_k^*} \\
\dot{\vec{p}}^{X_k} &= {}^{X_{k-1}}\vec{f}^{\,X_k^\ominus} + {}^{\mathrm{FT}}\vec{f}^{\,X_k^\ominus} + {}^{\mathrm{a}}\vec{f}^{\,X_k^{\mathrm{a}}} + {}^{\mathrm{g}}\vec{f}^{\,X_k^*}
\end{aligned} \tag{A.31}$$

while the following recursive relationships hold for the feedthrough loads on X_k:

$$\begin{aligned}
{}^{\mathrm{FT}}\vec{f}^{\,X_k^\ominus} &= {}^{\mathrm{FT}}\vec{f}^{\,X_{k+1}^\ominus} - \dot{\vec{p}}^{X_{k+1}} + {}^{\mathrm{a}}\vec{f}^{\,X_{k+1}^{\mathrm{a}}} + {}^{\mathrm{g}}\vec{f}^{\,X_{k+1}^*} \\
{}^{\mathrm{FT}}\vec{t}^{\,X_k^\ominus} &= {}^{\mathrm{FT}}\vec{t}^{\,X_{k+1}^\ominus} + {}^{X_k^\ominus}\vec{r}^{\,X_{k+1}^\ominus} \times {}^{\mathrm{FT}}\vec{f}^{\,X_k^\ominus} - {}^{X_{k+1}^\ominus}\dot{\vec{\hbar}}^{X_{k+1}} + {}^{\mathrm{a}}\vec{t}^{\,X_{k+1}^{\mathrm{a}}} + \\
&\qquad {}^{X_{k+1}^\ominus}\vec{r}^{\,X_{k+1}^{\mathrm{a}}} \times {}^{\mathrm{a}}\vec{f}^{\,X_{k+1}^{\mathrm{a}}} + {}^{X_{k+1}^\ominus}\vec{r}^{\,X_{k+1}^*} \times {}^{\mathrm{g}}\vec{f}^{\,X_{k+1}^*}
\end{aligned} \tag{A.32}$$

Of course, these recursive relationships do not hold for the final element $k_{\mathrm{L}}(m)$ in subcomponent m. The feedthrough loading now comes from the first element $k_1(m+1)$ of

the next subcomponent $m+1$ and works on $X_{k_{\mathrm{L}}(m)}$ in its *exit* point. The equations of motions now are (compare with Eq. A.31):

$$\begin{aligned}
{}^{X^{\ominus}_{k_{\mathrm{L}}(m)}}\dot{\vec{h}}^{X_{k_{\mathrm{L}}(m)}} &= {}^{X_{k_{\mathrm{L}}(m)-1}}\vec{t}^{\,X^{\ominus}_{k_{\mathrm{L}}(m)}} + {}^{\mathrm{FT}}\vec{t}^{\,X^{\oplus}_{k_1(m+1)-1}} + {}^{X^{\ominus}_{k_{\mathrm{L}}(m)}}\vec{r}^{\,X^{\oplus}_{k_{\mathrm{L}}(m)}} \times \\
{}^{\mathrm{FT}}\vec{f}^{\,X^{\oplus}_{k_1(m+1)-1}} + {}^{\mathrm{a}}\vec{t}^{\,X^{\mathrm{a}}_{k_{\mathrm{L}}(m)}} + {}^{X^{\ominus}_{k_{\mathrm{L}}(m)}}\vec{r}^{\,X^{\mathrm{a}}_{k_{\mathrm{L}}(m)}} \times {}^{\mathrm{a}}\vec{f}^{\,X^{\mathrm{a}}_{k_{\mathrm{L}}(m)}} + {}^{X^{\ominus}_{k_{\mathrm{L}}(m)}}\vec{r}^{\,X^{*}_{k_{\mathrm{L}}(m)}} \times {}^{\mathrm{g}}\vec{f}^{\,X^{*}_{k_{\mathrm{L}}(m)}} \\
\dot{\vec{p}}^{\,X_{k_{\mathrm{L}}(m)}} &= {}^{X_{k_{\mathrm{L}}(m)-1}}\vec{f}^{\,X^{\ominus}_{k_{\mathrm{L}}(m)}} + {}^{\mathrm{FT}}\vec{f}^{\,X^{\oplus}_{k_1(m+1)-1}} + {}^{\mathrm{a}}\vec{f}^{\,X^{\mathrm{a}}_{k_{\mathrm{L}}(m)}} + {}^{\mathrm{g}}\vec{f}^{\,X^{*}_{k_{\mathrm{L}}(m)}}
\end{aligned} \tag{A.33}$$

Note that index $k_1(m+1)-1$ equals $k_{\mathrm{L}}(m)$ but the first notation is associated with subcomponent $m+1$ and the second with m.

The feedthrough loads from subcomponent m to $m-1$ are determined as follows:

$$\begin{aligned}
{}^{\mathrm{FT}}\vec{f}^{\,X_{\mathrm{PP}(m)}} \triangleq {}^{\mathrm{FT}}\vec{f}^{\,X^{\oplus}_{k_1(m)-1}} &= {}^{\mathrm{FT}}\vec{f}^{\,X^{\ominus}_{k_1(m)}} - \dot{\vec{p}}^{\,X_{k_1(m)}} + {}^{\mathrm{a}}\vec{f}^{\,X^{\mathrm{a}}_{k_1(m)}} + {}^{\mathrm{g}}\vec{f}^{\,X^{*}_{k_1(m)}} \\
{}^{\mathrm{FT}}\vec{t}^{\,X_{\mathrm{PP}(m)}} \triangleq {}^{\mathrm{FT}}\vec{t}^{\,X^{\oplus}_{k_1(m)-1}} &= {}^{\mathrm{FT}}\vec{t}^{\,X^{\ominus}_{k_1(m)}} - {}^{X^{\ominus}_{k_1(m)}}\dot{\vec{h}}^{X_{k_1(m)}} + {}^{\mathrm{a}}\vec{t}^{\,X^{\mathrm{a}}_{k_1(m)}} + \\
&\quad {}^{X^{\ominus}_{k_1(m)}}\vec{r}^{\,X^{\mathrm{a}}_{k_1(m)}} \times {}^{\mathrm{a}}\vec{f}^{\,X^{\mathrm{a}}_{k_1(m)}} + {}^{X^{\ominus}_{k_1(m)}}\vec{r}^{\,X^{*}_{k_1(m)}} \times {}^{\mathrm{g}}\vec{f}^{\,X^{*}_{k_1(m)}}
\end{aligned} \tag{A.34}$$

The feedthrough loads in the *entry* point of the last element $X_{k_{\mathrm{L}}(m)}$ of a subcomponent m are defined zero; the feedthrough loads from the next subcomponent are added to the external loads to the last element of the actual subcomponent.

The expressions for the feedthrough loads from the blade flange onto the rotor centre are obtained from Eq. A.34 (take $m=1$). Note that subcomponent '0' of the rotor blade is the 'blade base' that is set up by 'dummy element' X_0. Element X_0 only provides a spanwise offset over the blade root radius R_{root} from the rotor centre (along $\vec{e}_y^{\,X_0}$). The entry point of X_0 coincides with the rotor centre $R^{\mathrm{c}}_{\mathrm{r}}$ and the exit point with the blade flange's entry point $X_1^{\ominus}$. Thus, the rotor centre is loaded by the rotor blade X as follows:

$$\begin{aligned}
{}^{\mathrm{FT}}\vec{f}^{\,X^{\ominus}_0} &= {}^{\mathrm{FT}}\vec{f}^{\,X_{\mathrm{PP}(2)}} - \dot{\vec{p}}^{\,X_1} + {}^{\mathrm{a}}\vec{f}^{\,X^{\mathrm{a}}_1} + {}^{\mathrm{g}}\vec{f}^{\,X^{*}_1} \\
{}^{\mathrm{FT}}\vec{t}^{\,X^{\ominus}_0} &= {}^{\mathrm{FT}}\vec{t}^{\,X_{\mathrm{PP}(2)}} - {}^{X^{\ominus}_1}\dot{\vec{h}}^{X_1} + {}^{\mathrm{a}}\vec{t}^{\,X^{\mathrm{a}}_1} + \\
&\quad {}^{X^{\ominus}_1}\vec{r}^{\,X^{\mathrm{a}}_1} \times {}^{\mathrm{a}}\vec{f}^{\,X^{\mathrm{a}}_1} + {}^{X^{\ominus}_1}\vec{r}^{\,X^{*}_1} \times {}^{\mathrm{g}}\vec{f}^{\,X^{*}_1} + R_{\mathrm{root}} \cdot \vec{e}_y^{\,X_0} \times {}^{\mathrm{FT}}\vec{f}^{\,X^{\ominus}_0}
\end{aligned} \tag{A.35}$$

The coordinate system $\vec{e}^{\,X_0}_{x,y,z}$ follows from the coordinate system on the rotor shaft & hub $\vec{e}^{\,R_{\mathrm{r}}}_{x,y,z}$ after rotation along the x-axis over the blade root azimuth offset angle $2\pi\cdot(b-1)/B$ for rotor blade X_b with $X_b = D, E, F$ for $b = 1, 2, 3$.

Summarised angular and linear vector impulse equations

Before the equations of motions are formulated as scalar equations in coordinates along the axes of the intermediate coordinate systems, the angular and linear vector impulse equations are slightly reformulated. For each blade element the loads in the entry point are subdivided in 'responsive loads', 'feedthrough loads' and 'external loads', respectively marked with prefixes RS, FT and EX):

$$\begin{aligned}
{}^{X^{\ominus}_k}\dot{\vec{h}}^{X_k} &= {}^{\mathrm{RS}}\vec{t}^{\,X^{\ominus}_k} + {}^{\mathrm{FT}}\vec{t}^{\,X^{\ominus}_k} + {}^{\mathrm{EX}}\vec{t}^{\,X^{\ominus}_k} \\
\dot{\vec{p}}^{\,X_k} &= {}^{\mathrm{RS}}\vec{f}^{\,X^{\ominus}_k} + {}^{\mathrm{FT}}\vec{f}^{\,X^{\ominus}_k} + {}^{\mathrm{EX}}\vec{f}^{\,X^{\ominus}_k}
\end{aligned} \tag{A.36}$$

The external loads follows from the gravitation and aerodynamic conversion while these loads for the last element in a subcomponent are augmented with the feedthrough loads

from the next subcomponent:

$$\begin{aligned}
{}^{\mathrm{EX}}\vec{f}^{\,X_k^{\ominus}} &\triangleq {}^{\mathrm{a}}\vec{f}^{\,X_k^{\mathrm{a}}} + {}^{\mathrm{g}}\vec{f}^{\,X_k^{*}} + \delta_{k,k_{\mathrm{L}(m)}} \cdot {}^{\mathrm{FT}}\vec{f}^{\,X_{\mathrm{PP}(m+1)}} \\
{}^{\mathrm{EX}}\vec{t}^{\,X_k^{\ominus}} &\triangleq {}^{\mathrm{a}}\vec{t}^{\,X_k^{\mathrm{a}}} + {}^{X_k^{\ominus}\!\!\rightarrow}\vec{r}^{\,X_k^{\mathrm{a}}} \times {}^{\mathrm{a}}\vec{f}^{\,X_k^{\mathrm{a}}} + {}^{X_k^{\ominus}\!\!\rightarrow}\vec{r}^{\,X_k^{*}} \times {}^{\mathrm{g}}\vec{f}^{\,X_k^{*}} + \\
&\qquad \delta_{k,k_{\mathrm{L}(m)}} \cdot \left({}^{\mathrm{FT}}\vec{t}^{\,X_{\mathrm{PP}(m+1)}} + {}^{X_k^{\ominus}\!\!\rightarrow}\vec{r}^{\,X_k^{\oplus}} \times {}^{\mathrm{FT}}\vec{f}^{\,X_{\mathrm{PP}(m+1)}} \right)
\end{aligned} \tag{A.37}$$

Note that ${}^{\mathrm{FT}}\vec{f}^{\,X_{\mathrm{PP}(m+1)}}$ and ${}^{\mathrm{FT}}\vec{t}^{\,X_{\mathrm{PP}(m+1)}}$ equal $\vec{0}$ for $k_{\mathrm{L}}(m) = N$ ($m = 2$).

The expressions for the feedthrough loads onto the last element of a subcomponent differ from those on the foregoing elements:

$$\begin{aligned}
{}^{\mathrm{FT}}\vec{f}^{\,X_k^{\ominus}} &= \begin{cases} \vec{0} & \text{for } k = k_{\mathrm{L}}(m) \\ {}^{\mathrm{FT}}\vec{f}^{\,X_{k+1}^{\ominus}} - \dot{\vec{p}}^{\,X_{k+1}} + {}^{\mathrm{EX}}\vec{f}^{\,X_{k+1}^{\ominus}} & \text{for } k < k_{\mathrm{L}}(m) \end{cases} \\
{}^{\mathrm{FT}}\vec{t}^{\,X_k^{\ominus}} &= \begin{cases} \vec{0} & \text{for } k = k_{\mathrm{L}}(m) \\ {}^{\mathrm{FT}}\vec{t}^{\,X_{k+1}^{\ominus}} + {}^{X_k^{\ominus}\!\!\rightarrow}\vec{r}^{\,X_k^{\oplus}} \times {}^{\mathrm{FT}}\vec{f}^{\,X_k^{\ominus}} - {}^{X_{k+1}^{\ominus}}\dot{\vec{h}}^{\,X_{k+1}} + {}^{\mathrm{EX}}\vec{t}^{\,X_{k+1}^{\ominus}} & \text{for } k < k_{\mathrm{L}}(m) \end{cases}
\end{aligned} \tag{A.38}$$

The expressions for the blade loads on the rotor centre are reformulated as:

$$\begin{aligned}
{}^{\mathrm{FT}}\vec{f}^{\,X_0^{\ominus}} &= {}^{\mathrm{FT}}\vec{f}^{\,X_1^{\ominus}} - \dot{\vec{p}}^{\,X_1} + {}^{\mathrm{EX}}\vec{f}^{\,X_1^{\ominus}} \\
{}^{\mathrm{FT}}\vec{t}^{\,X_0^{\ominus}} &= {}^{\mathrm{FT}}\vec{t}^{\,X_1^{\ominus}} - {}^{X_1^{\ominus}}\dot{\vec{h}}^{\,X_1} + {}^{\mathrm{EX}}\vec{t}^{\,X_1^{\ominus}} + R_{\mathrm{root}} \cdot \vec{e}_y^{\,X_0} \times {}^{\mathrm{FT}}\vec{f}^{\,X_0^{\ominus}}
\end{aligned} \tag{A.39}$$

The responsive loads ${}^{\mathrm{RS}}\vec{f}^{\,X_k^{\ominus}}$ and ${}^{\mathrm{RS}}\vec{t}^{\,X_k^{\ominus}}$ are the loads from the preceeding element X_{k-1} on element X_k. A responsive load coordinate in the entry point is a visco/elastic load or actuation load from a control device if a degree of freedom has been defined 'along the coordinate direction'; otherwise it is just a contact force from the preceeding element. If a responsive load coordinate pertains to a degree of freedom, then its dependency on that degree of freedom and its time derivative or on other degrees of freedom is explicitely defined. Such a defined dependency tells that an scalar equation of motion exists along the concerning 'load coordinate direction'.

A.2.2 Equations of motion for rotor blade profile & structure X_{p}

The first four paragraphs in this subsection give a summary of the involved variables in the coordinate vectors for the impulse of the blade elements X_2 up to X_N and for the aerodynamic, gravitation and responsive loading on those elements. The subsequent paragraphs (v) list the needed input variables to profile & structure X_{p}, (vi) describe the derivation of the system matrices in the state space model for X_{p} and (vii) lists the required output variables from X_{p} and links them to the state and input variables via additional system matrices.

The (blade-generic) subcomponent model for the structure & profile X_{p} is obtained by a call to TBUX2SUBEOM() in function TBUBLADEEOM(), which in turn is called to from function TBUAEROEOM(). The model for X_{p} exists as structure variable sysX2sub. The fields in sysX2sub are 2D matrices A, B, C, K, the parameterisation of the first order state space representation, and cell arrays with lists of input, output and state variable names. Point of departure for model creation by function TBUX2SUBEOM() is the availability for blade elements $X_2 \ldots X_N$ of ((f).c.s.: (final) coordinate system, $k = 2 \ldots N$):

- means and sensitivities of angular and linear impulse vectors (along f.c.s. of X_k in actual position)

- means and sensitivities of aerodynamic and gravitation loads (along f.c.s., conversion c.s. and annulus wise c.s. of X_k in actual position; see par. **(vii)**)
- sensitivities of displacement vectors relative to rotor centre in average position (along f.c.s. of X_0 in average position)
- transformation matrices and their sensitivities to rotational dofs
- stiffness and damper values in the connection points between two elements
- element length, location of c.o.g. and aerodynamic conversion point
- bottom-up ranking of rotation and translation axes in the connnection points
- flags for angular and linear dofs in the connection points

The mentioned sensitivities belong to the 'motion and load formulations' and map all motion and load variations to input variables from the blade flange, the drive-train the wake, or the environment (wind, gravitation). These are provided by preceeding function calls in TBUAEREOM() to TBUBLADEKIN() etc. (see section 2.2.1).

Functionality TBUX2SUBEOM() (f.c.s: final coordinate system, $k = 2 \ldots N$)::

- definition of input name lists; each list contains the names of the input subvectors from a specific source (G, W, R, X1sub (= blade flange X_{f}));
- definition of output name lists; eahc list containts the names of the output subvectors to a specific destination (G, W, X1sub);
- lumping together the aerodynamic and gravitation loads to equivalent force and torque load formulation in the entry points of each blade elements X_k (call TBUXSUBFTEX(); coordinates along actual f.c.s.of X_k);
- transform the feedthrough loading from outward elements within the subcomponent ($X_{k+1} \ldots X_N$) on the *exit* point of element X_k to equivalent force and torque load formulations in the *entry* point of X_k (call TBUSYSFTFT(); coordinates along actual f.c.s. of X_k; define 'equal to zero' for X_N; see also Eq. A.38);
- definition of the sensitivities of the responsive (visco/elastic) loads in the entry points of X_k to the dofs (call TBUQRESPNOCP());
- derive the mass, spring and damper matrix for the equations of motion for the blade element set $X_2 \ldots X_N$ ($\boldsymbol{M}, \boldsymbol{S}, \boldsymbol{D}$; call TBUSYSMDSMX());
- derive load formulations for feedthrough force and torque loading on the blade flange exit (exit point of final element of preceeding subcomponent; call TBUSYSFTPP; coordinates along actual f.c.s. of X_1);
- derive the input matrix for the mass/spring/damper formulation of the blade model as well as output matrices on the dofs and their time derivatives and the feedthrough matrix ($\boldsymbol{G}, \boldsymbol{H}, \boldsymbol{L}, \boldsymbol{K}$; call TBUSYSGHLKMX())
- transform the mass/spring/damper model formulation $\{\boldsymbol{M}, \boldsymbol{S}, \boldsymbol{D}, \boldsymbol{G}, \boldsymbol{H}, \boldsymbol{L}, \boldsymbol{K}\}$ to the first order state space formulation $\{\boldsymbol{A}, \boldsymbol{B}, \boldsymbol{C}, \boldsymbol{K}\}$ (call TBUSYSMDS2FSR())

(i) Linear and angular impulse

Equation B.133in section B.3.2 gives the overall expressions for the coordinate vectors along the coordinate system of element X_k of the linear and angular impulse. The expressions contain mean values and sensitivities to output variables from the blade flange or rotor shaft & hub and to internal degrees of freedom. Equation B.133 tells:

$$\begin{aligned} {}^{X_k^{\ominus}}\underline{\dot{h}}^{X_k} &= {}^{X_k^{\ominus}}\bar{\underline{\dot{h}}}^{X_k} + \sum_{(\underline{z})} \frac{\partial {}^{X_k^{\ominus}}\underline{\dot{h}}^{X_k}}{\partial \underline{z}} \cdot \delta \underline{z} \\ \underline{\dot{p}}^{X_k} &= \bar{\underline{\dot{p}}}^{X_k} + \sum_{(\underline{z})} \frac{\partial \underline{\dot{p}}^{X_k}}{\partial \underline{z}} \cdot \delta \underline{z} \end{aligned} \tag{A.40}$$

The reactive variation as represented by the summation over $\underline{z}$ involves

- output from the flange X_{f}: $\underline{\omega}^{X_{\mathrm{FF}}}$, $\underline{\alpha}^{X_{\mathrm{FF}}}$, $\underline{a}^{X_{\mathrm{FF}}^{\oplus}}$;
- degrees of freedom in X_{p}, encapsulated by: $\underline{\phi}^X$, $\underline{\dot{\varphi}}^X$, $\underline{\ddot{\varphi}}^X$, $\underline{\dot{\varrho}}^X$ and $\underline{\ddot{\varrho}}^X$.

The partial derivatives to $\underline{\phi}^X$, $\underline{\dot{\varphi}}^X$, $\underline{\ddot{\varphi}}^X$, $\underline{\dot{\varrho}}^X$ and $\underline{\ddot{\varrho}}^X$ only may contain non-zero elements when they pertain to elements X_2 up to X_N.

(ii) Aerodynamic loading

Equation B.217In section B.7.3 gives the overall expressions for the coordinate vectors along the coordinate system of X_k of the concentrated aerodynamic loads ${}^{\mathrm{a}}\underline{f}^{X_k^{\mathrm{a}}}$ and ${}^{\mathrm{a}}\underline{t}^{X_k^{\mathrm{a}}}$ in the aerodynamic conversion points X_k^{a} of element X_k. The expressions contain mean values, sensitivities to the longitudinal turbulence in the intersection of blade X with the rotor annuli (${}^{\mathrm{t}}\underline{u}^{W/X}$), sensitivities to the periodic wind speed variations on blade X ($\underline{u}^X_{\mathrm{per}}$) and sensitivities to output variables from the blade flange, wake and rotor shaft & hub and to the degrees of freedom in the blade profile & structure (through $\underline{z}$). Equation B.217 tells:

$$\begin{aligned} {}^{\mathrm{a}}\underline{f}^{X_k^{\mathrm{a}}} &= {}^{\mathrm{a}}\bar{\underline{f}}^{X_k^{\mathrm{a}}} + \frac{\partial {}^{\mathrm{a}}\underline{f}^{X_k^{\mathrm{a}}}}{\partial \underline{u}^X_{\mathrm{per}}} \cdot \delta \underline{u}^X_{\mathrm{per}} + \frac{\partial {}^{\mathrm{a}}\underline{f}^{X_k^{\mathrm{a}}}}{\partial {}^{\mathrm{t}}\underline{u}^{W/X}} \cdot {}^{\mathrm{t}}\underline{u}^{W/X} + \sum_{(\underline{z})} \frac{\partial {}^{\mathrm{a}}\underline{f}^{X_k^{\mathrm{a}}}}{\partial \underline{z}} \cdot \delta \underline{z} \\ {}^{\mathrm{a}}\underline{t}^{X_k^{\mathrm{a}}} &= {}^{\mathrm{a}}\bar{\underline{t}}^{X_k^{\mathrm{a}}} + \frac{\partial {}^{\mathrm{a}}\underline{t}^{X_k^{\mathrm{a}}}}{\partial \underline{u}^X_{\mathrm{per}}} \cdot \delta \underline{u}^X_{\mathrm{per}} + \frac{\partial {}^{\mathrm{a}}\underline{t}^{X_k^{\mathrm{a}}}}{\partial {}^{\mathrm{t}}\underline{u}^{W/X}} \cdot {}^{\mathrm{t}}\underline{u}^{W/X} + \sum_{(\underline{z})} \frac{\partial {}^{\mathrm{a}}\underline{t}^{X_k^{\mathrm{a}}}}{\partial \underline{z}} \cdot \delta \underline{z} \end{aligned} \tag{A.41}$$

The reactive variation as represented by the summation over $\underline{z}$ involves

- output from the flange X_{f}: ${}^{\mathrm{a}}\underline{q}_{\mathrm{f}}^{X_{\mathrm{FF}}}$, $\underline{v}^{X_{\mathrm{FF}}^{\oplus}}$, $\underline{\omega}^{X_{\mathrm{FF}}^{\oplus}}$, $\underline{\phi}^{X_{\mathrm{FF}}}$
- output from the wake W: $\underline{u}^W_{\mathrm{i_m}}$
- processed output from the rotor shaft & hub R: $\underline{u}^{X_{\mathrm{FF}(0)}}_{\mathrm{ori}}$.
- degrees of freedom in X_{p}, encapsulated by: $\underline{\phi}^X$, $\underline{\dot{\varphi}}^X$, $\underline{\dot{\varrho}}^X$

The partial derivatives to $\underline{\phi}^X$, $\underline{\dot{\varphi}}^X$ and $\underline{\dot{\varrho}}^X$ only may contain non-zero elements when they pertain to elements X_2 up to X_N.

The actual output $\underline{u}^R_{\mathrm{ori}}$ of R_{r} is a coordinate vector along the coordinate system of R_{r}. It represents the wind speed variation relative to the rotor plane through the orientation change of the mean wind velocity as caused by deformation and deviation of the support structure and drive-drive train (see section B.5.2 up to Eq. B.167). The mapping to the processed output $\underline{u}^{X_{\mathrm{FF}(0)}}_{\mathrm{ori}}$ consists of the rotation along the x-axis over the blade root azimuth offset angle $2\pi\cdot(b-1)/B$ ($b = 1, 2, 3$ for X_b=D, E, F); see paragraph (vi) in section A.1.

(iii) Gravitation loading

Equation B.293 gives the overall expressions for the coordinate vectors along the coordinate system of X_k of the gravitation load ${}^{\mathrm{a}}\underline{f}^{X_k^*}$ in the centre of gravity X_k* of element X_k. Equation B.293 tells:

$$ {}^{\mathrm{g}}\underline{f}^{X_k^*} = {}^{\mathrm{g}}\underline{\bar{f}}^{X_k^*} + \frac{\partial {}^{\mathrm{g}}\underline{f}^{X_k^*}}{\partial \underline{g}^{R}_{\mathrm{per}}} \cdot \delta \underline{g}^{R}_{\mathrm{per}} + \frac{\partial {}^{\mathrm{g}}\underline{f}^{X_k^*}}{\partial \underline{g}^{X_{\mathrm{FF}}}_{\mathrm{ori}}} \cdot \delta \underline{g}^{X_{\mathrm{FF}}}_{\mathrm{ori}} + \frac{\partial {}^{\mathrm{g}}\underline{f}^{X_k^*}}{\partial \underline{\phi}^{X}} \cdot \delta \underline{\phi}^{X} \qquad \text{(A.42)} $$

The periodic variation $\delta \underline{g}^{R}_{\mathrm{per}}$ represents the periodic varying coordinates of the graviation vector $\vec{g}$ along the y- and z-axis of the coordinate system in the rotor centre.

The reactive variaton involves:

- output from the flange X_{f}: $\underline{g}^{X_{\mathrm{FF}}}_{\mathrm{ori}}$
- degrees of freedom in X_{p}, encapsulated by: $\underline{\phi}^{X}$

The variation $\delta \underline{g}^{X_{\mathrm{FF}}}_{\mathrm{ori}}$ represents the variation of the gravitation vector relative to the final element of the foregoing substructure through orientation changes. That is to say for the blade profile & structure X_{p}, it describes the coordinate variations along the coordinate system of X_1, caused by deformation and deviation of the support structure, drive-train and blade flange.

(iv) Responsive loads

Under the assumption of six degrees of freedom in the entry point of the blade elements X_k ($k = 2 \ldots N$), the responsive force and torque loads are visco/elastic in three directions each. The defined bottom-up ranking of the deformation directions is distorsion, flatwise bending, edgewise bending (see section 3.6.1).

The point of departure for the derivation of the equations of motion is the vector formulation of loads and motion according to Eq. A.26. Therefore we define the responsive load coordinate vectors ${}^{\mathrm{RS}}\underline{f}^{X_k}$ and ${}^{\mathrm{RS}}\underline{t}^{X_k}$ as follows:

$$ {}^{\mathrm{RS}}\underline{f}^{X_k} = \begin{bmatrix} {}^{\mathrm{RS}}f_1^{X_k} \\ {}^{\mathrm{RS}}f_2^{X_k} \\ {}^{\mathrm{RS}}f_3^{X_k} \end{bmatrix} \triangleq \begin{bmatrix} {}^{\mathrm{RS}}f_{\mathrm{x}}^{X_k^2} \\ {}^{\mathrm{RS}}f_{\mathrm{y}}^{X_k^1} \\ {}^{\mathrm{RS}}f_{\mathrm{z}}^{X_k^3} \end{bmatrix} \quad \text{and} \quad {}^{\mathrm{RS}}\underline{t}^{X_k} = \begin{bmatrix} {}^{\mathrm{RS}}t_1^{X_k} \\ {}^{\mathrm{RS}}t_2^{X_k} \\ {}^{\mathrm{RS}}t_3^{X_k} \end{bmatrix} \triangleq \begin{bmatrix} {}^{\mathrm{RS}}t_{\mathrm{x}}^{X_k^3} \\ {}^{\mathrm{RS}}t_{\mathrm{y}}^{X_k^1} \\ {}^{\mathrm{RS}}t_{\mathrm{z}}^{X_k^2} \end{bmatrix} \qquad \text{(A.43)} $$

The intermediate and final coordinate systems on the blade elements approximate the elastic neutral axes (see section 3.3 and 3.6.1. This implies the following:

- The angular and linear visco/elastic loads

$$ \begin{aligned} {}^{\mathrm{RS}}t_1^{X_k} \triangleq {}^{\mathrm{RS}}t_{\mathrm{x}}^{X_k^3} &= -s^{X_k}_{\mathrm{t_x\phi_x}} \cdot (\bar{\phi}_3^{X_k} + \delta\phi_3^{X_k}) - d^{X_k}_{\mathrm{t_x\phi_x}} \cdot \dot{\varphi}_3^{X_k} \\ {}^{\mathrm{RS}}f_3^{X_k} \triangleq {}^{\mathrm{RS}}f_{\mathrm{z}}^{X_k^3} &= -s^{X_k}_{\mathrm{f_z\rho_z}} \cdot (\bar{\rho}_3^{X_k} + \delta\rho_3^{X_k}) - d^{X_k}_{\mathrm{f_z\rho_z}} \cdot \dot{\varrho}_3^{X_k} \end{aligned} \qquad \text{(A.44)} $$

  point along the x- and z-axis of the 3rd intermediate (=final) coordinate system of X_k and represent the edgwise responsive torque and force in $X_k^{\ominus}$.

- The angular and linear visco/elastic loads

$$\begin{aligned} {}^{\mathrm{RS}}t_3^{X_k} \triangleq {}^{\mathrm{RS}}t_{\mathrm{z}}^{X_k^2} &= -s_{\mathrm{t_z}\phi_{\mathrm{z}}}^{X_k} \cdot (\bar{\phi}_2^{X_k} + \delta\phi_2^{X_k}) - d_{\mathrm{t_z}\phi_{\mathrm{z}}}^{X_k} \cdot \dot{\varphi}_2^{X_k} \\ {}^{\mathrm{RS}}f_1^{X_k} \triangleq {}^{\mathrm{RS}}f_{\mathrm{x}}^{X_k^2} &= -s_{\mathrm{f_x}\rho_{\mathrm{x}}}^{X_k} \cdot (\bar{\rho}_2^{X_k} + \delta\rho_2^{X_k}) - d_{\mathrm{f_x}\rho_{\mathrm{x}}}^{X_k} \cdot \dot{\varrho}_2^{X_k} \end{aligned} \tag{A.45}$$

  point along the z- and x-axis of the 2$^{\mathrm{nd}}$ intermediate coordinate system of X_k and represent the flatwise responsive torque and force in $X_k^{\ominus}$.

- The angular and linear visco/elastic loads

$$\begin{aligned} {}^{\mathrm{RS}}t_2^{X_k} \triangleq {}^{\mathrm{RS}}f_{\mathrm{y}}^{X_k^1} &= -s_{\mathrm{t_y}\phi_{\mathrm{y}}}^{X_k} \cdot (\bar{\phi}_1^{X_k} + \delta\phi_1^{X_k}) - d_{\mathrm{t_y}\phi_{\mathrm{y}}}^{X_k} \cdot \dot{\varphi}_1^{X_k} \\ {}^{\mathrm{RS}}f_2^{X_k} \triangleq {}^{\mathrm{RS}}t_{\mathrm{y}}^{X_k^1} &= -s_{\mathrm{f_y}\rho_{\mathrm{y}}}^{X_k} \cdot (\bar{\rho}_1^{X_k} + \delta\rho_1^{X_k}) - d_{\mathrm{f_y}\rho_{\mathrm{y}}}^{X_k} \cdot \dot{\varrho}_1^{X_k} \end{aligned} \tag{A.46}$$

  both point along the y-axis of the 1$^{\mathrm{st}}$ intermediate coordinate system of X_k and represent the co-axial responsive torque and force in $X_k^{\ominus}$.

The associated linearised expressions for the responsive loads are:

$$\begin{aligned} {}^{\mathrm{RS}}\underline{f}^{X_k} &= {}^{\mathrm{RS}}\bar{\underline{f}}^{X_k} + \frac{\partial^{\mathrm{RS}}\underline{f}^{X_k}}{\partial\underline{\rho}^X} \cdot \delta\underline{\rho}^X + \frac{\partial^{\mathrm{RS}}\underline{f}^{X_k}}{\partial\underline{\dot{\varrho}}^X} \cdot \underline{\dot{\varrho}}^X \\ {}^{\mathrm{RS}}\underline{t}^{X_k} &= {}^{\mathrm{RS}}\bar{\underline{t}}^{X_k} + \frac{\partial^{\mathrm{RS}}\underline{t}^{X_k}}{\partial\underline{\phi}^X} \cdot \delta\underline{\phi}^X + \frac{\partial^{\mathrm{RS}}\underline{t}^{X_k}}{\partial\underline{\dot{\varphi}}^X} \cdot \underline{\dot{\varphi}}^X \end{aligned} \tag{A.47}$$

For the means holds:

$$\begin{aligned} {}^{\mathrm{RS}}\bar{\underline{f}}^{X_k} &= \left[-s_{\mathrm{f_x}\rho_{\mathrm{x}}}^{X_k} \cdot \bar{\rho}_2^{X_k} \quad -s_{\mathrm{f_y}\rho_{\mathrm{y}}}^{X_k} \cdot \bar{\rho}_1^{X_k} \quad -s_{\mathrm{f_z}\rho_{\mathrm{z}}}^{X_k} \cdot \bar{\rho}_3^{X_k}\right]^{\mathrm{T}} \\ {}^{\mathrm{RS}}\bar{\underline{t}}^{X_k} &= \left[-s_{\mathrm{t_x}\phi_{\mathrm{x}}}^{X_k} \cdot \bar{\phi}_3^{X_k} \quad -s_{\mathrm{t_y}\phi_{\mathrm{y}}}^{X_k} \cdot \bar{\phi}_1^{X_k} \quad -s_{\mathrm{t_z}\phi_{\mathrm{z}}}^{X_k} \cdot \bar{\phi}_2^{X_k}\right]^{\mathrm{T}} \end{aligned} \tag{A.48}$$

For the sensitivities to the dof position variations hold:

$$\frac{\partial^{\mathrm{RS}}\underline{f}^{X_k}}{\partial\underline{\rho}^X} = \begin{pmatrix} -s_{\mathrm{f_x}\rho_{\mathrm{x}}}^{X_k} \cdot [\ 0_{(1)} \ldots 0_{((k-1)*3)} \quad 0 \quad 1 \quad 0 \quad 0_{((k*3)+1)} \ldots 0_{(N*3)}\ ] \\ -s_{\mathrm{f_y}\rho_{\mathrm{y}}}^{X_k} \cdot [\ 0_{(1)} \ldots 0_{((k-1)*3)} \quad 1 \quad 0 \quad 0 \quad 0_{((k*3)+1)} \ldots 0_{(N*3)}\ ] \\ -s_{\mathrm{f_z}\rho_{\mathrm{z}}}^{X_k} \cdot [\ 0_{(1)} \ldots 0_{((k-1)*3)} \quad 0 \quad 0 \quad 1 \quad 0_{((k*3)+1)} \ldots 0_{(N*3)}\ ] \end{pmatrix}$$

and

$$\frac{\partial^{\mathrm{RS}}\underline{t}^{X_k}}{\partial\underline{\phi}^X} = \begin{pmatrix} -s_{\mathrm{t_x}\phi_{\mathrm{x}}}^{X_k} \cdot [\ 0_{(1)} \ldots 0_{((k-1)*3)} \quad 0 \quad 0 \quad 1 \quad 0_{((k*3)+1)} \ldots 0_{(N*3)}\ ] \\ -s_{\mathrm{t_y}\phi_{\mathrm{y}}}^{X_k} \cdot [\ 0_{(1)} \ldots 0_{((k-1)*3)} \quad 1 \quad 0 \quad 0 \quad 0_{((k*3)+1)} \ldots 0_{(N*3)}\ ] \\ -s_{\mathrm{t_z}\phi_{\mathrm{z}}}^{X_k} \cdot [\ 0_{(1)} \ldots 0_{((k-1)*3)} \quad 0 \quad 1 \quad 0 \quad 0_{((k*3)+1)} \ldots 0_{(N*3)}\ ] \end{pmatrix} \tag{A.49}$$

The sensitivities to the dof speeds are obtained from the ones above by just replacing $s_{(.)}^{X_k}$ by $d_{(.)}^{X_k}$.

If less than six degrees of freedom apply in an entry point then some viso/elastic load expressions are not valid (infinite stiffness and damper values would apply). However, this is of no importance because these expressions are skipped when the equations of motions are being derived.

(v) Input variables

The input that is required by the blade profile & structure X_{p} is the envelope of all variables that are involved with the impulse vectors, aerodynamic and gravitation loads and output vectors, except of course the internal variables. So the following input applies:

- distributed aerodynamic force loads on final flange element: ${}^{\mathrm{a}}\underline{q}^{X_{\mathrm{FF}(1)}}$, ${}^{\mathrm{a_L}}\underline{q}^{X_{\mathrm{FF}(1)}}$
- kinematic vectors on flange exit: $\underline{\omega}^{X_{\mathrm{FF}(1)}}$, $\underline{\alpha}^{X_{\mathrm{FF}(1)}}$, $\underline{v}^{X^{\oplus}_{\mathrm{FF}(1)}}$, $\underline{a}^{X^{\oplus}_{\mathrm{FF}(1)}}$
- dof angular position variations in blade flange: $\underline{\phi}^{X_{\mathrm{FF}(1)}}$
- wind speed variation by orientation change up till hub: $\underline{u}_{\mathrm{ori}}^{X_{\mathrm{FF}(0)}}$.
- gravitation variation by orientation change up till flange: $\underline{g}_{\mathrm{ori}}^{X_{\mathrm{FF}(1)}}$
- displacement vectors on flange exit: $\underline{\xi}^{X_{\mathrm{FF}(1)}}$, $\underline{x}^{X_{\mathrm{FF}(1)}}$
- induction speed variation in rotor annuli: $\underline{u}_{\mathrm{i_m}}^{W}$
- periodic wind speed variation on blade: $\underline{u}_{\mathrm{per}}^{X}$
- periodic gravitation variation on blade base : $\underline{g}_{\mathrm{per}}^{X_0}$
- stochastic wind speed variation in intersection annuli/blade: $\underline{u}_{\mathrm{sto}}^{W/X}$

The input vector $\underline{v}^{X_{\mathrm{P}}}$ of the blade profile & structure has the following composition:

$$\underline{v}^{X_{\mathrm{p}}} = \begin{bmatrix} \underline{v}^{X_{\mathrm{p}}G} \\ \underline{v}^{X_{\mathrm{p}}W} \\ \underline{v}^{X_{\mathrm{p}}R} \\ \underline{v}^{X_{\mathrm{p}}X_{\mathrm{f}}} \end{bmatrix} \quad \text{with} \quad \underline{v}^{X_{\mathrm{p}}G} = \begin{bmatrix} \underline{u}_{\mathrm{per}}^{X} \\ \underline{g}_{\mathrm{per}}^{X_0} \\ \underline{u}_{\mathrm{sto}}^{W/X} \end{bmatrix}$$

$$\text{and} \quad \underline{v}^{X_{\mathrm{p}}W} = \begin{bmatrix} \underline{u}_{\mathrm{i_m}}^{W} \end{bmatrix} \;;\; \underline{v}^{X_{\mathrm{p}}R} = \begin{bmatrix} \underline{u}_{\mathrm{ori}}^{X_{\mathrm{FF}(0)}} \end{bmatrix} \;;\; \underline{v}^{X_{\mathrm{p}}X_{\mathrm{f}}} = \begin{bmatrix} \underline{\omega}^{X_{\mathrm{FF}(1)}} \\ \underline{\alpha}^{X_{\mathrm{FF}(1)}} \\ \underline{v}^{X^{\oplus}_{\mathrm{FF}(1)}} \\ \underline{a}^{X^{\oplus}_{\mathrm{FF}(1)}} \\ \underline{\phi}^{X_{\mathrm{FF}(1)}} \\ {}^{\mathrm{a}}\underline{q}^{X_{\mathrm{FF}(1)}} \\ {}^{\mathrm{a_L}}\underline{q}^{X_{\mathrm{FF}(1)}} \\ \underline{g}_{\mathrm{ori}}^{X_{\mathrm{FF}(1)}} \\ \underline{\xi}^{X_{\mathrm{FF}(1)}} \\ \underline{x}^{X_{\mathrm{FF}(1)}} \end{bmatrix} \tag{A.50}$$

For the composition of the 'independent' input subvectors $\underline{u}_{\mathrm{per}}^{X}$, $\underline{g}_{\mathrm{per}}^{X_0}$ and $\underline{u}_{\mathrm{sto}}^{W/X}$, and the wake induction vector $\underline{u}_{\mathrm{i_m}}^{W}$ see section 3.4.2 and also Eq. B.175, B.182 and B.279.

(vi) Equations of motion and 2nd order vector state equation

The availabe partial derivatives for the impulse vectors and the external, feedthrough and responsive loads enable to formulate the equations of motion as a second order state space model. The 'state equation' has a mass, damper and spring matrix on the left hand side and an input matrix on the right hand side. The left hand side matrices are partitionend in

accordance with the angular dofs and linear dofs while the input matrix is partitioned in accordance with the subvectors in the input vector:

$$\left[\boldsymbol{M}_{\varphi}^{X_{\mathrm{p}}} \mid \boldsymbol{M}_{\varrho}^{X_{\mathrm{p}}}\right] \cdot \begin{bmatrix} \underline{\ddot{\varphi}}^{X} \\ \underline{\ddot{\varrho}}^{X} \end{bmatrix} + \left[\boldsymbol{D}_{\varphi}^{X_{\mathrm{p}}} \mid \boldsymbol{D}_{\varrho}^{X_{\mathrm{p}}}\right] \cdot \begin{bmatrix} \underline{\dot{\varphi}}^{X} \\ \underline{\dot{\varrho}}^{X} \end{bmatrix} +$$

$$\left[\boldsymbol{S}_{\varphi}^{X_{\mathrm{p}}} \mid \boldsymbol{S}_{\varrho}^{X_{\mathrm{p}}}\right] \cdot \begin{bmatrix} \underline{\varphi}^{X} \\ \underline{\varrho}^{X} \end{bmatrix} = \left[\boldsymbol{G}^{X_{\mathrm{p}}G} \mid \boldsymbol{G}^{X_{\mathrm{p}}W} \mid \boldsymbol{G}^{X_{\mathrm{p}}R} \mid \boldsymbol{G}^{X_{\mathrm{p}}X_{\mathrm{f}}}\right] \cdot \begin{bmatrix} \underline{v}^{X_{\mathrm{p}}G} \\ \underline{v}^{X_{\mathrm{p}}W} \\ \underline{v}^{X_{\mathrm{p}}R} \\ \underline{v}^{X_{\mathrm{p}}X_{\mathrm{f}}} \end{bmatrix} \tag{A.51}$$

These matrices are derived by considering the vector impulse equations in expressions A.36 up to A.39 for the elements $X_N \ldots X_2$ in their respective sets of three coordinate systems. We start in element X_N and consider in the third intermediate coordinate system the x-coordinate of the angular impulse and the z-coordinate of the linear impulse. We denote these vector equation coordinates as the $3\mathrm{rd}$ *scalar angular and linear impulse equation for element* X_N. See also the paragraph on the responsive loads.

Afterwards, the z-coordinate of the angular impulse equation and the x-coordinate of the linear impulse equaton are considered in the second intermediate coordinate system (i.c.s.). These coordinates set up the $2\mathrm{nd}$ scalar angular and linear impulse equation for X_N. Finally, the y-coordinates of the angular and linear impulse are dealt with in the first i.c.s. and these set up the $1\mathrm{st}$ scalar angular and linear impulse equation for X_N.

When going from X_N to X_{N-1} the (sensitivities of the) feedthrough loads in $X_{N-1}^{\ominus}$ are expressed in the final coordinate system of X_{N-1}.

The w^{th} scalar angular impulse equation for element X_k sets up the row with ranking number $6(k-1)+2(w-1)+1$ of the belonging system matrices. The involved system matrix rows are denoted as (w is the ranking number of the involved intermediate coordinate system and thus corresponds to the x, z and y-axis for $w = 3, 2, 1$):

- $\underline{\boldsymbol{m}}_{h\varphi_w}^{X_k}$ and $\underline{\boldsymbol{m}}_{h\varrho_w}^{X_k}$ to mass matrix partitions $\boldsymbol{M}_{\varphi}^{X_{\mathrm{p}}}$ and $\boldsymbol{M}_{\varrho}^{X_{\mathrm{p}}}$;
- $\underline{\boldsymbol{d}}_{h\varphi_w}^{X_k}$ and $\underline{\boldsymbol{d}}_{h\varrho_w}^{X_k}$ to damping matrix partitions $\boldsymbol{D}_{\varphi}^{X_{\mathrm{p}}}$ and $\boldsymbol{D}_{\varrho}^{X_{\mathrm{p}}}$;
- $\underline{\boldsymbol{s}}_{h\varphi_w}^{X_k}$ and $\underline{\boldsymbol{s}}_{h\varrho_w}^{X_k}$ to stiffness matrix partitions $\boldsymbol{S}_{\varphi}^{X_{\mathrm{p}}}$ and $\boldsymbol{S}_{\varrho}^{X_{\mathrm{p}}}$;
- $\underline{\boldsymbol{g}}_{h_w}^{X_k G}$, $\underline{\boldsymbol{g}}_{h_w}^{X_k W}$, $\underline{\boldsymbol{g}}_{h_w}^{X_k R}$ and $\underline{\boldsymbol{g}}_{h_w}^{X_k X_{\mathrm{f}}}$ to input matrix partitions $\boldsymbol{G}^{X_{\mathrm{p}}G}$, $\boldsymbol{G}^{X_{\mathrm{p}}W}$, $\boldsymbol{G}^{X_{\mathrm{p}}R}$ and $\boldsymbol{G}^{X_{\mathrm{p}}X_{\mathrm{f}}}$.

The w^{th} scalar linear impulse equation for element X_k yields the row with ranking number $6(k-1)+2(w-1)+2$ of the belonging system matrices The involved system matrix rows are denoted as (i.c.s. ranking number w now corresponds to the z, x and y-axis for $w = 3, 2, 1$):

- $\underline{\boldsymbol{m}}_{p\varphi_w}^{X_k}$ and $\underline{\boldsymbol{m}}_{p\varrho_w}^{X_k}$ to mass matrix partitions $\boldsymbol{M}_{\varphi}^{X_{\mathrm{p}}}$ and $\boldsymbol{M}_{\varrho}^{X_{\mathrm{p}}}$;
- $\underline{\boldsymbol{d}}_{p\varphi_w}^{X_k}$ and $\underline{\boldsymbol{d}}_{p\varrho_w}^{X_k}$ to damping matrix partitions $\boldsymbol{D}_{\varphi}^{X_{\mathrm{p}}}$ and $\boldsymbol{D}_{\varrho}^{X_{\mathrm{p}}}$;
- $\underline{\boldsymbol{s}}_{p\varphi_w}^{X_k}$ and $\underline{\boldsymbol{s}}_{p\varrho_w}^{X_k}$ to stiffness matrix partitions $\boldsymbol{S}_{\varphi}^{X_{\mathrm{p}}}$ and $\boldsymbol{D}_{\varrho}^{X_{\mathrm{p}}}$;
- $\underline{\boldsymbol{g}}_{p_w}^{X_k G}$, $\underline{\boldsymbol{g}}_{p_w}^{X_k W}$, $\underline{\boldsymbol{g}}_{p_w}^{X_k R}$ and $\underline{\boldsymbol{g}}_{p_w}^{X_k X_{\mathrm{f}}}$ to input matrix partitions $\boldsymbol{G}^{X_{\mathrm{p}}G}$, $\boldsymbol{G}^{X_{\mathrm{p}}W}$, $\boldsymbol{G}^{X_{\mathrm{p}}R}$ and $\boldsymbol{G}^{X_{\mathrm{p}}X_{\mathrm{f}}}$.

Above mentioned rows in the left hand side matrices are obtained from the partial derivatives of the scalar impulse equations to the *internal* variables $\underline{\ddot{\varphi}}^{X}$, $\underline{\ddot{\varrho}}^{X}$, $\underline{\dot{\varphi}}^{X}$, $\underline{\dot{\varrho}}^{X}$, $\underline{\varphi}^{X}$ and $\underline{\varrho}^{X}$. The rows in the right hand side matrices follow from the partial derivatives of the scalar impulse equations to the input variables $\underline{v}^{X_{\mathrm{p}}G}$, $\underline{v}^{X_{\mathrm{p}}W}$, $\underline{v}^{X_{\mathrm{p}}R}$ and $\underline{v}^{X_{\mathrm{p}}X_{\mathrm{f}}}$.

Two complications seem to occur:

- only $6(N-1)$ rows but $6N$ columns in left hand system matrices;
- non-valid rows in left hand system matrices for scalar impulse equations that pertain to a 'non-dof-direction'.

However, these are no real complications because the first three columns of both matrix partitions in each left hand side matrix are deleted. The influence of these blade dofs 'comes in' via the input matrix partitions that pertain to the 'feed forward' dofs $\underline{\phi}^{X_{\mathrm{FF}}}$ from the blade flange or to the other 'feed forward' inputs from the flange that also depend on the dofs in the blade flange. Besides, each non-valid row and the corresponding column, which pertains to the 'non-dof' element of $\underline{\phi}^{X}$ or $\underline{\rho}^{X}$, is deleted. Of course, the corresponding row in the right hand side input matrix is also deleted! This yields a second order system equation with square left hand side matrices and adequately dimensioned input matrix.

Note that a 'non-valid row' $6(k-1)+2(w-1)+1$ pertains to the **rotation** $\phi_{w}^{X_k}$ and thus to the column $3\cdot(k-1)+w$ in the **left** partition of the left hand system matrices, while a 'non-valid row' $6(k-1)+2(w-1)+2$ pertains to the **translation** $\rho_{w}^{X_k}$ and thus to the column $3\cdot(k-1)+w$ in the **right** partition.

We end up this paragraph with the formulation of the three scalar angular and linear impulse equations and their explicit relationship with the row vectors in the system matrices of Eq. A.51.

The third scalar angular impulse equation pertains to the x-axis and the linear one to the z-axis of the third intermediate coordinate system. It holds:

$$\begin{aligned}
[\,1\,0\,0\,]\cdot {}^{X_k^{\ominus}}\dot{\underline{h}}^{X_k} &= [\,1\,0\,0\,]\cdot {}^{\mathrm{RS}}\underline{t}^{X_k^{\ominus}} + [\,1\,0\,0\,]\cdot {}^{\mathrm{FT}}\underline{t}^{X_k^{\ominus}} + [\,1\,0\,0\,]\cdot {}^{\mathrm{EX}}\underline{t}^{X_k^{\ominus}} \\
[\,0\,0\,1\,]\cdot \underline{\dot{p}}^{X_k} &= [\,0\,0\,1\,]\cdot {}^{\mathrm{RS}}\underline{f}^{X_k^{\ominus}} + [\,0\,0\,1\,]\cdot {}^{\mathrm{FT}}\underline{f}^{X_k^{\ominus}} + [\,0\,0\,1\,]\cdot {}^{\mathrm{EX}}\underline{f}^{X_k^{\ominus}}
\end{aligned} \tag{A.52}$$

The second scalar angular and linear impulse equation pertain to the z-axis and x-axis of the second intermediate coordinate system. It holds:

$$\begin{aligned}
{}^{X_k^2}\Phi_{(3,:)}^{X_k}\cdot {}^{X_k^{\ominus}}\dot{\underline{h}}^{X_k} &= [\,0\,0\,1\,]\cdot {}^{\mathrm{RS}}\underline{t}^{X_k^{\ominus}} + {}^{X_k^2}\Phi_{(3,:)}^{X_k}\cdot {}^{\mathrm{FT}}\underline{t}^{X_k^{\ominus}} + {}^{X_k^2}\Phi_{(3,:)}^{X_k}\cdot {}^{\mathrm{EX}}\underline{t}^{X_k^{\ominus}} \\
{}^{X_k^2}\Phi_{(1,:)}^{X_k}\cdot \underline{\dot{p}}^{X_k} &= [\,1\,0\,0\,]\cdot {}^{\mathrm{RS}}\underline{f}^{X_k^{\ominus}} + {}^{X_k^2}\Phi_{(1,:)}^{X_k}\cdot {}^{\mathrm{FT}}\underline{f}^{X_k^{\ominus}} + {}^{X_k^2}\Phi_{(1,:)}^{X_k}\cdot {}^{\mathrm{EX}}\underline{f}^{X_k^{\ominus}}
\end{aligned} \tag{A.53}$$

The first scalar impulse equations both pertain to the y-axis of the first i.c.s.:

$$\begin{aligned}
{}^{X_k^1}\Phi_{(2,:)}^{X_k}\cdot {}^{X_k^{\ominus}}\dot{\underline{h}}^{X_k} &= [\,0\,1\,0\,]\cdot {}^{\mathrm{RS}}\underline{t}^{X_k^{\ominus}} + {}^{X_k^1}\Phi_{(2,:)}^{X_k}\cdot {}^{\mathrm{FT}}\underline{t}^{X_k^{\ominus}} + {}^{X_k^1}\Phi_{(2,:)}^{X_k}\cdot {}^{\mathrm{EX}}\underline{t}^{X_k^{\ominus}} \\
{}^{X_k^1}\Phi_{(2,:)}^{X_k}\cdot \underline{\dot{p}}^{X_k} &= [\,0\,1\,0\,]\cdot {}^{\mathrm{RS}}\underline{f}^{X_k^{\ominus}} + {}^{X_k^1}\Phi_{(2,:)}^{X_k}\cdot {}^{\mathrm{FT}}\underline{f}^{X_k^{\ominus}} + {}^{X_k^1}\Phi_{(2,:)}^{X_k}\cdot {}^{\mathrm{EX}}\underline{f}^{X_k^{\ominus}}
\end{aligned} \tag{A.54}$$

Equations A.47 up to A.49 specifiy the responsive load coordinate vectors ${}^{\mathrm{RS}}\underline{t}^{X_k^{\ominus}}$ and ${}^{\mathrm{RS}}\underline{f}^{X_k^{\ominus}}$

The external load coordinate vectors follow straightforward from Eq. A.37:

$$\begin{aligned}
{}^{\mathrm{EX}}\underline{f}^{X_k^{\ominus}} &\triangleq {}^{\mathrm{a}}\underline{f}^{X_k^{\mathrm{a}}} + {}^{\mathrm{g}}\underline{f}^{X_k^{*}} \\
{}^{\mathrm{EX}}\underline{t}^{X_k^{\ominus}} &\triangleq {}^{\mathrm{a}}\underline{t}^{X_k^{\mathrm{a}}} + {}^{X_k^{\ominus}}\underline{r}^{X_k^{\mathrm{a}}} \times {}^{\mathrm{a}}\underline{f}^{X_k^{\mathrm{a}}} + {}^{X_k^{\ominus}}\underline{r}^{X_k^{*}} \times {}^{\mathrm{g}}\underline{f}^{X_k^{*}}
\end{aligned} \tag{A.55}$$

The expressions for the feedthrough load coordinate vectors are ($2 \leq k \leq N$):

$$
{}^{\mathrm{FT}}\underline{f}^{X_k^{\ominus}} = \begin{cases} \underline{0} & (k = N) \\ {}^{X_k}\Phi^{X_{k+1}} \cdot \left({}^{\mathrm{FT}}\underline{f}^{X_{k+1}^{\ominus}} - \underline{\dot{p}}^{X_{k+1}} + {}^{\mathrm{EX}}\underline{f}^{X_{k+1}^{\ominus}} \right) & (k < N) \end{cases}
$$

$$
{}^{\mathrm{FT}}\underline{t}^{X_k^{\ominus}} = \begin{cases} \underline{0} & (k = N) \\ {}^{X_k^{\ominus}}\underline{r}^{X_k^{\oplus}} \times {}^{\mathrm{FT}}\underline{f}^{X_k^{\ominus}} + {}^{X_k}\Phi^{X_{k+1}} \cdot \left({}^{\mathrm{FT}}\underline{t}^{X_{k+1}^{\ominus}} - {}^{X_{k+1}^{\ominus}}\underline{\dot{h}}^{X_{k+1}} + {}^{\mathrm{EX}}\underline{t}^{X_{k+1}^{\ominus}} \right) & (k < N) \end{cases}
$$

(A.56)

The linearised expressions for the aerodynamic and gravitation load coordinate vectors were listed in the second and third paragraph of this subsection. The expressions for the external load coordinate vectors comprise the envelope of dependencies:

$$
\begin{aligned}
{}^{\mathrm{EX}}\underline{f}^{X_k^{\ominus}} &= {}^{\mathrm{EX}}\bar{\underline{f}}^{X_k^{\ominus}} + \frac{\partial^{\mathrm{EX}}\underline{f}^{X_k^{\ominus}}}{\partial \underline{u}_{\mathrm{per}}^{X}} \cdot \underline{u}_{\mathrm{per}}^{X} + \frac{\partial^{\mathrm{EX}}\underline{f}^{X_k^{\ominus}}}{\partial \underline{g}_{\mathrm{per}}^{X_0}} \cdot \underline{g}_{\mathrm{per}}^{X_0} + \frac{\partial^{\mathrm{EX}}\underline{f}^{X_k^{\ominus}}}{\partial {}^{\mathrm{t}}\underline{u}^{W/X}} \cdot {}^{\mathrm{t}}\underline{u}^{W/X} + \sum_{(\underline{z})} \frac{\partial^{\mathrm{EX}}\underline{f}^{X_k^{\ominus}}}{\partial \underline{z}} \cdot \delta\underline{z} \\
{}^{\mathrm{EX}}\underline{t}^{X_k^{\ominus}} &= {}^{\mathrm{EX}}\bar{\underline{t}}^{X_k^{\ominus}} + \frac{\partial^{\mathrm{EX}}\underline{t}^{X_k^{\ominus}}}{\partial \underline{u}_{\mathrm{per}}^{X}} \cdot \underline{u}_{\mathrm{per}}^{X} + \frac{\partial^{\mathrm{EX}}\underline{t}^{X_k^{\ominus}}}{\partial \underline{g}_{\mathrm{per}}^{X_0}} \cdot \underline{g}_{\mathrm{per}}^{X_0} + \frac{\partial^{\mathrm{EX}}\underline{t}^{X_k^{\ominus}}}{\partial {}^{\mathrm{t}}\underline{u}^{W/X}} \cdot {}^{\mathrm{t}}\underline{u}^{W/X} + \sum_{(\underline{z})} \frac{\partial^{\mathrm{EX}}\underline{t}^{X_k^{\ominus}}}{\partial \underline{z}} \cdot \delta\underline{z}
\end{aligned}
$$

(A.57)

The reactive variation as represented by the summation over $\underline{z}$ involves

- output from the flange X_{f}: ${}^{\mathrm{a}}\underline{q}_{\mathrm{f}}^{X_{\mathrm{FF}}}$, $\underline{v}^{X_{\mathrm{FF}}^{\oplus}}$, $\underline{\omega}^{X_{\mathrm{FF}}^{\oplus}}$, $\underline{\phi}^{X_{\mathrm{FF}}}$
- output from the wake W: $\underline{u}_{\mathrm{i_m}}^{W}$
- processed output from the rotor shaft & hub R: $\underline{u}_{\mathrm{ori}}^{X_{\mathrm{FF}(0)}}$
- output from the flange X_{f}: $\underline{g}_{\mathrm{ori}}^{X_{\mathrm{FF}(1)}}$
- degrees of freedom in X_{p}, encapsulated by: $\underline{\phi}^{X}$, $\underline{\dot{\varphi}}^{X}$, $\underline{\dot{\varrho}}^{X}$

The expressions for the mean external load vectors are just the overlined versions of those in Eq. A.55. For the sensitivities hold (of course only if $\underline{q}$ applies in a right hand side partial derivative):

$$
\begin{aligned}
\frac{\partial^{\mathrm{EX}}\underline{f}^{X_k^{\ominus}}}{\partial \underline{q}} &= \frac{\partial^{\mathrm{a}}\underline{f}^{X_k^{\mathrm{a}}}}{\partial \underline{q}} + \frac{\partial^{\mathrm{g}}\underline{f}^{X_k^{*}}}{\partial \underline{q}} \\
\frac{\partial^{\mathrm{EX}}\underline{t}^{X_k^{\ominus}}}{\partial \underline{q}} &= \frac{\partial^{\mathrm{a}}\underline{t}^{X_k^{\mathrm{a}}}}{\partial \underline{q}} + \mathrm{J}^3_{v=1}\left({}^{X_k^{\ominus}}\underline{r}^{X_k^{\mathrm{a}}} \times \underline{e}_v \right) \cdot \frac{\partial^{\mathrm{a}}\underline{f}^{X_k^{\mathrm{a}}}}{\partial \underline{q}} + \mathrm{J}^3_{v=1}\left({}^{X_k^{\ominus}}\underline{r}^{X_k^{*}} \times \underline{e}_v \right) \cdot \frac{\partial^{\mathrm{g}}\underline{f}^{X_k^{*}}}{\partial \underline{q}}
\end{aligned}
$$

(A.58)

The expressions for the feed through coordinate vectors comprises the envelope of dependencies for the external loads and the impulse vectors:

$$
\begin{aligned}
{}^{\mathrm{FT}}\underline{f}^{X_k^{\ominus}} &= {}^{\mathrm{FT}}\bar{\underline{f}}^{X_k^{\ominus}} + \frac{\partial^{\mathrm{FT}}\underline{f}^{X_k^{\ominus}}}{\partial \underline{u}_{\mathrm{per}}^{X}} \cdot \underline{u}_{\mathrm{per}}^{X} + \frac{\partial^{\mathrm{FT}}\underline{f}^{X_k^{\ominus}}}{\partial \underline{g}_{\mathrm{per}}^{R}} \cdot \underline{g}_{\mathrm{per}}^{R} + \frac{\partial^{\mathrm{FT}}\underline{f}^{X_k^{\ominus}}}{\partial {}^{\mathrm{t}}\underline{u}^{W/X}} \cdot {}^{\mathrm{t}}\underline{u}^{W/X} + \sum_{(\underline{z})} \frac{\partial^{\mathrm{FT}}\underline{f}^{X_k^{\ominus}}}{\partial \underline{z}} \cdot \delta\underline{z} \\
{}^{\mathrm{FT}}\underline{t}^{X_k^{\ominus}} &= {}^{\mathrm{FT}}\bar{\underline{t}}^{X_k^{\ominus}} + \frac{\partial^{\mathrm{FT}}\underline{t}^{X_k^{\ominus}}}{\partial \underline{u}_{\mathrm{per}}^{X}} \cdot \underline{u}_{\mathrm{per}}^{X} + \frac{\partial^{\mathrm{FT}}\underline{t}^{X_k^{\ominus}}}{\partial \underline{g}_{\mathrm{per}}^{R}} \cdot \underline{g}_{\mathrm{per}}^{R} + \frac{\partial^{\mathrm{FT}}\underline{t}^{X_k^{\ominus}}}{\partial {}^{\mathrm{t}}\underline{u}^{W/X}} \cdot {}^{\mathrm{t}}\underline{u}^{W/X} + \sum_{(\underline{z})} \frac{\partial^{\mathrm{FT}}\underline{t}^{X_k^{\ominus}}}{\partial \underline{z}} \cdot \delta\underline{z}
\end{aligned}
$$

(A.59)

The reactive variation as represented by the summation over $\underline{z}$ involves the ones for the external loads, extended with

- output from the flange X_{f}: $\underline{\alpha}^{X_{\mathrm{FF}}}$, $\underline{a}^{X_{\mathrm{FF}}^{\oplus}}$;

- degrees of freedom in X_{p}, encapsulated by: $\underline{\ddot{\varphi}}^{X}$, $\underline{\ddot{o}}^{X}$.

For the sake of the pursued linearised expressions we define the average values of the feed-through loads in the *exit* of element X_k in the coordinate system of X_{k+1} ($k < N$):

$$\begin{aligned} {}^{\mathrm{FT}}\underline{\bar{f}}^{X_k^{\oplus}/X_{k+1}} &= {}^{\mathrm{FT}}\underline{\bar{f}}^{X_{k+1}^{\ominus}} - \underline{\bar{\dot{p}}}^{X_{k+1}} + {}^{\mathrm{EX}}\underline{f}^{X_{k+1}^{\ominus}} \\ {}^{\mathrm{FT}}\underline{\bar{t}}^{X_k^{\oplus}/X_{k+1}} &= {}^{\mathrm{FT}}\underline{\bar{t}}^{X_{k+1}^{\ominus}} - {}^{X_{k+1}^{\ominus}}\underline{\dot{\bar{h}}}^{X_{k+1}} + {}^{\mathrm{EX}}\underline{\bar{t}}^{X_{k+1}^{\ominus}} \end{aligned} \tag{A.60}$$

For the mean values of the feedthrough loads in the *entry* point of X_k holds:

$$\begin{aligned} {}^{\mathrm{FT}}\underline{\bar{f}}^{X_k^{\ominus}} &= {}^{X_k}\bar{\Phi}^{X_{k+1}} \cdot {}^{\mathrm{FT}}\underline{\bar{f}}^{X_k^{\oplus}/X_{k+1}} \\ {}^{\mathrm{FT}}\underline{\bar{t}}^{X_k^{\ominus}} &= {}^{X_k^{\ominus}}\underline{r}^{X_k^{\oplus}} \times {}^{\mathrm{FT}}\underline{\bar{f}}^{X_k^{\ominus}} + {}^{X_k}\bar{\Phi}^{X_{k+1}} \cdot {}^{\mathrm{FT}}\underline{\bar{t}}^{X_k^{\oplus}/X_{k+1}} \end{aligned} \tag{A.61}$$

For the corresponding variations the following expressions apply:

$$\begin{aligned} \delta^{\mathrm{FT}}\underline{f}^{X_k^{\ominus}} &= {}^{X_k}\bar{\Phi}^{X_{k+1}} \cdot \left(\delta^{\mathrm{FT}}\underline{f}^{X_{k+1}^{\ominus}} - \delta\underline{\dot{p}}^{X_{k+1}} + \delta^{\mathrm{EX}}\underline{f}^{X_{k+1}^{\ominus}}\right) + \delta^{X_k}\Phi^{X_{k+1}} \cdot {}^{\mathrm{FT}}\underline{\bar{f}}^{X_k^{\oplus}/X_{k+1}} \\ \delta^{\mathrm{FT}}\underline{\bar{t}}^{X_k^{\ominus}} &= {}^{X_k^{\ominus}}\underline{r}^{X_k^{\oplus}} \times \delta^{\mathrm{FT}}\underline{f}^{X_k^{\ominus}} + \\ &\quad {}^{X_k}\bar{\Phi}^{X_{k+1}} \cdot \left(\delta^{\mathrm{FT}}\underline{t}^{X_{k+1}^{\ominus}} - \delta^{X_{k+1}^{\ominus}}\underline{\dot{h}}^{X_{k+1}} + \delta^{\mathrm{EX}}\underline{t}^{X_{k+1}^{\ominus}}\right) + \delta^{X_k}\Phi^{X_{k+1}} \cdot {}^{\mathrm{FT}}\underline{\bar{t}}^{X_k^{\oplus}/X_{k+1}} \end{aligned} \tag{A.62}$$

For the sensitivities to the variabels $\underline{q}$ holds:

$$\begin{aligned} \frac{\partial^{\mathrm{FT}}\underline{f}^{X_k^{\ominus}}}{\partial \underline{q}} &= {}^{X_k}\bar{\Phi}^{X_{k+1}} \cdot \left(\frac{\partial^{\mathrm{FT}}\underline{f}^{X_{k+1}^{\ominus}}}{\partial \underline{q}} - \frac{\partial \underline{\dot{p}}^{X_{k+1}}}{\partial \underline{q}} + \frac{\partial^{\mathrm{EX}}\underline{f}^{X_{k+1}^{\ominus}}}{\partial \underline{q}}\right) + \\ &\quad \delta_{\underline{q}\,\underline{\phi}^{X}} \cdot \left[\, \mathrm{O}_{(1)} \ldots \mathrm{O}_{(k)} \;\; \mathrm{J}_{v=1}^{3}\Big(\frac{\partial^{X_k}\Phi^{X_{k+1}}}{\partial \phi_v^{X_{k+1}}} \cdot {}^{\mathrm{FT}}\underline{\bar{f}}^{X_k^{\oplus}/X_{k+1}}\Big) \;\; \mathrm{O}_{(k+2)} \ldots \mathrm{O}_{(N)} \,\right] \\ \frac{\partial^{\mathrm{FT}}\underline{\bar{t}}^{X_k^{\ominus}}}{\partial \underline{q}} &= \mathrm{J}_{v=1}^{3}\Big({}^{X_k^{\ominus}}\underline{r}^{X_k^{\oplus}} \times \underline{e}_v\Big) \cdot \frac{\partial^{\mathrm{FT}}\underline{f}^{X_k^{\ominus}}}{\partial \underline{q}} + {}^{X_k}\bar{\Phi}^{X_{k+1}} \cdot \frac{\partial\left({}^{\mathrm{FT}}\underline{t}^{X_{k+1}^{\ominus}} - {}^{X_{k+1}^{\ominus}}\underline{\dot{h}}^{X_{k+1}} + {}^{\mathrm{EX}}\underline{t}^{X_{k+1}^{\ominus}}\right)}{\partial \underline{q}} + \\ &\quad \delta_{\underline{q}\,\underline{\phi}^{X}} \cdot \left[\, \mathrm{O}_{(1)} \ldots \mathrm{O}_{(k)} \;\; \mathrm{J}_{v=1}^{3}\Big(\frac{\partial^{X_k}\Phi^{X_{k+1}}}{\partial \phi_v^{X_{k+1}}} \cdot {}^{\mathrm{FT}}\underline{\bar{t}}^{X_k^{\oplus}/X_{k+1}}\Big) \;\; \mathrm{O}_{(k+2)} \ldots \mathrm{O}_{(N)} \,\right] \end{aligned} \tag{A.63}$$

Note that the last term in the right hand side of both equations only applies if $\underline{q}$ equals $\underline{\phi}^{X}$!

The pairs of rows $\{\underline{\boldsymbol{m}}_{h\varphi_w}^{X_k}, \underline{\boldsymbol{m}}_{p\varphi_w}^{X_k} | w = 3, 2, 1\}$, with ranking numbers $6(k-1)+2(w-1)+1$ and $6(k-1)+2(w-1)+2$ in the mass matrix partition $\boldsymbol{M}_{\varphi}^{X_{\mathrm{p}}}$, are now determined as follows (the partial derivatives in the right hand side only apply if they are defined for the 'independent variable'; in this case $\underline{\ddot{\varphi}}^{X}$):

- for $w = 3$:

$$\begin{aligned} \underline{\boldsymbol{m}}_{h\varphi_3}^{X_k} &= -[\,1\,0\,0\,] \cdot \frac{\partial^{\mathrm{RS}}\underline{t}^{X_k^{\ominus}}}{\partial \underline{\ddot{\varphi}}^{X}} + [\,1\,0\,0\,] \cdot \Big(\frac{\partial^{X_k^{\ominus}}\underline{\dot{h}}^{X_k}}{\partial \underline{\ddot{\varphi}}^{X}} - \frac{\partial^{\mathrm{FT}}\underline{t}^{X_k^{\ominus}}}{\partial \underline{\ddot{\varphi}}^{X}} - \frac{\partial^{\mathrm{EX}}\underline{t}^{X_k^{\ominus}}}{\partial \underline{\ddot{\varphi}}^{X}}\Big) \\ \underline{\boldsymbol{m}}_{p\varphi_3}^{X_k} &= -[\,0\,0\,1\,] \cdot \frac{\partial^{\mathrm{RS}}\underline{f}^{X_k^{\ominus}}}{\partial \underline{\ddot{\varphi}}^{X}} + [\,0\,0\,1\,] \cdot \Big(\frac{\partial \underline{\dot{p}}^{X_k}}{\partial \underline{\ddot{\varphi}}^{X}} - \frac{\partial^{\mathrm{FT}}\underline{f}^{X_k^{\ominus}}}{\partial \underline{\ddot{\varphi}}^{X}} - \frac{\partial^{\mathrm{EX}}\underline{f}^{X_k^{\ominus}}}{\partial \underline{\ddot{\varphi}}^{X}}\Big) \end{aligned} \tag{A.64}$$

- for $w = 2$:

$$\begin{aligned} \underline{\boldsymbol{m}}_{h\varphi_2}^{X_k} &= -[\,0\,0\,1\,] \cdot \frac{\partial^{\mathrm{RS}}\underline{t}^{X_k^{\ominus}}}{\partial \underline{\ddot{\varphi}}^{X}} + {}^{X_k^2}\bar{\Phi}_{(3,:)}^{X_k} \cdot \Big(\frac{\partial^{X_k^{\ominus}}\underline{\dot{h}}^{X_k}}{\partial \underline{\ddot{\varphi}}^{X}} - \frac{\partial^{\mathrm{FT}}\underline{t}^{X_k^{\ominus}}}{\partial \underline{\ddot{\varphi}}^{X}} - \frac{\partial^{\mathrm{EX}}\underline{t}^{X_k^{\ominus}}}{\partial \underline{\ddot{\varphi}}^{X}}\Big) \\ \underline{\boldsymbol{m}}_{p\varphi_2}^{X_k} &= -[\,1\,0\,0\,] \cdot \frac{\partial^{\mathrm{RS}}\underline{f}^{X_k^{\ominus}}}{\partial \underline{\ddot{\varphi}}^{X}} + {}^{X_k^2}\bar{\Phi}_{(1,:)}^{X_k} \cdot \Big(\frac{\partial \underline{\dot{p}}^{X_k}}{\partial \underline{\ddot{\varphi}}^{X}} - \frac{\partial^{\mathrm{FT}}\underline{f}^{X_k^{\ominus}}}{\partial \underline{\ddot{\varphi}}^{X}} - \frac{\partial^{\mathrm{EX}}\underline{f}^{X_k^{\ominus}}}{\partial \underline{\ddot{\varphi}}^{X}}\Big) \end{aligned} \tag{A.65}$$

- for $w = 1$:

$$\begin{aligned}
\underline{\boldsymbol{m}}_{h\varphi_1}^{X_k} &= -[\,0\,1\,0\,]\cdot\frac{\partial^{\mathrm{RS}}\underline{t}^{X_k^{\ominus}}}{\partial\underline{\ddot{\varphi}}^{X}} + {}^{X_k^1}\bar{\Phi}_{(2,:)}^{X_k}\cdot\Big(\frac{\partial^{X_k^{\ominus}}\dot{\underline{h}}^{X_k}}{\partial\underline{\ddot{\varphi}}^{X}} - \frac{\partial^{\mathrm{FT}}\underline{t}^{X_k^{\ominus}}}{\partial\underline{\ddot{\varphi}}^{X}} - \frac{\partial^{\mathrm{EX}}\underline{t}^{X_k^{\ominus}}}{\partial\underline{\ddot{\varphi}}^{X}}\Big)\\
\underline{\boldsymbol{m}}_{p\varphi_1}^{X_k} &= -[\,0\,1\,0\,]\cdot\frac{\partial^{\mathrm{RS}}\underline{f}^{X_k^{\ominus}}}{\partial\underline{\ddot{\varphi}}^{X}} + {}^{X_k^1}\bar{\Phi}_{(2,:)}^{X_k}\cdot\Big(\frac{\partial\underline{\dot{p}}^{X_k}}{\partial\underline{\ddot{\varphi}}^{X}} - \frac{\partial^{\mathrm{FT}}\underline{f}^{X_k^{\ominus}}}{\partial\underline{\ddot{\varphi}}^{X}} - \frac{\partial^{\mathrm{EX}}\underline{f}^{X_k^{\ominus}}}{\partial\underline{\ddot{\varphi}}^{X}}\Big)
\end{aligned} \tag{A.66}$$

The corresponding rows in the mass matrix partition $\boldsymbol{M}_{\varrho}^{X_{\mathrm{P}}}$ are obtained by taking the sensitivities to $\underline{\ddot{\varrho}}^{X}$ instead of $\underline{\ddot{\varphi}}^{X}$. For the rows in both damping matrix partitions $\boldsymbol{D}_{\varphi}^{X_{\mathrm{P}}}$ and $\boldsymbol{D}_{\varrho}^{X_{\mathrm{P}}}$ and in the stiffness matrix partition $\boldsymbol{S}_{\varrho}^{X_{\mathrm{P}}}$, take the sensitivities to $\underline{\dot{\varphi}}^{X}$ and $\underline{\dot{\varrho}}^{X}$ and $\underline{\varrho}^{X}$. For the remaining stiffness matrix partition $\boldsymbol{S}_{\varphi}^{X_{\mathrm{P}}}$ the same scheme applies for $w = 3$ but differs for $w = 2$ and $w = 1$:

- for $w = 2$:

$$\begin{aligned}
\underline{\boldsymbol{s}}_{h\varphi_2}^{X_k} &= -[\,0\,0\,1\,]\cdot\frac{\partial^{\mathrm{RS}}\underline{t}^{X_k^{\ominus}}}{\partial\underline{\phi}^{X}} + {}^{X_k^2}\bar{\Phi}_{(3,:)}^{X_k}\cdot\Big(\frac{\partial^{X_k^{\ominus}}\dot{\underline{h}}^{X_k}}{\partial\underline{\phi}^{X}} - \frac{\partial^{\mathrm{FT}}\underline{t}^{X_k^{\ominus}}}{\partial\underline{\phi}^{X}} - \frac{\partial^{\mathrm{EX}}\underline{t}^{X_k^{\ominus}}}{\partial\underline{\phi}^{X}}\Big) +\\
&\quad [\,\mathrm{O}_{(1\ldots k-1)}\;\;\mathrm{J}_{v=1}^{3}\Big(\frac{\partial^{X_k^2}\Phi_{(3,:)}^{X_k}}{\partial\phi_v^{X_k}}\cdot\Big({}^{X_k^{\ominus}}\dot{\bar{\underline{h}}}^{X_k} - {}^{\mathrm{FT}}\bar{\underline{t}}^{X_k^{\ominus}} - {}^{\mathrm{EX}}\bar{\underline{t}}^{X_k^{\ominus}}\Big)\Big)\;\;\mathrm{O}_{(k+1\ldots N)}\,]\\
\underline{\boldsymbol{s}}_{p\varphi_2}^{X_k} &= -[\,1\,0\,0\,]\cdot\frac{\partial^{\mathrm{RS}}\underline{f}^{X_k^{\ominus}}}{\partial\underline{\phi}^{X}} + {}^{X_k^2}\bar{\Phi}_{(1,:)}^{X_k}\cdot\Big(\frac{\partial\underline{\dot{p}}^{X_k}}{\partial\underline{\phi}^{X}} - \frac{\partial^{\mathrm{FT}}\underline{f}^{X_k^{\ominus}}}{\partial\underline{\phi}^{X}} - \frac{\partial^{\mathrm{EX}}\underline{f}^{X_k^{\ominus}}}{\partial\underline{\phi}^{X}}\Big) +\\
&\quad [\,\mathrm{O}_{(1\ldots k-1)}\;\;\mathrm{J}_{v=1}^{3}\Big(\frac{\partial^{X_k^2}\Phi_{(1,:)}^{X_k}}{\partial\phi_v^{X_k}}\cdot\Big({}^{X_k^{\ominus}}\bar{\underline{p}}^{X_k} - {}^{\mathrm{FT}}\bar{\underline{f}}^{X_k^{\ominus}} - {}^{\mathrm{EX}}\bar{\underline{f}}^{X_k^{\ominus}}\Big)\Big)\;\;\mathrm{O}_{(k+1\ldots N)}\,]
\end{aligned} \tag{A.67}$$

- for $w = 1$:

$$\begin{aligned}
\underline{\boldsymbol{s}}_{h\varphi_1}^{X_k} &= -[\,0\,1\,0\,]\cdot\frac{\partial^{\mathrm{RS}}\underline{t}^{X_k^{\ominus}}}{\partial\underline{\phi}^{X}} + {}^{X_k^1}\bar{\Phi}_{(2,:)}^{X_k}\cdot\Big(\frac{\partial^{X_k^{\ominus}}\dot{\underline{h}}^{X_k}}{\partial\underline{\phi}^{X}} - \frac{\partial^{\mathrm{FT}}\underline{t}^{X_k^{\ominus}}}{\partial\underline{\phi}^{X}} - \frac{\partial^{\mathrm{EX}}\underline{t}^{X_k^{\ominus}}}{\partial\underline{\phi}^{X}}\Big) +\\
&\quad [\,\mathrm{O}_{(1\ldots k-1)}\;\;\mathrm{J}_{v=1}^{3}\Big(\frac{\partial^{X_k^1}\Phi_{(2,:)}^{X_k}}{\partial\phi_v^{X_k}}\cdot\Big({}^{X_k^{\ominus}}\dot{\bar{\underline{h}}}^{X_k} - {}^{\mathrm{FT}}\bar{\underline{t}}^{X_k^{\ominus}} - {}^{\mathrm{EX}}\bar{\underline{t}}^{X_k^{\ominus}}\Big)\Big)\;\;\mathrm{O}_{(k+1\ldots N)}\,]\\
\underline{\boldsymbol{s}}_{p\varphi_1}^{X_k} &= -[\,0\,1\,0\,]\cdot\frac{\partial^{\mathrm{RS}}\underline{f}^{X_k^{\ominus}}}{\partial\underline{\phi}^{X}} + {}^{X_k^1}\bar{\Phi}_{(2,:)}^{X_k}\cdot\Big(\frac{\partial\underline{\dot{p}}^{X_k}}{\partial\underline{\phi}^{X}} - \frac{\partial^{\mathrm{FT}}\underline{f}^{X_k^{\ominus}}}{\partial\underline{\phi}^{X}} - \frac{\partial^{\mathrm{EX}}\underline{f}^{X_k^{\ominus}}}{\partial\underline{\phi}^{X}}\Big) +\\
&\quad [\,\mathrm{O}_{(1\ldots k-1)}\;\;\mathrm{J}_{v=1}^{3}\Big(\frac{\partial^{X_k^1}\Phi_{(2,:)}^{X_k}}{\partial\phi_v^{X_k}}\cdot\Big({}^{X_k^{\ominus}}\bar{\underline{p}}^{X_k} - {}^{\mathrm{FT}}\bar{\underline{f}}^{X_k^{\ominus}} - {}^{\mathrm{EX}}\bar{\underline{f}}^{X_k^{\ominus}}\Big)\Big)\;\;\mathrm{O}_{(k+1\ldots N)}\,]
\end{aligned} \tag{A.68}$$

The pairs of rows $\{\underline{\boldsymbol{g}}_{h_w}^{X_k X_{\mathrm{f}}}, \underline{\boldsymbol{g}}_{p_w}^{X_k X_{\mathrm{f}}} | w = 3, 2, 1\}$, with ranking numbers $6(k-1)+2(w-1)+1$ and $6(k-1)+2(w-1)+2$ in the input matrix partition $\boldsymbol{G}^{X_{\mathrm{P}} X_{\mathrm{f}}}$, are determined as follows (the partial derivatives in the right hand side only apply if they are defined for the 'independent variable'; in this case $\underline{z}$):

- for $w = 3$:

$$\begin{aligned}
\underline{\boldsymbol{g}}_{h_3}^{X_k X_{\mathrm{f}}} &= \mathrm{J}_{(\underline{z})}\Big([\,1\,0\,0\,]\cdot\frac{\partial^{\mathrm{RS}}\underline{t}^{X_k^{\ominus}}}{\partial\underline{z}} + [\,1\,0\,0\,]\cdot\Big(-\frac{\partial^{X_k^{\ominus}}\dot{\underline{h}}^{X_k}}{\partial\underline{z}} + \frac{\partial^{\mathrm{FT}}\underline{t}^{X_k^{\ominus}}}{\partial\underline{z}} + \frac{\partial^{\mathrm{EX}}\underline{t}^{X_k^{\ominus}}}{\partial\underline{z}}\Big)\Big)\\
\underline{\boldsymbol{g}}_{p_3}^{X_k X_{\mathrm{f}}} &= \mathrm{J}_{(\underline{z})}\Big([\,0\,0\,1\,]\cdot\frac{\partial^{\mathrm{RS}}\underline{f}^{X_k^{\ominus}}}{\partial\underline{z}} + [\,0\,0\,1\,]\cdot\Big(-\frac{\partial\underline{\dot{p}}^{X_k}}{\partial\underline{z}} + \frac{\partial^{\mathrm{FT}}\underline{f}^{X_k^{\ominus}}}{\partial\underline{z}} + \frac{\partial^{\mathrm{EX}}\underline{f}^{X_k^{\ominus}}}{\partial\underline{z}}\Big)\Big)
\end{aligned} \tag{A.69}$$

- for $w = 2$:

$$\begin{aligned}
\underline{\boldsymbol{g}}_{h_2}^{X_k X_\mathrm{f}} &= \mathrm{J}_{(\underline{z})}\Big([\,0\,0\,1\,] \cdot \frac{\partial^{\mathrm{RS}} \underline{t}^{X_k^{\ominus}}}{\partial \underline{z}} + {}^{X_k^2}\bar{\Phi}^{X_k}_{(3,:)} \cdot \big(- \frac{\partial^{X_k^{\ominus}} \underline{\dot{h}}^{X_k}}{\partial \underline{z}} + \frac{\partial^{\mathrm{FT}} \underline{t}^{X_k^{\ominus}}}{\partial \underline{z}} + \frac{\partial^{\mathrm{EX}} \underline{t}^{X_k^{\ominus}}}{\partial \underline{z}} \big) \Big) \\
\underline{\boldsymbol{g}}_{p_2}^{X_k X_\mathrm{f}} &= \mathrm{J}_{(\underline{z})}\Big([\,1\,0\,0\,] \cdot \frac{\partial^{\mathrm{RS}} \underline{f}^{X_k^{\ominus}}}{\partial \underline{z}} + {}^{X_k^2}\bar{\Phi}^{X_k}_{(1,:)} \cdot (- \frac{\partial \underline{\dot{p}}^{X_k}}{\partial \underline{z}} + \frac{\partial^{\mathrm{FT}} \underline{f}^{X_k^{\ominus}}}{\partial \underline{z}} + \frac{\partial^{\mathrm{EX}} \underline{f}^{X_k^{\ominus}}}{\partial \underline{z}}) \Big)
\end{aligned} \tag{A.70}$$

- for $w = 1$:

$$\begin{aligned}
\underline{\boldsymbol{g}}_{h_1}^{X_k X_\mathrm{f}} &= \mathrm{J}_{(\underline{z})}\Big([\,0\,1\,0\,] \cdot \frac{\partial^{\mathrm{RS}} \underline{t}^{X_k^{\ominus}}}{\partial \underline{z}} + {}^{X_k^1}\bar{\Phi}^{X_k}_{(2,:)} \cdot \big(- \frac{\partial^{X_k^{\ominus}} \underline{\dot{h}}^{X_k}}{\partial \underline{z}} + \frac{\partial^{\mathrm{FT}} \underline{t}^{X_k^{\ominus}}}{\partial \underline{z}} + \frac{\partial^{\mathrm{EX}} \underline{t}^{X_k^{\ominus}}}{\partial \underline{z}} \big) \Big) \\
\underline{\boldsymbol{g}}_{p_1}^{X_k} &= \mathrm{J}_{(\underline{z})}\Big([\,0\,1\,0\,] \cdot \frac{\partial^{\mathrm{RS}} \underline{f}^{X_k^{\ominus}}}{\partial \underline{z}} + {}^{X_k^1}\bar{\Phi}^{X_k}_{(2,:)} \cdot (- \frac{\partial \underline{\dot{p}}^{X_k}}{\partial \underline{z}} + \frac{\partial^{\mathrm{FT}} \underline{f}^{X_k^{\ominus}}}{\partial \underline{z}} + \frac{\partial^{\mathrm{EX}} \underline{f}^{X_k^{\ominus}}}{\partial \underline{z}}) \Big)
\end{aligned} \tag{A.71}$$

The notation $\mathrm{J}_{(\underline{z})}(.)$ means that the partial derivatives to the involved subvector variables are to be put next to each other. These are (see also Eq. A.50):

- kinematic vectors on flange exit: $\underline{\omega}^{X_{\mathrm{FF}(1)}}$, $\underline{\alpha}^{X_{\mathrm{FF}(1)}}$, $\underline{v}^{X^{\oplus}_{\mathrm{FF}(1)}}$, $\underline{a}^{X^{\oplus}_{\mathrm{FF}(1)}}$
- dof angular position variations in blade flange: $\underline{\phi}^{X_{\mathrm{FF}(1)}}$
- distributed aerodynamic force loads on final flange element: ${}^{\mathrm{a}}\underline{q}^{X_{\mathrm{FF}(1)}}$, ${}^{\mathrm{aL}}\underline{q}^{X_{\mathrm{FF}(1)}}$
- gravitation variation by orientation change up till flange: $\underline{g}_{\mathrm{ori}}^{X_{\mathrm{FF}(1)}}$

The rows in the input matrix partition $\boldsymbol{G}^{X_\mathrm{p} G}$ for the 'exogeneous' input variables are obtained by taking the partial derivatives to:

- periodic wind speed variation on blade: $\underline{u}^{X}_{\mathrm{per}}$
- periodic gravitation variation on blade base: $\underline{g}^{X_0}_{\mathrm{per}}$
- stochastic wind speed variation in intersection annuli/blade: ${}^{\mathrm{t}}\underline{u}^{W/X}$

For the rows in the input matrix partition $\boldsymbol{G}^{X_\mathrm{p} W}$: for the input variables from the wake take the partial derivatives to the induction speed variations $\underline{u}^{W}_{\mathrm{im}}$ in the rotor annuli; for the input matrix partition $\boldsymbol{G}^{X_\mathrm{p} R}$ the partial derivative to the wind speed variation $\underline{u}_{\mathrm{ori}}^{X_{\mathrm{FF}(0)}}$ by orientation change up till the hub applies.

(vii) Output variables and vector output equation in 2nd order model

The blade profile & structure X_p needs to provide the following output:

- aerodynamic force load reactions to wake W:
  ${}^{\mathrm{aL}}\underline{f}^{W_m/X_k}$ for $k = 2 \ldots N$ (along actual annulus-wise c.s. for X_k)
- distributed aerodynamic force loads on X_2 to flange X_f:
  ${}^{\mathrm{a}}\underline{q}^{X_{\mathrm{PP}(2)}}$, ${}^{\mathrm{aL}}\underline{q}^{X_{\mathrm{PP}(2)}}$ (along actual conversion c.s. for X_2)
- variations in angular dofs on X_2 to flange X_f: $\underline{\phi}^{X_{\mathrm{PP}(2)}}$
- feedthrough force and torque on flange exit $X_1^{\oplus}$:
  ${}^{\mathrm{FT}}\underline{f}^{X_{\mathrm{PP}(2)}}$, ${}^{\mathrm{FT}}\underline{t}^{X_{\mathrm{PP}(2)}}$ (= ${}^{\mathrm{FT}}\underline{f}^{X_1^{\oplus}}$, ${}^{\mathrm{FT}}\underline{t}^{X_1^{\oplus}}$, along actual f.c.s. for X_1)

- exit point displacements relative to rotor centre in average position:
  $\delta^{\bar{X}_0^{\ominus}} \underline{r}^{X_k^{\oplus}/\bar{X}_0}$ for $k = 2 \ldots N$ (along average c.s. of blade base X_0).

The output vector $\underline{y}^{X_\mathrm{P}}$ of the blade profile & structure has the following composition:

$$\underline{y}^{X_\mathrm{P}} = \begin{bmatrix} \underline{y}^{GX_\mathrm{P}} \\ \underline{y}^{WX_\mathrm{P}} \\ \underline{y}^{X_\mathrm{f}X_\mathrm{P}} \end{bmatrix} \quad \text{with} \quad \underline{y}^{GX_\mathrm{P}} = \begin{bmatrix} \delta^{\bar{X}_0^{\ominus}} \underline{r}^{X_2^{\oplus}/\bar{X}_0} \\ \vdots \\ \delta^{\bar{X}_0^{\ominus}} \underline{r}^{X_N^{\oplus}/\bar{X}_0} \end{bmatrix}$$

$$\text{and} \quad \underline{y}^{WX_\mathrm{P}} = \begin{bmatrix} {}^{\mathrm{a_L}}\underline{f}^{W_m/X_2} \\ \vdots \\ {}^{\mathrm{a_L}}\underline{f}^{W_m/X_N} \end{bmatrix} \; ; \; \underline{y}^{X_\mathrm{f}X_\mathrm{P}} = \begin{bmatrix} {}^{\mathrm{FT}}\underline{f}^{X_{\mathrm{PP}(2)}} \\ {}^{\mathrm{FT}}\underline{t}^{X_{\mathrm{PP}(2)}} \\ {}^{\mathrm{a}}\underline{q}^{X_{\mathrm{PP}(2)}} \\ {}^{\mathrm{a_L}}\underline{q}^{X_{\mathrm{PP}(2)}} \\ \underline{\phi}^{X_{\mathrm{PP}(2)}} \end{bmatrix} \tag{A.72}$$

The reaction load from element X_k is to be supplied to the wake subsystem W as a coordinate vector along the annulus wise coordinate system in the intersection of blade element X_k and rotor annulus W_m.

The coordinate vector ${}^{\mathrm{a_L}}\underline{f}^{W_m/X_k}$ is the reaction load from blade element X_k on the wake. It is supplied as a coordinate vector along the annulus wise coordinate system in the intersection of blade element X_k and rotor annulus W_m. It equals minus the concentrated force load on X_k, *but only as concerns the force component caused by lift.* The linearised expression involves dependency on the same variables as for the force load ${}^{\mathrm{a}}\underline{f}^{X_k}$ by Eq. A.41 except that the distributed import load from the flange is now 'lift-only' (${}^{\mathrm{a_L}}\underline{q}^{X_{\mathrm{FF}(1)}}$ instead of ${}^{\mathrm{a}}\underline{q}^{X_{\mathrm{FF}(1)}}$).

The concenctrated load outpus to the blade flange consist of coordinates along the final coordinate system of X_1. The coordinates of the disributed export loads ${}^{\mathrm{a}}\underline{q}^{X_{\mathrm{PP}(2)}^{\ominus}}$ and ${}^{\mathrm{a_L}}\underline{q}^{X_{\mathrm{PP}(2)}^{\ominus}}$ to the blade flange are along the conversion coordiante system of X_2. Therefore the rotation dof position variations of the profile's first element, in subvector $\underline{\phi}^{X_{\mathrm{PP}(2)}}$, are also output to the flange. The distributed export loads depend on the same variables as the concentrated force load ${}^{\mathrm{a}}\underline{f}^{X_k}$ does, except that the dependency on ${}^{\mathrm{a}}\underline{q}^{X_{\mathrm{FF}(1)}}$ is excluded (see section B.7.2, Eq. B.203). Chapter Appendix B does not contain expressions for the feedthrough loads ${}^{\mathrm{FT}}\underline{f}^{X_1^{\oplus}}$ and ${}^{\mathrm{FT}}\underline{t}^{X_1^{\oplus}}$ to the blade flange. Equation A.34, together with the expressions for the external loads in Eq. A.55, yields the expressions for the feedthrough loads, which are transformed to the coordinate system of X_1:

$$\begin{aligned} {}^{\mathrm{FT}}\underline{f}^{X_1^{\oplus}} &= {}^{X_1}\Phi^{X_2} \cdot \left({}^{\mathrm{FT}}\underline{f}^{X_2^{\ominus}} - \underline{\dot{p}}^{X_2} + {}^{\mathrm{EX}}\underline{f}^{X_2} \right) \\ {}^{\mathrm{FT}}\underline{t}^{X_1^{\oplus}} &= {}^{X_1}\Phi^{X_2} \cdot \left({}^{\mathrm{FT}}\underline{t}^{X_2^{\ominus}} - {}^{X_2^{\ominus}}\underline{\dot{h}}^{X_2} + {}^{\mathrm{EX}}\underline{t}^{X_2} \right) \end{aligned} \tag{A.73}$$

The feedthrough loads to the flange thus depend on the envelope of variables on which the aerodynamic loads, gravitation loads and impulse vectors depend. The linearised expressions are:

$$\begin{aligned} {}^{\mathrm{FT}}\underline{f}^{X_1^{\oplus}} &= {}^{\mathrm{FT}}\bar{\underline{f}}^{X_1^{\oplus}} + \sum_{(\underline{q})} \frac{\partial {}^{\mathrm{FT}}\underline{f}^{X_1^{\oplus}}}{\partial \underline{q}} \cdot \delta \underline{q} \\ {}^{\mathrm{FT}}\underline{t}^{X_1^{\oplus}} &= {}^{\mathrm{FT}}\bar{\underline{t}}^{X_1^{\oplus}} + \sum_{(\underline{q})} \frac{\partial {}^{\mathrm{FT}}\underline{t}^{X_1^{\oplus}}}{\partial \underline{q}} \cdot \delta \underline{q} \end{aligned} \tag{A.74}$$

The summation over $(\underline{q})$ involves:

- exogeneous periodic wind speed and gravition input: $\underline{u}^{X}_{\mathrm{per}}$, $\underline{g}^{R}_{\mathrm{per}}$
- exogenous stochastic wind speed input: $\underline{u}^{W/X}_{\mathrm{sto}}$
- output from wake W: $\underline{u}^{W}_{\mathrm{i_m}}$
- processed output from rotor shaft & hub R: $\underline{u}^{X_{\mathrm{FF}(0)}}_{\mathrm{ori}}$
- output from flange X_{f}: $\underline{\omega}^{X^{\oplus}_{\mathrm{FF}(1)}}$, $\underline{\alpha}^{X_{\mathrm{FF}(1)}}$, $\underline{v}^{X^{\oplus}_{\mathrm{FF}(1)}}$, $\underline{a}^{X^{\oplus}_{\mathrm{FF}(1)}}$, $\underline{\phi}^{X_{\mathrm{FF}(1)}}$, ${}^{\mathrm{a}}\underline{q}_{\mathrm{f}}^{X_{\mathrm{FF}(1)}}$, $\underline{g}_{\mathrm{ori}}^{X_{\mathrm{FF}(1)}}$
- degrees of freedom in X_{p}, encapsulated by: $\underline{\phi}^{X}$, $\underline{\dot{\varphi}}^{X}$, $\underline{\ddot{\varphi}}^{X}$, $\underline{\dot{o}}^{X}$ $\underline{\ddot{o}}^{X}$.

The means are obtained by just taking the overlined version of the expressions above. This corresponds to the transformation of the auxiliary variables by Eq. A.58 (for $k = 1$) to the coordinate system of X_1:

$$\begin{aligned} {}^{\mathrm{FT}}\underline{\bar{f}}^{X^{\oplus}_1} &= {}^{X_1}\bar{\Phi}^{X_2} \cdot {}^{\mathrm{FT}}\underline{\bar{f}}^{X^{\oplus}_1/X_2} \\ {}^{\mathrm{FT}}\underline{\bar{t}}^{X^{\oplus}_1} &= {}^{X_1}\bar{\Phi}^{X_2} \cdot {}^{\mathrm{FT}}\underline{\bar{t}}^{X^{\oplus}_1/X_2} \end{aligned} \tag{A.75}$$

For the sensitivities to the variables $\underline{q}$ holds:

$$\begin{aligned} \frac{\partial {}^{\mathrm{FT}}\underline{f}^{X^{\oplus}_1}}{\partial \underline{q}} &= {}^{X_1}\bar{\Phi}^{X_2} \cdot \Big(\frac{\partial {}^{\mathrm{FT}}\underline{f}^{X^{\ominus}_2}}{\partial \underline{q}} - \frac{\partial \underline{\dot{p}}^{X_2}}{\partial \underline{q}} + \frac{\partial {}^{\mathrm{EX}}\underline{f}^{X^{\ominus}_2}}{\partial \underline{q}}\Big) + \\ &\quad \delta_{\underline{q}\,\underline{\phi}^X} \cdot \big[\, \mathrm{O}_{(1)} \;\; \mathrm{J}^3_{v=1}\Big(\frac{\partial {}^{X_1}\Phi^{X_2}}{\partial \phi_v^{X_2}} \cdot {}^{\mathrm{FT}}\underline{\bar{f}}^{X^{\oplus}_1/X_2}\Big) \;\; \mathrm{O}_{(3)} \ldots \mathrm{O}_{(N)} \,\big] \\ \frac{\partial {}^{\mathrm{FT}}\underline{t}^{X^{\oplus}_1}}{\partial \underline{q}} &= {}^{X_1}\bar{\Phi}^{X_2} \cdot \Big(\frac{\partial {}^{\mathrm{FT}}\underline{t}^{X^{\ominus}_2}}{\partial \underline{q}} - \frac{\partial {}^{X^{\ominus}_2}\underline{h}^{X_2}}{\partial \underline{q}} + \frac{\partial {}^{\mathrm{EX}}\underline{t}^{X^{\ominus}_2}}{\partial \underline{q}}\Big) + \\ &\quad \delta_{\underline{q}\,\underline{\phi}^X} \cdot \big[\, \mathrm{O}_{(1)} \;\; \mathrm{J}^3_{v=1}\Big(\frac{\partial {}^{X_1}\Phi^{X_2}}{\partial \phi_v^{X_2}} \cdot {}^{\mathrm{FT}}\underline{\bar{t}}^{X^{\oplus}_1/X_2}\Big) \;\; \mathrm{O}_{(3)} \ldots \mathrm{O}_{(N)} \,\big] \end{aligned} \tag{A.76}$$

Note that the last term in the right hand side of both equations only applies if $\underline{q}$ equals $\underline{\phi}^X$!

The displacement variations of the exit points $X^{\oplus}_k$ relative to rotor centre in average position $\bar{X}^{\ominus}_0$ are used for describing the mode shapes. They depend on the variations in position dofs $\underline{\phi}^X$ and $\underline{\rho}^X$ and on the displacement variations $\underline{\xi}^{X_{\mathrm{FF}(1)}}$ and $\underline{x}^{X_{\mathrm{FF}(1)}}$ at the blade flange exit. For the displacement variation vector $\delta^{\bar{X}^{\ominus}_0}\underline{r}^{X^{\oplus}_k/\bar{X}_0}$ with coordinates along the blade base in its average position $\bar{X}_0$, holds:

$$\delta^{\bar{X}^{\ominus}_0}\underline{r}^{X^{\oplus}_k/\bar{X}_0} = \sum_{(\underline{z})} \frac{\partial^{\bar{X}^{\ominus}_0}\underline{r}^{X^{\oplus}_k/\bar{X}_0}}{\partial \underline{z}} \cdot \delta \underline{z} \qquad (\underline{z} = \underline{\phi}^X, \underline{\rho}^X, \underline{\xi}^{X_{\mathrm{FF}(1)}}, \underline{x}^{X_{\mathrm{FF}(1)}}) \tag{A.77}$$

with:

$$\begin{aligned} \frac{\partial^{\bar{X}^{\ominus}_0}\underline{r}^{X^{\oplus}_k/\bar{X}_0}}{\partial \underline{\xi}^{X_{\mathrm{FF}}}} &= \big[\, \mathrm{J}^3_{v=1}\Big({}^{X_0}\bar{\Phi}^{X_k} \cdot \sum_{j=2}^{k} {}^{X_k}\bar{\Phi}^{X_j} \cdot \big({}^{X_j}\underline{\bar{\Phi}}_v^{X_1} \times {}^{X^{\ominus}_j}\underline{r}^{X^{\oplus}_j}\Big) \,\big] \quad \text{for } k = 2 \ldots N \\ \frac{\partial^{\bar{X}^{\ominus}_0}\underline{r}^{X^{\oplus}_k/\bar{X}_0}}{\partial \underline{x}^{X_{\mathrm{FF}}}} &= \big[\, {}^{X_0}\Phi^{X_1} \,\big] \quad \text{for } k = 2 \ldots N \end{aligned} \tag{A.78}$$

and

$$\begin{aligned} \frac{\partial^{\bar{X}^{\ominus}_0}\underline{r}^{X^{\oplus}_k/\bar{X}_0}}{\partial \underline{\phi}^X} &= \big[\, \mathrm{O}_{(1)} \;\; \mathrm{J}^k_{i=2}\Big(\mathrm{J}^3_{v=1}\Big(\sum_{j=i}^{k} \frac{\partial {}^{X_0}\Phi^{X_j}}{\partial \phi_v^{X_i}} \cdot {}^{X^{\ominus}_j}\underline{r}^{X^{\oplus}_j}\Big)\Big) \;\; \mathrm{O}_{(k+1)} \ldots \mathrm{O}_{(N)} \,\big] \quad \text{for } k = 2 \ldots N \\ \frac{\partial^{\bar{X}^{\ominus}_0}\underline{r}^{X^{\oplus}_k/\bar{X}_0}}{\partial \underline{\rho}^X} &= \big[\, \mathrm{O}_{(1)} \;\; \mathrm{J}^k_{i=2}\Big({}^{X_0}\Phi^{X_i} \cdot {}^{X_i}\Phi^{X_i^{\mathrm{t}}}\Big) \;\; \mathrm{O}_{(k+1)} \ldots \mathrm{O}_{(N)} \,\big] \quad \text{for } k = 2 \ldots N \end{aligned} \tag{A.79}$$

The coordinate vectors $\{{}^{X_j^{\ominus}}\underline{r}^{X_j^{\oplus}}\}$ are invariant. They only contains the spanwise length of X_j in the final coordinate system of X_j.

It can be proved that ($i \leq k$):

$$\mathrm{J}^3_{v=1}\Big(\sum_{j=i}^{k}\frac{\partial^{X_0}\Phi^{X_j}}{\partial\phi_v^{X_i}}\cdot{}^{X_j^{\ominus}}\underline{r}^{X_j^{\oplus}}\Big)=\mathrm{J}^3_{v=1}\Big({}^{X_0}\bar{\Phi}^{X_k}\cdot\sum_{j=i}^{k}{}^{X_k}\bar{\Phi}^{X_j}\cdot\big({}^{X_j}\bar{\Phi}^{X_i}\cdot{}^{X_i}\underline{\bar{\Phi}}_v^{\iota_{\mathrm{r}}X_i}\times{}^{X_j^{\ominus}}\underline{r}^{X_j^{\oplus}}\big)\Big) \tag{A.80}$$

The expressions above are based on the property that when rotation variations are considered as *vectors*, the linearisation error applies. Since the linearisation error for variations is the point of departure for TURBU Offshore, this is fully accepted. Then the displacement sensitivities to the position variations are exactly the same as the velocity sensitivities to the rate of change in the position variations. Thus it holds (see Eq. B.113, B.124 and B.127):

$$\begin{aligned}\frac{\partial^{\bar{X}_0^{\ominus}}\underline{r}^{X_k^{\oplus}/\bar{X}_0}}{\partial\underline{\xi}^{X_{\mathrm{FF}}}}&=&{}^{X_0}\bar{\Phi}^{X_k}\cdot\frac{\partial\underline{v}^{X_k^{\oplus}}}{\partial\underline{\omega}^{X_{\mathrm{FF}}}}\\ \frac{\partial^{\bar{X}_0^{\ominus}}\underline{r}^{X_k^{\oplus}/\bar{X}_0}}{\partial\underline{\phi}^{X}}&=&{}^{X_0}\bar{\Phi}^{X_k}\cdot\frac{\partial\underline{v}^{X_k^{\oplus}}}{\partial\underline{\dot{\varphi}}^{X}}\end{aligned} \tag{A.81}$$

The mean values of the (remaining) output variables follow straightforward from the equations above and from those referenced in chapter Appendix B. For the variations the output vector equation on the 2nd order state space model is formulated as follows:

$$\begin{bmatrix}\underline{y}^{GX_{\mathrm{p}}}\\ \underline{y}^{WX_{\mathrm{p}}}\\ \underline{y}^{X_{\mathrm{f}}X_{\mathrm{p}}}\end{bmatrix}=\begin{bmatrix}\boldsymbol{H}_{\varphi}^{GX_{\mathrm{p}}}&\boldsymbol{H}_{\varrho}^{GX_{\mathrm{p}}}\\ \boldsymbol{H}_{\varphi}^{WX_{\mathrm{p}}}&\boldsymbol{H}_{\varrho}^{WX_{\mathrm{p}}}\\ \boldsymbol{H}_{\varphi}^{X_{\mathrm{f}}X_{\mathrm{p}}}&\boldsymbol{H}_{\varrho}^{X_{\mathrm{f}}X_{\mathrm{p}}}\end{bmatrix}\cdot\begin{bmatrix}\underline{\varphi}^{X}\\ \underline{\varrho}^{X}\end{bmatrix}+\begin{bmatrix}\boldsymbol{L}_{\varphi}^{GX_{\mathrm{p}}}&\boldsymbol{L}_{\varrho}^{GX_{\mathrm{p}}}\\ \boldsymbol{L}_{\varphi}^{WX_{\mathrm{p}}}&\boldsymbol{L}_{\varrho}^{WX_{\mathrm{p}}}\\ \boldsymbol{L}_{\varphi}^{X_{\mathrm{f}}X_{\mathrm{p}}}&\boldsymbol{L}_{\varrho}^{X_{\mathrm{f}}X_{\mathrm{p}}}\end{bmatrix}\cdot\begin{bmatrix}\dot{\underline{\varphi}}^{X}\\ \dot{\underline{\varrho}}^{X}\end{bmatrix}+$$

$$\begin{bmatrix}\boldsymbol{K}^{GX_{\mathrm{p}}G}&\boldsymbol{K}^{GX_{\mathrm{p}}W}&\boldsymbol{K}^{GX_{\mathrm{p}}R}&\boldsymbol{K}^{GX_{\mathrm{p}}X_{\mathrm{f}}}\\ \boldsymbol{K}^{WX_{\mathrm{p}}G}&\boldsymbol{K}^{WX_{\mathrm{p}}W}&\boldsymbol{K}^{WX_{\mathrm{p}}R}&\boldsymbol{K}^{WX_{\mathrm{p}}X_{\mathrm{f}}}\\ \boldsymbol{K}^{X_{\mathrm{f}}X_{\mathrm{p}}G}&\boldsymbol{K}^{X_{\mathrm{f}}X_{\mathrm{p}}W}&\boldsymbol{K}^{X_{\mathrm{f}}X_{\mathrm{p}}R}&\boldsymbol{K}^{X_{\mathrm{f}}X_{\mathrm{p}}X_{\mathrm{f}}}\end{bmatrix}\cdot\begin{bmatrix}\underline{v}^{X_{\mathrm{p}}G}\\ \underline{v}^{X_{\mathrm{p}}W}\\ \underline{v}^{X_{\mathrm{p}}R}\\ \underline{v}^{X_{\mathrm{p}}X_{\mathrm{f}}}\end{bmatrix} \tag{A.82}$$

Before the matrices that map states and inputs to outputs are specified, the vector state equation is reformulated in explicit expressions for the dof accelerations:

$$\begin{bmatrix}\ddot{\underline{\varphi}}^{X}\\ \ddot{\underline{\varrho}}^{X}\end{bmatrix}=\begin{bmatrix}\big(\boldsymbol{M}^{X_{\mathrm{p}}}\big)^{-1}_{\varphi}\\ \big(\boldsymbol{M}^{X_{\mathrm{p}}}\big)^{-1}_{\varphi}\end{bmatrix}\cdot\Big(-\Big[\boldsymbol{D}_{\varphi}^{X_{\mathrm{p}}}\mid\boldsymbol{D}_{\varrho}^{X_{\mathrm{p}}}\Big]\cdot\begin{bmatrix}\dot{\underline{\varphi}}^{X}\\ \dot{\underline{\varrho}}^{X}\end{bmatrix}-\Big[\boldsymbol{S}_{\varphi}^{X_{\mathrm{p}}}\mid\boldsymbol{S}_{\varrho}^{X_{\mathrm{p}}}\Big]\cdot\begin{bmatrix}\underline{\varphi}^{X}\\ \underline{\varrho}^{X}\end{bmatrix}+$$

$$\big[\boldsymbol{G}^{X_{\mathrm{p}}G}\mid\boldsymbol{G}^{X_{\mathrm{p}}W}\mid\boldsymbol{G}^{X_{\mathrm{p}}R}\mid\boldsymbol{G}^{X_{\mathrm{p}}X_{\mathrm{f}}}\big]\cdot\begin{bmatrix}\underline{v}^{X_{\mathrm{p}}G}\\ \underline{v}^{X_{\mathrm{p}}W}\\ \underline{v}^{X_{\mathrm{p}}R}\\ \underline{v}^{X_{\mathrm{p}}X_{\mathrm{f}}}\end{bmatrix}\Big) \tag{A.83}$$

Note that the inverse mass matrix is partitioned in two sets of rows (block row matrix). The upper block maps the dofs, the dof speeds and the inputs to the angular dof accelerations while the lower block performs this mapping to the linear dof accelerations.

Be aware that the non-valid rows have been deleted from all system matrices and also the corresponding columns in the mass, damper and stiffness matrix; non-valid rows arise at scalar impulse equations 'in non-dof directions' (see paragraph (vi) at 'Two complications seem ...').

The reformulated state equation makes clear that the mapping from the dof position variations to the outputs into the blade flange is established via matrices $\boldsymbol{H}_{\varphi}^{X_{\mathrm{f}}X_{\mathrm{p}}}$ and

$\boldsymbol{H}_{\varrho}^{X_{\mathrm{f}}X_{\mathrm{p}}}$ given by:

$$\begin{aligned}\boldsymbol{H}_{\varphi}^{X_{\mathrm{f}}X_{\mathrm{p}}} &= \frac{\partial \underline{y}^{X_{\mathrm{f}}X_{\mathrm{p}}}}{\partial \underline{\phi}^{X}} - \left(\frac{\partial \underline{y}^{X_{\mathrm{f}}X_{\mathrm{p}}}}{\partial \underline{\ddot{\varphi}}^{X}} \cdot \left(\boldsymbol{M}^{X_{\mathrm{p}}}\right)_{\varphi}^{-1} + \frac{\partial \underline{y}^{X_{\mathrm{f}}X_{\mathrm{p}}}}{\partial \underline{\ddot{\varrho}}^{X}} \cdot \left(\boldsymbol{M}^{X_{\mathrm{p}}}\right)_{\varrho}^{-1}\right) \cdot \boldsymbol{S}_{\varphi}^{X_{\mathrm{p}}} \\ \boldsymbol{H}_{\varrho}^{X_{\mathrm{f}}X_{\mathrm{p}}} &= \frac{\partial \underline{y}^{X_{\mathrm{f}}X_{\mathrm{p}}}}{\partial \underline{\rho}^{X}} - \left(\frac{\partial \underline{y}^{X_{\mathrm{f}}X_{\mathrm{p}}}}{\partial \underline{\ddot{\varphi}}^{X}} \cdot \left(\boldsymbol{M}^{X_{\mathrm{p}}}\right)_{\varphi}^{-1} + \frac{\partial \underline{y}^{X_{\mathrm{f}}X_{\mathrm{p}}}}{\partial \underline{\ddot{\varrho}}^{X}} \cdot \left(\boldsymbol{M}^{X_{\mathrm{p}}}\right)_{\varrho}^{-1}\right) \cdot \boldsymbol{S}_{\varrho}^{X_{\mathrm{p}}}\end{aligned} \tag{A.84}$$

The mapping matrices $\boldsymbol{L}_{\varphi}^{X_{\mathrm{f}}X_{\mathrm{p}}}$ and $\boldsymbol{L}_{\varphi}^{X_{\mathrm{f}}X_{\mathrm{p}}}$ for the dof speeds are obtained via these equations by

(i) taking partial deriviatives to $\underline{\dot{\varphi}}^{X}$ and $\underline{\dot{\varrho}}^{X}$ instead of to $\underline{\phi}^{X}$ and $\underline{\rho}^{X}$;

(ii) replacing the stiffness matrices $\boldsymbol{S}_{\varphi}^{X_{\mathrm{p}}}$ and $\boldsymbol{S}_{\varrho}^{X_{\mathrm{p}}}$ by damping matrices $\boldsymbol{D}_{\varphi}^{X_{\mathrm{p}}}$ and $\boldsymbol{D}_{\varrho}^{X_{\mathrm{p}}}$.

A partial derivative of the output subvector $\underline{y}^{X_{\mathrm{f}}X_{\mathrm{p}}}$, composed of 'elementary' subvectors $\{\underline{z}_{\mathrm{y}}\}$, to an elementary subvector $\underline{q}$ is obtained by putting above each other (stacking) the partial derivatives of the involved output elementary subvectors. For this we introduce the operator $\mathrm{S}(.)$ (see Eq. A.72):

$$\frac{\partial \underline{y}^{X_{\mathrm{f}}X_{\mathrm{p}}}}{\partial \underline{q}} = \mathrm{S}_{(\underline{z}_{\mathrm{y}})}\left(\frac{\partial \underline{z}_{\mathrm{y}}}{\partial \underline{q}}\right) = \begin{bmatrix} \partial^{\mathrm{FT}} \underline{f}^{X_1^{\oplus}} / \partial \underline{q} \\ \partial^{\mathrm{FT}} \underline{t}^{X_1^{\oplus}} / \partial \underline{q} \\ \partial^{\mathrm{a}} \underline{q}^{X_{\mathrm{PP}(2)}^{\ominus}} / \partial \underline{q} \\ \partial^{\mathrm{a_L}} \underline{q}^{X_{\mathrm{PP}(2)}^{\ominus}} / \partial \underline{q} \\ \partial \underline{\phi}^{X_{\mathrm{PP}(2)}} / \partial \underline{q} \end{bmatrix} \tag{A.85}$$

The mapping from the 'exogenous' input subvector to the output subvector into the blade flange occurs via matrix $\boldsymbol{K}^{X_{\mathrm{f}}X_{\mathrm{p}}G}$ given by:

$$\boldsymbol{K}^{X_{\mathrm{f}}X_{\mathrm{p}}G} = \frac{\partial \underline{y}^{X_{\mathrm{f}}X_{\mathrm{p}}}}{\partial \underline{v}^{X_{\mathrm{p}}G}} - \left(\frac{\partial \underline{y}^{X_{\mathrm{f}}X_{\mathrm{p}}}}{\partial \underline{\ddot{\varphi}}^{X}} \cdot \left(\boldsymbol{M}^{X_{\mathrm{p}}}\right)_{\varphi}^{-1} + \frac{\partial \underline{y}^{X_{\mathrm{f}}X_{\mathrm{p}}}}{\partial \underline{\ddot{\varrho}}^{X}} \cdot \left(\boldsymbol{M}^{X_{\mathrm{p}}}\right)_{\varrho}^{-1}\right) \cdot \boldsymbol{G}^{X_{\mathrm{p}}G} \tag{A.86}$$

Be aware that all columns in the output sensitivities to the degree of freedoms that pertain to non-dof directions as concerns X_{p} are to be deleted before using them in the parametrisation of the vector output equation.

The partial derivative of the composed output subvector $\underline{y}^{X_{\mathrm{f}}X_{\mathrm{p}}}$ to the input subvector $\underline{v}^{X_{\mathrm{p}}G}$, composed of 'elementary' subvectors $\{\underline{q}_{\mathrm{v}}\}$, is obtained by (i) putting above each other ('stacking') the partial derivatives of the output elementary subvectors to an input elementary subvector, and (ii) doing this for all elementary input subvectors and putting next to each other the obtained 'stacks'. With elementary output subvectors $\{\underline{z}_{\mathrm{y}}\}$ the

expression becomes: (see Eq. A.50):

$$\frac{\partial \underline{y}^{X_\mathrm{f} X_\mathrm{p}}}{\partial \underline{v}^{X_\mathrm{p} G}} = \mathrm{J}_{(\underline{q}_\mathrm{v})}\Big(\mathrm{S}_{(\underline{z}_\mathrm{y})}\big(\frac{\partial \underline{z}_\mathrm{y}}{\partial \underline{q}_\mathrm{v}}\big)\Big) = \begin{bmatrix} \frac{\partial^{\mathrm{FT}} \underline{f}^{X_1^\oplus}}{\partial \underline{u}^{X}_{\mathrm{per}}} & \frac{\partial^{\mathrm{FT}} \underline{f}^{X_1^\oplus}}{\partial \underline{g}^{X_0}_{\mathrm{per}}} & \frac{\partial^{\mathrm{FT}} \underline{f}^{X_1^\oplus}}{\partial^{\mathrm{t}} \underline{u}^{W/X}} \\ \frac{\partial^{\mathrm{FT}} \underline{t}^{X_1^\oplus}}{\partial \underline{u}^{X}_{\mathrm{per}}} & \frac{\partial^{\mathrm{FT}} \underline{t}^{X_1^\oplus}}{\partial \underline{g}^{X_0}_{\mathrm{per}}} & \frac{\partial^{\mathrm{FT}} \underline{t}^{X_1^\oplus}}{\partial^{\mathrm{t}} \underline{u}^{W/X}} \\ \frac{\partial^{\mathrm{a}} \underline{q}^{X_{\mathrm{PP}(2)}^\ominus}}{\partial \underline{u}^{X}_{\mathrm{per}}} & \frac{\partial^{\mathrm{a}} \underline{q}^{X_{\mathrm{PP}(2)}^\ominus}}{\partial \underline{g}^{X_0}_{\mathrm{per}}} & \frac{\partial^{\mathrm{a}} \underline{q}^{X_{\mathrm{PP}(2)}^\ominus}}{\partial^{\mathrm{t}} \underline{u}^{W/X}} \\ \frac{\partial^{\mathrm{a_L}} \underline{q}^{X_{\mathrm{PP}(2)}^\ominus}}{\partial \underline{u}^{X}_{\mathrm{per}}} & \frac{\partial^{\mathrm{a_L}} \underline{q}^{X_{\mathrm{PP}(2)}^\ominus}}{\partial \underline{g}^{X_0}_{\mathrm{per}}} & \frac{\partial^{\mathrm{a_L}} \underline{q}^{X_{\mathrm{PP}(2)}^\ominus}}{\partial^{\mathrm{t}} \underline{u}^{W/X}} \\ \frac{\partial \underline{\phi}^{X_{\mathrm{PP}(2)}}}{\partial \underline{u}^{X}_{\mathrm{per}}} & \frac{\partial \underline{\phi}^{X_{\mathrm{PP}(2)}}}{\partial \underline{g}^{X_0}_{\mathrm{per}}} & \frac{\partial \underline{\phi}^{X_{\mathrm{PP}(2)}}}{\partial^{\mathrm{t}} \underline{u}^{W/X}} \end{bmatrix} \tag{A.87}$$

The mapping from the input subvectors from the wake, rotor shaft & hub and blade flange itself to the output subvector into the blade flange occurs via matrices $\boldsymbol{K}^{X_\mathrm{f} X_\mathrm{p} W}$, $\boldsymbol{K}^{X_\mathrm{f} X_\mathrm{p} R}$ and $\boldsymbol{K}^{X_\mathrm{f} X_\mathrm{p} X_\mathrm{f}}$. These matrices are determined in accordance with Eq. A.86:

(i) replace output sensitivity to $\underline{v}^{X_\mathrm{p} G}$ by the one to $\underline{v}^{X_\mathrm{p} W}$, $\underline{v}^{X_\mathrm{p} R}$ and $\underline{v}^{X_\mathrm{p} X_\mathrm{f}}$;

(ii) replace input matrix partition $\boldsymbol{G}^{X_\mathrm{p} G}$ by $\boldsymbol{G}^{X_\mathrm{p} W}$, $\boldsymbol{G}^{X_\mathrm{p} R}$ and $\boldsymbol{G}^{X_\mathrm{p} X_\mathrm{f}}$.

The partial derivative of the *output* subvector to the flange to the *input* subvector from the flange is then composed as follows:

$$\frac{\partial \underline{y}^{X_\mathrm{f} X_\mathrm{p}}}{\partial \underline{v}^{X_\mathrm{p} X_\mathrm{f}}} = \mathrm{J}_{(\underline{q}_\mathrm{v})}\Big(\mathrm{S}_{(\underline{z}_\mathrm{y})}\big(\frac{\partial \underline{z}_\mathrm{y}}{\partial \underline{q}_\mathrm{v}}\big)\Big) = \begin{bmatrix} \frac{\partial \underline{z}_{\mathrm{y}_1}}{\partial \underline{q}_{\mathrm{v}_1}} & \cdots & \frac{\partial \underline{z}_{\mathrm{y}_1}}{\partial \underline{q}_{\mathrm{v}_9}} \\ \vdots & \vdots & \vdots \\ \frac{\partial \underline{z}_{\mathrm{y}_5}}{\partial \underline{q}_{\mathrm{v}_1}} & \cdots & \frac{\partial \underline{z}_{\mathrm{y}_5}}{\partial \underline{q}_{\mathrm{v}_9}} \end{bmatrix} \tag{A.88}$$

in which $\underline{z}_{\mathrm{y}_i}$ involves ${}^{\mathrm{FT}}\underline{f}^{X_1^\oplus}$, ${}^{\mathrm{FT}}\underline{t}^{X_1^\oplus}$, ${}^{\mathrm{a}}\underline{q}^{X_{\mathrm{PP}(2)}^\ominus}$, ${}^{\mathrm{a_L}}\underline{q}^{X_{\mathrm{PP}(2)}^\ominus}$ and $\underline{\phi}^{X_{\mathrm{PP}(2)}}$ while $\underline{q}_{\mathrm{v}_j}$ involves $\underline{\omega}^{X_{\mathrm{FF}(1)}}$, $\underline{\alpha}^{X_{\mathrm{FF}(1)}}$, $\underline{v}^{X_{\mathrm{FF}(1)}^\oplus}$, $\underline{a}^{X_{\mathrm{FF}(1)}^\oplus}$, $\underline{\phi}^{X_{\mathrm{FF}(1)}}$, ${}^{\mathrm{a}}\underline{q}^{X_{\mathrm{FF}(1)}}$, ${}^{\mathrm{a_L}}\underline{q}^{X_{\mathrm{FF}(1)}}$, $\underline{g}_{\mathrm{ori}}^{X_{\mathrm{FF}(1)}}$, $\underline{\xi}^{X_{\mathrm{FF}(1)}}$, and $\underline{x}^{X_{\mathrm{FF}(1)}}$.

A.2.3 Equations of motion for rotor blade flange X_f

The first four paragraphs in this subsection give a summary of the involved variables in the coordinate vectors for the impulse of the blade element X_1 and for the aerodynamic, gravitation and responsive loading on this elements. The subsequent paragraphs (v) list the needed input variables to the flang X_f, (vi) describe the derivation of the system matrices in the state space model for X_f, (vii) lists the required output variables from X_f and links them to the state and input variables via additional system matrices and (viii) describes the submodel for the pitch control system and the incorporation in the flange model.

The (blade-generic) subcomponent model for the flange X_f and pitch control system $X_{\mathrm{f_c}}$ are obtained by a call to TBUX1SUBEOM() and TBUXCSUBEOM() in function TBUBLADEEOM(), which in turn is called to from function TBUAEROEOM(). The models for X_f and $X_{\mathrm{f_c}}$ exist as structure variables sysX1sub and sysXCsub. The fields in sysX1sub and sysXCsub are 2D matrices A, B, C, K, the parameterisation of the first order state space representation, and cell arrays with lists of input, output and state variable

names. Point of departure for the flange model creation by function TBUX1SUBEOM() is the availability for blade element X_1 of (f.c.s: final coordinate system):

- means and sensitivities of angular and linear impulse vector (along f.c.s. of X_1 in actual position);
- means and sensitivities of aerodynamic and gravitation loads (along f.c.s., conversion c.s. and annulus wise c.s. of X_k in actual position; see par. **(vii)**);
- means of feedthrough loads from blade structure & profile on blade flange exit (along f.c.s. of X_1 in actual position);
- sensitivities of displacement vectors relative to rotor centre in average position (along f.c.s. of X_0 in average position);
- sensitivities of kinematic vectors at blade flange exit (along f.c.s. of X_1 in actual position);
- sensitivities of gravitation by orientation change at blade flange exit (along f.c.s. of X_1 in actual position);
- sensitivities of displacement vectors at blade flange exit relative to rotor centre in average position (along f.c.s. of X_1 in average position);
- transformation matrices and their sensitivities to rotational dofs;
- stiffness and damper values in the connection point with the blade base X_0;
- element length, location of c.o.g. and aerodynamic conversion point;
- bottom-up ranking of rotation and translation axes in the connnection point;
- flags for angular and linear dofs in the connection point.

The mentioned sensitivities belong to the 'motion and load formulations' and map all motion and load variations to input variables from the blade profile & structure, the drive-train, the wake, or the environment (wind, gravitation). These are provided by preceeding function calls in TBUAEREOM() (see section 2.2.1).

Functionality TBUX1SUBEOM() ((f.)c.s: (final) coordinate system):

- definition of input name lists; each list contains the names of the input subvectors from a specific source (G, W, R, X2sub (= blade profile & structure X_{p}), XCsub (= pitch control $X_{\mathrm{f_c}}$);
- definition of output name lists; each list containts the names of the output subvectors to a specific destination (G, W, R, X2sub, XCsub);
- lumping together the aerodynamic, gravitation loads and the feedthrough loads from the blade profile & structure to equivalent force and torque load formulation in the entry point of element X_1 (call TBUXSUBFTEX(); coordinates along actual f.c.s. of X_1);
- define 'equal to zero' the feedthrough loading from outward elements within the 'flange subcomponent' (there are no) in the *entry* point of X_1 (call TBUSYSFTFT());
- definition of the sensitivities of the responsive (visco/elastic or control-driven) loads in the entry point of X_1 to the dofs or control output (call TBUQRESPNOCP());
- derive the mass, spring and damper matrix for the equations of motion for the blade element X_1 ($\boldsymbol{M}, \boldsymbol{S}, \boldsymbol{D}$; call TBUSYSMDSMX());
- derive load formulations for feedthrough force and torque loading on the rotor centre (exit point of final element of preceeding subcomponent; call TBUSYSFTPP; coordinates along actual c.s of blade base X_0);

- derive the input matrix for the mass/spring/damper formulation of the flange model as well as output matrices on the dofs and their time derivatives and the feedthrough matrix ($\boldsymbol{G}, \boldsymbol{H}, \boldsymbol{L}, \boldsymbol{K}$; call TBUSYSGHLKMX())
- transform the mass/spring/damper model formulation $\{\boldsymbol{M}, \boldsymbol{S}, \boldsymbol{D}, \boldsymbol{G}, \boldsymbol{H}, \boldsymbol{L}, \boldsymbol{K}\}$ to the first order state space formulation $\{\boldsymbol{A}, \boldsymbol{B}, \boldsymbol{C}, \boldsymbol{K}\}$ (call TBUSYSMDS2FSR())

Point of departure for the pitch control model creation by function TBUXCSUBEOM() is the availability of:

- parameters for filtering, dynamic inflow compensation and PID feedback of the rotational speed to the pitch angle setpoint
- parameters for PD feedback of the pitch angle tracking error to the actuation torque

Functionality TBUXCSUBEOM():

- definition of input name lists; each list contains the names of the input subvectors from a specific source (R, X1sub (= blade flang X_{f})
- definition of output name lists; each list containts the names of the output subvectors to a specific destination (G, X1sub);
- parametrisation of the transfer function formulations for the outer and inner control loop
- convert transfer function models to first order state space models (call TF2SS())
- connect both state space models to the pitch control system model via the pitch angle setpoint (call CONNECT())

(i) Linear and angular impulse

Equation B.133 also applies for the the linear and angular impulse of the 'one-element' blade flange subcomponent X_{f}. However, the reactive variation as represented by the summation over $\underline{z}$ now involves

- processed output from the rotor shaft & hub R: $\underline{\omega}^{X_{\mathrm{FF}(0)}}$ $\underline{\alpha}^{X^{\oplus}_{\mathrm{FF}(0)}}$, $\underline{a}^{X^{\oplus}_{\mathrm{FF}(0)}}$
- degrees of freedom in X_{f}, encapsulated by: $\underline{\phi}^{X}$, $\underline{\dot{\varphi}}^{X}$, $\underline{\ddot{\varphi}}^{X}$, $\underline{\dot{\varrho}}^{X}$ and $\underline{\ddot{\varrho}}^{X}$.

The partial derivatives to $\underline{\phi}^{X}$, $\underline{\dot{\varphi}}^{X}$, $\underline{\ddot{\varphi}}^{X}$, $\underline{\dot{\varrho}}^{X}$ and $\underline{\ddot{\varrho}}^{X}$. only may contain non-zero elements when they pertain to element X_1. The processed output vectors from R apply in the entry point of the blade flange, that is to say the exit point $X_0^{\oplus}$ of the blade base. However, the actual output vectors of R are related to the rotor centre $R_{\mathrm{r}}^{\mathrm{c}}$. So, the mapping involves the coordinate transformation over the azimuth offset $2\pi\cdot(b-1)/B$ ($b = 1, 2, 3$) as well as the spanwise offset over the root radius R_{root}. See paragraph (vi) in section A.1.

(ii) Aerodynamic loading

Equation A.41 also applies for the aerodynamic loads on the 'one-element' blade flange subcomponent X_{f}. However, the reactive variation as represented by the summation over $\underline{z}$ now involves

- output from the blade structure & profile X_{p}: ${}^{\mathrm{a}}\underline{q}_{\mathrm{f}}^{X_{\mathrm{PP}}}$, $\underline{\phi}^{X_{\mathrm{PP}(2)}}$,
- processed output from the rotor shaft & hub R: $\underline{u}_{\mathrm{ori}}^{X_{\mathrm{FF}(0)}}$, $\underline{v}^{X^{\oplus}_{\mathrm{FF}(0)}}$, $\underline{\omega}^{X_{\mathrm{FF}(0)}}$

- output from the wake W: $\underline{u}_{\mathrm{im}}^{W}$
- degrees of freedom in X_{f}, encapsulated by: $\underline{\phi}^{X}$, $\underline{\dot{\varphi}}^{X}$, $\underline{\dot{\varrho}}^{X}$

The partial derivatives to $\underline{\phi}^{X}$, $\underline{\dot{\varphi}}^{X}$ and $\underline{\dot{\varrho}}^{X}$ only may contain non-zero elements when they pertain to element X_1.

(iii) Gravitation loading

Equation A.41 also applies for the gravitation loads on the 'one-element' blade flange subcomponent X_{f}. However, the reactive variaton now involves:

- processed output from the rotor shaft & hub R: $\underline{g}_{\mathrm{ori}}^{X_{\mathrm{FF}(0)}}$
- degrees of freedom in X_{f}, encapsulated by: $\underline{\phi}^{X}$

The variation $\delta\underline{g}_{\mathrm{ori}}^{X_{\mathrm{FF}(0)}}$ represents the reactive variation of the gravitation vector relative to the blade base coordinate system. It is obtained from the output $\delta\underline{g}_{\mathrm{ori}}^{R}$ of R_{r}; see paragraph (vi) in section A.1.

(iv) Responsive loads

Under the assumption of six degrees of freedom in the entry point of the blade element X_1, the responsive force and torque loads are visco/elastic in three directions each. The defined bottom-up ranking of the deformation directions is flapwise hinging or coning, pitching, edgewise hinging or δ_3-deviation (see section 3.6.1). The following holds for the responsive loads (note $k = 1$ and assume 'passive pitching by viso/elastic behaviour'):

- The angular and linear visco/elastic loads

$$\begin{aligned} {}^{\mathrm{RS}}t_1^{X_k^3} &= -s_{\mathrm{t_x}\phi_{\mathrm{x}}}^{X_k} \cdot (\bar{\phi}_3^{X_k} + \delta\phi_3^{X_k}) - d_{\mathrm{t_x}\phi_{\mathrm{x}}}^{X_k} \cdot \dot{\varphi}_3^{X_k} \\ {}^{\mathrm{RS}}f_3^{X_k^3} &= -s_{\mathrm{f_z}\rho_{\mathrm{z}}}^{X_k} \cdot (\bar{\rho}_3^{X_k} + \delta\rho_3^{X_k}) - d_{\mathrm{f_z}\rho_{\mathrm{z}}}^{X_k} \cdot \dot{\varrho}_3^{X_k} \end{aligned} \tag{A.89}$$

  point along the x- and z-axis of the 3$^{\mathrm{rd}}$ intermediate (=final) coordinate system of X_1 and represent the edgwise hinging torque and force in $X_1^{\ominus}$.

- The angular and linear visco/elastic loads

$$\begin{aligned} {}^{\mathrm{RS}}t_2^{X_k^2} &= -s_{\mathrm{t_y}\phi_{\mathrm{y}}}^{X_k} \cdot (\bar{\phi}_2^{X_k} + \delta\phi_2^{X_k}) - d_{\mathrm{t_y}\phi_{\mathrm{y}}}^{X_k} \cdot \dot{\varphi}_2^{X_k} \\ {}^{\mathrm{RS}}f_2^{X_k^2} &= -s_{\mathrm{f_y}\rho_{\mathrm{y}}}^{X_k} \cdot (\bar{\rho}_2^{X_k} + \delta\rho_2^{X_k}) - d_{\mathrm{f_y}\rho_{\mathrm{y}}}^{X_k} \cdot \dot{\varrho}_2^{X_k} \end{aligned} \tag{A.90}$$

  both point along the y-axis of the 2$^{\mathrm{nd}}$ intermediate coordinate system of X_1 and represent the co-axial responsive torque and force in $X_1^{\ominus}$.

- The angular and linear visco/elastic loads

$$\begin{aligned} {}^{\mathrm{RS}}t_3^{X_k^1} &= -s_{\mathrm{t_z}\phi_{\mathrm{z}}}^{X_k} \cdot (\bar{\phi}_1^{X_k} + \delta\phi_1^{X_k}) - d_{\mathrm{t_z}\phi_{\mathrm{z}}}^{X_k} \cdot \dot{\varphi}_1^{X_k} \\ {}^{\mathrm{RS}}f_1^{X_k^1} &= -s_{\mathrm{f_x}\rho_{\mathrm{x}}}^{X_k} \cdot (\bar{\rho}_1^{X_k} + \delta\rho_1^{X_k}) - d_{\mathrm{f_x}\rho_{\mathrm{x}}}^{X_k} \cdot \dot{\varrho}_1^{X_k} \end{aligned} \tag{A.91}$$

  point along the z- and x-axis of the 1$^{\mathrm{st}}$ intermediate coordinate system of X_1 and represent the flatwise responsive torque and force in $X_1^{\ominus}$.

The point of departure for the derivation of the equations of motion is the vector formulation of loads and motion according to Eq. A.26. Therefore we define the responsive load coordinate vectors ${}^{\mathrm{RS}}\underline{f}^{X_1}$ and ${}^{\mathrm{RS}}\underline{t}^{X_1}$ as follows ($k = 1$):

$$ {}^{\mathrm{RS}}\underline{f}^{X_1} \triangleq \begin{bmatrix} {}^{\mathrm{RS}}f_{\mathrm{x}}^{X_1^1} \\ {}^{\mathrm{RS}}f_{\mathrm{y}}^{X_1^2} \\ {}^{\mathrm{RS}}f_{\mathrm{z}}^{X_1^3} \end{bmatrix} = \begin{bmatrix} {}^{\mathrm{RS}}f_1^{X_1^1} \\ {}^{\mathrm{RS}}f_2^{X_1^2} \\ {}^{\mathrm{RS}}f_3^{X_1^3} \end{bmatrix} \quad \text{and} \quad {}^{\mathrm{RS}}\underline{t}^{X_1} \triangleq \begin{bmatrix} {}^{\mathrm{RS}}t_{\mathrm{x}}^{X_1^3} \\ {}^{\mathrm{RS}}t_{\mathrm{y}}^{X_1^2} \\ {}^{\mathrm{RS}}t_{\mathrm{z}}^{X_1^1} \end{bmatrix} = \begin{bmatrix} {}^{\mathrm{RS}}t_1^{X_1^3} \\ {}^{\mathrm{RS}}t_2^{X_1^2} \\ {}^{\mathrm{RS}}t_3^{X_1^1} \end{bmatrix} \tag{A.92} $$

The associated linearised expressions are:

$$ \begin{aligned} {}^{\mathrm{RS}}\underline{f}^{X_1} &= {}^{\mathrm{RS}}\bar{\underline{f}}^{X_1} + \frac{\partial^{\mathrm{RS}}\underline{f}^{X_1}}{\partial \underline{\rho}^X} \cdot \delta\underline{\rho}^X + \frac{\partial^{\mathrm{RS}}\underline{f}^{X_1}}{\partial \dot{\underline{\rho}}^X} \cdot \dot{\underline{\rho}}^X \\ {}^{\mathrm{RS}}\underline{t}^{X_1} &= {}^{\mathrm{RS}}\bar{\underline{t}}^{X_1} + \frac{\partial^{\mathrm{RS}}\underline{t}^{X_1}}{\partial \underline{\phi}^X} \cdot \delta\underline{\phi}^X + \frac{\partial^{\mathrm{RS}}\underline{t}^{X_1}}{\partial \dot{\underline{\varphi}}^X} \cdot \dot{\underline{\varphi}}^X \end{aligned} \tag{A.93} $$

For the means holds:

$$ \begin{aligned} {}^{\mathrm{RS}}\bar{\underline{f}}^{X_1} &= \begin{bmatrix} -s_{\mathrm{f_x}\rho_{\mathrm{x}}}^{X_1} \cdot \bar{\rho}_1^{X_1} & -s_{\mathrm{f_y}\rho_{\mathrm{y}}}^{X_1} \cdot \bar{\rho}_2^{X_1} & -s_{\mathrm{f_z}\rho_{\mathrm{z}}}^{X_1} \cdot \bar{\rho}_3^{X_1} \end{bmatrix}^{\mathrm{T}} \\ {}^{\mathrm{RS}}\bar{\underline{t}}^{X_1} &= \begin{bmatrix} -s_{\mathrm{t_x}\phi_{\mathrm{x}}}^{X_1} \cdot \bar{\phi}_3^{X_1} & -s_{\mathrm{t_y}\phi_{\mathrm{y}}}^{X_1} \cdot \bar{\phi}_2^{X_1} & -s_{\mathrm{t_z}\phi_{\mathrm{z}}}^{X_1} \cdot \bar{\phi}_1^{X_1} \end{bmatrix}^{\mathrm{T}} \end{aligned} \tag{A.94} $$

For the sensitivities to the dof position variations holds:

$$ \frac{\partial^{\mathrm{RS}}\underline{f}^{X_1}}{\partial \underline{\rho}^X} = \begin{pmatrix} -s_{\mathrm{f_x}\rho_{\mathrm{x}}}^{X_1} \cdot [\ 1 & 0 & 0 & 0_{((1*3)+1)} \ldots 0_{(N*3)}\ ] \\ -s_{\mathrm{f_y}\rho_{\mathrm{y}}}^{X_1} \cdot [\ 0 & 1 & 0 & 0_{((1*3)+1)} \ldots 0_{(N*3)}\ ] \\ -s_{\mathrm{f_z}\rho_{\mathrm{z}}}^{X_1} \cdot [\ 0 & 0 & 1 & 0_{((1*3)+1)} \ldots 0_{(N*3)}\ ] \end{pmatrix} $$

and

$$ \frac{\partial^{\mathrm{RS}}\underline{t}^{X_1}}{\partial \underline{\phi}^X} = \begin{pmatrix} -s_{\mathrm{t_x}\phi_{\mathrm{x}}}^{X_1} \cdot [\ 0 & 0 & 1 & 0_{((1*3)+1)} \ldots 0_{(N*3)}\ ] \\ -s_{\mathrm{t_y}\phi_{\mathrm{y}}}^{X_1} \cdot [\ 0 & 1 & 0 & 0_{((1*3)+1)} \ldots 0_{(N*3)}\ ] \\ -s_{\mathrm{t_z}\phi_{\mathrm{z}}}^{X_1} \cdot [\ 1 & 0 & 0 & 0_{((1*3)+1)} \ldots 0_{(N*3)}\ ] \end{pmatrix} \tag{A.95} $$

The sensitivities to the dof speeds are obtained from the ones above by just replacing $s_{(.)}^{X_1}$ by $d_{(.)}^{X_1}$.

Next to pitching, the degrees of freedom of the blade flange can be used on the one side for modelling elastic hinges in the blade root and on the other side for tuning the natural frequencies of rotor blade deformation modes to measurements. If less than six degrees of freedom apply in the entry point $X_1^{\ominus}$ then the non-valid corresponding visco/elastic expressions are skipped when the equations of motions are being derived.

In case of active pitch control, the responsive torque load ${}^{\mathrm{RS}}t_2^{X_1^2}$ results from the inner loop of the pitch control, which is 'driven' by the pitch angle setpoint, which in turn results from the outer loop driven by the rotor speed 'measurement'. Actually, ${}^{\mathrm{RS}}t_2^{X_1^2}$ then amounts to minus the 'nose-up pitch angle adjustment torque' $t_{\mathrm{pt}}^{X_1}$. For the sensitivities of the responsive torque loading to the dof position variations then holds:

$$ \frac{\partial^{\mathrm{RS}}\underline{t}^{X_1}}{\partial \underline{\phi}^X} = \begin{pmatrix} -s_{\mathrm{t_x}\phi_{\mathrm{x}}}^{X_1} \cdot [\ 0 & 0 & 1 & 0_{((1*3)+1)} \ldots 0_{(N*3)}\ ] \\ [\ 0 & 0 & 0 & 0_{((1*3)+1)} \ldots 0_{(N*3)}\ ] \\ -s_{\mathrm{t_z}\phi_{\mathrm{z}}}^{X_1} \cdot [\ 1 & 0 & 0 & 0_{((1*3)+1)} \ldots 0_{(N*3)}\ ] \end{pmatrix} \tag{A.96} $$

The sensitivities to the dof speeds are obtained from the ones above by just replacing $s_{(.)}^{X_1}$ by $d_{(.)}^{X_1}$.

However, in addition the sensitivity to the pitch actuation torque $t_{\mathrm{pt}}^{X_1}$ then applies:

$$\frac{\partial^{\mathrm{RS}}\underline{t}^{X_1}}{\partial t_{\mathrm{pt}}^{X_1}} = \begin{pmatrix} 0 \\ -1 \\ 0 \end{pmatrix} \tag{A.97}$$

The pitch control behaviour only applies in the equations of motion if the variations *around* the equilibrium conditions are considered (EOM). When evaluating the equations of motion in the equilibrium conditions (EOE), the rotation $\bar{\phi}_2^{X_1}$ is set fixed to minus the average value of the pitch angle ϕ_{pt}^{X}, which follows from the aerodynamic equilibrium assessment. See section 3.6.2 for the pitch control algorithm that emits the pitch actuation torque $t_{\mathrm{pt}}^{X_1}$.

(v) Input variables

The input that is required by the blade flange X_{f} is the envelope of all variables that are involved with the impulse vectors, aerodynamic and gravitation loads and output vectors, except of course the internal variables. So the following input applies (see also Eq. A.13 up to A.18):

- feedthrough force and torque from profile & structure X_{p}:
  ${}^{\mathrm{FT}}\underline{f}^{X_{\mathrm{PP}(2)}}$, ${}^{\mathrm{FT}}\underline{t}^{X_{\mathrm{PP}(2)}}$ (= ${}^{\mathrm{FT}}\underline{f}^{X_1^{\oplus}}$, ${}^{\mathrm{FT}}\underline{t}^{X_1^{\oplus}}$)
- distributed aerodynamic force loads on X_2 from X_{p}: ${}^{\mathrm{a}}\underline{q}^{X_{\mathrm{PP}(2)}^{\ominus}}$, ${}^{\mathrm{a_L}}\underline{q}^{X_{\mathrm{PP}(2)}^{\ominus}}$
- variations in angular dofs on X_k^2 from X_{p}: $\underline{\phi}^{X_{\mathrm{PP}(2)}}$
- kinematic vectors on blade blase exit: $\underline{\omega}^{X_{\mathrm{FF}(0)}}$, $\underline{\alpha}^{X_{\mathrm{FF}(0)}}$, $\underline{v}^{X_{\mathrm{FF}(0)}^{\oplus}}$, $\underline{a}^{X_{\mathrm{FF}(0)}^{\oplus}}$
- wind speed variation by orientation change up till hub: $\underline{u}_{\mathrm{ori}}^{X_{\mathrm{FF}(0)}}$.
- gravitation variation by orientation change up till hub: $\underline{g}_{\mathrm{ori}}^{X_{\mathrm{FF}(0)}}$
- displacement vectors on blade blase exit: $\underline{\xi}^{X_{\mathrm{FF}(0)}}$, $\underline{x}^{X_{\mathrm{FF}(0)}}$
- induction speed variation in rotor annuli: $\underline{u}_{\mathrm{im}}^{W}$
- periodic wind speed variation on blade: $\underline{u}_{\mathrm{per}}^{X}$
- periodic gravitation variation on blade base: $\underline{g}_{\mathrm{per}}^{X_0}$
- stochastic wind speed variation in intersection annuli/blade: $\underline{u}_{\mathrm{sto}}^{W/X}$
- pitch actuation torque: $t_{\mathrm{pt}}^{X_1}$

The input vector $\underline{v}^{X_\mathrm{f}}$ of the blade flange has the following composition:

$$\underline{v}^{X_\mathrm{f}} = \begin{bmatrix} \underline{v}^{X_\mathrm{f}G} \\ \underline{v}^{X_\mathrm{f}W} \\ \underline{v}^{X_\mathrm{f}R} \\ \underline{v}^{X_\mathrm{f}X_\mathrm{p}} \\ \underline{v}^{X_\mathrm{f}X_\mathrm{fc}} \end{bmatrix} \quad \text{with} \quad \underline{v}^{X_\mathrm{f}G} = \begin{bmatrix} \underline{u}^{X}_{\mathrm{per}} \\ \underline{g}^{X_0}_{\mathrm{per}} \\ \underline{u}^{W/X}_{\mathrm{sto}} \end{bmatrix}$$

$$\text{and} \quad \underline{v}^{X_\mathrm{f}W} = \begin{bmatrix} \underline{u}^{W}_{\mathrm{i_m}} \end{bmatrix} \; ; \; \underline{v}^{X_\mathrm{f}R} = \begin{bmatrix} \underline{\omega}^{X_{\mathrm{FF}(0)}} \\ \underline{\alpha}^{X_{\mathrm{FF}(0)}} \\ \underline{v}^{X^{\oplus}_{\mathrm{FF}(0)}} \\ \underline{a}^{X^{\oplus}_{\mathrm{FF}(0)}} \\ \underline{u}^{X_{\mathrm{FF}(0)}}_{\mathrm{ori}} \\ \underline{g}^{X_{\mathrm{FF}(0)}}_{\mathrm{ori}} \\ \underline{\xi}^{X_{\mathrm{FF}(0)}} \\ \underline{x}^{X_{\mathrm{FF}(0)}} \end{bmatrix} \; ; \; \underline{v}^{X_\mathrm{f}X_\mathrm{p}} = \begin{bmatrix} {}^{\mathrm{FT}}\underline{f}^{X_{\mathrm{PP}(2)}} \\ {}^{\mathrm{FT}}\underline{t}^{X_{\mathrm{PP}(2)}} \\ {}^{\mathrm{a}}\underline{q}^{X_{\mathrm{PP}(2)}} \\ {}^{\mathrm{a_L}}\underline{q}^{X_{\mathrm{PP}(2)}} \\ \underline{\phi}^{X_{\mathrm{PP}(2)}} \end{bmatrix} \tag{A.98}$$

The *internal* control input subvector $\underline{v}^{X_\mathrm{f}X_\mathrm{fc}}$ only applies if the blade flange incorporates a pitch control system. The pitch control system is modelled as a submodel within the scope of the flange (see section 3.6.2 and paragraph (viii) and emits the pitch actuation torque to the flange element (see end of paragraph (iv)):

$$\underline{v}^{X_\mathrm{f}X_\mathrm{fc}} = \begin{bmatrix} t^{X_1}_{\mathrm{pt}} \end{bmatrix} \tag{A.99}$$

This input subvector will disappear when the flange element model and the pitch control system are integrated.

For the composition of the 'independent' input subvectors $\underline{u}^{X}_{\mathrm{per}}$, $\underline{g}^{X_0}_{\mathrm{per}}$ and ${}^{\mathrm{t}}\underline{u}^{W/X}$, and the wake induction vector $\underline{u}^{W}_{\mathrm{i_m}}$ see Eq. B.175, B.182 and B.279.

(vi) Equations of motion and 2nd order vector state equation

Just as for the element X_2 up to X_N in te blade profile and structure X_p, the equations of motion for the blade element X_1 are also formulated as a second order vector state equation. This state equation also consists of a partitioned mass, damper and spring matrix in the left hand side, in accordance with the angular dofs and linear dofs, and of a partitioned input input matrix in the right hand side, in accordance with the subvectors in the input vector:

$$\left[\boldsymbol{M}^{X_\mathrm{f}}_{\varphi} \mid \boldsymbol{M}^{X_\mathrm{f}}_{\varrho}\right] \cdot \begin{bmatrix} \ddot{\underline{\varphi}}^{X} \\ \ddot{\underline{\varrho}}^{X} \end{bmatrix} + \left[\boldsymbol{D}^{X_\mathrm{f}}_{\varphi} \mid \boldsymbol{D}^{X_\mathrm{f}}_{\varrho}\right] \cdot \begin{bmatrix} \dot{\underline{\varphi}}^{X} \\ \dot{\underline{\varrho}}^{X} \end{bmatrix} + \left[\boldsymbol{S}^{X_\mathrm{f}}_{\varphi} \mid \boldsymbol{S}^{X_\mathrm{f}}_{\varrho}\right] \cdot \begin{bmatrix} \underline{\varphi}^{X} \\ \underline{\varrho}^{X} \end{bmatrix} =$$

$$\left[\boldsymbol{G}^{X_\mathrm{f}G} \mid \boldsymbol{G}^{X_\mathrm{f}W} \mid \boldsymbol{G}^{X_\mathrm{f}R} \mid \boldsymbol{G}^{X_\mathrm{f}X_\mathrm{d}} \mid \boldsymbol{G}^{X_\mathrm{f}X_\mathrm{fc}}\right] \cdot \begin{bmatrix} \underline{v}^{X_\mathrm{f}G} \\ \underline{v}^{X_\mathrm{f}W} \\ \underline{v}^{X_\mathrm{f}R} \\ \underline{v}^{X_\mathrm{f}X_\mathrm{f}} \\ \underline{v}^{X_\mathrm{f}X_\mathrm{fc}} \end{bmatrix} \tag{A.100}$$

Note that the input matrix partition for the internal control input subvector $\underline{v}^{X_\mathrm{f}X_\mathrm{fc}}$ only applies if the blade flange incorporates a pitch servo.

The system matrices are derived from the scalar angular and linear impulse equation for the element X_1. First we consider in the the third intermediate coordinate system (i.c.s.) the x-coordinate of the angular impulse and the z-coordinate of the linear impulse. Afterwards, the y-coordinates of the angular and linear impulse equation are dealt with

in the second i.c.s. These set up the $2\mathrm{nd}$ scalar angular and linear impulse equation for X_N. Finally, the $1\mathrm{st}$ scalar angular and linear impulse equation for X_1 are derived from respectively the z and x-coordinate of the angular and linear impulse equation in the $1\mathrm{st}$ i.c.s.

The w^{th} scalar angular impulse equation for element X_k sets up the rows with ranking number $6(k-1)+2(w-1)+1$ in the system matrices (note: $k=1$ only!). These rows are denoted as (i.c.s. ranking number w corresponds to the x, y and z-axis for $w=3,2,1$):

- $\underline{\boldsymbol{m}}_{h\varphi_w}^{X_1}$ and $\underline{\boldsymbol{m}}_{h\varrho_w}^{X_1}$ to mass matrix partitions $\boldsymbol{M}_{\varphi}^{X_{\mathrm{P}}}$ and $\boldsymbol{M}_{\varrho}^{X_{\mathrm{P}}}$;
- $\underline{\boldsymbol{d}}_{h\varphi_w}^{X_1}$ and $\underline{\boldsymbol{d}}_{h\varrho_w}^{X_1}$ to damping matrix partitions $\boldsymbol{D}_{\varphi}^{X_{\mathrm{P}}}$ and $\boldsymbol{D}_{\varrho}^{X_{\mathrm{P}}}$;
- $\underline{\boldsymbol{s}}_{h\varphi_w}^{X_1}$ and $\underline{\boldsymbol{s}}_{h\varrho_w}^{X_1}$ to stiffness matrix partitions $\boldsymbol{S}_{\varphi}^{X_{\mathrm{P}}}$ and $\boldsymbol{S}_{\varrho}^{X_{\mathrm{P}}}$;
- $\underline{\boldsymbol{g}}_{h_w}^{X_1 G}$, $\underline{\boldsymbol{g}}_{h_w}^{X_1 W}$, $\underline{\boldsymbol{g}}_{h_w}^{X_1 R}$ $\underline{\boldsymbol{g}}_{h_w}^{X_1 X_{\mathrm{f}}}$, and $\underline{\boldsymbol{g}}_{h_w}^{X_1 X_{\mathrm{f_c}}}$ to input matrix partitions $\boldsymbol{G}^{X_{\mathrm{f}} G}$, $\boldsymbol{G}^{X_{\mathrm{f}} W}$, $\boldsymbol{G}^{X_{\mathrm{f}} R}$, $\boldsymbol{G}^{X_{\mathrm{f}} X_{\mathrm{f}}}$, $\boldsymbol{G}^{X_{\mathrm{f}} X_{\mathrm{f_c}}}$.

The w^{th} scalar linear impulse equation for element X_1 yields the rows with ranking number $2(w-1)+2$ in the system matrices. These rows are denoted as (i.c.s. ranking number w now corresponds to the z, y and x-axis for $w=3,2,1$):

- $\underline{\boldsymbol{m}}_{p\varphi_w}^{X_1}$ and $\underline{\boldsymbol{m}}_{p\varrho_w}^{X_1}$ to mass matrix partitions $\boldsymbol{M}_{\varphi}^{X_{\mathrm{P}}}$ and $\boldsymbol{M}_{\varrho}^{X_{\mathrm{P}}}$;
- $\underline{\boldsymbol{d}}_{p\varphi_w}^{X_1}$ and $\underline{\boldsymbol{d}}_{p\varrho_w}^{X_1}$ to damping matrix partitions $\boldsymbol{D}_{\varphi}^{X_{\mathrm{P}}}$ and $\boldsymbol{D}_{\varrho}^{X_{\mathrm{P}}}$;
- $\underline{\boldsymbol{s}}_{p\varphi_w}^{X_1}$ and $\underline{\boldsymbol{s}}_{p\varrho_w}^{X_1}$ to stiffness matrix partitions $\boldsymbol{S}_{\varphi}^{X_{\mathrm{P}}}$ and $\boldsymbol{D}_{\varrho}^{X_{\mathrm{P}}}$;
- $\underline{\boldsymbol{g}}_{p_w}^{X_1 G}$, $\underline{\boldsymbol{g}}_{p_w}^{X_1 W}$, $\underline{\boldsymbol{g}}_{p_w}^{X_1 R}$ $\underline{\boldsymbol{g}}_{p_w}^{X_1 X_{\mathrm{f}}}$, and $\underline{\boldsymbol{g}}_{p_w}^{X_1 X_{\mathrm{f_c}}}$ to input matrix partitions $\boldsymbol{G}^{X_{\mathrm{f}} G}$, $\boldsymbol{G}^{X_{\mathrm{f}} W}$, $\boldsymbol{G}^{X_{\mathrm{f}} R}$, $\boldsymbol{G}^{X_{\mathrm{f}} X_{\mathrm{f}}}$, $\boldsymbol{G}^{X_{\mathrm{f}} X_{\mathrm{f_c}}}$.

Above mentioned rows in the left hand side matrices are obtained from the partial derivatives of the scalar impulse equations to the *internal* variables $\underline{\ddot{\varphi}}^X$, $\underline{\ddot{\varrho}}^X$, $\underline{\dot{\varphi}}^X$, $\underline{\dot{\varrho}}^X$, $\underline{\varphi}^X$ and $\underline{\varrho}^X$. The rows in the right hand side matrices follow from the partial derivatives of the scalar impulse equations to the input variables $\underline{v}^{X_{\mathrm{f}} G}$,$\underline{v}^{X_{\mathrm{f}} X_{\mathrm{f_c}}}$, $\underline{v}^{X_{\mathrm{f}} W}$, $\underline{v}^{X_{\mathrm{f}} R}$ and $\underline{v}^{X_{\mathrm{f}} X_{\mathrm{P}}}$.

Note that all columns but the first three of the rows of the left hand side matrix partitions are deleted. The influence of the belonging blade dofs 'comes in' via the input matrix partitions that pertain to the feedthrough loads from the profile & structure. Besides, each non-valid row and the corresponding column, which pertains to the 'non-dof' element of $\underline{\phi}^X$ or $\underline{\rho}^X$ *as concerns* X_{f}, is deleted. The input matrix is cleaned up accordingly (of course rows only). This yields a second order system equation with square left hand side matrices and adequately dimensioned input matrix.

Note that a 'non-valid row' $2(w-1)+1$ pertains to the **rotation** $\phi_w^{X_1}$ and thus to the column w in the **left** partition of the left hand system matrices, while a 'non-valid row' $2(w-1)+2$ pertains to the **translation** $\rho_w^{X_1}$ and thus to the column w in the **right** partition.

We end up this paragraph with the formulation of the three scalar angular and linear impulse equations and their explicit relationship with the row vectors in the system matrices of Eq. A.100.

The third scalar angular impulse equation pertains to the x-axis and the linear one to the z-axis of the third intermediate coordinate system. It holds:

$$\begin{aligned}
[\,1\,0\,0\,]\cdot {}^{X_1^{\ominus}}\underline{\dot{h}}^{X_1} &= [\,1\,0\,0\,]\cdot {}^{\mathrm{RS}}\underline{t}^{X_1^{\ominus}} + [\,1\,0\,0\,]\cdot {}^{\mathrm{FT}}\underline{t}^{X_1^{\ominus}} + [\,1\,0\,0\,]\cdot {}^{\mathrm{EX}}\underline{t}^{X_1^{\ominus}} \\
[\,0\,0\,1\,]\cdot \underline{\dot{p}}^{X_1} &= [\,0\,0\,1\,]\cdot {}^{\mathrm{RS}}\underline{f}^{X_1^{\ominus}} + [\,0\,0\,1\,]\cdot {}^{\mathrm{FT}}\underline{f}^{X_1^{\ominus}} + [\,0\,0\,1\,]\cdot {}^{\mathrm{EX}}\underline{f}^{X_1^{\ominus}}
\end{aligned} \tag{A.101}$$

The second scalar impulse equations both pertain to the y-axis of the second i.c.s.:

$$\begin{aligned}
{}^{X_1^2}\Phi^{X_1}_{(2,:)}\cdot {}^{X_1^{\ominus}}\underline{\dot{h}}^{X_1} &= [\,0\,1\,0\,]\cdot {}^{\mathrm{RS}}\underline{t}^{X_1^{\ominus}} + {}^{X_1^2}\Phi^{X_1}_{(2,:)}\cdot {}^{\mathrm{FT}}\underline{t}^{X_1^{\ominus}} + {}^{X_1^2}\Phi^{X_1}_{(2,:)}\cdot {}^{\mathrm{EX}}\underline{t}^{X_1^{\ominus}} \\
{}^{X_1^2}\Phi^{X_1}_{(2,:)}\cdot \underline{\dot{p}}^{X_1} &= [\,0\,1\,0\,]\cdot {}^{\mathrm{RS}}\underline{f}^{X_1^{\ominus}} + {}^{X_1^2}\Phi^{X_1}_{(2,:)}\cdot {}^{\mathrm{FT}}\underline{f}^{X_1^{\ominus}} + {}^{X_1^2}\Phi^{X_1}_{(2,:)}\cdot {}^{\mathrm{EX}}\underline{f}^{X_1^{\ominus}}
\end{aligned} \tag{A.102}$$

The first scalar angular and linear impulse equation pertain to the z-axis and x-axis of the first i.c.s.:

$$\begin{aligned}
{}^{X_1^1}\Phi^{X_1}_{(3,:)}\cdot {}^{X_1^{\ominus}}\underline{\dot{h}}^{X_1} &= [\,0\,0\,1\,]\cdot {}^{\mathrm{RS}}\underline{t}^{X_1^{\ominus}} + {}^{X_1^2}\Phi^{X_1}_{(3,:)}\cdot {}^{\mathrm{FT}}\underline{t}^{X_1^{\ominus}} + {}^{X_1^2}\Phi^{X_1}_{(3,:)}\cdot {}^{\mathrm{EX}}\underline{t}^{X_1^{\ominus}} \\
{}^{X_1^1}\Phi^{X_1}_{(1,:)}\cdot \underline{\dot{p}}^{X_1} &= [\,1\,0\,0\,]\cdot {}^{\mathrm{RS}}\underline{f}^{X_1^{\ominus}} + {}^{X_1^2}\Phi^{X_1}_{(1,:)}\cdot {}^{\mathrm{FT}}\underline{f}^{X_1^{\ominus}} + {}^{X_1^2}\Phi^{X_1}_{(1,:)}\cdot {}^{\mathrm{EX}}\underline{f}^{X_1^{\ominus}}
\end{aligned} \tag{A.103}$$

Equations A.92 up to A.95 specifiy the responsive load coordinate vectors ${}^{\mathrm{RS}}\underline{t}^{X_1^{\ominus}}$ and ${}^{\mathrm{RS}}\underline{f}^{X_1^{\ominus}}$

The external load coordinate vectors follow from Eq. A.37 while in addition they include the feedthrough loads from the profile & structure X_{p}, which also pertain to the f.c.s. of X_1:

$$\begin{aligned}
{}^{\mathrm{EX}}\underline{f}^{X_1^{\ominus}} &\triangleq {}^{\mathrm{a}}\underline{f}^{X_1^{\mathrm{a}}} + {}^{\mathrm{g}}\underline{f}^{X_1^{*}} + {}^{\mathrm{FT}}\underline{f}^{X_{\mathrm{PP}(2)}} \\
{}^{\mathrm{EX}}\underline{t}^{X_1^{\ominus}} &\triangleq {}^{\mathrm{a}}\underline{t}^{X_1^{\mathrm{a}}} + {}^{X_k^{\ominus}}\underline{r}^{X_1^{\mathrm{a}}} \times {}^{\mathrm{a}}\underline{f}^{X_1^{\mathrm{a}}} + {}^{X_1^{\ominus}}\underline{r}^{X_1^{*}} \times {}^{\mathrm{g}}\underline{f}^{X_1^{*}} + {}^{X_1^{\ominus}}\underline{r}^{X_1^{\oplus}} \times {}^{\mathrm{FT}}\underline{f}^{X_{\mathrm{PP}(2)}} + {}^{\mathrm{FT}}\underline{t}^{X_{\mathrm{PP}(2)}}
\end{aligned} \tag{A.104}$$

The feedthrough loads ${}^{\mathrm{FT}}\underline{f}^{X_1^{\ominus}}$ and ${}^{\mathrm{FT}}\underline{t}^{X_1^{\ominus}}$ from the 'next element within the subcomponent' do not apply because the flange X_{f} is a one-element subcomponent.

The expressions for the external load coordinate vectors comprise the envelope of dependencies for the aerodynamic and gravitation load coordinate vectors. The linearised expressions are:

$$\begin{aligned}
{}^{\mathrm{EX}}\underline{f}^{X_1^{\ominus}} &= {}^{\mathrm{EX}}\bar{\underline{f}}^{X_1^{\ominus}} + \sum_{(\underline{q})} \frac{\partial {}^{\mathrm{EX}}\underline{f}^{X_1^{\ominus}}}{\partial \underline{q}}\cdot \delta\underline{q} \\
{}^{\mathrm{EX}}\underline{t}^{X_1^{\ominus}} &= {}^{\mathrm{EX}}\bar{\underline{t}}^{X_1^{\ominus}} + \sum_{(\underline{q})} \frac{\partial {}^{\mathrm{EX}}\underline{t}^{X_1^{\ominus}}}{\partial \underline{q}}\cdot \delta\underline{q}
\end{aligned} \tag{A.105}$$

The summation over $(\underline{q})$ involves:

- exogeneous periodic wind speed and gravition input: $\underline{u}^{X}_{\mathrm{per}}$, $\underline{g}^{X_0}_{\mathrm{per}}$
- exogenous stochastic wind speed input: $\underline{u}^{W/X}_{\mathrm{sto}}$
- feedthrough loads from X_{p} in exit point $X_{\mathrm{f}}^{\oplus}$: ${}^{\mathrm{FT}}\underline{f}^{X_{\mathrm{PP}(2)}}$, ${}^{\mathrm{FT}}\underline{t}^{X_{\mathrm{PP}(2)}}$
- output from wake W: $\underline{u}^{W}_{\mathrm{im}}$
- processed output from rotor shaft & hub R: $\underline{\omega}^{X^{\oplus}_{\mathrm{FF}(0)}}$, $\underline{\alpha}^{X_{\mathrm{FF}(0)}}$, $\underline{v}^{X^{\oplus}_{\mathrm{FF}(0)}}$, $\underline{a}^{X^{\oplus}_{\mathrm{FF}(0)}}$, $\underline{u}^{X_{\mathrm{FF}(0)}}_{\mathrm{ori}}$, $\underline{g}^{X_{\mathrm{FF}(0)}}_{\mathrm{ori}}$
- output from profile & structure X_{p}: ${}^{\mathrm{a}}\underline{q}_{\mathrm{f}}^{X_{\mathrm{PP}(2)}}$,

- degrees of freedom in X_{f}, encapsulated by: $\underline{\phi}^{X}$, $\underline{\dot{\varphi}}^{X}$, $\underline{\ddot{\varphi}}^{X}$, $\underline{\dot{\varrho}}^{X}$ $\underline{\ddot{\varrho}}^{X}$.

The expressions for the mean external load vectors are just the overlined versions of those in Eq. A.104. The sensitivities are obtained from Eq. A.58 with $k = 1$.

We do not need to derive expressions for feedthrough loads to 'inner' elements because the flange is a one-element subcomponent.

The pairs of rows $\{\underline{\boldsymbol{m}}^{X_1}_{h\varphi_w}, \underline{\boldsymbol{m}}^{X_1}_{p\varphi_w} | w = 3, 2, 1\}$, with ranking numbers $2(w-1)+1$ and $2(w-1)+2$ in the mass matrix partition $\boldsymbol{M}^{X_{\mathrm{f}}}_{\varphi}$, are now determined as follows (the partial derivatives in the right hand side only apply if they are defined for the 'independent variable'; in this case $\underline{\ddot{\varphi}}^{X}$):

- for $w = 3$:

$$\begin{aligned}
\underline{\boldsymbol{m}}^{X_1}_{h\varphi_3} &= -[\,1\,0\,0\,] \cdot \frac{\partial^{\mathrm{RS}} \underline{t}^{X_1^{\ominus}}}{\partial \underline{\ddot{\varphi}}^{X}} + [\,1\,0\,0\,] \cdot \Big(\frac{\partial^{X_1^{\ominus}} \underline{\dot{h}}^{X_1}}{\partial \underline{\ddot{\varphi}}^{X}} - \frac{\partial^{\mathrm{EX}} \underline{t}^{X_1^{\ominus}}}{\partial \underline{\ddot{\varphi}}^{X}} \Big) \\
\underline{\boldsymbol{m}}^{X_1}_{p\varphi_3} &= -[\,0\,0\,1\,] \cdot \frac{\partial^{\mathrm{RS}} \underline{f}^{X_1^{\ominus}}}{\partial \underline{\ddot{\varphi}}^{X}} + [\,0\,0\,1\,] \cdot \Big(\frac{\partial \underline{\dot{p}}^{X_1}}{\partial \underline{\ddot{\varphi}}^{X}} - \frac{\partial^{\mathrm{EX}} \underline{f}^{X_1^{\ominus}}}{\partial \underline{\ddot{\varphi}}^{X}} \Big)
\end{aligned} \tag{A.106}$$

- for $w = 2$:

$$\begin{aligned}
\underline{\boldsymbol{m}}^{X_1}_{h\varphi_2} &= -[\,0\,1\,0\,] \cdot \frac{\partial^{\mathrm{RS}} \underline{t}^{X_1^{\ominus}}}{\partial \underline{\ddot{\varphi}}^{X}} + {}^{X_1^2}\bar{\Phi}^{X_1}_{(2,:)} \cdot \Big(\frac{\partial^{X_1^{\ominus}} \underline{\dot{h}}^{X_1}}{\partial \underline{\ddot{\varphi}}^{X}} - \frac{\partial^{\mathrm{EX}} \underline{t}^{X_1^{\ominus}}}{\partial \underline{\ddot{\varphi}}^{X}} \Big) \\
\underline{\boldsymbol{m}}^{X_1}_{p\varphi_2} &= -[\,0\,1\,0\,] \cdot \frac{\partial^{\mathrm{RS}} \underline{f}^{X_1^{\ominus}}}{\partial \underline{\ddot{\varphi}}^{X}} + {}^{X_1^2}\bar{\Phi}^{X_1}_{(2,:)} \cdot \Big(\frac{\partial \underline{\dot{p}}^{X_1}}{\partial \underline{\ddot{\varphi}}^{X}} - \frac{\partial^{\mathrm{EX}} \underline{f}^{X_1^{\ominus}}}{\partial \underline{\ddot{\varphi}}^{X}} \Big)
\end{aligned} \tag{A.107}$$

- for $w = 1$:

$$\begin{aligned}
\underline{\boldsymbol{m}}^{X_1}_{h\varphi_1} &= -[\,0\,0\,1\,] \cdot \frac{\partial^{\mathrm{RS}} \underline{t}^{X_1^{\ominus}}}{\partial \underline{\ddot{\varphi}}^{X}} + {}^{X_1^1}\bar{\Phi}^{X_1}_{(3,:)} \cdot \Big(\frac{\partial^{X_1^{\ominus}} \underline{\dot{h}}^{X_1}}{\partial \underline{\ddot{\varphi}}^{X}} - \frac{\partial^{\mathrm{EX}} \underline{t}^{X_1^{\ominus}}}{\partial \underline{\ddot{\varphi}}^{X}} \Big) \\
\underline{\boldsymbol{m}}^{X_1}_{p\varphi_1} &= -[\,1\,0\,0\,] \cdot \frac{\partial^{\mathrm{RS}} \underline{f}^{X_1^{\ominus}}}{\partial \underline{\ddot{\varphi}}^{X}} + {}^{X_1^1}\bar{\Phi}^{X_1}_{(1,:)} \cdot \Big(\frac{\partial \underline{\dot{p}}^{X_1}}{\partial \underline{\ddot{\varphi}}^{X}} - \frac{\partial^{\mathrm{EX}} \underline{f}^{X_1^{\ominus}}}{\partial \underline{\ddot{\varphi}}^{X}} \Big)
\end{aligned} \tag{A.108}$$

The corresponding rows in the mass matrix partition $\boldsymbol{M}^{X_{\mathrm{f}}}_{\varrho}$ are obtained by taking the sensitivities to $\underline{\ddot{\varrho}}^{X}$ instead of $\underline{\ddot{\varphi}}^{X}$. For the rows in both damping matrix partitions $\boldsymbol{D}^{X_{\mathrm{f}}}_{\varphi}$ and $\boldsymbol{D}^{X_{\mathrm{f}}}_{\varrho}$ and in the stiffness matrix partition $\boldsymbol{S}^{X_{\mathrm{f}}}_{\varrho}$, take the sensitivities to $\underline{\dot{\varphi}}^{X}$ and $\underline{\dot{\varrho}}^{X}$ and $\underline{\varrho}^{X}$. For the remaining stiffness matrix partition $\boldsymbol{S}^{X_{\mathrm{f}}}_{\varphi}$ the same scheme applies for $w = 3$ but differs for $w = 2$ and $w = 1$:

- for $w = 2$:

$$\begin{aligned}
\underline{\boldsymbol{s}}^{X_1}_{h\varphi_2} &= -[\,0\,1\,0\,] \cdot \frac{\partial^{\mathrm{RS}} \underline{t}^{X_1^{\ominus}}}{\partial \underline{\phi}^{X}} + {}^{X_1^2}\bar{\Phi}^{X_1}_{(2,:)} \cdot \Big(\frac{\partial^{X_1^{\ominus}} \underline{\dot{h}}^{X_1}}{\partial \underline{\phi}^{X}} - \frac{\partial^{\mathrm{EX}} \underline{t}^{X_1^{\ominus}}}{\partial \underline{\phi}^{X}} \Big) + \\
&\quad [\;\mathrm{J}^{3}_{v=1} \Big(\frac{\partial^{X_1^2} \Phi^{X_1}_{(2,:)}}{\partial \phi_v^{X_1}} \cdot \Big({}^{X_1^{\ominus}}\bar{\underline{\dot{h}}}^{X_1} - {}^{\mathrm{EX}}\bar{\underline{t}}^{X_1^{\ominus}} \Big) \Big) \;\; \mathrm{O}_{(2\ldots N)} \;] \\
\underline{\boldsymbol{s}}^{X_1}_{p\varphi_2} &= -[\,0\,1\,0\,] \cdot \frac{\partial^{\mathrm{RS}} \underline{f}^{X_1^{\ominus}}}{\partial \underline{\phi}^{X}} + {}^{X_1^2}\bar{\Phi}^{X_1}_{(2,:)} \cdot \Big(\frac{\partial \underline{\dot{p}}^{X_1}}{\partial \underline{\phi}^{X}} - \frac{\partial^{\mathrm{EX}} \underline{f}^{X_1^{\ominus}}}{\partial \underline{\phi}^{X}} \Big) + \\
&\quad [\;\mathrm{J}^{3}_{v=1} \Big(\frac{\partial^{X_1^2} \Phi^{X_1}_{(2,:)}}{\partial \phi_v^{X_1}} \cdot \Big({}^{X_1^{\ominus}}\bar{\underline{\dot{p}}}^{X_1} - {}^{\mathrm{EX}}\bar{\underline{f}}^{X_1^{\ominus}} \Big) \Big) \;\; \mathrm{O}_{(2\ldots N)} \;]
\end{aligned} \tag{A.109}$$

- for $w = 1$:

$$\begin{aligned}
\underline{\boldsymbol{s}}_{h\varphi_1}^{X_1} &= -[\,0\,0\,1\,]\cdot\frac{\partial^{\mathrm{RS}}\underline{t}^{X_1^{\ominus}}}{\partial\underline{\phi}^{X}} + {}^{X_1^1}\bar{\Phi}_{(3,:)}^{X_1}\cdot\Big(\frac{\partial^{X_1^{\ominus}}\underline{\dot{h}}^{X_1}}{\partial\underline{\phi}^{X}} - \frac{\partial^{\mathrm{EX}}\underline{t}^{X_1^{\ominus}}}{\partial\underline{\phi}^{X}}\Big) + \\
&\quad [\;\mathrm{J}_{v=1}^{3}\Big(\frac{\partial^{X_1^1}\Phi_{(3,:)}^{X_1}}{\partial\phi_v^{X_1}}\cdot\Big({}^{X_1^{\ominus}}\bar{\dot{h}}^{X_1} - {}^{\mathrm{EX}}\bar{\underline{t}}^{X_1^{\ominus}}\Big)\Big)\;\mathrm{O}_{(2\ldots N)}\;] \\
\underline{\boldsymbol{s}}_{p\varphi_1}^{X_1} &= -[\,1\,0\,0\,]\cdot\frac{\partial^{\mathrm{RS}}\underline{f}^{X_1^{\ominus}}}{\partial\underline{\phi}^{X}} + {}^{X_1^1}\bar{\Phi}_{(1,:)}^{X_1}\cdot\Big(\frac{\partial\underline{\dot{p}}^{X_1}}{\partial\underline{\phi}^{X}} - \frac{\partial^{\mathrm{EX}}\underline{f}^{X_1^{\ominus}}}{\partial\underline{\phi}^{X}}\Big) + \\
&\quad [\;\mathrm{J}_{v=1}^{3}\Big(\frac{\partial^{X_1^1}\Phi_{(1,:)}^{X_1}}{\partial\phi_v^{X_1}}\cdot\Big({}^{X_1^{\ominus}}\bar{\underline{p}}^{X_1} - {}^{\mathrm{EX}}\bar{\underline{f}}^{X_1^{\ominus}}\Big)\Big)\;\mathrm{O}_{(2\ldots N)}\;]
\end{aligned} \tag{A.110}$$

The pairs of rows $\{\underline{\boldsymbol{g}}_{h_w}^{X_1 X_\mathrm{p}}, \underline{\boldsymbol{g}}_{p_w}^{X_1 X_\mathrm{p}} | w = 3, 2, 1\}$, with ranking numbers $2(w-1)+1$ and $2(w-1)+2$ in the input matrix partition $\boldsymbol{G}^{X_\mathrm{f} X_\mathrm{p}}$, are determined as follows (the partial derivatives in the right hand side only apply if they are defined for the 'independent variable'; in this case $\underline{z}$):

- for $w = 3$:

$$\begin{aligned}
\underline{\boldsymbol{g}}_{h_3}^{X_1 X_\mathrm{p}} &= \mathrm{J}_{(\underline{z})}\Big([\,1\,0\,0\,]\cdot\frac{\partial^{\mathrm{RS}}\underline{t}^{X_1^{\ominus}}}{\partial\underline{z}} + [\,1\,0\,0\,]\cdot\Big(-\frac{\partial^{X_1^{\ominus}}\underline{\dot{h}}^{X_1}}{\partial\underline{z}} + \frac{\partial^{\mathrm{EX}}\underline{t}^{X_1^{\ominus}}}{\partial\underline{z}}\Big)\Big) \\
\underline{\boldsymbol{g}}_{p_3}^{X_1 X_\mathrm{p}} &= \mathrm{J}_{(\underline{z})}\Big([\,0\,0\,1\,]\cdot\frac{\partial^{\mathrm{RS}}\underline{f}^{X_1^{\ominus}}}{\partial\underline{z}} + [\,0\,0\,1\,]\cdot\Big(-\frac{\partial\underline{\dot{p}}^{X_1}}{\partial\underline{z}} + \frac{\partial^{\mathrm{EX}}\underline{f}^{X_1^{\ominus}}}{\partial\underline{z}}\Big)\Big)
\end{aligned} \tag{A.111}$$

- for $w = 2$:

$$\begin{aligned}
\underline{\boldsymbol{g}}_{h_2}^{X_1 X_\mathrm{p}} &= \mathrm{J}_{(\underline{z})}\Big([\,0\,1\,0\,]\cdot\frac{\partial^{\mathrm{RS}}\underline{t}^{X_1^{\ominus}}}{\partial\underline{z}} + {}^{X_1^2}\bar{\Phi}_{(2,:)}^{X_1}\cdot\Big(-\frac{\partial^{X_1^{\ominus}}\underline{\dot{h}}^{X_1}}{\partial\underline{z}} + \frac{\partial^{\mathrm{EX}}\underline{t}^{X_1^{\ominus}}}{\partial\underline{z}}\Big)\Big) \\
\underline{\boldsymbol{g}}_{p_2}^{X_1 X_\mathrm{p}} &= \mathrm{J}_{(\underline{z})}\Big([\,0\,1\,0\,]\cdot\frac{\partial^{\mathrm{RS}}\underline{f}^{X_1^{\ominus}}}{\partial\underline{z}} + {}^{X_1^2}\bar{\Phi}_{(2,:)}^{X_1}\cdot\Big(-\frac{\partial\underline{\dot{p}}^{X_1}}{\partial\underline{z}} + \frac{\partial^{\mathrm{EX}}\underline{f}^{X_1^{\ominus}}}{\partial\underline{z}}\Big)\Big)
\end{aligned} \tag{A.112}$$

- for $w = 1$:

$$\begin{aligned}
\underline{\boldsymbol{g}}_{h_1}^{X_1 X_\mathrm{p}} &= \mathrm{J}_{(\underline{z})}\Big([\,0\,0\,1\,]\cdot\frac{\partial^{\mathrm{RS}}\underline{t}^{X_1^{\ominus}}}{\partial\underline{z}} + {}^{X_1^1}\bar{\Phi}_{(3,:)}^{X_1}\cdot\Big(-\frac{\partial^{X_1^{\ominus}}\underline{\dot{h}}^{X_1}}{\partial\underline{z}} + \frac{\partial^{\mathrm{EX}}\underline{t}^{X_1^{\ominus}}}{\partial\underline{z}}\Big)\Big) \\
\underline{\boldsymbol{g}}_{p_1}^{X_1} &= \mathrm{J}_{(\underline{z})}\Big([\,1\,0\,0\,]\cdot\frac{\partial^{\mathrm{RS}}\underline{f}^{X_1^{\ominus}}}{\partial\underline{z}} + {}^{X_1^1}\bar{\Phi}_{(1,:)}^{X_1}\cdot\Big(-\frac{\partial\underline{\dot{p}}^{X_1}}{\partial\underline{z}} + \frac{\partial^{\mathrm{EX}}\underline{f}^{X_1^{\ominus}}}{\partial\underline{z}}\Big)\Big)
\end{aligned} \tag{A.113}$$

The notation $\mathrm{J}_{(\underline{z})}\big(.\big)$ means that the partial derivatives to the involved elementary subvectors are to be put next to each other. These are (see also Eq. A.50):

- feedthrough force and torque from profile & structure X_p: ${}^{\mathrm{FT}}\underline{f}^{X_{\mathrm{PP}(2)}}$, ${}^{\mathrm{FT}}\underline{t}^{X_{\mathrm{PP}(2)}}$;
- distributed aerodynamic force load on X_2 from X_p: ${}^{\mathrm{a}}\underline{q}^{X_{\mathrm{PP}(2)}^{\ominus}}$

The rows in the input matrix partition $\boldsymbol{G}^{X_\mathrm{f} G}$ for the 'exogeneous' input variables are obtained by taking the partial derivatives to:

- periodic wind speed variation on blade: $\underline{u}_{\mathrm{per}}^{X}$

- periodic gravitation variation on hub: $\underline{g}_{\mathrm{per}}^{X_0}$
- stochastic wind speed variation in intersection annuli/blade: ${}^{\mathrm{t}}\underline{u}^{W/X}$

For the rows in the input matrix partition $\boldsymbol{G}^{X_{\mathrm{f}}W}$: for the input variables from the wake take the partial derivatives to the induction speed variations $\underline{u}_{\mathrm{im}}^{W}$ in the rotor annuli; for the input matrix partition $\boldsymbol{G}^{X_{\mathrm{f}}R}$ the partial derivative to the following elementary input subvectors applies:

- kinematic vectors on blade blase exit: $\underline{\omega}^{X_{\mathrm{FF}(0)}}$, $\underline{\alpha}^{X_{\mathrm{FF}(0)}}$, $\underline{v}^{X_{\mathrm{FF}(0)}^{\oplus}}$, $\underline{a}^{X_{\mathrm{FF}(0)}^{\oplus}}$
- wind speed variation by orientation change up till hub: $\underline{u}_{\mathrm{ori}}^{X_{\mathrm{FF}(0)}}$.
- gravitation variation by orientation change up till hub: $\underline{g}_{\mathrm{ori}}^{X_{\mathrm{FF}(0)}}$

Finally the rows in the input matrix partition $\boldsymbol{G}^{X_{\mathrm{f}}X_{\mathrm{f_c}}}$ are built up from the the partial derivatives to the internal control signal from the pitch actuator. This input vector only contains the actuation torque $t_{\mathrm{pt}}^{X_1}$ 'along the y-axis angular dof direction of X_1' and has opposite orientation. So for the rows $\{\underline{\boldsymbol{g}}_{h_w}^{X_1X_{\mathrm{f_c}}}, \underline{\boldsymbol{g}}_{p_w}^{X_1X_{\mathrm{f_c}}} | w = 3, 2, 1\}$, with ranking numbers $2(w-1)+1$ and $2(w-1)+2$ holds:

$$
\begin{array}{lll}
\text{for } w=3: & \left\{ \begin{array}{lcl} \underline{\boldsymbol{g}}_{h_3}^{X_1X_{\mathrm{f_c}}} & = & [\ 0\ ] \\ \underline{\boldsymbol{g}}_{p_3}^{X_1X_{\mathrm{f_c}}} & = & [\ 0\ ] \end{array} \right. & \\
\text{for } w=2: & \left\{ \begin{array}{lcl} \underline{\boldsymbol{g}}_{h_2}^{X_1X_{\mathrm{f_c}}} & = & [\ \partial^{\mathrm{RS}} t_2^{X_1^2}/\partial t_{\mathrm{pt}}^{X_1}\ ] = [\ -1\ ] \\ \underline{\boldsymbol{g}}_{p_2}^{X_1X_{\mathrm{f_c}}} & = & [\ 0\ ] \end{array} \right. & \text{(A.114)} \\
\text{for } w=1: & \left\{ \begin{array}{lcl} \underline{\boldsymbol{g}}_{h_1}^{X_1X_{\mathrm{f_c}}} & = & [\ 0\ ] \\ \underline{\boldsymbol{g}}_{p_1}^{X_1X_{\mathrm{f_c}}} & = & [\ 0\ ] \end{array} \right. &
\end{array}
$$

(vii) Output variables and vector output equation in 2nd order model
The blade flange X_{f} needs to provide the following output:

- aerodynamic force load reaction to wake W:
  ${}^{\mathrm{a_L}}\underline{f}^{W_m/X_1}$ (along actual annulus-wise c.s. for X_1)
- distributed aerodynamic force loads on X_1 to profile & structure:
  ${}^{\mathrm{a}}\underline{q}^{X_{\mathrm{FF}(1)}}$, ${}^{\mathrm{a_L}}\underline{q}^{X_{\mathrm{FF}(1)}}$ (along actual conversion c.s. for X_1)
- kinematic vectors on exit point $X_1^{\oplus}$ to profile & structure:
  $\underline{\omega}^{X_{\mathrm{FF}(1)}}$, $\underline{\alpha}^{X_{\mathrm{FF}(1)}}$, $\underline{v}^{X_{\mathrm{FF}(1)}^{\oplus}}$, $\underline{a}^{X_{\mathrm{FF}(1)}^{\oplus}}$ (along actual f.c.s. for X_1)
- dof angular position variations in blade flange: $\underline{\phi}^{X_{\mathrm{FF}(1)}}$
- gravitation variation by orientation change up till flange:
  $\underline{g}_{\mathrm{ori}}^{X_{\mathrm{FF}(1)}}$ (along actual f.c.s. for X_1)
- exit point displacement relative to average rotor centre to profile & structure:
  $\underline{\xi}^{X_{\mathrm{FF}(1)}}$, $\underline{x}^{X_{\mathrm{FF}(1)}^{\oplus}}$ (along average f.c.s. X_1)
- feedthrough force and torque on rotor centre $X_0^{\ominus}$:
  ${}^{\mathrm{FT}}\underline{f}^{X_{\mathrm{PP}(1)}}$, ${}^{\mathrm{FT}}\underline{t}^{X_{\mathrm{PP}(1)}}$ (= ${}^{\mathrm{FT}}\underline{f}^{X_0^{\ominus}}$, ${}^{\mathrm{FT}}\underline{t}^{X_0^{\ominus}}$; along actual c.s. blade base X_0)

- force and torque loading on blade flange entry $X_1^{\ominus}$:
  $\underline{f}^{X_1^{\ominus}/X_0}$, $\underline{t}^{X_1^{\ominus}/X_0}$ (along actual c.s. blade base X_0)
- exit point displacement relative to rotor centre in average position :
  $\delta^{\bar{X}_0^{\ominus}} \underline{r}^{X_1^{\oplus}/\bar{X}_0}$ (along average c.s. blade base X_0)
- pitchwise position varation to pitch control system $X_{\mathrm{f_c}}$: $\varphi_2^{X_1}$

Note that the determination of the *flapg, lead and setting angle* in the profile & structure X_{p} requires the angular position variations $\underline{\phi}^{X_{\mathrm{FF}(1)}}$ in the blade flange X_{f} (see section B.4.1). In general this means that all angular dofs in preceeding subcomponents of a rotor blade are to be fed into a next subcomponent!

The output vector $\underline{y}^{X_{\mathrm{f}}}$ of the blade flange has the following composition:

$$\underline{y}^{X_{\mathrm{f}}} = \begin{bmatrix} \underline{y}^{GX_{\mathrm{f}}} \\ \underline{y}^{WX_{\mathrm{f}}} \\ \underline{y}^{RX_{\mathrm{f}}} \\ \underline{y}^{X_{\mathrm{p}}X_{\mathrm{f}}} \\ \underline{y}^{X_{\mathrm{f_c}}X_{\mathrm{f}}} \end{bmatrix} \quad \text{with} \quad \underline{y}^{GX_{\mathrm{f}}} = \begin{bmatrix} \delta^{X_1^{\ominus}} \underline{r}^{X_1^{\oplus}/X_0} \\ \underline{f}^{X_1^{\ominus}/X_0} \\ \underline{t}^{X_1^{\ominus}/X_0} \end{bmatrix}$$

$$\text{and} \quad \underline{y}^{WX_{\mathrm{f}}} = \begin{bmatrix} {}^{\mathrm{aL}}\underline{f}^{W_m/X_1} \end{bmatrix} \; ; \; \underline{y}^{RX_{\mathrm{f}}} = \begin{bmatrix} {}^{\mathrm{FT}}\underline{f}^{X_{\mathrm{PP}(1)}} \\ {}^{\mathrm{FT}}\underline{t}^{X_{\mathrm{PP}(1)}} \end{bmatrix} \; ; \; \underline{y}^{X_{\mathrm{p}}X_{\mathrm{f}}} = \begin{bmatrix} \underline{\omega}^{X_{\mathrm{FF}(1)}} \\ \underline{\alpha}^{X_{\mathrm{FF}(1)}} \\ \underline{v}^{X_{\mathrm{FF}(1)}^{\oplus}} \\ \underline{a}^{X_{\mathrm{FF}(1)}^{\oplus}} \\ \underline{\phi}^{X_{\mathrm{FF}(1)}} \\ {}^{\mathrm{a}}\underline{q}^{X_{\mathrm{FF}(1)}} \\ {}^{\mathrm{aL}}\underline{q}^{X_{\mathrm{FF}(1)}} \\ \underline{g}_{\mathrm{ori}}^{X_{\mathrm{FF}(1)}} \\ \underline{\xi}^{X_{\mathrm{FF}(1)}} \\ \underline{x}^{X_{\mathrm{FF}(1)}^{\oplus}} \end{bmatrix} \tag{A.115}$$

The *internal* output subvector $\underline{y}^{X_{\mathrm{f_c}}X_{\mathrm{f}}}$ only applies if the blade flange incorporates a pitch control system. The pitch servo requires the angular dof position varation and speed along the y-axis of the flange as 'measurement signals' (see paragraph (vii)):

$$\underline{y}^{X_{\mathrm{f_c}}X_{\mathrm{f}}} = \left[\varphi_2^{X_1}\right] \tag{A.116}$$

This output subvector will disappear when the flange element model and the pitch actuator servo model are integrated.

The reaction load ${}^{\mathrm{aL}}\underline{f}^{W_m/X_1}$ from element X_1 to the wake subsystem W is supplied as a coordinate vector along the annulus wise coordinate system in the intersection of blade element X_1 and rotor annulus W_m. The linearised expression involves dependency on the same variables as for the force load ${}^{\mathrm{a}}\underline{f}^{X_k}$ by Eq. A.41 except that the distributed import load from the profile & structure is now 'lift-only' (${}^{\mathrm{aL}}\underline{q}^{X_{\mathrm{PP}(2)}}$ instead of ${}^{\mathrm{a}}\underline{q}^{X_{\mathrm{PP}(2)}}$).

The feedthrough kinematic vectors $\underline{\omega}^{X_{\mathrm{FF}(1)}}$, $\underline{\alpha}^{X_{\mathrm{FF}(1)}}$, $\underline{v}^{X_{\mathrm{FF}(1)}^{\oplus}}$ and $\underline{a}^{X_{\mathrm{FF}(1)}^{\oplus}}$ to the profile & structure X_{p} are supplied as coordinate vectors along the f.c.s. $\vec{e}^{\,X_1}$. The expression for the means and variations follow from Eq. B.101 up to B.105 and from Eq. B.120 up to B.130 by setting '$k = 1$' and '$X_{\mathrm{FF}} = X_{\mathrm{FF}(0)}$' and considering the point $X_k^{\oplus}$ instead of X_k^* for $\underline{v}^{X_{\mathrm{FF}(1)}^{\oplus}}$ and $\underline{a}^{X_{\mathrm{FF}(1)}^{\oplus}}$.

The feedthrough 'variation by orientation change' vector $\underline{g}_{\mathrm{ori}}^{X_{\mathrm{FF}(1)}}$ is also expressed along $\vec{e}^{\,X_1}$; Eq. B.297 and B.298 are used with '$X_{\mathrm{FF}} = X_{\mathrm{FF}(1)}$' (i.e. $\delta\underline{g}_{\mathrm{ori}}^{X_{\mathrm{FF}}} = \delta\underline{g}_{\mathrm{ori}}^{X_{\mathrm{f}}}$).

The feedthrough loads ${}^{\mathrm{FT}}\underline{f}^{X_{\mathrm{PP}(1)}} \equiv {}^{\mathrm{FT}}\underline{f}^{X_0^{\ominus}}$, ${}^{\mathrm{FT}}\underline{t}^{X_{\mathrm{PP}(1)}} \equiv {}^{\mathrm{FT}}\underline{t}^{X_0^{\ominus}}$ on rotor centre $X_0^{\ominus}$ depend on the envelope of variables on which the aerodynamic loads, gravitation loads and impulse vector depend (see Eq. A.39, A.34 and A.32). Their coordinates are along the coordinate system of the blade blase X_0. All output variables to the blade flange consist of coordinates along the final coordinate system of X_1.

Chapter Appendix B does not contain expressions for the feedthrough loads to the rotor centre. Equation A.39, yields the expressions for the feedthrough loads, which are transformed to the coordinate system of X_0:

$$\begin{aligned}
\left[\ {}^{\mathrm{FT}}\underline{f}^{X_0^{\ominus}} \equiv {}^{\mathrm{FT}}\underline{f}^{X_{b\,\mathrm{PP}(1)}^{\ominus}}\ \right] &= {}^{X_0}\Phi^{X_1}\cdot\left(-\underline{\dot{p}}^{X_1} + {}^{\mathrm{EX}}\underline{f}^{X_1^{\ominus}}\right)\\
\left[\ {}^{\mathrm{FT}}\underline{t}^{X_0^{\ominus}} \equiv {}^{\mathrm{FT}}\underline{t}^{X_{b\,\mathrm{PP}(1)}^{\ominus}}\ \right] &= {}^{X_0}\Phi^{X_1}\cdot\left(-{}^{X_1^{\ominus}}\underline{\dot{h}}^{X_1} + {}^{\mathrm{EX}}\underline{t}^{X_1^{\ominus}}\right) + R_{\mathrm{root}}\cdot\underline{e}_2 \times {}^{\mathrm{FT}}\underline{f}^{X_0^{\ominus}}
\end{aligned} \tag{A.117}$$

The feedthrough loads to the flange thus depend on the envelope of variables on which the aerodynamic loads, gravitation loads and impulse vectors depend. The linearised expressions are:

$$\begin{aligned}
{}^{\mathrm{FT}}\underline{f}^{X_0^{\ominus}} &= {}^{\mathrm{FT}}\bar{\underline{f}}^{X_0^{\ominus}} + \sum_{(\underline{q})}\frac{\partial^{\mathrm{FT}}\underline{f}^{X_0^{\ominus}}}{\partial\underline{q}}\cdot\delta\underline{q}\\
{}^{\mathrm{FT}}\underline{t}^{X_0^{\ominus}} &= {}^{\mathrm{FT}}\bar{\underline{t}}^{X_0^{\ominus}} + \sum_{(\underline{q})}\frac{\partial^{\mathrm{FT}}\underline{t}^{X_0^{\ominus}}}{\partial\underline{q}}\cdot\delta\underline{q}
\end{aligned} \tag{A.118}$$

The summation over $(\underline{q})$ involves:

- exogeneous periodic wind speed and gravition input: $\underline{u}_{\mathrm{per}}^{X}$, $\underline{g}_{\mathrm{per}}^{X_0}$
- exogenous stochastic wind speed input: $\underline{u}_{\mathrm{sto}}^{W/X}$
- output from wake W: $\underline{u}_{\mathrm{i_m}}^{W}$
- processed output from rotor shaft & hub R: $\underline{\omega}^{X_{\mathrm{FF}(0)}^{\oplus}}$, $\underline{\alpha}^{X_{\mathrm{FF}(0)}}$, $\underline{v}^{X_{\mathrm{FF}(0)}^{\oplus}}$, $\underline{a}^{X_{\mathrm{FF}(0)}^{\oplus}}$, $\underline{u}_{\mathrm{ori}}^{X_{\mathrm{FF}(0)}}$, $\underline{g}_{\mathrm{ori}}^{X_{\mathrm{FF}(0)}}$
- output from profile & structure X_{p}: ${}^{\mathrm{a}}\underline{q}_{\mathrm{f}}^{X_{\mathrm{PP}(2)}}$, ${}^{\mathrm{FT}}\underline{f}^{X_{\mathrm{PP}(2)}}$, ${}^{\mathrm{FT}}\underline{t}^{X_{\mathrm{PP}(2)}}$
- degrees of freedom in X_{f}, encapsulated by: $\underline{\phi}^{X}$, $\underline{\dot{\varphi}}^{X}$, $\underline{\ddot{\varphi}}^{X}$, $\underline{\dot{o}}^{X}$ $\underline{\ddot{o}}^{X}$.

The means are obtained by just taking the overlined version of the expressions above.

$$\begin{aligned}
{}^{\mathrm{FT}}\bar{\underline{f}}^{X_0^{\ominus}} &= {}^{X_0}\bar{\Phi}^{X_1}\cdot\left(-\bar{\underline{\dot{p}}}^{X_1} + {}^{\mathrm{EX}}\bar{\underline{f}}^{X_1^{\ominus}}\right)\\
{}^{\mathrm{FT}}\bar{\underline{t}}^{X_0^{\ominus}} &= {}^{X_0}\bar{\Phi}^{X_1}\cdot\left(-{}^{X_1^{\ominus}}\bar{\underline{\dot{h}}}^{X_1} + {}^{\mathrm{EX}}\bar{\underline{t}}^{X_1^{\ominus}}\right) + R_{\mathrm{root}}\cdot\underline{2}\times{}^{\mathrm{FT}}\bar{\underline{f}}^{X_0^{\ominus}}
\end{aligned} \tag{A.119}$$

Define the mean feedthrough loads in the blade base *exit* along the coordinate system of X_1:

$$\begin{aligned}
{}^{\mathrm{FT}}\bar{\underline{f}}^{X_0^{\oplus}/X_1} &= -\bar{\underline{\dot{p}}}^{X_1} + {}^{\mathrm{EX}}\bar{\underline{f}}^{X_1^{\ominus}}\\
{}^{\mathrm{FT}}\bar{\underline{t}}^{X_0^{\oplus}/X_1} &= -{}^{X_1^{\ominus}}\bar{\underline{\dot{h}}}^{X_1} + {}^{\mathrm{EX}}\bar{\underline{t}}^{X_1^{\ominus}}
\end{aligned} \tag{A.120}$$

For the sensitivities to the variables $\underline{q}$ holds:

$$\begin{aligned}
\frac{\partial^{\mathrm{FT}}\underline{f}^{X_0^{\ominus}}}{\partial \underline{q}} &= {}^{X_0}\bar{\Phi}^{X_1}\cdot\Big(-\frac{\partial \underline{\dot{p}}^{X_1}}{\partial \underline{q}}+\frac{\partial^{\mathrm{EX}}\underline{f}^{X_1^{\ominus}}}{\partial \underline{q}}\Big)+\\
&\quad \delta_{\underline{q}\,\underline{\phi}^X}\cdot\Big[\ \mathrm{J}_{v=1}^{3}\Big(\frac{\partial^{X_0}\Phi^{X_1}}{\partial \phi_v^{X_1}}\cdot {}^{\mathrm{FT}}\underline{\bar{f}}^{X_0^{\oplus}/X_1}\Big)\ \mathrm{O}_{(2)}\ldots\mathrm{O}_{(N)}\ \Big]\\
\frac{\partial^{\mathrm{FT}}\underline{t}^{X_0^{\ominus}}}{\partial \underline{q}} &= {}^{X_0}\bar{\Phi}^{X_1}\cdot\Big(-\frac{\partial^{X_1^{\ominus}}\underline{h}^{X_1}}{\partial \underline{q}}+\frac{\partial^{\mathrm{EX}}\underline{t}^{X_1^{\ominus}}}{\partial \underline{q}}\Big)+\\
&\quad \delta_{\underline{q}\,\underline{\phi}^X}\cdot\Big[\ \mathrm{J}_{v=1}^{3}\Big(\frac{\partial^{X_0}\Phi^{X_1}}{\partial \phi_v^{X_1}}\cdot {}^{\mathrm{FT}}\underline{\bar{t}}^{X_0^{\oplus}/X_1}\Big)\ \mathrm{O}_{(2)}\ldots\mathrm{O}_{(N)}\ \Big]+\\
&\quad \mathrm{J}_{v=1}^{3}\Big(R_{\mathrm{root}}\cdot\underline{e}_2\times\underline{e}_v\Big)\cdot\frac{\partial^{\mathrm{FT}}\underline{f}^{X_0^{\ominus}}}{\partial \underline{q}}
\end{aligned}\tag{A.121}$$

Note that the last term in the right hand side of both equations only applies if $\underline{q}$ equals $\underline{\phi}^X$!

The disributed export loads ${}^{\mathrm{a}}\underline{q}^{X_{\mathrm{FF}(1)}}$ and ${}^{\mathrm{aL}}\underline{q}^{X_{\mathrm{FF}(1)}}$ to the blade profile & structure depend on the same variables as the concentrated force load ${}^{\mathrm{a}}\underline{f}^{X_1}$ does, except that the dependency on ${}^{\mathrm{a}}\underline{q}^{X_{\mathrm{PP}(2)}^{\ominus}}$ is excluded (see section B.7.2, Eq. B.203). Their are coordinates are along the final coordinate system of X_1.

For the blade flange loads, which are expressed in the actual coordinate system of the blade base and which are 'user-output', holds:

$$\begin{aligned}
\underline{\bar{f}}^{X_1^{\ominus}/X_0} &= {}^{X_0}\bar{\Phi}^{X_1}\cdot\big(-\underline{\bar{\dot{p}}}^{X_1}+{}^{\mathrm{EX}}\underline{\bar{f}}^{X_1^{\ominus}}\big)\\
\underline{\bar{t}}^{X_1^{\ominus}/X_0} &= {}^{X_0}\bar{\Phi}^{X_1}\cdot\big(-{}^{X_1^{\ominus}}\underline{\bar{\dot{h}}}^{X_1}+{}^{\mathrm{EX}}\underline{\bar{t}}^{X_1^{\ominus}}\big)
\end{aligned}\tag{A.122}$$

and

$$\begin{aligned}
\frac{\partial \underline{f}^{X_1^{\ominus}/X_0}}{\partial \underline{q}} &= {}^{X_0}\bar{\Phi}^{X_1}\cdot\Big(-\frac{\partial \underline{\dot{p}}^{X_1}}{\partial \underline{q}}+\frac{\partial^{\mathrm{EX}}\underline{f}^{X_1^{\ominus}}}{\partial \underline{q}}\Big)+\\
&\quad \delta_{\underline{q}\,\underline{\phi}^X}\cdot\Big[\ \mathrm{J}_{v=1}^{3}\Big(\frac{\partial^{X_0}\Phi^{X_1}}{\partial \phi_v^{X_1}}\cdot {}^{\mathrm{FT}}\underline{\bar{f}}^{X_0^{\oplus}/X_1}\Big)\ \mathrm{O}_{(2)}\ldots\mathrm{O}_{(N)}\ \Big]\\
\frac{\partial \underline{t}^{X_1^{\ominus}/X_0}}{\partial \underline{q}} &= {}^{X_0}\bar{\Phi}^{X_1}\cdot\Big(-\frac{\partial^{X_1^{\ominus}}\underline{h}^{X_1}}{\partial \underline{q}}+\frac{\partial^{\mathrm{EX}}\underline{t}^{X_1^{\ominus}}}{\partial \underline{q}}\Big)+\\
&\quad \delta_{\underline{q}\,\underline{\phi}^X}\cdot\Big[\ \mathrm{J}_{v=1}^{3}\Big(\frac{\partial^{X_0}\Phi^{X_1}}{\partial \phi_v^{X_1}}\cdot {}^{\mathrm{FT}}\underline{\bar{t}}^{X_0^{\oplus}/X_1}\Big)\ \mathrm{O}_{(2)}\ldots\mathrm{O}_{(N)}\ \Big]
\end{aligned}\tag{A.123}$$

Note that the last term in the right hand side of both equations only applies if $\underline{q}$ equals $\underline{\phi}^X$! The same variables for '$\underline{q}$' apply as for the feedthrough loads to the rotor centre (see under Eq. A.118).

The displacement variation of the exit point $X_1^{\oplus}$ relative to rotor centre in average position $\bar{X}_0^{\ominus}$ is used for describing the mode shapes. It depends on the variations in position dofs $\underline{\phi}^X$ and $\underline{\rho}^X$ and on the displacement variations $\underline{\xi}^{X_{\mathrm{FF}(0)}}$ and $\underline{x}^{X_{\mathrm{FF}(0)}}$ at the blade flange entry. See section A.1, par. (vi), header *Drive-train outputs in the rotor blades*, for the mapping of displacement variables from the rotor centre to the blade flange entry.

For the displacement variation vector $\delta^{\bar{X}_0^{\ominus}}\underline{r}^{X_1^{\oplus}/\bar{X}_0}$ with coordinates along the average c.s. of the blade base $\bar{X}_0$, holds:

$$\delta^{\bar{X}_0^{\ominus}}\underline{r}^{X_1^{\oplus}/\bar{X}_0} = \sum_{(\underline{z})}\frac{\partial^{\bar{X}_0^{\ominus}}\underline{r}^{X_1^{\oplus}/\bar{X}_0}}{\partial \underline{z}}\cdot\delta\underline{z} \qquad (\underline{z}=\underline{\phi}^X,\underline{\rho}^X,\underline{\xi}^{X_{\mathrm{FF}(0)}},\underline{x}^{X_{\mathrm{FF}(0)}}) \tag{A.124}$$

with (see discussion from Eq. A.77 and see Eq. B.105, B.113, B.124 and B.127):

$$\begin{aligned}
\frac{\partial \underline{r}^{X_1^{\oplus}/\bar{X}_0}}{\partial \underline{\xi}^{X_{\mathrm{FF}(0)}}} &= {}^{X_0}\bar{\Phi}^{X_1} \cdot \frac{\partial \underline{v}^{X_1^{\oplus}}}{\partial \underline{\omega}^{X_{\mathrm{FF}(0)}}} \quad ; \quad \frac{\partial \underline{r}^{X_1^{\oplus}/\bar{X}_0}}{\partial \underline{\phi}^{X}} = {}^{X_0}\bar{\Phi}^{X_1} \cdot \frac{\partial \underline{v}^{X_1^{\oplus}}}{\partial \underline{\varphi}^{X}} \\
\frac{\partial \underline{r}^{X_1^{\oplus}/\bar{X}_0}}{\partial \underline{x}^{X_{\mathrm{FF}(0)}}} &= {}^{X_0}\bar{\Phi}^{X_1} \cdot \frac{\partial \underline{v}^{X_1^{\oplus}}}{\partial \underline{v}^{X_{\mathrm{FF}(0)}}} \quad ; \quad \frac{\partial \underline{r}^{X_1^{\oplus}/\bar{X}_0}}{\partial \underline{\varrho}^{X}} = {}^{X_0}\bar{\Phi}^{X_1} \cdot \frac{\partial \underline{v}^{X_1^{\oplus}}}{\partial \underline{\varrho}^{X}}
\end{aligned} \tag{A.125}$$

For the displacement outputs to the profile & structure then holds the following sensitivities (coordinates along average f.c.s. of X_1):

$$\begin{aligned}
\frac{\partial \underline{x}^{X_{\mathrm{FF}(1)}}}{\partial \underline{\xi}^{X_{\mathrm{FF}(0)}}} &= \frac{\partial \underline{v}^{X_1^{\oplus}}}{\partial \underline{\omega}^{X_{\mathrm{FF}(0)}}} \quad ; \quad \frac{\partial \underline{x}^{X_{\mathrm{FF}(1)}}}{\partial \underline{\phi}^{X}} = \frac{\partial \underline{v}^{X_1^{\oplus}}}{\partial \underline{\varphi}^{X}} \\
\frac{\partial \underline{x}^{X_{\mathrm{FF}(1)}}}{\partial \underline{x}^{X_{\mathrm{FF}(0)}}} &= \frac{\partial \underline{v}^{X_1^{\oplus}}}{\partial \underline{v}^{X_{\mathrm{FF}(0)}}} \quad ; \quad \frac{\partial \underline{x}^{X_{\mathrm{FF}(1)}}}{\partial \underline{\varrho}^{X}} = \frac{\partial \underline{v}^{X_1^{\oplus}}}{\partial \underline{\varrho}^{X}} \\
\frac{\partial \underline{\xi}^{X_{\mathrm{FF}(1)}}}{\partial \underline{\xi}^{X_{\mathrm{FF}(0)}}} &= \frac{\partial \underline{\omega}^{X_1}}{\partial \underline{\omega}^{X_{\mathrm{FF}(0)}}} \quad ; \quad \frac{\partial \underline{\xi}^{X_{\mathrm{FF}(1)}}}{\partial \underline{\phi}^{X}} = \frac{\partial \underline{\omega}^{X_1^{\oplus}}}{\partial \underline{\varphi}^{X}}
\end{aligned} \tag{A.126}$$

The mean values of the output variables follow straightforward from the equations above and from those referenced in chapter Appendix B. For the variations hold:

$$\begin{bmatrix} \underline{y}^{GX_{\mathrm{f}}} \\ \underline{y}^{WX_{\mathrm{f}}} \\ \underline{y}^{RX_{\mathrm{f}}} \\ \underline{y}^{X_{\mathrm{p}}X_{\mathrm{f}}} \\ \underline{y}^{X_{\mathrm{f_c}}X_{\mathrm{f}}} \end{bmatrix} = \begin{bmatrix} \boldsymbol{H}_{\varphi}^{GX_{\mathrm{f}}} & \boldsymbol{H}_{\varrho}^{GX_{\mathrm{f}}} \\ \boldsymbol{H}_{\varphi}^{WX_{\mathrm{f}}} & \boldsymbol{H}_{\varrho}^{WX_{\mathrm{f}}} \\ \boldsymbol{H}_{\varphi}^{RX_{\mathrm{f}}} & \boldsymbol{H}_{\varrho}^{RX_{\mathrm{f}}} \\ \boldsymbol{H}_{\varphi}^{X_{\mathrm{p}}X_{\mathrm{f}}} & \boldsymbol{H}_{\varrho}^{X_{\mathrm{p}}X_{\mathrm{f}}} \\ \boldsymbol{H}_{\varphi}^{X_{\mathrm{f_c}}X_{\mathrm{f}}} & \boldsymbol{H}_{\varrho}^{X_{\mathrm{f_c}}X_{\mathrm{f}}} \end{bmatrix} \cdot \begin{bmatrix} \underline{\varphi}^{X} \\ \underline{\varrho}^{X} \end{bmatrix} + \begin{bmatrix} \boldsymbol{L}_{\varphi}^{GX_{\mathrm{f}}} & \boldsymbol{L}_{\varrho}^{GX_{\mathrm{f}}} \\ \boldsymbol{L}_{\varphi}^{WX_{\mathrm{f}}} & \boldsymbol{L}_{\varrho}^{WX_{\mathrm{f}}} \\ \boldsymbol{L}_{\varphi}^{RX_{\mathrm{f}}} & \boldsymbol{L}_{\varrho}^{WX_{\mathrm{f}}} \\ \boldsymbol{L}_{\varphi}^{X_{\mathrm{p}}X_{\mathrm{f}}} & \boldsymbol{L}_{\varrho}^{X_{\mathrm{p}}X_{\mathrm{f}}} \\ \boldsymbol{L}_{\varphi}^{X_{\mathrm{f_c}}X_{\mathrm{f}}} & \boldsymbol{L}_{\varrho}^{X_{\mathrm{f}}X_{\mathrm{f}}} \end{bmatrix} \cdot \begin{bmatrix} \dot{\underline{\varphi}}^{X} \\ \dot{\underline{\varrho}}^{X} \end{bmatrix} +$$

$$\begin{bmatrix} \boldsymbol{K}^{GX_{\mathrm{f}}G} & \boldsymbol{K}^{GX_{\mathrm{f}}W} & \boldsymbol{K}^{GX_{\mathrm{f}}R} & \boldsymbol{K}^{GX_{\mathrm{f}}X_{\mathrm{p}}} & \boldsymbol{K}^{GX_{\mathrm{f}}X_{\mathrm{f_c}}} \\ \boldsymbol{K}^{WX_{\mathrm{f}}G} & \boldsymbol{K}^{WX_{\mathrm{f}}W} & \boldsymbol{K}^{WX_{\mathrm{f}}R} & \boldsymbol{K}^{WX_{\mathrm{f}}X_{\mathrm{p}}} & \boldsymbol{K}^{WX_{\mathrm{f}}X_{\mathrm{f_c}}} \\ \boldsymbol{K}^{RX_{\mathrm{f}}G} & \boldsymbol{K}^{RX_{\mathrm{f}}W} & \boldsymbol{K}^{RX_{\mathrm{f}}R} & \boldsymbol{K}^{RX_{\mathrm{f}}X_{\mathrm{p}}} & \boldsymbol{K}^{RX_{\mathrm{f}}X_{\mathrm{f_c}}} \\ \boldsymbol{K}^{X_{\mathrm{p}}X_{\mathrm{f}}G} & \boldsymbol{K}^{X_{\mathrm{p}}X_{\mathrm{f}}W} & \boldsymbol{K}^{X_{\mathrm{p}}X_{\mathrm{f}}R} & \boldsymbol{K}^{X_{\mathrm{p}}X_{\mathrm{f}}X_{\mathrm{p}}} & \boldsymbol{K}^{X_{\mathrm{p}}X_{\mathrm{f}}X_{\mathrm{f_c}}} \\ \boldsymbol{K}^{X_{\mathrm{f_c}}X_{\mathrm{f}}G} & \boldsymbol{K}^{X_{\mathrm{f_c}}X_{\mathrm{f}}W} & \boldsymbol{K}^{X_{\mathrm{f_c}}X_{\mathrm{f}}R} & \boldsymbol{K}^{X_{\mathrm{f_c}}X_{\mathrm{f}}X_{\mathrm{p}}} & \boldsymbol{K}^{X_{\mathrm{f_c}}X_{\mathrm{f}}X_{\mathrm{f_c}}} \end{bmatrix} \cdot \begin{bmatrix} \underline{v}^{X_{\mathrm{f}}G} \\ \underline{v}^{X_{\mathrm{f}}W} \\ \underline{v}^{X_{\mathrm{f}}R} \\ \underline{v}^{X_{\mathrm{f}}X_{\mathrm{p}}} \\ \underline{v}^{X_{\mathrm{f}}X_{\mathrm{f_c}}} \end{bmatrix} \tag{A.127}$$

The 2nd order vector state equation is reformulated for determination of the partitions in the output matrices $\boldsymbol{H}^{X_{\mathrm{f}}}$ and $\boldsymbol{L}^{X_{\mathrm{f}}}$, and feedthrough matrix $\boldsymbol{K}^{X_{\mathrm{f}}}$:

$$\begin{bmatrix} \ddot{\underline{\varphi}}^{X} \\ \ddot{\underline{\varrho}}^{X} \end{bmatrix} = \begin{bmatrix} \left(\boldsymbol{M}^{X_{\mathrm{f}}}\right)_{\varphi}^{-1} \\ \left(\boldsymbol{M}^{X_{\mathrm{f}}}\right)_{\varphi}^{-1} \end{bmatrix} \cdot \Big(- \left[\boldsymbol{D}_{\varphi}^{X_{\mathrm{f}}} \mid \boldsymbol{D}_{\varrho}^{X_{\mathrm{f}}}\right] \cdot \begin{bmatrix} \dot{\underline{\varphi}}^{X} \\ \dot{\underline{\varrho}}^{X} \end{bmatrix} - \left[\boldsymbol{S}_{\varphi}^{X_{\mathrm{f}}} \mid \boldsymbol{S}_{\varrho}^{X_{\mathrm{f}}}\right] \cdot \begin{bmatrix} \underline{\varphi}^{X} \\ \underline{\varrho}^{X} \end{bmatrix} +$$

$$\left[\boldsymbol{G}^{X_{\mathrm{f}}G} \mid \boldsymbol{G}^{X_{\mathrm{f}}W} \mid \boldsymbol{G}^{X_{\mathrm{f}}R} \mid \boldsymbol{G}^{X_{\mathrm{f}}X_{\mathrm{p}}} \mid \boldsymbol{G}^{X_{\mathrm{f}}X_{\mathrm{f_c}}}\right] \cdot \begin{bmatrix} \underline{v}^{X_{\mathrm{f}}G} \\ \underline{v}^{X_{\mathrm{f}}W} \\ \underline{v}^{X_{\mathrm{f}}R} \\ \underline{v}^{X_{\mathrm{f}}X_{\mathrm{p}}} \\ \underline{v}^{X_{\mathrm{f}}X_{\mathrm{f_c}}} \end{bmatrix} \Big) \tag{A.128}$$

The upper block in the inverse mass matrix maps dofs, dof speeds and inputs to angular dof accelerations; the lower block to linear dof accelerations.

Be aware that the non-valid rows [and corresponding columns], which arise from 'non-dof directions' have been deleted from all system matrices (see paragraph (vi) at 'Two complications seem ...**').**

For the output matrix partitions $\boldsymbol{H}_{\varphi}^{X_{\mathrm{p}}X_{\mathrm{f}}}$ and $\boldsymbol{H}_{\varrho}^{X_{\mathrm{p}}X_{\mathrm{f}}}$, which map angular and linear dof position variations to the outputs into the blade profile & structure thus holds:

$$\begin{aligned}\boldsymbol{H}_{\varphi}^{X_{\mathrm{p}}X_{\mathrm{f}}} &= \frac{\partial \underline{y}^{X_{\mathrm{p}}X_{\mathrm{f}}}}{\partial \underline{\phi}^{X}} - \left(\frac{\partial \underline{y}^{X_{\mathrm{p}}X_{\mathrm{f}}}}{\partial \underline{\ddot{\varphi}}^{X}} \cdot \left(\boldsymbol{M}^{X_{\mathrm{f}}}\right)_{\varphi}^{-1} + \frac{\partial \underline{y}^{X_{\mathrm{p}}X_{\mathrm{f}}}}{\partial \underline{\ddot{\varrho}}^{X}} \cdot \left(\boldsymbol{M}^{X_{\mathrm{f}}}\right)_{\varrho}^{-1}\right) \cdot \boldsymbol{S}_{\varphi}^{X_{\mathrm{f}}} \\ \boldsymbol{H}_{\varrho}^{X_{\mathrm{p}}X_{\mathrm{f}}} &= \frac{\partial \underline{y}^{X_{\mathrm{p}}X_{\mathrm{f}}}}{\partial \underline{\rho}^{X}} - \left(\frac{\partial \underline{y}^{X_{\mathrm{p}}X_{\mathrm{f}}}}{\partial \underline{\ddot{\varphi}}^{X}} \cdot \left(\boldsymbol{M}^{X_{\mathrm{f}}}\right)_{\varphi}^{-1} + \frac{\partial \underline{y}^{X_{\mathrm{p}}X_{\mathrm{f}}}}{\partial \underline{\ddot{\varrho}}^{X}} \cdot \left(\boldsymbol{M}^{X_{\mathrm{f}}}\right)_{\varrho}^{-1}\right) \cdot \boldsymbol{S}_{\varrho}^{X_{\mathrm{f}}}\end{aligned} \tag{A.129}$$

The output matrices $\boldsymbol{L}_{\varphi}^{X_{\mathrm{p}}X_{\mathrm{f}}}$ and $\boldsymbol{L}_{\varphi}^{X_{\mathrm{p}}X_{\mathrm{f}}}$ are obtained in the same way as described just after Eq. A.84 for the blade profile & structure X_{p}.

The partial derivative of the output subvector $\underline{y}^{X_{\mathrm{p}}X_{\mathrm{f}}}$, which is composed of 'elementary' subvectors $\{\underline{z}_{\mathrm{y}}\}$, to an elementary subvector $\underline{q}$ like $\underline{\phi}^{X}$ is obtained by putting above each other ('stacking') the partial derivatives of the involved output elementary subvectors (see Eq. A.85 and A.115):

$$\begin{aligned}\frac{\partial \underline{y}^{X_{\mathrm{p}}X_{\mathrm{f}}}}{\partial \underline{q}} &= \mathrm{S}_{(\underline{z}_{\mathrm{y}})}\left(\frac{\partial \underline{z}_{\mathrm{y}}}{\partial \underline{q}}\right) \qquad \text{for } \underline{z}_{\mathrm{y}} = \underline{\omega}^{X_{\mathrm{FF}(1)}}, \underline{\alpha}^{X_{\mathrm{FF}(1)}}, \underline{v}^{X_{\mathrm{FF}(1)}^{\oplus}}, \underline{a}^{X_{\mathrm{FF}(1)}^{\oplus}}, \\ &\qquad \underline{\phi}^{X_{\mathrm{FF}(1)}}, {}^{\mathrm{a}}\underline{q}^{X_{\mathrm{FF}(1)}}, {}^{\mathrm{aL}}\underline{q}^{X_{\mathrm{FF}(1)}}, \underline{g}_{\mathrm{ori}}^{X_{\mathrm{FF}(1)}}, \underline{\xi}^{X_{\mathrm{FF}(1)}}, \underline{x}^{X_{\mathrm{FF}(1)}^{\oplus}}\end{aligned} \tag{A.130}$$

For the feedthrough matrix partition $\boldsymbol{K}^{X_{\mathrm{p}}X_{\mathrm{f}}G}$, that maps the 'exogenous' input subvector to the output subvector into the blade profile & structure X_{p} holds:

$$\boldsymbol{K}^{X_{\mathrm{p}}X_{\mathrm{f}}G} = \frac{\partial \underline{y}^{X_{\mathrm{p}}X_{\mathrm{f}}}}{\partial \underline{v}^{X_{\mathrm{f}}G}} - \left(\frac{\partial \underline{y}^{X_{\mathrm{p}}X_{\mathrm{f}}}}{\partial \underline{\ddot{\varphi}}^{X}} \cdot \left(\boldsymbol{M}^{X_{\mathrm{f}}}\right)_{\varphi}^{-1} + \frac{\partial \underline{y}^{X_{\mathrm{p}}X_{\mathrm{f}}}}{\partial \underline{\ddot{\varrho}}^{X}} \cdot \left(\boldsymbol{M}^{X_{\mathrm{f}}}\right)_{\varrho}^{-1}\right) \cdot \boldsymbol{G}^{X_{\mathrm{f}}G} \tag{A.131}$$

Be aware that all columns in the output sensitivities to the degree of freedoms that pertain to non-dof directions as concerns X_{f} are deleted before use.

The input subvector $\underline{v}^{X_{\mathrm{f}}G}$ is now composed by itself of 'elementary' subvectors $\{\underline{q}_{\mathrm{v}}\}$. The partial derivative of the composed output subvector $\underline{y}^{X_{\mathrm{p}}X_{\mathrm{f}}}$ to this input vector is obtained by (i) stacking the partial derivatives of the output elementary subvectors to an input elementary subvector, and (ii) doing this for all elementary input subvectors and putting next to each other the obtained 'stacks'. With elementary output subvectors $\{\underline{z}_{\mathrm{y}}\}$ the expression becomes (see Eq. A.88):

$$\frac{\partial \underline{y}^{X_{\mathrm{p}}X_{\mathrm{f}}}}{\partial \underline{v}^{X_{\mathrm{p}}G}} = \mathrm{J}_{(\underline{q}_{\mathrm{v}})}\left(\mathrm{S}_{(\underline{z}_{\mathrm{y}})}\left(\frac{\partial \underline{z}_{\mathrm{y}}}{\partial \underline{q}_{\mathrm{v}}}\right)\right) \quad \text{with:} \quad \begin{cases} \underline{q}_{\mathrm{v}} = \underline{u}_{\mathrm{per}}^{X}, \underline{g}_{\mathrm{per}}^{R}, {}^{\mathrm{t}}\underline{u}^{W/X} \\ \underline{z}_{\mathrm{y}} = \underline{\omega}^{X_{\mathrm{FF}(1)}}, \underline{\alpha}^{X_{\mathrm{FF}(1)}}, \underline{v}^{X_{\mathrm{FF}(1)}^{\oplus}}, \underline{a}^{X_{\mathrm{FF}(1)}^{\oplus}}, \\ \underline{\phi}^{X_{\mathrm{FF}(1)}}, {}^{\mathrm{a}}\underline{q}^{X_{\mathrm{FF}(1)}}, {}^{\mathrm{aL}}\underline{q}^{X_{\mathrm{FF}(1)}}, \underline{g}_{\mathrm{ori}}^{X_{\mathrm{FF}(1)}}, \underline{\xi}^{X_{\mathrm{FF}(1)}}, \underline{x}^{X_{\mathrm{FF}(1)}^{\oplus}} \end{cases} \tag{A.132}$$

The mapping from the input subvectors from the control, wake, rotor shaft & hub, profile & structure X_{p} itself, and from the pith servo $X_{\mathrm{f_c}}$ to the output subvector into X_{p} occurs via matrices $\boldsymbol{K}^{X_{\mathrm{p}}X_{\mathrm{f}}W}$, $\boldsymbol{K}^{X_{\mathrm{p}}X_{\mathrm{f}}R}$, $\boldsymbol{K}^{X_{\mathrm{p}}X_{\mathrm{f}}X_{\mathrm{p}}}$ and $\boldsymbol{K}^{X_{\mathrm{p}}X_{\mathrm{f}}X_{\mathrm{f_c}}}$. These matrices are determined in accordance with Eq. A.131 by replacing the:

(i) output sensitivity to $\underline{v}^{X_{\mathrm{f}}G}$ by those to $\underline{v}^{X_{\mathrm{f}}W}$, $\underline{v}^{X_{\mathrm{f}}R}$, $\underline{v}^{X_{\mathrm{f}}X_{\mathrm{p}}}$, and $\underline{v}^{X_{\mathrm{f}}X_{\mathrm{f_c}}}$;

(ii) input matrix partition $\boldsymbol{G}^{X_{\mathrm{f}}G}$ by $\boldsymbol{G}^{X_{\mathrm{f}}W}$, $\boldsymbol{G}^{X_{\mathrm{f}}R}$, $\boldsymbol{G}^{X_{\mathrm{f}}X_{\mathrm{p}}}$, and $\boldsymbol{G}^{X_{\mathrm{f}}X_{\mathrm{f_c}}}$.

The partial derivatives of the 'composed' output subvectors to the 'composed' input subvectors are determined in accordance with Eq. A.132.

(viii) Pitch control system equations and 1st order state space model

The pitch model equations and in section 3.6.2 can be transformated into a first order state space representations and linked together:

$$\begin{aligned}
\underline{\dot{x}}^{X_{\mathrm{fc}}} &= \boldsymbol{A}^{X_{\mathrm{fc}}} \cdot \underline{x}^{X_{\mathrm{fc}}} + \boldsymbol{B}^{X_{\mathrm{fc}}} \cdot \underline{v}^{X_{\mathrm{fc}}} \quad \text{with input vector} \quad \underline{v}^{X_{\mathrm{fc}}} = [\ \phi_2^{X_1}\ \ \omega_1^{X_{\mathrm{FF}(0)}}\ ]^{\mathrm{T}} \\
\underline{y}^{X_{\mathrm{fc}}} &= \boldsymbol{C}^{X_{\mathrm{fc}}} \cdot \underline{x}^{X_{\mathrm{fc}}} + \boldsymbol{K}^{X_{\mathrm{fc}}} \cdot \underline{v}^{X_{\mathrm{fc}}} \quad \text{with output vector} \quad \underline{y}^{X_{\mathrm{fc}}} = [\ \phi_{\mathrm{pt_r}}^{X_1}\ \ t_{\mathrm{pt}}^{X_1}\ ]
\end{aligned} \tag{A.133}$$

The 'transfer function formulations' in Eq. A.2.3 and 3.40 are transformed into state space representations via a basic MATLAB function (TF2SS()). The inner and outer loop models are connected through the pitch angle setpoint, also via a basic MATLAB function (CONNECT()). The involved procedure is dealt with in detail below, but now as concerns the connection of the pitch control to the flange model.

(ix) Connection of pitch control to blade flange model

The state equation and output equation of the pitch control system model are rewritten

$$\begin{aligned}
\underline{\dot{x}}^{X_{\mathrm{fc}}} &= \boldsymbol{A}^{X_{\mathrm{fc}}} \cdot \underline{x}^{X_{\mathrm{fc}}} + [\ \boldsymbol{B}^{X_{\mathrm{fc}}R} \mid \boldsymbol{B}^{X_{\mathrm{fc}}X_{\mathrm{f}}}\ ] \cdot \begin{bmatrix} \underline{v}^{X_{\mathrm{f}}R} \\ \underline{y}^{X_{\mathrm{fc}}X_{\mathrm{f}}} \end{bmatrix} \\
\underline{y}^{X_{\mathrm{fc}}} &= \boldsymbol{C}^{X_{\mathrm{fc}}} \cdot \underline{x}^{X_{\mathrm{fc}}} + [\ \boldsymbol{K}^{X_{\mathrm{fc}}R} \mid \boldsymbol{K}^{X_{\mathrm{fc}}X_{\mathrm{f}}}\ ] \cdot \begin{bmatrix} \underline{v}^{X_{\mathrm{f}}R} \\ \underline{y}^{X_{\mathrm{fc}}X_{\mathrm{f}}} \end{bmatrix}
\end{aligned} \tag{A.134}$$

We also have to write the flange model as a first order state space representation. Point of departure is the compact form of the rewritten state equation and the output equation for the pitch control system. The angular and linear degrees of freedom are clustered in the 'position state vector' $\underline{x}_{\mathrm{p}}^{X_{\mathrm{f}}}$; the input and output subvectors that do not interact with the pitch servo are clustered in the 'external input and ouput vectors' $\underline{v}^{X_{\mathrm{f}}E}$ and $\underline{y}^{EX_{\mathrm{f}}}$:

$$\underline{x}_{\mathrm{p}}^{X_{\mathrm{f}}} \triangleq \begin{bmatrix} \underline{\varphi}^{X} \\ \underline{o}^{X} \end{bmatrix} \quad ; \quad \underline{v}^{X_{\mathrm{f}}E} \triangleq \begin{bmatrix} \underline{v}^{X_{\mathrm{f}}G} \\ \underline{v}^{X_{\mathrm{f}}W} \\ \underline{v}^{X_{\mathrm{f}}R} \\ \underline{v}^{X_{\mathrm{f}}X_{\mathrm{p}}} \end{bmatrix} \quad ; \quad \underline{y}^{EX_{\mathrm{f}}} \triangleq \begin{bmatrix} \underline{y}^{GX_{\mathrm{f}}} \\ \underline{y}^{WX_{\mathrm{f}}} \\ \underline{y}^{RX_{\mathrm{f}}} \\ \underline{y}^{X_{\mathrm{p}}X_{\mathrm{f}}} \end{bmatrix} \tag{A.135}$$

The matrices in the vector state and output equation A.128 and A.127 are clustered accordingly:

$$\begin{aligned}
\boldsymbol{G}^{X_{\mathrm{f}}} &= \begin{bmatrix} \boldsymbol{G}^{X_{\mathrm{f}}E} & \boldsymbol{G}^{X_{\mathrm{f}}X_{\mathrm{fc}}} \end{bmatrix} \\
\boldsymbol{K}^{X_{\mathrm{f}}} &= \begin{bmatrix} \boldsymbol{K}^{EX_{\mathrm{f}}E} & \boldsymbol{K}^{EX_{\mathrm{f}}X_{\mathrm{fc}}} \\ \boldsymbol{K}^{X_{\mathrm{fc}}X_{\mathrm{f}}E} & \boldsymbol{K}^{X_{\mathrm{fc}}X_{\mathrm{f}}X_{\mathrm{fc}}} \end{bmatrix} \quad ; \quad \boldsymbol{H}^{X_{\mathrm{f}}} = \begin{bmatrix} \boldsymbol{H}^{EX_{\mathrm{f}}} \\ \boldsymbol{H}^{X_{\mathrm{fc}}X_{\mathrm{f}}} \end{bmatrix} \quad ; \quad \boldsymbol{L}^{X_{\mathrm{f}}} = \begin{bmatrix} \boldsymbol{L}^{EX_{\mathrm{f}}} \\ \boldsymbol{L}^{X_{\mathrm{fc}}X_{\mathrm{f}}} \end{bmatrix}
\end{aligned} \tag{A.136}$$

Further, the inverse mass matrix and the stiffness and damper matrix are not yet partitioned any more. The state and output equation for the flange element then becomes:

$$\begin{aligned}
\underline{\ddot{x}}_{\mathrm{p}}^{X_{\mathrm{f}}} &= \left(\boldsymbol{M}^{X_{\mathrm{f}}}\right)^{-1} \cdot \left(-\boldsymbol{D}^{X_{\mathrm{f}}} \cdot \underline{\dot{x}}_{\mathrm{p}}^{X_{\mathrm{f}}} - \boldsymbol{S}^{X_{\mathrm{f}}} \cdot \underline{x}_{\mathrm{p}}^{X_{\mathrm{f}}} + \begin{bmatrix} \boldsymbol{G}^{X_{\mathrm{f}}E} & \boldsymbol{G}^{X_{\mathrm{f}}X_{\mathrm{fc}}} \end{bmatrix} \cdot \begin{bmatrix} \underline{v}^{X_{\mathrm{f}}E} \\ \underline{v}^{X_{\mathrm{f}}X_{\mathrm{fc}}} \end{bmatrix} \right) \\
\begin{bmatrix} \underline{y}^{EX_{\mathrm{f}}} \\ \underline{y}^{X_{\mathrm{fc}}X_{\mathrm{f}}} \end{bmatrix} &= \begin{bmatrix} \boldsymbol{H}^{EX_{\mathrm{f}}} \\ \boldsymbol{H}^{X_{\mathrm{fc}}X_{\mathrm{f}}} \end{bmatrix} \cdot \underline{x}_{\mathrm{p}}^{X_{\mathrm{f}}} + \begin{bmatrix} \boldsymbol{L}^{EX_{\mathrm{f}}} \\ \boldsymbol{L}^{X_{\mathrm{fc}}X_{\mathrm{f}}} \end{bmatrix} \cdot \underline{\dot{x}}_{\mathrm{p}}^{X_{\mathrm{f}}} + \begin{bmatrix} \boldsymbol{K}^{EX_{\mathrm{f}}E} & \boldsymbol{K}^{EX_{\mathrm{f}}X_{\mathrm{fc}}} \\ \boldsymbol{K}^{X_{\mathrm{fc}}X_{\mathrm{f}}E} & \boldsymbol{K}^{X_{\mathrm{fc}}X_{\mathrm{f}}X_{\mathrm{fc}}} \end{bmatrix} \cdot \begin{bmatrix} \underline{v}^{X_{\mathrm{f}}E} \\ \underline{v}^{X_{\mathrm{f}}X_{\mathrm{fc}}} \end{bmatrix}
\end{aligned} \tag{A.137}$$

The first order state space representation is now obtained via the 'speed state vector' $\underline{x}_{\mathrm{s}}^{X_{\mathrm{f}}}$, in which includes the time derivatives of the angular and linear dofs are clustered (use short-hand superscript 'fce' instead of $X_{\mathrm{f}}X_{\mathrm{f_c}}E$ etc.)

$$\begin{aligned}
\begin{bmatrix} \dot{\underline{x}}_{\mathrm{p}}^{\mathrm{f}} \\ \dot{\underline{x}}_{\mathrm{s}}^{\mathrm{f}} \end{bmatrix} &= \begin{bmatrix} \mathrm{O} & \boldsymbol{I} \\ \boldsymbol{A}_{\mathrm{p}}^{\mathrm{f}} & \boldsymbol{A}_{\mathrm{s}}^{\mathrm{f}} \end{bmatrix} \cdot \begin{bmatrix} \underline{x}_{\mathrm{p}}^{\mathrm{f}} \\ \underline{x}_{\mathrm{s}}^{\mathrm{f}} \end{bmatrix} + \begin{bmatrix} \mathrm{O} & \mathrm{O} \\ \boldsymbol{B}^{\mathrm{fe}} & \boldsymbol{B}^{\mathrm{fc}} \end{bmatrix} \cdot \begin{bmatrix} \underline{v}^{\mathrm{fe}} \\ \underline{v}^{\mathrm{fc}} \end{bmatrix} \\
\begin{bmatrix} \underline{y}^{\mathrm{ef}} \\ \underline{y}^{\mathrm{cf}} \end{bmatrix} &= \begin{bmatrix} \boldsymbol{C}_{\mathrm{p}}^{\mathrm{ef}} & \boldsymbol{C}_{\mathrm{s}}^{\mathrm{ef}} \\ \boldsymbol{C}_{\mathrm{p}}^{\mathrm{cf}} & \boldsymbol{C}_{\mathrm{s}}^{\mathrm{cf}} \end{bmatrix} \cdot \begin{bmatrix} \underline{x}_{\mathrm{p}}^{\mathrm{f}} \\ \underline{x}_{\mathrm{s}}^{\mathrm{f}} \end{bmatrix} + \begin{bmatrix} \boldsymbol{K}^{\mathrm{efe}} & \boldsymbol{K}^{\mathrm{efc}} \\ \boldsymbol{K}^{\mathrm{cfe}} & \boldsymbol{K}^{\mathrm{cfc}} \end{bmatrix} \cdot \begin{bmatrix} \underline{v}^{\mathrm{fe}} \\ \underline{v}^{\mathrm{fc}} \end{bmatrix}
\end{aligned} \tag{A.138}$$

with the following relationships between the state transition, input and output matrix A,B,C on the one side and the system matrices M,D,S,G on the other side:

$$\begin{aligned}
\boldsymbol{A}_{\mathrm{p}}^{\mathrm{f}} &= -\left(\boldsymbol{M}^{X_{\mathrm{f}}}\right)^{-1} \cdot \boldsymbol{S}^{X_{\mathrm{f}}} \quad ; \quad \boldsymbol{A}_{\mathrm{s}}^{\mathrm{f}} = -\left(\boldsymbol{M}^{X_{\mathrm{f}}}\right)^{-1} \cdot \boldsymbol{D}^{X_{\mathrm{f}}} \\
\boldsymbol{B}^{\mathrm{fe}} &= \left(\boldsymbol{M}^{X_{\mathrm{f}}}\right)^{-1} \cdot \boldsymbol{G}^{X_{\mathrm{f}}E} \quad ; \quad \boldsymbol{B}^{\mathrm{fc}} = \left(\boldsymbol{M}^{X_{\mathrm{f}}}\right)^{-1} \cdot \boldsymbol{G}^{X_{\mathrm{f}}X_{\mathrm{f_c}}} \\
\boldsymbol{C}_{\mathrm{p}}^{\mathrm{ef}} &= \boldsymbol{H}^{EX_{\mathrm{f}}} \quad ; \quad \boldsymbol{C}_{\mathrm{s}}^{\mathrm{ef}} = \boldsymbol{L}^{EX_{\mathrm{f}}} \\
\boldsymbol{C}_{\mathrm{p}}^{\mathrm{cf}} &= \boldsymbol{H}^{X_{\mathrm{f_c}}X_{\mathrm{f}}} \quad ; \quad \boldsymbol{C}_{\mathrm{s}}^{\mathrm{cf}} = \boldsymbol{L}^{X_{\mathrm{f_c}}X_{\mathrm{f}}}
\end{aligned} \tag{A.139}$$

The state space representation of the pitch control system model is written in the same format, in which we also assume an 'external output vector'. Of course, this model does not include a 'position' and 'speed' state (sub)vector but only *the* 'ordinary' state vector $\underline{x}_{\mathrm{o}}^{\mathrm{c}}$ in the by nature first order vector state equation ($\underline{x}_{\mathrm{o}}^{\mathrm{c}} = \underline{x}^{X_{\mathrm{f_c}}}$):

$$\begin{aligned}
\dot{\underline{x}}_{\mathrm{o}}^{\mathrm{c}} &= \boldsymbol{A}_{\mathrm{o}}^{\mathrm{c}} \cdot \underline{x}_{\mathrm{o}}^{\mathrm{c}} + \begin{bmatrix} \boldsymbol{B}^{\mathrm{ce}} & \boldsymbol{B}^{\mathrm{cf}} \end{bmatrix} \cdot \begin{bmatrix} \underline{v}^{\mathrm{ce}} \\ \underline{v}^{\mathrm{cf}} \end{bmatrix} \\
\begin{bmatrix} \underline{y}^{\mathrm{ec}} \\ \underline{y}^{\mathrm{fc}} \end{bmatrix} &= \begin{bmatrix} \boldsymbol{C}_{\mathrm{o}}^{\mathrm{ec}} \\ \boldsymbol{C}_{\mathrm{o}}^{\mathrm{fc}} \end{bmatrix} \cdot \underline{x}_{\mathrm{o}}^{\mathrm{c}} + \begin{bmatrix} \boldsymbol{K}^{\mathrm{ece}} & \boldsymbol{K}^{\mathrm{ecf}} \\ \boldsymbol{K}^{\mathrm{fce}} & \boldsymbol{K}^{\mathrm{fcf}} \end{bmatrix} \cdot \begin{bmatrix} \underline{v}^{\mathrm{ce}} \\ \underline{v}^{\mathrm{cf}} \end{bmatrix}
\end{aligned} \tag{A.140}$$

The 'connection conditions' are:

$$\underline{v}^{\mathrm{fc}} = \underline{y}^{\mathrm{fc}} \quad \text{and} \quad \underline{v}^{\mathrm{cf}} = \underline{y}^{\mathrm{cf}} \tag{A.141}$$

Substitution of the connection conditions in the 'lower part' in the output equation of both models yields the explicit expression for the 'internal' output subvectors in the state (sub)vectors and the 'external' input subvectors:

$$\begin{aligned}
\begin{bmatrix} \underline{y}^{\mathrm{fc}} \\ \underline{y}^{\mathrm{cf}} \end{bmatrix} &= \boldsymbol{Q} \cdot \left(\begin{bmatrix} \mathrm{O} & \mathrm{O} & \boldsymbol{C}_{\mathrm{o}}^{\mathrm{fc}} \\ \boldsymbol{C}_{\mathrm{p}}^{\mathrm{cf}} & \boldsymbol{C}_{\mathrm{s}}^{\mathrm{cf}} & \mathrm{O} \end{bmatrix} \cdot \begin{bmatrix} \underline{x}_{\mathrm{p}}^{\mathrm{f}} \\ \underline{x}_{\mathrm{s}}^{\mathrm{f}} \\ \underline{x}_{\mathrm{o}}^{\mathrm{c}} \end{bmatrix} + \begin{bmatrix} \mathrm{O} & \boldsymbol{K}^{\mathrm{fce}} \\ \boldsymbol{K}^{\mathrm{cfe}} & \mathrm{O} \end{bmatrix} \cdot \begin{bmatrix} \underline{v}^{\mathrm{fe}} \\ \underline{v}^{\mathrm{ce}} \end{bmatrix} \right) \\
\text{with} \quad \boldsymbol{Q} &= \begin{bmatrix} \boldsymbol{I} & -\boldsymbol{K}^{\mathrm{fcf}} \\ -\boldsymbol{K}^{\mathrm{cfc}} & \boldsymbol{I} \end{bmatrix}^{-1} .
\end{aligned} \tag{A.142}$$

Now collect both vector state equations and output equations into one state and one output equation and substitute the result above for the internal output vectors. This yields the

following state space representation for the blade flange with pitch servo:

$$\begin{bmatrix} \dot{\underline{x}}_{\mathrm{p}}^{\mathrm{f}} \\ \dot{\underline{x}}_{\mathrm{s}}^{\mathrm{f}} \\ \dot{\underline{x}}_{\mathrm{o}}^{\mathrm{c}} \end{bmatrix} = \begin{bmatrix} \mathrm{O} & \boldsymbol{I} & \mathrm{O} \\ \boldsymbol{A}_{\mathrm{p}}^{\mathrm{ff}} & \boldsymbol{A}_{\mathrm{s}}^{\mathrm{ff}} & \boldsymbol{A}_{\mathrm{o}}^{\mathrm{fc}} \\ \boldsymbol{A}_{\mathrm{p}}^{\mathrm{cf}} & \boldsymbol{A}_{\mathrm{s}}^{\mathrm{cf}} & \boldsymbol{A}_{\mathrm{o}}^{\mathrm{cc}} \end{bmatrix} \cdot \begin{bmatrix} \dot{\underline{x}}_{\mathrm{p}}^{\mathrm{f}} \\ \dot{\underline{x}}_{\mathrm{s}}^{\mathrm{f}} \\ \dot{\underline{x}}_{\mathrm{o}}^{\mathrm{c}} \end{bmatrix} + \begin{bmatrix} \mathrm{O} & \mathrm{O} \\ \boldsymbol{B}^{\mathrm{ffe}} & \boldsymbol{B}^{\mathrm{fce}} \\ \boldsymbol{B}^{\mathrm{cfe}} & \boldsymbol{B}^{\mathrm{cce}} \end{bmatrix} \cdot \begin{bmatrix} \underline{v}^{\mathrm{fe}} \\ \underline{v}^{\mathrm{ce}} \end{bmatrix}$$

$$\begin{bmatrix} \underline{y}^{\mathrm{ef}} \\ \underline{y}^{\mathrm{ec}} \end{bmatrix} = \begin{bmatrix} \boldsymbol{C}_{\mathrm{p}}^{\mathrm{eff}} & \boldsymbol{C}_{\mathrm{s}}^{\mathrm{eff}} & \boldsymbol{C}_{\mathrm{o}}^{\mathrm{fc}} \\ \boldsymbol{C}_{\mathrm{p}}^{\mathrm{ecf}} & \boldsymbol{C}_{\mathrm{s}}^{\mathrm{ecf}} & \boldsymbol{C}_{\mathrm{o}}^{\mathrm{cc}} \end{bmatrix} \cdot \begin{bmatrix} \dot{\underline{x}}_{\mathrm{p}}^{\mathrm{f}} \\ \dot{\underline{x}}_{\mathrm{s}}^{\mathrm{f}} \\ \dot{\underline{x}}_{\mathrm{o}}^{\mathrm{c}} \end{bmatrix} + \begin{bmatrix} \boldsymbol{K}^{\mathrm{effe}} & \boldsymbol{K}^{\mathrm{efce}} \\ \boldsymbol{K}^{\mathrm{ecfe}} & \boldsymbol{K}^{\mathrm{ecce}} \end{bmatrix} \cdot \begin{bmatrix} \underline{v}^{\mathrm{fe}} \\ \underline{v}^{\mathrm{ce}} \end{bmatrix} \tag{A.143}$$

For the partitions in the 'closed loop' state transition matrix and input matrix holds:

$$\begin{bmatrix} \boldsymbol{A}_{\mathrm{p}}^{\mathrm{ff}} & \boldsymbol{A}_{\mathrm{s}}^{\mathrm{ff}} & \boldsymbol{A}_{\mathrm{o}}^{\mathrm{fc}} \\ \boldsymbol{A}_{\mathrm{p}}^{\mathrm{cf}} & \boldsymbol{A}_{\mathrm{s}}^{\mathrm{cf}} & \boldsymbol{A}_{\mathrm{o}}^{\mathrm{cc}} \end{bmatrix} = \begin{bmatrix} \boldsymbol{A}_{\mathrm{p}}^{\mathrm{f}} & \boldsymbol{A}_{\mathrm{s}}^{\mathrm{f}} & \mathrm{O} \\ \mathrm{O} & \mathrm{O} & \boldsymbol{A}_{\mathrm{o}}^{\mathrm{c}} \end{bmatrix} + \begin{bmatrix} \boldsymbol{B}^{\mathrm{fc}} & \mathrm{O} \\ \mathrm{O} & \boldsymbol{B}^{\mathrm{cf}} \end{bmatrix} \cdot \boldsymbol{Q} \cdot \begin{bmatrix} \mathrm{O} & \mathrm{O} & \boldsymbol{C}_{\mathrm{o}}^{\mathrm{fc}} \\ \boldsymbol{C}_{\mathrm{p}}^{\mathrm{cf}} & \boldsymbol{C}_{\mathrm{s}}^{\mathrm{cf}} & \mathrm{O} \end{bmatrix}$$

$$\begin{bmatrix} \boldsymbol{B}^{\mathrm{ffe}} & \boldsymbol{B}^{\mathrm{fce}} \\ \boldsymbol{B}^{\mathrm{cfe}} & \boldsymbol{B}^{\mathrm{cce}} \end{bmatrix} = \begin{bmatrix} \boldsymbol{B}^{\mathrm{fe}} & \mathrm{O} \\ \mathrm{O} & \boldsymbol{B}^{\mathrm{ce}} \end{bmatrix} + \begin{bmatrix} \boldsymbol{B}^{\mathrm{fc}} & \mathrm{O} \\ \mathrm{O} & \boldsymbol{B}^{\mathrm{cf}} \end{bmatrix} \cdot \boldsymbol{Q} \cdot \begin{bmatrix} \mathrm{O} & \boldsymbol{K}^{\mathrm{fce}} \\ \boldsymbol{K}^{\mathrm{cfe}} & \mathrm{O} \end{bmatrix} \tag{A.144}$$

For the partitions in the 'closed loop' output and feedthrough matrix holds:

$$\begin{bmatrix} \boldsymbol{C}_{\mathrm{p}}^{\mathrm{eff}} & \boldsymbol{C}_{\mathrm{s}}^{\mathrm{eff}} & \boldsymbol{C}_{\mathrm{o}}^{\mathrm{fc}} \\ \boldsymbol{C}_{\mathrm{p}}^{\mathrm{ecf}} & \boldsymbol{C}_{\mathrm{s}}^{\mathrm{ecf}} & \boldsymbol{C}_{\mathrm{o}}^{\mathrm{cc}} \end{bmatrix} = \begin{bmatrix} \boldsymbol{C}_{\mathrm{p}}^{\mathrm{ef}} & \boldsymbol{C}_{\mathrm{s}}^{\mathrm{ef}} & \mathrm{O} \\ \mathrm{O} & \mathrm{O} & \boldsymbol{C}_{\mathrm{o}}^{\mathrm{ec}} \end{bmatrix} + \begin{bmatrix} \boldsymbol{K}^{\mathrm{efc}} & \mathrm{O} \\ \mathrm{O} & \boldsymbol{K}^{\mathrm{ecf}} \end{bmatrix} \cdot \boldsymbol{Q} \cdot \begin{bmatrix} \mathrm{O} & \mathrm{O} & \boldsymbol{C}_{\mathrm{o}}^{\mathrm{fc}} \\ \boldsymbol{C}_{\mathrm{p}}^{\mathrm{cf}} & \boldsymbol{C}_{\mathrm{s}}^{\mathrm{cf}} & \mathrm{O} \end{bmatrix}$$

$$\begin{bmatrix} \boldsymbol{K}^{\mathrm{effe}} & \boldsymbol{K}^{\mathrm{efce}} \\ \boldsymbol{K}^{\mathrm{ecfe}} & \boldsymbol{K}^{\mathrm{ecce}} \end{bmatrix} = \begin{bmatrix} \boldsymbol{K}^{\mathrm{efe}} & \mathrm{O} \\ \mathrm{O} & \boldsymbol{K}^{\mathrm{ece}} \end{bmatrix} + \begin{bmatrix} \boldsymbol{K}^{\mathrm{efc}} & \mathrm{O} \\ \mathrm{O} & \boldsymbol{K}^{\mathrm{ecf}} \end{bmatrix} \cdot \boldsymbol{Q} \cdot \begin{bmatrix} \mathrm{O} & \boldsymbol{K}^{\mathrm{fce}} \\ \boldsymbol{K}^{\mathrm{cfe}} & \mathrm{O} \end{bmatrix} \tag{A.145}$$

Finally we rewrite the first order state space reprentation for the overall flange model as follows:

$$\begin{bmatrix} \dot{\underline{x}}_{\mathrm{p}}^{X_{\mathrm{f}}} \\ \dot{\underline{x}}_{\mathrm{s}}^{X_{\mathrm{f}}} \\ \dot{\underline{x}}_{\mathrm{o}}^{X_{\mathrm{f}}} \end{bmatrix} = \begin{bmatrix} \mathrm{O} & \boldsymbol{I} & \mathrm{O} \\ \boldsymbol{A}_{\mathrm{sp}}^{X_{\mathrm{f}}} & \boldsymbol{A}_{\mathrm{ss}}^{X_{\mathrm{f}}} & \boldsymbol{A}_{\mathrm{so}}^{X_{\mathrm{f}}} \\ \boldsymbol{A}_{\mathrm{op}}^{X_{\mathrm{f}}} & \boldsymbol{A}_{\mathrm{os}}^{X_{\mathrm{f}}} & \boldsymbol{A}_{\mathrm{oo}}^{X_{\mathrm{f}}} \end{bmatrix} \cdot \begin{bmatrix} \underline{x}_{\mathrm{p}}^{X_{\mathrm{f}}} \\ \underline{x}_{\mathrm{s}}^{X_{\mathrm{f}}} \\ \underline{x}_{\mathrm{o}}^{X_{\mathrm{f}}} \end{bmatrix} + \begin{bmatrix} \mathrm{O} & \mathrm{O} & \mathrm{O} & \mathrm{O} \\ \boldsymbol{B}_{\mathrm{s}}^{X_{\mathrm{f}}G} & \boldsymbol{B}_{\mathrm{s}}^{X_{\mathrm{f}}W} & \boldsymbol{B}_{\mathrm{s}}^{X_{\mathrm{f}}R} & \boldsymbol{B}_{\mathrm{s}}^{X_{\mathrm{f}}X_{\mathrm{p}}} \\ \boldsymbol{B}_{\mathrm{o}}^{X_{\mathrm{f}}G} & \boldsymbol{B}_{\mathrm{o}}^{X_{\mathrm{f}}W} & \boldsymbol{B}_{\mathrm{o}}^{X_{\mathrm{f}}R} & \boldsymbol{B}_{\mathrm{o}}^{X_{\mathrm{f}}X_{\mathrm{p}}} \end{bmatrix} \cdot \begin{bmatrix} \underline{v}^{X_{\mathrm{f}}G} \\ \underline{v}^{X_{\mathrm{f}}W} \\ \underline{v}^{X_{\mathrm{f}}R} \\ \underline{v}^{X_{\mathrm{f}}X_{\mathrm{p}}} \end{bmatrix} \tag{A.146}$$

and

$$\begin{bmatrix} \underline{y}^{GX_\mathrm{f}} \\ \underline{y}^{WX_\mathrm{f}} \\ \underline{y}^{RX_\mathrm{f}} \\ \underline{y}^{X_\mathrm{p}X_\mathrm{f}} \end{bmatrix} = \begin{bmatrix} \boldsymbol{C}_\mathrm{p}^{GX_\mathrm{f}} & \boldsymbol{C}_\mathrm{s}^{GX_\mathrm{f}} & \boldsymbol{C}_\mathrm{o}^{GX_\mathrm{f}} \\ \boldsymbol{C}_\mathrm{p}^{WX_\mathrm{f}} & \boldsymbol{C}_\mathrm{s}^{WX_\mathrm{f}} & \boldsymbol{C}_\mathrm{o}^{WX_\mathrm{f}} \\ \boldsymbol{C}_\mathrm{p}^{RX_\mathrm{f}} & \boldsymbol{C}_\mathrm{s}^{RX_\mathrm{f}} & \boldsymbol{C}_\mathrm{o}^{RX_\mathrm{f}} \\ \boldsymbol{C}_\mathrm{p}^{X_\mathrm{p}X_\mathrm{f}} & \boldsymbol{C}_\mathrm{s}^{X_\mathrm{p}X_\mathrm{f}} & \boldsymbol{C}_\mathrm{o}^{X_\mathrm{p}X_\mathrm{f}} \end{bmatrix} \cdot \begin{bmatrix} \dot{\underline{x}}_\mathrm{p}^\mathrm{f} \\ \dot{\underline{x}}_\mathrm{s}^\mathrm{f} \\ \dot{\underline{x}}_\mathrm{o}^\mathrm{c} \end{bmatrix} + \begin{bmatrix} \boldsymbol{K}_\mathrm{c}^{GX_\mathrm{f}G} & \boldsymbol{K}_\mathrm{c}^{GX_\mathrm{f}W} & \boldsymbol{K}_\mathrm{c}^{GX_\mathrm{f}R} & \boldsymbol{K}_\mathrm{c}^{GX_\mathrm{f}X_\mathrm{p}} \\ \boldsymbol{K}_\mathrm{c}^{WX_\mathrm{f}G} & \boldsymbol{K}_\mathrm{c}^{WX_\mathrm{f}W} & \boldsymbol{K}_\mathrm{c}^{WX_\mathrm{f}R} & \boldsymbol{K}_\mathrm{c}^{WX_\mathrm{f}X_\mathrm{p}} \\ \boldsymbol{K}_\mathrm{c}^{RX_\mathrm{f}G} & \boldsymbol{K}_\mathrm{c}^{RX_\mathrm{f}W} & \boldsymbol{K}_\mathrm{c}^{RX_\mathrm{f}R} & \boldsymbol{K}_\mathrm{c}^{RX_\mathrm{f}X_\mathrm{p}} \\ \boldsymbol{K}_\mathrm{c}^{X_\mathrm{p}X_\mathrm{f}G} & \boldsymbol{K}_\mathrm{c}^{X_\mathrm{p}X_\mathrm{f}W} & \boldsymbol{K}_\mathrm{c}^{X_\mathrm{p}X_\mathrm{f}R} & \boldsymbol{K}_\mathrm{c}^{X_\mathrm{p}X_\mathrm{f}X_\mathrm{p}} \end{bmatrix} \cdot \begin{bmatrix} \underline{v}^{X_\mathrm{f}G} \\ \underline{v}^{X_\mathrm{f}W} \\ \underline{v}^{X_\mathrm{f}R} \\ \underline{v}^{X_\mathrm{f}X_\mathrm{p}} \end{bmatrix} \tag{A.147}$$

The state transition submatrices are equal to those in Eq. A.143.

The output submatrices are composed of the corresponding rows in the output submatrices in Eq. A.143 (only the upper block matrices apply!).

All input submatrices are composed of the corresponding columns in the input submatrices $\boldsymbol{B}^{\mathrm{ffe}}$ and $\boldsymbol{B}^{\mathrm{cfe}}$ in Eq. A.146.

All feedthrough submatrices are composed of the corresonding row & column combinations in submatrix $\boldsymbol{K}^{\mathrm{effe}}$ (the lower block $\boldsymbol{K}^{\mathrm{ecfe}}$ is empty!). De subscript 'c' is used in the feedthrough matrix partitions because they cater for the 'closed loop' behaviour of flange; they differ from the feedthrough matrix partitions in Eq. A.127!

A.2.4 First order state space representation rotor blade X

The first of the three paragraphs in this subsection deals with the transformation of the model for the blade profile & structure X_p into a first order state space model. In paragraph (ii) the input and output vectors of the models of X_f and X_p are reorganised in order to make them 'systematically connectable'. Paragraph (iii) deals with the actual connection procedure.

(i) First order state space representation for blade profile & structure

The vector state and output equation A.83 and A.82 enable straighforward reformulation of the model for the blade profile & structure X_p in a first order state space representation. For this, the angular and linear degree of freedom position variations are clustered in 'position' state subvector $\underline{x}_\mathrm{p}^{X_\mathrm{p}}$ and their time derivatives in 'speed' state subvector $\underline{x}_\mathrm{p}^{X_\mathrm{s}}$. The state and output equation then look like:

$$\begin{bmatrix} \dot{\underline{x}}_\mathrm{p}^{X_\mathrm{p}} \\ \dot{\underline{x}}_\mathrm{s}^{X_\mathrm{p}} \end{bmatrix} = \begin{bmatrix} \mathrm{O} & \boldsymbol{I} \\ \boldsymbol{A}_\mathrm{sp}^{X_\mathrm{p}} & \boldsymbol{A}_\mathrm{ss}^{X_\mathrm{p}} \end{bmatrix} \cdot \begin{bmatrix} \underline{x}_\mathrm{p}^{X_\mathrm{p}} \\ \underline{x}_\mathrm{s}^{X_\mathrm{p}} \end{bmatrix} + \begin{bmatrix} \mathrm{O} & \mathrm{O} & \mathrm{O} & \mathrm{O} \\ \boldsymbol{B}_\mathrm{s}^{X_\mathrm{p}G} & \boldsymbol{B}_\mathrm{s}^{X_\mathrm{p}W} & \boldsymbol{B}_\mathrm{s}^{X_\mathrm{p}R} & \boldsymbol{B}_\mathrm{s}^{X_\mathrm{p}X_\mathrm{f}} \end{bmatrix} \cdot \begin{bmatrix} \underline{v}^{X_\mathrm{p}G} \\ \underline{v}^{X_\mathrm{p}W} \\ \underline{v}^{X_\mathrm{p}R} \\ \underline{v}^{X_\mathrm{p}X_\mathrm{f}} \end{bmatrix} \tag{A.148}$$

$$\begin{bmatrix} \underline{y}^{GX_\mathrm{p}} \\ \underline{y}^{WX_\mathrm{p}} \\ \underline{y}^{X_\mathrm{f}X_\mathrm{p}} \end{bmatrix} = \begin{bmatrix} \boldsymbol{C}_\mathrm{p}^{GX_\mathrm{p}} & \boldsymbol{C}_\mathrm{s}^{GX_\mathrm{p}} \\ \boldsymbol{C}_\mathrm{p}^{WX_\mathrm{p}} & \boldsymbol{C}_\mathrm{s}^{WX_\mathrm{p}} \\ \boldsymbol{C}_\mathrm{p}^{X_\mathrm{f}X_\mathrm{p}} & \boldsymbol{C}_\mathrm{s}^{X_\mathrm{f}X_\mathrm{p}} \end{bmatrix} \cdot \begin{bmatrix} \dot{\underline{x}}_\mathrm{p}^{X_\mathrm{p}} \\ \dot{\underline{x}}_\mathrm{s}^{X_\mathrm{p}} \end{bmatrix} + \begin{bmatrix} \boldsymbol{K}^{GX_\mathrm{p}G} & \boldsymbol{K}^{GX_\mathrm{p}W} & \boldsymbol{K}^{GX_\mathrm{p}R} & \boldsymbol{K}^{GX_\mathrm{p}X_\mathrm{f}} \\ \boldsymbol{K}^{WX_\mathrm{p}G} & \boldsymbol{K}^{WX_\mathrm{p}W} & \boldsymbol{K}^{WX_\mathrm{p}R} & \boldsymbol{K}^{WX_\mathrm{p}X_\mathrm{f}} \\ \boldsymbol{K}^{X_\mathrm{f}X_\mathrm{p}G} & \boldsymbol{K}^{X_\mathrm{f}X_\mathrm{p}W} & \boldsymbol{K}^{X_\mathrm{f}X_\mathrm{p}R} & \boldsymbol{K}^{X_\mathrm{f}X_\mathrm{p}X_\mathrm{f}} \end{bmatrix} \cdot \begin{bmatrix} \underline{v}^{X_\mathrm{p}G} \\ \underline{v}^{X_\mathrm{p}W} \\ \underline{v}^{X_\mathrm{p}R} \\ \underline{v}^{X_\mathrm{p}X_\mathrm{f}} \end{bmatrix} \tag{A.149}$$

The partitions in the state transition matrix, input matrix and output matrix have the following relationship with the mass, spring, damper and input and output matrix partitions in the second order model formulation by Eq. A.83 and Eq. A.82:

$$\begin{aligned} \boldsymbol{A}_\mathrm{sp}^{X_\mathrm{p}} &= -\left(\boldsymbol{M}^{X_\mathrm{p}}\right)^{-1} \cdot \boldsymbol{S}^{X_\mathrm{p}} \quad ; \quad \boldsymbol{A}_\mathrm{ss}^{X_\mathrm{p}} = -\left(\boldsymbol{M}^{X_\mathrm{p}}\right)^{-1} \cdot \boldsymbol{D}^{X_\mathrm{p}} \\ \boldsymbol{B}_\mathrm{s}^{X_\mathrm{p}G} &= \left(\boldsymbol{M}^{X_\mathrm{p}}\right)^{-1} \cdot \boldsymbol{G}^{X_\mathrm{p}E} \quad ; \quad \boldsymbol{B}_\mathrm{s}^{X_\mathrm{p}W} = \left(\boldsymbol{M}^{X_\mathrm{p}}\right)^{-1} \cdot \boldsymbol{G}^{X_\mathrm{p}W} \quad \text{etc.} \\ \boldsymbol{C}_\mathrm{p}^{GX_\mathrm{f}} &= \boldsymbol{H}^{GX_\mathrm{f}} \quad ; \quad \boldsymbol{C}_\mathrm{p}^{WX_\mathrm{f}} = \boldsymbol{H}^{WX_\mathrm{f}} \quad \text{etc.} \\ \boldsymbol{C}_\mathrm{s}^{GX_\mathrm{f}} &= \boldsymbol{L}^{GX_\mathrm{f}} \quad ; \quad \boldsymbol{C}_\mathrm{s}^{WX_\mathrm{f}} = \boldsymbol{L}^{WX_\mathrm{f}} \quad \text{etc.} \end{aligned} \tag{A.150}$$

All feedthrough matrix partitions are equal to those in Eq. A.82.

(ii) Reorganisation of input and output vectors

We now cluster the input and output subvectors that do not interact with the blade flange in the external input and output vectors $\underline{v}^{X_\mathrm{p}E}$ and $\underline{y}^{EX_\mathrm{p}}$:

$$\underline{v}^{X_\mathrm{p}E} \triangleq \begin{bmatrix} \underline{v}^{X_\mathrm{p}G} \\ \underline{v}^{X_\mathrm{p}W} \\ \underline{v}^{X_\mathrm{p}R} \end{bmatrix} \quad ; \quad \underline{y}^{EX_\mathrm{p}} \triangleq \begin{bmatrix} \underline{y}^{GX_\mathrm{p}} \\ \underline{y}^{WX_\mathrm{p}} \end{bmatrix} \tag{A.151}$$

With a focus on connection to the flange model, thestate space representation is compactly formulated (use short-hand superscript 'fpe' instead of $X_\mathrm{f}X_\mathrm{p}E$ etc.)

$$\begin{aligned} \begin{bmatrix} \dot{\underline{x}}_\mathrm{p}^\mathrm{p} \\ \dot{\underline{x}}_\mathrm{s}^\mathrm{p} \end{bmatrix} &= \begin{bmatrix} \mathrm{O} & \boldsymbol{I} \\ \boldsymbol{A}_\mathrm{sp}^\mathrm{p} & \boldsymbol{A}_\mathrm{ss}^\mathrm{p} \end{bmatrix} \cdot \begin{bmatrix} \underline{x}_\mathrm{p}^\mathrm{p} \\ \underline{x}_\mathrm{s}^\mathrm{p} \end{bmatrix} + \begin{bmatrix} \mathrm{O} & \mathrm{O} \\ \boldsymbol{B}_\mathrm{s}^\mathrm{pe} & \boldsymbol{B}_\mathrm{s}^\mathrm{pf} \end{bmatrix} \cdot \begin{bmatrix} \underline{v}^\mathrm{pe} \\ \underline{v}^\mathrm{pf} \end{bmatrix} \\ \begin{bmatrix} \underline{y}^\mathrm{ep} \\ \underline{y}^\mathrm{fp} \end{bmatrix} &= \begin{bmatrix} \boldsymbol{C}_\mathrm{p}^\mathrm{ep} & \boldsymbol{C}_\mathrm{s}^\mathrm{ep} \\ \boldsymbol{C}_\mathrm{p}^\mathrm{fp} & \boldsymbol{C}_\mathrm{s}^\mathrm{fp} \end{bmatrix} \cdot \begin{bmatrix} \underline{x}_\mathrm{p}^\mathrm{p} \\ \underline{x}_\mathrm{s}^\mathrm{p} \end{bmatrix} + \begin{bmatrix} \boldsymbol{K}^\mathrm{epe} & \boldsymbol{K}^\mathrm{epf} \\ \boldsymbol{K}^\mathrm{fpe} & \boldsymbol{K}^\mathrm{fpf} \end{bmatrix} \cdot \begin{bmatrix} \underline{v}^\mathrm{pe} \\ \underline{v}^\mathrm{pf} \end{bmatrix} \end{aligned} \tag{A.152}$$

Note that te state transition matrix partitions equal are to those in Eq. A.148. The input matrix partition $\boldsymbol{B}^\mathrm{pe}$ clusters the first three input matrix partitions in Eq. A.148. The feedthrough matrix partition $\boldsymbol{K}^\mathrm{epe}$ clusters the first three columns in the first two rows of the feedthrough matrix in A.149. Etc.

We also cluster the input and output subvectors of the blade flange X_f that do not interact with the profile & structure in the external input and output vectors $\underline{v}^{X_\mathrm{f}E}$ and $\underline{y}^{EX_\mathrm{f}}$:

$$\underline{v}^{X_\mathrm{f}E} \triangleq \begin{bmatrix} \underline{v}^{X_\mathrm{f}G} \\ \underline{v}^{X_\mathrm{f}W} \\ \underline{v}^{X_\mathrm{f}R} \end{bmatrix} \quad ; \quad \underline{y}^{EX_\mathrm{f}} \triangleq \begin{bmatrix} \underline{y}^{GX_\mathrm{f}} \\ \underline{y}^{WX_\mathrm{f}} \\ \underline{y}^{RX_\mathrm{f}} \end{bmatrix} \tag{A.153}$$

The compact notation for the flange's state space representation by Eq. A.146 and A.147

then becomes (use short-hand superscript 'pfe' instead of $X_{\rm p}X_{\rm f}E$ etc.):

$$\begin{bmatrix} \underline{\dot{x}}^{\rm f}_{\rm p} \\ \underline{\dot{x}}^{\rm f}_{\rm s} \\ \underline{\dot{x}}^{\rm f}_{\rm o} \end{bmatrix} = \begin{bmatrix} {\rm O} & \boldsymbol{I} & {\rm O} \\ \boldsymbol{A}^{\rm f}_{\rm sp} & \boldsymbol{A}^{\rm f}_{\rm ss} & \boldsymbol{A}^{\rm f}_{\rm so} \\ \boldsymbol{A}^{\rm f}_{\rm op} & \boldsymbol{A}^{\rm f}_{\rm os} & \boldsymbol{A}^{\rm f}_{\rm oo} \end{bmatrix} \cdot \begin{bmatrix} \underline{x}^{\rm f}_{\rm p} \\ \underline{x}^{\rm f}_{\rm s} \\ \underline{x}^{\rm f}_{\rm o} \end{bmatrix} + \begin{bmatrix} {\rm O} & {\rm O} \\ \boldsymbol{B}^{\rm fe}_{\rm s} & \boldsymbol{B}^{\rm fp}_{\rm s} \\ \boldsymbol{B}^{\rm fe}_{\rm o} & \boldsymbol{B}^{\rm fp}_{\rm o} \end{bmatrix} \cdot \begin{bmatrix} \underline{v}^{\rm fe} \\ \underline{v}^{\rm fp} \end{bmatrix}$$

$$\begin{bmatrix} \underline{y}^{\rm ef} \\ \underline{y}^{\rm pf} \end{bmatrix} = \begin{bmatrix} \boldsymbol{C}^{\rm ef}_{\rm p} & \boldsymbol{C}^{\rm ef}_{\rm s} & \boldsymbol{C}^{\rm ef}_{\rm o} \\ \boldsymbol{C}^{\rm pf}_{\rm p} & \boldsymbol{C}^{\rm pf}_{\rm s} & \boldsymbol{C}^{\rm pf}_{\rm o} \end{bmatrix} \cdot \begin{bmatrix} \underline{x}^{\rm f}_{\rm p} \\ \underline{x}^{\rm f}_{\rm s} \\ \underline{x}^{\rm f}_{\rm o} \end{bmatrix} + \begin{bmatrix} \boldsymbol{K}^{\rm efe} & \boldsymbol{K}^{\rm efp} \\ \boldsymbol{K}^{\rm pfe} & \boldsymbol{K}^{\rm pfp} \end{bmatrix} \cdot \begin{bmatrix} \underline{v}^{\rm fe} \\ \underline{v}^{\rm fp} \end{bmatrix} \tag{A.154}$$

Note that te state transition matrix partitions are equal to those in Eq. A.146. The input matrix partition $\boldsymbol{B}^{\rm fe}_{\rm s}$ clusters the first four input matrix partitions in the second row of Eq. A.148. Etc.

(iii) Connection of the flange model with the profile & structure model

The connection conditions are

$$\underline{v}^{\rm fp} = \underline{y}^{\rm fp} \quad \text{and} \quad \underline{v}^{\rm pf} = \underline{y}^{\rm pf} \tag{A.155}$$

Substitution of the connection conditions in the 'lower part' in the output equation of both models yields the explicit expression for the 'internal' output subvectors in the state (sub)vectors and the 'external' input subvectors:

$$\begin{bmatrix} \underline{v}^{\rm fp} \\ \underline{v}^{\rm pf} \end{bmatrix} \overset{\substack{\text{connection}\\ \text{condition}}}{=} \begin{bmatrix} \underline{y}^{\rm fp} \\ \underline{y}^{\rm pf} \end{bmatrix} = \boldsymbol{Q} \cdot \Bigg(\begin{bmatrix} {\rm O} & \boldsymbol{C}^{\rm fp}_{\rm p} & {\rm O} & \boldsymbol{C}^{\rm fp}_{\rm s} & {\rm O} \\ \boldsymbol{C}^{\rm pf}_{\rm p} & {\rm O} & \boldsymbol{C}^{\rm pf}_{\rm s} & {\rm O} & \boldsymbol{C}^{\rm pf}_{\rm o} \end{bmatrix} \cdot \begin{bmatrix} \underline{x}^{\rm f}_{\rm p} \\ \underline{x}^{\rm p}_{\rm p} \\ \underline{x}^{\rm f}_{\rm s} \\ \underline{x}^{\rm p}_{\rm s} \\ \underline{x}^{\rm f}_{\rm o} \end{bmatrix} +$$

$$\begin{bmatrix} {\rm O} & \boldsymbol{K}^{\rm fpe} \\ \boldsymbol{K}^{\rm pfe} & {\rm O} \end{bmatrix} \cdot \begin{bmatrix} \underline{v}^{\rm fe} \\ \underline{v}^{\rm pe} \end{bmatrix} \Bigg) \quad \text{with} \quad \boldsymbol{Q} = \begin{bmatrix} \boldsymbol{I} & -\boldsymbol{K}^{\rm fpf} \\ -\boldsymbol{K}^{\rm pfp} & \boldsymbol{I} \end{bmatrix}^{-1} \cdot \tag{A.156}$$

The model connection is established by substition of the equation above in the state equation and in the 'external' output equation of the integrated model. For this we split up the input part in the integrated model formulation into the 'interaction part', driven by $\left[\underline{v}^{\rm fp\,T}\ \underline{v}^{\rm pf\,T}\right]^{\rm T}$, and the 'external' part, driven by $\underline{v}^{\rm e^*}$, which is the envelope of the subcomponent external input vectors $\underline{v}^{\rm fe}$ and $\underline{v}^{\rm pe}$:

$$\begin{bmatrix} \underline{\dot{x}}^{\rm f}_{\rm p} \\ \underline{\dot{x}}^{\rm p}_{\rm p} \\ \underline{\dot{x}}^{\rm f}_{\rm s} \\ \underline{\dot{x}}^{\rm p}_{\rm s} \\ \underline{\dot{x}}^{\rm f}_{\rm o} \end{bmatrix} = \begin{bmatrix} {\rm O} & {\rm O} & \boldsymbol{I} & {\rm O} & {\rm O} \\ {\rm O} & {\rm O} & {\rm O} & \boldsymbol{I} & {\rm O} \\ \boldsymbol{A}^{\rm f}_{\rm sp} & {\rm O} & \boldsymbol{A}^{\rm f}_{\rm ss} & {\rm O} & \boldsymbol{A}^{\rm f}_{\rm so} \\ {\rm O} & \boldsymbol{A}^{\rm p}_{\rm sp} & {\rm O} & \boldsymbol{A}^{\rm p}_{\rm ss} & {\rm O} \\ \boldsymbol{A}^{\rm f}_{\rm op} & {\rm O} & \boldsymbol{A}^{\rm f}_{\rm os} & {\rm O} & \boldsymbol{A}^{\rm f}_{\rm oo} \end{bmatrix} \cdot \begin{bmatrix} \underline{x}^{\rm f}_{\rm p} \\ \underline{x}^{\rm p}_{\rm p} \\ \underline{x}^{\rm f}_{\rm s} \\ \underline{x}^{\rm p}_{\rm s} \\ \underline{x}^{\rm f}_{\rm o} \end{bmatrix} +$$

$$\begin{bmatrix} {\rm O} & {\rm O} \\ {\rm O} & {\rm O} \\ \boldsymbol{B}^{\rm fp}_{\rm s} & {\rm O} \\ {\rm O} & \boldsymbol{B}^{\rm pf}_{\rm s} \\ \boldsymbol{B}^{\rm fp}_{\rm o} & {\rm O} \end{bmatrix} \cdot \begin{bmatrix} \underline{v}^{\rm fp} \\ \underline{v}^{\rm pf} \end{bmatrix} + \begin{bmatrix} {\rm O} \\ {\rm O} \\ \boldsymbol{B}^{\rm fe^*}_{\rm s} \\ \boldsymbol{B}^{\rm pe^*}_{\rm s} \\ \boldsymbol{B}^{\rm fe^*}_{\rm o} \end{bmatrix} \cdot \underline{v}^{\rm e^*}$$

and

$$\begin{bmatrix} \underline{y}^{\mathrm{ef}} \\ \underline{y}^{\mathrm{ep}} \end{bmatrix} = \begin{bmatrix} \boldsymbol{C}_{\mathrm{p}}^{\mathrm{ef}} & \mathrm{O} & \boldsymbol{C}_{\mathrm{s}}^{\mathrm{ef}} & \mathrm{O} & \boldsymbol{C}_{\mathrm{o}}^{\mathrm{ef}} \\ \mathrm{O} & \boldsymbol{C}_{\mathrm{p}}^{\mathrm{ep}} & \mathrm{O} & \boldsymbol{C}_{\mathrm{s}}^{\mathrm{ep}} & \mathrm{O} \end{bmatrix} \cdot \begin{bmatrix} \underline{x}_{\mathrm{p}}^{\mathrm{f}} \\ \underline{x}_{\mathrm{p}}^{\mathrm{p}} \\ \underline{x}_{\mathrm{s}}^{\mathrm{f}} \\ \underline{x}_{\mathrm{s}}^{\mathrm{p}} \\ \underline{x}_{\mathrm{o}}^{\mathrm{f}} \end{bmatrix} + \begin{bmatrix} \boldsymbol{K}^{\mathrm{efp}} & \mathrm{O} \\ \mathrm{O} & \boldsymbol{K}^{\mathrm{epf}} \end{bmatrix} \cdot \begin{bmatrix} \underline{v}^{\mathrm{fp}} \\ \underline{v}^{\mathrm{pf}} \end{bmatrix} + \begin{bmatrix} \boldsymbol{K}^{\mathrm{efe}^*} \\ \boldsymbol{K}^{\mathrm{epe}^*} \end{bmatrix} \cdot \underline{v}^{\mathrm{e}^*} \tag{A.157}$$

The input matrix $\boldsymbol{B}_{\mathrm{s}}^{\mathrm{pe}^*}$ is composed of $\boldsymbol{B}_{\mathrm{s}}^{\mathrm{pe}}$ and all-zero columns for all input variables that are in $\underline{v}^{\mathrm{fe}}$ but not in $\underline{v}^{\mathrm{pe}}$ (see Eq. A.50, A.98; interaction inputs excluded). The input matrices $\boldsymbol{B}_{\mathrm{s}}^{\mathrm{fe}^*}$ and $\boldsymbol{B}_{\mathrm{o}}^{\mathrm{fe}^*}$ do not differ from $\boldsymbol{B}_{\mathrm{s}}^{\mathrm{fe}}$ and $\boldsymbol{B}_{\mathrm{o}}^{\mathrm{fe}}$ because input vector $\underline{v}^{\mathrm{fe}}$ includes all elements of $\underline{v}^{\mathrm{pe}}$.

The feedthrough matrix $\boldsymbol{K}^{\mathrm{epe}^*}$ is composed of $\boldsymbol{K}^{\mathrm{epe}}$ and all-zero columns for all input variables that are in $\underline{v}^{\mathrm{fe}}$ but not in $\underline{v}^{\mathrm{pe}}$; $\boldsymbol{K}^{\mathrm{efe}^*}$ equals $\boldsymbol{K}^{\mathrm{efe}}$.

Substitution of Eq. A.156 in and clustering the 'position' and 'speed' state subvectors in $\underline{x}_{\mathrm{p}}^{X}$ and $\underline{x}_{\mathrm{s}}^{X}$ yields the pursued first order state space representation of the overall rotor blade model:

$$\begin{bmatrix} \underline{\dot{x}}_{\mathrm{p}}^{X} \\ \underline{\dot{x}}_{\mathrm{s}}^{X} \\ \underline{\dot{x}}_{\mathrm{o}}^{X} \end{bmatrix} = \begin{bmatrix} \mathrm{O} & \boldsymbol{I} & \mathrm{O} \\ \boldsymbol{A}_{\mathrm{sp}}^{X} & \boldsymbol{A}_{\mathrm{ss}}^{X} & \boldsymbol{A}_{\mathrm{so}}^{X} \\ \boldsymbol{A}_{\mathrm{op}}^{X} & \boldsymbol{A}_{\mathrm{os}}^{X} & \boldsymbol{A}_{\mathrm{oo}}^{X} \end{bmatrix} \cdot \begin{bmatrix} \underline{x}_{\mathrm{p}}^{X} \\ \underline{x}_{\mathrm{s}}^{X} \\ \underline{x}_{\mathrm{o}}^{X} \end{bmatrix} + \begin{bmatrix} \mathrm{O} & \mathrm{O} & \mathrm{O} \\ \boldsymbol{B}_{\mathrm{s}}^{XG} & \boldsymbol{B}_{\mathrm{s}}^{XW} & \boldsymbol{B}_{\mathrm{s}}^{XR} \\ \boldsymbol{B}_{\mathrm{o}}^{XG} & \boldsymbol{B}_{\mathrm{o}}^{XW} & \boldsymbol{B}_{\mathrm{o}}^{XR} \end{bmatrix} \cdot \begin{bmatrix} \underline{v}^{XG} \\ \underline{v}^{XW} \\ \underline{v}^{XR} \end{bmatrix}$$

$$\begin{bmatrix} \underline{y}^{GX} \\ \underline{y}^{WX} \\ \underline{y}^{RX} \end{bmatrix} = \begin{bmatrix} C_{\mathrm{p}}^{GX} & C_{\mathrm{s}}^{GX} & C_{\mathrm{o}}^{GX} \\ C_{\mathrm{p}}^{WX} & C_{\mathrm{s}}^{WX} & C_{\mathrm{o}}^{WX} \\ C_{\mathrm{p}}^{RX} & C_{\mathrm{s}}^{RX} & C_{\mathrm{o}}^{RX} \end{bmatrix} \cdot \begin{bmatrix} \underline{x}_{\mathrm{p}}^{X} \\ \underline{x}_{\mathrm{s}}^{X} \\ \underline{x}_{\mathrm{o}}^{X} \end{bmatrix} + \begin{bmatrix} K^{GXG} & K^{GXW} & K^{GXR} \\ K^{WXG} & K^{WXW} & K^{WXR} \\ K^{RXG} & K^{RXW} & K^{RXR} \end{bmatrix} \cdot \begin{bmatrix} \underline{v}^{XG} \\ \underline{v}^{XW} \\ \underline{v}^{XR} \end{bmatrix} \tag{A.158}$$

Note that the input subvectors are equal to those as specified for the flange in Eq. A.98.

The lower partitions of the state transition matrix $\boldsymbol{A}^{X}$ are obtained as:

$$\begin{bmatrix} \boldsymbol{A}_{\mathrm{sp}}^{X} & \boldsymbol{A}_{\mathrm{ss}}^{X} & \boldsymbol{A}_{\mathrm{so}}^{X} \\ \boldsymbol{A}_{\mathrm{op}}^{X} & \boldsymbol{A}_{\mathrm{os}}^{X} & \boldsymbol{A}_{\mathrm{oo}}^{X} \end{bmatrix} = \begin{bmatrix} \begin{bmatrix} \boldsymbol{A}_{\mathrm{sp}}^{\mathrm{f}} & \mathrm{O} \\ \mathrm{O} & \boldsymbol{A}_{\mathrm{sp}}^{\mathrm{p}} \end{bmatrix} & \begin{bmatrix} \boldsymbol{A}_{\mathrm{ss}}^{\mathrm{f}} & \mathrm{O} \\ \mathrm{O} & \boldsymbol{A}_{\mathrm{ss}}^{\mathrm{p}} \end{bmatrix} & \begin{bmatrix} \boldsymbol{A}_{\mathrm{so}}^{\mathrm{f}} \\ \mathrm{O} \end{bmatrix} \\ \begin{bmatrix} \boldsymbol{A}_{\mathrm{op}}^{\mathrm{f}} & \mathrm{O} \end{bmatrix} & \begin{bmatrix} \boldsymbol{A}_{\mathrm{os}}^{\mathrm{f}} & \mathrm{O} \end{bmatrix} & \begin{bmatrix} \boldsymbol{A}_{\mathrm{oo}}^{\mathrm{f}} \end{bmatrix} \end{bmatrix} + \begin{bmatrix} \begin{bmatrix} \boldsymbol{B}_{\mathrm{s}}^{\mathrm{fp}} & \mathrm{O} \\ \mathrm{O} & \boldsymbol{B}_{\mathrm{s}}^{\mathrm{pf}} \end{bmatrix} \\ \begin{bmatrix} \boldsymbol{B}_{\mathrm{o}}^{\mathrm{fp}} & \mathrm{O} \end{bmatrix} \end{bmatrix} \cdot \boldsymbol{Q} \cdot \begin{bmatrix} \begin{bmatrix} \mathrm{O} & \boldsymbol{C}_{\mathrm{p}}^{\mathrm{fp}} \\ \boldsymbol{C}_{\mathrm{p}}^{\mathrm{pf}} & \mathrm{O} \end{bmatrix} & \begin{bmatrix} \mathrm{O} & \boldsymbol{C}_{\mathrm{s}}^{\mathrm{fp}} \\ \boldsymbol{C}_{\mathrm{s}}^{\mathrm{pf}} & \mathrm{O} \end{bmatrix} & \begin{bmatrix} \mathrm{O} \\ \boldsymbol{C}_{\mathrm{o}}^{\mathrm{pf}} \end{bmatrix} \end{bmatrix} \tag{A.159}$$

The lower partitions of the input matrix $\boldsymbol{B}^{X}$ are obtained as:

$$\begin{bmatrix} \boldsymbol{B}_{\mathrm{s}}^{XG} & \dots & \boldsymbol{B}_{\mathrm{s}}^{XR} \\ \boldsymbol{B}_{\mathrm{o}}^{XG} & \dots & \boldsymbol{B}_{\mathrm{o}}^{XR} \end{bmatrix} \cdot = \begin{bmatrix} \begin{bmatrix} \boldsymbol{B}_{\mathrm{s}}^{\mathrm{fe}^*} \\ \boldsymbol{B}_{\mathrm{s}}^{\mathrm{pe}^*} \end{bmatrix} \\ \begin{bmatrix} \boldsymbol{B}_{\mathrm{o}}^{\mathrm{fe}^*} \end{bmatrix} \end{bmatrix} + \begin{bmatrix} \begin{bmatrix} \boldsymbol{B}_{\mathrm{s}}^{\mathrm{fp}} & \mathrm{O} \\ \mathrm{O} & \boldsymbol{B}_{\mathrm{s}}^{\mathrm{pf}} \end{bmatrix} \\ \begin{bmatrix} \boldsymbol{B}_{\mathrm{o}}^{\mathrm{fp}} & \mathrm{O} \end{bmatrix} \end{bmatrix} \cdot \boldsymbol{Q} \cdot \begin{bmatrix} \boldsymbol{K}^{\mathrm{fpe}^*} \\ \boldsymbol{K}^{\mathrm{pfe}^*} \end{bmatrix} \tag{A.160}$$

The feedthrough matrix $\boldsymbol{K}^{\mathrm{fpe}^*}$ is composed of $\boldsymbol{K}^{\mathrm{fpe}}$ and all-zero columns for all input variables that are in $\underline{v}^{\mathrm{fe}}$ but not in $\underline{v}^{\mathrm{pe}}$; $\boldsymbol{K}^{\mathrm{pfe}^*}$ equals $\boldsymbol{K}^{\mathrm{pfe}}$.

Similar expressions hold for the output and feedthroug matrix. However, first the following intermediate output and feedthrough matrices are calcualted:

$$\begin{bmatrix} \boldsymbol{C}_{\mathrm{p}}^{\mathrm{ef}X} & \boldsymbol{C}_{\mathrm{s}}^{\mathrm{ef}X} & \boldsymbol{C}_{\mathrm{o}}^{\mathrm{ef}X} \\ \boldsymbol{C}_{\mathrm{p}}^{\mathrm{pf}X} & \boldsymbol{C}_{\mathrm{s}}^{\mathrm{pf}X} & \boldsymbol{C}_{\mathrm{o}}^{\mathrm{pf}X} \end{bmatrix} = \left[\begin{bmatrix} \boldsymbol{C}_{\mathrm{p}}^{\mathrm{ef}} & \mathrm{O} \\ \mathrm{O} & \boldsymbol{C}_{\mathrm{p}}^{\mathrm{ep}} \end{bmatrix} \begin{bmatrix} \boldsymbol{C}_{\mathrm{s}}^{\mathrm{ef}} & \mathrm{O} \\ \mathrm{O} & \boldsymbol{C}_{\mathrm{s}}^{\mathrm{ep}} \end{bmatrix} \begin{bmatrix} \boldsymbol{C}_{\mathrm{o}}^{\mathrm{ef}} \\ \mathrm{O} \end{bmatrix} \right] + \begin{bmatrix} \boldsymbol{K}^{\mathrm{efp}} & \mathrm{O} \\ \mathrm{O} & \boldsymbol{K}^{\mathrm{epf}} \end{bmatrix} \cdot \boldsymbol{Q} \cdot \left[\begin{bmatrix} \mathrm{O} & \boldsymbol{C}_{\mathrm{p}}^{\mathrm{fp}} \\ \boldsymbol{C}_{\mathrm{p}}^{\mathrm{pf}} & \mathrm{O} \end{bmatrix} \begin{bmatrix} \mathrm{O} & \boldsymbol{C}_{\mathrm{s}}^{\mathrm{fp}} \\ \boldsymbol{C}_{\mathrm{s}}^{\mathrm{pf}} & \mathrm{O} \end{bmatrix} \begin{bmatrix} \mathrm{O} \\ \boldsymbol{C}_{\mathrm{o}}^{\mathrm{pf}} \end{bmatrix} \right] \tag{A.161}$$

and

$$\begin{bmatrix} \boldsymbol{K}_{\mathrm{c}}^{\mathrm{efe}^*} \\ \boldsymbol{K}_{\mathrm{c}}^{\mathrm{epe}^*} \end{bmatrix} = \begin{bmatrix} \boldsymbol{K}^{\mathrm{efe}^*} \\ \boldsymbol{K}^{\mathrm{epe}^*} \end{bmatrix} + \begin{bmatrix} \boldsymbol{K}^{\mathrm{efp}} & \mathrm{O} \\ \mathrm{O} & \boldsymbol{K}^{\mathrm{epf}} \end{bmatrix} \cdot \boldsymbol{Q} \cdot \begin{bmatrix} \boldsymbol{K}^{\mathrm{fpe}^*} \\ \boldsymbol{K}^{\mathrm{pfe}^*} \end{bmatrix} \tag{A.162}$$

Afterward the rows of these matrices have to be interchanged in order to reorganise the output vector from $[\ \underline{y}^{\mathrm{ef}\mathrm{T}}\ \ \underline{y}^{\mathrm{ep}\mathrm{T}}\ ]^{\mathrm{T}}$, into $[\ \underline{y}^{GX\mathrm{T}}\ \ \underline{y}^{WX\mathrm{T}}\ \ \underline{y}^{RX\mathrm{T}}\ ]^{\mathrm{T}}$, and thus to obtain the output and feedthrough matrix by Eq. A.158. The differently organised output vectors are given by (see Eq. A.72 and A.115 for the variables in the subvectors):

$$\begin{bmatrix} \underline{y}^{\mathrm{ef}} \\ \underline{y}^{\mathrm{ep}} \end{bmatrix} = \begin{bmatrix} \underline{y}^{GX_{\mathrm{f}}} \\ \underline{y}^{WX_{\mathrm{f}}} \\ \underline{y}^{RX_{\mathrm{f}}} \\ \underline{y}^{GX_{\mathrm{p}}} \\ \underline{y}^{WX_{\mathrm{p}}} \end{bmatrix} \quad ; \quad \begin{bmatrix} \underline{y}^{GX} \\ \underline{y}^{WX} \\ \underline{y}^{RX} \end{bmatrix} = \begin{bmatrix} y_1^{GX_{\mathrm{f}}} \\ \vdots \\ y_3^{GX_{\mathrm{f}}} \\ \underline{y}^{GX_{\mathrm{p}}} \\ y_4^{GX_{\mathrm{f}}} \\ \vdots \\ y_9^{GX_{\mathrm{f}}} \\ y_{10}^{GX_{\mathrm{f}}} \\ \underline{y}^{WX_{\mathrm{f}}} \\ \underline{y}^{WX_{\mathrm{p}}} \\ \underline{y}^{RX_{\mathrm{f}}} \end{bmatrix} \tag{A.163}$$

The exogeneous and interaction inputs for the overall blade model are described in section 3.4.2 and section A.1, paragraph (ii).

A.3 Wake model

The model for the dynamic wake behaviour is obtained with M-function tbuwakeeom(). The state vector consists of the 'ensemble average' axial induction speed variations in the rotor annuli (average over B instantaneous values) and optionally also the 'ensemble average' tangental induction speed variations. For the modelling equations see section **??**.

A.3.1 Equations of motion for the rotor annuli

This section includes three paragraphs.In paragraph (i) the required exogeneous and interaction input variables are derived from the 'influcence variables' in the linearised equations. In paragraph (ii) the vector state equation is derived for the transient behaviour. Finally the vector output equation is derived in in paragraph (iv) and the vector state and output equation are lumped together to the first order state space representation of the 'dynamic wake model'.

The component model for the wake W is obtained by a call to TBUWAKEEOM() in function TBUAEROEOM(). The model exists as structure variables sysW. The fields in are 2D matrices A, B, C, K, the parameterisation of the first order state space representation, and cell arrays with lists of input, output and state variable names. Point of departure for the wake model creation by function TBUWAKEEOM() is the availability of (c.s: final coordinate system):

- means and sensitivities of angular and linear impulse vector in the rotor annuli (along f.c.s. of X_1 in actual position);
- means and sensitivities of Prandtl's correction factor and transportation velocity in the rotor annuli;
- means of aerodynamic reaction forces on the wake on blade elements $X_1 \ldots X_n$ (lift only; along annulus wise c.s. of X_k in actual position);
- means of axial and tangential induction speeds in the rotor annuli;
- radius and width of the rotor annuli and number of rotor blades;
- mapping table between blade elements and rotor annuli;
- flag for wake modelling (equilibrium, frozen, ECN differential equation wake model);
- multiplier for the time constants for the tangential induction speed transients relative to the axial induction speed transients in the rotor annuli (0.1 implies ten times as fast transient behaviour for the tangential induction speed).

The mentioned sensitivities belong to the 'motion and load formulations' and map all motion and load variations to input variables from the support structure (wind orientation change) or the environment (wind turbulence, tower shadow, shear). These are provided by a preceeding function call in TBUAEREOM() to TBUWAKEFLOW() (see section 2.2.1).

Functionality TBUWAKEEOM():

- definition of input name lists; each list contains the names of the input subvectors from a specific source (G, D, E, F, S);
- definition of output name lists; each list containts the names of the output subvectors to a specific destination (G, D, E, F);
- calculate average overall axial and tangential forces on the rotor annuli;
- assemble state transition, input and output matrix $\{\boldsymbol{A}, \boldsymbol{B}, \boldsymbol{C}\}$ for the wake model and feedthrough matrix $\boldsymbol{K} := \mathrm{O}$ (see par. (iii) and (iv));
- create name lists for the *individual elements* in the input and output subvectors;
- if flag for equilibrium wake ON : $\boldsymbol{K} := -\boldsymbol{C} \cdot \boldsymbol{A}^{-1} \cdot \boldsymbol{B}$ and $\boldsymbol{C} := \mathrm{O}$;
- if flag for frozen wake ON : $\boldsymbol{C} := \mathrm{O}$.

(i) Input variables

The differential equation in Eq. 3.24 and the algebraic equation or differential equation for the tangential induction speed in Eq. 3.26 implicetely tell which input variables are required.

The variations in the axial and tangential lift force reactions from the rotor blades are inputs that are provided via the output subvectors $\underline{y}^{WD}$, $\underline{y}^{WE}$, $\underline{y}^{WF}$ of the rotor blade state space model.

The variations in Prandtl's correction factor and the transportion speed depend on the axial, transverse and vertical ('undisturbed') wind speed variations in the intersection of the blade elements with the rotor plane, and on the axial induction speed (see section B.8, Eq. 3.30). The undisturbed wind speed variations are partially exogeneous and partially a result of the dynamic deformation, vizually the tilting and yawing of the rotor plane through tower deformation. section B.8.1 yields the following expression for the undisturbed variations:

$$\delta \underline{u}^{W_m/X/R_{\rm fx}} \triangleq \begin{bmatrix} \delta U_{\rm ax}^{W_m/X} \\ \delta U_{\rm yaw}^{W_m/X} \\ \delta U_{\rm tilt}^{W_m/X} \end{bmatrix} = \frac{\partial \underline{u}^{W_m/X/R_{\rm fx}}}{\partial \underline{u}_{\rm sto}^{W/X/R_{\rm fx}}} \cdot \underline{u}_{\rm sto}^{W/X/R_{\rm fx}} + \frac{\partial \underline{u}^{W_m/X/R_{\rm fx}}}{\partial \underline{u}_{\rm per}^{X/R_{\rm fx}}} \cdot \underline{u}_{\rm per}^{X/R_{\rm fx}} + \underline{u}_{\rm ori}^{S_{\rm n}} \tag{A.164}$$

The sensitivity to the overall turbulence vector $\underline{u}_{\rm sto}^{W/X}$ in the intersection of blade X with the annuli selects the appropriate annulus. The periodic variations $\underline{u}_{\rm per}^{X/R_{\rm fx}}$ are already expressed in the rotor plane directions so that the sensitivity matrix only selects the appropriate blade element. These periodic variations are only caused by the tower stagnation and wind shear (${}^{\rm r}u^{X_k^{\rm a}}$ and by the axial induction variation from oblique inflow ($-U_{\rm iobl}^{X_k}$).

The undisturbed oblique inflow average wind speed components now contribute to the average *transverse and vertical wind speed. The modulation with the rotational speed only occurs when the oblique inflow is considered 'blade relative'. The average oblique inflow then contributes to the* periodic *wind speed variatons on the blade profile!*

The wind speed variation $\underline{u}_{\rm ori}^{S_{\rm n}}$ is caused by the orientation change of the rotor plane relative to the average longitudinal wind speed. The orientation of the rotor plane coincides with that of the nacelle $S_{\rm n}$, so the variation $\underline{u}_{\rm ori}^{S_{\rm n}}$ is caused by angular position variations in all elements of the support structure. The tilting and yawing of the rotor plane by shaft bending is neglected because it introduces periodic coefficients that pertain to degrees of freedom in the *rotating part* of the windturbine. These cannot be eliminated via the Coleman transformation.

The composition of the input vector $\underline{v}^W$ to the wake model is (see also paragraph (ii) in section A.1):

$$\underline{v}^W = \begin{bmatrix} \underline{v}^{WG} \\ \underline{v}^{WD} \\ \underline{v}^{WE} \\ \underline{v}^{WF} \\ \underline{v}^{WS} \end{bmatrix} \quad \text{with} \quad \underline{v}^{WG} = \begin{bmatrix} \underline{u}_{\rm per}^{D/R_{\rm fx}} \\ \underline{u}_{\rm per}^{E/R_{\rm fx}} \\ \underline{u}_{\rm per}^{F/R_{\rm fx}} \\ \underline{u}_{\rm sto}^{W/D/R_{\rm fx}} \\ \underline{u}_{\rm sto}^{W/E/R_{\rm fx}} \\ \underline{u}_{\rm sto}^{W/F/R_{\rm fx}} \end{bmatrix} \; ; \; \underline{v}^{WS} = \begin{bmatrix} \underline{u}_{\rm ori}^{S_{\rm n}} \end{bmatrix} \quad \text{and}$$

$$\underline{v}^{WD} = \begin{bmatrix} {}^{\rm a_L}\underline{f}^{W_m/D_1} \\ \vdots \\ {}^{\rm a_L}\underline{f}^{W_m/D_N} \end{bmatrix} \; ; \; \underline{v}^{WE} = \begin{bmatrix} {}^{\rm a_L}\underline{f}^{W_m/E_1} \\ \vdots \\ {}^{\rm a_L}\underline{f}^{W_m/E_N} \end{bmatrix} \; ; \; \underline{v}^{WF} = \begin{bmatrix} {}^{\rm a_L}\underline{f}^{W_m/F_1} \\ \vdots \\ {}^{\rm a_L}\underline{f}^{W_m/F_N} \end{bmatrix} \tag{A.165}$$

(ii) First order vector state equation

The available partial derivatives for Prandtl's correction factor and the transportation speed enable to formulate the equations of motion for the as a first order vector state equation. The input matrix is partitioned in accordance with the organisation of the input vector $\underline{v}^W$

in exogeneous and interaction input subvectors. If we also assume transient behaviour for the tangential induction the state equation is:

$$\begin{aligned} \underline{\dot{x}}_{\mathrm{o}}^{W} &= \boldsymbol{A}^{W} \cdot \underline{x}_{\mathrm{o}}^{W} + [\ \boldsymbol{B}^{WG}\ \boldsymbol{B}^{WD}\ \boldsymbol{B}^{WE}\ \boldsymbol{B}^{WF}\ \boldsymbol{B}^{WS}\ ] \cdot \begin{bmatrix} \underline{v}^{WG} \\ \underline{v}^{WD} \\ \underline{v}^{WE} \\ \underline{v}^{WF} \\ \underline{v}^{WS} \end{bmatrix} \\ \text{with} \quad \underline{x}_{\mathrm{o}}^{W} &= [\ U^{W_1}\ V^{W_1}\ \ldots\ U^{W_P}\ V^{W_P}\ ]^{\mathrm{T}} \end{aligned} \tag{A.166}$$

The subscript 'o' is attributed to the state vector because the state equations are by nature of the first order.

The rows $\underline{\boldsymbol{a}}_{\mathrm{ax}}^{W_m}$, with ranking numbers $2(\mathrm{m}-1)+1$ in the state transition matrix $\boldsymbol{A}^{W}$, are determined as follows (see Eq. B.8.3 and B.255 for the partial derivatives of $F_{\mathrm{p}}^{W_m}$ and $U_{\mathrm{tr}}^{W_m}$) :

$$\begin{aligned} \underline{\boldsymbol{a}}_{\mathrm{ax}}^{W_m} = & \left(-\frac{\bar{U}_{\mathrm{tr}}^{W_m}}{\bar{R}^{W_m} \cdot \bar{\mathcal{F}}_{\mathrm{a}}^{W_m}} + \sum_{k=k_1(m)}^{k_{\mathrm{end}}(m)} \left(\frac{B \cdot {}^{\mathrm{a}}\mathrm{L}\, \bar{f}_1^{X_k}}{4B\rho\pi \bar{r}^{W_m} \Delta\bar{r}^{W_m} \bar{R}^{W_m} \bar{\mathcal{F}}_{\mathrm{a}}^{W_m} (\bar{F}_{\mathrm{p}}^{W_m})^2} \right) \cdot \frac{\partial F_{\mathrm{p}}^{W_m}}{\partial U_{\mathrm{im}}^{W_m}} - \right. \\ & \left. \frac{\bar{U}_{\mathrm{i}}^{W_m}}{\bar{R}^{W_m} \cdot \bar{\mathcal{F}}_{\mathrm{a}}^{W_m}} \cdot \frac{\partial U_{\mathrm{tr}}^{W_m}}{\partial U_{\mathrm{im}}^{W_m}} \right) \cdot \left[0_{(1)}\ \ldots\ 0_{(2m-2)}\quad 1\ \ 0\quad 0_{(2m+1)}\ \ldots\ 0_{2P} \right] \end{aligned} \tag{A.167}$$

For the rows $\underline{\boldsymbol{a}}_{\mathrm{tg}}^{W_m}$, with ranking numbers $2(\mathrm{m}-1)+2$ in matrix $\boldsymbol{A}^{W}$, holds:

$$\underline{\boldsymbol{a}}_{\mathrm{tg}}^{W_m} = \left(-\frac{\gamma \cdot \bar{U}_{\mathrm{tr}}^{W_m}}{\bar{R}^{W_m} \cdot \bar{\mathcal{F}}_{\mathrm{a}}^{W_m}} \right) \cdot \left[0_{(1)}\ \ldots\ 0_{(2m-2)}\quad 0\ \ 1\quad 0_{(2m+1)}\ \ldots\ 0_{2P} \right] \tag{A.168}$$

The rows $\underline{\boldsymbol{b}}_{\mathrm{ax}}^{W_m G}$, with ranking numbers $2(\mathrm{m}-1)+1$ in the input matrix partition $\boldsymbol{B}^{WG}$, are determined as follows

$$\begin{aligned} \underline{\boldsymbol{b}}_{\mathrm{ax}}^{W_m G} = & \left(\sum_{k=k_1(m)}^{k_{\mathrm{end}}(m)} \left(\frac{B \cdot {}^{\mathrm{a}}\mathrm{L}\, \bar{f}_1^{X_k}}{4B\rho\pi \bar{r}^{W_m} \Delta\bar{r}^{W_m} \bar{R}^{W_m} \bar{\mathcal{F}}_{\mathrm{a}}^{W_m} (\bar{F}_{\mathrm{p}}^{W_m})^2} \right) \cdot \frac{\partial F_{\mathrm{p}}^{W_m}}{\partial \underline{u}^{W_m/X/R_{\mathrm{fx}}}} - \right. \\ & \left. \frac{\bar{U}_{\mathrm{i}}^{W_m}}{B \cdot \bar{R}^{W_m} \bar{\mathcal{F}}_{\mathrm{a}}^{W_m}} \cdot \frac{\partial U_{\mathrm{tr}}^{W_m}}{\partial \underline{u}^{W_m/X/R_{\mathrm{fx}}}} \right) \cdot \\ & \Big[\big(\mathrm{O}_{(1)}\ \ldots \mathrm{O}_{(k_1(m)-1)}\ \ \epsilon_{k_1(m)}\boldsymbol{I} \ldots\ \epsilon_{k_{\mathrm{end}}(m)}\boldsymbol{I}\ \ \mathrm{O}_{(k_{\mathrm{end}}(m)+1)}\ \ldots\ \mathrm{O}_{(N)} \big) \mid \ldots \\ & \big(\mathrm{O}_{(1)}\ \ldots \mathrm{O}_{(k_1(m)-1)}\ \ \epsilon_{k_1(m)}\boldsymbol{I} \ldots\ \epsilon_{k_{\mathrm{end}}(m)}\boldsymbol{I}\ \ \mathrm{O}_{(k_{\mathrm{end}}(m)+1)}\ \ldots\ \mathrm{O}_{(N)} \big) \mid \ldots \\ & \big(\mathrm{O}_{(1)}\ \ldots \mathrm{O}_{(k_1(m)-1)}\ \ \epsilon_{k_1(m)}\boldsymbol{I} \ldots\ \epsilon_{k_{\mathrm{end}}(m)}\boldsymbol{I}\ \ \mathrm{O}_{(k_{\mathrm{end}}(m)+1)}\ \ldots\ \mathrm{O}_{(N)} \big) \mid \ldots \\ & \big(\mathrm{O}_{(1)}\ \ldots\ \mathrm{O}_{(m-1)}\ \ \boldsymbol{I}\ \ \mathrm{O}_{(m+1)}\ \ldots\ \mathrm{O}_{(P)} \big) \mid \ldots \\ & \big(\mathrm{O}_{(1)}\ \ldots\ \mathrm{O}_{(m-1)}\ \ \boldsymbol{I}\ \ \mathrm{O}_{(m+1)}\ \ldots\ \mathrm{O}_{(P)} \big) \mid \ldots \\ & \big(\mathrm{O}_{(1)}\ \ldots\ \mathrm{O}_{(m-1)}\ \ \boldsymbol{I}\ \ \mathrm{O}_{(m+1)}\ \ldots\ \mathrm{O}_{(P)} \big) \Big] \end{aligned} \tag{A.169}$$

We used Eq. B.252 and B.256 and also B.243 and B.245 for the sensitivity of Prandtl's correction factor and the transportation speed on the periodic and stochastic wind speed variations.

The rows $\underline{\boldsymbol{b}}_{\mathrm{tg}}^{W_m G}$ with ranking numbers $2(\mathrm{m}-1)+2$ in $\boldsymbol{B}^{WG}$ are determined similar to the ones in Eq. A.169. Just replace $\bar{U}_{\mathrm{i}}^{W_m}$ by $\bar{V}_{\mathrm{i}}^{W_m}$ and multiply by γ:

$$\underline{\boldsymbol{b}}_{\mathrm{tg}}^{W_m G} = \gamma \cdot \frac{\bar{V}_{\mathrm{i}}^{W_m}}{\bar{U}_{\mathrm{i}}^{W_m}} \cdot \underline{\boldsymbol{b}}_{\mathrm{ax}}^{W_m G} \tag{A.170}$$

The rows in the input matrix partition $\boldsymbol{B}^{WS}$ for the wind speed variations $\underline{u}_{\mathrm{ori}}^{S_{\mathrm{n}}}$ by orientation change of the support structure just consist of the 'first part' of the row vector expressions above multiplied with the number of blades B:

$$\begin{aligned}
\underline{\boldsymbol{b}}_{\mathrm{ax}}^{W_m S} &= \sum_{k=k_1(m)}^{k_{\mathrm{end}}(m)} \left(\frac{B \cdot {}^{\mathrm{a_L}}\bar{f}_1^{X_k}}{4B\rho\pi\,\bar{r}^{W_m}\Delta\bar{r}^{W_m}\bar{R}^{W_m}\bar{\mathcal{F}}_{\mathrm{a}}^{W_m}(\bar{F}_{\mathrm{p}}^{W_m})^2} \right) \cdot \frac{\partial F_{\mathrm{p}}^{W_m}}{\partial \underline{u}^{W_m/X/R_{\mathrm{fx}}}} - \frac{\bar{U}_{\mathrm{i}}^{W_m}}{\bar{R}^{W_m}\bar{\mathcal{F}}_{\mathrm{a}}^{W_m}} \cdot \frac{\partial U_{\mathrm{tr}}^{W_m}}{\partial \underline{u}^{W_m/X/R_{\mathrm{fx}}}} \\
\underline{\boldsymbol{b}}_{\mathrm{tg}}^{W_m S} &= \gamma \cdot \frac{\bar{V}_{\mathrm{i}}^{W_m}}{\bar{U}_{\mathrm{i}}^{W_m}} \cdot \underline{\boldsymbol{b}}_{\mathrm{ax}}^{W_m S}
\end{aligned} \tag{A.171}$$

For the input matrix rows with respect to the lift force reactions from the blades, which are provides by the rotor blade model as *minus* the aerodynamic blade forces, holds ($X = D, E, F$):

$$\begin{aligned}
\underline{\boldsymbol{b}}_{\mathrm{ax}}^{W_m X} &= \frac{-1}{\rho \cdot 4\pi\bar{r}^{W_m}\Delta\bar{r}^{W_m} \cdot \bar{R}^{W_m}\bar{\mathcal{F}}_{\mathrm{a}}^{W_m}\bar{F}^{W_m}} \cdot [\,1\;\;0\;\;0\,] \cdot \\
&\quad \left[\, \mathrm{O}_{(1)} \;\ldots \mathrm{O}_{(k_1(m)-1)} \;\; \epsilon_{k_1(m)}\boldsymbol{I} \ldots \; \epsilon_{k_{\mathrm{end}}(m)}\boldsymbol{I} \;\; \mathrm{O}_{(k_{\mathrm{end}}(m)+1)} \;\ldots\; \mathrm{O}_{(N)} \right] \\
\underline{\boldsymbol{b}}_{\mathrm{tg}}^{W_m X} &= \frac{-\gamma}{\rho \cdot 4\pi\bar{r}^{W_m}\Delta\bar{r}^{W_m} \cdot \bar{R}^{W_m}\bar{\mathcal{F}}_{\mathrm{a}}^{W_m}\bar{F}^{W_m}} \cdot [\,0\;\;0\;\;1\,] \cdot \\
&\quad \left[\, \mathrm{O}_{(1)} \;\ldots \mathrm{O}_{(k_1(m)-1)} \;\; \epsilon_{k_1(m)}\boldsymbol{I} \ldots \; \epsilon_{k_{\mathrm{end}}(m)}\boldsymbol{I} \;\; \mathrm{O}_{(k_{\mathrm{end}}(m)+1)} \;\ldots\; \mathrm{O}_{(N)} \right]
\end{aligned} \tag{A.172}$$

(iii) Output variables and first order state space representation

The wake model needs to provide the following interaction output:

- induction speed variation in rotor annuli: $\underline{u}_{\mathrm{i_m}}^{W}$

The wake induction vector $\underline{u}_{\mathrm{i_m}}^{W}$ contains for each rotor annulus *minus* the 'annulus-average' axial and tangential induction speed in the first and third location of the subvectors $\{\underline{u}_{\mathrm{i_m}}^{W_m} | w = 1 \ldots P\}$. This vector is input to all rotor blades.

The output vector $\underline{y}^{W}$ of the wake has the following composition:

$$\underline{y}^{W} = \begin{bmatrix} \underline{y}^{GW} \\ \underline{y}^{XW} \end{bmatrix} \quad \text{with } \underline{y}^{XW} = \begin{bmatrix} \underline{u}_{\mathrm{i_m}}^{W} \end{bmatrix} = \begin{bmatrix} \underline{u}_{\mathrm{i_m}}^{W_1} \\ \vdots \\ \underline{u}_{\mathrm{i_m}}^{W_P} \end{bmatrix} \quad \text{where } \underline{u}_{\mathrm{i_m}}^{W_m} = \delta \begin{bmatrix} -U_{\mathrm{i_m}}^{W_m} \\ 0 \\ -V_{\mathrm{i_m}}^{W_m} \end{bmatrix} \tag{A.173}$$

The 'exogeneous' output subvector $\underline{y}^{GW}$ is equal to the 'interaction' output subvector $\underline{y}^{XW}$.

For the state equation that includes transient behaviour of both the axial and tangential induction, the vector output equation becomes:

$$\begin{bmatrix} \underline{y}^{GW} \\ \underline{y}^{XW} \end{bmatrix} = \begin{bmatrix} \boldsymbol{C}^{GW} \\ \boldsymbol{C}^{XW} \end{bmatrix} \cdot \underline{x}_{\mathrm{o}}^{W} \quad \text{with } \boldsymbol{C}^{GW} = \boldsymbol{C}^{XW} = \mathrm{diag}^{(P)}\Big(\begin{bmatrix} -1 & 0 \\ 0 & 0 \\ 0 & -1 \end{bmatrix} \Big) \tag{A.174}$$

The '$\mathrm{diag}^{(P)}(.)$' operator creates a 'P-block' diagonal-like matrix with $3P$ rows and $2P$ columns.

The first order state space representation for the wake model with axial and tangential induction transients then becomes:

$$\begin{aligned} \dot{\underline{x}}_{\mathrm{o}}^{W} &= \boldsymbol{A}^{W} \cdot \underline{x}_{\mathrm{o}}^{W} + [\, \boldsymbol{B}^{WG}\ \boldsymbol{B}^{WD}\ \boldsymbol{B}^{WE}\ \boldsymbol{B}^{WF}\ \boldsymbol{B}^{WS} \,] \cdot \begin{bmatrix} \underline{v}^{WG} \\ \underline{v}^{WD} \\ \underline{v}^{WE} \\ \underline{v}^{WF} \\ \underline{v}^{WS} \end{bmatrix} \\ \begin{bmatrix} \underline{y}^{GW} \\ \underline{y}^{XW} \end{bmatrix} &= \begin{bmatrix} \boldsymbol{C}^{GW} \\ \boldsymbol{C}^{XW} \end{bmatrix} \cdot \underline{x}_{\mathrm{o}}^{W} \end{aligned} \tag{A.175}$$

If only axial induction transients are to be taken into account then all even numbered rows in the vector state equation are deleted as well as the second column in the output matrix. However, the feedthrough matrix $\boldsymbol{K}^{W}$ will appear, which will change the output equation into:

$$\begin{bmatrix} \underline{y}^{GW} \\ \underline{y}^{XW} \end{bmatrix} = \begin{bmatrix} \boldsymbol{C}_{\mathrm{ax}}^{GW} \\ \boldsymbol{C}_{\mathrm{ax}}^{XW} \end{bmatrix} \cdot \underline{x}_{\mathrm{o}}^{W} + \begin{bmatrix} \boldsymbol{K}_{\mathrm{ax}}^{GWG} & \boldsymbol{K}_{\mathrm{ax}}^{GWD} & \boldsymbol{K}_{\mathrm{ax}}^{GWE} & \boldsymbol{K}_{\mathrm{ax}}^{GWF} & \boldsymbol{K}_{\mathrm{ax}}^{GWS} \\ \boldsymbol{K}_{\mathrm{ax}}^{XWG} & \boldsymbol{K}_{\mathrm{ax}}^{XWD} & \boldsymbol{K}_{\mathrm{ax}}^{XWE} & \boldsymbol{K}_{\mathrm{ax}}^{XWF} & \boldsymbol{K}_{\mathrm{ax}}^{XWS} \end{bmatrix} \cdot \begin{bmatrix} \underline{v}^{WG} \\ \underline{v}^{WD} \\ \underline{v}^{WE} \\ \underline{v}^{WF} \\ \underline{v}^{WS} \end{bmatrix} \tag{A.176}$$

The algebraic equation 3.25 for the tangential induction speed variation completely defines the non-zero elements in the feedthrough matrix partitions.

A.4 Drive-train model

The drive-train consist of four one-element subcomponents: the gearbox house R_{h}, the slow shaft system of the gearbox R_{s}, the fast shaft and generator rotor R_{f} and the rotor shaft & hub R_{r}. Since the gearbox house stands still in average sense, the model of this subcomponent is added to the support structure model, which is subject of section A.5. The gearbox slow shaft is assumed massless and only serves as step-up in the derivation of the kinematic vectors for rotor shaft & hub and the rotor blades (see section B.2.1). We only need to derive the equations of motions and the belonging state space models for the generator rotor R_{f} and the hub R_{r}. The models for these subcomponents are derived in sections A.4.2 and A.4.1.

The main shaft flexibility can be modelled with up to *six* degrees of freedom in the rotor centre. With six dofs, the integration of the models for the rotating and standstill part could also be performed manually. So called 'algebraic loops over the main rotation' are then avoided: the six springs and dampers allow to express any tower loading from the blades in linear functions of the degrees of freedom. At less than six dofs, at least any *inertia load by the rotor* is by nature proportionally fed back to the tower loading. The part of the fedback inertia loads that is caused by tower acceleration establishes an algebraic loop over the main rotation: the acceleration is fed forward to the rotor blades *after modulation* and fed back to the tower again *after demodulation* **without any dynamic relationship**. In case of a 2- or 1-bladed rotor the connection of the standstill to rotating part has to be performed manually. The 'manual elimination' of the algebraic loops mentioned above is a very nasty job. In case of 3 or more rotor blades, it is allowed to perform *automatic* connection of the rotating and standstill part. This is done for an arbitrary value of the azimut angle, *accompanied by the Coleman transformation on the state variables as well as on the input and output variables for that same azimut angle in accordance with section 4.2*.

A.4.1 Equations of motion for rotor shaft & hub R_r

The model for R_r includes 3D mechanic impulse conservation of the rotor hub and linear shaft deformation. The shaft deformation is assumed mass-less and is based on the slender beam theory; it may include co-axial deformation and bending, which is modelled by means of up to six spring-damper pairs in the rotor centre 'between the *rigidized* shaft and the hub'. During the parametrisation of the drive-train via function TBUDRIVTRPAR() the spring-damper pairs can be dimensioned such that they incorporate the effect of a radial shaft bearing and of a rigid span between the rotor centre and 'end of the flexible part of the main shaft'. The mass properties of the main shaft are moved to the rotor hub, which yields enlarged moments of inertia and a co-axial shift of the centre of gravity.

The mean values and sensitivities of the impulse vectors as formulated in section B.2.2, paragraph on *Rotor shaft & hub* R_r, apply and do not need further discussion. This also holds for the gravitation loading on R_r by section B.10.3. The responsive loading is dealt with in paragraph (i), cleared up by a disussion on the modelling of the shaft flexibility. The required input variables from other components and from the generator rotor & fast shaft subcomponent R_f are subject of paragraph (ii). The derivation method for the second order state equation for the blade flange in section A.2.3 holds for R_r in a slightly modified way, which is discussed in paragraph (iii). The output variables to other components and to the preceeding subcomponent R_f are subject of paragraph (iv), togehter with the involved output equation.

The subcomponent model for the rotor shaft & hub R_r is obtained by a call to TBUR3SUBEOM() in function TBUDRIVTREOM(). The model for R_r exists as structure variable sysR3sub. The fields in sysR3sub are 2D matrices A, B, C, K, the parameterisation of the first order state space representation, and cell arrays with lists of input, output and state variable names. Point of departure for the rotor shaft model creation by function TBUR3SUBEOM() is the availability for the one-element subcomponet R_r of ((f.)c.s: (final) coordinate system):

- means and sensitivities of angular and linear impulse vector and gravition loads (along f.c.s. of R_r in actual position);
- means of feedthrough loads from the rotor blades on the rotor centre (along c.s. of blade bases $\{X_0\}$ in actual position);
- sensitivities of displacement vectors relative to rotor centre in average position (along f.c.s. of R_r in average position);
- sensitivities of kinematic vectors in rotor centre (= exit point and entry point of R_r; along f.c.s. of R_r in actual position);
- sensitivities of wind speed and gravitation by orientation change in rotor centre (along f.c.s. of R_r in actual position);
- transformation matrices and their sensitivities to rotational dofs relative to the slow shaft exit of gearbox house R_s (forward and backward);
- stiffness and damper values in the connection point with the blade base entries (=rotor centre);
- location of c.o.g. relative to rotor centre;
- bottom-up ranking of rotation and translation axes in the connnection point;
- flags for angular and linear dofs in the connection point;
- number of blades and gearbox ratio

The mentioned sensitivities belong to the 'motion formulations' and map all motion variations to input variables from the generator rotor subcomponent $R_{\rm f}$, from the support structure or from the environment (gravitation). These are provided by preceeding calls in TBUDRIVTREOM() to functions TBUDRIVTRCONS(), TBUDRIVTRKIN(), TBUDRIVTRIMP(). Note that outputs from the support structure are assumed to be modulated with the main azimut angle (See section A.1, par. (vi), header *Support structure outputs into the drive-train*).

Functionality TBUR3SUBEOM() ((f.)c.s: (final) coordinate system):

- definition of input name lists; each list contains the names of the input subvectors from a specific source (G, S, D, E, F, R2sub (= generator rotor $R_{\rm f}$);
- definition of output name lists; each list contains the names of the output subvectors to a specific destination (G, S, D, E, F, R2sub);
- lumping together the gravitation loads and the feedthrough loads from the rotor blades to equivalent force and torque load formulations in the rotor centre $R_{\rm r}^{\rm c}$ (coordinates along actual f.c.s. of $R_{\rm r}$);
- define 'equal to zero' the feedthrough loading from outward elements within the 'rotor shaft subcomponent' (there are no) in the rotor centre $R_{\rm r}^{\rm c}$ (call TBUSYSFTFT());
- definition of the sensitivities of the responsive (visco/elastic) loads in the rotor centre $R_{\rm r}^{\rm c}$ to the dofs by straightforward use of 4 sets of 3×3 stiffness and damper matrices (see par. (i));
- derive the mass, spring and damper matrix for the equations of motion for the rotor shaft $R_{\rm r}$ ($\boldsymbol{M}, \boldsymbol{S}, \boldsymbol{D}$; call TBUSYSMDSMX());
- derive load formulations for feedthrough force and torque loading on the nacelle and on the generator rotor (exit point of final element of preceeding subcomponent, which coincides with the rotor centre; call TBUSYSFTPP and 'extract' fraction $1/i_{\rm gb}$ of co-axial torque for generator loading; coordinates along actual c.s of slow gearbox exit $R_{\rm s}$);
- derive the input matrix for the mass/spring/damper formulation of $R_{\rm r}$ as well as the output matrices on the dofs and their time derivatives and the feedthrough matrix ($\boldsymbol{G}, \boldsymbol{H}, \boldsymbol{L}, \boldsymbol{K}$; call TBUSYSGHLKMX());
- transform the mass/spring/damper model formulation $\{\boldsymbol{M}, \boldsymbol{S}, \boldsymbol{D}, \boldsymbol{G}, \boldsymbol{H}, \boldsymbol{L}, \boldsymbol{K}\}$ to the first order state space formulation $\{\boldsymbol{A}, \boldsymbol{B}, \boldsymbol{C}, \boldsymbol{K}\}$ (call TBUSYSMDS2FSR()).

(i) Responsive loading

As described in paragraph (ii) in section 3.7.2 the responsive loading for the rotor shaft involves viso-elastic loads for up to six degrees of freedom. The sensitivity matrices to the 'full dof vectors' of the drive-train are *just the* 3×3 *matrices* $\frac{\partial^{\rm RS}\underline{t}^{R_{\rm r}}}{\partial \underline{\varphi}^{R_{\rm r}}}$, $\frac{\partial^{\rm RS}\underline{t}^{R_{\rm r}}}{\partial \underline{\varrho}^{R_{\rm r}}}$, $\frac{\partial^{\rm RS}\underline{f}^{R_{\rm r}}}{\partial \underline{\varphi}^{R_{\rm r}}}$ and $\frac{\partial^{\rm RS}\underline{f}^{R_{\rm r}}}{\partial \underline{\varrho}^{R_{\rm r}}}$ as specified in Eq. 3.72 in section 3.7.2. In the implementation it is faked as if the overall drive-train model consists of only *one* subcomponent; the subcomponent counter m is set to 1 i.s.o. 3. This is the only way in which can be deal with the 'rather strange' drive-train elements via the generic functions tbusysmdsmx(), tbusysghlkmx() etc. The price to be payed for it is that the names of the input and output variables of $R_{\rm r}$ to the generator rotor, rotor blades and to the support structure are to be modified as concerns the *source counter* m. This is established by setting the so called 'offset variable' `mshift4subcmp` equal to 2; like wise the offset variables `mshift4inff, mshift4inpp, mshift4outff, mshift4outpp` are set equal to 0, -1, -1 and 0; see tbusysmdsghlkmx() and tbur3subeom().

(ii) Input variables

The input vector to the rotor shaft & hub has the following composition:

$$\underline{v}^{R_\mathrm{r}} = \begin{bmatrix} \underline{v}^{R_\mathrm{r}G} \\ \underline{v}^{R_\mathrm{r}D} \\ \underline{v}^{R_\mathrm{r}E} \\ \underline{v}^{R_\mathrm{r}F} \\ \underline{v}^{R_\mathrm{r}S} \\ \underline{v}^{R_\mathrm{r}R_\mathrm{f}} \end{bmatrix} \tag{A.177}$$

All subvectors but $\underline{v}^{R_\mathrm{r}R_\mathrm{f}}$ are the same as the subvectors in $\underline{v}^{R}$ by Eq. A.5 in section A.1. The input subvector $\underline{v}^{R_\mathrm{r}R_\mathrm{f}}$ from the generator rotor contains the angular deviation variation, speed and acceleration of R_f relative to the nacelle:

$$\underline{v}^{R_\mathrm{r}R_\mathrm{f}} = \begin{bmatrix} \varphi_\mathrm{x}^{R_\mathrm{f}} \\ \dot{\varphi}_\mathrm{x}^{R_\mathrm{f}} \\ \ddot{\varphi}_\mathrm{x}^{R_\mathrm{f}} \end{bmatrix} \tag{A.178}$$

(iii) Equations of motion and 2$^{\mathrm{nd}}$ order vector state equation

Just as in the implementation of impulse vectors and load vector for R_r (see Eq. B.94, B.289 and the previous pargraph (i)), the implementation of the 2$^{\mathrm{nd}}$ order state vector equation is based on encapsulating dof vectors. However, they are now restricted to R_r and *not* to the whole drive train component. That is to say, the mass, spring and damper matrix arise from partial derivatives of impulse and load vectors to the dof vectors $\underline{\phi}^{R_\mathrm{r}}$ and $\underline{\varrho}^{R_\mathrm{r}}$. The implementation for R_r thus differs from the one for the rotor blade subcomponent models, in which the partial derivatives to the *overall* encapsulating dof vectors are considered (paragraph (v) in section A.2.2 and section A.2.3). Point of departure is the full-size vector state equation (6×6-matrices):

$$\left[\boldsymbol{M}_{\varphi}^{R_\mathrm{r}} \mid \boldsymbol{M}_{\varrho}^{R_\mathrm{r}}\right] \cdot \begin{bmatrix} \ddot{\underline{\varphi}}^{R_\mathrm{r}} \\ \ddot{\underline{\varrho}}^{R_\mathrm{r}} \end{bmatrix} + \left[\boldsymbol{D}_{\varphi}^{R_\mathrm{r}} \mid \boldsymbol{D}_{\varrho}^{R_\mathrm{r}}\right] \cdot \begin{bmatrix} \dot{\underline{\varphi}}^{R_\mathrm{r}} \\ \dot{\underline{\varrho}}^{R_\mathrm{r}} \end{bmatrix} + \left[\boldsymbol{S}_{\varphi}^{R_\mathrm{r}} \mid \boldsymbol{S}_{\varrho}^{R_\mathrm{r}}\right] \cdot \begin{bmatrix} \underline{\varphi}^{R_\mathrm{r}} \\ \underline{\varrho}^{R_\mathrm{r}} \end{bmatrix} =$$

$$\left[\boldsymbol{G}^{R_\mathrm{r}G} \mid \boldsymbol{G}^{R_\mathrm{r}D} \mid \boldsymbol{G}^{R_\mathrm{r}E} \mid \boldsymbol{G}^{R_\mathrm{r}F} \mid \boldsymbol{G}^{R_\mathrm{r}S} \mid \boldsymbol{G}^{R_\mathrm{r}R_\mathrm{f}}\right] \cdot \begin{bmatrix} \underline{v}^{R_\mathrm{r}G} \\ \underline{v}^{R_\mathrm{r}D} \\ \underline{v}^{R_\mathrm{r}E} \\ \underline{v}^{R_\mathrm{r}F} \\ \underline{v}^{R_\mathrm{r}S} \\ \underline{v}^{R_\mathrm{r}R_\mathrm{f}} \end{bmatrix} \tag{A.179}$$

These matrices are derived by considering the angular and linear vector impulse equation for the one-element subcomponent R_r in its set of three coordinate systems. We start with the y-coordinate of the angular impulse and the z-coordinate of the linear impulse in the 3rd intermediate coordinate system (i.c.s.). Afterwards, the respective z-coordinate and y-coordinate are considered in the 2nd i.c.s. Finally, both x-coordinates are dealt with in the 1st i.c.s. The pairs of rows $\{\underline{\boldsymbol{m}}_{h\varphi_w}^{R_\mathrm{r}}, \underline{\boldsymbol{m}}_{p\varphi_w}^{R_\mathrm{r}} | w = 3, 2, 1\}$, with ranking numbers $2(w-1)+1$ and $2(w-1)+2$ in the mass matrix partition $\boldsymbol{M}_{\varphi}^{R_\mathrm{r}}$, are now determined as follows (the partial derivatives in the right hand side only apply if they are defined for the 'independent variable' $\ddot{\underline{\varphi}}^{R_\mathrm{r}}$):

- for $w = 3$:

$$\begin{aligned} \underline{\boldsymbol{m}}_{h\varphi_3}^{R_\mathrm{r}} &= -[\,0\,1\,0\,] \cdot \frac{\partial^{\mathrm{RS}} \underline{t}^{R_\mathrm{r}^\mathrm{c}}}{\partial \ddot{\underline{\varphi}}^{R_\mathrm{r}}} + [\,0\,1\,0\,] \cdot \left(\frac{\partial^{R_\mathrm{r}^\mathrm{c}} \dot{\underline{h}}^{R_\mathrm{r}}}{\partial \ddot{\underline{\varphi}}^{R_\mathrm{r}}} - \frac{\partial^{\mathrm{EX}} \underline{t}^{R_\mathrm{r}^\mathrm{c}}}{\partial \ddot{\underline{\varphi}}^{R_\mathrm{r}}} \right) \\ \underline{\boldsymbol{m}}_{p\varphi_3}^{R_\mathrm{r}} &= -[\,0\,0\,1\,] \cdot \frac{\partial^{\mathrm{RS}} \underline{f}^{R_\mathrm{r}^\mathrm{c}}}{\partial \ddot{\underline{\varphi}}^{R_\mathrm{r}}} + [\,0\,0\,1\,] \cdot \left(\frac{\partial \dot{\underline{p}}^{R_\mathrm{r}}}{\partial \ddot{\underline{\varphi}}^{R_\mathrm{r}}} - \frac{\partial^{\mathrm{EX}} \underline{f}^{R_\mathrm{r}^\mathrm{c}}}{\partial \ddot{\underline{\varphi}}^{R_\mathrm{r}}} \right) \end{aligned} \tag{A.180}$$

- for $w = 2$:

$$\begin{aligned}
\underline{\boldsymbol{m}}_{h\varphi_2}^{R_\mathrm{r}} &= -[\,0\,0\,1\,]\cdot\frac{\partial^{\mathrm{RS}}\underline{t}^{R_\mathrm{r}^\mathrm{c}}}{\partial\underline{\ddot{\varphi}}^{R_\mathrm{r}}} + {}^{R_\mathrm{r}^2}\bar{\Phi}_{(3,:)}^{R_\mathrm{r}}\cdot\Big(\frac{\partial^{R_\mathrm{r}^\mathrm{c}}\dot{\underline{h}}^{R_\mathrm{r}}}{\partial\underline{\ddot{\varphi}}^{R_\mathrm{r}}} - \frac{\partial^{\mathrm{EX}}\underline{t}^{R_\mathrm{r}^\mathrm{c}}}{\partial\underline{\ddot{\varphi}}^{R_\mathrm{r}}}\Big)\\
\underline{\boldsymbol{m}}_{p\varphi_2}^{R_\mathrm{r}} &= -[\,0\,1\,0\,]\cdot\frac{\partial^{\mathrm{RS}}\underline{f}^{R_\mathrm{r}^\mathrm{c}}}{\partial\underline{\ddot{\varphi}}^{R_\mathrm{r}}} + {}^{R_\mathrm{r}^2}\bar{\Phi}_{(2,:)}^{R_\mathrm{r}}\cdot\Big(\frac{\partial\underline{\dot{p}}^{R_\mathrm{r}}}{\partial\underline{\ddot{\varphi}}^{R_\mathrm{r}}} - \frac{\partial^{\mathrm{EX}}\underline{f}^{R_\mathrm{r}^\mathrm{c}}}{\partial\underline{\ddot{\varphi}}^{R_\mathrm{r}}}\Big)
\end{aligned} \tag{A.181}$$

- for $w = 1$:

$$\begin{aligned}
\underline{\boldsymbol{m}}_{h\varphi_1}^{R_\mathrm{r}} &= -[\,1\,0\,0\,]\cdot\frac{\partial^{\mathrm{RS}}\underline{t}^{R_\mathrm{r}^\mathrm{c}}}{\partial\underline{\ddot{\varphi}}^{R_\mathrm{r}}} + {}^{R_\mathrm{r}^1}\bar{\Phi}_{(1,:)}^{R_\mathrm{r}}\cdot\Big(\frac{\partial^{R_\mathrm{r}^\mathrm{c}}\dot{\underline{h}}^{R_\mathrm{r}}}{\partial\underline{\ddot{\varphi}}^{R_\mathrm{r}}} - \frac{\partial^{\mathrm{EX}}\underline{t}^{R_\mathrm{r}^\mathrm{c}}}{\partial\underline{\ddot{\varphi}}^{R_\mathrm{r}}}\Big)\\
\underline{\boldsymbol{m}}_{p\varphi_1}^{R_\mathrm{r}} &= -[\,1\,0\,0\,]\cdot\frac{\partial^{\mathrm{RS}}\underline{f}^{R_\mathrm{r}^\mathrm{c}}}{\partial\underline{\ddot{\varphi}}^{R_\mathrm{r}}} + {}^{R_\mathrm{r}^1}\bar{\Phi}_{(1,:)}^{R_\mathrm{r}}\cdot\Big(\frac{\partial\underline{\dot{p}}^{R_\mathrm{r}}}{\partial\underline{\ddot{\varphi}}^{R_\mathrm{r}}} - \frac{\partial^{\mathrm{EX}}\underline{f}^{R_\mathrm{r}^\mathrm{c}}}{\partial\underline{\ddot{\varphi}}^{R_\mathrm{r}}}\Big)
\end{aligned} \tag{A.182}$$

Note that NO feedthrough loading exists from other elements within the one-element subcomponent R_r. The loading from the rotor blades is considered as external loading for R_r and included in ${}^{\mathrm{EX}}\underline{t}^{R_\mathrm{r}^\mathrm{c}}$ and ${}^{\mathrm{EX}}\underline{f}^{R_\mathrm{r}^\mathrm{c}}$.

The deformation along the z- and y-axis are assumed zero-mean in TURBU Offshore (no prebended rotor shaft). Then the transformation matrices ${}^{R_\mathrm{r}^2}\bar{\Phi}_{(1,:)}^{R_\mathrm{r}}$ and ${}^{R_\mathrm{r}^1}\bar{\Phi}_{(1,:)}^{R_\mathrm{r}}$ are both the identity.

The corresponding rows in the mass matrix partition $\boldsymbol{M}_{\varrho}^{R_\mathrm{r}}$ are obtained by taking the sensitivities to $\underline{\ddot{\varrho}}^{R_\mathrm{r}}$ instead of $\underline{\ddot{\varphi}}^{R_\mathrm{r}}$. For the rows in both damping matrix partitions $\boldsymbol{D}_{\varphi}^{R_\mathrm{r}}$ and $\boldsymbol{D}_{\varrho}^{R_\mathrm{r}}$ and in the stiffness matrix partition $\boldsymbol{S}_{\varrho}^{R_\mathrm{r}}$, take the sensitivities to $\underline{\dot{\varphi}}^{R_\mathrm{r}}$ and $\underline{\dot{\varrho}}^{R_\mathrm{r}}$ and $\underline{\varrho}^{R_\mathrm{r}}$. For the remaining stiffness matrix partition $\boldsymbol{S}_{\varphi}^{R_\mathrm{r}}$ the same scheme applies for $w = 3$ but differs for $w = 2$ and $w = 1$:

- for $w = 2$:

$$\begin{aligned}
\underline{\boldsymbol{s}}_{h\varphi_2}^{R_\mathrm{r}} &= -[\,0\,0\,1\,]\cdot\frac{\partial^{\mathrm{RS}}\underline{t}^{R_\mathrm{r}^\mathrm{c}}}{\partial\underline{\phi}^{R_\mathrm{r}}} + {}^{R_\mathrm{r}^2}\bar{\Phi}_{(3,:)}^{R_\mathrm{r}}\cdot\Big(\frac{\partial^{R_\mathrm{r}^\mathrm{c}}\dot{\underline{h}}^{R_\mathrm{r}}}{\partial\underline{\phi}^{R_\mathrm{r}}} - \frac{\partial^{\mathrm{EX}}\underline{t}^{R_\mathrm{r}^\mathrm{c}}}{\partial\underline{\phi}^{R_\mathrm{r}}}\Big) +\\
&\quad [\,\mathrm{J}_{v=1}^{3}\Big(\frac{\partial^{R_\mathrm{r}^2}\Phi_{(3,:)}^{R_\mathrm{r}}}{\partial\phi_v^{R_\mathrm{r}}}\cdot\Big({}^{R_\mathrm{r}^\mathrm{c}}\bar{\dot{\underline{h}}}^{R_\mathrm{r}} - {}^{\mathrm{EX}}\bar{\underline{t}}^{R_\mathrm{r}^\mathrm{c}}\Big)\Big)\,]\\
\underline{\boldsymbol{s}}_{p\varphi_2}^{R_\mathrm{r}} &= -[\,0\,1\,0\,]\cdot\frac{\partial^{\mathrm{RS}}\underline{f}^{R_\mathrm{r}^\mathrm{c}}}{\partial\underline{\phi}^{R_\mathrm{r}}} + {}^{R_\mathrm{r}^2}\bar{\Phi}_{(2,:)}^{R_\mathrm{r}}\cdot\Big(\frac{\partial\underline{\dot{p}}^{R_\mathrm{r}}}{\partial\underline{\phi}^{R_\mathrm{r}}} - \frac{\partial^{\mathrm{EX}}\underline{f}^{R_\mathrm{r}^\mathrm{c}}}{\partial\underline{\phi}^{R_\mathrm{r}}}\Big) +\\
&\quad [\,\mathrm{J}_{v=1}^{3}\Big(\frac{\partial^{R_\mathrm{r}^2}\Phi_{(2,:)}^{R_\mathrm{r}}}{\partial\phi_v^{R_\mathrm{r}}}\cdot\Big({}^{R_\mathrm{r}^\mathrm{c}}\bar{\underline{\dot{p}}}^{R_\mathrm{r}} - {}^{\mathrm{EX}}\bar{\underline{f}}^{R_\mathrm{r}^\mathrm{c}}\Big)\Big)\,]
\end{aligned} \tag{A.183}$$

- for $w = 1$:

$$\begin{aligned}
\underline{\boldsymbol{s}}_{h\varphi_1}^{R_\mathrm{r}} &= -[\,1\,0\,0\,]\cdot\frac{\partial^{\mathrm{RS}}\underline{t}^{R_\mathrm{r}^\mathrm{c}}}{\partial\underline{\phi}^{R_\mathrm{r}}} + {}^{R_\mathrm{r}^1}\bar{\Phi}_{(1,:)}^{R_\mathrm{r}}\cdot\Big(\frac{\partial^{R_\mathrm{r}^\mathrm{c}}\dot{\underline{h}}^{R_\mathrm{r}}}{\partial\underline{\phi}^{R_\mathrm{r}}} - \frac{\partial^{\mathrm{EX}}\underline{t}^{R_\mathrm{r}^\mathrm{c}}}{\partial\underline{\phi}^{R_\mathrm{r}}}\Big) +\\
&\quad [\,\mathrm{J}_{v=1}^{3}\Big(\frac{\partial^{R_\mathrm{r}^1}\Phi_{(1,:)}^{R_\mathrm{r}}}{\partial\phi_v^{R_\mathrm{r}}}\cdot\Big({}^{R_\mathrm{r}^\mathrm{c}}\bar{\dot{\underline{h}}}^{R_\mathrm{r}} - {}^{\mathrm{EX}}\bar{\underline{t}}^{R_\mathrm{r}^\mathrm{c}}\Big)\Big)\,]\\
\underline{\boldsymbol{s}}_{p\varphi_1}^{R_\mathrm{r}} &= -[\,1\,0\,0\,]\cdot\frac{\partial^{\mathrm{RS}}\underline{f}^{R_\mathrm{r}^\mathrm{c}}}{\partial\underline{\phi}^{R_\mathrm{r}}} + {}^{R_\mathrm{r}^1}\bar{\Phi}_{(1,:)}^{R_\mathrm{r}}\cdot\Big(\frac{\partial\underline{\dot{p}}^{R_\mathrm{r}}}{\partial\underline{\phi}^{R_\mathrm{r}}} - \frac{\partial^{\mathrm{EX}}\underline{f}^{R_\mathrm{r}^\mathrm{c}}}{\partial\underline{\phi}^{R_\mathrm{r}}}\Big) +\\
&\quad [\,\mathrm{J}_{v=1}^{3}\Big(\frac{\partial^{R_\mathrm{r}^1}\Phi_{(2,:)}^{R_\mathrm{r}}}{\partial\phi_v^{R_\mathrm{r}}}\cdot\Big({}^{R_\mathrm{r}^\mathrm{c}}\bar{\underline{\dot{p}}}^{R_\mathrm{r}} - {}^{\mathrm{EX}}\bar{\underline{f}}^{R_\mathrm{r}^\mathrm{c}}\Big)\Big)\,]
\end{aligned} \tag{A.184}$$

The pairs of rows $\{\underline{\boldsymbol{g}}_{h_w}^{R_\mathrm{r}S}, \underline{\boldsymbol{g}}_{p_w}^{R_\mathrm{r}S} | w = 3,2,1\}$, with ranking numbers $2(w-1)+1$ and $2(w-1)+2$ in the input matrix partition $\boldsymbol{G}^{R_\mathrm{r}S}$, are determined as follows (the partial

derivatives in the right hand side only apply if they are defined for the 'independent variable'; in this case $\underline{z}$):

- for $w = 3$:

$$\begin{aligned}
\underline{\boldsymbol{g}}_{h3}^{R_\mathrm{r}S} &= \mathrm{J}_{(\underline{z})}\Big([\,0\,1\,0\,]\cdot\frac{\partial^{\mathrm{RS}}\underline{t}^{R_\mathrm{r}^\mathrm{c}}}{\partial\underline{z}}+[\,0\,1\,0\,]\cdot(-\frac{\partial^{R_\mathrm{r}^\mathrm{c}}\dot{\underline{h}}^{R_\mathrm{r}}}{\partial\underline{z}}+\frac{\partial^{\mathrm{EX}}\underline{t}^{R_\mathrm{r}^\mathrm{c}}}{\partial\underline{z}})\Big)\\
\underline{\boldsymbol{g}}_{p3}^{R_\mathrm{r}S} &= \mathrm{J}_{(\underline{z})}\Big([\,0\,0\,1\,]\cdot\frac{\partial^{\mathrm{RS}}\underline{f}^{R_\mathrm{r}^\mathrm{c}}}{\partial\underline{z}}+[\,0\,0\,1\,]\cdot(-\frac{\partial\dot{\underline{p}}^{R_\mathrm{r}}}{\partial\underline{z}}+\frac{\partial^{\mathrm{EX}}\underline{f}^{R_\mathrm{r}^\mathrm{c}}}{\partial\underline{z}})\Big)
\end{aligned}\tag{A.185}$$

- for $w = 2$:

$$\begin{aligned}
\underline{\boldsymbol{g}}_{h2}^{R_\mathrm{r}S} &= \mathrm{J}_{(\underline{z})}\Big([\,0\,0\,1\,]\cdot\frac{\partial^{\mathrm{RS}}\underline{t}^{R_\mathrm{r}^\mathrm{c}}}{\partial\underline{z}}+{}^{R_\mathrm{r}^2}\bar{\Phi}^{R_\mathrm{r}}_{(3,:)}\cdot\Big(-\frac{\partial^{R_\mathrm{r}^\mathrm{c}}\dot{\underline{h}}^{R_\mathrm{r}}}{\partial\underline{z}}+\frac{\partial^{\mathrm{EX}}\underline{t}^{R_\mathrm{r}^\mathrm{c}}}{\partial\underline{z}}\Big)\Big)\\
\underline{\boldsymbol{g}}_{p2}^{R_\mathrm{r}S} &= \mathrm{J}_{(\underline{z})}\Big([\,0\,1\,0\,]\cdot\frac{\partial^{\mathrm{RS}}\underline{f}^{R_\mathrm{r}^\mathrm{c}}}{\partial\underline{z}}+{}^{R_\mathrm{r}^2}\bar{\Phi}^{R_\mathrm{r}}_{(2,:)}\cdot(-\frac{\partial\dot{\underline{p}}^{R_\mathrm{r}}}{\partial\underline{z}}+\frac{\partial^{\mathrm{EX}}\underline{f}^{R_\mathrm{r}^\mathrm{c}}}{\partial\underline{z}})\Big)
\end{aligned}\tag{A.186}$$

- for $w = 1$:

$$\begin{aligned}
\underline{\boldsymbol{g}}_{h1}^{R_\mathrm{r}S} &= \mathrm{J}_{(\underline{z})}\Big([\,1\,0\,0\,]\cdot\frac{\partial^{\mathrm{RS}}\underline{t}^{R_\mathrm{r}^\mathrm{c}}}{\partial\underline{z}}+{}^{R_\mathrm{r}^1}\bar{\Phi}^{R_\mathrm{r}}_{(1,:)}\cdot\Big(-\frac{\partial^{R_\mathrm{r}^\mathrm{c}}\dot{\underline{h}}^{R_\mathrm{r}}}{\partial\underline{z}}+\frac{\partial^{\mathrm{EX}}\underline{t}^{R_\mathrm{r}^\mathrm{c}}}{\partial\underline{z}}\Big)\Big)\\
\underline{\boldsymbol{g}}_{p1}^{R_\mathrm{r}S} &= \mathrm{J}_{(\underline{z})}\Big([\,1\,0\,0\,]\cdot\frac{\partial^{\mathrm{RS}}\underline{f}^{R_\mathrm{r}^\mathrm{c}}}{\partial\underline{z}}+{}^{R_\mathrm{r}^1}\bar{\Phi}^{R_\mathrm{r}}_{(1,:)}\cdot(-\frac{\partial\dot{\underline{p}}^{R_\mathrm{r}}}{\partial\underline{z}}+\frac{\partial^{\mathrm{EX}}\underline{f}^{R_\mathrm{r}^\mathrm{c}}}{\partial\underline{z}})\Big)
\end{aligned}\tag{A.187}$$

The notation $\mathrm{J}_{(\underline{z})}(.)$ means that the partial derivatives to the involved subvector variables are to be put next to each other. These are for the submatrices $\boldsymbol{G}^{R_\mathrm{r}G}$, $\{\boldsymbol{G}^{R_\mathrm{r}D}$, $\boldsymbol{G}^{R_\mathrm{r}E}$, $\boldsymbol{G}^{R_\mathrm{r}F}\}$, $\boldsymbol{G}^{R_\mathrm{r}S}$, and $\boldsymbol{G}^{R_\mathrm{r}R_\mathrm{f}}$:

- periodic gravitation load vector $\underline{g}_{\mathrm{per}}^{R_\mathrm{r}}$;
- feedthrough loads from the rotor blades $D, E, F \equiv \{X_b | b = 1\ldots3\}$:
  $\{{}^{\mathrm{FT}}\underline{f}^{X_{b_{\mathrm{PP}(1)}}}, {}^{\mathrm{FT}}\underline{t}^{X_{b_{\mathrm{PP}(1)}}} | b = 1\ldots3\}$
- processed kinematic vectors from support structure and gravitation variation:
  $\underline{\omega}^{S_{\mathrm{FF}(4)}}$, $\underline{\alpha}^{S_{\mathrm{FF}(4)}}$, $\underline{v}^{S^{\oplus}_{\mathrm{FF}(4)}}$, $\underline{a}^{S^{\oplus}_{\mathrm{FF}(4)}}$ $\underline{g}_{\mathrm{ori}}^{S_{\mathrm{FF}(4)}}$
- co-axial angular variables from the generator rotor: $\varphi_\mathrm{x}^{R_\mathrm{f}}$, $\dot{\varphi}_\mathrm{x}^{R_\mathrm{f}}$, $\ddot{\varphi}_\mathrm{x}^{R_\mathrm{f}}$;

Note that each non-valid row and the corresponding column, which pertains to a 'non-dof' element of $\underline{\varphi}^{R_\mathrm{r}}$ or $\underline{\varrho}^{R_\mathrm{r}}$, is deleted from the mass, damper and stiffness matrix. Of course, the corresponding row in the input matrix is also deleted! This yields a second order system equation with square left hand side matrices and adequately dimensioned input matrix.

The external load coordinate vectors include the gravition loading and the feedthrough loads from the rotor blades in the rotor centre (see also Eq. A.20):

$$\begin{aligned}
{}^{\mathrm{EX}}\underline{f}^{R_\mathrm{r}^\mathrm{c}} &\triangleq {}^{\mathrm{g}}\underline{f}^{R_\mathrm{r}^*}+\sum_{b=1}^{3}\Phi_{1b}\cdot{}^{\mathrm{FT}}\underline{f}^{X_{b_{\mathrm{PP}(1)}}}\\
{}^{\mathrm{EX}}\underline{t}^{R_\mathrm{r}^\mathrm{c}} &\triangleq {}^{R_\mathrm{r}^\mathrm{c}}\underline{r}^{R_\mathrm{r}^*}\times{}^{\mathrm{g}}\underline{f}^{R_\mathrm{r}^*}+\sum_{b=1}^{3}\Phi_{1b}\cdot{}^{\mathrm{FT}}\underline{t}^{X_{b_{\mathrm{PP}(1)}}}
\end{aligned}\tag{A.188}$$

The linearised expressions for gravitation load coordinate vectors are listed in section B.10.3, Eq. B.290, B.291, and B.292. The expressions for the external load coordinate vectors comprise the envelope of dependencies:

$$
\begin{aligned}
{}^{\mathrm{EX}}\underline{f}^{R_\mathrm{r}^\mathrm{c}} &= {}^{\mathrm{EX}}\bar{\underline{f}}^{R_\mathrm{r}^\mathrm{c}} + \frac{\partial^{\mathrm{EX}}\underline{f}^{R_\mathrm{r}^\mathrm{c}}}{\partial \underline{g}^{R}_{\mathrm{per}}} \cdot \underline{g}^{R}_{\mathrm{per}} + \frac{\partial^{\mathrm{EX}}\underline{f}^{R_\mathrm{r}^\mathrm{c}}}{\partial \underline{\varphi}^{R_\mathrm{r}}} \cdot \underline{\varphi}^{R_\mathrm{r}} + \frac{\partial^{\mathrm{EX}}\underline{f}^{R_\mathrm{r}^\mathrm{c}}}{\partial \underline{g}^{S_{\mathrm{FF}(4)}}_{\mathrm{ori}}} \cdot \underline{g}^{S_{\mathrm{FF}(4)}}_{\mathrm{ori}} + \sum_{b=1}^{3} \frac{\partial^{\mathrm{EX}}\underline{f}^{R_\mathrm{r}^\mathrm{c}}}{\partial^{\mathrm{FT}}\underline{f}^{X_{b_{\mathrm{PP}(1)}}}} \cdot \delta^{\mathrm{FT}}\underline{f}^{X_{b_{\mathrm{PP}(1)}}} \\
{}^{\mathrm{EX}}\underline{t}^{R_\mathrm{r}^\mathrm{c}} &= {}^{\mathrm{EX}}\bar{\underline{t}}^{R_\mathrm{r}^\mathrm{c}} + \frac{\partial^{\mathrm{EX}}\underline{t}^{R_\mathrm{r}^\mathrm{c}}}{\partial \underline{g}^{R}_{\mathrm{per}}} \cdot \underline{g}^{R}_{\mathrm{per}} + \frac{\partial^{\mathrm{EX}}\underline{t}^{R_\mathrm{r}^\mathrm{c}}}{\partial \underline{\varphi}^{R_\mathrm{r}}} \cdot \underline{\varphi}^{R_\mathrm{r}} + \frac{\partial^{\mathrm{EX}}\underline{t}^{R_\mathrm{r}^\mathrm{c}}}{\partial \underline{g}^{S_{\mathrm{FF}(4)}}_{\mathrm{ori}}} \cdot \underline{g}^{S_{\mathrm{FF}(4)}}_{\mathrm{ori}} + \sum_{b=1}^{3} \frac{\partial^{\mathrm{EX}}\underline{t}^{R_\mathrm{r}^\mathrm{c}}}{\partial^{\mathrm{FT}}\underline{t}^{X_{b_{\mathrm{PP}(1)}}}} \cdot \delta^{\mathrm{FT}}\underline{t}^{X_{b_{\mathrm{PP}(1)}}}
\end{aligned}
\tag{A.189}
$$

The expressions for the mean external load vectors are just the overlined versions of those in Eq. A.188. For the sensitivities to $\underline{g}^{R}_{\mathrm{per}}$, $\underline{\varphi}^{R_\mathrm{r}}$ and $\underline{g}^{S_{\mathrm{FF}(4)}}_{\mathrm{ori}}$ holds :

$$
\begin{aligned}
\frac{\partial^{\mathrm{EX}}\underline{f}^{R_\mathrm{r}^\mathrm{c}}}{\partial \underline{q}} &= \frac{\partial^{\mathrm{g}}\underline{f}^{R_\mathrm{r}^*}}{\partial \underline{q}} \\
\frac{\partial^{\mathrm{EX}}\underline{t}^{R_\mathrm{r}^\mathrm{c}}}{\partial \underline{q}} &= \mathrm{J}^{3}_{v=1}\big({}^{R_\mathrm{r}^\mathrm{c}}\underline{r}^{R_\mathrm{r}^*} \times \underline{e}_v\big) \cdot \frac{\partial^{\mathrm{g}}\underline{f}^{R_\mathrm{r}^*}}{\partial \underline{q}}
\end{aligned}
\tag{A.190}
$$

Further it holds:

$$
\frac{\partial^{\mathrm{EX}}\underline{f}^{R_\mathrm{r}^\mathrm{c}}}{\partial^{\mathrm{FT}}\underline{f}^{X_{b_{\mathrm{PP}(1)}}}} = \frac{\partial^{\mathrm{EX}}\underline{t}^{R_\mathrm{r}^\mathrm{c}}}{\partial^{\mathrm{FT}}\underline{t}^{X_{b_{\mathrm{PP}(1)}}}} = \Phi_{1b} \equiv \Phi_{\mathrm{x}}^{\mathrm{T}}\big(\tfrac{2\pi(b-1)}{B}\big) \tag{A.191}
$$

(iv) Output variables and vector output equation in 2nd order model

It is allowed to assume that all interaction with the generator rotor R_r and the gearbox house R_h occurs in the rotor centre R_r^c; R_h, in turn interacts with the nacelle in the same point (see section A.5.1). The loading on R_h equals the visco/elastic reaction by the springs and dampers for the shaft flexibility in $R_\mathrm{r}^{\oplus}$ **minus** the torque consumption by the acceleration of the generator rotor. The latter equals the fraction $1/i_{\mathrm{gb}}$ of minus the responsive co-axial torque component ${}^{\mathrm{RS}}t_1^{R_\mathrm{r}^\mathrm{c}}$ in the rotor centre.

The output vector $\underline{y}^{R}$ of the drive-train has the following composition:

$$
\underline{y}^{R_\mathrm{r}} = \begin{bmatrix} \underline{y}^{GR_\mathrm{r}} \\ \underline{y}^{XR_\mathrm{r}} \\ \underline{y}^{SR_\mathrm{r}} \\ \underline{y}^{R_\mathrm{f}R_\mathrm{r}} \end{bmatrix} \tag{A.192}
$$

Only the output subvector $\underline{y}^{XR_\mathrm{r}}$ is the same as in $\underline{v}^{R}$ by Eq. A.6 in section A.1.

The expressions for the means and sensitivities of the feedthrough kinematic and orientation vectors to the rotor blades in $\underline{y}^{XR_\mathrm{r}}$ are listed in section B.2.1 and via Eq. B.167 and Eq. B.281. This concerns $\underline{\omega}^{R_\mathrm{r}}$, $\underline{\alpha}^{R_\mathrm{r}}$, $\underline{v}^{R_\mathrm{r}^\mathrm{c}}$, $\underline{a}^{R_\mathrm{r}^\mathrm{c}}$, $\underline{u}^{R_\mathrm{r}}_{\mathrm{ori}}$, and $\underline{g}^{R_\mathrm{r}}_{\mathrm{ori}}$. The expressions pertain to the actual final coordinate system $\vec{e}^{\,R_\mathrm{r}}$ of the rotor hub.

The exogeneous output subvector $\underline{y}^{GR_\mathrm{r}}$ provides the linear and angular displacements and the torque load in the centre of the hub (section 3.4.3):

$$
\underline{y}^{GR_\mathrm{r}} = \begin{bmatrix} {}^{\bar{R}_\mathrm{r}^\mathrm{c}}\underline{r}^{R_\mathrm{r}^\mathrm{c}/\bar{R}_\mathrm{r}} \\ \underline{\xi}^{R_\mathrm{r}^\mathrm{c}/\bar{R}_\mathrm{r}} \\ {}^{\mathrm{FT}}\underline{t}^{R_\mathrm{r}^\mathrm{c}} \end{bmatrix} \tag{A.193}
$$

For the torque load ${}^{\mathrm{FT}}\underline{t}^{R_\mathrm{r}^\mathrm{c}}$ in the centre of the hub holds:

$$
{}^{\mathrm{FT}}\underline{t}^{R_\mathrm{r}^\mathrm{c}} = {}^{\mathrm{EX}}\underline{t}^{R_\mathrm{r}^\mathrm{c}} \text{(see Eq. A.188 etc.)} \tag{A.194}
$$

The 'user-output' displacements ${}^{\bar{R}^{\mathrm{c}}_{\mathrm{r}}}\underline{r}^{R^{\mathrm{c}}_{\mathrm{r}}/\bar{R}_{\mathrm{r}}}$ and $\underline{\xi}^{R^{\mathrm{c}}_{\mathrm{r}}/\bar{R}_{\mathrm{r}}}$ equal the feedthrough displacements $\underline{x}^{R^{\mathrm{c}}_{\mathrm{r}}}$ and $\underline{\xi}^{R^{\mathrm{c}}_{\mathrm{r}}}$ to the rotor blades. These are coordinate vectors along the rotor hub coordinate system in its *average* position $\vec{e}^{\,\bar{R}_{\mathrm{r}}}$. It holds:

$$\begin{aligned} \underline{\xi}^{R^{\mathrm{c}}_{\mathrm{r}}} &= \underline{\xi}^{R_{\tilde{\mathrm{h}}"}} + \underline{\varphi}^{R_{\mathrm{r}}} + \begin{pmatrix} \varphi_{\mathrm{x}}^{R_{\mathrm{f}}} \\ 0 \\ 0 \end{pmatrix} \\ \underline{x}^{R^{\mathrm{c}}_{\mathrm{r}}} &= \underline{x}^{R_{\tilde{\mathrm{h}}"}} + \underline{\varrho}^{R_{\mathrm{r}}} \end{aligned} \tag{A.195}$$

The output subvector $\underline{y}^{R_{\mathrm{f}}R_{\mathrm{r}}}$ to the generator rotor contains the co-axial torque to the fast shaft; the output subvector $\underline{y}^{SR_{\mathrm{r}}}$ to the nacelle differs from the overall output vector of the drive-train in the co-axial torque: the torque on the fast shaft is not transmitted to the nacelle.

For the overall feedthrough loading from the drive-train along the coordinate system of the slow gearbox shaft R_{s} holds:

$$\begin{aligned} {}^{\mathrm{FT}}\underline{f}^{R_{\mathrm{s}}} &= {}^{R_{\mathrm{s}}}\Phi^{R_{\mathrm{r}}} \cdot (-\underline{\dot{p}}^{R_{\mathrm{r}}} + {}^{\mathrm{EX}}\underline{f}^{R^{\mathrm{c}}_{\mathrm{r}}}) \\ {}^{\mathrm{FT}}\underline{t}^{R_{\mathrm{s}}} &= {}^{R_{\mathrm{s}}}\Phi^{R_{\mathrm{r}}} \cdot (-{}^{R^{\mathrm{c}}_{\mathrm{r}}}\underline{\dot{h}}^{R_{\mathrm{r}}} + {}^{\mathrm{EX}}\underline{t}^{R^{\mathrm{c}}_{\mathrm{r}}}) \end{aligned} \tag{A.196}$$

These overall loads are mapped to the nacelle and generator loading by:

$$\begin{aligned} \underline{y}^{SR_{\mathrm{r}}} &= \begin{bmatrix} {}^{\mathrm{FT}}\underline{f}^{S^{\oplus}_{\tilde{\mathrm{n}}}R_{\mathrm{r}}} \\ {}^{\mathrm{FT}}\underline{t}^{S^{\oplus_{\mathrm{r}}}_{\tilde{\mathrm{n}}}R_{\mathrm{r}}} \end{bmatrix} = \begin{pmatrix} \boldsymbol{I} & \mathrm{O} \\ \mathrm{O} & \boldsymbol{T}_{\mathrm{gb_s}} \end{pmatrix} \cdot \begin{bmatrix} {}^{\mathrm{FT}}\underline{f}^{R_{\mathrm{s}}} \\ {}^{\mathrm{FT}}\underline{t}^{R_{\mathrm{s}}} \end{bmatrix} \text{ with } \boldsymbol{T}_{\mathrm{gb_s}} = \begin{pmatrix} \frac{i_{\mathrm{gb}}-1}{i_{\mathrm{gb}}} & 0 & 0 \\ 0 & 1 & 0 \\ 0 & 0 & 1 \end{pmatrix} \\ \underline{y}^{R_{\mathrm{f}}R_{\mathrm{r}}} &= \begin{bmatrix} {}^{\mathrm{FT}}t_{\mathrm{x}}^{R_{\mathrm{f}}} \end{bmatrix} = \begin{pmatrix} \frac{1}{i_{\mathrm{gb}}} & 0 & 0 \end{pmatrix} \cdot {}^{\mathrm{FT}}\underline{t}^{R_{\mathrm{s}}} \end{aligned} \tag{A.197}$$

The feedthrough loads to the slow gearbox shaft by Eq. A.196 thus depend on the envelope of variables on which external loads and impulse vectors depend. The linearised expressions are:

$$\begin{aligned} {}^{\mathrm{FT}}\underline{f}^{R_{\mathrm{s}}} &= {}^{\mathrm{FT}}\bar{\underline{f}}^{R_{\mathrm{s}}} + \sum_{(\underline{q})} \frac{\partial {}^{\mathrm{FT}}\underline{f}^{R_{\mathrm{s}}}}{\partial \underline{q}} \cdot \delta\underline{q} \\ {}^{\mathrm{FT}}\underline{t}^{R_{\mathrm{s}}} &= {}^{\mathrm{FT}}\bar{\underline{t}}^{R_{\mathrm{s}}} + \sum_{(\underline{q})} \frac{\partial {}^{\mathrm{FT}}\underline{t}^{R_{\mathrm{s}}}}{\partial \underline{q}} \cdot \delta\underline{q} \end{aligned}$$

$$\text{for } \underline{q} = \underline{g}^{R}_{\mathrm{per}}, \{{}^{\mathrm{FT}}\underline{f}^{X_{b_{\mathrm{PP}(1)}}}, {}^{\mathrm{FT}}\underline{t}^{X_{b_{\mathrm{PP}(1)}}} | b = 1 \ldots 3\}, \underline{\omega}^{S^{\oplus}_{\mathrm{FF}(4)}}, \underline{\alpha}^{S_{\mathrm{FF}(4)}}, \underline{a}^{S^{\oplus}_{\mathrm{FF}(4)}}, \underline{g}^{S_{\mathrm{FF}(4)}}_{\mathrm{ori}}$$
$$\varphi_{\mathrm{x}}^{R_{\mathrm{f}}}, \dot{\varphi}_{\mathrm{x}}^{R_{\mathrm{f}}}, \ddot{\varphi}_{\mathrm{x}}^{R_{\mathrm{f}}}; \underline{\varphi}^{R_{\mathrm{r}}}, \underline{\dot{\varphi}}^{R_{\mathrm{r}}}, \underline{\ddot{\varphi}}^{R_{\mathrm{r}}}, \underline{\dot{\varrho}}^{R_{\mathrm{r}}} \underline{\ddot{\varrho}}^{R_{\mathrm{r}}}$$

(A.198)

The means are obtained by just taking the overlined version of the expressions above.

$$\begin{aligned} {}^{\mathrm{FT}}\bar{\underline{f}}^{R_{\mathrm{s}}} &= {}^{R_{\mathrm{s}}}\bar{\Phi}^{R_{\mathrm{r}}} \cdot (-\bar{\underline{\dot{p}}}^{R_{\mathrm{r}}} + {}^{\mathrm{EX}}\bar{\underline{f}}^{R^{\mathrm{c}}_{\mathrm{r}}}) \\ {}^{\mathrm{FT}}\bar{\underline{t}}^{R_{\mathrm{s}}} &= {}^{R_{\mathrm{s}}}\bar{\Phi}^{R_{\mathrm{r}}} \cdot (-{}^{R^{\mathrm{c}}_{\mathrm{r}}}\bar{\underline{\dot{h}}}^{R_{\mathrm{r}}} + {}^{\mathrm{EX}}\bar{\underline{t}}^{R^{\mathrm{c}}_{\mathrm{r}}}) \end{aligned} \tag{A.199}$$

For the sensitivities to the variables $\underline{q}$ holds:

$$\begin{aligned}
\frac{\partial^{\mathrm{FT}}\underline{f}^{R_\mathrm{s}}}{\partial \underline{q}} &= {}^{R_\mathrm{s}}\bar{\Phi}^{R_\mathrm{r}} \cdot \left(-\frac{\partial \underline{\dot{p}}^{R_\mathrm{r}}}{\partial \underline{q}} + \frac{\partial^{\mathrm{EX}}\underline{f}^{R_\mathrm{c}}_\mathrm{r}}{\partial \underline{q}}\right) + \\
&\qquad \delta_{\underline{q}\underline{\phi}^{R_\mathrm{r}}} \cdot \left[\ \mathrm{J}^3_{v=1}\Big(\frac{\partial^{R_\mathrm{s}}\Phi^{R_\mathrm{r}}}{\partial \phi_v^{R_\mathrm{r}}} \cdot \left(-\bar{\underline{p}}^{R_\mathrm{r}} + {}^{\mathrm{EX}}\bar{\underline{f}}^{R^\mathrm{c}_\mathrm{r}}\right)\Big)\ \right] \\
\frac{\partial^{\mathrm{FT}}\underline{t}^{R_\mathrm{s}}}{\partial \underline{q}} &= {}^{R_\mathrm{s}}\bar{\Phi}^{R_\mathrm{r}} \cdot \left(-\frac{\partial^{R^\mathrm{c}_\mathrm{r}}\underline{h}^{R_\mathrm{r}}}{\partial \underline{q}} + \frac{\partial^{\mathrm{EX}}\underline{t}^{R^\mathrm{c}_\mathrm{r}}}{\partial \underline{q}}\right) + \\
&\qquad \delta_{\underline{q}\underline{\phi}^{R_\mathrm{r}}} \cdot \left[\ \mathrm{J}^3_{v=1}\Big(\frac{\partial^{R_\mathrm{s}}\Phi^{R_\mathrm{r}}}{\partial \phi_v^{R_\mathrm{r}}} \cdot \left(-{}^{R^\mathrm{c}_\mathrm{r}}\bar{\underline{\dot{h}}}^{R_\mathrm{r}} + {}^{\mathrm{EX}}\bar{\underline{t}}^{R^\mathrm{c}_\mathrm{r}}\right)\Big)\ \right]
\end{aligned} \tag{A.200}$$

Note that the last term in the right hand side of both equations only applies if $\underline{q}$ equals $\underline{\phi}^{R_\mathrm{r}}$!

The output equation that belongs to the 2$^{\mathrm{nd}}$ order state equation is:

$$\underline{y}^{R_\mathrm{r}} = \left[\boldsymbol{H}^{R_\mathrm{r}}_{\varphi} \ \ \boldsymbol{H}^{R_\mathrm{r}}_{\varrho}\right] \cdot \begin{bmatrix} \underline{\varphi}^{R_\mathrm{r}} \\ \underline{\varrho}^{R_\mathrm{r}} \end{bmatrix} + \left[\boldsymbol{L}^{R_\mathrm{r}}_{\varphi} \ \ \boldsymbol{L}^{R_\mathrm{r}}_{\varrho}\right] \cdot \begin{bmatrix} \underline{\dot{\varphi}}^{R_\mathrm{r}} \\ \underline{\dot{\varrho}}^{R_\mathrm{r}} \end{bmatrix} + \boldsymbol{K}^{R_\mathrm{r}} \cdot \underline{v}^{R_\mathrm{r}} \tag{A.201}$$

For the output matrix partitions $\boldsymbol{H}^{R_\mathrm{r}}_{\varphi}$ and $\boldsymbol{H}^{R_\mathrm{r}}_{\varrho}$, which map angular and linear dof position variations to the outputs thus holds:

$$\begin{aligned}
\boldsymbol{H}^{R_\mathrm{r}}_{\varphi} &= \frac{\partial \underline{y}^{R_\mathrm{r}}}{\partial \underline{\phi}^{R_\mathrm{r}}} - \left(\frac{\partial \underline{y}^{R_\mathrm{r}}}{\partial \underline{\ddot{\varphi}}^{R_\mathrm{r}}} \cdot \left(\boldsymbol{M}^{R_\mathrm{r}}\right)^{-1}_{\varphi} + \frac{\partial \underline{y}^{R_\mathrm{r}}}{\partial \underline{\ddot{\varrho}}^{R_\mathrm{r}}} \cdot \left(\boldsymbol{M}^{R_\mathrm{r}}\right)^{-1}_{\varrho}\right) \cdot \boldsymbol{S}^{R_\mathrm{r}}_{\varphi} \\
\boldsymbol{H}^{R_\mathrm{r}}_{\varrho} &= \frac{\partial \underline{y}^{R_\mathrm{r}}}{\partial \underline{\rho}^{R_\mathrm{r}}} - \left(\frac{\partial \underline{y}^{R_\mathrm{r}}}{\partial \underline{\ddot{\varphi}}^{R_\mathrm{r}}} \cdot \left(\boldsymbol{M}^{R_\mathrm{r}}\right)^{-1}_{\varphi} + \frac{\partial \underline{y}^{R_\mathrm{r}}}{\partial \underline{\ddot{\varrho}}^{R_\mathrm{r}}} \cdot \left(\boldsymbol{M}^{R_\mathrm{r}}\right)^{-1}_{\varrho}\right) \cdot \boldsymbol{S}^{R_\mathrm{r}}_{\varrho}
\end{aligned} \tag{A.202}$$

The rows of the matrix partitions $\left(\boldsymbol{M}^{R_\mathrm{r}}\right)^{-1}_{\varphi}$ and $\left(\boldsymbol{M}^{R_\mathrm{r}}\right)^{-1}_{\varrho}$ of the inverse mass matrix respectively yield the expression for the subvector $\underline{\ddot{\varphi}}^{R_\mathrm{r}}$ and $\underline{\ddot{\varrho}}^{R_\mathrm{r}}$ similarly to exspression A.128 for the blade flange X_f.

The output matrices $\boldsymbol{L}^{R_\mathrm{r}}_{\varphi}$ and $\boldsymbol{L}^{R_\mathrm{r}}_{\varphi}$ are obtained by using the direct sensitivities $\partial \underline{y}^{R_\mathrm{r}}/\partial \underline{\dot{\varphi}}^{R_\mathrm{r}}$ and $\partial \underline{y}^{R_\mathrm{r}}/\partial \underline{\dot{\varrho}}^{R_\mathrm{r}}$ instead of $\partial \underline{y}^{R_\mathrm{r}}/\partial \underline{\phi}^{R_\mathrm{r}}$ and $\partial \underline{y}^{R_\mathrm{r}}/\partial \underline{\rho}^{R_\mathrm{r}}$, and by replacing the stiffness matrix partitions $\boldsymbol{S}^{R_\mathrm{r}}_{\varphi}$ and $\boldsymbol{S}^{R_\mathrm{r}}_{\varrho}$ by the damper matrix partitions $\boldsymbol{D}^{R_\mathrm{r}}_{\varphi}$ and $\boldsymbol{D}^{R_\mathrm{r}}_{\varrho}$.

The partial derivative of the output vector $\underline{y}^{R_\mathrm{r}}$, which is composed of subvectors $\{\underline{z}_\mathrm{y}\}$, to a subvector $\underline{q}$ like $\underline{\phi}^{R_\mathrm{r}}$ is obtained by putting above each other ('stacking') the partial derivatives of the involved output elementary subvectors (see also Eq. A.85 and A.115):

$$\begin{aligned}
\frac{\partial \underline{y}^{R_\mathrm{r}}}{\partial \underline{q}} &= \mathrm{S}_{(\underline{z}_\mathrm{y})}\left(\frac{\partial \underline{z}_\mathrm{y}}{\partial \underline{q}}\right) \qquad \text{for } \underline{z}_\mathrm{y} = {}^{\bar{R}^\mathrm{c}_\mathrm{r}}\underline{r}^{R^\mathrm{c}_\mathrm{r}/\bar{R}_\mathrm{r}}, \underline{\xi}^{R^\mathrm{c}_\mathrm{r}/\bar{R}_\mathrm{r}}, {}^{\mathrm{FT}}\underline{t}^{R^\mathrm{c}_\mathrm{r}}, \underline{\omega}^{R_\mathrm{r}}, \underline{\alpha}^{R_\mathrm{r}}, \underline{v}^{R^\mathrm{c}_\mathrm{r}}, \underline{a}^{R^\mathrm{c}_\mathrm{r}}, \underline{\xi}^{R^\mathrm{c}_\mathrm{r}}, \underline{x}^{R^\mathrm{c}_\mathrm{r}} \\
&\qquad \underline{u}^{R_\mathrm{r}}_{\mathrm{ori}}, \underline{g}^{R_\mathrm{r}}_{\mathrm{ori}}, \underline{\xi}^{R_\mathrm{r}}, \underline{x}^{R^\mathrm{c}_\mathrm{r}\mathrm{FT}}\underline{f}^{S^{\oplus\mathrm{r}}_{\tilde{\mathrm{n}}}}, {}^{\mathrm{FT}}\underline{t}^{S^{\oplus\mathrm{r}}_{\tilde{\mathrm{n}}}R_\mathrm{r}}, {}^{\mathrm{FT}}t^{R_\mathrm{f}}_{\mathrm{x}}
\end{aligned} \tag{A.203}$$

For the feedthrough matrix partition $\boldsymbol{K}^{R_\mathrm{r}}$ holds:

$$\boldsymbol{K}^{R_\mathrm{r}} = \frac{\partial \underline{y}^{R_\mathrm{r}}}{\partial \underline{v}^{R_\mathrm{r}}} - \left(\frac{\partial \underline{y}^{R_\mathrm{r}}}{\partial \underline{\ddot{\varphi}}^{R_\mathrm{r}}} \cdot \left(\boldsymbol{M}^{R_\mathrm{r}}\right)^{-1}_{\varphi} + \frac{\partial \underline{y}^{R_\mathrm{r}}}{\partial \underline{\ddot{\varrho}}^{R_\mathrm{r}}} \cdot \left(\boldsymbol{M}^{R_\mathrm{r}}\right)^{-1}_{\varrho}\right) \cdot \boldsymbol{G}^{R_\mathrm{r}} \tag{A.204}$$

Note that the partial derivatives to the dof vectors are cleaned up before use in the determination of the output and feedthrough matrices: columns that pertain to non-dof directions as concerns R_r are removed.

The input vector $\underline{v}^{R_\mathrm{r}}$ is composed of subvectors $\{\underline{q}_\mathrm{v}\}$. The partial derivative of the composed output vector $\underline{y}^{R_\mathrm{r}}$ to this input vector is obtained by (i) stacking the partial derivatives of the output subvectors to an input subvector, and (ii) doing this for all input

subvectors and putting next to each other the obtained 'stacks'. With output subvectors $\{\underline{z}_{\mathrm{y}}\}$ the expression becomes (see e.g. also Eq. A.88):

$$\frac{\partial \underline{y}^{R_{\mathrm{r}}}}{\partial \underline{v}^{R_{\mathrm{r}}}} = \mathrm{J}_{(\underline{q}_{\mathrm{v}})}\Big(\mathrm{S}_{(\underline{z}_{\mathrm{y}})}\Big(\frac{\partial \underline{z}_{\mathrm{y}}}{\partial \underline{q}_{\mathrm{v}}}\Big)\Big) \quad \text{with} \quad \begin{cases} \underline{q}_{\mathrm{v}} = \underline{g}^{R}_{\mathrm{per}}, \{{}^{\mathrm{FT}}\underline{f}^{X_{b_{\mathrm{PP}(1)}}}, {}^{\mathrm{FT}}\underline{t}^{X_{b_{\mathrm{PP}(1)}}} | b = 1 \ldots 3\}, \\ \quad \underline{\omega}^{S^{\oplus}_{\mathrm{FF}(4)}}, \underline{\alpha}^{S_{\mathrm{FF}(4)}}, \underline{v}^{S^{\oplus}_{\mathrm{FF}(4)}}, \underline{a}^{S^{\oplus}_{\mathrm{FF}(4)}}, \underline{u}^{S_{\mathrm{FF}(4)}}_{\mathrm{ori}}, \underline{g}^{S_{\mathrm{FF}(4)}}_{\mathrm{ori}}, \\ \quad \underline{\xi}^{S_{\mathrm{FF}(4)}}, \underline{x}^{S_{\mathrm{FF}(4)}}, \varphi^{R_{\mathrm{f}}}_{\mathrm{x}}, \dot{\varphi}^{R_{\mathrm{f}}}_{\mathrm{x}}, \ddot{\varphi}^{R_{\mathrm{f}}}_{\mathrm{x}} \\ \underline{z}_{\mathrm{y}} \text{ as in Eq. A.203} \end{cases} \tag{A.205}$$

A.4.2 Equation of motion for fast shaft & generator rotor R_{f}

The model for R_{f} only includes co-axial angular impulse conservation of the generator rotor. All remaining first order inertia effects are taken into account in the model for the nacelle. This includes gyroscopic tilt- and yawwise effects. The counter torque by the electric system (responsive loading) may be either incorporated in the model of R_{f} itself, as a function of the variation in the main azimut angle and / or its time derivative, or it may be imported from the subcomponent $R_{\mathrm{f_c}}$ with a specific model for the generator torque control system. This is specified during the parametrisation of the drive-train via function TUBDRIVTRPAR().

The mean values and sensitivities of the impulse vectors as formulated in section B.2.2, paragraph on *Generator rotor & fast shaft* R_{f}, apply and do not need further discussion. Because the mass parameter is moved to the nacelle, there is no gravitation loading. The responsive loading is dealt with in paragraph (i), which includes the option for generator toruqe control. The required input variables are subject of paragraph (ii). Then, the second order state equation for the generator rotor is formulated in paragraph (iii), followed by the required output equation in paragraph (iv). Finally, paragraph (v) describes the submodel for the generator torque control system.

The subcomponent model for the generator rotor & fast shaft R_{f} is obtained by a call to TBUR2SUBEOM() in function TBUDRIVTREOM(). The model for R_{f} exists as structure variable sysR2sub. The fields in sysR2sub are 2D matrices A, B, C, K, the parameterisation of the first order state space representation, and cell arrays with lists of input, output and state variable names. Point of departure for the generator rotor model creation by function TBUR2SUBEOM() is the availability for the one-element subcomponent R_{f} of ((f.)c.s: (final) coordinate system):

- means and sensitivities of angular and linear impulse vector of R_{f} (along f.c.s. of R_{f} in actual position);
- mean co-axial feedthrough torque from the rotor shaft & hub (along c.s. of gearbox slow shaft $\{R\mathrm{s}\}$ in actual position);
- transformation matrices and their sensitivities to rotational dofs relative to the slow shaft exit of the gearbox R_{s} (forward and backward);
- co-axial stiffness and damper value
- bottom-up ranking of rotation and translation axes in the connnection point;
- flags for co-axial angular dof and for feedthrough of azimut deviation[4];
- gearbox ratio

[4]If this flag equals 0 then variations in the main rotational speed do *NOT* affect the azimut position of the tubine rotor.

The mentioned sensitivities belong to the 'motion formulations' and map all motion variations to input variables from the support structure or to dofs in the generator rotor. These are provided by a preceeding call in TBUDRIVTREOM() to function TBUDRIVTRIMP(). Note that outputs from the support structure are assumed to be modulated with the main azimut angle (See section A.1, par. (vi), header *Support structure outputs into the drive-train*).

Functionality TBUR2SUBEOM() ((f.)c.s: (final) coordinate system):

- definition of input name lists; each list contains the names of the input subvectors from a specific source (S, R3sub, RCsub (= generator torque control system));
- definition of output name lists; each list contains the names of the output subvectors to a specific destination (G, S, R3sub, RCsub);
- assemble the 'extern torque load formulation' from the coaxial feedthrough loading from the rotor shaft & hub (coordinates along actual f.c.s. of R_{f});
- define 'equal to zero' the feedthrough loading from outward elements within the 'generator rotor subcomponent' (there are no) (call TBUSYSFTFT());
- definition of the sensitivities of the responsive (visco/elastic) torque (and dummy force) loads the dofs or the input from the generator torque control system (see par. (i));
- derive the mass, spring and damper matrix for the equations of motion for the generator rotor R_{f} ($\boldsymbol{M}, \boldsymbol{S}, \boldsymbol{D}$; call TBUSYSMDSMX());
- derive load formulations for feedthrough torque loading on the nacelle (call TBUSYSFTPP; along actual c.s of slow gearbox exit R_{s});
- derive the input matrix for the mass/spring/damper formulation of R_{f} as well as the output matrices on the dofs and their time derivatives and the feedthrough matrix ($\boldsymbol{G}, \boldsymbol{H}, \boldsymbol{L}, \boldsymbol{K}$; call TBUSYSGHLKMX());
- transform the mass/spring/damper model formulation $\{\boldsymbol{M}, \boldsymbol{S}, \boldsymbol{D}, \boldsymbol{G}, \boldsymbol{H}, \boldsymbol{L}, \boldsymbol{K}\}$ to the first order state space formulation $\{\boldsymbol{A}, \boldsymbol{B}, \boldsymbol{C}, \boldsymbol{K}\}$ (call TBUSYSMDS2FSR()).

The model for the generator torque control system exists in structure variable sysRCsub. It is created with TBURCSUBEOM() via call from function TBUDRIVTREOM(). Point of departure for the torque controller model creation by TBURCSUBEOM() is the availability of:

- parameters for torque servo behaviour of the electric system;
- steepness of the torque/speed curve in the actual working conditions and parameters for low-pass filtering;
- feedback gain for damping of drive-train distorsion and parameters for high- or band-pass filtering.

Functionality TBURCSUBEOM():

- definition of input name lists; each list contains the names of the input subvectors from a specific source (R2sub)
- definition of output name lists; each list containts the names of the output subvectors to a specific destination (R2sub);
- parametrisation of the transfer function formulations for the torque servo behaviour, torque/speed control and drive-train damping

- connect transfer function models (call SERIES(), PARALLEL());
- convert transfer function models to first order state space models (call TF2SS())

(i) Responsive loading

The only responsive loading that matters is the co-axial torque from the electric system. With the defined bottum-up ranked rotation order along the y-, z- and x-axis, the expression for the reponsive torque vector becomes:

$$ {}^{\mathrm{RS}}\underline{t}^{R_{\mathrm{f}}} \triangleq \begin{bmatrix} {}^{\mathrm{RS}}t_{\mathrm{x}}^{R_{\mathrm{f}}3} \\ {}^{\mathrm{RS}}t_{\mathrm{y}}^{R_{\mathrm{f}}1} \\ {}^{\mathrm{RS}}t_{\mathrm{z}}^{R_{\mathrm{f}}2} \end{bmatrix} = {}^{\mathrm{RS}}\underline{\bar{t}}^{R_{\mathrm{f}}} + \frac{\partial^{\mathrm{RS}}\underline{t}^{R_{\mathrm{f}}}}{\partial \underline{\varphi}^{R_{\mathrm{f}}}} \cdot \underline{\varphi}^{R_{\mathrm{f}}} + \frac{\partial^{\mathrm{RS}}\underline{t}^{R_{\mathrm{f}}}}{\partial \underline{\dot{\varphi}}^{R_{\mathrm{f}}}} \cdot \underline{\dot{\varphi}}^{R_{\mathrm{f}}} + \frac{\partial^{\mathrm{RS}}\underline{t}^{R_{\mathrm{f}}}}{\partial t_{\mathrm{e}}} \cdot \delta t_{\mathrm{e}} \tag{A.206} $$

Note that in case of a direct-coupled asynchronous or synchronous machine, which does not allow a generator torque control system, one of the first two terms in the left hand side applies, while in case of a variable speed system only the third term applies. In the latter case, the generator torque control system yields a 'counter torque': if > 0 then it will slow down the rotational speed.

For the sensitivities to the angular dof vectors and to the control torque from $R_{\mathrm{f_c}}$ then holds:

$$ \frac{\partial^{\mathrm{RS}}\underline{t}^{R_{\mathrm{f}}}}{\partial \underline{\varphi}^{R_{\mathrm{f}}}} = -\begin{pmatrix} 0 & 0 & s_{\mathrm{t_x}\phi_{\mathrm{x}}}^{R_{\mathrm{f}}} \\ 0 & 0 & 0 \\ 0 & 0 & 0 \end{pmatrix} \quad ; \quad \frac{\partial^{\mathrm{RS}}\underline{t}^{R_{\mathrm{f}}}}{\partial \underline{\dot{\varphi}}^{R_{\mathrm{f}}}} = -\begin{pmatrix} 0 & 0 & d_{\mathrm{t_x}\phi_{\mathrm{x}}}^{R_{\mathrm{f}}} \\ 0 & 0 & 0 \\ 0 & 0 & 0 \end{pmatrix} \quad ; \quad \frac{\partial^{\mathrm{RS}}\underline{t}^{R_{\mathrm{f}}}}{\partial t_{\mathrm{e}}} = \begin{pmatrix} -1 \\ 0 \\ 0 \end{pmatrix} \tag{A.207} $$

As described in paragraph (ii) in section 3.7.2 the responsive loading for the rotor shaft involves viso-elastic loads for up to six degrees of freedom. Similar to the rotor shaft subcomponent model, the sensitivity matrices to the 'full dof vectors' of the drive-train are now *just the* 3×3 *matrices* $\frac{\partial^{\mathrm{RS}}\underline{t}^{R_{\mathrm{f}}}}{\partial \underline{\varphi}^{R_{\mathrm{f}}}}$, $\frac{\partial^{\mathrm{RS}}\underline{t}^{R_{\mathrm{f}}}}{\partial \underline{o}^{R_{\mathrm{f}}}}$, $\frac{\partial^{\mathrm{RS}}\underline{f}^{R_{\mathrm{f}}}}{\partial \underline{\varphi}^{R_{\mathrm{f}}}}$ and $\frac{\partial^{\mathrm{RS}}\underline{f}^{R_{\mathrm{f}}}}{\partial \underline{o}^{R_{\mathrm{f}}}}$ as specified in Eq. A.207 for the non-zero ones. In the implementation it is faked as if the overall drive-train model consists of only *one* subcomponent; the subcomponent counter m is set to 1 i.s.o. 2. This is the only way in which can be deal with the 'rather strange' drive-train elements via the generic functions tbusysmdsmx(), tbusysghlkmx() etc. The price to be payed for it is that the names of the input and output variables of R_{f} to the rotor shaft&hub are to be modified as concerns the *source counter* m. This is established by setting the so called 'offset variable' `mshift4subcmp` equal to 1 (the offset variables `mshift4inff, mshift4inpp, mshift4outff, mshift4outpp` are all set equal to 0; see tbusysmdsghlkmx() and tbur2subeom().

mshift4subcmp=1;

(ii) Input variables

The input vector for R_{f} has the following composition:

$$ \underline{v}^{R_{\mathrm{f}}} = \begin{bmatrix} \underline{v}^{R_{\mathrm{f}}S} \\ \underline{v}^{R_{\mathrm{f}}R_{\mathrm{r}}} \\ \underline{v}^{R_{\mathrm{f}}R_{\mathrm{f_c}}} \end{bmatrix} \tag{A.208} $$

with

$$ \underline{v}^{R_{\mathrm{f}}S} = \begin{bmatrix} \underline{\alpha}^{S_{\mathrm{FF}(4)}} \end{bmatrix} \quad ; \quad \underline{v}^{R_{\mathrm{f}}R_{\mathrm{r}}} = \begin{bmatrix} {}^{\mathrm{FT}}t_{\mathrm{x}}^{R_{\mathrm{f}}} \end{bmatrix} \quad ; \quad \underline{v}^{R_{\mathrm{f}}R_{\mathrm{f_c}}} = \begin{bmatrix} t_{\mathrm{e}} \end{bmatrix} $$

(iii) Equations of motion and 2$^{\mathrm{nd}}$ order vector state equation

The derivation method for the second order state equation for the rotor shaft R_{r} also holds for R_{f}, but in a much more simple way. The generator rotor R_{f} moves in co-axial angular sense only with respect to the nacelle. This means that only one equation of motion for R_{f} is to be taken into account in the drive-train model. The governing equation pertains to the angular impulse coordinate along the x-axis. All remaining dynamic effects of R_{f} are moved to the nacelle. The implementation via function TBUSYSMDSMX() is nevertheless based on the encapsulating dof vectors $\underline{\phi}^{R_{\mathrm{f}}}$ and $\underline{\rho}^{R_{\mathrm{f}}}$. with 6×6-matrices:

$$\left[\boldsymbol{M}_{\varphi}^{R_{\mathrm{f}}} \mid \boldsymbol{M}_{\varrho}^{R_{\mathrm{f}}}\right] \cdot \begin{bmatrix} \underline{\ddot{\varphi}}^{R_{\mathrm{f}}} \\ \underline{\ddot{\varrho}}^{R_{\mathrm{f}}} \end{bmatrix} + \left[\boldsymbol{D}_{\varphi}^{R_{\mathrm{f}}} \mid \boldsymbol{D}_{\varrho}^{R_{\mathrm{f}}}\right] \cdot \begin{bmatrix} \underline{\dot{\varphi}}^{R_{\mathrm{f}}} \\ \underline{\dot{\varrho}}^{R_{\mathrm{f}}} \end{bmatrix} + \left[\boldsymbol{S}_{\varphi}^{R_{\mathrm{f}}} \mid \boldsymbol{S}_{\varrho}^{R_{\mathrm{f}}}\right] \cdot \begin{bmatrix} \underline{\varphi}^{R_{\mathrm{f}}} \\ \underline{\varrho}^{R_{\mathrm{f}}} \end{bmatrix} = \left[\boldsymbol{G}^{R_{\mathrm{f}}S} \mid \boldsymbol{G}^{R_{\mathrm{f}}R_{\mathrm{r}}} \mid \boldsymbol{G}^{R_{\mathrm{f}}R_{\mathrm{fc}}}\right] \cdot \begin{bmatrix} \underline{v}^{R_{\mathrm{f}}S} \\ \underline{v}^{R_{\mathrm{f}}R_{\mathrm{r}}} \\ \underline{v}^{R_{\mathrm{f}}R_{\mathrm{fc}}} \end{bmatrix} \tag{A.209}$$

These matrices are derived by considering the angular and linear vector impulse equation for the one-element subcomponent R_{f} in its set of three coordinate systems. Since each non-valid row and the corresponding column, which pertains to a 'non-dof' element of $\underline{\varphi}^{R_{\mathrm{f}}}$ or $\underline{\varrho}^{R_{\mathrm{f}}}$, is deleted from the mass, damper, stiffnes and input matrix, we have only to consider the *angular* scalar impulse equation along the x-axis. The rotations in R_{f} are bottom-up ranked along the y-, z and x-axis. So we start (and also end up) with the x-coordinate of the angular impulse in the 3rd intermediate coordinate system. The row $\underline{\boldsymbol{m}}_{h\varphi_w}^{R_{\mathrm{f}}}$ for $w = 3$, with ranking numbers $2(w-1)+1$ in the mass matrix partition $\boldsymbol{M}_{\varphi}^{R_{\mathrm{f}}}$ is now determined as follows (the partial derivatives in the right hand side only apply if they are defined for the 'independent variable' $\underline{\ddot{\varphi}}^{R_{\mathrm{f}}}$):

- for $w = 3$:

$$\underline{\boldsymbol{m}}_{h\varphi_3}^{R_{\mathrm{f}}} = -[\,1\,0\,0\,] \cdot \frac{\partial^{\mathrm{RS}}\underline{t}^{R_{\mathrm{f}}}}{\partial \underline{\ddot{\varphi}}^{R_{\mathrm{f}}}} + [\,1\,0\,0\,] \cdot \left(\frac{\partial^{R_{\mathrm{f}}^*}\underline{\dot{h}}^{R_{\mathrm{f}}}}{\partial \underline{\ddot{\varphi}}^{R_{\mathrm{f}}}} - \frac{\partial^{\mathrm{EX}}\underline{t}^{R_{\mathrm{f}}}}{\partial \underline{\ddot{\varphi}}^{R_{\mathrm{f}}}}\right) \tag{A.210}$$

Note that NO feedthrough loading exists from other elements within the one-element subcomponent R_{f}. The loading from the rotor shaft & hub R_{r} is considered as external loading for R_{f} and included in ${}^{\mathrm{EX}}\underline{t}^{R_{\mathrm{f}}}$.

For the corresponding row in the damping matrix partition $\boldsymbol{D}_{\varphi}^{R_{\mathrm{f}}}$ and stiffness matrix partition $\boldsymbol{S}_{\varphi}^{R_{\mathrm{f}}}$, take the sensitivities to $\underline{\dot{\varphi}}^{R_{\mathrm{f}}}$ and $\underline{\varphi}^{R_{\mathrm{f}}}$.

The row $\underline{\boldsymbol{g}}_{h_w}^{R_{\mathrm{f}}S}$ for $w = 3$, with ranking number $2(w-1)+1$ in the input matrix partition $\boldsymbol{G}^{R_{\mathrm{f}}S}$, is determined as follows (the partial derivatives in the right hand side only apply if they are defined for the 'independent variable'; in this case $\underline{z}$):

- for $w = 3$:

$$\underline{\boldsymbol{g}}_{h3}^{R_{\mathrm{f}}S} = [\,1\,0\,0\,] \cdot \frac{\partial^{\mathrm{RS}}\underline{t}^{R_{\mathrm{f}}}}{\partial \underline{z}} + [\,1\,0\,0\,] \cdot \left(-\frac{\partial^{R_{\mathrm{f}}^*}\underline{\dot{h}}^{R_{\mathrm{f}}}}{\partial \underline{z}} + \frac{\partial^{\mathrm{EX}}\underline{t}^{R_{\mathrm{f}}}}{\partial \underline{z}}\right) \tag{A.211}$$

The involved subvectors $\underline{z}$ for the submatrices $\boldsymbol{G}^{R_{\mathrm{f}}S}$, $\boldsymbol{G}^{R_{\mathrm{f}}R_{\mathrm{r}}}$, $\boldsymbol{G}^{R_{\mathrm{f}}R_{\mathrm{fc}}}$ are:

- co-axial feedthrough torque from the rotor shaft & hub: $[\,{}^{\mathrm{FT}}t_{\mathrm{x}}^{R_{\mathrm{f}}}\,]$
- processed angular acceleratoin vector from support structure: $\underline{\alpha}^{S_{\mathrm{FF}(4)}}$
- co-axial electric torque from the generator torque control system : $[\,t_{\mathrm{e}}\,]$

The external load coordinate vector only includes the feedthrough loading from the rotor shaft & hub: (see also Eq. A.20):

$$ {}^{\mathrm{EX}}\underline{t}^{R_\mathrm{f}} \quad = \quad \begin{bmatrix} {}^{\mathrm{FT}}t_\mathrm{x}^{R_\mathrm{f}} \\ 0 \\ 0 \end{bmatrix} \tag{A.212} $$

The expressions for the mean external torque vector is just the overlined versions A.188. As the (co-axial) variation $\underline{\varphi_3}^{R_\mathrm{f}}$ in the main rotation is the only potential dof in R_f, the mean feedthrough load from R_f, which is also co-axial, does not result in load variations on R_f because of the dofs in R_f.

(iv) Output variables and vector output equation in 2nd order model

The output vector of R_f has the following composition:

$$ \underline{y}^{R_\mathrm{f}} = \begin{bmatrix} \underline{y}^{GR_\mathrm{f}} \\ \underline{y}^{SR_\mathrm{f}} \\ \underline{y}^{R_\mathrm{r}R_\mathrm{f}} \\ \underline{y}^{R_{\mathrm{f_c}}R_\mathrm{f}} \end{bmatrix} $$

with

$$ \underline{y}^{GR_\mathrm{f}} = \begin{bmatrix} \dot{\varphi}_\mathrm{x}^{R_\mathrm{f}} \\ t_\mathrm{e} \end{bmatrix} \quad ; \quad \underline{y}^{SR_\mathrm{f}} = \begin{bmatrix} {}^{\mathrm{FT}}\underline{t}^{S\oplus_\mathrm{n}R_\mathrm{f}} \end{bmatrix} \quad ; \quad \underline{y}^{R_\mathrm{r}R_\mathrm{f}} = \begin{bmatrix} \varphi_\mathrm{x}^{R_\mathrm{f}} \\ \dot{\varphi}_\mathrm{x}^{R_\mathrm{f}} \\ \ddot{\varphi}_\mathrm{x}^{R_\mathrm{f}} \end{bmatrix} \quad ; \quad \underline{y}^{R_{\mathrm{f_c}}R_\mathrm{f}} = \begin{bmatrix} \dot{\varphi}_\mathrm{x}^{R_\mathrm{f}} \end{bmatrix} \tag{A.213} $$

For the feedthrough torque ${}^{\mathrm{FT}}\underline{t}^{S\oplus_\mathrm{n}R_\mathrm{f}}$ to the support structure holds (along slow gearbox shaft c.s. $\vec{e}^{\,R_\mathrm{s}}$):

$$ {}^{\mathrm{FT}}\underline{t}^{S\oplus_\mathrm{n}R_\mathrm{f}} = {}^{R_\mathrm{s}}\Phi^{R_\mathrm{f}} \cdot (-{}^{R_\mathrm{f}^*}\dot{\underline{h}}^{R_\mathrm{f}} + {}^{\mathrm{EX}}\underline{t}^{R_\mathrm{f}}) \tag{A.214} $$

This torque thus depends on the envelope of variables on which the external torque and angular impulse vectors depend. The linearised expression is:

$$ \begin{aligned} {}^{\mathrm{FT}}\underline{t}^{S\oplus_\mathrm{n}R_\mathrm{f}} \quad &= \quad {}^{\mathrm{FT}}\bar{\underline{t}}^{S\oplus_\mathrm{n}R_\mathrm{f}} + \sum_{(\underline{q})} \frac{\partial {}^{\mathrm{FT}}\underline{t}^{S\oplus_\mathrm{n}R_\mathrm{f}}}{\partial \underline{q}} \cdot \delta\underline{q} \\ &\text{for } \underline{q} = \underline{\alpha}^{S_{\mathrm{FF}(4)}}, [{}^{\mathrm{FT}}t_\mathrm{x}^{R_\mathrm{f}}], \underline{\ddot{\varphi}}^{R_\mathrm{f}} \end{aligned} \tag{A.215} $$

The rate of change in the angular impulse of R_f is zero-mean. The only non-zero mean external torque loading results from the co-axial feedthrough torque from the rotor shaft & hub R_r by Eq. A.212 and A.197, so that:

$$ {}^{\mathrm{FT}}\bar{\underline{t}}^{S\oplus_\mathrm{n}R_\mathrm{f}} = \boldsymbol{T}_{\mathrm{gb_f}} \cdot {}^{\mathrm{FT}}\bar{\underline{t}}^{R_\mathrm{s}} \text{ with } \boldsymbol{T}_{\mathrm{gb_f}} = \begin{pmatrix} \frac{1}{i_\mathrm{gb}} & 0 & 0 \\ 0 & 0 & 0 \\ 0 & 0 & 0 \end{pmatrix} \tag{A.216} $$

with ${}^{\mathrm{FT}}\bar{\underline{t}}^{R_\mathrm{s}}$ by Eq. A.199

Because of non-zero torque loading and angular dofs along the x-axis *only*, it simply holds for the sensitivities:

$$ \frac{\partial {}^{\mathrm{FT}}\underline{t}^{S\oplus_\mathrm{n}R_\mathrm{f}}}{\partial \underline{q}} \quad = \quad {}^{R_\mathrm{s}}\bar{\Phi}^{R_\mathrm{f}} \cdot (-\frac{\partial {}^{R_\mathrm{f}^*}\dot{\underline{h}}^{R_\mathrm{f}}}{\partial \underline{q}} + \frac{\partial {}^{\mathrm{EX}}\underline{t}^{R_\mathrm{f}}}{\partial \underline{q}}) \tag{A.217} $$

For 'user-output' counter torque holds:

$$ t_\mathrm{e} = [\,1 \;\; 0 \;\; 0\,] \cdot {}^{\mathrm{FT}}\underline{t}^{S\oplus_\mathrm{n}R_\mathrm{f}} \tag{A.218} $$

For the sensitivities of the output subvector to the rotor shaft & hub holds (bottom-up ranked rotations along $y-$, $z-$ and $x-$axis):

$$\begin{aligned}
\frac{\partial \underline{y}^{R_\mathrm{r}R_\mathrm{f}}}{\partial \underline{\varphi}^{R_\mathrm{f}}} &= \begin{pmatrix} 0 & 0 & \delta_{1\psi}\cdot\frac{1}{i_\mathrm{gb}} \\ 0 & 0 & 0 \\ 0 & 0 & 0 \end{pmatrix} \\
\frac{\partial \underline{y}^{R_\mathrm{r}R_\mathrm{f}}}{\partial \dot{\underline{\varphi}}^{R_\mathrm{f}}} &= \begin{pmatrix} 0 & 0 & 0 \\ 0 & 0 & \frac{1}{i_\mathrm{gb}} \\ 0 & 0 & 0 \end{pmatrix} \\
\frac{\partial \underline{y}^{R_\mathrm{r}R_\mathrm{f}}}{\partial \ddot{\underline{\varphi}}^{R_\mathrm{f}}} &= \begin{pmatrix} 0 & 0 & 0 \\ 0 & 0 & 0 \\ 0 & 0 & \frac{1}{i_\mathrm{gb}} \end{pmatrix}
\end{aligned} \tag{A.219}$$

The kronecker delta $\delta_{1\psi}$ implies the option for the azimut deviation flag being 1 or 0. If this flag equals 0 then the azimut variation by the variation in the main rotational speed is *NOT* fed through in the azimut position of the rotor shaft and rotor blade.

The output equation that belongs to the 2$^{\mathrm{nd}}$ order state equation is (angular dofs only):

$$\underline{y}^{R_\mathrm{f}} = \boldsymbol{H}_{\varphi}^{R_\mathrm{f}}\cdot\underline{\varphi}^{R_\mathrm{f}} + \boldsymbol{L}_{\varphi}^{R_\mathrm{f}}\cdot\dot{\underline{\varphi}}^{R_\mathrm{f}} + \boldsymbol{K}^{R_\mathrm{f}}\cdot\underline{v}^{R_\mathrm{f}} \tag{A.220}$$

For the output matrix partitions $\boldsymbol{H}_{\varphi}^{R_\mathrm{f}}$ and $\boldsymbol{L}_{\varphi}^{R_\mathrm{f}}$, which map angular dof position and speed variations to the outputs hold:

$$\begin{aligned}
\boldsymbol{H}_{\varphi}^{R_\mathrm{f}} &= \frac{\partial \underline{y}^{R_\mathrm{f}}}{\partial \underline{\phi}^{R_\mathrm{f}}} - \frac{\partial \underline{y}^{R_\mathrm{f}}}{\partial \ddot{\underline{\varphi}}^{R_\mathrm{f}}}\cdot\left(\boldsymbol{M}^{R_\mathrm{f}}\right)_{\varphi}^{-1}\cdot\boldsymbol{S}_{\varphi}^{R_\mathrm{f}} \\
\boldsymbol{L}_{\varphi}^{R_\mathrm{f}} &= \frac{\partial \underline{y}^{R_\mathrm{f}}}{\partial \underline{\varphi}^{R_\mathrm{f}}} - \frac{\partial \underline{y}^{R_\mathrm{f}}}{\partial \ddot{\underline{\varphi}}^{R_\mathrm{f}}}\cdot\left(\boldsymbol{M}^{R_\mathrm{f}}\right)_{\varphi}^{-1}\cdot\boldsymbol{D}_{\varphi}^{R_\mathrm{f}}
\end{aligned} \tag{A.221}$$

For the feedthrough matrix partition $\boldsymbol{K}^{R_\mathrm{f}}$ holds (angular dofs only):

$$\boldsymbol{K}^{R_\mathrm{f}} = \frac{\partial \underline{y}^{R_\mathrm{f}}}{\partial \underline{v}^{R_\mathrm{f}}} - \frac{\partial \underline{y}^{R_\mathrm{f}}}{\partial \ddot{\underline{\varphi}}^{R_\mathrm{f}}}\cdot\left(\boldsymbol{M}^{R_\mathrm{f}}\right)_{\varphi}^{-1}\cdot\boldsymbol{G}^{R_\mathrm{f}} \tag{A.222}$$

The partial derivatives to the dof vectors are cleaned up before use in the determination of the output and feedthrough matrices: columns that pertain to non-dof directions as concerns R_f are removed.

The partial derivative of the composed output vector $\underline{y}^{R_\mathrm{f}}$ to the composed input vector is obtained by (i) stacking the partial derivatives of the output subvectors to an input subvector, and (ii) doing this for all input subvectors and putting next to each other the obtained 'stacks'. The generic expression for the overall partial derivative matrix is (see e.g. also Eq. A.88):

$$\frac{\partial \underline{y}^{R_\mathrm{f}}}{\partial \underline{v}^{R_\mathrm{f}}} = \mathrm{J}_{(\underline{q}_\mathrm{v})}\left(\mathrm{S}_{(\underline{z}_\mathrm{y})}\left(\frac{\partial \underline{z}_\mathrm{y}}{\partial \underline{q}_\mathrm{v}}\right)\right) \quad \text{with} \quad \begin{cases} \underline{q}_\mathrm{v} = \underline{\alpha}^{S_{\mathrm{FF}(4)}}, {}^{\mathrm{FT}}t_\mathrm{x}^{R_\mathrm{f}}, \ddot{\underline{\varphi}}^{R_\mathrm{f}} \\ \underline{z}_\mathrm{y} = t_\mathrm{e}, {}^{\mathrm{FT}}\underline{t}^{S_\mathrm{n}^{\oplus}R_\mathrm{f}}, \varphi_\mathrm{x}^{R_\mathrm{f}}, \dot{\varphi}_\mathrm{x}^{R_\mathrm{f}}, \ddot{\varphi}_\mathrm{x}^{R_\mathrm{f}} \end{cases} \tag{A.223}$$

(v) Generator torque control system equations and 1$^{\mathrm{st}}$ order state space model
The implemented generator torque control system is described in paragraph (i) of section 3.7.2.

The multiplcation and summation of 'transfer function formulations' in Eq. 3.67 of section 3.7.2 result into one transfer function via basic MATLAB functions SERIES and

PARALLEL(). Afterwards this transfer function is transformed into state space format with M-function TF2SS():

$$\begin{aligned} \dot{\underline{x}}^{R_{\mathrm{f_c}}} &= \boldsymbol{A}^{R_{\mathrm{f_c}}} \cdot \underline{x}^{R_{\mathrm{f_c}}} + \boldsymbol{B}^{R_{\mathrm{f_c}}} \cdot \underline{v}^{R_{\mathrm{f_c}}} \quad \text{with input vector} \quad \underline{v}^{R_{\mathrm{f_c}}} = [\ \dot{\varphi}_{\mathrm{x}}^{R_{\mathrm{f}}}\ ]^{\mathrm{T}} \\ \underline{y}^{R_{\mathrm{f_c}}} &= \boldsymbol{C}^{R_{\mathrm{f_c}}} \cdot \underline{x}^{R_{\mathrm{f_c}}} + \boldsymbol{K}^{R_{\mathrm{f_c}}} \cdot \underline{v}^{R_{\mathrm{f_c}}} \quad \text{with output vector} \quad \underline{y}^{R_{\mathrm{f_c}}} = [\ t_{\mathrm{e}}\ ] \end{aligned} \tag{A.224}$$

The connection of the models for the generator torque controller $R_{\mathrm{f_c}}$ and the generator rotor R_{f} is similar to that for pitch controller and blade flange in paragraph (ix) in section A.2.3.

A.5 Support structure model

The submodel for the dynamic support structure behaviour is obtained with tbusupstreom(). M-function tbusupstreom() also includes the dynamic behaviour of the standstill part of the drive-train, the gearbox house R_{h}. The overall support structure submodel is thus composed of seperate models of:

- one-element subcomponent R_{h} for the gearbox house [including control];
- one-element subcomponent S_{n} for the nacelle (S_M) [including control];
- multi-element subcomponent S_{t} for the (tubular) tower ($S_{2\ldots M-1}$) ;
- one-element subcomponent model S_{f} for the foundation (S_1).

The equations of motion and its accomodation in first order state space model representations are dealt with in subsections section A.5.1 up to section A.5.4 for the respective subcomponents R_{h}, S_{n}, S_{t} and S_{f}. The expressions for the mean loads on the support structure as caused by the drive-train and rotor were listed in the chapter on load calculation in section 4.1.

A.5.1 Equations of motion for the gearbox house R_{h}

The gearbox house R_{h} moves in co-axial angular sense only with respect to the nacelle. This means that only one equation of motion is to be taken into account for R_{h} specifically. The governing equation pertains to the angular impulse coordinate along the x-axis. All remaining first order inertia effects are taken into account in the model for the nacelle.

The co-axial gearbox support torque (responsive loading) may be either incorporated in the model of R_{h} itself, as a function of the variation in the relative rotation and / or its time derivative, or it may be imported from the subcomponent $R_{\mathrm{h_c}}$ with a specific model for the gearbox support torque control system. This is specified during the parametrisation of the support structure via function TBUSUPSTRPAR().

The sensitivities of the impulse vectors as formulated in section B.2.2, paragraph on *Gearbox house* R_{h}, apply and do not need further discussion. Because the mass parameter is moved to the nacelle, there is no gravitation loading. The responsive loading is dealt with in paragraph (i), which includes the option for gearbox support torque control. The required input variables are subject of paragraph (ii). Then, the second order state equation for the gearbox house is formulated in paragraph (iii), followed by the required output equation in paragraph (iv). Finally, paragraph (v) describes the submodel for the support torque control system.

The subcomponent model for the gearbox house R_{h} is obtained by a call to TBUS4SUBEOM() in function TBUSUPSTREOM(). The model for R_{h} exists as structure variable sysS4sub. The fields in sysS4sub are 2D matrices A, B, C, K, the parameterisation of the first

order state space representation, and cell arrays with lists of input, output and state variable names. Point of departure for the gearbox house model creation by function TBUS4SUBEOM() is the availability for the one-element subcomponent R_{h} of ((f.)c.s: (final) coordinate system):

- sensitivities of angular and linear impulse vector of R_{h} (along f.c.s. of R_{h} in actual position: $\vec{e}^{\,R_{\mathrm{h}}}$);
- means of feedthrough forces and torques from drive-train (along $\vec{e}^{\,R_{\mathrm{h}}}$);
- sensitivities of displacement vectors relative to rotor centre in average position (along 'feedthrough' f.c.s. of R_{h} in average position: $\vec{e}^{\,\bar{R}_{\mathrm{h}"}}$);
- sensitivities of kinematic vectors in rotor centre (= exit and entry point of R_{h}; along 'feedthrough' f.c.s. of R_{h} in actual position: $\vec{e}^{\,R_{\mathrm{h}"}}$);
- sensitivities of wind speed and gravitation by orientation change in rotor centre (along $\vec{e}^{\,R_{\mathrm{h}"}}$);
- transformation matrices and their sensitivities to rotational dofs relative to the exit point of the nacelle (forward and backward);
- co-axial angular stiffness and damper value
- bottom-up ranking of rotation and translation axes in the exit point of the nacelle.

The mentioned sensitivities belong to the 'motion formulations' and map all motion variations to input variables from the nacelle or to dofs in the gearbox house. These already have been obtained when assembling the drive-train model via calls in TBUDRIVTREOM() to functions TBUDRIVTRCONS(), TBUDRIVTRKIN(), and TBUDRIVTRIMP(). Note that output variables from the (rotating part of the) drive train are assumed to be *de*modulated with the main azimut angle (See section A.1, par. (vi), header *Drive train outputs into the support structure*).

Functionality TBUS4SUBEOM() ((f.)c.s: (final) coordinate system):

- definition of input name lists; each list contains the names of the input subvectors from a specific source (R, S3sub, S4Csub (= gearbox torque control system));
- definition of output name lists; each list contains the names of the output subvectors to a specific destination (G, R, S3sub, S4Csub);
- assemble the 'extern torque and force load formulation' from the feedthrough loading from the drive-train (coordinates along actual f.c.s. of R_{h});
- define 'equal to zero' the feedthrough loading from outward elements within the 'gearbox house subcomponent' (there are no) (call TBUSYSFTFT());
- definition of the sensitivities of the responsive (visco/elastic) torque (and dummy force) loads the dofs or the input from the gearbox support torque control system (see par. (i));
- derive the mass, spring and damper matrix for the equations of motion for the generator rotor R_{f} ($\boldsymbol{M}, \boldsymbol{S}, \boldsymbol{D}$; call TBUSYSMDSMX());
- derive load formulations for feedthrough torques and forces on the nacelle (call TBUSYSFTPP; along actual f.c.s. of the nacelle element S_M);
- derive the input matrix for the mass/spring/damper formulation of R_{h} as well as the output matrices on the dofs and their time derivatives and the feedthrough matrix ($\boldsymbol{G}, \boldsymbol{H}, \boldsymbol{L}, \boldsymbol{K}$; call TBUSYSGHLKMX());

- transform the mass/spring/damper model formulation $\{\boldsymbol{M}, \boldsymbol{S}, \boldsymbol{D}, \boldsymbol{G}, \boldsymbol{H}, \boldsymbol{L}, \boldsymbol{K}\}$ to the first order state space formulation $\{\boldsymbol{A}, \boldsymbol{B}, \boldsymbol{C}, \boldsymbol{K}\}$ (call TBUSYSMDS2FSR()).

The model for the gearbox support torque control system exists in structure variable sysS4Csub. It is created with TBUS4CSUBEOM() via a call from function TBUSUPSTREOM(). Point of departure for the gearbox torque controller model creation by TBUS4CSUBEOM() is the availability of:

- parameters for torque servo behaviour of the flexible gearbox support;
- parameters for feedback and low-pass filtering of gearbox house co-axial deviation φ_{gb}.

Functionality TBUS4CSUBEOM():

- definition of input name lists; each list contains the names of the input subvectors from a specific source (S4sub)
- definition of output name lists; each list containts the names of the output subvectors to a specific destination (S4sub);
- parametrisation of the transfer function formulations for the torque servo behaviour and co-axial deviation control;
- connect transfer function models (call SERIES(), PARALLEL());
- convert transfer function models to first order state space models (call TF2SS())

(i) Responsive loading

The only responsive loading that matters is the co-axial torque from the gearbox support system. With the defined bottum-up ranked rotation order along the y-, z- and x-axis, the expression for the reponsive torque vector becomes:

$$ {}^{\mathrm{RS}}\underline{t}^{R_{\mathrm{h}}} \triangleq \begin{bmatrix} {}^{\mathrm{RS}}t_{\mathrm{x}}^{R_{\mathrm{h}}^3} \\ {}^{\mathrm{RS}}t_{\mathrm{y}}^{R_{\mathrm{h}}^1} \\ {}^{\mathrm{RS}}t_{\mathrm{z}}^{R_{\mathrm{h}}^2} \end{bmatrix} = {}^{\mathrm{RS}}\underline{\bar{t}}^{R_{\mathrm{h}}} + \frac{\partial {}^{\mathrm{RS}}\underline{t}^{R_{\mathrm{h}}}}{\partial \underline{\varphi}^{R_{\mathrm{h}}}} \cdot \underline{\varphi}^{R_{\mathrm{h}}} + \frac{\partial {}^{\mathrm{RS}}\underline{t}^{R_{\mathrm{h}}}}{\partial \underline{\dot{\varphi}}^{R_{\mathrm{h}}}} \cdot \underline{\dot{\varphi}}^{R_{\mathrm{h}}} + \frac{\partial {}^{\mathrm{RS}}\underline{t}^{R_{\mathrm{h}}}}{\partial t_{\mathrm{gb}}} \cdot \delta t_{\mathrm{gb}} $$

(A.225)

Note that in case of passive flexible gearbox support (visco-elastic) the first two terms in the left hand side apply, while in case of a gearbox torque control system the third term applies. In the latter case, the control system yields a co-axial 'counter torque' t_{gb} on the gearbox house: if > 0 it will turn the gearbox house back towards its initial position when the actual deviation $\varphi_{\mathrm{gb}} > 0$.

For the sensitivities to the angular dof vectors and to the control torque from $R_{\mathrm{h_c}}$ then holds:

$$ \frac{\partial {}^{\mathrm{RS}}\underline{t}^{R_{\mathrm{h}}}}{\partial \underline{\varphi}^{R_{\mathrm{h}}}} = -\begin{pmatrix} 0 & 0 & s_{\mathrm{t_x}\phi_{\mathrm{x}}}^{R_{\mathrm{h}}} \\ 0 & 0 & 0 \\ 0 & 0 & 0 \end{pmatrix} \quad ; \quad \frac{\partial {}^{\mathrm{RS}}\underline{t}^{R_{\mathrm{h}}}}{\partial \underline{\dot{\varphi}}^{R_{\mathrm{h}}}} = -\begin{pmatrix} 0 & 0 & d_{\mathrm{t_x}\phi_{\mathrm{x}}}^{R_{\mathrm{h}}} \\ 0 & 0 & 0 \\ 0 & 0 & 0 \end{pmatrix} \quad ; \quad \frac{\partial {}^{\mathrm{RS}}\underline{t}^{R_{\mathrm{h}}}}{\partial t_{\mathrm{gb}}} = \begin{pmatrix} -1 \\ 0 \\ 0 \end{pmatrix} $$

(A.226)

(ii) Input variables

The input vector for R_{h} has the following composition:

$$\underline{v}^{R_{\mathrm{h}}} = \begin{bmatrix} \underline{v}^{R_{\mathrm{h}}R} \\ \underline{v}^{R_{\mathrm{h}}S_{\mathrm{n}}} \\ \underline{v}^{R_{\mathrm{h}}R_{\mathrm{hc}}} \end{bmatrix}$$

with

$$\underline{v}^{R_{\mathrm{h}}R} = \begin{bmatrix} {}^{\mathrm{FT}}\underline{f}^{S_{\mathrm{n}}^{\oplus}R_{\mathrm{r}}} \\ {}^{\mathrm{FT}}\underline{t}^{S_{\mathrm{n}}^{\oplus}R_{\mathrm{r}}} \\ {}^{\mathrm{FT}}\underline{t}^{S_{\mathrm{n}}^{\oplus}R_{\mathrm{f}}} \end{bmatrix} \quad ; \quad \underline{v}^{R_{\mathrm{h}}S_{\mathrm{n}}} = \begin{bmatrix} \underline{\omega}^{S_{\mathrm{FF(3)}}} \\ \underline{\alpha}^{S_{\mathrm{FF(3)}}} \\ \underline{v}^{S_{\mathrm{FF(3)}}^{\oplus}} \\ \underline{a}^{S_{\mathrm{FF(3)}}^{\oplus}} \\ \underline{u}_{\mathrm{ori}}^{S_{\mathrm{FF(3)}}} \\ \underline{g}_{\mathrm{ori}}^{S_{\mathrm{FF(3)}}} \\ \underline{\xi}^{S_{\mathrm{FF(3)}}} \\ \underline{x}^{S_{\mathrm{FF(3)}}^{\oplus}} \end{bmatrix} \quad ; \quad \underline{v}^{R_{\mathrm{h}}R_{\mathrm{hc}}} = \begin{bmatrix} t_{\mathrm{gb}} \end{bmatrix}$$

(A.227)

(iii) Equations of motion and 2nd order vector state equation

The derivation method for the second order state equation for the gearbox house R_{h} is very similar to that for the generator rotor R_{f}. For R_{h} also only one equation of motion is to be taken into account in, vizually the angular impulse coordinate along the x-axis, while all remaining dynamic effects of R_{h} are moved to the nacelle. The implementation via function TBUSYSMDSMX() is nevertheless based on the encapsulating dof vectors $\underline{\phi}^{R_{\mathrm{h}}}$ and $\underline{\rho}^{R_{\mathrm{h}}}$. with 6×6-matrices:

$$\left[\boldsymbol{M}_{\varphi}^{R_{\mathrm{h}}} \mid \boldsymbol{M}_{\varrho}^{R_{\mathrm{h}}}\right] \cdot \begin{bmatrix} \underline{\ddot{\varphi}}^{R_{\mathrm{h}}} \\ \underline{\ddot{\varrho}}^{R_{\mathrm{h}}} \end{bmatrix} + \left[\boldsymbol{D}_{\varphi}^{R_{\mathrm{h}}} \mid \boldsymbol{D}_{\varrho}^{R_{\mathrm{h}}}\right] \cdot \begin{bmatrix} \underline{\dot{\varphi}}^{R_{\mathrm{h}}} \\ \underline{\dot{\varrho}}^{R_{\mathrm{h}}} \end{bmatrix} + \left[\boldsymbol{S}_{\varphi}^{R_{\mathrm{h}}} \mid \boldsymbol{S}_{\varrho}^{R_{\mathrm{h}}}\right] \cdot \begin{bmatrix} \underline{\varphi}^{R_{\mathrm{h}}} \\ \underline{\varrho}^{R_{\mathrm{h}}} \end{bmatrix} = \left[\boldsymbol{G}^{R_{\mathrm{h}}R} \mid \boldsymbol{G}^{R_{\mathrm{h}}S_{\mathrm{n}}} \mid \boldsymbol{G}^{R_{\mathrm{h}}R_{\mathrm{hc}}}\right] \cdot \begin{bmatrix} \underline{v}^{R_{\mathrm{h}}R} \\ \underline{v}^{R_{\mathrm{h}}S_{\mathrm{n}}} \\ \underline{v}^{R_{\mathrm{h}}R_{\mathrm{hc}}} \end{bmatrix}$$

(A.228)

These matrices are derived by considering the angular and linear vector impulse equation for the one-element subcomponent R_{h} in its set of three coordinate systems. Since each row and corresponding column that pertains to a 'non-dof' element of $\underline{\varphi}^{R_{\mathrm{h}}}$ or $\underline{\varrho}^{R_{\mathrm{h}}}$ is deleted from the mass, damper, stiffnes and input matrix, we only list the *angular* scalar impulse equation along the x-axis. The rotations in R_{h} are bottom-up ranked along the y-, z and x-axis. So we start (and also end up) with the x-coordinate of the angular impulse in the 3rd intermediate coordinate system. The row $\underline{\boldsymbol{m}}_{h\varphi_w}^{R_{\mathrm{h}}}$ for $w = 3$, with ranking numbers $2(w-1)+1$ in the mass matrix partition $\boldsymbol{M}_{\varphi}^{R_{\mathrm{h}}}$ is now determined as follows (the partial derivatives in the right hand side only apply if they are defined for the 'independent variable' $\underline{\ddot{\varphi}}^{R_{\mathrm{h}}}$):

- for $w = 3$:

$$\underline{\boldsymbol{m}}_{h\varphi_3}^{R_{\mathrm{h}}} = -[\,1\,0\,0\,] \cdot \frac{\partial^{\mathrm{RS}}\underline{t}^{R_{\mathrm{h}}}}{\partial \underline{\ddot{\varphi}}^{R_{\mathrm{h}}}} + [\,1\,0\,0\,] \cdot \left(\frac{\partial^{R_{\mathrm{h}}^{*}}\underline{\dot{h}}^{R_{\mathrm{h}}}}{\partial \underline{\ddot{\varphi}}^{R_{\mathrm{h}}}} - \frac{\partial^{\mathrm{EX}}\underline{t}^{R_{\mathrm{h}}}}{\partial \underline{\ddot{\varphi}}^{R_{\mathrm{h}}}}\right) \qquad \text{(A.229)}$$

Note that NO feedthrough loading exists from other elements within the one-element subcomponent R_{h}. The loading from the drive-train is considered as external loading for R_{h} and included in ${}^{\mathrm{EX}}\underline{t}^{R_{\mathrm{h}}}$.

For the corresponding row in the damping matrix partition $\boldsymbol{D}_{\varphi}^{R_{\mathrm{h}}}$ and stiffness matrix partition $\boldsymbol{S}_{\varphi}^{R_{\mathrm{h}}}$, take the sensitivities to $\underline{\dot{\varphi}}^{R_{\mathrm{h}}}$ and $\underline{\varphi}^{R_{\mathrm{h}}}$.

The row $\underline{\boldsymbol{g}}_{h_w}^{R_\mathrm{h} R}$ for $w = 3$, with ranking number $2(w-1)+1$ in the input matrix partition $\boldsymbol{G}^{R_\mathrm{h} R}$, is determined as follows (the partial derivatives in the right hand side only apply if they are defined for the 'independent variable'; in this case $\underline{z}$):

- for $w = 3$:

$$\underline{\boldsymbol{g}}_{h_3}^{R_\mathrm{h} R} = [\,1\,0\,0\,] \cdot \frac{\partial^{\mathrm{RS}} \underline{t}^{R_\mathrm{h}}}{\partial \underline{z}} + [\,1\,0\,0\,] \cdot \left(-\frac{\partial^{R_\mathrm{h}^*} \underline{\dot{h}}^{R_\mathrm{h}}}{\partial \underline{z}} + \frac{\partial^{\mathrm{EX}} \underline{t}^{R_\mathrm{h}}}{\partial \underline{z}}\right) \tag{A.230}$$

The involved subvectors $\underline{z}$ for the submatrices $\boldsymbol{G}^{R_\mathrm{h} R}$, $\boldsymbol{G}^{R_\mathrm{h} S_\mathrm{n}}$, $\boldsymbol{G}^{R_\mathrm{h} R_\mathrm{hc}}$ are:

- feedthrough torques from shaftR_r and generator rotor R_f: ${}^{\mathrm{FT}}\underline{t}^{S_\mathrm{n}^\oplus R_\mathrm{r}}$, ${}^{\mathrm{FT}}\underline{t}^{S_\mathrm{n}^\oplus R_\mathrm{f}}$;
- angular acceleratoin vector from the nacelle: $\underline{\alpha}^{S_{\mathrm{FF}(3)}}$
- co-axial support torque from the gearbox torque control system : $[\ t_\mathrm{gb}\ ]$

Although not yet required (see also next paragraph), both the external force and torque coordinate vectors are listed. They only include the feedthrough loading from the drive-train:

$$\begin{aligned} {}^{\mathrm{EX}}\underline{f}^{R_\mathrm{h}^*} &= {}^{\mathrm{FT}}\underline{f}^{S_\mathrm{n}^\oplus R_\mathrm{r}} \\ {}^{\mathrm{EX}}\underline{t}^{R_\mathrm{h}^*} &= {}^{\mathrm{FT}}\underline{t}^{S_\mathrm{n}^\oplus R_\mathrm{r}} + {}^{\mathrm{FT}}\underline{t}^{S_\mathrm{n}^\oplus R_\mathrm{f}} \end{aligned} \tag{A.231}$$

As there is only one potential dof in R_h, vizually the co-axial variation $\varphi_3^{R_\mathrm{h}}$, the orientation op the mean feedthrough torque from the drive-train cannot be affected by another dof in R_h when considering the co-axial angular impulse conservation. So there is no 'stiffening effect' by dofs in R_h via the mean external loading.

(iv) Output variables and vector output equation in 2nd order model
The gearbox house R_h needs to provide the following output:

- co-axial deviation angle and support torque (if control included): φ_gb, t_gb
- feedthrough force and torque on nacelle exit $S_M^\oplus$:
  ${}^{\mathrm{FT}}\underline{f}^{S_{\mathrm{PP}(4)}}$, ${}^{\mathrm{FT}}\underline{t}^{S_{\mathrm{PP}(4)}}$ ($\equiv {}^{\mathrm{FT}}\underline{f}^{S_\mathrm{n}^\oplus R_\mathrm{h}}$, ${}^{\mathrm{FT}}\underline{t}^{S_\mathrm{n}^\oplus R_\mathrm{h}}$, along actual f.c.s. of S_M)
- kinematic vectors in exit of R_h ($\equiv S_M^\oplus$) to drive train:
  $\underline{\omega}^{S_{\mathrm{FF}(4)}}$, $\underline{\alpha}^{S_{\mathrm{FF}(4)}}$, $\underline{v}^{S_{\mathrm{FF}(4)}^\oplus}$, $\underline{a}^{S_{\mathrm{FF}(4)}^\oplus}$ ($\equiv \underline{\omega}^{R_\mathrm{h"}}$, $\underline{\alpha}^{R_\mathrm{h"}}$, $\underline{v}^{S_\mathrm{n}^\oplus}$, $\underline{a}^{S_\mathrm{n}^\oplus}$; along $\vec{e}^{\,R_\mathrm{h"}}$)
- wind speed and gravitation variation by orientation change up till R_h:
  $\underline{u}_\mathrm{ori}^{S_{\mathrm{FF}(4)}}$, $\underline{g}_\mathrm{ori}^{S_{\mathrm{FF}(4)}}$ ($\equiv \underline{u}_\mathrm{ori}^{R_\mathrm{h"}}$, $\underline{g}_\mathrm{ori}^{R_\mathrm{h"}}$; along actual feedthrough f.c.s. $\vec{e}^{\,R_\mathrm{h"}}$)
- exit point displacement relative to average rotor centre to drive-train:
  $\underline{\xi}^{S_{\mathrm{FF}(4)}}$, $\underline{x}^{S_{\mathrm{FF}(4)}^\oplus}$ ($\equiv \underline{\xi}^{R_\mathrm{h}^"}$, $\underline{x}^{S_\mathrm{n}^\oplus}$; along average feedthrough f.c.s. $\vec{e}^{\,\bar{R}_\mathrm{h"}}$)

Note that the exit point $S_\mathrm{n}^\oplus$ of the nacelle coincides with the entry point of the gearbox house, which in turn coincides with the rotor centre R_r^c.

Note that the average 'feedthrough' f.c.s. $\vec{e}^{\,\bar{R}_\mathrm{h"}}$ of the gearbox house coincides with its 'real' average f.c.s. $\vec{e}^{\,\bar{R}_\mathrm{h}}$, which in turn coincides with the average f.c.s. $\vec{e}^{\,\bar{S}_M}$ of the nacelle.

The output vector from R_{h} has the following composition:

$$\underline{y}^{R_{\mathrm{h}}} = \begin{bmatrix} \underline{y}^{GR_{\mathrm{h}}} \\ \underline{y}^{RR_{\mathrm{h}}} \\ \underline{y}^{S_{\mathrm{n}}R_{\mathrm{h}}} \\ \underline{y}^{R_{\mathrm{hc}}R_{\mathrm{h}}} \end{bmatrix}$$

with

$$\underline{y}^{GR_{\mathrm{h}}} = \begin{bmatrix} \varphi_{\mathrm{gb}} \\ t_{\mathrm{gb}} \end{bmatrix}; \quad \underline{y}^{S_{\mathrm{n}}R_{\mathrm{h}}} = \begin{bmatrix} {}^{\mathrm{FT}}\underline{f}^{S_{\mathrm{PP}(4)}} \\ {}^{\mathrm{FT}}\underline{t}^{S_{\mathrm{PP}(4)}} \end{bmatrix}; \quad \underline{y}^{RR_{\mathrm{h}}} = \begin{bmatrix} \underline{\omega}^{S_{\mathrm{FF}(4)}} \\ \underline{\alpha}^{S_{\mathrm{FF}(4)}} \\ \underline{v}^{S^{\oplus}_{\mathrm{FF}(4)}} \\ \underline{a}^{S^{\oplus}_{\mathrm{FF}(4)}} \\ \underline{u}_{\mathrm{ori}}^{S_{\mathrm{FF}(4)}} \\ \underline{g}_{\mathrm{ori}}^{S_{\mathrm{FF}(4)}} \\ \underline{\xi}^{S_{\mathrm{FF}(4)}} \\ \underline{x}^{S^{\oplus}_{\mathrm{FF}(4)}} \end{bmatrix}; \quad \underline{y}^{R_{\mathrm{hc}}R_{\mathrm{h}}} = \begin{bmatrix} \varphi_{\mathrm{gb}} \end{bmatrix} \tag{A.232}$$

The feedthrough kinematic vectors $\underline{\omega}^{S_{\mathrm{FF}(4)}}$, $\underline{\alpha}^{S_{\mathrm{FF}(4)}}$, $\underline{v}^{S^{\oplus}_{\mathrm{FF}(4)}}$ and $\underline{a}^{S^{\oplus}_{\mathrm{FF}(4)}}$ to the drive-train are supplied as coordinate vectors along the feedthrough f.c.s. $\vec{e}^{\,R_{\mathrm{h}}"}$. See equation B.34 for the variations in $\underline{\omega}^{S_{\mathrm{FF}(4)}}$ and $\underline{\alpha}^{S_{\mathrm{FF}(4)}}$. The variations in $\underline{v}^{S^{\oplus}_{\mathrm{FF}(4)}}$, $\underline{a}^{S^{\oplus}_{\mathrm{FF}(4)}}$ are equal to the input kinematic vectors $\underline{v}^{S^{\oplus}_{\mathrm{FF}(3)}}$, $\underline{a}^{S^{\oplus}_{\mathrm{FF}(3)}}$ from the nacelle.

The feedthrough 'orientation change vectors' $\underline{u}_{\mathrm{ori}}^{S_{\mathrm{FF}(4)}}$ and $\underline{g}_{\mathrm{ori}}^{S_{\mathrm{FF}(4)}}$ are also expressed along $\vec{e}^{\,R_{\mathrm{h}}"}$ (see Eq. B.164 and B.277).

The feedthrough loads along the actual f.c.s. of S_M to the nacelle are given by (external loads by Eq. A.231):

$$\begin{aligned} {}^{\mathrm{FT}}\underline{f}^{S_{\mathrm{PP}(4)}} &= {}^{S_{\mathrm{n}}}\Phi^{R_{\mathrm{h}}} \cdot \left(-\underline{\dot{p}}^{R_{\mathrm{h}}} + {}^{\mathrm{EX}}\underline{f}^{R^*_{\mathrm{h}}}\right) \\ {}^{\mathrm{FT}}\underline{t}^{S_{\mathrm{PP}(4)}} &= {}^{S_{\mathrm{n}}}\Phi^{R_{\mathrm{h}}} \cdot \left(-{}^{R^*_{\mathrm{h}}}\underline{\dot{h}}^{R_{\mathrm{h}}} + {}^{\mathrm{EX}}\underline{t}^{R^*_{\mathrm{h}}}\right) \end{aligned} \tag{A.233}$$

Since the mass $m^{R_{\mathrm{h}}}$ is moved to the nacelle, the c.o.g. R^*_{h} can be chosen anywhere *as concerns the behaviour of* R_{h}. We let R^*_{h} coincide with the nacelle exit point $S^{\oplus}_{\mathrm{n}}$, which lays in the rotor centre. Note that the rate of change in the

- linear impulse equals zero because of mass $m^{R_{\mathrm{h}}}$ moved to S_{n};
- angular impulse is non-zero in co-axial sense only because inertia parameters $m^{R_{\mathrm{h}}}$, $J^{R_{\mathrm{h}}}_{\mathrm{y,z}}$ moved to S_{n}.

Of course, the time-average rate change in the impulse vectors of R_{h} equals zero. The mean feedthrough loads to the nacelle are then given by (see section 4.1 for mean feedthrough loads from the drive-train):

$$\begin{aligned} {}^{\mathrm{FT}}\bar{\underline{f}}^{S_{\mathrm{PP}(4)}} &= {}^{S_{\mathrm{n}}}\bar{\Phi}^{R_{\mathrm{h}}} \cdot {}^{\mathrm{FT}}\bar{\underline{f}}^{S^{\oplus}_{\mathrm{n}}R_{\mathrm{r}}} \\ {}^{\mathrm{FT}}\bar{\underline{t}}^{S_{\mathrm{PP}(4)}} &= {}^{S_{\mathrm{n}}}\bar{\Phi}^{R_{\mathrm{h}}} \cdot \left({}^{\mathrm{FT}}\bar{\underline{t}}^{S^{\oplus}_{\mathrm{n}}R_{\mathrm{r}}} + {}^{\mathrm{FT}}\bar{\underline{t}}^{S^{\oplus}_{\mathrm{n}}R_{\mathrm{f}}}\right) \end{aligned} \tag{A.234}$$

The variation of the feedthrough loads to the nacelle are given by:

$$\begin{aligned} \delta{}^{\mathrm{FT}}\underline{f}^{S_{\mathrm{PP}(4)}} &= \sum_{(\underline{q})} \frac{\partial {}^{\mathrm{FT}}\underline{f}^{S_{\mathrm{PP}(4)}}}{\partial \underline{q}} \cdot \delta\underline{q} \quad \text{for } \underline{q} = {}^{\mathrm{FT}}\underline{f}^{S^{\oplus}_{\mathrm{n}}R_{\mathrm{r}}}, \underline{\varphi}^{R_{\mathrm{h}}} \\ \delta{}^{\mathrm{FT}}\underline{t}^{S_{\mathrm{PP}(4)}} &= \sum_{(\underline{q})} \frac{\partial {}^{\mathrm{FT}}\underline{t}^{S_{\mathrm{PP}(4)}}}{\partial \underline{q}} \cdot \delta\underline{q} \quad \text{for } \underline{q} = {}^{\mathrm{FT}}\underline{t}^{S^{\oplus}_{\mathrm{n}}R_{\mathrm{r}}}, {}^{\mathrm{FT}}\underline{t}^{S^{\oplus}_{\mathrm{n}}R_{\mathrm{f}}}, \underline{\omega}^{S^{\oplus}_{\mathrm{FF}(3)}}, \underline{\alpha}^{S_{\mathrm{FF}(3)}}, \underline{\varphi}^{R_{\mathrm{h}}} \end{aligned} \tag{A.235}$$

For the sensitivities to the variables $\underline{q}$ holds:

$$\begin{aligned}
\frac{\partial^{\mathrm{FT}} \underline{f}^{S_{\mathrm{PP}(4)}}}{\partial \underline{q}} &= {}^{S_{\mathrm{n}}}\bar{\Phi}^{R_{\mathrm{h}}} \cdot \left(\frac{\partial^{\mathrm{EX}} \underline{f}^{R_{\mathrm{h}}^*}}{\partial \underline{q}}\right) + \delta_{\underline{q}\,\underline{\phi}^{R_{\mathrm{h}}}} \cdot \left[\, \mathrm{J}_{v=1}^{3}\Big(\frac{\partial^{S_{\mathrm{n}}}\Phi^{R_{\mathrm{h}}}}{\partial \phi_v^{R_{\mathrm{h}}}} \cdot \left({}^{\mathrm{EX}}\bar{\underline{f}}^{R_{\mathrm{h}}^*}\right)\Big)\,\right] \\
\frac{\partial^{\mathrm{FT}} \underline{t}^{S_{\mathrm{PP}(4)}}}{\partial \underline{q}} &= {}^{S_{\mathrm{n}}}\bar{\Phi}^{R_{\mathrm{h}}} \cdot \left(-\frac{\partial^{R_{\mathrm{h}}^*} \underline{h}^{R_{\mathrm{h}}}}{\partial \underline{q}} + \frac{\partial^{\mathrm{EX}} \underline{t}^{R_{\mathrm{h}}^*}}{\partial \underline{q}}\right) + \delta_{\underline{q}\,\underline{\phi}^{R_{\mathrm{h}}}} \cdot \left[\; \mathrm{J}_{v=1}^{3}\Big(\frac{\partial^{S_{\mathrm{n}}}\Phi^{R_{\mathrm{h}}}}{\partial \phi_v^{R_{\mathrm{h}}}} \cdot \left({}^{\mathrm{EX}}\bar{\underline{t}}^{R_{\mathrm{h}}^*}\right)\Big)\,\right]
\end{aligned} \tag{A.236}$$

Note that the last term in the right hand side of both equations only applies if $\underline{q}$ equals $\underline{\phi}^{R_{\mathrm{h}}}$!

For the displacement outputs to the drive-train holds (the bottom-up ranked rotations for R_{h} are along the y, z- and x-axis; zero-average $\bar{\phi}_{\mathrm{gb}}$):

$$\begin{aligned}
\underline{\xi}^{S_{\mathrm{FF}(4)}} &= \underline{\xi}^{S_{\mathrm{FF}(3)}} + \begin{pmatrix} 0 & 0 & \frac{i_{\mathrm{gb}}-1}{i_{\mathrm{gb}}} \\ 1 & 0 & 0 \\ 0 & 1 & 0 \end{pmatrix} \cdot \begin{pmatrix} 0 \\ 0 \\ \varphi_{\mathrm{gb}} \end{pmatrix} \\
\underline{x}^{S_{\mathrm{FF}(4)}} &= \underline{x}^{S_{\mathrm{FF}(3)}}
\end{aligned} \tag{A.237}$$

The output equation that belongs to the 2$^{\mathrm{nd}}$ order state equation is (angular dofs only):

$$\underline{y}^{R_{\mathrm{h}}} = \boldsymbol{H}_{\varphi}^{R_{\mathrm{h}}} \cdot \underline{\varphi}^{R_{\mathrm{h}}} + \boldsymbol{L}_{\varphi}^{R_{\mathrm{h}}} \cdot \dot{\underline{\varphi}}^{R_{\mathrm{h}}} + \boldsymbol{K}^{R_{\mathrm{h}}} \cdot \underline{v}^{R_{\mathrm{h}}} \tag{A.238}$$

For the output matrix partitions $\boldsymbol{H}_{\varphi}^{R_{\mathrm{h}}}$ and $\boldsymbol{L}_{\varphi}^{R_{\mathrm{h}}}$, which map angular dof position and speed variations to the outputs hold:

$$\begin{aligned}
\boldsymbol{H}_{\varphi}^{R_{\mathrm{h}}} &= \frac{\partial \underline{y}^{R_{\mathrm{h}}}}{\partial \underline{\phi}^{R_{\mathrm{h}}}} - \frac{\partial \underline{y}^{R_{\mathrm{h}}}}{\partial \underline{\ddot{\varphi}}^{R_{\mathrm{h}}}} \cdot \left(\boldsymbol{M}^{R_{\mathrm{h}}}\right)_{\varphi}^{-1} \cdot \boldsymbol{S}_{\varphi}^{R_{\mathrm{h}}} \\
\boldsymbol{L}_{\varphi}^{R_{\mathrm{h}}} &= \frac{\partial \underline{y}^{R_{\mathrm{h}}}}{\partial \dot{\underline{\varphi}}^{R_{\mathrm{h}}}} - \frac{\partial \underline{y}^{R_{\mathrm{h}}}}{\partial \underline{\ddot{\varphi}}^{R_{\mathrm{h}}}} \cdot \left(\boldsymbol{M}^{R_{\mathrm{h}}}\right)_{\varphi}^{-1} \cdot \boldsymbol{D}_{\varphi}^{R_{\mathrm{h}}}
\end{aligned} \tag{A.239}$$

For the feedthrough matrix partition $\boldsymbol{K}^{R_{\mathrm{h}}}$ holds (angular dofs only):

$$\boldsymbol{K}^{R_{\mathrm{h}}} = \frac{\partial \underline{y}^{R_{\mathrm{h}}}}{\partial \underline{v}^{R_{\mathrm{h}}}} - \frac{\partial \underline{y}^{R_{\mathrm{h}}}}{\partial \underline{\ddot{\varphi}}^{R_{\mathrm{h}}}} \cdot \left(\boldsymbol{M}^{R_{\mathrm{h}}}\right)_{\varphi}^{-1} \cdot \boldsymbol{G}^{R_{\mathrm{h}}} \tag{A.240}$$

The partial derivatives to the dof vectors are cleaned up before use in the determination of the output and feedthrough matrices: columns that pertain to non-dof directions as concerns R_{h} are removed.

The partial derivative of the composed output vector $\underline{y}^{R_{\mathrm{h}}}$ to the composed input vector is obtained by (i) stacking the partial derivatives of the output subvectors to an input subvector, and (ii) doing this for all input subvectors and putting next to each other the obtained 'stacks'. The generic expression for the overall partial derivative matrix is (see e.g. also Eq. A.88):

$$\frac{\partial \underline{y}^{R_{\mathrm{h}}}}{\partial \underline{v}^{R_{\mathrm{h}}}} = \mathrm{J}_{(\underline{q}_{\mathrm{v}})}\Big(\mathrm{S}_{(\underline{z}_{\mathrm{y}})}\left(\frac{\partial \underline{z}_{\mathrm{y}}}{\partial \underline{q}_{\mathrm{v}}}\right)\Big) \quad \text{with} \quad \begin{cases}
\underline{q}_{\mathrm{v}} = {}^{\mathrm{FT}}\underline{f}^{S_{\mathrm{n}}^{\oplus}R_{\mathrm{r}}}, {}^{\mathrm{FT}}\underline{t}^{S_{\mathrm{n}}^{\oplus}R_{\mathrm{r}}}, {}^{\mathrm{FT}}\underline{t}^{S_{\mathrm{n}}^{\oplus}R_{\mathrm{f}}}, \underline{\omega}^{S_{\mathrm{FF}(3)}^{\oplus}}, \underline{\alpha}^{S_{\mathrm{FF}(3)}}, \\
\quad \underline{v}^{S_{\mathrm{FF}(3)}^{\oplus}}, \underline{a}^{S_{\mathrm{FF}(3)}}, \underline{u}_{\mathrm{ori}}^{S_{\mathrm{FF}(3)}}, \underline{g}_{\mathrm{ori}}^{S_{\mathrm{FF}(3)}}, \underline{\xi}^{S_{\mathrm{FF}(3)}}, \underline{x}^{S_{\mathrm{FF}(3)}}, t_{\mathrm{gb}} \\
\underline{z}_{\mathrm{y}} = t_{\mathrm{gb}}, \varphi_{\mathrm{gb}}, \underline{\omega}^{S_{\mathrm{FF}(4)}^{\oplus}}, \underline{\alpha}^{S_{\mathrm{FF}(4)}}, \underline{v}^{S_{\mathrm{FF}(4)}^{\oplus}}, \underline{a}^{S_{\mathrm{FF}(4)}^{\oplus}}, \underline{u}_{\mathrm{ori}}^{S_{\mathrm{FF}(4)}}, \\
\quad \underline{g}_{\mathrm{ori}}^{S_{\mathrm{FF}(4)}}, \underline{\xi}^{S_{\mathrm{FF}(4)}}, \underline{x}^{S_{\mathrm{FF}(4)}}, {}^{\mathrm{FT}}\underline{f}^{S_{\mathrm{PP}(4)}}, {}^{\mathrm{FT}}\underline{t}^{S_{\mathrm{PP}(4)}}, \varphi_{\mathrm{gb}}
\end{cases} \tag{A.241}$$

(v) Gearbox torque control system equations and 1$^{\mathrm{st}}$ order state space model
The implemented gearbox torque control system is listed in paragraph (ii) of section 3.8.2.

The multiplication and summation of 'transfer function formulations' in Eq. 3.92 result into one transfer function via basic MATLAB functions SERIES and PARALLEL(). Afterwards this transfer function is transformed into state space format with M-function TF2SS():

$$\begin{aligned} \dot{\underline{x}}^{R_{\mathrm{hc}}} &= \boldsymbol{A}^{R_{\mathrm{hc}}} \cdot \underline{x}^{R_{\mathrm{hc}}} + \boldsymbol{B}^{R_{\mathrm{hc}}} \cdot \underline{v}^{R_{\mathrm{hc}}} \quad \text{with input vector} \quad \underline{v}^{R_{\mathrm{hc}}} = [\ \varphi_{\mathrm{gb}}\ ]^{\mathrm{T}} \\ \underline{y}^{R_{\mathrm{hc}}} &= \boldsymbol{C}^{R_{\mathrm{hc}}} \cdot \underline{x}^{R_{\mathrm{hc}}} + \boldsymbol{K}^{R_{\mathrm{hc}}} \cdot \underline{v}^{R_{\mathrm{hc}}} \quad \text{with output vector} \quad \underline{y}^{R_{\mathrm{hc}}} = [\ t_{\mathrm{gb}}\ ] \end{aligned} \tag{A.242}$$

The connection of the models for the gearbox torque controller R_{hc} and the gearbox house R_{h} is similar to that for pitch controller and blade flange in paragraph (ix) in section A.2.3.

A.5.2 Equations of motion for the nacelle S_{n}

The nacelle S_{n} has been implemented as a one-element subcomponent, set up by support structure element S_M, which allows the full six degrees of freedom. Yawing is the prinicple dof, but the inclusion of naying and nodding (tilting) dofs enable on the one side to tune the natural frequencies of wind turbine 'system deformation modes' to measurements and on the other side to model non-coaxial elastic gearbox support.

The yaw actuation torque (responsive loading) may be either incorporated in the model of S_{n} itself, as a function of the variation in the relative rotation and / or its time derivative, or it may be imported from the subcomponent $S_{\mathrm{n_c}}$ with a specific model for the yawing torque control system. This is specified during the parametrisation of the support structure via function TBUSUPSTRPAR().

The impulse vectors of the nacelle also include the non-coaxial inertia effects of the gearbox house and generator rotor. The latter also add some (minor) first order gyroscopic effects because of the main rotational speed of the generator rotor:

> The tilt- and yawwise angular motions of the generator rotor do not differ from those of the nacelle. So it is permitted to add the sensitivity of the rate of change in the involved angular impulse coordinates to these angular motions ($\partial^{R_{\mathrm{f}}^*} \dot{\underline{h}}^{R_{\mathrm{f}}} / \partial \underline{\omega}^{R_{\mathrm{f}}}$) to sensitivity of the rate of change in the nacelle's angular impulse coordinates to its own angular velocity $\partial^{S \ominus_M} \dot{\underline{h}}^{S_M} / \partial \underline{\omega}^{S_M}$).

In addition to these gyroscopic inertia effects, the mass and non-coxial inertia moments of the generator rotor and gearbox house are added to the corresponding inertia parameters of the nacelle, which affect the dependency of the inertia behaviour on the *acceleration* variables. See section B.1.2, paragraph on *Nacelle* S_{n}, for the sensitivities of the impulse vectors.

The mean value and sensitivity of the gravitation loading as formulated in section B.10.2 apply and do not need further discussion.

The responsive loading is dealt with in paragraph (i). The required input variables are subject of paragraph (ii). Then, the second order state equation for the nacelle is formulated in paragraph (iii), followed by the required output equation in paragraph (iv). Finally, paragraph (v) describes the submodel for the yawing torque control system.

The responsive loading is dealt with in paragraph (i), which includes the option for gearbox support torque control. The required input variables are subject of paragraph (ii). Then, the second order state equation for the gearbox house is formulated in paragraph

(iii), followed by the required output equation in paragraph (iv). Finally, paragraph (v) describes the submodel for the support torque control system.

The subcomponent model for the nacelle S_{n} is obtained by a call to TBUS3SUBEOM() in function TBUSUPSTREOM(). The model for S_{n} exists as structure variable sysS3sub. The fields in sysS3sub are 2D matrices A, B, C, K, the parameterisation of the first order state space representation, and cell arrays with lists of input, output and state variable names. Point of departure for the gearbox house model creation by function TBUS3SUBEOM() is the availability for the one-element subcomponent S_{n} of ((f.)c.s: (final) coordinate system):

- sensitivities of angular and linear impulse vector of S_M (along f.c.s. of S_M in actual position: $\vec{e}^{\,S_M}$);
- means of feedthrough forces and torques from gearbox house (along $\vec{e}^{\,S_M}$);
- sensitivities of displacement vectors relative to the (fixed) tower base (along tower base c.s. $\vec{e}^{\,B}$);
- sensitivities of kinematic vectors in rotor centre (= exit point of S_{m}; along $\vec{e}^{\,S_M}$);
- sensitivities of wind speed and gravitation by orientation change in rotor centre along $\vec{e}^{\,S_M}$);
- transformation matrices and their sensitivities to rotational dofs relative to the exit point of the tower (forward and backward);
- angular stiffness and damper values;
- bottom-up ranking of rotation and translation axes in the exit point of the tower;

The mentioned sensitivities belong to the 'motion formulations' and map all motion variations to input variables from the tower or to dofs in the nacelle. These are obtained via calls in TBUSUPSTREOM() to functions TBUSUPSTRCONS(), TBUSUPSTRKIN(), and TBUSUPSTRIMP().

Functionality TBUS3SUBEOM() ((f.)c.s: (final) coordinate system):

- definition of input name lists; each list contains the names of the input subvectors from a specific source (S4sub, S2sub, S3Csub (= yawing torque control system));
- definition of output name lists; each list contains the names of the output subvectors to a specific destination (G, S4sub, S2sub, S3Csub);
- lumping together the gravitation loads and the feedthrough loads from the gearbox house to equivalent force and torque load formulations in the yaw bearing centre (= nacelle entry point; call TBUSSUBFTEX(); coordinates along actual f.c.s. of S_M);
- define 'equal to zero' the feedthrough loading from outward elements within the 'nacelle subcomponent' (there are no) (call TBUSYSFTFT());
- definition of the sensitivities of the responsive (visco/elastic) torque and force loads to the dofs and/or the input from the yawing torque control system (see par. (i));
- derive the mass, spring and damper matrix for the equations of motion for the nacelle S_{n} ($\boldsymbol{M}, \boldsymbol{S}, \boldsymbol{D}$; call TBUSYSMDSMX());
- derive load formulations for feedthrough torques and forces on the tower (call TBUSYS-FTPP; along actual f.c.s. of S_M);
- derive the input matrix for the mass/spring/damper formulation of S_{n} as well as the output matrices on the dofs and their time derivatives and the feedthrough matrix ($\boldsymbol{G}, \boldsymbol{H}, \boldsymbol{L}, \boldsymbol{K}$; call TBUSYSGHLKMX());

- transform the mass/spring/damper model formulation $\{\boldsymbol{M}, \boldsymbol{S}, \boldsymbol{D}, \boldsymbol{G}, \boldsymbol{H}, \boldsymbol{L}, \boldsymbol{K}\}$ to the first order state space formulation $\{\boldsymbol{A}, \boldsymbol{B}, \boldsymbol{C}, \boldsymbol{K}\}$ (call TBUSYSMDS2FSR()).

The model for the yawing torque control system exists in structure variable sysS3Csub. It is created with TBUS3CSUBEOM() via a call from function TBUSUPSTREOM(). Point of departure for the gearbox torque controller model creation by TBUS3CSUBEOM() is the availability of:

- parameters for yawing torque servo behaviour of the flexible yawing actuator;
- parameters for feedback and low-pass filtering of yawing deviation angle φ_{yw}.

Functionality TBUS3CSUBEOM():

- definition of input name lists; each list contains the names of the input subvectors from a specific source (S3sub)
- definition of output name lists; each list containts the names of the output subvectors to a specific destination (S3sub);
- parametrisation of the transfer function formulations for the torque servo behaviour and co-axial deviation control;
- connect transfer function models (call SERIES(), PARALLEL());
- convert transfer function models to first order state space models (call TF2SS())

(i) Responsive loads

The defined bottom-up ranking of the angular deviation directions for the nacelle is yawing, naying and noddding (see section 3.8.1). So the involved rotation axes are in the z-, x- and y-direction for the 1st, 2nd and 3rd intermediate coordinate system. The corresponding translation axes are chosen in z-, y- and x-direction. The responsive force and torque loads can be visco/elastic in three directions each while the responsive torque along the (co-axial) z-axis is the yaw actuation torque t_{yw} if active yaw control control is applied. No cross couplings are assumed between a pair of an angular and linear dof on the one side and a pair of a visco/elastic responsive force and torque on the other side. For the responsive load coordinate vectors then holds:

$$
\begin{aligned}
{}^{\mathrm{RS}}\underline{f}^{S_M} &= \begin{bmatrix} {}^{\mathrm{RS}}f_1^{S_M} \\ {}^{\mathrm{RS}}f_2^{S_M} \\ {}^{\mathrm{RS}}f_3^{S_M} \end{bmatrix} \triangleq \begin{bmatrix} {}^{\mathrm{RS}}f_{\mathrm{x}}^{S3_M} \\ {}^{\mathrm{RS}}f_{\mathrm{y}}^{S2_M} \\ {}^{\mathrm{RS}}f_{\mathrm{z}}^{S1_M} \end{bmatrix} = {}^{\mathrm{RS}}\bar{\underline{f}}^{S_M} + \frac{\partial^{\mathrm{RS}}\underline{f}^{S_M}}{\partial \underline{\rho}^{S}} \cdot \delta\underline{\rho}^{S} + \frac{\partial^{\mathrm{RS}}\underline{f}^{S_M}}{\partial \underline{\dot{\rho}}^{S}} \cdot \underline{\dot{\rho}}^{S} \\
{}^{\mathrm{RS}}\underline{t}^{S_M} &= \begin{bmatrix} {}^{\mathrm{RS}}t_1^{S_M} \\ {}^{\mathrm{RS}}t_2^{S_M} \\ {}^{\mathrm{RS}}t_3^{S_M} \end{bmatrix} \triangleq \begin{bmatrix} {}^{\mathrm{RS}}t_{\mathrm{x}}^{S2_M} \\ {}^{\mathrm{RS}}t_{\mathrm{y}}^{S3_M} \\ {}^{\mathrm{RS}}t_{\mathrm{z}}^{S1_M} \end{bmatrix} = {}^{\mathrm{RS}}\bar{\underline{t}}^{S_M} + \frac{\partial^{\mathrm{RS}}\underline{t}^{S_M}}{\partial \underline{\phi}^{S}} \cdot \delta\underline{\phi}^{S} + \frac{\partial^{\mathrm{RS}}\underline{t}^{S_M}}{\partial \underline{\dot{\varphi}}^{S}} \cdot \underline{\dot{\varphi}}^{S} + \frac{\partial^{\mathrm{RS}}\underline{t}^{S_M}}{\partial t_{\mathrm{yw}}} \cdot \delta t_{\mathrm{yw}}
\end{aligned}
\tag{A.243}
$$

For the mean responsive loads holds (no active yaw control):

$$
\begin{aligned}
{}^{\mathrm{RS}}\bar{\underline{f}}^{S_M} &= \left[-s_{\mathrm{f_x}\rho_{\mathrm{x}}}^{S_M} \cdot \bar{\rho}_3^{S_M} \quad -s_{\mathrm{f_y}\rho_{\mathrm{y}}}^{S_M} \cdot \bar{\rho}_2^{S_M} \quad -s_{\mathrm{f_z}\rho_{\mathrm{z}}}^{S_M} \cdot \bar{\rho}_1^{S_M} \right]^{\mathrm{T}} \\
{}^{\mathrm{RS}}\bar{\underline{t}}^{S_M} &= \left[-s_{\mathrm{t_x}\phi_{\mathrm{x}}}^{S_M} \cdot \bar{\phi}_2^{S_M} \quad -s_{\mathrm{t_y}\phi_{\mathrm{y}}}^{S_M} \cdot \bar{\phi}_3^{S_M} \quad -s_{\mathrm{t_z}\phi_{\mathrm{z}}}^{S_M} \cdot \bar{\phi}_1^{S_M} \right]^{\mathrm{T}}
\end{aligned}
\tag{A.244}
$$

For the sensitivities to the dof position variations hold (no active yaw control):

$$\frac{\partial^{\mathrm{RS}}\underline{f}^{S_M}}{\partial \underline{\rho}^{\mathrm{X}}} = \begin{pmatrix} -s^{S_M}_{\mathrm{f_x}\rho_\mathrm{x}} \cdot [\, 0_{(1\ldots3M-3)} & 0\,0\,1\,] \\ -s^{S_M}_{\mathrm{f_y}\rho_\mathrm{y}} \cdot [\, 0_{(1\ldots3M-3)} & 0\,1\,0\,] \\ -s^{S_M}_{\mathrm{f_z}\rho_\mathrm{z}} \cdot [\, 0_{(1\ldots3M-3)} & 1\,0\,0\,] \end{pmatrix} ; \quad \frac{\partial^{\mathrm{RS}}\underline{t}^{S_M}}{\partial \underline{\phi}^{\mathrm{X}}} = \begin{pmatrix} -s^{S_M}_{\mathrm{t_x}\phi_\mathrm{x}} \cdot [\, 0_{(1\ldots3M-3)} & 0\,1\,0\,] \\ -s^{S_M}_{\mathrm{t_y}\phi_\mathrm{y}} \cdot [\, 0_{(1\ldots3M-3)} & 0\,0\,1\,] \\ -s^{S_M}_{\mathrm{t_z}\phi_\mathrm{z}} \cdot [\, 0_{(1\ldots3M-3)} & 1\,0\,0\,] \end{pmatrix} \tag{A.245}$$

The sensitivities to the dof speeds are obtained from the ones above by just replacing $s^{S_M}_{(.)}$ by $d^{S_M}_{(.)}$.

If less than six degrees of freedom apply in an entry point then some reponsive load expressions are not valid (infinite stiffness and damper values would apply). However, this is of no importance because these expressions are skipped when the equations of motions are being derived.

In case of active yaw control, the control system yields a co-axial 'counter torque' t_{yw} on the nacelle: if > 0 it will turn the nacelle back towards its initial position when the actual deviation $\varphi_{\mathrm{yw}} > 0$ (clockwise deviation at top-down view on tower). The responsive torque load ${}^{\mathrm{RS}}t_3^{S_M}$ then amounts to minus the 'counter clockwise oriented yaw actuation torque' t_{yw} and the third row in the sensitivity matrix for the visco/elastic responsive torque loading then equals zero:

$$\frac{\partial^{\mathrm{RS}}\underline{t}^{S_M}}{\partial \underline{\phi}^{S}} = \begin{pmatrix} -s^{S_M}_{\mathrm{t_x}\phi_\mathrm{x}} \cdot [\, 0_{(1\ldots3M-3)} & 0\,1\,0\,] \\ -s^{S_M}_{\mathrm{t_y}\phi_\mathrm{y}} \cdot [\, 0_{(1\ldots3M-3)} & 0\,0\,1\,] \\ [\, 0_{1\ldots3M-3)} & 0\,0\,0\,] \end{pmatrix} \quad ; \quad \frac{\partial^{\mathrm{RS}}\underline{t}^{S_M}}{\partial t_{\mathrm{yw}}} = \begin{pmatrix} 0 \\ 0 \\ -1 \end{pmatrix} \tag{A.246}$$

The sensitivities to the dof speeds are obtained from the ones above to the dof positions by just replacing $s^{S_M}_{(.)}$ by $d^{S_M}_{(.)}$.

The yaw control behaviour only applies in the equations of motion if the variations *around* the equilibrium conditions are considered (EOM). When evaluating the equations of motion in the equilibrium conditions (EOE), the rotation $\bar{\phi}_3^{S_M}$ is set fixed to the average value of the yaw angle ϕ_{yw}, which is a user defined setpoint.

(ii) Input variables

The input vector for S_{n} has the following composition:

$$\underline{v}^{S_{\mathrm{n}}} = \begin{bmatrix} \underline{v}^{S_{\mathrm{n}}R_{\mathrm{h}}} \\ \underline{v}^{S_{\mathrm{n}}S_{\mathrm{t}}} \\ \underline{v}^{S_{\mathrm{n}}S_{\mathrm{n_c}}} \end{bmatrix}$$

with

$$\underline{v}^{S_{\mathrm{n}}R_{\mathrm{h}}} = \begin{bmatrix} {}^{\mathrm{FT}}\underline{f}^{S_{\mathrm{PP}(4)}} \\ {}^{\mathrm{FT}}\underline{t}^{S_{\mathrm{PP}(4)}} \end{bmatrix} ; \quad \underline{v}^{S_{\mathrm{n}}S_{\mathrm{t}}} = \begin{bmatrix} \underline{\omega}^{S_{\mathrm{FF}(2)}} \\ \underline{\alpha}^{S_{\mathrm{FF}(2)}} \\ \underline{v}^{S^{\oplus}_{\mathrm{FF}(2)}} \\ \underline{a}^{S^{\oplus}_{\mathrm{FF}(2)}} \\ \underline{u}_{\mathrm{ori}}^{S_{\mathrm{FF}(2)}} \\ \underline{g}_{\mathrm{ori}}^{S_{\mathrm{FF}(2)}} \\ \underline{\xi}^{S_{\mathrm{FF}(2)}} \\ \underline{x}^{S^{\oplus}_{\mathrm{FF}(2)}} \end{bmatrix} ; \quad \underline{v}^{S_{\mathrm{n}}S_{\mathrm{n_c}}} = [\, t_{\mathrm{yw}} \,] \tag{A.247}$$

(iii) Equations of motion and 2nd order vector state equation

Just as for the rotor blade subcomponents, the implementation of the 2nd order state vector equation for the nacelle $S_{\rm n}$ is based on the overall encapsulating dof vectors. That is to say, the mass, spring and damper matrix arise from partial derivatives of impulse and load vectors to the dof vectors $\underline{\varphi}^S$ and $\underline{\varrho}^S$. Point of departure is the full-size vector state equation ($6M \times 6M$-matrices):

$$\left[\boldsymbol{M}_{\varphi}^{S_{\rm n}} \mid \boldsymbol{M}_{\varrho}^{S_{\rm n}}\right] \cdot \begin{bmatrix} \ddot{\underline{\varphi}}^S \\ \ddot{\underline{\varrho}}^S \end{bmatrix} + \left[\boldsymbol{D}_{\varphi}^{S_{\rm n}} \mid \boldsymbol{D}_{\varrho}^{S_{\rm n}}\right] \cdot \begin{bmatrix} \dot{\underline{\varphi}}^S \\ \dot{\underline{\varrho}}^S \end{bmatrix} + \left[\boldsymbol{S}_{\varphi}^{S_{\rm n}} \mid \boldsymbol{S}_{\varrho}^{S_{\rm n}}\right] \cdot \begin{bmatrix} \underline{\varphi}^S \\ \underline{\varrho}^S \end{bmatrix} = \left[\, \boldsymbol{G}^{S_{\rm n} R_{\rm h}} \mid \boldsymbol{G}^{S_{\rm n} S_{\rm t}} \mid \boldsymbol{G}^{S_{\rm n} S_{\rm n_c}} \,\right] \cdot \begin{bmatrix} \underline{v}^{S_{\rm n} R_{\rm h}} \\ \underline{v}^{S_{\rm n} S_{\rm t}} \\ \underline{v}^{S_{\rm n} S_{\rm n_c}} \end{bmatrix} \tag{A.248}$$

The one-element subcomponent $S_{\rm n}$ is set up by support structure element S_M. The required matrices are derived by considering the vector impulse equations for element S_M in its set of three coordinate systems. The bottum-up ranked rotation axes for $S_{\rm n}$ are the z-, y- and x-axis; the z-axis is co-axial for the tower. Thus we start with the x- and y-coordinate of the angular and linear impulse in the 3rd intermediate coordinate system (i.c.s.). Afterwards, the respective y-coordinate and x-coordinate are considered in the 2nd i.c.s. Finally, both z-coordinates are dealt with in the 1st i.c.s.

The pairs of rows $\{\underline{\boldsymbol{m}}_{h\varphi_w}^{S_M}, \underline{\boldsymbol{m}}_{p\varphi_w}^{S_M} | w = 3, 2, 1\}$, with ranking numbers $6(M-1)+2(w-1)+1$ and $6(M-1)+2(w-1)+2$ in the mass matrix partition $\boldsymbol{M}_{\varphi}^{S_{\rm n}}$, are now determined as follows (the partial derivatives in the right hand side only apply if they are defined for the 'independent variable' $\ddot{\underline{\varphi}}^S$):

- for $w = 3$:

$$\begin{aligned} \underline{\boldsymbol{m}}_{h\varphi_3}^{S_M} &= -[\,1\,0\,0\,] \cdot \frac{\partial^{\rm RS} \underline{t}^{S_M^{\ominus}}}{\partial \ddot{\underline{\varphi}}^S} + [\,1\,0\,0\,] \cdot \Big(\frac{\partial^{S_M^{\ominus}} \dot{\underline{h}}^{S_M}}{\partial \ddot{\underline{\varphi}}^S} - \frac{\partial^{\rm EX} \underline{t}^{S_M^{\ominus}}}{\partial \ddot{\underline{\varphi}}^S} \Big) \\ \underline{\boldsymbol{m}}_{p\varphi_3}^{S_M} &= -[\,0\,1\,0\,] \cdot \frac{\partial^{\rm RS} \underline{f}^{S_M^{\ominus}}}{\partial \ddot{\underline{\varphi}}^S} + [\,0\,1\,0\,] \cdot \Big(\frac{\partial \dot{\underline{p}}^{S_M}}{\partial \ddot{\underline{\varphi}}^S} - \frac{\partial^{\rm EX} \underline{f}^{S_M^{\ominus}}}{\partial \ddot{\underline{\varphi}}^S} \Big) \end{aligned} \tag{A.249}$$

- for $w = 2$:

$$\begin{aligned} \underline{\boldsymbol{m}}_{h\varphi_2}^{S_M} &= -[\,0\,1\,0\,] \cdot \frac{\partial^{\rm RS} \underline{t}^{S_M^{\ominus}}}{\partial \ddot{\underline{\varphi}}^S} + {}^{S_M^2}\bar{\Phi}_{(2,:)}^{S_M} \cdot \Big(\frac{\partial^{S_M^{\ominus}} \dot{\underline{h}}^{S_M}}{\partial \ddot{\underline{\varphi}}^S} - \frac{\partial^{\rm EX} \underline{t}^{S_M^{\ominus}}}{\partial \ddot{\underline{\varphi}}^S} \Big) \\ \underline{\boldsymbol{m}}_{p\varphi_2}^{S_M} &= -[\,1\,0\,0\,] \cdot \frac{\partial^{\rm RS} \underline{f}^{S_M^{\ominus}}}{\partial \ddot{\underline{\varphi}}^S} + {}^{S_M^2}\bar{\Phi}_{(1,:)}^{S_M} \cdot \Big(\frac{\partial \dot{\underline{p}}^{S_M}}{\partial \ddot{\underline{\varphi}}^S} - \frac{\partial^{\rm EX} \underline{f}^{S_M^{\ominus}}}{\partial \ddot{\underline{\varphi}}^S} \Big) \end{aligned} \tag{A.250}$$

- for $w = 1$:

$$\begin{aligned} \underline{\boldsymbol{m}}_{h\varphi_1}^{S_M} &= -[\,0\,0\,1\,] \cdot \frac{\partial^{\rm RS} \underline{t}^{S_M^{\ominus}}}{\partial \ddot{\underline{\varphi}}^S} + {}^{S_M^1}\bar{\Phi}_{(3,:)}^{S_M} \cdot \Big(\frac{\partial^{S_M^{\ominus}} \dot{\underline{h}}^{S_M}}{\partial \ddot{\underline{\varphi}}^S} - \frac{\partial^{\rm EX} \underline{t}^{S_M^{\ominus}}}{\partial \ddot{\underline{\varphi}}^S} \Big) \\ \underline{\boldsymbol{m}}_{p\varphi_1}^{S_M} &= -[\,0\,0\,1\,] \cdot \frac{\partial^{\rm RS} \underline{f}^{S_M^{\ominus}}}{\partial \ddot{\underline{\varphi}}^S} + {}^{S_M^1}\bar{\Phi}_{(3,:)}^{S_M} \cdot \Big(\frac{\partial \dot{\underline{p}}^{S_M}}{\partial \ddot{\underline{\varphi}}^S} - \frac{\partial^{\rm EX} \underline{f}^{S_M^{\ominus}}}{\partial \ddot{\underline{\varphi}}^S} \Big) \end{aligned} \tag{A.251}$$

Note that NO feedthrough loading exists from other elements within the one-element subcomponent $S_{\rm n}$. The loading from the gearbox house $R_{\rm h}$ is considered as external loading for $S_{\rm n}$ and included in ${}^{\rm EX}\underline{t}^{S_M^{\ominus}}$ and ${}^{\rm EX}\underline{f}^{S_M^{\ominus}}$.

The corresponding rows in the mass matrix partition $\boldsymbol{M}_{\varrho}^{S_{\rm n}}$ are obtained by taking the sensitivities to $\ddot{\underline{\varrho}}^S$ instead of $\ddot{\underline{\varphi}}^S$. For the rows in both damping matrix partitions $\boldsymbol{D}_{\varphi}^{S_{\rm n}}$ and

$\boldsymbol{D}_{\underline{\varrho}}^{S_{\mathrm{n}}}$ and in the stiffness matrix partition $\boldsymbol{S}_{\underline{\varrho}}^{S_{\mathrm{n}}}$, take the sensitivities to $\underline{\dot{\varphi}}^{S}$ and $\underline{\dot{\varrho}}^{S}$ and $\underline{\varrho}^{S}$. For the remaining stiffness matrix partition $\boldsymbol{S}_{\underline{\varphi}}^{S_{\mathrm{n}}}$ the same scheme applies for $w = 3$ but differs for $w = 2$ and $w = 1$:

- for $w = 2$:

$$\begin{aligned}
\underline{\boldsymbol{s}}_{h\varphi_2}^{S_M} &= -[\,0\,1\,0\,]\cdot\frac{\partial^{\mathrm{RS}}\underline{t}^{S_M^{\ominus}}}{\partial\underline{\phi}^{S}} + {}^{S_M^2}\bar{\Phi}_{(2,:)}^{S_M}\cdot\Big(\frac{\partial^{S_M^{\ominus}}\underline{\dot{h}}^{S_M}}{\partial\underline{\phi}^{S}} - \frac{\partial^{\mathrm{EX}}\underline{t}^{S_M^{\ominus}}}{\partial\underline{\phi}^{S}}\Big) + \\
&\qquad [\,\mathrm{O}_{(1\ldots M-1)}\;\; \mathrm{J}_{v=1}^{3}\Big(\frac{\partial^{S_M^2}\Phi_{(2,:)}^{S_M}}{\partial\phi_v^{S_M}}\cdot\Big({}^{S_M^{\ominus}}\bar{\underline{h}}^{S_M} - {}^{\mathrm{EX}}\bar{\underline{t}}^{S_M^{\ominus}}\Big)\Big)\,] \\
\underline{\boldsymbol{s}}_{p\varphi_2}^{S_M} &= -[\,1\,0\,0\,]\cdot\frac{\partial^{\mathrm{RS}}\underline{f}^{S_M^{\ominus}}}{\partial\underline{\phi}^{S}} + {}^{S_M^2}\bar{\Phi}_{(1,:)}^{S_M}\cdot\Big(\frac{\partial\underline{\dot{p}}^{S_M}}{\partial\underline{\phi}^{S}} - \frac{\partial^{\mathrm{EX}}\underline{f}^{S_M^{\ominus}}}{\partial\underline{\phi}^{S}}\Big) + \\
&\qquad [\,\mathrm{O}_{(1\ldots M-1)}\;\; \mathrm{J}_{v=1}^{3}\Big(\frac{\partial^{S_M^2}\Phi_{(1,:)}^{S_M}}{\partial\phi_v^{S_M}}\cdot\Big({}^{S_M^{\ominus}}\bar{\underline{p}}^{S_M} - {}^{\mathrm{EX}}\bar{\underline{f}}^{S_M^{\ominus}}\Big)\Big)\,]
\end{aligned} \tag{A.252}$$

- for $w = 1$:

$$\begin{aligned}
\underline{\boldsymbol{s}}_{h\varphi_1}^{S_M} &= -[\,0\,0\,1\,]\cdot\frac{\partial^{\mathrm{RS}}\underline{t}^{S_M^{\ominus}}}{\partial\underline{\phi}^{S}} + {}^{S_M^1}\bar{\Phi}_{(3,:)}^{S_M}\cdot\Big(\frac{\partial^{S_M^{\ominus}}\underline{\dot{h}}^{S_M}}{\partial\underline{\phi}^{S}} - \frac{\partial^{\mathrm{EX}}\underline{t}^{S_M^{\ominus}}}{\partial\underline{\phi}^{S}}\Big) + \\
&\qquad [\,\mathrm{O}_{(1\ldots M-1)}\;\; \mathrm{J}_{v=1}^{3}\Big(\frac{\partial^{S_M^1}\Phi_{(3,:)}^{S_M}}{\partial\phi_v^{S_M}}\cdot\Big({}^{S_M^{\ominus}}\bar{\underline{h}}^{S_M} - {}^{\mathrm{EX}}\bar{\underline{t}}^{S_M^{\ominus}}\Big)\Big)\,] \\
\underline{\boldsymbol{s}}_{p\varphi_1}^{S_M} &= -[\,0\,0\,1\,]\cdot\frac{\partial^{\mathrm{RS}}\underline{f}^{S_M^{\ominus}}}{\partial\underline{\phi}^{S}} + {}^{S_M^1}\bar{\Phi}_{(3,:)}^{S_M}\cdot\Big(\frac{\partial\underline{\dot{p}}^{S_M}}{\partial\underline{\phi}^{S}} - \frac{\partial^{\mathrm{EX}}\underline{f}^{S_M^{\ominus}}}{\partial\underline{\phi}^{S}}\Big) + \\
&\qquad [\,\mathrm{O}_{(1\ldots M-1)}\;\; \mathrm{J}_{v=1}^{3}\Big(\frac{\partial^{S_M^1}\Phi_{(3,:)}^{S_M}}{\partial\phi_v^{S_M}}\cdot\Big({}^{S_M^{\ominus}}\bar{\underline{p}}^{S_M} - {}^{\mathrm{EX}}\bar{\underline{f}}^{S_M^{\ominus}}\Big)\Big)\,]
\end{aligned} \tag{A.253}$$

The pairs of rows $\{\underline{\boldsymbol{g}}_{h_w}^{S_M R_{\mathrm{h}}}, \underline{\boldsymbol{g}}_{p_w}^{S_{\mathrm{n}} R_{\mathrm{h}}} | w = 3, 2, 1\}$, with ranking numbers $2(w-1)+1$ and $2(w-1)+2$ in the input matrix partition $\boldsymbol{G}^{S_{\mathrm{n}} R_{\mathrm{h}}}$, are determined as follows (the partial derivatives in the right hand side only apply if they are defined for the 'independent variable'; in this case $\underline{z}$):

- for $w = 3$:

$$\begin{aligned}
\underline{\boldsymbol{g}}_{h_3}^{S_M R_{\mathrm{h}}} &= \mathrm{J}_{(\underline{z})}\Big([\,1\,0\,0\,]\cdot\frac{\partial^{\mathrm{RS}}\underline{t}^{S_M^{\ominus}}}{\partial\underline{z}} + [\,1\,0\,0\,]\cdot(-\frac{\partial^{S_M^{\ominus}}\underline{\dot{h}}^{S_M}}{\partial\underline{z}} + \frac{\partial^{\mathrm{EX}}\underline{t}^{S_M^{\ominus}}}{\partial\underline{z}})\Big) \\
\underline{\boldsymbol{g}}_{p_3}^{S_M R_{\mathrm{h}}} &= \mathrm{J}_{(\underline{z})}\Big([\,0\,1\,0\,]\cdot\frac{\partial^{\mathrm{RS}}\underline{f}^{S_M^{\ominus}}}{\partial\underline{z}} + [\,0\,1\,0\,]\cdot(-\frac{\partial\underline{\dot{p}}^{S_M}}{\partial\underline{z}} + \frac{\partial^{\mathrm{EX}}\underline{f}^{S_M^{\ominus}}}{\partial\underline{z}})\Big)
\end{aligned} \tag{A.254}$$

- for $w = 2$:

$$\begin{aligned}
\underline{\boldsymbol{g}}_{h_2}^{S_M R_{\mathrm{h}}} &= \mathrm{J}_{(\underline{z})}\Big([\,0\,1\,0\,]\cdot\frac{\partial^{\mathrm{RS}}\underline{t}^{S_M^{\ominus}}}{\partial\underline{z}} + {}^{S_M^2}\bar{\Phi}_{(2,:)}^{S_M}\cdot\Big(-\frac{\partial^{S_M^{\ominus}}\underline{\dot{h}}^{S_M}}{\partial\underline{z}} + \frac{\partial^{\mathrm{EX}}\underline{t}^{S_M^{\ominus}}}{\partial\underline{z}}\Big)\Big) \\
\underline{\boldsymbol{g}}_{p_2}^{S_M R_{\mathrm{h}}} &= \mathrm{J}_{(\underline{z})}\Big([\,1\,0\,0\,]\cdot\frac{\partial^{\mathrm{RS}}\underline{f}^{S_M^{\ominus}}}{\partial\underline{z}} + {}^{S_M^2}\bar{\Phi}_{(1,:)}^{S_M}\cdot(-\frac{\partial\underline{\dot{p}}^{S_M}}{\partial\underline{z}} + \frac{\partial^{\mathrm{EX}}\underline{f}^{S_M^{\ominus}}}{\partial\underline{z}})\Big)
\end{aligned} \tag{A.255}$$

- for $w = 1$:

$$\begin{aligned}
\underline{\boldsymbol{g}}_{h_1}^{S_M R_{\mathrm{h}}} &= \mathrm{J}_{(\underline{z})}\Big([\,0\,0\,1\,]\cdot\frac{\partial^{\mathrm{RS}}\underline{t}^{S_M^{\ominus}}}{\partial\underline{z}} + {}^{S_M^1}\bar{\Phi}_{(3,:)}^{S_M}\cdot\Big(-\frac{\partial^{S_M^{\ominus}}\underline{\dot{h}}^{S_M}}{\partial\underline{z}} + \frac{\partial^{\mathrm{EX}}\underline{t}^{S_M^{\ominus}}}{\partial\underline{z}}\Big)\Big) \\
\underline{\boldsymbol{g}}_{p_1}^{S_M R_{\mathrm{h}}} &= \mathrm{J}_{(\underline{z})}\Big([\,0\,0\,1\,]\cdot\frac{\partial^{\mathrm{RS}}\underline{f}^{S_M^{\ominus}}}{\partial\underline{z}} + {}^{S_M^1}\bar{\Phi}_{(3,:)}^{S_M}\cdot(-\frac{\partial\underline{\dot{p}}^{S_M}}{\partial\underline{z}} + \frac{\partial^{\mathrm{EX}}\underline{f}^{S_M^{\ominus}}}{\partial\underline{z}})\Big)
\end{aligned} \tag{A.256}$$

The involved subvectors $\underline{z}$ for the submatrices $\boldsymbol{G}^{S_{\rm n}R}$, $\boldsymbol{G}^{S_{\rm n}S_{\rm n}}$, $\boldsymbol{G}^{S_{\rm n}S_{\rm nc}}$ are listed in Eq. A.247 in the previous paragraph.

Note that all columns but the last three of the rows of the mass, damper and stiffness matrix partitions are deleted. Besides each non-valid row together with the corresponding column , that is to say which pertains to a 'non-dof' element of $\underline{\varphi}^S$ or $\underline{\varrho}^S$ *as concerns* $S_{\rm n}$, is deleted . Of course, the corresponding row in the input matrix is also deleted. This yields a second order system equation with square left hand side matrices and adequately dimensioned input matrix.

The external load coordinate vectors, which pertain to the nacelle entry (=yaw bearing centre) and have coordinates along the f.c.s. of S_M, include the gravition loading and the feedthrough loads from the gearbox house in nacelle exit (= rotor centre):

$$\begin{aligned} {}^{\rm EX}\underline{f}^{S_M^{\ominus}} &\triangleq {}^{\rm g}\underline{f}^{S_{\rm n}^*} + {}^{\rm FT}\underline{f}^{S_{\rm PP(4)}} \\ {}^{\rm EX}\underline{t}^{S_M^{\ominus}} &\triangleq {}^{S_M^{\ominus}}\underline{r}^{S_M^*} \times {}^{\rm g}\underline{f}^{S_{\rm n}^*} + {}^{S_M^{\ominus}}\underline{r}^{S_M^{\oplus}} \times {}^{\rm FT}\underline{f}^{S_{\rm PP(4)}} + {}^{\rm FT}\underline{t}^{S_{\rm PP(4)}} \end{aligned} \tag{A.257}$$

The linearised expressions for the gravitation load coordinate vectors are listed in section B.10.3, Eq. B.285 and and B.286. The external load coordinate vectors are subdivided into means and sensitivities as:

$$\begin{aligned} {}^{\rm EX}\underline{f}^{S_M^{\ominus}} &= {}^{\rm EX}\bar{\underline{f}}^{S_M^{\ominus}} + \frac{\partial {}^{\rm EX}\underline{f}^{S_M^{\ominus}}}{\partial \underline{\varphi}^S}\cdot\underline{\varphi}^S + \frac{\partial {}^{\rm EX}\underline{f}^{S_M^{\ominus}}}{\partial \underline{g}_{\rm ori}^{S_{\rm FF(2)}}}\cdot\underline{g}_{\rm ori}^{S_{\rm FF(2)}} + \frac{\partial {}^{\rm EX}\underline{f}^{S_M^{\ominus}}}{\partial {}^{\rm FT}\underline{f}^{S_{\rm PP(4)}}}\cdot\delta^{\rm FT}\underline{f}^{S_{\rm PP(4)}} \\ {}^{\rm EX}\underline{t}^{S_M^{\ominus}} &= {}^{\rm EX}\bar{\underline{t}}^{S_M^{\ominus}} + \frac{\partial {}^{\rm EX}\underline{t}^{S_M^{\ominus}}}{\partial \underline{\varphi}^S}\cdot\underline{\varphi}^S + \frac{\partial {}^{\rm EX}\underline{t}^{S_M^{\ominus}}}{\partial \underline{g}_{\rm ori}^{S_{\rm FF(2)}}}\cdot\underline{g}_{\rm ori}^{S_{\rm FF(2)}} + \\ &\qquad \frac{\partial {}^{\rm EX}\underline{t}^{S_M^{\ominus}}}{\partial {}^{\rm FT}\underline{t}^{S_{\rm PP(4)}}}\cdot\delta^{\rm FT}\underline{t}^{S_{\rm PP(4)}} + \frac{\partial {}^{\rm EX}\underline{t}^{S_M^{\ominus}}}{\partial {}^{\rm FT}\underline{t}^{S_{\rm PP(4)}}}\cdot\delta^{\rm FT}\underline{t}^{S_{\rm PP(4)}} \end{aligned} \tag{A.258}$$

For the sensitivities to $\underline{\varphi}^S$ and $\underline{g}_{\rm ori}^{S_{\rm FF(2)}}$ holds :

$$\frac{\partial {}^{\rm EX}\underline{f}^{S_M^{\ominus}}}{\partial \underline{q}} = \frac{\partial {}^{\rm g}\underline{f}^{S_{\rm n}^*}}{\partial \underline{q}} \quad ; \quad \frac{\partial {}^{\rm EX}\underline{t}^{S_M^{\ominus}}}{\partial \underline{q}} = {\rm J}^3_{v=1}\left({}^{S_M^{\ominus}}\underline{r}^{S_{\rm n}^*}\times\underline{e}_v\right)\cdot\frac{\partial {}^{\rm g}\underline{f}^{S_{\rm n}^*}}{\partial \underline{q}} \tag{A.259}$$

Further it holds:

$$\frac{\partial {}^{\rm EX}\underline{f}^{S_M^{\ominus}}}{\partial {}^{\rm FT}\underline{f}^{S_{\rm PP(4)}}} = \boldsymbol{I} \quad ; \quad \frac{\partial {}^{\rm EX}\underline{t}^{S_M^{\ominus}}}{\partial {}^{\rm FT}\underline{t}^{S_{\rm PP(4)}}} = \boldsymbol{I} \quad ; \quad \frac{\partial {}^{\rm EX}\underline{t}^{S_M^{\ominus}}}{\partial {}^{\rm FT}\underline{f}^{S_{\rm PP(4)}}} = {\rm J}^3_{v=1}\left({}^{S_M^{\ominus}}\underline{r}^{S_{\rm n}^{\oplus}}\times\underline{e}_v\right) \tag{A.260}$$

(iv) Output variables and vector output equation in 2nd order model
The nacelle $S_{\rm n}$ needs to provide the following output:

- yaw angle deviation (if control included): $\varphi_{\rm yw}$;
- exit point displacement relative to the (fixed) position of the turbine base:
  $\delta^{\bar{S}_0^{\ominus}}\underline{r}^{S_M^{\oplus}/B}$ (along fixed c.s. $\vec{e}^{\,\bar{S}_0} \equiv \vec{e}^{\,B}$)
- feedthrough force and torque on tower top $S_{M-1}^{\oplus}$:
  ${}^{\rm FT}\underline{f}^{S_{\rm PP(3)}}$, ${}^{\rm FT}\underline{t}^{S_{\rm PP(3)}}$ ($\equiv {}^{\rm FT}\underline{f}^{S_{M-1}^{\oplus}}$, ${}^{\rm FT}\underline{t}^{S_{M-1}^{\oplus}}$, along actual c.s. $\vec{e}^{\,S_{M-1}}$)
- kinematic vectors in nacelle exit $S_M^{\oplus}$ to gearbox house:
  $\underline{\omega}^{S_{\rm FF(3)}}$, $\underline{\alpha}^{S_{\rm FF(3)}}$, $\underline{v}^{S_{\rm FF(3)}^{\oplus}}$, $\underline{a}^{S_{\rm FF(3)}^{\oplus}}$ (along actual c.s. $\vec{e}^{\,S_M}$)

- wind speed and gravitation variation by orientation change up till exit $S_{\rm n}^{\oplus}$:
  $\underline{u}_{\rm ori}^{S_{\rm FF(3)}}, \underline{g}_{\rm ori}^{S_{\rm FF(3)}}$ (along actual c.s. $\vec{e}^{\,S_M}$)
- exit point displacement relative to average position nacelle exit:
  $\underline{\xi}^{S_{\rm FF(3)}}, \underline{x}^{S_{\rm FF(3)}^{\oplus}}$ (along average f.c.s. $\vec{e}^{\,S_M}$)

The output vector from $S_{\rm n}$ has the following composition:

$$\underline{y}^{S_{\rm n}} = \begin{bmatrix} \underline{y}^{GS_{\rm n}} \\ \underline{y}^{R_{\rm h}S_{\rm n}} \\ \underline{y}^{S_{\rm t}S_{\rm n}} \\ \underline{y}^{S_{\rm nc}S_{\rm n}} \end{bmatrix}$$

with

$$\underline{y}^{GS_{\rm n}} = \begin{bmatrix} \varphi_{\rm yw} \\ t_{\rm yw} \end{bmatrix}; \quad \underline{y}^{S_{\rm t}S_{\rm n}} = \begin{bmatrix} {}^{\rm FT}\underline{f}^{S_{\rm PP(3)}} \\ {}^{\rm FT}\underline{t}^{S_{\rm PP(3)}} \end{bmatrix}; \quad \underline{y}^{R_{\rm h}S_{\rm n}} = \begin{bmatrix} \underline{\omega}^{S_{\rm FF(3)}} \\ \underline{\alpha}^{S_{\rm FF(3)}} \\ \underline{v}^{S_{\rm FF(3)}^{\oplus}} \\ \underline{a}^{S_{\rm FF(3)}^{\oplus}} \\ \underline{u}_{\rm ori}^{S_{\rm FF(3)}} \\ \underline{g}_{\rm ori}^{S_{\rm FF(3)}} \\ \underline{\xi}^{S_{\rm FF(3)}} \\ \underline{x}^{S_{\rm FF(3)}^{\oplus}} \end{bmatrix}; \quad \underline{y}^{S_{\rm nc}S_{\rm n}} = \begin{bmatrix} \varphi_{\rm yw} \end{bmatrix} \tag{A.261}$$

The (zero-mean) feedthrough kinematic vectors $\underline{\omega}^{S_{\rm FF(3)}}$, $\underline{\alpha}^{S_{\rm FF(3)}}$, $\underline{v}^{S_{\rm FF(3)}^{\oplus}}$ and $\underline{a}^{S_{\rm FF(3)}^{\oplus}}$ to the gearbox house $R_{\rm h}$ are supplied as coordinate vectors along the f.c.s. $\vec{e}^{\,S_M}$. The expression for the variations follow from Eq. B.1 up to B.7 by setting '$k = M$' and '$S_{\rm FF} = S_{\rm FF(2)}$' and considering the point $S_M^{\oplus}$ instead of S_M^* for $\underline{v}^{S_{\rm FF(3)}^{\oplus}}$ and $\underline{a}^{S_{\rm FF(3)}^{\oplus}}$.

The feedthrough 'orientation change vectors' $\underline{u}_{\rm ori}^{S_{\rm FF(3)}}$ and $\underline{g}_{\rm ori}^{S_{\rm FF(3)}}$ ($\equiv \underline{u}_{\rm ori}^{S_{\rm n}}$, $\underline{g}_{\rm ori}^{S_{\rm n}}$) are also expressed along $\vec{e}^{\,S_M}$ (see Eq. B.164 and B.287, B.288).

For the displacement variation vector $\delta^{\bar{S}_0^{\ominus}}\underline{r}^{S_M^{\oplus}/B}$ with coordinates along the fixed c.s. of the turbine base $B \equiv \bar{S}_0$, holds:

$$\delta^{\bar{S}_0^{\ominus}}\underline{r}^{S_M^{\oplus}/B} = \sum_{(\underline{z})} \frac{\partial^{\bar{S}_0^{\ominus}}\underline{r}^{S_M^{\oplus}/B}}{\partial \underline{z}} \cdot \delta \underline{z} \qquad (\underline{z} = \underline{\phi}^S, \underline{\rho}^S, \underline{\xi}^{S_{\rm FF(2)}}, \underline{x}^{S_{\rm FF(2)}}) \tag{A.262}$$

with (see discussion from Eq. A.77):

$$\begin{aligned} \frac{\partial^{\bar{S}_0^{\ominus}}\underline{r}^{S_M^{\oplus}/B}}{\partial \underline{\xi}^{S_{\rm FF(2)}}} &= {}^{S_0}\bar{\Phi}^{S_M} \cdot \frac{\partial \underline{v}^{S_M^{\oplus}}}{\partial \underline{\omega}^{S_{\rm FF(2)}}} \quad ; \quad \frac{\partial^{\bar{S}_0^{\ominus}}\underline{r}^{S_M^{\oplus}/B}}{\partial \underline{\phi}^S} = {}^{S_0}\bar{\Phi}^{S_M} \cdot \frac{\partial \underline{v}^{S_M^{\oplus}}}{\partial \dot{\underline{\varphi}}^S} \\ \frac{\partial^{\bar{S}_0^{\ominus}}\underline{r}^{S_M^{\oplus}/B}}{\partial \underline{x}^{S_{\rm FF(2)}}} &= {}^{S_0}\bar{\Phi}^{S_M} \cdot \frac{\partial \underline{v}^{S_M^{\oplus}}}{\partial \underline{v}^{S_{\rm FF(2)}}} \quad ; \quad \frac{\partial^{\bar{S}_0^{\ominus}}\underline{r}^{S_M^{\oplus}/B}}{\partial \underline{\rho}^S} = {}^{S_0}\bar{\Phi}^{S_M} \cdot \frac{\partial \underline{v}^{S_M^{\oplus}}}{\partial \dot{\underline{\rho}}^S} \end{aligned} \tag{A.263}$$

For the displacement outputs to the gearbox house then holds the following sensitivities (coordinates along average f.c.s. of S_M):

$$\begin{aligned}
\frac{\partial \underline{x}^{S_{\mathrm{FF}(3)}}}{\partial \underline{\xi}^{S_{\mathrm{FF}(2)}}} &= \frac{\partial \underline{v}^{S_M^{\oplus}}}{\partial \underline{\omega}^{S_{\mathrm{FF}(2)}}} \quad ; \quad \frac{\partial \underline{x}^{S_{\mathrm{FF}(3)}}}{\partial \underline{\phi}^{S}} = \frac{\partial \underline{v}^{S_M^{\oplus}}}{\partial \dot{\underline{\varphi}}^{S}} \\
\frac{\partial \underline{x}^{S_{\mathrm{FF}(3)}}}{\partial \underline{x}^{S_{\mathrm{FF}(2)}}} &= \frac{\partial \underline{v}^{S_M^{\oplus}}}{\partial \underline{v}^{S_{\mathrm{FF}(2)}}} \quad ; \quad \frac{\partial \underline{x}^{S_{\mathrm{FF}(3)}}}{\partial \underline{\varrho}^{S}} = \frac{\partial \underline{v}^{S_M^{\oplus}}}{\partial \dot{\underline{\varrho}}^{S}} \\
\frac{\partial \underline{\xi}^{S_{\mathrm{FF}(3)}}}{\partial \underline{\xi}^{S_{\mathrm{FF}(2)}}} &= \frac{\partial \underline{\omega}^{S_M}}{\partial \underline{\omega}^{S_{\mathrm{FF}(2)}}} \quad ; \quad \frac{\partial \underline{\xi}^{S_{\mathrm{FF}(3)}}}{\partial \underline{\phi}^{S}} = \frac{\partial \underline{\omega}^{S_M^{\oplus}}}{\partial \dot{\underline{\varphi}}^{S}}
\end{aligned} \tag{A.264}$$

The feedthrough loads along the actual f.c.s. of S_{M-1} to the tower top are given by (external loads by Eq. A.231):

$$\begin{aligned}
{}^{\mathrm{FT}}\underline{f}^{S_{\mathrm{PP}(3)}} &= {}^{S_{M-1}}\Phi^{S_M} \cdot (-\underline{\dot{p}}^{S_M} + {}^{\mathrm{EX}}\underline{f}^{S_M^{\ominus}}) \\
{}^{\mathrm{FT}}\underline{t}^{S_{\mathrm{PP}(3)}} &= {}^{S_{M-1}}\Phi^{S_M} \cdot (-{}^{S_M^{\ominus}}\underline{\dot{h}}^{S_M} + {}^{\mathrm{EX}}\underline{t}^{S_M^{\ominus}})
\end{aligned} \tag{A.265}$$

Of course, the time-average rate change in the impulse vectors of S_M equals zero. The mean feedthrough loads to the tower top are then given by (see section 4.1 for mean feedthrough loads from the drive-train):

$$\begin{aligned}
{}^{\mathrm{FT}}\bar{\underline{f}}^{S_{\mathrm{PP}(3)}} &= {}^{S_{M-1}}\bar{\Phi}^{S_M} \,.\, {}^{\mathrm{EX}}\bar{\underline{f}}^{S_M} \\
{}^{\mathrm{FT}}\bar{\underline{t}}^{S_{\mathrm{PP}(3)}} &= {}^{S_{M-1}}\bar{\Phi}^{S_M} \,.\, {}^{\mathrm{EX}}\bar{\underline{t}}^{S_M}
\end{aligned} \tag{A.266}$$

The variation of the feedthrough loads to the tower top are given by:

$$\begin{aligned}
\delta {}^{\mathrm{FT}}\underline{f}^{S_{\mathrm{PP}(3)}} &= \sum_{(\underline{q})} \frac{\partial {}^{\mathrm{FT}}\underline{f}^{S_{\mathrm{PP}(3)}}}{\partial \underline{q}} \cdot \delta \underline{q} \quad \text{for } \underline{q} = {}^{\mathrm{FT}}\underline{f}^{S_{\mathrm{PP}(4)}}, \underline{\alpha}^{S_{\mathrm{FF}(2)}}, \\
&\qquad \underline{a}^{S_{\mathrm{FF}(2)}}, \underline{g}_{\mathrm{ori}}^{S_{\mathrm{FF}(2)}}, \underline{\varphi}^{S}, \ddot{\underline{\varphi}}^{S}, \ddot{\underline{\varrho}}^{S} \\
\delta {}^{\mathrm{FT}}\underline{t}^{S_{\mathrm{PP}(3)}} &= \sum_{(\underline{q})} \frac{\partial {}^{\mathrm{FT}}\underline{t}^{S_{\mathrm{PP}(3)}}}{\partial \underline{q}} \cdot \delta \underline{q} \quad \text{for } \underline{q} = {}^{\mathrm{FT}}\underline{t}^{S_{\mathrm{PP}(4)}}, {}^{\mathrm{FT}}\underline{f}^{S_{\mathrm{PP}(4)}}, \underline{\alpha}^{S_{\mathrm{FF}(2)}}, \\
&\qquad \underline{a}^{S_{\mathrm{FF}(2)}}, \underline{g}_{\mathrm{ori}}^{S_{\mathrm{FF}(2)}}, \underline{\varphi}^{S}, \ddot{\underline{\varphi}}^{S}, \ddot{\underline{\varrho}}^{S}
\end{aligned} \tag{A.267}$$

For the sensitivities to the variables $\underline{q}$ holds:

$$\begin{aligned}
\frac{\partial {}^{\mathrm{FT}}\underline{f}^{S_{\mathrm{PP}(3)}}}{\partial \underline{q}} &= {}^{S_{M-1}}\bar{\Phi}^{S_M} \cdot (-\frac{\partial \underline{\dot{p}}^{S_M}}{\partial \underline{q}} + \frac{\partial {}^{\mathrm{EX}}\underline{f}^{S_M^{\ominus}}}{\partial \underline{q}}) + \\
&\qquad \delta_{\underline{q}\underline{\phi}^{S}} \cdot [\, \mathrm{O}_{(1)} \ldots \mathrm{O}_{(M-1)} \;\; \mathrm{J}^3_{v=1}\big(\frac{\partial {}^{S_{M-1}}\Phi^{S_M}}{\partial \phi_v^{S_M}} \cdot ({}^{\mathrm{EX}}\bar{\underline{f}}^{S_M^{\ominus}})\big) \,] \\
\frac{\partial {}^{\mathrm{FT}}\underline{t}^{S_{\mathrm{PP}(3)}}}{\partial \underline{q}} &= {}^{S_{M-1}}\bar{\Phi}^{S_M} \cdot (-\frac{\partial {}^{S_M^{\ominus}}\underline{\dot{h}}^{S_M}}{\partial \underline{q}} + \frac{\partial {}^{\mathrm{EX}}\underline{t}^{S_M^{\ominus}}}{\partial \underline{q}}) + \\
&\qquad \delta_{\underline{q}\underline{\phi}^{S}} \cdot [\, \mathrm{O}_{(1)} \ldots \mathrm{O}_{(M-1)} \;\; \mathrm{J}^3_{v=1}\big(\frac{\partial {}^{S_{M-1}}\Phi^{S_M}}{\partial \phi_v^{S_M}} \cdot ({}^{\mathrm{EX}}\bar{\underline{t}}^{S_M^{\ominus}})\big) \,]
\end{aligned} \tag{A.268}$$

Note that the last term in the right hand side of both equations only applies if $\underline{q}$ equals $\underline{\phi}^{S}$!

The output equation that belongs to the 2nd order state equation is:

$$\underline{y}^{S_{\mathrm{n}}} = \big[\boldsymbol{H}_{\varphi}^{S_{\mathrm{n}}} \;\; \boldsymbol{H}_{\varrho}^{S_{\mathrm{n}}}\big] \cdot \begin{bmatrix} \underline{\varphi}^{S} \\ \underline{\varrho}^{S} \end{bmatrix} + \big[\boldsymbol{L}_{\varphi}^{S_{\mathrm{n}}} \;\; \boldsymbol{L}_{\varrho}^{S_{\mathrm{n}}}\big] \cdot \begin{bmatrix} \dot{\underline{\varphi}}^{S} \\ \dot{\underline{\varrho}}^{S} \end{bmatrix} + \boldsymbol{K}^{S_{\mathrm{n}}} \cdot \underline{v}^{S_{\mathrm{n}}} \tag{A.269}$$

The matrix partitions $\boldsymbol{H}_{\varphi}^{S_{\mathrm{n}}}$ and $\boldsymbol{L}_{\varphi}^{S_{\mathrm{n}}}$ map the *angular* dof position and speed variations:

$$\begin{aligned}
\boldsymbol{H}_{\varphi}^{S_{\mathrm{n}}} &= \frac{\partial \underline{y}^{S_{\mathrm{n}}}}{\partial \underline{\phi}^{S}} - \big(\frac{\partial \underline{y}^{S_{\mathrm{n}}}}{\partial \ddot{\underline{\varphi}}^{S}} \cdot \big(\boldsymbol{M}^{S_{\mathrm{n}}}\big)_{\varphi}^{-1} + \frac{\partial \underline{y}^{S_{\mathrm{n}}}}{\partial \ddot{\underline{\varrho}}^{S}} \cdot \big(\boldsymbol{M}^{S_{\mathrm{n}}}\big)_{\varrho}^{-1} \big) \cdot \boldsymbol{S}_{\varphi}^{S_{\mathrm{n}}} \\
\boldsymbol{L}_{\varphi}^{S_{\mathrm{n}}} &= \frac{\partial \underline{y}^{S_{\mathrm{n}}}}{\partial \dot{\underline{\varphi}}^{S}} - \big(\frac{\partial \underline{y}^{S_{\mathrm{n}}}}{\partial \ddot{\underline{\varphi}}^{S}} \cdot \big(\boldsymbol{M}^{S_{\mathrm{n}}}\big)_{\varphi}^{-1} + \frac{\partial \underline{y}^{S_{\mathrm{n}}}}{\partial \ddot{\underline{\varrho}}^{S}} \cdot \big(\boldsymbol{M}^{S_{\mathrm{n}}}\big)_{\varrho}^{-1} \big) \cdot \boldsymbol{D}_{\varphi}^{S_{\mathrm{n}}}
\end{aligned} \tag{A.270}$$

The matrix partitions $\boldsymbol{H}_{\varrho}^{S_\mathrm{n}}$ and $\boldsymbol{L}_{\varrho}^{S_\mathrm{n}}$ map the *linear* dof position and speed variations:

$$\begin{aligned}
\boldsymbol{H}_{\varrho}^{S_\mathrm{n}} &= \frac{\partial \underline{y}^{S_\mathrm{n}}}{\partial \underline{\varrho}^{S}} - \Big(\frac{\partial \underline{y}^{S_\mathrm{n}}}{\partial \underline{\ddot{\varphi}}^{S}} \cdot \Big(\boldsymbol{M}^{S_\mathrm{n}}\Big)_{\varphi}^{-1} + \frac{\partial \underline{y}^{S_\mathrm{n}}}{\partial \underline{\ddot{\varrho}}^{S}} \cdot \Big(\boldsymbol{M}^{S_\mathrm{n}}\Big)_{\varrho}^{-1} \Big) \cdot \boldsymbol{S}_{\varrho}^{S_\mathrm{n}} \\
\boldsymbol{L}_{\varrho}^{S_\mathrm{n}} &= \frac{\partial \underline{y}^{S_\mathrm{n}}}{\partial \underline{\dot{\varrho}}^{S}} - \Big(\frac{\partial \underline{y}^{S_\mathrm{n}}}{\partial \underline{\ddot{\varphi}}^{S}} \cdot \Big(\boldsymbol{M}^{S_\mathrm{n}}\Big)_{\varphi}^{-1} + \frac{\partial \underline{y}^{S_\mathrm{n}}}{\partial \underline{\ddot{\varrho}}^{S}} \cdot \Big(\boldsymbol{M}^{S_\mathrm{n}}\Big)_{\varrho}^{-1} \Big) \cdot \boldsymbol{D}_{\varrho}^{S_\mathrm{n}}
\end{aligned} \tag{A.271}$$

For the feedthrough matrix $\boldsymbol{K}^{S_\mathrm{n}}$ holds:

$$\boldsymbol{K}^{S_\mathrm{n}} = \frac{\partial \underline{y}^{S_\mathrm{n}}}{\partial \underline{v}^{S_\mathrm{n}}} - \Big(\frac{\partial \underline{y}^{S_\mathrm{n}}}{\partial \underline{\ddot{\varphi}}^{S}} \cdot \Big(\boldsymbol{M}^{S_\mathrm{n}}\Big)_{\varphi}^{-1} + \frac{\partial \underline{y}^{S_\mathrm{n}}}{\partial \underline{\ddot{\varrho}}^{S}} \cdot \Big(\boldsymbol{M}^{S_\mathrm{n}}\Big)_{\varrho}^{-1} \Big) \cdot \boldsymbol{G}^{S_\mathrm{n}} \tag{A.272}$$

The partial derivatives to the dof vectors are cleaned up before use in the determination of the output and feedthrough matrices: columns that pertain to non-dof directions as concerns S_n are removed.

The partial derivative of the composed output vector $\underline{y}^{S_\mathrm{n}}$ to the composed input vector is obtained by (i) stacking the partial derivatives of the output subvectors to an input subvector, and (ii) doing this for all input subvectors and putting next to each other the obtained 'stacks'. The generic expression for the overall partial derivative matrix is (see e.g. also Eq. A.88):

$$\frac{\partial \underline{y}^{S_\mathrm{n}}}{\partial \underline{v}^{S_\mathrm{n}}} = \mathrm{J}_{(\underline{q}_\mathrm{v})}\Big(\mathrm{S}_{(\underline{z}_\mathrm{y})}\Big(\frac{\partial \underline{z}_\mathrm{y}}{\partial \underline{q}_\mathrm{v}}\Big)\Big) \quad \text{with} \quad \left\{ \begin{array}{l} \underline{q}_\mathrm{v} = {}^{\mathrm{FT}}\underline{f}^{S_{\mathrm{PP}(4)}}, {}^{\mathrm{FT}}\underline{t}^{S_{\mathrm{PP}(4)}}, \underline{\omega}^{S^{\oplus}_{\mathrm{FF}(2)}}, \underline{\alpha}^{S_{\mathrm{FF}(2)}}, \\ \qquad \underline{v}^{S^{\oplus}_{\mathrm{FF}(2)}}, \underline{a}^{S_{\mathrm{FF}(2)}}, \underline{u}_{\mathrm{ori}}^{S_{\mathrm{FF}(2)}}, \underline{g}_{\mathrm{ori}}^{S_{\mathrm{FF}(2)}}, \underline{\xi}^{S_{\mathrm{FF}(2)}}, \underline{x}^{S_{\mathrm{FF}(2)}}, t_{\mathrm{yw}} \\ \underline{z}_\mathrm{y} = t_{\mathrm{yw}}, \varphi_{\mathrm{yw}}, \underline{\omega}^{S^{\oplus}_{\mathrm{FF}(3)}}, \underline{\alpha}^{S_{\mathrm{FF}(3)}}, \underline{v}^{S^{\oplus}_{\mathrm{FF}(3)}}, \underline{a}^{S^{\oplus}_{\mathrm{FF}(3)}}, \underline{u}_{\mathrm{ori}}^{S_{\mathrm{FF}(3)}}, \\ \qquad \underline{g}_{\mathrm{ori}}^{S_{\mathrm{FF}(3)}}, \underline{\xi}^{S_{\mathrm{FF}(3)}}, \underline{x}^{S_{\mathrm{FF}(3)}}, {}^{\mathrm{FT}}\underline{f}^{S_{\mathrm{PP}(3)}}, {}^{\mathrm{FT}}\underline{t}^{S_{\mathrm{PP}(3)}}, \varphi_{\mathrm{yw}} \end{array} \right. \tag{A.273}$$

(v) Yawing torque control system equations and 1st order state space model
For the implemented yawing torque control system see paragraph (iii) in section 3.8.2.

The multiplication and summation of 'transfer function formulations' in Eq. 3.91 result into one transfer function via basic MATLAB functions SERIES and PARALLEL(). Afterwards this transfer function is transformed into state space format with M-function TF2SS():

$$\begin{aligned}
\underline{\dot{x}}^{S_{\mathrm{n_c}}} &= \boldsymbol{A}^{S_{\mathrm{n_c}}} \cdot \underline{x}^{S_{\mathrm{n_c}}} + \boldsymbol{B}^{S_{\mathrm{n_c}}} \cdot \underline{v}^{S_{\mathrm{n_c}}} \quad \text{with input vector} \quad \underline{v}^{S_{\mathrm{n_c}}} = [\ \varphi_{\mathrm{yw}}\ ]^{\mathrm{T}} \\
\underline{y}^{S_{\mathrm{n_c}}} &= \boldsymbol{C}^{S_{\mathrm{n_c}}} \cdot \underline{x}^{S_{\mathrm{n_c}}} + \boldsymbol{K}^{S_{\mathrm{n_c}}} \cdot \underline{v}^{S_{\mathrm{n_c}}} \quad \text{with output vector} \quad \underline{y}^{S_{\mathrm{n_c}}} = [\ t_{\mathrm{yw}}\ ]
\end{aligned} \tag{A.274}$$

The connection of the models for the yawing torque controller $S_{\mathrm{n_c}}$ and the nacelle S_n is similar to that for pitch controller and blade flange in paragraph (ix) in section A.2.3.

A.5.3 Equations of motions for the tower S_t

The tower S_t has been implemented as a multi-element subcomponent, set up by support structure elements $\{S_k | k = 2 \ldots M-1\}$. Each element allows up to six degrees of freedom of which usually five directions are active: the co-axial linear deformation is neglected.

The sensitivities of the (zero-mean) impulse vectors for the tower elements as formulated in section B.1.2, paragraph on *Tower* S_t, apply and do not need further discussion. The linearised expressions for the (zero-mean) hydrodynamic loads on the underwater elements

are listed in section B.9.1, Eq. 3.101 and 3.102, and in section **??**, Eq. B.260 up to B.263. For the gravitation loads see B.10.2, Eq. B.286 up to B.288.

The responsive loading on the tower elements is dealt with in paragraph (i). The required input variables are subject of paragraph (ii). Then, the second order state equation for the tower is formulated in paragraph (iii), followed by the required output equation in paragraph (iv).

The subcomponent model for the tower S_{t} is obtained by a call to TBUS2SUBEOM() in function TBUSUPSTREOM(). The model for S_{t} exists as structure variable sysS2sub. The fields in sysS2sub are 2D matrices A, B, C, K, the parameterisation of the first order state space representation, and cell arrays with lists of input, output and state variable names. Point of departure for the gearbox house model creation by function TBUS2SUBEOM() is the availability for the one-element subcomponent S_{t} of ((f.)c.s: (final) coordinate system):

- sensitivities of angular and linear impulse vectors (along f.c.s. of S_k in actual position: $\vec{e}^{\,S_k}$);
- means sensitivities of gravitation loads (along $\vec{e}^{\,S_k}$);
- sensitivities of hydrodynamic loads (along $\vec{e}^{\,S_k}$);
- means of feedthrough forces and torques from nacelle (along $\vec{e}^{\,S_{M-1}}$);
- sensitivities of displacement vectors relative to the (fixed) tower base (along tower base c.s. $\vec{e}^{\,B}$);
- sensitivities of kinematic vectors in tower top (= exit point of S_{t}; along $\vec{e}^{\,S_{M-1}}$);
- sensitivities of wind speed and gravitation by orientation change in tower tp along $\vec{e}^{\,S_{M-1}}$);
- transformation matrices and their sensitivities to rotational dofs;
- stiffness and damper values in the connection points between the elements;
- bottom-up ranking of rotation and translation axes in the connection points;

The mentioned sensitivities belong to the 'motion and load formulations' and map all motion and load variations to exogeneous input variables of to input variables from the foundation or to dofs in the tower. These are obtained via calls in TBUSUPSTREOM() to functions TBUSUPSTRCONS(), TBUSUPSTRKIN(), and TBUSUPSTRIMP(). Functionality TBUS2SUBEOM() ((f.)c.s: (final) coordinate system):

- definition of input name lists; each list contains the names of the input subvectors from a specific source (G, S3sub, S1sub);
- definition of output name lists; each list contains the names of the output subvectors to a specific destination (G, S3sub, S1sub);
- lumping together the hydrodynamic and gravitation loads to equivalent force and torque load formulations in the entry points of each tower element S_k; also includes feedthrough loading from nacelle for S_{M-1} (call TBUSSUBFTEX(); coordinates along actual f.c.s.of S_k);
- transform the feedthrough loading from outward elements within the subcomponent ($S_{k+1} \ldots S_{M-1}$) on the *exit* point of element S_k to equivalent force and torque load formulations in the *entry* point of S_k (call TBUSYSFTFT(); coordinates along actual f.c.s. of S_k; define 'equal to zero' for S_{m-1}; see also Eq. A.289);

- definition of the sensitivities of the responsive (visco/elastic) loads in the entry points of S_k to the dofs (call TBUQRESPNOCP());
- derive the mass, spring and damper matrix for the equations of motion for the tower S_{t} ($\boldsymbol{M}, \boldsymbol{S}, \boldsymbol{D}$; call TBUSYSMDSMX());
- derive load formulations for feedthrough torques and forces on the foundation (call TBUSYSFTPP; along actual f.c.s. of S_2);
- derive the input matrix for the mass/spring/damper formulation of S_{t} as well as the output matrices on the dofs and their time derivatives and the feedthrough matrix ($\boldsymbol{G}, \boldsymbol{H}, \boldsymbol{L}, \boldsymbol{K}$; call TBUSYSGHLKMX());
- transform the mass/spring/damper model formulation $\{\boldsymbol{M}, \boldsymbol{S}, \boldsymbol{D}, \boldsymbol{G}, \boldsymbol{H}, \boldsymbol{L}, \boldsymbol{K}\}$ to the first order state space formulation $\{\boldsymbol{A}, \boldsymbol{B}, \boldsymbol{C}, \boldsymbol{K}\}$ (call TBUSYSMDS2FSR()).

(i) Responsive loads

Under the assumption of six degrees of freedom in the entry point of the tower elements S_k ($k = 2 \ldots M-1$), the responsive force and torque loads are visco/elastic in three directions each. The defined bottom-up ranking of the deformation directions is distorsion, sideward bending and fore-aft bending (see section 3.8.1). So the involved rotation axes are in the z-, x- and y-direction for the 1st, 2nd and 3rd intermediate coordinate system, with corresponding translation axes in z-, y- and x-direction. The rotation axes approximate the elastic neutral axes on the tower elements very well. For the responsive load coordinate vectors then holds:

$$
\begin{aligned}
{}^{\mathrm{RS}}\underline{f}^{S_k} &= \begin{bmatrix} {}^{\mathrm{RS}}f_1^{S_k} \\ {}^{\mathrm{RS}}f_2^{S_k} \\ {}^{\mathrm{RS}}f_3^{S_k} \end{bmatrix} \quad \triangleq \quad \begin{bmatrix} {}^{\mathrm{RS}}f_{\mathrm{x}}^{S_k^3} \\ {}^{\mathrm{RS}}f_{\mathrm{y}}^{S_k^2} \\ {}^{\mathrm{RS}}f_{\mathrm{z}}^{S_k^1} \end{bmatrix} \quad = \quad {}^{\mathrm{RS}}\bar{\underline{f}}^{S_k} + \frac{\partial^{\mathrm{RS}}\underline{f}^{S_k}}{\partial \underline{\rho}^{S}} \cdot \delta\underline{\rho}^{S} + \frac{\partial^{\mathrm{RS}}\underline{f}^{S_k}}{\partial \underline{\dot{\rho}}^{S}} \cdot \underline{\dot{\rho}}^{S} \\
{}^{\mathrm{RS}}\underline{t}^{S_k} &= \begin{bmatrix} {}^{\mathrm{RS}}t_1^{S_k} \\ {}^{\mathrm{RS}}t_2^{S_k} \\ {}^{\mathrm{RS}}t_3^{S_k} \end{bmatrix} \quad \triangleq \quad \begin{bmatrix} {}^{\mathrm{RS}}t_{\mathrm{x}}^{S_k^2} \\ {}^{\mathrm{RS}}t_{\mathrm{y}}^{S_k^3} \\ {}^{\mathrm{RS}}t_{\mathrm{z}}^{S_k^1} \end{bmatrix} \quad = \quad {}^{\mathrm{RS}}\bar{\underline{t}}^{S_k} + \frac{\partial^{\mathrm{RS}}\underline{t}^{S_k}}{\partial \underline{\phi}^{S}} \cdot \delta\underline{\phi}^{S} + \frac{\partial^{\mathrm{RS}}\underline{t}^{S_k}}{\partial \underline{\dot{\varphi}}^{S}} \cdot \underline{\dot{\varphi}}^{S}
\end{aligned}
\tag{A.275}
$$

For the mean responsive loads holds:

$$
\begin{aligned}
{}^{\mathrm{RS}}\bar{\underline{f}}^{S_k} &= \left[-s_{\mathrm{f_x}\rho_{\mathrm{x}}}^{S_k} \cdot \bar{\rho}_3^{S_k} \quad - s_{\mathrm{f_y}\rho_{\mathrm{y}}}^{S_k} \cdot \bar{\rho}_2^{S_k} \quad - s_{\mathrm{f_z}\rho_{\mathrm{z}}}^{S_k} \cdot \bar{\rho}_1^{S_k} \right]^{\mathrm{T}} \\
{}^{\mathrm{RS}}\bar{\underline{t}}^{S_k} &= \left[-s_{\mathrm{t_x}\phi_{\mathrm{x}}}^{S_k} \cdot \bar{\phi}_2^{S_k} \quad - s_{\mathrm{t_y}\phi_{\mathrm{y}}}^{S_k} \cdot \bar{\phi}_3^{S_k} \quad - s_{\mathrm{t_z}\phi_{\mathrm{z}}}^{S_k} \cdot \bar{\phi}_1^{S_k} \right]^{\mathrm{T}}
\end{aligned}
\tag{A.276}
$$

For the sensitivities to the dof position variations hold:

$$
\frac{\partial^{\mathrm{RS}}\underline{f}^{S_k}}{\partial \underline{\rho}^{X}} = \begin{pmatrix} -s_{\mathrm{f_x}\rho_{\mathrm{x}}}^{S_k} \cdot [\ 0_{(1)} \ldots 0_{((k-1)*3)} \quad 0 \quad 1 \quad 0 \quad 0_{((k*3)+1)} \ldots 0_{(M*3)}\ ] \\ -s_{\mathrm{f_y}\rho_{\mathrm{y}}}^{S_k} \cdot [\ 0_{(1)} \ldots 0_{((k-1)*3)} \quad 0 \quad 0 \quad 1 \quad 0_{((k*3)+1)} \ldots 0_{(M*3)}\ ] \\ -s_{\mathrm{f_z}\rho_{\mathrm{z}}}^{S_k} \cdot [\ 0_{(1)} \ldots 0_{((k-1)*3)} \quad 1 \quad 0 \quad 0 \quad 0_{((k*3)+1)} \ldots 0_{(M*3)}\ ] \end{pmatrix}
$$

and

$$
\frac{\partial^{\mathrm{RS}}\underline{t}^{S_k}}{\partial \underline{\phi}^{X}} = \begin{pmatrix} -s_{\mathrm{t_x}\phi_{\mathrm{x}}}^{S_k} \cdot [\ 0_{(1)} \ldots 0_{((k-1)*3)} \quad 0 \quad 0 \quad 1 \quad 0_{((k*3)+1)} \ldots 0_{(M*3)}\ ] \\ -s_{\mathrm{t_y}\phi_{\mathrm{y}}}^{S_k} \cdot [\ 0_{(1)} \ldots 0_{((k-1)*3)} \quad 0 \quad 1 \quad 0 \quad 0_{((k*3)+1)} \ldots 0_{(M*3)}\ ] \\ -s_{\mathrm{t_z}\phi_{\mathrm{z}}}^{S_k} \cdot [\ 0_{(1)} \ldots 0_{((k-1)*3)} \quad 1 \quad 0 \quad 0 \quad 0_{((k*3)+1)} \ldots 0_{(M*3)}\ ] \end{pmatrix}
\tag{A.277}
$$

The sensitivities to the dof speeds are obtained from the ones above by just replacing $s_{(.)}^{S_k}$ by $d_{(.)}^{S_k}$.

If less than six degrees of freedom apply in an entry point then some viso/elastic load expressions are not valid (infinite stiffness and damper values would apply). However, this is of no importance because these expressions are skipped when the equations of motions are being derived.

(ii) Input variables

The input vector for S_t has the following composition:

$$\underline{v}^{S_\mathrm{t}} = \begin{bmatrix} \underline{v}^{S_\mathrm{n}G} \\ \underline{v}^{S_\mathrm{n}S_\mathrm{t}} \\ \underline{v}^{S_\mathrm{n}S_\mathrm{f}} \end{bmatrix}$$

with

$$\underline{v}^{S_\mathrm{t}G} = \begin{bmatrix} \underline{w}^{S}_{\mathrm{horz}} \\ \underline{\dot{w}}^{S}_{\mathrm{horz}} \end{bmatrix} \;;\; \underline{v}^{S_\mathrm{t}S_\mathrm{n}} = \begin{bmatrix} {}^{\mathrm{FT}}\underline{f}^{S_{\mathrm{PP}(3)}} \\ {}^{\mathrm{FT}}\underline{t}^{S_{\mathrm{PP}(3)}} \end{bmatrix} \;;\; \underline{v}^{S_\mathrm{t}S_\mathrm{f}} = \begin{bmatrix} \underline{\omega}^{S_{\mathrm{FF}(1)}} \\ \underline{\alpha}^{S_{\mathrm{FF}(1)}} \\ \underline{v}^{S^{\oplus}_{\mathrm{FF}(1)}} \\ \underline{a}^{S^{\oplus}_{\mathrm{FF}(1)}} \\ \underline{u}^{S_{\mathrm{FF}(1)}}_{\mathrm{ori}} \\ \underline{g}^{S_{\mathrm{FF}(1)}}_{\mathrm{ori}} \\ \underline{\xi}^{S_{\mathrm{FF}(1)}} \\ \underline{x}^{S^{\oplus}_{\mathrm{FF}(1)}} \\ {}^{\mathrm{h}}\underline{q}^{S_{\mathrm{FF}(1)}} \end{bmatrix} \tag{A.278}$$

(iii) Equations of motion and 2$^{\mathrm{nd}}$ order vector state equation

The implementation of the 2^{nd} order state vector equation for the tower S_t is based on the overall encapsulating dof vectors for the support structure. That is to say, the mass, spring and damper matrix arise from partial derivatives of impulse and load vectors to the dof vectors $\underline{\varphi}^S$ and $\underline{\varrho}^S$. Point of departure is the full-size vector state equation ($6M \times 6M$-matrices):

$$\left[\boldsymbol{M}_{\varphi}^{S_\mathrm{t}} \mid \boldsymbol{M}_{\varrho}^{S_\mathrm{t}}\right] \cdot \begin{bmatrix} \ddot{\underline{\varphi}}^S \\ \ddot{\underline{\varrho}}^S \end{bmatrix} + \left[\boldsymbol{D}_{\varphi}^{S_\mathrm{t}} \mid \boldsymbol{D}_{\varrho}^{S_\mathrm{t}}\right] \cdot \begin{bmatrix} \dot{\underline{\varphi}}^S \\ \dot{\underline{\varrho}}^S \end{bmatrix} + \left[\boldsymbol{S}_{\varphi}^{S_\mathrm{t}} \mid \boldsymbol{S}_{\varrho}^{S_\mathrm{t}}\right] \cdot \begin{bmatrix} \underline{\varphi}^S \\ \underline{\varrho}^S \end{bmatrix} = \left[\boldsymbol{G}^{S_\mathrm{t}G} \mid \boldsymbol{G}^{S_\mathrm{t}S_\mathrm{n}} \mid \boldsymbol{G}^{S_\mathrm{t}S_\mathrm{f}}\right] \cdot \begin{bmatrix} \underline{v}^{S_\mathrm{t}G} \\ \underline{v}^{S_\mathrm{t}S_\mathrm{n}} \\ \underline{v}^{S_\mathrm{t}S_\mathrm{f}} \end{bmatrix} \tag{A.279}$$

The support structure elements $\{S_k | k = 2 \ldots M-1\}$ set up the multi-element subcomponent S_t. The required matrices are derived by considering the vector impulse equations for elements $\{S_k\}$ in their sets of three coordinate systems. The bottum-up ranked rotation axes for S_t are the z-, y- and x-axis; the z-axis is co-axial for the tower. Thus we start with the x- and y-coordinate of the angular and linear impulse in the $3\mathrm{rd}$ intermediate coordinate system (i.c.s.). Afterwards, the respective y-coordinate and x-coordinate are considered in the $2\mathrm{nd}$ i.c.s. Finally, both z-coordinates are dealt with in the $1\mathrm{st}$ i.c.s.

The pairs of rows $\{\underline{\boldsymbol{m}}^{S_k}_{h\varphi_w}, \underline{\boldsymbol{m}}^{S_k}_{p\varphi_w} | w = 3, 2, 1\}$, with ranking numbers $6(k-1)+2(w-1)+1$ and $6(k-1)+2(w-1)+2$ in the mass matrix partition $\boldsymbol{M}_{\varphi}^{S_\mathrm{t}}$, are now determined as follows (the partial derivatives in the right hand side only apply if they are defined for the 'independent variable'; in this case $\ddot{\underline{\varphi}}^S$):

- for $w = 3$:

$$\begin{aligned}
\underline{\boldsymbol{m}}_{h\varphi_3}^{S_k} &= -[\,1\,0\,0\,]\cdot\frac{\partial^{\mathrm{RS}}\underline{t}^{S_k^{\ominus}}}{\partial\underline{\ddot{\varphi}}^{S}} + [\,1\,0\,0\,]\cdot\Big(\frac{\partial^{S_k^{\ominus}}\underline{\dot{h}}^{S_k}}{\partial\underline{\ddot{\varphi}}^{S}} - \frac{\partial^{\mathrm{FT}}\underline{t}^{S_k^{\ominus}}}{\partial\underline{\ddot{\varphi}}^{S}} - \frac{\partial^{\mathrm{EX}}\underline{t}^{S_k^{\ominus}}}{\partial\underline{\ddot{\varphi}}^{S}}\Big)\\
\underline{\boldsymbol{m}}_{p\varphi_3}^{S_k} &= -[\,0\,1\,0\,]\cdot\frac{\partial^{\mathrm{RS}}\underline{f}^{S_k^{\ominus}}}{\partial\underline{\ddot{\varphi}}^{S}} + [\,0\,1\,0\,]\cdot\Big(\frac{\partial\underline{\dot{p}}^{S_k}}{\partial\underline{\ddot{\varphi}}^{S}} - \frac{\partial^{\mathrm{FT}}\underline{f}^{S_k^{\ominus}}}{\partial\underline{\ddot{\varphi}}^{S}} - \frac{\partial^{\mathrm{EX}}\underline{f}^{S_k^{\ominus}}}{\partial\underline{\ddot{\varphi}}^{S}}\Big)
\end{aligned} \tag{A.280}$$

- for $w = 2$:

$$\begin{aligned}
\underline{\boldsymbol{m}}_{h\varphi_2}^{S_k} &= -[\,0\,1\,0\,]\cdot\frac{\partial^{\mathrm{RS}}\underline{t}^{S_k^{\ominus}}}{\partial\underline{\ddot{\varphi}}^{S}} + {}^{S_k^2}\bar{\Phi}^{S_k}_{(2,:)}\cdot\Big(\frac{\partial^{S_k^{\ominus}}\underline{\dot{h}}^{S_k}}{\partial\underline{\ddot{\varphi}}^{S}} - \frac{\partial^{\mathrm{FT}}\underline{t}^{S_k^{\ominus}}}{\partial\underline{\ddot{\varphi}}^{S}} - \frac{\partial^{\mathrm{EX}}\underline{t}^{S_k^{\ominus}}}{\partial\underline{\ddot{\varphi}}^{S}}\Big)\\
\underline{\boldsymbol{m}}_{p\varphi_2}^{S_k} &= -[\,1\,0\,0\,]\cdot\frac{\partial^{\mathrm{RS}}\underline{f}^{S_k^{\ominus}}}{\partial\underline{\ddot{\varphi}}^{S}} + {}^{S_k^2}\bar{\Phi}^{S_k}_{(1,:)}\cdot\Big(\frac{\partial\underline{\dot{p}}^{S_k}}{\partial\underline{\ddot{\varphi}}^{S}} - \frac{\partial^{\mathrm{FT}}\underline{f}^{S_k^{\ominus}}}{\partial\underline{\ddot{\varphi}}^{S}} - \frac{\partial^{\mathrm{EX}}\underline{f}^{S_k^{\ominus}}}{\partial\underline{\ddot{\varphi}}^{S}}\Big)
\end{aligned} \tag{A.281}$$

- for $w = 1$:

$$\begin{aligned}
\underline{\boldsymbol{m}}_{h\varphi_1}^{S_k} &= -[\,0\,0\,1\,]\cdot\frac{\partial^{\mathrm{RS}}\underline{t}^{S_k^{\ominus}}}{\partial\underline{\ddot{\varphi}}^{S}} + {}^{S_k^1}\bar{\Phi}^{S_k}_{(3,:)}\cdot\Big(\frac{\partial^{S_k^{\ominus}}\underline{\dot{h}}^{S_k}}{\partial\underline{\ddot{\varphi}}^{S}} - \frac{\partial^{\mathrm{FT}}\underline{t}^{S_k^{\ominus}}}{\partial\underline{\ddot{\varphi}}^{S}} - \frac{\partial^{\mathrm{EX}}\underline{t}^{S_k^{\ominus}}}{\partial\underline{\ddot{\varphi}}^{S}}\Big)\\
\underline{\boldsymbol{m}}_{p\varphi_1}^{S_k} &= -[\,0\,0\,1\,]\cdot\frac{\partial^{\mathrm{RS}}\underline{f}^{S_k^{\ominus}}}{\partial\underline{\ddot{\varphi}}^{S}} + {}^{S_k^1}\bar{\Phi}^{S_k}_{(3,:)}\cdot\Big(\frac{\partial\underline{\dot{p}}^{S_k}}{\partial\underline{\ddot{\varphi}}^{S}} - \frac{\partial^{\mathrm{FT}}\underline{f}^{S_k^{\ominus}}}{\partial\underline{\ddot{\varphi}}^{S}} - \frac{\partial^{\mathrm{EX}}\underline{f}^{S_k^{\ominus}}}{\partial\underline{\ddot{\varphi}}^{S}}\Big)
\end{aligned} \tag{A.282}$$

The corresponding rows in the mass matrix partition $\boldsymbol{M}_{\varrho}^{S_{\mathrm{t}}}$ are obtained by taking the sensitivities to $\underline{\ddot{\varrho}}^{S}$ instead of $\underline{\ddot{\varphi}}^{S}$. For the rows in both damping matrix partitions $\boldsymbol{D}_{\varphi}^{S_{\mathrm{t}}}$ and $\boldsymbol{D}_{\varrho}^{S_{\mathrm{t}}}$ and in the stiffness matrix partition $\boldsymbol{S}_{\varrho}^{S_{\mathrm{t}}}$, take the sensitivities to $\underline{\dot{\varphi}}^{S}$ and $\underline{\dot{\varrho}}^{S}$ and $\underline{\varrho}^{S}$. For the remaining stiffness matrix partition $\boldsymbol{S}_{\varphi}^{S_{\mathrm{t}}}$ the same scheme applies for $w = 3$ but differs for $w = 2$ and $w = 1$:

- for $w = 2$:

$$\begin{aligned}
\underline{\boldsymbol{s}}_{h\varphi_2}^{S_k} &= -[\,0\,1\,0\,]\cdot\frac{\partial^{\mathrm{RS}}\underline{t}^{S_k^{\ominus}}}{\partial\underline{\phi}^{S}} + {}^{S_k^2}\bar{\Phi}^{S_k}_{(2,:)}\cdot\Big(\frac{\partial^{S_k^{\ominus}}\underline{\dot{h}}^{S_k}}{\partial\underline{\phi}^{S}} - \frac{\partial^{\mathrm{FT}}\underline{t}^{S_k^{\ominus}}}{\partial\underline{\phi}^{S}} - \frac{\partial^{\mathrm{EX}}\underline{t}^{S_k^{\ominus}}}{\partial\underline{\phi}^{S}}\Big) +\\
&\quad [\,\mathrm{O}_{(1\ldots k-1)}\;\; \mathrm{J}^{3}_{v=1}\Big(\frac{\partial^{S_k^2}\Phi^{S_k}_{(2,:)}}{\partial\phi_v^{S_k}}\cdot\Big({}^{S_k^{\ominus}}\underline{\dot{h}}^{S_k} - {}^{\mathrm{FT}}\underline{\bar{t}}^{S_k^{\ominus}} - {}^{\mathrm{EX}}\underline{\bar{t}}^{S_k^{\ominus}}\Big)\Big)\;\; \mathrm{O}_{(k+1\ldots M)}\,]\\
\underline{\boldsymbol{s}}_{p\varphi_2}^{S_k} &= -[\,1\,0\,0\,]\cdot\frac{\partial^{\mathrm{RS}}\underline{f}^{S_k^{\ominus}}}{\partial\underline{\phi}^{S}} + {}^{S_k^2}\bar{\Phi}^{S_k}_{(1,:)}\cdot\Big(\frac{\partial\underline{\dot{p}}^{S_k}}{\partial\underline{\phi}^{S}} - \frac{\partial^{\mathrm{FT}}\underline{f}^{S_k^{\ominus}}}{\partial\underline{\phi}^{S}} - \frac{\partial^{\mathrm{EX}}\underline{f}^{S_k^{\ominus}}}{\partial\underline{\phi}^{S}}\Big) +\\
&\quad [\,\mathrm{O}_{(1\ldots k-1)}\;\; \mathrm{J}^{3}_{v=1}\Big(\frac{\partial^{S_k^2}\Phi^{S_k}_{(1,:)}}{\partial\phi_v^{S_k}}\cdot\Big({}^{S_k^{\ominus}}\underline{\dot{p}}^{S_k} - {}^{\mathrm{FT}}\underline{\bar{f}}^{S_k^{\ominus}} - {}^{\mathrm{EX}}\underline{\bar{f}}^{S_k^{\ominus}}\Big)\Big)\;\; \mathrm{O}_{(k+1\ldots M)}\,]
\end{aligned} \tag{A.283}$$

- for $w = 1$:

$$\begin{aligned}
\underline{\boldsymbol{s}}_{h\varphi_1}^{S_k} &= -[\,0\,0\,1\,]\cdot\frac{\partial^{\mathrm{RS}}\underline{t}^{S_k^{\ominus}}}{\partial\underline{\phi}^{S}} + {}^{S_k^1}\bar{\Phi}^{S_k}_{(3,:)}\cdot\Big(\frac{\partial^{S_k^{\ominus}}\underline{\dot{h}}^{S_k}}{\partial\underline{\phi}^{S}} - \frac{\partial^{\mathrm{FT}}\underline{t}^{S_k^{\ominus}}}{\partial\underline{\phi}^{S}} - \frac{\partial^{\mathrm{EX}}\underline{t}^{S_k^{\ominus}}}{\partial\underline{\phi}^{S}}\Big) +\\
&\quad [\,\mathrm{O}_{(1\ldots k-1)}\;\; \mathrm{J}^{3}_{v=1}\Big(\frac{\partial^{S_k^1}\Phi^{S_k}_{(3,:)}}{\partial\phi_v^{S_k}}\cdot\Big({}^{S_k^{\ominus}}\underline{\dot{h}}^{S_k} - {}^{\mathrm{FT}}\underline{\bar{t}}^{S_k^{\ominus}} - {}^{\mathrm{EX}}\underline{\bar{t}}^{S_k^{\ominus}}\Big)\Big)\;\; \mathrm{O}_{(k+1\ldots M)}\,]\\
\underline{\boldsymbol{s}}_{p\varphi_1}^{S_k} &= -[\,0\,0\,1\,]\cdot\frac{\partial^{\mathrm{RS}}\underline{f}^{S_k^{\ominus}}}{\partial\underline{\phi}^{S}} + {}^{S_k^1}\bar{\Phi}^{S_k}_{(3,:)}\cdot\Big(\frac{\partial\underline{\dot{p}}^{S_k}}{\partial\underline{\phi}^{S}} - \frac{\partial^{\mathrm{FT}}\underline{f}^{S_k^{\ominus}}}{\partial\underline{\phi}^{S}} - \frac{\partial^{\mathrm{EX}}\underline{f}^{S_k^{\ominus}}}{\partial\underline{\phi}^{S}}\Big) +\\
&\quad [\,\mathrm{O}_{(1\ldots k-1)}\;\; \mathrm{J}^{3}_{v=1}\Big(\frac{\partial^{S_k^1}\Phi^{S_k}_{(3,:)}}{\partial\phi_v^{S_k}}\cdot\Big({}^{S_k^{\ominus}}\underline{\dot{p}}^{S_k} - {}^{\mathrm{FT}}\underline{\bar{f}}^{S_k^{\ominus}} - {}^{\mathrm{EX}}\underline{\bar{f}}^{S_k^{\ominus}}\Big)\Big)\;\; \mathrm{O}_{(k+1\ldots M)}\,]
\end{aligned} \tag{A.284}$$

The pairs of rows $\{\underline{\boldsymbol{g}}_{h_w}^{S_k S_\mathrm{f}}, \underline{\boldsymbol{g}}_{p_w}^{S_k S_\mathrm{f}} | w = 3, 2, 1\}$, with ranking numbers $6(k-1)+2(w-1)+1$ and $6(k-1)+2(w-1)+2$ in the input matrix partition $\boldsymbol{G}^{S_\mathrm{t} S_\mathrm{f}}$, are determined as follows (the partial derivatives in the right hand side only apply if they are defined for the 'independent variable'; in this case $\underline{z}$):

- for $w = 3$:

$$\begin{aligned}
\underline{\boldsymbol{g}}_{h_3}^{S_k S_\mathrm{f}} &= \mathrm{J}_{(\underline{z})}\Big([\,1\,0\,0\,] \cdot \frac{\partial^{\mathrm{RS}} \underline{t}^{S_k^\ominus}}{\partial \underline{z}} + [\,1\,0\,0\,] \cdot (-\frac{\partial^{S_k^\ominus} \underline{\dot{h}}^{S_k}}{\partial \underline{z}} + \frac{\partial^{\mathrm{FT}} \underline{t}^{S_k^\ominus}}{\partial \underline{z}} + \frac{\partial^{\mathrm{EX}} \underline{t}^{S_k^\ominus}}{\partial \underline{z}}) \Big) \\
\underline{\boldsymbol{g}}_{p_3}^{S_k S_\mathrm{f}} &= \mathrm{J}_{(\underline{z})}\Big([\,0\,1\,0\,] \cdot \frac{\partial^{\mathrm{RS}} \underline{f}^{S_k^\ominus}}{\partial \underline{z}} + [\,0\,1\,0\,] \cdot (-\frac{\partial \underline{\dot{p}}^{S_k}}{\partial \underline{z}} + \frac{\partial^{\mathrm{FT}} \underline{f}^{S_k^\ominus}}{\partial \underline{z}} + \frac{\partial^{\mathrm{EX}} \underline{f}^{S_k^\ominus}}{\partial \underline{z}}) \Big)
\end{aligned} \tag{A.285}$$

- for $w = 2$:

$$\begin{aligned}
\underline{\boldsymbol{g}}_{h_2}^{S_k S_\mathrm{f}} &= \mathrm{J}_{(\underline{z})}\Big([\,0\,1\,0\,] \cdot \frac{\partial^{\mathrm{RS}} \underline{t}^{S_k^\ominus}}{\partial \underline{z}} + {}^{S_k^2}\bar{\Phi}_{(2,:)}^{S_k} \cdot \big(-\frac{\partial^{S_k^\ominus} \underline{\dot{h}}^{S_k}}{\partial \underline{z}} + \frac{\partial^{\mathrm{FT}} \underline{t}^{S_k^\ominus}}{\partial \underline{z}} + \frac{\partial^{\mathrm{EX}} \underline{t}^{S_k^\ominus}}{\partial \underline{z}}) \Big) \\
\underline{\boldsymbol{g}}_{p_2}^{S_k S_\mathrm{f}} &= \mathrm{J}_{(\underline{z})}\Big([\,1\,0\,0\,] \cdot \frac{\partial^{\mathrm{RS}} \underline{f}^{S_k^\ominus}}{\partial \underline{z}} + {}^{S_k^2}\bar{\Phi}_{(1,:)}^{S_k} \cdot (-\frac{\partial \underline{\dot{p}}^{S_k}}{\partial \underline{z}} + \frac{\partial^{\mathrm{FT}} \underline{f}^{S_k^\ominus}}{\partial \underline{z}} + \frac{\partial^{\mathrm{EX}} \underline{f}^{S_k^\ominus}}{\partial \underline{z}}) \Big)
\end{aligned} \tag{A.286}$$

- for $w = 1$:

$$\begin{aligned}
\underline{\boldsymbol{g}}_{h_1}^{S_k S_\mathrm{f}} &= \mathrm{J}_{(\underline{z})}\Big([\,0\,0\,1\,] \cdot \frac{\partial^{\mathrm{RS}} \underline{t}^{S_k^\ominus}}{\partial \underline{z}} + {}^{S_k^1}\bar{\Phi}_{(3,:)}^{S_k} \cdot \big(-\frac{\partial^{S_k^\ominus} \underline{\dot{h}}^{S_k}}{\partial \underline{z}} + \frac{\partial^{\mathrm{FT}} \underline{t}^{S_k^\ominus}}{\partial \underline{z}} + \frac{\partial^{\mathrm{EX}} \underline{t}^{S_k^\ominus}}{\partial \underline{z}}) \Big) \\
\underline{\boldsymbol{g}}_{p_1}^{S_k} &= \mathrm{J}_{(\underline{z})}\Big([\,0\,0\,1\,] \cdot \frac{\partial^{\mathrm{RS}} \underline{f}^{S_k^\ominus}}{\partial \underline{z}} + {}^{S_k^1}\bar{\Phi}_{(3,:)}^{S_k} \cdot (-\frac{\partial \underline{\dot{p}}^{S_k}}{\partial \underline{z}} + \frac{\partial^{\mathrm{FT}} \underline{f}^{S_k^\ominus}}{\partial \underline{z}} + \frac{\partial^{\mathrm{EX}} \underline{f}^{S_k^\ominus}}{\partial \underline{z}}) \Big)
\end{aligned} \tag{A.287}$$

The notation $\mathrm{J}_{(\underline{z})}\big(.\big)$ means that the partial derivatives to the involved subvector variables are to be put next to each other. The involved subvectors $\underline{z}$ for the submatrices $\boldsymbol{G}^{S_\mathrm{t} G}$, $\boldsymbol{G}^{S_\mathrm{t} S_\mathrm{n}}$ and $\boldsymbol{G}^{S_\mathrm{t} S_\mathrm{f}}$ are listed in Eq. A.278 in the previous paragraph.

The external load coordinate vectors include hydrodynamic loading, gravitation loading and, for the tower top element, feedthrough loading from the nacelle (see also Eq. A.37):

$$\begin{aligned}
{}^{\mathrm{EX}}\underline{f}^{S_k^\ominus} &\triangleq {}^{\mathrm{h}}\underline{f}^{S_k^\mathrm{h}} + {}^{\mathrm{g}}\underline{f}^{S_k^*} + \delta_{k,M-1} \cdot {}^{\mathrm{FT}}\underline{f}^{S_{\mathrm{PP}(3)}} \\
{}^{\mathrm{EX}}\underline{t}^{S_k^\ominus} &\triangleq {}^{\mathrm{h}}\underline{t}^{S_k^\mathrm{h}} + {}^{S_k^\ominus}\underline{r}^{S_k^\mathrm{h}} \times {}^{\mathrm{h}}\underline{f}^{S_k^\mathrm{h}} + {}^{S_k^\ominus}\underline{r}^{S_k^*} \times {}^{\mathrm{g}}\underline{f}^{S_k^*} + \\
&\qquad \delta_{k,M-1} \cdot \big({}^{\mathrm{FT}}\underline{t}^{S_{\mathrm{PP}(3)}} + {}^{S_k^\ominus}\underline{r}^{S_k^*} \times {}^{\mathrm{FT}}\underline{f}^{S_{\mathrm{PP}(3)}} \big)
\end{aligned} \tag{A.288}$$

The expressions for the feedthrough load coordinate vectors are ($2 \leq k \leq M-1$):

$${}^{\mathrm{FT}}\underline{f}^{S_k^\ominus} = \begin{cases} \underline{0} & (k = M-1) \\ {}^{S_k}\Phi^{S_{k+1}} \cdot \big({}^{\mathrm{FT}}\underline{f}^{S_{k+1}^\ominus} - \underline{\dot{p}}^{S_{k+1}} + {}^{\mathrm{EX}}\underline{f}^{S_{k+1}^\ominus} \big) & (k < M-1) \end{cases}$$

$${}^{\mathrm{FT}}\underline{t}^{S_k^\ominus} = \begin{cases} \underline{0} & (k = M-1) \\ {}^{S_k^\ominus}\underline{r}^{S_k^\oplus} \times {}^{\mathrm{FT}}\underline{f}^{S_k^\ominus} + {}^{S_k}\Phi^{S_{k+1}} \cdot \big({}^{\mathrm{FT}}\underline{t}^{S_{k+1}^\ominus} - {}^{S_{k+1}^\ominus}\underline{\dot{h}}^{S_{k+1}} + {}^{\mathrm{EX}}\underline{t}^{S_{k+1}^\ominus} \big) & (k < M-1) \end{cases} \tag{A.289}$$

The expressions for the external load coordinate vectors comprise the envelope of dependencies:

$$\begin{aligned}
{}^{\mathrm{EX}}\underline{f}^{S_k^{\ominus}} &= {}^{\mathrm{EX}}\bar{\underline{f}}^{S_k^{\ominus}} + \frac{\partial^{\mathrm{EX}}\underline{f}^{S_k^{\ominus}}}{\partial \underline{w}^{S}_{\mathrm{horz}}} \cdot \underline{w}^{S}_{\mathrm{horz}} + \frac{\partial^{\mathrm{EX}}\underline{f}^{S_k^{\ominus}}}{\partial \underline{\dot{w}}^{S}_{\mathrm{horz}}} \cdot \underline{\dot{w}}^{S}_{\mathrm{horz}} + \sum_{(\underline{z})} \frac{\partial^{\mathrm{EX}}\underline{f}^{S_k^{\ominus}}}{\partial \underline{z}} \cdot \delta\underline{z} \\
{}^{\mathrm{EX}}\underline{t}^{S_k^{\ominus}} &= {}^{\mathrm{EX}}\bar{\underline{t}}^{S_k^{\ominus}} + \frac{\partial^{\mathrm{EX}}\underline{t}^{S_k^{\ominus}}}{\partial \underline{w}^{S}_{\mathrm{horz}}} \cdot \underline{w}^{S}_{\mathrm{horz}} + \frac{\partial^{\mathrm{EX}}\underline{t}^{S_k^{\ominus}}}{\partial \underline{\dot{w}}^{S}_{\mathrm{horz}}} \cdot \underline{\dot{w}}^{S}_{\mathrm{horz}} + \sum_{(\underline{z})} \frac{\partial^{\mathrm{EX}}\underline{t}^{S_k^{\ominus}}}{\partial \underline{z}} \cdot \delta\underline{z}
\end{aligned} \tag{A.290}$$

The reactive variation as represented by the summation over $\underline{z}$ involves

- [output from the nacelle S_{n}: ${}^{\mathrm{FT}}\underline{f}^{S_{\mathrm{PP}(3)}}$, ${}^{\mathrm{FT}}\underline{t}^{S_{\mathrm{PP}(3)}}$];
- output from the foundation S_{f}: ${}^{\mathrm{h}}\underline{q}_{\mathrm{f}}^{S_{\mathrm{FF}}}$, $\underline{v}^{S_{\mathrm{FF}}^{\oplus}}$, $\underline{\omega}^{S_{\mathrm{FF}}^{\oplus}}$, $\underline{v}^{S_{\mathrm{FF}}^{\oplus}}$, $\underline{a}^{S_{\mathrm{FF}}^{\oplus}}$, $\underline{g}_{\mathrm{ori}}^{S_{\mathrm{FF}(1)}}$
- degrees of freedom in S_{t}, encapsulated by: $\underline{\varphi}^{S}$, $\underline{\dot{\varphi}}^{S}$, $\underline{\dot{\varrho}}^{S}$, $\underline{\ddot{\varphi}}^{S}$, $\underline{\ddot{\varrho}}^{S}$

The expressions for the sensitivities of the external load vectors are (of course only if $\underline{q}$ applies in a right hand side partial derivative):

$$\begin{aligned}
\frac{\partial^{\mathrm{EX}}\underline{f}^{S_k^{\ominus}}}{\partial \underline{q}} &= \frac{\partial^{\mathrm{h}}\underline{f}^{S_k^{\mathrm{h}}}}{\partial \underline{q}} + \frac{\partial^{\mathrm{g}}\underline{f}^{S_k^{*}}}{\partial \underline{q}} \\
\frac{\partial^{\mathrm{EX}}\underline{t}^{S_k^{\ominus}}}{\partial \underline{q}} &= \frac{\partial^{\mathrm{h}}\underline{t}^{S_k^{\mathrm{h}}}}{\partial \underline{q}} + \mathrm{J}^3_{v=1}\big({}^{S_k^{\ominus}}\underline{r}^{S_k^{\mathrm{a}}} \times \underline{e}_v\big) \cdot \frac{\partial^{\mathrm{h}}\underline{f}^{S_k^{\mathrm{h}}}}{\partial \underline{q}} + \mathrm{J}^3_{v=1}\big({}^{S_k^{\ominus}}\underline{r}^{S_k^{*}} \times \underline{e}_v\big) \cdot \frac{\partial^{\mathrm{g}}\underline{f}^{S_k^{*}}}{\partial \underline{q}}
\end{aligned} \tag{A.291}$$

Further it holds:

$$\frac{\partial^{\mathrm{EX}}\underline{f}^{S_{M-1}^{\ominus}}}{\partial^{\mathrm{FT}}\underline{f}^{S_{\mathrm{PP}(3)}}} = \boldsymbol{I} \;\; ; \;\; \frac{\partial^{\mathrm{EX}}\underline{t}^{S_{M-1}^{\ominus}}}{\partial^{\mathrm{FT}}\underline{t}^{S_{\mathrm{PP}(3)}}} = \boldsymbol{I} \;\; ; \;\; \frac{\partial^{\mathrm{EX}}\underline{t}^{S_{M-1}^{\ominus}}}{\partial^{\mathrm{FT}}\underline{f}^{S_{\mathrm{PP}(3)}}} = \mathrm{J}^3_{v=1}\big({}^{S_{M-1}^{\ominus}}\underline{r}^{S_{M-1}^{\oplus}} \times \underline{e}_v\big) \tag{A.292}$$

The expressions for the feedthrough coordinate vectors comprises the envelope of dependencies for the external loads and the impulse vectors:

$$\begin{aligned}
{}^{\mathrm{FT}}\underline{f}^{S_k^{\ominus}} &= {}^{\mathrm{FT}}\bar{\underline{f}}^{S_k^{\ominus}} + \frac{\partial^{\mathrm{FT}}\underline{f}^{S_k^{\ominus}}}{\partial \underline{w}^{S}_{\mathrm{horz}}} \cdot \underline{w}^{S}_{\mathrm{horz}} + \frac{\partial^{\mathrm{FT}}\underline{f}^{S_k^{\ominus}}}{\partial \underline{\dot{w}}^{S}_{\mathrm{horz}}} \cdot \underline{\dot{w}}^{S}_{\mathrm{horz}} + \sum_{(\underline{z})} \frac{\partial^{\mathrm{FT}}\underline{f}^{S_k^{\ominus}}}{\partial \underline{z}} \cdot \delta\underline{z} \\
{}^{\mathrm{FT}}\underline{t}^{S_k^{\ominus}} &= {}^{\mathrm{FT}}\bar{\underline{t}}^{S_k^{\ominus}} + \frac{\partial^{\mathrm{FT}}\underline{t}^{S_k^{\ominus}}}{\partial \underline{w}^{S}_{\mathrm{horz}}} \cdot \underline{w}^{S}_{\mathrm{horz}} + \frac{\partial^{\mathrm{FT}}\underline{t}^{S_k^{\ominus}}}{\partial \underline{\dot{w}}^{S}_{\mathrm{horz}}} \cdot \underline{\dot{w}}^{S}_{\mathrm{horz}} + \sum_{(\underline{z})} \frac{\partial^{\mathrm{FT}}\underline{t}^{S_k^{\ominus}}}{\partial \underline{z}} \cdot \delta\underline{z}
\end{aligned} \tag{A.293}$$

The reactive variation as represented by the summation over $\underline{z}$ involves the ones for the external loads. For the sake of the pursued linearised expressions we define the average values of the feed-through loads in the *exit* of element S_k in the coordinate system of S_{k+1} ($k < M-1$):

$$\begin{aligned}
{}^{\mathrm{FT}}\bar{\underline{f}}^{S_k^{\oplus}/S_{k+1}} &= {}^{\mathrm{FT}}\bar{\underline{f}}^{S_{k+1}^{\ominus}} - \bar{\underline{p}}^{S_{k+1}} + {}^{\mathrm{EX}}\bar{\underline{f}}^{S_{k+1}^{\ominus}} \\
{}^{\mathrm{FT}}\bar{\underline{t}}^{S_k^{\oplus}/S_{k+1}} &= {}^{\mathrm{FT}}\bar{\underline{t}}^{S_{k+1}^{\ominus}} - {}^{S_{k+1}^{\ominus}}\dot{\bar{\underline{h}}}^{S_{k+1}} + {}^{\mathrm{EX}}\bar{\underline{t}}^{S_{k+1}^{\ominus}}
\end{aligned} \tag{A.294}$$

For the mean values of the feedthrough loads in the *entry* point of S_k holds:

$$\begin{aligned}
{}^{\mathrm{FT}}\bar{\underline{f}}^{S_k^{\ominus}} &= {}^{S_k}\bar{\Phi}^{S_{k+1}} \,.\, {}^{\mathrm{FT}}\bar{\underline{f}}^{S_k^{\oplus}/S_{k+1}} \\
{}^{\mathrm{FT}}\bar{\underline{t}}^{S_k^{\ominus}} &= {}^{S_k^{\ominus}}\underline{r}^{S_k^{\oplus}} \times {}^{\mathrm{FT}}\bar{\underline{f}}^{S_k^{\ominus}} + {}^{S_k}\bar{\Phi}^{S_{k+1}} \,.\, {}^{\mathrm{FT}}\bar{\underline{t}}^{S_k^{\oplus}/S_{k+1}}
\end{aligned} \tag{A.295}$$

For the corresponding variations the following expressions apply:

$$\begin{aligned}
\delta^{\mathrm{FT}}\underline{f}^{S_k^{\ominus}} &= {}^{S_k}\bar{\Phi}^{S_{k+1}}\cdot\left(\delta^{\mathrm{FT}}\underline{f}^{S_{k+1}^{\ominus}} - \delta\underline{\dot{p}}^{S_{k+1}} + \delta^{\mathrm{EX}}\underline{f}^{S_{k+1}^{\ominus}}\right) + \delta^{S_k}\Phi^{S_{k+1}}\cdot{}^{\mathrm{FT}}\bar{\underline{f}}^{S_k^{\oplus}/S_{k+1}} \\
\delta^{\mathrm{FT}}\underline{t}^{S_k^{\ominus}} &= {}^{S_k^{\ominus}}\underline{r}^{S_k^{\oplus}}\times\delta^{\mathrm{FT}}\underline{f}^{S_k^{\ominus}} + \\
&\quad {}^{S_k}\bar{\Phi}^{S_{k+1}}\cdot\left(\delta^{\mathrm{FT}}\underline{t}^{S_{k+1}^{\ominus}} - \delta^{S_{k+1}^{\ominus}}\underline{\dot{h}}^{S_{k+1}} + \delta^{\mathrm{EX}}\underline{t}^{S_{k+1}^{\ominus}}\right) + \delta^{S_k}\Phi^{S_{k+1}}\cdot{}^{\mathrm{FT}}\bar{\underline{t}}^{S_k^{\oplus}/S_{k+1}}
\end{aligned} \tag{A.296}$$

For the sensitivities to the variabels $\underline{q}$ holds:

$$\begin{aligned}
\frac{\partial^{\mathrm{FT}}\underline{f}^{S_k^{\ominus}}}{\partial\underline{q}} &= {}^{S_k}\bar{\Phi}^{S_{k+1}}\cdot\left(\frac{\partial^{\mathrm{FT}}\underline{f}^{S_{k+1}^{\ominus}}}{\partial\underline{q}} - \frac{\partial\underline{p}^{S_{k+1}}}{\partial\underline{q}} + \frac{\partial^{\mathrm{EX}}\underline{f}^{S_{k+1}^{\ominus}}}{\partial\underline{q}}\right) + \\
&\quad \delta_{\underline{q}\,\underline{\phi}^S}\cdot\left[\,\mathrm{O}_{(1)}\ldots\mathrm{O}_{(k)}\;\;\mathrm{J}^3_{v=1}\Big(\frac{\partial^{S_k}\Phi^{S_{k+1}}}{\partial\phi_v^{S_{k+1}}}\cdot{}^{\mathrm{FT}}\bar{\underline{f}}^{S_k^{\oplus}/S_{k+1}}\Big)\;\;\mathrm{O}_{(k+2)}\ldots\mathrm{O}_{(M)}\,\right] \\
\frac{\partial^{\mathrm{FT}}\underline{t}^{S_k^{\ominus}}}{\partial\underline{q}} &= \mathrm{J}^3_{v=1}\Big({}^{S_k^{\ominus}}\underline{r}^{S_k^{\oplus}}\times\underline{e}_v\Big)\cdot\frac{\partial^{\mathrm{FT}}\underline{f}^{S_k^{\ominus}}}{\partial\underline{q}} + {}^{S_k}\bar{\Phi}^{S_{k+1}}\cdot\frac{\partial({}^{\mathrm{FT}}\underline{t}^{S_{k+1}^{\ominus}} - {}^{S_{k+1}^{\ominus}}\underline{\dot{h}}^{S_{k+1}} + {}^{\mathrm{EX}}\underline{t}^{S_{k+1}^{\ominus}})}{\partial\underline{q}} + \\
&\quad \delta_{\underline{q}\,\underline{\phi}^S}\cdot\left[\,\mathrm{O}_{(1)}\ldots\mathrm{O}_{(k)}\;\;\mathrm{J}^3_{v=1}\Big(\frac{\partial^{S_k}\Phi^{S_{k+1}}}{\partial\phi_v^{S_{k+1}}}\cdot{}^{\mathrm{FT}}\bar{\underline{t}}^{S_k^{\oplus}/S_{k+1}}\Big)\;\;\mathrm{O}_{(k+2)}\ldots\mathrm{O}_{(M)}\,\right]
\end{aligned} \tag{A.297}$$

Note that the last term in the right hand side of both equations only applies if $\underline{q}$ equals $\underline{\phi}^S$!

(iv) Output variables and vector output equation in 2nd order model

The tower S_{t} needs to provide the following output:

- exit point displacements relative to the (fixed) position of the turbine base:
  $\delta^{S_0^{\ominus}}\underline{r}^{S_k^{\oplus}/B}$ for $k = 2\ldots M-1$ (along fixed c.s. $\vec{e}^{\,S_0} \equiv \vec{e}^{\,B}$);
- feedthrough force and torque on foundation element exit $S_1^{\oplus}$:
  ${}^{\mathrm{FT}}\underline{f}^{S_{\mathrm{PP}(2)}}$, ${}^{\mathrm{FT}}\underline{t}^{S_{\mathrm{PP}(2)}}$ (along actual c.s. $\vec{e}^{\,S_1}$)
- distributed hydrodynamic force load on S_2 to foundation S_{f}:
  ${}^{\mathrm{h}}\underline{q}^{S_{\mathrm{PP}(2)}}$ (along actual c.s. $\vec{e}^{\,S_2}$);
- kinematic vectors in tower top $S_{M-1}^{\oplus}$ to nacelle:
  $\underline{\omega}^{S_{\mathrm{FF}(2)}}$, $\underline{\alpha}^{S_{\mathrm{FF}(2)}}$, $\underline{v}^{S^{\oplus}_{\mathrm{FF}(2)}}$, $\underline{a}^{S^{\oplus}_{\mathrm{FF}(2)}}$ (along actual c.s. $\vec{e}^{\,S_{M-1}}$)
- wind speed and gravitation variation by orientation change up till exit S_{M-1}:
  $\underline{u}_{\mathrm{ori}}^{S_{\mathrm{FF}(2)}}$, $\underline{g}_{\mathrm{ori}}^{S_{\mathrm{FF}(2)}}$ (along actual c.s. $\vec{e}^{\,S_{M-1}}$)
- exit point displacement tower top relative to average position tower top:
  $\underline{\xi}^{S_{\mathrm{FF}(2)}}$, $\underline{x}^{S^{\oplus}_{\mathrm{FF}(2)}}$ (along average f.c.s. $\vec{e}^{\,\bar{S}_{M-1}}$).

The output vector from S_t has the following composition:

$$\underline{y}^{S_\mathrm{t}} = \begin{bmatrix} \underline{y}^{S_\mathrm{t} G} \\ \underline{y}^{S_\mathrm{t} S_\mathrm{n}} \\ \underline{y}^{S_\mathrm{n} S_\mathrm{f}} \end{bmatrix}$$

with

$$\underline{y}^{G S_\mathrm{t}} = \begin{bmatrix} \delta^{\bar{S}_0^\ominus} \underline{r}^{S_2^\oplus / B} \\ \vdots \\ \delta^{\bar{S}_0^\ominus} \underline{r}^{S_{M-1}^\oplus / B} \end{bmatrix}; \quad \underline{y}^{S_\mathrm{f} S_\mathrm{t}} = \begin{bmatrix} {}^{\mathrm{FT}}\underline{f}^{S_{\mathrm{PP}(2)}} \\ {}^{\mathrm{FT}}\underline{t}^{S_{\mathrm{PP}(2)}} \\ {}^{\mathrm{h}}\underline{q}^{S_{\mathrm{PP}(2)}} \end{bmatrix}; \quad \underline{y}^{S_\mathrm{n} S_\mathrm{t}} = \begin{bmatrix} \underline{\omega}^{S_{\mathrm{FF}(2)}} \\ \underline{\alpha}^{S_{\mathrm{FF}(2)}} \\ \underline{v}^{S_{\mathrm{FF}(2)}^\oplus} \\ \underline{a}^{S_{\mathrm{FF}(2)}^\oplus} \\ \underline{u}_{\mathrm{ori}}^{S_{\mathrm{FF}(2)}} \\ \underline{g}_{\mathrm{ori}}^{S_{\mathrm{FF}(2)}} \\ \underline{\xi}^{S_{\mathrm{FF}(2)}} \\ \underline{x}^{S_{\mathrm{FF}(2)}^\oplus} \end{bmatrix} \tag{A.298}$$

The (zero-mean) feedthrough kinematic vectors $\underline{\omega}^{S_{\mathrm{FF}(2)}}$, $\underline{\alpha}^{S_{\mathrm{FF}(2)}}$, $\underline{v}^{S_{\mathrm{FF}(2)}^\oplus}$ and $\underline{a}^{S_{\mathrm{FF}(2)}^\oplus}$ to the nacelle S_n are supplied as coordinate vectors along the f.c.s. $\vec{e}^{\,S_{M-1}}$. The expression for the variations follow from Eq. B.1 up to B.7 by setting '$k = M-1$' and '$S_{\mathrm{FF}} = S_{\mathrm{FF}(1)}$' and considering the point $S_{M-1}^\oplus$ instead of S_{M-1}^* for $\underline{v}^{S_{\mathrm{FF}(2)}^\oplus}$ and $\underline{a}^{S_{\mathrm{FF}(2)}^\oplus}$.

The feedthrough 'orientation change vectors' $\underline{u}_{\mathrm{ori}}^{S_{\mathrm{FF}(2)}}$ and $\underline{g}_{\mathrm{ori}}^{S_{\mathrm{FF}(2)}}$ ($\equiv \underline{u}_{\mathrm{ori}}^{S_\mathrm{t}}$, $\underline{g}_{\mathrm{ori}}^{S_\mathrm{t}}$) are also expressed along $\vec{e}^{\,S_{M-1}}$ (see Eq. B.164 and B.287, B.288).

For the displacement variation vector $\delta^{\bar{S}_0^\ominus} \underline{r}^{S_k^\oplus / B}$ with coordinates along the fixed c.s. of the turbine base $B \equiv \bar{S}_0$, holds:

$$\delta^{\bar{S}_0^\ominus} \underline{r}^{S_k^\oplus / B} = \sum_{(\underline{z})} \frac{\partial^{\bar{S}_0^\ominus} \underline{r}^{S_1^\oplus / B}}{\partial \underline{z}} \cdot \delta \underline{z} \qquad (\underline{z} = \underline{\phi}^S, \underline{\rho}^S, \underline{\xi}^{S_{\mathrm{FF}(1)}}, \underline{x}^{S_{\mathrm{FF}(1)}}) \tag{A.299}$$

with (see discussion from Eq. A.77):

$$\begin{aligned} \frac{\partial^{\bar{S}_0^\ominus} \underline{r}^{S_k^\oplus / B}}{\partial \underline{\xi}^{S_{\mathrm{FF}(1)}}} &= {}^{S_0}\bar{\Phi}^{S_k} \cdot \frac{\partial \underline{v}^{S_k^\oplus}}{\partial \underline{\omega}^{S_{\mathrm{FF}(1)}}} \quad ; \quad \frac{\partial^{\bar{S}_0^\ominus} \underline{r}^{S_k^\oplus / B}}{\partial \underline{\phi}^S} = {}^{S_0}\bar{\Phi}^{S_k} \cdot \frac{\partial \underline{v}^{S_k^\oplus}}{\partial \dot{\underline{\varphi}}^S} \\ \frac{\partial^{\bar{S}_0^\ominus} \underline{r}^{S_k^\oplus / B}}{\partial \underline{x}^{S_{\mathrm{FF}(1)}}} &= {}^{S_0}\bar{\Phi}^{S_k} \cdot \frac{\partial \underline{v}^{S_k^\oplus}}{\partial \underline{v}^{S_{\mathrm{FF}(1)}}} \quad ; \quad \frac{\partial^{\bar{S}_0^\ominus} \underline{r}^{S_k^\oplus / B}}{\partial \underline{\rho}^S} = {}^{S_0}\bar{\Phi}^{S_k} \cdot \frac{\partial \underline{v}^{S_k^\oplus}}{\partial \dot{\underline{\rho}}^S} \end{aligned} \tag{A.300}$$

For the displacement outputs to the gearbox house then holds the following sensitivities (coordinates along average f.c.s. of S_{M-1}):

$$\begin{aligned} \frac{\partial \underline{x}^{S_{\mathrm{FF}(2)}}}{\partial \underline{\xi}^{S_{\mathrm{FF}(1)}}} &= \frac{\partial \underline{v}^{S_{M-1}^\oplus}}{\partial \underline{\omega}^{S_{\mathrm{FF}(1)}}} \quad ; \quad \frac{\partial \underline{x}^{S_{\mathrm{FF}(2)}}}{\partial \underline{\phi}^S} = \frac{\partial \underline{v}^{S_{M-1}^\oplus}}{\partial \dot{\underline{\varphi}}^S} \\ \frac{\partial \underline{x}^{S_{\mathrm{FF}(2)}}}{\partial \underline{x}^{S_{\mathrm{FF}(1)}}} &= \frac{\partial \underline{v}^{S_{M-1}^\oplus}}{\partial \underline{v}^{S_{\mathrm{FF}(1)}}} \quad ; \quad \frac{\partial \underline{x}^{S_{\mathrm{FF}(2)}}}{\partial \underline{\rho}^S} = \frac{\partial \underline{v}^{S_{M-1}^\oplus}}{\partial \dot{\underline{\rho}}^S} \\ \frac{\partial \underline{\xi}^{S_{\mathrm{FF}(2)}}}{\partial \underline{\xi}^{S_{\mathrm{FF}(1)}}} &= \frac{\partial \underline{\omega}^{S_{M-1}}}{\partial \underline{\omega}^{S_{\mathrm{FF}(1)}}} \quad ; \quad \frac{\partial \underline{\xi}^{S_{\mathrm{FF}(2)}}}{\partial \underline{\phi}^S} = \frac{\partial \underline{\omega}^{S_{M-1}^\oplus}}{\partial \dot{\underline{\varphi}}^S} \end{aligned} \tag{A.301}$$

The feedthrough loads along the actual f.c.s. of S_1 to the foundation are given by (external loads by Eq. A.231):

$$\begin{aligned} {}^{\mathrm{FT}}\underline{f}^{S_{\mathrm{PP}(2)}} &= {}^{S_1}\Phi^{S_2} \cdot ({}^{\mathrm{FT}}\underline{f}^{S_2^\ominus} - \dot{\underline{p}}^{S_2} + {}^{\mathrm{EX}}\underline{f}^{S_2^\ominus}) \\ {}^{\mathrm{FT}}\underline{t}^{S_{\mathrm{PP}(2)}} &= {}^{S_1}\Phi^{S_2} \cdot ({}^{\mathrm{FT}}\underline{t}^{S_2^\ominus} + -^{S_2^\ominus}\dot{\underline{h}}^{S_2} + {}^{\mathrm{EX}}\underline{t}^{S_2^\ominus}) \end{aligned} \tag{A.302}$$

Of course, the time-average rate change in the impulse vectors of S_M equals zero. The mean feedthrough loads to the foundation are then given by:

$$\begin{aligned} {}^{\mathrm{FT}}\underline{f}^{S_{\mathrm{PP}(2)}} &= {}^{S_1}\bar{\Phi}^{S_2} \cdot \left({}^{\mathrm{FT}}\underline{\bar{f}}^{S_2^{\ominus}} + {}^{\mathrm{EX}}\underline{\bar{f}}^{S_2}\right) \\ {}^{\mathrm{FT}}\underline{t}^{S_{\mathrm{PP}(2)}} &= {}^{S_1}\bar{\Phi}^{S_2} \cdot \left({}^{\mathrm{FT}}\underline{\bar{t}}^{S_2^{\ominus}} + {}^{\mathrm{EX}}\underline{\bar{t}}^{S_2}\right) \end{aligned} \tag{A.303}$$

The variation of the feedthrough loads to the foundation are given by:

$$\begin{aligned} \delta^{\mathrm{FT}}\underline{f}^{S_{\mathrm{PP}(2)}} &= \sum_{(\underline{q})} \frac{\partial^{\mathrm{FT}}\underline{f}^{S_{\mathrm{PP}(2)}}}{\partial \underline{q}} \cdot \delta\underline{q} \quad \text{for } \underline{q} = \underline{w}^S_{\mathrm{horz}}, \dot{\underline{w}}^S_{\mathrm{horz}}, {}^{\mathrm{FT}}\underline{f}^{S_{\mathrm{PP}(3)}}, \underline{\omega}^{S_{\mathrm{FF}(1)}}, \underline{\alpha}^{S_{\mathrm{FF}(1)}}, \\ &\qquad \underline{v}^{S_{\mathrm{FF}(1)}}, \underline{a}^{S_{\mathrm{FF}(1)}}, \underline{g}_{\mathrm{ori}}^{S_{\mathrm{FF}(1)}}, {}^{\mathrm{h}}\underline{q}^{S_{\mathrm{FF}(1)}}, \underline{\varphi}^S, \dot{\underline{\varphi}}^S, \dot{\underline{\varrho}}^S, \ddot{\underline{\varphi}}^S, \ddot{\underline{\varrho}}^S \\ \delta^{\mathrm{FT}}\underline{t}^{S_{\mathrm{PP}(2)}} &= \sum_{(\underline{q})} \frac{\partial^{\mathrm{FT}}\underline{t}^{S_{\mathrm{PP}(2)}}}{\partial \underline{q}} \cdot \delta\underline{q} \quad \text{for } \underline{q} = \underline{w}^S_{\mathrm{horz}}, \dot{\underline{w}}^S_{\mathrm{horz}}, {}^{\mathrm{FT}}\underline{t}^{S_{\mathrm{PP}(3)}}, {}^{\mathrm{FT}}\underline{f}^{S_{\mathrm{PP}(3)}}, \underline{\omega}^{S_{\mathrm{FF}(1)}}, \underline{\alpha}^{S_{\mathrm{FF}(1)}}, \\ &\qquad \underline{v}^{S_{\mathrm{FF}(1)}}, \underline{a}^{S_{\mathrm{FF}(1)}}, \underline{g}_{\mathrm{ori}}^{S_{\mathrm{FF}(1)}}, {}^{\mathrm{h}}\underline{q}^{S_{\mathrm{FF}(1)}}, \underline{\varphi}^S, \dot{\underline{\varphi}}^S, \dot{\underline{\varrho}}^S, \ddot{\underline{\varphi}}^S, \ddot{\underline{\varrho}}^S \end{aligned} \tag{A.304}$$

For the sensitivities to the variables $\underline{q}$ holds:

$$\begin{aligned} \frac{\partial^{\mathrm{FT}}\underline{f}^{S_{\mathrm{PP}(2)}}}{\partial \underline{q}} &= {}^{S_1}\bar{\Phi}^{S_2} \cdot \left(\frac{\partial^{\mathrm{FT}}\underline{f}^{S_2^{\ominus}}}{\partial \underline{q}} - \frac{\partial \underline{\dot{p}}^{S_2}}{\partial \underline{q}} + \frac{\partial^{\mathrm{EX}}\underline{f}^{S_2^{\ominus}}}{\partial \underline{q}}\right) + \\ &\qquad \delta_{\underline{q}\underline{\phi}^S} \cdot \left[\ \mathrm{O}_{(1)} \ \ \mathrm{J}^3_{v=1}\Big(\frac{\partial^{S_1}\Phi^{S_2}}{\partial \phi_v^{S_2}} \cdot \left({}^{\mathrm{FT}}\underline{\bar{f}}^{S_2^{\ominus}} + {}^{\mathrm{EX}}\underline{\bar{f}}^{S_2^{\ominus}}\right)\Big) \ \ \mathrm{O}_{(3)} \ldots \mathrm{O}_{(M)} \ \right] \\ \frac{\partial^{\mathrm{FT}}\underline{t}^{S_{\mathrm{PP}(2)}}}{\partial \underline{q}} &= {}^{S_1}\bar{\Phi}^{S_2} \cdot \left(\frac{\partial^{\mathrm{FT}}\underline{f}^{S_2^{\ominus}}}{\partial \underline{q}} - \frac{\partial^{S_2^{\ominus}}\underline{h}^{S_2}}{\partial \underline{q}} + \frac{\partial^{\mathrm{EX}}\underline{t}^{S_2^{\ominus}}}{\partial \underline{q}}\right) + \\ &\qquad \delta_{\underline{q}\underline{\phi}^S} \cdot \left[\ \mathrm{O}_{(1)} \ \ \mathrm{J}^3_{v=1}\Big(\frac{\partial^{S_1}\Phi^{S_2}}{\partial \phi_v^{S_2}} \cdot \left({}^{\mathrm{FT}}\underline{\bar{t}}^{S_2^{\ominus}} + {}^{\mathrm{EX}}\underline{\bar{t}}^{S_2^{\ominus}}\right)\Big) \ \ \mathrm{O}_{(3)} \ldots \mathrm{O}_{(M)} \ \right] \end{aligned} \tag{A.305}$$

Note that the last term in the right hand side of both equations only applies if $\underline{q}$ equals $\underline{\phi}^S$!

The output equation that belongs to the 2nd order state equation is:

$$\underline{y}^{S_{\mathrm{t}}} = \left[\boldsymbol{H}_{\varphi}^{S_{\mathrm{t}}} \ \ \boldsymbol{H}_{\varrho}^{S_{\mathrm{t}}}\right] \cdot \begin{bmatrix} \underline{\varphi}^S \\ \underline{\varrho}^S \end{bmatrix} + \left[\boldsymbol{L}_{\varphi}^{S_{\mathrm{t}}} \ \ \boldsymbol{L}_{\varrho}^{S_{\mathrm{t}}}\right] \cdot \begin{bmatrix} \dot{\underline{\varphi}}^S \\ \dot{\underline{\varrho}}^S \end{bmatrix} + \boldsymbol{K}^{S_{\mathrm{t}}} \cdot \underline{v}^{S_{\mathrm{t}}} \tag{A.306}$$

The matrix partitions $\boldsymbol{H}_{\varphi}^{S_{\mathrm{t}}}$ and $\boldsymbol{L}_{\varphi}^{S_{\mathrm{t}}}$ map the *angular* dof position and speed variations:

$$\begin{aligned} \boldsymbol{H}_{\varphi}^{S_{\mathrm{t}}} &= \frac{\partial \underline{y}^{S_{\mathrm{t}}}}{\partial \underline{\phi}^S} - \Big(\ \frac{\partial \underline{y}^{S_{\mathrm{t}}}}{\partial \ddot{\underline{\varphi}}^S} \cdot \left(\boldsymbol{M}^{S_{\mathrm{t}}}\right)^{-1}_{\varphi} + \frac{\partial \underline{y}^{S_{\mathrm{t}}}}{\partial \ddot{\underline{\varrho}}^S} \cdot \left(\boldsymbol{M}^{S_{\mathrm{t}}}\right)^{-1}_{\varrho} \Big) \cdot \boldsymbol{S}_{\varphi}^{S_{\mathrm{t}}} \\ \boldsymbol{L}_{\varphi}^{S_{\mathrm{t}}} &= \frac{\partial \underline{y}^{S_{\mathrm{t}}}}{\partial \underline{\varphi}^S} - \Big(\ \frac{\partial \underline{y}^{S_{\mathrm{t}}}}{\partial \ddot{\underline{\varphi}}^S} \cdot \left(\boldsymbol{M}^{S_{\mathrm{t}}}\right)^{-1}_{\varphi} + \frac{\partial \underline{y}^{S_{\mathrm{t}}}}{\partial \ddot{\underline{\varrho}}^S} \cdot \left(\boldsymbol{M}^{S_{\mathrm{t}}}\right)^{-1}_{\varrho} \Big) \cdot \boldsymbol{D}_{\varphi}^{S_{\mathrm{t}}} \end{aligned} \tag{A.307}$$

The matrix partitions $\boldsymbol{H}_{\varrho}^{S_{\mathrm{t}}}$ and $\boldsymbol{L}_{\varrho}^{S_{\mathrm{t}}}$ map the *linear* dof position and speed variations:

$$\begin{aligned} \boldsymbol{H}_{\varrho}^{S_{\mathrm{t}}} &= \frac{\partial \underline{y}^{S_{\mathrm{t}}}}{\partial \underline{\varrho}^S} - \Big(\ \frac{\partial \underline{y}^{S_{\mathrm{t}}}}{\partial \ddot{\underline{\varphi}}^S} \cdot \left(\boldsymbol{M}^{S_{\mathrm{t}}}\right)^{-1}_{\varphi} + \frac{\partial \underline{y}^{S_{\mathrm{t}}}}{\partial \ddot{\underline{\varrho}}^S} \cdot \left(\boldsymbol{M}^{S_{\mathrm{t}}}\right)^{-1}_{\varrho} \Big) \cdot \boldsymbol{S}_{\varrho}^{S_{\mathrm{t}}} \\ \boldsymbol{L}_{\varrho}^{S_{\mathrm{t}}} &= \frac{\partial \underline{y}^{S_{\mathrm{t}}}}{\partial \dot{\underline{\varrho}}^S} - \Big(\ \frac{\partial \underline{y}^{S_{\mathrm{t}}}}{\partial \ddot{\underline{\varphi}}^S} \cdot \left(\boldsymbol{M}^{S_{\mathrm{t}}}\right)^{-1}_{\varphi} + \frac{\partial \underline{y}^{S_{\mathrm{t}}}}{\partial \ddot{\underline{\varrho}}^S} \cdot \left(\boldsymbol{M}^{S_{\mathrm{t}}}\right)^{-1}_{\varrho} \Big) \cdot \boldsymbol{D}_{\varrho}^{S_{\mathrm{t}}} \end{aligned} \tag{A.308}$$

For the feedthrough matrix $\boldsymbol{K}^{S_{\mathrm{t}}}$ holds:

$$\boldsymbol{K}^{S_{\mathrm{t}}} = \frac{\partial \underline{y}^{S_{\mathrm{t}}}}{\partial \underline{v}^{S_{\mathrm{t}}}} - \Big(\ \frac{\partial \underline{y}^{S_{\mathrm{t}}}}{\partial \ddot{\underline{\varphi}}^S} \cdot \left(\boldsymbol{M}^{S_{\mathrm{t}}}\right)^{-1}_{\varphi} + \frac{\partial \underline{y}^{S_{\mathrm{t}}}}{\partial \ddot{\underline{\varrho}}^S} \cdot \left(\boldsymbol{M}^{S_{\mathrm{t}}}\right)^{-1}_{\varrho} \Big) \cdot \boldsymbol{G}^{S_{\mathrm{t}}} \tag{A.309}$$

The partial derivatives to the dof vectors are cleaned up before use in the determination of the output and feedthrough matrices: columns that pertain to non-dof directions as concerns S_{t} are removed.

The partial derivative of the composed output vector $\underline{y}^{S_\mathrm{t}}$ to the composed input vector is obtained by (i) stacking the partial derivatives of the output subvectors to an input subvector, and (ii) doing this for all input subvectors and putting next to each other the obtained 'stacks'. The generic expression for the overall partial derivative matrix is (see e.g. also Eq. A.88):

$$\frac{\partial \underline{y}^{S_\mathrm{t}}}{\partial \underline{v}^{S_\mathrm{t}}} = \mathrm{J}_{(\underline{q}_\mathrm{v})}\Big(\mathrm{S}_{(\underline{z}_\mathrm{y})}\Big(\frac{\partial \underline{z}_\mathrm{y}}{\partial \underline{q}_\mathrm{v}}\Big)\Big) \quad \text{with} \quad \left\{ \begin{array}{l} \underline{q}_\mathrm{v} = \underline{w}^S_\mathrm{horz}, \underline{\dot{w}}^S_\mathrm{horz}, {}^\mathrm{FT}\underline{f}^{S_\mathrm{PP(3)}}, {}^\mathrm{FT}\underline{t}^{S_\mathrm{PP(3)}}, \underline{\omega}^{S^\oplus_\mathrm{FF(1)}}, \underline{\alpha}^{S_\mathrm{FF(1)}}, \\ \quad \underline{v}^{S^\oplus_\mathrm{FF(1)}}, \underline{a}^{S_\mathrm{FF(1)}}, \underline{u}^{S_\mathrm{FF(1)}}_\mathrm{ori}, \underline{g}^{S_\mathrm{FF(1)}}_\mathrm{ori}, \underline{\xi}^{S_\mathrm{FF(1)}}, \underline{x}^{S_\mathrm{FF(1)}}, {}^\mathrm{h}\underline{q}^{S_\mathrm{FF(1)}} \\ \underline{z}_\mathrm{y} = \delta^{\bar{S}^\ominus_0}\underline{r}^{S^\oplus_2/B} \ldots \delta^{\bar{S}^\ominus_0}\underline{r}^{S^\oplus_{M-1}/B}, \underline{\omega}^{S^\oplus_\mathrm{FF(2)}}, \underline{\alpha}^{S_\mathrm{FF(2)}}, \underline{v}^{S^\oplus_\mathrm{FF(2)}}, \underline{a}^{S^\oplus_\mathrm{FF(2)}}, \\ \quad \underline{u}^{S_\mathrm{FF(2)}}_\mathrm{ori}, \underline{g}^{S_\mathrm{FF(2)}}_\mathrm{ori}, \underline{\xi}^{S_\mathrm{FF(2)}}, \underline{x}^{S_\mathrm{FF(2)}}, {}^\mathrm{FT}\underline{f}^{S_\mathrm{PP(2)}}, {}^\mathrm{FT}\underline{t}^{S_\mathrm{PP(2)}}, {}^\mathrm{h}\underline{q}^{S_\mathrm{PP(2)}} \end{array} \right. \tag{A.310}$$

A.5.4 Equations of motions for the foundation S_f

The foundation S_f has been implemented as a one-element subcomponent, set up by support structur element S_1. Up to six degrees of freedom are allowed for modelling the soil compliance in each direction.

The sensitivities of the (zero-mean) impulse vectors for the foundation element as formulated in section B.1.2, paragraph on *Foundation* S_f, apply and do not need further discussion. The linearised expressions for the (zero-mean) hydrodynamic loading is listed in section 3.8.3, Eq. 3.101 and 3.102, and in section B.9.1, Eq. B.260 up to B.263. For the gravitation load see B.10.2, Eq. B.286 up to B.288.

The responsive loading on the foundation element is dealt with in paragraph (i). The required input variables are subject of paragraph (ii). Then, the second order state equation for the foundaiton is formulated in paragraph (iii), followed by the required output equation in paragraph (iv).

The subcomponent model for the tower S_t is obtained by a call to TBUS1SUBEOM() in function TBUSUPSTREOM(). The model for S_f exists as structure variable sysS1sub. The fields in sysS2sub are 2D matrices A, B, C, K, the parameterisation of the first order state space representation, and cell arrays with lists of input, output and state variable names. Point of departure for the gearbox house model creation by function TBUS2SUBEOM() is the availability for the one-element subcomponent S_f of ((f.)c.s: (final) coordinate system):

- sensitivities of angular and linear impulse vector (along f.c.s. of S_1 in actual position: $\vec{e}^{\,S_1}$);
- means and sensitivities of gravitation load (along $\vec{e}^{\,S_1}$);
- sensitivities of hydrodynamic load (along $\vec{e}^{\,S_1}$);
- means of feedthrough forces and torques from tower (along $\vec{e}^{\,S_1}$);
- sensitivities of displacement vectors relative to the (fixed) tower base (along tower base c.s. $\vec{e}^{\,B}$);
- sensitivities of kinematic vectors in tower bottom (= exit point of S_f; along $\vec{e}^{\,S_1}$);
- sensitivities of wind speed and gravitation by orientation change for feedthrough into the tower bottom (along $\vec{e}^{\,S_1}$);
- transformation matrices and their sensitivities to rotational dofs;

- stiffness and damper values in the foundation entry;
- bottom-up ranking of rotation and translation axes in the foundation entry.

The mentioned sensitivities belong to the 'motion and load formulations' and map all motion and load variations to exogeneous input variables of to input variables from the tower or to dofs in the foundation. These are obtained via calls in TBUSUPSTREOM() to functions TBUSUPSTRCONS(), TBUSUPSTRKIN(), and TBUSUPSTRIMP(). Functionality TBUS1SUBEOM() ((f.)c.s: (final) coordinate system):

- definition of input name lists; each list contains the names of the input subvectors from a specific source (G, S2sub);
- definition of output name lists; each list contains the names of the output subvectors to a specific destination (G, S2sub);
- lumping together the hydrodynamic and gravitation loads to equivalent force and torque load formulations in the entry point of foundation element S_1; also includes feedthrough loading from tower (call TBUSSUBFTEX(); coordinates along actual f.c.s.of S_1);
- define 'equal to zero' the feedthrough loading from outward elements within the 'foundation subcomponent' (there are no) (call TBUSYSFTFT());
- definition of the sensitivities of the responsive (visco/elastic) loads in the entry point of S_1 to the dofs (use of results obtained earlier with TBUSUPSTRPAR(), see paragraph (i));
- derive the mass, spring and damper matrix for the equations of motion for the foundation S_f ($\boldsymbol{M}, \boldsymbol{S}, \boldsymbol{D}$; call TBUSYSMDSMX());
- derive load formulations for feedthrough torques and forces on the tower base (call TBUSYSFTPP; along fixed c.s. of tower base B);
- derive the input matrix for the mass/spring/damper formulation of S_t as well as the output matrices on the dofs and their time derivatives and the feedthrough matrix ($\boldsymbol{G}, \boldsymbol{H}, \boldsymbol{L}, \boldsymbol{K}$; call TBUSYSGHLKMX());
- transform the mass/spring/damper model formulation $\{\boldsymbol{M}, \boldsymbol{S}, \boldsymbol{D}, \boldsymbol{G}, \boldsymbol{H}, \boldsymbol{L}, \boldsymbol{K}\}$ to the first order state space formulation $\{\boldsymbol{A}, \boldsymbol{B}, \boldsymbol{C}, \boldsymbol{K}\}$ (call TBUSYSMDS2FSR()).

(i) Responsive loading

The responsive loading in the turbine foundation subcomponent S_f is modelled by viso-elastic loads that correspond to tower extension *below* the earth surface. See paragraph (i) in 3.8.2.

The pursued sensitivity matrices of the responsive torque and force loads in the foundation element S_1 to the overall dof vectors for S are assembled as (see Eq. 3.86 for the involved non-zero 3×3 submatrices):

$$\begin{aligned}
\frac{\partial^{\mathrm{RS}} \underline{t}^{S_1}}{\partial \underline{\varphi}^{S}} &= [\, \frac{\partial^{\mathrm{RS}} \underline{t}^{S_1}}{\partial \underline{\varphi}^{S_1}} \;\; \mathrm{O}_{(2)} \;\; \ldots \;\; \mathrm{O}_{(M)} \,] \quad ; \quad \frac{\partial^{\mathrm{RS}} \underline{t}^{S_1}}{\partial \underline{\varrho}^{S}} = [\, \frac{\partial^{\mathrm{RS}} \underline{t}^{S_1}}{\partial \underline{\varrho}^{S_1}} \;\; \mathrm{O}_{(2)} \;\; \ldots \;\; \mathrm{O}_{(M)} \,] \\
\frac{\partial^{\mathrm{RS}} \underline{f}^{S_1}}{\partial \underline{\varphi}^{S}} &= [\, \frac{\partial^{\mathrm{RS}} \underline{f}^{S_1}}{\partial \underline{\varphi}^{S_1}} \;\; \mathrm{O}_{(2)} \;\; \ldots \;\; \mathrm{O}_{(M)} \,] \quad ; \quad \frac{\partial^{\mathrm{RS}} \underline{f}^{S_1}}{\partial \underline{\varrho}^{S}} = [\, \frac{\partial^{\mathrm{RS}} \underline{f}^{S_1}}{\partial \underline{\varrho}^{S_1}} \;\; \mathrm{O}_{(2)} \;\; \ldots \;\; \mathrm{O}_{(M)} \,]
\end{aligned} \tag{A.311}$$

(ii) Input variables

The input vector for S_{f} has the following composition:

$$\underline{v}^{S_{\mathrm{f}}} = \begin{bmatrix} \underline{v}^{S_{\mathrm{f}}G} \\ \underline{v}^{S_{\mathrm{f}}S_{\mathrm{t}}} \end{bmatrix}$$

with

$$\underline{v}^{S_{\mathrm{f}}G} = \begin{bmatrix} \underline{w}^{S}_{\mathrm{horz}} \\ \underline{\dot{w}}^{S}_{\mathrm{horz}} \end{bmatrix} \;;\; \underline{v}^{S_{\mathrm{f}}S_{\mathrm{t}}} = \begin{bmatrix} {}^{\mathrm{FT}}\underline{f}^{S_{\mathrm{PP(2)}}} \\ {}^{\mathrm{FT}}\underline{t}^{S_{\mathrm{PP(2)}}} \\ {}^{\mathrm{h}}\underline{q}^{S_{\mathrm{PP(2)}}} \end{bmatrix} \tag{A.312}$$

(iii) Equations of motion and 2$^{\mathrm{nd}}$ order vector state equation

The implementation of the 2$^{\mathrm{nd}}$ order state vector equation for the foundation S_{f} is based on the overall encapsulating dof vectors of the support structure. That is to say, the mass, spring and damper matrix arise from partial derivatives of impulse and load vectors to the dof vectors $\underline{\varphi}^{S}$ and $\underline{\varrho}^{S}$. Point of departure is the full-size vector state equation ($6M \times 6M$-matrices):

$$\left[\boldsymbol{M}_{\varphi}^{S_{\mathrm{f}}} \mid \boldsymbol{M}_{\varrho}^{S_{\mathrm{f}}}\right] \cdot \begin{bmatrix} \underline{\ddot{\varphi}}^{S} \\ \underline{\ddot{\varrho}}^{S} \end{bmatrix} + \left[\boldsymbol{D}_{\varphi}^{S_{\mathrm{f}}} \mid \boldsymbol{D}_{\varrho}^{S_{\mathrm{f}}}\right] \cdot \begin{bmatrix} \underline{\dot{\varphi}}^{S} \\ \underline{\dot{\varrho}}^{S} \end{bmatrix} + \left[\boldsymbol{S}_{\varphi}^{S_{\mathrm{f}}} \mid \boldsymbol{S}_{\varrho}^{S_{\mathrm{f}}}\right] \cdot \begin{bmatrix} \underline{\varphi}^{S} \\ \underline{\varrho}^{S} \end{bmatrix} = \left[\, \boldsymbol{G}^{S_{\mathrm{f}}G} \mid \boldsymbol{G}^{S_{\mathrm{f}}S_{\mathrm{t}}} \,\right] \cdot \begin{bmatrix} \underline{v}^{S_{\mathrm{f}}G} \\ \underline{v}^{S_{\mathrm{f}}S_{\mathrm{t}}} \end{bmatrix} \tag{A.313}$$

The one-element subcomponent S_{f} is set up by support structure element S_1. The required matrices are derived by considering the vector impulse equations for element S_1 in its set of three coordinate systems. The bottum-up ranked rotation axes for S_{f} are the z-, y- and x-axis; the z-axis is co-axial for the tower. Thus we start with the x- and y-coordinate of the angular and linear impulse in the 3rd intermediate coordinate system (i.c.s.). Afterwards, the respective y-coordinate and x-coordinate are considered in the 2nd i.c.s. Finally, both z-coordinates are dealt with in the 1st i.c.s.

The pairs of rows $\{\underline{\boldsymbol{m}}^{S_1}_{h\varphi_w}, \underline{\boldsymbol{m}}^{S_1}_{p\varphi_w} | w = 3,2,1\}$, with ranking numbers $2(w-1)+1$ and $2(w-1)+2$ in the mass matrix partition $\boldsymbol{M}_{\varphi}^{S_{\mathrm{f}}}$, are now determined as follows (the partial derivatives in the right hand side only apply if they are defined for the 'independent variable' $\underline{\ddot{\varphi}}^{S}$):

- for $w = 3$:

$$\begin{aligned} \underline{\boldsymbol{m}}^{S_1}_{h\varphi_3} &= -[\,1\,0\,0\,] \cdot \frac{\partial^{\mathrm{RS}}\underline{t}^{S_1^{\ominus}}}{\partial \underline{\ddot{\varphi}}^{S}} + [\,1\,0\,0\,] \cdot \Big(\frac{\partial^{S_1^{\ominus}}\underline{\dot{h}}^{S_1}}{\partial \underline{\ddot{\varphi}}^{S}} - \frac{\partial^{\mathrm{EX}}\underline{t}^{S_1^{\ominus}}}{\partial \underline{\ddot{\varphi}}^{S}} \Big) \\ \underline{\boldsymbol{m}}^{S_1}_{p\varphi_3} &= -[\,0\,1\,0\,] \cdot \frac{\partial^{\mathrm{RS}}\underline{f}^{S_1^{\ominus}}}{\partial \underline{\ddot{\varphi}}^{S}} + [\,0\,1\,0\,] \cdot \Big(\frac{\partial \underline{\dot{p}}^{S_1}}{\partial \underline{\ddot{\varphi}}^{S}} - \frac{\partial^{\mathrm{EX}}\underline{f}^{S_1^{\ominus}}}{\partial \underline{\ddot{\varphi}}^{S}} \Big) \end{aligned} \tag{A.314}$$

- for $w = 2$:

$$\begin{aligned} \underline{\boldsymbol{m}}^{S_1}_{h\varphi_2} &= -[\,0\,1\,0\,] \cdot \frac{\partial^{\mathrm{RS}}\underline{t}^{S_1^{\ominus}}}{\partial \underline{\ddot{\varphi}}^{S}} + {}^{S_1^2}\bar{\Phi}^{S_1}_{(2,:)} \cdot \Big(\frac{\partial^{S_1^{\ominus}}\underline{\dot{h}}^{S_1}}{\partial \underline{\ddot{\varphi}}^{S}} - \frac{\partial^{\mathrm{EX}}\underline{t}^{S_1^{\ominus}}}{\partial \underline{\ddot{\varphi}}^{S}} \Big) \\ \underline{\boldsymbol{m}}^{S_1}_{p\varphi_2} &= -[\,1\,0\,0\,] \cdot \frac{\partial^{\mathrm{RS}}\underline{f}^{S_1^{\ominus}}}{\partial \underline{\ddot{\varphi}}^{S}} + {}^{S_1^2}\bar{\Phi}^{S_1}_{(1,:)} \cdot \Big(\frac{\partial \underline{\dot{p}}^{S_1}}{\partial \underline{\ddot{\varphi}}^{S}} - \frac{\partial^{\mathrm{EX}}\underline{f}^{S_1^{\ominus}}}{\partial \underline{\ddot{\varphi}}^{S}} \Big) \end{aligned} \tag{A.315}$$

- for $w = 1$:

$$\begin{aligned}
\underline{\boldsymbol{m}}_{h\varphi_1}^{S_1} &= -[\,0\,0\,1\,]\cdot\frac{\partial^{\mathrm{RS}}\underline{t}^{S_1^{\ominus}}}{\partial\underline{\ddot{\varphi}}^{S}} + {}^{S_1^1}\bar{\Phi}_{(3,:)}^{S_1}\cdot\Big(\frac{\partial^{S_1^{\ominus}}\underline{\dot{h}}^{S_1}}{\partial\underline{\ddot{\varphi}}^{S}} - \frac{\partial^{\mathrm{EX}}\underline{t}^{S_1^{\ominus}}}{\partial\underline{\ddot{\varphi}}^{S}}\Big)\\
\underline{\boldsymbol{m}}_{p\varphi_1}^{S_1} &= -[\,0\,0\,1\,]\cdot\frac{\partial^{\mathrm{RS}}\underline{f}^{S_1^{\ominus}}}{\partial\underline{\ddot{\varphi}}^{S}} + {}^{S_1^1}\bar{\Phi}_{(3,:)}^{S_1}\cdot\Big(\frac{\partial\underline{\dot{p}}^{S_1}}{\partial\underline{\ddot{\varphi}}^{S}} - \frac{\partial^{\mathrm{EX}}\underline{f}^{S_1^{\ominus}}}{\partial\underline{\ddot{\varphi}}^{S}}\Big)
\end{aligned} \tag{A.316}$$

Note that NO feedthrough loading exists from other elements within the one-element subcomponent S_f. The loading from the tower S_t is considered as external loading for S_f and included in ${}^{\mathrm{EX}}\underline{t}^{S_1^{\ominus}}$ and ${}^{\mathrm{EX}}\underline{f}^{S_1^{\ominus}}$.

The corresponding rows in the mass matrix partition $\boldsymbol{M}_{\varrho}^{S_\mathrm{f}}$ are obtained by taking the sensitivities to $\underline{\ddot{\varrho}}^{S}$ instead of $\underline{\ddot{\varphi}}^{S}$. For the rows in both damping matrix partitions $\boldsymbol{D}_{\varphi}^{S_\mathrm{f}}$ and $\boldsymbol{D}_{\varrho}^{S_\mathrm{f}}$ and in the stiffness matrix partition $\boldsymbol{S}_{\varrho}^{S_\mathrm{f}}$, take the sensitivities to $\underline{\dot{\varphi}}^{S}$ and $\underline{\dot{\varrho}}^{S}$ and $\underline{\varrho}^{S}$. For the remaining stiffness matrix partition $\boldsymbol{S}_{\varphi}^{S_\mathrm{f}}$ the same scheme applies for $w = 3$ but differs for $w = 2$ and $w = 1$:

- for $w = 2$:

$$\begin{aligned}
\underline{\boldsymbol{s}}_{h\varphi_2}^{S_1} &= -[\,0\,1\,0\,]\cdot\frac{\partial^{\mathrm{RS}}\underline{t}^{S_1^{\ominus}}}{\partial\underline{\phi}^{S}} + {}^{S_1^2}\bar{\Phi}_{(2,:)}^{S_1}\cdot\Big(\frac{\partial^{S_1^{\ominus}}\underline{\dot{h}}^{S_1}}{\partial\underline{\phi}^{S}} - \frac{\partial^{\mathrm{EX}}\underline{t}^{S_1^{\ominus}}}{\partial\underline{\phi}^{S}}\Big) +\\
&\qquad [\,\mathrm{J}_{v=1}^{3}\Big(\frac{\partial^{S_1^2}\Phi_{(2,:)}^{S_1}}{\partial\phi_v^{S_1^1}}\cdot\Big({}^{S_1^{\ominus}}\underline{\dot{h}}^{S_1} - {}^{\mathrm{EX}}\underline{\bar{t}}^{S_1^{\ominus}}\Big)\ \mathrm{O}_{(2\ldots M)}\,]\\
\underline{\boldsymbol{s}}_{p\varphi_2}^{S_1} &= -[\,1\,0\,0\,]\cdot\frac{\partial^{\mathrm{RS}}\underline{f}^{S_1^{\ominus}}}{\partial\underline{\phi}^{S}} + {}^{S_1^2}\bar{\Phi}_{(1,:)}^{S_1}\cdot\Big(\frac{\partial\underline{\dot{p}}^{S_1}}{\partial\underline{\phi}^{S}} - \frac{\partial^{\mathrm{EX}}\underline{f}^{S_1^{\ominus}}}{\partial\underline{\phi}^{S}}\Big) +\\
&\qquad [\,\mathrm{J}_{v=1}^{3}\Big(\frac{\partial^{S_1^2}\Phi_{(1,:)}^{S_1}}{\partial\phi_v^{S_1^1}}\cdot\Big({}^{S_1^{\ominus}}\underline{\bar{p}}^{S_1} - {}^{\mathrm{EX}}\underline{\bar{f}}^{S_1^{\ominus}}\Big)\Big)\ \mathrm{O}_{(2\ldots M)}\,]
\end{aligned} \tag{A.317}$$

- for $w = 1$:

$$\begin{aligned}
\underline{\boldsymbol{s}}_{h\varphi_1}^{S_1} &= -[\,0\,0\,1\,]\cdot\frac{\partial^{\mathrm{RS}}\underline{t}^{S_1^{\ominus}}}{\partial\underline{\phi}^{S}} + {}^{S_1^1}\bar{\Phi}_{(3,:)}^{S_1}\cdot\Big(\frac{\partial^{S_1^{\ominus}}\underline{\dot{h}}^{S_1}}{\partial\underline{\phi}^{S}} - \frac{\partial^{\mathrm{EX}}\underline{t}^{S_1^{\ominus}}}{\partial\underline{\phi}^{S}}\Big) +\\
&\qquad [\,\mathrm{J}_{v=1}^{3}\Big(\frac{\partial^{S_1^1}\Phi_{(3,:)}^{S_1}}{\partial\phi_v^{S_1^1}}\cdot\Big({}^{S_1^{\ominus}}\underline{\dot{h}}^{S_1} - {}^{\mathrm{EX}}\underline{\bar{t}}^{S_1^{\ominus}}\Big)\ \mathrm{O}_{(2\ldots M)}\,]\\
\underline{\boldsymbol{s}}_{p\varphi_1}^{S_1} &= -[\,0\,0\,1\,]\cdot\frac{\partial^{\mathrm{RS}}\underline{f}^{S_1^{\ominus}}}{\partial\underline{\phi}^{S}} + {}^{S_1^1}\bar{\Phi}_{(3,:)}^{S_1}\cdot\Big(\frac{\partial\underline{\dot{p}}^{S_1}}{\partial\underline{\phi}^{S}} - \frac{\partial^{\mathrm{EX}}\underline{f}^{S_1^{\ominus}}}{\partial\underline{\phi}^{S}}\Big) +\\
&\qquad [\,\mathrm{J}_{v=1}^{3}\Big(\frac{\partial^{S_1^1}\Phi_{(3,:)}^{S_1}}{\partial\phi_v^{S_1^1}}\cdot\Big({}^{S_1^{\ominus}}\underline{\bar{p}}^{S_1} - {}^{\mathrm{EX}}\underline{\bar{f}}^{S_1^{\ominus}}\Big)\Big)\ \mathrm{O}_{(2\ldots M)}\,]
\end{aligned} \tag{A.318}$$

The pairs of rows $\{\underline{\boldsymbol{g}}_{h_w}^{S_1 S_\mathrm{t}}, \underline{\boldsymbol{g}}_{p_w}^{S_1 S_\mathrm{t}} | w = 3, 2, 1\}$, with ranking numbers $2(w-1)+1$ and $2(w-1)+2$ in the input matrix partition $\boldsymbol{G}^{S_\mathrm{f} S_\mathrm{t}}$, are determined as follows (the partial derivatives in the right hand side only apply if they are defined for the 'independent variable'; in this case $\underline{z}$):

- for $w = 3$:

$$\begin{aligned}
\underline{\boldsymbol{g}}_{h_3}^{S_1 S_\mathrm{t}} &= \mathrm{J}_{(\underline{z})}\Big([\,1\,0\,0\,]\cdot\frac{\partial^{\mathrm{RS}}\underline{t}^{S_1^{\ominus}}}{\partial\underline{z}} + [\,1\,0\,0\,]\cdot\Big(-\frac{\partial^{S_1^{\ominus}}\underline{\dot{h}}^{S_1}}{\partial\underline{z}} + \frac{\partial^{\mathrm{EX}}\underline{t}^{S_1^{\ominus}}}{\partial\underline{z}}\Big)\Big)\\
\underline{\boldsymbol{g}}_{p_3}^{S_1 S_\mathrm{t}} &= \mathrm{J}_{(\underline{z})}\Big([\,0\,1\,0\,]\cdot\frac{\partial^{\mathrm{RS}}\underline{f}^{S_1^{\ominus}}}{\partial\underline{z}} + [\,0\,1\,0\,]\cdot\Big(-\frac{\partial\underline{\dot{p}}^{S_1}}{\partial\underline{z}} + \frac{\partial^{\mathrm{EX}}\underline{f}^{S_1^{\ominus}}}{\partial\underline{z}}\Big)\Big)
\end{aligned} \tag{A.319}$$

- for $w = 2$:

$$\begin{aligned}
\underline{\boldsymbol{g}}_{h_2}^{S_1 S_\mathrm{t}} &= \mathrm{J}_{(\underline{z})}\Big([\,0\,1\,0\,] \cdot \frac{\partial^{\mathrm{RS}} \underline{t}^{S_1^\ominus}}{\partial \underline{z}} + {}^{S_1^2}\bar{\Phi}^{S_1}_{(2,:)} \cdot \big(- \frac{\partial^{S_1^\ominus} \dot{\underline{h}}^{S_1}}{\partial \underline{z}} + \frac{\partial^{\mathrm{EX}} \underline{t}^{S_1^\ominus}}{\partial \underline{z}}\big)\Big) \\
\underline{\boldsymbol{g}}_{p_2}^{S_1 S_\mathrm{t}} &= \mathrm{J}_{(\underline{z})}\Big([\,1\,0\,0\,] \cdot \frac{\partial^{\mathrm{RS}} \underline{f}^{S_1^\ominus}}{\partial \underline{z}} + {}^{S_1^2}\bar{\Phi}^{S_1}_{(1,:)} \cdot (-\frac{\partial \dot{\underline{p}}^{S_1}}{\partial \underline{z}} + \frac{\partial^{\mathrm{EX}} \underline{f}^{S_1^\ominus}}{\partial \underline{z}})\Big)
\end{aligned} \tag{A.320}$$

- for $w = 1$:

$$\begin{aligned}
\underline{\boldsymbol{g}}_{h_1}^{S_1 S_\mathrm{t}} &= \mathrm{J}_{(\underline{z})}\Big([\,0\,0\,1\,] \cdot \frac{\partial^{\mathrm{RS}} \underline{t}^{S_1^\ominus}}{\partial \underline{z}} + {}^{S_1^1}\bar{\Phi}^{S_1}_{(3,:)} \cdot \big(- \frac{\partial^{S_1^\ominus} \dot{\underline{h}}^{S_1}}{\partial \underline{z}} + \frac{\partial^{\mathrm{EX}} \underline{t}^{S_1^\ominus}}{\partial \underline{z}}\big)\Big) \\
\underline{\boldsymbol{g}}_{p_1}^{S_1 S_\mathrm{t}} &= \mathrm{J}_{(\underline{z})}\Big([\,0\,0\,1\,] \cdot \frac{\partial^{\mathrm{RS}} \underline{f}^{S_1^\ominus}}{\partial \underline{z}} + {}^{S_1^1}\bar{\Phi}^{S_1}_{(3,:)} \cdot (-\frac{\partial \dot{\underline{p}}^{S_1}}{\partial \underline{z}} + \frac{\partial^{\mathrm{EX}} \underline{f}^{S_1^\ominus}}{\partial \underline{z}})\Big)
\end{aligned} \tag{A.321}$$

The involved subvectors $\underline{z}$ for the submatrices $\boldsymbol{G}^{S_\mathrm{f} G}$ and $\boldsymbol{G}^{S_\mathrm{f} S_\mathrm{t}}$ are listed in Eq. A.312 in the previous paragraph.

Note that all columns but the first three of the rows of the mass, damper and stiffness matrix partitions are deleted. Besides each non-valid row together with the corresponding column , that is to say which pertains to a 'non-dof' element of $\underline{\varphi}^S$ or $\underline{\varrho}^S$ *as concerns* S_f, is deleted . Of course, the corresponding row in the input matrix is also deleted. This yields a second order system equation with square left hand side matrices and adequately dimensioned input matrix.

The external load coordinate vectors, which pertain to the foundation entry (=tower bse) and have coordinates along the f.c.s. of S_1, include the hydrodynamic and gravition loading as well as the feedthrough loads from the tower in the foundation exit (= tower bottom):

$$\begin{aligned}
{}^{\mathrm{EX}}\underline{f}^{S_1^\ominus} &\triangleq {}^{\mathrm{g}}\underline{f}^{S_1^*} + {}^{\mathrm{h}}\underline{f}^{S_1^\mathrm{h}} + {}^{\mathrm{FT}}\underline{f}^{S_{\mathrm{PP}(2)}} \\
{}^{\mathrm{EX}}\underline{t}^{S_1^\ominus} &\triangleq {}^{S_1^\ominus}\underline{r}^{S_1^*} \times {}^{\mathrm{g}}\underline{f}^{S_1^*} + {}^{S_1^\ominus}\underline{r}^{S_1^\mathrm{h}} \times {}^{\mathrm{h}}\underline{f}^{S_1^\mathrm{h}} + {}^{\mathrm{h}}\underline{t}^{S_1^\mathrm{h}} + {}^{S_1^\ominus}\underline{r}^{S_1^\oplus} \times {}^{\mathrm{FT}}\underline{f}^{S_{\mathrm{PP}(2)}} + {}^{\mathrm{FT}}\underline{t}^{S_{\mathrm{PP}(2)}}
\end{aligned} \tag{A.322}$$

The expressions for the external load coordinate vectors comprise the envelope of dependencies:

$$\begin{aligned}
{}^{\mathrm{EX}}\underline{f}^{S_1^\ominus} &= {}^{\mathrm{EX}}\bar{\underline{f}}^{S_1^\ominus} + \frac{\partial^{\mathrm{EX}} \underline{f}^{S_1^\ominus}}{\partial \underline{w}^S_{\mathrm{horz}}} \cdot \underline{w}^S_{\mathrm{horz}} + \frac{\partial^{\mathrm{EX}} \underline{f}^{S_1^\ominus}}{\partial \dot{\underline{w}}^S_{\mathrm{horz}}} \cdot \dot{\underline{w}}^S_{\mathrm{horz}} + \sum_{(\underline{z})} \frac{\partial^{\mathrm{EX}} \underline{f}^{S_1^\ominus}}{\partial \underline{z}} \cdot \delta \underline{z} \\
{}^{\mathrm{EX}}\underline{t}^{S_1^\ominus} &= {}^{\mathrm{EX}}\bar{\underline{t}}^{S_1^\ominus} + \frac{\partial^{\mathrm{EX}} \underline{t}^{S_1^\ominus}}{\partial \underline{w}^S_{\mathrm{horz}}} \cdot \underline{w}^S_{\mathrm{horz}} + \frac{\partial^{\mathrm{EX}} \underline{t}^{S_1^\ominus}}{\partial \dot{\underline{w}}^S_{\mathrm{horz}}} \cdot \dot{\underline{w}}^S_{\mathrm{horz}} + \sum_{(\underline{z})} \frac{\partial^{\mathrm{EX}} \underline{t}^{S_1^\ominus}}{\partial \underline{z}} \cdot \delta \underline{z}
\end{aligned} \tag{A.323}$$

The reactive variation as represented by the summation over $\underline{z}$ involves

- output from the tower S_t: ${}^{\mathrm{h}}\underline{q}_\mathrm{f}^{S_{\mathrm{PP}(2)}}$, ${}^{\mathrm{FT}}\underline{f}^{S_{\mathrm{PP}(2)}}$, ${}^{\mathrm{FT}}\underline{t}^{S_{\mathrm{PP}(2)}}$
- degrees of freedom in S_f, encapsulated by: $\underline{\varphi}^S$, $\dot{\underline{\varphi}}^S$, $\dot{\underline{\varrho}}^S$, $\ddot{\underline{\varphi}}^S$, $\ddot{\underline{\varrho}}^S$

The expressions for the sensitivities of the external load vectors are (of course only if $\underline{q}$ applies in a right hand side partial derivative):

$$\begin{aligned}
\frac{\partial^{\mathrm{EX}} \underline{f}^{S_1^\ominus}}{\partial \underline{q}} &= \frac{\partial^{\mathrm{h}} \underline{f}^{S_1^\mathrm{h}}}{\partial \underline{q}} + \frac{\partial^{\mathrm{g}} \underline{f}^{S_1^*}}{\partial \underline{q}} + \\
\frac{\partial^{\mathrm{EX}} \underline{t}^{S_1^\ominus}}{\partial \underline{q}} &= \frac{\partial^{\mathrm{h}} \underline{t}^{S_1^\mathrm{h}}}{\partial \underline{q}} + \mathrm{J}^3_{v=1}\big({}^{S_1^\ominus}\underline{r}^{S_1^\mathrm{h}} \times \underline{e}_v \big) \cdot \frac{\partial^{\mathrm{h}} \underline{f}^{S_1^\mathrm{h}}}{\partial \underline{q}} + \mathrm{J}^3_{v=1}\big({}^{S_1^\ominus}\underline{r}^{S_1^*} \times \underline{e}_v \big) \cdot \frac{\partial^{\mathrm{g}} \underline{f}^{S_1^*}}{\partial \underline{q}}
\end{aligned} \tag{A.324}$$

Further it holds:

$$\frac{\partial^{\mathrm{EX}}\underline{f}^{S_1^{\ominus}}}{\partial^{\mathrm{FT}}\underline{f}^{S_{\mathrm{PP}(2)}}} = \boldsymbol{I} \;;\; \frac{\partial^{\mathrm{EX}}\underline{t}^{S_1^{\ominus}}}{\partial^{\mathrm{FT}}\underline{t}^{S_{\mathrm{PP}(2)}}} = \boldsymbol{I} \;;\; \frac{\partial^{\mathrm{EX}}\underline{t}^{S_1^{\ominus}}}{\partial^{\mathrm{FT}}\underline{f}^{S_{\mathrm{PP}(2)}}} = \mathrm{J}^3_{v=1}\big({}^{S_1^{\ominus}}\underline{r}^{S_1^{\oplus}} \times \underline{e}_v\big) \tag{A.325}$$

(iv) Output variables and vector output equation in 2nd order model
The foundation S_{f} needs to provide the following output:

- exit point displacements relative to the (fixed) position of the turbine base:
  $\delta^{\bar{S}_0^{\ominus}}\underline{r}^{S_1^{\oplus}/B}$ (along fixed c.s. $\vec{e}^{\,\bar{S}_0} \equiv \vec{e}^{\,B}$);
- force and torque loads on the foundation entry $S_1^{\ominus}$: ${}^{\mathrm{FT}}\underline{f}^{S_1^{\ominus}/B}$, ${}^{\mathrm{FT}}\underline{t}^{S_1^{\ominus}/B}$ (along fixed c.s. $\vec{e}^{\,\bar{S}_0}$);
- distributed hydrodynamic force load on S_1 to tower S_{t}:
  ${}^{\mathrm{h}}\underline{q}^{S_{\mathrm{FF}(1)}}$ (along actual c.s. $\vec{e}^{\,S_1}$);
- kinematic vectors in foundation exit $S_1^{\oplus}$ to tower:
  $\underline{\omega}^{S_{\mathrm{FF}(1)}}$, $\underline{\alpha}^{S_{\mathrm{FF}(1)}}$, $\underline{v}^{S_{\mathrm{FF}(1)}^{\oplus}}$, $\underline{a}^{S_{\mathrm{FF}(1)}^{\oplus}}$ (along actual c.s. $\vec{e}^{\,S_1}$)
- wind speed and gravitation variation by orientation change up till exit $S_{\mathrm{f}}^{\oplus}$:
  $\underline{u}_{\mathrm{ori}}^{S_{\mathrm{FF}(1)}}$, $\underline{g}_{\mathrm{ori}}^{S_{\mathrm{FF}(1)}}$ (along actual c.s. $\vec{e}^{\,S_1}$)
- exit point displacement foundation relative to average position foundation exit:
  $\underline{\xi}^{S_{\mathrm{FF}(1)}}$, $\underline{x}^{S_{\mathrm{FF}(1)}^{\oplus}}$ (along average f.c.s. $\vec{e}^{\,\bar{S}_1}$).

The output vector from S_{f} has the following composition:

$$\underline{y}^{S_{\mathrm{f}}} = \begin{bmatrix} \underline{y}^{GS_{\mathrm{f}}} \\ \underline{y}^{S_{\mathrm{t}}S_{\mathrm{f}}} \end{bmatrix}$$

with

$$\underline{y}^{GS_{\mathrm{f}}} = \begin{bmatrix} \delta^{\bar{S}_0^{\ominus}}\underline{r}^{S_1^{\oplus}/B} \\ {}^{\mathrm{FT}}\underline{f}^{S_1^{\ominus}/B} \\ {}^{\mathrm{FT}}\underline{t}^{S_1^{\ominus}/B} \end{bmatrix}; \quad \underline{y}^{S_{\mathrm{t}}S_{\mathrm{f}}} = \begin{bmatrix} \underline{\omega}^{S_{\mathrm{FF}(1)}} \\ \underline{\alpha}^{S_{\mathrm{FF}(1)}} \\ \underline{v}^{S_{\mathrm{FF}(1)}^{\oplus}} \\ \underline{a}^{S_{\mathrm{FF}(1)}^{\oplus}} \\ \underline{u}_{\mathrm{ori}}^{S_{\mathrm{FF}(1)}} \\ \underline{g}_{\mathrm{ori}}^{S_{\mathrm{FF}(1)}} \\ \underline{\xi}^{S_{\mathrm{FF}(1)}} \\ \underline{x}^{S_{\mathrm{FF}(1)}^{\oplus}} \\ {}^{\mathrm{h}}\underline{q}^{S_{\mathrm{FF}(1)}} \end{bmatrix} \tag{A.326}$$

The (zero-mean) feedthrough kinematic vectors $\underline{\omega}^{S_{\mathrm{FF}(1)}}$, $\underline{\alpha}^{S_{\mathrm{FF}(1)}}$, $\underline{v}^{S_{\mathrm{FF}(1)}^{\oplus}}$ and $\underline{a}^{S_{\mathrm{FF}(1)}^{\oplus}}$ to the tower S_{t} are supplied as coordinate vectors along the f.c.s. $\vec{e}^{\,S_1}$. The expression for the variations follow from Eq. B.1 up to B.7 by setting '$k = 1$' (S_{FF} does not apply because of 'tower base rigidity', that is to say the foundation entry point $S_1^{\ominus}$ does not move) and considering the point $S_1^{\oplus}$ instead of S_1^* for $\underline{v}^{S_{\mathrm{FF}(1)}^{\oplus}}$ and $\underline{a}^{S_{\mathrm{FF}(1)}^{\oplus}}$.

The feedthrough 'orientation change vectors' $\underline{u}_{\mathrm{ori}}^{S_{\mathrm{FF}(1)}}$ and $\underline{g}_{\mathrm{ori}}^{S_{\mathrm{FF}(1)}}$ ($\equiv \underline{u}_{\mathrm{ori}}^{S_{\mathrm{f}}}$, $\underline{g}_{\mathrm{ori}}^{S_{\mathrm{f}}}$) are also expressed along $\vec{e}^{\,S_1}$ (see Eq. B.164 and B.287, B.288).

For the tower base loads, which are expressed in the (fixed) coordinate system of the tower base and which are 'user-output', holds:

$$\begin{aligned} {}^{\mathrm{FT}}\underline{f}^{S_1^{\ominus}/B} &= {}^{S_0}\bar{\Phi}^{S_1}\cdot\left({}^{\mathrm{EX}}\underline{f}^{S_1^{\ominus}}\right) \\ {}^{\mathrm{FT}}\underline{t}^{S_1^{\ominus}/B} &= {}^{S_0}\bar{\Phi}^{S_1}\cdot\left({}^{\mathrm{EX}}\underline{t}^{S_1^{\ominus}}\right) \end{aligned} \tag{A.327}$$

and

$$\begin{aligned} \frac{\partial^{\mathrm{FT}}\underline{f}^{S_1^{\ominus}/B}}{\partial\underline{q}} &= {}^{S_0}\bar{\Phi}^{S_1}\cdot\left(-\frac{\partial\underline{\dot{p}}^{S_1}}{\partial\underline{q}}+\frac{\partial^{\mathrm{EX}}\underline{f}^{S_1^{\ominus}}}{\partial\underline{q}}\right)+ \\ &\quad \delta_{\underline{q}\,\underline{\phi}^S}\cdot\left[\ \mathrm{J}_{v=1}^{3}\Big(\frac{\partial^{S_0}\Phi^{S_1}}{\partial\phi_v^{S_1}}\cdot{}^{\mathrm{FT}}\underline{f}^{S_1^{\ominus}/B}\Big)\ \mathrm{O}_{(2)}\ldots\mathrm{O}_{(M)}\ \right] \\ \frac{\partial^{\mathrm{FT}}\underline{t}^{S_1^{\ominus}/B}}{\partial\underline{q}} &= {}^{S_0}\bar{\Phi}^{S_1}\cdot\left(-\frac{\partial^{S_1^{\ominus}}\underline{h}^{S_1}}{\partial\underline{q}}+\frac{\partial^{\mathrm{EX}}\underline{t}^{S_1^{\ominus}}}{\partial\underline{q}}\right)+ \\ &\quad \delta_{\underline{q}\,\underline{\phi}^S}\cdot\left[\ \mathrm{J}_{v=1}^{3}\Big(\frac{\partial^{S_0}\Phi^{S_1}}{\partial\phi_v^{S_1}}\cdot{}^{\mathrm{FT}}\underline{t}^{S_1^{\ominus}/B}\Big)\ \mathrm{O}_{(2)}\ldots\mathrm{O}_{(M)}\ \right] \end{aligned} \tag{A.328}$$

Note that the last term in the right hand side of both equations only applies if $\underline{q}$ equals $\underline{\phi}^S$!

For the displacement variation vector $\delta^{S_0^{\ominus}}\underline{r}^{S_1^{\oplus}/B}$ with coordinates along the fixed c.s. of the turbine base $B\equiv\bar{S}_0$, holds:

$$\delta^{S_0^{\ominus}}\underline{r}^{S_1^{\oplus}/B} = \sum_{(\underline{z})}\frac{\partial^{S_0^{\ominus}}\underline{r}^{S_1^{\oplus}/B}}{\partial\underline{z}}\cdot\delta\underline{z} \qquad (\underline{z}=\underline{\phi}^S,\underline{\rho}^S) \tag{A.329}$$

with (see discussion from Eq. A.77):

$$\frac{\partial^{S_0^{\ominus}}\underline{r}^{S_1^{\oplus}/B}}{\partial\underline{\phi}^S} = {}^{S_0}\bar{\Phi}^{S_1}\cdot\frac{\partial\underline{v}^{S_1^{\oplus}}}{\partial\underline{\dot{\varphi}}^S}\quad;\quad\frac{\partial^{S_0^{\ominus}}\underline{r}^{S_1^{\oplus}/B}}{\partial\underline{\rho}^S} = {}^{S_0}\bar{\Phi}^{S_1}\cdot\frac{\partial\underline{v}^{S_1^{\oplus}}}{\partial\underline{\dot{\varrho}}^S} \tag{A.330}$$

For the displacement outputs to the tower then holds the following sensitivities (coordinates along average f.c.s. of S_1):

$$\begin{aligned} \frac{\partial\underline{x}^{S_{\mathrm{FF}(1)}}}{\partial\underline{\phi}^S} &= \frac{\partial\underline{v}^{S_1^{\oplus}}}{\partial\underline{\dot{\varphi}}^S}\quad;\quad\frac{\partial\underline{\xi}^{S_{\mathrm{FF}(1)}}}{\partial\underline{\phi}^S} = \frac{\partial\underline{\omega}^{S_1^{\oplus}}}{\partial\underline{\dot{\varphi}}^S} \\ \frac{\partial\underline{x}^{S_{\mathrm{FF}(1)}}}{\partial\underline{\rho}^S} &= \frac{\partial\underline{v}^{S_1^{\oplus}}}{\partial\underline{\dot{\varrho}}^S} \end{aligned} \tag{A.331}$$

The output equation that belongs to the 2$^{\mathrm{nd}}$ order state equation is:

$$\underline{y}^{S_{\mathrm{f}}} = \left[\boldsymbol{H}_{\varphi}^{S_{\mathrm{f}}}\ \ \boldsymbol{H}_{\varrho}^{S_{\mathrm{f}}}\right]\cdot\begin{bmatrix}\underline{\varphi}^S\\ \underline{\varrho}^S\end{bmatrix}+\left[\boldsymbol{L}_{\varphi}^{S_{\mathrm{f}}}\ \ \boldsymbol{L}_{\varrho}^{S_{\mathrm{f}}}\right]\cdot\begin{bmatrix}\underline{\dot{\varphi}}^S\\ \underline{\dot{\varrho}}^S\end{bmatrix}+\boldsymbol{K}^{S_{\mathrm{f}}}\cdot\underline{v}^{S_{\mathrm{f}}} \tag{A.332}$$

The matrix partitions $\boldsymbol{H}_{\varphi}^{S_{\mathrm{f}}}$ and $\boldsymbol{L}_{\varphi}^{S_{\mathrm{f}}}$ map the *angular* dof position and speed variations:

$$\begin{aligned} \boldsymbol{H}_{\varphi}^{S_{\mathrm{f}}} &= \frac{\partial\underline{y}^{S_{\mathrm{f}}}}{\partial\underline{\phi}^S}-\Big(\frac{\partial\underline{y}^{S_{\mathrm{f}}}}{\partial\underline{\ddot{\varphi}}^S}\cdot\left(\boldsymbol{M}^{S_{\mathrm{f}}}\right)_{\varphi}^{-1}+\frac{\partial\underline{y}^{S_{\mathrm{f}}}}{\partial\underline{\ddot{\varrho}}^S}\cdot\left(\boldsymbol{M}^{S_{\mathrm{f}}}\right)_{\varrho}^{-1}\Big)\cdot\boldsymbol{S}_{\varphi}^{S_{\mathrm{f}}} \\ \boldsymbol{L}_{\varphi}^{S_{\mathrm{f}}} &= \frac{\partial\underline{y}^{S_{\mathrm{f}}}}{\partial\underline{\dot{\varphi}}^S}-\Big(\frac{\partial\underline{y}^{S_{\mathrm{f}}}}{\partial\underline{\ddot{\varphi}}^S}\cdot\left(\boldsymbol{M}^{S_{\mathrm{f}}}\right)_{\varphi}^{-1}+\frac{\partial\underline{y}^{S_{\mathrm{f}}}}{\partial\underline{\ddot{\varrho}}^S}\cdot\left(\boldsymbol{M}^{S_{\mathrm{f}}}\right)_{\varrho}^{-1}\Big)\cdot\boldsymbol{D}_{\varphi}^{S_{\mathrm{f}}} \end{aligned} \tag{A.333}$$

The matrix partitions $\boldsymbol{H}_{\varrho}^{S_{\mathrm{f}}}$ and $\boldsymbol{L}_{\varrho}^{S_{\mathrm{f}}}$ map the *linear* dof position and speed variations:

$$\begin{aligned} \boldsymbol{H}_{\varrho}^{S_{\mathrm{f}}} &= \frac{\partial\underline{y}^{S_{\mathrm{f}}}}{\partial\underline{\rho}^S}-\Big(\frac{\partial\underline{y}^{S_{\mathrm{f}}}}{\partial\underline{\ddot{\varphi}}^S}\cdot\left(\boldsymbol{M}^{S_{\mathrm{f}}}\right)_{\varphi}^{-1}+\frac{\partial\underline{y}^{S_{\mathrm{f}}}}{\partial\underline{\ddot{\varrho}}^S}\cdot\left(\boldsymbol{M}^{S_{\mathrm{f}}}\right)_{\varrho}^{-1}\Big)\cdot\boldsymbol{S}_{\varrho}^{S_{\mathrm{f}}} \\ \boldsymbol{L}_{\varrho}^{S_{\mathrm{f}}} &= \frac{\partial\underline{y}^{S_{\mathrm{f}}}}{\partial\underline{\dot{\varrho}}^S}-\Big(\frac{\partial\underline{y}^{S_{\mathrm{f}}}}{\partial\underline{\ddot{\varphi}}^S}\cdot\left(\boldsymbol{M}^{S_{\mathrm{f}}}\right)_{\varphi}^{-1}+\frac{\partial\underline{y}^{S_{\mathrm{f}}}}{\partial\underline{\ddot{\varrho}}^S}\cdot\left(\boldsymbol{M}^{S_{\mathrm{f}}}\right)_{\varrho}^{-1}\Big)\cdot\boldsymbol{D}_{\varrho}^{S_{\mathrm{f}}} \end{aligned} \tag{A.334}$$

For the feedthrough matrix $\boldsymbol{K}^{S_\mathrm{f}}$ holds:

$$\boldsymbol{K}^{S_\mathrm{f}} \;=\; \frac{\partial \underline{y}^{S_\mathrm{f}}}{\partial \underline{v}^{S_\mathrm{f}}} - \Big(\frac{\partial \underline{y}^{S_\mathrm{f}}}{\partial \underline{\dot{v}}^{S}} \cdot \Big(\boldsymbol{M}^{S_\mathrm{f}}\Big)_{\varphi}^{-1} + \frac{\partial \underline{y}^{S_\mathrm{f}}}{\partial \underline{\ddot{v}}^{S}} \cdot \Big(\boldsymbol{M}^{S_\mathrm{f}}\Big)_{\varrho}^{-1} \Big) \cdot \boldsymbol{G}^{S_\mathrm{f}} \qquad \text{(A.335)}$$

The partial derivatives to the dof vectors are cleaned up before use in the determination of the output and feedthrough matrices: columns that pertain to non-dof directions as concerns S_f are removed.

The partial derivative of the composed output vector $\underline{y}^{S_\mathrm{f}}$ to the composed input vector is obtained by (i) stacking the partial derivatives of the output subvectors to an input subvector, and (ii) doing this for all input subvectors and putting next to each other the obtained 'stacks'. The generic expression for the overall partial derivative matrix is (see e.g. also Eq. A.88):

$$\frac{\partial \underline{y}^{S_\mathrm{f}}}{\partial \underline{v}^{S_\mathrm{f}}} = \mathrm{J}_{(\underline{q}_\mathrm{v})}\Big(\mathrm{S}_{(\underline{z}_\mathrm{y})}\Big(\frac{\partial \underline{z}_\mathrm{y}}{\partial \underline{q}_\mathrm{v}}\Big)\Big) \quad \text{with} \quad \left\{ \begin{array}{l} \underline{q}_\mathrm{v} = \underline{w}^{S}_{\mathrm{horz}}, \underline{\dot{w}}^{S}_{\mathrm{horz}}, {}^{\mathrm{FT}}\underline{f}^{S_{\mathrm{PP}(2)}}, {}^{\mathrm{FT}}\underline{t}^{S_{\mathrm{PP}(2)}}, {}^{\mathrm{h}}\underline{q}^{S_{\mathrm{PP}(2)}} \\ \underline{z}_\mathrm{y} = \delta^{S^{\ominus}_{0}}\underline{r}^{S^{\oplus/B}_{1}}, {}^{\mathrm{FT}}\underline{f}^{S^{\ominus/B}_{1}}, {}^{\mathrm{FT}}\underline{t}^{S^{\ominus/B}_{1}}, \underline{\omega}^{S^{\oplus}_{\mathrm{FF}(1)}}, \underline{\alpha}^{S_{\mathrm{FF}(1)}}, \\ \qquad \underline{v}^{S^{\oplus}_{\mathrm{FF}(1)}}, \underline{a}^{S^{\oplus}_{\mathrm{FF}(1)}}, \underline{u}^{S_{\mathrm{FF}(1)}}_{\mathrm{ori}}, \underline{g}^{S_{\mathrm{FF}(1)}}_{\mathrm{ori}}, \underline{\xi}^{S_{\mathrm{FF}(1)}}, \underline{x}^{S_{\mathrm{FF}(1)}}, {}^{\mathrm{h}}\underline{q}^{S_{\mathrm{FF}(1)}} \end{array} \right. \qquad \text{(A.336)}$$

APPENDIX B. MOTION AND LOADING

The equations of motion for a subcomponent of a substructure (e.g. the tower in the support structure) follow from the linearised coordinates of the impulse vector equations along the local coordinate systems on the elements. The impulse equations are established by motions and loads. This appendix provides the expressions for the means and variations in terms of average coordinate values and their sensitivities to degrees of freedom and inputs in the required coordinate systems.

The linearised expressions in the motion and loading formulations were obtained by approximation through the basic principle only: neglect all products that consist of two or more variations in the degrees of freedom within a subcomponent and or the inputs from another subcomponent or 'from outside' (wind, wave or periodic gravity load). The background behind the linearised approach to the formulation of kinematic quantities is given in chapter 4 in [5]. The remaining sections of this chapter deal with the expressions for the mean and variation of those quantities that are required for the parametrisation of the equations of motion. The expressions are focused on the applied substructures and their subdivisions in subcomponents. They pertain to the:

- angular and linear velocity and acceleration, as well as the rate of change of the angular and linear impulse, of the elements of the support structure, drive-train and rotor blades (section B.1, B.2, B.3);
- flap, lead and setting angle of the blade elements, the relative wind speed in the aerodynamic conversion points and the inflow angle and angle of attack (section B.4, B.5, B.6);
- aerodynamic loads in the conversion points of the blade elements (section B.7)
- transportation speed and Prandtl's correction factor in the rotor annuli (section B.8);
- hydrodynamic loads in the conversion points of the support structure elements (section B.9)
- gravitation loads on all elements (section B.10)

The sections section B.1, B.2 and B.3 also comprise the partitioning of the three (main) turbine components in subcomponents.

B.1 Support structure motion

For the layout of the support structure model S see section 3.8.1. Expressions for the means and sensitivity functions for the kinematic quantitites are given in section B.1.1 while this is done for the angular and linear impulse in section B.1.2. The means and sensitivities are calculated and stored as fields in structure variables by calls to M-functions TBUSUPSTRKIN() and TBUSUPSTRIMP() from TBUSUPSTREOM(). A 'sensitivity field' is a structure variable by itself: the 'subfields' contain the actual partial derivatives.

B.1.1 Support structure kinematics

The expressions for the kinematic quantities are summarized as sums of matrix/vector products of partial derivatives and column vectors with time derivatives of degrees of freedom or with kinematic quantities of the final element in the foregoing subcomponent. This final foregoing element is typed as S_{FF} and is the turbine base for foundation S_{f}, the

element S_1 for the tower S_t and the element S_{M-1} for the nacelle S_n. Only *variations* apply in the kinematics of the support structure. For the angular kinematic vectors hold:

$$\begin{aligned} \delta\underline{\omega}^{S_k} &= \frac{\partial \underline{\omega}^{S_k}}{\partial \underline{\omega}^{S_{\mathrm{FF}}}} \cdot \delta\underline{\omega}^{S_{\mathrm{FF}}} + \frac{\partial \underline{\omega}^{S_k}}{\partial \underline{\dot{\varphi}}^{S}} \cdot \underline{\dot{\varphi}}^{S} \\ \delta\underline{\alpha}^{S_k} &= \frac{\partial \underline{\alpha}^{S_k}}{\partial \underline{\alpha}^{S_{\mathrm{FF}}}} \cdot \delta\underline{\alpha}^{S_{\mathrm{FF}}} + \frac{\partial \underline{\alpha}^{S_k}}{\partial \underline{\dot{\varphi}}^{S}} \cdot \underline{\ddot{\varphi}}^{S} \end{aligned} \tag{B.1}$$

For the linear kinematic vectors for a centre of gravity hold:

$$\begin{aligned} \delta\underline{v}^{S_k^*} &= \frac{\partial \underline{v}^{S_k^*}}{\partial \underline{v}^{S_{\mathrm{FF}}}} \cdot \delta\underline{v}^{S_{\mathrm{FF}}^{\oplus}} + \frac{\partial \underline{v}^{S_k^*}}{\partial \underline{\omega}^{S_{\mathrm{FF}}}} \cdot \delta\underline{\omega}^{S_{\mathrm{FF}}} + \frac{\partial \underline{v}^{S_k^*}}{\partial \underline{\dot{\varphi}}^{S}} \cdot \underline{\dot{\varphi}}^{S} + \frac{\partial \underline{v}^{S_k^*}}{\partial \underline{\dot{\varrho}}^{S}} \cdot \underline{\dot{\varrho}}^{S} \\ \delta\underline{a}^{S_k^*} &= \frac{\partial \underline{a}^{S_k^*}}{\partial \underline{a}^{S_{\mathrm{FF}}}} \cdot \delta\underline{a}^{S_{\mathrm{FF}}^{\oplus}} + \frac{\partial \underline{a}^{S_k^*}}{\partial \underline{\omega}^{S_{\mathrm{FF}}}} \cdot \delta\underline{\omega}^{S_{\mathrm{FF}}} + \frac{\partial \underline{a}^{S_k^*}}{\partial \underline{\dot{\varphi}}^{S}} \cdot \underline{\ddot{\varphi}}^{S} + \frac{\partial \underline{a}^{S_k^*}}{\partial \underline{\dot{\varrho}}^{S}} \cdot \underline{\ddot{\varrho}}^{S} \end{aligned} \tag{B.2}$$

All the involved partial derivatives are eventually composed of the average transformation matrices within the support structure and place vectors on the elements. The expressions below however contain $\boldsymbol{G}$- and $\boldsymbol{R}$-type matrices. $\boldsymbol{R}$-matrices consist of 'place column vectors' that map rotation dofs, or rotations of S_{FF}, to a linear kinematic vector. $\boldsymbol{G}$-matrices consist of 'gain column vectors' that map rotations to an angular kinematic vector or translations to a linear kinematic vector.

$$\frac{\partial \underline{\omega}^{S_k}}{\partial \underline{\omega}^{S_{\mathrm{FF}}}} \equiv \frac{\partial \underline{\alpha}^{S_k}}{\partial \underline{\alpha}^{S_{\mathrm{FF}}}} \equiv \frac{\partial \underline{v}^{S_k^*}}{\partial \underline{v}^{S_{\mathrm{FF}}}} \equiv \frac{\partial \underline{a}^{S_k^*}}{\partial \underline{a}^{S_{\mathrm{FF}}}} = \begin{cases} \mathrm{O} & (k=1) \\ {}^{S_k}\bar{\Phi}^{S_1} & (k=2\ldots M-1, \text{use Eq. 3.80}) \\ {}^{S_M}\bar{\Phi}^{S_{M-1}} & (k=M, \text{use Eq. 3.80}) \end{cases} \tag{B.3}$$

For the remaining partial derivatives holds:

$$\frac{\partial \underline{v}^{S_k^*}}{\partial \underline{\omega}^{S_{\mathrm{FF}}}} \equiv \frac{\partial \underline{a}^{S_k^*}}{\partial \underline{\alpha}^{S_{\mathrm{FF}}}} = \begin{cases} \mathrm{O} & (k=1) \\ \boldsymbol{R}_{k\mathrm{f}}^{S_{\mathrm{t}}^*} & (k=2\ldots M-1, \text{use Eq. B.15}) \\ \boldsymbol{R}_{M\mathrm{t}}^{S_{\mathrm{n}}^*} & (k=M, \text{use Eq. B.19}) \end{cases} \tag{B.4}$$

and

$$\frac{\partial \underline{\omega}^{S_k}}{\partial \underline{\dot{\varphi}}^{S}} \equiv \frac{\partial \underline{\alpha}^{S_k}}{\partial \underline{\ddot{\varphi}}^{S}} = \begin{cases} \left(\boldsymbol{G}_{11}^{S_{\mathrm{f}}^{\mathrm{r}}} \;\; \mathrm{O}_{(2)} \ldots \mathrm{O}_{(M)}\right) & (k=1, \text{use Eq. B.8}) \\ \left(\mathrm{O} \;\; \mathrm{J}_{i=2}^{k}(\boldsymbol{G}_{ki}^{S_{\mathrm{t}}^{\mathrm{r}}}) \;\; \mathrm{O}_{(k+1)} \ldots \mathrm{O}_{(M)}\right) & (k=2\ldots M-1, \text{use Eq. B.14}) \\ \left(\mathrm{O}_{(1)} \ldots \mathrm{O}_{(M-1)} \;\; \boldsymbol{G}_{MM}^{S_{\mathrm{n}}^{\mathrm{r}}}\right) & (k=M, \text{use Eq. B.19}) \end{cases} \tag{B.5}$$

and

$$\frac{\partial \underline{v}^{S_k^*}}{\partial \underline{\dot{\varrho}}^{S}} \equiv \frac{\partial \underline{a}^{S_k^*}}{\partial \underline{\ddot{\varrho}}^{S}} = \begin{cases} \left(\boldsymbol{G}_{11}^{S_{\mathrm{f}}^{\mathrm{t}}} \;\; \mathrm{O}_{(2)} \ldots \mathrm{O}_{(M)}\right) & (k=1, \text{use Eq. B.10}) \\ \left(\mathrm{O} \;\; \mathrm{J}_{i=2}^{k}(\boldsymbol{G}_{ki}^{S_{\mathrm{t}}^{\mathrm{t}}}) \;\; \mathrm{O}_{(k+1)} \ldots \mathrm{O}_{(M)}\right) & (k=2\ldots M-1, \text{use Eq. B.14}) \\ \left(\mathrm{O}_{(1)} \ldots \mathrm{O}_{(M)}\right) & (k=M) \end{cases} \tag{B.6}$$

and

$$\frac{\partial \underline{v}^{S_k^*}}{\partial \underline{\dot{\varphi}}^{S}} \equiv \frac{\partial \underline{a}^{S_k^*}}{\partial \underline{\ddot{\varphi}}^{S}} = \begin{cases} \left(\boldsymbol{R}_{11}^{S_{\mathrm{f}}^*} \;\; \mathrm{O}_{(2)} \ldots \mathrm{O}_{(M)}\right) & (k=1, \text{use Eq. B.10}) \\ \left(\mathrm{O} \;\; \mathrm{J}_{i=2}^{k}(\boldsymbol{R}_{ki}^{S_{\mathrm{t}}^*}) \;\; \mathrm{O}_{(k+1)} \ldots \mathrm{O}_{(M)}\right) & (k=2\ldots M-1, \text{use Eq. B.15}) \\ \left(\mathrm{O}_{(1)} \ldots \mathrm{O}_{(M-1)} \;\; \boldsymbol{R}_{MM}^{S_{\mathrm{n}}^*}\right) & (k=M, \text{use Eq. B.19}) \end{cases} \tag{B.7}$$

The operator expression $\mathrm{J}_{i=2}^{k}(\boldsymbol{P}_i)$ implies that the matrices $\boldsymbol{P}_i$ are put next to each other from left ro right for $i = 2 \ldots k$.

All $\boldsymbol{G}$- and $\boldsymbol{R}$-matrices are dealt with in the three subparagraphs below.

Kinematics foundation S_f
The angular velocity and acceleration of the one-element subcomponent S_f are obtained by (zero-mean; linearised variation):

$$\begin{aligned} \delta\underline{\omega}^{S_1} &= \sum_{v=1}^{3} {}^{S_1}\underline{\bar{\Phi}}_v^{S_1^{\iota\mathrm{r}}} \cdot \dot{\varphi}_v^{S_1} = {}^{S_1}\bar{\Phi}^{S_1^{\iota\mathrm{r}}} \cdot \underline{\dot{\varphi}}^{S_1} = \boldsymbol{G}_{11}^{S_\mathrm{f}^\mathrm{r}} \cdot \underline{\dot{\varphi}}^{S_1} \\ \delta\underline{\alpha}^{S_1} &= \sum_{v=1}^{3} {}^{S_1}\underline{\bar{\Phi}}_v^{S_1^{\iota\mathrm{r}}} \cdot \dot{\varphi}_v^{S_1} = {}^{S_1}\bar{\Phi}^{S_1^{\iota\mathrm{r}}} \cdot \underline{\ddot{\varphi}}^{S_1} = \boldsymbol{G}_{11}^{S_\mathrm{f}^\mathrm{r}} \cdot \underline{\ddot{\varphi}}^{S_1} \end{aligned} \tag{B.8}$$

with the internal rotation transformation matrix for rotation order 'z,y,x' given by:

$${}^{S_1}\bar{\Phi}^{S_1^{\iota\mathrm{r}}} = \left[{}^{S_1}\bar{\Phi}^{S_1^2} \cdot {}^{S_1^2}\underline{\bar{\Phi}}_3^{S_1^1} \quad {}^{S_1}\underline{\bar{\Phi}}_2^{S_1^2} \quad \underline{e}_1 \right] = \left[\Phi_\mathrm{x}(\bar{\phi}_3^{S_1}) \cdot \underline{\Phi}_{\mathrm{y}_3}(\bar{\phi}_2^{S_1}) \quad \underline{\Phi}_{\mathrm{x}_2}(\bar{\phi}_3^{S_1}) \quad \underline{e}_1 \right] \tag{B.9}$$

The linear velocity and acceleration in the centre of gravity are obtained by (zero-mean; linearised varation):

$$\begin{aligned} \delta\underline{v}^{S_1^*} &= \sum_{v=1}^{3} {}^{S_1}\underline{\bar{\Phi}}_v^{S_1^{\iota\mathrm{r}}} \times {}^{S_1^\ominus}\underline{r}^{S_1^*} \cdot \dot{\varphi}_v^{S_1} + {}^{S_1}\bar{\Phi}^{S_1^{\iota\mathrm{t}}} \cdot \underline{\dot{\varrho}}^{S_1} = \boldsymbol{R}_{11}^{S_\mathrm{f}^*} \cdot \underline{\dot{\varphi}}^{S_1} + \boldsymbol{G}_{11}^{S_\mathrm{f}^\mathrm{t}} \cdot \underline{\dot{\varrho}}^{S_1} \\ \delta\underline{a}^{S_1^*} &= \sum_{v=1}^{3} {}^{S_1}\underline{\bar{\Phi}}_v^{S_1^{\iota\mathrm{r}}} \times {}^{S_1^\ominus}\underline{r}^{S_1^*} \cdot \ddot{\varphi}_v^{S_1} + {}^{S_1}\bar{\Phi}^{S_1^{\iota\mathrm{t}}} \cdot \underline{\ddot{\varrho}}^{S_1} = \boldsymbol{R}_{11}^{S_\mathrm{f}^*} \cdot \underline{\ddot{\varphi}}^{S_1} + \boldsymbol{G}_{11}^{S_\mathrm{f}^\mathrm{t}} \cdot \underline{\ddot{\varrho}}^{S_1} \end{aligned} \tag{B.10}$$

with internal transformation matrix ${}^{S_1}\bar{\Phi}^{S_1^{\iota\mathrm{t}}}$ for translation order 'z,x,y' given by:

$${}^{S_1}\bar{\Phi}^{S_1^{\iota\mathrm{t}}} = \left[{}^{S_1}\bar{\Phi}^{S_1^2} \cdot {}^{S_1^2}\underline{\bar{\Phi}}_3^{S_1^1} \quad {}^{S_1}\underline{\bar{\Phi}}_1^{S_1^2} \quad \underline{e}_2 \right] = \left[\Phi_\mathrm{x}(\bar{\phi}_3^{S_1}) \cdot \underline{\Phi}_{\mathrm{y}_3}(\bar{\phi}_2^{S_1}) \quad \underline{\Phi}_{\mathrm{x}_1}(\bar{\phi}_3^{S_1}) \quad \underline{e}_2 \right] \tag{B.11}$$

The expressions for the linear velocity and acceleration in hydrodynamic conversion point S_1^h are the same as for the centre of gravity, except S_1^* is replaced by S_1^h. This also holds for the exit point $S_1^\oplus$, where S_1 is replaced by $S_1^\oplus$.

The exit point of the final element of the foundation ($S_\mathrm{f}^\oplus$) coincides with the exit point $S_1^\oplus$. The angular and linear velocity and acceleration on the (exit point of the) final foundation element are typed as $\underline{\omega}^{S_\mathrm{f}^\oplus}$, $\underline{\alpha}^{S_\mathrm{f}^\oplus}$, $\underline{v}^{S_\mathrm{f}^\oplus}$, and $\underline{a}^{S_\mathrm{f}^\oplus}$.

Kinematics tower S_t
The angular velocity and acceleration of the elements $S_{2\ldots M-1}$ in subcomponent S_t are obtained by (zero-mean; linearised variation):

$$\begin{aligned} \delta\underline{\omega}^{S_k} &= {}^{S_k}\bar{\Phi}^{S_1} \cdot \underline{\omega}^{S_\mathrm{f}^\oplus} + \sum_{i=2}^{k} \boldsymbol{G}_{ki}^{S_\mathrm{t}^\mathrm{r}} \cdot \underline{\dot{\varphi}}^{S_i} \\ \delta\underline{\alpha}^{S_k} &= {}^{S_k}\bar{\Phi}^{S_1} \cdot \underline{\alpha}^{S_\mathrm{f}^\oplus} + \sum_{i=2}^{k} \boldsymbol{G}_{ki}^{S_\mathrm{t}^\mathrm{r}} \cdot \underline{\ddot{\varphi}}^{S_i} \end{aligned} \tag{B.12}$$

The linear velocity and acceleration in the centre of gravity of the tower elements $S_{2\ldots M-1}$

are obtained by (zero-mean; linearised varation):

$$\begin{aligned}
\delta\underline{v}^{S_k^*} &= {}^{S_k}\bar{\Phi}^{S_1}\cdot\underline{v}^{S_{\mathrm{f}}^{\oplus}} + \boldsymbol{R}_{k\mathrm{f}}^{S_{\mathrm{t}}^*}\cdot\underline{\omega}^{S_{\mathrm{f}}^{\oplus}} + \sum_{i=2}^{k}\boldsymbol{R}_{ki}^{S_{\mathrm{t}}^*}\cdot\underline{\dot{\varphi}}^{S_i} + \boldsymbol{G}_{ki}^{S_{\mathrm{t}}^{\mathrm{t}}}\cdot\underline{\dot{\varrho}}^{S_i} \\
\delta\underline{a}^{S_k^*} &= {}^{S_k}\bar{\Phi}^{S_1}\cdot\underline{a}^{S_{\mathrm{f}}^{\oplus}} + \boldsymbol{R}_{k\mathrm{f}}^{S_{\mathrm{t}}^*}\cdot\underline{\alpha}^{S_{\mathrm{f}}^{\oplus}} + \sum_{i=2}^{k}\boldsymbol{R}_{ki}^{S_{\mathrm{t}}^*}\cdot\underline{\ddot{\varphi}}^{S_i} + \boldsymbol{G}_{ki}^{S_{\mathrm{t}}^{\mathrm{t}}}\cdot\underline{\ddot{\varrho}}^{S_i}
\end{aligned} \tag{B.13}$$

The 'gain' matrix $\boldsymbol{G}_{ki}^{S_{\mathrm{t}}^{\mathrm{r}}}$ maps the rotation degrees of freedom for element S_i to contributions to the x-, y- and z component of the angular kinematic vector on element S_k in the final coordinate system of S_k. The 'gain' matrix $\boldsymbol{G}_{ki}^{S_{\mathrm{t}}^{\mathrm{t}}}$ maps *translation* degrees of freedom to a *linear* kinematic vector. It holds:

$$\begin{aligned}
\boldsymbol{G}_{ki}^{S_{\mathrm{t}}^{\mathrm{r}}} &= {}^{S_k}\bar{\Phi}^{S_i}\,.\,{}^{S_i}\bar{\Phi}^{S_i^{\iota\mathrm{r}}} \\
\boldsymbol{G}_{ki}^{S_{\mathrm{t}}^{\mathrm{t}}} &= {}^{S_k}\bar{\Phi}^{S_i}\,.\,{}^{S_i}\bar{\Phi}^{S_i^{\iota\mathrm{t}}}
\end{aligned} \tag{B.14}$$

Use equation B.9 and B.11 for the interntal rotation and translation transformation matrix ${}^{S_i}\bar{\Phi}^{S_i^{\iota\mathrm{r}}}$ and ${}^{S_i}\bar{\Phi}^{S_i^{\iota\mathrm{t}}}$ through subtitution of S_1 by S_i.

The 'place vector' matrix $\boldsymbol{R}_{ki}^{S_{\mathrm{t}}^*}$ maps the rotation degrees of freedom for element S_i to contributions to the x-, y- and z component of the linear kinematic vector in the centre of gravity of element S_k in the final coordinate system of S_k; place vector matrix $\boldsymbol{R}_{k\mathrm{f}}^{S_{\mathrm{t}}^*}$ maps the angular kinematic vector of the final element of the foregoing subcomponent, the foundation, to the linear kinematic vector under consideration. It holds :

$$\begin{aligned}
\boldsymbol{R}_{ki}^{S_{\mathrm{t}}^*} &= \sum_{p=i}^{k}{}^{S_k}\bar{\Phi}^{S_p}\cdot\mathrm{J}_{v=1}^{3}\big({}^{S_p}\bar{\Phi}^{S_i}\,.\,{}^{S_i}\underline{\bar{\Phi}}_{v}^{S_i^{\iota\mathrm{r}}}\times{}^{S_p^{\ominus}}\underline{r}^{S_{p|k}^{\oplus|*}}\big) \\
\boldsymbol{R}_{k\mathrm{f}}^{S_{\mathrm{t}}^*} &= \sum_{p=2}^{k}{}^{S_k}\bar{\Phi}^{S_p}\cdot\mathrm{J}_{v=1}^{3}\big({}^{S_p}\underline{\bar{\Phi}}_{v}^{S_1}\times{}^{S_p^{\ominus}}\underline{r}^{S_{p|k}^{\oplus|*}}\big)
\end{aligned} \tag{B.15}$$

The operator expression $\mathrm{J}_{v=1}^{3}(\underline{q}_v)$ implies that the coordinate vectors $\underline{q}_v$ are put next to each other from left ro right for $v = 1, 2, 3,$.

The place vector ${}^{S_p^{\ominus}}\underline{r}^{S_{p|k}^{\oplus|*}}$ runs to the exit point if $p < k$ and to the centre of gravity if $p = k$.

Note that only two translation dofs wil be involved: ρ_2 along the x-axis and ρ_3 along the y-axis, which pertain to fore-aft and sideward tower bending (ϕ_2 along y-axis, ϕ_3 along x-axis!).

The expressions for the linear kinematic quantities in S_k^{h} and $S_k^{\oplus}$ are obtained from those for S_k^* through substituion of '*' by 'h' (for $k = 2 \ldots N_{\mathrm{uw}}$) or '$\oplus$' (for $k = 2 \ldots M-1$).

The angular and linear velocity and acceleration on the (exit point of the) final tower element are typed as $\underline{\omega}^{S_{\mathrm{t}}^{\oplus}}$, $\underline{\alpha}^{S_{\mathrm{t}}^{\oplus}}$, $\underline{v}^{S_{\mathrm{t}}^{\oplus}}$, and $\underline{a}^{S_{\mathrm{t}}^{\oplus}}$.

Kinematics nacelle S_{n}
The angular velocity and acceleration of the one element subcomponent S_{n} are obtained by (zero-mean; linearised variation):

$$\begin{aligned}
\delta\underline{\omega}^{S_M} &= {}^{S_M}\bar{\Phi}^{S_{M-1}}\cdot\underline{\omega}^{S_{\mathrm{t}}^{\oplus}} + \boldsymbol{G}_{MM}^{S_{\mathrm{n}}^{\mathrm{r}}}\cdot\underline{\dot{\varphi}}^{S_M} \\
\delta\underline{\alpha}^{S_M} &= {}^{S_M}\bar{\Phi}^{S_{M-1}}\cdot\underline{\alpha}^{S_{\mathrm{t}}^{\oplus}} + \boldsymbol{G}_{MM}^{S_{\mathrm{n}}^{\mathrm{r}}}\cdot\underline{\ddot{\varphi}}^{S_M}
\end{aligned} \tag{B.16}$$

The linear velocity and acceleration in the centre of gravity of the tower elements $S_{2\ldots M-1}$ are obtained by (zero-mean; linearised varation):

$$\begin{aligned} \delta\underline{v}^{S_M^*} &= {}^{S_M}\bar{\Phi}^{S_{M-1}} \cdot \underline{v}^{S_{\mathrm{t}}^{\oplus}} + \boldsymbol{R}_{M\mathrm{t}}^{S_{\mathrm{n}}^*} \cdot \underline{\omega}^{S_{\mathrm{t}}^{\oplus}} + \boldsymbol{R}_{MM}^{S_{\mathrm{n}}^*} \cdot \dot{\underline{\varphi}}^{S_M} \\ \delta\underline{a}^{S_M^*} &= {}^{S_M}\bar{\Phi}^{S_{M-1}} \cdot \underline{a}^{S_{\mathrm{t}}^{\oplus}} + \boldsymbol{R}_{M\mathrm{t}}^{S_{\mathrm{n}}^*} \cdot \underline{\alpha}^{S_{\mathrm{t}}^{\oplus}} + \boldsymbol{R}_{MM}^{S_{\mathrm{n}}^*} \cdot \ddot{\underline{\varphi}}^{S_M} \end{aligned} \tag{B.17}$$

Note that no translation dofs are involved in the nacelle.

The internal rotation transformation matrix of the nacelle is given by (rotation order 'z,y,x'; rotation along x-axis $\equiv 0$):

$${}^{S_M}\bar{\Phi}^{S_M^{\iota\mathrm{r}}} = \left[{}^{S_M}\bar{\Phi}^{S_M^2} \cdot {}^{S_M^2}\underline{\Phi}_3^{S_M^1} \quad {}^{S_M}\underline{\Phi}_2^{S_M^2} \quad \underline{e}_1 \right] = \left[\Phi_{\mathrm{x}}(0) \cdot \underline{\Phi}_{\mathrm{y}_3}(-\phi_{\mathrm{ti}}^S) \quad \underline{\Phi}_{\mathrm{x}_2}(0) \quad \underline{e}_1 \right] \tag{B.18}$$

For the place and gain vector sets in matrix-types $\boldsymbol{R}$ and $\boldsymbol{G}$ holds:

$$\begin{aligned} \boldsymbol{G}_{MM}^{S_{\mathrm{t}}^{\mathrm{r}}} &= {}^{S_M}\bar{\Phi}^{S_M^{\iota\mathrm{r}}} \\ \boldsymbol{R}_{MM}^{S_{\mathrm{n}}^*} &= \mathrm{J}_{v=1}^{3}({}^{S_M}\underline{\bar{\Phi}}_v^{S_M^{\iota\mathrm{r}}} \times {}^{S_M^{\ominus}}\underline{r}^{S_M^*}) \\ \boldsymbol{R}_{M\mathrm{t}}^{S_{\mathrm{t}}^*} &= \mathrm{J}_{v=1}^{3}({}^{S_M}\underline{\bar{\Phi}}_v^{S_{M-1}} \times {}^{S_M^{\ominus}}\underline{r}^{S_M^*}) \end{aligned} \tag{B.19}$$

The expressions for the linear kinematic quantities in the exit point to the rotor centre $S_M^{\oplus\mathrm{r}}$ are obtained from those for S_k^* through substitution of '*' by '$\oplus$r'.

The angular and linear velocity and acceleration on the (exit point to the rotor centre of the) final nacelle element are typed as $\underline{\omega}^{S_{\mathrm{n}}^{\oplus\mathrm{r}}}$, $\underline{\alpha}^{S_{\mathrm{n}}^{\oplus\mathrm{r}}}$, $\underline{v}^{S_{\mathrm{n}}^{\oplus\mathrm{r}}}$, and $\underline{a}^{S_{\mathrm{n}}^{\oplus\mathrm{r}}}$.

B.1.2 Support structure impulse

Just as the kinematic quantities, the angular and linear impulse vectors $\vec{h}$ and $\vec{p}$ for a support structure element S_k are expressed in coordinates along the local coordinate system of S_k . The angular impulse is taken relative to the moving entry point $S_k^{\ominus}$. Actually we use the *biased* angular impulse ${}^{S_k^{\ominus}}\vec{\not{h}}^{S_k}$, which excludes the term that is set up by the linear acceleration of the reference point $S_k^{\ominus}$. The time derivative relative to the (non-moving) earth G of this biased angular impulse equals the torque load in $S_k^{\ominus}$ (see discussion in §5.1.3 of [5]). It holds:

$${}^{S_k^{\ominus}}\underline{\dot{\not{h}}}^{S_k} \triangleq \left({}^{(G)}\frac{\mathrm{d}}{\mathrm{d}t}\left({}^{S_k^{\ominus}}\vec{\not{h}}^{S_k} \right) \right)^{S_k} = {}^{S_k^{\ominus}}\underline{r}^{S_k^*} \times m^{S_k}\underline{a}^{S_k^*} + \boldsymbol{I}^{S_k} \cdot \underline{\alpha}^{S_k} + \underline{\omega}^{S_k} \times \boldsymbol{I}^{S_k} \cdot \underline{\omega}^{S_k} \tag{B.20}$$

The inertia matrix $\boldsymbol{I}^{S_k}$ contains the inertia moments and products relative to the centre of gravity of S_k and applies along the axes of the final coordinate system of S_k. For the foundation and tower elements, the principle x- and y-axis coincide with the neutral bending elastic x and y-axis, the matrix $\boldsymbol{I}^{S_k}$ is simply the diagonal of the priniciple moments of inertia $J_{x,y,z}^{S_k}$:

$$\boldsymbol{I}^{S_k} = \begin{pmatrix} J_x^{S_k} & 0 & 0 \\ 0 & J_x^{S_k} & 0 \\ 0 & 0 & J_x^{S_k} \end{pmatrix} \quad \text{for } k = 1 \ldots M-1 \tag{B.21}$$

The principle axes of the nacelle S_{n} are assumed to coincide with the axes of the final coordinate system of the last tower element S_{M-1} *after the yaw rotation*; the belonging priniciple moments of inertia are $J_{x,y,z}^{S_{\mathrm{n}}}$. As the expression for the nacelle's angular impulse applies in the final coordinate system of S_M, the inertia matrix $\boldsymbol{I}^{S_M}$ is obtained from the principle moments of inertia after transformation over minus the tilt angle ϕ_{ti}^S along the y-axis (note: $(I \bullet \alpha)^{S_M} = {}^{S_M}\Phi^{S_M^2} \cdot (I \bullet \vec{\alpha})^{S_M^2} = {}^{S_M}\Phi^{S_M^2} \cdot (I)^{S_M^2} \cdot ({}^{S_M}\Phi^{S_M^2})^{\mathrm{T}} \cdot {}^{S_M}\Phi^{S_M^2} \bullet (\vec{\alpha})^{S_M^2}$

with ${}^{S_M}\Phi^{S^2_M} = \Phi_{\rm y}(-\phi^S_{\rm ti})$). In addition the inertia matrix is augmented with the principle moments of inertia relative to the y and $z-axis$ of the gearbox house ($J^{R_{\rm h}}_{y,z}$ see section B.2.2); these moments of inertia apply along the *tilted* y- and z-axis:

$$\boldsymbol{I}^{S_M} = \Phi_{\rm y}(-\phi^S_{\rm ti}) \cdot \begin{pmatrix} J_x^{S_{\rm n}} & 0 & 0 \\ 0 & J_y^{S_{\rm n}} & 0 \\ 0 & 0 & J_z^{S_{\rm n}} \end{pmatrix} \cdot \Phi^{\rm T}_{\rm y}(-\phi^S_{\rm ti}) \;+\; \begin{pmatrix} 0 & 0 & 0 \\ 0 & J_y^{R_{\rm h}} & 0 \\ 0 & 0 & J_z^{R_{\rm h}} \end{pmatrix} \tag{B.22}$$

In section B.2.2 is motivated that the right hand side of the equation above is to be augmented ('summed') with the (non-coaxial) inertia parameters $J^{R_{\rm f}}_{\rm y}$ and $J^{R_{\rm f}}_{\rm z}$ from $R_{\rm f}$ *when the sensitivity of the impulse vectors of* $S_{\rm n}$ *to acceleration variables is considered.*

The inertia parameters of $R_{\rm f}$ are dealt with in another way *when the sensitivity of the angular impulse to the angular speed is considered.* Visually, the non-zero mean angular speed $i_{\rm gb}\cdot\bar{\boldsymbol{\Omega}}$ of $R_{\rm f}$ may cause yaw- or tiltwise 'inertia torques' via $J^{R_{\rm f}}_{\rm y} - J^{R_{\rm f}}_{\rm x}$ or $J^{R_{\rm f}}_{\rm x} - J^{R_{\rm f}}_{\rm z}$ at tilt- or yawwise angular motion. It is allowed to deal with these gyroscopic effects in the equations of motion of the nacelle. This yields the following additional sensitivity for the angular impulse:

$$\Delta\frac{\partial^{S^{\ominus}_{\rm n}}\underline{\dot{\boldsymbol{\mathcal{h}}}}^{S_{\rm n}}}{\partial\underline{\boldsymbol{\omega}}^{S_{\rm n}}} = \frac{\partial^{R^*_{\rm f}}\underline{\dot{\boldsymbol{\mathcal{h}}}}^{R_{\rm f}}}{\partial\underline{\boldsymbol{\omega}}^{R_{\rm f}}} = \left[\;\; \begin{bmatrix} 0 \\ 0 \\ 0 \end{bmatrix} \;\; \begin{bmatrix} 0 \\ 0 \\ i_{\rm gb}\bar{\boldsymbol{\Omega}}(J^{R_{\rm f}}_{\rm y} - J^{R_{\rm f}}_{\rm x}) \end{bmatrix} \;\; \begin{bmatrix} 0 \\ i_{\rm gb}\bar{\boldsymbol{\Omega}}(J^{R_{\rm f}}_{\rm x} - J^{R_{\rm f}}_{\rm z}) \\ 0 \end{bmatrix} \;\right] \tag{B.23}$$

Since the model for the gearbox house $R_{\rm h}$ is derived from the angular co-axial impulse coordinate only, the non-coaxial inertia parameters of $R_{\rm h}$ also are to be catered for in the model of the nacelle $S_{\rm n}$. But, in contrast to the generator rotor, the mean rotational speed $\bar{\boldsymbol{\Omega}}$ does not play a role in $R_{\rm h}$. Thus only second order gyroscopic effects exist. These are neglected in the linear approach. So it satisfies to include its non-coaxial inertia parameters in the sensitivity of the impulse vectors of $S_{\rm n}$ to the acceleration variables. See Eq. B.30 and B.25 for the inertia augmentation.

The expression for the (absolute) time derivative of the linear impulse $\vec{p}$ for element S_k is:

$$\underline{\dot{p}}^{S_k} \;\triangleq\; \left({}^{(G)}\tfrac{\rm d}{{\rm d}t}\left(\vec{p}^{\,S_k}\right)\right)^{S_k} \;=\; m^{S_k}\underline{a}^{S^*_k} \tag{B.24}$$

The nacelle mass $m^{S_{\rm n}}$ is augmented with the generator rotor mass $m^{R_{\rm f}}$ and gearbox house mass $m^{R_{\rm h}}$ (see section B.2.2) so that for the mass of element S_M holds:

$$m^{S_M} = m^{S_{\rm n}} + m^{R_{\rm f}} + m^{R_{\rm h}} \tag{B.25}$$

According to section B.1.1, all kinematic quantities of the support structure are zero-mean. This implies the following for the time derivatives of the (biased) angular impulse and the linear impulse (see Eq. B.1, B.2):

$$\begin{aligned}
{}^{S^{\ominus}_k}\underline{\dot{\boldsymbol{\mathcal{h}}}}^{S_k} \;&=\; \frac{\partial^{S^{\ominus}_k}\underline{\dot{\boldsymbol{\mathcal{h}}}}^{S_k}}{\partial\underline{a}^{S^{\oplus}_{\rm FF}}}\cdot\delta\underline{a}^{S^{\oplus}_{\rm FF}} + \frac{\partial^{S^{\ominus}_k}\underline{\dot{\boldsymbol{\mathcal{h}}}}^{S_k}}{\partial\underline{\boldsymbol{\alpha}}^{S_{\rm FF}}}\cdot\delta\underline{\boldsymbol{\alpha}}^{S_{\rm FF}} + \frac{\partial^{S^{\ominus}_k}\underline{\dot{\boldsymbol{\mathcal{h}}}}^{S_k}}{\partial\underline{\ddot{\boldsymbol{\varphi}}}^{S}}\cdot\delta\underline{\ddot{\boldsymbol{\varphi}}}^{S} + \frac{\partial^{S^{\ominus}_k}\underline{\dot{\boldsymbol{\mathcal{h}}}}^{S_k}}{\partial\underline{\ddot{\varrho}}^{S}}\cdot\delta\underline{\ddot{\varrho}}^{S} + \\
&\qquad \delta_{k,M}\cdot\frac{\partial^{S^{\ominus}_{\rm n}}\underline{\dot{\boldsymbol{\mathcal{h}}}}^{S_{\rm n}}}{\partial\underline{\boldsymbol{\omega}}^{S_{\rm FF}}}\cdot\delta\underline{\boldsymbol{\omega}}^{S_{\rm FF}} + \delta_{k,M}\cdot\frac{\partial^{S^{\ominus}_{\rm n}}\underline{\dot{\boldsymbol{\mathcal{h}}}}^{S_{\rm n}}}{\partial\underline{\dot{\boldsymbol{\varphi}}}^{S}}\cdot\delta\underline{\dot{\boldsymbol{\varphi}}}^{S} \\
{}^{S^{\ominus}_k}\underline{\dot{p}}^{S_k} \;&=\; \frac{\partial\underline{\dot{p}}^{S_k}}{\partial\underline{a}^{S^{\oplus}_{\rm FF}}}\cdot\delta\underline{a}^{S^{\oplus}_{\rm FF}} + \frac{\partial\underline{\dot{p}}^{S_k}}{\partial\underline{\boldsymbol{\alpha}}^{S_{\rm FF}}}\cdot\delta\underline{\boldsymbol{\alpha}}^{S_{\rm FF}} + \frac{\partial\underline{\dot{p}}^{S_k}}{\partial\underline{\ddot{\boldsymbol{\varphi}}}^{S}}\cdot\delta\underline{\ddot{\boldsymbol{\varphi}}}^{S} + \frac{\partial\underline{\dot{p}}^{S_k}}{\partial\underline{\ddot{\varrho}}^{S}}\cdot\delta\underline{\ddot{\varrho}}^{S}
\end{aligned} \tag{B.26}$$

The sensitivity of the rate of change in the angular impulse to $\underline{\boldsymbol{\alpha}}^{S_{\rm FF}}$ and $\underline{\ddot{\boldsymbol{\varphi}}}^{S}$ involve the direct partial derivatives of the angular impulse to $\underline{\boldsymbol{\alpha}}^{S_k}$ and $\underline{a}^{S^*_k}$:

$$\frac{\partial^{S^{\ominus}_k}\underline{\dot{\boldsymbol{\mathcal{h}}}}^{S_k}}{\partial\underline{z}} \;=\; \frac{\partial^{S^{\ominus}_k}\underline{\dot{\boldsymbol{\mathcal{h}}}}^{S_k}}{\partial\underline{\boldsymbol{\alpha}}^{S_k}}\cdot\frac{\partial\underline{\boldsymbol{\alpha}}^{S_k}}{\partial\underline{z}} \;+\; \frac{\partial^{S^{\ominus}_k}\underline{\dot{\boldsymbol{\mathcal{h}}}}^{S_k}}{\partial\underline{a}^{S^*_k}}\cdot\frac{\partial\underline{a}^{S^*_k}}{\partial\underline{z}} \qquad \text{for } \underline{z} = \underline{\boldsymbol{\alpha}}^{S_{\rm FF}}, \underline{\ddot{\boldsymbol{\varphi}}}^{S} \tag{B.27}$$

The sensitivity to $\underline{a}^{S_{\mathrm{FF}}^{\oplus}}$ and $\underline{\ddot{o}}^{S}$ involves the partial derivative to only $\underline{a}^{S_k^*}$:

$$\frac{\partial^{S_k^{\ominus}} \underline{\dot{h}}^{S_k}}{\partial \underline{z}} = \frac{\partial^{S_k^{\ominus}} \underline{\dot{h}}^{S_k}}{\partial \underline{a}^{S_k^*}} \cdot \frac{\partial \underline{a}^{S_k^*}}{\partial \underline{z}} \quad \text{for } \underline{z} = \underline{a}^{S_{\mathrm{FF}}^{\oplus}}, \underline{\ddot{o}}^{S} \tag{B.28}$$

The direct partial derivatives of the angular impulse change are given by:

$$\begin{aligned} \frac{\partial^{S_k^{\ominus}} \underline{\dot{h}}^{S_k}}{\partial \underline{\alpha}^{S_k}} &= \boldsymbol{I}^{S_k} \\ \frac{\partial^{S_k^{\ominus}} \underline{\dot{h}}^{S_k}}{\partial \underline{a}^{S_k^*}} &= \mathrm{J}_{w=1}^{3}\left({}^{S_k^{\ominus}}\underline{r}^{S_k^*} \times m^{S_k} \cdot \underline{e}_w\right) \end{aligned} \tag{B.29}$$

Note that for the nacelle the 'inertia matrix for the angular acceleration', typed as $\boldsymbol{I}_{\alpha}^{S_M}$, is composed as follows (see Eq. B.30 for $\boldsymbol{I}^{S_M}$):

$$\boldsymbol{I}_{\alpha}^{S_M} = \boldsymbol{I}^{S_M} + \begin{pmatrix} 0 & 0 & 0 \\ 0 & J_y^{R_{\mathrm{f}}} & 0 \\ 0 & 0 & J_z^{R_{\mathrm{f}}} \end{pmatrix} \tag{B.30}$$

The sensitivity of the rate of change in the angular impulse of the nacelle to $\underline{\omega}^{S_{\mathrm{FF}}}$ from the tower and to $\underline{\dot{\varphi}}^{S}$ involves the direct partial derivative of the angular impulse to $\underline{\omega}^{S_M}$ (see Eq. B.23):

$$\frac{\partial^{S_{\mathrm{n}}^{\ominus}} \underline{\dot{h}}^{S_{\mathrm{n}}}}{\partial \underline{z}} = \frac{\partial^{S_{\mathrm{n}}^{\ominus}} \underline{\dot{h}}^{S_{\mathrm{n}}}}{\partial \underline{\omega}^{S_{\mathrm{n}}}} \cdot \frac{\partial \underline{\omega}^{S_{\mathrm{n}}}}{\partial \underline{z}} \quad \text{for } \underline{z} = \underline{\omega}^{S_{\mathrm{FF}}}, \underline{\dot{\varphi}}^{S} \tag{B.31}$$

The sensitivity of the rate of change of the linear impulse to all variables only involves the direct partial derivative to $\underline{a}^{S_k^*}$:

$$\frac{\partial \underline{\dot{p}}^{S_k}}{\partial \underline{z}} = \underline{m}^{S_k} \cdot \frac{\partial \underline{a}^{S_k^*}}{\partial \underline{z}} \quad \text{for } \underline{z} = \underline{\alpha}^{S_{\mathrm{FF}}}, \underline{a}^{S_{\mathrm{FF}}^{\oplus}}, \underline{\ddot{\varphi}}^{S}, \underline{\ddot{o}}^{S} \tag{B.32}$$

Note that the (underwater) element masses in the impulse vectors are NOT extended with water mass. The water mass influence is catered for in the dependency of the hydrodynamic loading on the element acceleration.

B.2 Drive train motion

The layout of the drive-train model R is described in section 3.7.1. The layout of the drive-train model R is defined through the 'one-element subcomponents' and the element configuration via rotations and translations. Expressions for the mean and sensitivity functions for the kinematic quantitites are given in section B.2.1 while this is done for the angular and linear impulse in section B.2.2.

The means and sensitivities are calculated and stored as fields in structure variables. A 'sensitivity field' contains 'subfields' with the actual partial derivatives. For the gearbox house, generator rotor and rotor shaft & hub subcomponents R_{h}, R_{f} and R_{r} this occurs by calls to M-functions TBUDRIVTRKIN() and TBUDRIVTRIMP() from TBUDRIVTREOM(). The kinematic vectors for the gearbox slow shaft R_{s} are not explicitely avialable as structure variables; they are 'intermediate results' for the kinematic vectors of the rotor shaft & hub R_{r}.

B.2.1 Drive train kinematics

Kinematics gearbox house R_{h}
The gearbox only moves in co-axial sense relative to the nacelle; all inertia parameters

except the co-axial moment of inertia are moved to the nacelle. Only the co-axial angular acceleration of $R_{\rm h}$ is relevant for the equation of motion:

$$\delta\alpha_1^{R_{\rm h}} \;=\; \delta\alpha_1^{S_{\rm n}^{\oplus {\rm r}}} + \ddot{\varphi}_3^{R_{\rm h}} \tag{B.33}$$

Furthermore, the angular velocity and acceleration vector *as fed through* to the slow shaft are relevant kinematic vectors for the gearbox house (see Eq. 3.62 for $\phi_3^{R_{\rm h"}}$):

$$\begin{aligned} \delta\underline{\omega}^{R_{\rm h"}} &= \Phi_{\rm x}(\bar{\phi}_3^{R_{\rm h"}})\cdot\delta\underline{\omega}^{S_{\rm n}^{\oplus {\rm r}}} + \dot{\varphi}_3^{R_{\rm h"}}\cdot\underline{e}_1 \\ \delta\underline{\alpha}^{R_{\rm h"}} &= \Phi_{\rm x}(\bar{\phi}_3^{R_{\rm h"}})\cdot\delta\underline{\alpha}^{S_{\rm n}^{\oplus {\rm r}}} + \ddot{\varphi}_3^{R_{\rm h"}}\cdot\underline{e}_1 \end{aligned} \tag{B.34}$$

The gearbox house kinematic vectors are not explicitely available as structure variables; the expressions are just incorporated in the ones for the impulse vectors (see next subsection).

Kinematics slow gearbox shaft $R_{\rm s}$
The massless and rigid subcomponent $R_{\rm s}$ does not require an equation of motion. The gearbox slow shaft kinematics are only used as step-up to the expressions for the rotor shaft & hub kinematic vectors. In this context we also define the 'feed-through' kinematic vectors from the stand still to the rotating partition of the wind turbine in the coordinate system of $R_{\rm s}$ (see Eq. 3.65):

$$\begin{aligned} \delta\underline{\omega}^{R_{\tilde{\rm h}"}} &\triangleq \left(\vec{\omega}^{R_{\rm h"}}\right)^{R_{\rm s}} &&= (\Phi_{\rm d}+\Phi_{\rm c}\cdot\cos\bar{\Omega}t+\Phi_{\rm s}\cdot\sin\bar{\Omega}t)\cdot\delta\underline{\omega}^{R_{\rm h"}} \\ \delta\underline{\alpha}^{R_{\tilde{\rm h}"}} &\triangleq \left(\vec{\alpha}^{R_{\rm h"}}\right)^{R_{\rm s}} &&= (\Phi_{\rm d}+\Phi_{\rm c}\cdot\cos\bar{\Omega}t+\Phi_{\rm s}\cdot\sin\bar{\Omega}t)\cdot\delta\underline{\alpha}^{R_{\rm h"}} \\ \delta\underline{v}^{S_{\tilde{\rm n}}^{\oplus {\rm r}}} &\triangleq \left(\vec{\delta v}^{S_{\rm n}^{\oplus {\rm r}}}\right)^{R_{\rm s}} &&= (\Phi_{\rm d}+\Phi_{\rm c}\cdot\cos\bar{\Omega}t+\Phi_{\rm s}\cdot\sin\bar{\Omega}t)\cdot\Phi_{\rm x}(\bar{\phi}_3^{R_{\rm h"}})\cdot\delta\underline{v}^{S_{\rm n}^{\oplus {\rm r}}} \\ \delta\underline{a}^{S_{\tilde{\rm n}}^{\oplus {\rm r}}} &\triangleq \left(\vec{\delta a}^{S_{\rm n}^{\oplus {\rm r}}}\right)^{R_{\rm s}} &&= (\Phi_{\rm d}+\Phi_{\rm c}\cdot\cos\bar{\Omega}t+\Phi_{\rm s}\cdot\sin\bar{\Omega}t)\cdot\Phi_{\rm x}(\bar{\phi}_3^{R_{\rm h"}})\cdot\delta\underline{a}^{S_{\rm n}^{\oplus {\rm r}}} \end{aligned} \tag{B.35}$$

From now on, the kinematic vectors will first be expressed indepedent of a coordinate system while afterwards the expressions are derived for the linearised approximations in the (final) coordinate system of the element under consideration.

For the angular velocity and acceleration of the slow shaft holds:

$$\begin{aligned} \vec{\omega}^{R_{\rm s}} &= \vec{\omega}^{R_{\rm h"}} + {}^{R_{\rm h"}}\vec{\omega}^{R_{\rm s}} \\ \vec{\alpha}^{R_{\rm s}} &= \vec{\alpha}^{R_{\rm h"}} + \tfrac{\rm d}{{\rm d}t}\left({}^{R_{\rm h"}}\vec{\omega}^{R_{\rm s}}\right) = \vec{\alpha}^{R_{\rm h"}} + {}^{(R_{\rm h"})}\tfrac{\rm d}{{\rm d}t}\left({}^{R_{\rm h"}}\vec{\omega}^{R_{\rm s}}\right) + \vec{\omega}^{R_{\rm h"}} \times {}^{R_{\rm h"}}\vec{\omega}^{R_{\rm s}} \\ &\text{with } {}^{R_{\rm h"}}\vec{\omega}^{R_{\rm s}} = (\bar{\Omega}+\delta\Omega)\cdot\vec{e}_1^{R_{\rm h"}} \text{ and } {}^{(R_{\rm h"})}\tfrac{\rm d}{{\rm d}t}\left({}^{R_{\rm h"}}\vec{\omega}^{R_{\rm s}}\right) = \dot{\Omega}\cdot\vec{e}_1^{R_{\rm h"}} \end{aligned} \tag{B.36}$$

We collect the rotation and translation dofs of the rotor shaft and for the variable speed option in column vectors $\underline{\varphi}^R$ and $\underline{\varrho}^R$:

$$\underline{\varphi}^R = \begin{pmatrix} \varphi_3^{R_{\rm f}} \\ \varphi_1^{R_{\rm r}} \\ \varphi_2^{R_{\rm r}} \\ \varphi_3^{R_{\rm r}} \end{pmatrix} \qquad \underline{\varrho}^R = \begin{pmatrix} \varrho_1^{R_{\rm r}} \\ \varrho_2^{R_{\rm r}} \\ \varrho_3^{R_{\rm r}} \end{pmatrix} \tag{B.37}$$

with

$$\varphi_3^{R_{\rm f}} = \phi_3^{R_{\rm f}} - i_{\rm gb}\cdot\bar{\Omega}t \tag{B.38}$$

The correponding linearised coordinate expresssions along $\vec{e}^{\,R_{\rm s}}$ of the angular speed and acceleartion of the slow gearbox shaft are:

$$\begin{aligned} \underline{\omega}^{R_{\rm s}} &\overset{\text{(orde 0,1)}}{=} \bar{\underline{\omega}}^{R_{\rm s}} + \frac{\partial\underline{\omega}^{R_{\rm s}}}{\partial\underline{\omega}^{R_{\tilde{\rm h}"}}}\cdot\delta\underline{\omega}^{R_{\tilde{\rm h}"}} + \frac{\partial\underline{\omega}^{R_{\rm s}}}{\partial\underline{\dot{\varphi}}^R}\cdot\underline{\dot{\varphi}}^R \\ \delta\underline{\alpha}^{R_{\rm s}} &\overset{\text{(orde 0,1)}}{=} \frac{\partial\underline{\alpha}^{R_{\rm s}}}{\partial\underline{\alpha}^{R_{\tilde{\rm h}"}}}\cdot\delta\underline{\alpha}^{R_{\tilde{\rm h}"}} + \frac{\partial\underline{\alpha}^{R_{\rm s}}}{\partial\underline{\omega}^{R_{\tilde{\rm h}"}}}\cdot\delta\underline{\omega}^{R_{\tilde{\rm h}"}} + \frac{\partial\underline{\alpha}^{R_{\rm s}}}{\partial\underline{\ddot{\varphi}}^R}\cdot\underline{\ddot{\varphi}}^R \end{aligned} \tag{B.39}$$

with mean

$$\bar{\underline{\omega}}^{R_\mathrm{s}} = \bar{\boldsymbol{\Omega}} \cdot \underline{e}_1 \tag{B.40}$$

while for the sensitivity matrices holds:

$$\begin{aligned} \frac{\partial \underline{\omega}^{R_\mathrm{s}}}{\partial \underline{\omega}^{R_\mathrm{h}}} &\equiv \frac{\partial \underline{\alpha}^{R_\mathrm{s}}}{\partial \underline{\alpha}^{R_\mathrm{h}}} = \begin{pmatrix} 1 & 0 & 0 \\ 0 & 1 & 0 \\ 0 & 0 & 1 \end{pmatrix} \\ \frac{\partial \underline{\omega}^{R_\mathrm{s}}}{\partial \underline{\dot{\varphi}}^{R}} &\equiv \frac{\partial \underline{\alpha}^{R_\mathrm{s}}}{\partial \underline{\ddot{\varphi}}^{R}} = \begin{pmatrix} 1/i_\mathrm{gb} & 0 & 0 & 0 \\ 0 & 0 & 0 & 0 \\ 0 & 0 & 0 & 0 \end{pmatrix} \end{aligned} \tag{B.41}$$

and

$$\frac{\partial \underline{\alpha}^{R_\mathrm{s}}}{\partial \underline{\omega}^{R_\mathrm{h}}} = \mathrm{J}^3_{v=1}(\underline{e}_v \times \bar{\boldsymbol{\Omega}} \cdot \underline{e}_1) = \begin{pmatrix} 0 & 0 & 0 \\ 0 & 0 & \bar{\Omega} \\ 0 & -\bar{\Omega} & 0 \end{pmatrix} \tag{B.42}$$

The slow gearbox shaft kinematic vectors are not explicitely available as structure variables; the expressions are just incorporated in the ones for the kinematic vectors of the rotor shaft & hub R_r (see paragraph on R_r in this subsection).

Kinematics generator rotor R_f
Just as for the gearbox house, only the co-axial angular acceleration is relevant for the generator rotor as concerns it equations of motion:

$$\delta\alpha_1^{R_\mathrm{h}} = \delta\alpha_1^{S_\mathrm{n}^{\oplus \mathrm{r}}} + \ddot{\varphi}_3^{R_\mathrm{f}} \tag{B.43}$$

However, also the *non*-coaxial angular motion of the generator rotor must be considered because of first order gyroscopic effects (see also B.2.2). For this, we define the 'feed-through' angular kinematic vectors of the nacelle in the coordinate system of R_f:

$$\begin{aligned} \delta\underline{\omega}^{S_\tilde{\mathrm{n}}} &\triangleq \left(\vec{\omega}^{S_\mathrm{n}}\right)^{R_\mathrm{f}} = (\Phi_\mathrm{d} + \Phi_\mathrm{c} \cdot \cos\bar{\boldsymbol{\Omega}}t + \Phi_\mathrm{s} \cdot \sin\bar{\boldsymbol{\Omega}}t) \cdot \delta\underline{\omega}^{S_\mathrm{n}} \\ \delta\underline{\alpha}^{S_\tilde{\mathrm{n}}} &\triangleq \left(\vec{\alpha}^{S_\mathrm{n}}\right)^{R_\mathrm{f}} = (\Phi_\mathrm{d} + \Phi_\mathrm{c} \cdot \cos\bar{\boldsymbol{\Omega}}t + \Phi_\mathrm{s} \cdot \sin\bar{\boldsymbol{\Omega}}t) \cdot \delta\underline{\alpha}^{S_\mathrm{n}} \end{aligned} \tag{B.44}$$

For the angular velocity and acceleration of the fast shaft holds:

$$\begin{aligned} \vec{\omega}^{R_\mathrm{f}} &= \vec{\omega}^{S_\mathrm{n}} + {}^{S_\mathrm{n}}\vec{\omega}^{R_\mathrm{f}} \\ \vec{\alpha}^{R_\mathrm{s}} &= \vec{\alpha}^{S_\mathrm{n}} + \frac{\mathrm{d}}{\mathrm{d}t}\left({}^{S_\mathrm{n}}\vec{\omega}^{R_\mathrm{f}}\right) = \vec{\alpha}^{S_\mathrm{n}} + {}^{(S_\mathrm{n})}\frac{\mathrm{d}}{\mathrm{d}t}\left({}^{S_\mathrm{n}}\vec{\omega}^{R_\mathrm{f}}\right) + \vec{\omega}^{S_\mathrm{n}} \times {}^{S_\mathrm{n}}\vec{\omega}^{R_\mathrm{f}} \\ \text{with } {}^{S_\mathrm{n}}\vec{\omega}^{R_\mathrm{f}} &= i_\mathrm{gb} \cdot (\bar{\boldsymbol{\Omega}} + \delta\boldsymbol{\Omega}) \cdot \vec{e}_1^{\,S_\mathrm{n}} \text{ and } {}^{(S_\mathrm{n})}\frac{\mathrm{d}}{\mathrm{d}t}\left({}^{S_\mathrm{n}}\vec{\omega}^{R_\mathrm{f}}\right) = \ddot{\varphi}_3^{R_\mathrm{f}} \cdot \vec{e}_1^{\,S_\mathrm{n}} \end{aligned} \tag{B.45}$$

The correponding linearised coordinate expresssions along $\vec{e}^{\,R_\mathrm{f}}$ are:

$$\begin{aligned} \underline{\omega}^{R_\mathrm{f}} &\overset{\text{(orde 0,1)}}{=} \bar{\underline{\omega}}^{R_\mathrm{f}} + \frac{\partial \underline{\omega}^{R_\mathrm{f}}}{\partial \underline{\omega}^{S_\tilde{\mathrm{n}}}} \cdot \delta\underline{\omega}^{S_\tilde{\mathrm{n}}} + \frac{\partial \underline{\omega}^{R_\mathrm{f}}}{\partial \underline{\dot{\varphi}}^{R}} \cdot \underline{\dot{\varphi}}^{R} \\ \delta\underline{\alpha}^{R_\mathrm{f}} &\overset{\text{(orde 0,1)}}{=} \frac{\partial \underline{\alpha}^{R_\mathrm{f}}}{\partial \underline{\alpha}^{S_\tilde{\mathrm{n}}}} \cdot \delta\underline{\alpha}^{S_\tilde{\mathrm{n}}} + \frac{\partial \underline{\alpha}^{R_\mathrm{f}}}{\partial \underline{\omega}^{S_\tilde{\mathrm{n}}}} \cdot \delta\underline{\omega}^{S_\tilde{\mathrm{n}}} + \frac{\partial \underline{\alpha}^{R_\mathrm{f}}}{\partial \underline{\ddot{\varphi}}^{R}} \cdot \underline{\ddot{\varphi}}^{R} \end{aligned} \tag{B.46}$$

with mean ($\bar{\dot{\phi}}_3^{R_\mathrm{f}} = i_\mathrm{gb} \cdot \bar{\boldsymbol{\Omega}}$):

$$\bar{\underline{\omega}}^{R_\mathrm{f}} = i_\mathrm{gb} \cdot \bar{\boldsymbol{\Omega}} \cdot \underline{e}_1 \tag{B.47}$$

while for the sensitivity matrices holds:

$$\begin{aligned} \frac{\partial \underline{\omega}^{R_\mathrm{f}}}{\partial \underline{\omega}^{S_\tilde{\mathrm{n}}}} &\equiv \frac{\partial \underline{\alpha}^{R_\mathrm{f}}}{\partial \underline{\alpha}^{S_\tilde{\mathrm{n}}}} = \begin{pmatrix} 1 & 0 & 0 \\ 0 & 1 & 0 \\ 0 & 0 & 1 \end{pmatrix} \\ \frac{\partial \underline{\omega}^{R_\mathrm{f}}}{\partial \underline{\dot{\varphi}}^{R}} &\equiv \frac{\partial \underline{\alpha}^{R_\mathrm{f}}}{\partial \underline{\ddot{\varphi}}^{R}} = \begin{pmatrix} 1 & 0 & 0 & 0 \\ 0 & 0 & 0 & 0 \\ 0 & 0 & 0 & 0 \end{pmatrix} \end{aligned} \tag{B.48}$$

and

$$\frac{\partial \underline{\alpha}^{R_{\rm f}}}{\partial \underline{\omega}^{S_{\tilde{\rm n}}}} \;=\; {\rm J}^3_{v=1}(\underline{e}_v \times i_{\rm gb}\bar{\boldsymbol{\Omega}}\cdot\underline{e}_1) = \begin{pmatrix} 0 & 0 & 0 \\ 0 & 0 & i_{\rm gb}\bar{\boldsymbol{\Omega}} \\ 0 & -i_{\rm gb}\bar{\boldsymbol{\Omega}} & 0 \end{pmatrix} \tag{B.49}$$

Neither all non-coaxial motion, nor the linear co-axial motion have to be taken into account in the equation of motion for the generator rotor. All these excluded motions are added to the nacelle, which has already been mentioned in section B.1.2, paragraph on the nacelle $S_{\rm n}$ (eq B.23) and which will be cleared up in detail in section B.2.2, paragraph on $R_{\rm f}$. The generator rotor kinematic vectors are not explicitely available as structure variables; the expressions are just incorporated in the ones for the impulse vectors (see next subsection).

Kinematics rotor shaft & hub $R_{\rm r}$

We first give the expressions for the internal rotation and translation transformation matrices under rotation order 'x,z,y' for $R_{\rm r}$ (distorsion along x-axis, $\bar{\phi}_2^{R_{\rm r}}=0$ and $\bar{\phi}_3^{R_{\rm r}}=0$ for zero-mean bending) :

$$\begin{aligned}
{}^{R_{\rm r}}\bar{\Phi}^{R_{\rm r}^{\iota {\rm r}}} \;&=\; \Big[{}^{R_{\rm r}}\bar{\Phi}^{R_{\rm r}^2}\cdot{}^{R_{\rm r}^2}\bar{\Phi}^{R_{\rm r}^1} \quad {}^{R_{\rm r}}\bar{\Phi}^{R_{\rm r}^2}_3 \quad \underline{e}_2\Big] = \ldots \\
&\qquad \Big[\Phi_{\rm y}(\bar{\phi}_3^{R_{\rm r}})\cdot\underline{\Phi}_{\rm z_1}(\bar{\phi}_2^{R_{\rm r}}) \quad \underline{\Phi}_{\rm y_3}(\bar{\phi}_3^{R_{\rm r}}) \quad \underline{e}_2\Big] = \begin{pmatrix} 1 & 0 & 0 \\ 0 & 0 & 1 \\ 0 & 1 & 0 \end{pmatrix} \\
{}^{R_{\rm r}}\bar{\Phi}^{R_{\rm r}^{\iota {\rm t}}} \;&=\; \Big[{}^{R_{\rm r}}\bar{\Phi}^{R_{\rm r}^2}\cdot{}^{R_{\rm r}^2}\bar{\Phi}^{R_{\rm r}^1} \quad {}^{R_{\rm r}}\bar{\Phi}^{R_{\rm r}^2}_2 \quad \underline{e}_3\Big] = \ldots \\
&\qquad \Big[\Phi_{\rm y}(\bar{\phi}_3^{R_{\rm r}})\cdot\underline{\Phi}_{\rm z_1}(\bar{\phi}_2^{R_{\rm r}}) \quad \underline{\Phi}_{\rm y_2}(\bar{\phi}_3^{R_{\rm r}}) \quad \underline{e}_3\Big] = \begin{pmatrix} 1 & 0 & 0 \\ 0 & 1 & 0 \\ 0 & 0 & 1 \end{pmatrix}
\end{aligned} \tag{B.50}$$

For the angular velocity and acceleration of the rotor shaft & hub $R_{\rm r}$ at the 'hub-side' holds:

$$\begin{aligned}
\vec{\omega}^{R_{\rm r}} \;&=\; \vec{\omega}^{R_{\rm s}} + {}^{R_{\rm s}}\vec{\omega}^{R_{\rm r}} \\
\vec{\alpha}^{R_{\rm r}} \;&=\; \vec{\alpha}^{R_{\rm s}} + \frac{{\rm d}}{{\rm d}t}\Big({}^{R_{\rm s}}\vec{\omega}^{R_{\rm r}}\Big) \;=\; \vec{\alpha}^{R_{\rm s}} + {}^{(R_{\rm s})}\frac{{\rm d}}{{\rm d}t}\Big({}^{R_{\rm s}}\vec{\omega}^{R_{\rm r}}\Big) + \vec{\omega}^{R_{\rm s}} \times {}^{R_{\rm s}}\vec{\omega}^{R_{\rm r}} \\
&\text{with } {}^{R_{\rm s}}\vec{\omega}^{R_{\rm r}} \;=\; \dot{\varphi}_1^{R_{\rm r}}\cdot\vec{e}_1^{R_{\rm s}} + \dot{\varphi}_2^{R_{\rm r}}\cdot\vec{e}_3^{R_{\rm r}^1} + \dot{\varphi}_3^{R_{\rm r}}\cdot\vec{e}_2^{R_{\rm r}^2}
\end{aligned} \tag{B.51}$$

The linearised coordinate expressions for the 'rotational increments' ${}^{R_{\rm s}}\vec{\omega}^{R_{\rm r}}$ and ${}^{(R_{\rm s})}\frac{{\rm d}}{{\rm d}t}\Big({}^{R_{\rm s}}\vec{\omega}^{R_{\rm r}}\Big)$ along $\vec{e}^{R_{\rm r}}$ are:

$$\begin{aligned}
{}^{R_{\rm s}}\underline{\omega}^{R_{\rm r}} \;&\triangleq\; \Big({}^{R_{\rm s}}\vec{\omega}^{R_{\rm r}}\Big)^{R_{\rm r}} \;\overset{\text{(orde 0,1)}}{=}\; \Big[\underline{0} \quad {}^{R_{\rm r}}\bar{\Phi}^{R_{\rm r}^{\iota {\rm r}}}\Big]\cdot\dot{\underline{\varphi}}^R \\
{}^{(R_{\rm s})}\frac{{\rm d}}{{\rm d}t}\Big({}^{R_{\rm s}}\underline{\omega}^{R_{\rm r}}\Big) \;&\triangleq\; \Big({}^{(R_{\rm s})}\frac{{\rm d}}{{\rm d}t}\Big({}^{R_{\rm s}}\vec{\omega}^{R_{\rm r}}\Big)\Big)^{R_{\rm r}} \;\overset{\text{(orde 0,1)}}{=}\; \Big[\underline{0} \quad {}^{R_{\rm r}}\bar{\Phi}^{R_{\rm r}^{\iota {\rm r}}}\Big]\cdot\ddot{\underline{\varphi}}^R
\end{aligned} \tag{B.52}$$

The corresponding linearised coordinate expressions for the angular velocity and acceleration along $\vec{e}^{R_{\rm r}}$ then become:

$$\begin{aligned}
\underline{\omega}^{R_{\rm r}} \;&\overset{\text{(orde 0,1)}}{=}\; \bar{\underline{\omega}}^{R_{\rm r}} + \frac{\partial \underline{\omega}^{R_{\rm r}}}{\partial \underline{\omega}^{R_{\tilde{\rm h}"}}}\cdot\delta\underline{\omega}^{R_{\tilde{\rm h}"}} + \frac{\partial \underline{\omega}^{R_{\rm r}}}{\partial \dot{\underline{\varphi}}^R}\cdot\dot{\underline{\varphi}}^R + \frac{\partial \underline{\omega}^{R_{\rm r}}}{\partial \underline{\phi}^R}\cdot\delta\underline{\phi}^R \\
\delta\underline{\alpha}^{R_{\rm r}} \;&\overset{\text{(orde 0,1)}}{=}\; \frac{\partial \underline{\alpha}^{R_{\rm r}}}{\partial \underline{\alpha}^{R_{\tilde{\rm h}"}}}\cdot\delta\underline{\alpha}^{R_{\tilde{\rm h}"}} + \frac{\partial \underline{\alpha}^{R_{\rm r}}}{\partial \underline{\omega}^{R_{\tilde{\rm h}"}}}\cdot\delta\underline{\omega}^{R_{\tilde{\rm h}"}} + \frac{\partial \underline{\alpha}^{R_{\rm r}}}{\partial \dot{\underline{\varphi}}^R}\cdot\dot{\underline{\varphi}}^R + \frac{\partial \underline{\alpha}^{R_{\rm r}}}{\partial \ddot{\underline{\varphi}}^R}\cdot\ddot{\underline{\varphi}}^R
\end{aligned} \tag{B.53}$$

with mean

$$\bar{\underline{\omega}}^{R_{\rm r}} = {}^{R_{\rm r}}\bar{\Phi}^{R_{\rm s}}\cdot\bar{\boldsymbol{\Omega}}\underline{e}_1 = \bar{\Phi}_{\rm x}(\bar{\phi}_1^{R_{\rm r}})\cdot\bar{\boldsymbol{\Omega}}\underline{e}_1 = \bar{\boldsymbol{\Omega}}\underline{e}_1 \tag{B.54}$$

while for the sensitivity matrices holds (use Eq. B.41, B.50):

$$\begin{aligned}
\frac{\partial \underline{\omega}^{R_{\rm r}}}{\partial \underline{\omega}^{R_{\tilde{\rm h}"}}} \;&\equiv\; \frac{\partial \underline{\alpha}^{R_{\rm r}}}{\partial \underline{\alpha}^{R_{\tilde{\rm h}"}}} \;=\; {}^{R_{\rm r}}\bar{\Phi}^{R_{\rm s}}\cdot\frac{\partial \underline{\omega}^{R_{\rm s}}}{\partial \underline{\omega}^{R_{\tilde{\rm h}"}}} \;=\; \bar{\Phi}_{\rm x}(\bar{\phi}_1^{R_{\rm r}}) \\
\frac{\partial \underline{\omega}^{R_{\rm r}}}{\partial \dot{\underline{\varphi}}^R} \;&\equiv\; \frac{\partial \underline{\alpha}^{R_{\rm r}}}{\partial \ddot{\underline{\varphi}}^R} \;=\; \Big[1/i_{\rm gb}\cdot\underline{e}_1 \quad {}^{R_{\rm r}}\bar{\Phi}^{R_{\rm r}^{\iota {\rm r}}}\Big] \;=\; \begin{pmatrix} 1/i_{\rm gb} & 1 & 0 & 0 \\ 0 & 0 & 0 & 1 \\ 0 & 0 & 1 & 0 \end{pmatrix}
\end{aligned} \tag{B.55}$$

and (use Eq. B.42):

$$\begin{aligned}
\frac{\partial \underline{\alpha}^{R_\mathrm{r}}}{\partial \underline{\omega}^{R_\mathrm{r}}_{\tilde{\mathrm{h}}''}} &= {}^{R_\mathrm{r}}\bar{\Phi}^{R_\mathrm{s}} \cdot \frac{\partial \underline{\alpha}^{R_\mathrm{s}}}{\partial \underline{\omega}^{R_\mathrm{r}}_{\tilde{\mathrm{h}}''}} = \bar{\Phi}_\mathrm{x}(\bar{\phi}_1^{R_\mathrm{r}}) \cdot \begin{pmatrix} 0 & 0 & 0 \\ 0 & 0 & \bar{\Omega} \\ 0 & -\bar{\Omega} & 0 \end{pmatrix} \\
\frac{\partial \underline{\alpha}^{R_\mathrm{r}}}{\partial \underline{\dot{\rho}}^{R}} &= \left[\underline{0} \;\; \mathrm{J}^3_{v=1}({}^{R_\mathrm{r}}\bar{\Phi}^{R_\mathrm{s}} \cdot \bar{\Omega}\underline{e}_1 \times {}^{R_\mathrm{r}}\underline{\bar{\Phi}}^{\iota_{R_\mathrm{r}}}_v)\right] = \begin{pmatrix} 0 & 0 & 0 & 0 \\ 0 & 0 & -\bar{\Omega} & 0 \\ 0 & 0 & 0 & \bar{\Omega} \end{pmatrix} \\
\frac{\partial \underline{\omega}^{R_\mathrm{r}}}{\partial \underline{\dot{\phi}}^{R}} &= \left[\underline{0} \;\; \mathrm{J}^3_{v=1}(\frac{\partial {}^{R_\mathrm{r}}\underline{\Phi}^{R_\mathrm{s}}}{\partial \phi_v^{R_\mathrm{r}}} \cdot \bar{\Omega}\underline{e}_1)\right] = \begin{pmatrix} 0 & 0 & 0 & 0 \\ 0 & 0 & -\bar{\Omega} & 0 \\ 0 & 0 & 0 & \bar{\Omega} \end{pmatrix}
\end{aligned} \tag{B.56}$$

The linear velocity and acceleration in point 'p' at the hub-side of R_r can be expressed as follows (coordinate system independent; note that $S^{\oplus\mathrm{r}}_\mathrm{n}$ coincides with $R^{\ominus}_\mathrm{r}$):

$$\begin{aligned}
\vec{v}^{\,R^\mathrm{p}_\mathrm{r}} &= \vec{v}^{\,S^{\oplus\mathrm{r}}_\mathrm{n}} + \frac{\mathrm{d}}{\mathrm{d}t}\Big({}^{R^{\ominus}_\mathrm{r}}\vec{r}^{\,R^\mathrm{p}_\mathrm{r}}\Big) = \vec{v}^{\,S^{\oplus\mathrm{r}}_\mathrm{n}} + {}^{(R_\mathrm{r})}\frac{\mathrm{d}}{\mathrm{d}t}\Big({}^{R^{\ominus}_\mathrm{r}}\vec{r}^{\,R^\mathrm{p}_\mathrm{r}}\Big) + \vec{\omega}^{\,R_\mathrm{r}} \times {}^{R^{\ominus}_\mathrm{r}}\vec{r}^{\,R^\mathrm{p}_\mathrm{r}} \\
\vec{a}^{\,R^\mathrm{p}_\mathrm{r}} &= \vec{a}^{\,S^{\oplus\mathrm{r}}_\mathrm{n}} + \frac{\mathrm{d}}{\mathrm{d}t}\Big({}^{(R_\mathrm{r})}\frac{\mathrm{d}}{\mathrm{d}t}\Big({}^{R^{\ominus}_\mathrm{r}}\vec{r}^{\,R^\mathrm{p}_\mathrm{r}}\Big)\Big) + \frac{\mathrm{d}}{\mathrm{d}t}\Big(\vec{\omega}^{\,R_\mathrm{r}} \times {}^{R^{\ominus}_\mathrm{r}}\vec{r}^{\,R^\mathrm{p}_\mathrm{r}}\Big) \\
&= \vec{a}^{\,S^{\oplus\mathrm{r}}_\mathrm{n}} + \vec{\alpha}^{\,R_\mathrm{r}} \times {}^{R^{\ominus}_\mathrm{r}}\vec{r}^{\,R^\mathrm{p}_\mathrm{r}} + \vec{\omega}^{\,R_\mathrm{r}} \times (\vec{\omega}^{\,R_\mathrm{r}} \times {}^{R^{\ominus}_\mathrm{r}}\vec{r}^{\,R^\mathrm{p}_\mathrm{r}}) + \ldots \\
&\qquad 2\vec{\omega}^{\,R_\mathrm{r}} \times {}^{(R_\mathrm{r})}\frac{\mathrm{d}}{\mathrm{d}t}\Big({}^{R^{\ominus}_\mathrm{r}}\vec{r}^{\,R^\mathrm{p}_\mathrm{r}}\Big) + {}^{(R_\mathrm{r})}\frac{\mathrm{d}^2}{\mathrm{d}t^2}\Big({}^{R^{\ominus}_\mathrm{r}}\vec{r}^{\,R^\mathrm{p}_\mathrm{r}}\Big)
\end{aligned} \tag{B.57}$$

The linearised coordinate expressions for the 'translation' increments along $\vec{e}^{\,R_\mathrm{r}}$ are (use Eq. B.52):

$$\begin{aligned}
{}^{(R_\mathrm{r})}\frac{\mathrm{d}}{\mathrm{d}t}\Big({}^{R^{\ominus}_\mathrm{r}}\underline{r}^{R^\mathrm{p}_\mathrm{r}}\Big) &\triangleq \Big({}^{(R_\mathrm{r})}\frac{\mathrm{d}}{\mathrm{d}t}\Big({}^{R^{\ominus}_\mathrm{r}}\vec{r}^{\,R^\mathrm{p}_\mathrm{r}}\Big)\Big)^{R_\mathrm{r}} = \left[\underline{0} \;\; {}^{R_\mathrm{r}}\bar{\Phi}^{\iota_{R^\mathrm{t}_\mathrm{r}}}\right] \cdot \underline{\dot{\varrho}}^{R} \\
{}^{(R_\mathrm{r})}\frac{\mathrm{d}^2}{\mathrm{d}t^2}\Big({}^{R^{\ominus}_\mathrm{r}}\underline{r}^{R^\mathrm{p}_\mathrm{r}}\Big) &\triangleq \Big({}^{(R_\mathrm{r})}\frac{\mathrm{d}^2}{\mathrm{d}t^2}\Big({}^{R^{\ominus}_\mathrm{r}}\vec{r}^{\,R^\mathrm{p}_\mathrm{r}}\Big)\Big)^{R_\mathrm{r}} = \left[\underline{0} \;\; {}^{R_\mathrm{r}}\bar{\Phi}^{\iota_{R^\mathrm{t}_\mathrm{r}}}\right] \cdot \underline{\ddot{\varrho}}^{R}
\end{aligned} \tag{B.58}$$

The translation dofs $\{\rho_v\}$ are included in the model only for valid structural dynamics through stiffness, damping and inertia effects. The influence of $\{\rho_v\}$ on orientation and length of the place vector is very small: the typical products 'rotation variations times element length' are much larger than even the average translation sizes $\{\bar{\rho}_v\}$.

Neglecting the influence of translations dofs yields invariant coordinates for place vectors between points on an element:

$${}^{R^{\ominus}_\mathrm{r}}\underline{r}^{R^\mathrm{p}_\mathrm{r}} \triangleq \Big({}^{R^{\ominus}_\mathrm{r}}\vec{r}^{\,R^\mathrm{p}_\mathrm{r}}\Big)^{R_\mathrm{r}} \equiv \overline{\Big({}^{R^{\ominus}_\mathrm{r}}\vec{r}^{\,R^\mathrm{p}_\mathrm{r}}\Big)^{R_\mathrm{r}}} \quad \text{(invariant)} \tag{B.59}$$

For invariant ${}^{R^{\ominus}_\mathrm{r}}\underline{r}^{R^\mathrm{p}_\mathrm{r}}$, with short-form $\underline{r}^\mathrm{p}$, the following (intermediate) linearised coordinate expressions along $\vec{e}^{\,R_\mathrm{r}}$ apply for the linear velocity and acceleration:

$$\begin{aligned}
\underline{v}^{R^\mathrm{p}_\mathrm{r}} &= \bar{\underline{\omega}}^{R_\mathrm{r}} \times \underline{r}^\mathrm{p} + {}^{R_\mathrm{r}}\bar{\Phi}^{R_\mathrm{s}} \cdot \delta\underline{v}^{S^{\oplus\mathrm{r}}_\mathrm{n}} + \delta\underline{\omega}^{R_\mathrm{r}} \times \underline{r}^\mathrm{p} + {}^{(R_\mathrm{r})}\frac{\mathrm{d}}{\mathrm{d}t}\Big(\underline{r}^\mathrm{p}\Big) \\
\underline{a}^{R^\mathrm{p}_\mathrm{r}} &= \bar{\underline{\omega}}^{R_\mathrm{r}} \times (\bar{\underline{\omega}}^{R_\mathrm{r}} \times \underline{r}^\mathrm{p}) + {}^{R_\mathrm{r}}\bar{\Phi}^{R_\mathrm{s}} \cdot \delta\underline{a}^{S^{\oplus\mathrm{r}}_\mathrm{n}} + \delta\underline{\alpha}^{R_\mathrm{r}} \times \underline{r}^\mathrm{p} + \\
&\quad \delta\underline{\omega}^{R_\mathrm{r}} \times (\bar{\underline{\omega}}^{R_\mathrm{r}} \times \underline{r}^\mathrm{p}) + \bar{\underline{\omega}}^{R_\mathrm{r}} \times (\delta\underline{\omega}^{R_\mathrm{r}} \times \underline{r}^\mathrm{p}) + 2\bar{\underline{\omega}}^{R_\mathrm{r}} \times {}^{(R_\mathrm{r})}\frac{\mathrm{d}}{\mathrm{d}t}\Big(\underline{r}^\mathrm{p}\Big) + {}^{(R_\mathrm{r})}\frac{\mathrm{d}^2}{\mathrm{d}t^2}\Big(\underline{r}^\mathrm{p}\Big)
\end{aligned} \tag{B.60}$$

Examining equations B.53 and B.58, the expressions above are transformed into the

desired form as follows:

$$\begin{aligned}
\underline{v}^{R_{\mathrm{r}}^{\mathrm{p}}} &= \bar{\underline{v}}^{R_{\mathrm{r}}^{\mathrm{p}}} + \frac{\partial \underline{v}^{R_{\mathrm{r}}^{\mathrm{p}}}}{\partial \underline{v}^{S_{\tilde{\mathrm{n}}}^{\oplus \mathrm{r}}}} \cdot \delta \underline{v}^{S_{\tilde{\mathrm{n}}}^{\oplus \mathrm{r}}} + \frac{\partial \underline{v}^{R_{\mathrm{r}}^{\mathrm{p}}}}{\partial \underline{\omega}^{R_{\tilde{\mathrm{h}}"}^{\oplus \mathrm{r}}}} \cdot \delta \underline{\omega}^{R_{\tilde{\mathrm{h}}"}^{\oplus \mathrm{r}}} + \ldots \\
&\qquad \frac{\partial \underline{v}^{R_{\mathrm{r}}^{\mathrm{p}}}}{\partial \underline{\phi}^{R}} \cdot \delta \underline{\phi}^{R} + \frac{\partial \underline{v}^{R_{\mathrm{r}}^{\mathrm{p}}}}{\partial \dot{\underline{\varphi}}^{R}} \cdot \dot{\underline{\varphi}}^{R} + \frac{\partial \underline{v}^{R_{\mathrm{r}}^{\mathrm{p}}}}{\partial \dot{\underline{\varrho}}^{R}} \cdot \dot{\underline{\varrho}}^{R} \\
\underline{a}^{R_{\mathrm{r}}^{\mathrm{p}}} &= \bar{\underline{a}}^{R_{\mathrm{r}}^{\mathrm{p}}} + \frac{\partial \underline{a}^{R_{\mathrm{r}}^{\mathrm{p}}}}{\partial \underline{a}^{S_{\tilde{\mathrm{n}}}^{\oplus \mathrm{r}}}} \cdot \delta \underline{a}^{S_{\tilde{\mathrm{n}}}^{\oplus \mathrm{r}}} + \frac{\partial \underline{a}^{R_{\mathrm{r}}^{\mathrm{p}}}}{\partial \underline{\alpha}^{R_{\tilde{\mathrm{h}}"}^{\oplus \mathrm{r}}}} \cdot \delta \underline{\alpha}^{R_{\tilde{\mathrm{h}}"}^{\oplus \mathrm{r}}} + \frac{\partial \underline{a}^{R_{\mathrm{r}}^{\mathrm{p}}}}{\partial \underline{\omega}^{R_{\tilde{\mathrm{h}}"}^{\oplus \mathrm{r}}}} \cdot \delta \underline{\omega}^{R_{\tilde{\mathrm{h}}"}^{\oplus \mathrm{r}}} + \ldots \\
&\quad \frac{\partial \underline{a}^{R_{\mathrm{r}}^{\mathrm{p}}}}{\partial \underline{\phi}^{R}} \cdot \delta \underline{\phi}^{R} + \frac{\partial \underline{a}^{R_{\mathrm{r}}^{\mathrm{p}}}}{\partial \dot{\underline{\varphi}}^{R}} \cdot \dot{\underline{\varphi}}^{R} + \frac{\partial \underline{a}^{R_{\mathrm{r}}^{\mathrm{p}}}}{\partial \ddot{\underline{\varphi}}^{R}} \cdot \ddot{\underline{\varphi}}^{R} + \frac{\partial \underline{a}^{R_{\mathrm{r}}^{\mathrm{p}}}}{\partial \dot{\underline{\varrho}}^{R}} \cdot \dot{\underline{\varrho}}^{R} + \frac{\partial \underline{a}^{R_{\mathrm{r}}^{\mathrm{p}}}}{\partial \ddot{\underline{\varrho}}^{R}} \cdot \ddot{\underline{\varrho}}^{R}
\end{aligned} \tag{B.61}$$

For the mean values holds:

$$\begin{aligned}
\bar{\underline{v}}^{R_{\mathrm{r}}^{\mathrm{p}}} &= \bar{\boldsymbol{\Omega}} \underline{e}_1 \times \underline{r}^{\mathrm{p}} = \bar{\boldsymbol{\Omega}} \begin{bmatrix} 0 \\ -r_3 \\ r_2 \end{bmatrix} \\
\bar{\underline{a}}^{R_{\mathrm{r}}^{\mathrm{p}}} &= \bar{\boldsymbol{\Omega}} \underline{e}_1 \times (\bar{\boldsymbol{\Omega}} \underline{e}_1 \times \underline{r}^{\mathrm{p}}) = \bar{\boldsymbol{\Omega}}^2 \begin{bmatrix} 0 \\ -r_2 \\ -r_3 \end{bmatrix}
\end{aligned} \tag{B.62}$$

The following 'intermediate sensitivity functions' are frequently used in the expressions for the sensitivity functions in Eq. B.60:

$$\begin{aligned}
\frac{\partial \underline{a}^{R_{\mathrm{r}}^{\mathrm{p}}}}{\partial \underline{\alpha}^{R_{\mathrm{r}}}} &\equiv \frac{\partial \underline{v}^{R_{\mathrm{r}}^{\mathrm{p}}}}{\partial \underline{\omega}^{R_{\mathrm{r}}}} = \mathrm{J}^3_{v=1}(\underline{e}_v \times \underline{r}^{\mathrm{p}}) = \begin{pmatrix} 0 & r_3 & -r_2 \\ -r_3 & 0 & r_1 \\ r_2 & -r_1 & 0 \end{pmatrix} \\
\frac{\partial \underline{a}^{R_{\mathrm{r}}^{\mathrm{p}}}}{\partial \underline{\omega}^{R_{\mathrm{r}}}} &= \mathrm{J}^3_{v=1}(\underline{e}_v \times (\bar{\underline{\omega}}^{R_{\mathrm{r}}} \times \underline{r}^{\mathrm{p}}) + \bar{\underline{\omega}}^{R_{\mathrm{r}}} \times (\underline{e}_v \times \underline{r}^{\mathrm{p}})) = \bar{\boldsymbol{\Omega}} \begin{pmatrix} 0 & r_2 & r_3 \\ -2r_2 & r_1 & 0 \\ -2r_3 & 0 & r_1 \end{pmatrix}
\end{aligned} \tag{B.63}$$

For the sensitivity functions to the 'fed-in' kinematic vectors from the stand still partition holds (use Eq. B.55, B.60):

$$\begin{aligned}
\frac{\partial \underline{v}^{R_{\mathrm{r}}^{\mathrm{p}}}}{\partial \underline{v}^{S_{\tilde{\mathrm{n}}}^{\oplus \mathrm{r}}}} &\equiv \frac{\partial \underline{a}^{R_{\mathrm{r}}^{\mathrm{p}}}}{\partial \underline{a}^{S_{\tilde{\mathrm{n}}}^{\oplus \mathrm{r}}}} = {}^{R_{\mathrm{r}}}\bar{\Phi}^{R_{\mathrm{s}}} = \Phi_{\mathrm{x}}(\bar{\phi}_1^{R_{\mathrm{r}}}) \\
\frac{\partial \underline{v}^{R_{\mathrm{r}}^{\mathrm{p}}}}{\partial \underline{\omega}^{R_{\tilde{\mathrm{h}}"}^{\oplus \mathrm{r}}}} &\equiv \frac{\partial \underline{a}^{R_{\mathrm{r}}^{\mathrm{p}}}}{\partial \underline{\alpha}^{R_{\tilde{\mathrm{h}}"}^{\oplus \mathrm{r}}}} = \frac{\partial \underline{v}^{R_{\mathrm{r}}^{\mathrm{p}}}}{\partial \underline{\omega}^{R_{\mathrm{r}}}} \cdot \frac{\partial \underline{\omega}^{R_{\mathrm{r}}}}{\partial \underline{\omega}^{R_{\tilde{\mathrm{h}}"}^{\oplus \mathrm{r}}}} = \begin{pmatrix} 0 & r_3 & -r_2 \\ -r_3 & 0 & r_1 \\ r_2 & -r_1 & 0 \end{pmatrix} \cdot \Phi_{\mathrm{x}}(\bar{\phi}_1^{R_{\mathrm{r}}})
\end{aligned} \tag{B.64}$$

and (use Eq. B.63, Eq. B.56 for $\partial \underline{\alpha}^{R_{\mathrm{r}}} / \partial \underline{\omega}^{R_{\tilde{\mathrm{h}}"}^{\oplus \mathrm{r}}}$, allowed interchange of order of multiplication, and Eq. B.55 for $\partial \underline{\omega}^{R_{\mathrm{r}}} / \partial \underline{\omega}^{R_{\tilde{\mathrm{h}}"}^{\oplus \mathrm{r}}}$):

$$\frac{\partial \underline{a}^{R_{\mathrm{r}}^{\mathrm{p}}}}{\partial \underline{\omega}^{R_{\tilde{\mathrm{h}}"}^{\oplus \mathrm{r}}}} = \frac{\partial \underline{a}^{R_{\mathrm{r}}^{\mathrm{p}}}}{\partial \underline{\alpha}^{R_{\mathrm{r}}}} \cdot \frac{\partial \underline{\alpha}^{R_{\mathrm{r}}}}{\partial \underline{\omega}^{R_{\tilde{\mathrm{h}}"}^{\oplus \mathrm{r}}}} + \frac{\partial \underline{a}^{R_{\mathrm{r}}^{\mathrm{p}}}}{\partial \underline{\omega}^{R_{\mathrm{r}}}} \cdot \frac{\partial \underline{\omega}^{R_{\mathrm{r}}}}{\partial \underline{\omega}^{R_{\tilde{\mathrm{h}}"}^{\oplus \mathrm{r}}}} = \begin{pmatrix} 0 & 2r_2 & 2r_3 \\ -2r_2 & 0 & 0 \\ -2r_3 & 0 & 0 \end{pmatrix} \cdot \bar{\boldsymbol{\Omega}} \cdot \Phi_{\mathrm{x}}(\bar{\phi}_1^{R_{\mathrm{r}}}) \quad , \tag{B.65}$$

For the sensitivity functions to the degrees of freedom in R holds (use Eq. B.63):

$$\begin{aligned}
\frac{\partial \underline{v}^{R_{\mathrm{r}}^{\mathrm{p}}}}{\partial \dot{\underline{\varphi}}^{R}} &\equiv \frac{\partial \underline{a}^{R_{\mathrm{r}}^{\mathrm{p}}}}{\partial \ddot{\underline{\varphi}}^{R}} = \frac{\partial \underline{v}^{R_{\mathrm{r}}^{\mathrm{p}}}}{\partial \underline{\omega}^{R_{\mathrm{r}}}} \cdot \frac{\partial \underline{\omega}^{R_{\mathrm{r}}}}{\partial \dot{\underline{\varphi}}^{R}} = \begin{pmatrix} 0 & 0 & -r_2 & r_3 \\ -r_3/i_{\mathrm{gb}} & -r_3 & r_1 & 0 \\ r_2/i_{\mathrm{gb}} & r_2 & 0 & -r_1 \end{pmatrix} \\
\frac{\partial \underline{v}^{R_{\mathrm{r}}^{\mathrm{p}}}}{\partial \dot{\underline{\varrho}}^{R}} &\equiv \frac{\partial \underline{a}^{R_{\mathrm{r}}^{\mathrm{p}}}}{\partial \ddot{\underline{\varrho}}^{R}} = {}^{R_{\mathrm{r}}}\bar{\Phi}^{R_{\mathrm{r}}^{t\mathrm{t}}} = \begin{pmatrix} 1 & 0 & 0 \\ 0 & 1 & 0 \\ 0 & 0 & 1 \end{pmatrix}
\end{aligned} \tag{B.66}$$

and (use Eq. B.56, B.63):

$$\begin{aligned}
\frac{\partial \underline{v}^{R_{\mathrm{r}}^{\mathrm{p}}}}{\partial \underline{\phi}^{R}} &= \frac{\partial \underline{v}^{R_{\mathrm{r}}^{\mathrm{p}}}}{\partial \underline{\omega}^{R_{\mathrm{r}}}} \cdot \frac{\partial \underline{\omega}^{R_{\mathrm{r}}}}{\partial \underline{\phi}^{R}} = \bar{\Omega} \begin{pmatrix} 0 & 0 & -r_3 & -r_2 \\ 0 & 0 & 0 & r_1 \\ 0 & 0 & r_1 & 0 \end{pmatrix} \\
\frac{\partial \underline{a}^{R_{\mathrm{r}}^{\mathrm{p}}}}{\partial \underline{\phi}^{R}} &= \frac{\partial \underline{a}^{R_{\mathrm{r}}^{\mathrm{p}}}}{\partial \underline{\omega}^{R_{\mathrm{r}}}} \cdot \frac{\partial \underline{\omega}^{R_{\mathrm{r}}}}{\partial \underline{\phi}^{R}} = \bar{\Omega}^2 \begin{pmatrix} 0 & 0 & -r_2 & r_3 \\ 0 & 0 & -r_1 & 0 \\ 0 & 0 & 0 & r_1 \end{pmatrix}
\end{aligned} \tag{B.67}$$

and (use Eq. B.50, B.55, B.56, B.63):

$$\begin{aligned}
\frac{\partial \underline{a}^{R_{\mathrm{r}}^{\mathrm{p}}}}{\partial \ddot{\underline{\varphi}}^{R}} &= \frac{\partial \underline{a}^{R_{\mathrm{r}}^{\mathrm{p}}}}{\partial \underline{\alpha}^{R_{\mathrm{r}}}} \cdot \frac{\partial \underline{\alpha}^{R_{\mathrm{r}}}}{\partial \ddot{\underline{\varphi}}^{R}} + \frac{\partial \underline{a}^{R_{\mathrm{r}}^{\mathrm{p}}}}{\partial \underline{\omega}^{R_{\mathrm{r}}}} \cdot \frac{\partial \underline{\omega}^{R_{\mathrm{r}}}}{\partial \ddot{\underline{\varphi}}^{R}} = \bar{\Omega} \begin{pmatrix} 0 & 0 & 0 & 0 \\ -2r_2/i_{\mathrm{gb}} & -2r_2 & 0 & 2r_1 \\ -2r_3/i_{\mathrm{gb}} & -2r_3 & 2r_1 & 0 \end{pmatrix} \\
\frac{\partial \underline{a}^{R_{\mathrm{r}}^{\mathrm{p}}}}{\partial \dot{\underline{\varrho}}^{R}} &= \mathrm{J}_{v=1}^{3}(2\underline{\bar{\omega}}^{R_{\mathrm{r}}} \times {}^{R_{\mathrm{r}}}\underline{\bar{\Phi}}_{v}^{R_{\mathrm{r}}^{\iota_{\mathrm{t}}}}) = 2\bar{\Omega} \begin{pmatrix} 0 & 0 & 0 \\ 0 & 0 & -1 \\ 0 & 1 & 0 \end{pmatrix}
\end{aligned} \tag{B.68}$$

The linear velocity and acceleration in the exit point $X_0^{\oplus}$ of the blades bases (=$X_{\mathrm{f}}^{\ominus}$) have similar dependencies as above. But, replace R_{p} by $X_0^{\oplus}$ and premultiply the dependencies with the transformation matrix ${}^{X_0}\bar{\Phi}^{R_{\mathrm{r}}}$ by Eq. 3.63.

The kinematic and impulse vector formulations for the subcomponents in the support structure and rotor blades alllow to apply a generic procedure for the derivation of the equations of motions. In order to facilitate this generic procedure also for the rotor shaft & hub subcomponent the implementation of the kinematic vectors slightly differs from the formulations above. In M-function TBUDRIVTRKIN(), the dependency on the potential angular degrees of freedom in the drive-train is split-up into dependency on the angulars dofs in R_{r} and on co-axial angular output variables from R_{f}. For the angular acceleration of R_{r} the following mappings apply (similar for the other kinematic vectors):

$$\begin{aligned}
\frac{\partial \underline{\alpha}^{R_{\mathrm{r}}}}{\partial \underline{\phi}^{R}} \cdot \delta\underline{\phi}^{R} &\mapsto \frac{\partial \underline{\alpha}^{R_{\mathrm{r}}}}{\partial \underline{\phi}^{R_{\mathrm{r}}}} \cdot \delta\underline{\phi}^{R_{\mathrm{r}}} + \frac{\partial \underline{\alpha}^{R_{\mathrm{r}}}}{\partial \phi_{\mathrm{x}}^{R_{\mathrm{f}}}} \cdot \delta\phi_{\mathrm{x}}^{R_{\mathrm{f}}} \\
\frac{\partial \underline{\alpha}^{R_{\mathrm{r}}}}{\partial \dot{\underline{\varphi}}^{R}} \cdot \delta\dot{\underline{\varphi}}^{R} &\mapsto \frac{\partial \underline{\alpha}^{R_{\mathrm{r}}}}{\partial \dot{\underline{\varphi}}^{R_{\mathrm{r}}}} \cdot \delta\dot{\underline{\varphi}}^{R_{\mathrm{r}}} + \frac{\partial \underline{\alpha}^{R_{\mathrm{r}}}}{\partial \dot{\varphi}_{\mathrm{x}}^{R_{\mathrm{f}}}} \cdot \delta\dot{\varphi}_{\mathrm{x}}^{R_{\mathrm{f}}} \\
\frac{\partial \underline{\alpha}^{R_{\mathrm{r}}}}{\partial \ddot{\underline{\varphi}}^{R}} \cdot \delta\ddot{\underline{\varphi}}^{R} &\mapsto \frac{\partial \underline{\alpha}^{R_{\mathrm{r}}}}{\partial \ddot{\underline{\varphi}}^{R_{\mathrm{r}}}} \cdot \delta\ddot{\underline{\varphi}}^{R_{\mathrm{r}}} + \frac{\partial \underline{\alpha}^{R_{\mathrm{r}}}}{\partial \ddot{\varphi}_{\mathrm{x}}^{R_{\mathrm{f}}}} \cdot \delta\ddot{\varphi}_{\mathrm{x}}^{R_{\mathrm{f}}}
\end{aligned} \tag{B.69}$$

The following relationships hold between the now applying variables and the overall dof vectors by Eq. B.70 ($\underline{y}^{R_{\mathrm{r}}R_{\mathrm{f}}}$ is output vector from generator rotor R_{f} to shaft & hub R_{r}):

$$\begin{aligned}
\underline{\varphi}^{R_{\mathrm{r}}} &= \begin{pmatrix} \varphi_1^{R_{\mathrm{r}}} \\ \varphi_2^{R_{\mathrm{r}}} \\ \varphi_3^{R_{\mathrm{r}}} \end{pmatrix} = \begin{pmatrix} \varphi_2^{R} \\ \varphi_3^{R} \\ \varphi_4^{R} \end{pmatrix} \\
\underline{y}^{R_{\mathrm{r}}R_{\mathrm{f}}} &= \begin{pmatrix} \varphi_{\mathrm{x}}^{R_{\mathrm{f}}} \\ \dot{\varphi}_{\mathrm{x}}^{R_{\mathrm{f}}} \\ \ddot{\varphi}_{\mathrm{x}}^{R_{\mathrm{f}}} \end{pmatrix} \triangleq \begin{pmatrix} 1/i_{\mathrm{gb}} \cdot \phi_3^{R_{\mathrm{f}}} - \bar{\Omega} \cdot t \\ 1/i_{\mathrm{gb}} \cdot \dot{\phi}_3^{R_{\mathrm{f}}} - \bar{\Omega} \\ 1/i_{\mathrm{gb}} \cdot \ddot{\phi}_3^{R_{\mathrm{f}}} \end{pmatrix} = \frac{1}{i_{\mathrm{gb}}} \begin{pmatrix} \varphi_3^{R_{\mathrm{f}}} \\ \dot{\varphi}_3^{R_{\mathrm{f}}} \\ \ddot{\varphi}_3^{R_{\mathrm{f}}} \end{pmatrix} = \frac{1}{i_{\mathrm{gb}}} \begin{pmatrix} \varphi_1^{R} \\ \dot{\varphi}_1^{R} \\ \ddot{\varphi}_1^{R} \end{pmatrix}
\end{aligned} \tag{B.70}$$

The bottum-up ranking of the rotation dofs in R_{r} is distorsion (along x-axis), 'yaw0-wise' bending (along z-axis) and 'tilt0-wise' bending (along y-axis).

B.2.2 Drive train impulse

The angular and linear impulse vectors $\vec{h}$ and $\vec{p}$ for a one-element drive train subcomponent $R_{<\mathrm{sc}>}$ are expressed in coordinates along the local coordinate system of that

subcomponent. Actually, the full two vector expressions only apply in case of the rotor shaft & hub $R_{\rm r}$. Expressions for the impulse of the slow gearbox shaft system $R_{\rm s}$ do not apply because $R_{\rm s}$ is assumed mass-less.

Gearbox house $R_{\rm h}$
Since the gearbox house $R_{\rm h}$ only rotates in co-axial sense relative to the nacelle and does not involve translation dofs, only the angular impulse coordinate along the x-axis applies. With zero-mean angular velocity, the linearised expression for the angular impulse coordinate along the x-axis becomes (taken relative to the c.o.g, irrelevant because of moved mass to nacelle):

$$\begin{aligned} {}^{R_{\rm h}^*}\dot{\not{h}}_1^{R_{\rm h}} &= J_x^{R_{\rm h}} \cdot \delta\alpha_1^{R_{\rm h}} \\ \text{so (see Eq. B.33):} & \\ {}^{R_{\rm h}^*}\dot{\not{h}}_1^{R_{\rm h}} &= \frac{\partial {}^{R_{\rm h}^*}\dot{\not{h}}_1^{R_{\rm h}}}{\partial \alpha_1^{S_{\rm n}}} \cdot \delta\alpha_1^{S_{\rm n}} + \frac{\partial {}^{R_{\rm h}^*}\dot{\not{h}}_1^{R_{\rm h}}}{\partial \ddot{\varphi}_3^{R_{\rm h}}} \cdot \ddot{\varphi}_3^{R_{\rm h}} \end{aligned} \tag{B.71}$$

with sensitivities:

$$\frac{\partial {}^{R_{\rm h}^*}\dot{\not{h}}_1^{R_{\rm h}}}{\partial \alpha_1^{S_{\rm n}}} = \frac{\partial {}^{R_{\rm h}^*}\dot{\not{h}}_1^{R_{\rm h}}}{\partial \ddot{\varphi}_3^{R_{\rm h}}} = J_x^{R_{\rm h}} \tag{B.72}$$

where $J_x^{R_{\rm h}}$ is the co-axial moment of inertia of the gearbox house. As already mentioned at the nacelle's impulse coordinate vectors in section B.1.2, the mass of $R_{\rm h}$ and *non*-coaxial moments of inertia $J_{y,z}^{R_{\rm h}}$ are added to the inertia matrix of the nacelle.

Just as for the kinematic vectors of the rotor shaft & hub the implementation of the impulse vectors for the gearbox house slightly differs from the formulations above for 'generic' derivation of the equations of motions. In M-function TBUDRIVTRIMP(), the dependency on the (only) potential co-axial angular degree of freedom is extended with depedencies on the (never applying) remaining two angular degrees of freedom and all three linear degrees of freedom in $R_{\rm h}$. Taking into account the 'moved inertia to the nacelle', the implementation then comprises:

$$\begin{aligned} {}^{R_{\rm h}^*}\dot{\underline{\not{h}}}^{R_{\rm h}} &= \frac{\partial {}^{R_{\rm h}^*}\dot{\underline{\not{h}}}^{R_{\rm h}}}{\partial \underline{\alpha}^{S_{\tilde{\rm n}}}} \cdot \delta\underline{\alpha}^{S_{\tilde{\rm n}}} + \frac{\partial {}^{R_{\rm h}^*}\dot{\underline{\not{h}}}^{R_{\rm h}}}{\partial \underline{\ddot{\varphi}}^{R_{\rm h}}} \cdot \underline{\ddot{\varphi}}^{R_{\rm h}} + \frac{\partial {}^{R_{\rm h}^*}\dot{\underline{\not{h}}}^{R_{\rm h}}}{\partial \underline{\ddot{\varrho}}^{R_{\rm h}}} \cdot \underline{\ddot{\varrho}}^{R_{\rm h}} \\ \dot{\underline{p}}^{R_{\rm h}} &= \frac{\partial \dot{\underline{p}}^{R_{\rm h}}}{\partial \underline{\ddot{\varphi}}^{R_{\rm h}}} \cdot \underline{\ddot{\varphi}}^{R_{\rm h}} + \frac{\partial \dot{\underline{p}}^{R_{\rm h}}}{\partial \underline{\ddot{\varrho}}^{R_{\rm h}}} \cdot \underline{\ddot{\varrho}}^{R_{\rm h}} \end{aligned} \tag{B.73}$$

with

$$\begin{aligned} \frac{\partial {}^{R_{\rm h}^*}\dot{\underline{\not{h}}}^{R_{\rm h}}}{\partial \underline{\alpha}^{S_{\tilde{\rm n}}}} &= \begin{pmatrix} J_x^{R{\rm h}} & 0 & 0 \\ 0 & 0 & 0 \\ 0 & 0 & 0 \end{pmatrix} \\ \frac{\partial {}^{R_{\rm h}^*}\dot{\underline{\not{h}}}^{R_{\rm h}}}{\partial \underline{\ddot{\varphi}}^{R_{\rm h}}} &= \begin{pmatrix} 0 & 0 & J_x^{R{\rm h}} \\ 0 & 0 & 0 \\ 0 & 0 & 0 \end{pmatrix} \quad ; \quad \frac{\partial {}^{R_{\rm h}^*}\dot{\underline{\not{h}}}^{R_{\rm h}}}{\partial \underline{\ddot{\varrho}}^{R_{\rm h}}} = \begin{pmatrix} 0 & 0 & 0 \\ 0 & 0 & 0 \\ 0 & 0 & 0 \end{pmatrix} \\ \frac{\partial \dot{\underline{p}}^{R_{\rm h}}}{\partial \underline{\ddot{\varphi}}^{R_{\rm h}}} &= \begin{pmatrix} 0 & 0 & 0 \\ 0 & 0 & 0 \\ 0 & 0 & 0 \end{pmatrix} \quad ; \quad \frac{\partial \dot{\underline{p}}^{R_{\rm h}}}{\partial \underline{\ddot{\varrho}}^{R_{\rm h}}} = \begin{pmatrix} 0 & 0 & 0 \\ 0 & 0 & 0 \\ 0 & 0 & 0 \end{pmatrix} \end{aligned} \tag{B.74}$$

The bottum-up ranked rotation axes for dofs in $R_{\rm h}$ are the y-, z- and x-axis; angular and linear dofs along the y- and z-axis do never apply, just as the linear dof along the x-axis.

Generator rotor $R_{\rm f}$
Just as for the gearbox house all non-coaxial angular inertia effects are moved to the nacelle. However, these also include first order gyroscopic effects due to the non-zero

mean angular speed $i_{\mathrm{gb}} \cdot \bar{\Omega}$. In order to enable extension of the nacelle model with these effects, also the *non*-coaxial angular impulse coordinates of the generator rotor must be considered. The linearised expression for the angular impulse coordinate vector, which is taken relative to the centre of gravity, is derived from the following first order approximation:

$$ {}^{R_{\mathrm{f}}^*}\underline{\dot{\boldsymbol{h}}}^{R_{\mathrm{f}}} = \boldsymbol{I}^{R_{\mathrm{f}}} \cdot \delta\underline{\alpha}^{R_{\mathrm{f}}} + \underline{\bar{\omega}}^{R_{\mathrm{f}}} \times \boldsymbol{I}^{R_{\mathrm{f}}} \cdot \underline{\bar{\omega}}^{R_{\mathrm{f}}} + \underline{\bar{\omega}}^{R_{\mathrm{f}}} \times \boldsymbol{I}^{R_{\mathrm{f}}} \cdot \delta\underline{\omega}^{R_{\mathrm{f}}} + \delta\underline{\omega}^{R_{\mathrm{f}}} \times \boldsymbol{I}^{R_{\mathrm{f}}} \cdot \underline{\bar{\omega}}^{R_{\mathrm{f}}} \tag{B.75} $$

The inertia matrix $\boldsymbol{I}^{R_{\mathrm{f}}}$ is simply the diagonal of the priniciple moments of inertia $J_{x,y,z}^{R_{\mathrm{f}}}$ because we assume that the principle axes coincide with the coordinate system on R_{f}:

$$ \boldsymbol{I}^{R_{\mathrm{f}}} = \begin{pmatrix} J_x^{R\mathrm{f}} & 0 & 0 \\ 0 & J_y^{R_{\mathrm{f}}} & 0 \\ 0 & 0 & J_z^{R\mathrm{f}} \end{pmatrix} \tag{B.76} $$

Since $\boldsymbol{I}^{R_{\mathrm{f}}}$ is diagonal, the vector product $\underline{\bar{\omega}}^{R_{\mathrm{f}}} \times \boldsymbol{I}^{R_{\mathrm{f}}} \cdot \underline{\bar{\omega}}^{R_{\mathrm{f}}}$ of the mean angular velocities will be zero because $\underline{\bar{\omega}}^{R_{\mathrm{f}}}$ only has the non-zero coordinate $i_{\mathrm{gb}}\bar{\Omega}$ along the x-axis (see Eq. B.47).

The pursued expression for the angular impulse involves sensitivities to any variable upon which $\underline{\alpha}^{R_{\mathrm{f}}}$ or $\underline{\omega}^{R_{\mathrm{f}}}$ depends (see Eq. B.46). This yields:

$$ {}^{R_{\mathrm{f}}^*}\underline{\dot{\boldsymbol{h}}}^{R_{\mathrm{f}}} = \frac{\partial {}^{R_{\mathrm{f}}^*}\underline{\dot{\boldsymbol{h}}}^{R_{\mathrm{f}}}}{\partial \underline{\omega}^{S_{\tilde{\mathrm{n}}}}} \cdot \delta\underline{\omega}^{S_{\tilde{\mathrm{n}}}} + \frac{\partial {}^{R_{\mathrm{f}}^*}\underline{\dot{\boldsymbol{h}}}^{R_{\mathrm{f}}}}{\partial \underline{\alpha}^{S_{\tilde{\mathrm{n}}}}} \cdot \delta\underline{\alpha}^{S_{\tilde{\mathrm{n}}}} + \frac{\partial {}^{R_{\mathrm{f}}^*}\underline{\dot{\boldsymbol{h}}}^{R_{\mathrm{f}}}}{\partial \underline{\dot{\varphi}}^{R}} \cdot \underline{\dot{\varphi}}^{R} + \frac{\partial {}^{R_{\mathrm{f}}^*}\underline{\dot{\boldsymbol{h}}}^{R_{\mathrm{f}}}}{\partial \underline{\ddot{\varphi}}^{R}} \cdot \underline{\ddot{\varphi}}^{R} \tag{B.77} $$

with sensitivities (see Eq. B.48, B.49):

$$ \begin{aligned} \frac{\partial {}^{R_{\mathrm{f}}^*}\underline{\dot{\boldsymbol{h}}}^{R_{\mathrm{f}}}}{\partial \underline{\omega}^{S_{\tilde{\mathrm{n}}}}} &= \frac{\partial {}^{R_{\mathrm{f}}^*}\underline{\dot{\boldsymbol{h}}}^{R_{\mathrm{f}}}}{\partial \underline{\alpha}^{R_{\mathrm{f}}}} \cdot \frac{\partial \underline{\alpha}^{R_{\mathrm{f}}}}{\partial \underline{\omega}^{S_{\tilde{\mathrm{n}}}}} + \frac{\partial {}^{R_{\mathrm{f}}^*}\underline{\dot{\boldsymbol{h}}}^{R_{\mathrm{f}}}}{\partial \underline{\omega}^{R_{\mathrm{f}}}} \cdot \frac{\partial \underline{\omega}^{R_{\mathrm{f}}}}{\partial \underline{\omega}^{S_{\tilde{\mathrm{n}}}}} \\ \frac{\partial {}^{R_{\mathrm{f}}^*}\underline{\dot{\boldsymbol{h}}}^{R_{\mathrm{f}}}}{\partial \underline{\alpha}^{S_{\tilde{\mathrm{n}}}}} &= \frac{\partial {}^{R_{\mathrm{f}}^*}\underline{\dot{\boldsymbol{h}}}^{R_{\mathrm{f}}}}{\partial \underline{\alpha}^{R_{\mathrm{f}}}} \cdot \frac{\partial \underline{\alpha}^{R_{\mathrm{f}}}}{\partial \underline{\alpha}^{S_{\tilde{\mathrm{n}}}}} \end{aligned} \tag{B.78} $$

and:

$$ \begin{aligned} \frac{\partial {}^{R_{\mathrm{f}}^*}\underline{\dot{\boldsymbol{h}}}^{R_{\mathrm{f}}}}{\partial \underline{\dot{\varphi}}^{R}} &= \frac{\partial {}^{R_{\mathrm{f}}^*}\underline{\dot{\boldsymbol{h}}}^{R_{\mathrm{f}}}}{\partial \underline{\omega}^{R_{\mathrm{f}}}} \cdot \frac{\partial \underline{\omega}^{R_{\mathrm{f}}}}{\partial \underline{\dot{\varphi}}^{R}} \\ \frac{\partial {}^{R_{\mathrm{f}}^*}\underline{\dot{\boldsymbol{h}}}^{R_{\mathrm{f}}}}{\partial \underline{\ddot{\varphi}}^{R}} &= \frac{\partial {}^{R_{\mathrm{f}}^*}\underline{\dot{\boldsymbol{h}}}^{R_{\mathrm{f}}}}{\partial \underline{\alpha}^{R_{\mathrm{f}}}} \cdot \frac{\partial \underline{\alpha}^{R_{\mathrm{f}}}}{\partial \underline{\ddot{\varphi}}^{R}} \end{aligned} \tag{B.79} $$

in which the direct partial derivatives of the angular impulse are given by:

$$ \begin{aligned} \frac{\partial {}^{R_{\mathrm{f}}^*}\underline{\dot{\boldsymbol{h}}}^{R_{\mathrm{f}}}}{\partial \underline{\omega}^{R_{\mathrm{f}}}} &= \mathrm{J}_{w=1}^{3}\big(\underline{\bar{\omega}}^{R_{\mathrm{f}}} \times \boldsymbol{I}^{R_{\mathrm{f}}} \cdot \underline{e}_w + \underline{e}_w \times \boldsymbol{I}^{R_{\mathrm{f}}} \cdot \underline{\bar{\omega}}^{R_{\mathrm{f}}}\big) \\ \frac{\partial {}^{R_{\mathrm{f}}^*}\underline{\dot{\boldsymbol{h}}}^{R_{\mathrm{f}}}}{\partial \underline{\alpha}^{R_{\mathrm{f}}}} &= \boldsymbol{I}^{R_{\mathrm{f}}} \end{aligned} \tag{B.80} $$

The equations of motion for the generator rotor R_{f} only comprises the co-axial rotation. It is allowed to add the inertia effects of the (non-coaxial) inertia parameters of R_{f} to the impulse vectors of the nacelle S_{n}. The way these parameters are eventually dealt with is also included in section B.1.2. The text below gives a discussion on this 'inertia transfer' and explains why the generator rotor model can be limited to co-axial rotation only.

The (non-coaxial) inertia parameters from R_{f} have to be summed to the corresonding nacelle parameters when the sensitivity of the impulse vectors of S_{n} to acceleration variables is considered. This concerns augmentation of the nacelle mass with $m^{R_{\mathrm{f}}}$ and of the nacelle's inertia moments relative to the y- and z-axis in the final coordinate system with the non-coaxial moments of inertia $J_{\mathrm{y}}^{R_{\mathrm{f}}}$ and $J_{\mathrm{z}}^{R_{\mathrm{f}}}$, which are equal due to axi-symmetry.

The inertia parameters of $R_{\rm f}$ are dealt with in another way when the sensitivity of the angular impulse to the angular speed is considerd. Visually, the non-zero mean angular speed $i_{\rm gb}\cdot\bar{\Omega}$ of $R_{\rm f}$ may cause yaw- or tiltwise 'inertia torques' via $J_{\rm y}^{R_{\rm f}}-J_{\rm x}^{R_{\rm f}}$ or $J_{\rm x}^{R_{\rm f}}-J_{\rm z}^{R_{\rm f}}$ at tilt- or yawwise angular motion. It is allowed to deal with these gyroscopic effects in the equations of motion of the nacelle.

Actually, the generator rotor has the following angular impulse sensitivity to its angular velocity vector (see and elaborate Eq. B.79):

$$\frac{\partial^{R_{\rm f}^*}\underline{\dot{\hbar}}^{R_{\rm f}}}{\partial\underline{\omega}^{R_{\rm f}}} \;=\; \left[\;\left[\begin{array}{c}0\\0\\0\end{array}\right]\;\left[\begin{array}{c}0\\0\\i_{\rm gb}\bar{\Omega}(J_{\rm y}^{R_{\rm f}}-J_{\rm x}^{R_{\rm f}})\end{array}\right]\;\left[\begin{array}{c}0\\i_{\rm gb}\bar{\Omega}(J_{\rm x}^{R_{\rm f}}-J_{\rm z}^{R_{\rm f}})\\0\end{array}\right]\;\right] \tag{B.81}$$

It is clear that only the tilt- and yawwise motions of the generator rotor play a role; these do not differ from those of the nacelle. As $J_{\rm y}^{R_{\rm f}}=J_{\rm z}^{R_{\rm f}}$ because of axi-symmetry, it can be proven that ($\tilde{\Phi}=\Phi_{\rm x}(\bar{\Omega}t)$):

$$\Big(\;\tilde{\Phi}^{\rm T}\cdot(\frac{\partial^{R_{\rm f}^*}\underline{\dot{\hbar}}^{R_{\rm f}}}{\partial\underline{\omega}^{R_{\rm f}}}\cdot\delta\underline{\omega}^{R_{\rm f}})\;=\;\tilde{\Phi}^{\rm T}\cdot(\frac{\partial^{R_{\rm f}^*}\underline{\dot{\hbar}}^{R_{\rm f}}}{\partial\underline{\omega}^{R_{\rm f}}}\cdot(\tilde{\Phi}\cdot\delta\underline{\omega}^{S_{\rm n}})\;\Big)\;=\;\frac{\partial^{R_{\rm f}^*}\underline{\dot{\hbar}}^{R_{\rm f}}}{\partial\underline{\omega}^{R_{\rm f}}}\cdot\delta\underline{\omega}^{S_{\rm n}} \tag{B.82}$$

This equality tells that adding $\partial^{R_{\rm f}^*}\underline{\dot{\hbar}}^{R_{\rm f}}/\partial\underline{\omega}^{R_{\rm f}}$ to the sensitivity of the nacelle's angular impulse to the angular velocity, considered in the final coordinate system of the nacelle, exactly caters of the gyroscopic effects of the generator rotor.

Just as for the kinematic vectors of the rotor shaft & hub the implementation of the impulse vectors for the generator rotor slightly differs from the formulations above for 'generic' derivation of the equations of motions. In M-function TBUDRIVTRIMP(), the dependency on the (only) potential co-axial angular degree of freedom is extended with depedencies on the (never applying) remaining two angular degrees of freedom and all three linear degrees of freedom in $R_{\rm f}$. Taking into account the 'moved inertia to the nacelle', the implementation then comprises:

$$\begin{aligned}
{}^{R_{\rm f}^*}\underline{\dot{\hbar}}^{R_{\rm f}} &= \frac{\partial^{R_{\rm f}^*}\underline{\dot{\hbar}}^{R_{\rm f}}}{\partial\underline{\alpha}^{S_{\tilde{\rm n}}}}\cdot\delta\underline{\alpha}^{S_{\tilde{\rm n}}}+\frac{\partial^{R_{\rm f}^*}\underline{\dot{\hbar}}^{R_{\rm f}}}{\partial\underline{\varphi}^{R_{\rm f}}}\cdot\underline{\dot{\varphi}}^{R_{\rm f}}+\frac{\partial^{R_{\rm f}^*}\underline{\dot{\hbar}}^{R_{\rm f}}}{\partial\underline{\varrho}^{R_{\rm f}}}\cdot\underline{\dot{\varrho}}^{R_{\rm f}}\\
\dot{\underline{p}}^{R_{\rm f}} &= \frac{\partial\dot{\underline{p}}^{R_{\rm f}}}{\partial\underline{\dot{\varphi}}^{R_{\rm f}}}\cdot\underline{\dot{\varphi}}^{R_{\rm f}}+\frac{\partial\dot{\underline{p}}^{R_{\rm f}}}{\partial\underline{\dot{\varrho}}^{R_{\rm f}}}\cdot\underline{\dot{\varrho}}^{R_{\rm f}}
\end{aligned} \tag{B.83}$$

with

$$\begin{aligned}
\frac{\partial^{R_{\rm f}^*}\underline{\dot{\hbar}}^{R_{\rm f}}}{\partial\underline{\alpha}^{S_{\tilde{\rm n}}}} &= \left(\begin{array}{ccc}J_x^{Rf}&0&0\\0&0&0\\0&0&0\end{array}\right)\\
\frac{\partial^{R_{\rm f}^*}\underline{\dot{\hbar}}^{R_{\rm f}}}{\partial\underline{\dot{\varphi}}^{R_{\rm f}}} &= \left(\begin{array}{ccc}0&0&J_x^{Rf}\\0&0&0\\0&0&0\end{array}\right)\;;\;\frac{\partial^{R_{\rm f}^*}\underline{\dot{\hbar}}^{R_{\rm f}}}{\partial\underline{\dot{\varrho}}^{R_{\rm f}}}=\left(\begin{array}{ccc}0&0&0\\0&0&0\\0&0&0\end{array}\right)\\
\frac{\partial\dot{\underline{p}}^{R_{\rm f}}}{\partial\underline{\dot{\varphi}}^{R_{\rm f}}} &= \left(\begin{array}{ccc}0&0&0\\0&0&0\\0&0&0\end{array}\right)\;;\;\frac{\partial\dot{\underline{p}}^{R_{\rm f}}}{\partial\underline{\dot{\varrho}}^{R_{\rm f}}}=\left(\begin{array}{ccc}0&0&0\\0&0&0\\0&0&0\end{array}\right)
\end{aligned} \tag{B.84}$$

The bottum-up ranked rotation axes for dofs in $R_{\rm f}$ are the y-, z- and x-axis; angular and linear dofs along the y- and z-axis do never apply, just as the linear dof along the x-axis.

Rotor shaft & hub $R_{\rm r}$
Since the degrees of freedom of $R_{\rm r}$ are modelled in the rotor centre $R_{\rm r}^{\rm c}$, the angular impulse of $R_{\rm r}$ is also considered relative to $R_{\rm r}^{\rm c}$. The linearised expression for the angular

impulse coordinate vector is derived from the following first order approximation:

$$\begin{aligned} {}^{R_{\mathrm{r}}^{\mathrm{c}}}\dot{\underline{\boldsymbol{h}}}^{R_{\mathrm{r}}} &= {}^{R_{\mathrm{r}}^{\mathrm{c}}}\underline{r}^{R_{\mathrm{r}}^{*}} \times m^{R_{\mathrm{r}}}(\bar{\underline{a}}^{R_{\mathrm{r}}^{*}} + \delta\underline{a}^{R_{\mathrm{r}}^{*}}) + \boldsymbol{I}^{R_{\mathrm{r}}} \cdot \delta\underline{\alpha}^{R_{\mathrm{r}}} + \\ & \bar{\underline{\omega}}^{R_{\mathrm{r}}} \times \boldsymbol{I}^{R_{\mathrm{r}}} \cdot \bar{\underline{\omega}}^{R_{\mathrm{r}}} + \bar{\underline{\omega}}^{R_{\mathrm{r}}} \times \boldsymbol{I}^{R_{\mathrm{r}}} \cdot \delta\underline{\omega}^{R_{\mathrm{r}}} + \delta\underline{\omega}^{R_{\mathrm{r}}} \times \boldsymbol{I}^{R_{\mathrm{r}}} \cdot \bar{\underline{\omega}}^{R_{\mathrm{r}}} \end{aligned} \tag{B.85}$$

The inertia matrix $\boldsymbol{I}^{R_{\mathrm{r}}}$ contains the inertia moments and products relative to the centre of gravity of R_{r} and applies along the axes of the final coordinate system of R_{r}. These are assumed to coincide with the priniciple inertia axes, so the matrix $\boldsymbol{I}^{R_{\mathrm{r}}}$ is simply the diagonal of the priniciple moments of inertia $J_{x,y,z}^{R_{\mathrm{r}}}$.

The pursued expression for the angular impulse involves sensitivities to any variable upon which $\underline{a}^{R_{\mathrm{r}}^{*}}$, $\underline{\alpha}^{R_{\mathrm{r}}}$ or $\underline{\omega}^{R_{\mathrm{r}}}$ depends; for the linear impulse this only concerns $\underline{a}^{R_{\mathrm{r}}^{*}}$. The linearised expressions are written in compact form:

$$\begin{aligned} {}^{R_{\mathrm{r}}^{\mathrm{c}}}\dot{\underline{h}}^{R_{\mathrm{r}}} &= {}^{R_{\mathrm{r}}^{\mathrm{c}}}\bar{\dot{\underline{h}}}^{R_{\mathrm{r}}} + \sum_{(\underline{z})} \frac{\partial {}^{R_{\mathrm{r}}^{\mathrm{c}}}\dot{\underline{h}}^{R_{\mathrm{r}}}}{\partial \underline{z}} \cdot \delta\underline{z} \\ \underline{\dot{p}}^{R_{\mathrm{r}}} &= \bar{\underline{\dot{p}}}^{R_{\mathrm{r}}} + \sum_{(\underline{z})} \frac{\partial \underline{\dot{p}}^{R_{\mathrm{r}}}}{\partial \underline{z}} \cdot \delta\underline{z} \end{aligned} \tag{B.86}$$

Equations B.61 and B.53 tell that the summuation over $\underline{z}$ concerns $\underline{\omega}^{R_{\tilde{\mathrm{n}}"}}$, $\underline{\alpha}^{R_{\tilde{\mathrm{n}}"}}$, $\underline{a}^{S_{\tilde{\mathrm{n}}}^{\oplus}}$, $\underline{\phi}^{R}$, $\underline{\dot{\varphi}}^{R}$, $\underline{\ddot{\varphi}}^{R}$, $\underline{\dot{\varrho}}^{R}$ and $\underline{\ddot{\varrho}}^{R}$.

Just as for the generator rotor R_{f} the vector product $\bar{\underline{\omega}}^{R_{\mathrm{r}}} \times \boldsymbol{I}^{R_{\mathrm{r}}} \cdot \bar{\underline{\omega}}^{R_{\mathrm{r}}}$ will be zero because the inertia matrix is diagonal and the mean angular velocity only has the non-zero coordiante $\bar{\boldsymbol{\Omega}}$ along the x-axis (see Eq. B.54). The expressions for the mean impulse values aree:

$$\begin{aligned} {}^{R_{\mathrm{r}}^{\mathrm{c}}}\bar{\dot{\underline{h}}}^{R_{\mathrm{r}}} &= {}^{R_{\mathrm{r}}^{\mathrm{c}}}\underline{r}^{R_{\mathrm{r}}^{*}} \times m^{R_{\mathrm{r}}}\bar{\underline{a}}^{R_{\mathrm{r}}^{*}} \\ \bar{\underline{\dot{p}}}^{R_{\mathrm{r}}} &= m^{R_{\mathrm{r}}}\bar{\underline{a}}^{R_{\mathrm{r}}^{*}} \end{aligned} \tag{B.87}$$

while equation B.62 tells that the means may only be non-zero in case of eccentricity of the hub.

The sensitivity of the rate of change in the angular impulse to $\underline{\omega}^{R_{\tilde{\mathrm{n}}"}}$ and $\underline{\dot{\varphi}}^{R}$ involve the direct partial derivatives of the angular impulse to $\underline{\omega}^{R_{\mathrm{r}}}$, $\underline{\alpha}^{R_{\mathrm{r}}}$ and $\underline{a}^{R_{\mathrm{r}}^{*}}$:

$$\frac{\partial {}^{R_{\mathrm{r}}^{\mathrm{c}}}\dot{\underline{h}}^{R_{\mathrm{r}}}}{\partial \underline{z}} = \frac{\partial {}^{R_{\mathrm{r}}^{\mathrm{c}}}\dot{\underline{h}}^{R_{\mathrm{r}}}}{\partial \underline{\omega}^{R_{\mathrm{r}}}} \cdot \frac{\partial \underline{\omega}^{R_{\mathrm{r}}}}{\partial \underline{z}} + \frac{\partial {}^{R_{\mathrm{r}}^{\mathrm{c}}}\dot{\underline{h}}^{R_{\mathrm{r}}}}{\partial \underline{\alpha}^{R_{\mathrm{r}}}} \cdot \frac{\partial \underline{\alpha}^{R_{\mathrm{r}}}}{\partial \underline{z}} + \frac{\partial {}^{R_{\mathrm{r}}^{\mathrm{c}}}\dot{\underline{h}}^{R_{\mathrm{r}}}}{\partial \underline{a}^{R_{\mathrm{r}}^{*}}} \cdot \frac{\partial \underline{a}^{R_{\mathrm{r}}^{*}}}{\partial \underline{z}} \quad \text{for } \underline{z} = \underline{\omega}^{R_{\tilde{\mathrm{n}}"}}, \underline{\dot{\varphi}}^{R} \tag{B.88}$$

The sensitivity to $\underline{\phi}^{R}$ involves the direct partial derivatives to $\underline{\omega}^{R_{\mathrm{r}}}$ and $\underline{a}^{R_{\mathrm{r}}^{*}}$:

$$\frac{\partial {}^{R_{\mathrm{r}}^{\mathrm{c}}}\dot{\underline{h}}^{R_{\mathrm{r}}}}{\partial \underline{z}} = \frac{\partial {}^{R_{\mathrm{r}}^{\mathrm{c}}}\dot{\underline{h}}^{R_{\mathrm{r}}}}{\partial \underline{\omega}^{R_{\mathrm{r}}}} \cdot \frac{\partial \underline{\omega}^{R_{\mathrm{r}}}}{\partial \underline{z}} + \frac{\partial {}^{R_{\mathrm{r}}^{\mathrm{c}}}\dot{\underline{h}}^{R_{\mathrm{r}}}}{\partial \underline{a}^{R_{\mathrm{r}}^{*}}} \cdot \frac{\partial \underline{a}^{R_{\mathrm{r}}^{*}}}{\partial \underline{z}} \quad \text{for } \underline{z} = \underline{\phi}^{R} \tag{B.89}$$

The sensitivity to $\underline{\alpha}^{R_{\tilde{\mathrm{n}}"}}$ and $\underline{\ddot{\varphi}}^{R}$ involves direct partial derivatives to $\underline{\alpha}^{R_{\mathrm{r}}}$ and $\underline{a}^{R_{\mathrm{r}}^{*}}$:

$$\frac{\partial {}^{R_{\mathrm{r}}^{\mathrm{c}}}\dot{\underline{h}}^{R_{\mathrm{r}}}}{\partial \underline{z}} = \frac{\partial {}^{R_{\mathrm{r}}^{\mathrm{c}}}\dot{\underline{h}}^{R_{\mathrm{r}}}}{\partial \underline{\alpha}^{R_{\mathrm{r}}}} \cdot \frac{\partial \underline{\alpha}^{R_{\mathrm{r}}}}{\partial \underline{z}} + \frac{\partial {}^{R_{\mathrm{r}}^{\mathrm{c}}}\dot{\underline{h}}^{R_{\mathrm{r}}}}{\partial \underline{a}^{R_{\mathrm{r}}^{*}}} \cdot \frac{\partial \underline{a}^{R_{\mathrm{r}}^{*}}}{\partial \underline{z}} \quad \text{for } \underline{z} = \underline{\alpha}^{R_{\tilde{\mathrm{n}}"}}, \underline{\ddot{\varphi}}^{R} \tag{B.90}$$

The sensitivity to $\underline{a}^{S_{\tilde{\mathrm{n}}}^{\oplus}}$, $\underline{\dot{\varrho}}^{R}$ and $\underline{\ddot{\varrho}}^{R}$ involves the partial derivative to only $\underline{a}^{R_{\mathrm{r}}^{*}}$:

$$\frac{\partial {}^{R_{\mathrm{r}}^{\mathrm{c}}}\dot{\underline{h}}^{R_{\mathrm{r}}}}{\partial \underline{z}} = \frac{\partial {}^{R_{\mathrm{r}}^{\mathrm{c}}}\dot{\underline{h}}^{R_{\mathrm{r}}}}{\partial \underline{a}^{R_{\mathrm{r}}^{*}}} \cdot \frac{\partial \underline{a}^{R_{\mathrm{r}}^{*}}}{\partial \underline{z}} \quad \text{for } \underline{z} = \underline{a}^{S_{\tilde{\mathrm{n}}}^{\oplus}}, \underline{\dot{\varrho}}^{R}, \underline{\ddot{\varrho}}^{R} \tag{B.91}$$

The direct partial derivatives of the angular impulse change are given by:

$$\begin{aligned}
\frac{\partial {}^{R_\mathrm{r}^\mathrm{c}}\dot{\underline{\underline{h}}}^{R_\mathrm{r}}}{\partial \underline{\omega}^{R_\mathrm{r}}} &= \mathrm{J}_{w=1}^{3}\left(\bar{\underline{\omega}}^{R_\mathrm{r}} \times \boldsymbol{I}^{R_\mathrm{r}} \cdot \underline{e}_w + \underline{e}_w \times \boldsymbol{I}^{R_\mathrm{r}} \cdot \bar{\underline{\omega}}^{R_\mathrm{r}}\right) \\
\frac{\partial {}^{R_\mathrm{r}^\mathrm{c}}\dot{\underline{\underline{h}}}^{R_\mathrm{r}}}{\partial \underline{\alpha}^{R_\mathrm{r}}} &= \boldsymbol{I}^{R_\mathrm{r}} \\
\frac{\partial {}^{R_\mathrm{r}^\mathrm{c}}\dot{\underline{\underline{h}}}^{R_\mathrm{r}}}{\partial \underline{a}^{R_\mathrm{r}^*}} &= \mathrm{J}_{w=1}^{3}\left({}^{R_\mathrm{r}^\mathrm{c}}\underline{r}^{R_\mathrm{r}^*} \times m^{R_\mathrm{r}} \cdot \underline{e}_w\right)
\end{aligned} \tag{B.92}$$

The sensitivity of the rate of change of the linear impulse to all variables only involves the direct partial derivative to $\underline{a}^{R_\mathrm{r}^*}$:

$$\frac{\partial \dot{\underline{p}}^{R_\mathrm{r}}}{\partial \underline{z}} = \underline{m}^{R_\mathrm{r}} \cdot \frac{\partial \underline{a}^{R_\mathrm{r}^*}}{\partial \underline{z}} \quad \text{for } \underline{z} = \underline{\omega}^{R_{\tilde{\mathrm{n}}"}}, \underline{\alpha}^{R_{\tilde{\mathrm{n}}"}}, \underline{a}^{S^{\oplus}_{\tilde{\mathrm{n}}}}, \underline{\phi}^{R}, \underline{\dot{\varphi}}^{R}, \underline{\ddot{\varphi}}^{R}, \underline{\dot{\varrho}}^{R}, \underline{\ddot{\varrho}}^{R} \tag{B.93}$$

Just as for the impulse vector of the generator rotor R_f, the implementation slightly differs from the formulations above in order to facilitate generic derivation of the equations of motions. In M-function TUBDRIVTRIMP(), the dependency on the potential angular degrees of freedom in the drive-train is split-up into dependency on the angulars dofs in R_r and on co-axial angular output variables from R_f. For the rate of change in the angular impulse of R_r the following mappings then apply (see also Eq. B.69, B.70; similar expressions for linear impulse):

$$\begin{aligned}
\frac{\partial {}^{R_\mathrm{r}^\mathrm{c}}\dot{\underline{\underline{h}}}^{R_\mathrm{r}}}{\partial \underline{\phi}^{R}} \cdot \delta\underline{\phi}^{R} &\mapsto \frac{\partial {}^{R_\mathrm{r}^\mathrm{c}}\dot{\underline{\underline{h}}}^{R_\mathrm{r}}}{\partial \underline{\phi}^{R_\mathrm{r}}} \cdot \delta\underline{\phi}^{R_\mathrm{r}} + \frac{\partial {}^{R_\mathrm{r}^\mathrm{c}}\dot{\underline{\underline{h}}}^{R_\mathrm{r}}}{\partial \phi_\mathrm{x}^{R_\mathrm{f}}} \cdot \delta\phi_\mathrm{x}^{R_\mathrm{f}} \\
\frac{\partial {}^{R_\mathrm{r}^\mathrm{c}}\dot{\underline{\underline{h}}}^{R_\mathrm{r}}}{\partial \underline{\dot{\varphi}}^{R}} \cdot \delta\underline{\dot{\varphi}}^{R} &\mapsto \frac{\partial {}^{R_\mathrm{r}^\mathrm{c}}\dot{\underline{\underline{h}}}^{R_\mathrm{r}}}{\partial \underline{\dot{\varphi}}^{R_\mathrm{r}}} \cdot \delta\underline{\dot{\varphi}}^{R_\mathrm{r}} + \frac{\partial {}^{R_\mathrm{r}^\mathrm{c}}\dot{\underline{\underline{h}}}^{R_\mathrm{r}}}{\partial \dot{\varphi}_\mathrm{x}^{R_\mathrm{f}}} \cdot \delta\dot{\varphi}_\mathrm{x}^{R_\mathrm{f}} \\
\frac{\partial {}^{R_\mathrm{r}^\mathrm{c}}\dot{\underline{\underline{h}}}^{R_\mathrm{r}}}{\partial \underline{\ddot{\varphi}}^{R}} \cdot \delta\underline{\ddot{\varphi}}^{R} &\mapsto \frac{\partial {}^{R_\mathrm{r}^\mathrm{c}}\dot{\underline{\underline{h}}}^{R_\mathrm{r}}}{\partial \underline{\ddot{\varphi}}^{R_\mathrm{r}}} \cdot \delta\underline{\ddot{\varphi}}^{R_\mathrm{r}} + \frac{\partial {}^{R_\mathrm{r}^\mathrm{c}}\dot{\underline{\underline{h}}}^{R_\mathrm{r}}}{\partial \ddot{\varphi}_\mathrm{x}^{R_\mathrm{f}}} \cdot \delta\ddot{\varphi}_\mathrm{x}^{R_\mathrm{f}}
\end{aligned} \tag{B.94}$$

B.3 Rotor blade motion

For the layout of the rotor blade model X see section 3.6.1. Expressions for the mean and sensitivity functions for the kinematic quantitites are given in section B.3.1 while this is done for the angular and linear impulse in section B.3.2. The means and sensitivities are calculated and stored in structure variables by calls to M-functions TBUBLADEKIN() and TBUBLADEIMP() from TBUAEREOM().

B.3.1 Rotor blade kinematics

The kinematic vectors for any blade element X_k depend on the degrees of freedom within the blade subcomponent (flange, structure & profile) and on kinematic vectors of the final element in the foregoing subcomponent (X_FF). The final foregoing element X_FF is the blade base element X_0 for the blade flange X_f and is the 'final' flange element X_1 for the blade structure & profile X_p. Denote the element number of X_FF as k_FF and the first element of a subcomponent as $k^{\oplus}_\mathrm{FF}$.

Before continuing with the kinematic vectors, we give the expressions for the internal rotation and transformation matrices. For the flange element X_1 only rotation dofs may apply, under rotation order 'z,y,x', so:

$${}^{X_1}\bar{\Phi}^{X_1^{\iota_\mathrm{r}}} = \left[{}^{X_1}\bar{\Phi}^{X_1^2} \,.\, {}^{X_1^2}\underline{\bar{\Phi}}_3^{X_1^1} \quad {}^{X_1}\underline{\bar{\Phi}}_2^{X_1^2} \quad \underline{e}_1\right] = \left[\Phi_\mathrm{x}(\bar{\phi}_3^{X_1}) \cdot \underline{\Phi}_{\mathrm{y}_3}(\bar{\phi}_2^{X_1}) \quad \underline{\Phi}_{\mathrm{x}_2}(\bar{\phi}_3^{X_1}) \quad \underline{e}_2\right] \tag{B.95}$$

For blade profile elements $X_{2\ldots N}$ both rotation and translation dofs may apply, under rotation order 'y,z,x' and corresponding translation order 'y,x,z':

$$
\begin{aligned}
{}^{x_k}\bar{\Phi}^{x_k^{\iota_r}} &= \left[{}^{x_k}\bar{\Phi}^{x_k^2} \cdot {}^{x_k^2}\underline{\Phi}_2^{x_k^1} \quad {}^{x_k}\underline{\Phi}_3^{x_k^2} \quad \underline{e}_1 \right] = \left[\Phi_{\mathrm{x}}(\bar{\phi}_3^{x_k}) \cdot \underline{\Phi}_{\mathrm{z}_2}(\bar{\phi}_2^{x_k}) \quad \underline{\Phi}_{\mathrm{x}_3}(\bar{\phi}_3^{x_k}) \quad \underline{e}_1 \right] \\
{}^{x_k}\bar{\Phi}^{x_k^{\iota_t}} &= \left[{}^{x_k}\bar{\Phi}^{x_k^2} \cdot {}^{x_k^2}\underline{\Phi}_2^{x_k^1} \quad {}^{x_k}\underline{\Phi}_1^{x_k^2} \quad \underline{e}_3 \right] = \left[\Phi_{\mathrm{x}}(\bar{\phi}_3^{x_k}) \cdot \underline{\Phi}_{\mathrm{z}_2}(\bar{\phi}_2^{x_k}) \quad \underline{\Phi}_{\mathrm{x}_1}(\bar{\phi}_3^{x_k}) \quad \underline{e}_3 \right]
\end{aligned}
\tag{B.96}
$$

For the angular kinematic vectors for element X_k hold:

$$
\begin{aligned}
\vec{\omega}^{x_k} &= \vec{\omega}^{x_{\mathrm{FF}}} + {}^{x_{\mathrm{FF}}}\vec{\omega}^{x_m} = \vec{\omega}^{x_{\mathrm{FF}}} + \sum_{m=k_{\mathrm{FF}}^{\oplus}}^{k} {}^{x_{m-1}}\vec{\omega}^{x_m} \\
\vec{\alpha}^{x_k} &= \vec{\alpha}^{x_{\mathrm{FF}}} + \vec{\omega}^{x_{\mathrm{FF}}} \times {}^{x_{\mathrm{FF}}}\vec{\omega}^{x_m} + {}^{(x_{\mathrm{FF}})}\tfrac{\mathrm{d}}{\mathrm{d}t}\Big({}^{x_{\mathrm{FF}}}\vec{\omega}^{x_m} \Big) \\
\text{with } {}^{x_{m-1}}\vec{\omega}^{x_m} &= \begin{cases} \dot{\varphi}_1^{x_k} \cdot \vec{e}_3^{\,x_k} + \dot{\varphi}_2^{x_k} \cdot \vec{e}_2^{\,x_k} + \dot{\varphi}_3^{x_k} \cdot \vec{e}_1^{\,x_k} & \text{for } k = 1 \\ \dot{\varphi}_1^{x_k} \cdot \vec{e}_2^{\,x_k} + \dot{\varphi}_2^{x_k} \cdot \vec{e}_3^{\,x_k} + \dot{\varphi}_3^{x_k} \cdot \vec{e}_1^{\,x_k} & \text{for } k = 2 \ldots N \end{cases}
\end{aligned}
\tag{B.97}
$$

The angular velocity increments ${}^{x_{m-1}}\vec{\omega}^{x_m}$ are all zero-mean. For the third term in the right hand side of the expression for $\vec{\alpha}^{x_k}$ thus holds:

$$
\begin{aligned}
{}^{(x_{\mathrm{FF}})}\tfrac{\mathrm{d}}{\mathrm{d}t}\Big({}^{x_{\mathrm{FF}}}\vec{\omega}^{x_m} \Big) &= \sum_{m=k_{\mathrm{FF}}^{\oplus}}^{k} \Big({}^{x_{\mathrm{FF}}}\vec{\omega}^{x_{m-1}} \times {}^{x_{m-1}}\vec{\omega}^{x_m} + {}^{(x_{m-1})}\tfrac{\mathrm{d}}{\mathrm{d}t}\Big({}^{x_{m-1}}\vec{\omega}^{x_m} \Big) \Big) \\
&\overset{\text{(orde 0,1)}}{=} \sum_{m=k_{\mathrm{FF}}^{\oplus}}^{k} {}^{(x_{m-1})}\tfrac{\mathrm{d}}{\mathrm{d}t}\Big({}^{x_{m-1}}\vec{\omega}^{x_m} \Big)
\end{aligned}
\tag{B.98}
$$

The linearised coordinate expressions for the 'rotational increments' along $\vec{e}^{\,x_k}$ are:

$$
\begin{aligned}
{}^{x_{\mathrm{FF}}}\underline{\omega}^{x_m} &\triangleq \Big({}^{x_{\mathrm{FF}}}\vec{\omega}^{x_m} \Big)^{x_k} = \\
&\Big[\mathrm{O}_{(1)} \ldots \mathrm{O}_{(k_{\mathrm{FF}})} \quad \mathrm{J}_{i=k_{\mathrm{FF}}^{\oplus}}^{k} \big({}^{x_k}\bar{\Phi}^{x_i} \cdot {}^{x_i}\bar{\Phi}^{x_i^{\iota_r}} \big) \quad \mathrm{O}_{(k+1)} \ldots \mathrm{O}_{(N)} \Big] \cdot \underline{\dot{\varphi}}^{X} \\
{}^{(x_{\mathrm{FF}})}\tfrac{\mathrm{d}}{\mathrm{d}t}\Big({}^{x_{\mathrm{FF}}}\underline{\omega}^{x_m} \Big) &\triangleq \Big({}^{(x_{\mathrm{FF}})}\tfrac{\mathrm{d}}{\mathrm{d}t}\Big({}^{x_{\mathrm{FF}}}\vec{\omega}^{x_m} \Big) X_k \Big) = \\
&\Big[\mathrm{O}_{(1)} \ldots \mathrm{O}_{(k_{\mathrm{FF}})} \quad \mathrm{J}_{i=k_{\mathrm{FF}}^{\oplus}}^{k} \big({}^{x_k}\bar{\Phi}^{x_i} \cdot {}^{x_i}\bar{\Phi}^{x_i^{\iota_r}} \big) \quad \mathrm{O}_{(k+1)} \ldots \mathrm{O}_{(N)} \Big] \cdot \underline{\ddot{\varphi}}^{X}
\end{aligned}
\tag{B.99}
$$

The following intermediate linearised coordinate expressions along $\vec{e}^{\,x_k}$ apply for $\underline{\omega}^{x_k}$ and $\underline{\omega}^{x_k}$:

$$
\begin{aligned}
\underline{\omega}^{x_k} &= {}^{x_k}\bar{\Phi}^{x_{\mathrm{FF}}} \cdot \bar{\underline{\omega}}^{x_{\mathrm{FF}}} + {}^{x_k}\bar{\Phi}^{x_{\mathrm{FF}}} \cdot \delta\underline{\omega}^{x_{\mathrm{FF}}} + \delta^{x_k}\Phi^{x_{\mathrm{FF}}} \cdot \bar{\underline{\omega}}^{x_{\mathrm{FF}}} + {}^{x_{\mathrm{FF}}}\underline{\omega}^{x_m} \\
\underline{\alpha}^{x_k} &= {}^{x_k}\bar{\Phi}^{x_{\mathrm{FF}}} \cdot \delta\underline{\alpha}^{x_{\mathrm{FF}}} + {}^{x_k}\bar{\Phi}^{x_{\mathrm{FF}}} \cdot \bar{\underline{\omega}}^{x_{\mathrm{FF}}} \times {}^{x_{\mathrm{FF}}}\underline{\omega}^{x_m} + {}^{(x_{\mathrm{FF}})}\tfrac{\mathrm{d}}{\mathrm{d}t}\Big({}^{x_{\mathrm{FF}}}\underline{\omega}^{x_m} \Big)
\end{aligned}
\tag{B.100}
$$

Examining equation B.99, the expressions above are transformed as follows into the desired form:

$$
\begin{aligned}
\underline{\omega}^{x_k} &\overset{\text{(orde 0,1)}}{=} \bar{\underline{\omega}}^{x_k} + \frac{\partial \underline{\omega}^{x_k}}{\partial \underline{\omega}^{x_{\mathrm{FF}}}} \cdot \delta\underline{\omega}^{x_{\mathrm{FF}}} + \frac{\partial \underline{\omega}^{x_k}}{\partial \underline{\phi}^{X}} \cdot \delta\underline{\phi}^{X} + \frac{\partial \underline{\omega}^{x_k}}{\partial \underline{\dot{\varphi}}^{X}} \cdot \underline{\dot{\varphi}}^{X} \\
\delta\underline{\alpha}^{x_k} &\overset{\text{(orde 0,1)}}{=} \frac{\partial \underline{\alpha}^{x_k}}{\partial \underline{\alpha}^{x_{\mathrm{FF}}}} \cdot \delta\underline{\alpha}^{x_{\mathrm{FF}}} + \frac{\partial \underline{\alpha}^{x_k}}{\partial \underline{\dot{\varphi}}^{X}} \cdot \delta\underline{\dot{\varphi}}^{X} + \frac{\partial \underline{\alpha}^{x_k}}{\partial \underline{\ddot{\varphi}}^{X}} \cdot \underline{\ddot{\varphi}}^{X}
\end{aligned}
\tag{B.101}
$$

with mean

$$
\bar{\underline{\omega}}^{x_k} = \begin{cases} {}^{x_1}\bar{\Phi}^{x_0} \cdot \bar{\underline{\omega}}^{x_0} & \text{for } k = 1 \\ {}^{x_k}\bar{\Phi}^{x_1} \cdot \bar{\underline{\omega}}^{x_1} & \text{for } k = 2 \ldots N \end{cases}
\tag{B.102}
$$

while for the sensitivity matrices holds:

$$\frac{\partial \underline{\omega}^{X_k}}{\partial \underline{\omega}^{X_{\mathrm{FF}}}} \equiv \frac{\partial \underline{\alpha}^{X_k}}{\partial \underline{\alpha}^{X_{\mathrm{FF}}}} = \begin{cases} {}^{X_1}\bar{\Phi}^{X_0} & \text{for } k=1 \\ {}^{X_k}\bar{\Phi}^{X_1} & \text{for } k=2\ldots N \end{cases}$$

$$\frac{\partial \underline{\omega}^{X_k}}{\partial \underline{\dot{\varphi}}^{X}} \equiv \frac{\partial \underline{\alpha}^{X_k}}{\partial \underline{\ddot{\varphi}}^{X}} = \begin{cases} \left[\boldsymbol{G}_{11}^{X_{\mathrm{f}}^{\mathrm{r}}} \;\; \mathrm{O}_{(2)} \ldots \mathrm{O}_{(N)}\right] & \text{for } k=1 \\ \left[\mathrm{O}_{(1)} \;\; \mathrm{J}_{i=2}^{k}(\boldsymbol{G}_{ki}^{X_{\mathrm{P}}^{\mathrm{r}}}) \;\; \mathrm{O}_{(k+1)} \ldots \mathrm{O}_{(N)}\right] & \text{for } k=2\ldots N \end{cases} \tag{B.103}$$

and:

$$\frac{\partial \underline{\alpha}^{X_k}}{\partial \underline{\dot{\varphi}}^{X}} = \begin{cases} \left[\mathrm{J}_{v=1}^{3}({}^{X_1}\bar{\Phi}^{X_0} \cdot \underline{\bar{\omega}}^{X_0} \times \underline{\boldsymbol{G}}_{11_v}^{X_{\mathrm{f}}^{\mathrm{r}}}) \;\; \mathrm{O}_{(2)} \ldots \mathrm{O}_{(N)}\right] & \text{for } k=1 \\ \left[\mathrm{O}_{(1)} \;\; \mathrm{J}_{i=2}^{k}\big(\mathrm{J}_{v=1}^{3}({}^{X_k}\bar{\Phi}^{X_1} \cdot \underline{\bar{\omega}}^{X_1} \times \underline{\boldsymbol{G}}_{ki_v}^{X_{\mathrm{P}}^{\mathrm{r}}})\big) \;\; \mathrm{O}_{(k+1)} \ldots \mathrm{O}_{(N)}\right] & \text{for } k=2\ldots N \end{cases}$$

$$\frac{\partial \underline{\omega}^{X_k}}{\partial \underline{\phi}^{X}} = \begin{cases} \left[\mathrm{J}_{v=1}^{3}(\frac{\partial^{X_1}\Phi^{X_0}}{\partial \phi_v^{X_1}} \cdot \underline{\bar{\omega}}^{X_0}) \;\; \mathrm{O}_{(2)} \ldots \mathrm{O}_{(N)}\right] & \text{for } k=1 \\ \left[\mathrm{O}_{(1)} \;\; \mathrm{J}_{i=2}^{k}\big(\mathrm{J}_{v=1}^{3}(\frac{\partial^{X_k}\bar{\Phi}^{X_1}}{\partial \phi_v^{X_i}} \cdot \underline{\bar{\omega}}^{X_1})\big) \;\; \mathrm{O}_{(k+1)} \ldots \mathrm{O}_{(N)}\right] & \text{for } k=2\ldots N \end{cases} \tag{B.104}$$

The 'gain vector' matrix $\boldsymbol{G}_{ki}^{X_{\mathrm{SC}}^{\mathrm{r}}}$, with columns $\{\underline{\boldsymbol{G}}_{ki_v}^{X_{\mathrm{SC}}^{\mathrm{r}}}\}$, maps rotation dofs on blade element X_i to angular kinematic vectors on X_k for subcompont X_{SC}. We here also define the gain matrix $\boldsymbol{G}_{ki}^{X_{\mathrm{SC}}^{\mathrm{r}}}$, which maps translation dofs on X_i to linear kinematic vectors on X_k of X_{SC}. It holds (see Eq. B.99 and Eq. B.109):

$$\begin{aligned} \boldsymbol{G}_{ki}^{X_{\mathrm{SC}}^{\mathrm{r}}} &= {}^{X_k}\bar{\Phi}^{X_i} \,.\, {}^{X_i}\bar{\Phi}^{\iota_i^{\mathrm{r}}} \\ \boldsymbol{G}_{ki}^{X_{\mathrm{SC}}^{\mathrm{t}}} &= {}^{X_k}\bar{\Phi}^{X_i} \,.\, {}^{X_i}\bar{\Phi}^{\iota_i^{\mathrm{t}}} \end{aligned} \tag{B.105}$$

The coordinate system independent expressions for the linear velocity and acceleration in the centre of gravity of a blade element are similar to those for a point on the rotor hub (see Eq. B.57); the only difference is that we use the final foregoing element X_{FF} as reference for the non-absolute time derivatives instead of the actual element X_k:

$$\begin{aligned} \vec{v}^{\,X_k^*} &= \vec{v}^{\,X_{\mathrm{FF}}^{\oplus}} + {}^{(X_{\mathrm{FF}})}\frac{\mathrm{d}}{\mathrm{d}t}\Big({}^{X_{\mathrm{FF}}^{\oplus}}\vec{r}^{\,X_k^*}\Big) + \vec{\omega}^{\,X_{\mathrm{FF}}} \times {}^{X_{\mathrm{FF}}^{\oplus}}\vec{r}^{\,X_k^*} \\ \vec{a}^{\,X_k^*} &= \vec{a}^{\,X_{\mathrm{FF}}^{\oplus}} + \vec{\alpha}^{\,X_{\mathrm{FF}}} \times {}^{X_{\mathrm{FF}}^{\oplus}}\vec{r}^{\,X_k^*} + \vec{\omega}^{\,X_{\mathrm{FF}}} \times (\vec{\omega}^{\,X_{\mathrm{FF}}} \times {}^{X_{\mathrm{FF}}^{\oplus}}\vec{r}^{\,X_k^*}) + \ldots \\ &\qquad 2\vec{\omega}^{\,X_{\mathrm{FF}}} \times {}^{(X_{\mathrm{FF}})}\frac{\mathrm{d}}{\mathrm{d}t}\Big({}^{X_{\mathrm{FF}}^{\oplus}}\vec{r}^{\,X_k^*}\Big) + {}^{(X_{\mathrm{FF}})}\frac{\mathrm{d}^2}{\mathrm{d}t^2}\Big({}^{X_{\mathrm{FF}}^{\oplus}}\vec{r}^{\,X_k^*}\Big) \end{aligned} \tag{B.106}$$

In order to obtain linearised expressions for the translation increments ${}^{(X_{\mathrm{FF}})}\frac{\mathrm{d}}{\mathrm{d}t}\Big({}^{X_{\mathrm{FF}}^{\oplus}}\vec{r}^{\,X_k^*}\Big)$ and ${}^{(X_{\mathrm{FF}})}\frac{\mathrm{d}^2}{\mathrm{d}t^2}\Big({}^{X_{\mathrm{FF}}^{\oplus}}\vec{r}^{\,X_k^*}\Big)$, the place vector ${}^{X_{\mathrm{FF}}^{\oplus}}\vec{r}^{\,X_k^*}$ is decomposed in place vector increments over the elements and the reference for the non-aboluste time derivatives 'is fit to the concerning blade elements in the decomposition':

$$\begin{aligned} {}^{X_{\mathrm{FF}}^{\oplus}}\vec{r}^{\,X_k^*} &= \sum_{m=k_{\mathrm{FF}}^{\oplus}}^{k} {}^{X_m^{\ominus}}\vec{r}^{\,X_{m|k}^{\oplus|*}} \\ {}^{(X_{\mathrm{FF}})}\frac{\mathrm{d}}{\mathrm{d}t}\Big({}^{X_{\mathrm{FF}}^{\oplus}}\vec{r}^{\,X_k^*}\Big) &= \sum_{m=k_{\mathrm{FF}}^{\oplus}}^{k} {}^{X_{\mathrm{FF}}}\vec{\omega}^{\,X_m} \times {}^{X_m^{\ominus}}\vec{r}^{\,X_{m|k}^{\oplus|*}} + {}^{(X_m)}\frac{\mathrm{d}}{\mathrm{d}t}\Big({}^{X_m^{\ominus}}\vec{r}^{\,X_{m|k}^{\oplus|*}}\Big) \end{aligned} \tag{B.107}$$

This decomposition and 'fit of reference for the time derivatives' is also applied to the acceleration translation increment. Both the rotation increment ${}^{X_{\mathrm{FF}}}\vec{\omega}^{\,X_m}$ and translation

increment ${}^{(X_m)}\frac{\mathrm{d}}{\mathrm{d}t}\Big(x_m^{\ominus\rightarrow} r^{X^{\oplus|*}_{m|k}}\Big)$ are zero-mean. This implies that all products of these increments that appear in the obtained expression for the acceleration translation increment are to be neglected in the linearised approach. It then holds (see Eq. 3.64 for the first term in the right hand side):

$$ {}^{(X_{\mathrm{FF}})}\frac{\mathrm{d}^2}{\mathrm{d}t^2}\Big(x_{\mathrm{FF}}^{\oplus\rightarrow} r^{X^*_k}\Big) \quad \overset{\text{(orde 1)}}{=} \quad \sum_{m=k^{\oplus}_{\mathrm{FF}}}^{k} {}^{(X_{\mathrm{FF}})}\frac{\mathrm{d}}{\mathrm{d}t}\Big(x_{\mathrm{FF}}\vec{\omega}^{X_m}\Big) \times x_m^{\ominus\rightarrow} r^{X^{\oplus|*}_{m|k}} + {}^{(X_m)}\frac{\mathrm{d}^2}{\mathrm{d}t^2}\Big(x_m^{\ominus\rightarrow} r^{X^{\oplus|*}_{m|k}}\Big) \tag{B.108} $$

For the linearised coordinate expressions along e^{X_k} for the second term in the right hand side of equations B.107 and B.108 holds:

$$ \Big(\sum_{m=k^{\oplus}_{\mathrm{FF}}}^{k} {}^{(X_m)}\frac{\mathrm{d}}{\mathrm{d}t}\Big(x_m^{\ominus\rightarrow} r^{X^{\oplus|*}_{m|k}}\Big)\Big)^{X_k} = \Big[\mathrm{O}_{(1)}\ldots\mathrm{O}_{(k_{\mathrm{FF}})} \;\; \mathrm{J}^{k}_{i=k^{\oplus}_{\mathrm{FF}}}\big({}^{X_k}\bar{\Phi}^{X_i}\cdot{}^{X_i}\bar{\Phi}^{X_i^{\iota_{\mathrm{t}}}}\big) \;\; \mathrm{O}_{(k+1)}\ldots\mathrm{O}_{(N)}\Big]\cdot\underline{\dot{\varrho}}^{X} $$

$$ \Big(\sum_{m=k^{\oplus}_{\mathrm{FF}}}^{k} {}^{(X_m)}\frac{\mathrm{d}^2}{\mathrm{d}t^2}\Big(x_m^{\ominus\rightarrow} r^{X^{\oplus|*}_{m|k}}\Big)\Big)^{X_k} = \Big[\mathrm{O}_{(1)}\ldots\mathrm{O}_{(k_{\mathrm{FF}})} \;\; \mathrm{J}^{k}_{i=k^{\oplus}_{\mathrm{FF}}}\big({}^{X_k}\bar{\Phi}^{X_i}\cdot{}^{X_i}\bar{\Phi}^{X_i^{\iota_{\mathrm{t}}}}\big) \;\; \mathrm{O}_{(k+1)}\ldots\mathrm{O}_{(N)}\Big]\cdot\underline{\ddot{\varrho}}^{X} \tag{B.109} $$

while for the linearised coordinates for the first term in the RHS of of equations B.107 and B.108 holds:

$$ \Big(\sum_{m=k^{\oplus}_{\mathrm{FF}}}^{k} {}^{X_{\mathrm{FF}}}\vec{\omega}^{X_m}\times x_m^{\ominus\rightarrow} r^{X^{\oplus|*}_{m|k}}\Big)^{X_k} = \Big[\mathrm{O}_{(1)}\ldots\mathrm{O}_{(k_{\mathrm{FF}})} \; \mathrm{J}^{k}_{i=k^{\oplus}_{\mathrm{FF}}}\Big(\sum_{m=i}^{k} {}^{X_k}\bar{\Phi}^{X_m}\cdot\mathrm{J}^{3}_{v=1}\big({}^{X_m}\bar{\Phi}^{X_i}\cdot{}^{X_i}\underline{\bar{\Phi}}_{v}^{X_i^{\iota_{\mathrm{r}}}}\times x_m^{\ominus}\underline{r}^{X^{\oplus|*}_{m|k}}\big)\Big) \; \mathrm{O}_{(k+1)}\ldots\mathrm{O}_{(N)}\Big]\cdot\underline{\dot{\varphi}}^{X} $$

$$ \Big(\sum_{m=k^{\oplus}_{\mathrm{FF}}}^{k} {}^{(X_{\mathrm{FF}})}\frac{\mathrm{d}}{\mathrm{d}t}\Big({}^{X_{\mathrm{FF}}}\vec{\omega}^{X_m}\Big)\times x_m^{\ominus\rightarrow} r^{X^{\oplus|*}_{m|k}}\Big)^{X_k} = \Big[\mathrm{O}_{(1)}\ldots\mathrm{O}_{(k_{\mathrm{FF}})} \; \mathrm{J}^{k}_{i=k^{\oplus}_{\mathrm{FF}}}\Big(\sum_{m=i}^{k} {}^{X_k}\bar{\Phi}^{X_m}\cdot\mathrm{J}^{3}_{v=1}\big({}^{X_m}\bar{\Phi}^{X_i}\cdot{}^{X_i}\underline{\bar{\Phi}}_{v}^{X_i^{\iota_{\mathrm{r}}}}\times x_m^{\ominus}\underline{r}^{X^{\oplus|*}_{m|k}}\big)\Big) \; \mathrm{O}_{(k+1)}\ldots\mathrm{O}_{(N)}\Big]\cdot\underline{\ddot{\varphi}}^{X} \tag{B.110} $$

The linearised coordinate expressions for the overall translation increments along $\vec{e}^{\,X_k}$ are now obtained from equations B.107 and B.108 by use of the intermediate results above:

$$ \begin{aligned} {}^{(X_{\mathrm{FF}})}\frac{\mathrm{d}}{\mathrm{d}t}\Big(x_{\mathrm{FF}}^{\oplus}\underline{r}^{X^*_k}\Big) &\triangleq \Big({}^{(X_{\mathrm{FF}})}\frac{\mathrm{d}}{\mathrm{d}t}\Big(x_{\mathrm{FF}}^{\oplus\rightarrow} r^{X^*_k}\Big)\Big)^{X_k} \overset{\text{(orde 1)}}{=} \\ &\Big[\mathrm{O}_{(1)}\ldots\mathrm{O}_{(k_{\mathrm{FF}})} \;\; \mathrm{J}^{k}_{i=k^{\oplus}_{\mathrm{FF}}}\big(\boldsymbol{G}_{ki}^{X^{\mathrm{t}}_{\mathrm{SC}}}\big) \;\; \mathrm{O}_{(k+1)}\ldots\mathrm{O}_{(N)}\Big]\cdot\underline{\dot{\varrho}}^{X} + \\ &\Big[\mathrm{O}_{(1)}\ldots\mathrm{O}_{(k_{\mathrm{FF}})} \;\; \mathrm{J}^{k}_{i=k^{\oplus}_{\mathrm{FF}}}\big(\boldsymbol{R}_{ki}^{X^{*}_{\mathrm{SC}}}\big) \;\; \mathrm{O}_{(k+1)}\ldots\mathrm{O}_{(N)}\Big]\cdot\underline{\dot{\varphi}}^{X} \end{aligned} \tag{B.111} $$

$$ \begin{aligned} {}^{(X_{\mathrm{FF}})}\frac{\mathrm{d}^2}{\mathrm{d}t^2}\Big(x_{\mathrm{FF}}^{\oplus}\underline{r}^{X^*_k}\Big) &\triangleq \Big({}^{(X_{\mathrm{FF}})}\frac{\mathrm{d}^2}{\mathrm{d}t^2}\Big(x_{\mathrm{FF}}^{\oplus\rightarrow} r^{X^*_k}\Big)\Big)^{X_k} \overset{\text{(orde 1)}}{=} \\ &\Big[\mathrm{O}_{(1)}\ldots\mathrm{O}_{(k_{\mathrm{FF}})} \;\; \mathrm{J}^{k}_{i=k^{\oplus}_{\mathrm{FF}}}\big(\boldsymbol{G}_{ki}^{X^{\mathrm{t}}_{\mathrm{SC}}}\big) \;\; \mathrm{O}_{(k+1)}\ldots\mathrm{O}_{(N)}\Big]\cdot\underline{\ddot{\varrho}}^{X} + \\ &\Big[\mathrm{O}_{(1)}\ldots\mathrm{O}_{(k_{\mathrm{FF}})} \;\; \mathrm{J}^{k}_{i=k^{\oplus}_{\mathrm{FF}}}\big(\boldsymbol{R}_{ki}^{X^{*}_{\mathrm{SC}}}\big) \;\; \mathrm{O}_{(k+1)}\ldots\mathrm{O}_{(N)}\Big]\cdot\underline{\ddot{\varphi}}^{X} \end{aligned} \tag{B.112} $$

The 'gain vector' matrix $\boldsymbol{G}_{ki}^{X^{\mathrm{t}}_{\mathrm{SC}}}$ has already been defined in Eq. B.36. The 'place vector' matrix $\boldsymbol{R}_{ki}^{X^{*}_{\mathrm{SC}}}$ maps rotation dofs in element X_i of subcomponent X_{SC} to linear kinematic

vectors of the c.o.g. of element X_k. We here also define the place vector matrix $\boldsymbol{R}_{k\mathrm{FF}}^{X^*_{\mathrm{SC}}}$ that maps the angular kinematic vectors of the final foregoing element X_{FF} to linear kinematic vectors of X^*_k of X_{SC}:

$$\begin{aligned}
\boldsymbol{R}_{ki}^{X^*_{\mathrm{SC}}} &= \sum_{m=i}^{k} {}^{X_k}\bar{\Phi}^{X_m} \cdot \mathrm{J}^3_{v=1}\big({}^{X_m}\bar{\Phi}^{X_i} \cdot {}^{X_i}\underline{\Phi}_v^{X_i^{\mathrm{tr}}} \times {}^{X_m^{\ominus}}\underline{r}^{X^{\oplus|*}_{m|k}}\big) \\
\boldsymbol{R}_{k\mathrm{FF}}^{X^*_{\mathrm{SC}}} &= \sum_{m=k^{\oplus}_{\mathrm{FF}}}^{k} {}^{X_k}\bar{\Phi}^{X_m} \cdot \mathrm{J}^3_{v=1}\big({}^{X_m}\bar{\Phi}_v^{X_{k_{\mathrm{FF}}}} \times {}^{X_m^{\ominus}}\underline{r}^{X^{\oplus|*}_{m|k}}\big)
\end{aligned} \tag{B.113}$$

The place vector ${}^{X_m^{\ominus}\!\!\rightarrow}r^{X^{\oplus|*}_{m|k}}$ runs to the exit point if $m < k$ and to the centre of gravity if $m = k$.

Just as in the drive train model, the translation dofs $\{\rho_v\}$ are included in the blade model only for valid structural dynamic behaviour through stiffness, damping and inertia effects. The influence of $\{\rho_v\}$ on orientation and length of the place vector is neglected. Then a place vector between two points on one element, say X_k, has invariant coordinates along the final coordinate system on X_k. This coordinate system $\vec{e}^{\,X_k}$ is actually obtained *after* the coordinate system transformations caused by the rotation dofs of X_k in the entry point $X_k^{\ominus}$. E.g. for the place vectors from the entry point to the c.o.g. and to the exit point holds (short form $\underline{r}^{m|k}$):

$$\underline{r}^{m|k} \triangleq \left({}^{X_m^{\ominus}\!\!\rightarrow}r^{X^{\oplus|*}_{m|k}}\right)^{X_m} \Rightarrow \begin{cases} {}^{X_k^{\ominus}}\underline{r}^{X_k^*} \triangleq \left({}^{X_k^{\ominus}\!\!\rightarrow}r^{X_k^*}\right)^{X_k} \equiv \overline{\left({}^{X_k^{\ominus}\!\!\rightarrow}r^{X_k^*}\right)^{X_k}} \\ {}^{X_m^{\ominus}}\underline{r}^{X_m^{\oplus}} \triangleq \left({}^{X_m^{\ominus}\!\!\rightarrow}r^{X_m^{\oplus}}\right)^{X_m} \equiv \overline{\left({}^{X_m^{\ominus}\!\!\rightarrow}r^{X_m^{\oplus}}\right)^{X_m}} \end{cases} \tag{B.114}$$

With the additional short forms:

$$\begin{array}{llcll}
\underline{v}^k & \triangleq \left(\vec{v}^{\,X_k^*}\right)^{X_k} & ; & \underline{a}^k & \triangleq \left(\vec{a}^{\,X_k^*}\right)^{X_k} \\
\underline{v}^{\mathrm{FF}} & \triangleq \left(\vec{v}^{\,X_{\mathrm{FF}}^{\oplus}}\right)^{X_{\mathrm{FF}}} & ; & \underline{a}^{\mathrm{FF}} & \triangleq \left(\vec{a}^{\,X_{\mathrm{FF}}^{\oplus}}\right)^{X_{\mathrm{FF}}} \\
\underline{\omega}^{\mathrm{FF}} & \triangleq \left(\vec{\omega}^{\,X_{\mathrm{FF}}^{\oplus}}\right)^{X_{\mathrm{FF}}} & ; & \underline{\alpha}^{\mathrm{FF}} & \triangleq \left(\vec{\alpha}^{\,X_{\mathrm{FF}}^{\oplus}}\right)^{X_{\mathrm{FF}}} \\
{}^k\bar{\Phi}^{\mathrm{FF}} & \triangleq {}^{X_k}\bar{\Phi}^{X_{\mathrm{FF}}} & ; & \delta^k\Phi^{\mathrm{FF}} & \triangleq \delta^{X_k}\Phi^{X_{\mathrm{FF}}} \\
{}^{(\mathrm{FF})}\frac{\mathrm{d}}{\mathrm{d}t}\left({}^{\mathrm{FF}}\underline{r}^k\right) & \triangleq \left({}^{(X\mathrm{FF})}\frac{\mathrm{d}}{\mathrm{d}t}\left({}^{X^{\oplus}_{k_{\mathrm{FF}}}}\vec{r}^{\,X_k^*}\right)\right)^{X_k} & ; & {}^{(\mathrm{FF})}\frac{\mathrm{d}^2}{\mathrm{d}t^2}\left({}^{\mathrm{FF}}\underline{r}^k\right) & \triangleq \left({}^{(X\mathrm{FF})}\frac{\mathrm{d}^2}{\mathrm{d}t^2}\left({}^{X^{\oplus}_{k_{\mathrm{FF}}}}\vec{r}^{\,X_k^*}\right)\right)^{X_k} \\
{}^{\mathrm{FF}}\underline{r}^k & \triangleq {}^{X^{\oplus}_{k_{\mathrm{FF}}}}\underline{r}^{X_k^*} \triangleq \left({}^{X^{\oplus}_{k_{\mathrm{FF}}}}\vec{r}^{\,X_k^*}\right)^{X_k} = \displaystyle\sum_{m=k^{\oplus}_{\mathrm{FF}}}^{k} {}^{X_k}\Phi^{X_m} \cdot \underline{r}^{m|k} & & &
\end{array} \tag{B.115}$$

we can write the intermediate linearised coordinate expressions for the linear velocity and acceleration as follows:

$$\begin{aligned}
\underline{v}^k &= {}^k\bar{\Phi}^{\mathrm{FF}} \cdot \bar{\underline{v}}^{\mathrm{FF}} + {}^k\bar{\Phi}^{\mathrm{FF}} \cdot \bar{\underline{\omega}}^{\mathrm{FF}} \times {}^{\mathrm{FF}}\bar{\underline{r}}^k + {}^k\bar{\Phi}^{\mathrm{FF}} \cdot \delta\underline{v}^{\mathrm{FF}} + {}^k\bar{\Phi}^{\mathrm{FF}} \cdot \delta\underline{\omega}^{\mathrm{FF}} \times {}^{\mathrm{FF}}\bar{\underline{r}}^k + \\
&\qquad \delta^k\Phi^{\mathrm{FF}} \cdot \bar{\underline{v}}^{\mathrm{FF}} + \delta^k\Phi^{\mathrm{FF}} \cdot \bar{\underline{\omega}}^{\mathrm{FF}} \times {}^{\mathrm{FF}}\bar{\underline{r}}^k + + {}^k\bar{\Phi}^{\mathrm{FF}} \cdot \bar{\underline{\omega}}^{\mathrm{FF}} \times \delta^{\mathrm{FF}}\underline{r}^k + {}^{(\mathrm{FF})}\frac{\mathrm{d}}{\mathrm{d}t}\left({}^{\mathrm{FF}}\underline{r}^k\right) \\
\underline{a}^k &= {}^k\bar{\Phi}^{\mathrm{FF}} \cdot \bar{\underline{a}}^{\mathrm{FF}} + {}^k\bar{\Phi}^{\mathrm{FF}} \cdot \bar{\underline{\omega}}^{\mathrm{FF}} \times \left({}^k\bar{\Phi}^{\mathrm{FF}} \cdot \bar{\underline{\omega}}^{\mathrm{FF}} \times {}^{\mathrm{FF}}\bar{\underline{r}}^k\right) + {}^k\bar{\Phi}^{\mathrm{FF}} \cdot \delta\underline{a}^{\mathrm{FF}} + \\
&\qquad {}^k\bar{\Phi}^{\mathrm{FF}} \cdot \delta\underline{\alpha}^{\mathrm{FF}} \times {}^{\mathrm{FF}}\bar{\underline{r}}^k + \delta^k\Phi^{\mathrm{FF}} \cdot \bar{\underline{a}}^{\mathrm{FF}} + \delta\left({}^k\Phi^{\mathrm{FF}} \cdot \underline{\omega}^{\mathrm{FF}} \times \left({}^k\Phi^{\mathrm{FF}} \cdot \underline{\omega}^{\mathrm{FF}} \times {}^{\mathrm{FF}}\underline{r}^k\right)\right) + \\
&\qquad 2\,{}^k\bar{\Phi}^{\mathrm{FF}} \cdot \bar{\underline{\omega}}^{\mathrm{FF}} \times {}^{(\mathrm{FF})}\frac{\mathrm{d}}{\mathrm{d}t}\left({}^{\mathrm{FF}}\underline{r}^k\right) + {}^{(\mathrm{FF})}\frac{\mathrm{d}^2}{\mathrm{d}t^2}\left({}^{\mathrm{FF}}\underline{r}^k\right)
\end{aligned} \tag{B.116}$$

Since linear algebray tells

$$\begin{aligned} \underline{a} \times (\underline{b} \times \underline{c}) \;&=\; (\sum_{w=1}^{3} a_w \cdot \underline{e}_w) \times (\underline{b} \times \underline{c}) \;= \\ & \mathrm{J}^3_{w=1}(\underline{e}_w \times (\underline{b} \times \underline{c})) \cdot \underline{a} \;=\; \mathrm{J}^3_{w=1}(\underline{a} \times (\underline{e}_w \times \underline{c})) \cdot \underline{b} \end{aligned} \tag{B.117}$$

the sixth term in the expression for the acceleration can be written as:

$$\begin{aligned} &\delta({}^{k}\Phi^{\mathrm{FF}}\underline{\omega}^{\mathrm{FF}} \times ({}^{k}\Phi^{\mathrm{FF}}\underline{\omega}^{\mathrm{FF}} \times {}^{\mathrm{FF}}\underline{r}^{k})) \;= \\ &\mathrm{J}^3_{w=1}\big(\underline{e}_w \times ({}^{k}\bar{\Phi}^{\mathrm{FF}}\bar{\underline{\omega}}^{\mathrm{FF}} \times {}^{\mathrm{FF}}\bar{\underline{r}}^{k}) + {}^{k}\bar{\Phi}^{\mathrm{FF}}\bar{\underline{\omega}}^{\mathrm{FF}} \times (\underline{e}_w \times {}^{\mathrm{FF}}\bar{\underline{r}}^{k})\big)\cdot \\ &\qquad ({}^{k}\bar{\Phi}^{\mathrm{FF}} \cdot \delta\underline{\omega}^{\mathrm{FF}} + \delta{}^{k}\Phi^{\mathrm{FF}} \cdot \bar{\underline{\omega}}^{\mathrm{FF}}) + {}^{k}\bar{\Phi}^{\mathrm{FF}}\bar{\underline{\omega}}^{\mathrm{FF}} \times ({}^{k}\bar{\Phi}^{\mathrm{FF}}\bar{\underline{\omega}}^{\mathrm{FF}} \times \delta{}^{\mathrm{FF}}\underline{r}^{k}) \end{aligned} \tag{B.118}$$

We already mentioned that translation dofs $\{\rho_v^{X_k}\}$ do not affect the length and orientation of place vectors on an element (eq. B.114). As ${}^{\mathrm{FF}}\underline{r}^k$ is then composed of invariant coordinate vectors $\underline{r}^{m|k}$ while the rotation dofs in elements $X_{m+1\ldots k}$ affect the coordinates along $\vec{e}^{\,X_k}$ (eq. B.115, 3.4), the expression for the place vector coordinate variations $\delta{}^{\mathrm{FF}}\underline{r}^k$ is:

$$\begin{aligned} \delta{}^{\mathrm{FF}}\underline{r}^k \;&=\; \sum_{m=k^{\oplus}_{\mathrm{FF}}}^{k}\sum_{i=m+1}^{k}\sum_{v=1}^{3}\frac{\partial^{X_k}\Phi^{X_m}}{\partial\phi_v^{X_i}}\cdot\underline{r}^{m|k}\cdot\delta\phi_v^{X_i} = \sum_{i=k^{\oplus}_{\mathrm{FF}}}^{k}\sum_{v=1}^{3}\sum_{m=k^{\oplus}_{\mathrm{FF}}}^{i-1}(.)\cdot\delta\phi_v^{X_i} \;= \\ &[\mathrm{O}_{(1)}\ldots\mathrm{O}_{(k_{\mathrm{FF}})}\;\; \mathrm{J}^k_{i=k^{\oplus}_{\mathrm{FF}}}\big(\mathrm{J}^3_{v=1}(\sum_{m=k^{\oplus}_{\mathrm{FF}}}^{i-1}\frac{\partial^{X_k}\Phi^{X_m}}{\partial\phi_v^{X_i}}\cdot\underline{r}^{m|k})\big)\;\; \mathrm{O}_{(k+1)}\ldots\mathrm{O}_{(N)}]\cdot\delta\underline{\phi}^{X} \end{aligned} \tag{B.119}$$

Examining equations B.111 and B.112 for the translation increments and the expressions above, the desired form for the linearised coordinate expressions along $\vec{e}^{\,X_k}$ for $\vec{v}^{\,X_k^*}$ and $\vec{a}^{\,X_k^*}$ becomes

$$\begin{aligned} \underline{v}^{X_k^*} \;&=\; \bar{\underline{v}}^{X_k^*} + \frac{\partial\underline{v}^{X_k^*}}{\partial\underline{v}^{X^{\oplus}_{\mathrm{FF}}}}\cdot\delta\underline{v}^{X^{\oplus}_{\mathrm{FF}}} + \frac{\partial\underline{v}^{X_k^*}}{\partial\underline{\omega}^{X^{\oplus}_{\mathrm{FF}}}}\cdot\delta\underline{\omega}^{X^{\oplus}_{\mathrm{FF}}} + \frac{\partial\underline{v}^{X_k^*}}{\partial\underline{\phi}^{X}}\cdot\delta\underline{\phi}^{X} + \frac{\partial\underline{v}^{X_k^*}}{\partial\underline{\dot{\varphi}}^{X}}\cdot\underline{\dot{\varphi}}^{X} + \frac{\partial\underline{v}^{X_k^*}}{\partial\underline{\dot{\varrho}}^{X}}\cdot\underline{\dot{\varrho}}^{X} \\ \underline{a}^{X_k^*} \;&=\; \bar{\underline{a}}^{X_k^*} + \frac{\partial\underline{a}^{X_k^*}}{\partial\underline{a}^{X^{\oplus}_{\mathrm{FF}}}}\cdot\delta\underline{a}^{X^{\oplus}_{\mathrm{FF}}} + \frac{\partial\underline{a}^{X_k^*}}{\partial\underline{\alpha}^{X^{\oplus}_{\mathrm{FF}}}}\cdot\delta\underline{\alpha}^{X^{\oplus}_{\mathrm{FF}}} + \frac{\partial\underline{a}^{X_k^*}}{\partial\underline{\omega}^{X^{\oplus}_{\mathrm{FF}}}}\cdot\delta\underline{\omega}^{X^{\oplus}_{\mathrm{FF}}} + \frac{\partial\underline{a}^{X_k^*}}{\partial\underline{\phi}^{X}}\cdot\delta\underline{\phi}^{X} + \\ &\qquad \frac{\partial\underline{a}^{X_k^*}}{\partial\underline{\dot{\varphi}}^{X}}\cdot\underline{\dot{\varphi}}^{X} + \frac{\partial\underline{a}^{X_k^*}}{\partial\underline{\dot{\varrho}}^{X}}\cdot\underline{\dot{\varrho}}^{X} + \frac{\partial\underline{a}^{X_k^*}}{\partial\underline{\ddot{\varphi}}^{X}}\cdot\underline{\ddot{\varphi}}^{X} + \frac{\partial\underline{a}^{X_k^*}}{\partial\underline{\ddot{\varrho}}^{X}}\cdot\underline{\ddot{\varrho}}^{X} \end{aligned} \tag{B.120}$$

For the mean linear velocity and acceleration hold (use Eq. B.113):

$$\begin{aligned} \bar{\underline{v}}^{X_k^*} \;&=\; \begin{cases} {}^{X_1}\bar{\Phi}^{X_0}\cdot\bar{\underline{v}}^{X_0^{\oplus}} + \boldsymbol{R}^{X_{\mathrm{f}}^*}_{1X_0}\cdot\bar{\underline{\omega}}^{X_0} & \text{for } k=1 \\ {}^{X_k}\bar{\Phi}^{X_1}\cdot\bar{\underline{v}}^{X_1^{\oplus}} + + \boldsymbol{R}^{X_{\mathrm{p}}^*}_{kX_{\mathrm{f}}}\cdot\bar{\underline{\omega}}^{X_1} & \text{for } k=2\ldots N \end{cases} \\ \bar{\underline{a}}^{X_k^*} \;&=\; \begin{cases} {}^{X_1}\bar{\Phi}^{X_0}\cdot\bar{\underline{a}}^{X_0^{\oplus}} + {}^{X_1}\bar{\Phi}^{X_0}\cdot\bar{\underline{\omega}}^{X_0}\times\boldsymbol{R}^{X_{\mathrm{f}}^*}_{1X_0}\cdot\bar{\underline{\omega}}^{X_0} & \text{for } k=1 \\ {}^{X_k}\bar{\Phi}^{X_1}\cdot\bar{\underline{a}}^{X_1^{\oplus}} + {}^{X_k}\bar{\Phi}^{X_1}\cdot\bar{\underline{\omega}}^{X_1}\times\boldsymbol{R}^{X_{\mathrm{p}}^*}_{kX_{\mathrm{f}}}\cdot\bar{\underline{\omega}}^{X_1} & \text{for } k=2\ldots N \end{cases} \end{aligned} \tag{B.121}$$

The sensitivity functions are derived from the right hand sides of Eq. B.116. The $\boldsymbol{G}$- and $\boldsymbol{R}$-matrices as defined in Eq. B.105 and B.113 are used in the expressions. An 'intermediate sensitivity' function is defined as (see Eq. B.118 and B.102):

$$\begin{aligned} \frac{\partial\underline{a}^{X_k^*}}{\partial\underline{\omega}^{X_{\mathrm{FF}}/X_k}} \;&\triangleq\; \mathrm{J}^3_{w=1}\big(\underline{e}_w \times ({}^{k}\bar{\Phi}^{\mathrm{FF}}\bar{\underline{\omega}}^{\mathrm{FF}} \times {}^{\mathrm{FF}}\bar{\underline{r}}^{k}) + {}^{k}\bar{\Phi}^{\mathrm{FF}}\bar{\underline{\omega}}^{\mathrm{FF}} \times (\underline{e}_w \times {}^{\mathrm{FF}}\bar{\underline{r}}^{k})\big) \;= \\ &\qquad \mathrm{J}^3_{w=1}\big({}^{X^{\oplus}_{\mathrm{FF}}}\bar{r}_w^{X_k^*}\cdot\bar{\underline{\omega}}^{X_k} - 2\bar{\omega}_w^{X_k}\cdot{}^{X^{\oplus}_{\mathrm{FF}}}\bar{\underline{r}}^{X_k^*} + (\bar{\underline{\omega}}^{X_k}\bullet{}^{X^{\oplus}_{\mathrm{FF}}}\bar{\underline{r}}^{X_k^*})\cdot\underline{e}_w\big) \end{aligned} \tag{B.122}$$

in which the linear algebra 'triple outer product' rule is used:

$$\underline{a} \times (\underline{b} \times \underline{c}) = (\underline{a} \bullet \underline{c}) \cdot \underline{b} - (\underline{a} \bullet \underline{b}) \cdot \underline{c} \tag{B.123}$$

For the sensitivities to the 'fed-in' kinematic vectors from the foregoing subcomponent hold:

$$\begin{aligned}
\frac{\partial \underline{v}^{X_k^*}}{\partial \underline{v}^{X_{\mathrm{FF}}^{\oplus}}} \equiv \frac{\partial \underline{a}^{X_k^*}}{\partial \underline{a}^{X_{\mathrm{FF}}^{\oplus}}} &= \begin{cases} {}^{X_1}\bar{\Phi}^{X_0} & \text{for } k = 1 \\ {}^{X_k}\bar{\Phi}^{X_1} & \text{for } k = 2 \ldots N \end{cases} \\
\frac{\partial \underline{v}^{X_k^*}}{\partial \underline{\omega}^{X_{\mathrm{FF}}}} \equiv \frac{\partial \underline{a}^{X_k^*}}{\partial \underline{\alpha}^{X_{\mathrm{FF}}}} &= \begin{cases} \boldsymbol{R}_{1X_0}^{X_{\mathrm{f}}^*} & \text{for } k = 1 \\ \boldsymbol{R}_{kX_{\mathrm{f}}}^{X_{\mathrm{p}}^*} & \text{for } k = 2 \ldots N \end{cases}
\end{aligned} \tag{B.124}$$

and, arising from the term $\delta({}^{k}\Phi^{\mathrm{FF}} \cdot \underline{\omega}^{\mathrm{FF}} \times ({}^{k}\Phi^{\mathrm{FF}} \cdot \underline{\omega}^{\mathrm{FF}} \times {}^{\mathrm{FF}}\underline{r}^{k}))$:

$$\frac{\partial \underline{a}^{X_k^*}}{\partial \underline{\omega}^{X_{\mathrm{FF}}}} = \begin{cases} \frac{\partial \underline{a}^{X_1^*}}{\partial \underline{\omega}^{X_0/X_1}} \cdot {}^{X_1}\bar{\Phi}^{X_0} & \text{for } k = 1 \\ \frac{\partial \underline{a}^{X_k^*}}{\partial \underline{\omega}^{X_1/X_k}} \cdot {}^{X_k}\bar{\Phi}^{X_1} & \text{for } k = 2 \ldots N \end{cases} \tag{B.125}$$

Sensitivities to the degrees of freedom in X arise from the terms ${}^{(\mathrm{FF})}\frac{\mathrm{d}}{\mathrm{d}t}\left({}^{\mathrm{FF}}\underline{r}^{k}\right)$ and ${}^{(\mathrm{FF})}\frac{\mathrm{d}^2}{\mathrm{d}t^2}\left({}^{\mathrm{FF}}\underline{r}^{k}\right)$ (use Eq. B.111 and B.112):

$$\frac{\partial \underline{v}^{X_k^*}}{\partial \underline{\dot{\varphi}}^{X}} \equiv \frac{\partial \underline{a}^{X_k^*}}{\partial \underline{\ddot{\varphi}}^{X}} = \begin{cases} \left[\boldsymbol{R}_{11}^{X_{\mathrm{f}}^*} \;\; \mathrm{O}_{(2)} \ldots \mathrm{O}_{(N)}\right] & \text{for } k = 1 \\ \left[\mathrm{O}_{(1)} \;\; \mathrm{J}_{i=2}^{k}(\boldsymbol{R}_{ki}^{X_{\mathrm{p}}^*}) \;\; \mathrm{O}_{(k+1)} \ldots \mathrm{O}_{(N)}\right] & \text{for } k = 2 \ldots N \end{cases} \tag{B.126}$$

$$\frac{\partial \underline{v}^{X_k^*}}{\partial \underline{\dot{\varrho}}^{X}} \equiv \frac{\partial \underline{a}^{X_k^*}}{\partial \underline{\ddot{\varrho}}^{X}} = \begin{cases} \left[\boldsymbol{G}_{11}^{X_{\mathrm{f}}^{\mathrm{t}}} \;\; \mathrm{O}_{(2)} \ldots \mathrm{O}_{(N)}\right] & \text{for } k = 1 \\ \left[\mathrm{O}_{(1)} \;\; \mathrm{J}_{i=2}^{k}(\boldsymbol{G}_{ki}^{X_{\mathrm{p}}^{\mathrm{t}}}) \;\; \mathrm{O}_{(k+1)} \ldots \mathrm{O}_{(N)}\right] & \text{for } k = 2 \ldots N \end{cases} \tag{B.127}$$

and from the term $2^{k}\bar{\Phi}^{\mathrm{FF}} \cdot \bar{\underline{\omega}}^{\mathrm{FF}} \times {}^{(\mathrm{FF})}\frac{\mathrm{d}}{\mathrm{d}t}\left({}^{\mathrm{FF}}\underline{r}^{k}\right)$ (use Eq. B.102 and B.111):

$$\begin{aligned}
\frac{\partial \underline{a}^{X_k^*}}{\partial \underline{\dot{\varphi}}^{X}} &= \begin{cases} \left[\mathrm{J}_{v=1}^{3}(\bar{\underline{\omega}}^{X_k} \times \underline{\boldsymbol{R}}_{11_v}^{X_{\mathrm{f}}^*}) \;\; \mathrm{O}_{(2)} \ldots \mathrm{O}_{(N)}\right] & \text{for } k = 1 \\ \left[\mathrm{O}_{(1)} \;\; \mathrm{J}_{i=2}^{k}\left(\mathrm{J}_{v=1}^{3}(\bar{\underline{\omega}}^{X_k} \times \underline{\boldsymbol{R}}_{ki_v}^{X_{\mathrm{p}}^*})\right) \;\; \mathrm{O}_{(k+1)} \ldots \mathrm{O}_{(N)}\right] & \text{for } k = 2 \ldots N \end{cases} \\
\frac{\partial \underline{a}^{X_k^*}}{\partial \underline{\dot{\varrho}}^{X}} &= \begin{cases} \left[\mathrm{J}_{v=1}^{3}(\bar{\underline{\omega}}^{X_k} \times \underline{\boldsymbol{G}}_{11_v}^{X_{\mathrm{f}}^{\mathrm{t}}}) \;\; \mathrm{O}_{(2)} \ldots \mathrm{O}_{(N)}\right] & \text{for } k = 1 \\ \left[\mathrm{O}_{(1)} \;\; \mathrm{J}_{i=2}^{k}\left(\mathrm{J}_{v=1}^{3}(\bar{\underline{\omega}}^{X_k} \times \underline{\boldsymbol{G}}_{ki_v}^{X_{\mathrm{p}}^{\mathrm{t}}})\right) \;\; \mathrm{O}_{(k+1)} \ldots \mathrm{O}_{(N)}\right] & \text{for } k = 2 \ldots N \end{cases}
\end{aligned} \tag{B.128}$$

and from the terms $\delta^{k}\Phi^{\mathrm{FF}} \cdot \bar{\underline{v}}^{\mathrm{FF}}$, $\delta^{k}\Phi^{\mathrm{FF}} \cdot \bar{\underline{\omega}}^{\mathrm{FF}} \times {}^{\mathrm{FF}}\bar{\underline{r}}^{k}$ and ${}^{k}\bar{\Phi}^{\mathrm{FF}} \cdot \bar{\underline{\omega}}^{\mathrm{FF}} \times \delta^{\mathrm{FF}}\underline{r}^{k}$:

$$\frac{\partial \underline{v}^{X_k^*}}{\partial \underline{\phi}^{X}} = \begin{cases} \left[\mathrm{J}_{v=1}^{3}\left(\frac{\partial^{X_1}\Phi^{X_0}}{\partial \phi_v^{X_1}} \cdot \bar{\underline{v}}^{X_0^{\oplus}} + \frac{\partial^{X_1}\Phi^{X_0}}{\partial \phi_v^{X_1}} \cdot \bar{\underline{\omega}}^{X_0} \times {}^{X_0^{\oplus}}\bar{\underline{r}}^{X_k^*}\right) \;\; \mathrm{O}_{(2)} \ldots \mathrm{O}_{(N)}\right] & \text{for } k = 1 \\ \Bigg[\mathrm{O}_{(2)} \;\; \mathrm{J}_{i=2}^{k}\Big(\mathrm{J}_{v=1}^{3}\Big(\frac{\partial^{X_k}\Phi^{X_1}}{\partial \phi_v^{X_i}} \cdot \bar{\underline{v}}^{X_1^{\oplus}} + \frac{\partial^{X_k}\Phi^{X_1}}{\partial \phi_v^{X_i}} \cdot \bar{\underline{\omega}}^{X_1} \times {}^{X_0^{\oplus}}\bar{\underline{r}}^{X_k^*} + \\ \qquad \bar{\underline{\omega}}^{X_k} \times \sum_{m=2}^{i-1} \frac{\partial^{X_k}\Phi^{X_m}}{\partial \phi_v^{X_1}} \cdot {}^{X_m^{\ominus}}\bar{\underline{r}}^{X_m^{\oplus}}\Big)\Big) \;\; \mathrm{O}_{(k+1)} \ldots \mathrm{O}_{(N)}\Bigg] & \text{for } k = 2 \ldots N \end{cases} \tag{B.129}$$

and from the terms $\delta^k\Phi^{\mathrm{FF}}\cdot\underline{\bar{a}}^{\mathrm{FF}}$ and $\delta({}^k\Phi^{\mathrm{FF}}\cdot\underline{\omega}^{\mathrm{FF}}\times({}^k\Phi^{\mathrm{FF}}\cdot\underline{\omega}^{\mathrm{FF}}\times{}^{\mathrm{FF}}\underline{r}^k))$:

$$\frac{\partial\underline{a}^{X_k^*}}{\partial\underline{\phi}^X} = \begin{cases} \left[\mathrm{J}_{v=1}^{3}\Big(\frac{\partial^{X_1}\Phi^{X_0}}{\partial\phi_v^{X_1}}\cdot\underline{\bar{a}}^{X_0^{\oplus}}+\frac{\partial\underline{a}^{X_1^*}}{\partial\underline{\omega}^{X_0/X_1}}\cdot\frac{\partial^{X_1}\Phi^{X_0}}{\partial\phi_v^{X_1}}\cdot\underline{\bar{\omega}}^{X_0}\Big)\ \mathrm{O}_{(2)}\ldots\mathrm{O}_{(N)}\right] & \text{for } k=1 \\ \Big[\mathrm{O}_{(2)}\ \mathrm{J}_{i=2}^{k}\Big(\mathrm{J}_{v=1}^{3}\Big(\frac{\partial^{X_k}\Phi^{X_1}}{\partial\phi_v^{X_i}}\cdot\underline{\bar{a}}^{X_1^{\oplus}}+\frac{\partial\underline{a}^{X_k^*}}{\partial\underline{\omega}^{X_1/X_k}}\cdot\frac{\partial^{X_k}\Phi^{X_k}}{\partial\phi_v^{X_2}}\cdot\underline{\bar{\omega}}^{X_1}+ \\ \qquad\underline{\bar{\omega}}^{X_k}\times(\underline{\bar{\omega}}^{X_k}\times\sum_{m=2}^{i-1}\frac{\partial^{X_k}\Phi^{X_m}}{\partial\phi_v^{X_1}}\cdot{}^{X_m^{\ominus}}\underline{\bar{r}}^{X_m^{\oplus}})\Big)\Big)\ \mathrm{O}_{(k+1)}\ldots\mathrm{O}_{(N)}\Big] & \text{for } k=2\ldots N \end{cases} \tag{B.130}$$

B.3.2 Rotor blade impulse

Since the degrees of freedom of the blade elements are modelled in the entry point $X_k^{\ominus}$, the angular impulse of X_k is also considered relative to $X_k^{\ominus}$. The linearised expression for the angular impulse coordinate vector is derived from the following first order approximation:

$$\begin{aligned} {}^{X_k^{\ominus}}\dot{\underline{h}}^{X_k} &= {}^{X_k^{\ominus}}\underline{r}^{X_k^*}\times m^{X_k}(\underline{\bar{a}}^{X_k^*}+\delta\underline{a}^{X_k^*})+\boldsymbol{I}^{X_k}\cdot\delta\underline{\alpha}^{X_k}+ \\ &\quad\underline{\bar{\omega}}^{X_k}\times\boldsymbol{I}^{X_k}\cdot\underline{\bar{\omega}}^{X_k}+\underline{\bar{\omega}}^{X_k}\times\boldsymbol{I}^{X_k}\cdot\delta\underline{\omega}^{X_k}+\delta\underline{\omega}^{X_k}\times\boldsymbol{I}^{X_k}\cdot\underline{\bar{\omega}}^{X_k} \end{aligned} \tag{B.131}$$

The inertia matrix $\boldsymbol{I}^{X_k}$ contains the inertia moments and products relative to the centre of gravity of X_k and applies along the axes of the final coordinate system of X_k. The matrix $\boldsymbol{I}^{X_k}$ follows from the principle moments of inertia $J_{x,y,z}^{X_k}$ for the concerning blade element. The mapping depends on the relative orientation of the principle axes and the neutral elastic axes, since the latter set up the final coordinate system. The y-axis $\vec{e}_y^{\,X_k}$ of the final coordinate system coincides with the spanwise coordinate of X_k.

The rotation from the blade-neutral z-axis $\vec{e}_z^{\,X_0}$ over the angle $\phi_{\mathrm{ez}}^{X_k}$ along $\vec{e}_y^{\,X_k}$ yeilds the direction of the bending neutral elastic z-axis *in case of zero pitch angle and no blade deformation*. When looking from the blade root to the tip this rotation is in counter clockwise sense if $\phi_{\mathrm{pz}}^{X_k}>0$. The bending neutral elastic x-axis is perpendicular to the z-axis and $\vec{e}_y^{\,X_k}$. For zero-deformation, these z- and x-axis coincide with $\vec{e}_z^{\,X_k}$ and $\vec{e}_x^{\,X_k}$.

The principle y-axis of a blade element X_k is assumed to coincide with $\vec{e}_y^{\,X_k}$. The principle z-axis of X_k is obtained by rotation from $\vec{e}_z^{\,X_0}$ over the angle $\phi_{\mathrm{pz}}^{X_k}$ along $\vec{e}_y^{\,X_k}$ (no pitch, no deformation; equal sign convention as for $\phi_{\mathrm{ez}}^{X_k}$). The principle x-axis is perpendicular to the principle y- and z-axis.

Note that both $\phi_{\mathrm{pz}}^{X_k}$ and $\phi_{\mathrm{ez}}^{X_k}$ have reverse orientation as concerns the direction of rotation along $\vec{e}_y^{\,X_k}$. The inertia matrix $\boldsymbol{I}^{X_k}$ is then obtained from the principle moments of inertia after transformation over the rotation $\Delta\phi_{\mathrm{ez}\leftarrow\mathrm{pr}}^{X_k}$ along $\vec{e}_y^{\,X_k}$ (see also section B.1.2 near eq. B.30):

$$\begin{aligned} \boldsymbol{I}^{X_k} &= \Phi_{\mathrm{y}}(\Delta\phi_{\mathrm{ez}\leftarrow\mathrm{pr}}^{X_k})\cdot\begin{pmatrix} J_x^{S_{\mathrm{n}}} & 0 & 0 \\ 0 & J_y^{S_{\mathrm{n}}} & 0 \\ 0 & 0 & J_z^{S_{\mathrm{n}}} \end{pmatrix}\cdot\Phi_{\mathrm{y}}^{\mathrm{T}}(\Delta\phi_{\mathrm{ez}\leftarrow\mathrm{pr}}^{X_k}) \\ \text{with } \Delta\phi_{\mathrm{ez}\leftarrow\mathrm{pr}}^{X_k} &= -(\,(-\phi_{\mathrm{pz}}^{X_k})\,-\,(-\phi_{\mathrm{ez}}^{X_k})\,) \end{aligned} \tag{B.132}$$

The pursued expression for the angular impulse involves sensitivities to any variable upon which $\underline{a}^{X_k^*}$, $\underline{\alpha}^{X_k}$ or $\underline{\omega}^{X_k}$ depends; for the linear impulse this only concerns $\underline{a}^{X_k^*}$. The

linearised expressions are written in compact form:

$$\begin{aligned} {}^{x_k^{\ominus}}\underline{\dot{\boldsymbol{h}}}^{X_k} &= {}^{x_k^{\ominus}}\underline{\bar{\dot{\boldsymbol{h}}}}^{X_k} + \sum_{(\underline{z})} \frac{\partial {}^{x_k^{\ominus}}\underline{\dot{\boldsymbol{h}}}^{X_k}}{\partial \underline{z}} \cdot \delta \underline{z} \\ \underline{\dot{p}}^{X_k} &= \underline{\bar{\dot{p}}}^{X_k} + \sum_{(\underline{z})} \frac{\partial \underline{\dot{p}}^{X_k}}{\partial \underline{z}} \cdot \delta \underline{z} \end{aligned} \tag{B.133}$$

Equations B.120 and B.100 tell that the summuation over $\underline{z}$ concerns $\underline{\omega}^{X_{\mathrm{FF}}}$, $\underline{\alpha}^{X_{\mathrm{FF}}}$, $\underline{a}^{X_{\mathrm{FF}}^{\oplus}}$, $\underline{\phi}^{X}$, $\underline{\dot{\varphi}}^{X}$, $\underline{\ddot{\varphi}}^{X}$, $\underline{\dot{\varrho}}^{X}$ and $\underline{\ddot{\varrho}}^{X}$.

The expressions for the mean impulse values are:

$$\begin{aligned} {}^{x_k^{\ominus}}\underline{\bar{\boldsymbol{h}}}^{X_k} &= {}^{x_k^{\ominus}}\underline{r}^{x_k^*} \times m^{X_k} \underline{\bar{a}}^{x_k^*} + \underline{\bar{\omega}}^{X_k} \times \boldsymbol{I}^{X_k} \cdot \underline{\bar{\omega}}^{X_k} \\ \underline{\bar{p}}^{X_k} &= m^{X_k} \underline{\bar{a}}^{x_k^*} \end{aligned} \tag{B.134}$$

The sensitivity of the rate of change in the angular impulse to $\underline{\omega}^{X_{\mathrm{FF}}}$ and $\underline{\dot{\varphi}}^{X}$ involve the direct partial derivatives of the angular impulse to $\underline{\omega}^{X_k}$, $\underline{\alpha}^{X_k}$ and $\underline{a}^{x_k^*}$:

$$\frac{\partial {}^{x_k^{\ominus}}\underline{\dot{\boldsymbol{h}}}^{X_k}}{\partial \underline{z}} = \frac{\partial {}^{x_k^{\ominus}}\underline{\dot{\boldsymbol{h}}}^{X_k}}{\partial \underline{\omega}^{X_k}} \cdot \frac{\partial \underline{\omega}^{X_k}}{\partial \underline{z}} + \frac{\partial {}^{x_k^{\ominus}}\underline{\dot{\boldsymbol{h}}}^{X_k}}{\partial \underline{\alpha}^{X_k}} \cdot \frac{\partial \underline{\alpha}^{X_k}}{\partial \underline{z}} + \frac{\partial {}^{x_k^{\ominus}}\underline{\dot{\boldsymbol{h}}}^{X_k}}{\partial \underline{a}^{x_k^*}} \cdot \frac{\partial \underline{a}^{x_k^*}}{\partial \underline{z}} \quad \text{for } \underline{z} = \underline{\omega}^{X_{\mathrm{FF}}}, \underline{\dot{\varphi}}^{X} \tag{B.135}$$

The sensitivity to $\underline{\phi}^{X}$ involves the direct partial derivatives to $\underline{\omega}^{X_k}$ and $\underline{a}^{x_k^*}$:

$$\frac{\partial {}^{x_k^{\ominus}}\underline{\dot{\boldsymbol{h}}}^{X_k}}{\partial \underline{z}} = \frac{\partial {}^{x_k^{\ominus}}\underline{\dot{\boldsymbol{h}}}^{X_k}}{\partial \underline{\omega}^{X_k}} \cdot \frac{\partial \underline{\omega}^{X_k}}{\partial \underline{z}} + \frac{\partial {}^{x_k^{\ominus}}\underline{\dot{\boldsymbol{h}}}^{X_k}}{\partial \underline{a}^{x_k^*}} \cdot \frac{\partial \underline{a}^{x_k^*}}{\partial \underline{z}} \quad \text{for } \underline{z} = \underline{\phi}^{X} \tag{B.136}$$

The sensitivity to $\underline{\alpha}^{X_{\mathrm{FF}}}$ and $\underline{\ddot{\varphi}}^{X}$ involves direct partial derivatives to $\underline{\alpha}^{X_k}$ and $\underline{a}^{x_k^*}$:

$$\frac{\partial {}^{x_k^{\ominus}}\underline{\dot{\boldsymbol{h}}}^{X_k}}{\partial \underline{z}} = \frac{\partial {}^{x_k^{\ominus}}\underline{\dot{\boldsymbol{h}}}^{X_k}}{\partial \underline{\alpha}^{X_k}} \cdot \frac{\partial \underline{\alpha}^{X_k}}{\partial \underline{z}} + \frac{\partial {}^{x_k^{\ominus}}\underline{\dot{\boldsymbol{h}}}^{X_k}}{\partial \underline{a}^{x_k^*}} \cdot \frac{\partial \underline{a}^{x_k^*}}{\partial \underline{z}} \quad \text{for } \underline{z} = \underline{\alpha}^{X_{\mathrm{FF}}}, \underline{\ddot{\varphi}}^{X} \tag{B.137}$$

The sensitivity to $\underline{a}^{X_{\mathrm{FF}}^{\oplus}}$, $\underline{\dot{\varrho}}^{X}$ and $\underline{\ddot{\varrho}}^{X}$ involves the partial derivative to only $\underline{a}^{x_k^*}$:

$$\frac{\partial {}^{x_k^{\ominus}}\underline{\dot{\boldsymbol{h}}}^{X_k}}{\partial \underline{z}} = \frac{\partial {}^{x_k^{\ominus}}\underline{\dot{\boldsymbol{h}}}^{X_k}}{\partial \underline{a}^{x_k^*}} \cdot \frac{\partial \underline{a}^{x_k^*}}{\partial \underline{z}} \quad \text{for } \underline{z} = \underline{a}^{X_{\mathrm{FF}}^{\oplus}}, \underline{\dot{\varrho}}^{X}, \underline{\ddot{\varrho}}^{X} \tag{B.138}$$

The direct partial derivatives of the angular impulse change are given by:

$$\begin{aligned} \frac{\partial {}^{x_k^{\ominus}}\underline{\dot{\boldsymbol{h}}}^{X_k}}{\partial \underline{\omega}^{X_k}} &= \mathrm{J}_{w=1}^{3}\left(\underline{\bar{\omega}}^{X_k} \times \boldsymbol{I}^{X_k} \cdot \underline{e}_w + \underline{e}_w \times \boldsymbol{I}^{X_k} \cdot \underline{\bar{\omega}}^{X_k}\right) \\ \frac{\partial {}^{x_k^{\ominus}}\underline{\dot{\boldsymbol{h}}}^{X_k}}{\partial \underline{\alpha}^{X_k}} &= \boldsymbol{I}^{X_k} \\ \frac{\partial {}^{x_k^{\ominus}}\underline{\dot{\boldsymbol{h}}}^{X_k}}{\partial \underline{a}^{x_k^*}} &= \mathrm{J}_{w=1}^{3}\left({}^{x_k^{\ominus}}\underline{r}^{x_k^*} \times m^{X_k} \cdot \underline{e}_w\right) \end{aligned} \tag{B.139}$$

The sensitivity of the rate of change of the linear impulse to all variables only involves the direct partial derivative to $\underline{a}^{x_k^*}$:

$$\frac{\partial \underline{\dot{p}}^{X_k}}{\partial \underline{z}} = \underline{m}^{X_k} \cdot \frac{\partial \underline{a}^{x_k^*}}{\partial \underline{z}} \quad \text{for } \underline{z} = \underline{\omega}^{X_{\mathrm{FF}}}, \underline{\alpha}^{X_{\mathrm{FF}}}, \underline{a}^{X_{\mathrm{FF}}^{\oplus}}, \underline{\phi}^{X}, \underline{\dot{\varphi}}^{X}, \underline{\ddot{\varphi}}^{X}, \underline{\dot{\varrho}}^{X}, \underline{\ddot{\varrho}}^{X} \tag{B.140}$$

B.4 Flap, lead and setting angle on rotor blades

General expressions for the flap, lead and setting angle for a rotor blade X are derived in subsection B.4.1. Means and sensitivity functions for the blade flange X_{p} and blade structure & profile X_{f} are listed in section B.4.2.

B.4.1 General expressions flap, lead and setting angle

The element cone or flap angle β^{X_k} and lead angle ζ^{X_k} define the transformation from the axial and leadwise direction of the blade root to the 'normal' and 'leadwise' direction of the aerodynamic force loading on blade element X_k. The latter are identified as the x- and z-axis of the so called 'conversion' coordinate system $\vec{e}^{\,X_k{}^{c_v}}$:

- $\vec{e}_x^{\,X_k^{cv}}$ lays in the plane spanned by the x- and y-axis of the unpitched blade flange coordinate system $\vec{e}^{\,X_0}$ and points 'flapwise backward';
- $\vec{e}_z^{\,X_k^{cv}}$ lays in the plane spanned by the z- and y-axes of the unpitched blade flange (rotor plane) and points 'leadwise relative to the blade-element'.

Fig. B.1 shows the orientation of coordinate system in the rotor plane for the blade element D_μ. The transformation involves rotation over minus the element cone or flap angle β^{X_k} and over plus the element lead angle ζ^{X_k}.

The blade element flap angle $\beta^{X_{k=1\ldots N}}$ is the rotation from the blade-neutral y-axis $\vec{e}_y^{\,X_0}$ to the projection of the elastic axis of X_k in the blade-neutral xy-plane (spanned by $\vec{e}_{x,y}^{\,X_0}$) (>0 at backward orientation).

$$\begin{aligned}
\beta^{X_k} &= \arctan\frac{\vec{e}_y^{\,X_k}\bullet\vec{e}_x^{\,X_0}}{\vec{e}_y^{\,X_k}\bullet\vec{e}_y^{\,X_0}} &&= \arctan\frac{{}^{X_k}\Phi_{21}^{X_0}}{{}^{X_k}\Phi_{22}^{X_0}}\\
\cos\beta^{X_k} &= \frac{\vec{e}_y^{\,X_k}\bullet\vec{e}_y^{\,X_0}}{\sqrt{(\vec{e}_y^{\,X_k}\bullet\vec{e}_x^{\,X_0})^2+(\vec{e}_y^{\,X_k}\bullet\vec{e}_y^{\,X_0})^2}} &&= \frac{{}^{X_k}\Phi_{22}^{X_0}}{\sqrt{({}^{X_k}\Phi_{21}^{X_0})^2+({}^{X_k}\Phi_{22}^{X_0})^2}}\\
\sin\beta^{X_k} &= \frac{\vec{e}_y^{\,X_k}\bullet\vec{e}_x^{\,X_0}}{\sqrt{(\vec{e}_y^{\,X_k}\bullet\vec{e}_x^{\,X_0})^2+(\vec{e}_y^{\,X_k}\bullet\vec{e}_y^{\,X_0})^2}} &&= \frac{{}^{X_k}\Phi_{21}^{X_0}}{\sqrt{({}^{X_k}\Phi_{21}^{X_0})^2+({}^{X_k}\Phi_{22}^{X_0})^2}}
\end{aligned} \tag{B.141}$$

The blade element lead angle $\zeta^{X_{k=1\ldots N}}$ is the rotation from the projection of the elastic axis of X_k in the blade-neutral xy-plane to the actual elastic axis of X_k (>0 at clockwise orientation in fore-to-aft view)

$$\begin{aligned}
\zeta^{X_k} &= \arctan\frac{\vec{e}_y^{\,X_k}\bullet\vec{e}_z^{\,X_0}}{\sqrt{(\vec{e}_y^{\,X_k}\bullet\vec{e}_x^{\,X_0})^2+(\vec{e}_y^{\,X_k}\bullet\vec{e}_y^{\,X_0})^2}} &&= \arctan\frac{{}^{X_k}\Phi_{23}^{X_0}}{\sqrt{({}^{X_k}\Phi_{21}^{X_0})^2+({}^{X_k}\Phi_{22}^{X_0})^2}}\\
\cos\zeta^{X_k} &= \sqrt{(\vec{e}_y^{\,X_k}\bullet\vec{e}_x^{\,X_0})^2+(\vec{e}_y^{\,X_k}\bullet\vec{e}_y^{\,X_0})^2} &&= \sqrt{({}^{X_k}\Phi_{21}^{X_0})^2+({}^{X_k}\Phi_{22}^{X_0})^2}\\
\sin\zeta^{X_k} &= \vec{e}_y^{\,X_k}\bullet\vec{e}_z^{\,X_0} &&= {}^{X_k}\Phi_{23}^{X_0}
\end{aligned} \tag{B.142}$$

The linearised approximations for variatons in flap and lead angle are (${}^{k}\Phi_{ij}^{0}$ short form of ${}^{X_k}\Phi_{ij}^{X_0}$):

$$\begin{aligned}
\delta\beta^{X_k} &= \sum_{i=1}^{k}\sum_{v=1}^{3}\frac{\partial\beta^{X_k}}{\partial\phi_v^{X_i}}\cdot\delta\phi_v^{X_i}\\
\delta\zeta^{X_k} &= \sum_{i=1}^{k}\sum_{v=1}^{3}\frac{\partial\zeta^{X_k}}{\partial\phi_v^{X_i}}\cdot\delta\phi_v^{X_i}
\end{aligned} \tag{B.143}$$

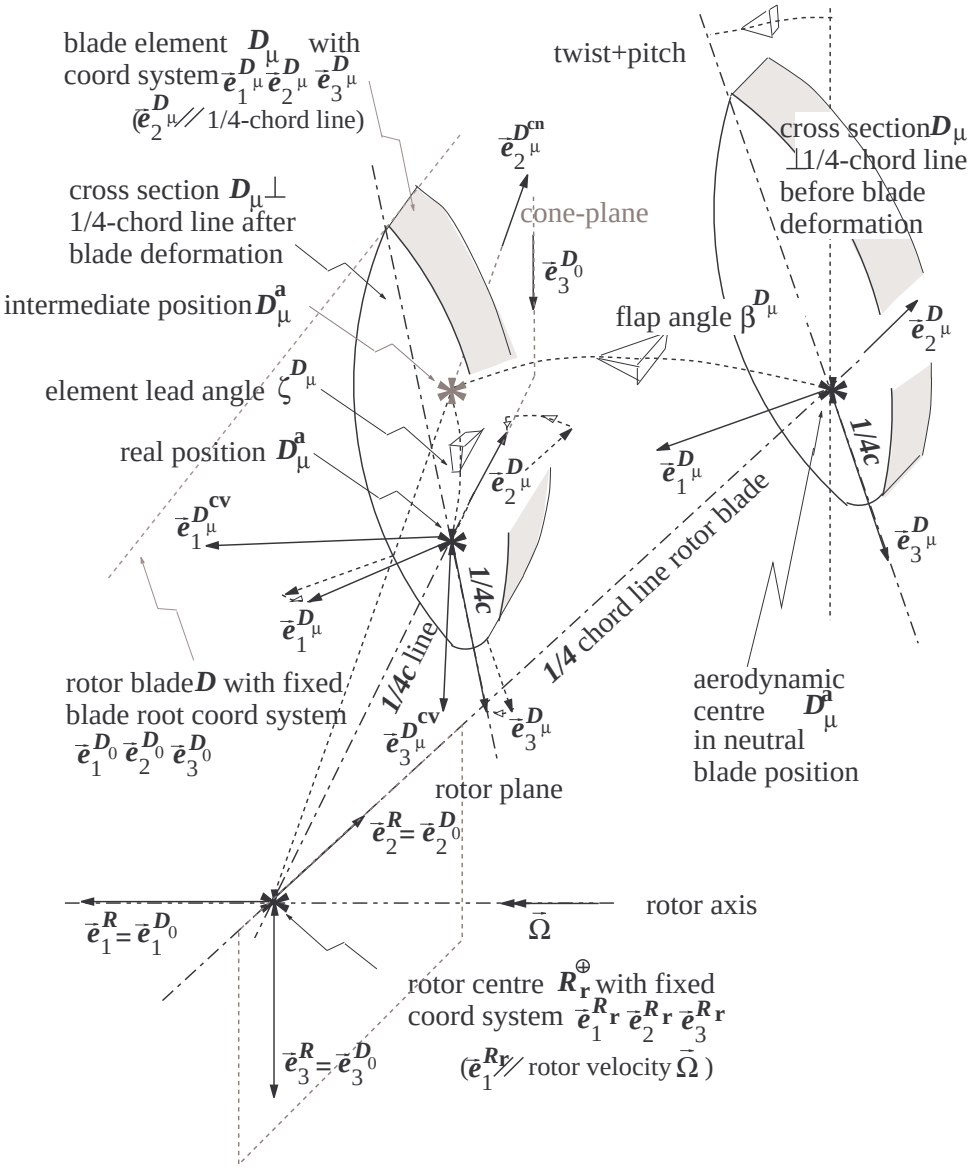

Figure B.1 *Coordinate systems on 'neutral blade' and blade with prebending and deformation ($\vec{e}_{1,2,3}^{\,D_\mu} = \vec{e}_{x,y,z}^{\,D_\mu}$)*

with:

$$\frac{\partial \beta^{X_k}}{\partial \phi_v^{X_i}} = \frac{({}^k\bar{\Phi}^0_{22} \cdot \frac{\partial {}^k\Phi^0_{21}}{\partial \phi_v^{X_i}} - {}^k\bar{\Phi}^0_{21} \cdot \frac{\partial {}^k\Phi^0_{22}}{\partial \phi_v^{X_i}})}{({}^k\bar{\Phi}^0_{21})^2 + ({}^k\bar{\Phi}^0_{22})^2}$$

$$\frac{\partial \zeta^{X_k}}{\partial \phi_v^{X_i}} = \frac{([({}^k\bar{\Phi}^0_{21})^2 + ({}^k\bar{\Phi}^0_{22})^2] \cdot \frac{\partial {}^k\Phi^0_{23}}{\partial \phi_v^{X_i}} - {}^k\bar{\Phi}^0_{23} \cdot {}^k\bar{\Phi}^0_{21} \cdot \frac{\partial {}^k\Phi^0_{21}}{\partial \phi_v^{X_i}} - {}^k\bar{\Phi}^0_{23} \cdot {}^k\bar{\Phi}^0_{22} \cdot \frac{\partial {}^k\Phi^0_{22}}{\partial \phi_v^{X_i}})}{[({}^k\bar{\Phi}^0_{21})^2 + ({}^k\bar{\Phi}^0_{22})^2 + ({}^k\bar{\Phi}^0_{23})^2] \cdot \sqrt{({}^k\bar{\Phi}^0_{21})^2 + ({}^k\bar{\Phi}^0_{22})^2}} \tag{B.144}$$

The blade element setting angle $\phi_{\text{set}}^{X_{k=1\ldots N}}$ is the rotation from the leadwise axis of blade element X_k to its chord line for the actual pitch angle and blade deformation state (>0 at counter clockwise orientation in root-to-tip view). For its expression in dofs, we introduce

the chord-wise blade coordinate system $\vec{e}^{\,X_k^{\rm set}}$ with the z-axis along the chord line of X_k. By this definition, $\vec{e}^{\,X_k^{\rm set}}$ origins from *the* coordinate system $\vec{e}^{\,X_k}$ by rotation along the y-axis over $-(\phi_{\rm tw}^{X_k} - \phi_{\rm ez}^{X_k})$. The setting angle actually is the angle between the chord line and the lead direction of the blade element. The expression for the setting angle is:

$$\begin{aligned}
\phi_{\rm set}^{X_k} &= -\arctan\frac{\vec{e}_z^{\,X_k^{\rm set}} \bullet \vec{e}_x^{\,X_k^{\rm cv}}}{\vec{e}_z^{\,X_k^{\rm set}} \bullet \vec{e}_z^{\,X_k^{\rm cv}}} = -\arctan\frac{{}^{X_k^{\rm set}}\Phi^{X_k}_{(3,:)} \cdot {}^{X_k}\Phi^{X_0} \cdot {}^{X_0}\Phi^{X_k^{\rm cv}}_{(:,1)}}{{}^{X_k^{\rm set}}\Phi^{X_k}_{(3,:)} \cdot {}^{X_k}\Phi^{X_0} \cdot {}^{X_0}\Phi^{X_k^{\rm cv}}_{(:,3)}} \\
&\text{because} \quad {}^{X_k^{\rm set}}\Phi^{X_k^{\rm cv}}_{pq} = {}^{X_k^{\rm set}}\Phi^{X_k}_{(p,:)} \cdot {}^{X_k}\Phi^{X_k^0} \cdot {}^{X_0}\Phi^{X_k^{\rm cv}}_{(:,q)}
\end{aligned} \tag{B.145}$$

For the transformation matrices ${}^{X_k^{\rm set}}\Phi^{X_k}$ and ${}^{X_0}\Phi^{X_k^{\rm cv}}$ hold:

$$\begin{aligned}
{}^{X_k^{\rm set}}\Phi^{X_k} &\overset{\text{(invariant)}}{=} \Phi_{\rm y}(-(\phi_{\rm tw}^{X_k} - \phi_{\rm ez}^{X_k})) \\
{}^{X_0}\Phi^{X_k^{\rm cv}} &= \Phi_{\rm z}^{\rm T}(-\beta^{X_k}) \cdot \Phi_{\rm x}^{\rm T}(\zeta^{X_k})
\end{aligned} \tag{B.146}$$

The linear approximation for the variaton in column q of ${}^{X_k}\Phi^{X_k^{\rm cv}}$ can be expressed as follows:

$$\begin{aligned}
\frac{\partial {}^{X_k}\Phi^{X_k^{\rm cv}}_{(:,q)}}{\partial \underline{\phi}^X} \cdot \delta\underline{\phi}^X &= \Big([\frac{\partial {}^{X_k}\Phi^{X_0}}{\partial \underline{\phi}^X} \cdot ({}^{X_0}\bar{\Phi}^{X_k^{\rm cv}} \cdot \underline{e}_q)] + \\
&{}^{X_k}\bar{\Phi}^{X_0} \cdot \left[-\frac{\mathrm{d}\Phi_{\rm z}^{\rm T}}{\mathrm{d}\phi}\Big|_{-\bar{\beta}^{X_k}} \cdot \Phi_{\rm x}^{\rm T}|_{\bar{\zeta}^{X_k}} \cdot \underline{e}_q \;\Big|\; \Phi_{\rm z}^{\rm T}|_{-\bar{\beta}^{X_k}} \cdot \frac{\mathrm{d}\Phi_{\rm x}^{\rm T}}{\mathrm{d}\phi}\Big|_{\bar{\zeta}^{X_k}} \cdot \underline{e}_q \right] \cdot \begin{bmatrix} \frac{\partial \beta^{X_k}}{\partial \underline{\phi}^X} \\ \frac{\partial \zeta^{X_k}}{\partial \underline{\phi}^X} \end{bmatrix} \Big) \cdot \delta\underline{\phi}^X
\end{aligned} \tag{B.147}$$

The linearised variation of the setting angle can be expressed in the sensitivities of the variation in columns of ${}^{X_k}\Phi^{X_k^{\rm cv}}$ to the rotation dofs:

$$\delta\phi_{\rm set}^{X_k} = \sum_{i=1}^{k}\sum_{v=1}^{3} \frac{\partial \phi_{\rm set}^{X_k}}{\partial \phi_v^{X_i}} \cdot \delta\phi_v^{X_i} \tag{B.148}$$

with

$$\frac{\partial \phi_{\rm set}^{X_k}}{\partial \phi_v^{X_i}} = \frac{{}^{X_k^{\rm set}}\bar{\Phi}_{31}^{X_k^{\rm cv}} \cdot ({}^{X_k^{\rm set}}\Phi^{X_k}_{(3,:)} \cdot \frac{\partial^{X_k}\Phi^{X_k^{\rm cv}}_{(:,3)}}{\partial \phi_v^{X_i}}) - {}^{X_k^{\rm set}}\bar{\Phi}_{33}^{X_k^{\rm cv}} \cdot ({}^{X_k^{\rm set}}\Phi^{X_k}_{(3,:)} \cdot \frac{\partial^{X_k}\Phi^{X_k^{\rm cv}}_{(:,1)}}{\partial \phi_v^{X_i}})}{({}^{X_k^{\rm set}}\bar{\Phi}_{31}^{X_k^{\rm cv}})^2 + ({}^{X_k^{\rm set}}\bar{\Phi}_{33}^{X_k^{\rm cv}})^2} \tag{B.149}$$

B.4.2 Mean and sensitivities of flap, lead and setting angle

The following linearised expressions hold for the flap, lead and setting angle of blade element X_k:

$$\begin{aligned}
\beta^{X_k} &= \bar{\beta}^{X_k} + \frac{\partial \beta^{X_k}}{\partial \underline{\phi}^X} \cdot \delta\underline{\phi}^X + \frac{\partial \beta^{X_k}}{\partial \underline{\phi}^{X_{\rm FF}}} \cdot \delta\underline{\phi}^{X_{\rm FF}} \\
\zeta^{X_k} &= \bar{\zeta}^{X_k} + \frac{\partial \zeta^{X_k}}{\partial \underline{\phi}^X} \cdot \delta\underline{\phi}^X + \frac{\partial \zeta^{X_k}}{\partial \underline{\phi}^{X_{\rm FF}}} \cdot \delta\underline{\phi}^{X_{\rm FF}} \\
\phi_{\rm set}^{X_k} &= \bar{\phi}_{\rm set}^{X_k} + \frac{\partial \phi_{\rm set}^{X_k}}{\partial \underline{\phi}^X} \cdot \delta\underline{\phi}^X + \frac{\partial \phi_{\rm set}^{X_k}}{\partial \underline{\phi}^{X_{\rm FF}}} \cdot \delta\underline{\phi}^{X_{\rm FF}}
\end{aligned} \tag{B.150}$$

The mean values are given by (see Eq. B.146 for ${}^{X_k^{\rm set}}\bar{\Phi}^{X_k}$ and ${}^{X_0}\bar{\Phi}^{X_k^{\rm cv}}$):

$$\bar{\beta}^{X_k} = \begin{cases} \arctan({}^{X_1}\bar{\Phi}_{21}^{X_0} / {}^{X_1}\bar{\Phi}_{22}^{X_0}) & \text{for k=1} \\ \arctan({}^{X_k}\bar{\Phi}_{21}^{X_0} / {}^{X_k}\bar{\Phi}_{22}^{X_0}) & \text{for k=2...N} \end{cases}$$

$$\bar{\zeta}^{X_k} = \begin{cases} \arctan({}^{X_1}\bar{\Phi}_{23}^{X_0} / \sqrt{({}^{X_1}\bar{\Phi}_{21}^{X_0})^2 + ({}^{X_1}\bar{\Phi}_{22}^{X_0})^2}) & \text{for k=1} \\ \arctan({}^{X_k}\bar{\Phi}_{23}^{X_0} / \sqrt{({}^{X_k}\bar{\Phi}_{21}^{X_0})^2 + ({}^{X_k}\bar{\Phi}_{22}^{X_0})^2}) & \text{for k=2...N} \end{cases}$$

$$\bar{\phi}_{\rm set}^{X_k} = \begin{cases} -\arctan({}^{X_1^{\rm set}}\bar{\Phi}_{(3,:)}^{X_1} \cdot {}^{X_1}\bar{\Phi}^{X_0} \cdot {}^{X_0}\bar{\Phi}_{(:,1)}^{X_1^{\rm cv}} / {}^{X_1^{\rm set}}\bar{\Phi}_{(3,:)}^{X_1} \cdot {}^{X_1}\bar{\Phi}^{X_0} \cdot {}^{X_0}\bar{\Phi}_{(:,3)}^{X_1^{\rm cv}}) & \text{for k=1} \\ -\arctan({}^{X_k^{\rm set}}\bar{\Phi}_{(3,:)}^{X_k} \cdot {}^{X_k}\bar{\Phi}^{X_0} \cdot {}^{X_0}\bar{\Phi}_{(:,1)}^{X_k^{\rm cv}} / {}^{X_k^{\rm set}}\bar{\Phi}_{(3,:)}^{X_k} \cdot {}^{X_k}\bar{\Phi}^{X_0} \cdot {}^{X_0}\bar{\Phi}_{(:,3)}^{X_k^{\rm cv}}) & \text{for k=2...N} \end{cases} \tag{B.151}$$

and sensitivity functions (see Eq. B.144 for $\partial\beta^{X_k}/\partial\phi_v^{X_i}$ and $\partial\zeta^{X_k}/\partial\phi_v^{X_i}$):

$$\frac{\partial\beta^{X_k}}{\partial\underline{\phi}^{X}} = \begin{cases} \left[\mathrm{J}_{v=1}^{3}(\partial\beta^{X_1}/\partial\phi_v^{X_1})\ \ \mathrm{O}_{(2)}\ldots\mathrm{O}_{(N)}\right] & \text{for k=1} \\ \left[\mathrm{O}_{(1)}\ \ \mathrm{J}_{i=2}^{k}\big(\mathrm{J}_{v=1}^{3}(\partial\beta^{X_k}/\partial\phi_v^{X_i})\big)\ \ \mathrm{O}_{(k+1)}\ldots\mathrm{O}_{(N)}\right] & \text{for k=2...N} \end{cases}$$

$$\frac{\partial\beta^{X_k}}{\partial\underline{\phi}^{X_{\rm FF}}} = \begin{cases} \text{<does not exist>} & \text{for k=1} \\ \mathrm{J}_{v=1}^{3}(\partial\beta^{X_k}/\partial\phi_v^{X_1}) & \text{for k=2...N} \end{cases} \tag{B.152}$$

and

$$\frac{\partial\zeta^{X_k}}{\partial\underline{\phi}^{X}} = \begin{cases} \left[\mathrm{J}_{v=1}^{3}(\partial\zeta^{X_1}/\partial\phi_v^{X_1})\ \ \mathrm{O}_{(2)}\ldots\mathrm{O}_{(N)}\right] & \text{for k=1} \\ \left[\mathrm{O}_{(1)}\ \ \mathrm{J}_{i=2}^{k}\big(\mathrm{J}_{v=1}^{3}(\partial\zeta^{X_k}/\partial\phi_v^{X_i})\big)\ \ \mathrm{O}_{(k+1)}\ldots\mathrm{O}_{(N)}\right] & \text{for k=2...N} \end{cases}$$

$$\frac{\partial\zeta^{X_k}}{\partial\underline{\phi}^{X_{\rm FF}}} = \begin{cases} \text{<does not exist>} & \text{for k=1} \\ \mathrm{J}_{v=1}^{3}(\partial\zeta^{X_k}/\partial\phi_v^{X_1}) & \text{for k=2...N} \end{cases} \tag{B.153}$$

and (see Eq. B.147 and B.149 for $\partial\phi_{\rm set}^{X_k}/\partial\phi_v^{X_i}$):

$$\frac{\partial\phi_{\rm set}^{X_k}}{\partial\underline{\phi}^{X}} = \begin{cases} \left[\mathrm{J}_{v=1}^{3}(\partial\phi_{\rm set}^{X_1}/\partial\phi_v^{X_1})\ \ \mathrm{O}_{(2)}\ldots\mathrm{O}_{(N)}\right] & \text{for k=1} \\ \left[\mathrm{O}_{(1)}\ \ \mathrm{J}_{i=2}^{k}\big(\mathrm{J}_{v=1}^{3}(\partial\phi_{\rm set}^{X_k}/\partial\phi_v^{X_i})\big)\ \ \mathrm{O}_{(k+1)}\ldots\mathrm{O}_{(N)}\right] & \text{for k=2...N} \end{cases}$$

$$\frac{\partial\phi_{\rm set}^{X_k}}{\partial\underline{\phi}^{X_{\rm FF}}} = \begin{cases} \text{<does not exist>} & \text{for k=1} \\ \mathrm{J}_{v=1}^{3}(\partial\phi_{\rm set}^{X_k}/\partial\phi_v^{X_1}) & \text{for k=2...N} \end{cases} \tag{B.154}$$

B.5 Blade relative wind speed

The general expression for the wind speed $\underline{u}^{X_k}$, as experienced by the rotating and deforming rotor blade in the blade element's normal, radial and lead direction, is derived in subsection B.5.1. The point of the departure is set up by the mean wind speed, described relative to the rotating hub, and by the wind speed variations from turbulence and tower stagnation and wind shear. The mean wind speed is expressed along the coordinate system of the hub in section B.5.2. The mean, sensitivity functions and input variations for the blade-relative wind speed on the blade flange and blade structure & profile elements are given in section B.5.3.

B.5.1 General expression for coordinates and magnitude

The relative wind speed vector $\underline{u}$ for blade element X_k comprises the wind velocity component $U_{\rm n}$ in normal direction and minus U_ℓ in lead direction in the aerodynamic

conversion point X_k^{a}. These depend on the undisturbed wind field velocity $\underline{U}$ and the blade velocity $\underline{v}$ in X_k^{a} as well as on the axial and tangential induction speeds U_{i} and V_{i} in the cross section of rotor annulus W_m and blade element X_k:

$$\underline{u}^{X_k} \triangleq \begin{bmatrix} U_{\mathrm{n}} \\ U_{\mathrm{r}} \\ -U_{\ell} \end{bmatrix}^{X_k^{\mathrm{a}}} = {}^{X_k^{\mathrm{cv}}}\Phi^{A} \cdot \underline{U}^{X_k^{\mathrm{a}}} + {}^{X_k^{\mathrm{cv}}}\Phi^{X_k} \cdot (-\underline{v}^{X_k^{\mathrm{a}}}) + {}^{X_k^{\mathrm{cv}}}\Phi^{W_m/X_k} \cdot \underline{u}_{\mathrm{i}}^{W_m/X_k}$$

$$\text{with: } \underline{u}_{\mathrm{i}}^{W_m/X_k} \triangleq \begin{bmatrix} -U_{\mathrm{i}}^{W_m/X_k} \\ 0 \\ -V_{\mathrm{i}}^{W_m/X_k} \end{bmatrix} \tag{B.155}$$

The undisturbed wind velocity points along the x-axis of the 'aerodynamic coordinate system' $\vec{e}^{\,A}$ and is composed of the mean value $\bar{U}$, the perodic value ${}^{\mathrm{r}}u^{X_k^{\mathrm{a}}}$, and the turbulence ${}^{\mathrm{t}}u^{W_m/X_k^{\mathrm{a}}}(t)$ in the cross section of W_m with X in point X_k^{a}:

$$\underline{U}^{X_k^{\mathrm{a}}} = \left(\vec{U}_{\mathrm{u}}^{X_k^{\mathrm{a}}}\right)^{A} \text{ with } \vec{U}^{X_k^{\mathrm{a}}} = \left(\bar{U} + {}^{\mathrm{r}}u^{X_k^{\mathrm{a}}}(t) + {}^{\mathrm{t}}u^{W_m/X_k^{\mathrm{a}}}(t)\right) \cdot \vec{e}_x^{\,A} \tag{B.156}$$

For the mean coordinates of the blade relative wind velocity vector along $\vec{e}^{\,X_k^{\mathrm{cv}}}$ holds (see Eq. B.164):

$$\begin{aligned} \bar{\underline{u}}^{X_k} &= {}^{X_k^{\mathrm{cv}}}\bar{\Phi}^{R_{\mathrm{h''}}} \cdot \bar{\underline{u}}^{R_{\mathrm{h''}}} - {}^{X_k^{\mathrm{cv}}}\bar{\Phi}^{X_k} \cdot \bar{\underline{v}}^{X_k^{\mathrm{a}}} + {}^{X_k^{\mathrm{cv}}}\bar{\Phi}^{W_m/X_k} \cdot \bar{\underline{u}}_{\mathrm{i}}^{W_m/X_k} \\ \text{with } {}^{X_k^{\mathrm{cv}}}\bar{\Phi}^{R_{\mathrm{h''}}} &= {}^{X_k^{\mathrm{cv}}}\bar{\Phi}^{X_0} \cdot {}^{X_0}\bar{\Phi}^{R_{\mathrm{r}}} \cdot {}^{R_{\mathrm{r}}}\bar{\Phi}^{R_{\mathrm{s}}} \cdot {}^{R_{\mathrm{s}}}\bar{\Phi}^{R_{\mathrm{h''}}} \quad ({}^{R_{\mathrm{s}}}\bar{\Phi}^{R_{\mathrm{h''}}} = \Phi_{\mathrm{d}}) \end{aligned} \tag{B.157}$$

The mean wind speed coordinate vector $\bar{\underline{u}}^{R_{\mathrm{h''}}}$ pertains to the the coordinate system of the gearbox house. It is derived from the average longitudinal winds speed $\bar{U}$ via the orientation between the turbine base and the wind field and via the average compliance of the support structure and gearbox house. The transformation matrix ${}^{R_{\mathrm{h''}}}\bar{\Phi}^{A}$ is involved. A detailed treatment is given in section B.5.2. The linearised expression for the variation $\delta\underline{u}^{X_k}$ is built up from a purely stochastic and periodic contribution ($\delta\underline{u}_{\mathrm{sto}}^{X_k}$ and $\delta\underline{u}_{\mathrm{per}}^{X_k}$) and from a reactive contribution that is caused by structural motion and induction varation on the one side ($\delta\underline{u}_{\mathrm{mot}}^{X_k}$) and by orientation changes on the other side ($\delta\underline{u}_{\mathrm{ori}}^{X_k}$):

$$\delta\underline{u}^{X_k} = \delta\underline{u}_{\mathrm{sto}}^{X_k} + \delta\underline{u}_{\mathrm{per}}^{X_k} + \delta\underline{u}_{\mathrm{mot}}^{X_k} + \delta\underline{u}_{\mathrm{ori}}^{X_k} \tag{B.158}$$

Figure B.2 shows the assembly of contributions to the wind speed on a blade element, however without the contribution driven by structural motion and induction varation. The periodic axial induction speed by oblique inflow, $U_{\mathrm{i_o}}^{X_k}$, is included in the scheme as well; in linearised sense, it is a purely periodic 'external input'.

For the stochastic contribution holds (see Eq. 3.63 and 3.65 and use Eq. B.164; see also section 3.4.2):

$$\begin{aligned} \delta\underline{u}_{\mathrm{sto}}^{X_k} &\triangleq \underline{u}_{\mathrm{sto}}^{W_m/X_k^{\mathrm{a}}} = \\ &{}^{X_k^{\mathrm{cv}}}\bar{\Phi}^{X_0} \cdot \Phi_{\mathrm{x}}({}^{R}\psi^{X_0} + \bar{\phi}_1^{R_{\mathrm{r}}}) \cdot (\Phi_{\mathrm{d}} + \Phi_{\mathrm{c}} \cdot \cos\bar{\Omega}t + \Phi_{\mathrm{s}} \cdot \sin\bar{\Omega}t) \cdot {}^{R_{\mathrm{h''}}}\widetilde{\underline{\Phi}}_1^{\bar{A}/X} \cdot {}^{\mathrm{t}}\underline{u}^{W_m/X_k^{\mathrm{a}}} \end{aligned} \tag{B.159}$$

For the periodic contribution holds:

$$\delta\underline{u}_{\mathrm{per}}^{X_k} = \delta\underline{u}_{\mathrm{obl}}^{X_k} + \delta\underline{u}_{\mathrm{stag}}^{X_k} + \delta\underline{u}_{\mathrm{i_{obl}}}^{X_k}$$

with:

$$\begin{aligned} \delta\underline{u}_{\mathrm{obl}}^{X_k} &= {}^{X_k^{\mathrm{cv}}}\bar{\Phi}^{X_0} \cdot \Phi_{\mathrm{x}}({}^{R}\psi^{X_0}) \cdot \delta\underline{u}_{\mathrm{obl}}^{R} \quad \text{(use Eq. B.168)} \\ \delta\underline{u}_{\mathrm{stag}}^{X_k} &= {}^{X_k^{\mathrm{cv}}}\bar{\Phi}^{X_0} \cdot \Phi_{\mathrm{x}}({}^{R}\psi^{X_0} + \bar{\phi}_1^{R_{\mathrm{r}}}) \cdot (\Phi_{\mathrm{d}} + \Phi_{\mathrm{c}}\cos\bar{\Omega}t + \Phi_{\mathrm{s}}\sin\bar{\Omega}t) \cdot {}^{R_{\mathrm{h''}}}\bar{\underline{\Phi}}_1^{A} \cdot {}^{\mathrm{r}}u^{X_k^{\mathrm{a}}} \\ \delta\underline{u}_{\mathrm{i_{obl}}}^{X_k} &= -{}^{X_k^{\mathrm{cv}}}\bar{\Phi}^{X_0} \cdot U_{\mathrm{i_{obl}}}^{X_k} \cdot \underline{e}_1 \end{aligned} \tag{B.160}$$

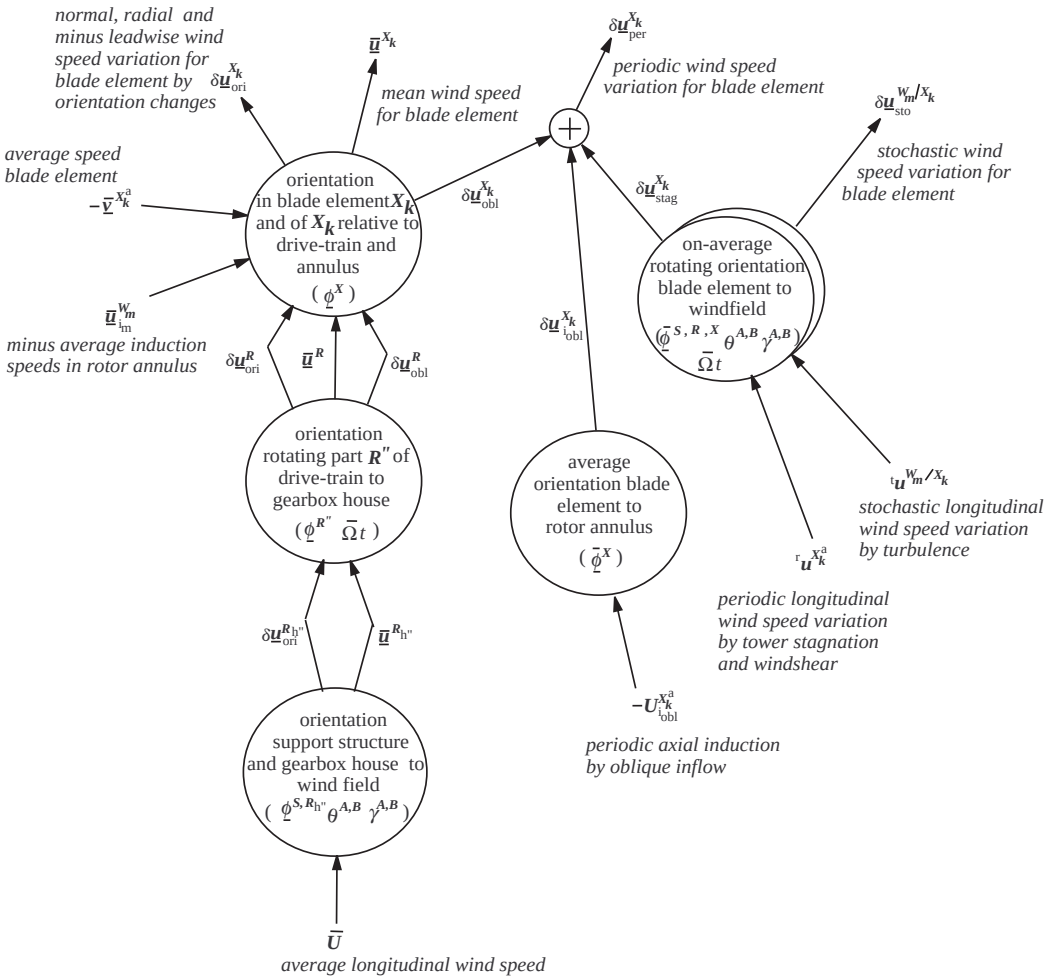

Figure B.2 *Wind speed coordinates on blade element from mean longitudinal wind speed and from turbulence, tower stagnation & wind shear and inductive reaction on oblique-inflow*

The periodic wind speed variation contains the contribution $\delta\underline{u}_{\mathrm{obl}}^{X_k}$ from undisturbed oblique inflow. This is caused by 'modulation' of the mean transverse and vertical wind speed components in the rotor plane by means of the main rotation of the rotor blades (see section B.5.2, Eq.B.168). The contribution $\delta\underline{u}_{\mathrm{i_{obl}}}^{X_k}$ is caused by the azimut-periodic axial induction speed varation by oblique inflow ($U_{\mathrm{i_{obl}}}^{X_k}$) as defined in section B.8.1 by Eq. B.248.

For the contribution related to motion holds:

$$\begin{aligned}\delta\underline{u}_{\mathrm{mot}}^{X_k} \;=\; -{}^{X_k^{\mathrm{cv}}}\bar{\Phi}^{X_k}\cdot\Big(&\frac{\partial\underline{v}^{X_k^{\mathrm{a}}}}{\partial\underline{\omega}^{X_0}}\cdot\delta\underline{\omega}^{X_0}+\frac{\partial\underline{v}^{X_k^{\mathrm{a}}}}{\partial\underline{v}_0^{X_0^{\oplus}}}\cdot\delta\underline{v}_0^{X_0^{\oplus}}+\ldots\\ &\frac{\partial\underline{v}^{X_k^{\mathrm{a}}}}{\partial\underline{\varphi}^{X}}\cdot\dot{\underline{\varphi}}^{X}+\frac{\partial\underline{v}^{X_k^{\mathrm{a}}}}{\partial\underline{\varrho}^{X}}\cdot\dot{\underline{\varrho}}^{X}\Big)+{}^{X_k^{\mathrm{cv}}}\bar{\Phi}^{W_m/X_k}\cdot\delta\underline{u}_{\mathrm{i_m}}^{W_m}\end{aligned}\tag{B.161}$$

We use $\underline{u}_{\mathrm{i_m}}^{W_m}$ instead of $\underline{u}_{\mathrm{i_m}}^{W_m/X}$ because the non-oblique-inflow component of the induction speed has been assumed independent of the azimut position in an annulus in section A.3.1.

Figure B.3 shows the assembly of contributions to the mean wind speed on a blade element,

to the periodic wind speed caused by undisturbed oblique inflow and to the reactive wind speed variation caused by orientation changes.

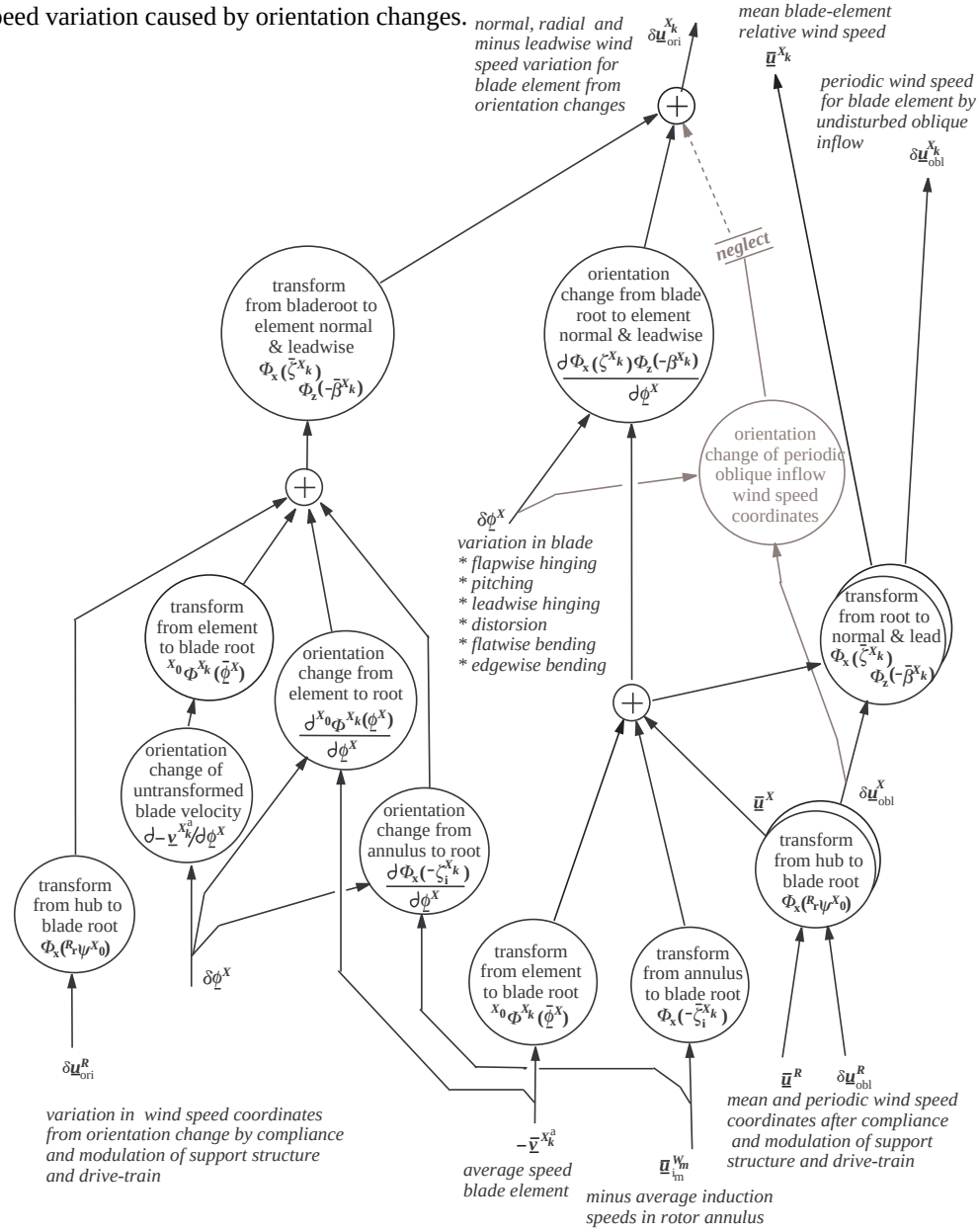

Figure B.3 *Wind speed coordinates on blade element from mean longitudinal wind speed, mean induction speed and mean blade speed*

For the contribution related to orientation changes holds (use Eq. B.168, B.167):

$$\begin{aligned}\delta \underline{u}_{\mathrm{ori}}^{X_k} \;=\; & {}^{X_k^{\mathrm{cv}}}\bar{\Phi}^{X_0} \cdot {}^{X_0}\bar{\Phi}^{R_r} \cdot \delta \underline{u}_{\mathrm{ori}}^{R} + \\ & {}^{X_k^{\mathrm{cv}}}\bar{\Phi}^{X_0} \cdot \Big(-{}^{X_0}\bar{\Phi}^{X_k} \cdot \frac{\partial \underline{v}^{X_k^{\mathrm{a}}}}{\partial \underline{\phi}^{X}} - \Big[\frac{\partial^{X_0}\Phi^{X_k}}{\partial \underline{\phi}^{X}} \cdot \bar{\underline{v}}^{X_k^{\mathrm{a}}}\Big] + \Big[\frac{\partial^{X_0}\Phi^{W_m/X_k}}{\partial \underline{\phi}^{X}} \cdot \bar{\underline{u}}_{\mathrm{i_m}}^{W_m}\Big]\Big) \cdot \delta \underline{\phi}^{X} + \\ & \Big[\frac{\partial^{X_k^{\mathrm{cv}}}\Phi^{X_0}}{\partial \underline{\phi}^{X}} \cdot \Big(-{}^{X_0}\bar{\Phi}^{X_k} \cdot \bar{\underline{v}}^{X_k^{\mathrm{a}}} + {}^{X_0}\bar{\Phi}^{W_m/X_k} \cdot \bar{\underline{u}}_{\mathrm{i_m}}^{W_m} + {}^{X_0}\bar{\Phi}^{R_r} \cdot \bar{\underline{u}}^{R}\Big)\Big] \cdot \delta \underline{\phi}^{X}\end{aligned} \tag{B.162}$$

The expressions for the magnitude $||\underline{u}^{X_k}||$ of the blade relative wind speed and the

linearised expression for its variation are:

$$\begin{aligned} ||\underline{u}^{X_k}|| &= \sqrt{(U_{\mathrm{n}}^{X_k})^2 + (U_{\ell}^{X_k})^2} \\ \delta||\underline{u}^{X_k}|| &= \frac{2\bar{U}_{\mathrm{n}}^{X_k}\cdot\delta U_{\mathrm{n}}^{X_k} + 2\bar{U}_{\ell}^{X_k}\cdot\delta U_{\ell}^{X_k}}{2\sqrt{(\bar{U}_{\mathrm{n}}^{X_k})^2+(\bar{U}_{\ell}^{X_k})^2}} = \frac{(\bar{\underline{u}}^{X_k})^{\mathrm{T}}}{||\bar{\underline{u}}^{X_k}||}\cdot\delta\underline{u}^{X_k} \end{aligned} \tag{B.163}$$

The terms ${}^{X_k^{\mathrm{cv}}}\bar{\Phi}^{X_0}\cdot{}^{X_0}\bar{\Phi}^{R}\cdot\delta\underline{u}_{\mathrm{ori}}^{R}$ and $\left[{}^{X_0}\bar{\Phi}^{R}\cdot\bar{\underline{u}}^{R}\right]\cdot\delta\underline{\phi}^{X}$ are caused, respectivley influenced, by the compliance and angular configuration of the drive-train and support structure. These 'feedthrough-terms are' treated in more detail in section B.5.2.

B.5.2 Feedthrough-terms from drive-train by orientation changes

The compliance and configuration of the drive-train and support structure cause wind speed variations in the coordinate system on the rotor hub purely from the orientation difference between the axial direction of the wind plane and the longitudinal windspeed direction. In the linearised approximation it is allowed to split up these variations into a purely periodic part $\delta\underline{u}_{\mathrm{obl}}^{R}$ and reactive part $\delta\underline{u}_{\mathrm{rea}}^{R}$. The reactive part is caused by motion and by configuration changes. The 'motion part' influences the blade relative wind speed via the blade root velocity vectors $\delta\underline{\omega}^{X_0}$ and $\delta\underline{v}^{X_0^{\oplus}}$ by equation B.161; the 'orientation part' $\delta\underline{u}_{\mathrm{ori}}^{R}$ via the position variations $\delta\underline{\phi}^{S}$, $\delta\phi_3^{R_{\mathrm{h}"}}$ and and $\delta\underline{\phi}^{R_{\mathrm{r}}}$ of the rotation dofs.

Figure B.4 shows at the right side the modulation of the mean transverse and vertical wind speed components, which results in the periodic wind speed coordinates on the rotor hub by undisturbed oblique inflow. In the middle it shows the appearance of the mean wind speed coordinates on the hub.

The periodic part follows from the average transverse and vertical wind speed components in the rotor plane. These non-axial components result from the average compliance and the configuration angles of the support structure and gearbox house, together with the relative orientation of the wind field to the turbine base. The rotations for the support structure are collected in $\underline{\phi}^{S}$. Note that only the part $(i_{\mathrm{gb}}-1)/i_{\mathrm{gb}}$ of the co-axial gearbox house rotation affects the main shaft rotation, identified as $\phi_3^{R_{\mathrm{h}"}}$. The axial, transverse and vertical wind speed components are collected in coordinate vector $\underline{u}^{R_{\mathrm{h}"}}$. For the mean value $\bar{\underline{u}}^{R_{\mathrm{h}"}}$ and for the linearised approximation $\delta\underline{u}_{\mathrm{ori}}^{R_{\mathrm{h}"}}$ of its variation by orientation change holds:

$$\bar{\underline{u}}^{R_{\mathrm{h}"}} \triangleq \begin{bmatrix} \bar{U}_{\mathrm{ax}}^{"} \\ \bar{U}_{\mathrm{yaw}}^{"} \\ \bar{U}_{\mathrm{tilt}}^{"} \end{bmatrix} = {}^{R_{\mathrm{h}"}}\bar{\underline{\Phi}}_1^{A}\cdot\bar{U}$$

$$\delta\underline{u}_{\mathrm{ori}}^{R_{\mathrm{h}"}} \triangleq \begin{bmatrix} \delta U_{\mathrm{ax}}^{"} \\ \delta U_{\mathrm{yaw}}^{"} \\ \delta U_{\mathrm{tilt}}^{"} \end{bmatrix} = \frac{\partial\underline{u}_{\mathrm{ori}}^{R_{\mathrm{h}"}}}{\partial\phi_3^{R_{\mathrm{h}"}}}\cdot\delta\phi_3^{R_{\mathrm{h}"}} + \delta\underline{u}_{\mathrm{ori}}^{S_{\mathrm{n}}}$$

$$\begin{aligned} \text{with}\quad {}^{R_{\mathrm{h}"}}\bar{\Phi}^{A} &= \Phi_{\mathrm{x}}(\bar{\phi}_3^{R_{\mathrm{h}"}})\cdot{}^{S_M}\Phi^{S_0}(\bar{\underline{\phi}}^{S})\cdot\Phi_{\mathrm{y}}(-\theta^{B})\cdot\Phi_{\mathrm{z}}(\gamma^{B})\cdot\Phi_{\mathrm{z}}^{\mathrm{T}}(\gamma^{A})\cdot\Phi_{\mathrm{y}}^{\mathrm{T}}(\theta^{A}) \\ \frac{\partial\underline{u}_{\mathrm{ori}}^{R_{\mathrm{h}"}}}{\partial\phi_3^{R_{\mathrm{h}"}}} &= \left.\frac{\mathrm{d}\Phi_{\mathrm{x}}}{\mathrm{d}\phi}\right|_{\bar{\phi}_1^{R_{\mathrm{h}"}}}\cdot{}^{S_M}\bar{\underline{\Phi}}_1^{A}\cdot\bar{U} \end{aligned} \tag{B.164}$$

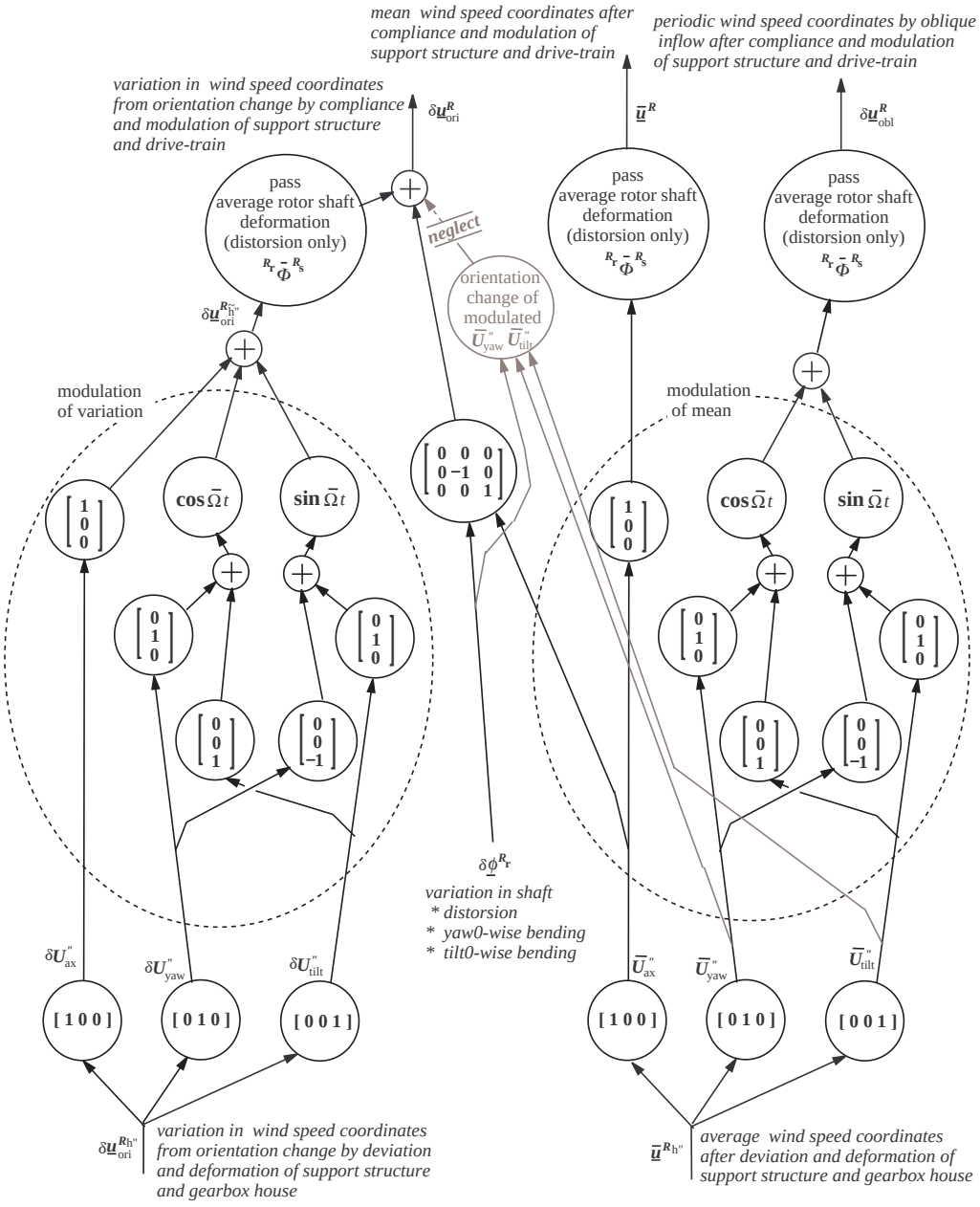

Figure B.4 *Wind speed coordinates on rotor hub from mean longitudinal wind speed*

while:

$$\delta \underline{u}_{\mathrm{ori}}^{S_{\mathrm{n}}} = \frac{\partial \underline{u}_{\mathrm{ori}}^{S_{\mathrm{n}}}}{\partial \underline{\phi}^{S}} \cdot \delta \underline{\phi}^{S} + {}^{S_M}\bar{\Phi}^{S_{M-1}} \cdot \delta \underline{u}_{\mathrm{ori}}^{S_{\mathrm{t}}}$$

$$\delta \underline{u}_{\mathrm{ori}}^{S_{\mathrm{t}}} = \frac{\partial \underline{u}_{\mathrm{ori}}^{S_{\mathrm{t}}}}{\partial \underline{\phi}^{S}} \cdot \delta \underline{\phi}^{S} + {}^{S_{M-1}}\bar{\Phi}^{S_1} \cdot \delta \underline{u}_{\mathrm{ori}}^{S_{\mathrm{f}}}$$

$$\delta \underline{u}_{\mathrm{ori}}^{S_{\mathrm{f}}} = \frac{\partial \underline{u}_{\mathrm{ori}}^{S_{\mathrm{f}}}}{\partial \underline{\phi}^{S}} \cdot \delta \underline{\phi}^{S}$$

with:

$$\begin{aligned}
\frac{\partial \underline{u}_{\mathrm{ori}}^{S_{\mathrm{n}}}}{\partial \underline{\phi}^{S}} &= [\mathrm{O}_{(1)} \ldots \mathrm{O}_{(M-1)} \;\; \mathrm{J}_{v=1}^{3}(\frac{\partial {}^{S_M}\Phi^{S_{M-1}}}{\partial \phi_v^{S_M}} \cdot {}^{S_{M-1}}\underline{\bar{\Phi}}_1^{A} \cdot \bar{U})] \\
\frac{\partial \underline{u}_{\mathrm{ori}}^{S_{\mathrm{t}}}}{\partial \underline{\phi}^{S}} &= [\mathrm{O}_{(1)} \;\; \mathrm{J}_{i=2}^{M-1}\big(\mathrm{J}_{v=1}^{3}(\frac{\partial {}^{S_{M-1}}\Phi^{S_1}}{\partial \phi_v^{S_i}} \cdot {}^{S_1}\underline{\bar{\Phi}}_1^{A} \cdot \bar{U})\big) \;\; \mathrm{O}_{(M)}] \\
\frac{\partial \underline{u}_{\mathrm{ori}}^{S_{\mathrm{f}}}}{\partial \underline{\phi}^{S}} &= [\mathrm{J}_{v=1}^{3}(\frac{\partial {}^{S_1}\Phi^{S_0}}{\partial \phi_v^{S_1}} \cdot {}^{B}\underline{\Phi}_1^{A} \cdot \bar{U}) \;\; \mathrm{O}_{(2)} \ldots \mathrm{O}_{(M)}]
\end{aligned}$$

We also define the 'feedthrough variation by orientation change' of the gearbox house in the *rotating* coordinate system on the slow gearbox shaft (see Eq. B.35 and 3.65):

$$\delta \underline{u}_{\mathrm{ori}}^{R_{\tilde{\mathrm{h}}"}} \;\triangleq\; \big(\delta \vec{u}_{\mathrm{ori}}^{R_{\mathrm{h}"}}\big)^{R_{\mathrm{s}}} \;=\; (\Phi_{\mathrm{d}} + \Phi_{\mathrm{c}} \cdot \cos \bar{\Omega} t + \Phi_{\mathrm{s}} \cdot \sin \bar{\Omega} t) \cdot \delta \underline{u}_{\mathrm{ori}}^{R_{\mathrm{h}"}} \qquad \text{(B.165)}$$

Figure B.4 shows at the left side the feed-through of the variations $\delta \underline{u}_{\mathrm{ori}}^{S"}$ related to the orientation change of the support structure and gearbox house. It also shows the contribution of the varying shaft deformation $\delta \underline{\phi}^{R_{\mathrm{r}}}$ to the reactive wind speed variation on the rotor hub via the axial and the modulated transverse and vertical mean wind speed components. The ranking order of shaft deformations is distorsion in $\phi_1^{R_{\mathrm{r}}}$, yaw0-wise bending in $\phi_2^{R_{\mathrm{r}}}$ and tilt0-wise bending in $\phi_3^{R_{\mathrm{r}}}$. Taking into account this ranking order and assuming zero-mean main shaft bending the contribution of $\delta \underline{\phi}^{R_{\mathrm{r}}}$ to $\delta \underline{u}_{\mathrm{ori}}^{R}$ becomes (only the average distorsion $\bar{\phi}_1^{R_{\mathrm{r}}}$ contributes to ${}^{R_{\mathrm{r}}}\bar{\Phi}^{R_{\mathrm{s}}}$).

$$\begin{aligned}
\frac{\partial \underline{u}_{\mathrm{ori}}^{R}}{\partial \underline{\phi}^{R_{\mathrm{r}}}} \cdot \delta \underline{\phi}^{R_{\mathrm{r}}} &= \bar{U}_{\mathrm{ax}}^{"} \cdot \begin{pmatrix} 0 & 0 & 0 \\ 0 & -1 & 0 \\ 0 & 0 & 1 \end{pmatrix} \cdot \delta \underline{\phi}^{R_{\mathrm{r}}} + \\
&\left(\bar{U}_{\mathrm{yaw}}^{"} \cdot \begin{pmatrix} 0 & \cos & \sin \\ -\sin & 0 & 0 \\ -\cos & 0 & 0 \end{pmatrix}_{\bar{\phi}_1^{R_{\mathrm{r}}}} + \bar{U}_{\mathrm{tilt}}^{"} \cdot \begin{pmatrix} 0 & \sin & -\cos \\ \cos & 0 & 0 \\ -\sin & 0 & 0 \end{pmatrix}_{\bar{\phi}_1^{R_{\mathrm{r}}}} \right) \cdot \cos \bar{\Omega} t \cdot \delta \underline{\phi}^{R_{\mathrm{r}}} + \\
&\left(-\bar{U}_{\mathrm{yaw}}^{"} \cdot \begin{pmatrix} 0 & \sin & -\cos \\ \cos & 0 & 0 \\ -\sin & 0 & 0 \end{pmatrix}_{\bar{\phi}_1^{R_{\mathrm{r}}}} + \bar{U}_{\mathrm{tilt}}^{"} \cdot \begin{pmatrix} 0 & \cos & \sin \\ -\sin & 0 & 0 \\ -\cos & 0 & 0 \end{pmatrix}_{\bar{\phi}_1^{R_{\mathrm{r}}}} \right) \cdot \sin \bar{\Omega} t \cdot \delta \underline{\phi}^{R_{\mathrm{r}}}
\end{aligned} \qquad \text{(B.166)}$$

The orientation change by shaft bending via the modulated mean transverse and vertical wind speed components is neglected because of numerical treatment: it is not possible to eliminate periodic coefficients on 'rotating degrees of freedom like shaft bending' from the homogeneous model equations. This would make it necessary to apply Floquent analysis for 3 bladed wind turbines also. As the non-axial wind speed components are much smaller than the axial one, the modulated coefficients in the second and third term are also much smaller than the non-modulated ones.

The approximated expression for the overall 'orientation part' of the wind speed variation on the rotor hub then becomes ($\phi_1^R = \psi - \bar{\Omega} t$, see Eq. B.37; both variation ϕ_1^R in the main shaft rotation and main shaft distorsion ϕ_2^R along the x-axis!):

$$\delta \underline{u}_{\mathrm{ori}}^{R} \;=\; \frac{\partial \underline{u}_{\mathrm{ori}}^{R}}{\partial \underline{\phi}^{R}} \cdot \delta \underline{\phi}^{R} + \Phi_{\mathrm{x}}(\bar{\phi}_1^{R_{\mathrm{r}}}) \cdot \delta \underline{u}_{\mathrm{ori}}^{R_{\tilde{\mathrm{h}}"}} \quad \text{with} \quad \frac{\partial \underline{u}_{\mathrm{ori}}^{R}}{\partial \underline{\phi}^{R}} = \bar{U}_{\mathrm{ax}}^{"} \cdot \begin{pmatrix} 0 & 0 & 0 & 0 \\ 0 & 0 & -1 & 0 \\ 0 & 0 & 0 & 1 \end{pmatrix} \qquad \text{(B.167)}$$

Note that $\delta \phi_1^R$ equals variation $\varphi_{\mathrm{x}}^{R_{\mathrm{f}}}$ in the main shaft rotation and $\delta[\phi_2^R \phi_3^R \phi_4^R]'$ equals the deformation vector $\underline{\varphi}^{R_{\mathrm{r}}}$ of the rotor shaft & hub.

The matrix/vector notations for the periodic wind speed variations and for the mean wind

speed on the rotor hub along the rotating coordinate system $\vec{e}^{\,R_\mathrm{r}}$ are (see Eq. 3.65):

$$\begin{aligned}\delta\underline{u}^{R}_{\mathrm{obl}} &= {}^{R_\mathrm{r}}\bar{\Phi}^{R_\mathrm{s}}\cdot\left({}^{R_\mathrm{s}}\tilde{\Phi}^{R_\mathrm{h"}}-{}^{R_\mathrm{s}}\bar{\Phi}^{R_\mathrm{h"}}\right)\cdot\bar{\underline{u}}^{R_\mathrm{h"}} = \\ &\qquad \Phi_\mathrm{x}(\bar{\phi}_1^{R_\mathrm{r}})\cdot(\Phi_\mathrm{c}\cdot\bar{\underline{u}}^{R_\mathrm{h"}}\cdot\cos\bar{\Omega}t+\Phi_\mathrm{s}\cdot\bar{\underline{u}}^{R_\mathrm{h"}}\cdot\sin\bar{\Omega}t) \qquad \text{(B.168)}\\ \bar{\underline{u}}^{R} &= {}^{R_\mathrm{r}}\bar{\Phi}^{R_\mathrm{s}}\,.\,{}^{R_\mathrm{s}}\bar{\Phi}^{R_\mathrm{h"}}\cdot\bar{\underline{u}}^{R_\mathrm{h"}} = \Phi_\mathrm{x}(\bar{\phi}_1^{R_\mathrm{r}})\cdot\Phi_\mathrm{d}\cdot\bar{\underline{u}}^{R_\mathrm{h"}}\end{aligned}$$

The reactive wind speed variation on a blade element by orientation changes includes the fed-through rotor hub varation $\delta\underline{u}^{R}_{\mathrm{ori}}$. In additon, the *average* wind velocity $\bar{\underline{u}}^{R}$ on the rotor hub influences this 'orientation part': via the position variation $\delta\underline{\phi}^{X}$ of the blade rotaton dofs (last term in Eq. B.162). As a matter of fact, the periodic part $\delta\underline{u}^{R}_{\mathrm{obl}}$ does also! The full expression for the 'orientation part' by $\delta\underline{\phi}^{X}$ actually is:

$$\frac{\partial\underline{u}^{X_k}_{\mathrm{ori}}}{\partial\underline{\phi}^{X}}\cdot\delta\underline{\phi}^{X}=\left[\frac{\partial^{X_k^{\mathrm{cv}}}\Phi^{X_0}}{\partial\underline{\phi}^{X}}\cdot\left({}^{X_0}\bar{\Phi}^{R_\mathrm{r}}\cdot\bar{\underline{u}}^{R}+{}^{X_0}\bar{\Phi}^{R_\mathrm{r}}\cdot\delta\underline{u}^{R}_{\mathrm{obl}}\right)\right]\cdot\delta\underline{\phi}^{X} \qquad \text{(B.169)}$$

The contribution by the modulated varation of $\underline{\phi}^{X}$ is neglected for the same reason as is done for the the modulated varation of $\underline{\phi}^{R}$.

B.5.3 Mean, sensitivities and input variations for blade relative wind speed

We have to derive expressions for the mean values and sensitivity functions of the blade relative wind speed within the scope of the subcomponents X_f and X_p. For this, we (re)compose the overall reactive wind speed variation $\delta\underline{u}^{X_k}_{\mathrm{rea}}$ from the 'motion-partition' $\delta\underline{u}^{X_k}_{\mathrm{mot}}$ and 'orientation-partition' $\delta\underline{u}^{X_k}_{\mathrm{ori}}$ (eq. B.161 and B.162). We also take together all the terms that origin from the coordinate variations of the blade speed $\underline{v}^{X_k^\mathrm{a}}$ along $\vec{e}^{\,X_k}$ and the products of (variations) of transformation matrices. We then obtain:

$$\begin{aligned}\delta\underline{u}^{X_k}_{\mathrm{rea}} &= {}^{X_k^{\mathrm{cv}}}\bar{\Phi}^{W_m/X_k}\cdot\delta\underline{u}^{W_m}_{\mathrm{i_m}}-{}^{X_k^{\mathrm{cv}}}\bar{\Phi}^{X_k}\cdot\delta\underline{v}^{X_k^\mathrm{a}}+{}^{X_k^{\mathrm{cv}}}\bar{\Phi}^{X_0}\,.\,{}^{X_0}\bar{\Phi}^{R_\mathrm{r}}\cdot\delta\underline{u}^{R}_{\mathrm{ori}}+\\ &\left[\frac{\partial^{X_k^{\mathrm{cv}}}\bar{\Phi}^{W_m/X_k}}{\partial\underline{\phi}^{X}}\cdot\bar{\underline{u}}^{W_m}_{\mathrm{i_m}}\right]\cdot\delta\underline{\phi}^{X}-\left[\frac{\partial^{X_k^{\mathrm{cv}}}\bar{\Phi}^{X_k}}{\partial\underline{\phi}^{X}}\cdot\bar{\underline{v}}^{X_k^\mathrm{a}}\right]\cdot\delta\underline{\phi}^{X}+\left[\frac{\partial^{X_k^{\mathrm{cv}}}\Phi^{X_0}}{\partial\underline{\phi}^{X}}\cdot{}^{X_0}\bar{\Phi}^{R_\mathrm{r}}\cdot\bar{\underline{u}}^{R}\right]\cdot\delta\underline{\phi}^{X}\end{aligned} \qquad \text{(B.170)}$$

Matrix ${}^{X_k^{\mathrm{cv}}}\Phi^{W_m/X_k}$ transforms coordinates along the 'annulus wise coordinate system' $\vec{e}^{\,W_m/X_k}$, with x-axis perpendicular to the rotor plane ($//\vec{e}^{\,X_0}$ and z-axis pointing leadwise with 'induction lead angle offset' ζ_i as 'defined' in fig B.5), to coordinates along $\vec{e}^{\,X_k^{\mathrm{cv}}}$.

Although the element lead angle ζ will differ from the induction lead angle ζ_i, this difference is relatively small and both angles are very small in absolute sense. It then holds (see Eq. B.146):

$${}^{X_k^{\mathrm{cv}}}\Phi^{W_m/X_k}={}^{X_k^{\mathrm{cv}}}\Phi^{W_m/X_0}\,.\,{}^{X_0}\Phi^{W_m/X_k} = \Phi_\mathrm{x}(\zeta^{X_k})\cdot\Phi_\mathrm{z}(-\beta^{X_k})\cdot\Phi_\mathrm{x}^\mathrm{T}(\zeta_\mathrm{i}^{X_k}) \simeq \Phi_\mathrm{z}(-\beta^{X_k}) \qquad \text{(B.171)}$$

Now write the reactive variation in the relative wind speed as follows:

$$\delta\underline{u}^{X_k}_{\mathrm{rea}} = {}^{X_k^{\mathrm{cv}}}\bar{\Phi}^{W_m/X_k}\cdot\delta\underline{u}^{W_m}_{\mathrm{i_m}}-{}^{X_k^{\mathrm{cv}}}\bar{\Phi}^{X_k}\cdot\delta\underline{v}^{X_k^\mathrm{a}}+\sum_{i=1}^{k}\sum_{v=1}^{3}\frac{\partial\underline{u}^{X_k}_{\mathrm{rea"}}}{\partial\phi_v^{X_i}}\cdot\delta\phi_v^{X_i} \qquad \text{(B.172)}$$

We used the 'offset partial derivative' $\partial\underline{u}^{X_k}_{\mathrm{rea"}}/\partial\phi_v^{X_i}$ instead of the complete partial derivative $\partial\underline{u}^{X_k}_{\mathrm{rea}}/\partial\phi_v^{X_i}$. The latter also includes the dependency of the blade element's velocity variation $\delta\underline{v}^{X_k^\mathrm{a}}$ on the rotation dof positions:

$$\frac{\partial\underline{u}^{X_k}_{\mathrm{rea}}}{\partial\phi_v^{X_i}} = \frac{\partial\underline{u}^{X_k}_{\mathrm{rea"}}}{\partial\phi_v^{X_i}}+\left(-{}^{X_k^{\mathrm{cv}}}\bar{\Phi}^{X_k}\cdot\frac{\partial\underline{v}^{X_k^\mathrm{a}}}{\partial\phi_v^{X_i}}\right) \qquad \text{(B.173)}$$

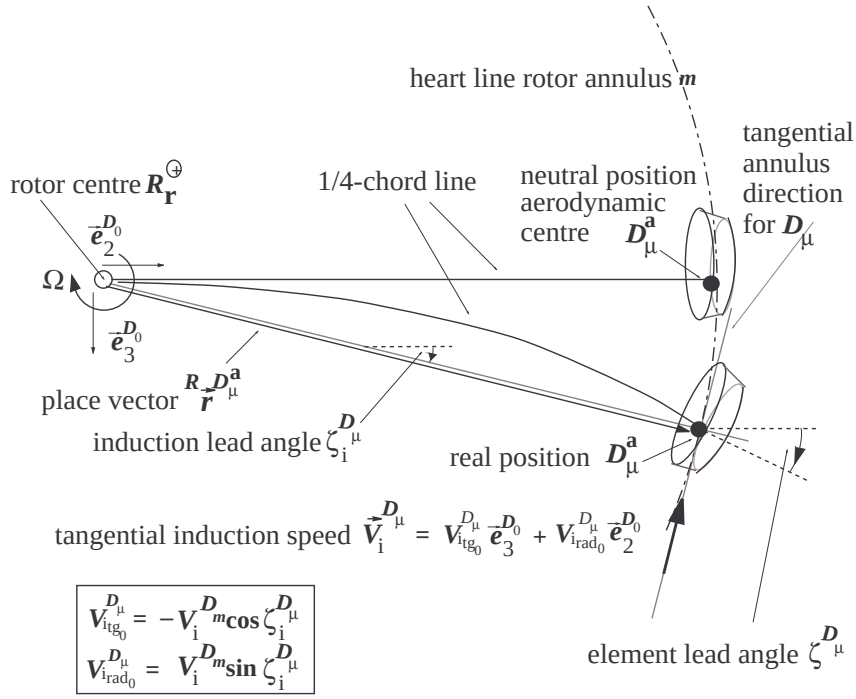

Figure B.5 *Leadwise orientation of blade element D_μ and tangential direction of cross section rotor annulus A_m with D_μ ($\vec{e}^{D_\mu}_{1,2,3} = \vec{e}^{D_\mu}_{x,y,z}$)*

Using a similar linear approximation as in Eq. B.147, the 'offset sensitivity' of the reactive wind speed varation to the rotation dof positions becomes (see Eq. B.144 for $\partial \beta^{X_k} / \partial \phi_v^{X_i}$ and $\partial \zeta^{X_k} / \partial \phi_v^{X_i}$):

$$\frac{\partial \underline{u}^{X_k}_{i_{rea}}}{\partial \phi_v^{X_i}} = \left[-\left.\frac{d\Phi_z}{d\phi}\right|_{-\bar{\beta}^{X_k}} \cdot \underline{\bar{u}}^{W_m}_{i_m} - \Phi_x|_{\bar{\zeta}^{X_k}} \cdot \left.\frac{d\Phi_z}{d\phi}\right|_{-\bar{\beta}^{X_k}} \cdot \left({}^{X_0}\bar{\Phi}^{R_r} \cdot \underline{\bar{u}}^{R} - {}^{X_0}\bar{\Phi}^{X_k} \cdot \underline{\bar{v}}^{X^a_k} \right) \right| \dots$$

$$\left.\frac{d\Phi_x}{d\phi}\right|_{\bar{\zeta}^{X_k}} \cdot \Phi_z|_{-\bar{\beta}^{X_k}} \cdot \left({}^{X_0}\bar{\Phi}^{R_r} \cdot \underline{\bar{u}}^{R} - {}^{X_0}\bar{\Phi}^{X_k} \cdot \underline{\bar{v}}^{X^a_k} \right) \Bigg] \cdot \begin{bmatrix} \frac{\partial \beta^{X_k}}{\partial \phi_v^{X_i}} \\ \frac{\partial \zeta^{X_k}}{\partial \phi_v^{X_i}} \end{bmatrix} - {}^{X^{cv}_k}\bar{\Phi}^{X_0} \cdot \frac{\partial {}^{X_0}\Phi^{X_k}}{\partial \phi_v^{X_i}} \cdot \underline{\bar{v}}^{X^a_k} \tag{B.174}$$

Equation B.170 tells that the reactive wind speed variation depends on the induction and blade element velocity and on the orientation change of the support structure and drive train via $\delta \underline{u}^{R_r}_{ori}$ and of the blade via $\delta \underline{\phi}^{X}$ (see Eq. B.167, B.165 and B.164 for $\delta \underline{u}^{R_r}_{ori}$).

We collect the annulus specific induction velocity coordinates in the overall coordinate vectors $\underline{u}^{W}_{i_m}$:

$$\underline{u}^{W}_{i_m} = \begin{bmatrix} \underline{u}^{W_1}_{i_m} \\ \vdots \\ \underline{u}^{W_P}_{i_m} \end{bmatrix} \tag{B.175}$$

For the induction velocity coordinates on element X_k then holds (O is 3×3 all-zero matrix; I is 3×3 identity matrix):

$$\underline{u}^{W_m/X_k}_{i_m} = [\; O_{(1)} \; \dots \; O_{(m(k)-1)} \; I \; O_{(m(k)+1)} \; \dots \; O_{(P)} \;] \cdot \underline{u}^{W}_{i_m} \tag{B.176}$$

As we assume the number of elements N an integer multiple of the number of rotor annuli

P, the dependency of annulus number m on element number k becomes:

$$m(k) = \text{ceil}\left(\tfrac{k}{N/P}\right) \qquad (\text{ceil}(x) \text{ yields smallest integer} \geq x) \tag{B.177}$$

The blade relative wind speed can be expressed as:

$$\underline{u}^{X_k} = \underline{\bar{u}}^{X_k} + \frac{\partial \underline{u}^{X_k}}{\partial \underline{u}^{X}_{\text{per}}} \cdot \underline{u}^{X}_{\text{per}} + \frac{\partial \underline{u}^{X_k}}{\partial \underline{u}^{W/X}_{\text{sto}}} \cdot \underline{u}^{W/X}_{\text{sto}} + \sum_{(\underline{z})} \frac{\partial \underline{u}^{X_k}}{\partial \underline{z}} \cdot \delta \underline{z} \tag{B.178}$$

in which the summation over $\underline{z}$ involves $\underline{v}^{X^{\oplus}_{\text{FF}}}$, $\underline{\omega}^{X_{\text{FF}}}$, $\underline{\phi}^{X_{\text{FF}}}$, $\underline{\phi}^{X}$, $\underline{\dot{\varphi}}^{X}$, $\underline{\dot{\varrho}}^{X}$, $\underline{u}^{W}_{\text{i}_{\text{m}}}$, and $\underline{u}^{R_{\text{r}}}_{\text{ori}}$ (see of Eq. B.120 and B.158).

The mean relative wind speed $\underline{\bar{u}}^{X_k}$ is expressed as follows in the average longitudinal wind speed, the blade element velocity and the induction speeds (use Eq. B.157 and B.164):

$$\underline{\bar{u}}^{X_k} = {}^{X^{\text{cv}}_k}\bar{\Phi}^{R_{\text{s}}} \cdot \Phi_{\text{d}} \cdot {}^{R_{\text{h}^{\text{u}}}}\underline{\bar{\Phi}}^{A}_{1} \cdot \bar{U} - {}^{X^{\text{cv}}_k}\bar{\Phi}^{X_k} \cdot \underline{\bar{v}}^{X^{\text{a}}_k} + {}^{X^{\text{cv}}_k}\bar{\Phi}^{W_m/X_k} \cdot \underline{\bar{u}}^{W_m/X_k}_{\text{i}} \tag{B.179}$$

The stochastic variation in equation B.159 actually is a function of the longitudinal turbulence ${}^{\text{t}}u^{W_m/X_k}$ in the intersection of the blade element with the related rotor annulus. This relationship is given in section 3.4.2. However, the blade model input is the turbulence in the rotating conversion coordinate systems of the blade elements so that: The periodic variation sensitivity of the blade relative wind speed then becomes:

$$\frac{\partial \underline{u}^{X_k}}{\partial \underline{u}^{W/X}_{\text{sto}}} = [\, \text{O}_{(1)} \ \ldots \ \text{O}_{(k-1)} \ \boldsymbol{I} \ \text{O}_{(k+1)} \ \ldots \ \text{O}_{(N)} \,] \tag{B.180}$$

The periodic variation is the blade element specific variation $\delta \underline{u}^{X_k}_{\text{per}}$ and is expressed in the

- modulated transverse and vertical components of the average wind velocity ($\delta u^{R_{\text{r}}}_{\text{obl}}$),
- longitudinal wind speed variation by shear and tower stagnation (${}^{\text{r}}u^{X^{\text{a}}_k}$)
- azimut-periodic axial induction speed varation by oblique inflow ($U^{X_k}_{\text{i}_{\text{obl}}}$)

This yields by combination eq. B.160 and B.168 (see eq. B.248 in section B.8.1 for $U^{X_k}_{\text{i}_{\text{obl}}}$):

$$\begin{aligned}\delta \underline{u}^{X_k}_{\text{per}} = {}& {}^{X^{\text{cv}}_k}\bar{\Phi}^{R_{\text{s}}} \cdot \Phi_{\text{d}} \cdot {}^{\text{r}}u^{X^{\text{a}}_k} + {}^{X^{\text{cv}}_k}\bar{\Phi}^{R_{\text{s}}} \cdot (\Phi_{\text{c}} \cos \bar{\boldsymbol{\Omega}} t + \Phi_{\text{s}} \sin \bar{\boldsymbol{\Omega}} t) \cdot \\ & ({}^{R_{\text{h}^{\text{u}}}}\underline{\bar{\Phi}}^{A}_{1} \cdot \bar{U} + {}^{\text{r}}u^{X^{\text{a}}_k}) - {}^{X^{\text{cv}}_k}\bar{\Phi}^{X_0} \cdot U^{X_k}_{\text{i}_{\text{obl}}} \cdot \underline{e}_1\end{aligned} \tag{B.181}$$

The expression for the blade relative wind speed involves the periodic variation sensitivity to the *overall* periodic wind speed coordinate vector $\underline{u}^{X}_{\text{per}}$ for blade X, which is composed as:

$$\underline{u}^{X}_{\text{per}} = \begin{bmatrix} \underline{u}^{X_1}_{\text{per}} \\ \vdots \\ \underline{u}^{X_N}_{\text{per}} \end{bmatrix} \tag{B.182}$$

The periodic variation sensitivity of the blade relative wind speed then becomes:

$$\frac{\partial \underline{u}^{X_k}}{\partial \underline{u}^{X}_{\text{per}}} = [\, \text{O}_{(1)} \ \ldots \ \text{O}_{(k-1)} \ \boldsymbol{I} \ \text{O}_{(k+1)} \ \ldots \ \text{O}_{(N)} \,] \tag{B.183}$$

For the sensitivities to the outputs of the final element of the foregoing subcomponent hold (see Eq. B.124 for $\partial \underline{v}^{X_k^{\mathrm{a}}} / \partial \underline{v}^{X_{\mathrm{FF}}^{\oplus}}$ and $\partial \underline{v}^{X_k^{\mathrm{a}}} / \partial \underline{\omega}^{X_{\mathrm{FF}}}$, and Eq. B.174 for $\partial \underline{u}_{\mathrm{rea"}}^{X_k} / \partial \phi_v^{X_i}$):

$$\begin{aligned}
\frac{\partial \underline{u}^{X_k}}{\partial \underline{v}^{X_{\mathrm{FF}}^{\oplus}}} &= -{}^{X_k^{\mathrm{cv}}}\bar{\Phi}^{X_k} \cdot \frac{\partial \underline{v}^{X_k^{\mathrm{a}}}}{\partial \underline{v}^{X_{\mathrm{FF}}^{\oplus}}} \\
\frac{\partial \underline{u}^{X_k}}{\partial \underline{\omega}^{X_{\mathrm{FF}}}} &= -{}^{X_k^{\mathrm{cv}}}\bar{\Phi}^{X_k} \cdot \frac{\partial \underline{v}^{X_k^{\mathrm{a}}}}{\partial \underline{\omega}^{X_{\mathrm{FF}}^{\oplus}}} \\
\frac{\partial \underline{u}^{X_k}}{\partial \underline{\phi}^{X_{\mathrm{FF}}}} &= \begin{cases} \text{<does not exist>} & \text{for k=1} \\ \mathrm{J}^3_{v=1}\left(\partial \underline{u}_{\mathrm{rea"}}^{X_k} / \partial \phi_v^{X_1}\right) & \text{for k=2...N} \end{cases}
\end{aligned} \tag{B.184}$$

For the sensitivities to the degrees of freedom in the concerning subcomponent hold (see Eq. B.174 for $\partial \underline{u}_{\mathrm{rea"}}^{X_k} / \partial \phi_v^{X_i}$ and Eq. B.129 for $\partial \underline{v}^{X_k^{\mathrm{a}}} / \partial \underline{\phi}^{X}$, and Eq. B.127 for $\partial \underline{v}^{X_k^{\mathrm{a}}} / \partial \dot{\underline{\varphi}}^{X}$ and $\partial \underline{v}^{X_k^{\mathrm{a}}} / \partial \dot{\underline{\varrho}}^{X}$):

$$\begin{aligned}
\frac{\partial \underline{u}^{X_k}}{\partial \underline{\phi}^{X}} &= -{}^{X_k^{\mathrm{cv}}}\bar{\Phi}^{X_k} \cdot \frac{\partial \underline{v}^{X_k^{\mathrm{a}}}}{\partial \underline{\phi}^{X}} + \begin{cases} \left[\mathrm{J}^3_{v=1}\left(\frac{\partial \underline{u}_{\mathrm{rea"}}^{X_1}}{\partial \phi_v^{X_1}}\right) \;\; \mathrm{O}_{(2)} \ldots \mathrm{O}_{(N)} \right] & \text{for k=1} \\ \left[\mathrm{O}_{(1)} \;\; \mathrm{J}^k_{i=2}\Big(\mathrm{J}^3_{v=1}\left(\frac{\partial \underline{u}_{\mathrm{rea"}}^{X_k}}{\partial \phi_v^{X_i}}\right)\Big) \;\; \mathrm{O}_{(k+1)} \ldots \mathrm{O}_{(N)} \right] & \text{for k=2...N} \end{cases} \\
\frac{\partial \underline{u}^{X_k}}{\partial \dot{\underline{\varphi}}^{X}} &= -{}^{X_k^{\mathrm{cv}}}\bar{\Phi}^{X_k} \cdot \frac{\partial \underline{v}^{X_k^{\mathrm{a}}}}{\partial \dot{\underline{\varphi}}^{X}} \\
\frac{\partial \underline{u}^{X_k}}{\partial \dot{\underline{\varrho}}^{X}} &= -{}^{X_k^{\mathrm{cv}}}\bar{\Phi}^{X_k} \cdot \frac{\partial \underline{v}^{X_k^{\mathrm{a}}}}{\partial \dot{\underline{\varrho}}^{X}}
\end{aligned} \tag{B.185}$$

For the sensitivities to the induction velocity varation and the orientation change of support structure and drive-train hold (see Eq. B.170, B.171, B.176 and B.146):

$$\begin{aligned}
\frac{\partial \underline{u}^{X_k}}{\partial \underline{u}_{\mathrm{im}}^{W}} &\simeq \left[\mathrm{O}_{(1)} \;\; \ldots \;\; \mathrm{O}_{(m(k)-1)} \;\; \Phi_{\mathrm{z}}(-\bar{\beta}^{X_k}) \;\; \mathrm{O}_{(m(k)+1)} \;\; \ldots \;\; \mathrm{O}_{(P)} \right] \\
\frac{\partial \underline{u}^{X_k}}{\partial \underline{u}_{\mathrm{ori}}^{R_{\mathrm{r}}}} &= {}^{X_k^{\mathrm{cv}}}\bar{\Phi}^{X_0} \cdot \Phi_{\mathrm{x}}\left({}^{R_{\mathrm{r}}}\psi^{X_0}\right)
\end{aligned} \tag{B.186}$$

B.6 Inflow angle and angle of attack

General expressions for the inflow angle and angle of attack for a rotor blade X are derived in subsection B.6.1. Means, sensitivity functions and input variations for the angle of attack on the blade flange X_{p} and blade structure & profile X_{f} are listed in section B.6.2.

B.6.1 General expressions inflow angle and angle of attack

The inflow angle $\phi_{\mathrm{inf}}^{X_k}$ equals the arctangent of the normal and leadwise blade-relative wind speed components U_{n} and U_{ℓ}; the latter are the *first* and *minus third* coordinates of the blade-relative wind speed coordinate vector $\underline{u}^{X_k}$. For the inflow angle and the linearised approximation of its variation holds:

$$\begin{aligned}
\phi_{\mathrm{inf}}^{X_k} &= \arctan \frac{U_{\mathrm{n}}^{X_k}}{U_{\ell}^{X_k}} \\
\delta\phi_{\mathrm{inf}}^{X_k} &= \frac{1}{1+(\bar{U}_{\mathrm{n}}^{X_k}/\bar{U}_{\ell}^{X_k})^2} \cdot \left(\frac{\delta U_{\mathrm{n}}^{X_k}}{\bar{U}_{\ell}^{X_k}} - \frac{\bar{U}_{\mathrm{n}}^{X_k} \cdot \delta U_{\ell}^{X_k}}{(\bar{U}_{\ell}^{X_k})^2} \right) \\
&= \frac{(\bar{\underline{u}}^{X_k})^{\mathrm{T}}}{||\bar{\underline{u}}^{X_k}||^2} \cdot \mathrm{P}_{\phi_{\mathrm{inf}}} \cdot \delta \underline{u}^{X_k} \qquad \text{with} \quad \mathrm{P}_{\phi_{\mathrm{inf}}} = \begin{pmatrix} 0 & 0 & 1 \\ 0 & 0 & 0 \\ -1 & 0 & 0 \end{pmatrix}
\end{aligned} \tag{B.187}$$

The angle of attack $\phi_{\mathrm{a}_{\frac{3}{4}_c}}^{X_k}$ ($\equiv$ $\phi_{\mathrm{a}"}^{X_k}$) on the 3/4 chord position equals the difference between the inflow angle and the setting angle, augmented with a correction term for the cone-angle:

$$\phi_{\mathrm{a}"}^{X_k} = \phi_{\mathrm{inf}}^{X_k} - \phi_{\mathrm{set}}^{X_k} + \frac{1/2\, c^{X_k}}{r^{W_m/X_k}} \cdot \sin\beta^{X_k} \tag{B.188}$$

The previous section yielded expressions for the linearised variation of the element setting angle and cone-angle. Together with the expression above for the variation in the inflow angle, the variation of the angle of attack can then be expressed as:

$$\delta\phi_{\mathrm{a}"}^{X_k} = \frac{(\underline{\bar{u}}^{X_k})^{\mathrm{T}}}{||\underline{\bar{u}}^{X_k}||^2} \cdot \mathrm{P}_{\phi_{\mathrm{inf}}} \cdot \delta\underline{u}^{X_k} + \sum_{i=1}^{k}\sum_{v=1}^{3}\left(-\frac{\partial\phi_{\mathrm{set}}^{X_k}}{\partial\phi_v^{X_i}} + \frac{1/2\, c^{X_k}}{r^{W_m/X_k}} \cdot \cos\bar{\beta}^{X_k} \cdot \frac{\partial\beta^{X_k}}{\partial\phi_v^{X_i}} \right) \cdot \delta\underline{\phi}_v^{X_i} \tag{B.189}$$

Make an explicit definition for the (intermediate) sensitivity function to the blade relative wind speed:

$$\frac{\partial\phi_{\mathrm{a}"}^{X_k}}{\partial\underline{u}^{X_k}} = \frac{(\underline{\bar{u}}^{X_k})^{\mathrm{T}}}{||\underline{\bar{u}}^{X_k}||^2} \cdot \begin{pmatrix} 0 & 0 & 1 \\ 0 & 0 & 0 \\ -1 & 0 & 0 \end{pmatrix} \tag{B.190}$$

B.6.2 Means, sensitivities and input variations for angle of attack

The following linearised expression holds for the angle of attack on the 3/4-chord position of a blade element X_k:

$$\phi_{\mathrm{a}"}^{X_k} = \bar{\phi}_{\mathrm{a}"}^{X_k} + \frac{\partial\phi_{\mathrm{a}"}^{X_k}}{\partial\underline{u}_{\mathrm{per}}^{X}} \cdot \delta\underline{u}_{\mathrm{per}}^{X} + \frac{\partial\phi_{\mathrm{a}"}^{X_k}}{\partial^{\mathrm{t}}\underline{u}^{W/X}} \cdot {}^{\mathrm{t}}\underline{u}^{W/X} + \sum_{(\underline{z})} \frac{\partial\phi_{\mathrm{a}"}^{X_k}}{\partial\underline{z}} \cdot \delta\underline{z} \tag{B.191}$$

in which the summation over $\underline{z}$ involves $\underline{v}^{X_{\mathrm{FF}}^{\oplus}}$, $\underline{\omega}^{X_{\mathrm{FF}}}$, $\underline{\phi}^{X_{\mathrm{FF}}}$, $\underline{\phi}^{X}$, $\underline{\dot{\varphi}}^{X}$, $\underline{\dot{\varrho}}^{X}$, $\underline{u}_{\mathrm{i_m}}^{W}$, and $\underline{u}_{\mathrm{ori}}^{R_{\mathrm{r}}}$ (see Eq. B.178 for $\underline{u}^{X_k}$ and eq. B.150 for β^{X_k} and $\phi_{\mathrm{set}}^{X_k}$).

The expression for the mean value is (see Eq. B.179 for $\bar{\underline{u}}^{X_k}$ and Eq. B.151 for $\bar{\phi}_{\mathrm{set}}^{X_k}$ and $\bar{\beta}^{X_k}$):

$$\bar{\phi}_{\mathrm{a}"}^{X_k} = \arctan\left(\frac{\bar{u}_1^{X_k}}{-\bar{u}_3^{X_k}}\right) - \bar{\phi}_{\mathrm{set}}^{X_k} + \frac{1/2\, c^{X_k}}{\bar{r}^{W_m}} \cdot \sin\bar{\beta}^{X_k} \tag{B.192}$$

For the stochastic and periodic input variation sensitivity holds (see B.180 and B.183):

$$\frac{\partial\phi_{\mathrm{a}"}^{X_k}}{\partial\underline{u}_{\mathrm{per}}^{X}} = \frac{\partial\phi_{\mathrm{a}"}^{X_k}}{\partial\underline{u}^{X_k}} \cdot \frac{\partial\underline{u}^{X_k}}{\partial\underline{u}_{\mathrm{per}}^{X}} \quad \text{and} \quad \frac{\partial\phi_{\mathrm{a}"}^{X_k}}{\partial^{\mathrm{t}}\underline{u}^{W/X}} = \frac{\partial\phi_{\mathrm{a}"}^{X_k}}{\partial\underline{u}^{X_k}} \cdot \frac{\partial\underline{u}^{X_k}}{\partial\underline{u}_{\mathrm{sto}}^{W/X}} \tag{B.193}$$

For the reactive sensitivities holds (see Eq. B.184, B.185 for the partial deriviatives of the blade relative wind speed $\underline{u}^{X_k}$):

$$\begin{aligned}
\frac{\partial\phi_{\mathrm{a}"}^{X_k}}{\partial\underline{v}^{X_{\mathrm{FF}}^{\oplus}}} &= \frac{\partial\phi_{\mathrm{a}"}^{X_k}}{\partial\underline{u}^{X_k}} \cdot \frac{\partial\underline{u}^{X_k}}{\partial\underline{v}^{X_{\mathrm{FF}}^{\oplus}}} \quad ; \quad \frac{\partial\phi_{\mathrm{a}"}^{X_k}}{\partial\underline{\omega}^{X_{\mathrm{FF}}}} = \frac{\partial\phi_{\mathrm{a}"}^{X_k}}{\partial\underline{u}^{X_k}} \cdot \frac{\partial\underline{u}^{X_k}}{\partial\underline{\omega}^{X_{\mathrm{FF}}}} \\
\frac{\partial\phi_{\mathrm{a}"}^{X_k}}{\partial\underline{\dot{\varphi}}^{X}} &= \frac{\partial\phi_{\mathrm{a}"}^{X_k}}{\partial\underline{u}^{X_k}} \cdot \frac{\partial\underline{u}^{X_k}}{\partial\underline{\dot{\varphi}}^{X}} \quad ; \quad \frac{\partial\phi_{\mathrm{a}"}^{X_k}}{\partial\underline{\dot{\varrho}}^{X}} = \frac{\partial\phi_{\mathrm{a}"}^{X_k}}{\partial\underline{u}^{X_k}} \cdot \frac{\partial\underline{u}^{X_k}}{\partial\underline{\dot{\varrho}}^{X}} \\
\frac{\partial\phi_{\mathrm{a}"}^{X_k}}{\partial\underline{u}_{\mathrm{i_m}}^{W}} &= \frac{\partial\phi_{\mathrm{a}"}^{X_k}}{\partial\underline{u}^{X_k}} \cdot \frac{\partial\underline{u}^{X_k}}{\partial\underline{u}_{\mathrm{i_m}}^{W}} \quad ; \quad \frac{\partial\phi_{\mathrm{a}"}^{X_k}}{\partial\underline{u}_{\mathrm{ori}}^{R_{\mathrm{r}}}} = \frac{\partial\phi_{\mathrm{a}"}^{X_k}}{\partial\underline{u}^{X_k}} \cdot \frac{\partial\underline{u}^{X_k}}{\partial\underline{u}_{\mathrm{ori}}^{R_{\mathrm{r}}}}
\end{aligned} \tag{B.194}$$

and (see Eq. B.152, B.154 for the partial deriviatives of $\phi_{\mathrm{set}}^{X_k}$ and β^{X_k}):

$$\begin{aligned}
\frac{\partial\phi_{\mathrm{a}"}^{X_k}}{\partial\underline{\phi}^{X_{\mathrm{FF}}}} &= \frac{\partial\phi_{\mathrm{a}"}^{X_k}}{\partial\underline{u}^{X_k}} \cdot \frac{\partial\underline{u}^{X_k}}{\partial\underline{\phi}^{X_{\mathrm{FF}}}} - \frac{\partial\phi_{\mathrm{set}}^{X_k}}{\partial\underline{\phi}^{X_{\mathrm{FF}}}} + \frac{1/2\, c^{X_k \cdot \cos\bar{\beta}^{X_k}}}{\bar{r}^{W_m}} \cdot \frac{\partial\beta^{X_k}}{\partial\underline{\phi}^{X_{\mathrm{FF}}}} \\
\frac{\partial\phi_{\mathrm{a}"}^{X_k}}{\partial\underline{\phi}^{X}} &= \frac{\partial\phi_{\mathrm{a}"}^{X_k}}{\partial\underline{u}^{X_k}} \cdot \frac{\partial\underline{u}^{X_k}}{\partial\underline{\phi}^{X}} - \frac{\partial\phi_{\mathrm{set}}^{X_k}}{\partial\underline{\phi}^{X}} + \frac{1/2\, c^{X_k \cdot \cos\bar{\beta}^{X_k}}}{\bar{r}^{W_m}} \cdot \frac{\partial\beta^{X_k}}{\partial\underline{\phi}^{X}}
\end{aligned} \tag{B.195}$$

B.7 Aerodynamic loads

This section gives the implemented expressions for the mean, sensitivities and input variations for concentrated forces and torques that are caused by the distributed aerodynamic lift, drag and moment loading.

The general expressions for the distributed aerodynamic loads on the blades and the mapping mechanism to concentrated loads were given in paragraph (i) and (ii) of section 3.6.3. The expressions for the mean values, sensitivities and variations by stochastic and periodic inputs are listed in section B.7.1. The concentrated loads on a subcomponent appear also to depend on distributed loading on a *neighbouring* subcomponent. Section B.7.2 gives the means, sensitivities and input variations for these distributed 'export loads from neighbouring subcomponents'. Eventually, section B.7.3 lists the expressions for the means, sensitivities and input variations of the pursued concentrated aerodynamic loads. In addition, section B.7.4 tives the means, sensitivities and input variations for the closely related reaction force loads on the rotor annuli.

B.7.1 Mean, sensitivities and input variations for distributed loads

The linearised expressions for the distributed aerodynamic loads follow straigthforward from the expressions for the blade relative windspeed in section B.5.3 and for the angle of attack in section B.6.2. The overall expressions are:

$$\begin{aligned}
{}^{\mathrm{a}}\underline{q}_{\mathrm{f}}^{X_k^{\mathrm{cv}}} &= {}^{\mathrm{a}}\overline{\underline{q}}_{\mathrm{f}}^{X_k^{\mathrm{cv}}} + \frac{\partial \underline{q}_{\mathrm{f}}^{X_k}}{\partial {}^{\mathrm{t}}\underline{u}^{W/X}} \cdot {}^{\mathrm{t}}\underline{u}^{W/X} + \frac{\partial {}^{\mathrm{a}}\underline{q}_{\mathrm{f}}^{X_k^{\mathrm{cv}}}}{\partial \underline{u}_{\mathrm{per}}^{X}} \cdot \delta\underline{u}_{\mathrm{per}}^{X} + \sum_{(\underline{z})} \frac{\partial {}^{\mathrm{a}}\underline{q}_{\mathrm{f}}^{X_k^{\mathrm{cv}}}}{\partial \underline{z}} \cdot \delta\underline{z} \\
{}^{\mathrm{a}}\underline{q}_{\mathrm{t}}^{X_k^{\mathrm{cv}}} &= {}^{\mathrm{a}}\overline{\underline{q}}_{\mathrm{t}}^{X_k^{\mathrm{cv}}} + \frac{\partial \underline{q}_{\mathrm{f}}^{X_k}}{\partial \underline{u}_{\mathrm{sto}}^{W/X}} \cdot \underline{u}_{\mathrm{sto}}^{W/X} + \frac{\partial {}^{\mathrm{a}}\underline{q}_{\mathrm{t}}^{X_k^{\mathrm{cv}}}}{\partial \underline{u}_{\mathrm{per}}^{X}} \cdot \delta\underline{u}_{\mathrm{per}}^{X} + \sum_{(\underline{z})} \frac{\partial {}^{\mathrm{a}}\underline{q}_{\mathrm{t}}^{X_k^{\mathrm{cv}}}}{\partial \underline{z}} \cdot \delta\underline{z}
\end{aligned} \tag{B.196}$$

in which the summation over $\underline{z}$ involves $\underline{v}^{X_{\mathrm{FF}}^{\oplus}}$, $\underline{\omega}^{X_{\mathrm{FF}}}$, $\underline{\phi}^{X_{\mathrm{FF}}}$, $\underline{\phi}^{X}$, $\dot{\underline{\varphi}}^{X}$, $\dot{\underline{\varrho}}^{X}$, $\underline{u}_{\mathrm{im}}^{W}$, and $\underline{u}_{\mathrm{ori}}^{R_{\mathrm{r}}}$.

For the mean values hold (see Eq. B.179, B.192 for $\bar{\underline{u}}^{X_k}$ and $\bar{\phi}_{\mathrm{a''}}^{X_k}$):

$$\begin{aligned}
{}^{\mathrm{a}}\overline{\underline{q}}_{\mathrm{f}}^{X_k^{\mathrm{cv}}} &= \tfrac{1}{2}\rho c^{X_k} \cdot ||\bar{\underline{u}}^{X_k}|| \cdot \boldsymbol{C}_{\mathrm{LD}}^{X_k}(\bar{\phi}_{\mathrm{a''}}^{X_k}) \cdot \bar{\underline{u}}^{X_k} \\
{}^{\mathrm{a}}\overline{\underline{q}}_{\mathrm{t}}^{X_k^{\mathrm{cv}}} &= \tfrac{1}{2}\rho (c^{X_k})^2 \cdot ||\bar{\underline{u}}^{X_k}||^2 \cdot \underline{\boldsymbol{C}}_{\mathrm{M}}^{X_k}(\bar{\phi}_{\mathrm{a''}}^{X_k}) \\
&\text{with } ||\bar{\underline{u}}^{X_k}|| = \sqrt{(\bar{u}_1^{X_k})^2 + (\bar{u}_3^{X_k})^2}
\end{aligned} \tag{B.197}$$

For the periodic variation sensitivities hold (see B.181, B.183):

$$\begin{aligned}
\frac{\partial {}^{\mathrm{a}}\underline{q}_{\mathrm{f}}^{X_k^{\mathrm{cv}}}}{\partial \underline{u}_{\mathrm{per}}^{X_k}} &= \Big(\frac{\partial {}^{\mathrm{a}}\underline{q}_{\mathrm{f}}^{X_k^{\mathrm{cv}}}}{\partial \underline{u}^{X_k}} + \frac{\partial {}^{\mathrm{a}}\underline{q}_{\mathrm{f}}^{X_k^{\mathrm{cv}}}}{\partial \phi_{\mathrm{a''}}^{X_k}} \cdot \frac{\partial \phi_{\mathrm{a''}}^{X_k}}{\partial \underline{u}^{X_k}}\Big) \cdot \frac{\partial \underline{u}^{X_k}}{\partial \underline{u}_{\mathrm{per}}^{X_k}} \\
\frac{\partial {}^{\mathrm{a}}\underline{q}_{\mathrm{t}}^{X_k^{\mathrm{cv}}}}{\partial \underline{u}_{\mathrm{per}}^{X_k}} &= \Big(\frac{\partial {}^{\mathrm{a}}\underline{q}_{\mathrm{t}}^{X_k^{\mathrm{cv}}}}{\partial \underline{u}^{X_k}} + \frac{\partial {}^{\mathrm{a}}\underline{q}_{\mathrm{t}}^{X_k^{\mathrm{cv}}}}{\partial \phi_{\mathrm{a''}}^{X_k}} \cdot \frac{\partial \phi_{\mathrm{a''}}^{X_k}}{\partial \underline{u}^{X_k}}\Big) \cdot \frac{\partial \underline{u}^{X_k}}{\partial \underline{u}_{\mathrm{per}}^{X_k}}
\end{aligned} \tag{B.198}$$

For the stochastic variation sensitivities holds (see Eq. B.193):

$$\begin{aligned}
\frac{\partial \underline{q}_{\mathrm{f}}^{X_k}}{\partial \underline{u}_{\mathrm{sto}}^{W/X}} &= \Big(\frac{\partial {}^{\mathrm{a}}\underline{q}_{\mathrm{f}}^{X_k^{\mathrm{cv}}}}{\partial \underline{u}^{X_k}} + \frac{\partial {}^{\mathrm{a}}\underline{q}_{\mathrm{f}}^{X_k^{\mathrm{cv}}}}{\partial \phi_{\mathrm{a''}}^{X_k}} \cdot \frac{\partial \phi_{\mathrm{a''}}^{X_k}}{\partial \underline{u}^{X_k}}\Big) \cdot \frac{\partial \underline{u}^{X_k}}{\partial \underline{u}_{\mathrm{sto}}^{W/X}} \\
\frac{\partial \underline{q}_{\mathrm{t}}^{X_k}}{\partial \underline{u}_{\mathrm{sto}}^{W/X}} &= \Big(\frac{\partial {}^{\mathrm{a}}\underline{q}_{\mathrm{t}}^{X_k^{\mathrm{cv}}}}{\partial \underline{u}^{X_k}} + \frac{\partial {}^{\mathrm{a}}\underline{q}_{\mathrm{t}}^{X_k^{\mathrm{cv}}}}{\partial \phi_{\mathrm{a''}}^{X_k}} \cdot \frac{\partial \phi_{\mathrm{a''}}^{X_k}}{\partial \underline{u}^{X_k}}\Big) \cdot \frac{\partial \underline{u}^{X_k}}{\partial \underline{u}_{\mathrm{sto}}^{W/X}}
\end{aligned} \tag{B.199}$$

For the sensitivity to the rotation dof positions of the actual subcomponent holds (use Eq. B.195 and see Eq. B.184, B.185, B.152, B.154 for the partial deriviatives of $\underline{u}^{X_k}$, $\phi_{\mathrm{set}}^{X_k}$

and β^{X_k}):

$$\begin{aligned}
\frac{\partial^{\mathrm{a}} \underline{q}_{\mathrm{f}}^{X_k^{\mathrm{cv}}}}{\partial \underline{\phi}^{X}} &= \Big(\frac{\partial^{\mathrm{a}} \underline{q}_{\mathrm{f}}^{X_k^{\mathrm{cv}}}}{\partial \underline{u}^{X_k}} + \frac{\partial^{\mathrm{a}} \underline{q}_{\mathrm{f}}^{X_k^{\mathrm{cv}}}}{\partial \phi_{\mathrm{a}''}^{X_k}} \cdot \frac{\partial \phi_{\mathrm{a}''}^{X_k}}{\partial \underline{u}^{X_k}}\Big) \cdot \frac{\partial \underline{u}^{X_k}}{\partial \underline{\phi}^{X}} + \frac{\partial^{\mathrm{a}} \underline{q}_{\mathrm{f}}^{X_k^{\mathrm{cv}}}}{\partial \phi_{\mathrm{a}''}^{X_k}} \cdot \Big(\frac{\frac{1}{2}\, c^{X_k} \cdot \cos \bar{\beta}^{X_k}}{\bar{r}^{W_m}} \cdot \frac{\partial \beta^{X_k}}{\partial \underline{\phi}^{X}} - \frac{\partial \phi_{\mathrm{set}}^{X_k}}{\partial \underline{\phi}^{X}}\Big) \\
\frac{\partial^{\mathrm{a}} \underline{q}_{\mathrm{t}}^{X_k^{\mathrm{cv}}}}{\partial \underline{\phi}^{X}} &= \Big(\frac{\partial^{\mathrm{a}} \underline{q}_{\mathrm{t}}^{X_k^{\mathrm{cv}}}}{\partial \underline{u}^{X_k}} + \frac{\partial^{\mathrm{a}} \underline{q}_{\mathrm{t}}^{X_k^{\mathrm{cv}}}}{\partial \phi_{\mathrm{a}''}^{X_k}} \cdot \frac{\partial \phi_{\mathrm{a}''}^{X_k}}{\partial \underline{u}^{X_k}}\Big) \cdot \frac{\partial \underline{u}^{X_k}}{\partial \underline{\phi}^{X}} + \frac{\partial^{\mathrm{a}} \underline{q}_{\mathrm{t}}^{X_k^{\mathrm{cv}}}}{\partial \phi_{\mathrm{a}''}^{X_k}} \cdot \Big(\frac{\frac{1}{2}\, c^{X_k} \cdot \cos \bar{\beta}^{X_k}}{\bar{r}^{W_m}} \cdot \frac{\partial \beta^{X_k}}{\partial \underline{\phi}^{X}} - \frac{\partial \phi_{\mathrm{set}}^{X_k}}{\partial \underline{\phi}^{X}}\Big)
\end{aligned} \tag{B.200}$$

The same expression holds for the sensitivity to the rotation dof positions of the foregoing subcomponent $\underline{\phi}^{X_{\mathrm{FF}}}$.

For the remaining sensitivities hold ($\underline{z} = \underline{v}^{X_{\mathrm{FF}}^{\oplus}}, \underline{\omega}^{X_{\mathrm{FF}}^{\oplus}}, \dot{\underline{\varphi}}^{X}, \dot{\underline{\varrho}}^{X}, \underline{u}_{\mathrm{im}}^{W}, \underline{u}_{\mathrm{ori}}^{R}$; use Eq. B.194 and see Eq. 3.47, B.184, B.185, B.186):

$$\begin{aligned}
\frac{\partial^{\mathrm{a}} \underline{q}_{\mathrm{f}}^{X_k^{\mathrm{cv}}}}{\partial \underline{z}} &= \Big(\frac{\partial^{\mathrm{a}} \underline{q}_{\mathrm{f}}^{X_k^{\mathrm{cv}}}}{\partial \underline{u}^{X_k}} + \frac{\partial^{\mathrm{a}} \underline{q}_{\mathrm{f}}^{X_k^{\mathrm{cv}}}}{\partial \phi_{\mathrm{a}''}^{X_k}} \cdot \frac{\partial \phi_{\mathrm{a}''}^{X_k}}{\partial \underline{u}^{X_k}}\Big) \cdot \frac{\partial \underline{u}^{X_k}}{\partial \underline{z}} \\
\frac{\partial^{\mathrm{a}} \underline{q}_{\mathrm{t}}^{X_k^{\mathrm{cv}}}}{\partial \underline{z}} &= \Big(\frac{\partial^{\mathrm{a}} \underline{q}_{\mathrm{t}}^{X_k^{\mathrm{cv}}}}{\partial \underline{u}^{X_k}} + \frac{\partial^{\mathrm{a}} \underline{q}_{\mathrm{t}}^{X_k^{\mathrm{cv}}}}{\partial \phi_{\mathrm{a}''}^{X_k}} \cdot \frac{\partial \phi_{\mathrm{a}''}^{X_k}}{\partial \underline{u}^{X_k}}\Big) \cdot \frac{\partial \underline{u}^{X_k}}{\partial \underline{z}}
\end{aligned} \tag{B.201}$$

B.7.2 Mean, sensitivities and variations for distributed 'export' loads

Consider the subcomponent with ranking number n, with elements $X_{k_1(n)}$ up to and including $X_{k_{\mathrm{L}}(n)}$. The concentrated aerodynamic loads on the last element of the foregoing subcomponent, with ranking number $n-1$, depends on the distributed force load on $X_{k_1(n)}$. In a similar way, the concentrated loads on the first element of the subsequent subcomponent (no. $n+1$) depends on the distribued load on $X_{k_{\mathrm{L}}(n)}$.

So, in general, a subcomponent n has to export the distributed loads on its first and last element $k_1(n)$ and $k_{\mathrm{L}}(n)$ and to import the distributed loads on the last element $k_{\mathrm{L}}(n-1)$ of the foregoing subcomponent and on the first element $k_1(n+1)$ of the subsequent subcomponent. The used notations are:

- ${}^{\mathrm{a}}\underline{q}_{\mathrm{f}}^{X_{\mathrm{PP}(n)}^{\ominus}}$ and ${}^{\mathrm{a}}\underline{q}_{\mathrm{f}}^{X_{\mathrm{FF}(n)}}$ for export loads from $k_1(n)$ and $k_{\mathrm{L}}(n)$
- ${}^{\mathrm{a}}\underline{q}_{\mathrm{f}}^{X_{\mathrm{FF}(n-1)}}$ and ${}^{\mathrm{a}}\underline{q}_{\mathrm{f}}^{X_{\mathrm{PP}(n+1)}^{\ominus}}$ for import loads from $k_{\mathrm{L}}(n-1)$ and $k_1(n+1)$.

The mnemonics FF and PP stand for 'Final Foregoing' and 'Primary Post' (see discussion in section 3.6.3 above Eq. 3.52).

The rotor blades are subdivided into only two subcomponents: no. 1, the blade flange X_{f} and no. 2, the blade structure & profile X_{p}, so that:

- flange X_{f} only imports ${}^{\mathrm{a}}\underline{q}_{\mathrm{f}}^{X_{\mathrm{PP}(2)}^{\ominus}}$ from structure & profile X_{p};
- structure & profile X_{p} only imports ${}^{\mathrm{a}}\underline{q}_{\mathrm{f}}^{X_{\mathrm{FF}(1)}^{\ominus}}$ from flange X_{f}.

As already mentioned in section 3.6.3, the both export loads are expressed in coordinates along the conversion coordinate systems, so it simply holds:

$$\begin{aligned}
{}^{\mathrm{a}}\underline{q}_{\mathrm{f}}^{X_{\mathrm{PP}(n)}^{\ominus}} &\triangleq {}^{\mathrm{a}}\underline{q}_{\mathrm{f}}^{X_{k_1(n)}^{\mathrm{cv}}} \\
{}^{\mathrm{a}}\underline{q}_{\mathrm{f}}^{X_{\mathrm{FF}(n)}} &\triangleq {}^{\mathrm{a}}\underline{q}_{\mathrm{f}}^{X_{k_{\mathrm{L}}(n)}^{\mathrm{cv}}}
\end{aligned} \tag{B.202}$$

The linearised expression for both export loads is:

$$
\begin{aligned}
{}^{\mathrm{a}}\underline{q}_{\mathrm{f}}^{\,X_{\mathrm{PP}}} &= {}^{\mathrm{a}}\overline{\underline{q}}_{\mathrm{f}}^{\,X_{\mathrm{PP}}} + \frac{\partial^{\mathrm{a}}\underline{q}_{\mathrm{f_{per}}}^{\,X^{\ominus}_{\mathrm{PP}}}}{\partial \underline{u}_{\mathrm{per}}^{\,X_{k_1}}} \cdot \delta \underline{u}_{\mathrm{per}}^{\,X_{k_1}} + \frac{\partial^{\mathrm{a}}\underline{q}_{\mathrm{f}}^{\,X^{\ominus}_{\mathrm{PP}}}}{\partial \underline{u}_{\mathrm{sto}}^{\,W/X}} \cdot \underline{u}_{\mathrm{sto}}^{\,W/X} + \sum_{(\underline{z})} \frac{\partial^{\mathrm{a}}\underline{q}_{\mathrm{f}}^{\,X_{\mathrm{PP}}}}{\partial \underline{z}} \cdot \delta \underline{z} \\
{}^{\mathrm{a}}\underline{q}_{\mathrm{f}}^{\,X_{\mathrm{FF}}} &= {}^{\mathrm{a}}\overline{\underline{q}}_{\mathrm{f}}^{\,X_{\mathrm{FF}}} + \frac{\partial^{\mathrm{a}}\underline{q}_{\mathrm{f_{per}}}^{\,X_{\mathrm{PP}}}}{\partial \underline{u}_{\mathrm{per}}^{\,X_{k_r mL}}} \cdot \delta \underline{u}_{\mathrm{per}}^{\,X_{k_r mL}} + \frac{\partial^{\mathrm{a}}\underline{q}_{\mathrm{f}}^{\,X_{\mathrm{FF}}}}{\partial \underline{u}_{\mathrm{sto}}^{\,W/X}} \cdot \underline{u}_{\mathrm{sto}}^{\,W/X} + \sum_{(\underline{z})} \frac{\partial^{\mathrm{a}}\underline{q}_{\mathrm{f}}^{\,X_{\mathrm{FF}}}}{\partial \underline{z}} \cdot \delta \underline{z}
\end{aligned}
\tag{B.203}
$$

The summation over $\underline{z}$ involves $\underline{v}^{X^{\oplus}_{\mathrm{FF}}}$, $\underline{\omega}^{X^{\oplus}_{\mathrm{FF}}}$, $\underline{\phi}^{X_{\mathrm{FF}}}$, $\underline{\phi}^{X}$, $\underline{\dot{\varphi}}^{X}$, $\underline{\dot{\varrho}}^{X}$, $\underline{u}_{\mathrm{i_m}}^{W}$ and $\underline{u}_{\mathrm{ori}}^{R}$.

For the mean values hold (see Eq. B.197):

$$
\begin{aligned}
{}^{\mathrm{a}}\overline{\underline{q}}_{\mathrm{f}}^{\,X_{\mathrm{PP}}} &= {}^{\mathrm{a}}\overline{\underline{q}}_{\mathrm{f}}^{\,X^{\mathrm{cv}}_{k_1}} \\
{}^{\mathrm{a}}\overline{\underline{q}}_{\mathrm{f}}^{\,X_{\mathrm{FF}}} &= {}^{\mathrm{a}}\overline{\underline{q}}_{\mathrm{f}}^{\,X^{\mathrm{cv}}_{k_{\mathrm{L}}}}
\end{aligned}
\tag{B.204}
$$

For the periodic variation sensitivities holds: (see B.198):

$$
\begin{aligned}
\frac{\partial^{\mathrm{a}}\underline{q}_{\mathrm{f_{per}}}^{\,X^{\ominus}_{\mathrm{PP}}}}{\partial \underline{u}_{\mathrm{per}}^{\,X_{k_1}}} &= \frac{\partial \underline{q}_{\mathrm{f_{per}}}^{\,X_{k_1}}}{\partial \underline{u}_{\mathrm{per}}^{\,X_{k_1}}} \\
\frac{\partial^{\mathrm{a}}\underline{q}_{\mathrm{f_{per}}}^{\,X_{\mathrm{FF}}}}{\partial \underline{u}_{\mathrm{per}}^{\,X_{k_{\mathrm{L}}}}} &= \frac{\partial \underline{q}_{\mathrm{f_{per}}}^{\,X_{k_{\mathrm{L}}}}}{\partial \underline{u}_{\mathrm{per}}^{\,X_{k_{\mathrm{L}}}}}
\end{aligned}
\tag{B.205}
$$

and for the stochastic variation sensitivities (see Eq. B.199):

$$
\begin{aligned}
\frac{\partial^{\mathrm{a}}\underline{q}_{\mathrm{f}}^{\,X_{\mathrm{PP}}}}{\partial^{\mathrm{t}}\underline{u}^{W/X}} &= \frac{\partial \underline{q}_{\mathrm{f}}^{\,X_{k_1}}}{\partial^{\mathrm{t}}\underline{u}^{W/X}} \\
\frac{\partial^{\mathrm{a}}\underline{q}_{\mathrm{f}}^{\,X_{\mathrm{FF}}}}{\partial \underline{u}_{\mathrm{sto}}^{\,W/X}} &= \frac{\partial \underline{q}_{\mathrm{f}}^{\,X_{k_{\mathrm{L}}}}}{\partial \underline{u}_{\mathrm{sto}}^{\,W/X}}
\end{aligned}
\tag{B.206}
$$

For the sensitivities to $\underline{z} = \underline{v}^{X^{\oplus}_{\mathrm{FF}}}, \underline{\omega}^{X^{\oplus}_{\mathrm{FF}}}, \underline{\dot{\varphi}}^{X}, \underline{\dot{\varrho}}^{X}, \underline{u}_{\mathrm{i_m}}^{W}, \underline{u}_{\mathrm{ori}}^{R}$ holds (see Eq. B.201):

$$
\begin{aligned}
\frac{\partial^{\mathrm{a}}\underline{q}_{\mathrm{f}}^{\,X_{\mathrm{PP}}}}{\partial \underline{z}} &= \frac{\partial^{\mathrm{a}}\underline{q}_{\mathrm{f}}^{\,X^{\mathrm{cv}}_{k_1}}}{\partial \underline{z}} \\
\frac{\partial^{\mathrm{a}}\underline{q}_{\mathrm{f}}^{\,X_{\mathrm{FF}}}}{\partial \underline{z}} &= \frac{\partial^{\mathrm{a}}\underline{q}_{\mathrm{f}}^{\,X^{\mathrm{cv}}_{k_{\mathrm{L}}}}}{\partial \underline{z}}
\end{aligned}
\tag{B.207}
$$

For the sensitivities to the rotation dof positions holds (see Eq. B.200 and B.212) :

$$
\begin{aligned}
\frac{\partial^{\mathrm{a}}\underline{q}_{\mathrm{f}}^{\,X_{\mathrm{PP}}}}{\partial \phi_v^{\,X_i}} &= \frac{\partial^{\mathrm{a}}\underline{q}_{\mathrm{f}}^{\,X^{\mathrm{cv}}_{k_1}}}{\partial \phi_v^{\,X_i}} \\
\frac{\partial^{\mathrm{a}}\underline{q}_{\mathrm{f}}^{\,X_{\mathrm{FF}}}}{\partial \phi_v^{\,X_i}} &= \frac{\partial^{\mathrm{a}}\underline{q}_{\mathrm{f}}^{\,X^{\mathrm{cv}}_{k_{\mathrm{L}}}}}{\partial \phi_v^{\,X_i}}
\end{aligned}
\tag{B.208}
$$

so that for the elements in the subcompoments flange X_{f} and blade profile & structure X_{p} the sensitivities to the (internal) rotation dof vector $\underline{\phi}^{X}$ and to the output rotation dof vector $\underline{\phi}^{X_{\mathrm{FF}}}$ of the foregoing subcomponent are expressed as:

$$
\begin{aligned}
\frac{\partial^{\mathrm{a}}\underline{q}_{\mathrm{f}}^{\,X_{\mathrm{PP}}}}{\partial \underline{\phi}^{X}} &= \begin{cases} \left[\mathrm{J}^3_{v=1}\left(\partial^{\mathrm{a}}\underline{q}_{\mathrm{f}}^{\,X_{\mathrm{PP}}}/\partial \phi_v^{\,X_1}\right)\ \mathrm{O}_{(2)} \ldots \mathrm{O}_{(N)}\right] & \text{(for } X_{\mathrm{f}}\text{; <not used>)} \\ \left[\mathrm{O}_{(1)}\ \ \mathrm{J}^3_{v=1}\left(\partial^{\mathrm{a}}\underline{q}_{\mathrm{f}}^{\,X_{\mathrm{PP}}}/\partial \phi_v^{\,X_2}\right)\ \mathrm{O}_{(3)} \ldots \mathrm{O}_{(N)}\right] & \text{(for } X_{\mathrm{p}}\text{)} \end{cases} \\
\frac{\partial^{\mathrm{a}}\underline{q}_{\mathrm{f}}^{\,X_{\mathrm{PP}}}}{\partial \underline{\phi}^{X_{\mathrm{FF}}}} &= \begin{cases} \text{<does not exist>} & \text{(for } X_{\mathrm{f}}\text{; <not used>)} \\ \mathrm{J}^3_{v=1}\left(\partial^{\mathrm{a}}\underline{q}_{\mathrm{f}}^{\,X_{\mathrm{PP}}}/\partial \phi_v^{\,X_1}\right) & \text{(for } X_{\mathrm{p}}\text{)} \end{cases}
\end{aligned}
\tag{B.209}
$$

and

$$\frac{\partial^{\mathrm{a}} \underline{q}_{\mathrm{f}}^{X_{\mathrm{FF}}}}{\partial \underline{\phi}^{X}} = \begin{cases} \left[\mathrm{J}^{3}_{v=1}\left(\partial^{\mathrm{a}} \underline{q}_{\mathrm{f}}^{X_{\mathrm{FF}}} / \partial \phi_{v}^{X_1}\right) \;\; \mathrm{O}_{(2)} \ldots \mathrm{O}_{(N)} \right] & \text{(for } X_{\mathrm{f}}\text{)} \\ \left[\mathrm{O}_{(1)} \;\; \mathrm{J}^{N}_{i=2}\left(\mathrm{J}^{3}_{v=1}\left(\partial^{\mathrm{a}} \underline{q}_{\mathrm{f}}^{X_{\mathrm{FF}}} / \partial \phi_{v}^{X_2}\right)\right) \right] & \text{(for } X_{\mathrm{p}}\text{; <not used>)} \end{cases}$$

$$\frac{\partial^{\mathrm{a}} \underline{q}_{\mathrm{f}}^{X_{\mathrm{FF}}}}{\partial \underline{\phi}^{X_{\mathrm{FF}}}} = \begin{cases} \text{<does not exist>} & \text{(for } X_{\mathrm{f}}\text{)} \\ \mathrm{J}^{3}_{v=1}\left(\partial^{\mathrm{a}} \underline{q}_{\mathrm{f}}^{X_{\mathrm{FF}}} / \partial \phi_{v}^{X_1}\right) & \text{(for } X_{\mathrm{p}}\text{; <not used>)} \end{cases} \tag{B.210}$$

B.7.3 Mean, sensitivities and input variations for concentrated loads

Equations B.200 up to B.199 are straightforward used for the variation of the distributed loads on elements X_{k-1}, X_k and X_{k+1} in the epxressions for the concentrated load variations $\delta^{\mathrm{a}} \underline{f}^{X_k^{\mathrm{a}}}$ and $\delta^{\mathrm{a}} \underline{t}^{X_k^{\mathrm{a}}}$ as specified in 3.54 and 3.55 in section 3.6.3. The direct dependency of the concentrated loads on the rotation dof positions is derived from the expression for the sensitivity of the transformation matrix ${}^{X_k}\Phi^{X_k^{\mathrm{cv}}}$ from the conversion coordinate system to *the* coordinate system on element X_k as by eq. B.147. It holds:

$$\delta^{X_k}\Phi^{X_{k+j}^{\mathrm{cv}}} \cdot {}^{\mathrm{a}}\overline{\underline{q}}^{X_{k+j}^{\mathrm{cv}}} = \sum_{i=1}^{k+j} \sum_{v=1}^{3} \left({}^{X_k}\bar{\Phi}^{X_{k+j}} \cdot \frac{\partial^{X_{k+j}}\Phi^{X_{k+j}^{\mathrm{cv}}}}{\partial \phi_v^{X_i}} + \delta_{(i,k+\delta_{(j,1)})} \cdot \frac{\partial^{X_k}\Phi^{X_{k+j}}}{\partial \phi_v^{X_i}} \cdot {}^{X_{k+j}}\bar{\Phi}^{X_{k+j}^{\mathrm{cv}}} \right) \cdot {}^{\mathrm{a}}\overline{\underline{q}}^{X_{k+j}^{\mathrm{cv}}} \cdot \delta\phi_v^{X_i} \tag{B.211}$$

with the sensitivity of the transformation matrix ${}^{X_k}\Phi^{X_k^{\mathrm{cv}}}$ to a rotation dof $\phi_v^{X_i}$ given by (see Eq. B.147):

$$\frac{\partial^{X_k}\Phi^{X_k^{\mathrm{cv}}}}{\partial \phi_v^{X_i}} = \frac{\partial^{X_k}\Phi^{X_0}}{\partial \phi_v^{X_i}} \cdot {}^{X_0}\bar{\Phi}^{X_k^{\mathrm{cv}}} + {}^{X_k}\bar{\Phi}^{X_0} \cdot \mathrm{J}^{3}_{p=1}\left(\begin{bmatrix} -\left.\frac{\mathrm{d}\Phi_{\mathrm{z}}^{\mathrm{T}}}{\mathrm{d}\phi}\right|_{-\bar{\beta}^{X_k}} \cdot \left.\Phi^{\mathrm{T}}_{\mathrm{x}_{(:,p)}}\right|_{\bar{\zeta}^{X_k}} & \left| \; \left.\Phi_{\mathrm{z}}^{\mathrm{T}}\right|_{-\bar{\beta}^{X_k}} \cdot \left.\frac{\mathrm{d}\Phi^{\mathrm{T}}_{\mathrm{x}_{(:,p)}}}{\mathrm{d}\phi}\right|_{\bar{\zeta}^{X_k}} \right. \end{bmatrix} \cdot \begin{bmatrix} \partial\beta^{X_k}/\partial\phi_v^{X_i} \\ \partial\zeta^{X_k}/\partial\phi_v^{X_i} \end{bmatrix} \right) \tag{B.212}$$

The direct dependency of the concentrated loads on the rotation dofs can be derived by linking Eq. B.211 to the varation expressions 3.54 and 3.55. These direct dependencies do not yet include the sensitivity of the distributed loads to the rotation dofs. They are referred to as 'offset partial derivatives' and marked with a double quote subscript (").

$$\begin{aligned} \frac{\partial^{\mathrm{a}} \underline{f}_{"}^{X_k^{\mathrm{a}}}}{\partial \phi_v^{X_i}} = {} & \frac{\partial^{X_k}\Phi^{X_k^{\mathrm{cv}}}}{\partial \phi_v^{X_i}} \cdot {}^{\mathrm{a}}G^{\mathrm{F}}_{\mathrm{fq}_{k,0}} \cdot {}^{\mathrm{a}}\overline{\underline{q}}_{\mathrm{f}}^{X_k^{\mathrm{cv}}} + (\delta_{(k,k_{\mathrm{FF}}\oplus)} \cdot \delta_{k_{\mathrm{FF}}\downarrow 1} + \delta_{k\downarrow k^{\oplus}_{\mathrm{FF}}+1}) \cdot \\ & \left({}^{X_k}\bar{\Phi}^{X_{k-1}} \cdot \frac{\partial^{X_{k-1}}\Phi^{X_{k-1}^{\mathrm{cv}}}}{\partial \phi_v^{X_i}} + \delta_{(i,k)} \cdot \frac{\partial^{X_k}\Phi^{X_{k-1}}}{\partial \phi_v^{X_i}} \cdot {}^{X_{k-1}}\bar{\Phi}^{X_{k-1}^{\mathrm{cv}}} \right) \cdot {}^{\mathrm{a}}G^{\mathrm{F}}_{\mathrm{fq}_{k,-1}} \cdot {}^{\mathrm{a}}\overline{\underline{q}}_{\mathrm{f}}^{X_{k-1}^{\mathrm{cv}}} + \\ & \delta_{k\uparrow k^{\ominus}_{\mathrm{PP}}} \cdot \left({}^{X_k}\bar{\Phi}^{X_{k+1}} \cdot \frac{\partial^{X_{k+1}}\Phi^{X_{k+1}^{\mathrm{cv}}}}{\partial \phi_v^{X_i}} + \delta_{(i,k+1)} \cdot \frac{\partial^{X_k}\Phi^{X_{k+1}}}{\partial \phi_v^{X_i}} \cdot {}^{X_{k+1}}\bar{\Phi}^{X_{k+1}^{\mathrm{cv}}} \right) \cdot {}^{\mathrm{a}}G^{\mathrm{F}}_{\mathrm{fq}_{k,+1}} \cdot {}^{\mathrm{a}}\overline{\underline{q}}_{\mathrm{f}}^{X_{k+1}^{\mathrm{cv}}} \end{aligned} \tag{B.213}$$

and

$$\frac{\partial^{\mathrm{a}}\underline{t}_{,,}^{X_k^{\mathrm{a}}}}{\partial\phi_v^{X_i}} = \frac{\partial^{X_k}\Phi^{X_k^{\mathrm{cv}}}}{\partial\phi_v^{X_i}}\cdot{}^{\mathrm{a}}G^{\mathrm{M}}_{\mathrm{tq}_{k,0}}\cdot{}^{\mathrm{a}}\underline{q}_{\mathrm{t}}^{X_k^{\mathrm{cv}}} + \frac{\partial^{X_k}\Phi^{X_k^{\mathrm{cv}}}}{\partial\phi_v^{X_i}}\cdot{}^{\mathrm{a}}G^{\mathrm{F}}_{\mathrm{tq}_{k,0}}\cdot{}^{\mathrm{a}}\underline{q}_{\mathrm{f}}^{X_k^{\mathrm{cv}}} +$$
$$(\delta_{(k,k_{\mathrm{FF}}\oplus)}\cdot\delta_{k_{\mathrm{FF}}\downarrow 1}+\delta_{k\downarrow k^{\oplus}_{\mathrm{FF}}+1})\cdot$$
$$\left({}^{X_k}\bar{\Phi}^{X_{k-1}}\cdot\frac{\partial^{X_{k-1}}\Phi^{X_{k-1}^{\mathrm{cv}}}}{\partial\phi_v^{X_i}}+\delta_{(i,k)}\cdot\frac{\partial^{X_k}\Phi^{X_{k-1}}}{\partial\phi_v^{X_i}}\cdot{}^{X_{k-1}}\bar{\Phi}^{X_{k-1}^{\mathrm{cv}}}\right)\cdot{}^{\mathrm{a}}G^{\mathrm{F}}_{\mathrm{tq}_{k,-1}}\cdot{}^{\mathrm{a}}\underline{q}_{\mathrm{f}}^{X_{k-1}^{\mathrm{cv}}} +$$
$$\delta_{k\uparrow k^{\ominus}_{\mathrm{PP}}}\cdot\left({}^{X_k}\bar{\Phi}^{X_{k+1}}\cdot\frac{\partial^{X_{k+1}}\Phi^{X_{k+1}^{\mathrm{cv}}}}{\partial\phi_v^{X_i}}+\delta_{(i,k+1)}\cdot\frac{\partial^{X_k}\Phi^{X_{k+1}}}{\partial\phi_v^{X_i}}\cdot{}^{X_{k+1}}\bar{\Phi}^{X_{k+1}^{\mathrm{cv}}}\right)\cdot{}^{\mathrm{a}}G^{\mathrm{F}}_{\mathrm{tq}_{k,+1}}\cdot{}^{\mathrm{a}}\underline{q}_{\mathrm{f}}^{X_{k+1}^{\mathrm{cv}}} \tag{B.214}$$

For the elements in the subcompoments flange X_{f} and blade profile & structure X_{p} the offset sensitivities to the (internal) rotation dof vector $\underline{\phi}^{X}$ and the output rotation dof vector $\underline{\phi}^{X_{\mathrm{FF}}}$ of the foregoing subcomponent follow from the two equations above (see eq. B.212 for $\partial^{X_p}\Phi^{X_p^{\mathrm{cv}}}/\partial\phi_v^{X_i}$ in the expressions for $\partial^{\mathrm{a}}\underline{f}_{,,}^{X_k^{\mathrm{a}}}/\partial\phi_v^{X_i}$ and $\partial^{\mathrm{a}}\underline{t}_{,,}^{X_k^{\mathrm{a}}}/\partial\phi_v^{X_i}$)

$$\frac{\partial^{\mathrm{a}}\underline{f}_{,,}^{X_k^{\mathrm{a}}}}{\partial\underline{\phi}^{X}} = \begin{cases}\left[\mathrm{J}^3_{v=1}(\partial^{\mathrm{a}}\underline{f}_{,,}^{X_k^{\mathrm{a}}}/\partial\phi_v^{X_1})\ \ \mathrm{O}_{(2)}\ldots\mathrm{O}_{(N)}\right] & \text{for k=1}\\ \left[\mathrm{O}_{(1)}\ \ \mathrm{J}^k_{i=2}\big(\mathrm{J}^3_{v=1}(\partial^{\mathrm{a}}\underline{f}_{,,}^{X_k^{\mathrm{a}}}/\partial\phi_v^{X_i})\big)\ \ \mathrm{O}_{(k+1)}\ldots\mathrm{O}_{(N)}\right] & \text{for k=2...N}\end{cases}$$
$$\frac{\partial^{\mathrm{a}}\underline{f}_{,,}^{X_k^{\mathrm{a}}}}{\partial\underline{\phi}^{X_{\mathrm{FF}}}} = \begin{cases}\text{<does not exist>} & \text{for k=1}\\ \mathrm{J}^3_{v=1}(\partial^{\mathrm{a}}\underline{f}_{,,}^{X_k^{\mathrm{a}}}/\partial\phi_v^{X_1}) & \text{for k=2...N}\end{cases}$$
$$\frac{\partial^{\mathrm{a}}\underline{f}_{,,}^{X_k^{\mathrm{a}}}}{\partial\underline{\phi}^{X_{\mathrm{PP}}}} = \begin{cases}\mathrm{J}^3_{v=1}(\partial^{\mathrm{a}}\underline{f}_{,,}^{X_k^{\mathrm{a}}}/\partial\phi_v^{X_2}) & \text{for k=1}\\ \text{<does not exist>} & \text{for k=2...N}\end{cases} \tag{B.215}$$

and

$$\frac{\partial^{\mathrm{a}}\underline{t}_{,,}^{X_k^{\mathrm{a}}}}{\partial\underline{\phi}^{X}} = \begin{cases}\left[\mathrm{J}^3_{v=1}(\partial^{\mathrm{a}}\underline{t}_{,,}^{X_k^{\mathrm{a}}}/\partial\phi_v^{X_1})\ \ \mathrm{O}_{(2)}\ldots\mathrm{O}_{(N)}\right] & \text{for k=1}\\ \left[\mathrm{O}_{(1)}\ \ \mathrm{J}^k_{i=2}\big(\mathrm{J}^3_{v=1}(\partial^{\mathrm{a}}\underline{t}_{,,}^{X_k^{\mathrm{a}}}/\partial\phi_v^{X_i})\big)\ \ \mathrm{O}_{(k+1)}\ldots\mathrm{O}_{(N)}\right] & \text{for k=2...N}\end{cases}$$
$$\frac{\partial^{\mathrm{a}}\underline{t}_{,,}^{X_k^{\mathrm{a}}}}{\partial\underline{\phi}^{X_{\mathrm{FF}}}} = \begin{cases}\text{<does not exist>} & \text{for k=1}\\ \mathrm{J}^3_{v=1}(\partial^{\mathrm{a}}\underline{t}_{,,}^{X_k^{\mathrm{a}}}/\partial\phi_v^{X_1}) & \text{for k=2...N}\end{cases}$$
$$\frac{\partial^{\mathrm{a}}\underline{t}_{,,}^{X_k^{\mathrm{a}}}}{\partial\underline{\phi}^{X_{\mathrm{PP}}}} = \begin{cases}\mathrm{J}^3_{v=1}(\partial^{\mathrm{a}}\underline{t}_{,,}^{X_k^{\mathrm{a}}}/\partial\phi_v^{X_2}) & \text{for k=1}\\ \text{<does not exist>} & \text{for k=2...N}\end{cases} \tag{B.216}$$

The linearised expressions for the concentrated aerodynamic loads follow straigthforward from the expressions for the distributed loads in section B.7.1 and from the direct senstivities of the concentrated loads to the rotation dof positions (see $\partial^{\mathrm{a}}\underline{f}_{,,}^{X_k^{\mathrm{a}}}$, ${}^{\mathrm{a}}\underline{t}_{,,}^{X_k^{\mathrm{a}}}/\partial\underline{\phi}^{X}$, $\underline{\phi}^{X_{\mathrm{FF}}}$, $\underline{\phi}^{X_{\mathrm{PP}}}$ by Eq. B.215 and B.216). Equation 3.48 tells that concentrated loads on an element depend on the distributed loads on that very element *and* on the neighbouring elements. This implies that a concentrated load may depend on 'input distributed loads' from the most nearby elements of the neighbouring subcomponents, vizually ${}^{\mathrm{a}}\underline{q}_{\mathrm{f}}^{X_{\mathrm{FF}}}$, ${}^{\mathrm{a}}\underline{q}_{\mathrm{f}}^{X_{\mathrm{PP}}}$. It also implies that a concentrated load depends on up to three distributed loads within the actual subcomponent (${}^{\mathrm{a}}\underline{q}_{\mathrm{f}}^{X_{k\pm1}^{\mathrm{cv}}}$). The latter may make a concentrated load to depend on the induction wind velocity and turbulence in more than *one* rotor annulus: element X_{k-1} or X_{k+1} may intersect with another rotor annlus than X_k. This is the fundamental reason why we introduced the overall induction and turbulence coordinate vectors in Eq. B.175.

The overall expressions for the concentrated aerodynamic loads are:

$$\begin{aligned} {}^{\mathrm{a}}\underline{f}^{X_k^{\mathrm{a}}} &= {}^{\mathrm{a}}\bar{\underline{f}}^{X_k^{\mathrm{a}}} + \frac{\partial^{\mathrm{a}}\underline{f}^{X_k^{\mathrm{a}}}}{\partial \underline{u}_{\mathrm{per}}^{X}} \cdot \delta\underline{u}_{\mathrm{per}}^{X} + \frac{\partial^{\mathrm{a}}\underline{f}^{X_k^{\mathrm{a}}}}{\partial \underline{u}_{\mathrm{sto}}^{W/X}} \cdot \underline{u}_{\mathrm{sto}}^{W/X} + \sum_{(\underline{z})} \frac{\partial^{\mathrm{a}}\underline{f}^{X_k^{\mathrm{a}}}}{\partial \underline{z}} \cdot \delta\underline{z} \\ {}^{\mathrm{a}}\underline{t}^{X_k^{\mathrm{a}}} &= {}^{\mathrm{a}}\bar{\underline{t}}^{X_k^{\mathrm{a}}} + \frac{\partial^{\mathrm{a}}\underline{t}^{X_k^{\mathrm{a}}}}{\partial \underline{u}_{\mathrm{per}}^{X}} \cdot \delta\underline{u}_{\mathrm{per}}^{X} + \frac{\partial^{\mathrm{a}}\underline{t}^{X_k^{\mathrm{a}}}}{\partial \underline{u}_{\mathrm{sto}}^{W/X}} \cdot \underline{u}_{\mathrm{sto}}^{W/X} + \sum_{(\underline{z})} \frac{\partial^{\mathrm{a}}\underline{t}^{X_k^{\mathrm{a}}}}{\partial \underline{z}} \cdot \delta\underline{z} \end{aligned} \tag{B.217}$$

The summation over $\underline{z}$ involves ${}^{\mathrm{a}}\underline{q}_{\mathrm{f}}^{X_{\mathrm{FF}}}$, ${}^{\mathrm{a}}\underline{q}_{\mathrm{f}}^{X_{\mathrm{PP}}}$, $\underline{v}^{X_{\mathrm{FF}}^{\oplus}}$, $\underline{\omega}^{X_{\mathrm{FF}}^{\oplus}}$, $\underline{\phi}^{X_{\mathrm{FF}}}$, $\underline{\phi}^{X_{\mathrm{PP}}}$, $\underline{\phi}^{X}$, $\underline{\dot{\varphi}}^{X}$, $\underline{\dot{\varrho}}^{X}$, $\underline{u}_{\mathrm{im}}^{W}$ and $\underline{u}_{\mathrm{ori}}^{R}$.

For the mean values hold (see Eq. B.197) :

$$\begin{aligned} {}^{\mathrm{a}}\bar{\underline{f}}^{X_k^{\mathrm{a}}} &= {}^{X_k}\bar{\Phi}^{X_k^{\mathrm{cv}}} \cdot {}^{\mathrm{a}}G_{\mathrm{fq}_{k,0}}^{\mathrm{F}} \cdot {}^{\mathrm{a}}\overline{\underline{q}}_{\mathrm{f}}^{X_k^{\mathrm{cv}}} + \\ &\left(\delta_{(k,k_{\mathrm{FF}}\oplus)} \cdot \delta_{k_{\mathrm{FF}}\downarrow 1} \cdot {}^{X_k}\bar{\Phi}^{X_{k-1}^{\mathrm{cv}}} \cdot {}^{\mathrm{a}}G_{\mathrm{fq}_{k,-1}}^{\mathrm{F}} \cdot {}^{\mathrm{a}}\overline{\underline{q}}_{\mathrm{f}}^{X_{\mathrm{FF}}} + \delta_{k\downarrow k_{\mathrm{FF}}^{\oplus}+1} \cdot {}^{X_k}\bar{\Phi}^{X_{k-1}^{\mathrm{cv}}} \cdot {}^{\mathrm{a}}G_{\mathrm{fq}_{k,-1}}^{\mathrm{F}} \cdot {}^{\mathrm{a}}\overline{\underline{q}}_{\mathrm{f}}^{X_{k-1}^{\mathrm{cv}}}\right) + \\ &\left(\delta_{(k,k_{\mathrm{PP}}^{\ominus})} \cdot \delta_{k_{\mathrm{PP}}\uparrow N} \cdot {}^{X_k}\bar{\Phi}^{X_{k+1}^{\mathrm{cv}}} \cdot {}^{\mathrm{a}}G_{\mathrm{fq}_{k,+1}}^{\mathrm{F}} \cdot {}^{\mathrm{a}}\overline{\underline{q}}_{\mathrm{f}}^{X_{\mathrm{PP}}^{\ominus}} + \delta_{k\uparrow k_{\mathrm{PP}}^{\ominus}-1} \cdot {}^{X_k}\bar{\Phi}^{X_{k+1}^{\mathrm{cv}}} \cdot {}^{\mathrm{a}}G_{\mathrm{fq}_{k,+1}}^{\mathrm{F}} \cdot {}^{\mathrm{a}}\overline{\underline{q}}_{\mathrm{f}}^{X_{k+1}^{\mathrm{cv}}}\right) \end{aligned} \tag{B.218}$$

and:

$$\begin{aligned} {}^{\mathrm{a}}\bar{\underline{t}}^{X_k^{\mathrm{a}}} &= \left({}^{X_k}\bar{\Phi}^{X_k^{\mathrm{cv}}} \cdot {}^{\mathrm{a}}G_{\mathrm{tq}_k}^{\mathrm{M}} \cdot {}^{\mathrm{a}}\overline{\underline{q}}_{\mathrm{t}}^{X_k^{\mathrm{cv}}}\right) + \left({}^{X_k}\bar{\Phi}^{X_k^{\mathrm{cv}}} \cdot {}^{\mathrm{a}}G_{\mathrm{tq}_{k,0}}^{\mathrm{F}} \cdot {}^{\mathrm{a}}\overline{\underline{q}}_{\mathrm{f}}^{X_k^{\mathrm{cv}}}\right) + \\ &\left(\delta_{(k,k_{\mathrm{FF}}\oplus)} \cdot \delta_{k_{\mathrm{FF}}\downarrow 1} \cdot {}^{X_k}\bar{\Phi}^{X_{k-1}^{\mathrm{cv}}} \cdot {}^{\mathrm{a}}G_{\mathrm{fq}_{k,-1}}^{\mathrm{F}} \cdot {}^{\mathrm{a}}\overline{\underline{q}}_{\mathrm{f}}^{X_{\mathrm{FF}}} + \delta_{k\downarrow k_{\mathrm{FF}}^{\oplus}+1} \cdot {}^{X_k}\bar{\Phi}^{X_{k-1}^{\mathrm{cv}}} \cdot {}^{\mathrm{a}}G_{\mathrm{fq}_{k,-1}}^{\mathrm{F}} \cdot {}^{\mathrm{a}}\overline{\underline{q}}_{\mathrm{f}}^{X_{k-1}^{\mathrm{cv}}}\right) + \\ &\left(\delta_{(k,k_{\mathrm{PP}}^{\ominus})} \cdot \delta_{k_{\mathrm{PP}}\uparrow N} \cdot {}^{X_k}\bar{\Phi}^{X_{k+1}^{\mathrm{cv}}} \cdot {}^{\mathrm{a}}G_{\mathrm{fq}_{k,+1}}^{\mathrm{F}} \cdot {}^{\mathrm{a}}\overline{\underline{q}}_{\mathrm{f}}^{X_{\mathrm{PP}}^{\ominus}} + \delta_{k\uparrow k_{\mathrm{PP}}^{\ominus}-1} \cdot {}^{X_k}\bar{\Phi}^{X_{k+1}^{\mathrm{cv}}} \cdot {}^{\mathrm{a}}G_{\mathrm{fq}_{k,+1}}^{\mathrm{F}} \cdot {}^{\mathrm{a}}\overline{\underline{q}}_{\mathrm{f}}^{X_{k+1}^{\mathrm{cv}}}\right) \end{aligned} \tag{B.219}$$

For the stochastic variation sensitivity holds (use Eq. B.199 for $\partial {}^{\mathrm{a}}\underline{q}_{\mathrm{f}}^{X_{k[\pm 1]}}, {}^{\mathrm{a}}\underline{q}_{\mathrm{t}}^{X_k} / \partial \underline{u}_{\mathrm{sto}}^{W/X}$):

$$\begin{aligned} \frac{\partial^{\mathrm{a}}\underline{f}^{X_k^{\mathrm{a}}}}{\partial^{\mathrm{t}}\underline{u}^{W/X}} &= {}^{X_k}\bar{\Phi}^{X_k^{\mathrm{cv}}} \cdot {}^{\mathrm{a}}G_{\mathrm{fq}_{k,0}}^{\mathrm{F}} \cdot \frac{\partial^{\mathrm{a}}\underline{q}_{\mathrm{f}}^{X_k^{\mathrm{cv}}}}{\partial^{\mathrm{t}}\underline{u}^{W/X}} + \\ &\quad \delta_{k\downarrow k_{\mathrm{FF}}^{\oplus}+1} \cdot {}^{X_k}\bar{\Phi}^{X_{k-1}^{\mathrm{cv}}} \cdot {}^{\mathrm{a}}G_{\mathrm{fq}_{k,-1}}^{\mathrm{F}} \cdot \frac{\partial^{\mathrm{a}}\underline{q}_{\mathrm{f}}^{X_{k-1}^{\mathrm{cv}}}}{\partial \underline{u}_{\mathrm{sto}}^{W/X}} + \delta_{k\uparrow k_{\mathrm{PP}}^{\ominus}-1} \cdot {}^{X_k}\bar{\Phi}^{X_{k+1}^{\mathrm{cv}}} \cdot {}^{\mathrm{a}}G_{\mathrm{fq}_{k,+1}}^{\mathrm{F}} \cdot \frac{\partial^{\mathrm{a}}\underline{q}_{\mathrm{f}}^{X_{k+1}^{\mathrm{cv}}}}{\partial \underline{u}_{\mathrm{sto}}^{W/X}} \\ \frac{\partial^{\mathrm{a}}\underline{t}^{X_k^{\mathrm{a}}}}{\partial \underline{u}_{\mathrm{sto}}^{W/X}} &= {}^{X_k}\bar{\Phi}^{X_k^{\mathrm{cv}}} \cdot {}^{\mathrm{a}}G_{\mathrm{tq}_k}^{\mathrm{M}} \cdot \frac{\partial^{\mathrm{a}}\underline{q}_{\mathrm{t}}^{X_k^{\mathrm{cv}}}}{\partial \underline{u}_{\mathrm{sto}}^{W/X}} + {}^{X_k}\bar{\Phi}^{X_k^{\mathrm{cv}}} \cdot {}^{\mathrm{a}}G_{\mathrm{tq}_{k,0}}^{\mathrm{F}} \cdot \frac{\partial^{\mathrm{a}}\underline{q}_{\mathrm{f}}^{X_k^{\mathrm{cv}}}}{\partial \underline{u}_{\mathrm{sto}}^{W/X}} + \\ &\quad \delta_{k\downarrow k_{\mathrm{FF}}^{\oplus}+1} \cdot {}^{X_k}\bar{\Phi}^{X_{k-1}^{\mathrm{cv}}} \cdot {}^{\mathrm{a}}G_{\mathrm{fq}_{k,-1}}^{\mathrm{F}} \cdot \frac{\partial^{\mathrm{a}}\underline{q}_{\mathrm{f}}^{X_{k-1}^{\mathrm{cv}}}}{\partial \underline{u}_{\mathrm{sto}}^{W/X}} + \delta_{k\uparrow k_{\mathrm{PP}}^{\ominus}-1} \cdot {}^{X_k}\bar{\Phi}^{X_{k+1}^{\mathrm{cv}}} \cdot {}^{\mathrm{a}}G_{\mathrm{fq}_{k,+1}}^{\mathrm{F}} \cdot \frac{\partial^{\mathrm{a}}\underline{q}_{\mathrm{f}}^{X_{k+1}^{\mathrm{cv}}}}{\partial \underline{u}_{\mathrm{sto}}^{W/X}} \end{aligned} \tag{B.220}$$

and for the periodic variation (use Eq. B.198 for $\partial {}^{\mathrm{a}}\underline{q}_{\mathrm{f_{per}}}^{X_{k[\pm 1]}}, {}^{\mathrm{a}}\underline{q}_{\mathrm{t_{per}}}^{X_k} / \partial \underline{u}_{\mathrm{per}}^{X}$):

$$\begin{aligned} \frac{\partial^{\mathrm{a}}\underline{f}_{\mathrm{per}}^{X_k^{\mathrm{a}}}}{\partial \underline{u}_{\mathrm{per}}^{X}} &= {}^{X_k}\bar{\Phi}^{X_k^{\mathrm{cv}}} \cdot {}^{\mathrm{a}}G_{\mathrm{fq}_{k,0}}^{\mathrm{F}} \cdot \frac{\partial^{\mathrm{a}}\underline{q}_{\mathrm{f_{per}}}^{X_k^{\mathrm{cv}}}}{\partial \underline{u}_{\mathrm{per}}^{X}} + \\ &\quad \delta_{k\downarrow k_{\mathrm{FF}}^{\oplus}+1} \cdot {}^{X_k}\bar{\Phi}^{X_{k-1}^{\mathrm{cv}}} \cdot {}^{\mathrm{a}}G_{\mathrm{fq}_{k,-1}}^{\mathrm{F}} \cdot \frac{\partial^{\mathrm{a}}\underline{q}_{\mathrm{f_{per}}}^{X_{k-1}^{\mathrm{cv}}}}{\partial \underline{u}_{\mathrm{per}}^{X}} + \delta_{k\uparrow k_{\mathrm{PP}}^{\ominus}-1} \cdot {}^{X_k}\bar{\Phi}^{X_{k+1}^{\mathrm{cv}}} \cdot {}^{\mathrm{a}}G_{\mathrm{fq}_{k,+1}}^{\mathrm{F}} \cdot \frac{\partial^{\mathrm{a}}\underline{q}_{\mathrm{f_{per}}}^{X_{k+1}^{\mathrm{cv}}}}{\partial \underline{u}_{\mathrm{per}}^{X}} \end{aligned} \tag{B.221}$$

and:

$$\begin{aligned} \frac{\partial^{\mathrm{a}}\underline{t}_{\mathrm{per}}^{X_k^{\mathrm{a}}}}{\partial \underline{u}_{\mathrm{per}}^{X}} &= {}^{X_k}\bar{\Phi}^{X_k^{\mathrm{cv}}} \cdot {}^{\mathrm{a}}G_{\mathrm{tq}_k}^{\mathrm{M}} \cdot \frac{\partial^{\mathrm{a}}\underline{q}_{\mathrm{t_{per}}}^{X_k^{\mathrm{cv}}}}{\partial \underline{u}_{\mathrm{per}}^{X}} + {}^{X_k}\bar{\Phi}^{X_k^{\mathrm{cv}}} \cdot {}^{\mathrm{a}}G_{\mathrm{tq}_{k,0}}^{\mathrm{F}} \cdot \frac{\partial^{\mathrm{a}}\underline{q}_{\mathrm{f_{per}}}^{X_k^{\mathrm{cv}}}}{\partial \underline{u}_{\mathrm{per}}^{X}} + \\ &\quad \delta_{k\downarrow k_{\mathrm{FF}}^{\oplus}+1} \cdot {}^{X_k}\bar{\Phi}^{X_{k-1}^{\mathrm{cv}}} \cdot {}^{\mathrm{a}}G_{\mathrm{fq}_{k,-1}}^{\mathrm{F}} \cdot \frac{\partial^{\mathrm{a}}\underline{q}_{\mathrm{f_{per}}}^{X_{k-1}^{\mathrm{cv}}}}{\partial \underline{u}_{\mathrm{per}}^{X}} + \delta_{k\uparrow k_{\mathrm{PP}}^{\ominus}-1} \cdot {}^{X_k}\bar{\Phi}^{X_{k+1}^{\mathrm{cv}}} \cdot {}^{\mathrm{a}}G_{\mathrm{fq}_{k,+1}}^{\mathrm{F}} \cdot \frac{\partial^{\mathrm{a}}\underline{q}_{\mathrm{f_{per}}}^{X_{k+1}^{\mathrm{cv}}}}{\partial \underline{u}_{\mathrm{per}}^{X}} \end{aligned} \tag{B.222}$$

For the sensitivity to the distributed loads on the foregoing subcomponent holds:

$$\begin{aligned}\frac{\partial^{\mathrm{a}}\underline{f}^{X_k^{\mathrm{a}}}}{\partial^{\mathrm{a}}\underline{q}_{\mathrm{f}}^{X_{\mathrm{FF}}}} &= \delta_{(k,k_{\mathrm{FF}}\oplus)}\cdot\delta_{k_{\mathrm{FF}}\downarrow 1}\cdot {}^{X_k}\bar{\Phi}^{X_{k-1}^{\mathrm{cv}}}\cdot {}^{\mathrm{a}}G^{\mathrm{F}}_{\mathrm{fq}_{k,-1}}\\ \frac{\partial^{\mathrm{a}}\underline{t}^{X_k^{\mathrm{a}}}}{\partial^{\mathrm{a}}\underline{q}_{\mathrm{f}}^{X_{\mathrm{FF}}}} &= \delta_{(k,k_{\mathrm{FF}}\oplus)}\cdot\delta_{k_{\mathrm{FF}}\downarrow 1}\cdot {}^{X_k}\bar{\Phi}^{X_{k-1}^{\mathrm{cv}}}\cdot {}^{\mathrm{a}}G^{\mathrm{F}}_{\mathrm{tq}_{k,-1}}\end{aligned} \tag{B.223}$$

and to the distributed loads on the subsequent subomponent:

$$\begin{aligned}\frac{\partial^{\mathrm{a}}\underline{f}^{X_k^{\mathrm{a}}}}{\partial^{\mathrm{a}}\underline{q}_{\mathrm{f}}^{X_{\mathrm{PP}}}} &= {}^{X_k}\bar{\Phi}^{X_{k+1}^{\mathrm{cv}}}\cdot {}^{\mathrm{a}}G^{\mathrm{F}}_{\mathrm{fq}_{k,+1}}\cdot\delta_{(k,k^{\ominus}_{\mathrm{PP}})}\cdot\delta_{k_{\mathrm{PP}}\uparrow N}\\ \frac{\partial^{\mathrm{a}}\underline{t}^{X_k^{\mathrm{a}}}}{\partial^{\mathrm{a}}\underline{q}_{\mathrm{f}}^{X_{\mathrm{PP}}}} &= {}^{X_k}\bar{\Phi}^{X_{k+1}^{\mathrm{cv}}}\cdot {}^{\mathrm{a}}G^{\mathrm{F}}_{\mathrm{tq}_{k,+1}}\cdot\delta_{(k,k^{\ominus}_{\mathrm{PP}})}\cdot\delta_{k_{\mathrm{PP}}\uparrow N}\end{aligned} \tag{B.224}$$

For all remaining sensitivities except those to the rotation dof position holds ($\underline{z} = \underline{v}^{X^{\oplus}_{\mathrm{FF}}}, \underline{\omega}^{X^{\oplus}_{\mathrm{FF}}}, \underline{\dot{\varphi}}^{X}, \underline{\dot{\varrho}}^{X}, \underline{u}^{W}_{\mathrm{i_m}}, \underline{u}^{R}_{\mathrm{ori}}$; see Eq. B.201) :

$$\begin{aligned}\frac{\partial^{\mathrm{a}}\underline{f}^{X_k^{\mathrm{a}}}}{\partial\underline{z}} &= {}^{X_k}\bar{\Phi}^{X_k^{\mathrm{cv}}}\cdot {}^{\mathrm{a}}G^{\mathrm{F}}_{\mathrm{fq}_{k,0}}\cdot\frac{\partial^{\mathrm{a}}\underline{q}_{\mathrm{f}}^{X_k^{\mathrm{cv}}}}{\partial\underline{z}} +\\ &\delta_{k\downarrow k^{\oplus}_{\mathrm{FF}}+1}\cdot {}^{X_k}\bar{\Phi}^{X_{k-1}^{\mathrm{cv}}}\cdot {}^{\mathrm{a}}G^{\mathrm{F}}_{\mathrm{fq}_{k,-1}}\cdot\frac{\partial^{\mathrm{a}}\underline{q}_{\mathrm{f}}^{X_{k-1}^{\mathrm{cv}}}}{\partial\underline{z}} + \delta_{k\uparrow k^{\ominus}_{\mathrm{PP}}-1}\cdot {}^{X_k}\bar{\Phi}^{X_{k+1}^{\mathrm{cv}}}\cdot {}^{\mathrm{a}}G^{\mathrm{F}}_{\mathrm{fq}_{k,+1}}\cdot\frac{\partial^{\mathrm{a}}\underline{q}_{\mathrm{f}}^{X_{k+1}^{\mathrm{cv}}}}{\partial\underline{z}}\end{aligned} \tag{B.225}$$

and:

$$\begin{aligned}\frac{\partial^{\mathrm{a}}\underline{t}^{X_k^{\mathrm{a}}}}{\partial\underline{z}} &= {}^{X_k}\bar{\Phi}^{X_k^{\mathrm{cv}}}\cdot {}^{\mathrm{a}}G^{\mathrm{M}}_{\mathrm{tq}_k}\cdot\frac{\partial^{\mathrm{a}}\underline{q}_{\mathrm{t}}^{X_k^{\mathrm{cv}}}}{\partial\underline{z}} + {}^{X_k}\bar{\Phi}^{X_k^{\mathrm{cv}}}\cdot {}^{\mathrm{a}}G^{\mathrm{F}}_{\mathrm{tq}_{k,0}}\cdot\frac{\partial^{\mathrm{a}}\underline{q}_{\mathrm{f}}^{X_k^{\mathrm{cv}}}}{\partial\underline{z}} +\\ &\delta_{k\downarrow k^{\oplus}_{\mathrm{FF}}+1}\cdot {}^{X_k}\bar{\Phi}^{X_{k-1}^{\mathrm{cv}}}\cdot {}^{\mathrm{a}}G^{\mathrm{F}}_{\mathrm{tq}_{k,-1}}\cdot\frac{\partial^{\mathrm{a}}\underline{q}_{\mathrm{f}}^{X_{k-1}^{\mathrm{cv}}}}{\partial\underline{z}} + \delta_{k\uparrow k^{\ominus}_{\mathrm{PP}}-1}\cdot {}^{X_k}\bar{\Phi}^{X_{k+1}^{\mathrm{cv}}}\cdot {}^{\mathrm{a}}G^{\mathrm{F}}_{\mathrm{tq}_{k,+1}}\cdot\frac{\partial^{\mathrm{a}}\underline{q}_{\mathrm{f}}^{X_{k+1}^{\mathrm{cv}}}}{\partial\underline{z}}\end{aligned} \tag{B.226}$$

For the sensitivity to the rotation dof positions $\underline{\phi}^{X_{\mathrm{FF}}}$ that are input from the foregoing subcomponent holds (see Eq. B.215, B.216 and B.200) :

$$\begin{aligned}\frac{\partial^{\mathrm{a}}\underline{f}^{X_k^{\mathrm{a}}}}{\partial\underline{\phi}^{X_{\mathrm{FF}}}} &= \frac{\partial^{\mathrm{a}}\underline{f}_{,,}^{X_k^{\mathrm{a}}}}{\partial\underline{\phi}^{X_{\mathrm{FF}}}} + {}^{X_k}\bar{\Phi}^{X_k^{\mathrm{cv}}}\cdot {}^{\mathrm{a}}G^{\mathrm{F}}_{\mathrm{fq}_{k,0}}\cdot\frac{\partial^{\mathrm{a}}\underline{q}_{\mathrm{f}}^{X_k^{\mathrm{cv}}}}{\partial\underline{\phi}^{X_{\mathrm{FF}}}} +\\ &\delta_{k\downarrow k^{\oplus}_{\mathrm{FF}}+1}\cdot {}^{X_k}\bar{\Phi}^{X_{k-1}^{\mathrm{cv}}}\cdot {}^{\mathrm{a}}G^{\mathrm{F}}_{\mathrm{fq}_{k,-1}}\cdot\frac{\partial^{\mathrm{a}}\underline{q}_{\mathrm{f}}^{X_{k-1}^{\mathrm{cv}}}}{\partial\underline{\phi}^{X_{\mathrm{FF}}}} + \delta_{k\uparrow k^{\ominus}_{\mathrm{PP}}-1}\cdot {}^{X_k}\bar{\Phi}^{X_{k+1}^{\mathrm{cv}}}\cdot {}^{\mathrm{a}}G^{\mathrm{F}}_{\mathrm{fq}_{k,+1}}\cdot\frac{\partial^{\mathrm{a}}\underline{q}_{\mathrm{f}}^{X_{k+1}^{\mathrm{cv}}}}{\partial\underline{\phi}^{X_{\mathrm{FF}}}}\end{aligned} \tag{B.227}$$

and:

$$\begin{aligned}\frac{\partial^{\mathrm{a}}\underline{t}^{X_k^{\mathrm{a}}}}{\partial\underline{\phi}^{X_{\mathrm{FF}}}} &= \frac{\partial^{\mathrm{a}}\underline{t}_{,,}^{X_k^{\mathrm{a}}}}{\partial\underline{\phi}^{X_{\mathrm{FF}}}} + {}^{X_k}\bar{\Phi}^{X_k^{\mathrm{cv}}}\cdot {}^{\mathrm{a}}G^{\mathrm{M}}_{\mathrm{tq}_{k,0}}\cdot\frac{\partial^{\mathrm{a}}\underline{q}_{\mathrm{t}}^{X_k^{\mathrm{cv}}}}{\partial\underline{\phi}^{X_{\mathrm{FF}}}} + {}^{X_k}\bar{\Phi}^{X_k^{\mathrm{cv}}}\cdot {}^{\mathrm{a}}G^{\mathrm{F}}_{\mathrm{tq}_{k,0}}\cdot\frac{\partial^{\mathrm{a}}\underline{q}_{\mathrm{f}}^{X_k^{\mathrm{cv}}}}{\partial\underline{\phi}^{X_{\mathrm{FF}}}} +\\ &\delta_{k\downarrow k^{\oplus}_{\mathrm{FF}}+1}\cdot {}^{X_k}\bar{\Phi}^{X_{k-1}^{\mathrm{cv}}}\cdot {}^{\mathrm{a}}G^{\mathrm{F}}_{\mathrm{tq}_{k,-1}}\cdot\frac{\partial^{\mathrm{a}}\underline{q}_{\mathrm{f}}^{X_{k-1}^{\mathrm{cv}}}}{\partial\underline{\phi}^{X_{\mathrm{FF}}}} + \delta_{k\uparrow k^{\ominus}_{\mathrm{PP}}-1}\cdot {}^{X_k}\bar{\Phi}^{X_{k+1}^{\mathrm{cv}}}\cdot {}^{\mathrm{a}}G^{\mathrm{F}}_{\mathrm{tq}_{k,+1}}\cdot\frac{\partial^{\mathrm{a}}\underline{q}_{\mathrm{f}}^{X_{k+1}^{\mathrm{cv}}}}{\partial\underline{\phi}^{X_{\mathrm{FF}}}}\end{aligned} \tag{B.228}$$

The same expressions hold for the sensitivity to the rotation dof positions of the actual subcomponent ($\partial^{\mathrm{a}}\underline{f}^{X_k^{\mathrm{a}}}, {}^{\mathrm{a}}\underline{t}^{X_k^{\mathrm{a}}}/\partial\underline{\phi}^{X}$).

For the sensitivity to the rotation dof positions $\underline{\phi}^{X_{\mathrm{PP}}}$ that are input from the following subcomponent holds (see Eq. B.215, B.216 and B.200) :

$$\frac{\partial^{\mathrm{a}}\underline{f}^{X_k^{\mathrm{a}}}}{\partial\underline{\phi}^{X_{\mathrm{PP}}}} = \frac{\partial^{\mathrm{a}}\underline{f}_{,,}^{X_k^{\mathrm{a}}}}{\partial\underline{\phi}^{X_{\mathrm{PP}}}} \tag{B.229}$$

and:

$$\frac{\partial^{\mathrm{a}}\underline{t}^{X_k^{\mathrm{a}}}}{\partial\underline{\phi}^{X_{\mathrm{PP}}}} = \frac{\partial^{\mathrm{a}}\underline{t}_{,,}^{X_k^{\mathrm{a}}}}{\partial\underline{\phi}^{X_{\mathrm{PP}}}} \tag{B.230}$$

B.7.4 Mean, sensitivities and variations for reaction loads on annuli

See paragraph (iii) in section 3.6.3 for the general expression of the reaction force loading by the rotor blades on the rotor annuli, which are expressed in coordinates along the annulus wise coordinate system $\vec{e}^{\,W_m/X_k}$ in the intersection of blade element X_k and rotor annulus W_m.

Denote the direct sensitivity of the reaction force to a rotation dof position as $\partial^{\mathrm{a_L}}\underline{f}_{"}W_m/X_k/\partial\phi_v^{X_i}$: holds:

$$\begin{aligned}\frac{\partial^{\mathrm{a_L}}\underline{f}_{"}^{W_m/X_k}}{\partial\phi_v^{X_i}} &= -\Big(\frac{\partial^{W/X_k}\Phi^{X_k^{\mathrm{cv}}}}{\partial\phi_v^{X_i}}\cdot{}^{X_k^{\mathrm{cv}}}\bar{\Phi}^{X_0}\cdot{}^{X_0}\bar{\Phi}^{X_k}\cdot{}^{\mathrm{a_L}}\underline{\bar{f}}^{X_k^{\mathrm{a}}}+\\ &\quad {}^{W/X_k}\bar{\Phi}^{X_k^{\mathrm{cv}}}\cdot\frac{\partial^{X_k^{\mathrm{cv}}}\Phi^{X_0}}{\partial\phi_v^{X_i}}\cdot{}^{X_0}\bar{\Phi}^{X_k}\cdot{}^{\mathrm{a_L}}\underline{\bar{f}}^{X_k^{\mathrm{a}}}+{}^{W/X_k}\bar{\Phi}^{X_k^{\mathrm{cv}}}\cdot{}^{X_k^{\mathrm{cv}}}\bar{\Phi}^{X_0}\cdot\frac{\partial^{X_0}\Phi^{X_k}}{\partial\phi_v^{X_i}}\cdot{}^{\mathrm{a_L}}\underline{\bar{f}}^{X_k^{\mathrm{a}}}\Big)\end{aligned} \tag{B.231}$$

Equation B.171 tells that ${}^{W/X_k}\Phi^{X_k^{\mathrm{cv}}}$ can very well approximated by $\Phi_{\mathrm{z}}^{\mathrm{T}}(-\beta^{X_k})$. Further, ${}^{X_k^{\mathrm{cv}}}\bar{\Phi}^{X_0}$ is the product $\Phi_{\mathrm{x}}(\zeta^{X_k})\cdot\Phi_{\mathrm{z}}(-\beta^{X_k})$ of transformation matrices over the lead angle and minus the blade flap angle. The expression above can then be rewritten as:

$$\begin{aligned}\frac{\partial^{\mathrm{a_L}}\underline{f}_{"}^{W_m/X_k}}{\partial\phi_v^{X_i}} &= -\Big(\frac{\partial\Phi_{\mathrm{z}}^{\mathrm{T}}(-\beta^{X_k})}{\partial\phi_v^{X_i}}\cdot{}^{\mathrm{a_L}}\underline{\bar{f}}^{X_k^{\mathrm{a}}/\mathrm{cv}}+{}^{W/X_k}\Phi^{X_0}\cdot\frac{\partial^{X_0}\Phi^{X_k}}{\partial\phi_v^{X_i}}\cdot{}^{\mathrm{a_L}}\underline{\bar{f}}^{X_k^{\mathrm{a}}}+\\ &\quad \Phi_{\mathrm{z}}^{\mathrm{T}}(-\bar{\beta}^{X_k})\cdot\Big(\frac{\partial\Phi_{\mathrm{x}}(\zeta^{X_k})}{\partial\phi_v^{X_i}}\cdot\Phi_{\mathrm{z}}(-\bar{\beta}^{X_k})\cdot{}^{\mathrm{a_L}}\underline{\bar{f}}^{X_k^{\mathrm{a}}/0}+\Phi_{\mathrm{x}}(\bar{\zeta}^{X_k})\cdot\frac{\partial\Phi_{\mathrm{z}}(-\beta^{X_k})}{\partial\phi_v^{X_i}}\cdot{}^{\mathrm{a_L}}\underline{\bar{f}}^{X_k^{\mathrm{a}}/0}\Big)\Big)\end{aligned} \tag{B.232}$$

in which the following short hand notations are used:

$${}^{\mathrm{a_L}}\underline{\bar{f}}^{X_k^{\mathrm{a}}/\mathrm{cv}} = {}^{X_k^{\mathrm{cv}}}\bar{\Phi}^{X_0}\cdot{}^{X_0}\bar{\Phi}^{X_k}\cdot{}^{\mathrm{a_L}}\underline{\bar{f}}^{X_k^{\mathrm{a}}} \quad\text{and}\quad {}^{\mathrm{a_L}}\underline{\bar{f}}^{X_k^{\mathrm{a}}/0} = {}^{X_0}\bar{\Phi}^{X_k}\cdot{}^{\mathrm{a_L}}\underline{\bar{f}}^{X_k^{\mathrm{a}}}$$

For the sensitivities of the transformation matrices in the flap and lead angle holds:

$$\frac{\partial\Phi_{\mathrm{z}}(-\beta^{X_k})}{\partial\phi_v^{X_i}} = -\left.\frac{\mathrm{d}\Phi_{\mathrm{z}}}{\mathrm{d}\phi}\right|_{-\bar{\beta}^{X_k}}\cdot\frac{\partial\beta^{X_k}}{\partial\phi_v^{X_i}} \quad\text{and}\quad \frac{\partial\Phi_{\mathrm{x}}(\zeta^{X_k})}{\partial\phi_v^{X_i}} = \left.\frac{\mathrm{d}\Phi_{\mathrm{x}}}{\mathrm{d}\phi}\right|_{\bar{\zeta}^{X_k}}\cdot\frac{\partial\zeta^{X_k}}{\partial\phi_v^{X_i}}$$

The direct sensitivity of the force load reaction on the rotor annulus can be rewritten as:

$$\frac{\partial^{\mathrm{a_L}}\underline{f}_{"}^{W_m/X_k}}{\partial\phi_v^{X_i}} = \left[\frac{\partial^{\mathrm{a_L}}\underline{f}_{"}^{W_m/X_k}}{\partial\beta^{X_k}}\;\middle|\;\frac{\partial^{\mathrm{a_L}}\underline{f}_{"}^{W_m/X_k}}{\partial\zeta^{X_k}}\right]\cdot\begin{bmatrix}\dfrac{\partial\beta^{X_k}}{\partial\phi_v^{X_i}}\\[2ex]\dfrac{\partial\zeta^{X_k}}{\partial\phi_v^{X_i}}\end{bmatrix}-{}^{W/X_k}\bar{\Phi}^{X_0}\cdot\frac{\partial^{X_0}\Phi^{X_k}}{\partial\phi_v^{X_i}}\cdot{}^{\mathrm{a_L}}\underline{\bar{f}}^{X_k^{\mathrm{a}}} \tag{B.233}$$

with:

$$\begin{aligned}\frac{\partial^{\mathrm{a_L}}\underline{f}_{"}^{W_m/X_k}}{\partial\beta^{X_k}} &= \Phi_{\mathrm{z}}^{\mathrm{T}\prime}(-\bar{\beta}^{X_k})\cdot{}^{\mathrm{a_L}}\underline{\bar{f}}^{X_k^{\mathrm{a}}/\mathrm{cv}}+\Phi_{\mathrm{z}}^{\mathrm{T}}(-\bar{\beta}^{X_k})\cdot\Phi_{\mathrm{x}}(\bar{\zeta}^{X_k})\cdot\Phi_{\mathrm{z}}'(-\bar{\beta}^{X_k})\cdot{}^{\mathrm{a_L}}\underline{\bar{f}}^{X_k^{\mathrm{a}}/0}\\ \frac{\partial^{\mathrm{a_L}}\underline{f}_{"}^{W_m/X_k}}{\partial\zeta^{X_k}} &= -\Phi_{\mathrm{z}}^{\mathrm{T}}(-\bar{\beta}^{X_k})\cdot\Phi_{\mathrm{x}}'(\bar{\zeta}^{X_k})\cdot\Phi_{\mathrm{z}}(-\bar{\beta}^{X_k})\cdot{}^{\mathrm{a_L}}\underline{\bar{f}}^{X_k^{\mathrm{a}}/0}\end{aligned} \tag{B.234}$$

in which the following short hand notations are used:

$$\Phi_{\mathrm{z}}'(-\bar{\beta}^{X_k}) = \left.\frac{\mathrm{d}\Phi_{\mathrm{z}}}{\mathrm{d}\phi}\right|_{-\bar{\beta}^{X_k}} \quad\text{and}\quad \Phi_{\mathrm{z}}^{\mathrm{T}\prime}(-\bar{\beta}^{X_k}) = \left.\frac{\mathrm{d}\Phi_{\mathrm{z}}^{\mathrm{T}}}{\mathrm{d}\phi}\right|_{-\bar{\beta}^{X_k}} \quad\text{and}\quad \Phi_{\mathrm{x}}'(\bar{\zeta}^{X_k}) = \left.\frac{\mathrm{d}\Phi_{\mathrm{x}}}{\mathrm{d}\phi}\right|_{\bar{\zeta}^{X_k}}$$

The overall expression for the force load reaction on rotor annulus W_m in the intersection with blade element X_k is:

$${}^{\mathrm{a_L}}\underline{f}^{W_m/X_k} = {}^{\mathrm{a_L}}\underline{\bar{f}}^{W_m/X_k}+\frac{\partial^{\mathrm{a_L}}\underline{f}^{W_m/X_k}}{\partial\underline{u}_{\mathrm{per}}^{X}}\cdot\delta\underline{u}_{\mathrm{per}}^{X}+\frac{\partial^{\mathrm{a_L}}\underline{f}^{W_m/X_k}}{\partial\underline{u}_{\mathrm{sto}}^{W/X}}\cdot\underline{u}_{\mathrm{sto}}^{W/X}+\sum_{(\underline{z})}\frac{\partial^{\mathrm{a_L}}\underline{f}^{W_m/X_k}}{\partial\underline{z}}\cdot\delta\underline{z} \tag{B.235}$$

The summation over $\underline{z}$ involves ${}^{\mathrm{a_L}}\underline{q}_{\mathrm{f}}^{X_{\mathrm{FF}}}$, ${}^{\mathrm{a_L}}\underline{q}_{\mathrm{f}}^{X_{\mathrm{PP}}}$, $\underline{v}^{X_{\mathrm{FF}}^{\oplus}}$, $\underline{\omega}^{X_{\mathrm{FF}}^{\oplus}}$, $\underline{\phi}^{X_{\mathrm{FF}}}$, $\underline{\phi}^{X_{\mathrm{PP}}}$,$\underline{\phi}^{X}$, $\underline{\dot{\varphi}}^{X}$, $\underline{\dot{\varrho}}^{X}$, $\underline{u}_{\mathrm{im}}^{W}$ and $\underline{u}_{\mathrm{ori}}^{R}$.

For the mean values hold (see Eq. B.197) :

$$ {}^{\mathrm{a_L}}\bar{\underline{f}}^{W_m/X_k} \;=\; -^{W/X_k}\bar{\Phi}^{X_k} \,.\, {}^{\mathrm{a_L}}\bar{\underline{f}}^{X_k^{\mathrm{a}}} \tag{B.236} $$

For the periodic and stochastic variation sensitivities hold:

$$ \begin{aligned} \frac{\partial^{\mathrm{a_L}}\underline{f}^{W_m/X_k}}{\partial \underline{u}_{\mathrm{per}}^{X}} &= -^{W/X_k}\bar{\Phi}^{X_k} \cdot \frac{\partial^{\mathrm{a_L}}\underline{f}^{X_k^{\mathrm{a}}}}{\partial \underline{u}_{\mathrm{per}}^{X}} \\ \frac{\partial^{\mathrm{a_L}}\underline{f}^{W_m/X_k}}{\partial \underline{u}_{\mathrm{sto}}^{W/X}} &= -^{W/X_k}\bar{\Phi}^{X_k} \cdot \frac{\partial^{\mathrm{a_L}}\underline{f}^{X_k^{\mathrm{a}}}}{\partial \underline{u}_{\mathrm{sto}}^{W/X}} \end{aligned} \tag{B.237} $$

For the reactive sensitivities to $\underline{z} = {}^{\mathrm{a_L}}\underline{q}_{\mathrm{f}}^{X_{\mathrm{FF}}}$, ${}^{\mathrm{a_L}}\underline{q}_{\mathrm{f}}^{X_{\mathrm{PP}}}$, $\underline{v}^{X_{\mathrm{FF}}^{\oplus}}$, $\underline{\omega}^{X_{\mathrm{FF}}^{\oplus}}$, $\underline{\dot{\varphi}}^{X}$, $\underline{\dot{\varrho}}^{X}$, $\underline{u}_{\mathrm{im}}^{W}$ and $\underline{u}_{\mathrm{ori}}^{R}$ holds:

$$ \frac{\partial^{\mathrm{a_L}}\underline{f}^{W_m/X_k}}{\partial \underline{z}} \;=\; -^{W/X_k}\bar{\Phi}^{X_k} \cdot \frac{\partial^{\mathrm{a_L}}\underline{f}^{X_k^{\mathrm{a}}}}{\partial \underline{z}} \tag{B.238} $$

and for the sensitivities to $\underline{\phi}^{X_{\mathrm{FF}}}$, $\underline{\phi}^{X_{\mathrm{PP}}}$ and $\underline{\phi}^{X}$:

$$ \begin{aligned} \frac{\partial^{\mathrm{a_L}}\underline{f}^{W_m/X_k}}{\partial \underline{\phi}^{X_{\mathrm{FF}}}} &= -^{W/X_k}\bar{\Phi}^{X_k} \cdot \frac{\partial^{\mathrm{a_L}}\underline{f}^{X_k^{\mathrm{a}}}}{\partial \underline{\phi}^{X_{\mathrm{FF}}}} + \begin{cases} \text{<does not exist>} & \text{for k=1} \\ \mathrm{J}^{3}_{v=1}\left(\frac{\partial^{\mathrm{a_L}}\underline{f}_{,v}^{W_m/X_k}}{\partial \phi_v^{X_1}}\right) & \text{for k=2...N} \end{cases} \\ \frac{\partial^{\mathrm{a_L}}\underline{f}^{W_m/X_k}}{\partial \underline{\phi}^{X_{\mathrm{PP}}}} &= -^{W/X_k}\bar{\Phi}^{X_k} \cdot \frac{\partial^{\mathrm{a_L}}\underline{f}^{X_k^{\mathrm{a}}}}{\partial \underline{\phi}^{X_{\mathrm{PP}}}} \\ \frac{\partial^{\mathrm{a_L}}\underline{f}^{W_m/X_k}}{\partial \underline{\phi}^{X}} &= -^{W/X_k}\bar{\Phi}^{X_k} \cdot \frac{\partial^{\mathrm{a_L}}\underline{f}^{X_k^{\mathrm{a}}}}{\partial \underline{\phi}^{X}} + \begin{cases} \left[\mathrm{J}^{3}_{v=1}\left(\frac{\partial^{\mathrm{a_L}}\underline{f}_{,v}^{W_m/X_k}}{\partial \phi_v^{X_1}}\right) \;\; \mathrm{O}_{(2\ldots N)}\right] & \text{for k=1} \\ \left[\mathrm{O}_{(1)} \;\; \mathrm{J}^{k}_{i=2}\Big(\mathrm{J}^{3}_{v=1}\left(\frac{\partial^{\mathrm{a_L}}\underline{f}_{,v}^{W_m/X_k}}{\partial \phi_v^{X_i}}\right)\Big) \;\; \mathrm{O}_{(k+1\ldots N)}\right] & \text{for k=2...N} \end{cases} \end{aligned} \tag{B.239} $$

B.8 Transportation speed and Prandtl's correction factor

The general expression for the transportation speed $U^{W_m/X}$ through annulus W_m in the intersection with blade X, as well as for the beloning Prandtl's correction factor $F_{\mathrm{p}}^{W_m/X}$, were derived in section 3.5.2. The point of departure is set up by the mean wind speed, described relative to the coordinate system fixed to the (non-rotating) rotor plane and by the wind speed variations by turbulence and tower stagnation and wind shear. The mean wind speed is expressed along the (non-rotating) rotor plane's coordinate system in section B.8.1, in which the wind speed variations relative to the rotor plane are also dealt with. The mean, sensitivity functions and linearised input variations for Prandtl's correction factor are given in section B.8.2; this is done for the transportation speed in section B.8.3.

B.8.1 Wind speed coordinates in coordinate system fixed to the rotor plane

The average wind speed components in the 'fixed' coordinate system $\vec{e}^{\,R_{\mathrm{fx}}}$ result from the average compliance and the configuration angles of the support structure, together with the relative orientation of the wind field to the turbine base. The associated rotation dof

coordinate vector for the support structure S is $\underline{\phi}^{S}$. For the mean value $\underline{\bar{u}}^{R_{\rm fx}}$ holds:

$$\underline{\bar{u}}^{R_{\rm fx}} \triangleq \begin{bmatrix} \bar{U}_{\rm ax} \\ \bar{U}_{\rm yaw} \\ \bar{U}_{\rm tilt} \end{bmatrix} = \underline{\bar{u}}^{S_{\rm n}} = {}^{S_M}\Phi^{S_0}(\underline{\bar{\phi}}^{S}) \cdot {}^{B}\Phi^{A}_{(:,1)} \cdot \bar{U} \tag{B.240}$$

with:

$${}^{B}\Phi^{A} = \Phi_{\rm y}(-\theta^{B}) \cdot \Phi_{\rm z}(\gamma^{B}) \cdot \Phi^{\rm T}_{\rm z}(\gamma^{A}) \cdot \Phi^{\rm T}_{\rm y}(\theta^{A})$$

The linearised expression for the variation $\delta\underline{u}^{W_m/X/R_{\rm fx}}$ of the wind speed vector in the 'fixed' coordinate system $\vec{e}^{\,R_{\rm fx}}$ is built up from a purely stochastic and periodic contribution ($\delta\underline{u}^{X_k/R_{\rm fx}}_{\rm sto}$ and $\delta\underline{u}^{X_k/R_{\rm fx}}_{\rm per}$) and from a reactive contribution that is caused by by orientation changes ($\delta\underline{u}^{X_k/R_{\rm fx}}_{\rm ori}$):

$$\delta\underline{u}^{W_m/X/R_{\rm fx}} = \begin{bmatrix} \delta U^{W_m/X}_{\rm ax} \\ \delta U^{W_m/X}_{\rm yaw} \\ \delta U^{W_m/X}_{\rm tilt} \end{bmatrix} = \delta\underline{u}^{W_m/X/R_{\rm fx}}_{\rm sto} + \delta\underline{u}^{W_m/X/R_{\rm fx}}_{\rm per} + \delta\underline{u}^{W_m/X/R_{\rm fx}}_{\rm ori} \quad \text{(use Eq. B.242, B.246)} \tag{B.241}$$

Figure B.6 shows the assembly of contributions from the average wind speed, turbulence and periodic variations from the tower shadow and windshear (all longitudinal only). The periodic axial induction speed by oblique inflow, $U^{X_k}_{\rm i_o}$, is included in the scheme as well.

For the stochastic contributions to $\underline{u}^{W_m/X/R_{\rm fx}}$ see the stochastic wake model inputs in 3.4.2.

For the periodic contributions to $\underline{u}^{W_m/X/R_{\rm fx}}$ holds:

$$\delta\underline{u}^{W_m/X/R_{\rm fx}}_{\rm per} = \sum_{k=k_1(m)}^{k_{\rm end}(m)} \epsilon_{k(m)} \cdot \left({}^{S_M}\bar{\Phi}^{A}_{(:,1)} \cdot {}^{\rm r}u^{X^{\rm a}_k} - U^{X_k}_{\rm i_{obl}} \cdot \underline{e}_1 \right) \quad \text{(use Eq. B.248)} \tag{B.242}$$

For the stochastic variation sensitivity holds:

$$\frac{\partial\underline{u}^{W_m/X/R_{\rm fx}}}{\partial\underline{u}^{W/X/R_{\rm fx}}_{\rm sto}} = \left({\rm O}_{(1)} \ \ldots {\rm O}_{(m-1)} \ \boldsymbol{I} \ {\rm O}_{(m+1)} \ \ldots \ {\rm O}_{(P)} \right) \tag{B.243}$$

Just as for the blade relative wind speed, the element specific periodic wind speed variations relative to $R_{\rm fx}$ are collected in a large column vector $\underline{u}^{X/R_{\rm fx}}_{\rm per}$ for each blade:

$$\underline{u}^{X/R_{\rm fx}}_{\rm per} = \begin{bmatrix} \underline{u}^{X_1/R_{\rm fx}}_{\rm per} \\ \vdots \\ \underline{u}^{X_N/R_{\rm fx}}_{\rm per} \end{bmatrix} \tag{B.244}$$

The periodic variation sensitivity in the intersection of a rotor annulus with blade element X_k then becomes:

$$\frac{\partial\underline{u}^{W_m/X/R_{\rm fx}}}{\partial\underline{u}^{X/R_{\rm fx}}_{\rm per}} = \left({\rm O}_{(1)} \ \ldots {\rm O}_{(k_1(m)-1)} \ \epsilon_{k_1(m)}\boldsymbol{I} \ldots \epsilon_{k_{\rm end}(m)}\boldsymbol{I} \ {\rm O}_{(k_{\rm end}(m)+1)} \ \ldots \ {\rm O}_{(N)} \right) \tag{B.245}$$

The weighting factors $\epsilon_{k_1(m)} \ldots \epsilon_{k_{\rm end}(m)}$ specifiy the relative contribution of blade element k to annulus m. If the number of elements N amounts to twice the number of rotor annuli P then:

- for $m = 1$ holds $\epsilon_k = 1/3,\ 2/3$ with $k = 1,\ 2$;
- for $m > 1$ & $m < P$ holds $\epsilon_k = 1/2,\ 1/2$ with $k = 2(m-1)+1,\ 2m$;

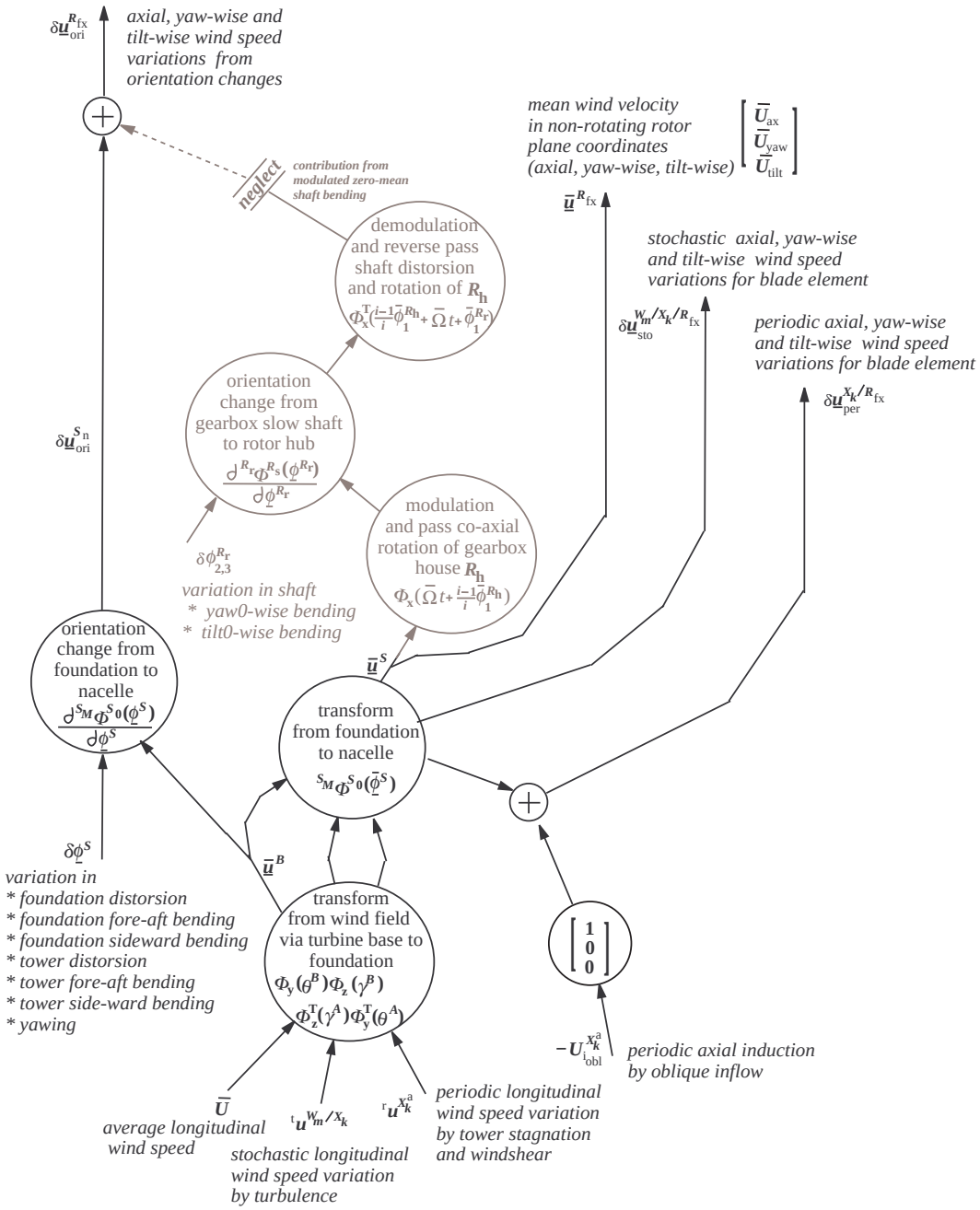

Figure B.6 *Wind speed coordinates in rotor plane from mean longitudinal wind speed and from turbulence, tower stagnation & wind shear and inductive reaction on oblique-inflow*

- for $m = P$ holds $\epsilon_k = {}_{2/3,\ 1/3}$ with $k = {}_{N-1,\ N}$.

AAs will be explained below, the rotation dof positions of only the *support structure* contribute to the 'orientation contributon' of the variation:

$$\delta \underline{u}_{\mathrm{ori}}^{W_m/X/R_{\mathrm{fx}}} \quad = \quad \delta \underline{u}_{\mathrm{ori}}^{S_{\mathrm{n}}} \qquad \text{(use Eq. B.164)} \tag{B.246}$$

No contribution by rotation dof positions of drive train:

- Next to the main rotation $\psi = \int^t \Omega t$, the rotor hub is deviated relative to the nacelle over the distorsion angle $\phi_1^{R_{\mathrm{r}}}$ and over the 'fed through' co-axial gearbox house rotation $\phi_3^{R_{\mathrm{h"}}}$. As we assume zero-mean main shaft bending, the rotations do *not* contribute to the *linearised* reactive wind speed variations along the axes of $\vec{e}^{\,R_{\mathrm{fx}}}$.
- While $\phi_1^{R_{\mathrm{r}}}$ and $\phi_3^{R_{\mathrm{h"}}}$ *do not* contribute to the reactive variations, the variations of the bending dofs $\phi_2^{R_{\mathrm{r}}}$ and $\phi_3^{R_{\mathrm{r}}}$ actually *do* contribute, but they are *modulated*:

$$\begin{aligned}
&\frac{\partial \underline{u}^{R_{\mathrm{fx}}}}{\partial \underline{\phi}^{R_{\mathrm{r}}}} \cdot \delta \underline{\phi}^{R_{\mathrm{r}}} \quad = \quad \cos \bar{\Omega} t \cdot \Phi_{\mathrm{x}}^{\mathrm{T}}(\bar{\phi}_1^{R_{\mathrm{r}}} + \bar{\phi}_3^{R_{\mathrm{h"}}}) \cdot \\
&\left(\left[\begin{array}{ccc|ccc|ccc} 0&0&0&0&\cos&-\sin&0&\sin&\cos \\ 0&0&0&1&0&0&0&0&0 \\ 0&0&0&0&0&0&1&0&0 \end{array} \right]_{\bar{\phi}_1^{R_{\mathrm{r}}}} \cdot (I_3 \otimes \Phi_{\mathrm{x}}(\phi_3^{R_{\mathrm{h"}}}) \cdot {}^{S_M}\bar{\Phi}^A_{(:,1)} \cdot \bar{U}) \right) \cdot \delta \underline{\bar{\phi}}^{R_{\mathrm{r}}} + \\
&\sin \bar{\Omega} t \cdot \Phi_{\mathrm{x}}^{\mathrm{T}}(\bar{\phi}_1^{R_{\mathrm{r}}} + \bar{\phi}_3^{R_{\mathrm{h"}}}) \cdot \\
&\left(\left[\begin{array}{ccc|ccc|ccc} 0&0&0&0&\sin&\cos&0&-\cos&\sin \\ 0&0&0&0&0&0&-1&0&0 \\ 0&0&0&1&0&0&0&0&0 \end{array} \right]_{\bar{\phi}_1^{R_{\mathrm{r}}}} \cdot (I_3 \otimes \Phi_{\mathrm{x}}(\bar{\phi}_3^{R_{\mathrm{h"}}}) \cdot {}^{S_M}\bar{\Phi}^A_{(:,1)} \cdot \bar{U}) \right) \cdot \delta \underline{\phi}^{R_{\mathrm{r}}}
\end{aligned} \tag{B.247}$$

The symbol '$\otimes$' implies the Kronecker product, which generates a 9×3 matrix with 3×1 columns equal to $\Phi_{\mathrm{x}}(\bar{\phi}_3^{R_{\mathrm{h"}}}) \cdot {}^{S_M}\bar{\Phi}^A_{(:,1)} \cdot \bar{U}$, diagonally ranked. The contribution by these modulated variations are neglected for the same reason as is done for their modulated contribution to the blade relative wind velocity (see 2nd and 3rd term in right hand side of Eq. B.166). Then, the 'orientation contribution' $\delta \underline{u}_{\mathrm{ori}}^{X_k/R_{\mathrm{fx}}}$ to the wind speed variation in the rotor plane becomes equal to the 'feedthrough windspeed variation by orientation change' $\delta \underline{u}_{\mathrm{ori}}^{S_{\mathrm{n}}}$ of the support structure, as in Eq. B.246.

In linearised sense, the periodic axial induction speed $U_{\mathrm{i_o}}^{X_k}$ is a purely periodic 'external input'. This is the case because we neglect the influence of the variation in the oblique-inflow angle χ^{X_k} and in the annulus-average axial induction speed $U_{\mathrm{i_m}}^{W_m}$. These both quantities would affect $U_{\mathrm{i_o}}^{X_k}$ *after modulation* by the 'on-average periodic' value-component of $U_{\mathrm{i_o}}^{X_k}$. We neglect the effect of these modulated variations for the same reason as mentioned above; their contribution is expected to be very small. The now

purely periodic assumed $U_{\mathrm{i_o}}^{W_m/X}$ is then determined as follows:

$$U_{\mathrm{i_o}}^{W_m/X} = \bar{U}_{\mathrm{i}}^{W_m} \cdot \begin{cases} \frac{15\pi}{64} \cdot \frac{\bar{r}^{W_m}}{\bar{R}} \cdot \tan(\bar{\chi}^{W_m}/2) \cdot \cos(\tilde{\boldsymbol{\Psi}}^X + \bar{\boldsymbol{\Psi}}_{\mathrm{off}}^{W_m}) & \text{(a)} \\ a_1 \cos(\tilde{\boldsymbol{\Psi}}^X + \bar{\boldsymbol{\Psi}}_{\mathrm{off}}^{W_k} - \Delta_1 \boldsymbol{\Psi}) + \\ \qquad a_2 \cos(2(\tilde{\boldsymbol{\Psi}}^X + \bar{\boldsymbol{\Psi}}_{\mathrm{off}}^{W_m}) - \Delta_2 \boldsymbol{\Psi}) & \text{(b)} \end{cases}$$

with:

$$\begin{aligned} \bar{\chi}^{W_m} &= \arctan \frac{\sqrt{(\bar{U}_{\mathrm{yaw}})^2 + (\bar{U}_{\mathrm{tilt}})^2}}{\bar{U}_{\mathrm{ax}} - \bar{U}_{\mathrm{i}}^{W_m}} \\ \tilde{\psi}^X &= \bar{\boldsymbol{\Omega}} \cdot t + \bar{\phi}_3^{R_{\mathrm{h}}} + \bar{\phi}_1^{R_{\mathrm{r}}} + {}^{R_{\mathrm{r}}}\psi^{X_0} \\ \bar{\psi}_{\mathrm{off}}^{W_m} &= -\arctan \frac{\bar{U}_{\mathrm{tilt}}}{\bar{U}_{\mathrm{yaw}}} \end{aligned} \tag{B.248}$$

Note:

- The axial, transverse and vertical components $\{U_{\mathrm{ax}}^{X_k},\ U_{\mathrm{yaw}}^{X_k},\ U_{\mathrm{tilt}}^{X_k} | X = D, E, F\}$ of the undisturbed wind speed on the rotor blade elements in rotor annulus m size the oblique inflow induction part $U_{\mathrm{i_o}}$ through the oblique inflow angle χ of rotor annulus m (case $B = 3$). The parameters in the right hand factor in the expression for $U_{\mathrm{i_o}}$ are the same as applied in PHATAS in function 'f_{skew}' [10]. Option (a) implies the parametrisation by Glauert while (b) implies a '2-harmonics engineering model' based on measured oblique inflow effects by Schepers and Vermeer [12].
- The oblique inflow induction contribution $U_{\mathrm{i_o}}$ becomes purely periodic because all inflow and wind turbine conditions are assumed constant in the expession for $U_{\mathrm{i_o}}$. Location and or time dependent variations in the undisturbed wind speed affect the oblique inflow angle χ as well as the azimut offset angle ψ_{off} for annulus W_m. The wake dynamics affect the ensemble average of the axial induction speed U_{i} in annulus W_m. The structural dynamic wind turbine behaviour affects the purely periodic course of the azimut angle ψ of rotor blade element X_k. If we took into account these effects, the oblique induction term $U_{\mathrm{i_o}}$ would cause modulated influences of variations in structural and input variables. These are an order of magnitude smaller than the periodic components in $U_{\mathrm{i_o}}$ and *will be neglected in TURBU Offshore*. We also neglect the variation of the azimut angle over the blade span. The now purely periodic assumed $U_{\mathrm{i_o}}^{W_m/X}$ is determined by Eq. B.248

B.8.2 Mean, sensitivities and input variations for Prandtl's correction factor

The following linearised expression holds for Prandtl's tip correction factor in the intersection of annulus W_m with blade element X_k (see section 3.4.2 for the relationship between the turbulence wake model input $\underline{u}_{\mathrm{sto}}^{W/X/R_{\mathrm{fx}}}$ and the annulus longitudinal wind speed vector ${}^{\mathrm{t}}\underline{u}^{W/X}$):

$$\begin{aligned} F_{\mathrm{p}}^{W_m/X} = \bar{F}_{\mathrm{p}}^{W_m} &+ \frac{\partial F_{\mathrm{p}}^{W_m/X}}{\partial \underline{u}_{\mathrm{sto}}^{W/X/R_{\mathrm{fx}}}} \cdot \underline{u}_{\mathrm{sto}}^{W/X/R_{\mathrm{fx}}} + \frac{\partial F_{\mathrm{p}}^{W_m/X}}{\partial \underline{u}_{\mathrm{per}}^{X/R_{\mathrm{fx}}}} \cdot \underline{u}_{\mathrm{per}}^{X/R_{\mathrm{fx}}} + \\ &\frac{\partial F_{\mathrm{p}}^{W_m/X}}{\partial \underline{u}_{\mathrm{ori}}^{S_{\mathrm{n}}}} \cdot \delta \underline{u}_{\mathrm{ori}}^{S_{\mathrm{n}}} + \frac{\partial F_{\mathrm{p}}^{W_m/X}}{\partial U_{\mathrm{i_m}}^{W_m}} \cdot \delta U_{\mathrm{i_m}}^{W_m} \end{aligned} \tag{B.249}$$

with the mean correction factor given by (see Eq. B.240 for $\bar{U}_{\mathrm{ax,yaw,tilt}}$):

$$\begin{aligned}\bar{F}_{\mathrm{p}}^{W_m} &= \tfrac{2}{\pi}\cdot\arccos\left(\mathrm{e}^{-(\bar{R}-\bar{r}^{W_m})\pi/\bar{d}^{W_m}}\right)\cdot\tfrac{2}{\pi}\cdot\arccos\left(\mathrm{e}^{-(\bar{r}^{W_m}-R_{\mathrm{root}})\pi/\bar{d}^{W_m}}\right)\\ \text{with}\quad \bar{d}^{W_m} &= \frac{2\pi\bar{r}^{W_m}}{B}\cdot\frac{\sqrt{(\bar{U}_{\mathrm{ax}}-\bar{U}_{\mathrm{im}}^{W_m})^2+(\bar{U}_{\mathrm{yaw}})^2+(\bar{U}_{\mathrm{tilt}})^2}}{\sqrt{\left(\bar{\Omega}\cdot\bar{r}^{W_m}\right)^2+(\bar{U}_{\mathrm{ax}}-\bar{U}_{\mathrm{im}}^{W_m})^2+(\bar{U}_{\mathrm{yaw}})^2+(\bar{U}_{\mathrm{tilt}})^2}}\end{aligned} \tag{B.250}$$

and the sensitivities to the orientation change and axial induction speed variation given by (see Eq. 3.30 for the right hand side partial derivatives):

$$\begin{aligned}\frac{\partial F_{\mathrm{p}}^{W_m/X}}{\partial \underline{u}_{\mathrm{ori}}^{S_{\mathrm{n}}}} &\equiv \frac{\partial F_{\mathrm{p}}^{W_m/X}}{\partial \underline{u}_{\mathrm{ori}}^{W_m/X/R_{\mathrm{fx}}}} = \frac{\mathrm{d}F_{\mathrm{p}}^{W_m/X}}{\mathrm{d}d^{W_m/X}}\cdot\frac{\mathrm{d}d^{W_m/X}}{\mathrm{d}U_{\mathrm{tr"}}^{W_m/X}}\cdot\frac{\partial U_{\mathrm{tr"}}^{W_m/X}}{\partial \underline{u}^{W_m/X/R_{\mathrm{fx}}}}\\ \frac{\partial F_{\mathrm{p}}^{W_m/X}}{\partial U_{\mathrm{im}}^{W_m}} &= \frac{\mathrm{d}F_{\mathrm{p}}^{W_m/X}}{\mathrm{d}d^{W_m/X}}\cdot\frac{\mathrm{d}d^{W_m/X}}{\mathrm{d}U_{\mathrm{tr"}}^{W_m/X}}\cdot\frac{\partial U_{\mathrm{tr"}}^{W_m/X}}{\partial U_{\mathrm{im}}^{W_m}}\end{aligned} \tag{B.251}$$

and stochastic and periodic variation sensitivities (see Eq. 3.30, B.243 and B.245):

$$\begin{aligned}\frac{\partial F_{\mathrm{p}}^{W_m/X}}{\partial \underline{u}_{\mathrm{sto}}^{W/X/R_{\mathrm{fx}}}} &= \left(\frac{\mathrm{d}F_{\mathrm{p}}^{W_m/X}}{\mathrm{d}d^{W_m/X}}\cdot\frac{\mathrm{d}d^{W_m/X}}{\mathrm{d}U_{\mathrm{tr"}}^{W_m/X}}\cdot\frac{\partial U_{\mathrm{tr"}}^{W_m/X}}{\partial \underline{u}^{W_m/X/R_{\mathrm{fx}}}}\right)\cdot\frac{\partial \underline{u}^{W_m/X/R_{\mathrm{fx}}}}{\partial \underline{u}_{\mathrm{sto}}^{W/X/R_{\mathrm{fx}}}}\\ \frac{\partial F_{\mathrm{p}}^{W_m/X}}{\partial \underline{u}_{\mathrm{per}}^{X/R_{\mathrm{fx}}}} &= \left(\frac{\mathrm{d}F_{\mathrm{p}}^{W_m/X}}{\mathrm{d}d^{W_m/X}}\cdot\frac{\mathrm{d}d^{W_m/X}}{\mathrm{d}U_{\mathrm{tr"}}^{W_m/X}}\cdot\frac{\partial U_{\mathrm{tr"}}^{W_m/X}}{\partial \underline{u}^{W_m/X/R_{\mathrm{fx}}}}\right)\cdot\frac{\partial \underline{u}^{W_m/X/R_{\mathrm{fx}}}}{\partial \underline{u}_{\mathrm{per}}^{X/R_{\mathrm{fx}}}}\end{aligned} \tag{B.252}$$

B.8.3 Mean, sensitivities and input variations for transportation speed

The following linearised expression holds for the transportation speed in the intersection of annulus W_m with blade element X_k:

$$\begin{aligned}U_{\mathrm{tr}}^{W_m/X} = \bar{U}_{\mathrm{tr}}^{W_m} &+ \frac{\partial U_{\mathrm{tr}}^{W_m/X}}{\partial \underline{u}_{\mathrm{sto}}^{W/X/R_{\mathrm{fx}}}}\cdot\underline{u}_{\mathrm{sto}}^{W/X/R_{\mathrm{fx}}} + \frac{\partial U_{\mathrm{tr}}^{W_m/X}}{\partial \underline{u}_{\mathrm{per}}^{X/R_{\mathrm{fx}}}}\cdot\underline{u}_{\mathrm{per}}^{X/R_{\mathrm{fx}}} +\\ &\frac{\partial U_{\mathrm{tr}}^{W_m/X}}{\partial \underline{u}_{\mathrm{ori}}^{S_{\mathrm{n}}}}\cdot\delta\underline{u}_{\mathrm{ori}}^{S_{\mathrm{n}}} + \frac{\partial U_{\mathrm{tr}}^{W_m/X}}{\partial U_{\mathrm{im}}^{W_m}}\cdot\delta U_{\mathrm{im}}^{W_m}\end{aligned} \tag{B.253}$$

with the mean transportation speed given by (see Eq. B.249 for $\bar{F}_{\mathrm{p}}^{W_m}$ and Eq. B.240 for $\bar{U}_{\mathrm{ax,yaw,tilt}}^{X_k}$):

$$\bar{U}_{\mathrm{tr}}^{W_m} = \sqrt{(\bar{U}_{\mathrm{ax}}-\bar{F}_{\mathrm{p}}^{W_m}\cdot\bar{U}_{\mathrm{im}}^{W_m})^2+(\bar{U}_{\mathrm{yaw}})^2+(\bar{U}_{\mathrm{tilt}})^2} \tag{B.254}$$

and the sensitivities to the orientation change and axial induction speed variation given by (see Eq. 3.31 and for the right hand side partial derivatives):

$$\begin{aligned}\frac{\partial U_{\mathrm{tr}}^{W_m/X}}{\partial \underline{u}_{\mathrm{ori}}^{S_{\mathrm{n}}}} &= \frac{\partial U_{\mathrm{tr}}^{W_m/X}}{\partial \underline{u}^{W_m/X/R_{\mathrm{fx}}}} + \frac{\partial U_{\mathrm{tr}}^{W_m/X}}{\partial F_{\mathrm{p}}^{W_m/X}}\cdot\frac{\partial F_{\mathrm{p}}^{W_m/X}}{\partial \underline{u}^{W_m/X/R_{\mathrm{fx}}}}\\ \frac{\partial U_{\mathrm{tr}}^{W_m/X}}{\partial U_{\mathrm{im}}^{W_m}} &= \frac{\partial U_{\mathrm{tr}}^{W_m/X}}{\partial U_{\mathrm{im}}^{W_m}} + \frac{\partial U_{\mathrm{tr}}^{W_m/X}}{\partial F_{\mathrm{p}}^{W_m/X}}\cdot\frac{\partial F_{\mathrm{p}}^{W_m/X}}{\partial U_{\mathrm{im}}^{W_m}}\end{aligned} \tag{B.255}$$

and stochastic and periodic variation sensitivities (see Eq. 3.31, , B.243, B.245):

$$\begin{aligned}\frac{\partial U_{\mathrm{tr}}^{W_m/X}}{\partial \underline{u}_{\mathrm{sto}}^{W/X/R_{\mathrm{fx}}}} &= \left(\frac{\partial U_{\mathrm{tr}}^{W_m/X}}{\partial \underline{u}^{W_m/X/R_{\mathrm{fx}}}} + \frac{\partial U_{\mathrm{tr}}^{W_m/X}}{\partial F_{\mathrm{p}}^{W_m/X}}\cdot\frac{\partial F_{\mathrm{p}}^{W_m/X}}{\partial \underline{u}^{W_m/X/R_{\mathrm{fx}}}}\right)\cdot\frac{\partial \underline{u}^{W_m/X/R_{\mathrm{fx}}}}{\partial \underline{u}_{\mathrm{sto}}^{W/X/R_{\mathrm{fx}}}}\\ \frac{\partial U_{\mathrm{tr}}^{W_m/X}}{\partial \underline{u}_{\mathrm{per}}^{X/R_{\mathrm{fx}}}} &= \left(\frac{\partial U_{\mathrm{tr}}^{W_m/X}}{\partial \underline{u}^{W_m/X/R_{\mathrm{fx}}}} + \frac{\partial U_{\mathrm{tr}}^{W_m/X}}{\partial F_{\mathrm{p}}^{W_m/X}}\cdot\frac{\partial F_{\mathrm{p}}^{W_m/X}}{\partial \underline{u}^{W_m/X/R_{\mathrm{fx}}}}\right)\cdot\frac{\partial \underline{u}^{W_m/X/R_{\mathrm{fx}}}}{\partial \underline{u}_{\mathrm{per}}^{X/R_{\mathrm{fx}}}}\end{aligned} \tag{B.256}$$

B.9 Hydrodynamic loads

This section gives expressions for the sensitivities and input variations for concentrated forces and torques that are caused by the (zero-mean assumed) distributed hydrodynamic mass and drag forces. The general expressions were given in 3.8.3.

The load formulations for the distributed loads are listed in section B.9.1. The concentrated loads on a subcomponent appear also to depend on distributed loading on a *neighbouring* subcomponent. Section B.9.2 gives the formulations for these distributed 'export loads from neighbouring subcomponents'. Eventually, section B.9.3 lists the formulations of the pursued concentrated hydrodynamic loads.

B.9.1 Sensitivities and input variations for distributed loads

The hydrodanimic loads only depend on the zero-mean stochastic horizonatal wave speed and acceleration and on the zero-mean linear speed and acceleration of the tower element. Just as for the turbulence, we collect the wave speeds and accelerations on the distinghuised under water levels in 'overall wave speed and acceleration coordinate vectors'. We assume as many distinghuised under water levels as there are under water support structure elements (M_{uw}):

$$\underline{w}^{S}_{\mathrm{horz}} = \begin{bmatrix} w^{S^{\mathrm{h}}_1}_{\mathrm{horz}} \\ \vdots \\ w^{S^{\mathrm{h}}_{M_{\mathrm{uw}}}}_{\mathrm{horz}} \end{bmatrix} \; ; \quad \underline{\dot{w}}^{S}_{\mathrm{horz}} = \begin{bmatrix} \dot{w}^{S^{\mathrm{h}}_1}_{\mathrm{horz}} \\ \vdots \\ \dot{w}^{S^{\mathrm{h}}_{M_{\mathrm{uw}}}}_{\mathrm{horz}} \end{bmatrix} \tag{B.257}$$

For the wave speed and acceleration on element S_k then holds:

$$\begin{aligned} w^{S^{\mathrm{h}}_k}_{\mathrm{horz}} &= [\; 0_{(1)} \; \ldots \; 0_{(k-1)} \; 1 \; 0_{(k+1)} \; \ldots \; 0_{(M_{\mathrm{uw}})} \;] \cdot \underline{w}^{S}_{\mathrm{horz}} \\ \dot{w}^{S^{\mathrm{h}}_k}_{\mathrm{horz}} &= [\; 0_{(1)} \; \ldots \; 0_{(k-1)} \; 1 \; 0_{(k+1)} \; \ldots \; 0_{(M_{\mathrm{uw}})} \;] \cdot \underline{\dot{w}}^{S}_{\mathrm{horz}} \end{aligned} \tag{B.258}$$

The linearised expression for the distributed hydrodynamic load on element S_k is:

$$\begin{aligned} \underline{q}_{\mathrm{f}}^{S^{\mathrm{h}}_k} = {} & \frac{\partial \underline{q}_{\mathrm{f}}^{S^{\mathrm{h}}_k}}{\partial \underline{w}^{S}_{\mathrm{horz}}} \cdot \underline{w}^{S}_{\mathrm{horz}} + \frac{\partial \underline{q}_{\mathrm{f}}^{S^{\mathrm{h}}_k}}{\partial \underline{\dot{w}}^{S}_{\mathrm{horz}}} \cdot \underline{\dot{w}}^{S}_{\mathrm{horz}} + \frac{\partial \underline{q}_{\mathrm{f}}^{S^{\mathrm{h}}_k}}{\partial \underline{v}^{S^{\oplus}_{\mathrm{FF}}}} \cdot \delta \underline{v}^{S^{\oplus}_{\mathrm{FF}}} + \frac{\partial \underline{q}_{\mathrm{f}}^{S^{\mathrm{h}}_k}}{\partial \underline{a}^{S^{\oplus}_{\mathrm{FF}}}} \cdot \delta \underline{a}^{S^{\oplus}_{\mathrm{FF}}} + \\ & \frac{\partial \underline{q}_{\mathrm{f}}^{S^{\mathrm{h}}_k}}{\partial \underline{\varphi}^{S}} \cdot \underline{\varphi}^{S} + \frac{\partial \underline{q}_{\mathrm{f}}^{S^{\mathrm{h}}_k}}{\partial \underline{\varrho}^{S}} \cdot \underline{\varrho}^{S} + \frac{\partial \underline{q}_{\mathrm{f}}^{S^{\mathrm{h}}_k}}{\partial \underline{\ddot{\varrho}}^{S}} \cdot \underline{\ddot{\varrho}}^{S} + \frac{\partial \underline{q}_{\mathrm{f}}^{S^{\mathrm{h}}_k}}{\partial \underline{\ddot{\varphi}}^{S}} \cdot \underline{\ddot{\varphi}}^{S} + \end{aligned} \tag{B.259}$$

For the stochastic variation sensitivities holds:

$$\begin{aligned} \frac{\partial \underline{q}_{\mathrm{f}}^{S^{\mathrm{h}}_k}}{\partial \underline{w}^{S}_{\mathrm{horz}}} &= \tfrac{1}{2}\rho_{\mathrm{H}} \cdot D^{S^{\mathrm{h}}_k} \cdot \underline{\boldsymbol{C}}^{S_k}_{\mathrm{V}_1} \cdot \sqrt{8/\pi} \cdot \sigma^{S^{\mathrm{h}}_k}_{w_{\mathrm{horz}}} \cdot [\; 0_{(1)} \; \ldots \; 0_{(k-1)} \; 1 \; 0_{(k+1)} \; \ldots \; 0_{(M_{\mathrm{uw}})} \;] \\ \frac{\partial \underline{q}_{\mathrm{f}}^{S^{\mathrm{h}}_k}}{\partial \underline{\dot{w}}^{S}_{\mathrm{horz}}} &= \tfrac{1}{4}\rho_{\mathrm{H}} \cdot \pi (D^{S^{\mathrm{h}}_k})^2 \cdot \underline{\boldsymbol{C}}^{S_k}_{\mathrm{M}_1} \cdot [\; 0_{(1)} \; \ldots \; 0_{(k-1)} \; 1 \; 0_{(k+1)} \; \ldots \; 0_{(M_{\mathrm{uw}})} \;] \end{aligned} \tag{B.260}$$

Coordinate vectors $\underline{\boldsymbol{C}}^{S_k}_{\mathrm{V}_1}$ and $\underline{\boldsymbol{C}}^{S_k}_{\mathrm{M}_1}$ represent the first column of the respective hydrodynamic coefficient matrices.

For the reactive sensitivities holds (see Eq. B.3, B.6 and B.5):

$$\begin{aligned} \frac{\partial \underline{q}_{\mathrm{f}}^{S^{\mathrm{h}}_k}}{\partial \underline{v}^{S^{\oplus}_{\mathrm{FF}}}} &= -\tfrac{1}{2}\rho_{\mathrm{H}} \cdot D^{S^{\mathrm{h}}_k} \cdot \boldsymbol{C}^{S_k}_{\mathrm{V}} \cdot \sqrt{8/\pi} \cdot \sigma^{S^{\mathrm{h}}_k}_{w_{\mathrm{horz}}} \cdot {}^{H}\bar{\Phi}^{S_k} \cdot \frac{\partial \underline{v}^{S^{\mathrm{h}}_k}}{\partial \underline{v}^{S^{\oplus}_{\mathrm{FF}}}} \\ \frac{\partial \underline{q}_{\mathrm{f}}^{S^{\mathrm{h}}_k}}{\partial \underline{a}^{S^{\oplus}_{\mathrm{FF}}}} &= -\tfrac{1}{4}\rho_{\mathrm{H}} \cdot \pi (D^{S^{\mathrm{h}}_k})^2 \cdot \boldsymbol{C}^{S_k}_{\mathrm{M}} \cdot \frac{C^{S^{\mathrm{h}}_k - 1}_{\mathrm{M}}}{C^{S^{\mathrm{h}}_k}_{\mathrm{M}}} \cdot {}^{H}\bar{\Phi}^{S_k} \cdot \frac{\partial \underline{a}^{S^{\mathrm{h}}_k}}{\partial \underline{a}^{S^{\oplus}_{\mathrm{FF}}}} \end{aligned} \tag{B.261}$$

and

$$\begin{aligned}\frac{\partial \underline{q}_{\mathrm{f}}^{S_k^{\mathrm{h}}}}{\partial \underline{\varphi}^{S}} &= -\tfrac{1}{2}\rho_{\mathrm{H}} \cdot D^{S_k^{\mathrm{h}}} \cdot \boldsymbol{C}_{\mathrm{V}}^{S_k} \cdot \sqrt{8/\pi} \cdot \sigma_{w_{\mathrm{horz}}}^{S_k^{\mathrm{h}}} \cdot {}^{H}\bar{\Phi}^{S_k} \cdot \frac{\partial \underline{v}^{S_k^{\mathrm{h}}}}{\partial \underline{\varphi}^{S}} \\ \frac{\partial \underline{q}_{\mathrm{f}}^{S_k^{\mathrm{h}}}}{\partial \underline{\varphi}^{S}} &= -\tfrac{1}{4}\rho_{\mathrm{H}} \cdot \pi (D^{S_k^{\mathrm{h}}})^2 \cdot \boldsymbol{C}_{\mathrm{M}}^{S_k} \cdot \frac{C_{\mathrm{M}}^{S_k^{\mathrm{h}}} - 1}{C_{\mathrm{M}}^{S_k^{\mathrm{h}}}} \cdot {}^{H}\bar{\Phi}^{S_k} \cdot \frac{\partial \underline{a}^{S_k^{\mathrm{h}}}}{\partial \underline{\varphi}^{S}}\end{aligned} \tag{B.262}$$

and

$$\begin{aligned}\frac{\partial \underline{q}_{\mathrm{f}}^{S_k^{\mathrm{h}}}}{\partial \underline{\varrho}^{S}} &= -\tfrac{1}{2}\rho_{\mathrm{H}} \cdot D^{S_k^{\mathrm{h}}} \cdot \boldsymbol{C}_{\mathrm{V}}^{S_k} \cdot \sqrt{8/\pi} \cdot \sigma_{w_{\mathrm{horz}}}^{S_k^{\mathrm{h}}} \cdot {}^{H}\bar{\Phi}^{S_k} \cdot \frac{\partial \underline{v}^{S_k^{\mathrm{h}}}}{\partial \underline{\varrho}^{S}} \\ \frac{\partial \underline{q}_{\mathrm{f}}^{S_k^{\mathrm{h}}}}{\partial \underline{\varrho}^{S}} &= -\tfrac{1}{4}\rho_{\mathrm{H}} \cdot \pi (D^{S_k^{\mathrm{h}}})^2 \cdot \boldsymbol{C}_{\mathrm{M}}^{S_k} \cdot \frac{C_{\mathrm{M}}^{S_k^{\mathrm{h}}} - 1}{C_{\mathrm{M}}^{S_k^{\mathrm{h}}}} \cdot {}^{H}\bar{\Phi}^{S_k} \cdot \frac{\partial \underline{a}^{S_k^{\mathrm{h}}}}{\partial \underline{\varrho}^{S}}\end{aligned} \tag{B.263}$$

The factor $\sqrt{8/\pi} \cdot \sigma_{w_{\mathrm{horz}}}^{S_k^{\mathrm{h}}}$ in the sensitivity to the relative water speed is mentioned and discussed in [5], appendix B.2.3. The standard deviation $\sigma_{w_{\mathrm{horz}}}^{S_k^{\mathrm{h}}}$ pertains to the horizontal wave speed on the underwater level corresponding to the average location of S_k^{h}.

B.9.2 Sensitivities and input variations for distributed 'export' loads

Just as a subcomponent in a rotor blade, the n^{th} subcomponent in the support structure has to 'export' the distributed loads on the first and last element $S_{k_1(n)}$ and $S_{k_{\mathrm{L}}(n)}$ (see section B.7.2). Besides it needs to import the distributed loads on the last element $k_{\mathrm{L}}(n-1)$ of the foregoing subcomponent and on the first element $k_1(n+1)$ of the subsequent subcomponent. The used notations for the hydrodynamic loads are:

- ${}^{\mathrm{h}}\underline{q}_{\mathrm{f}}^{S^{\ominus}_{\mathrm{PP}(n)}}$ and ${}^{\mathrm{h}}\underline{q}_{\mathrm{f}}^{S_{\mathrm{FF}(n)}}$ for export loads from $k_1(n)$ and $k_{\mathrm{L}}(n)$
- ${}^{\mathrm{h}}\underline{q}_{\mathrm{f}}^{S_{\mathrm{FF}(n-1)}}$ and ${}^{\mathrm{h}}\underline{q}_{\mathrm{f}}^{S^{\ominus}_{\mathrm{PP}(n+1)}}$ for import loads from $k_{\mathrm{L}}(n-1)$ and $k_1(n+1)$.

The mnemonics FF and PP stand for 'Final Foregoing' and 'Primary Post' (see discussion in section B.9.1 above Eq. 3.100).

Though the support structure is subdivided into three subcomponent, only the first two are involoved with hydrodynamic conversion: no. 1, the foundation S_{f} and no. 2, the tower S_{t}, so that:

- foundation S_{f} only imports ${}^{\mathrm{h}}\underline{q}_{\mathrm{f}}^{S^{\ominus}_{\mathrm{PP}(2)}}$ from tower S_{t};
- tower S_{t} only imports ${}^{\mathrm{h}}\underline{q}_{\mathrm{f}}^{S^{\ominus}_{\mathrm{FF}(1)}}$ from foundation S_{f}.

As already mentioned in section B.9.1, the export load from the first element to the foregoing subcomponent is to be expressed in coordinates along the final element of the foregoing subcomponent. This is not the case for the other export load. The following definitions thus hold:

$$\begin{aligned}{}^{\mathrm{h}}\underline{q}_{\mathrm{f}}^{S^{\ominus}_{\mathrm{PP}(n)}} &\triangleq \underline{q}_{\mathrm{f}}^{S_{k_1}^{\mathrm{h}}} \\ {}^{\mathrm{h}}\underline{q}_{\mathrm{f}}^{S_{\mathrm{FF}(n)}} &\triangleq \underline{q}_{\mathrm{f}}^{S_{k_{\mathrm{L}}}^{\mathrm{h}}}\end{aligned} \tag{B.264}$$

The linearised expression for both export loads is:

$$\begin{aligned}
{}^{\mathrm{h}}\underline{q}_{\mathrm{f}}^{S^{\ominus}_{\mathrm{PP}}} &= \frac{\partial^{\mathrm{h}}\underline{q}_{\mathrm{f}}^{S^{\ominus}_{\mathrm{PP}}}}{\partial \underline{w}^{S}_{\mathrm{horz}}} \cdot \delta\underline{w}^{S}_{\mathrm{horz}} + \frac{\partial^{\mathrm{h}}\underline{q}_{\mathrm{f}}^{S^{\ominus}_{\mathrm{PP}}}}{\partial \dot{\underline{w}}^{S}_{\mathrm{horz}}} \cdot \dot{\underline{w}}^{S}_{\mathrm{horz}} + \sum_{(\underline{z})} \frac{\partial^{\mathrm{a}}\underline{q}_{\mathrm{f}}^{S^{\ominus}_{\mathrm{BB}}}}{\partial \underline{z}} \cdot \delta\underline{z} \\
{}^{\mathrm{h}}\underline{q}_{\mathrm{f}}^{S_{\mathrm{FF}}} &= \frac{\partial^{\mathrm{h}}\underline{q}_{\mathrm{f}}^{S_{\mathrm{FF}}}}{\partial \underline{w}^{S}_{\mathrm{horz}}} \cdot \delta\underline{w}^{S}_{\mathrm{horz}} + \frac{\partial^{\mathrm{h}}\underline{q}_{\mathrm{f}}^{S_{\mathrm{FF}}}}{\partial \dot{\underline{w}}^{S}_{\mathrm{horz}}} \cdot \dot{\underline{w}}^{S}_{\mathrm{horz}} + \sum_{(\underline{z})} \frac{\partial^{\mathrm{a}}\underline{q}_{\mathrm{f}}^{S_{\mathrm{FF}}}}{\partial \underline{z}} \cdot \delta\underline{z}
\end{aligned} \tag{B.265}$$

The summation over $\underline{z}$ involves $\underline{v}^{S^{\oplus}_{\mathrm{FF}}}, \underline{a}^{S^{\oplus}_{\mathrm{FF}}}, \dot{\underline{\varphi}}^{S}, \dot{\underline{\varrho}}^{S}, \ddot{\underline{\varphi}}^{S}, \ddot{\underline{\varrho}}^{S}$.

For the stochastic variation sensitivities hold (see Eq. B.260 for $\partial \underline{q}_{\mathrm{f}}^{S^{\mathrm{h}}_{k}} / \partial \underline{w}^{S}_{\mathrm{horz}}$ and $\partial \underline{q}_{\mathrm{f}}^{S^{\mathrm{h}}_{k}} / \partial \dot{\underline{w}}^{S}_{\mathrm{horz}}$):

$$\begin{aligned}
\frac{\partial^{\mathrm{h}}\underline{q}_{\mathrm{f}}^{S^{\ominus}_{\mathrm{PP}}}}{\partial \underline{w}^{S}_{\mathrm{horz}}} &= {}^{S_{k_1-1}}\bar{\Phi}^{H} \cdot \frac{\partial \underline{q}_{\mathrm{f}}^{S^{\mathrm{h}}_{k_1}}}{\partial \underline{w}^{S}_{\mathrm{horz}}} \\
\frac{\partial^{\mathrm{h}}\underline{q}_{\mathrm{f}}^{S^{\ominus}_{\mathrm{PP}}}}{\partial \dot{\underline{w}}^{S}_{\mathrm{horz}}} &= {}^{S_{k_1-1}}\bar{\Phi}^{H} \cdot \frac{\partial \underline{q}_{\mathrm{f}}^{S^{\mathrm{h}}_{k_1}}}{\partial \dot{\underline{w}}^{S}_{\mathrm{horz}}} \\
\frac{\partial^{\mathrm{h}}\underline{q}_{\mathrm{f}}^{S_{\mathrm{FF}}}}{\partial \underline{w}^{S}_{\mathrm{horz}}} &= \frac{\partial \underline{q}_{\mathrm{f}}^{S^{\mathrm{h}}_{k_1}}}{\partial \underline{w}^{S}_{\mathrm{horz}}} \\
\frac{\partial^{\mathrm{h}}\underline{q}_{\mathrm{f}}^{S_{\mathrm{FF}}}}{\partial \dot{\underline{w}}^{S}_{\mathrm{horz}}} &= \frac{\partial \underline{q}_{\mathrm{f}}^{S^{\mathrm{h}}_{k_1}}}{\partial \dot{\underline{w}}^{S}_{\mathrm{horz}}}
\end{aligned} \tag{B.266}$$

For the reactive sensitivities holds (see Eq. B.261,B.262,B.263):

$$\begin{aligned}
\frac{\partial^{\mathrm{h}}\underline{q}_{\mathrm{f}}^{S^{\ominus}_{\mathrm{PP}}}}{\partial \underline{z}} &= \frac{\partial \underline{q}_{\mathrm{f}}^{S^{\mathrm{h}}_{k_1}}}{\partial \underline{z}} \\
\frac{\partial^{\mathrm{h}}\underline{q}_{\mathrm{f}}^{S_{\mathrm{FF}}}}{\partial \underline{z}} &= \frac{\partial \underline{q}_{\mathrm{f}}^{S^{\mathrm{h}}_{k_{\mathrm{L}}}}}{\partial \underline{z}}
\end{aligned} \tag{B.267}$$

B.9.3 Sensitivities and input variations for concentrated loads

The concentrated hydrodynamic loads on an element depend on the distributed loads on that very element *and* on the neighbouring elements. Thus a concentrated load may depend on 'input distributed loads' from the most nearby elements of the neighbouring subcomponents (${}^{\mathrm{h}}\underline{q}_{\mathrm{f}}^{S_{\mathrm{FF}}}$, ${}^{\mathrm{h}}\underline{q}_{\mathrm{f}}^{S^{\ominus}_{\mathrm{PP}}}$). A concentrated load also depends on one or two distributed loads within the actual subcomponent ($\underline{q}_{\mathrm{f}}^{S^{\mathrm{h}}_{k\pm1}}$). The latter makes a concentrated load to depend on the waves on more than *one* under water level. This made us to introduce the overall wave speed and acceleration coordinate vectors in Eq. B.257. The linearized expressions for the concentrated hydrodynamic loads are:

$$\begin{aligned}
{}^{\mathrm{h}}\underline{f}^{S^{\mathrm{h}}_{k}} &= \frac{\partial^{\mathrm{h}}\underline{f}^{S^{\mathrm{h}}_{k}}}{\partial \underline{w}^{S}_{\mathrm{horz}}} \cdot \underline{w}^{S}_{\mathrm{horz}} + \frac{\partial^{\mathrm{h}}\underline{f}^{S^{\mathrm{h}}_{k}}}{\partial \dot{\underline{w}}^{S}_{\mathrm{horz}}} \cdot \dot{\underline{w}}^{S}_{\mathrm{horz}} + \sum_{(\underline{z})} \frac{\partial^{\mathrm{h}}\underline{f}^{S^{\mathrm{h}}_{k}}}{\partial \underline{z}} \cdot \delta\underline{z} \\
{}^{\mathrm{h}}\underline{t}^{S^{\mathrm{h}}_{k}} &= \frac{\partial^{\mathrm{h}}\underline{t}^{S^{\mathrm{h}}_{k}}}{\partial \underline{w}^{S}_{\mathrm{horz}}} \cdot \underline{w}^{S}_{\mathrm{horz}} + \frac{\partial^{\mathrm{h}}\underline{t}^{S^{\mathrm{h}}_{k}}}{\partial \dot{\underline{w}}^{S}_{\mathrm{horz}}} \cdot \dot{\underline{w}}^{S}_{\mathrm{horz}} + \sum_{(\underline{z})} \frac{\partial^{\mathrm{h}}\underline{t}^{S^{\mathrm{h}}_{k}}}{\partial \underline{z}} \cdot \delta\underline{z}
\end{aligned} \tag{B.268}$$

in which $\underline{z}$ involves ${}^{\mathrm{h}}\underline{q}_{\mathrm{f}}^{S_{\mathrm{FF}}}$, ${}^{\mathrm{h}}\underline{q}_{\mathrm{f}}^{S^{\ominus}_{\mathrm{PP}}}$, $\underline{v}^{S^{\oplus}_{\mathrm{FF}}}$, $\underline{a}^{S^{\oplus}_{\mathrm{FF}}}$, $\dot{\underline{\varphi}}^{S}$, $\dot{\underline{\varrho}}^{S}$, $\ddot{\underline{\varphi}}^{S}$ and $\ddot{\underline{\varrho}}^{S}$.

For the stochastic variation sensitivities holds ($\underline{\zeta} = \underline{w}^{S}_{\mathrm{horz}},\ \underline{\dot{w}}^{S}_{\mathrm{horz}}$; see also Eq. B.260):

$$\frac{\partial^{\mathrm{h}}\underline{f}^{S^{\mathrm{h}}_k}}{\partial\underline{\zeta}} = {}^{S}{}_{k}\bar{\Phi}^{H}\cdot{}^{\mathrm{h}}G^{\mathrm{F}}_{\mathrm{fq}_{k,0}}\cdot\frac{\partial\underline{q}_{\mathrm{f}}^{S^{\mathrm{h}}_k}}{\partial\underline{\zeta}} + \delta_{k\downarrow k^{\oplus}_{\mathrm{FF}}+1}\cdot{}^{S}{}_{k}\bar{\Phi}^{H}\cdot{}^{\mathrm{h}}G^{\mathrm{F}}_{\mathrm{fq}_{k,-1}}\cdot\frac{\partial\underline{q}_{\mathrm{f}}^{S^{\mathrm{h}}_{k-1}}}{\partial\underline{\zeta}} + \delta_{k\uparrow k^{\ominus}_{\mathrm{PP}}-1}\cdot{}^{S}{}_{k}\bar{\Phi}^{H}\cdot{}^{\mathrm{h}}G^{\mathrm{F}}_{\mathrm{fq}_{k,+1}}\cdot\frac{\partial\underline{q}_{\mathrm{f}}^{S^{\mathrm{h}}_{k+1}}}{\partial\underline{\zeta}} \tag{B.269}$$

and

$$\frac{\partial^{\mathrm{h}}\underline{t}^{S^{\mathrm{h}}_k}}{\partial\underline{\zeta}} = {}^{S}{}_{k}\bar{\Phi}^{H}\cdot{}^{\mathrm{h}}G^{\mathrm{F}}_{\mathrm{tq}_{k,0}}\cdot\frac{\partial\underline{q}_{\mathrm{f}}^{S^{\mathrm{h}}_k}}{\partial\underline{\zeta}} + \delta_{k\downarrow k^{\oplus}_{\mathrm{FF}}+1}\cdot{}^{S}{}_{k}\bar{\Phi}^{H}\cdot{}^{\mathrm{h}}G^{\mathrm{F}}_{\mathrm{tq}_{k,-1}}\cdot\frac{\partial\underline{q}_{\mathrm{f}}^{S^{\mathrm{h}}_{k-1}}}{\partial\underline{\zeta}} + \delta_{k\uparrow k^{\ominus}_{\mathrm{PP}}-1}\cdot{}^{S}{}_{k}\bar{\Phi}^{H}\cdot{}^{\mathrm{h}}G^{\mathrm{F}}_{\mathrm{tq}_{k,+1}}\cdot\frac{\partial\underline{q}_{\mathrm{f}}^{S^{\mathrm{h}}_{k+1}}}{\partial\underline{\zeta}} \tag{B.270}$$

For the sensitivity to the distributed loads on the foregoing subcomponent holds:

$$\begin{aligned}\frac{\partial^{\mathrm{h}}\underline{f}^{S^{\mathrm{h}}_k}}{\partial^{\mathrm{h}}\underline{q}_{\mathrm{f}}^{S_{\mathrm{FF}}}} &= \delta_{(k,k_{\mathrm{FF}}\oplus)}\cdot\delta_{k_{\mathrm{FF}}\downarrow 1}\cdot{}^{S}{}_{k}\bar{\Phi}^{H}\cdot{}^{\mathrm{h}}G^{\mathrm{F}}_{\mathrm{fq}_{k,-1}}\\ \frac{\partial^{\mathrm{h}}\underline{t}^{S^{\mathrm{h}}_k}}{\partial^{\mathrm{h}}\underline{q}_{\mathrm{f}}^{S_{\mathrm{FF}}}} &= \delta_{(k,k_{\mathrm{FF}}\oplus)}\cdot\delta_{k_{\mathrm{FF}}\downarrow 1}\cdot{}^{S}{}_{k}\bar{\Phi}^{H}\cdot{}^{\mathrm{h}}G^{\mathrm{F}}_{\mathrm{tq}_{k,-1}}\end{aligned} \tag{B.271}$$

and to the distributed loads on the subsequent subomponent:

$$\begin{aligned}\frac{\partial^{\mathrm{h}}\underline{f}^{S^{\mathrm{h}}_k}}{\partial^{\mathrm{h}}\underline{q}_{\mathrm{f}}^{S^{\ominus}_{\mathrm{PP}}}} &= \delta_{(k,k^{\ominus}_{\mathrm{PP}})}\cdot\delta_{k_{\mathrm{PP}}\uparrow N}\cdot{}^{S}{}_{k}\Phi^{H}\cdot{}^{\mathrm{h}}G^{\mathrm{F}}_{\mathrm{fq}_{k,+1}}\\ \frac{\partial^{\mathrm{h}}\underline{t}^{S^{\mathrm{h}}_k}}{\partial^{\mathrm{h}}\underline{q}_{\mathrm{f}}^{S^{\ominus}_{\mathrm{PP}}}} &= \delta_{(k,k^{\ominus}_{\mathrm{PP}})}\cdot\delta_{k_{\mathrm{PP}}\uparrow N}\cdot{}^{S}{}_{k}\Phi^{H}\cdot{}^{\mathrm{h}}G^{\mathrm{F}}_{\mathrm{tq}_{k,+1}}\end{aligned} \tag{B.272}$$

For the remaining sensitivities holds ($\underline{z} = \underline{v}^{S^{\oplus}_{\mathrm{FF}}}, \underline{a}^{S^{\oplus}_{\mathrm{FF}}}, \underline{\dot{\varphi}}^{S}, \underline{\dot{\varrho}}^{S}, \underline{\ddot{\varphi}}^{S}, \underline{\ddot{\varrho}}^{S}$; see Eq. B.261,B.262,B.263) :

$$\frac{\partial^{\mathrm{h}}\underline{f}^{S^{\mathrm{h}}_k}}{\partial\underline{z}} = {}^{S}{}_{k}\bar{\Phi}^{H}\cdot{}^{\mathrm{h}}G^{\mathrm{F}}_{\mathrm{fq}_{k,0}}\cdot\frac{\partial\underline{q}_{\mathrm{f}}^{S^{\mathrm{h}}_k}}{\partial\underline{z}} + \delta_{k\downarrow k^{\oplus}_{\mathrm{FF}}+1}\cdot{}^{S}{}_{k}\bar{\Phi}^{H}\cdot{}^{\mathrm{h}}G^{\mathrm{F}}_{\mathrm{fq}_{k,-1}}\cdot\frac{\partial\underline{q}_{\mathrm{f}}^{S^{\mathrm{h}}_{k-1}}}{\partial\underline{z}} + \delta_{k\uparrow k^{\ominus}_{\mathrm{PP}}-1}\cdot{}^{S}{}_{k}\bar{\Phi}^{H}\cdot{}^{\mathrm{h}}G^{\mathrm{F}}_{\mathrm{fq}_{k,+1}}\cdot\frac{\partial\underline{q}_{\mathrm{f}}^{S^{\mathrm{h}}_{k+1}}}{\partial\underline{z}} \tag{B.273}$$

and:

$$\frac{\partial^{\mathrm{h}}\underline{t}^{S^{\mathrm{h}}_k}}{\partial\underline{z}} = {}^{S}{}_{k}\bar{\Phi}^{H}\cdot{}^{\mathrm{h}}G^{\mathrm{F}}_{\mathrm{tq}_{k,0}}\cdot\frac{\partial\underline{q}_{\mathrm{f}}^{S^{\mathrm{h}}_k}}{\partial\underline{z}} + \delta_{k\downarrow k^{\oplus}_{\mathrm{FF}}+1}\cdot{}^{S}{}_{k}\bar{\Phi}^{H}\cdot{}^{\mathrm{h}}G^{\mathrm{F}}_{\mathrm{tq}_{k,-1}}\cdot\frac{\partial\underline{q}_{\mathrm{f}}^{S^{\mathrm{h}}_{k-1}}}{\partial\underline{z}} + \delta_{k\uparrow k^{\ominus}_{\mathrm{PP}}-1}\cdot{}^{S}{}_{k}\bar{\Phi}^{H}\cdot{}^{\mathrm{h}}G^{\mathrm{F}}_{\mathrm{tq}_{k,+1}}\cdot\frac{\partial\underline{q}_{\mathrm{f}}^{S^{\mathrm{h}}_{k+1}}}{\partial\underline{z}} \tag{B.274}$$

B.10 Gravity loads

In section B.5 on the blade relative wind speed it was shown that its coordinates along the local coordinate systems of the blade elements were sensitive to orientation changes between the elements in the support structure, drive-train and rotor blade. This also holds in linearised sense because of the mean value of the longitudinal wind speed. Thus first

order variations in rotation degrees of freedom yield first order variations in the blade relative wind speed coordinates. The on-average rotation of the main shaft transforms the mean transverse and vertical wind speed components into periodic coordinates along the local coordinate systems.

The coordinates of the gravitation $\vec{g}$ along the elements' coordinate systems are subjected to a similar sensitivity on orientation changes. Linearised elaboration yields mean values and sensitivities to rotation dofs for the gravity force coordinate vectors on all elements. In addition, *periodic* gravity force coordinate variations appear for the rotor shaft & hub ($R_{\rm r}$) and the rotor blade elements.

The linearised expressions for the coordinate vectors of the gravitation along the coordinate systems of all elements is derived in section B.10.2. The corresponding gravity load coordinates follow straightforward from the gravitation coordinates. Sections B.10.2, B.10.3 and B.10.4 list the expessions for the mean, sensitivities (and periodic variations) of the gravity loads on the support structure, rotor shaft & hub, and rotor blades.

B.10.1 General expressions for gravition coordinates

The compliance and configuration of the support structure S cause variations in the gravition coordinate vector along the coordinate system on element S_k. This is caused by the orientation difference with the (fixed) geographic coordinate system $\vec{e}^{\,G}_{(.)}$. For the gravitation holds:

$$\vec{g} = {\rm g} \cdot \vec{e}^{\,G}_3 \qquad \text{(g: downward gravity acceleration)} \tag{B.275}$$

In the linearised approximation it is allowed to split up the gravitation coordinate vector $\underline{\rm g}^{S_k}$ (along the coordinate system of S_k) into a mean and reactive part. This reactive part depends on orientation changes via the position variation of the relevant rotation dofs in $\underline{\phi}^S$. For the linearised gravitation coordinates along any support structure element holds:

$$\begin{aligned} \underline{g}^{S_k} &= \bar{\underline{g}}^{S_k} + \delta \underline{g}^{S_k}_{\rm ori} \quad \text{with} \quad \bar{\underline{g}}^{S_k} = {}^{S_k}\Phi^{S_0} \cdot {}^{B}\underline{\Phi}^{G}_3 \cdot {\rm g} \quad \text{and} \quad \delta \underline{g}^{S_k}_{\rm ori} = \sum_{i=1}^{k} \sum_{v=1}^{3} \frac{\partial \underline{g}^{S_k}}{\partial \phi_v^{S_i}} \cdot \delta \phi_v^{S_i} \\ \text{while} \quad \frac{\partial \underline{g}^{S_k}}{\partial \phi_v^{S_i}} &= \frac{\partial {}^{S_k}\Phi^{S_0}}{\partial \phi_v^{S_i}} \cdot {}^{B}\underline{\Phi}^{G}_3 \cdot {\rm g} \quad \text{with} \quad {}^{B}\Phi^{G} = \Phi_{\rm y}(-\theta^B) \cdot \Phi_{\rm z}(\gamma^B) \end{aligned} \tag{B.276}$$

Section B.2 tells in the paragraphs on the kinematics of the gearbox house $R_{\rm h}$ and generator rotor $R_{\rm f}$ that all their mass parameters except the co-axial moment of inertia are moved to the nacelle. In addition the gearbox slow shaft $R_{\rm s}$ is assumed mass-less. So expressions for the gravity loads are not required for the subcomponents $R_{\rm h}$, $R_{\rm f}$ and $R_{\rm s}$. We only need the gravitation coordinates for the 'one element subcomponent' rotor shaft & hub $R_{\rm r}$. It appears that only the part $(i_{\rm gb}-1)/i_{\rm gb}$ of the co-axial gearbox house rotation is fed through into the main shaft rotation. Coordinate vector $\underline{g}^{R_{\rm h''}}$ contains the gravitation coordinates that are obtained after transformation over all rotation dofs in the support structure and over the fed-through gearbox house rotation $\phi_3^{R_{\rm h''}}$; these coordinates are identified as axial, transverse and vertical (see also section B.5.2).

For the mean value $\bar{\underline{g}}^{R_{\mathrm{h}"}}$ and linearised variation $\delta\underline{g}_{\mathrm{ori}}^{R_{\mathrm{h}"}}$ holds:

$$\begin{aligned}
\bar{\underline{g}}^{R_{\mathrm{h}"}} &\triangleq \begin{bmatrix} \bar{g}_{\mathrm{ax}}^{"} \\ \bar{g}_{\mathrm{yaw}}^{"} \\ \bar{g}_{\mathrm{tilt}}^{"} \end{bmatrix} &= {}^{R_{\mathrm{h}"}}\bar{\underline{\Phi}}_3^{G} \cdot \mathrm{g} \\
\delta\underline{g}_{\mathrm{ori}}^{R_{\mathrm{h}"}} &\triangleq \begin{bmatrix} \delta g_{\mathrm{ax}}^{"} \\ \delta g_{\mathrm{yaw}}^{"} \\ \delta g_{\mathrm{tilt}}^{"} \end{bmatrix} &= \frac{\partial \underline{g}^{R_{\mathrm{h}"}}}{\partial \phi_3^{R_{\mathrm{h}"}}} \cdot \delta\phi_3^{R_{\mathrm{h}"}} + \delta\underline{g}_{\mathrm{ori}}^{S_{\mathrm{n}}}
\end{aligned} \tag{B.277}$$

$$\begin{aligned}
\text{with} \quad {}^{R_{\mathrm{h}"}}\bar{\Phi}^{G} &= \Phi_{\mathrm{x}}(\bar{\phi}_3^{R_{\mathrm{h}"}}) \cdot {}^{S}{}_{M}\bar{\Phi}^{S_0} \cdot {}^{B}\Phi^{G} \\
\frac{\partial \underline{g}^{R_{\mathrm{h}"}}}{\partial \phi_3^{R_{\mathrm{h}"}}} &= \frac{\mathrm{d}\Phi_{\mathrm{x}}}{\mathrm{d}\phi}\bigg|_{\bar{\phi}_3^{R_{\mathrm{h}"}}} \cdot {}^{S}{}_{M}\bar{\underline{\Phi}}_3^{G} \cdot \mathrm{g}
\end{aligned}$$

The coordinate vector variation $\delta\underline{g}^{R_{\mathrm{h}"}}$ is fed forward to the (on-average rotating) rotor shaft & hub R_{r}. We also define the feed forward gravitation variaton in the rotating coordinate system on the slow gearbox shaft. Equation 3.65 shows the split-up of the transformation over the main rotation $\bar{\Omega}t$ into a constant part and harmonic part:

$$\delta\underline{g}_{\mathrm{ori}}^{R_{\tilde{\mathrm{h}}"}} \triangleq \left(\delta\vec{u}_{\mathrm{ori}}^{R_{\mathrm{h}"}}\right)^{R_{\mathrm{s}}} = (\Phi_{\mathrm{d}} + \Phi_{\mathrm{c}} \cdot \cos\bar{\Omega}t + \Phi_{\mathrm{s}} \cdot \sin\bar{\Omega}t) \cdot \delta\underline{g}_{\mathrm{ori}}^{R_{\mathrm{h}"}} \tag{B.278}$$

The gravitation coordinates $\underline{g}^{R_{\mathrm{r}}}$ on the rotor shaft & hub are assembled from:

- variations $\delta\underline{g}_{\mathrm{ori}}^{R_{\tilde{\mathrm{h}}"}}$ by the orientation changes in the support structure and gearbox house;
- variations by orientation changes via azimut variation $\psi - \bar{\Omega}t$ and shaft deformation $\underline{\phi}^{R_{\mathrm{r}}}$ (see Eq. B.37);
- mean gravitation coordinates along coordinate system $\vec{e}^{\,R_{\mathrm{h}"}}$ after transformation over main rotation $\bar{\Omega}t$.

Just as the implemented kinematics of & hub R_{r} in section B.2.1, the reactive gravity variation for R_{r} by the angulars dofs in the drive-train is split-up in its own angular dofs in $\underline{\varphi}^{R_{\mathrm{r}}}$ and the import angular dof $\underline{\phi}_{\mathrm{x}}^{R_{\mathrm{f}}}$ ($= \psi - \bar{\Omega}t$) from the generatoro rotor and fast shaft R_{f}.

The following linearised expression holds for $\underline{g}^{R_{\mathrm{r}}}$:

$$\begin{aligned}
\underline{g}^{R_{\mathrm{r}}} &= \bar{\underline{g}}^{R_{\mathrm{r}}} + \delta\underline{g}_{\mathrm{per}}^{R_{\mathrm{r}}} + \delta\underline{g}_{\mathrm{ori}}^{R_{\mathrm{r}}} \qquad \text{with} \\
\bar{\underline{g}}^{R_{\mathrm{r}}} &= {}^{R_{\mathrm{r}}}\bar{\Phi}^{R_{\mathrm{s}}} \cdot \Phi_{\mathrm{d}} \cdot \bar{\underline{g}}^{R_{\mathrm{h}"}} \\
\delta\underline{g}_{\mathrm{per}}^{R_{\mathrm{r}}} &= {}^{R_{\mathrm{r}}}\bar{\Phi}^{R_{\mathrm{s}}} \cdot (\Phi_{\mathrm{c}} \cdot \cos\bar{\Omega}t + \Phi_{\mathrm{s}} \cdot \sin\bar{\Omega}t) \cdot \bar{\underline{g}}^{R_{\mathrm{h}"}} \\
\delta\underline{g}_{\mathrm{ori}}^{R_{\mathrm{r}}} &= \frac{\partial \underline{g}^{R_{\mathrm{r}}}}{\partial \underline{\phi}^{R_{\mathrm{r}}}} \cdot \delta\underline{\phi}^{R_{\mathrm{r}}} + \frac{\partial \underline{g}^{R_{\mathrm{r}}}}{\partial \phi_{\mathrm{x}}^{R_{\mathrm{f}}}} \cdot \delta\phi_{\mathrm{x}}^{R_{\mathrm{f}}} + {}^{R_{\mathrm{r}}}\bar{\Phi}^{R_{\mathrm{s}}} \cdot \delta\underline{g}_{\mathrm{ori}}^{R_{\tilde{\mathrm{h}}"}}
\end{aligned} \tag{B.279}$$

The purely periodic variation follows from the average tiltwise (and minor yawwise) gravitation components in the rotor plane (see Eq. B.277).

Just as is shown in the left side of figure B.4 for the blade relative wind speed, the varying shaft deformation $\delta\underline{\phi}^{R_{\mathrm{r}}}$ contributes now to the reactive *gravitation* variation on the rotor hub. This occurs via the axial and modulated yaw- and tiltwise *mean* gravitation components. The ranking order of shaft deformations is distorsion in $\phi_1^{R_{\mathrm{r}}}$, yaw0-wise bending in $\phi_2^{R_{\mathrm{r}}}$ and tilt0-wise bending in $\phi_3^{R_{\mathrm{r}}}$. Under the assumed zero-mean shaft bending

the contribution of $\delta\underline{\phi}^{R_r}$ to $\delta\underline{g}^{R}_{\rm ori}$ becomes (only the average distorsion $\bar{\phi}_1^{R_r}$ contributes to ${}^{R_r}\bar{\Phi}^{R_s}$).

$$\frac{\partial \underline{g}^{R_r}}{\partial \underline{\phi}^{R_r}} \cdot \delta\underline{\phi}^{R_r} = \bar{g}^{"}_{\rm ax} \cdot \begin{pmatrix} 0 & 0 & 0 \\ 0 & -1 & 0 \\ 0 & 0 & 1 \end{pmatrix} \cdot \delta\underline{\phi}^{R_r} +$$

$$\left(\bar{g}^{"}_{\rm yaw} \cdot \begin{pmatrix} 0 & \cos & \sin \\ -\sin & 0 & 0 \\ -\cos & 0 & 0 \end{pmatrix}_{\bar{\phi}_1^{R_r}} + \bar{g}^{"}_{\rm tilt} \cdot \begin{pmatrix} 0 & \sin & -\cos \\ \cos & 0 & 0 \\ -\sin & 0 & 0 \end{pmatrix}_{\bar{\phi}_1^{R_r}} \right) \cdot \cos\bar{\Omega}t \cdot \delta\underline{\phi}^{R_r} +$$

$$\left(-\bar{g}^{"}_{\rm yaw} \cdot \begin{pmatrix} 0 & \sin & -\cos \\ \cos & 0 & 0 \\ -\sin & 0 & 0 \end{pmatrix}_{\bar{\phi}_1^{R_r}} + \bar{g}^{"}_{\rm tilt} \cdot \begin{pmatrix} 0 & \cos & \sin \\ -\sin & 0 & 0 \\ -\cos & 0 & 0 \end{pmatrix}_{\bar{\phi}_1^{R_r}} \right) \cdot \sin\bar{\Omega}t \cdot \delta\underline{\phi}^{R_r} \tag{B.280}$$

The orientation change by shaft bending via the modulated mean yaw- and tiltwise gravitation components is neglected because of numerical treatment: it is not possible to eliminate periodic coefficients on 'rotating degrees of freedom like shaft bending' from the homogeneous model equations. This would make it necessary to apply Floquent analysis for 3 bladed wind turbines also. The tiltwise gravitation component is dominant. If periodic (de)stiffening of the rotor shaft in vertical sense is a relevant phenonemon as concerns the overall dynamic behaviour, it will be no longer allowed to eliminate these periodic coefficients and Floquet analysis will be required.

The approximated expression for the sensitivity of the gravitation coordinates on the rotor hub to the rotation dofs in the drive-train then becomes (note that variation $\varphi_{\rm x}^{R_f}$ in the main shaft rotation and main shaft distorsion $\varphi_1^{R_r}$ are along the x-axis!):

$$\frac{\partial \underline{g}^{R_r}}{\partial \underline{\phi}^{R_r}} = \bar{g}^{"}_{\rm ax} \cdot \begin{pmatrix} 0 & 0 & 0 \\ 0 & -1 & 0 \\ 0 & 0 & 1 \end{pmatrix} \quad ; \quad \frac{\partial \underline{g}^{R_r}}{\partial \phi_{\rm x}^{R_f}} = \bar{g}^{"}_{\rm ax} \cdot \begin{pmatrix} 0 \\ 0 \\ 0 \end{pmatrix} \tag{B.281}$$

The gravitation coordinates $\underline{g}^{X_k}$ on a rotor blade element are assembled from:

- variations $\delta\underline{g}^{R_r}_{\rm ori}$ by the orientation changes in the support structure, gearbox house and main shaft & hub;
- variations by orientation changes via the rotation dofs $\underline{\phi}^{X}$ in the rotor blade;
- mean and periodic gravitation coordinates along coordinate system $\vec{e}^{\,R_r}$.

The linearised expression for $\underline{g}^{X_k}$ is:

$$\begin{aligned} \underline{g}^{X_k} &= \bar{\underline{g}}^{X_k} + \delta\underline{g}^{X_k}_{\rm per} + \delta\underline{g}^{X_k}_{\rm ori} \qquad \text{with} \\ \bar{\underline{g}}^{X_k} &= {}^{X_k}\bar{\Phi}^{X_0} \cdot {}^{X_0}\bar{\Phi}^{R_r} \cdot \bar{\underline{g}}^{R_r} \\ \delta\underline{g}^{X_k}_{\rm per} &= {}^{X_k}\bar{\Phi}^{X_0} \cdot \delta\underline{g}^{X}_{\rm per} \qquad (\delta\underline{g}^{X}_{\rm per} = {}^{X_0}\bar{\Phi}^{R_r} \cdot \delta\underline{g}^{R_r}_{\rm per}) \\ \delta\underline{g}^{X_k}_{\rm ori} &= \sum_{i=1}^{k}\sum_{v=1}^{3} \frac{\partial \underline{g}^{X_k}}{\partial \phi_v^{X_i}} \cdot \delta\phi_v^{X_i} + {}^{X_k}\bar{\Phi}^{X_0} \cdot {}^{X_0}\bar{\Phi}^{R_r} \cdot \delta\underline{g}^{R_r}_{\rm ori} \end{aligned} \tag{B.282}$$

The gravitation variation via $\delta\underline{\phi}^{X}$ occurs via the *average* gravitation coordinates $\bar{\underline{g}}^{R_r}$. As a matter of fact $\delta\underline{\phi}^{X}$ also cause gravitation variation via the purely periodic coordinates $\delta\underline{g}^{R_r}_{\rm per}$:

$$\frac{\partial \underline{g}^{X_k}}{\partial \phi_v^{X_i}} = \frac{\partial {}^{X_k}\Phi^{X_0}}{\partial \phi_v^{X_i}} \cdot ({}^{X_0}\bar{\Phi}^{R_r} \cdot \left(\bar{\underline{g}}^{R_r} + \delta\underline{g}^{X}_{\rm per}\right) \tag{B.283}$$

Because the tiltwise gravitation component is dominant, the modulated variation of $\underline{\phi}^X$, via $\delta \underline{u}_{\mathrm{per}}^{R_{\mathrm{r}}}$, models the periodical (de)stiffening of the rotor blades in lead-lag sense by the gravitation. If this is a relevant phenonemon for the dynamic behaviour, it will be required to take into account these periodic coefficients and apply Floquet analysis or Harmonic Balancing. Up till now, the contribution by the modulated variation of $\underline{\phi}^X$ is neglected for the same reason as is done for the the modulated varation of $\underline{\phi}^R$.

B.10.2 Mean and sensitivities for gravity loads on support structure

The linearised expression for the gravity force on element S_k is:

$$ {}^{\mathrm{g}}\underline{f}^{S_k^*} \;=\; {}^{\mathrm{g}}\underline{\bar{f}}^{S_k^*} + \frac{\partial\, {}^{\mathrm{g}}\underline{f}^{S_k^*}}{\partial \underline{g}_{\mathrm{ori}}^{S_{\mathrm{FF}}}} \cdot \delta \underline{g}_{\mathrm{ori}}^{S_{\mathrm{FF}}} + \frac{\partial\, {}^{\mathrm{g}}\underline{f}^{S_k^*}}{\partial \underline{\phi}^{S}} \cdot \delta \underline{\phi}^{S} \tag{B.284} $$

with mean (see Eq. B.277 for $\underline{\bar{g}}^{S_k}$):

$$ {}^{\mathrm{g}}\underline{\bar{f}}^{S_k^*} \;=\; m^{S_k} \cdot \underline{\bar{g}}^{S_k} \tag{B.285} $$

and sensitivities:

$$ \frac{\partial\, {}^{\mathrm{g}}\underline{f}^{S_k^*}}{\partial \underline{g}_{\mathrm{ori}}^{S_{\mathrm{FF}}}} \;=\; \begin{cases} \text{<does not exist>} & (\text{for } k=1) \\ m^{S_k} \cdot {}^{S_k}\bar{\Phi}^{S_1} & (\text{for } k=2\ldots M-1) \\ (m^{S_M} + m^{R_{\mathrm{h}}} + m^{R_{\mathrm{f}}}) \cdot {}^{S_M}\bar{\Phi}^{S_{M-1}} & (\text{for } k=M) \end{cases} $$

$$ \frac{\partial\, {}^{\mathrm{g}}\underline{f}^{S_k^*}}{\partial \underline{\phi}^{S}} \;=\; \begin{cases} [\,\mathrm{J}_{v=1}^{3}(\frac{\partial^{S_1}\Phi^{S_0}}{\partial \phi_v^{S_1}} \cdot {}^{B}\underline{\Phi}_3^{G} \cdot m^{S_1} \cdot \mathrm{g})\;\; \mathrm{O}_{(2)} \ldots \mathrm{O}_{(M)}\,] & (\text{for } k=1) \\ (\;\mathrm{O}_{(1)}\;\; \mathrm{J}_{i=2}^{k}\big(\mathrm{J}_{v=1}^{3}(\frac{\partial^{S_k}\Phi^{S_0}}{\partial \phi_v^{S_i}} \cdot {}^{B}\underline{\Phi}_3^{G} \cdot m^{S_k} \cdot \mathrm{g})\big)\;\; \mathrm{O}_{(k+1\ldots M)}\;) & (\text{for } k=2\ldots M-1) \\ (\;\mathrm{O}_{(1\ldots M-1)}\;\; \mathrm{J}_{v=1}^{3}(\frac{\partial^{S_M}\Phi^{S_0}}{\partial \phi_v^{S_M}} \cdot {}^{B}\underline{\Phi}_3^{G} \cdot (m^{S_M} + m^{R_{\mathrm{h}}} + m^{R_{\mathrm{f}}}) \cdot \mathrm{g})\;) & (\text{for } k=M) \end{cases} \tag{B.286} $$

while:

$$ \delta \underline{g}_{\mathrm{ori}}^{S_{\mathrm{FF}}} = \begin{cases} \delta \underline{g}_{\mathrm{ori}}^{S_{\mathrm{n}}} \;=\; \frac{\partial \underline{g}^{S_M}}{\partial \underline{\phi}^{S}} \cdot \delta \underline{\phi}^{S} + {}^{S_M}\bar{\Phi}^{S_{M-1}} \cdot \delta \underline{g}_{\mathrm{ori}}^{S_{\mathrm{t}}} & \text{for } \underline{g}_{\mathrm{ori}}^{R_{\mathrm{h}}"} \\ \delta \underline{g}_{\mathrm{ori}}^{S_{\mathrm{t}}} \;=\; \frac{\partial \underline{g}^{S_{M-1}}}{\partial \underline{\phi}^{S}} \cdot \delta \underline{\phi}^{S} + {}^{S_{M-1}}\bar{\Phi}^{S_1} \cdot \delta \underline{g}_{\mathrm{ori}}^{S_{\mathrm{f}}} & \text{for } {}^{\mathrm{g}}\underline{f}^{S_M} \\ \delta \underline{g}_{\mathrm{ori}}^{S_{\mathrm{f}}} \;=\; \frac{\partial \underline{g}_{\mathrm{ori}}^{S_1}}{\partial \underline{\phi}^{S}} \cdot \delta \underline{\phi}^{S} & \text{for } {}^{\mathrm{g}}\underline{f}^{S_{2\ldots M-1}} \end{cases} \tag{B.287} $$

with:

$$ \begin{aligned} \frac{\partial \underline{g}^{S_M}}{\partial \underline{\phi}^{S}} &= [\mathrm{O}_{(1)} \ldots \mathrm{O}_{(M-1)}\;\; \mathrm{J}_{v=1}^{3}(\frac{\partial^{S_M}\Phi^{S_{M-1}}}{\partial \phi_v^{S_M}} \cdot {}^{S_{M-1}}\underline{\bar{\Phi}}_3^{G} \cdot \mathrm{g})] \\ \frac{\partial \underline{g}^{S_{M-1}}}{\partial \underline{\phi}^{S}} &= [\mathrm{O}_{(1)}\;\; \mathrm{J}_{i=2}^{M-1}\big(\mathrm{J}_{v=1}^{3}(\frac{\partial^{S_{M-1}}\Phi^{S_1}}{\partial \phi_v^{S_i}} \cdot {}^{S_1}\underline{\bar{\Phi}}_3^{G} \cdot \mathrm{g})\big)\;\; \mathrm{O}_{(M)}] \\ \frac{\partial \underline{g}^{S_1}}{\partial \underline{\phi}^{S}} &= [\mathrm{J}_{v=1}^{3}(\frac{\partial^{S_1}\Phi^{S_0}}{\partial \phi_v^{S_1}} \cdot {}^{B}\underline{\Phi}_3^{G} \cdot \mathrm{g})\;\; \mathrm{O}_{(2)} \ldots \mathrm{O}_{(M)}] \end{aligned} \tag{B.288} $$

B.10.3 Mean, sensitivities and input variations for gravity loads on rotor hub

The linearised expression for the gravity force on the 'one element subcomponent' R_{r} is (see Eq. B.278 and B.277 for $\delta \underline{g}_{\mathrm{ori}}^{R_{\tilde{\mathrm{h}}"}}$):

$$ {}^{\mathrm{g}}\underline{f}^{R_{\mathrm{r}}^*} = {}^{\mathrm{g}}\bar{\underline{f}}^{R_{\mathrm{r}}^*} + \frac{\partial^{\mathrm{g}}\underline{f}_{\mathrm{per}}^{R_{\mathrm{r}}^*}}{\partial \underline{g}_{\mathrm{per}}^{R_{\mathrm{r}}}} \cdot \delta \underline{g}_{\mathrm{per}}^{R_{\mathrm{r}}} + \frac{\partial^{\mathrm{g}}\underline{f}^{R_{\mathrm{r}}^*}}{\partial \underline{g}_{\mathrm{ori}}^{R_{\tilde{\mathrm{h}}"}}} \cdot \delta \underline{g}_{\mathrm{ori}}^{R_{\tilde{\mathrm{h}}"}} + \frac{\partial^{\mathrm{g}}\underline{f}^{R_{\mathrm{r}}^*}}{\partial \underline{\phi}^{R_{\mathrm{r}}}} \cdot \delta \underline{\phi}^{R_{\mathrm{r}}} \tag{B.289} $$

with mean (use Eq. B.279 and see Eq. B.277 for $\bar{\underline{g}}^{R_{\mathrm{h}"}}$):

$$ {}^{\mathrm{g}}\bar{\underline{f}}^{R_{\mathrm{r}}^*} = m^{R_{\mathrm{r}}} \cdot {}^{R_{\mathrm{r}}}\bar{\Phi}^{R_{\mathrm{s}}} \cdot \Phi_{\mathrm{d}} \cdot \bar{\underline{g}}^{R_{\mathrm{h}"}} \tag{B.290} $$

and periodic variation sensitivity (see Eq. B.279 for $\underline{g}_{\mathrm{per}}^{R_{\mathrm{h}"}}$):

$$ \frac{\partial^{\mathrm{g}}\underline{f}_{\mathrm{per}}^{R_{\mathrm{r}}^*}}{\partial \underline{g}_{\mathrm{per}}^{R_{\mathrm{r}}}} = m^{R_{\mathrm{r}}} \tag{B.291} $$

and reactive sensitivities (use Eq. B.281):

$$ \begin{aligned} \frac{\partial^{\mathrm{g}}\underline{f}^{R_{\mathrm{r}}^*}}{\partial \underline{g}_{\mathrm{ori}}^{R_{\tilde{\mathrm{h}}"}}} &= {}^{R_{\mathrm{r}}}\bar{\Phi}^{R_{\mathrm{s}}} \cdot m^{R_{\mathrm{r}}} \\ \frac{\partial^{\mathrm{g}}\underline{f}^{R_{\mathrm{r}}^*}}{\partial \underline{\phi}^{R_{\mathrm{r}}}} &= m^{R_{\mathrm{r}}} \cdot \bar{g}_{\mathrm{ax}}^{"} \cdot \begin{pmatrix} 0 & 0 & 0 \\ 0 & -1 & 0 \\ 0 & 0 & 1 \end{pmatrix} \end{aligned} \tag{B.292} $$

B.10.4 Mean, sensitivities and input variations for gravity loads on blade elements

The linearised expression for the gravity force on blade element X_k is (see Eq. B.279 and B.281 for $\delta \underline{g}_{\mathrm{ori}}^{R_{\mathrm{r}}}$):

$$ {}^{\mathrm{g}}\underline{f}^{X_k^*} = {}^{\mathrm{g}}\bar{\underline{f}}^{X_k^*} + \frac{\partial^{\mathrm{g}}\underline{f}^{X_k^*}}{\partial \underline{g}_{\mathrm{per}}^{X}} \cdot \delta \underline{g}_{\mathrm{per}}^{R_{\mathrm{r}}} + \frac{\partial^{\mathrm{g}}\underline{f}^{X_k^*}}{\partial \underline{g}_{\mathrm{ori}}^{X_{\mathrm{FF}}}} \cdot \delta \underline{g}_{\mathrm{ori}}^{X_{\mathrm{FF}}} + \frac{\partial^{\mathrm{g}}\underline{f}^{X_k^*}}{\partial \underline{\phi}^{X}} \cdot \delta \underline{\phi}^{X} \tag{B.293} $$

with mean (use Eq. B.282, B.279 and see Eq. B.277 for $\bar{\underline{g}}^{R_{\mathrm{h}"}}$):

$$ {}^{\mathrm{g}}\bar{\underline{f}}^{X_k^*} = {}^{X_k}\bar{\Phi}^{X_0} \cdot {}^{X_0}\Phi^{R_{\mathrm{r}}} \cdot {}^{R_{\mathrm{r}}}\bar{\Phi}^{R_{\mathrm{s}}} \cdot \Phi_{\mathrm{d}} \cdot m^{X_k} \cdot \bar{\underline{g}}^{R_{\mathrm{h}"}} \tag{B.294} $$

and periodic variation sensitivity (see Eq. B.279 for $\delta \underline{g}_{\mathrm{per}}^{R_{\mathrm{r}}}$):

$$ \frac{\partial^{\mathrm{g}}\underline{f}_{\mathrm{per}}^{X_k^*}}{\partial \underline{g}_{\mathrm{per}}^{X}} = {}^{X_k}\bar{\Phi}^{X_0} \cdot m^{X_k} \tag{B.295} $$

and reactive sensitivities (use Eq. B.281, Eq. B.283):

$$ \begin{aligned} \frac{\partial^{\mathrm{g}}\underline{f}^{X_k^*}}{\partial \underline{g}_{\mathrm{ori}}^{X_{\mathrm{FF}}}} &= \begin{cases} m^{X_k} \cdot {}^{X_1}\bar{\Phi}^{X_0} & \text{for } k = 1 \\ m^{X_k} \cdot {}^{X_k}\bar{\Phi}^{X_1} & \text{for } k = 2 \ldots N \end{cases} \\ \frac{\partial^{\mathrm{g}}\underline{f}^{X_k^*}}{\partial \underline{\phi}^{X}} &= \begin{cases} \left(\mathrm{J}_{v=1}^{3}\left(\frac{\partial^{X_1}\Phi^{X_0}}{\partial \phi_v^{X_1}} \cdot {}^{X_0}\bar{\Phi}^{R_{\mathrm{r}}} \cdot m^{X_k} \cdot \bar{\underline{g}}^{R_{\mathrm{r}}}\right) \ \mathrm{O}_{(2)} \ldots \mathrm{O}_{(N)} \right) & \text{for } k = 1 \\ \left(\mathrm{O}_{(1)} \ \mathrm{J}_{i=2}^{k}\left(\mathrm{J}_{v=1}^{3}\left(\frac{\partial^{X_k}\Phi^{X_0}}{\partial \phi_v^{X_i}} \cdot {}^{X_0}\bar{\Phi}^{R_{\mathrm{r}}} \cdot m^{X_k} \cdot \bar{\underline{g}}^{R_{\mathrm{r}}}\right) \ \mathrm{O}_{(k+1\ldots N)} \right) & \text{for } k = 2 \ldots N \end{cases} \end{aligned} \tag{B.296} $$

while

$$\delta \underline{g}_{\mathrm{ori}}^{X_{\mathrm{FF}}} = \begin{cases} \delta \underline{g}_{\mathrm{ori}}^{X_{\mathrm{f}}} = \frac{\partial \underline{g}^{X_1}}{\partial \underline{\phi}^{X}} \cdot \delta \underline{\phi}^{X} + {}^{X_1}\bar{\Phi}^{R_{\mathrm{r}}} \cdot \delta \underline{g}_{\mathrm{ori}}^{R_{\mathrm{r}}} & \text{for } {}^{\mathrm{g}}\underline{f}^{X_{2\ldots N}} \\ {}^{X_0}\bar{\Phi}^{R_{\mathrm{r}}} \cdot \delta \underline{g}_{\mathrm{ori}}^{R_{\mathrm{r}}} & \text{for } {}^{\mathrm{g}}\underline{f}^{X_1} \end{cases} \tag{B.297}$$

with

$$\frac{\partial \underline{g}^{X_1}}{\partial \underline{\phi}^{X}} = \left(\mathrm{J}_{v=1}^{3} \left(\frac{\partial^{X_1}\Phi^{X_0}}{\partial \phi_v^{X_1}} \cdot {}^{X_0}\bar{\Phi}^{R_{\mathrm{r}}} \cdot \bar{\underline{g}}^{R_{\mathrm{r}}} \right) \ \mathrm{O}_{(2)} \ldots \mathrm{O}_{(N)} \right) \tag{B.298}$$

APPENDIX C. DISTRIBUTED AERODYNAMIC LOADING

```
%  SBBT-equivalent mapping of distributed to concentrated aerodynamic loads
%  ------------------------------------------------------------------------
%  As concerns the distributed aerodynamic loading we pursue the following:
%   * mb-element X10 behaves slender beam bending theory equivalent to
%     to physical blade partition P9 via connector @o10
%   * valid feedthrough of the aerodynamic loading on P9 towards P8
%
%  This is obtained  by translating the distributed aerodynamic loads on P9 into
%  concentrated aerodynamic forces and moments in the points X10a and X9a,
%  respectively located with ds9/2 and -ds9/2 spanwise offset to connector @o10.
%
%  We pursue the same for aerodynamic loading of mb-elements X9 ... X2 through the
%  same approach.
%
%    _____ _ _ _ _ _ _ _ _ _ _ _ _ _ _ _ _ _ _ _ _ _ _ _ _ _ _ _ _ _ _ _ _ _ _ _
%   /  ^  \      O X10a                                                        ^
%   |ds9/2|      !                                                           |
%   |  |  |      !                                                           |
%   | _v_ |_  __@o10 _                                                annulus 5|
%   |  ^  |      .              !                                            |
%   |  |  |      .              !                                            |
%   |ds9/2|      .              !                                            |
%   |__v__| P9   .   _____      !                                            |
%                  /  ^  \      O X9a                                        |
%                  |ds8/2|      !                                            |
%                  |  |  |      !                                            |
%                  | _v_ |_  __@o9__  _ _ _ _ _ _ _ _ _ _ _ _ _ _ _ _ _ _ _v
%                  |  ^  |      .              !                            ^
%                  |  |  |      .              !                            |
%                  |ds8/2|      .              !                            |
%                  |__v__| P8   .   _____      !                    annulus 4|
%                                 /  ^  \      O X8a                        |
%                                 |ds7/2|      !                            |
%                                 |  |  |      !                            |
%                                 | _v_ |_  __@o8__                         |
%                                 |  ^  |      .              !             |
%                                 |ds7/2|      .              !             |
%                                 |  |  |      .              !             |
%                                 |__v__| P7   .    _____     !             |
%                                              /  ^  \      O X7a            |
%                                              |ds6/2|      !             |
%                                              |  |  |      !             |
%                                              | _v_ |_  __@o7__ _ _ _  _ v_
%                                              |  ^  |      .             ^
%                                              |  |  |      .             |
%                                              |ds6/2|      .             |
%                                              |__v__| P6   .    annulus 3|
%
```

```
%  For a uniformly distributed load q over length S from the root to the tip of PHYB
%  partition with invariant bending  stiffness EI holds:
%    * translation at tipside        : q*S^4/8EI
%    * rotation at tipside           : +/- q*S^3/6EI
%    * feedthrough force at rootside : q*S
%    * feedthrough moment at rootside: +/- q/2*S^2
%
%  Actually, the upper and lower half of a partition P<n> are respectively loaded by
%  the distributed  aerodynamic loading on element X<k> and X<k-1> (k==n+1). This
%  concerns flat- and edgwise distributed loads qx_k an qz_k on X<k> and dito loads
%  qx_k-1 and qz_k-1 on X<k-1> (assumed uniformly). The  flat- and edgewise bending
%  stiffness values are EIz and EIx for partition P<n> (assumed invariant over P<n>).
%
%  It is equivalent to assume qx_k and qz_k over full span P<n> and the differences
%  qx_kmin - qx_k and qz_kmin - qz_k from the rootside to mu*ds<n> m tipward with
%  mu=0.5, n=k-1 and  kmin = k-1. The involved rotations and translations of P<n> are
%  (MuS = mu*ds<n>):
%   * flatwise translation qx_k*S^4/8EIz  at tip P<n> by  by full span load qx_k
%   * flatwise rotation   -qx_k*S^3/6EIz  at tip P<n> by  by full span load qx_k
%   * flatwise translation (qx_kmin-qx_k)*MuS^4/8EIz at MuS m tipward from root P<n>
%   * flatwise rotation   -(qx_kmin-qx_k)*MuS^3/6EIz at MuS m tipward from root P<n>
%   * edgewise translation qz_k*S^4/8EIx  at tip P<n> by  by full span load qx_k
%   * edgewise rotation    qz_k*S^3/6EIx  at tip P<n> by  by full span load qx_k
%   * edgewise translation (qz_kmin-qz_k)*MuS^4/8EIx at MuS m tipward from root P<n>
%   * edgewise rotation    (qz_kmin-qz_k)*MuS^3/6EIx at MuS m tipward from root P<n>
%
%  The rotations by load differences (qx_kmin-qx_k) and (qz_kmin-qz_k) at MuS m from
%  the rootside propagate to additional translations at the tipside of P<n>
%   * additional flatwise translation -(qx_kmin-qx_k)*(S-MuS)*MuS^3/6EIz
%   * additional edgewise translation  (qz_kmin-qz_k)*(S-MuS)*MuS^3/6EIx
%
%  Lumping together the rotations and translations yields at the tip of P<n>:
%   * flatwise translation qx_k*S^4/8EIz + (qx_kmin-qx_k)*MuS^4/8EIz + ...
%                                                (qx_kmin-qx_k)*(S-MuS)*MuS^3/6EIz
%   * edgewise translation qz_k*S^4/8EIx + (qz_kmin-qz_k)*MuS^4/8EIx + ...
%                                                (qz_kmin-qz_k)*(S-MuS)*MuS^3/6EIx
%   * flatwise rotation  -qx_k*S^3/6EIz - (qx_kmin-qx_k)*MuS^3/6EIz
%   * edgewise rotation   qz_k*S^3/6EIx + (qz_kmin-qz_k)*MuS^3/6EIx
%
%  Also the feedthrough of loads on P<n> to P<n-1> is specified for the loading of
%  P<n> from two distributed loads:
%   * flatwise force   qx_k*(S-MuS) + qx_kmin*MuS
%   * edgewise force   qz_k*(S-MuS) + qz_kmin*MuS
%   * flatwise moment -qx_k/2*S^2 - (qx_kmin-qx_k)/2*MuS^2
%   * edgewise moment  qz_k/2*S^2 + (qz_kmin-qz_k)/2*MuS^2
%
%  As mu=0.5, these expresions apply for MuS=S/2 and S-MuS=S/2. Then the following
%  holds for the translations and rotations of the tip of P<n> by its aerodynamic
%  deformation (i.e.: ... of the tip of P<n> through deformation of  P<n> only by only
%  aerodynamic loading on P<n>"):
%   * flatwise translation ux_n   = S^4/EIz*( 41/384 * qx_k + 7/384 * qx_kmin)
%   * edgewise translation uz_n   = S^4/EIx*( 41/384 * qz_k + 7/384 * qz_kmin)
%   * flatwise rotation    phiz_n = S^3/EIz*(-7/48 * qx_k - 1/48 * qx_kmin)
%   * edgewise rotation    phix_n = S^3/EIx*( 7/48 * qz_k + 1/48 * qz_kmin )
```

```
%
%  For the distributed aerodynamic loading on tip P<n-1> by aerodynamic feedthrough
%  from P<n> holds (i.e. "distributed aerodynamic loading on P<n> that is fed through
%  as concentrated loads at the tipside of P<n-1>"; note that MuS=S-MuS=S/2):
%   * flatwise force  Fax_n->n-1 =  (qx_k + qx_kmin)/2*S
%   * edgewise force  Faz_n->n-1 =  (qz_k + qz_kmin)/2*S
%   * flatwise moment Maz_n->n-1 = -(3*qx_k + qx_kmin)/8*S^2
%   * edgewise moment Max_n->n-1 =  (3*qz_k + qz_kmin)/8*S^2
%
%  Define on multi body model elements X<k> and X<k-1> so called aerodynamic
%  conversion points X<k>a and X<k-1>a. These points respectively have a 'tipward'
%  spanwise offset of +S<n>/2 and -S<n>/2 m to connector @o<k> of element X<k>. Thus,
%  the aerodynamic conversion points on MBBM elements X<k> and X<k-1> agree with the
%  tip- and rootside of PHYB partition P<n> for n==k-1. Assume concentrated loads in
%  these points, caused by only aerodynamic loading on X<k> only:
%   * flat- and edgewise forces Fax_k, Faz_k and moments Maz_k, Max_k in X<k>^a;
%   * dito forces Fax_k@kmin, Faz_k@kmin and moments Maz_k@kmin, Max_k@kmin in X<k-1>^a.
%
%  The resultant in conversion point X<k-1>a  from these concentrated loads must be
%  equal to the aerodynamic loading that is fed through from P<n> to the tip of P<n-1>
%  (i.e. Fax_n->n-1, etc. see above; note that S=S<n>; n=k-1):
%   * flatwise aero force   Fax_k + Fax_k@k-1           ==  (qx_k + qx_kmin)/2*S
%   * edgewise aero forces  Faz_k + Faz_k@k-1           ==  (qz_k + qz_kmin)/2*S
%   * flatwise aero moments Maz_k + Maz_k@k-1 - Fax_k*S  == -(3*qx_k + qx_kmin)/8*S^2
%   * edgewise aero moments Max_k + Max_k@k-1 + Faz_k*S  ==  (3*qz_k + qz_kmin)/8*S^2
%
%  Further, consider the flat- and edgewise rotations and translations of the
%  aerodynamic conversion point of X<k> by its aero deformation (i.e.: "... of
%  point X<k>a through degrees of freedom in only @o<k> by only the concentrated
%  aerodynamic loads in point X<k>a of element X<k>"). For these 'lumped deformations'
%  in MBBM element X<k> holds:
%   * flatwise translation ux_k = (1/srhox + S^2/4sphiz) * Fax_k - S/2sphiz * Maz_k
%   * edgewise translation uz_k = (1/srhoz + S^2/4sphix) * Faz_k + S/2sphix * Max_k
%   * flatwise rotation  phiz_k = 1/sphiz * (-S/2*Fax_k + Maz_k)
%   * edgewise rotation  phix_k = 1/sphix * ( S/2*Faz_k + Max_k)
%
%  These must agree with the translations and rotations of the tip of P<n> by its
%  aerodynamic deformation (i.e. ux_n, etc.; see above; note that n=k-1):
%
%   * flatwise translation (1/srhox + S^2/4sphiz) * Fax_k - S/2sphiz * Maz_k ==
%                                          S^4/EIz*(41/384 * qx_k + 7/384 * qx_kmin)
%   * edgewise translation (1/srhoz + S^2/4sphix) * Faz_k + S/2sphix * Max_k ==
%                                          S^4/EIx*(41/384 * qz_k + 7/384 * qz_kmin)
%   * flatwise rotation     1/sphiz * (-S/2*Fax_k + Maz_k) ==
%                                          S^3/EIz*(-7/48 * qx_k - 1/48 * qx_kmin)
%   * edgewise rotation     1/sphix * (S/2*Faz_k + Max_k)  ==
%                                          S^3/EIx*( 7/48 * qz_k + 1/48 * qz_kmin)
%
%  with srhox = srhox_k, etc. and S = S<n> and EIx = EIx<n>, etc, (n=k-1).
%
%  This agrees with an equality of matrix/vector products, which corresponds to a
%  linear mapping from the uniform flat- and edgewise load distributions qx_kmin, qx_k and
%  qz_kmin, qz_k  on blade partition P<n> to concentrated loads Fax_k ... Max_k in
%  conversion point X<k>a (n==k-1):
```

```
%                                                        -1
%   Sfm_k * |Fax_k| = Gq_n * |qx_k   | <=> |Fax_k| =  Sfm_k  * Sq_n*  |qx_k   |
%           |Faz_k|          |qz_k   |     |Faz_k|                    |qz_k   |
%           |Max_k|          |qx_kmin|     |Max_k|                    |qx_kmin|
%           |Max_k|          |qz_kmin|     |Max_k|                    |qz_kmin|
%
%   with:
%
%    Sfm_k = | (1/srhox + S^2/4sphiz)         0            -S/2sphiz       0    |
%            |          0            (1/srhoz + S^2/4sphix)    0       S/2sphix |
%            |     -S/2sphiz                  0             1/sphiz        0    |
%            |          0                S/2sphix             0       1/sphix  |
%
%     Sq_n = |   S^4*41/384EIz               0        S^4*7/384EIz         0    |
%            |      0                 S^4*41/384EIx      0        S^4*7/384EIx |
%            |   -S^3*7/48EIz                0       -S^3*1/48EIz          0    |
%            |      0                  S^3*7/48EIx       0        S^3*1/48EIx  |
%
%  The equivalence of the fedthrough aerodynamic loading from P<n> to P<n-1> on the
%  one side to concentrated aerodynamic loads in conversion points X<k>a and X<k-1>a
%  on the other side can also be written as a matrix/vector product equality.
%  Eventually, this equality corresponds to a linear mapping from the uniform flat-
%  and edgewise load distributions qx_k, qz_k, qx_kmin, qz_kmin on blade partition P<n> to
%  concentrated flat and edgewise loads Fax_k@k-1 ... Max_k@k-1 in conversion point
%  X<k-1>a (n==k-1):
%
%   |Fax_k@k-1| + Tfm_k&k-1*|Fax_k| = Gq2fm_n*|qx_k   |
%   |Faz_k@k-1|             |Faz_k|           |qz_k   |
%   |Maz_k@k-1|             |Maz_k|           |qx_kmin|
%   |Max_k@k-1|             |Max_k|           |qz_kmin|
%
%                                -1
%         <=> {use |Fax_k| = Sfm_k  * Sq_n * |qx_k   |}
%                  |Faz_k|                   |qz_k   |
%                  |Maz_k|                   |qx_kmin|
%                  |Max_k|                   |qz_kmin|
%
%                                            -1
%              |Fax_k@k-1| = [-Tfm_k&k-1 * Sfm_k  * Sq_n  +  Gq2fm_n] * |qx_k   |
%              |Maz_k@k-1|                                               |qz_k   |
%              |Faz_k@k-1|                                               |qx_kmin|
%              |Max_k@k-1|                                               |qz_kmin|
%
%   with:
%
%    Tfm_k&kmin = | 1  0  0  0 |  ;  Gq2fm_n = |  S/2     0      S/2     0   |
%                 | 0  1  0  0 |               |   0     S/2      0     S/2  |
%                 |-S  0  1  0 |               |-3S^2/8    0    -S^2/8   0   |
%                 | 0  S  0  1 |               |   0    3S^2/8    0    S^2/8 |
%
%  Now interchange columns and rows 2 and 3 in Sfm_k and Sq_n =>
%
%                           -1
%           |Fax_k| =  Sfm_k"  * Sq_n" *  |qx_k   |
```

```
%           |Maz_k|                       |qx_kmin|
%           |Faz_k|                       |qz_k   |
%           |Max_k|                       |qz_kmin|
%
%      with:
%
%      Sfm_k"= | (1/srhox + S^2/4sphiz)  -S/2sphiz           0                0   |
%              |     -S/2sphiz           1/sphiz             0                0   |
%              |          0                   0   (1/srhoz + S^2/4sphix)  S/2sphix |
%              |          0                   0         S/2sphix          1/sphix  |
%
%       Sq_n"= |   S^4*41/384EIz       S^4*7/384EIz         0               0     |
%              |   -S^3*7/48EIz        -S^3*1/48EIz         0               0     |
%              |      0                       0         S^4*41/384EIx S^4*7/384EIx |
%              |      0                       0         S^3*7/48EIx   S^3*1/48EIx  |
%
%
%  With sphiz = EIz/S; srhox = 12EIz/S^3 and sphix=EIx/S; srhoz=12EIx/S^3
%  it is clear that inv(Sfm_k)*Sq_n only depends on S! It holds:
%
%        Sfm_k"= | 1/EIz * |  S^3/3  -S^2/2 |             0       0     |
%                |         | -S^2/2      S  |             0       0     |
%                |              0        0    1/EIx * | S^3/3   S^2/2 | |
%                |              0        0            | S^2/2      S  | |
%
%   inv(Sfm_k")= | 12EIz * | 1/S^3   1/2S^2 |             0       0     |
%                |         | 1/2S^2  1/3S   |             0       0     |
%                |              0        0    12EIx * | 1/S^3  -1/2S^2| |
%                |              0        0            | -1/2S^2 1/3S  | |
%
%  inv(Sfm_k")*Sq_n" = |  156S/384    36S/384       0           0    |
%                      | 22S^2/384  10S^2/384       0           0    |
%                      |      0          0      156S/384     36S/384 |
%                      |      0          0    -22S^2/384  -10S^2/384 |
%
%  while:
%                           -1
%           |Fax_k| =  Sfm_k"  * Sq_n" *  |qx_k   |
%           |Maz_k|                       |qx_kmin|
%           |Faz_k|                       |qz_k   |
%           |Max_k|                       |qz_kmin|
%
%  Hence, changing rows 2 and 3 and columns 2 and 3 yields:
%
%   |Fax_k|  = |  156S/384      0       36S/384         0    | * |qx_k   |
%   |Faz_k|    |      0     156S/384       0         36S/384 |   |qz_k   |
%   |Maz_k|    | 22S^2/384      0     10S^2/384         0    |   |qx_kmin|
%   |Max_k|    |      0    -22S^2/384      0      -10S^2/384 |   |qz_kmin|
%
%  The gain  -Tfm_k&k-1 * inv(Sfm_k)  * Sq_n  +  Gq2fm_n can also be written
%  exclusively in S so that:
%
%   |Fax_k@k-1|  = |  36S/384       0      156S/384         0    | * |qx_k   |
%   |Faz_k@k-1|    |      0      36S/384       0        156S/384 |   |qz_k   |
```

```
%   |Maz_k@k-1|    |-10S^2/384      0    -22S^2/384         0    |   |qx_kmin|
%   |Max_k@k-1|    |      0     10S^2/384      0       22S^2/384 |   |qz_kmin|
%
%  Note that k=2,3,...,N!
%
%  Subst k@k-1 by k+1@k, introduce q_kplus and reshuffle q_k with q_kmin and q_kplus
%  with q_k, then:
%
%   |Fax_k|  = | 36S/384         0    156S/384      0         | * |qx_kmin|, (k=2...N)
%   |Faz_k|    | 0           36S/384     0       156S/384     |   |qz_kmin|
%   |Maz_k|    | 10S^2/384       0    22S^2/384      0        |   |qx_k   |
%   |Max_k|    |   0       -10S^2/384      0    -22S^2/384    |   |qz_k   |
%
%   |Fax_k+1@k|  = |156S/384         0     36S/384       0       | * |qx_k|, (k=1...N-
1)
%   |Faz_k+1@k|    |     0        156S/384      0      36S/384   |   |qz_k|
%   |Maz_k+1@k|    |-22S^2/384         0   -10S^2/384      0     |   |qx_kplus|
%   |Max_k+1@k|    |     0       22S^2/384       0     10S^2/384 |   |qz_kplus|
%
%  Define aerodynamic load vectors P_j, P_j+1@j and Q_m  as:
%   P_j     = |Fax_j     Faz_j     Maz_j     Max_j|'
%   P_j+1@j = |Fax_j+1@j Faz_j+1@j Maz_j+1@j Max_j+1@j|'
%   Q_m     = |qx_m qz_m |'
%
%  Define matrices Gpq = | GpqL GpqR | and Gpqsh = |GpqshL GpqshR| such that:
%   P_k     = | GpqL   GpqR   | * | Q_k-1  Q_k   |' (k=2...N)
%   P_k+1@k = | GpqshL GpqshR | * | Q_k    Q_k+1 |' (k=1...N-1)
%
%  For the resultant concentrated aerodynamic load vectors Pa^Xk in the aerodynamic
%  conversion points Xka then holds (k=1...N}:
%
%            {  | GpqshL GpqshR | * | Q_k  Q_{k+1} |'               ; k=1
%    Pa^Xk = {  | GpqL   GpqR+GpqshL GpqshR | * |Q_k-1 Q_k Q_k+1 |' ; k=2...N-1
%            {  | GpqL   GpqR   | * | Q_{k-1} Q_k  |'               ; k=N
%
%    with Pa^{Xk} = |Fa^Xk_x Fa^Xk_z Ma^Xk_z Ma^Xk_x|'
%         Q_k     = |q^Xk_x q^Xk_z |'
%
%  Note that for k=2...N the aero conv points are located 0.5*S tipward from connector
%  points @ok while for k=1  it lays in the connector point @o1.
%
%  Now take full coordinate vectors Fa^Xk and Ta^Xk for concentrated force and torque
%  loads and Qa^Xk for distrubed force loads, and take also into account the
%  distributed aerodynamic pitch-wise torque loading q^Xk_y.
%
%  For the concentrated force loads holds:
%
%          {|GfqshL GfqshR|*| Qfa^Xk'  Qfa^{X_{k+1}}' |' ; k=1
%   Fa^Xk = {|GfqL   GfqR+GfqshL GfqshR| * ...
%                                    |Qfa^{X_{k-1}}' Qfa^Xk' Qfa^{X_{k+1}}'|';k=2...N-
1
%          {|GfqL   GfqR  |*| Qfa^{X_{k-1}}' Qfa^Xk'  |' ;  k=N
%
%  with:
```

```
%           |Fa_x^Xk|                 | q_x^Xk|
%   Fa^Xk = |Fa_y^Xk|     ;  Qfa^Xk = |   0   |
%           |Fa_z^Xk|                 | q_z^Xk|
%
%     GfqL =   | 36S/384  0    0    | ; GfqR    = |156S/384  0     0    |
%              |    0     0    0    |             |    0     0     0    |
%              |    0     0 36S/384 |             |    0     0 156S/384 |
%
%     GfqshL = | 156S/384 0    0     | ; GfqshR = | 36S/384   0    0    |
%              |    0     0    0     |            |    0      0    0    |
%              |    0     0 156S/384 |            |    0      0 36S/384 |
%
%  For the concentrated torque loads holds:
%
%
%   Ta^Xk = Gtqp * Qta^Xk + ...
%
%     {|GtqshL GtqshR | * |Qfa^Xk’  Qfa^{X_{k+1}}’|’;k=1
%     {|GtqL   GtqR+GtqshL GtqshR | * |Qfa^{X_{k-1}}’ Qfa^X’k Qfa^{X_{k+1}}’|’;k=2...N-
1
%     {|GtqL   GtqR   | * |Qfa^{X_{k-1}}’ Qa^Xk’  |’;k=N
%
%  with:
%           |Ta_x^Xk|                 |   0   |
%   Ta^Xk = |Ta_y^Xk|     ;  Qta^Xk = | q_y^Xk|
%           |Ta_z^Xk|                 |   0   |
%
%     GtqL =   |     0     0 -10S^2/384  | ; GtqR =   |     0     0 -22S^2/384 |
%              |     0     0       0     |            |     0     0     0      |
%              | 10S^2/384 0       0     |            | 22S^2/384 0     0      |
%
%     GtqshL = |     0     0  22S^2/384  | ; GtqshR = |     0     0  10S^2/384 |
%              |     0     0          O  |            |     0     0     0      |
%              |-22S^2/384 0          0  |            |-10S^2/384 0     0      |
%
%              | 0  0  0 |
%     Gtqp   = | 0  S  0 |
%              | 0  0  0 |
%
%  In above expressions, the distributed aeroloads q^Xk_x [N/m], q^Xk_y [Nm/m] and
%  q^Xk_z [N/m] are along the axes of the elements ’structural’ coordinate system
%  e^Xk with x,y and z-axis pointing in edge-, span- and flatwise direction. The
%  dependency of the aerodynamic load distributions on the lift and dragcoeffient, on
%  the wind and blade speed and on the blade orientation angles yields expressions in
%  coordinates  along the so called ’conversion’ coordinate system e^{Xk^cv}. Though
%  the y-axes of e^{Xk^cv} and e^{Xk} coincide, the x- and z-axes do not:
%  * e_x^{Xk^cv} lays in the plane spanned by the x- and y-axis of the unpitched
%    blade flenge (coord. sys. e^X0) and points ’flapwise backward’;
%  * e_z^{Xk^cv} lays in the plane spanned by the z- and y-axes of the unpitched
%    blade flenge (rotor plane) and points ’leadwise relative to the blade-element’.
%
%  The 3*3-matrix Phi{Xk<-Xk^cv} transforms coordinates along e^{Xk^cv} to coordinates
%  along e^{Xk}. The matrix depends on increments in the flat- and edgewise angles,
%  in the blade-twist related neutral elastic z-axis angle, and in the angles in
```

```
%  the blade root. The latter caused by preconing or a flapwise hinge, by pitching, and
%  by delta_3 setting or a leadwise hinge. See Appendix B for details on matrix
%  Phi{Xk<-Xk^cv} and Appendix A for details on coordinate systems and rotations.
%
%  The next step is to include this transformation in the mapping from distributed
%  loads to concentrated forces. The 'input force vector' Qf^{Xk^cv} then includes
%  distributed force loads q^Xk_n in blade-normal and q^Xk_l blade-lead direction,
%  corresponding to the x- and z-axes of e^{Xk^cv};  input torque vector Qt^{Xk^cv}
%  only includes torque loading q^Xk_p in pitching direction, so along -e_y^{Xk^cv}:
%
%    Qf^{Xk^cv} = | q^Xk_n |  ;  Qt^{Xk^cv} = |    0    |
%                 |   0    |                  | -q^Xk_p |
%                 | q^Xk_l |                  |    0    |
%
%  For the mappings to the distributed loads along the structure coordinate system
%  e^Xk then holds:
%
%   Qfa^{X_{k-1}} = Phi{Xk<-X_{k-1}^cv} * Qf^{X_{k-1}^cv}
%   Qfa^{Xk}      = Phi{Xk<-Xk^cv}      * Qf^{Xk^cv}
%   Qfa^{X_{k+1}} = Phi{Xk<-X_{k+1}^cv} * Qf^{X_{k+1}^cv}
%
%  and:
%
%   Qta^Xk = Qt^{Xk^cv}
%
%  This yields the desired expressions for concentrated aerodynamic loads in conversion
%  points Xk^a from distributed aerodynamic loads on element Xk, k=1...N:
%
%    case k=1:
%
%     Fa^Xk = GfqshL * Phi{Xk<-Xk^cv} * Qf^{Xk^cv} + ...
%                                     GfqshR * Phi{Xk<-X_{k+1}^cv} * Qf^{X_{k+1}^cv}
%
%     Ta^Xk = Gtqp * Qta^Xk + GtqshL * Phi{Xk<-Xk^cv} * Qf^{Xk^cv} + ...
%                                     GtqshR * Phi{Xk<-X_{k+1}^cv} * Qf^{X_{k+1}^cv}
%    case k=2...N-1:
%
%     Fa^Xk = GfqL * Phi{Xk<-X_{k-1}^cv} * Qf^{X_{k-1}^cv} + ...
%                  (GfqR+GfqshL) * Phi{Xk<-Xk^cv} * Qf^{Xk^cv} +  ...
%                                      GfqshR * Phi{Xk<-X_{k+1}^cv} * Qf^{X_{k+1}^cv}
%
%     Ta^Xk = Gtqp * Qta^Xk + GtqL * Phi{Xk<-X_{k-1}^cv} * Qf^{X_{k-1}^cv} + ...
%                               (GtqR+GtqshL) * Phi{Xk<-Xk^cv} * Qf^{Xk^cv} +  ...
%                                      GtqshR * Phi{Xk<-X_{k+1}^cv} * Qf^{X_{k+1}^cv}
%    case k=N:
%
%     Fa^Xk = GfqL * Phi{Xk<-X_{k-1}^cv} * Qf^{X_{k-1}^cv} + ...
%                                             GfqR * Phi{Xk<-Xk^cv} * Qf^{Xk^cv}
%
%     Ta^Xk = Gtqp * Qta^Xk + GtqL * Phi{Xk<-X_{k-1}^cv} * Qf^{X_{k-1}^cv} + ...
%                                             GtqR * Phi{Xk<-Xk^cv} * Qf^{Xk^cv}
```

APPENDIX D. LOAD CALCULATION CONCEPT

This appendix describes the concept of the calculation of the steady state and the dynamic loading. The dynamic loading is subdivided into periodic and stochastic loading.

D.1 Definitions

$\vec{\not{h}}^{\,R}$: generalized impulse vector for turbine rotor R (angular and linear impulse)

$\underline{\not{h}}^{\,R}$: coordinates of impulse vector $\vec{\not{h}}^{\,R}$ for R along $\vec{e}^{\,R}$ (impulse coordinates)

$\left(\underline{\not{h}}^{\,R}\right)^{S}$: coordinates along $\vec{e}^{\,S}$ of impulse vector $\vec{\not{h}}^{\,R}$ for rotor R

${}^{\mathrm{ext}}\underline{\tilde{\not{h}}}^{\,R}$: extern harmonics (==0) of rotor impulse $\underline{\not{h}}^{\,R}$

$\vec{\not{h}}^{\,S}$: generalised impulse vector for support structure S (angular and linear impulse)

$\underline{\not{h}}^{\,S}$: coordinates of impulse vector $\vec{\not{h}}^{\,S}$ for S along axes of $\vec{e}^{\,S}$

$\underline{\bar{\not{h}}}^{\,R}$: mean of rotor impulse $\underline{\not{h}}^{\,R}$; mean part of $\vec{\not{h}}^{\,R}$ from mass- or inertia- asymmetry

$\widetilde{\left(\underline{\bar{\not{h}}}^{\,R}\right)}^{S}$: extern harmonics in $\vec{e}^{\,S}$ of mean of impulse $\underline{\not{h}}^{\,R}$

$\overline{\left(\underline{\bar{\not{h}}}^{\,R}\right)}^{S}$: mean in $\vec{e}^{\,S}$ (==0) of mean of rotor impulse $\underline{\not{h}}^{\,R}$

${}^{\mathrm{rea}}\underline{\tilde{\not{h}}}^{\,R}$: reactive harmonics of rotor impulse $\underline{\not{h}}^{\,R}$; periodic part of $\underline{\not{h}}^{\,R}$ from structural reaction on extern harmonics in $\underline{q}^{R}$

$\overline{\left({}^{\mathrm{rea}}\underline{\tilde{\not{h}}}^{\,R}\right)}^{S}$: mean in $\vec{e}^{\,S}$ (==0) of reactive harmonics of impulse $\underline{\not{h}}^{\,R}$

$\widetilde{\left({}^{\mathrm{rea}}\underline{\tilde{\not{h}}}^{\,R}\right)}^{S}$: reactive harmonics in $\vec{e}^{\,S}$ of reactive harmonics of impulse $\underline{\not{h}}^{\,R}$

${}^{\mathrm{rea}}\underline{\tilde{\not{h}}}^{\,R}$: reactive stochastics of rotor impulse $\underline{\not{h}}^{\,R}$; stochastic part of $\underline{\not{h}}^{\,R}$ from structural reaction on extern stochastics in $\underline{q}^{R}$ and $\underline{q}^{S}$

${}^{\mathrm{rea}}\underline{\tilde{\not{h}}}^{\,S}$: reactive harmonics of tower impulse $\underline{\not{h}}^{\,S}$; periodic part of $\underline{\not{h}}^{\,S}$ from structural reaction on extern harmonics in $\underline{q}^{R}$ and $\left(\underline{\bar{\not{h}}}^{\,R}\right)^{S}$

${}^{\mathrm{rea}}\underline{\tilde{\not{h}}}^{\,S}$: reactive stochastics of tower impulse $\underline{\not{h}}^{\,S}$; stochastic part of $\underline{\not{h}}^{\,S}$ from structural reaction on extern stochastics in $\underline{q}^{R}$ and $\underline{q}^{S}$

$\vec{q}^{\,R}$: generalised load vector on R caused by presence of gravity and air (force & torque)

$\underline{q}^{R}$: coordinates of load vector $\vec{q}^{\,R}$ for R along $\vec{e}^{\,R}$ (load coordinates)

$\left(\underline{q}^{R}\right)^{S}$: coordinates along $\vec{e}^{\,S}$ of load vector $\vec{q}^{\,R}$ for rotor R

${}^{\mathrm{ext}}\underline{\tilde{q}}^{R}$: extern harmonics in load coordinates $\underline{q}^{R}$; periodic part of $\underline{q}^{R}$ from gravity- and aero-load asymmetry, tower shadow, shear, oblique inflow

$\widetilde{\left({}^{\mathrm{ext}}\underline{\tilde{q}}^{R}\right)}^{S}$: extern harmonic coordinates along $\vec{e}^{\,S}$ of extern harmonics in $\underline{q}^{R}$

$\overline{\left({}^{\mathrm{ext}}\underline{\tilde{q}}^{R}\right)^{S}}$: mean coordinates along $\vec{e}^{\,S}$ of extern harmonics in $\underline{q}^{R}$

${}^{\mathrm{ext}}\underline{\check{q}}^{R}$: extern stochastics in load coordinates $\underline{q}^{R}$; stochastic part of $\underline{q}^{R}$ from turbulence

$\bar{\underline{q}}^{R}$: means in load coordinates $\underline{q}^{R}$; mean part of $\underline{q}^{R}$ from gravity and axial inflow

$\widetilde{\left(\bar{\underline{q}}^{R}\right)^{S}}$: extern harmonic coordinates along $\vec{e}^{\,S}$ of means in $\underline{q}^{R}$

$\overline{\left(\bar{\underline{q}}^{R}\right)^{S}}$: mean coordinates along $\vec{e}^{\,S}$ of means in $\underline{q}^{R}$

${}^{\mathrm{rea}}\underline{\tilde{q}}^{R}$: reactive harmonics in load coordinates $\underline{q}^{R}$; periodic part of $\vec{q}^{\,R}$ from structural and aerodynamic reaction on extern harmonics in $\underline{q}^{R}$

$\overline{\left({}^{\mathrm{rea}}\underline{\tilde{q}}^{R}\right)^{S}}$: mean in $\vec{e}^{\,S}$ of reactive harmonics of rotor load $\underline{q}^{R}$

$\widetilde{\left({}^{\mathrm{rea}}\underline{\tilde{q}}^{R}\right)^{S}}$: reactive harmonic coordinates along $\vec{e}^{\,S}$ of reactive harmonics in $\underline{q}^{R}$

${}^{\mathrm{rea}}\underline{\check{q}}^{R}$: reactive stochastics in load coordinates $\underline{q}^{R}$; stochastic part of $\underline{q}^{R}$ from structural and aerodynamic reaction on extern stochastics in $\underline{q}^{R}$ and $\underline{q}^{S}$

$\overline{\left((\underline{q}-\underline{\not{h}})^{R}\right)^{S}}$: mean coordinates along $\vec{e}^{\,S}$ of 'fed-through rotor load' $\vec{q}^{\,R}-\vec{\not{h}}^{\,R}$: $\overline{\left(\bar{\underline{q}}^{R}\right)^{S}}+\overline{\left({}^{\mathrm{ext}}\underline{\tilde{q}}^{R}\right)^{S}}+\overline{\left({}^{\mathrm{rea}}\underline{\tilde{q}}^{R}\right)^{S}}-\overline{\left({}^{\mathrm{rea}}\underline{\tilde{\not{h}}}^{R}\right)^{S}}$

$\widetilde{\left((\underline{q}-\underline{\not{h}})^{R}\right)^{S}}$: harmonic coordinates along $\vec{e}^{\,S}$ of fed-through rotor load $\vec{q}^{\,R}-\vec{\not{h}}^{\,R}$: $\widetilde{\left(\bar{\underline{q}}^{R}\right)^{S}}+\widetilde{\left({}^{\mathrm{ext}}\underline{\tilde{q}}^{R}\right)^{S}}+\widetilde{\left({}^{\mathrm{rea}}\underline{\tilde{q}}^{R}\right)^{S}}-\widetilde{\left(\bar{\underline{\not{h}}}^{R}\right)^{S}}-\widetilde{\left({}^{\mathrm{rea}}\underline{\tilde{\not{h}}}^{R}\right)^{S}}$

$\vec{q}^{\,S}$: generalized load vector on S caused by presence of gravity and water (force & torque)

$\underline{q}^{S}$: coordinates of load vector $\vec{q}^{\,S}$ for S along $\vec{e}^{\,S}$ (load coordinates)

${}^{\mathrm{ext}}\underline{\check{q}}^{S}$: extern stochastics in load coordinates $\underline{q}^{S}$; stochastic part of $\underline{q}^{S}$ from waves

${}^{\mathrm{rea}}\underline{\tilde{q}}^{S}$: reactive harmonics in load coordinates $\underline{q}^{S}$; periodic part of $\underline{q}^{S}$ from structural and hydrodynamic reaction on extern harmonics in $\underline{q}^{R}$ and $\left(\bar{\underline{\not{h}}}^{R}\right)^{S}$

${}^{\mathrm{rea}}\underline{\check{q}}^{S}$: reactive stochastics in load coordinates $\underline{q}^{S}$; stochastic part of $\underline{q}^{S}$ from structural and hydrodynamic reaction on extern stochastics in $\underline{q}^{R}$ and $\underline{q}^{S}$

R : turbine rotor (B blades, hub, drive-train) with 'mounted' rotating coord. sys. $\vec{e}^{\,R}$

S : support structure (foundation, tower, nacelle) with mounted standstill c.s. $\vec{e}^{\,S}$

D.2 Approach for periodic linear wind turbine model

The set-up of the linearised (frequency domain) load calculation program is based on the subdivision of load and impulse vectors into mean values, periodic variations and stochastic variations.

In this conceptual description for the load calculation the individual rotor blades, rotating parts of the drive-train and the wake are lumped together to (super)component 'rotor R' while the foundation, tower, nacelle, generator stator and gearbox house are lumped together to (super)component 'support structure S'. The loads on R caused by the presence of air and gravity are collected in load vector $\vec{q}^{\,R}$; the corresponding impulse values in vector $\vec{\not{h}}^{\,S}$. The loads on S as caused by gravity and waves surrounding S, so *not* fed-through from R, are collected in vector $\vec{q}^{\,S}$; the corresponding impulse values in $\vec{\not{h}}^{\,S}$. Note that loads and impulses are generalised: they contain both angular and linear quantities.

The linearised approach to the rotor and tower load vectors, $\vec{q}^{\,R}$ and $\vec{q}^{\,S}$, in a respective rotating and stand still coordinates system, $\vec{e}^{\,R}$ and $\vec{e}^{\,S}$, yields:

$$\begin{aligned} \underline{q}^R &= \underline{\bar{q}}^R + {}^{\mathrm{ext}}\underline{\tilde{q}}^R + {}^{\mathrm{rea}}\underline{\tilde{q}}^R + {}^{\mathrm{ext}}\underline{\check{q}}^R + {}^{\mathrm{rea}}\underline{\check{q}}^R \\ \underline{q}^S &= \underline{\overline{q}}^S + {}^{\mathrm{rea}}\underline{\tilde{q}}^S + {}^{\mathrm{ext}}\underline{\check{q}}^S + {}^{\mathrm{rea}}\underline{\check{q}}^S \end{aligned} \tag{D.1}$$

Each coordinate of the rotor load $\underline{q}^R$ (may) contain a mean, harmonic and stochastic part. The mean load coordinate vector is denoted as $\underline{\bar{q}}^R$ and follows from gravity and axial inflow. Both the harmonic and stochastic contributions to the rotor load vector are subdivided in an 'extern' and 'reactive' part. The extern part follows from the external conditions, the reactive part from the response behaviour:

- ${}^{\mathrm{ext}}\underline{\tilde{q}}^R$: extern harmonics in $\underline{q}^R$ caused by gravity- and aero-loading asymmetry and tower shadow, shear and oblique inflow (result from main rotation);
- ${}^{\mathrm{rea}}\underline{\tilde{q}}^R$: reactive harmonics in $\underline{q}^R$ caused by structural and aerodynamic reaction on extern harmonics in $\underline{q}^R$;
- ${}^{\mathrm{ext}}\underline{\check{q}}^R$: extern stochastics in $\underline{q}^R$ caused by turbulence;
- ${}^{\mathrm{rea}}\underline{\check{q}}^R$: reactive stochastics in $\underline{q}^R$ caused by structural and aerodynamic reaction on extern stochastics in $\underline{q}^R$ (turbulent loads) and $\underline{q}^S$ (wave loads).

Each coordinate of the tower load $\underline{q}^S$ (may) contain(s) a mean, harmonic and stochastic part (mean coordinate vector $\underline{\overline{q}}^S$; by gravity only). Extern harmonics in $\underline{q}^S$ do NOT exist; periodic tower loading only results from fed-through rotor load (and impulse). The stochastic part is subdivided in an 'extern' and 'reactive' part. Thus, the variations in the tower load vector are:

- ${}^{\mathrm{rea}}\underline{\tilde{q}}^S$: reactive harmonics in $\underline{q}^S$ caused by structural and hydrodynamic reaction on extern harmonics in $\underline{q}^R$ and in $\left(\underline{\bar{h}}^R\right)^S$ (the latter follows from mass- or inertia asymmetry in the rotor;
- ${}^{\mathrm{ext}}\underline{\check{q}}^S$: extern stochastics in $\underline{q}^S$ caused by waves
- ${}^{\mathrm{rea}}\underline{\check{q}}^S$: reactive stochastics in $\underline{q}^S$ caused by structural and hydrodynamic reaction on extern stochastics in $\underline{q}^R$ (turbulent loads) and $\underline{q}^S$ (wave loads).

Note that the extern harmonics in $\underline{q}^R$ may have both mean and harmonic coordinates along the stand still coordinate system $\vec{e}^{\,S}$; this also holds for the load-reactive harmonics:

- $\widetilde{\left({}^{\mathrm{ext}}\underline{\tilde{q}}^R\right)^S}$: extern harmonic coordinates along $\vec{e}^{\,S}$ of extern harmonics in $\underline{q}^R$
- $\overline{\left({}^{\mathrm{ext}}\underline{\tilde{q}}^R\right)^S}$: mean coordinates along $\vec{e}^{\,S}$ of extern harmonics in $\underline{q}^R$
- $\widetilde{\left({}^{\mathrm{rea}}\underline{\tilde{q}}^R\right)^S}$: reactive harmonic coordinates along $\vec{e}^{\,S}$ of reactive harmonics in $\underline{q}^R$
- $\overline{\left({}^{\mathrm{rea}}\underline{\tilde{q}}^R\right)^S}$: mean in $\vec{e}^{\,S}$ of reactive harmonics of rotor load $\underline{q}^R$

Mean coordinates $\overline{\left({}^{\mathrm{ext}}\underline{\tilde{q}}^R\right)^S}$ and $\overline{\left({}^{\mathrm{rea}}\underline{\tilde{q}}^R\right)^S}$ arise from transformation to $\vec{e}^{\,S}$ of harmonics in one time the angular rotor speed of periodic rotor loads ${}^{\mathrm{ext}}\underline{\tilde{q}}^R$. In addition, this 'demodulation' yields harmonics in two times the angular frequency.

Similarly, the mean values in $\underline{q}^R$ also have mean and harmonic coordinates along $\vec{e}^{\,S}$:

- $\widetilde{\left(\underline{\bar{q}}^{R}\right)}^{S}$: extern harmonic coordinates along $\vec{e}^{\,S}$ of means in $\underline{q}^{R}$
- $\overline{\left(\underline{\bar{q}}^{R}\right)}^{S}$: mean coordinates along $\vec{e}^{\,S}$ of means in $\underline{q}^{R}$

The fed-through of mean rotor loading into harmonic support structure loading is to be considered as arisen periodic tower loads from external conditions!! It is caused by asymmetry in gravity- and aero-loading on the rotor.

The linearised approach to the rotor and tower impulse vector, $\vec{\hbar}^{\,R}$ and $\vec{\hbar}^{\,S}$, in the rotating and stand still coordinates system, $\vec{e}^{\,R}$ and $\vec{e}^{\,S}$, yields:

$$\begin{aligned} \underline{\hbar}^{R} &= \underline{\bar{\hbar}}^{R} + {}^{\mathrm{rea}}\underline{\tilde{\hbar}}^{R} + {}^{\mathrm{rea}}\underline{\check{q}}^{R} \\ \underline{\hbar}^{S} &= {}^{\mathrm{rea}}\underline{\check{\hbar}}^{S} + {}^{\mathrm{rea}}\underline{\check{\hbar}}^{S} \end{aligned} \tag{D.2}$$

Each coordinate of the rotor impulse $\underline{\hbar}^{R}$ (may) contain a mean, harmonic and stochastic part. The mean impulse coordinate vector is denoted as $\underline{\bar{\hbar}}^{R}$; it follows from excentricity of the rotor centre of gravity or other inertia asymmetry on the rotor ('mass- or inertia-asymmetry'). Both the harmonic and stochastic part are *only* reactive and also depend on the tower top acceleration:

- ${}^{\mathrm{rea}}\underline{\tilde{\hbar}}^{R}$: reactive harmonics in $\underline{\hbar}^{R}$ from structural reaction on extern harmonics in $\underline{q}^{R}$;
- ${}^{\mathrm{rea}}\underline{\check{\hbar}}^{R}$: reactive stochastics in $\underline{\hbar}^{R}$ from structural reaction on extern stochastics in $\underline{q}^{R}$ and $\underline{q}^{S}$.

Each coordinate of the tower impulse $\underline{\hbar}^{S}$ (may) only contain a harmonic and stochastic part. Both the harmonic and stochastic part are ONLY reactive:

- ${}^{\mathrm{rea}}\underline{\tilde{\hbar}}^{S}$: reactive harmonics in $\underline{\hbar}^{S}$ from structural reaction on extern harmonic coordinates $\widetilde{\left(\underline{\bar{q}}^{R}\right)}^{S}$, $\widetilde{\left({}^{\mathrm{ext}}\underline{\tilde{q}}^{R}\right)}^{S}$ and $\widetilde{\left(\underline{\bar{\hbar}}^{R}\right)}^{S}$.
- ${}^{\mathrm{rea}}\underline{\check{\hbar}}^{S}$: reactive stochastics in $\underline{\hbar}^{S}$ from structural reaction on extern stochastic coordinates ${}^{\mathrm{ext}}\underline{\check{q}}^{R}$ and ${}^{\mathrm{ext}}\underline{\check{q}}^{S}$

Note that the mean values in $\underline{\hbar}^{R}$ will have only *harmonic* coordinates along $\vec{e}^{\,S}$; this also holds for the inertia-reactive harmonics in $\underline{\hbar}^{R}$:

- $\widetilde{\left(\underline{\bar{\hbar}}^{R}\right)}^{S}$: extern harmonics in $\vec{e}^{\,S}$ of mean of impulse $\underline{\hbar}^{R}$
- $\widetilde{\left({}^{\mathrm{rea}}\underline{\tilde{\hbar}}^{R}\right)}^{S}$: reactive harmonics in $\vec{e}^{\,S}$ of reactive harmonics of impulse $\underline{\hbar}^{R}$

The fed-through of (minus) the mean rotor impulse coordinates into harmonic coordinates along $\vec{e}^{\,S}$ is to be considered as arisen periodic tower loads from external conditions!! It is caused by mass- or intertia-asymmetry.

Finally, for the mean and harmonic coordinates along $\vec{e}^{\,S}$, $\overline{\left(\underline{q}^{R}\right)}^{S}$ and $\widetilde{\left((\underline{q}-\underline{\hbar})^{R}\right)}^{S}$, of the effective fed-through rotor load '$\vec{q}^{\,R}$-$\vec{\hbar}^{\,R}$' holds:

$$\begin{aligned} \overline{\left((\underline{q}-\underline{\hbar})^{R}\right)}^{S} &= \overline{\left(\underline{\bar{q}}^{R}\right)}^{S} + \overline{\left({}^{\mathrm{ext}}\underline{\tilde{q}}^{R}\right)}^{S} + \overline{\left({}^{\mathrm{rea}}\underline{\tilde{q}}^{R}\right)}^{S} \\ \widetilde{\left((\underline{q}-\underline{\hbar})^{R}\right)}^{S} &= \widetilde{\left(\underline{\bar{q}}^{R}\right)}^{S} + \widetilde{\left({}^{\mathrm{ext}}\underline{\tilde{q}}^{R}\right)}^{S} + \widetilde{\left({}^{\mathrm{rea}}\underline{\tilde{q}}^{R}\right)}^{S} - \widetilde{\left(\underline{\bar{\hbar}}^{R}\right)}^{S} - \widetilde{\left({}^{\mathrm{rea}}\underline{\tilde{\hbar}}^{R}\right)}^{S} \end{aligned} \tag{D.3}$$

D.3 Mean, periodic and stochastic state vectors

The mean $\underline{\bar{x}}^R$ along $\vec{e}^{\,R}$ of the rotor state depends on the rotor loading and impulse only:

$$\underline{\bar{x}}^R = \underline{\bar{x}}^R(\underline{\bar{q}}^R, \underline{\bar{\hbar}}^R) \tag{D.4}$$

The mean $\underline{\bar{x}}^S$ of the support structure state along $\vec{e}^{\,S}$ depends on loading only, but both from the rotor and tower:

$$\underline{\bar{x}}^S = \underline{\bar{x}}^S(\underline{\bar{q}}^S, \overline{\left(\underline{\bar{q}}^R\right)^S}, \overline{\left({}^{\mathrm{ext}}\underline{\tilde{q}}^R\right)^S} + \overline{\left({}^{\mathrm{rea}}\underline{\tilde{q}}^R\right)^S}) \tag{D.5}$$

The sum $\overline{\left({}^{\mathrm{ext}}\underline{\tilde{q}}^R\right)^S} + \overline{\left({}^{\mathrm{rea}}\underline{\tilde{q}}^R\right)^S}$ is the average tower loading from fed-through periodic rotor loading, that is to say it includes compensation for reactive harmonics in load coordinates $\underline{q}^R$.

Note that the consumption of periodic rotor loads by periodic rotor impulse has *no* effect on the effective fed-through *mean* loads along $\vec{e}^{\,S}$: on average, the rotor impulse along the stand-still coordinates *always* equals zero.

The dependency of the periodic rotor and support structure states $\underline{\tilde{x}}^R$, $\underline{\tilde{x}}^S$ along $\vec{e}^{\,R}$ and $\vec{e}^{\,S}$ on the loading and impulse defines the equations of motion for R and S to be simultaneously solved:

$$\begin{aligned}
\underline{\tilde{x}}^R &= \underline{\tilde{x}}^R({}^{\mathrm{ext}}\underline{\tilde{q}}^R + {}^{\mathrm{rea}}\underline{\tilde{q}}^R, {}^{\mathrm{rea}}\underline{\tilde{\hbar}}^R) \\
\underline{\tilde{x}}^S &= \underline{\tilde{x}}^S(\widetilde{\left({}^{\mathrm{ext}}\underline{\tilde{q}}^R\right)^S} + \widetilde{\left({}^{\mathrm{rea}}\underline{\tilde{q}}^R\right)^S} - \widetilde{\left({}^{\mathrm{rea}}\underline{\tilde{\hbar}}^R\right)^S}, \widetilde{\left(\underline{\bar{q}}^R\right)^S} - \widetilde{\left(\underline{\bar{\hbar}}^R\right)^S}, {}^{\mathrm{rea}}\underline{\tilde{q}}^S, {}^{\mathrm{rea}}\underline{\tilde{\hbar}}^S)
\end{aligned} \tag{D.6}$$

Causality problem:

- mean states $\underline{\bar{x}}^S$ and $\underline{\bar{x}}^R$ must be available for the calculation of periodic state variations $\underline{\tilde{x}}^S$ and $\underline{\tilde{x}}^R$ *but also*:
- load-reactive rotor harmonics ${}^{\mathrm{rea}}\underline{\tilde{q}}^R$ are required for calculation of mean support structure state $\underline{\bar{x}}^S$ whereas they are to be calculated from periodic rotor state $\underline{\tilde{x}}^R$

It is assumed that the contribution to the mean tower deformation by the load-reactive rotor harmonics in $\underline{q}^R$ is small in respect of the contribution by the mean and extern harmonics in $\underline{q}^R$.

In that case, it is allowed to first calculate $\underline{\bar{x}}^S$ only from $\underline{\bar{q}}^S$, $\overline{\left(\underline{\bar{q}}^R\right)^S}$ and $\overline{\left({}^{\mathrm{ext}}\underline{\tilde{q}}^R\right)^S}$; after calculation of the periodic turbine state, the average support structure state is recalculated with inclusion of the load-reactive rotor harmonics.

The dependency of the stochastic rotor and support structure states $\underline{\check{x}}^R$, $\underline{\check{x}}^S$ along $\vec{e}^{\,R}$ and $\vec{e}^{\,S}$ on the loading and impulse defines the equations of motion for R and S to be simultaneously solved:

$$\begin{aligned}
\underline{\check{x}}^R &= \underline{\check{x}}^R({}^{\mathrm{ext}}\underline{\check{q}}^R + {}^{\mathrm{rea}}\underline{\check{q}}^R, {}^{\mathrm{rea}}\underline{\check{\hbar}}^R) \\
\underline{\check{x}}^S &= \underline{\check{x}}^S(\left({}^{\mathrm{ext}}\underline{\check{q}}^R\right)^S + \left({}^{\mathrm{rea}}\underline{\check{q}}^R\right)^S - \left({}^{\mathrm{rea}}\underline{\check{\hbar}}^R\right)^S, {}^{\mathrm{ext}}\underline{\check{q}}^S, {}^{\mathrm{rea}}\underline{\check{q}}^S, {}^{\mathrm{rea}}\underline{\check{\hbar}}^S)
\end{aligned} \tag{D.7}$$

D.4 Average drive-train conditions

The average conditions in the drive-train pertain to rotating subcomponents on the one hand, vizually the E-machine rotor $R_{\rm f}$ and the rotor shaft & hub $R_{\rm r}$, and to a stand-still subcomponent on the other hand, the gearbox house $R_{\rm h}$. In order to anticipate during the determination of the equilibrium state on the periodic state, the involved deterministic drive-train loading from the rotor blades is split up in its average and periodic part:

$$\underline{\tilde{q}}^{R} = \overline{\underline{q}}^{R} + \underline{\tilde{q}}^{R} \tag{D.8}$$

while (superscript $\tilde{R}$ means coordinates along rotating coordinate system $\vec{e}^{\,\tilde{R}}$.

$$\underline{q}^{R} = \begin{bmatrix} \underline{t}^{R} \\ \underline{f}^{R} \end{bmatrix} \quad \text{with} \quad \begin{cases} \underline{t}^{R} &= \displaystyle\sum_{X=D}^{E,F} \left({}^{X_1}\vec{t}^{\,X_0^{\oplus}} + {}^{R_{\rm r}^{\oplus}}\vec{r}^{\,X_0^{\oplus}} \times {}^{X_1}\vec{f}^{\,X_0^{\oplus}} \right)^{\tilde{R}} + {}^{R_{\rm r}^{\oplus}}\underline{r}^{R_{\rm r}^{*}} \times {}^{\rm g}\underline{f}^{R_{\rm r}^{*}} \\ \underline{f}^{R} &= \displaystyle\sum_{X=D}^{E,F} \left({}^{X_1}\vec{f}^{\,X_0^{\oplus}} \right)^{\tilde{R}} + {}^{\rm g}\underline{f}^{R_{\rm r}^{*}} \end{cases} \tag{D.9}$$

A. Dealing with the average rotor loading $\overline{\underline{q}}^{R}$

Transform average coordinates $\overline{\underline{q}}^{R}$ in rotating coordinate system $\vec{e}^{\,\tilde{R}}$ of the resultant blade loading in the rotor centre $R_{\rm r}^{(+)}$ to

- average and periodic coordinates $\overline{\left(\underline{q}^{R}\right)^{R_{\rm fx}({\rm A})}}$ and $\widetilde{\left(\underline{q}^{R}\right)^{R_{\rm fx}({\rm A})}}$

in the associated stand-still coordinate system $\vec{e}^{\,R_{\rm fx}}$. The 'average-A' load coordinates $\overline{\left(\underline{q}^{R}\right)^{R_{\rm fx}({\rm A})}}$ are axially directed and are straightforward mapped to the average:

- co-axial torque and force loading on the gearbox house in point $R_{\rm h}^{(+{\rm s})}$
- co-axial fast shaft torque transmitted to the E-machine rotor in $R_{\rm f}^{(+{\rm s})}$

The accompanying deformation state of the rotor shaft and gearbox house follows from these loads via the stiffness of the co-axial linear and angular spring in the rotor centre $R_{\rm r}^{\oplus}$ (shaft) and in the mounting point $R_{\rm h}^{\ominus}$ of the gearbox to the nacelle (house). This yields the average values for the

- axial deviation degrees of freedom $\phi_x^{R_{\rm h}}$, $\rho_x^{R_{\rm h}}$ in mounting point $R_{\rm h}^{\ominus}$
- axial deformation degrees of freedom $\phi_x^{R_{\rm r}}$, $\rho_x^{R_{\rm r}}$ in rotor centre $R_{\rm r}^{\oplus}$

B. Dealing with the periodic rotor loading $\underline{\tilde{q}}^{R}$

Transform periodic coordinates $\underline{\tilde{q}}^{R}$ in rotating coordinate system $\vec{e}^{\,\tilde{R}}$ of the resultant blade loading in the rotor centre $R_{\rm r}^{(+)}$ to

- average and periodic coordinates $\overline{\left(\underline{\tilde{q}}^{R}\right)^{R_{\rm fx}({\rm B})}}$ and $\widetilde{\left(\underline{\tilde{q}}^{R}\right)^{R_{\rm fx}({\rm B})}}$

in the associated stand-still coordinate system $\vec{e}^{\,R_{\rm fx}}$. The 'average-B' load coordinates $\overline{\left(\underline{q}^{R}\right)^{R_{\rm fx}({\rm B})}}$ are perpendicular to the axial direction (yaw- and/or tiltwise). These loads are mapped to the average

- non-coaxial torque and force loading on the gearbox house in $R_{\rm h}^{(+{\rm s})}$,

- radial bearing force transmitted to the nacelle in $S_{\mathrm{n}}^{(+\mathrm{b})}$

This mapping is not so straightforward. It follows from the tilt- and yawwise deformation state of the rotor shaft and the gearbox house *while considering the rotor shaft's initial position as equilibrium*. This deformation state is obtained via a multi-body model of the rotor shaft, extended with 'cross coupled bending springs' in the gearbox slow shaft exit point $R_{\mathrm{s}}^{(-\mathrm{r})}$ ($\equiv R_{\mathrm{h}}^{(+\mathrm{s})}$). The latter result from yaw- and tiltwise flexible gearbox support in the mounting point $R_{\mathrm{h}}^{\ominus}$ to the nacelle. The inertia parameters of the multi-body model are moved to the rotor hub, while its elasto/viscous bending behaviour is transformed into bending springs that are fixed to the hub in the rotor centre $R_{\mathrm{r}}^{\oplus}$; note that the rotor shaft bending is constrained in radial sense by the main shaft bearing. The 'average-B' deformation state consists of the average values for the

- tilt- and yawwise deviation degree of freedom pairs $\{\phi_y^{R_{\mathrm{h}}}, \rho_z^{R_{\mathrm{h}}}\}$ and $\{\phi_z^{R_{\mathrm{h}}}, \rho_y^{R_{\mathrm{h}}}\}$ in in mounting point $R_{\mathrm{h}}^{\ominus}$

The calculation procedure also yields average values for the bending deformation degrees of freedom in the rotor centre. However these averages do not exist because the associated bending springs continuously rotate. Actually, the calculated values are the 'demodulations' of the '1p periodic value patterns' of the yaw0- and tilt0-wise[5] deformation degree of freedom pairs $\{\phi_z^{R_{\mathrm{r}}}, \rho_y^{R_{\mathrm{r}}}\}$ and $\{\phi_y^{R_{\mathrm{r}}}, \rho_z^{R_{\mathrm{r}}}\}$ in the rotor centre $R_{\mathrm{r}}^{\oplus}$.

In the calculation of the periodic state, the full periodic value patterns of the bending deformation degrees of freedom in $R_{\mathrm{r}}^{\oplus}$ arise from the dynamic response of the hub on the rotor loading $\underline{\tilde{q}}^R$. The periodic state of the gearbox house and support structure is correctly obtained if and only if:

- periodic load $\widetilde{\left(\underline{\overline{q}}^R\right)^{R_{\mathrm{fx}}(\mathrm{A})}}$ is injected in rotor centre $R_{\mathrm{r}}^{\oplus}$ at *shaft side*, NOT at *hub side*;
- average load $\overline{\left(-\underline{\tilde{q}}^R\right)^{R_{\mathrm{fx}}(\mathrm{B})}}$ is injected in rotor centre $R_{\mathrm{r}}^{\oplus}$ at *shaft side*, NOT at *hub side*.

The second 'load injection' prevents the appearance of undesired additional mean values in the gearbox house's deviation degrees of freedom that would coincide with the '1p periodic value patterns' of the bending deformation degrees of freedom in the rotor centre.

[5] yaw0-wise and tilt0-wise pertains to yaw and tilt orientation in the initial rotor shaft position

	Date: September 2004	**Report No.:** ECN-C--04-079
Title	TURBU Offshore, Computer Program for Frequency Domain Analysis of Horizontal Axis Offshore Wind Turbines; Implementation	
Author	T.G. van Engelen, H. Braam	
Principal(s)	Novem, Dutch Ministry of Economic Affairs	
ECN project number **Principal's order number**	7.5152 2020-01-12-10-001	
Programmes	Energieprogramma DEN, ARB	

Abstract

The design of offshore wind turbines requires to assess a huge amount of different sea-states and wind conditions. Therefor the calculational efficiency of a combined time/frequency domain approach is attractive. This was the reason for the development of the frequency domain tool TURBU Offshore. In addition, such a tool is very feasible for parameter studies; the dynamics of large offshore wind turbines use to be highly sensitive to the natural frequency values.

The implementation of TURBU Offshore is based on a modular linear model, with control loops included. The assumptions for structural and aerodynamic modelling are state of the art. A multi-blade transformation for three-bladed rotors eliminates the rotational coupling between the blades and the tower. Two-bladed rotors require a general handling of this coupling, which is however enabled by the model set-up. The program provides the mean loads, power spectra and periodic loads, which are merged to overall load histories for fatigue assessment. Besides, the power spectra make clear the relevance of poorly damped deformation modes.

Verification exercises point out that TURBU Offshore works well in stationary conditions and that it predicts damping rates and natural frequencies properly. It is expected that the use of TURBU Offshore in the design of wind turbines will yield substantial cost reduction for the nacelle, rotor and tower.

It is recommended to develop guidelines for the complementary use of TURBU Offshore with a time domain tool. The derivation of submodels for control design will be useful, just as the coupling of the linear structural dynamics model to an advanced aerodynamic code.

Keywords

wind turbine, offshore, frequency domain, computer programm, modelling, structural dynamics, wake dynamics

Authorization	Name	Signature	Date
Checked	D. Winkelaar		28/9/2004
Approved	H.B. Hendriks		28/9/2004
Authorised	H.J.M. Beurskens		28/9/2004